Dams and Appurtenant Hydraulic Structures

2nd Edition

Ljubomir Tanchev

CRC Press
Taylor & Francis Group
A BALKEMA BOOK

Dams and Appurtenant Hydraulic Structures

This page intentionally left blank

Dams and Appurtenant Hydraulic Structures

2nd Edition

Ljubomir Tanchev
University professor, retired


CRC Press
Taylor & Francis Group
Boca Raton London New York Leiden

CRC Press is an imprint of the
Taylor & Francis Group, an **informa** business
A BALKEMA BOOK

Illustration front cover:
Arch dam "Karun 3", 2004, Khuzestan Province, Iran, 205 m in height.

CRC Press/Balkema is an imprint of the Taylor & Francis Group, an informa business

Typeset by MPS Limited, Chennai, India
Printed and Bound by CPI Group (UK) Ltd, Croydon, CR0 4YY

Library of Congress Cataloging-in-Publication Data

Tanchev, Ljubomir, 1945–
[Brani i pridružni hidrotehnički objekti. English]
Dams and appurtenant hydraulic structures / Ljubomir Tanchev. — 2nd edition.
pages cm
"Translation of the publication which came out in Macedonian in 1999, with certain improvements and additions"—Preface.
First English edition: CRC Press/Balkema, 2005.
Summary: "Comprehensive and complete overview of all kinds of dams and appurtenant hydraulic structures, now in its second edition. Discusses various topics: general questions, design, construction, surveillance, maintenance and reconstruction of various embankment and concrete dams, hydromechanical equipment, spillway structures, bottom outlets, some special hydraulic structures, composition of structures in river hydraulic schemes, reservoirs, environmental effects of river hydraulic schemes and reservoirs and environmental protection. Special attention is paid to advanced methods of static and dynamic analysis of embankment dams. Richly-illustrated, fully revised, updated and expanded. Intended for senior students, researchers and professionals in civil, hydraulic, and environmental engineering and dam construction and exploitation"—Provided by publisher.
Includes bibliographical references and index.
ISBN 978-1-138-00006-3 (hardback) — ISBN 978-0-203-57705-9 (ebook PDF)
1. Dams. 2. Hydraulic structures. 3. Dams—Design and construction. I. Title.
TC540.T3713 2014
627'.8—dc23

2013050934

Published by: CRC Press/Balkema
P.O. Box 11320, 2301 EH Leiden, The Netherlands
e-mail: Pub.NL@taylorandfrancis.com
www.crcpress.com – www.taylorandfrancis.com

ISBN: 978-1-138-00006-3 (Hbk)
ISBN: 978-0-203-57705-9 (eBook PDF)

Table of contents

Preface

It is now more than ten years since the manuscript of the first edition was completed. This new (second) edition gave me a good opportunity to correct some errors, to update the text and references throughout, and, most importantly, to rewrite and enlarge parts of the text in response to some important developments in the field of dam design, analysis and construction. Major changes were imposed by the development in the field of embankment dam analysis (Chapters 8 and 9), concrete faced rockfill dams (Chapter 12), rockfill dams with a geomembrane facing (Chapter 13), rockfill dams with internal non-earth core (Chapter 14), roller-compacted concrete gravity dams, and hardfill dams (Chapter 18), and roller-compacted concrete arch dams (Chapter 20).

The main aim of the book remains the same as that of the first edition, i.e. to provide a complete and comprehensive picture of dams and the appurtenant hydraulic structures which are essential for their safe functioning, to: engineers specialising in the design, construction and exploitation of dams, to researchers and higher degree candidates in science, and to post-graduates in the fields of civil engineering, hydraulic engineering and environmental protection. The author also hopes that it will prove a useful text for students in their final year of undergraduate studies in the relevant disciplines.

The author would like to thank the publisher for the great effort made in providing the opportunity for this second edition.

Ljubomir Tanchev
Skopje, October 2013

This page intentionally left blank

Preface to the first edition

Water, one of the few natural resources without which there is no life, is distributed throughout the world unevenly in terms of place, season and quality. For this reason it is essential to construct dams on rivers, thus forming reservoirs for the storage and the even use of water. To date, forty-two thousand large dams have been built worldwide, and hundreds of thousands of smaller ones, which have made possible a rational use of a certain amount of river water – the most important water resource for human life and activity. Dams, together with their appurtenant hydraulic structures, belong among the most complex engineering works, above all because of their interaction with the water, their great influence on the environment and their high cost. Therefore great significance is given to theoretical research relating to dams, to improving the methods of analysing and constructing them, and to the knowledge gained in the course of their exploitation. In the past forty years great progress has been made in this respect.

More than twenty large dams and over a hundred smaller ones have been built in the Republic of Macedonia, which have still only partially exploited the available water, and flood control remains incomplete. The majority of the large dams were built in the period from 1952 to 1982 while, principally because of the lack of investment, the past twenty years have seen the construction mainly of smaller dams with a height of up to twenty metres and a reservoir volume of 300,000 cubic metres. In the next few years some two or three more large dams will be completed which will still not satisfy the need for water for the water supply, for irrigation and for the production of electrical energy, which are continually on the increase. The situation in all developing countries is similar, so that dams will continue to be built in the future despite the resistance on the part of devotees of the unobstructed flow of rivers.

The volume you have before you is a translation of the publication which came out in Macedonian in 1999, with certain improvements and additions. The text has been written with the intention of providing the reader with a comprehensive picture of dams and the appurtenant hydraulic structures which are essential for their safe functioning. The author hopes that it will prove useful to engineers specialising in the design, construction and exploitation of dams, to researchers and higher degree candidates in science, and to post-graduates in the fields of civil engineering, hydraulic engineering and environmental protection. Three years of experience of the Macedonian edition of the book have also demonstrated that a remarkable interest in it has also been shown by students in their final year of undergraduate studies in the relevant subjects.

Some 70% of the book is concerned with dams, while 30% is devoted to appurtenant hydraulic structures, hydromechanical equipment and to river hydraulic

schemes. The material is divided into five parts and thirty-five chapters. The *First Part* considers general questions about dams and appurtenant hydraulic structures (Chapters 1–5). The *Second Part* is devoted to embankment dams (Chapters 6–15) and the *Third Part* to concrete dams (Chapters 16–22). The *Fourth Part* deals with hydromechanical equipment and appurtenant hydraulic structures at dams (Chapters 23–30) while the *Fifth Part* is concerned with river hydraulic schemes as follows: Chapters 31 and 32 with the composition of structures in various different designs and types of hydraulic schemes, Chapter 33 with reservoirs, and Chapter 34 with the negative effects of river hydraulic schemes and with environmental protection, while Chapter 35 looks into questions of major importance relating to the repair and reconstruction of river hydraulic structures.

The most important achievements of the author's 25 years of research and practical work in the field of dams and hydraulic structures together with the achievements and experience of colleagues at the Department of Hydraulic Structures of the Faculty of Civil Engineering at the Ss. Cyril and Methodius University in Skopje have been incorporated into this book, and at appropriate points virtually all the more important dams in the Republic of Macedonia are described.

The list of people and institutions who have supported and assisted me in preparing this edition of the book is a long one. I would like to thank the *Fund of Waters* – Skopje, and the *Institute for Testing of Materials and New Technology 'Skopje'*, which financially supported the translation that was accomplished by Mr. Blagoja Neškoski and Prof. Graham Reid. I would also like to express my gratitude to the publisher who has made an English edition possible.

Ljubomir Tančev
Skopje, January 2005

Part I

Dams and appurtenant hydraulic structures – General

This page intentionally left blank

Chapter 1

Utilization of water resources by means of hydraulic structures

1.1 INTRODUCTION

Water plays an exceptionally significant role in the economy and in the life of all countries. It is of crucial importance to the existence of people, animals, and vegetation. The settling of people in different regions of the Earth has always been closely dependant on the possibilities for water supply, parallel with those for providing food, shelter, and heat. The increase in population, as well as the development and enrichment of mankind, in a number of places has reached a level at which the water supply, needed for the population, industry, irrigation, and production of electric power, has been brought to a critical point.

On the other hand, reserves of water on Earth are very large. They have been estimated to amount to 1.45 billion km^3 (Grishin et al., 1979). If we assume that the above quantity of water is uniformly spread over the Earth's surface, then the thickness of such a water layer would be almost 3,000 m. As much as 90% of that quantity is attributable to the water of oceans and seas, while the remainder of barely 10% belongs to lakes, rivers, underground waters, and glaciers, as well as moisture from water in the atmosphere. Only 1/5 of the freshwater, which is suitable for man's life and activities, is available for use.

The most significant place in water supply among usable waters is that of river courses. Some 2,000 km^3 of water belong to them, mainly appropriate to satisfy mankind's needs, which amount is not uniformly distributed over the continents: Europe (76 km^3), Asia (533), Africa (184), North America (236), South America (947), and Australia (24) (the percentage distribution of river water is presented in Fig. 1.1). The period of restoration of water in rivers taken on average amounts to 18–20 days[1], so that this most beneficial source of water provides on average about 38,000 km^3/year. Rivers, which are mainly fed from rainfall, satisfy the needs for water of 90% of the world's population.

River courses in the Republic of Macedonia take the most prominent place among waters usable for water supply Aegean, in which they flow out through the rivers Vardar and Strumica; then the Adriatic, to which they are taken away through the river Crn Drim (Black Drim); and the Black Sea, through the river Binachka Morava,

[1] Atmospheric humidity is usually replaced faster, on the average in 12 days, while underground waters need several hundred years for restoration.

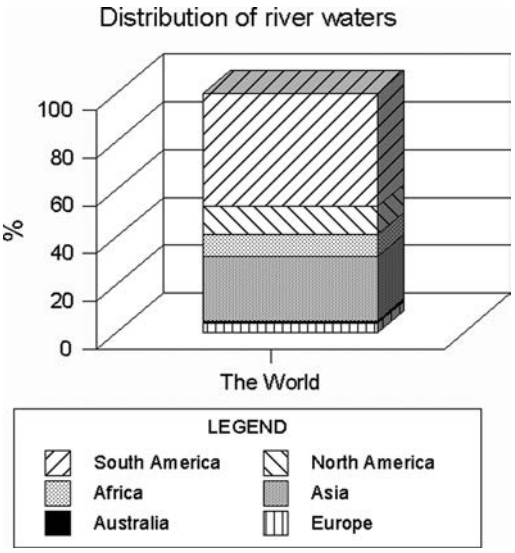

Figure 1.1 Distribution of river waters in the world.

which extends over an insignificant area. The largest is the catchment basin of the River Vardar, which extends some 20,525 km^2 or 80% of the territory of the Republic of Macedonia (Fig. 1.2). Taken on average, rivers in the Republic of Macedonia contain around 0.4 km^3 of water, i.e. a total of 7.5 km^3/year flows through these rivers. From this it is possible to conclude that each inhabitant of the Republic of Macedonia has half the quantity of river water in the world average.

An important unfavourable circumstance, which renders difficult a more complete utilization of water, is the fact that it is very not uniformly distributed on the Earth's surface – considering space, time, and quality. That is to say, particular countries and regions suffer from drought, while others possess too large quantities of water. Also, the very same region could, in the course of a particular period of the year, be exposed to drought, while suffering from floods in another period. In that way, water, that common nationwide wealth without which no life is possible, can be an irreplaceable friend to man, but also his great enemy if he is not able to utilize it in a correct manner and to keep it under control.

The uneven distribution of water regarding space, time, and quality, which is a characteristic feature also of the Republic of Macedonia, to a great extent renders difficult the utilization of water resources. This then imposes a need for the artificial redistribution of water by undertaking expensive engineering measures in order to obtain water for a given place and in a defined quantity, as well as at a pre-determined moment in time. The entirety of such engineering measures forms a separate part of the economy, which is called *water utilization*. We differentiate four basic water utilization branches, as follows:

1) Hydroenergetics, or the utilization of waterpower as a source of energy. The total annual output of hydroelectric power plants in the world amounts to 3,500

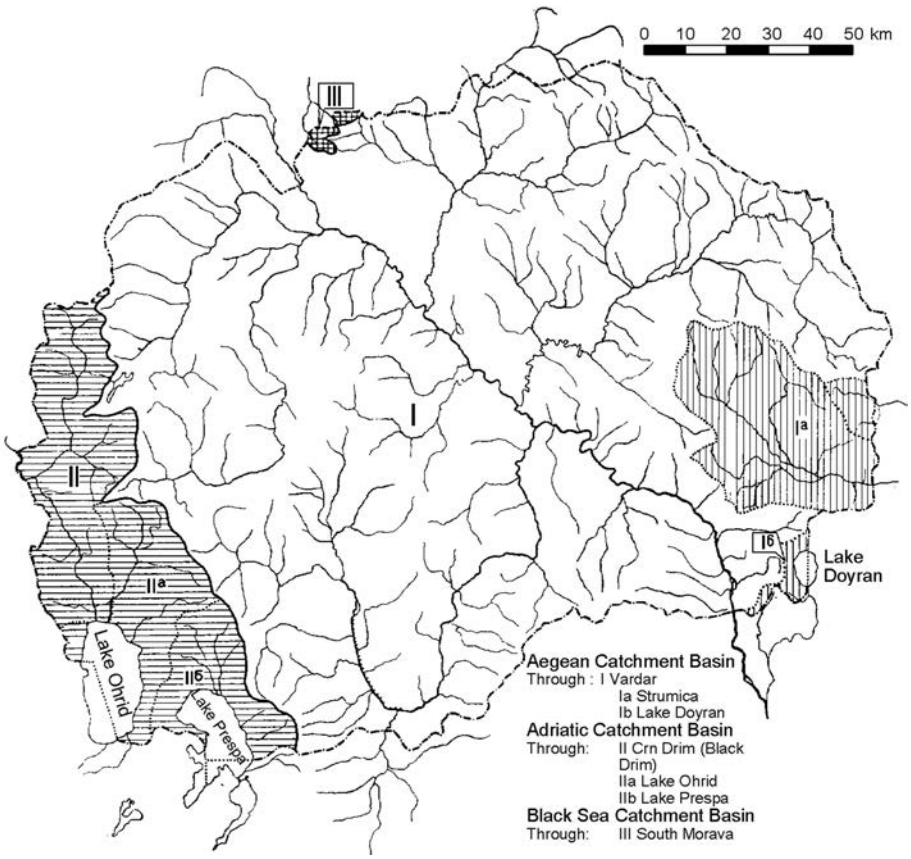

Figure 1.2 Catchment basins in the Republic of Macedonia.

TWh, which represents 20% of the overall consumption of electric power, i.e. 7% of the totally consumed energy from all power sources, along with noticeable variations from one country to another. Among the countries that have the highest percentage of production of electric power obtained from hydroelectric power plants are Norway (99%), Brazil (more than 90%), Albania (80%), Austria (70%), and Canada (more than 60%). The percentage in the Republic of Macedonia amounts to less than 15%. The total installed hydro capacity in the world amounts to 975,500 MW, while more than 176,000 MW are under construction (World Atlas, 2012).

2) Water transportation, or utilization of water as waterways, is the oldest and cheapest method of continental transportation, which is very important for a number of countries and represents an integral part of their transportation infrastructure. Water demands for navigation are usually for regulation of flow to maintain the minimum required water depth and the velocity below a safe maximum, as well as for water volume needed for passage through navigation locks.

3) Water supply and sewerage of inhabited places, industry, etc. – an area of vital importance for the life and economy of every country. Industrial demand, in many cases, is fairly constant throughout the year. Quantitative municipal demand has also little seasonal variation, but water supply for municipalities is closely interrelated with problems of water quality and potentially bad consequences of shortage.
4) Hydraulic land reclamation, i.e. irrigation of land, or else drainage of excess water from a specific territory. At the moment, irrigation systems cover approximately 270×10^6 ha, or 20% of the total cultivated areas. In many countries, especially in developing ones, increased food production is only possible by improving or increasing irrigation. The greatest amount of water is spent on irrigation – ¾ of total consumption in the world. Great efforts are made to develop effective ways of saving water by avoiding losses in distribution networks and by applying more skillful irrigation techniques.

In addition to the primary branches, there are also other water utilization branches, such as protection against floods, fish cultivation, maintenance of sanitary hygiene, and sports, recreation, etc. Among them, a very significant branch is protection against floods, which is always of particular interest to hydrotechnic engineers. Flood control is not a water use, but a demand for a more uniform time distribution of the flow. The most effective means to achieve this aim is reduction of flood peaks by storing the excess water in reservoirs. It is clear that there is a basic conflict between the objectives of flood control and of water conservation which has to be managed during operation of the reservoir.

It should be noted that in most cases, the very same watercourse is utilized for two or more water utilization branches. For example, a certain river could at the same time be utilized for water navigation, as well as for obtaining hydroelectric power. Or, water from a certain watercourse could be utilized for irrigation, water supply of an inhabited place, and for obtaining hydroelectric power. From this follows the fundamental principle of rational water utilization: water resources should be utilized in a complex way, in order to achieve the most effective and the most economical solution to water utilization problems, while at the same time taking into consideration not only the immediate but also future needs. Data required for the design of a multipurpose project are basically an aggregate of the data required for the various single purposes involved, but the method of analysis, although similar to those applied in design of single-purpose reservoirs, are more complex. The difficulties arise in the case of conflict of the requirements for the different purposes.

1.2 HYDRAULIC STRUCTURES (DEFINITION, CLASSIFICATION)

Civil engineering structures carried out for solving specific water utilization tasks are called *hydraulic structures*, while the applied science dealing with their general theory, design, construction, and operation is *hydotechnics* or *hydraulic engineering*.

The fundamental task of hydraulic engineering and hydraulic engineering structures is to adapt the actual natural water regime of rivers, lakes, underground waters, seas, etc. for the purpose of a worthwhile and economical water utilization for the

needs of the water utilization branch and for the protection of the environment from the harmful effects of water. Another task of hydrotechnics is the creation of artificial watercourses and reservoirs when there is a shortage of natural ones.

For fulfilling the above-mentioned tasks, two types of hydraulic engineering structures are usually constructed: *general hydraulic structures*, which are common to all water utilization branches; and *special hydraulic structures*, which serve the fulfilment of the purposes of separate water utilization branches.

General hydraulic engineering structures, according to their assignment, are divided into three different types:

1) *Water-retaining structures*, by means of which we raise the water level, for instance the riverbed, by constructing dams and specific types of embankments;
2) *Water-conveying structures*, by means of which artificial water courses are created, such as channels, tunnels, and pipelines (underground or surface and elevated structures, carried out by means of different materials). By means of these structures, water is conveyed in appropriate quantities for utilization for various purposes – for instance, for obtaining hydroelectric power in turbines of hydroelectric power plants, for water supply for inhabited places and the industry, for irrigation, and for draining water from surfaces, which are to be dried out, etc. Water-conveying structures can also be utilized for water navigation, and to encompass overflow and spillway structures, which serve for drawing off excess water from impounding reservoirs and its transfer downstream of the water-retaining structure;
3) *Intake structures*, which serve for intercepting water that, afterwards, is transported to users by means of water-conveying structures, depending on their needs.

Special hydraulic engineering structures are usually employed in only one or in part of water utilization branches, but not in all of them (otherwise they would be general structures). The following structures fall into this category:

- *special hydropower structures:* mechanical equipment buildings, reservoirs, chambers for water balancing, etc.;
- *special structures for water transportation:* water locks and lifting structures, harbors and wharves, quays, lighthouse structures, logways, etc.;
- *special structures of water supply systems:* specific intake structures, regular water intake structures, pump stations, water treatment plants, pipework structures for water supply (pressure relief chambers on head race structures, distribution shafts, shafts for aeration valves, etc.);
- *special structures for drainage and sewerage systems:* sewerage reticulation (catchment shafts and control manholes), pump stations, sewer cascade ramps, relief overflow weirs on collection mains, structures within water treatment plants (sedimentation tanks, biological stations, etc.);
- *special irrigation structures:* specific intakes, sedimentation tanks, structures on the channel network (inverted siphons, culverts, bridges, passages, distribution structures, cascades), structures on the pipework (shafts for aeration valves, outfall structures, distributing spreaders, etc.);

- *special structures used in drainage:* structures on the channel and drainage dewatering network (cascades, inverted siphons, culverts, bridges, core-walls for fixing the bottom, etc.);
- *structures for fishery economy:* fish passes (ladders), elevators, fishponds, spawner areas, etc.;
- *sporting recreational structures:* swimming pools, kayaking and rowing paths, etc.;
- *special structures for river regulation:* groynes and cut-off bunds, baffle piers, bank protection, etc.;
- *special structures for torrent regulation:* cascades, rustic structures, forestry-cultural measures (trenches, grassing, afforestation, etc.).

1.3 GENERAL FEATURES OF HYDRAULIC STRUCTURES

Water-retaining structures – dams. Dams are hydraulic structures for damming a riverbed in order to raise the water level and to create an artificial lake (impounding reservoir). According to their importance, dimensions, the complexity of the problems that should be solved during design and construction, their influence on the environment, etc., dams fall into the order of the most significant engineering structures in general.

They are built with local materials – clay, loam, sand, gravel, crushed stone, then concrete and reinforced concrete; particular structural elements require asphalt, steel, wood, plastic materials, etc. The most widespread are embankment dams, which are carried out with local materials; then, various kinds of concrete dams.

An enormous number of dams of various kinds have been built in the world. The Register of the International Commission on Large Dams (new version under preparation) lists around 45,000 large dams, i.e. dams higher than 15 m (or higher than 10 m, provided they fulfill certain other conditions, for which more details will be presented in Chapter 6).

Figure 1.3 presents the number of large dams constructed in the world in specific time periods, with (1) and without China (2), in which there are built more than half of all the large dams in the world, mainly of small height – up to 30 m. All the dams together form a total reservoir storage of more than 6,000 km^3, which is more than three times more than the volume of water that is contained in all rivers of the globe. Although the highest dam reaches 300 m, the majority of constructed dams are of considerably lower height. As such, 95% of all the large dams are lower than 60 m, 79% are lower than 30 m, while only 1% are higher than 100 m.

In spite of the great number of the dams constructed, more will have to be built, regardless of the fact that they have a certain negative influence on the environment and that day by day new opponents to the construction of dams appear, acting unitedly in various associations. That is to say, the population in developing countries is increasing rapidly and, towards the end of the century, it is expected to reach 10 billion inhabitants, Figure 1.4 (Pircher, 1993; Veltrop, 1991). That imposes the need for an urgent enlargement of the impounding reservoir space in most countries of the world.

In the period from 1990 to 2000, water interception in the world increased by a rate of 2–3%. Taking into consideration the present burden of the water resources,

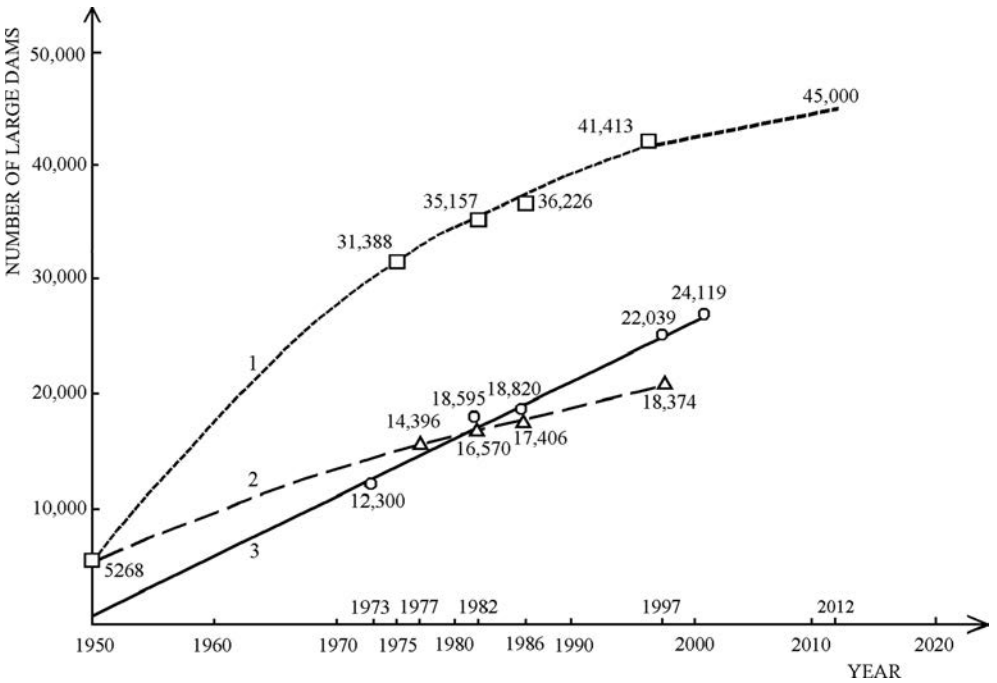

Figure 1.3 Total number of constructed dams in the world (after Jiazheng & Jing, 2000). (1) total number of large dams in the world; (2) number of large dams in the world except China; (3) number of large dams in China.

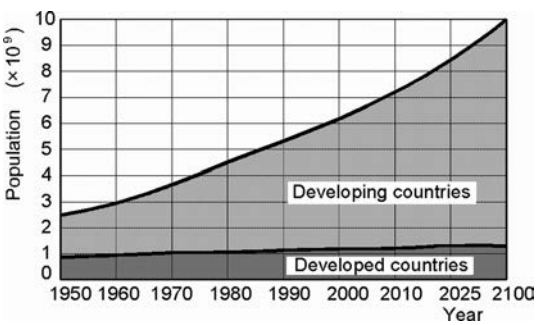

Figure 1.4 Increase of population in the world.

it is evident that the near future will also necessitate the construction of large dams, along with appropriate appurtenant hydraulic structures, which will make possible maximum utilization of river courses. The need for new dams and reservoirs applies in particular to the developing countries, which account for 70% of the world population, and for about 95% of annual population growth. It is estimated that at least 1.5 billion people have no access to a reliable source of drinking water and millions die from water-related diseases every year. Also, in regard to protection against flooding, dams, along

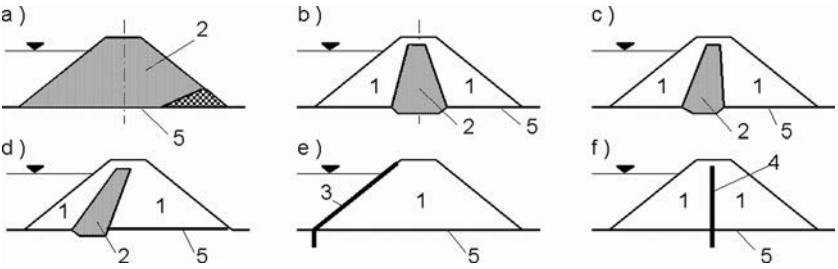

Figure 1.5 Various types of embankment dams. (a) Homogeneous; (b, c, d) zoned; (e) with impermeable face lining, and (f) with an internal core wall made of artificial material (1) Permeable earthfill material; (2) impervious earth material; (3) facing; (4) diaphragm wall (core) made of artificial material; (5) impervious foundation.

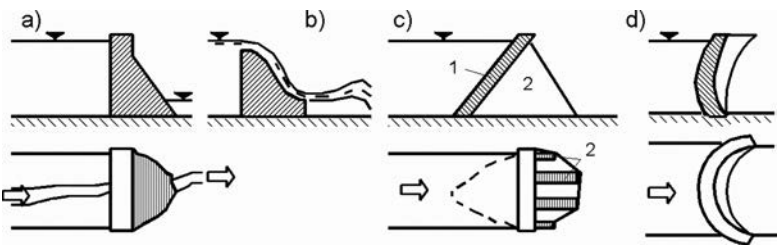

Figure 1.6 Schematic view of concrete dams.

with their appurtenant hydraulic structures, have an irreplaceable role. A number of dams in the world have been built, and will be built, for this purpose only.

Embankment dams are erected by means of placement and compaction of local earthfill and rockfill materials; their cross-section has the form of a trapezium (Fig. 1.5). They can be homogenous (a), when the dam body is made of more or less impervious material; or zoned (b, c, d), in which case there are constructed zones of various materials in the dam body, in which case impermeability is ensured by means of a relatively thin zone of cohesive material (2). There is also a third type of embankment dam (e, f), the impermeability of which is achieved by means of facing (3), or by means of an internal core wall made of artificial material (4) – concrete, reinforced concrete, asphalt, geosynthetics, or very rare steel. In Chapter 6 the classification of embankment dams will be discussed in more detail. Part Two of the book deals with the complex issues surrounding embankment dams.

Concrete dams (Fig. 1.6) are divided into massive (gravity) dams (a, b), buttress dams (c) and arch dams (d). At a rough estimate, the cross-section of a gravity dam has the form of a triangle and, as distinguished from an embankment dam (over which overflowing of water, as a rule, is not allowed), they can be constructed as no-overflow dams (a) or overflow dams (b). Part Three of this book is devoted to different types of concrete dams.

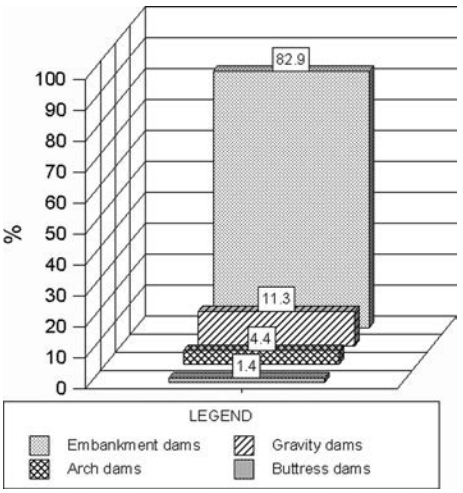

Figure 1.7 Particular kinds of dams in the world.

A common feature of embankment and gravity dams is that horizontal forces are resisted by their self-weight, i.e. they act as gravity dams. Buttress dams consist of a relatively thin slab (1) supported by buttresses (2) on the downstream side. The foundation of arch dams has a curved form, with the convex side turned towards the water, whereas their cross-section is a relatively thin, curved wall. They are constructed on a firm and sound rock, upon which is a restrained arch girder whereon they transmit their horizontal loading. Buttress and arch dams are also constructed as overflow dams, although much less frequently than the massive (gravity) dams are.

Concrete dams have yet another specific feature – water-conveying and outlet structures can be carried relatively simply out in the dam wall, and they are used for discharging the water from the impounding reservoir. Concrete dams are smaller in number than embankment dams – the representation of particular dams in the world, in accordance with data for 34,798 dams, registered in ICOLD in 1985, is presented in Figure 1.7. Should only higher dams be taken into consideration (for instance, higher than 100 m), then the picture essentially changes.

The potential of rivers in Macedonia is utilized to hardly 30%, and yet there is a permanent shortage of water for various purposes. The uneven distribution of water in time and space is strongly expressed, so that it is indispensably necessary to construct new impounding reservoirs for its equalization.

The construction of dams in the Republic of Macedonia (Fig. 1.10–1.13) dates from 1938, when the *Matka* (or Saint Andrea) arch dam was built, located on the River Treska, in the vicinity of Skopje. Until now, some 27 large dams have been built which enclose impounding reservoirs (Fig. 1.8, Table 1.1), as well as four dams forming tailings for industrial waste. The highest dam among them is the Kozyak, on the River Treska, commissioned in 2004, which has a structural height of 130 m (height above the terrain is 114 m). Two dams are higher than 100 m – Tikvesh (113.5 m) and Shpilje (112 m) – embankment dams, which were also the highest embankment dams in the

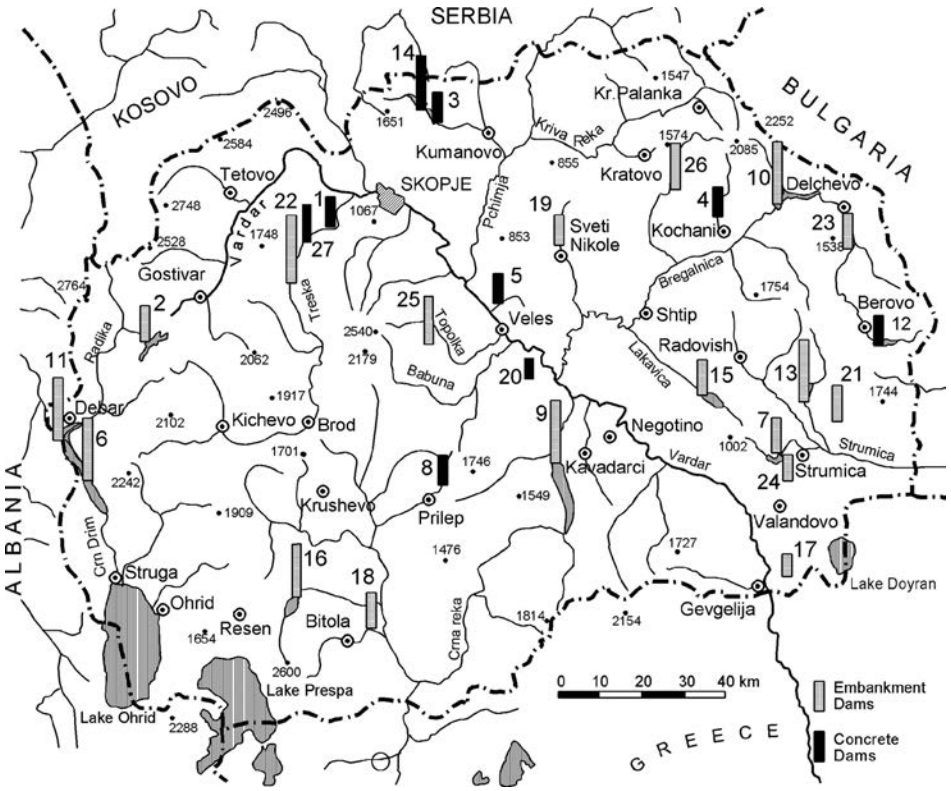

Figure 1.8 Dams in Macedonia. (1) Matka, $H_k = 38$ m; (2) Mavrovo, 62 m; (3) Lipkovo, 40 m; (4) Gratche, 43 m; (5) Mladost, 34 m; (6) Globochica, 90 m; (7) Vodocha, 48.7 m; (8) Prilep, 38.5 m; (9) Tikvesh, 113.5 m; (10) Kalimanci, 92 m; (11) Shpilje, 112 m; (12) Ratevska Reka, 53 m; (13) Turiya, 93 m; (14) Glazhnja, 80 m; (15) Mantovo, 49 m; (16) Strezhevo, 84.6 m; (17) Paljurci, 21.5 m; (18) Suvodol, 38.3 m; (19) Mavrovica, 24 m; (20) Podles, 22.5 m; (21) Ilovica, 29.8 m; (22) Kozyak, 130 m; (23) Loshana, 45.2 m; (24) Markova Reka, 30 m; (25) Lisiche, 76.9 m; (26) Knezhevo, 83 m; (27) Saint Petka, 64 m.

former Yugoslavia. Many small dams have also been constructed (more than 100), chiefly during the last twenty years[2].

Water-conveying structures. Channels fall into the group of water-conveying structures (Filjov et al., 1972; Fig. 1.9), and they are constructed by excavation into the ground (a), and can be formed by means of manmade embankments (b) or else, partially by excavation and partially with embankments (c). Also, *man-made course beds,* which are made of reinforced concrete and sometimes of wood or metal, are placed on the surface of the ground or elevated over supports (Fig. 1.9 d–f) and are employed when topographical and other conditions do not allow the construction of channels

[2]The Republic of Macedonia does not apply the ICOLD criterion, so that dams cited in Table 1.1 are in fact those treated as dams of particular interest to the country. Other dams higher than 15 m have also been constructed.

Table 1.1 Large dams in Macedonia.

Name	River	Year completed	Type	H [m]	H_S [m]	L [m]	V_D [$m^3 \times 10^3$]	V_R [$m^3 \times 10^6$]	Purpose
1. Matka	Treska	1938	AR	29.5	38	64	3	3.55	HEP
2. Mavrovo	Mavrovska	1952	EAR	54	62	210	777	357	HEP, IR
3. Lipkovo	Lipkovska	1958	AR	29.5	40	203	13	2.25	IR,WS
4. Gratche	Kochanska	1959	AR	29	43	150	12	2.4	WS, IR
5. Mladost	Otovica	1962	AR	27	34	73	2.56	8	IR
6. Globochica	Crn Drim	1965	E-R	82.5	90	196	998	58	HEP
7. Vodocha	Vodocha	1965	E-R	4	48.7	185	316.8	26.7	IR,WS
8. Prilep	Oreovechka	1966	MA	35	38.5	408.5	25.5	6	IR
9. Tikvesh	Crna Reka	1968	E-R	104	113.5	338	2722	475	IR, HEP
10. Kalimanci	Bregalnica	1969	E-R	85	92	240	1389	127	IR, HEP
11. Shpilje	Crn Drim	1969	E-R	101	112	330	2699	520	HEP
12. Ratevska	Ratevska	1972	AR	49	53	194	21.7	10.5	WS, IR
13. Turiya	Turiya	1972	E-R	77.5	93	417.3	1978	48	IR,WS, HP
14. Glaznja	Lipkovska	1972	AR	71.5	80	344	168	22	IR, HEP
15. Mantovo	Lakavica	1975	E-R	37.5	49	138	261	47.5	IR,WS
16. Strezevo	Shemnica	1982	E-R	76	84.6	632	4300	112	IR,WS, HEP
17. Paljurci	Luda Mara	1982	EAR	21.1	21.5	310	185	2.9	IR
18. Suvodol	Suvodolska	1982	EAR	33.9	38.3	941	1740	7.88	R,WS
19. Mavrovica	Mavrovica	1982	EAR	24	29	360	400	2.8	WS, IR
20. Podles	Vodnik	1985	AR	18	22.5	92	6.7	0.31	IR
21. Ilovica	Ilovichka	1999	E-R	27.8	29.8	274	131	0.5	WS, IR
22. Kozyak	Treska	2004	E-R	114	130	300	3340	550	R, HEP,WS
23. Loshana	Loshana	2006	R-F	41	45.2	165	260	1.08	WS
24. Markova R.	Markova R.	2006	E-R	26	30	72.5	64.6	0.66	WS
25. Lisiche	Topolka	2008	ERT	66	76.9	579.6	3295	23	WS, IR
26. Knezhevo	Zletovska	2011	E-R	75	83	290	1550	23.5	WS, IR, HEP
27. Saint Petka	Treska	2012	AR	41	64	115	32.5	9.1	HEP

Key: H – height above ground; H_s – structural height; L – length of dam crest; V_D – dam volume; V_R – maximum reservoir capacity; EAR – earthfill dam; E-R – earth-rock dam; R-F – rock-fill dam; AR – arch dam; MA – multiarch; WS – water supply; IR – irrigation; HEP – hydroelectric power; R – retention.

in the ground. *Tunnels* also fall into this group and they are built under the ground in those cases when very deep excavation would be necessary for the execution of channels, i.e. in cases of cutting into high hills (g, h). *Pipelines,* manmade closed course beds or troughs, most often made of steel or reinforced concrete, are placed on the surface of the ground, embedded or surrounded by concrete (i).

Intake structures. These hydraulic structures assist in the process of direct utilization of water from the water source. They are erected directly on the river course, or else in the case of an impounding reservoir, in which case they can be surface or underground, carried out in the dam wall or outside it. During their design and construction certain common problems must be solved, such as: controlled capture of needed water, elimination of sediment, silt and floating objects, the possibility of controlled operation at various water levels in the source of water capture, etc.

Hydraulic structures are constructed on rivers, lakes or seas, and are named accordingly: *river structures, lake structures, or sea structures*. This book deals with river hydraulic structures, which are of crucial importance for everyday human life.

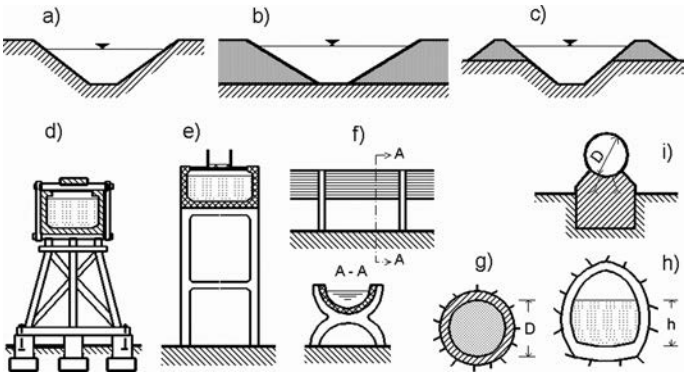

Figure 1.9 Examples of water-conveying structures. (a–c) Channels; man-made course beds; (d) wooden; (e, f) reinforced concrete; (g, h) tunnels; (i) pipelines.

Figure 1.10 Kozyak dam, the highest in Macedonia.

A group of hydraulic structures that are interconnected with conditions for joint work and with their location form *a hydraulic scheme*. Within the composition of the hydraulic scheme fall general and special hydraulic structures and, at the same time, they also are divided into *basic structures*, *auxiliary structures*, *and temporary structures*.

Basic hydraulic structures ensure the normal operation of the hydraulic scheme, create the required pressure and volume of the impounding reservoir and make possible

Figure 1.11 Turiya dam (Macedonia).

the realization of the special water utilization functions for which the hydraulic scheme has been created.

Auxiliary and *temporary* structures are necessary during the construction of the hydraulic scheme, as well as during its operation, when they are useful for the utilization of the basic structures. During that stage, auxiliary structures are non-hydraulic structures such as residential dwellings and administration buildings, roads, communications and lighting.

Within certain, usually large, territory hydraulic structures are very often interconnected. Such a complex of hydraulic structures, which are usually united into several hydraulic schemes with joint purposes, is named *a water utilization system* or *a hydro system*. There are hydro systems with only one function, as well as complex ones, which all satisfy the needs of a number of water utilization branches.

General hydraulic structures are necessary as appurtenant structures to the dams, and they are described in Part Four of this book, together with the hydromechanical equipment and some special hydraulic structures. Part Five of the book is devoted to the composition of the structures in the frame of different type of hydraulic schemes with dams.

Hydraulic structures, dams in particular, are characterized by a number of main features, which make them visibly different from most other engineering structures. Those features are:

1. *Action of water on the structure*. Water has a multiple effect on the hydraulic structure: (a) *mechanical action*, which consists of the pressure caused by water that is still and moves across the surface, or is percolating through the soil; (b) *physical–chemical action*, involving corrosion of metal parts, and damage to concrete; (c) *biological action*, which is demonstrated through the rotting of wooden parts. Water also acts indirectly on the structure through ice pressure and deposited

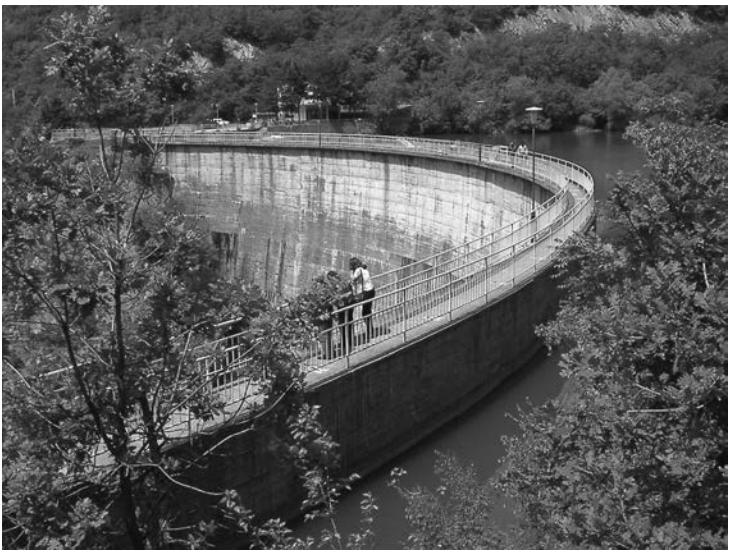

Figure 1.12 Gratche dam, one of the eight Macedonian arch dams.

detritus and sediments, as well as through the abrasive action of sediment, silt, and detritus, which water carries over the surface parts of the structure.

2. *Influence on the environment.* Hydraulic structures have a big influence on the environment, even causing significant changes in the nearby area. Dams raise the level of rivers, often at a considerable length in front of the structure, and at the same time and as a consequence, there is flooding of the riverbanks and also a raising of the underground water level. That imposes a requirement applicable during the construction of the hydraulic structures, especially dams: to take into account the conditions existing not only in the field where the structure is being constructed, but also much wider afield. Dams also have a noticeable influence on the quality of the water in a dammed river course, both upstream and downstream.
3. *Responsibility.* Consequences due to the failure of a hydraulic structure can be disastrous, which makes these structures very responsible and imposes the necessity during their dimensioning, to proceed with a high safety coefficient. Meanwhile, design, revision of design documentation, construction, and supervision control of works during construction should be at the highest level.
4. *Conditions for construction.* Conditions for construction of hydraulic structures are specific and are reflected in the following:

    a) In the course of construction it is necessary to solve the problem of giving passage to the water of the watercourse which can also be at a very high level in the case of the occurrence of flood waters;
    b) In some cases, construction work has to be performed under water;

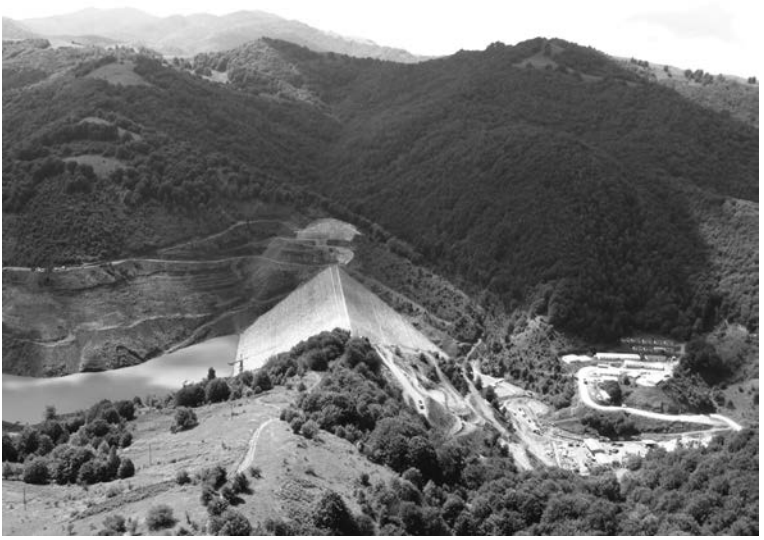

Figure 1.13 Knezhevo dam, first Macedonian embankment dam with asphaltic concrete core.

c) Hydraulic structures are most often located on ground that is far away from inhabited places, which makes organization of the works more difficult;
d) A powerful plant and equipment is necessary for such an enormous scope of construction work, especially earthworks, but also often necessary for concrete works; and
e) Stage construction is required in quite a number of cases, in order to facilitate faster implementation of certain facilities, which also complicates construction.

5. *Need for monitoring.* During construction, and especially in the course of utilization, hydraulic structures must be subjected to permanent, well-planned, and organized monitoring and surveillance. For that purpose, within the body of the structure dam wall, as well as in the surrounding ground, it is necessary to incorporate expensive equipment for measuring deformations, stresses, pore pressures, and seepage, as well as seismic occurrences. These safeguards ensure a permanent insight into the structure's condition, and that is very important from the viewpoint of safety and for the secure operation of the structure.
6. *Uniqueness and unrepeatedness.* The kind, construction, and dimensions of hydraulic structures – especially dams – are in close connection with local topographical, geological, and hydrological conditions. Taking into consideration that these conditions all, or some of them, differ from one site to another, it is obvious that every hydraulic structure will have its own individual characteristics and, in practice, is unique. Owing to that, in the design of such structures, any templated approach should be excluded. That is why it is necessary to perform a thorough analysis of the specific conditions that exist in the field.

7. *Cost*. In addition to the fact that investment expenditures for hydraulic structures are relatively high, which is stipulated due to the proportions and complexity of the structures – a dam above all – the high cost of hydro-mechanical equipment, special hydraulic structures, and operational costs are relatively low. Therefore, depending on the amount of credit interest rates, investments could be economically justified.

1.4 INTENT OF DAMS. ELEMENTS OF A DAM AND A RESERVOIR

Among general hydraulic structures, dams are the most important and the most expensive. They are constructed for two main purposes:

1. To raise the water level in a river to a certain elevation; and
2. To create an accumulation for gathering water.

Raising the water level in a river is necessary in order to make possible capture of water and its conducting away, as well as its utilization for irrigation, water supply, and obtaining hydroelectric power in the case of a headwater hydroelectric plant. Other purposes include creation of head for discharge hydroelectric power plants, improving conditions for navigation of the river, and sanitary reasons.

Dams forming an impounding reservoir are constructed in order to enable the regulation of a river course – during periods of abundant water, the water is impounded and stored in the impounding reservoir space in order to be utilized in the course of a drought period. In this way, a leveling is achieved, i.e. an equalization of the outflow in the course of time. Depending on the size of the impounding reservoir space, the equalization can be carried out in different time periods, i.e. it can be on a daily, weekly, yearly, or multi-year basis. Water from the accumulation is utilized in accordance with the intent for the needs of one or more water utilization branches. During the operational service of the hydraulic scheme, the water level in the impounding reservoir varies, so that the hydraulic scheme operates at variable pressure.

In general, we can differentiate three characteristic levels of water in the impounding reservoir (Fig. 1.14a): minimum water level (Min.W.L.), normal water level (N.W.L.), and maximum water level (M.W.L.).

These three levels divide the impounding reservoir space, formed by the dam (1), into three parts:

Dead storage I, which is not utilized and which is expected in the course of the operational structure's life (for example 50 years) to become filled with silt and deposits;

Live storage II, i.e. a part of the impounding reservoir capacity that is used for water utilization purposes. It is determined by taking into consideration of various economical, water utilization (i.e. water resources management), and other conditions, defined prior to the commencement of the dam's design;

Retention storage III, stored between the normal and maximum level, serving for the retention of flood water.

The maximum level is the highest possible level of the impounding reservoir and it rarely occurs at the outbreak of exclusively high waters (for instance with a probability

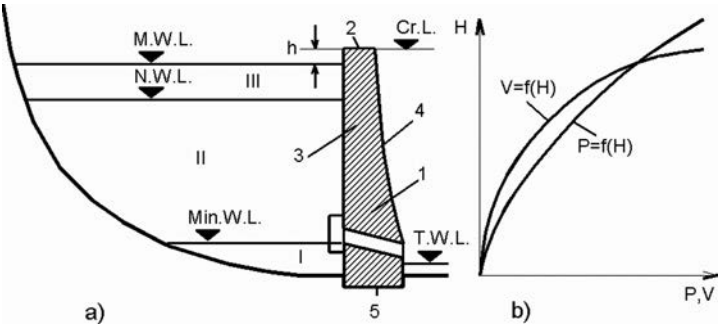

Figure 1.14 Elements of a dam and a reservoir.

of occurrence once in a thousand, or else, once in ten thousand years). At the same time, the overflow structures within the hydraulic scheme are completely open. The level of dead storage represents the lowest possible level of the water in the impounding reservoir and is connected with the bottom edge of the outlet structure.

Figure 1.14a denotes also the basic elements of the dam (1, shown schematically) as follows: crest of the dam (2) the highest horizontal surface of a no-overflow dam, raised over the maximum water level for the value of freeboard h; upstream side of dam (3), i.e. the side turned toward the impounding reservoir; downstream side of dam (4); foundation of dam (5); and tail water level (T.W.L.), i.e. the level of water in the riverbed downstream of the dam.

When designing dams which form impounding reservoirs, it is necessary to have two curves which outline the dependence of the impounding reservoir volume, i.e. the surface of the water table of the water level, $V = f(H)$ and $P = f(H)$ (Fig. 1.14b). These curves are generated over the surface of the water table for a certain water level of the impounding reservoir, earlier obtained by measuring an area by planimeter on the general layouts, for a known location of a dam site, and now, using much more advanced computer-based geodetic methods.

1.5 APPURTENANT HYDRAULIC STRUCTURES

For proper and safe service of a dam, it is indispensable, within its framework, to anticipate various general or special *appurtenant hydraulic structures*. The general (or common) structures serve all water economy branches. Among the general hydraulic structures, the most significant are the *spillway* and *outlet works* which, almost without exception, are constructed in every hydraulic scheme with a dam. In the frame of the hydraulic scheme, other ancillary facilities are incorporated as necessary during the dam construction and in the service period, like river-diversion structures, intake structures, etc.

The spillway structures have the task of evacuating flood waters from the reservoir at an assigned maximum level of the headwater and conveying them downstream in a safe manner. The structure and the type of the spillway works depend primarily on

Figure 1.15 Spillway works at concrete faced rockfill dam El Cajón (Mexico), $H = 189$ m, commissioned 2006, with controlled spillway, chute channel and flip bucket (courtesy Mr. Humberto Marengo).

the quantity of the flood water that should be evacuated, on the type of the dam, on the dam site topography and geology, and on other factors, described in Chapter 23.

The spillway contains several principal components: the spillweir or overflowing part of the dam, the spillway channel or tunnel with the purpose of conducting flood flows downstream of the dam and a stilling basin or other energy-dissipating structure. There are uncontrolled spillways, i.e. they function automatically as the water level rises above normal water level (NWL), or they may be controlled by gates. The different types of spillways are discussed in Chapters 26 and 27.

The maximum water quantity which should be evacuated by means of the spillway structures depends on the significance and size of the dam. A common practice for the spillways of large dams was to be dimensioned for flood water with a probability of 0.01% occurrence for embankment dams and 0.1% for concrete dams. This rule has been subject to serious revision over the past decades because of more cases of overflowing and failure of dams mainly as a consequence of an insufficient spillway capacity. As a result, in the USA, as well as in all other developed countries, an obligation has been introduced: for all more significant dams, the spillway structures should be dimensioned for the probable maximum flood – PMF (USCOLD, 1988). This tendency has spread to an increasing number of countries, and even already constructed dams are subject to revisions. The determination of the maximum flood water is an extremely complex problem and it should emerge from a detailed study, worked out separately for each specific case, and not through a linear application to water with a certain probability of occurrence. In the analysis one should particularly take into consideration the location of the dam, type of dam, procedure which is used for determination of design flood and the availability of measurements upon which the applied procedure is based.

Figure 1.16 Spillway and outlet work at the arch dam Karun 3 (Iran), $H = 205$ m, commissioned 2004.

The bottom outlet works serve to empty the reservoir (completely or to a certain level) in case of need for repairs to the structures of the hydraulic scheme or when there is danger of a failure of the dam. In some cases, especially at smaller dams, the bottom outlet also serves for discharging water from the reservoir to satisfy sanitary and water management requirements downstream of the hydraulic scheme. The above-described function of the outlet works dictates that it should be positioned low in relation to the crest of the dam, that is to say, close to the foundation. That is why, usually, it is called a bottom outlet. The construction and position of the bottom outlet depend, first of all, on the type of the dam, the purpose of the reservoir, and the quantity and depositing of silt. The level of the entrance edge of the outlets is most often dictated by the level of the dead storage in the reservoir, i.e. by the conditions for discharging the minimum quantity of water for satisfying the biological minimum in the river downstream of the dam.

The capacity of the outlet works is determined on the basis of the time which is necessary for emptying the reservoir and the necessity for water to satisfy the biological minimum in the river downstream of the dam. While the second condition gives a certain fixed quantity of water that should be conveyed through the outlet works, the first one – time necessary for emptying the reservoir – is determined separately for each hydraulic scheme, depending on local conditions. In that respect, a number of influential factors should be analyzed, such as: type and size of dam, volume of water storage, water head, the possibility during emptying the reservoir of also using water-conveying structures constructed for other purposes, inflow of the water in the reservoir during the emptying process, and conditions existing in the watercourse downstream from the hydraulic scheme. In some cases, the time required for emptying can be

2–3 days; in other cases, 2–3 weeks, while a month or two may be needed at larger reservoirs. At extremely large reservoirs (with volumes of billions m^3) it is practically impossible to significantly lower the water level in a reasonable time period by means of a bottom outlet structure. Various questions regarding the bottom outlet structures will be discussed in more detail in Chapter 28.

1.6 SHORT REVIEW OF THE HISTORICAL DEVELOPMENT OF HYDRAULIC STRUCTURES

The beginnings of construction of hydraulic structures go back to the ancient world, when civilizations were formed around big rivers (Smith, 1971). Initially, the Sumerians, who inhabited Mesopotamia, and afterwards the Assyrians and Babylonians, developed certain techniques and methods for defense against floods and for irrigation by utilizing the waters of the Tigris and the Euphrates, as did the ancient Egyptians, achieving fast drainage following flooding of the fertile land in the valley of the Nile.

The first dam, Sad el-Kafara, was built in Egypt about 2900 BC. It was constructed of earth material, 12 m high, and its remainders are visible even today (see Chapter 6). The Assyrians, in 1300 BC regulated the riverbed of the Tigris, fortifying the riverbanks with stone blocks and baked bricks, under the protection of a temporary dam (Van Asbeck, 1962).

Before our era, hydraulic structures were also built in other parts of the world such as Arabia, India, Sri Lanka and China. A well-known example is the Marib embankment dam, completed in Yemen around 750 BC for irrigation. This dam was raised to a final height of 20 m in several stages, during a rather long time period. From the same period dates the first significant masonry dam, 10 m high, built in Turkey. In Sri Lanka (Ceylon) even the ancient inhabitants built reservoirs in order to accumulate the water from monsoon rains for utilization in the course of drought periods. The first dam was built in 504 BC, and there has been continuous further construction since then, so that on this island there have been built over 30,000 mainly small reservoirs along with the abandoned ones, most of them in droughty and rainless areas where farming would not exist without irrigation.

In the period of the Roman Empire, a number of monumental hydraulic structures was built, which demonstrated the orientation of the Roman engineers to build strong, firm, and lasting structures. Dams have a particular place among them. For instance, in Spain, northeast of Merida, in the second century and during the period of the Emperor Augustus, the 20 m high dam Cornalvo was built. After its reconstruction in 1936, even nowadays it is still being utilized for irrigation. It is believed that the first arch dam was completed in the second century AD, in France. The Roman influence in dam construction in the Mediterranean countries was significant and long lasting.

The Japanese and Indian dam construction practice commenced around 750 AD, and was a notable contribution to the early development of embankment dams.

The period after 1000 AD is characterized by growth in the dams' height, as well as in the development of new concept. Of particular importance are more masonry dams built in Iran, including the first true arch dams (Kebar, 26 m high, Kurit, 43 m, etc.). Around the same time, smaller dams were being built in Europe, mainly below 10 m in height.

Feudal Europe did not bring any great progress in the construction of hydraulic structures, with certain rare exceptions, such as the invention of the ship lock, which meant a lot for the development of water transportation.

In the 16th century Spain made a considerable advance in the field of masonry dam construction. The Tibi gravity dam, 42 m high, was completed in 1594, and the Elche arch dam, 23 m in height, was completed in 1640. Then, the experience of Spanish dam-builders was transferred to Central and South America. After 1800 AD the dam design was improved by application of some empirical rules, combined with experience. Thus, dams steadily increased in size.

In the first half of the XIX century in Europe and the USA, a number of dams were built which made possible accumulation of water for water supply. The second half of the XIX century indicated brighter prospects for hydrotechnics, thanks to the invention of the steam-roller (1859), concrete, and reinforced concrete, as well as Darcy's law on flow through the porous earth medium. In that period, also rational methods of analysis for masonry dams were developed, mainly in France, Britain and in the US, enabling the construction of lots of such structures in different countries.

Hydraulic engineering has experienced an expansive development in the course of the last 80 years when an enormous increase in needs for water and energy for the population has occurred, as well as for industry, mining, and agriculture. This expansion, to a very great extent, has been assisted by the appearance and development of soil mechanics, by engineering, and by the manufacture of contemporary plants and equipment for carrying out large and complex civil engineering undertakings. The development of modern methods for static and dynamic analysis (dependent upon the development and availability of modern powerful computers), along with model testing investigation of structures, also played a significant role in the expansion of hydraulic engineering.

This page intentionally left blank

Chapter 2

Foundations of dams

2.1 FOUNDATIONS FOR HYDRAULIC STRUCTURES IN GENERAL

Hydraulic structures, like other civil engineering structures, are built on construction ground, i.e. on the topmost formations of the earth's crust. The well-known dam builder and French engineer, André Coyne,writes: "*There is no structure that is so firmly bonded to the foundation as the dam is . . . In other words, the dam consists of two parts: an artificial dam, made by the man, and a natural dam – the foundation upon which it is founded and which, at the same time, also represents its continuation and surrounding. The more significant part, of these two, is the latter, even though it is invisible.*" (André Coyne, *Cours de Barrages*, l'Ecole Nationale des Ponts et Chaussées, Paris, l939). Dam builders, of course, have always been aware of this fact; however, the variety of features of the foundation, until not long ago, has dictated the experiences, together with some empirical rules, to be used mainly in the calculations of dams.

The uppermost layer of the earth's crust, which is interesting from the point of view of civil engineering, generally consists of three parts: the surface soil or *topsoil*, having a very limited depth and originating in the disintegration of organic matter. Next is the *subsurface soil*, which is directly below the topsoil and consists of one or more layers originating from the disintegration of firm rocks. Finally, a *rock layer*, which serves as the firm part of the foundation.

All kinds of rocks and soils are aggregates of different minerals or broken remnants of the parent rock. Rocks and soils differ in strength that is determined as these are worked. Generally, rock materials are hard. Thus, for their manual working we use tools, such as a crowbar or a pick, or we resort to blasting operations. Soils usually are composed of sands, clays, peat and similar materials that can be cut with a spade. Both rocks and soils differ in mineralogical composition – which determines their chemical or salt composition – and in state (density, humidity, weathering etc.), as well as in structural and textural properties. The *structure* of rock or soil is understood to be the peculiar properties of their internal structure, governed by the size and shape of minerals composing the rock or soil and by the nature of bonds between their individual components. The structure determines the appearance of a rock or soil, such as solidity, uniformity, stratification and porosity (Bell, 1980; Maslov, 1987).

It is compulsory to remove the topsoil from the entire surface of the foundation of the hydraulic structure, so that it, in fact, does not represent construction soil. There are different classifications for foundations, by means of which they are divided

into groups having similar engineering-geological properties. The classification into three main kinds of foundations is widespread in civil engineering: *rock foundations*, *semi-rock foundations*, and *non-rock (soil) foundations*.

2.2 ROCK FOUNDATIONS

Rock foundations (bedrock) have a compressive strength in a waterlogged state greater than 5 MPa. Depending on the origination of the rock from which a foundation has been formed, it can consist of igneous (magmatic), sedimentary, or metamorphic rocks.

Igneous (magmatic) rocks originated by means of a cooling down of lava. Lava that has cooled down beneath the surface of the earth has formed *intrusive* (depth or plutonic) rocks, while lava cooled down on the earth's surface formed *effusive* (or volcanic) rocks. Basic representatives of igneous rocks are: *granite*, *synite*, *diorite*, *gabbro*, as well as their effusive analogies: *rhyolite*, *trachyte*, *andesite*, *basalt*, *diabase*, etc. Generally, igneous rocks have high strength characteristics, but they differ considerably in chemical composition, structure and texture.

The chemical composition of an igneous rock is determined by the composition of the minerals that constitute it. The particular rock species are mainly composed of *oxide* and *silicates*, main rock-forming minerals. *Oxides* include quartz, SiO_2 and free silica. *Silicates* are main components of most igneous (and metamorphic) rocks, representing complex compounds made up of Si, Al, Fe, Ca, Mg, Na, K, O and H occurring as various salts of silicic acids, like feldspars, micas, hornblende, augite. Depending on chemical composition and SiO_2 content, igneous rocks are classified as: *ultra-acidic, acidic, intermediate, basic* and *superbasic. Acidic* rocks contain 65–75% of SiO_2 (*granite* group), *intermediate* rocks 52–65% (*syenite* and *diorite* groups), *basic* rocks 40–52% (*gabbro* group). Ultra-acid and ultrabasic rocks have a very limited distribution. Table 2.1 presents a classification of principal igneous rocks according to their chemical composition, with some additional data on rocks of interest (Maslov, 1987).

Sedimentary rocks originated as a result of complex multi-stage processes. They are composed of consolidated particles which are the product of weathering and erosion of any previously existing rocks or soils, often followed by cementation. Weathering of rocks is caused by the action of atmospheric agents and of physical and chemical processes. According to their strength characteristics, sedimentary rocks are sometimes close to igneous rocks and, as a rule, are weaker than them. They can also be distinctively weaker, which depends on the kind of binding agent by means of which they have interconnected grains of sand, clay, gravel, and other materials from which sedimentary rocks have been formed. At the same time, the conditions during the formation of the rocks also have an influence. The sedimentary rocks are divided into four major groups (Maslov, 1987; McLean and Gribble, 1985):

1. Clastic or detrital sedimentary rocks (sometimes referred to as terrigenous), which are formed from minerals or rock fragments derived from the breakdown of preexisting rocks.
2. Chemical sedimentary rocks, which are formed from the precipitation of salts dissolved in water.

Table 2.1 Igneous rocks classification.

Acidity	Acid content [%]	Rocks: Intrusive (plutonic)	Rocks: Effusive (volcanic)	Colour	Fusibility	Mineralogical composition [%]: Quartz	Feldspars	Coloured minerals	Bulk density [kN/m^3]
Acid	>65	Granites	Quartz porphyries, liparites, obsidian, pumice	Grey, pink, reddish	Refractory	14–40	40–60	5–10 (micas, hornblende)	26–27
Intermediate	52–65	Syenites trachytes	Porphyries, Porphyries,	Grey, dark-grey, reddish	Medium	None or negligible	85–90	10–15 (hornblende, augite, biotite	27–29.5
		Diorites	Porphyries, andesites	Grey, dark-grey, dark-green			≈70	≈30 (hornblende, augite, biotite)	
Basic	40–52	Gabbro	Diabases, basalts	Dark-grey, black, dark-green	Pronounced	None	50	50 (augite, hornblende)	28–31

Table 2.2 Engineering properties of some unweathered sedimentary rocks (after McLean and Gribble, 1985).

Sedimentary Rock	Density [kN/m^3]	Porosity [%]	Water absorption [%]	Unconfined compressive strength [MN/m^2]
Conglomerate	25–28	1–20	–	–
Sandstone	19–26	5–25	<14.0	20–179
Siltstone	22–25	2–24	<6.0	–
Shale	20–24	10–35	<6.0	5–100
Hard limestone	25–27	0–10	<2.0	60–200
Soft limestone	23–25	5–50	<4.0	20–50
Dolomite	25–27.5	1–5	<1.5	30–200

3. Organic sedimentary rocks, which are formed from the skeletal remains of plants and animals and include coal and oil.
4. Limestones and dolomites, which are sedimentary rocks consisting of more than 50% carbonate, and can include chemical, clastic and biological material.

The properties of many sedimentary rocks, like porosity, water absorption and uniaxial compressive strength, are highly variable, depending upon how well the rock has been compacted or the grains cemented together. The engineering properties of some sedimentary rocks are given in Table 2.2, but they should serve only as a rough guide. The data for the natural rock involved in any hydraulic engineering scheme should always be gained by investigations.

Metamorphic rocks originated as a result of intense changes of igneous rocks, but generally of sedimentary rocks, caused by the action of high pressure and temperature, water vapour, chemically active gases, etc. The process of change is referred to as *metamorphism* of the original rock. There are three types of metamorphism, the first being

Table 2.3 Engineering properties of some common metamorphic rocks.

Metamorphic Rocks	*Density [kN/m^3]*	*Porosity [%]*	*Water absorption [%]*	*Unconfined compressive strength [kN/m^2]*
Slate	26–28	0.1–0.5	<0.5	70–200
Schist	26–28	0.1–1.5	<1.5	50–150
Gneiss	27–30	0.5–1.5	<1.0	50–200
Quartzite	26–27	0.1–0.5	<0.5	150–300
Marble	24–27	0.5–3.0	<1.0	70–150

dynamic metamorphism, when increased stress is the dominant agent. It is characteristic of narrow belts of movement, where the rocks on one side are being displaced relative to those on the other. Whether the rocks are simply crushed, or whether there is some growth of new crystals, depends largely on the temperature in the mass affected by dynamic metamorphism. In *thermal metamorphism*, increased temperature is the dominant agent causing change. It typically happens to rocks that lie at the margins of any large igneous intrusions and have been baked and altered by the hot magma. In large masses of granite, the changes extend outwards from the granite to distances in the order of 2 km. This zone of metamorphism is called the thermal aureole of the granite mass, and the types of new minerals formed anywhere within it depend on the temperature attained and the distance from the granite. The main agents causing *regional metamorphism* are temperature, load and directed pressure.

The degree of metamorphism is related to the conditions of temperature and pressure under which the new metamorphic rock has formed, and may be assessed by the appearance of certain new minerals. These index minerals, each of which indicates a particular temperature and pressure at the time it formed, are used to define the *metamorphic grade* of the rock in which they occur. Their presence and interpretation are conditional on the composition of the original parental rocks as well as on the grade of metamorphism. Textural changes also occur as metamorphic grade increases. These matters are discussed in more detail by McLean and Gribble (1985).

Basic representatives of the metamorphic rocks are: *slate, schist, gneiss*, *quartzite*, *marble*, *phyllites*, *amphibolites*, etc. Table 2.3 lists the engineering properties of some common metamorphic rocks (after McLean and Gribble, 1985).

An important property of rock foundations is *anisotropy.* Most rocks are anisotropic, which means that they have different properties in different directions. The basic characteristic is an almost regular appearance of fractures in the rock. Fractures are, in fact, *discontinuities*, originating from rupture in the rocks under the action of stresses, due to tension or to compression. A *joint* is a fracture that cuts off the rock by a small displacement of the adjacent parts. A *fault* is a fracture along whose length there is noticeable displacement of one side of the fracture in relation to the other side. Joints usually accompany faults. Fractures have a double negative role – they lower the strength of the rock and form paths for the circulation of underground water, which, in addition to water loss below the structure, could also have a negative mechanical and chemical effect upon the rocks (Chappell, 1990; Fell et al., 1992; Leps, 1989; Scavia, 1995).

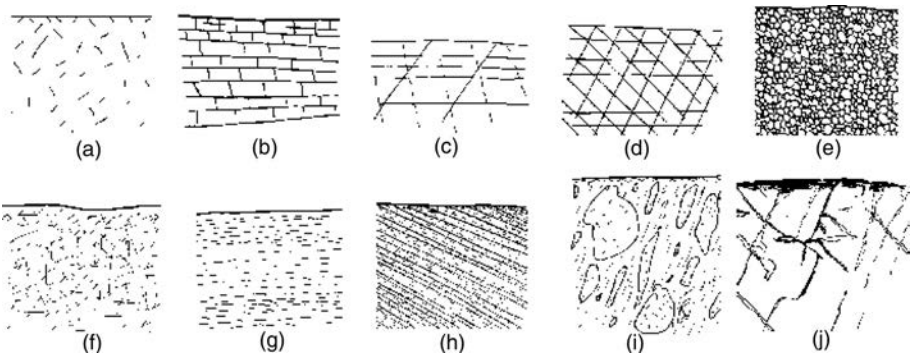

Figure 2.1 Kinds of rock mass attributes (after Goodman, 1995).

Anisotropy can be *primary anisotropy* or *secondary anisotropy*. Primary anisotropy is a consequence of processes that had been active during the formation of the rock mass, while secondary anisotropy is due to various subsequent processes, such as development of fractures, joints, and irregularities in different directions, due to the chemical effect of water. Secondary anisotropy can also exist in rocks with primary anisotropy, as well as in isotropic rocks.

From *structural* and *mechanical* points of view, rock foundations can be divided into nine classes (Goodman, 1995):

1. *Jointless rock* is found in many rock masses below the zone of weathering influences. This form is found, for example, in mass sandstone, granite rocks, and, in general, in non-foliated basement rocks (Fig. 2.1a). Rocks of this class may approach the reflective ideal material, which is: continuous, homogeneous, isotropic, and linearly elastic.
2. *Incompletely fractured rock* has fewer than three persistent joint sets so that, when excavated, the rock mass does not usually produce isolated blocks (Fig. 2.1b). For the analysis and computation of such rock masses, special methods of computation have been developed in rock mechanics, i.e. fracture mechanics. Non-convex excavations can produce blocks to be obtained from that rock class.
3. *Incipiently blocky rock* has fewer than three joint sets open or filled with soil but also additional joint sets that are currently healed or tightly closed (Fig. 2.1c). The reawakening of one of these incipient joint sets creates conditions for the occurrence of blocky rock. In some instances, the likelihood of joints reopening can sometimes be studied using numerical modelling or mathematical analysis.
4. *Blocky rock* contains three or more persistent joint sets clearly developed and open or filled with soil that lack appreciable tensile strength (Fig. 2.1d). This rock can be expected during use to produce blocks with a face on any excavated surface. Blocky rock includes rock masses, which are regularly cut by extensive joint sets in highly determined orientations, as well as rock masses that are variably and randomly cut by non-extensive joint sets, which do not extend too much. For analysis and computations of such rock masses, a *block theory* has been

developed in the last ten years, since methods of continuum mechanics are not well suited to such a medium.

5. *Highly porous rock*. Porosity significantly affects the mechanical behaviour of such rocks due to poro-elasticity, fluid content and its movement, as well as pore crushing under use, i.e. under distortion or contraction (Fig. 2.1e). Selected and refined methods of continuum mechanics apply to these rocks.
6. *Highly fissured rock* (Fig. 2.1f), has a number of closely spaced short fractures, which engender high brittleness, as well as great anisotropy, and significant non-linearity in virtually all mechanical properties. Investigation, sampling, and testing of these rocks are very difficult. These materials may resemble stiff-fissured soils in their mechanical behaviour.
7. *Squeezing* or *swelling rocks* generally contain active clay minerals whose reaction with water impress immediate or delayed cracking, volumetric changes, and distortions that may dominate rock mass behaviour (Fig. 2.1g). These rocks may soften appreciably, and soil mechanics methods may be applicable in such rocks.
8. *Mixtures of dissimilar rocks* include regular mixtures of masses achieved through rhythmical intimate interlayering of dissimilar rocks (for example, rhythmically-bedded sandstone and shale, Fig. 2.1h), or isotropic random mixtures, or else foliated random mixtures (for instance, serpentinite and melange i.e. other rock, Fig. 2.1i). Particular methods are being developed for the analysis of such materials.
9. *Cavernous rocks* are mainly soluble limestone, dolomite and gypsum, as well as clastic sedimentary rocks bonded by soluble cement material (Fig. 2.1j).

2.3 SEMI-ROCK AND SOIL FOUNDATIONS

Semi-rock foundations have been formed from rocks having compressive strength in waterlogged conditions less than 5 MPa. They are characterized by a noticeable deformability *(marlstones, siliceous clays,* etc.), lowered resistance to shearing, and submissiveness to softening under water *(gypsum, rock salt, gypsum-containing conglomerates,* and others, which are unsuitable as foundations for dams).

Semi-rock foundations are usually represented by moderately and highly weathered rock, sometimes also by completely weathered rock. Moderately weathered rock is discolored, with discontinuities that may be open and will have discolored surfaces with alteration starting to penetrate inwards. Intact rock is noticeably weaker, as is determined in the field, than the fresh rock. Highly weathered rock is discolored, with discontinuities that may be open and will have discolored surfaces. The original fabric of the rock near to the discontinuities may be altered and alteration penetrates deeply inwards, but corestones are still present. Completely weathered rock is discolored and changed to a soil but original fabric is mainly preserved. There may be occasional small corestones, and depending on the nature of the parent rock, this kind of foundation can be treated as a semi-rock.

Soil is the completely weathered material in the upper layers of the earth's crust, with no preserved original fabric. The science dealing with the equilibrium and motion of soil bodies is named *soil mechanics*. As was mentioned in the introductory part of this chapter, the difference between soil and rock is roughly that in soils it is possible

Table 2.4 Classification of soils.

Soil type	*Grain size min. [mm]*	*Grain size max. [mm]*
Clay		0.002
Silt	0.002	0.063
Sand	0.063	2
Gravel	2	63

to dig a trench with simple tools such as a spade, while in rock this is impossible, it must first be shattered with heavy equipment, or a mechanical drilling device.

The natural *weathering process* of rock is that under the long-term influence of sun, rain and wind, it degenerates into stones. This process is accelerated by fracturing of rock bodies by freezing and thawing of the water penetrating in the rock crevices. Thus, surface deposits are formed, called *residual soil deposits*. The coarse stones that are created in mountainous areas are transported downstream by gravity, often together with water in rivers. By impacts and by internal friction the stones are gradually reduced in size, so that the material becomes gradually finer. The material may be deposited in flowing rivers, the coarsest material at high velocities, but the finer material only at very low velocities. This means that gravel will be found in the upper reaches of a river bed, and finer material such as sand and silt in the lower reaches. This kind of soil is called *transported sediments*. Thus, the term "soil" includes residual sediments, water-transported sediments or *alluvium*, wind transported material or *dunes* and *loess*, sediment transported by glaciers or their meltwaters (*till* or *glacial drift*) and material moved downhill by gravity or *colluvium*.

Soils are classified into various types but in many cases these various types differ in mechanical properties. A simple, but popular subdivision of soils is on the basis of the grain size of the particles that constitute the soil. In this classification coarse granular material is denoted as *gravel* and finer material as *sand*. It has been agreed internationally to consider particles larger than 2 mm but smaller than 63 mm as gravel. Particles larger than 63 mm are denoted as *stones*. Sand is the material consisting of particles smaller than 2 mm, but larger than 0.063 mm. Particles smaller than 0.063 mm and larger than 0.002 mm are denoted as *silt*. Soil consisting of particles smaller than 0.002 mm, is termed *clay,* see Table 2.4.

The mechanical properties of the main types of soil – sand, clay and peat – are rather different. Clay is much less permeable by water than sand, but usually it is also much softer. Peat is rather light (sometimes slightly heavier than water), and strongly anisotropic because of the presence of fibers of organic material. Peat usually is also very compressible. Sand is rather permeable, and rather stiff, especially after a certain preloading. Also very characteristic of granular soils such as sand and gravel is that they cannot transfer tensile stresses.

The grain size may be useful as a first distinguishing property of soils, but it is not very useful for the mechanical properties. These can differ considerably for soils of the same grain size. For instance, sand consisting of round particles, can have a much lower strength than sand consisting of particles with sharp points. Also, soil samples consisting of a mixture of various grain sizes can have a very low permeability if the small particles just fit in the pores between the larger particles (Verruijt, 2012).

Soil foundations usually encompass complexes of dissimilar earth materials that, for hydraulic engineering purposes, can be divided into two characteristic types: *non-cohesive materials* and *cohesive materials*.

Non-cohesive earth materials are most often found in the form of *sand, gravel,* and a mixture of the two. Their properties depend on their origination and on the size of their particles. General characteristics are the absence of cohesion, a relatively large angle of internal friction, and significant water permeability.

Compacted sands are most often found having a porosity of 15–25%, $\varphi = 30–35^\circ$ and $\gamma = 17.5–19\,\text{kN/m}^3$. The coefficient of permeability ranges within the limits $10^{-1}–10^{-5}$ cm/s. An important property of non-cohesive soil materials is their easy and fast compacting following the application of loading, so that the subsequent settlements are negligible. Finegrained, silty, and clayey sands are disadvantageous, since during vibrational loadings considerable settlement occurs, which brings about a loosening of the material.

Coherent earth materials *(clay, loam,* i.e. *mild clay, loess)* are characterized by cohesion among the particles, greater compressibility under loading, a small angle of internal friction, and low water permeability. Settlement of the structure on such a foundation takes place slowly and is a continuing process. The porosity of clayey foundations amounts to 30–45%, cohesion 30–50 kN/m^2, with a coefficient of permeability of $k = 10^{-5}–10^{-8}$ cm/s.

In most cases, soil foundations are heterogeneous both across the surface and in depth. They very often include particular lenses and interbeds (intercalations) with different properties, which must be taken into consideration in selecting the structure of the work that will be carried out on them. In a number of cases, shallower lenses of poor material could be removed and replaced by means of a more suitable earth material.

2.4 REQUIREMENTS FOR THE FOUNDATION

In the design and construction of dams, the following three characteristics of the materials in the foundation are of crucial importance: *deformability, stability* and *water impermeability.*

Deformability greatly varies from one foundation to another. Both in earth foundations and in rock foundations three kinds of deformations appear: (1) *limited non-recoverable* deformations; (2) *recoverable* deformations, usually linear ones, which are named *elastic* deformations; and (3) *unlimited non-recoverable* deformations or, more often, limited by failure of the material. From a mechanical point of view, non-recoverable deformations are a result of two kinds of transformations of the material. The first one consists of *closing down the fractures* in the rock mass, while the second one represents a lowering the porosity of the earth layer, i.e. its *settlement*. In the second transformation, time can have a noticeable role, since it is in connection with pressing the water out of the pores of the earth material, i.e. with the process of *consolidation*.

In relation to water impermeability and to deformability, soil and rock clearly differ. The difference is mainly due to the considerable differences in the values of the moduli of elasticity, as well as the limit of elasticity. On account of that, the magnitude

of deformations among earth materials is larger, while reversible deformations are negligible.

When discussing *the stability* of the foundation, what is implied is its ability to resist external loads caused by the dam and the impounding reservoir, as well as the volumetric forces – self-weight and the effect of pore pressure. When considering the forces of water that act upon the foundation, it is important to understand the following:

1) The forces of water are completely equal, both in the earth soil and the rock masses, assuming that the groundwater flow originates from the same potential;
2) Only on a perfectly impermeable diaphragm wall can hydraulic pressure act with its full intensity. Once the water seepage flow has commenced, the pressure will act along the entire length of the water seepage path, having a value that will depend on the loss of pressure. At the same time, a greater part of the pressure will act on the most impermeable parts of the path, such as on the grout curtain or the zone in which fractures in the rock are closed due to the reaction of the foundation below the dam; and
3) Seepage flow in the dam foundation does not depend only on the water level in the impounding reservoir but also on the level of the tailwater, as well as on the natural level of the underground water in the slopes of the dam site, which is subject to temporary variations during rainy periods.

The instability of the foundation, under the action of the above-quoted loads, is exhibited in various ways. In the case of non-cohesive earth material or when non-cohesive earth material could fill the fractures in the rock, *progressive erosion* may take place. In foundations in which a zone of weaker material appears, usually in the form of a thin layer or interbed, it may lead to *a failure across the slipping surface,* precisely across such a weak layer. That is why it is of particular importance for such zones to be located beforehand.

In the case of homogeneous earth foundations, a failure could be expected over a *circular-cylindrical surface.* In a number of fractured rocks it is possible to expect similar phenomena. In any case, the *strength* of the material in the foundation is a limiting factor for stresses that can be accepted by the foundation, and thereby also for the height and dimensions of the dam.

Regarding stability, another significant condition for a safe operation of the dam is the stability of the contact of the dam and the foundation, i.e. the stability of the dam against its slipping across the foundation under the action of the total horizontal component W of the forces acting on the structure. Resistance of the structure against the force of slippage W is carried out by the force T, which is proportional to the vertical component V, i.e. $T = fV$. Here, f is a coefficient of friction that most often varies within the limits from 0.2 to 0.8 and depends upon the properties of the foundation, as well as on the material in the dam. The structure will be stable if $W \leq fV$, from which it is possible to understand the significance of the vertical forces, among which the greatest is the weight of the dam, as well as the significance of the kind of foundation, manifested through the coefficient f, which varies within broad limits.

Dams can generally be built on rock foundations, semi-rock foundations, and on non-rock foundations made up of materials having sufficient water impermeability, load-bearing capacity, stability, and limited deformability. Properties of the material

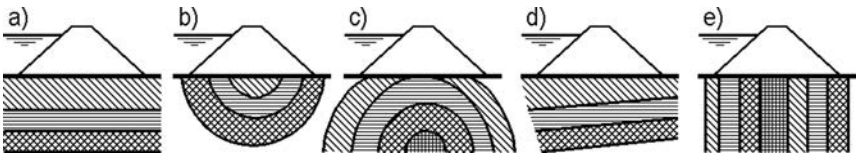

Figure 2.2 Disposition of extending layers.

in the foundation to a great extent influence the type and structure of the dam, as well as the technology of construction of works.

Of the embankment dams – earth-rock dams and rockfill dams are built primarily on rock foundations and semi-rock foundations, and sometimes even on foundations of gravel. For only small heights it would be feasible to carry them out also upon coarse-grained sand, clay, and compacted loam (mild clay). Unacceptable foundations for these types of dams are fine-grained sands, uncompacted clays and loams, peat, as well as rock foundations of gypsum and anhydrite. The same conditions apply to earth dams, as well as to low earth-rock dams.

Concrete dams transmit considerably larger stresses into the foundations, therefore the requirements for these dams are more rigorous. Arch dams require exclusively sound, hard, and firm rock. Something similar also applies to large gravity and buttress dams, while requirements for the quality of the rock can be moderated for such dams of moderate height. Only low gravity dams can be carried out upon soil foundations.

In assessing the evaluation for the quality of the rock foundations and soil foundations, the same factors do not apply. In this manner, when assessing the quality of rock foundations, it is necessary to pay attention to the following: (1) fractures filled with fine fractions of earth which could easily be washed out; (2) torn-off and sheared parts; and (3) weakened zones which, after saturation with water, could become unstable and fail (Fell et al., 1992; Scavia, 1995; Wahlstrom, 1974).

When appraising the quality of soil foundations, it is particularly necessary to take care and pay attention regarding the presence of: (1) earth materials, susceptible to erosion; (2) materials in which, following the construction of the dam, excess pore pressure could develop; (3) materials in which, under the action of the weight of the dam, it is possible that considerable unequal settlements could occur; and (4) low load-bearing capacity materials (having low values for the angle of internal friction and cohesion), which create interbeds where it is possible for a development of zones with plastic deformations to come about.

During the design of dams on rock foundations and semi-rock foundations one must also take into consideration the disposition of the extension of the layers. Preference should be given to dam sites with a *monocline* structure (Fig. 2.2a) or *syncline* structure (b), because in the case of *anticline* stratification (c) the rock is usually broken up and water-permeable. In the case of a monocline structure it is desirable that the layers should be horizontal (a) or else with a longwise inclination to the river channel, upstream of the water current (d). If the layers have been positioned vertically, or almost vertically, more favourable conditions exist when they extend across the river channel (e). In the case of a longitudinal disposition of layers, particular attention should be paid to the stability of the slopes of the valley during the filling of the reservoir.

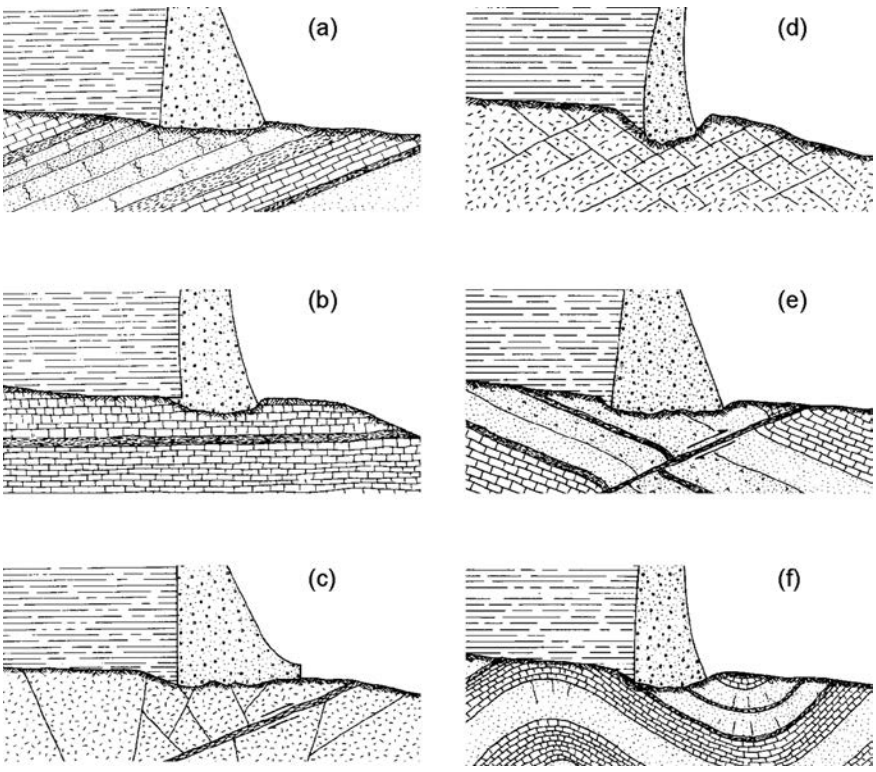

Figure 2.3 Possible adverse geological conditions in the foundation for concrete dam construction (after Wahlstrom, 1974).

Owing to their structure and nature, concrete dams require more rigorous conditions concerning the quality of rock in the foundation. Figure 2.3 represents possible geological conditions in the foundation, which are adverse for concrete dam construction because of the realistic hazard of the occurrence of failure in the foundation, which would cause failure of the dam. In example (a), fractured and brittle sandstone below the dam, placed on a weak shale layer, dipping downward towards the upstream side, indicates real conditions for a failure in the foundation. In diagram (b), horizontally-layered limestone rests on a weak shale layer, which extends downstream to a steep slope in the valley floor, creating conditions for slipping towards the downstream side. Diagram (c) illustrates fractured crystalline rocks that lie above a flat fault containing sheared gougy materials of very low strength. Intersecting strong conjugate joints (d) form a mass that, under the effect of shear forces, could easily cause mass shear dislocations. Similar conditions to these caused the well-known disaster of the Malpasset dam in France in l959. Conditions existing in example (e) are also adverse in which sedimentary rocks, dipping downward to the downstream side, are intersected by a fault containing materials of low strength. Folded rocks containing a thin weak layer of shale (f) also represent a potential hazard that may lead to foundation failure (Wahlstrom, 1974).

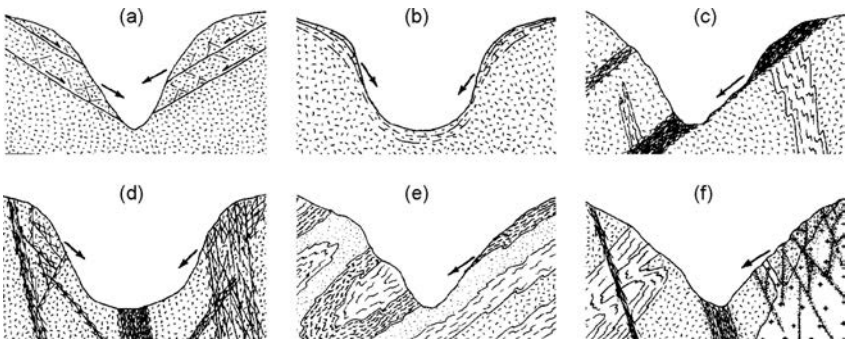

Figure 2.4 Some cases of possible unstable slope configurations in igneous and metamorphic rocks (after Wahlstrom, 1974).

The construction of a hydraulic scheme including an impounding reservoir regularly leads to changes in the environment. If it has been found that the change of the hydrogeological regime, caused by the construction of a dam, can cause sliding of the slopes, then appropriate precautionary measures will have to be undertaken, such as modifying and drainage of the slopes. Primary and secondary anisotropy in a number of cases contribute to instability of slopes in the river valley. Rock fissuring in particular causes disintegration and decomposition of the bedrock and slopes that have been stable during early stages of the excavation for the construction of works, and subsequently they become progressively unstable. Therefore, excavation in the river valley and modification of the slopes are usually alternate processes.

Identification of potentially unstable slopes in the river valley, which could fail as a consequence of the dam construction and filling of the impounding reservoir, or which could fail spontaneously in the service period of the hydraulic scheme, is essential. The early disclosure of potentially hazardous situations in the foundation below the slopes of the valley could well eliminate the dam site, without investing funds for further analyses and investigations.

Figures 2.4 and 2.5 illustrate several potentially hazardous situations in the foundation below the slopes of the river valley, which are only a small part of the variety of possible undesirable conditions in a rock foundation (Wahlstrom, 1974).

Figure 2.4 presents several kinds of unstable slope configurations in igneous and metamorphic rocks. In example (a), faults dip toward the valley and induce the hazard of gravity slipping, which could cause slope instability. Joints parallel to slopes (b), formed by long-term temperature changes, could also be a cause of instability. The condition in (c) appears when part of the material of the fault infill remains insecurely rested on the surface, while in (d), due to a significant degree of fractured rocks, its strength has been considerably decreased. A layer of mica schist in folded metamorphic terrain (e) presents a potential hazard, while thoroughly fractured and altered rocks, often associated with intrusive igneous rocks, produce a zone of weak rocks, which could lead to slope sliding, i.e. failure (f).

Figure 2.5 indicates several examples of potentially hazardous layers in a layered rock, which is often the case in sedimentary rocks, as well as in igneous rocks. In

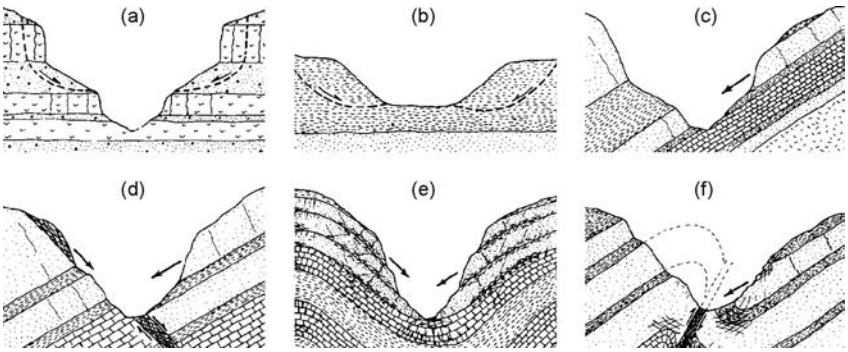

Figure 2.5 Examples of potentially hazardous situations in layered rocks (after Wahlstrom, 1974).

example (a) lava flows alternate with beds of volcanic ash. The slopes in horizontal shale layers may slip or fail, as is indicated in diagram (b), while in diagram (c), where a valley with inclined sediments is shown, instability is caused by a layer of sandstone above a layer of shale. In addition, a faulted and thereupon tilted sedimentary rock, as is shown in diagram (d), is a potential hazard for slope slippage or failure. Fractures resulting from slippage of layers past each other have reduced the competency of brittle rocks (e), whereas the active fault (f) often represents a potential hazard for the occurrence of collapse.

Water impermeability, an important property of the foundation, is rarely satisfied in natural foundations without there being a need for artificial measures for its improvement. However, water loss rarely plays a decisive role in the assessment of this property, and of more significant importance is the occurrence of uplift pressure beneath the dam, water pressure in the rock mass, pore pressure, and mechanical erosion of material in soil foundations (see following Chapters).

Water permeability in rock foundations can be either primary or secondary. *Primary water permeability* is determined by the mode of origin of the rock and is dependent upon its stratification. In general, underground water flow is greater in directions of layering than across the layers, in that it varies considerably, depending on the type of origin of the rock. *Secondary water permeability* is superimposed on a rock by the influence of a variety of natural processes, including dislocations by crustal movement, mechanical action due to weathering, and chemical alterations associated with solutions of dead-seated origin.

Moderate to high primary permeability exists in relatively few rocks. Notable exceptions are found in some medium- to coarse-grained clastic rocks. Crystalline igneous and meta-morphic rocks, partly to completely crystallized sedimentary rocks, and clastic rocks with grain interstices of grains filled with cement or clay, are generally essentially impermeable.

Interconnecting large to small channels of seepage flow, associated with secondary permeability, is of great concern in assessing potential leakage through the abutments of a dam site or beneath the dam. That is why there is no need to economise on efforts to identify and correctly evaluate these channels. Fractures that have formed in hard

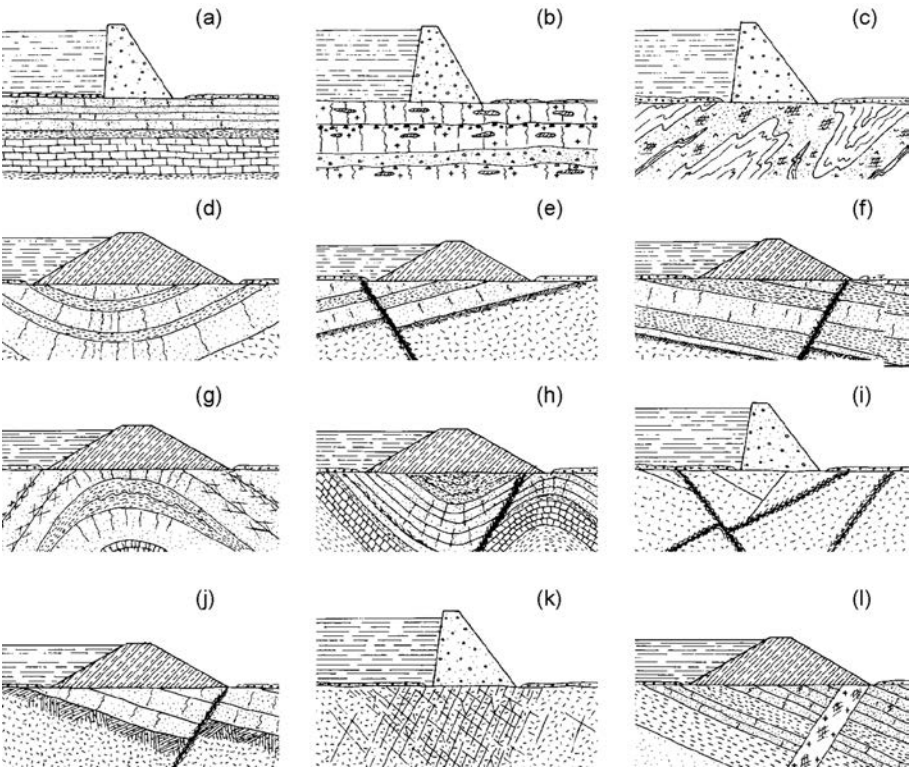

Figure 2.6 Idealized cross-sections of dams showing various kinds of zones of potential seepage in bedrock (after Wahlstrom, 1974).

brittle rocks are generally more continuous and more likely to be open to groundwater penetration than fractures in soft rocks.

Almost an infinite number of possibilities exist in which there is a potential hazard of seepage of water in the bedrock in the vicinities of dams and in the zones of an impounding reservoir. A few examples are shown in Figures 2.6 and 2.7 (Wahlstrom, 1974).

Figure 2.6 illustrates idealized cross-sections of dams showing various kinds of zones of potential seepage in bedrock where:

(a) Brittle, fractured sandstone lies in horizontal sedimentary sequence beneath a dam;
(b) A dam is situated on basaltic lava flows and interlayered pyroclastic deposits where the basaltic layers are fractured and contain open fractures so that seepage is very probable;
(c) A brittle layer of quartzite in tightly folded metamorphic rocks usually contains numerous intersecting fractures;
(d) Sandstone layers alternating with shale layers in a syncline fractures occur in the sandstone as a consequence of the syncline position;

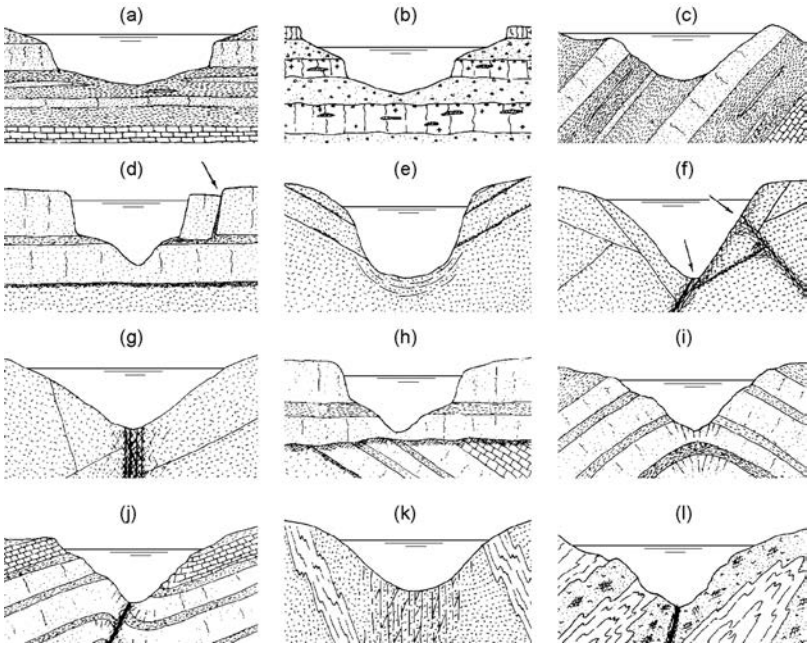

Figure 2.7 Idealized cross-sections of river valleys at a dam site and/or reservoir site (after Wahlstrom, 1974).

(e) A fault zone provides access of water to brittle sandstone layers, which dip in depth toward the upstream face;
(f) A fault provides egress for water moving through inclined, brittle sandstone layers;
(g) Brittle sandstone layers have been intensively fractured during the development of an anticline;
(h) Fractured sandstone in folded rocks is intersected by a fault zone that expedites ground-water movement to the surface beneath the dam;
(i) Faults in brittle crystalline rock provide channelways for groundwater circulation;
(j) Fractured sandstone, forming a weathered zone on granite beneath the sediment and a fault zone, create channelways for subsurface circulation of water;
(k) Extensively jointed crystalline rocks are permeable to groundwater flow; and
(l) A closely jointed igneous dike intersects a sedimentary sequence and provides a channel for groundwater movement.

Figure 2.7 presents idealized cross-sections of river valleys at a dam site and/or reservoir site where:

(a) Jointed sandstone presents a zone of potential seepage around the dam abutment when the reservoir is full;
(b) Basaltic lava flows (with open fractures) and layers of pyroclastic rocks create a potential for seepage;

(c) Fractured sandstones in the indicated position are prone to seepage flow;
(d) A subsided block, as shown with an arrow, has created an open channelway in a massive horizontal sandstone layer;
(e) Faults and fractures may cause gravity slippage;
(f) A strong fault system renders crystalline rocks permeable on one side of a valley;
(g) A wide fault zone promotes deep circulation of water beneath a dam;
(h) Fractured sandstone and a weathered zone beneath an angular unconformity enable easy circulation of groundwater;
(i) Fractured sandstone in an anticline creates a permeable zone parallel to the valley;
(j) Folded jointed rocks, along with a strong fault, create a potential for groundwater flow;
(k) A sheeted, jointed zone in crystalline rocks, creates a permeable zone; and
(l) Joints in a brittle quartzite layer and a fault produce channelways for underground water circulation.

In concluding this point, it must be said that bedrock containing water-soluble salts – chloride salts and sulphate–chloride salts that are more than 5% of the mass, sulphate salts more than 2% are not suitable for dam construction. Earth layers containing nonsoluble organic matter, such as leftovers of plants and roots, as well as passages dug out by animals, are removed from the foundation or are cut off with water-impervious members.

In all cases, when a foundation contains earth materials with poor strength characteristics, the possibility of their entire or partial removal must be considered for the improvement of the foundation, for which a decision is taken on the basis of a technical and economic comparison of the possible alternative solutions. In addition, it is always necessary to review the possibilities of decreasing the water permeability of the foundation, as well as decreasing the gradient of seepage flow. For that purpose, in rock foundations *grout curtains* are most often constructed, while *diaphragms* of various materials are used to cut off deposits and sediment materials.

Finally, it may be concluded that dams can be constructed not only in suitable geological conditions, but also on foundations containing specific deficiencies, provided that by means of technical analyses the essential technical measures for improvement of the foundation are correctly determined, and further provided that the most appropriate type of dam is selected.

2.5 INVESTIGATION WORKS REGARDING DAM FOUNDATIONS

In designing dams it is necessary to possess sufficiently substantial and abundant data on the geological and geotechnical features of the foundation in the zone of the dam site and the impounding reservoir. For that purpose, it is compulsory to conduct field engineering-geological and geotechnical investigation works and laboratory testing, in order to determine the geological history structure of the foundation, its tectonic geology, stratigraphy, faulting, foliation and jointing, as well as structural relationships, the permeability of the rock, the level of groundwater and its chemical composition, deformation characteristics and strength characteristics of the materials in the active zone of the dam foundation, etc.

By means of *the geological structure* of the ground in the zone of the impounding reservoir, it is necessary to establish the possibilities for storing water, as well as the consequences that such an action would have for the environment. At the same time, it is particularly important to determine the direction of the strike and dip of the permeable and impermeable layers and their position regarding the backwater and the banks of the river valley. Tectonic relationships and disturbances are also very important, particularly the existence and activities of faults and the degree of the disturbance of the layers in the zones of the fault. The knowledge gained by means of geological and tectonic investigations represents a basis for programming further investigations.

By means of geological mapping on the surface of the ground it is possible to obtain only a small part of the quoted necessary attainments and data, whereas for obtaining a complete understanding regarding the structure and properties of the material below the surface, indirect and direct investigation methods are applied.

Of particular significance are the deep investigation works, in connection with the selected dam site. Location, number, and depth of the boreholes is determined on the basis of preliminary geological studies, while investigations are carried out through the following methods: (1) sounding drillings by pulling out disturbed and undisturbed samples of earth materials and cores from the rock; (2) digging pits, trenches, adits and shafts, which enable direct insight into the materials, as well as sampling specimens; (3) measurements of the level of underground water in piezometers; (4) measurements of the permeability of the rock in particular sections of the sounding boreholes, of lengths from 2 to 5 meters, pressing water under pressure and measuring the flow; in the case of non-cohesive materials, measurements of permeability are much more delicate, while the results are less certain; (5) geophysical measurements, which enable one to forecast the spreading out of the layers between boreholes; and (6) measurements of the deformability and strength of rocks by means of trial loading. By applying a good combination of indirect and direct methods of investigations it is possible to achieve savings with regard to expensive drilling, without a visible loss in the quality of the obtained results.

2.5.1 Indirect investigation methods

Indirect methods of determining geological conditions and rock and soil mechanical data include a number of *geophysical* methods. The common deficiencies of all such methods are difficulties in interpreting the results because of the heterogeneity of rock and soil masses. Accordingly, their application has mainly an auxiliary character and is of minor importance compared to the direct field investigations. Out of a number of geophysical methods, the two most commonly used are:

(1) *geoseismic sounding*, which is used for measuring the velocity and spreading out of direct and reflected waves, caused by impact and weak explosions on the surface of the ground, or by means of sounding boreholes, and
(2) *geoelectrical sounding*, by means of which it is possible to measure the change of electrical resistance of the soil and rock formations at depth.

Within the first group the most common method is a *seismic refraction* measurement to identify boundaries between features with different physical properties. It is

Table 2.5 Approximate velocities of propagation of longitudinal elastic waves.

Medium	*Velocity of propagation [m/s]*
Air	330
Water	1400–1500
Residual soil	300–1500
Sand	300–1800
Clay	770–1900
Loess	770–2100
Sandstone, strongly jointed	340–440
Sandstone, jointed	700–1100
Sandstone	970–5300
Phyllite	1700–5000
Limestone	1600–6300
Dolomite	3200–7000
Gneiss	3700–6000
Granite	4300–6300
Basalt	5000–6400
Gabbro	5100–7600
Diabase	6200–6800
Peridotite	7800–8400

applied to find the bedrock below the overburden of soil, thus assessing the necessary depth of excavation. Because of easy handling and low costs, a seismic refraction survey is often applied to remote projects where difficulties arise in operating heavy machinery like drill rigs. Seismic waves are generated at a shot point at the surface by light blasting, by dropping a weight or by hitting a metal plate with a sledgehammer. The waves are reflected by a solid bed and monitored by geophones at the surface, or by hydrophones in water-covered areas. The geophones or hydrophones are arranged along a measuring profile at various distances from the source of the waves. These convert ground or water motions into a varying electrical current. The depth of the solid bed can be derived from the time of wave transfer between the source and the geophone, providing that the velocity of wave propagation in different layers is known, at least approximately, and providing that the layers are sufficiently isotropic. In general, the wave velocity increases with increasing strength and density of the penetrated medium. Thus, the reliability of the results increases with the differences of wave propagation within the penetrated layers and with the homogeneity of the layers. Therefore, in practice, the interpretation of the measurements is more difficult when differently weathered layers of rock exist between the surface and the solid bedrock. In these cases, it is necessary to calibrate the seismic measurements with the help of core drillings in order to correlate the seismic readings with the profile of boreholes. The spacing of the geophones depends on the number of different layers, on the consistency of layer thickness and on the homogeneity of each layer, and may be up to 50 m. Approximate values of wave velocities for some common media are given in Table 2.5.

Another geophysical tool is the measurement of *electrical resistance*. This method is based on the measurement of the property of resistivity, which is the electrical resistance between opposite faces of a unit cube of a given rock. The values of resistivity of rocks

and minerals range from 10^{-6} to over 10^{12} ohm-m, with no simple relationship in the spread of values to a genetic classification of rocks. Some minerals, like clays, conduct electricity well, but the predominant factor controlling the resistivity of most rocks and soils is the presence or absence of groundwater in them, and the relative concentration of dissolved salts, which acts as electrolyte. Crystalline rocks normally have high resistivity, except locally where they are broken by faults or joints and groundwater fills the voids. The method requires near horizontal stratification of a foundation. It can be used to determine the extent of a given layer. The reliability of the method depends again on the homogeneity and isotropy of the substrata – and, necessarily, on the experience of the measuring and interpreting team. Details of the application of this method are provided by McLean and Gribble, 2005.

2.5.2 Direct investigation methods

Direct investigation methods are: (1) *sounding drilling* for sampling specimens from the ground, and (2) *digging test pits, trenches, adits and shafts*. Now follows a brief description of the methods – details can be found in the books dealing with engineering geology and geotechnics (Bell, 1980; Fell et al. 1992, Maslov, 1987; Kutzner, 1997; McLean and Gribble, 2005).

2.5.2.1 Sounding drilling

Making a hole in soils and rocks is referred to conveniently as *drilling*. Sometimes making a hole in soil is called *boring*. Drilling is usually carried out using one of several available techniques: *rotary* drilling, *auger* drilling and *percussion* drilling.

1. *Rotary drilling* is performed using a so called rotary machine, and is suitable for both soil and rock investigation. Rotary drilling can involve either *core* or *non-core* drilling.

Core drilling is often called *diamond drilling*, and consists of a crown (either diamond-studded or made of tungsten carbide) rotated at the end of a hollow barrel which holds the cylinder of rock produced by the drill. High core recovery is important using this method, and this is influenced by core size and type of rock being drilled. Every effort is required to recover as much core as possible. Recovery in low strength, fractured rock and in the vicinity of faults is extremely poor, usually less than 30%, because of the brecciation of the rock. Drill bit sizes are chosen to suit the type of rock and depth of hole being drilled. In most engineering site investigation work, 75 mm diameter cored holes or larger are recommended. In soft rocks, to give a high core recovery, a double-tube core barrel is used, arranged in such a way that the inner tube is fixed while the outer one, in contact with the bit, rotates and water circulates between them. The hole size is about 75 mm diameter in total, and the rock core obtained is about 50 mm in diameter.

The drilled core is placed in boxes (Fig. 2.8), and logging of the core is performed. The logging should emphasize sections where core was not recovered as these may represent crucial zones in the foundation. It is recommended that each borehole log should contain the following information: (a) borehole identification, grid reference, contract details (client, contractor, site and reference number); (b) drilling method, inclination and equipment used; (c) drilling progress, rock resistance to drilling, *in situ*

Figure 2.8 The drilled core at one borehole below Knezhevo dam (Macedonia), depth 39 to 45 m.

tests; (d) groundwater levels and changes in standing water level; (e) detailed geological description including rock types, discontinuities encountered, core recovery, rock quality designation, degree of weathering and any simple field tests carried out.

Normally drilling is vertical, but in some instances, the drill holes may have to be angled to provide maximum information including the orientation of rock defects. Angled holes are slower to drill and slightly more expensive, but they should not present any problems to the professional driller.

The *non-core drilling* (or *wash boring*), involves the use of a solid roller, button or drag bit at the end of drill rods. The bits break up or grind the full face of the bottom of the hole and the fragments are removed by the circulating water. Samples from non-core rotary drilling through soil and rock are slurry of water and fine-grained material. This leads to uncertain identification of the materials. Non-coring bits can penetrate rock and care must be taken to change to coring methods as soon as resistance to penetration is encountered.

To support the hole sides when drilling in sandy soils above the water table and in soil below the water table, bentonite or chemical mud is used to assist in the recovery of drill cuttings. By maintaining a head of mud above the water table the excess pressure supports the sides of the hole.

2. *Auger drilling*. In this method a spiral flight auger is used to penetrate and remove the material below the surface. Auger drilling is suitable for weaker rocks and cohesive soils. The auger is a tool like a corkscrew rotated by hand or mechanically. With this dry drilling method a depth of 30 m can be reached using the common auger rig equipped with either solid or hollow flight augers. A steel blade 'V' bit will penetrate most fine-grained soils and extremely low strength rocks but usually refuses when faced with coarse gravel or low strength rock. A tungsten-carbide bit will grind slowly through low and medium strength rock. Inspecting disturbed samples of soil, conveyed to the surface, we can identify the stratification of the subsoil and the suitability of the material for dam construction. Therefore, the method is suitable to investigate embankment dam construction material deposits.

3. *Percussive drilling*. In the case of high strength rock, drill holes may be sunk using chisel drill bits and percussive hammers inside the hole to break the rock. Holes drilled in this way vary in diameter between approximately 110 mm and 80 mm (sometimes even less). Earlier, using traditional techniques, only small rock chips and dust were recovered for inspection so that information on the rock mass obtained by this method was limited. Recently a Swedish company has improved the method, involving lowering a miniature television camera into the hole and examining the rock quality and other properties of the rock mass, including fissures, joints, weathering and the location of any fault planes. It is clear that this technique works only if the hole is dry, i.e. without water (McLean and Gribble, 2005).

2.5.2.2 Digging test pits, trenches, adits and shafts

Test pits excavated by a rubber-tyred back-hoe or tracked excavator are relatively cheap, quick and effective in providing information on subsurface conditions. In the pit the subsurface profile is visible and can be logged and photographed. Material types, their boundaries and structure can be observed and recorded in three dimensions, as well as the presence and source of inflow of groundwater. Undisturbed samples can be taken from the pit's bottom and sides and *in situ* tests can be performed. Pit depth is limited by the reach of the machine and its ability to dig the material. Thus, the maximum depth is 4–6 m. Sometimes it is possible to dig cylindrical pits (or wells) manually, with a diameter of 80–100 cm, and a depth up to 12 m, if there is no groundwater.

Trenches are extensions of the use of test pits. They are excavated using either a tracked excavator or bulldozer and they provide virtually continuous exposures of the subsurface materials at sites. Trench exposures are logged and photographed in plan and elevation in a similar manner to test pits. The trenches practically have the same purpose as pits. In non-cohesive soils the excavating depth is limited by the groundwater. In cohesive soils it is usually limited by the risk of collapse. It must be emphasized that all pits or trenches must be adequately side-supported before any inspection is made.

Adits and shafts. Some sensitive and suspicious parts of the dam site at large important dams may impose the necessity of investigation by the excavation of adits or shafts into the area of concern. The adits and shafts provide the opportunity for direct observation of the ground conditions, measurement of orientation of defects and comparison with surface measurements, *in situ* testing, underground investigation drilling etc. Similar to test pits and trenches, the adits and shafts should be logged and photographed. As underground works, adits and shafts usually are expensive and slow to excavate, especially if they require support, ventilation and drainage. Thus, they should be carefully planned, located and designed. Very often exploratory adits have been incorporated in the final design of the dam, usually as drainage or grouting galleries.

2.5.3 Sampling

As was already said, during the execution of the investigation works samples are extracted from the ground. They are used to determine the spreading out and dip

of the layers, their composition and properties, the existence of faults and other discontinuities, as well as for establishing the physical and mechanical properties of the materials by means of laboratory testing.

Soil samples taken from boreholes, pits and trenches can be either disturbed or undisturbed. Disturbed samples are collected as representative of different material types of the investigated site. They are identified by location and depth and stored for laboratory testing. For cohesive soils about 3 kg of sample material is required for classification testing and 30 kg for compaction tests to evaluate probable performance as fill material in an embankment.

Undisturbed samples consist of material which is extracted from the site. Due to economic reasons soil samples usually have a cylindrical form, despite the ideal sample being a cube of approximately 0.3 m sides, hand cut from a test pit or trench, carefully packed and sealed to preserve the natural moisture. Samples prepared in such a way should be transported to the laboratory as soon as possible and with a minimum of disturbance.

To obtain samples of cohesive soils from boreholes, thin-walled steel tubes are used. The tubes are pushed into the soil using an adaptor connected to the drill rods. The drill hole should be cleaned out before sampling and the drilling water or mud level should be maintained during sampling to avoid "blowing" of material into the hole. The larger sample diameter is preferable because of lower probability of disturbance. Typical thin walled tube sizes are 50, 63 and 75 mm. The wall thickness and cutting edge shape are defined by codes to limit sample disturbance. Samples should be identified and sealed against moisture loss using either a sample tube sealing device or several layers of molten wax. Despite all preventive measures undisturbed samples can rust into the tube or dry out, therefore they should be transported to the laboratory and tested as soon as possible, preferably within two weeks.

The rock sample, taken for testing of strength and mineralogy, is usually a core. The core should be carefully stored (Figure 2.8), properly logged, photographed and sampled as soon as possible after drilling. A drill hole with full core recovery should present a complete linear profile through the rock mass below the ground surface. The core should be stored safely in the covered boxes because it serves to satisfy the needs of the site investigator, but also it should be used in the design and tendering period of the project realization. The core also provides samples for testing. A practical example of a stored part of a core is shown in Figure 2.8.

2.5.4 Testing

Extracted samples from the ground are used to determine the spreading out and dip of the layers, their composition and properties, the existence of faults and other discontinuities, as well as for establishing the physical and mechanical properties of the materials by means of laboratory testing.

Soil materials in the foundation beneath the dam are investigated by methods of soil mechanics. Whenever possible, it is necessary to investigate undisturbed samples of the material, while laboratory conditions of loading should be as realistic as possible in order to simulate the real conditions that will take place on the ground. There are a number of parameters and characteristics by means of which it is possible to

express the properties of the earth materials. These can all be divided into two basic groups:

1. *Physical and mechanical characteristics*, which enable one to predict the behaviour of the material under various forces and influences and which are used directly in calculating deformations, stability, seepage, etc.;
2. *Classification characteristics*, which aid in carrying out classification of the materials and thus assessing approximately the calculation characteristics by applying analogous and empirical relationships.

Among the physical and mechanical characteristics of earth materials, the most important are the following: unit weight, moisture, coefficient of compressibility, coefficient of lateral pressure, modulus of deformation, Poisson's ratio, coefficient of pore pressure, angle of internal friction, cohesion, coefficient of permeability, critical gradients at various kinds of seepage deformations, etc. Of the classification parameters, the most important are the granulometric composition (grain size distribution, as well as limits of plasticity or limits of consistency for clayey materials. For a determination of the strength characteristics of earth materials, tests for direct shearing and triaxial testing are being used, for which standard methods and apparatus have been developed. It is assumed that the readers are familiar with basic soil mechanics.

In many cases investigations of soil and rock in dam foundations are also carried out directly in the boreholes (*in situ*), through which are measured permeability, relative density, strength, and deformability of the layers at various depths in the boreholes. Of various *in situ* investigation methods, we will here mention the so called *penetration tests*. They serve mainly to find out the sequence of strata and the layer thickness and they are especially suitable to investigate potential deposits of embankment dam construction material. The *Standard penetration test* (SPT) is widely used all over world. It is useful to obtain estimates of the relative density, effective friction angle and deformation modulus (E) of cohesionless soils. With this method it is also possible to assess the liquefaction potential of saturated sands. The test is applied in a borehole. An alternative is the *cone penetration test*. This test has a similar purpose as SPT, but it is particularly useful in alluvial foundations where sandy soils are interlayered with clayey soils as the instrument is able to detect the layering better than most drilling and sampling techniques (Kutzner, 1997; Fell et al. 1992).

More tests are developed for in situ testing of rock. Well known and wide spread is the *water pressure permeability test,* which will be described in the next section. The topic of *in situ* testing of both soil and rock is very wide and rapidly developing and the readers are directed to the literature dealing with *engineering geology*, *geotechnics* and *soil mechanics*, cited in more places in the book.

2.6 IMPROVEMENT OF FOUNDATIONS

The rock foundation, upon which dam construction is anticipated, and which has some deficiencies, generally speaking, may be improved in two ways: (1) by *grouting* and (2) by *backfilling of fractures and tectonic zones*. In the case of soil foundations,

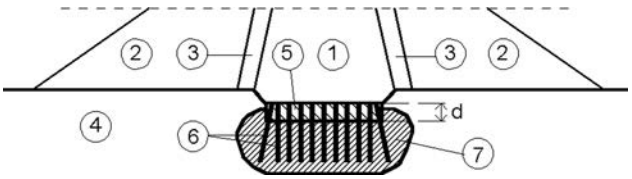

Figure 2.9 Consolidation grouting beneath the core of an embankment dam. (1) Clay core; (2) coarse grained material; (3) filter zones; (4) rock in the foundation; (5) concrete layer; (6) boreholes; and (7) consolidated foundation.

grouting is much more difficult and can be applied only in limited cases. In the case of soil foundations, separation elements in the form of *diaphragm walls* are more often constructed.

Grouting is a procedure in which a special pump within the foundation injects a suspension with different binding agents, solutions or artificial resins – either neat or with some infill and additions – clay, sand, stabilizing additions, etc. Grouting is carried out in appropriately positioned boreholes, so that the grouting mixture is backfilling fractures, voids, and pores in the rock mass. Three methods for improvement of the foundation by grouting are singled out: (1) *contact grouting,* (2) *consolidation grouting,* and (3) construction of a *grout curtain* (Nonveiller, 1989; Shroff & Shah, 1993).

Contact grouting causes possible gaps, voids and fractures at the contact between the rock and the hydraulic structure to be filled up, in order to obtain a monolithic bond between the concrete and the rock. The definition implies that it is a question of shallow grouting, by means of which it is possible to achieve a penetration into the rock of 0.5 to 1.5 m. It is particularly often applied for the backfilling of voids and gaps between the rock and the lining in the hydraulic tunnels. A cement–bentonite mixture is used exclusively for contact grouting.

Consolidation grouting is deep grouting as compared to the contact grouting and it is aimed at increasing the strength of the rock below the foundation of the dam in order to reduce seepage through it, to prevent insertion of fine particles from the core of the dam into the fractures of the foundation, and also to improve the bond between the foundation and the concrete structural members upon it. In the case of embankment dams, consolidation grouting is carried out only below the waterproof element, whereas in the case of concrete dams, it is beneath the entire dam.

The need for consolidation grouting and its depth depend on the condition of the rock and on the loading caused by the structure. The depth usually ranges from 5 to 15 m, and below the earth core of the highest embankment dam in the world, Nurek consolidation grouting has been carried out up to a depth of 20 m.

A concrete layer (Fig. 2.9) is used as bedding for consolidation grouting, which receives the required pressure and prevents the appearance of a water–cement mixture (laitance) on the surface. The thickness d of the concrete layer is determined by the condition: the weight of concrete should be larger than the pressure at grouting:

$$d = \frac{p \cdot 10^3}{k_s \gamma_b} \tag{2.1}$$

Table 2.6 Permissible relative loss of water q and permissible coefficient of permeability k.

Depth of headwater (m)	*Permissible relative loss of water q (m^3/s per m)*	*Permissible coefficient of permeability k (m/s)*
60	0.0834×10^{-5}	1×10^{-6}
60–100	0.0501×10^{-5}	6×10^{-7}
>100	0.0167×10^{-5}	2×10^{-7}

where p = maximum pressure at grouting (MPa); γ_b = weight by volume of the concrete (kN/m^3); k_s = safety coefficient, which allows some increase in p, and is usually assumed 1.5–2.

Consolidation grouting uses a solution of water, bentonite, and high-strength cement. For foundations beneath embankment dams a solution is prepared with maximum density in order to fill up only large fractures. In the case of foundations for arch dams, it is necessary to fill up even the smallest cracks in the rock mass, which is achieved by means of cement-colloidal solutions. Grouting itself is carried out through boreholes set up at a mutual spacing of 1.5 to 3 m.

Grout curtains are water-impermeable separations, constructed below the waterproof element of embankment dams (or at the upstream end, in the case of concrete dams). Grout curtains have the task of reducing the seepage water quantity through the foundation, increasing its stability, drawing down the water table line at lateral seepage in the banks of the structure, and lowering the seepage uplift pressure in the foundation (of concrete dams). They are made by the extrusion of grouting mixture into the fractures of the rock, through sounding boreholes and by the application of special equipment. Facilities and methods of work are selected depending on the structure, features, and conditions of the foundation, as well as on the purpose of such grouting. While injecting the grouting mixture, which can be from lean suspension to dense mortar, there is a rise in the pressure; this is necessary to enable the grout mixture to penetrate into the fracture, which tightens gradually. At the same time, grouting proceeds until it achieves the anticipated limit pressure, which is maintained up to lowering the mass flow to a certain specified quantity. The water from the grouting suspensions and mortars, under the action of the gradient of pressure, drains into the tightest fractures in the rock, so that in the other, larger fractures, what remains is a compacted mass with a binding agent that, in the course of time, will completely consolidate and harden.

A grouting curtain is obligatory in cases where the relative loss of water in the rock q and the coefficient of permeability k are larger than the permissible ones given in Table 2.1. The relative loss of water is the quantity pressed through 1 m of the length of the sounding borehole at a pressure of 0.01 MPa:

$$q = \frac{Q}{pL} \tag{2.2}$$

where Q = the loss of water in the investigated section having a length L, while p = the pressure by means of which water is being impressed.

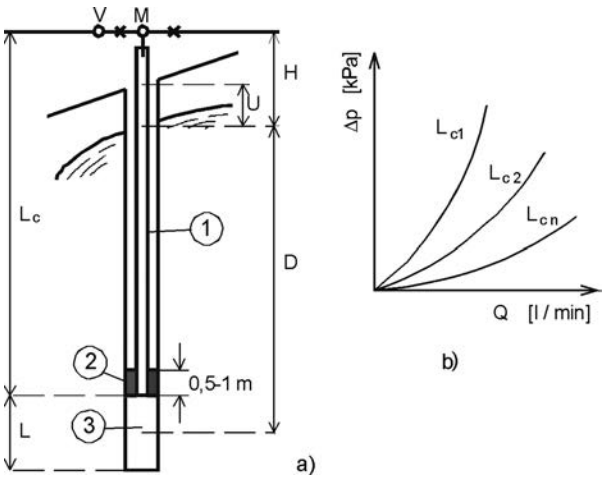

Figure 2.10 Schematic presentation of measurements of permeability according to Lugeon's method (a), and diagram of loss of pressure into the pipes (b).

In practice, the measurement of water permeability of rock is most often carried out according to the method of Lugeon, proposed in 1933. According to his method, the permeability of a fractured massif is assessed by the flow q expressed in l/min through 1 m of the borehole at a pressure of 1 MPa, while injecting water into a selected section of the borehole. Taking into consideration that water can only circulate through a rock through its fractures, then it is clear that the differences in the flow q in different investigated sections of the borehole through the same formation, show the degree of fracturing of the rock. In such a way, measurements according to Lugeon's method that are carried out in the course of investigation drilling, in addition to the degree of permeability, also enable an assessment of the homogeneity of the rock.

The measurement of permeability is carried out so that at the end of the selected measuring section (3), whose length usually is $L = 1–5$ m (Fig. 2.10a), boring ceases, while the section is isolated from the remaining part of the borehole by a special stopper (plug) (2), located at the end of the water supply pipe (1). That pipe, at ground surface, is connected to a pump, which presses water under pressure into the measuring section. Attached to the pipe is a pressure gauge (manometer) M for measuring the pressure and a water gauge V for measuring the flow. At the beginning water is pressed into the hole under low pressure as long as a constant flow has been established, and what follows afterwards is a record reading at several time intervals of 5 minutes each, as long as the difference between the flows is smaller than 10%.

For a calculation of the permeability, a mean value of measured flows is assumed. The procedure is repeated in the same section a number of times with higher pressures, up to $p = 1$ MPa, and again with smaller pressures, down to the lowest. In practice, sequences of pressure of 0.2, 0.4, 0.6, 0.8, 1 MPa and *vice versa,* are usually applied.

Pressure at the midpoint of the length of the measuring section is calculated by the pressure on the pressure gauge (manometer). This takes into consideration the level of

the pressure gauge, the elevation of the level of underground water, as well as hydraulic losses of pressure in the supply pipe of the pressure gauge to the end of pipe in the upper edge of the measuring section. The loss of pressure Δp should be determined prior to the test for different lengths of pipes and be given in a form of curves, depending on the flow Q, as is shown in Figure 2.10b.

The *Lugeon* permeability (LU, l/min/m) is calculated from the expression:

$$N = \frac{1000 \cdot Q}{p \cdot L \cdot \Delta t} \tag{2.3}$$

where Q = total flow in (l) in the course of measurement; Δt = time of measurement (min); L = length of measuring section (m); p = pressure of water at the midpoint of the measuring section (kPa).

The pressure at the midpoint of the measuring section, according to the markings in Figure 2.10a, will be:

$$p = p_{\mathrm{M}} + H \cdot \gamma_{\mathrm{w}} - \Delta p \tag{2.4}$$

where p_{M} = pressure in the pressure gauge (kPa); H = difference in elevation between the level of the pressure gauge and level of groundwater (m).

The capacity of the pump depends on the permeability of the rock, but it must be a minimum of 200 l/min at a pressure of 1 MPa. The level of underground water must be precisely determined prior to the test, whereas the stopper (plug) around the end of the pipe should be well inserted in order to prevent penetration of underground water into the measuring section.

In applying the Lugeon method as a criterion whether grouting is necessary or not, the value of 1 LU was valid until 1970. In the last ten years that limit has been moved up to 5 LU, except in cases of erodible filling of joints of the rock, when that criterion decreases to 3. This criterion has been applied in most new dams, and satisfactory results have been obtained, which implies a reduction of seepage water within acceptable limits from the viewpoint of the stability of the dam, and a loss of water from the impounding reservoir, as well as the life-duration of the dam.

Bear in mind that grouting works are expensive, so it is advisable that in adopting the criterion, a technical and economic analysis be performed so that a comparison can be made between the gains from grouting versus the cost of the works. New, more complex criteria have of late been proposed (Kutzner, 1991) in which the anisotropy of the rock is taken into consideration, the size of the fractures, the kind of dam to be built, and certain special conditions.

In the case of homogenous porosity of the rock, when there exists a danger of disturbances of the structure during the execution of testing, the *Lefrance* method is more suitable. For both methods, details are given in the textbook references (Nonveiller, 1989; Shroff & Shah, 1993).

Depending on the number of rows of sounding boreholes, the grout curtains can be *single-row grout curtains* or *multiple-row grout curtains*. Depending on their position in relation to the dam, they can be built in the riverbed below it, in the banks beneath the dam, or in the banks to the side of the dam. In the case of multiple-row curtains, the spacing between boreholes most often ranges from 1.5 to 3 m.

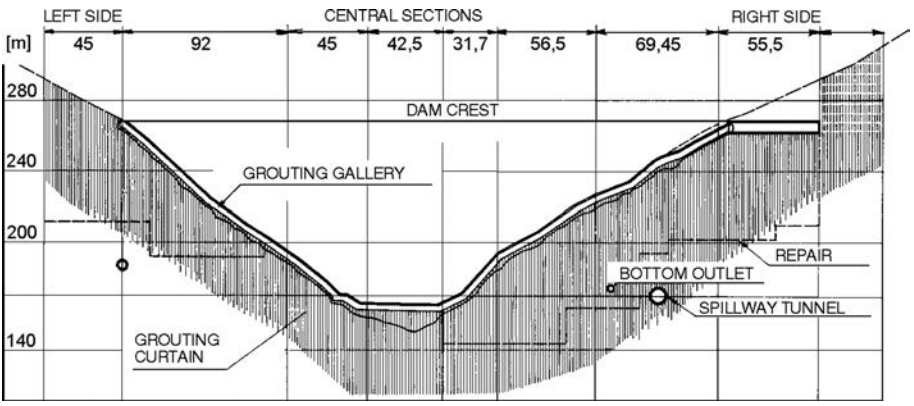

Figure 2.11 Unfolded section along the grout curtain at the Tikvesh dam.

The kind of material from which grout curtains are constructed depends on the characteristics of the dam foundation, as well as on the properties of the underground water. In that respect, we distinguish the materials as follows: cement grout curtains, clay–cement, chemical, bituminous, and other types of grout curtains.

Cement grout curtains have the most frequent application. They are made with a solution of cement in water and are applicable for fractures in the rock that are wider than 0.1 mm, provided the underground water moves with a velocity lower than 7×10^{-3} m/s and is not aggressive to the cement.

Clay–cement curtains are applied when most of the fractures are narrower than 0.1 mm. They are prepared from a cement and clay compound. Such a grout curtain has been constructed in the foundation of the highest dam in Macedonia – Tikvesh (Fig. 2.11; see also Chapter 11). The curtain extends into the riverbed, the banks, and continues at the side of the dam into both banks. The right bank is built of sericite–quartzite shale; phyllites are present in the riverbed, while amphibole shale occurs predominantly on the left bank. Occurrences of tectonic disintegration have been noticed in the foundation.

The grout curtain was first applied in two rows, mutually separated by 1.80 m, with boreholes alternately located, at distances of 3 m each. Grouting was performed from a gallery that had been built over a previously constructed concrete plug, below whose surface grouting has also been applied. The grout mixture consisted of 30% cement (PC 350), 65% clay, and 5% bentonite; it was mixed with water in the ratio 1:6–1:8. A denser compound was also employed. Once control borings and investigations had established that the required water impermeability had not been achieved in some parts, additional grouting was performed in a third row – in between the first two. The consumption of the dry mass amounted to around 330 kg per metre of the borehole, whereas the entire grouted mixture in all three rows amounted to 7,934 tons (YCOLD, 1970).

Chemical grout curtains are prepared with sodium silicate, calcium chloride, and other chemicals. They are used for fractures smaller than 0.1 mm.

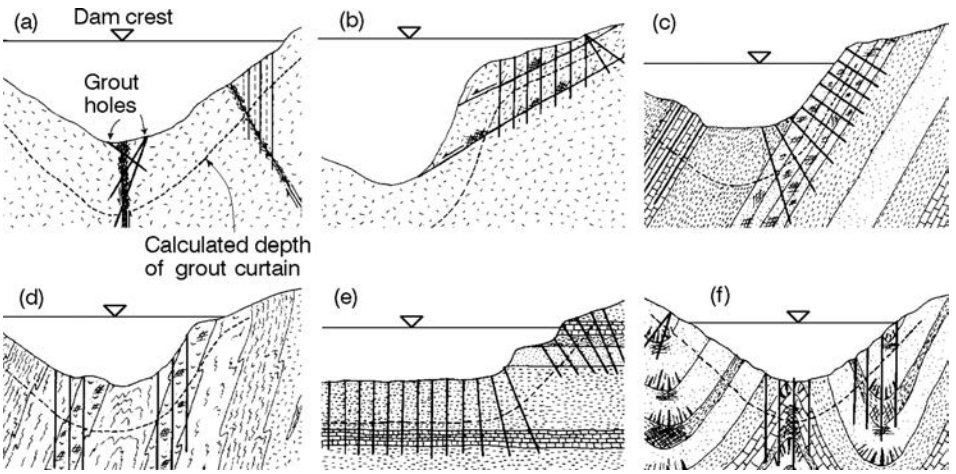

Figure 2.12 Curtain grout holes with a depth and situation determined by the local geological conditions existing in the foundation (after Wahlstrom, 1974).

The depth and thickness of a grout curtain depends on the kind and condition of the foundation rock below the dam, i.e. on its seepage characteristics. During the initial stage of design, the depth could be assumed to be $(0.50–0.75)H$. In cases when the positioning of fractures is rather irregular so that any rational analysis is not possible, the depth of grouting is assumed to be $(0.50–1.5)H$. The empirical formula $0.3H + C$ is also applied, in which C is a constant equal to 7.5 m for hard and sound rocks and 10.5 m for fractured rocks.

In practice, grout curtains have a depth of $(0.75–1)H$, regardless of the fact that theoretical analyses usually yield lower values. If the foundation is composed of karst limestone, marble or dolomite, then the depth of the suspended (hanging) curtain could amount to up to $3H$.

The depth of a curtain could be determined theoretically, while the specific conditions in the foundation determine the need for careful analysis of the geological conditions, so that grouting boreholes should be located in such a manner as to diminish or eliminate the potentially hazardous penetration of water below or around the theoretical grouting boundary. Figure 2.12, on which the theoretical boundary of grouting is shown by means of a dotted line, presents several cases in which the depth and attitudes of grouting boreholes are determined by the specific geological conditions, and not only by the calculated theoretical depth. The diagram represents only specially deepened or positioned boreholes, dictated by the geological conditions, and not normal ones, dictated by the theoretical line.

In the case (a), special inclined holes are aimed at intersecting a wide broken zone along a steep fault, and particular vertical pattern grout holes are deepened to intersect another fault in an abutment. The permeable zone in a steep-walled canyon (b) along gravity-slip faults is intersected by a row of grout holes. In diagram (c), pattern grout holes intersect a limestone layer and extend into an inclined layer of brittle fractured sandstone. In case (d), grouting holes are deepened to penetrate into fractured layers of

brittle quartzite in a metamorphic sequence containing schists and gneiss. In case (e), grout holes are extended beyond the theoretical formula depths in order to intersect the limestone layer. Diagram (f) presents a case in which deep grout holes probe highly fractured zones associated with tight folds in sedimentary rocks (Wahlstrom, 1974).

The procedure for grouting was invented and first applied by the French engineer Charles Berigny at the very beginning of the 19th century. By pressing plastic clay through wooden pipes of Ø8 cm, and by using a wooden ram (piston) and a heavy hammer, he stabilized the erosion-prone soil below the foundation of a structure in the harbour at Dieppe in France. There, he applied contact grouting with a suspension of pozzolan during the construction of a new structure in the same harbour.

Grouting of rock foundations beneath dams was initiated in the USA in the second half of the 19th century, and up to 1930 grouting had been applied only in some twenty dams. The systematic application and development of this procedure goes back to the construction of the arch-gravity Hoover Dam (also known as Boulder Dam), in 1932–1936, in which a grouting curtain and consolidation grouting had been applied below the entire foundation footing of the dam. At that time, precious experience was obtained from which standards for the grouting of rock foundations have been developed. In Macedonia after the Second World War, employing contemporary methods, plants, and equipment, grouting of a number of dams had been performed.

The other method for improving rock foundations – by *filling up fractures and tectonic zones* – has at its disposal a number of different possibilities, depending on specific local conditions. Wider fractures and tectonic zones in rock can be filled up with concrete or with a solution of cement and sand by applying various procedures, depending on their size and the kind of material used for filling them.

Fractures and tectonic zones with a thickness of 0.2–0.3 m are cleaned manually or by means of water jets and are filled in the upper part with a solution of cement, sand, and water. Through another possible method, to a certain depth, it is possible to dig out a manhole through the fracture, which will subsequently be filled with concrete. Tectonic zones with a thickness larger than 0.3 m are filled in with concrete wedges (keys). The most complete way is to clean the fractured zone as far as sound rock and then to fill the void with concrete.

Regarding the *soil foundations,* the development of methods for grouting has had a much more difficult advance. Namely, in the case of non-cohesive soils, composed of gravel and sand, difficulties occur during grouting, since larger parts of the suspension settle in the pores, thus preventing further penetration of the grouting mixture. In this, the pressure must not increase too much, in order to prevent any appearance of local penetrations and a moving up of the surface of the ground (Boulanger & Hayden, 1995). Certain developments have been achieved lately mainly by injecting water glass with an addition of agents (Nishigori & Takimoto, 1991). Practically, grouting in soil foundations is feasible only for deposits and formations of gravel or sandy gravel with a coefficient of seepage not lower than 5×10^{-4} cm/s. Here it is advantageous if the curtain penetrates into the water-impermeable layer, as is the case in Figure 2.13. If the curtain has been made as a suspension (hanging) curtain, it is necessary to achieve a depth of $\geq 1.0H$, in which H is the pressure on the dam (GCOLD, 2001).

Instead of using grouting, the water impermeability of soil foundations in hydraulic practice is more often achieved or improved with the construction of *diaphragm walls*

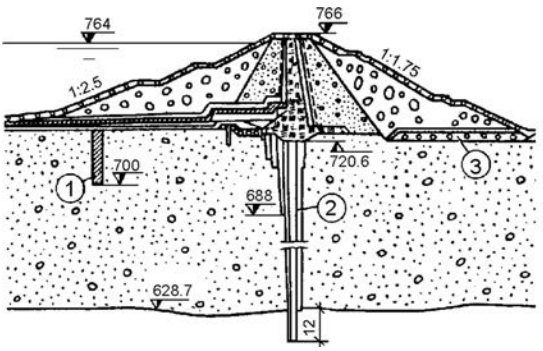

Figure 2.13 The Sylvenstein dam (Germany) with a grout curtain through deposit of gravel in the foundation (after Grishin et al., 1979). (1) Concrete cut-off trench for lengthening the seepage path; (2) grout curtain; (3) horizontal drainage for control of the curtain's effectiveness.

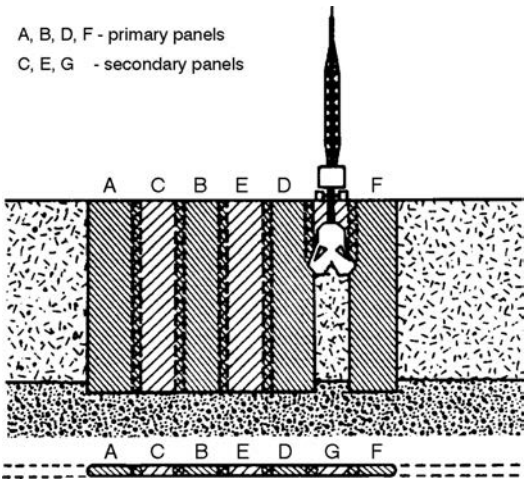

Figure 2.14 Construction of a cement–bentonite diaphragm wall (after Fell et al., 1992).

and *sheet piling*, which are made from various materials. Various kinds of diaphragm walls are used, depending on the structure of the dam and on the kind of soil foundation. Certain examples are reviewed at appropriate places in other chapters of this book, since a diaphragm wall can also be treated as an underground part of the dam. In continuation, we shall deal briefly with *cement–bentonite* and *concrete diaphragm walls*.

Cement–bentonite diaphragm walls are constructed in a trench, which is dug in continuation, in stretches, as shown in Figure 2.14. The dug out diaphragm stretch is kept stable, i.e. is backed, by means of cement–bentonite mortar, which is used for filling, immediately after digging out. Mortar is left in the trench to become cured and dried, in order to obtain a compressible, poorly water-permeable wall of low strength.

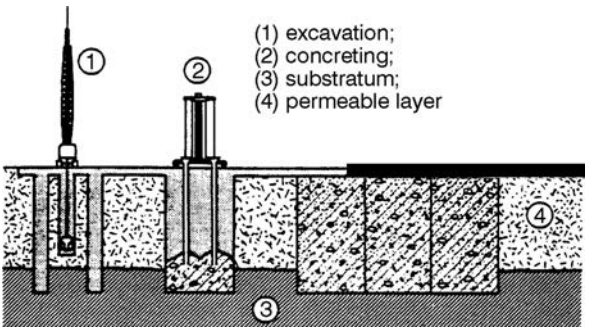

Figure 2.15 Concrete diaphragm wall (after Fell et al., 1992).

Diaphragm stretches are carried out in sequences, so that secondary diaphragm stretches are dug out only when the mortar in the primary diaphragm stretches is sufficiently hardened so as to carry itself; however, this should be done before it becomes too hardened. Thus, there is no need for supporting or shoring the end of the diaphragm stretch.

The trench can be 0.5–1.5 m wide, but most often it is near the lower limit, for economic reasons. The excavation is carried out by means of special plants and equipment, while the maximum depth of the diaphragm wall can exceed 50 m.

The cement–bentonite compound, according to some authors, in 1 m^3 could contain 80–350 kg cement and 30–50 kg bentonite, while, according to others, a typical compound contains 15–30% cement, 2–4% bentonite, 5–10% sand and gravel, and the rest water. Retarders are also added, in order to control the hardening process.

These diaphragm walls, in general, are of very low strength, as compared to concrete. In general, their strength amounts to 100 kPa at 28 days, and 150 kPa at 90 days. The water–cement ratio, as well as the type of cement, influences the strength. These diaphragm walls are plastic and they can adapt themselves to deformations in the foundation below the dam. Diaphragm walls can also be constructed of stiff or plastic concrete. Again, excavation is carried out in alternate diaphragm stretches (Fig. 2.15), providing the dug out excavated diaphragm stretch is kept stable with a filling of bentonite suspension. The stretches are cast with concrete or cement-bentonite concrete ("plastic concrete") (Fell et al., 1992).

The end of each diaphragm wall is shored with a special steel pipe, having a diameter the same as the width of the trench, which is pulled out following the setting of the concrete. Thus, a semicircular connection between any stretches has been formed, with better water-impermeability of the connection. Other joint systems can also be employed in order to improve water-impermeability of the diaphragm wall. Generally speaking, concrete diaphragm walls below the dam are not reinforced.

The thickness of concrete diaphragm walls, for depths up to 30 m, are most often assumed to be 0.6 m, being increased up to 1–1.2 m at a depth of 50 m. Conventional concrete can be used for their construction, however it is very stiff for this purpose and could crack, i.e. could be broken under the effect of the pressure of the surrounding earth. That is why plastic cement-bentonite concrete is more often used, with the

following participation of the constituent components in 1 m^3: 400–500 litres of bentonite suspension, 100–200 kg cement, 1300–1500 kg well-graded aggregate having a maximum grain smaller than 30 mm, and water–cement ratio 3.3:1. The bentonite suspension keeps the cement and aggregate in suspension during placing, and thus the concrete is provided with plasticity and a low permeability. The bentonite participation by weight in relation to water is 2–12%. In order to avoid segregation, the concrete is put in position by means of pipes or chutes (both conventional and plastic concrete). It is desirable to complete stretch concreting in less than 4 hours, in order to prevent noticeable hardening of the concrete.

More details of diaphragm walls that are used beneath dams can be found in the textbook references (Fell et al., 1992; Kutzner, 1997).

This page intentionally left blank

Chapter 3

Seepage through dams

3.1 ACTION OF SEEPAGE FLOW

The soil upon which dams are founded is porous and consists of a skeleton framework of solid particles with pores throughout. The penetration and movement of water through the porous medium, under the action of the gravitational potential occurring after the construction of water-retaining structures and the filling of the reservoir, is called *seepage*. Seepage may occur in the foundation beneath the dam (Fig. 3.1a), and in the banks beside the dam, as well as through the dam itself if it has been constructed with earth material, such as an earth dam (Fig. 3.1b). Owing to seepage, the following harmful effects may occur:

a) Loss of water in the impounding reservoir.
b) Pressure at the bottom of the dam, directed from below upwards and perpendicular to the bottom, which is called *uplift pressure*; this force is rather unfavourable, since it lightens the dam and reduces its resistance against the action of the horizontal forces.
c) Seepage water may take out fine earth particles from the foundation or from the body of the embankment dam, which leads to weakening of the foundation and body of the dam, as well as to possible damage downstream where those particles are carried. This phenomenon is called *mechanical erosion* and if it is of a progressive character, it can initiate the process of *piping,* which may be very dangerous, and even lead to failure of the foundation or to failure of the entire dam.
d) In addition to mechanical erosion, seepage water may also cause *chemical suffusion*, dissolving the rock salts in the foundation, which may lead to its progressive weakening.

In order to reduce the above harmful effects and to provide for the safety of the dam, it is essential to undertake special measures. Mainly, they consist of lengthening the path of the seepage, which reduces the velocity of the seepage, as well as the risk of erosion. By extending the seepage path, the larger part of the water potential will be spent on overcoming the frictional resistance of the flow through the earth medium on the way from the upstream face towards the downstream face of the dam. Vertical and horizontal water-impermeable elements are required for that purpose and are located in front of the dam and below it (Fig. 3.2a). The vertical elements (1) are constructed in

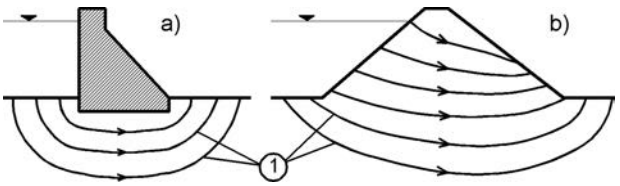

Figure 3.1 Seepage beneath a concrete dam (a), and through the body and foundation of an earth dam (b); (1) seepage.

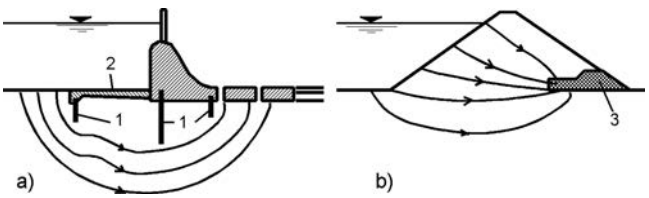

Figure 3.2 Measures for reducing the harmful effect of seepage. (a) By means of vertical partitions (1), and horizontal partitions (2); (b) by drainage.

a kind of sheet piling, then as a cement-grouting curtain, or as a diaphragm wall, most often a concrete or asphalt diaphragm wall. The horizontal elements are constructed in the kind of covering, i.e. blanket, in front of the dam, made of poorly permeable earth material, or else asphalt, concrete, or reinforced concrete.

For reducing the pressure in the bottom of hydraulic structures, as well as in the body of earth dams, *drainages* are an efficient means. They are structures in the form of an opening or a gallery in the dam, e.g. a pit or well, i.e. shaft, in the foundation. They can also be a member in the body of an embankment dam (3 in Fig. 3.2b), inserted into one or more permeable layers of sand, gravel or gritting material and placed in a horizontal, inclined or vertical position. Drainage facilitates taking away the water towards the downstream face of the dam and influences the velocity of the seepage and the magnitude of the uplift pressure.

3.2 MECHANICAL ACTION OF SEEPAGE FLOW ON THE EARTH'S SKELETON

It has been stated in the previous part that earth is a porous medium that consists of solid particles (the skeleton) with pores throughout. Pores can be filled with air, water, or else partially with air and partially with water. Analysing the mechanical action of seepage flow, the earth medium will be considered as being a two-phase system, i.e. it is assumed that the pores have been completely filled with water.

During seepage, the flow of water through pores in the earth medium is a laminar flow. Let us consider a part of the two-phase medium, which is shown greatly enlarged in Figure 3.3a. The earth particle *A* is surrounded by two streamlines (1) and (2).

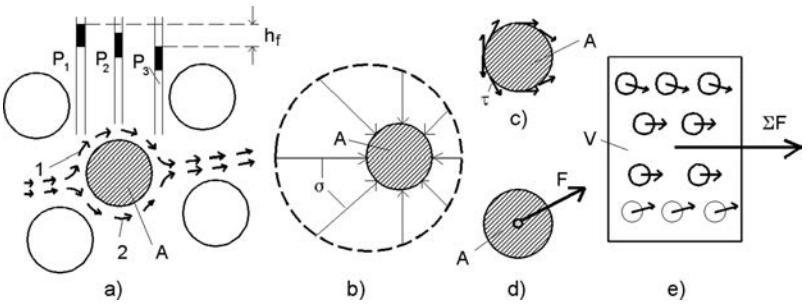

Figure 3.3 Mechanical action of seepage flow.

Because of the frictional resistance of the flow, there occurs a reduction of the pressure along the flow, shown by the level of the water in the piezometers P_1, P_2 and P_3, so that the normal pressure on particles is larger on the left side in relation to the right side (Fig. 3.3b).

In addition to the normal stress σ on the surface of the solid particle *A*, there are also tangential stresses τ (Fig. 3.3c). Should all of the elementary normal and tangential forces acting on the surface of particle *A* be added up, the force *F* is obtained (Fig. 3.3d), which tends to displace particle *A* in the direction of the seepage flow. This is called an *elementary force of hydraulic action* (Chugaev, 1985).

Let us imagine a larger volume of soil with more solid elementary particles (Fig. 3.3e). The force *F* acts on each of them, being different in relation to the intensity and direction, whereas their geometrical sum yields the summary force of hydraulic action Σ*F*, which tends to displace the entire considered volume *V*. The force acting from the side of the seepage flow on a unit of the volume is

$$F_s = \frac{\Sigma F}{V} \tag{3.1}$$

and is called a specific force of hydraulic action.

Let us assume that a unit of earth volume has been concentrated in point *M* (Fig. 3.4). One of the streamlines of the flow path (s) passes through point *M*. The specific force F_s can be broken down into the force F_t in the direction of the tangent (t) at point *M*, and a force F_w in the vertical direction. The force F_w is called a *specific force of hydrodynamic uplift pressure* and is equal to Archimedes' force:

$$F_w = (1 - n)\,\gamma_w \tag{3.2}$$

in which *n* is the porosity of soil, while γ_w is a unit weight of water.

The force F_t represents the *specific seepage force* and it is calculated from the following expression:

$$F_t = i\,\gamma_w \tag{3.3}$$

in which *i* is the hydraulic gradient at point *M*, given by the formula

$$i = \frac{\Delta h}{\Delta s} \tag{3.4}$$

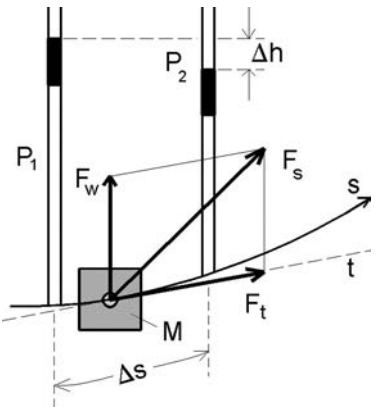

Figure 3.4 Forces acting on a unit of earth volume.

where Δh is loss of pressure along the elementary length Δs, denoted along the investigated streamline of the flow path. In this way, seepage force can be determined by means of the theory of seepage, which enables the determination of the hydraulic gradient i.

In the analysis of the possibility of originating deformations during seepage in an earth medium, it is necessary to take into consideration the forces F_w and F_t. For the sake of simplification, let us consider a unit volume of earth in the zone of seepage (Fig. 3.5a). Three forces act upon it: the unit weight of dry soil γ_d; the specific force of the hydrodynamic uplift pressure F_w; and the specific force of seepage F_t. Both vertical forces can be summed up, so that diagram (b) will be obtained instead of diagram (a), in which two volumetric forces act. In this case, it is:

$$\gamma' = \gamma_d - F_w \tag{3.5}$$

in which γ' is the buoyant unit weight of earth saturated in water. If we substitute the value for F_w from (3.2) into the formula (3.5), an expression for the calculation of γ' will be obtained:

$$\gamma' = \gamma_d - (1 - n)\,\gamma_w \tag{3.6}$$

It may be concluded that in the calculation of deformations, the earth – which is saturated with seepage water – should be considered as being immersed, having a buoyant unit weight γ'. It is also necessary to pay attention to the fact that the force F_t, too acts on each unit volume of such earth in the direction of the seepage.

Mechanical erosion of soil, as already mentioned in section 3.1, is a kind of seepage deformation in which seepage flow displaces separate fine particles by means of the elementary forces F. In this, the particles move independently from one another. If, during such movement, a particle comes across a relatively small pore through which it cannot pass, or else force F at some place is insufficient to be able to overcome the weight of the particle or the frictional resistance, then there occurs sedimentation

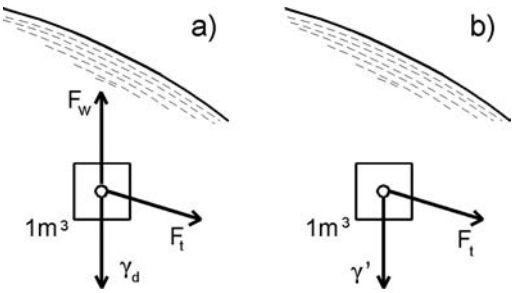

Figure 3.5 Forces acting on the unit volume of earth.

of the particle in a porous medium formed from coarser particles. The name of this phenomenon is *colmatation* (deposition of flow sediments).

Another consequence of the mechanical action of seepage flow which, together with the previous two falls into the group of microdeformations of a certain volume of earth, is the taking of fine particles out of the earth medium. This phenomenon is known as *external erosion*, as differentiated from *internal erosion*, where particles are not brought out of the earth medium. Seepage flow can also cause macro deformations of a particular volume of earth when, under the action of the summary force ΣF, there occurs a joint movement of all the particles forming that volume. In that way, there occurs a significant local deformation in the considered medium. An important case of such a local deformation occurs in the contact of different earth materials, for instance clay and some coarse-grained material. In such a case, the seepage forces fill fine particles of clay into the pores of the coarse-grained material.

From the description of the seepage mechanism, it arises that a mechanical erosion can originate only in the case of earth materials consisting of grains of different dimensions, whereas in the case of homogeneous earth materials, which consist of particles of equal size, only local seepage deformations are possible.

3.3 SEEPAGE RESISTANCE OF EARTH FOUNDATIONS AND STRUCTURES

By the term *seepage resistance* of earth foundations and structures is understood the ability of the earth material to resist seepage deformations. In that, one can distinguish:

1) *Normal seepage resistance*, which can be deranged in some particular weak spots and which can be appraised by means of calculations based on the rules of mechanics. Disturbance of the normal seepage resistance usually originates in the zone of the exit of the seepage flow in the downstream part of the dam, where local deformations may occur, or in the contact of fine-grained and coarse-grained material where noticeable erosion may occur.
2) *Random (casual) seepage resistance*, which can be deranged in some particular spots that are neither known in advance nor could be anticipated or evaluated by means of calculations, have an exclusively random (casual) nature. Casual seepage

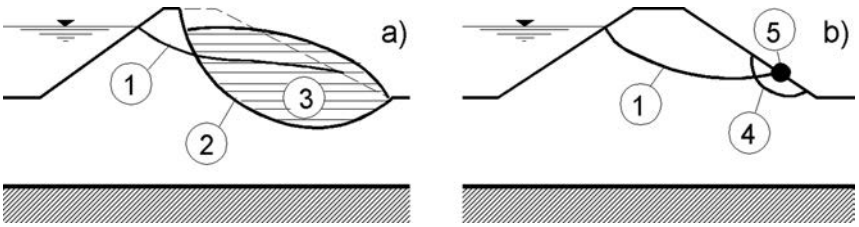

Figure 3.6 Complete failure of a dam slope (a), and local seepage deformation (b). (1) Seepage line; (2) surface slip circle; (3) slipped earth mass; (4) local landsliding; (5) exit point of the seepage line.

resistance can be disturbed when, for example, during the construction of an embankment dam, there is accidentally built in material of inadequate quality, or else if in the course of the service period there comes about an unforeseeable non-uniform settlement, which would accommodate forming a path of concentrated seepage. In order to eliminate or reduce to a minimum the risk from disturbing the casual seepage resistance, it is necessary during the dimensioning of the dam, to apply a safety coefficient, i.e. to anticipate a certain reserve.

One of the main properties of hydraulic structures is that during their construction and operation it is possible that there may be an occurrence of a number of casual factors that may significantly influence the operation of the structure. That is why the anticipation of some reserve, through the insertion of a safety coefficient, is an ordinary and often-used method in dimensioning such structures.

Both normal seepage resistance and random (casual) resistance can be local, when considering local deformations and damage at particular places in the dam, as well as general seepage resistance, when considering the ability of the dam to resist complete failure. Basic forms of possible damage to earth dams caused by seepage water that can be anticipated by means of calculations using the rules of mechanics are: a complete landslide, i.e. failure of the dam slope caused by the influence of forces due to weight and seepage (Fig. 3.6a), as well as local seepage deformations (Fig. 3.6b) in the zone of the exit point of the seepage line, originating under the action of seepage forces. All other damage, which cannot be analysed in accordance with the rules of mechanics, is of a casual nature.

Figure 3.6 clearly illustrates that sliding of the slope causes instantaneous and complete failure of the dam, while local deformation, as well as erosion (internal or external), does not put the dam out of operation. However, if such seepage deformations do not end in a certain period of time, then the final consequence could be failure of the dam.

3.4 THEORETICAL ASPECTS OF SEEPAGE

In the introductory part of this chapter, it was mentioned that earth is a porous material, so that water can flow through pores among the solid particles. The pressure of pore

water is measured in relation to the atmospheric pressure and the level at which the pressure is atmospheric, i.e. zero. It is defined as a water table or as a phreatic surface. It is assumed that below that level, the earth is completely saturated even though it is very probable that, due to the presence of a certain quantity of entrained air in the pores, the degree of saturation will be somewhat below 100%. Below the level of the water, pore water can be static – where the hydrostatic pressure depends on depth, or else it can flow through the earth under a certain hydraulic gradient, a situation that will be dealt with in this part.

If we use Bernoulli's theorem for the flow of pore water and take into consideration that, owing to the small velocity of flow, the velocity pressure is disregarded, then it follows that:

$$h = \frac{u}{\gamma_w} + z \tag{3.7}$$

where h = total head, u = pore water pressure, γ_w = unit weight of water, z = elevation head above a chosen plane.

Above the water table, it may come to a climbing and maintaining of the water under negative pressure with capillary tension, in which case climbing is larger if the dimensions of the pores are smaller. Negative pressure above the water table causes attracting forces among the particles, which are called 'suction forces,' and are a function of the size of pores and content of water.

The flow through a porous medium consisting of earth materials finer than gravel is always a laminar one and it can be represented empirically by Darcy's law:

$$q = Aki \tag{3.8}$$

or

$$v = \frac{q}{A} = ki \tag{3.9}$$

where q = flow quantity of water, A = area of cross-section through which the flow is performed, k = coefficient of permeability, i = hydraulic gradient, and v = flow velocity.

The coefficient of permeability (dimensions m/s) primarily depends on the average size of the pores, which on the other hand depends on the disposition of particles, their shape, and the earth's structure. Generally speaking, the smaller the dimensions of the particles, the smaller the average dimension of the pores, resulting in a coefficient of permeability that will be lower, i.e. the earth material will be less permeable. Even the presence of a small percentage of fine particles in coarse-grained earth will cause a considerable reduction of k. Soils consisting of layered deposits, have a larger permeability parallel to the layers than would be normal to them. In addition, fissures in clayey soils as a consequence result in much higher values of k in relation to the same material without fissures.

The value of k for various kinds of earth material ranges within the limits as denoted in Table 3.1 (Craig, 1978).

There are several empirical formulas for the determination of the coefficient of permeability, which are based on the granulometric composition of the earth material.

Table 3.1 Values of the coefficient of permeability (m/s).

1	10^{-1}	10^{-2}	10^{-3}	10^{-4}	10^{-5}	10^{-6}	10^{-7}	10^{-8}	10^{-9}	10^{-10}
Clean gravels		Clean sands and sand-gravel mixtures			Very fine sands, silts and clay-silt laminate		Unfissured clays and clay-silts (>20% clay)			
		Dessicated and fissured clays								

For example, according to Hazen, the approximate value of k can be determined from the expression:

$$k = 10^{-2} D_{10}^2 \quad [\text{m/s}] \tag{3.10}$$

where D_{10} = the diameter of the grains (in mm), represented by 10%.

More precisely, k is determined by means of laboratory tests on samples of the earth material, whereas for especially important projects the permeability is determined by means of investigations *in situ*.[1]

Let us now examine the case of two-dimensional seepage, assuming that the earth material through which seepage takes place, is homogeneous and isotropic in relation to the permeability, having a coefficient of permeability k. In the plane $x-z$, Darcy's law can be written in the following general form:

$$v_x = k i_x = -k \frac{\partial h}{\partial x} \tag{3.11}$$

$$v_z = k i_z = -k \frac{\partial h}{\partial z} \tag{3.12}$$

in which the total pressure h decreases in the direction of v_x and v_z. We consider an element of completely saturated earth having the dimensions $\mathrm{d}x$, $\mathrm{d}y$, $\mathrm{d}z$ in the directions x, y, z, with seepage taking place in the plane $x-z$ (Fig. 3.7). The components of discharge velocity of the water which enters the element are v_x and v_z, while the changes of the velocity of seepage through the element are $\partial v_x/\partial x$ and $\partial v_z/\partial z$, respectively. The volume of water entering the element in a unit time is:

$$V_\mathrm{e} = v_x \mathrm{d}y\mathrm{d}z + v_z \mathrm{d}x\mathrm{d}y \tag{3.13}$$

while the volume of water leaving the element in unit time amounts to:

$$V_\mathrm{l} = \left(v_x + \frac{\partial v_x}{\partial x}\mathrm{d}x\right)\mathrm{d}y\mathrm{d}z + \left(v_z + \frac{\partial v_z}{\partial z}\mathrm{d}z\right)\mathrm{d}x\mathrm{d}y \tag{3.14}$$

[1]These questions are treated in detail in the field of Soil Mechanics.

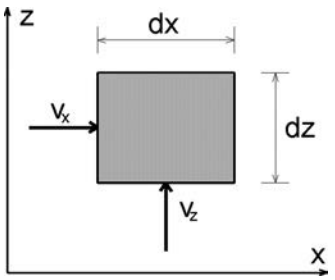

Figure 3.7 Seepage in the plane *x*–*z* for completely saturated earth element.

If an element is not susceptible to volume changes, and assuming that the water is not compressible, then $V_e = V_l$, which is represented:

$$\frac{\partial v_x}{\partial x} + \frac{\partial v_z}{\partial z} = 0 \tag{3.15}$$

The last expression represents an *equation of the continuity* in a plane.

While considering a two-dimensional seepage field, the potential can be represented by means of the potential function $\varphi(x, z)$, which is shown by:

$$\frac{\partial \varphi}{\partial x} = v_x = -k\frac{\partial h}{\partial x} \tag{3.16}$$

$$\frac{\partial \varphi}{\partial z} = v_z = -k\frac{\partial h}{\partial z} \tag{3.17}$$

From equations (3.15), (3.16), and (3.17) is then obtained:

$$\frac{\partial^2 \varphi}{\partial x^2} + \frac{\partial^2 \varphi}{\partial z^2} = 0 \tag{3.18}$$

i.e. that the potential function $\varphi(x, z)$ satisfies Laplace's differential equation.[2]

By integrating equation (3.18), the following will be obtained:

$$\varphi\,(x, z) = -kh(x, z) + \mathrm{C} \tag{3.19}$$

where C is a constant. If the function $\varphi(x, z)$ is given with a constant value, for instance $\varphi 1$, then it will represent a curved line, along which the potential $h1$, which is constant. Otherwise, if the function $\varphi(x, z)$ is given in a series of constant values φ_1, φ_2, $\varphi_3 \ldots$, then it will represent a family of curved lines having a constant potential along each of them. These curves are called *equipotentials*.

[2]In 1880 Forheimer indicated that the distribution of the pressure and velocity of water in a seepage medium is represented by means of Laplace's differential equation.

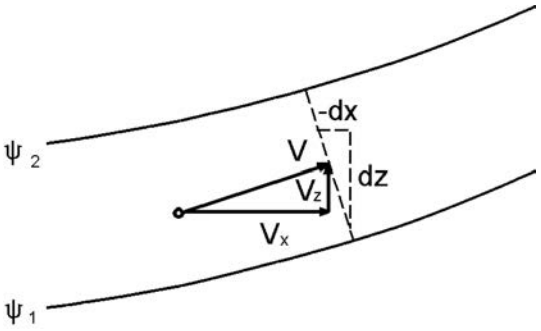

Figure 3.8 Seepage between two flow lines.

Another function in the seepage field, is *the flow function* $\psi(x, z)$, for which:

$$-\frac{\partial \psi}{\partial x} = v_z = -k\frac{\partial h}{\partial z} \tag{3.20}$$

$$\frac{\partial \psi}{\partial z} = v_x = -k\frac{\partial h}{\partial x} \tag{3.21}$$

and for which it is possible to demonstrate that it also satisfies Laplace's differential equation.

Total differential of the function $\psi(x, z)$ is:

$$\mathrm{d}\psi = \frac{\partial \psi}{\partial x}\mathrm{d}x + \frac{\partial \psi}{\partial z}\mathrm{d}z = -v_z\mathrm{d}x + v_x\mathrm{d}z \tag{3.22}$$

If the function $\psi(x, z)$ is given a constant value ψ_1, then $\mathrm{d}\psi = 0$, and:

$$\frac{\mathrm{d}z}{\mathrm{d}x} = \frac{v_z}{v_x} \tag{3.23}$$

In that way, the tangent at any point of the curve, represented by the function

$$\psi(x, z) = \psi_1 \tag{3.24}$$

determines the direction of the resultant discharge velocity at that point. That is why the curve represents the path of flow. If the function $\psi(x, z)$ is given with a series of constant values ψ_1, ψ_2, ψ_3, …, then a second family of curves is obtained, each of which represents a flow path. These curves are called flow lines.

The flow per unit time between two flow lines for which are given values of the functions of flow ψ_1 and ψ_2, is given by means of the expression (Fig. 3.8):

$$q = \int_{\psi_1}^{\psi_2} \left(-v_z\mathrm{d}x + v_x\mathrm{d}z\right) = \int_{\psi_1}^{\psi_2} \left(\frac{\partial \psi}{\partial x}\mathrm{d}x + \frac{\partial \psi}{\partial z}\mathrm{d}z\right) = \psi_2 - \psi_1 \tag{3.25}$$

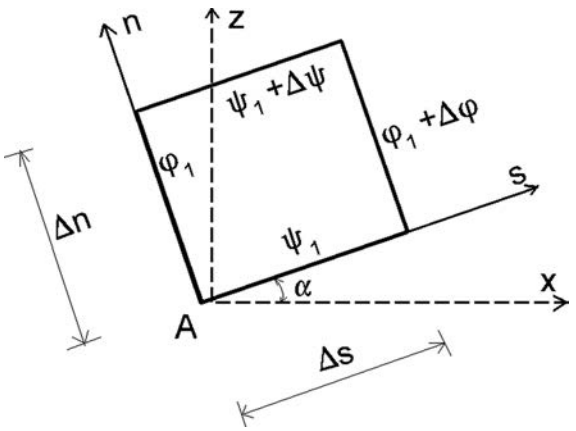

Figure 3.9 Intersection of two adjacent flow lines and equipotentials (after Craig, 1978).

This last expression shows that the flow through the seepage channel formed by two adjacent flow lines is constant.

The total differential of the function of the potential is:

$$\mathrm{d}\varphi = \frac{\partial \varphi}{\partial x}\mathrm{d}x + \frac{\partial \varphi}{\partial z}\mathrm{d}z = v_x \mathrm{d}x + v_z \mathrm{d}z \tag{3.26}$$

If $\varphi(x, z)$ is constant, then $\mathrm{d}\varphi = 0$, and

$$\frac{\mathrm{d}z}{\mathrm{d}x} = -\frac{v_x}{v_z} \tag{3.27}$$

By comparing equations (3.23) and (3.27), it is clear that the flow lines and the equipotentials intersect each other at right angles.

Let us consider now two flow lines ψ_1 and $(\psi_1 + \Delta\psi)$ at a reciprocal distance Δn, which are intersected normally by two equipotentials φ_1 and $(\varphi_1 + \Delta\varphi)$ at a reciprocal distance Δs (Fig. 3.9). Directions s and n are inclined at an angle a towards x, i.e. from the z axle.

At point A, the velocity of flow in direction s is v_s, while the components of v_s in directions x and z, are:

$$v_x = v_s \cos\alpha \quad v_z = v_s \sin\alpha \tag{3.28}$$

Now it is:

$$\frac{\partial \varphi}{\partial s} = \frac{\partial \varphi}{\partial x}\frac{\partial x}{\partial s} + \frac{\partial \varphi}{\partial z}\frac{\partial z}{\partial s} = v_s \cos^2\alpha + v_s \sin^2\alpha = v_s \tag{3.29}$$

$$\frac{\partial \psi}{\partial n} = \frac{\partial \psi}{\partial x}\frac{\partial x}{\partial n} + \frac{\partial \psi}{\partial z}\frac{\partial z}{\partial n} = -v_s \sin\alpha\,(-\sin\alpha) + v_s \cos^2\alpha = v_s \tag{3.30}$$

From here, it follows that:

$$\frac{\partial \psi}{\partial n} = \frac{\partial \varphi}{\partial s} \tag{3.31}$$

or

$$\frac{\Delta \psi}{\Delta n} = \frac{\Delta \varphi}{\Delta s} \tag{3.32}$$

i.e. the increase of the function of flow on the distance between two adjacent lines of flow is equal to the increase of the function of the potential on the distance between two adjacent lines of the potential. This property of the curves of families of the function of flow and the function of the potential is utilized in the practical solving of the problem of seepage.

3.5 PRACTICAL SOLUTION OF THE PROBLEM OF SEEPAGE

Laplace's differential equation can be integrated analytically for the simplest geometry and boundary conditions of the examined field. The solution is obtained in the form of families of flow lines and equipotentials, which jointly form a flow net. For more complex cases, which usually occur in practice, the solution is carried out by means of approximate methods, as follows: by the application of hydraulic models on a reduced scale, by analogous models, by a numerical way of solving problems, and by means of a graphical solution.

Hydraulic models on a reduced scale (usually 1:25) represent the seepage medium and enable establishment of the water level of the upstream face and downstream face. After stabilization of streaming by means of a system of built-in piezometers, the potential at particular points is measured and, with those results, equipotentials are reconstructed (by interpolation) and flow lines are constructed.

Flow lines can be made visible in the model by means of impressing concentrated colours at the entrance of the flow and, on the basis of that, drawing the flow net. The method of using hydraulic models gives the best results; however, it also has a deficiency: the manufacture of the model, by means of which the conditions of the ground will be truly reproduced, is a complex and expensive work. That is why doing so is rarely applied in the design of dams.

Analogous models are more often used in practice. *The electrical analogy model* takes a distinguished place and it also enables solving much more complex problems. The solution is possible on a two-dimensional or three-dimensional electrical model having the same geometrical shape as the earth through the water filtrates. The porous medium is replaced with an electric conductor, while the boundary conditions are established by means of electrical potential at the beginning and at the end of the seepage flow. By a drop in the potential throughout the model, there is made a simulation of the drop of the potential of the water flow in the prototype. The measurements are performed by means of Wheatstone's bridge and by means of a potential gauge. This model can also simulate changes in the permeability coefficient in particular zones of the earth medium through the changes of the electrical conductivity coefficient.

The application of the electrical analogy model is based on the analogy in expressing the seepage water quantity by means of Darcy's law (3.33) and the flow of electricity by means of Ohm's law (3.34):

Darcy's law		Ohm's law	
$Q = \frac{kAh}{l}$	(3.33)	$I = \frac{CA'E}{l'}$	(3.34)
Q = quantity of seepage		I = rate of flow of electricity	
k = coefficient of permeability		C = electric conductivity coefficient	
A = cross-sectional area		A' = cross-sectional area	
h = pressure head		E = electrical potential (voltage)	
l = length of seepage path		l' = length of path of electric current	

Numerical methods for the approximate solution of the problem of seepage originated some half a century ago, however their development and large-scale application has taken place in the last 30 years, along with the swift progress of computer technology. The best results have been achieved by using the method of finite differences (Kalkani, 1989) and, lately, by the use of the finite element method. The first method uses a mathematical approximation of the differentials, whereas the second one uses a physical approximation of the porous medium through which seepage takes place, and in this case a system of a considerable number of algebraic equations are obtained, so that a powerful computer system is needed for their solution. These two contemporary numerical methods are especially suitable for solving complex problems involving seepage through a non-homogeneous medium and in complex boundary conditions, both for plane problems and for spatial problems (Desai & Christian, 1977).

A *graphic solution* involving the construction of a flow net was developed at the very beginning of the last century in Germany by Forheimer and in England by Richardson, and even now represents a powerful weapon in the engineers' hands. The method is simple and with its application a relatively fast solution of practical problems of seepage is possible, without the need for working out expensive hydraulic or analogous models or the use of a powerful computer system. Accuracy coincides with the accuracy of the soil mechanics parameters used as input in solving the problems of seepage.

A graphical construction of the flow net is illustrated by the example of seepage below a concrete gravity dam through a porous stratum that lies on a water-impermeable rock (Fig. 3.10a). From the upstream face, the height of the water layer is $H = 15$ m, while from the downstream face the depth of water is small and so, is disregarded. The depth of the porous stratum below the dam is 20 m.

A graphical construction of the flow net is determined by a number of trials and by a gradual approximation to the best solution, paying attention to the theoretical aspects, as set out in section 3.4. The basic condition that has to be satisfied in the flow net is that each section between the flow line and the equipotential line should be at a right angle. Furthermore, for practical reasons, it is good to construct such a network, in which $\Delta\psi$ will have the same value between any two adjacent flow lines, while $\Delta\varphi$ will have the same value between any two adjacent equipotentials. It is also

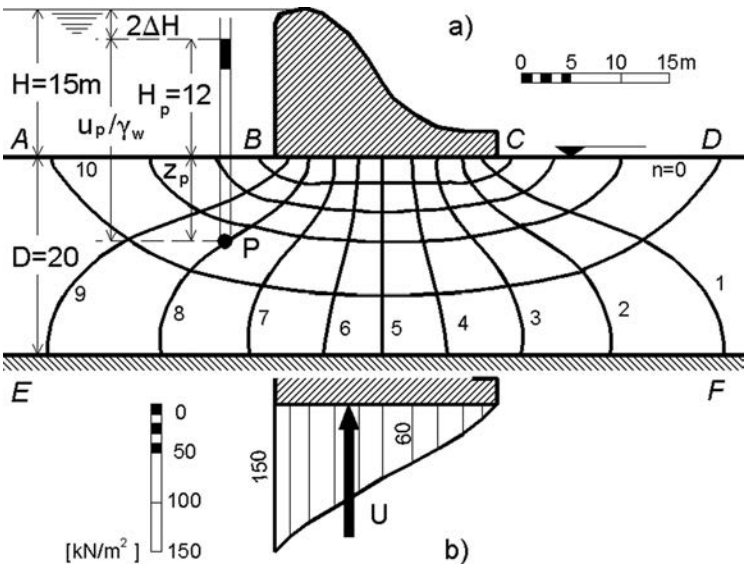

Figure 3.10 Flow net beneath a gravity dam.

advantageous to adopt Δs being $= \Delta n$ (in equation 3.32). In this way, the flow lines and the equipotentials will form a network of 'curvilinear squares,' and for each square the following conditions will apply:

$$\Delta\psi = \Delta\varphi \tag{3.35}$$

First of all, let us define the boundary conditions in the seepage zone. In order to define potential head at particular points, we select a reference plane or datum. It is usual with dams for the water level from the downstream face to be adopted as a reference plane or, if there is no water, to assume the terrain on the downstream face, as has been done in our example. At each point along the boundary *AB* the potential is constant, equal to the total head *H*, which means that *AB* is a boundary equipotential line. In a similar manner, it could be concluded that *CD* is also a boundary equipotential line, having zero potential. From the point *B*, water must flow towards *C* (below the water impermeable dam), so that the line *BC* is a boundary flow line. Also, during seepage water must flow from point *E* towards point *F* along the water-impermeable layer, so that line *EF* is the second boundary flow line. The other flow lines must be between the boundary lines *BC* and *EF*.

Figure 3.10a shows a flow net, made up according to the principles laid out in this part. Between the two last flow lines (at the lower boundary), squares need not be formed; however, the ratio of the length and width of each figure along this seepage channel must be constant.

In constructing the flow net there is no need to draw too many flow lines. Usually, quite satisfactory results are obtained by means of 4–6 seepage channels (a seepage channel is formed by means of two adjacent flow lines). There are altogether

11 equipotentials in the constructed flow net, denoted by the numbers $n = 0$ at the downstream boundary, and up to 10 at the upstream boundary. The drop of potential ΔH between any two adjacent equipotentials is:

$$\Delta H = \frac{H}{N_d} \tag{3.36}$$

in which N_d is the number of equipotential drops. In our example, it will be $\Delta H = 15/10 = 1.5$ m. The potential along an equipotential line, denoted by the number n, will be $n \times \Delta H$. For example, the potential at point P will be $H_p = n_p \times \Delta H = 8 \times 1.5 = 12$ m, i.e. water will rise in the piezometer 12 metres above the reference plane. Point P is at a distance z_p below the reference plane, i.e. it has an elevation head $-z_p$. The pore pressure u_p at point P can be calculated in accordance with Bernoulli's theorem:

$$u_p = \gamma_w[H_p - (-z_p)] = \gamma_w(H_p + z_p) \tag{3.37}$$

By means of the expression (3.37) and by using the flow net, it is also possible to calculate pore pressure at any point on the seepage medium. In this way, one can obtain a diagram of net water pressure distribution below the concrete dam (Fig. 3.10b), the area that gives the value of the force of uplift pressure, acting at the centre of gravity of the diagram and being directed upwards.

The flow net also enables us to calculate seepage water quantity through the seepage medium and for unit dimension in the y-direction. If we assume that the medium is homogeneous and isotropic, then by means of Darcy's law, it is possible to express the seepage water quantity through any seepage channel and for any unit length of the dam by:

$$q = Aki \tag{3.38}$$

In accordance with Figure 3.9, the area of the cross-section of the seepage channel will be:

$$A = \Delta n \times 1 \tag{3.39}$$

while the hydraulic gradient is:

$$i = \frac{\Delta H}{\Delta s} \tag{3.40}$$

Taking into consideration that at the network of squares, it is:

$$\Delta n = \Delta s \tag{3.41}$$

then it follows that:

$$q = k \times \Delta H \tag{3.42}$$

If N_f denotes the number of flow channels, and N_d denotes the number of equipotential drops ΔH, then:

$$Q = q \times N_f \quad H = \Delta H \times N_d \tag{3.43}$$

in which Q is total seepage water quantity on unit length beneath the dam. From equations (3.40) and (3.43) it can be determined that:

$$Q = kH\frac{N_f}{N_d} \tag{3.44}$$

From the expression (3.44), it can be seen that total seepage water quantity is a function of the ratio N_f/N_d, i.e. it depends on the number of flow lines and equipotentials. For the examined example, assuming that $k = 2.0 \times 10^{-6}$ m/s, it will be:

$$Q = 2.0 \times 10^{-6} \times 15 \times \frac{4.6}{10} = 13.8 \times 10^{-6} \quad [\mathrm{m}^3/\mathrm{s/m}]$$

3.6 SEEPAGE IN ANISOTROPIC SOIL CONDITIONS

The majority of the natural earth deposits are anisotropic in relation to water permeability, having a coefficient of permeability of maximum value in the direction of the layers, and of minimum value in the direction perpendicular to the layers. If these directions are denoted by x and z, then it will be (Craig 1978):

$$k_x = k_{\max} \quad k_z = k_{\min} \tag{3.45}$$

For this case, Darcy's law can be presented in the following general form:

$$v_x = k_x i_x = -k_x \frac{\partial h}{\partial x} \tag{3.46}$$

$$v_z = k_z i_z = -k_z \frac{\partial h}{\partial z} \tag{3.47}$$

In an arbitrary direction s, inclined at an angle a in relation to the x-direction, the coefficient of permeability is determined by means of the equation:

$$v_s = -k_s \frac{\partial h}{\partial s} \tag{3.48}$$

Proceeding onward:

$$\frac{\partial h}{\partial s} = \frac{\partial h}{\partial x}\frac{\partial x}{\partial s} + \frac{\partial h}{\partial z}\frac{\partial z}{\partial s} \tag{3.49}$$

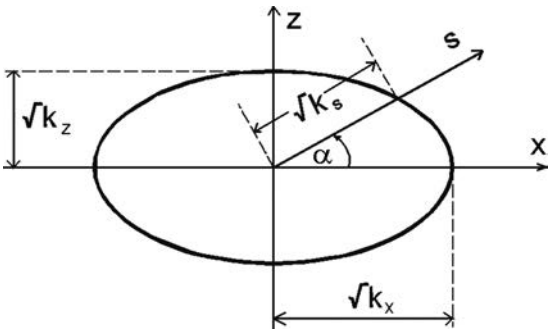

Figure 3.11 Ellipse of change of permeability.

i.e.

$$\frac{v_s}{k_s} = \frac{v_x}{k_x}\cos\alpha + \frac{v_z}{k_z}\sin\alpha \tag{3.50}$$

The components of the velocities of flow behave as follows:

$$v_x = v_s\cos\alpha \quad v_z = v_s\sin\alpha \tag{3.51}$$

Therefore:

$$\frac{1}{k_s} = \frac{\cos^2\alpha}{k_x} + \frac{\sin^2\alpha}{k_z} \tag{3.52}$$

or:

$$\frac{s^2}{k_s} = \frac{x^2}{k_x} + \frac{z^2}{k_z} \tag{3.53}$$

The expression in equation (3.53) describes the change of permeability in various directions, represented by an ellipse, and is shown in Figure 3.11.

Taking into consideration Darcy's law in a general form (3.43), (3.44), the equation of continuity (3.15) will be:

$$k_x\frac{\partial^2 h}{\partial x^2} + k_z\frac{\partial^2 h}{\partial z^2} = 0 \tag{3.54}$$

i.e.

$$\frac{\partial^2 h}{\left(\frac{k_z}{k_x}\right)\partial x^2} + \frac{\partial^2 h}{\partial z^2} = 0 \tag{3.55}$$

Performing the substitution:

$$x_t = x\sqrt{\frac{k_z}{k_x}} \tag{3.56}$$

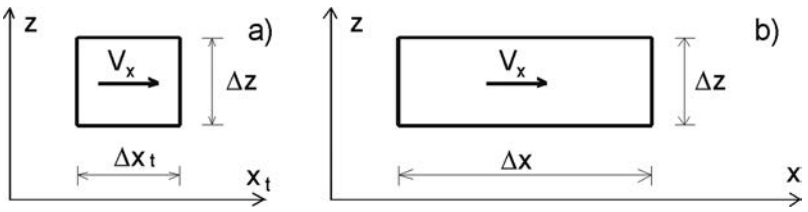

Figure 3.12 Elementary field of flow net (after Craig, 1978). (a) Transformed; (b) natural.

the equation of continuity will be:

$$\frac{\partial^2 h}{\partial x_t^2} + \frac{\partial^2 h}{\partial z^2} = 0 \tag{3.57}$$

which represents an equation of continuity for an isotropic medium in the plane $x_t - z$ (Craig, 1978).

Using equation (3.56), the factor of transformation is determined by means of which in the x-direction a given anisotropic seepage range is transformed into a fictitious isotropic seepage range, for which Laplace's equation is valid. If the flow net, which represents a solution to Laplace's equation, has been drawn for a transformed range, then the flow net for the natural range can be obtained by the application of the inverse value of the factor of transformation. Also, the required transformation could be carried out in the z-direction.

The value of the coefficient of permeability, applied to the transformed range, is called the *equivalent isotropic coefficient* and is obtained from the expression:

$$k' = \sqrt{k_x k_z} \tag{3.58}$$

The accuracy of the previous expression can be demonstrated on an elementary field of flow net through which seepage is taking place in the x-direction. The field is drawn in a transformed and natural scale (Fig. 3.12a, b), by means of transformation carried out in the x-direction.

The velocity of flow v_x could be expressed by either k', or by k_x:

$$v_x = -k' \frac{\partial h}{\partial x_t} = -k_x \frac{\partial h}{\partial x} \tag{3.59}$$

in which:

$$\frac{\partial h}{\partial x_t} = \frac{\partial h}{\sqrt{\frac{k_z}{k_x}}\partial x} \tag{3.60}$$

and from here:

$$k' = k_x\sqrt{\frac{k_z}{k_x}} = \sqrt{k_x k_z} \tag{3.61}$$

3.7 SEEPAGE IN NON-HOMOGENEOUS SOIL CONDITIONS

Let us now examine the case where the seepage medium consists of two isotropic earth layers, having thickness H_1, i.e. H_2 and coefficients of permeability k_1 and k_2, separated in between with a horizontal boundary (Fig. 3.13). That means that we have a case of non-homogeneous soil conditions. Both layers could be treated as one homogeneous anisotropic layer, having thickness $(H_1 + H_2)$, in which the coefficients of permeability, parallel, and perpendicular to the stratification, are k_x and k_z, respectively (after Craig, 1978).

For one-dimensional seepage in a horizontal direction, the equipotentials in any layer are vertical. If h_1 and h_2 represent the potential at two points in the first and the second layer respectively, then for a joint point that lies on the boundary, it will be $h_1 = h_2$. That is why whichever vertical line passes through those two layers is a common equipotential line. In that way, the hydraulic gradient in both layers and in the equivalent single layer, is equal and will be denoted by i_x. Total flow in the horizontal direction will be:

$$\overline{q}_x = (H_1 + H_2)\,\overline{k}_x i_x = \left(H_1 k_1 + H_2 k_2\right) i_x \tag{3.62}$$

in which

$$\overline{k}_x = \frac{H_1 k_1 + H_2 k_2}{H_1 + H_2} \tag{3.63}$$

For one-dimensional seepage in a vertical direction, the velocity of flow in each layer, and also in the equivalent single layer, must be equal in order to satisfy the conditions of continuity. In such a case, it follows that:

$$v_z = \overline{k}_z \bar{i}_z = k_1 i_1 = k_2 i_2 \tag{3.64}$$

in which $\bar{i}_z$ is average hydraulic gradient through the depth $(H_1 + H_2)$, i.e.

$$i_1 = \frac{\overline{k}_z}{k_1}\bar{i}_z \quad i_2 = \frac{\overline{k}_z}{k_2}\bar{i}_z \tag{3.65}$$

Now the loss in potential through the total depth $(H_1 + H_2)$ is equal to the sum of the losses in total head in the individual layers, i.e.:

$$\bar{i}_z(H_1 + H_2) = i_1 H_1 + i_2 H_2 = \overline{k}_z \bar{i}_z \left(\frac{H_1}{k_1} + \frac{H_2}{k_2}\right) \tag{3.66}$$

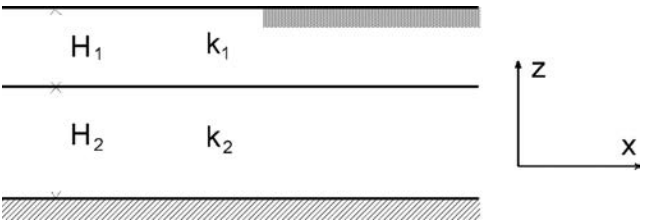

Figure 3.13 Seepage through non-homogeneous soil conditions.

in which:

$$\bar{k}_z = \frac{H_1 + H_2}{\frac{H_1}{k_1} + \frac{H_2}{k_2}} \tag{3.67}$$

3.8 SEEPAGE OF WATER THROUGH ROCK FOUNDATIONS

Seepage of water also takes place in rock foundations of dams; however, Darcy's law does not apply in this case. Namely, the rocks are distinguished with low porosity, so that seepage takes place through fissures and fractures, created as a result of various tectonic processes, and further due to erosion and excavation of foundation pits by means of blasting.

Fissures and fractures can have very different dimensions, ranging from parts of a millimetre up to a number of tens of centimetres. If they are filled up with fine fractions from weathered minerals, then they will be poorly water-permeable, but they could also remain partially filled, i.e. open.

By moving through fissures of the rock, seepage flow loses a part of its potential, the same as seepage in a porous earth medium. In such a case, it is not possible to apply the theory of potential flow of underground waters, so that the law according to which reduction of the potential takes place is unknown.

Seepage flow causes a force of uplift pressure at the bottom of a concrete dam, which lightens the dam, thus lowering its stability. Since seepage takes place through the pores and fissures of the rock, it is clear that the force of uplift pressure will not act across the entire surface of the bottom of the dam, but along the surface of the relevant pores and fissures. If α_2 denotes the coefficient of reduction of the surface upon which the force of uplift pressure is transmitted, then the area upon which that force will act will be $\alpha_2 B$, in which B is an area of 1 metre of the length of the dam. The value of the coefficient α_2 depends on the rock characteristics, as well as the dimensions of the fissures. The Russian hydraulic engineer M.M. Grishin recommends that we assume $\alpha_2 = 0.7-0.95$; however, experimental investigations have also shown lower results. It is often assumed as $\alpha_2 = \mathbf{1}$, which is on the safe side, although it is physically impossible (Grishin et al., 1979).

Figure 3.14 illustrates a diagram of a concrete gravity dam with a depth of headwater H_1, and a depth of tail water H_2. The total force of the uplift pressure consists of the sum of the force U_1, whose diagram is obtained through the depth of the tail

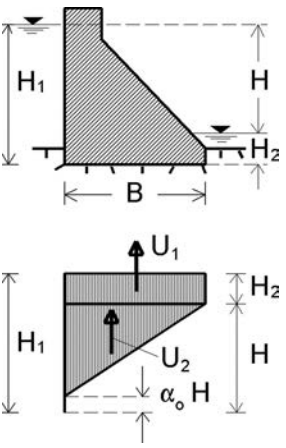

Figure 3.14 Uplift forces on a concrete dam on rock foundations.

water H_2, and the force U_2, caused by seepage of water in the rock. The diagram of the force U_1, in the case of a flat-bottom dam, is assumed to be rectangular, while for a complex shaped bottom, it is formed according to the contour. Thus, for a rectangular diagram it is:

$$U_1 = \alpha_2 \gamma_w H_2 B \tag{3.68}$$

The diagram of the force of seepage U_2 is assumed to change in a straight line, because the true shape cannot be obtained theoretically, while the results from observation indicate that such an approximation is good and makes a contribution to safety. The force U_2 can be calculated from the expression:

$$U_2 = 0.5\gamma_w(1 - \alpha_0)B\alpha_2 \tag{3.69}$$

in which α_0 is a coefficient of loss of pressure at the seepage path in a rock foundation, which, in regular calculations, is disregarded ($\alpha_0 \approx 0-0.1$).

The force of seepage uplift pressure increases the dimensions of the dam, and that is why measures are taken for its lowering. This is accomplished through the construction of a grout curtain and vertical drainages, positioned behind the curtain, which enable lowering the pressure left over behind the curtain. Depending on the materials from which they are constructed, grout curtains can be made of cement, clay–cement, bituminous etc. They are located at the upstream end of the dam in order to be able to effect as large a reduction of the seepage force, as possible (Fig. 3.15).

A diagram of the force U_2 is constructed depending on the kind of grout curtain and existence of drainage. For a cement curtain, the specific seepage uplift pressure falls to the value $\alpha_1 H$, in which α_1 is a coefficient of reduction of pressure equal to 0.3–0.6, depending on the depth of curtain and on the ratio of the permeability of the

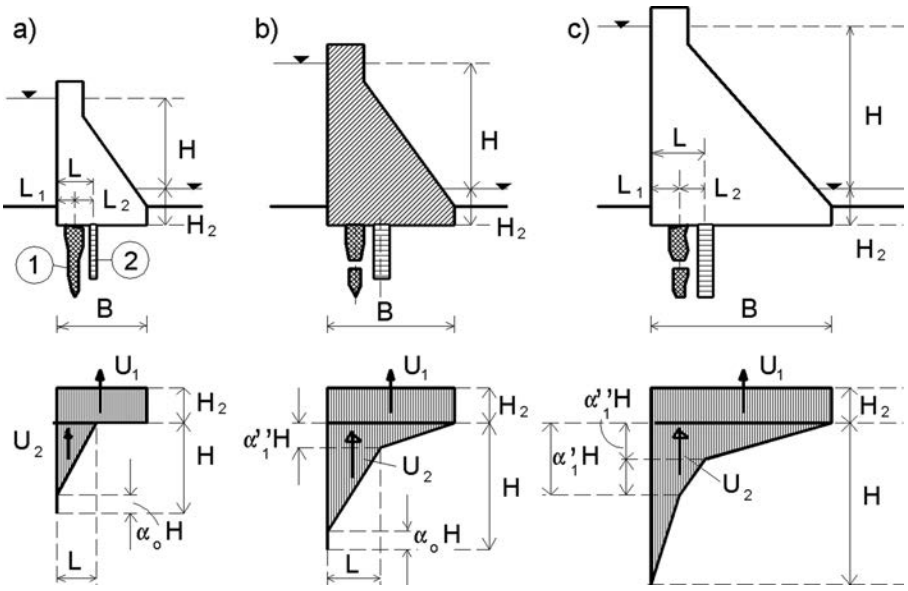

Figure 3.15 Diagram of uplift pressure in rock foundations when there is a grout curtain (1) and drainage (2).

curtain versus that of the foundation. If there is a drainage system below the curtain, then α_1 goes down to 0.1–0.3.

The question of seepage through rock foundations is still being investigated, so that a calculation of the force of uplift pressure in such a case is usually carried out in accordance with the requirements and recommendations as specified in the standards of particular countries. Russian standards recommend that the seepage uplift pressure at the bottom of concrete dams, having a grout curtain and drainage, be determined in the following way:

1) For dams having low head ($H < 25$ m) (Fig. 3.15a):

$$U_2 = 0.5\gamma_w(1 - \alpha_0)L\alpha_2 \tag{3.70}$$

2) For dams having medium head ($H < 25 < 75$ m) (Fig. 3.15b)

$$U_2 = 0.5\gamma_w H\left[L(1 - \alpha_0) + B\alpha_1''\right]\alpha_2 \tag{3.71}$$

3) For dams having high head ($H > 75$ m) (Fig. 3.15c):

$$U_2 = 0.5\gamma_w H\left[L_1\left(1 + \alpha_1' - \alpha_1''\right) + L_2\alpha_1' + B\alpha_1''\right]\alpha_2 \tag{3.72}$$

in which α_1' and α_1'' have values as given in Table 3.2.

Table 3.2 Values of coefficients α_1' and α_1''.

Type of dam	α_1'	α_1''
Gravity concrete dam		
– Low	0.3	0
– Medium	0.4	0.15
– High	0.5	0.25
Massive head buttress dam	0.4	0
Arch concrete dam	0.5	0.25

Seepage water can also cause chemical erosion, provided the rock foundation consists of easily soluble materials – gypsum, anhydrite, or rock salt. Because of that, dams are not permitted to be constructed on such foundations, since in such cases there are no measures for protection against the destructive action of the chemical erosion.

3.9 LATERAL SEEPAGE

Concrete water-retaining structures, with their lateral parts, reach to the banks of the valley or are composite with the earth parts of the dam, which is more rarely the case. In the zone of these joints there occurs a lateral seepage without any pressure, where a spatial picture of the movement of the seepage flow is obtained, which connects with the seepage flow under pressure below the dam. The lateral seepage causes a force that acts upon the joint of the impermeable structure with the original ground (or embankment) and has an influence on the enlargement of its dimensions. To reduce the pressure of the seepage flow in the zone of the joint, it is necessary to lower the

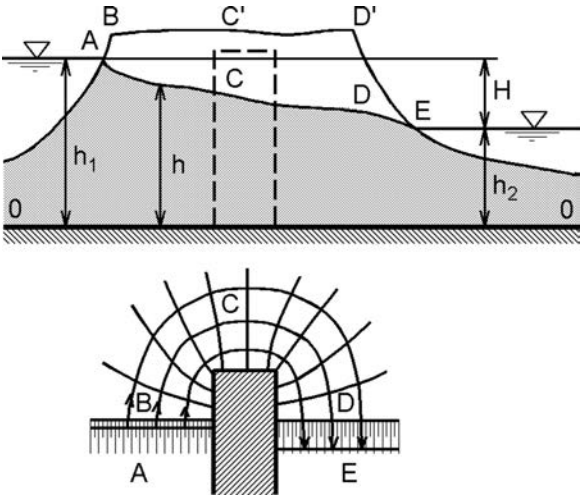

Figure 3.16 Schematic representation of lateral seepage.

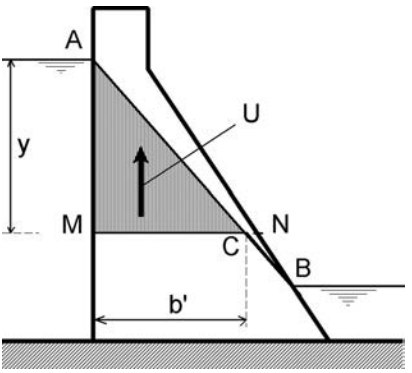

Figure 3.17 Seepage through a concrete dam.

water table. The construction of extended walls, impermeable diaphragm walls, and application of drainage systems achieves this.

In the joint zone between the concrete structure and the earth bank (Fig. 3.16), seepage of water occurs around the structure (lateral or side seepage), from the upstream face towards the downstream face. Initially, the level of the seepage water at the beginning was at the same elevation as the headwater, while moving around the structure gradually it goes down to the level of the tail water. Figure 3.16 shows the draw down curve (water table slope) of flow *ABCDE*. In a case where the water impermeable layer 0–0 is horizontal, and provided there is not an inflow of underground water from outside, the task can be solved in a classical way by applying Laplace's differential equation. In more complex cases, three-dimensional analysis is indispensable, by applying contemporary numerical methods (Desai et al., 1977).

3.10 SEEPAGE THROUGH THE BODY OF CONCRETE DAMS

Depending on the composition and grade, concrete used for the construction of concrete dams contains a certain percentage of pores, so that they lead to seepage of water in the course of servicing of the structure. This seepage has both a physical and a chemical influence on the concrete and it plays a noticeable role on the state of stresses and the stability of the dam (Fauchet et al., 1992). The particles of concrete are subjected to pressure from all sides as well as to uplift pressure in accordance with Archimedes' law. The pressure from all the sides upon the particles causes entirely insignificant deformations and is disregarded, while the action of uplift pressure in any section below the seepage line AB (Fig. 3.17) must be taken into consideration, also with a possible addition of the zone of capillary rising. For the horizontal section MN, the magnitude of the force of uplift pressure is determined by means of the diagram AMC, i.e. it amounts to

$$U = \frac{\alpha_2 y b' \gamma_w}{2} \tag{3.73}$$

in which the coefficient α_2 has an analogous meaning, the same as with the seepage in rock foundations. Investigations have stated that α_2 ranges from 0.43 to 0.95, in which it has smaller values at higher compressive stresses in concrete and vice versa, maximum values of α_2 should be taken for tensile stresses.

In order to reduce the harmful effect of seepage in the dam body, drainage galleries are built and located at various elevations in the vicinity of the upstream face, which are vertically connected one with another. These will be discussed in more detail in the chapter on gravity concrete dams. Also in use are vertical drainage holes in the upstream part of the dam body.

An efficient, although more expensive, measure is the construction of a waterproofing layer at the surface of the upstream face, made of special dense concrete, epoxy mortar, geomembrane, or other insulation material. Such a waterproofing layer reduces the penetration of water into the dam's body to a minimum.

This page intentionally left blank

Chapter 4

Forces and loadings on dams

4.1 FORCES AND LOADINGS ON DAMS IN GENERAL

Dams and appurtenant hydraulic structures, along with the foundation upon which they are built, must preserve their stability and invulnerability during various conditions, i.e. circumstances and possible cases of loadings occurring in the course of their construction and operation. Because of that, the form and dimensions of separate structural members, as well as the structure as a whole, are in close dependence upon the possible conditions of loading.

Dams and other hydraulic structures exhibit a complex response regarding their external and internal loadings and influences, which is in great contrast to their seemingly simple structural form. In fact, they are in most cases, asymmetric three-dimensional structures, constructed with materials exhibiting complex physical-mechanical properties. They are most often built on non-homogeneous anisotropic formations. This causes a complex interaction between the dam and its foundation, a response of both the structure and its foundation, especially when they are subjected to variable influences of the main loadings and to progressive saturation with water.

Some of the loadings are clearly defined in relation to their distribution, magnitude, and direction. Obvious examples are the self-weight of the structure and the hydrostatic pressure. The other main loadings, some of which are equally as significant as the two just quoted, are more difficult to define and can also be variable in the course of time. Examples might include but are not limited to pore pressure of the seepage water, and the thermal effect caused by hydration of the cement.

Loadings acting upon dams are usually divided into *primary*, *secondary*, and *exceptional loadings*. Such a classification has been made depending on the probability of occurrence and the relative significance of the loadings.

Primary loadings are of the utmost importance for all kinds of dams and other hydraulic structures. Here belong the forces from the *hydrostatic pressure* (most often horizontal; however, they can also be vertical – W_1, W_2, W_3 and W_4 in Fig. 4.1), the self-weight of the structure (G),determined through the appropriate volume weight of the structure and forces due to seepage (U_1 and U_2 in Fig. 4.1), which have already been discussed in Chapter 3. Here also belong forces due to seepage, appearing in the body of the dam and which are presented in the diagram.

Secondary loadings act on various kinds of dams, and have smaller magnitude than primary loadings, or else have a significant importance, but only for a certain

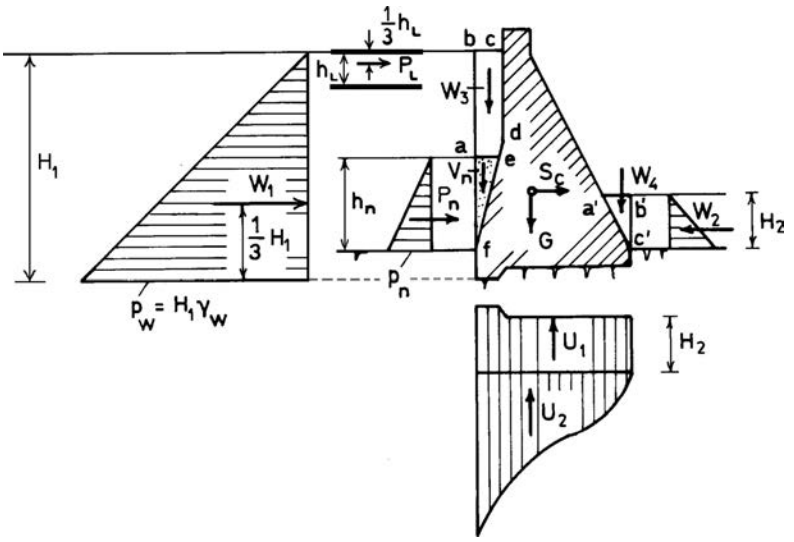

Figure 4.1 Forces acting on a concrete dam.

type of dam. Here belong the loadings from the deposit, i.e. sediment P_n, ice P_L, from the impact of the waves P_w, the thermal effect (in concrete dams, not illustrated in Fig. 4.1), the interaction effect (internal loading caused by the relative stiffness, as well as differential deformations of the dam and its foundation), and hydrostatic pressure in the banks (internal loading of seepage water on the rock mass in the banks, which is significant for arch dams).

Exceptional loadings have been so named on the basis of their low probability of occurrence. *Seismic forces* belong to this group – horizontal and vertical inertial forces from the mass of the dam and the impounded water of the storage lake, originating from seismic influence (Fig. 4.1 symbolically represents only the horizontal force of the mass of the dam S_c, having the point of force application at the centre of gravity).

During dimensioning and control calculations for embankment and concrete dams, depending on the specific conditions and the stage of design, appropriate loading combinations are selected for which there is a real probability that they would occur at the same time. It is obvious that some of the loadings exclude each other. For example, simultaneous action on the dam by both a force caused by ice and a force from wave impact is not possible.

In section 1.3, the influence of water on hydraulic structures was briefly explained, whereas the influence of seepage flow was examined in more detail in Chapter 3. In continuation, we shall dwell upon the subject of other forces and influences, which are significant in calculations for dams and other hydraulic structures.

Forces will be represented per one metre of the length of the dam; that is to say, they will be determined for a two-dimensional cross-section of the dam, having a unit thickness parallel to the axis of the dam. Two-dimensional treatment of problems in dams is a common practice since, in most cases, it yields sufficiently accurate results and

for practical purposes. At the same time, it is much simpler than the three-dimensional treatment, which is used in cases when the structure has an exceptional spatial character such as, for example, arch dams.

As an illustration of the calculation of the forces for a two-dimensional treatment of the problems, we shall present the determination of the force due to self-weight of the dam *G*,which is generally known in practice. That force acts at the centre of gravity of the cross-section of the dam *A*,and it amounts to:

$$G = \gamma \times A \times 1.0 \tag{4.1}$$

in which γ is the unit weight of the concrete; in the case in Figure 4.1, if there are no specific laboratory investigations and testing, it can be assumed as 23.5–24 kN/m^3.

4.2 FORCES FROM HYDROSTATIC AND HYDRODYNAMIC PRESSURE

It is rational to determine the forces of the hydrostatic and hydrodynamic pressure by breaking them up into horizontal and vertical components. Calculation of the upstream and downstream components of hydrostatic pressure W_1 and W_2 (Fig. 4.1) is carried out by means of appropriate diagrams composed of specific pressures at separate points. The vertical components W_3 and W_4 are equal to the weight of the water in the corresponding prism having unit length (*abcde* for W_3, i.e. $a'b'c'$ for W_4). The point at which forces converge is at the centre of gravity of the diagram, while the volume weight of water is $\gamma = 9.81$ kN/m^3 which, in practical calculations, could be taken to be 10 kN/m^3. Determination of the forces from uplift pressure, U_1 and U_2, caused by the seepage of water beneath the dam was discussed in Chapter 3. Water that percolates through certain members of the hydraulic structure causes forces that represent a sum of tangential and normal stresses. The tangential stresses are directed the same as the flow and they have a noteworthy value for only very high velocities of flow. Normal stresses are dependent on the weight of the liquid and on the changes in the direction of flow at the surge of the water flow on members of the structure. The force of hydrodynamic pressure upon a structure, i.e. member (for instance, upon a column), is determined from the formula:

$$W_d = \frac{C_x \Omega \rho v^2}{2} \tag{4.2}$$

where C_x is the coefficient of frontal resistance, dependent on the shape of the body through which water flows. If the jet hits the body and reflects back without the possibility of lateral circulation, then $C_x = 1$. On the contrary, it obtains adequately lower values, depending on the shape of the body that it hits, the direction of the circulation, etc. Or, it may be determined experimentally: Ω = area of the cross-section of the flow, $\rho = \gamma_w/g$ = density of water, and v = mean velocity of flow (Grishin et al., 1979).

The force of hydrodynamic pressure at the end of the flip bucket (Fig. 4.2a), reflection, i.e. buffer slab (Fig. 4.2b), or at a part of an intake tunnel under pressure

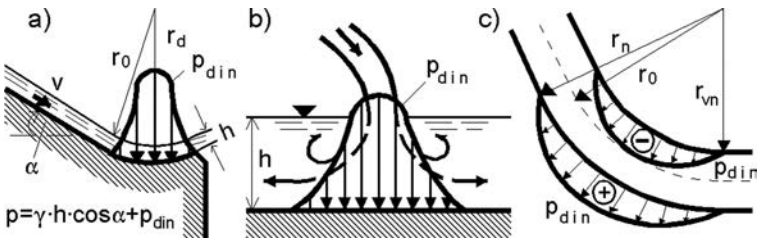

Figure 4.2 Diagrams of hydrodynamic components of pressure p_{din}, that water flow causes on the elements of a structure.

(Fig. 4.2c), is determined from the diagram of pressure. In determining the pressure at some point on the surface of the structure, the total pressure can be represented as the sum of the hydrostatic pressure and the pressure caused by the movement of the water:

$$p = p_{st} + p_{din} \tag{4.3}$$

Total pressure at a given moment can be determined as the sum of the mean value of the total pressure $\overline{p}$ in the course of time and the pulsating component p', so that it follows:

$$p = \overline{p} + p' = p_{st} + \overline{p}_{din} + p' \tag{4.4}$$

in which a dash over p denotes the average value.

The hydrodynamic pressure p_{din} and the pulsating component p' are represented by means of parts of the velocity pressure:

$$p_{din} = C_p \rho \frac{v^2}{2} \tag{4.5}$$

$$p' = \delta \rho \frac{v^2}{2} \tag{4.6}$$

where C_p is a coefficient of the pressure, and δ = coefficient of pulsation. The coefficient of pulsation is determined from formulae obtained in an analytical way, with semi-empirical formulae, or directly from laboratory experiments.

The magnitude of the pulsating component changes in the course of time from zero to extreme values, equal to the amplitude of pulsations of the pressure. In that way, the force of hydrodynamic pressure will be:

$$W_{din} = \overline{W}_{din} \pm W' = F(\overline{p}_{din} \pm p') \tag{4.7}$$

in which F = area of action of the force.

In a number of cases, in dimensioning the structures, it is not sufficient to know the average or maximum values of the hydrodynamic force, since hydrodynamic pressure acts with some frequency, which causes oscillations of the structure or of some of its

members that could lead to resonance (coincidence of the force frequency with the natural frequency of the system). Methods of calculation of the force of hydrodynamic pressure are not yet perfect which, in dimensioning, is compensated for by assuming a somewhat larger force than the real one. An incorrect assumption of hydrodynamic forces in calculations can lead to a failure of the structure, and that had already been happening in hydraulic practice.

4.3 INFLUENCE OF CAVITATION AND AERATION ON HYDRAULIC STRUCTURES

Cavitation in water-conveying structures occurs due to a local fall of pressure in the flow up to the critical value, when a phenomenon of cold 'boiling' turbulence, i.e. whirl, appears in the water. In cavitation, very tiny bubbles are formed that are filled with vapour. Their movement to places with higher pressure leads to a condensation of the vapour, repeated entrainment of bubbles into the fluid, with which it strikes into the hard boundaries of the structure. As a result, it leads to local damages of the material, a phenomenon that is called *cavitational erosion*, while the processes of development, transfer, and entrainment of bubbles into the fluid is called cavitation. In addition to erosion of the material, cavitation also causes changes in the character of the fluid's movement, loss of energy, vibrations, and noise. The time of entrainment of bubbles filled with vapour is very short (thousandth parts of a second) and is followed by the forming of an impact wave of high pressure, which causes erosion, deformations and, in some cases, destruction of the material of the water-conveying structure (Galjperin et al., 1977; Grishin et al., 1979).

As water flows with high velocity through water-conveying structures, cavitational erosion may appear at the overflow part of a concrete dam (1), at the structural member for energy dissipation (2, 3), at the sides of the lateral guide walls (4) (Fig. 4.3a), at the entrance (5), at the exit (6), in the lateral guide wall of closed water-conveying members under pressure (7) (Fig. 4.3b), and in parts of the water conveying structure behind the high pressure gates (8) (Fig. 4.3c).

If, in some part of the water-conveying structural member, there appears pressure that is higher than the critical one, then local reduction of pressure up to the critical pressure occurs as a result of the action of centrifugal forces or the deflection of the flow and at unevenness on the surface (Fig. 4.3d).

The danger of the appearance of cavitational erosion can be appraised through the coefficient of cavitation σ, which, at a given point, is determined from the expression:

$$\sigma = \frac{\dfrac{p_{abs}}{\gamma_w} - \dfrac{p_{cr}}{\gamma_w}}{\dfrac{v^2}{2g}} \tag{4.8}$$

in which p_{abs} = absolute pressure at a given point; p_{cr} = critical pressure of the water vapour, which depends on the fluid temperature and for water at 20°C it amounts to 3.25 kPa, and that corresponds to a water column of 0.24 m; and v = velocity of flow.

If $\sigma \leq \sigma_{cr}$, which could be the case at high velocities and low pressure at a considered point, then there is a danger of cavitation, while at $\sigma > \sigma_{cr}$ there is no such a

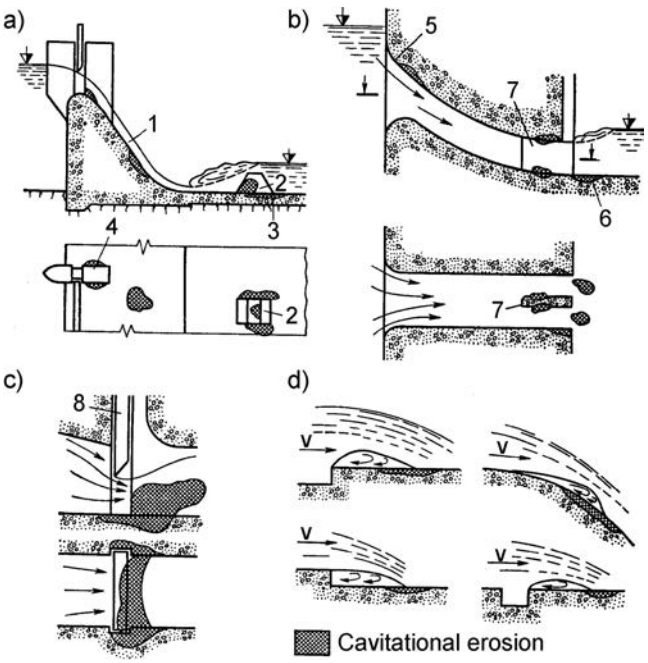

Figure 4.3 Cavitational erosion of water-conveying structures.

danger. The critical value of the coefficient of cavitation σ_{cr} is determined by means of laboratory investigations and testing. Depending on the form and dimensions of the unevenness, it can have a value ranging from 0 to 4.

In fighting cavitation, the following measuring are being employed: air feeding in the zones which are subjected to or susceptible to cavitation, construction of flat and smooth surfaces through which water flows, use of special resistant linings etc. (Abbasoglu & Okay, 1992; Galjperin et al., 1977). Regarding this significant question of cavitation in hydraulic structures and the actions for reducing damage that it causes, more attention will be paid in several places in Part Four of this book.

Aeration is a process in which a water stream flowing with a high velocity entrains air, which can evolve from various situations, for instance as a result of a demolition of the free water surface (Fig. 4.4a), during discharge below a gate in a closed water-conveying structural member (b), or at throwing out the jet into the atmosphere (c). Aeration causes a reduction in the permeability of water-conveying structural members, derangement of the stability of the flow, and it imposes the necessity for increasing the depth of the open flow, which requires a greater height of the lateral guide walls. For a determination of the flow parameters at which air entrainment begins, as well as for a determination of the quantity of the entrained air, empirical formulae are used.

Aeration of the flow can also cause certain positive consequences, such as in the case shown in Figure 4.4c when it contributes to dissipation of the energy of a thrown out jet. Aeration also plays a significant role in eliminating cavitation.

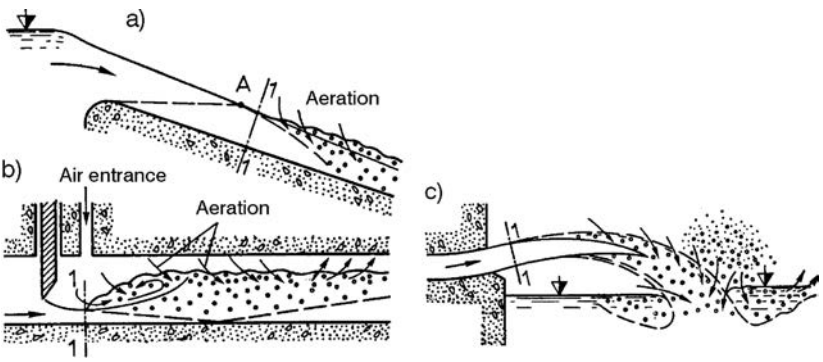

Figure 4.4 Aeration of the flow. (a) Beginning of turbulence; and (1–1) entrance section for air entrainment.

4.4 INFLUENCE FROM WAVES

Each derangement of water equilibrium causes waves on the surface of the water. Such a derangement can be caused by navigation vessels with their movements, underwater displacement in the earth's crust during earthquakes, high tides, etc. Waves are most often caused by wind blowing over the water surface. Waves caused by the wind have a visible influence on navigation, banks, and particularly on hydraulic structures, so that the attention paid to this problem is understandable. The way towards the correct solution of the problem was first traced by the great physicists, Kelvin and Helmholz, at the end of the last century and the beginning of this one.

Figure 4.5 illustrates and explains the elements of a wave caused by wind. The ratio of the wave height and its length (h_w/λ) is called the *steepness* of the wave, while the time interval in which the ridge of the wave displaces in a horizontal direction as much as is the length of the wave, is called the *period* of the wave.

Waves are classified as *progressive waves* and *standing waves*. In the case of standing waves, there is no change of parameters in a certain time period. They appear at a higher depth of water and as a frontal approach of regular waves toward a vertical wall.

The kind of wave and the values of its parameters (height h_w, period τ, length λ – Fig. 4.5) depend on the factors forming the wave, and those are wind velocity V and duration t, depth of the storage lake, i.e. the impounding reservoir H, length of front of the wind blowing L, and shape of the bank line. The length of the front of the wind blowing is the distance that is measured along a straight line from the bank to the structure, while the velocity of the wind in that direction is determined in accordance with a wind-rose (Fig. 4.6).

Depending on the degree of influence of the water depth Hon the kind of wave and on its parameters, the following zones are differentiated in the direction of the wind blowing from the storage lake space towards the bank (Fig. 4.7): *deep zone* (1), at $H > \lambda/2$, in which the bottom in practice does not influence the wave parameters, and *the shallow zone* (2), at $\lambda/2 > H > H_{cr}$, in which the depth has an influence on the

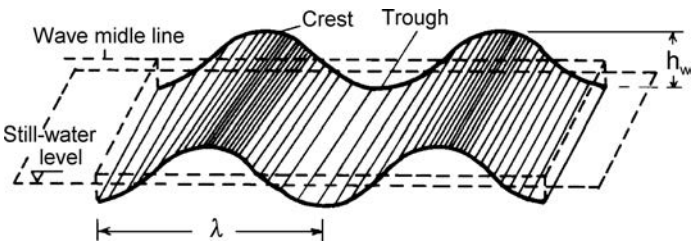

Figure 4.5 Parameters of a wave.

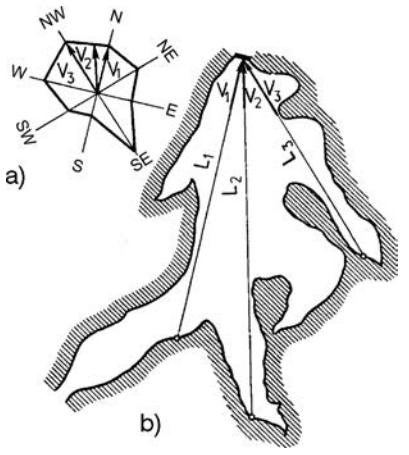

Figure 4.6 Wind-rose (a), and length of blowing of the wind (b).

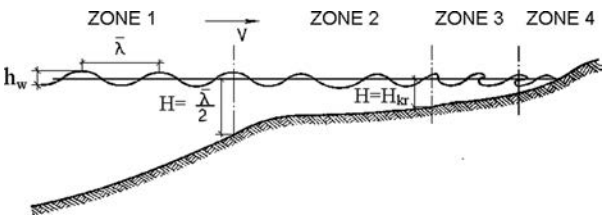

Figure 4.7 Division into zones according to the depth of water.

wave shape, as well as on its parameters; while at $H = H_{cr}$, a breaking-up of the wave commences; *zone of breaking up* (3), at $H < H_{cr}$, in which the waves are deformed and broken up; and *coastal zone* (4), in which the waves are definitely broken up and lap the shore (Grishin et al., 1979).

Since waves are formed in the deepest part of the storage lake, they are usually located in the deep zone. Regarding waves, the nature of wave action is different depending on the inclination of the slope. If it is steep, the wave does not break up but

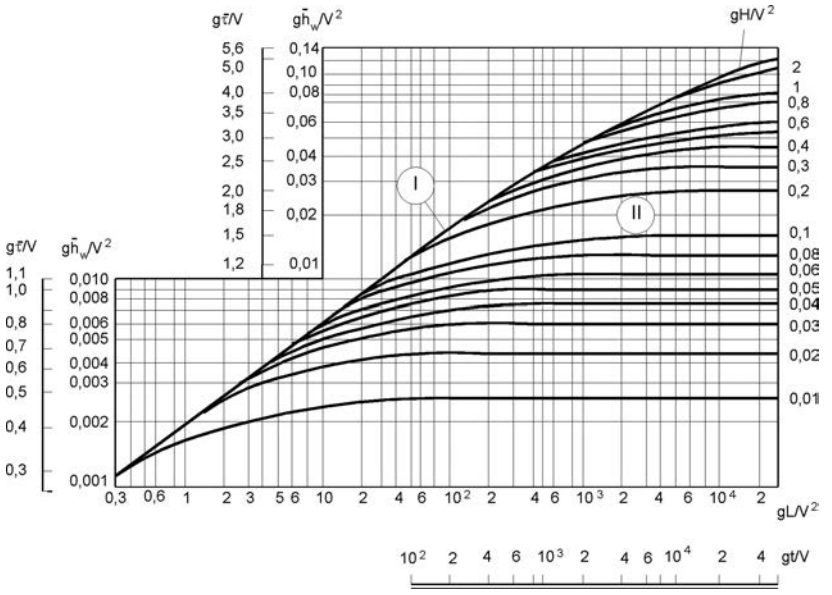

Figure 4.8 Diagrams for the determination of the parameters of waves in a deep zone (I) and a shallow zone (II) at (bottom) grade of $I \leq 0.001$ (according to Russian norms).

forms a *standing wave*, considerably higher than an *approaching wave*. In the case of moderate slopes, the wave is deformed and it crawls along the slope.

For the determination of the height of a wave, there are a number of empirical formulae. The best known is the formula of Stephenson, modified by Molitor:

$$h_w = 0.032\sqrt{VL} + 0.76 - 0.27\sqrt[4]{L} \quad (L < 32\,\text{km}) \tag{4.9}$$

$$h_w = 0.032\sqrt{VL} \quad (L > 32\,\text{km}) \tag{4.10}$$

in which V is the wind velocity and is introduced in km/h, L is the length of the front of blowing in km, while h_w is obtained in m. In the above calculations, as a governing value is taken the wind velocity at a height of 10 m above the water table, with a probability of occurrence in a certain period, dependent on the size and importance of the structure.

In the formula of Stephenson and Molitor the time duration of the wind (t), which is also an essential factor, is not taken into account.

Up until now, sufficiently accurate hydrodynamic and energy methods have not been discovered for a determination of wave parameters, by taking into consideration all of the factors that influence the formation of a wave; that is why various empirical relationships are in use, obtained through measurement data. Figure 4.8 presents diagrams from which it is possible to determine mean values of the height h_w and the period τ depending upon V (m/s), L (km), t (h) and H (m). These diagrams have been drawn by means of empirical formulae, derived by means of using the methods

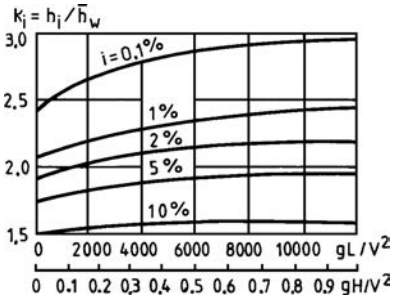

Figure 4.9 Diagram for determination of k_i (according to Russian norms).

of mathematical statistics, and the spectral theory of waves caused by wind. On the abscissa-axis on separate scales, there are applied the non-dimensional values gt/V and gL/V^2, in which g is the earth acceleration (m/s^2). On the ordinate-axis on separate scales, there are applied the non-dimensional values gh_w/V^2 and $\bar{g}\tau/V$. If for some non-dimensional values V, L and t, the value of gt/V is found to the left of the value gL/V^2, the wave develops, i.e. grows along with the increase in time duration of the wind. In such a case, the parameters of the wave are determined from the time duration of the wind, which is to say from the value gt/V. If the value of gt/V is situated to the right of the value of gL/V^2, then the wave is completely developed, so the increase in t does not cause an enlargement of the wave's dimensions. In such a case, the wave parameters are determined from the value of L. As soon as a governing scale on the abscissa-axis has been selected for a deep zone, the values gh_w/V^2 and $g\bar{\tau}/V$ will be determined along the envelope of the family of curves with determined values of gH/V^2, so that mean values of h_w and τ are obtained. The length of the wave is calculated from the expression:

$$\bar{\lambda} = \frac{g\bar{\tau}^2}{2\pi} \tag{4.11}$$

For a shallow zone having a bottom grade of $i \leq 0.001\, g\, h_w/V^2$, $g\bar{\tau}$ and corresponding values i, h_w and $\bar{\tau}$ can be determined from the curves according to the values of gH/V^2,while the length of the wave also in that case is determined from the formula (4.11). For a bottom grade larger than 0.001, it is necessary to also take into consideration the change in parameters of the wave owing to the decrease of depth, as well as the refraction of the wave (Grishin et al., 1979).

The height of the providing wave *i (%)* in the deep zone can be determined by multiplying the mean velocity of the wave h_w by the coefficient k_i, which can be obtained from the graph shown in Figure 4.9.

In calculating the stability and resistance of hydraulic structures, the height of waves is determined for a provision of 1–2%. In zones I and II, the waves coming frontally towards a vertical or almost vertical wall, convert into standing waves (waves

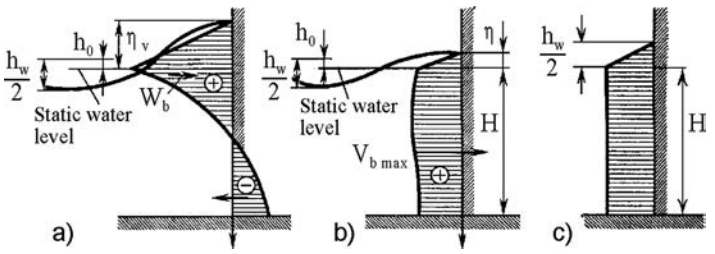

Figure 4.10 Diagrams of pressure for standing waves on a vertical wall.

which do not displace in the space), if it is in front of the structure $H > 1.5h_w$. If otherwise, in front of the wall at a section not shorter than 0.5λ, the depth is $H < H_{cr}$, then broken up waves act upon the wall (zone III).

Determination of the action of standing waves upon the structure consists of a calculation of the rising of the wave surface above the static water level, a calculation of the pressure of the waves on the structure, as well as a determination of the overturning moment caused by those forces. For rough calculations only, the force from wave impact can be taken as an additional horizontal static force acting along the line of the static level of the water, in accordance with the following empirical formula:

$$P_w = 2\gamma_w h_{ws}^2 \tag{4.12}$$

Calculation of the pressure from the waves at various points in water-retaining structures is carried out according to formulae that have been obtained through methods of hydromechanics. Figure 4.10 presents diagrams of the pressure of waves on a vertical wall. During a maximum rising of the water level, in the lower part of the wall there may occur a negative pressure caused by the waves (a). The diagram that corresponds to the maximum value of the force from the pressure of the wave has a positive sign along the entire height (b), whereas case (c) gives a schematic representation of the diagram.

For a calculation of the pressure of standing frontal waves on a vertical wall, one of the best methods and also one of the most complicated methods, is the method of Zagradskaya, which can be applied to both shallow zones and deep zones. The essentiality of the method is briefly presented in continuation (Grishin et al., 1979).

The maximum raising or lowering of the surface of the wave in a water-retaining structure above the static level is:

$$\eta_v = k_{\eta v} h_w \qquad \eta_n = -k_{\eta n} h_w \tag{4.13}$$

At the moment when a maximum force from wave pressure appears, the raising of the surface of the wave is:

$$\eta_p = k_{\eta p} h_w \tag{4.14}$$

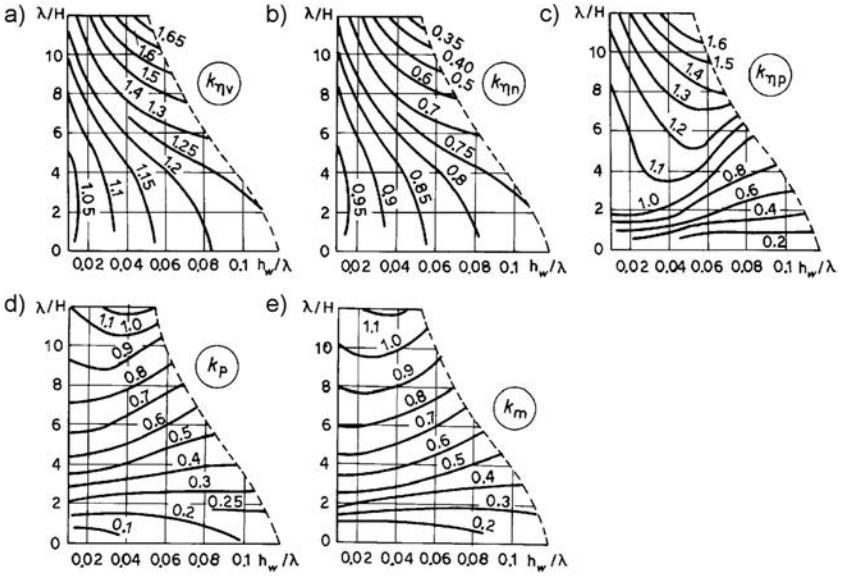

Figure 4.11 Diagrams for determination of the coefficient $k_i = f(\lambda/H, h_w/\lambda)$ in the formulae for calculation of the influence from waves on a vertical wall (Grishin et al., 1979).

while the maximum force from wave pressure at 1 metre length of the wall at $\eta = \eta_p$ is:

$$P_{max} = k_p \gamma_w h_w \left(H + \frac{h_w}{2} \right) \tag{4.15}$$

The moment from the force of wave pressure in relation to the bottom of the structure will be:

$$M_{max} = k_m \gamma_w h_w \left(\frac{h_w^2}{6} + \frac{h_w H}{2} + \frac{H^2}{2} \right) \tag{4.16}$$

The coefficients $k_{\eta v}, k_{\eta n}$, $k_{\eta p}$, k_p and k_m depend on the ratios h_w/λ and λ/H and are determined from the diagrams shown in Figure 4.11. The coefficients k_p and k_m, which appear in expressions (4.15) and (4.16) are coefficients for correction of the maximum force and moment, relating to the schematic diagram of pressure Fig. 4.10c.

For deep zones, the Mozhevitinov formula gives better results:

$$P_w = \frac{1}{2} \gamma_w h_w \left(\frac{\lambda}{\pi} + \frac{h_0}{2} \right) \tag{4.17}$$

in which $h_0 = \pi h_w^2/\lambda$. The distance of force P_w from the static level of the water is obtained from the expression:

$$y_c = \frac{\lambda}{2\pi} - \frac{3}{8} h_w \tag{4.18}$$

4.5 INFLUENCE OF ICE AND WATER SEDIMENT

Ice can cause a static and dynamic effect on the hydraulic structure. Static influence originates from the temperature expansion of the ice cover in front of the structure, as well as from the heaping of an ice field on the structure. In addition to this, a vertical force can also act on the structure, which is directed downwards or upwards from the ice cover stuck to the structure, at a variety of water levels. Dynamic pressure originates at the impact of moving ice on the hydraulic structure.

Mutual action of the ice and the hydraulic structure is a very complex phenomenon, which up to now has not been sufficiently and accurately clarified. That is why, in determining the pressure of the ice, empirical expressions and data are obtained from observations of existing structures.

Force from the static pressure of ice. During freezing, water expands its volume by 9%; however, during formation, the ice field causes an insignificant pressure. A further decrease in air temperature leads to a lowering of the ice temperature and a decrease in its volume, while a rise in temperature leads to expansion, the same as with every other solid body. Pressure of the ice upon the structure occurs at moments when the shore from the opposite side opposes expansion of the ice field. The ice force in this case can be calculated by means of the expression:

$$P_{\mathrm{L}} = k_{\mathrm{L}} b h_{\mathrm{L}} p \tag{4.19}$$

where b = width of the contact between ice and the structure; h_{L} = maximum depth of ice with a probability of occurrence once in 100 years; k_{L} = coefficient by means of which one could decrease the force of ice pressure versus the increase of the length l of the ice cover from the structure up to the opposite shore, given in Table 4.1; p = specific pressure of the ice which, depending on climatic conditions, could be taken as 0.15–0.30 MPa.

The force from the ice field that is heaped next to the hydraulic structure under the effect of wind, water flow below the ice, as well as a consequence of the inclination of the flow, is determined according to the formula (Grishin et al., 1979):

$$P_{\mathrm{l}} = 0.01\left(0.5v^2 + 50\frac{h_{\mathrm{i}}}{l}v^2 + 920h_{\mathrm{i}}i + 0.002V^2\right)\omega \quad [\mathrm{kN}] \tag{4.20}$$

in which v = velocity of flow of water below the ice (m/s); V = velocity of wind (m/s); i = inclination of the flow surface; h_{i} = thickness of the ice field, equal to $0.8h_{\mathrm{L}}$, in meters; ω = area of the ice field.

The expression in parentheses in equation (4.20) represents the following four forces relating to a unit volume of the ice field: frictional force of the flow from the

Table 4.1 Values of coefficient k_{L}.

Length of ice cover l (m)	*50*	*70*	*90*	*120*	*≥150*
k_{L}	1	0.9	0.8	0.7	0.6

bottom surface of the field, hydrodynamic pressure at the edge of the field, a force caused by the action of the inclination of the flow surface, and a frictional force of the air at the upper surface of the ice cover (Grishin et al., 1979).

It is assumed that the above-described horizontal forces from the pressure of the ice act at a distance 0.3 from the thickness of the ice below the water level.

Pressure from water sediment. In the upper courses of rivers dammed with lower dams, there occurs a normal precipitation of coarse-grained deposits (sand and gravel), while in the case of deep storage lakes fine-grained deposit (silt particles) are precipitated near the dam. The diagram of pressure from the deposit has a triangular form (Fig. 4.1) and, at a thickness of the layer h_n,the specific horizontal pressure will be:

$$p_n = \gamma'_n h_n k_n \tag{4.21}$$

in which k_n = coefficient of pressure from the deposit, and γ_n = volume weight of deposit in a saturated state.

The coefficient of pressure depends on the properties of the deposit, as well as on the possibilities of displacement of the structure under the loading. For loose sand, a coefficient k_n can be taken as 0.64; for moderately compacted sand, 0.52; for compacted sand, 0.49; and for clay, 0.67–1.

Coulomb's expression can also be applied:

$$k_n = \tan^2\left(45 - \frac{\varphi}{2}\right) \tag{4.22}$$

in which φ = angle of internal friction of the sediment material. In that case, the total horizontal force from the pressure of the deposit will be:

$$P_n = 0.5\gamma'_n h_n^2 \tan^2\left(45 - \frac{\varphi}{2}\right) \tag{4.23}$$

The vertical component of the force from river deposit V_n is equal to the weight of the volume of the earth deposit *aef* in its unsaturated state (Fig. 4.1).

In a flow with high velocity and in the case of a larger quantity of tractioned deposit, it is possible that a damaging of the surface part of particular members of the hydraulic structures may occur, owing to the abrasion action of the deposit material, especially of sand and gravel. Because of that, it is necessary to anticipate protection of the surfaces, which are potentially susceptible to abrasion. Such protection is offered by means of a surface layer of special hard concrete, or else by means of slabs made of hard stone mineral, steel, or reinforced concrete.

The deposit material also has a harmful abrasion effect upon the discharge parts of siphon pipes and turbines. Noticeable damage can arise during a shorter or longer period of operation, depending on the quantity and mineral composition of the deposit.

4.6 SEISMIC FORCES

Seismic influences caused by earthquakes, are an important element in the design and determination of the stability of structures. An earthquake can be caused by various

phenomena, i.e. events (explosions, volcanic activities, failure or cave-in of the vaults of caves and caverns); however, from an engineering point of view, earthquakes of *tectonic origin* are the most significant ones, and they can encompass a large territory and release enormous energy.

Even the ancient philosophers were interested in and dealt with the causes of the occurrence of earthquakes. Nevertheless, up to now this interesting problem has not been completely explained and clarified. The ancient Greek philosopher Aristotle considered the cause of earthquakes to be the movement of the 'spirit' (πνευμα) of solid matter that goes out from the bosom of the Earth. He had seen proof of his hypothesis in the volcanic activities that were frequent on the Balkans Peninsula, as well as on adjacent islands – a zone in which, as well, there had been and still are occurring earthquakes.

Today, the most widespread theory is that earthquakes appear due to displacement of the plates of which the Earth's crust consists, especially when it comes to slippage along geological faults. Most earthquakes originate at a depth of up to 30 km, but there have been earthquakes registered at a depth larger than 600 km, in which there are no conditions for geological faults. Some authors (Bell, 1980) divide earthquakes into *shallow earthquakes,* at a depth of up to 70 km; *middle deep earthquakes,* at a depth of 70–300 km; and *deep earthquakes,* at depths of 300–700 km beneath the Earth's surface.

Severe earthquakes cause impact waves that spread out over the earth. The point in the Earth's crust from which the first seismic waves arising from an earthquake originate is called the *hypocentre* (also used are the expressions *focus, seismic origin, centre)* of the earthquake. The *epicentre* (or *epifocus)* is a vertical projection of the hypocentre on the surface of the Earth.

In the absence of data, obtained through measurements with instruments, the position of the epicentre is often established on the basis of observed and recorded damage, as a point at which the earthquake shock has been the most intensive. In many cases, this point does not completely coincide with the epicentre as determined by means of instruments. The expression *epicentral distance* is used as a term for the distance from a certain point, called a *station,* to the epicentre of the earthquake.

The *magnitude* of an earthquake is a measure of released energy, while its intensity is a measure of the local destructive power of the earthquake. This means that the magnitude has only one value and it relates to the hypocentre of the earthquake, while the intensity is a variable value, dependent upon the distance from the station. For expressing the magnitude (*M*), the Richter *scale,* according to which the strongest recorded earthquake had 8.9 degrees, is most often used. For expressing the intensity, there are a number of scales and almost all of them are rather arbitrary and subjective ones. The most widespread is the use of the *Mercalli scale,* which has twelve degrees (for more details, see Chapter 9).

The intensity of vibrations in shallow earthquakes rapidly declines as they move away from the epicentre, while the shocks from deep earthquakes spread over a large territory but are felt with weaker intensity. The main shocks of the earthquake, in many cases, are indicated and foretold by preliminary weaker shocks, while in the post-earthquake period they are followed by hundreds or even thousands of 'calming down' or 'tranquillising' earthquake shocks.

Table 4.2 Values of the seismic acceleration τ [mm/s^2].

Intensity of earthquake	VII	VIII	IX
Type of foundation			
Weak – clay, soft marls, heterogeneous	300	600	1200
Medium – homogeneous sand, preconsolidated clayey and marly foundations, moderately heterogeneous clayey-sandy-gravel foundations	250	500	1000
Good – hard and firm rock and homogeneous gravel	200	400	800

The state of stress-deformations – and that also relates to the stability of hydraulic structures during an earthquake – depends on the nature of the movement of the foundation, structure of the work, and its *inertial, stiffness,* and *damping* properties. The most important parameters for calculation of structures subject to seismic forces are acceleration, displacement, and the period of oscillating of the foundation. The assigning of these parameters is beset with considerable difficulties since seismic oscillations of the earth are of a complex nature. Ground oscillations, at a certain point, depend on numerous factors hard to calculate, such as the energy mechanism of the earthquake, the distance and depth of the epicentre, the spectral composition and direction of ripple, and composition and structural features of the corresponding part of the earth's crust through which the seismic waves pass (Newmark & Rosenblueth, 1971).

The basic characteristic of earthquakes that is used for the dimensioning of structures is the *coefficient of seismicity* k_c, which is assigned through the *coefficient of seismic acceleration of the foundation* τ and the Earth's acceleration g; that is to say:

$$k_c = \frac{\tau}{g} \tag{4.24}$$

Within the range of intensities from degree VII to degree IX according to the Mercalli scale that are of practical meaning in the seismic designing of structures, values of the seismic acceleration τ [mm/s^2] can be taken from Table 4.2.

Data on the maximum intensity of an earthquake, which could occur within an area of the anticipated hydraulic structure, are taken from the appropriate seismologic maps.

Owing to the quoted difficulties in determining parameters for dimensioning the structures subjected to seismic effects, what is called the *pseudostatic method,* is still in significant use (Leshchinsky & San, 1994), while *dynamic methods,* which have experienced a speeded up development in the last years, are used for more significant structures and mainly for the final stage of their design.

The seismic force, assumed to be a static one, can be either horizontal or vertical. In designing hydraulic structures, only the horizontal component is taken into consideration. Exceptions are structures in which the state of stresses depends on vertical displacements, such as for instance at some types of arch dams. The vertical component is considered, along with the horizontal one, in the checkup of the stability of the structure.

Forces caused by an earthquake fall within the group of *inertial forces;* that is to say, they are proportional to the mass of the structure G/g, where G is the weight of the structure. In its simplest form, the seismic force S_c can be obtained from the expression:

$$S_c = k_c G \tag{4.25}$$

The force S_c acts at the centre of gravity of the structure (or structural member), whereas its direction and course can be arbitrary; however, in hydraulic structures they are chosen so as to give the most unfavourable case of loading. Regarding dams, it is the horizontal direction with a course towards the downstream face at a filled storage lake, and towards the upstream face in the case of an empty storage lake, as well as the vertical direction with a course from below upwards.

The expression (4.25) can be made even more realistic if we take into consideration the influence of the foundation and the height of the dam upon the inertial force through the coefficients α, i.e. β, in which case it will be:

$$S_c = k_c \alpha \beta G \tag{4.26}$$

For foundations composed of rock (bedrock) it could be taken as $\alpha = 0.5$; for semi-rock minerals, 0.75; for compacted clays and coarse-grained soils, 1.0; for dry sand, 1.75; and for sand saturated with water and for plastic clay, 2.0. The coefficient β ranges from 1.0, for smaller structures and low dams, up to 2.0 for high dams, in which it could be taken as being variable along the height (1.0 near the foundation and 2.0 at the crest).

During the seismic effect there comes about an oscillation, not only of the hydraulic structure, but also of the nearby water medium, which acts upon the structure with what is called hydroseismic *pressure*. Its magnitude depends not only on the parameters for oscillation of the structure, but also on the configuration of the storage lake (the shape of cross-sections and the foundation, and length of any ambient extension(s)). The phenomenon of the interactive action of the structure and the adjacent water ambience is very complex and it has not yet been sufficiently clarified, so that in a number of cases simplified methods are used. Within the framework of the static theory, such a solution is given by Westergaard for concrete dams having a vertical upstream face, so that under such conditions the diagram of the force has the shape of a parabola (Fig. 4.12a), represented by the equation (Golzé, 1977; Shuljman, 1976):

$$x = \frac{\frac{7}{8}\sqrt{H_1 y}}{1 - 3.38\left(\frac{H_1}{1000}\right)^2} \tag{4.27}$$

whereas the pressure at any point will be:

$$p_c = k_c \gamma_w \frac{\frac{7}{8}\sqrt{H_1 y}}{1 - 3.38\left(\frac{H_1}{1000}\right)^2} \tag{4.28}$$

The total seismic force from the hydrodynamic pressure of the water acting at a distance $0.43H_1$ from the foundation, is equal to the area of the diagram and can be calculated from the expression:

$$S_w = 0.54 k_c \gamma_w H_1^2 \tag{4.29}$$

In cases when there is an inclined upstream face of the concrete dam, the hydrodynamic pressure at separate points at a depth y can be calculated from the expression (Fig. 4.12b):

$$p_c = C k_c \gamma_w y \tag{4.30}$$

where C is a non-dimensional coefficient, which can be obtained from the expression:

$$C = \frac{C_m}{2}\left[\frac{y}{H_1}\left(2 - \frac{y}{H_1}\right) + \sqrt{\frac{y}{H_1}\left(2 - \frac{y}{H_1}\right)}\right] \tag{4.31}$$

in which C_m represents the maximum value of C for a given inclination of the upstream face of the dam and can be obtained from diagrams given in Figure 4.13.

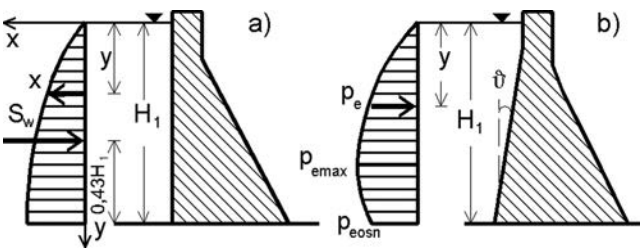

Figure 4.12 Seismic force caused by water.

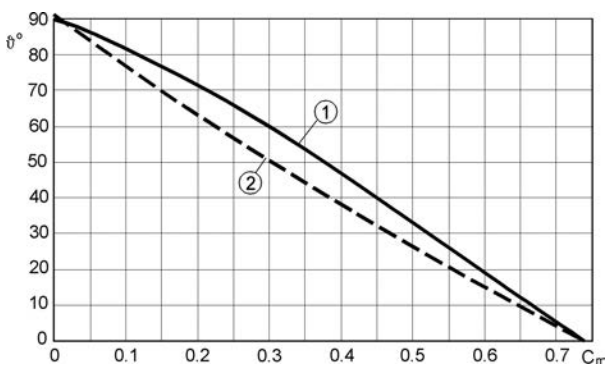

Figure 4.13 Diagram for determination of the coefficient C_m (after Golzé, 1977). (1) Maximum values of C_m; (2) values of C_m in the dam foundation.

4.7 TEMPERATURE EFFECTS

Temperature effects play a significant role in hydraulic structures, especially for dams which, in the course of their construction and operation, partially or as a whole, are permanently exposed to temperature variations. These variations might arise from variations of the temperature in the adjacent environment (air, water); artificial cooling or heating, from release of heat during settling of the concrete; breaking through of heat from the earth's foundation, etc.

Heat and temperature variations have a negative influence on hydraulic structures. They complicate and make more expensive their construction and operation, so that these factors should be carefully analysed at the initial stage of design.

4.7.1 Temperature effects on embankment dams

Regarding embankment dams and dykes made of local earth material, low, as well as high temperatures, can have a negative influence.

Low temperatures cause a freezing of earth materials, the consequence of which could be an occurrence of cracks and/or fractures in those materials, as well as a lowering of their strength at defrosting, i.e. thawing. Freezing of earth materials in the downstream part of an embankment dam could raise the seepage line from position 1 to position 2 (Fig. 4.14), owing to eliminating drainage from its function, which would be hazardous to the stability of the downstream slope provided there is fast defrosting in the spring period. In order to prevent this, drainage should be designed so as to enable the seepage line along its entire length to be below the depth of freezing of the earth materials (see Chapter 10).

In the case of embankment dams having a facing made of artificial materials, temperature variations have a significant influence on the part of the facing above the water level or on the entire facing, prior to filling up the impounding reservoir. At the surface of the facing during any summer period, temperatures could reach even higher than 60°C, which, to a large or small extent, has a harmful influence upon all kinds of facings. For instance, asphalt facings soften at high temperatures and have a reduced resistance to flow (creep) along the slope, whereas at low temperatures they become stiff and exhibit a low resistance against creation of cracks and/or fractures. During the design process, there should be endeavours to compose such an asphalt compound as would be resistant to temperature effects; however, it is also possible to use various protections in the form of thermal insulation. Among the most efficient ones is a coating of white paint, which reflects sunbeams. This has been shown successful during experiments on restoration of the asphalt facing of the El Grib dam (Algeria), constructed before World War II (Fig. 4.15).

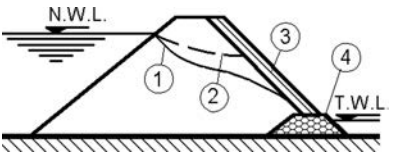

Figure 4.14 Rising of the seepage line at freezing of the downstream slope. (1) Seepage line prior to freezing, and (2) after freezing; (3) layer of frozen earth; (4) drainage.

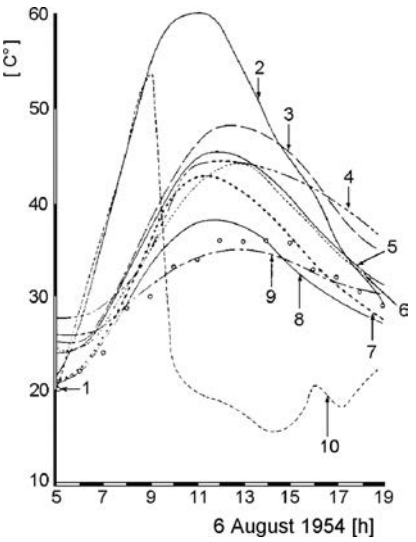

Figure 4.15 Experiments on selecting a thermal insulation layer at El Grib dam (after Van Asbeck, 1962). Temperature of: (1) air in the shade; (2) unprotected asphalt surface; (3) 6 cm below an unprotected surface; (4) 12 cm below an unprotected asphalt surface; (5) 3 cm below the surface of porous concrete; (6) 3 cm below the surface of porous concrete with asbestos fibres; (7) 2.5 cm below the surface of a concrete layer; (8) below synthetic resin – 4 mm; (9) coating of white paint; (10) a surface sprinkled with water.

4.7.2 Temperature effects on concrete structures

From the theory of structures, it is known that in the case of thin members of statically determinate structures, temperature variations do not cause stresses, but only displacements, while in the case of statically indeterminate structures there occur both stresses and displacements. At the same time, in the case of thin members, the non-uniformity of temperature variations in the cross-section is not taken into consideration, and those temperature variations, in practice, follow variations of the outdoor temperature.

Massive non-reinforced blocks behave in a different way, and they are used during the construction of gravity dams. The temperature of the concrete mixture built in to the block usually differs from the temperature of the nearby air, which is lower in winter and higher in summer. This difference further varies due to the exothermic heating of the concrete during simultaneous cooling of the block's surface, a situation that is retarded by the construction of adjacent blocks. The entire process is increasingly complicated owing to the natural variation of the outdoor temperature or by undertaking measures for artificial cooling of the structure.

Following the construction of a structure, the temperature regime is dictated from ten variations of the outside temperature and working conditions of the structure. Permanent variations of the temperature also cause permanent changes in the state of stresses and deformations in a massive concrete structure. Regarding dams, excessive stresses can cause cracks in concrete, while deformations can damage sealants in joints

between blocks and derange the normal operation of separate structural members, even of the dam as a whole. This imposes the necessity that for such structures during the design stage the temperature regime be defined, and measures be taken to modify the influence of temperature variations, deformations, and stresses caused by them and determined by means of the theory of thermoelasticity. Recently such calculations have been carried out by means of contemporary numerical methods. There are also endeavours, with the invention of new materials and a new construction technology of placement, to decrease thermal problems associated with concrete dams. These questions are dealt with in more detail in the chapters devoted to concrete dams, in Part Three of this book.

This page intentionally left blank

Chapter 5

Designing hydraulic structures

5.1 BASIC STAGES IN THE PROCESS OF THE CREATION AND USE OF HYDRAULIC STRUCTURES

The process of creation and use of hydraulic structures, especially dams, is long, troublesome, painstaking, and costly. What precedes this process is a *water utilization design* for the hydraulic system or the hydraulic scheme to which the dam, or the hydraulic structure that is to be built, belongs. This phase is highly significant, since the water economies are being set increasingly more complex tasks, caused by increasingly large demands made on water resources as a result of increased consumption of water, reduction of available waters, as well as increased demands in relation to the efficiency of hydraulic systems.

A water utilization design helps in selecting a solution to the water utilization problem, in which case we adopt parameters and configurations of the hydraulic system or scheme (number of storage reservoirs, size of available storage capacity, characteristic elevations of the water level, installed capacity, areas for irrigation, etc.), with a simultaneous determination of the regime of utilization of water in the service period. The water utilization design is a very important phase in the realization of a hydraulic system and its separate parts, since by having such a design, one can define the strategic orientation – where possible mistakes cannot in practice be eliminated later on – irrespective of the quality of the hydraulic part of the design.

Following elaboration of the water utilization design, we come to the realization of the individual structures (dam and/or appurtenant hydraulic structures), a process, which, generally speaking, can be divided into four stages:

1. *Investigation.* In the first stage, it is necessary to obtain all the necessary data on natural conditions of the region and the place of the more immediate location of the structure. Here, there belongs data on the topography of the terrain, its geological structure, seismicity of the ground, hydrological conditions of the catchment area and the watercourse, climatic particularities of the region, availability of local materials, economic and water utilization conditions and needs, etc.
2. *Design.* In this stage, on the basis of the design task and the requirements that have been set up with the water utilization assignment for the future water regime of the structure, and taking into consideration the data obtained from investigations, we establish the dimensions of the structure and the structural elements,

Figure 5.1 Kozyak dam (Macedonia) – early construction stage.

then work out the necessary plans and schemes, determine the methods of construction, as well as the necessary plant and equipment. Thus, it is possible to obtain the economic indicators for a structure that has been anticipated for construction.

3. *Construction (Fig. 5.1).* The third stage encompasses all the works concerning the organization of the construction of the structures, as well as the mechanization of the process of execution of the works. Then comes the construction of the structures, dismantling of the construction plant and equipment and of the temporary structures that have served in the course of the construction and, in the end, handing over the structure for operation.
4. *Operation/Service (Fig. 5.2).* The last stage encompasses all the works regarding the operation, i.e. service of the structure – management of its operation, supervision of the fulfilment of the requirements specified by the design, as well as the condition of the structure and equipment. What follows is an analysis of results from surveillance (monitoring, i.e. observation) measurements, periodic new analyses of static and dynamic stability, employment of the most sophisticated methods and newly-acquired parameters, checking the rate of flow, i.e. capacity of the overflow structures on the basis of new knowledge and criteria, regular maintenance, and capital overhaul of the structure.

This book, in relevant chapters, considers the most significant aspects of all four cited stages while the second one – design – will be analysed in more detail here.

Figure 5.2 Globochica dam (Macedonia), some 20 years after its construction (service period).

5.2 INVESTIGATION FOR DESIGN AND CONSTRUCTION OF HYDRAULIC STRUCTURES

Prior to designing hydraulic structures, it is essential to carry out the following investigative works:

- Topographic investigation works, in which, on the basis of geodetic measurements a locality plan is worked out and data for drawing various profiles and sections in the zone of the structure and the storage reservoir space, is obtained. By means of the topographic investigation works one can obtain:

  a) General regional maps, scaled 1:200,000–1:100,000, with contour lines at a vertical (contour) interval of 20 to 40 m, which serve for plotting the entire catchment area of the watercourse on which the hydraulic structures are located; nowadays, for most countries in the world, there are also available satellite photographs scaled 1:250,000;
  b) Ordinance maps 1:50,000–1:25,000, with contours at a vertical contour interval of 10 m, which serve for setting up the solutions, a survey of the entire area of the storage reservoir for comprehension of the general location of the structures;

c) Levelling (elevation network) and a tachometrically-surveyed longitudinal profile of the watercourse, in a convenient distorted scale (different for heights and lengths), to serve as a representation of the position of the structures in longitudinal and height respect;
d) Geodetic location plans scaled 1:200–1:2500, with a contour line at 1 to 2 m, to represent the layout solutions of the structures in various phases of the design; and
e) Detailed tachometric survey photographs of longitudinal and cross-profiles in the zone of the most important structures, scaled 1:100–1:200. In the case of a larger storage reservoir, it is also desirable to have air survey photographs of the entire storage reservoir space in a scale 1:10,000. One should take into consideration that photogrammetric photographs are not always appropriate when it is a question of steep terrain, with points and spots having considerable elevation differences. General regional maps and ordinance maps are worked out for the whole territory of the country and they can be obtained for use from authorized institutions.

- *Engineering-geological and hydro-geological investigation works*, the aim of which is to throw light on the geological structure of the region of a hydraulic scheme, the physical and mechanical properties of its minerals, hydro-geological conditions, and to determine occurrences of natural materials for construction of the structures. These investigative works can commence with the analysis and interpretation of satellite photographs, which enable a wide view of the project location. Such photographs can yield an indication of the geological formations in the region, the position of geological boundaries and faults, as well as give a global presentation of the relationship of the regional geology and the forms of the ground, drainage, vegetation and utilization of the land. These criteria can be beneficial in planning approach roads to and in the zone of the structures, discovering potential borrowing pits of local materials for construction, and for appraisal of filling the storage reservoir with sediment. For each design, it is necessary to create high-quality geological maps, for which purpose one can use all existing data and investigations and also undertake special investigations by means of intermediary and direct methods. Intermediary methods include *geophysical investigations* (seismic refraction, seismic reflection, electrical resistivity, etc.), while direct methods are conducted through the digging of wells, trenches, and manholes, as well as deep borings, which all facilitate investigations *in situ* and sampling specimens for laboratory testing. These issues will be elaborated in more detail in relevant places in this book.
- *Geotechnical investigation works*, by means of which we can determine the elastic and deformational characteristics of the rock materials at the dam site and in the foundations of some more significant structures, as well as of the rock materials which will be used for construction of the dam's body; they are effectuated through field and laboratory investigations. They should be carried out very carefully, since they yield invaluable data for the performance of the foundation below the structures of the hydraulic scheme and the body of earth–rock dams and rockfill dams (Vaughan et al., 1991). When it is a question of the foundation, geotechnical investigations are particularly significant in constructing arch dams

and other kinds of concrete dams, as well as in the cases of larger embankment dams.

- *Geomechanical investigation works*, which determine the characteristics of non-rock (soil) materials in the foundation, as well as in the borrow pits for local earth materials. For their realization, field and laboratory equipment has been developed, as well as precisely described methods and procedures. In cases of earthfill and earth–rock dams, it is also necessary to perform geomechanical investigations for defining the properties of non-rock (soil) foundations.
- *Hydrological investigation works*, which are useful for studying the hydrological regime of a watercourse planned for utilization, in which we can determine flows of the watercourse and their variation, the regime of flow in different seasons, and processes in the riverbed. At the same time, an investigation is performed of the climatic regime of the area in order to obtain data on the atmospheric precipitation (rainfall), air temperature and its variations, direction and duration of winds, etc. These are very important, since to a large extent, depending on them is the operation and profitability of the planned hydraulic scheme.
- *Constructional output investigation works*, which make it possible to obtain data that are necessary in the realization of the construction works, for instance, for conditions leading to connection of the construction site with the existing traffic network, for sources of supply of construction materials, water and electric power, conditions for settling down, supply and the living accommodation of workers, etc.
- *Other investigation works*, which help clarify the existing water utilization of the considered water resource. Then comes abundance of the river with fish and conditions for fishing, kinds of soil and vegetation in the region in which the hydraulic structure might be set up, as well as basic economic branches (industries) in the zone in which the planned hydraulic scheme will have an influence.

In a large number of practical cases, a need arises for further extending of the investigation, such as, with physical–chemical, radioactive and bacteriological investigation of the water, establishing the risk to the storage reservoir regarding erosion and sediment, hydraulic model investigations, statically-dynamic model investigations, etc.

The scope of necessary investigative works varies depending on the size and importance of a hydraulic scheme, i.e. on the structure, the design phase for which the investigative works are carried out, the size of the catchment area and future storage space, the character and structure of the ground of the future impounding reservoir, the geological structure of the dam site, the possible type of planned dam, and its appurtenant structures.

On the scope of investigative works that will be undertaken, an influence can also be the degree of previous investigation of the location for the needs of the subject structure, or else for some other designs, accomplished or not. In utilizing old data, it is necessary to verify its credibility, the way it has been obtained, as well as the methods applied. Site investigative works are, as a rule, expensive; however, when it is a question of hydraulic schemes with a dam, most often they do not extend to a significant part of the total investment expenditure. On the other hand, mistakes made in investigations and their insufficient scope, can lead to considerable failures in the realization of a hydraulic scheme with a dam, and that is a sufficient reason for not to save on them without an especially convincing reason.

5.3 CONTENTS OF THE HYDRAULIC DESIGN AND DESIGN PHASES

On the basis of data obtained from investigations and the objectives that have to be accomplished with a water utilization structure, in the second stage of the realization of the structure, we move to work out a *design*, which implies a variety of well-thought-over and coordinated activities such as would lead to the realization of the specific concept. The following major constituent elements come into the design for a hydraulic scheme with a dam:

- Elaboration and definition of the future hydrological and water utilization regime of the hydraulic structure, which includes determination of characteristic elevations of the tail-water and headwater, determination of area of submersion, and volume of the impounding reservoir, etc.;
- Selection of types, schematic structure of the works and materials for their construction and equipping, way of founding and structural interventions in the foundation and, finally, constructing the works;
- Hydraulic dimensioning of the structures and seepage calculations for the water-tight elements, structure, and foundation;
- Static and dynamic dimensioning and control, which verify the strength and stability of the designed structures and a foundation for the effects of all possible forces;
- Execution of solution and selection of surveillance instrumentation (monitoring) of the structure in the course of construction and operation;
- Elaboration of methods for organization of works with a time schedule, i.e. program and progress schedule, period of completion of structures, etc.;
- Preparation of technical specifications for construction and control of quality of materials and their placement;
- Preparation of Bill of Quantities and Estimate for the works along with determination of the total cost and the technical-economical indicators for the structure.

In addition, in cases of very large and significant structures, especially if they are not executed in the most favourable ground conditions – and that happens often in hydraulic engineering – within the framework of the design it is also possible to include a part of the scientific and investigative works for proving the justification of the selected structure and dimensions of the structure if, by means of the usual methods and existing theories, it cannot be proved. Here also belong model investigations of structures (hydraulic, seepage, static, and dynamic).

The process of designing a hydraulic structure is usually carried out in three phases. The first phase consists of preparing a *basic design for the watercourse*, which is a study by means of which we set up a technical concept for a complex utilization of the water of the considered watercourse. In general, the objective of the first phase is to present the designed hydraulic structures, approximately indicate their dimensions, the scope of the works and the quantity of necessary materials, necessary equipment, cost of structures and, most importantly, to prove the technical possibility, as well as the economic and commercial usefulness and justifiability of the structures. On the basis of that study, structures can be included in the plans for further elaboration and financing.

The second phase involves working out a *preliminary design* for the structures, in which, on the basis of more detailed data from the investigative works and detailed requirements, we determine the water utilization regime, as well as the type and basic details of the structures. It contains more accurate hydraulic, seepage, and static calculations and checks, elaborate drawings, and gives methods for the organization and execution of the works. In addition, a more detailed Bill of Quantities and Estimate of works is carried out. The Preliminary design should be a basis for precise determination of the investment value of the structures, in order to be able to serve as preparation of an investment program, and for closing the financial structure for construction of the structures, that is to say for making the decision for construction.

The third phase implies preparation of a *main* and *constructional design*, in which, on the basis of additional investigative works and more accurate data, final hydraulic, seepage, static and dynamic calculations are made, and detailed execution drawings for all structures and structural elements are prepared. Also, this phase finally elaborates the methods for organization of the works, anticipates the necessary plant and equipment, issues technical specifications for construction and control of quality and placement of materials, anticipates instruments and methods for surveillance (monitoring) of the structures in the course of construction and operation, performs detailing, and makes a more accurate Bill of Quantities.

On the basis of this worked out and accepted main design, a building permit is obtained so that the construction of works can commence. In this, owing to the complexity of hydraulic structures, especially dams, the relatively large territory on which they extend, which renders impossible investigative works in detail to define the characteristics of the foundation, the complexity of the conditions for construction (presence of water, need for diverting the watercourse, etc.), almost always implies the need for the design to go on even after the completion of the main design. Namely, following the opening of the construction pit and the commencement of construction, there often occur conditions that, to a large or small extent, differ from anticipated ones. Because of that, a need is imposed for performing alterations and amendments to the design. That is why designers should be in touch with everything that happens during the realization of the main design, in order to be able to react and respond in the right manner and at the right moment.

The above-described three phases of design occur with all large and more significant hydraulic structures. In the cases of small structures, the design can be performed in two phases, in which the first one and the second one are usually combined. In some cases, it is possible to go directly into preparation of the main design, if field conditions enable an experienced engineer, on the basis of analysis of data from investigative works, field prospecting, and small analysis, the ability to give an evaluation of the justification of the construction, type, and structure of the works.

On the basis of material brought up in this chapter, it is evident that individual phases of the stages of creation of hydraulic works mutually interlock. The process of creation of a hydraulic scheme with a dam and storage reservoir, from concept to completion of construction, could advance according to the chart and timetable, as given in the diagram in Figure 5.3 (Novak et al., 2001).

Following the early concepts of a design, that is to say after its initiation, there follows the need to become acquainted with the ground in a broader sense of the word – collect existing basic data, prepare maps of the area that will be occupied by the future

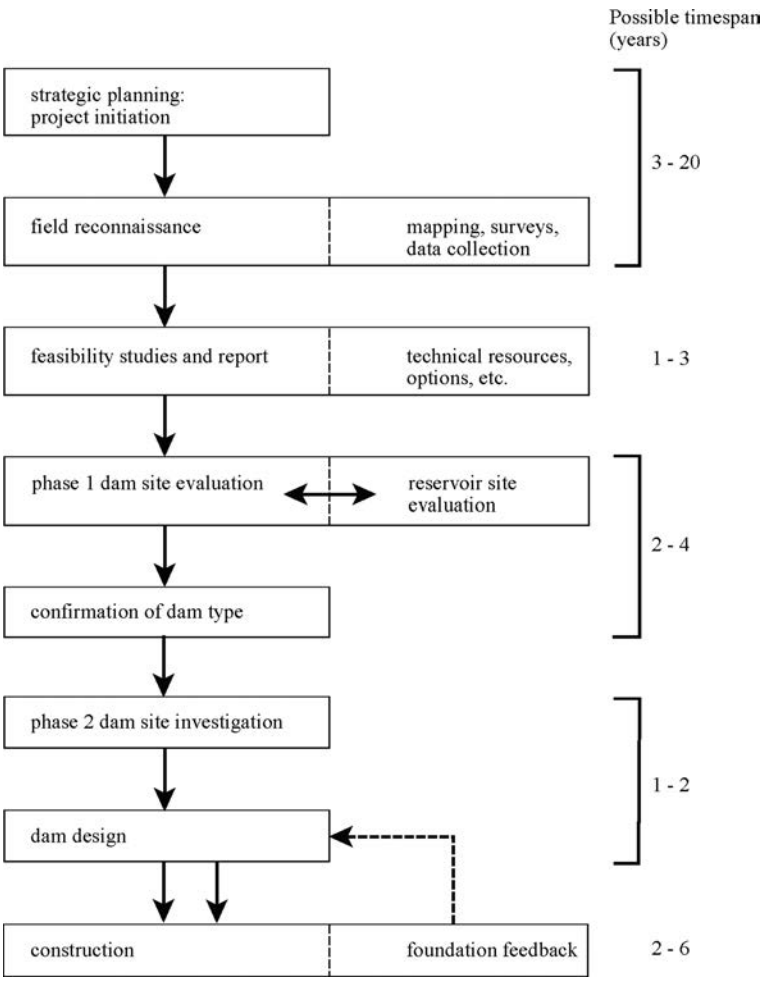

Figure 5.3 The process of the creation of a hydraulic scheme with a dam (after Novak et al., 2001).

dam, the impounding reservoir, and appurtenant structures. This phase is usually the longest of all, so it is a rare case when a more significant hydraulic scheme with a dam and storage reservoir, from its initial concept and early investigations, has reached the phase of design in a period shorter than three years, whereas often initial ideas and comprehension have matured for decades. The main purpose of this phase is to collect appropriate topographic, geological, and hydrological data. Existing maps and data, from formerly performed investigations and measurements, are a precious base to start with; however, we regularly need more detailed site surveys, investigations, and measurements. Photogrammetric surveys of the broader territory of the hydraulic scheme, amended by modern airplane surveys, with the application of sensitive sensors, facilitate the preparation of essential geodetic plans (scaled 1:5000 and larger). Here it should be noted that a skilled interpreter of air survey photographs could also elicit

useful data on the geologic structure of possible dam sites, as well as on the probability of occurrences of materials for construction of the dam. The hydrological investigations are directed towards a determination of the rainfall and characteristics of water runoff, as well as data on floodwaters in the past.

The basic study, i.e. the study that verifies the justifiability of the construction of a planned hydraulic scheme, encompasses different possibilities for its realization and utilization and lasts 1–3 years. It is a conclusion of the first phase, combining and interpreting the available information, data and results from measurements. It yields initial recommendations in relation to the technical and economic justification of the hydraulic scheme. It contains proposed alternatives in relation to the location, height, and type of dam. Comparisons are made regarding the cost, time of realization, and similar parameters. On the basis of this study, a decision is made concerning further, more detailed, investigative works, necessary for proving the correctness of the proposed locations, size of the dam and impounding reservoir. Then there follows a delicate phase in design: the final selection of the dam site and its evaluation, along with a detailed review of its influence on the selection, layout, technical effectiveness, and economy of appurtenant structures.

In close connection with selection of the dam site is the evaluation of the values of the storage space, formed by means of a dam located at the anticipated site, as well as its influence on the environment. These two moments – the selection of a dam site and the values of the impounding reservoir – are in close mutual conjunction and bestow a mutual influence on each other.

This phase is followed by additional investigative works, directed to proving the water-tightness and stability of the zone of the dam and impounding reservoir, in relation to future water retention. For that purpose, a thorough geological assessment is indispensable, especially in karst and similar formations. During this phase, an extension and amendment of the hydrological studies should also be performed.

The following step is also complex: determination of the dam type. It is in close dependence on a large part of the previously completed activities, and it must be performed with maximum studiousness and conscientiousness, since the correct selection of the type of dam, to a large extent, depends on the safety, economy, and regular operation of the entire hydraulic scheme. This step, along with the previous one, can last two to four years. Then, there follows the second phase of the investigations of the dam site, which will in detail determine its characteristics so that in the next step it will be possible to work out final designs, both for the dam and for appurtenant structures. This phase is mainly of a technical nature and it should not last more than two years. Following the acceptance of the designs and possession of the required permits, we come to the construction of the dam and the appurtenant structures.

An especially important topic that occurs in the course of completion of the design documentation, is the closure of the financial structure. In the first chapter, it was pointed out that one of the particularities of hydraulic structures is the need for a relatively high capital investment in their realization. On the other hand, clients invest in a particular project, motivated by financial profit; that is to say, by expectations of a return of more funds than those they invested and of the financial effect being greater than that expected from alternative capital investments. The accomplishment of this assumption requires the fulfilment of a number of conditions, which aggravates the possibility of providing financial resources. In any case,

it is best, prior to commencement of construction, that the financial construction be fully closed, since a possible longer interruption in construction works and a need for preservation of partially carried out works for hydraulic structures, can be very costly.

Following the opening of the construction pit, it is possible to find out if conditions in the foundation are different from those anticipated on the basis of investigative works (Yildiz & Yildiz, 1994). This can impose a revision of the design for the dam and its appurtenant structures; that is to say, there can appear a need for *design in the course of construction of the hydraulic scheme*. In such a case, it is most often a question of minor alterations, connected with the way of founding the dam and its appurtenant hydraulic structures, in which the solution is either simplified or else complicated. Sometimes interventions are considerable and they influence, not only the founding of the structures, but also the entire structures of certain works. In extreme cases, there can appear a need for a serious re-examination and alteration of certain structural solutions.

5.4 PROJECT MANAGEMENT AND THE ROLE OF LEGISLATION

The complexity of problems occurring in designing large dams, the duration of the process, and the significant investments necessary for realization of the project impose a vital need for highly professional management of the project in all its phases. The designers of dams, especially the one in charge, manage and coordinate the entire design and are obliged to be thoroughly acquainted with the latest world achievements within this dynamic engineering field, which constantly develops and advances. Such progress is not taking place abruptly, in leaps, but is rather a continuous and relatively long-lasting process, so that the acceptance of novelties and their applications must be performed on the basis of profound professional, technical, and material preparations. In the cases of economically weaker states, the acceptance and application of the latest world achievements in the local conditions, as a rule proceeds with difficulties.

In connection with this, a question can also be raised concerning the character and role of technical regulations in the process of the creation and operation of the hydraulic schemes with dams. The issuance of regulations in designing dams and appurtenant hydraulic structures has been solved in different ways in various countries. In general, it can be said that in most countries there are no strict regulations, within the framework of which one can place the designing of hydraulic schemes with a dam. This, of course, is all right since the individual nature that each dam site possesses, requires freedom for the designers which will enable them a complete expression of their creative abilities, by the help of which they will adapt the structures as much as is possible to the local conditions.

Macedonia is too young to have its own technical regulations, and in the standards of former Yugoslavia the problems of design, construction, and maintenance of dams and appurtenant hydraulic structures has received relatively little attention. On the other hand, the former practice of design, construction, and operation of dams and appurtenant hydraulic structures is rather widespread in our country, so that it has acquired a respectable base for the preparation of future technical regulations

using, besides worldwide knowledge, our own accomplishments, as well. Our technical regulations should encompass the most important elements of design and most of the questions should be treated on principle. Main efforts should be directed toward maintaining the high technical culture of engineering personnel, followed by a permanent broadening of their knowledge. This would facilitate a rational application of new world achievements in our practice and draw the maximum amount of useful conclusions from our own experience.

Somewhat different is that of the construction, maintenance, and operation of dams and appurtenant hydraulic structures, as well as their influence on the environment. Here, necessary rigorous regulations, which guarantee quality construction and maintenance of structures, as well as their safe operation, would be useful. Such an approach has been accepted by one great construction power – France. Its strict regulations for the construction and maintenance of dams originate from the end of the 19th century and are permanently being developed and renovated. They were especially tightened up in 1966 as a result of the disaster of the Malpasset arch dam in 1959. These technical regulations are clear and precise, while their implementation and enforcement is administered and controlled by bodies at state level.

Great Britain has less rigorous technical regulations, without detailed prescribed specifications for design, construction, and maintenance, with a minimum engagement of state bodies, but with, however, an emphasis on the competency and responsibilities of institutions and engineers responsible for specific structures (Novak et al., 2001). In working out our technical regulations for dams and appurtenant hydraulic structures, taking into consideration our mentality, the French model is preferred (Tančev, 1995, 1996).

Within the framework of this question, it is also necessary to consider the important aspect of classification of dams in relation to the hazard they initiate and cause, necessary measures for achieving maximum safety and responsibility for their safe operation, which should be borne by the organizations and persons in charge of the design, construction, and operation of dams. The references present examples of how these questions are approached and how they are regulated in certain countries (Heigerth et al., 1994; Kuusiniemi et al., 1994; Larsen, 1994; Lempérière, 1999; Salmon & Hartford, 1995a, b; Sandilands, 2000; Sieber, 2000; Solvik & Skoglund, 1994; Thomas, 1976; Walz, 1989).

In the phase of realization of a hydraulic project, a lot of risks and hazards can be expected which, depending on the reasons that have caused them, can be: economic, political, technological, social, environmental, etc. Risks are practically impossible to avoid, and that is why risk management is a very important topic. It is known that the construction of dams is carried out under difficult conditions of:

- Influence of a great number of external factors, such as topographic, geological, hydrological, impact on the environment, cultural and economic wealth, etc.;
- Construction of structures that require a heterogeneous organizational resource background;
- Numerous socio-economic factors (due to the long-lasting realization of projects), such as changes in economic policy, legal regulatory rules, prices of materials and resources, etc.;

- State of dislocation of the construction site from the head office of the construction company executing the works and, rather often, its considerable remoteness from large centres, where the infrastructure and accompanying production facilities exist.

On account of all that, it is very important that risk be perceived, evaluated, and, if possible, assessed. The general classification of risks and hazards starts from the place of their origin, so that they can be either *external* or *internal*.

External risks are defined as risks to the surroundings, and they encompass: political and legal, as well as economic risks, risks caused by acts of God, and ecological risks. Political, legal, and economic risks are related to the stability of the country in which construction works are carried out, and they are manifest in a change of fiscal policy, negative effects of inflation, risks in the change of legal regulations, etc. Risks caused by acts of God are earthquakes and other natural disasters, wars, revolutions, riots and disorders, radioactive and other radiation, contamination, disturbances and unrest, strikes, vandalism, great fires, etc.

Internal risks are directly associated with the realization of the project and can be generated from the contract, of a technical or financial nature, and from project management. Most often, internal risks originate because of: incorrect evaluation of the periods for construction, i.e. completion, quantities of works, insufficient degree of investigation of the conditions and technology of construction, bad assessment of the references of the contractor and the supervising engineer, breakdowns of the plant and equipment, non-coordination of the designs and alterations therein, changes in the technology of construction, errors in the placed materials and equipment, irregular cash flow of financial resources, altered conditions of financing, difficult foundation conditions (unforeseen in the design), and outstanding obligations in the name of other participating contractors, etc.

Project Risk Management is of considerable importance to the successful realization of a dam design and project. The basic concept of risk management is based on a prediction of events in order to reduce risk, to ease consequences arising from risk, and to prevent events that can cause risk, i.e. hazards.

Here, it is also considered necessary to look back at the exceptionally beneficial practice of our colleagues – the architects. In their cases, *no design for a significant structure can pass without its public presentation and acceptance*. Such an approach is perfectly suited when it is a question of the design and construction of dams. Namely, dams are very expensive and valuable structures, so that each irrational solution and failure can have far-reaching consequences, even for the economy of an entire country. Furthermore, large dams artificially raise the water level, which *creates a potential danger* for a certain broad region, so that the inhabitants of that region are interested in their safety. Finally, an impounding reservoir is formed with each large dam and, in the event that it is not properly designed, it causes *damage to the environment*, which in some cases, can have far-reaching consequences. The obligation of public presentation and acceptance of a design would drastically increase the responsibility of the client, i.e. the owner, and would also reduce the possibility of some of the cited undesirable consequences occurring.

Part 2

Embankment dams

This page intentionally left blank

Chapter 6

Embankment dams – general

6.1 INTRODUCTION, TERMINOLOGY, AND CLASSIFICATION

Embankment dams are the most widespread kind of water-retaining structures. They can be defined as dams constructed of natural material obtained from borrow pits located in the vicinity of the dam site. Material obtained from excavation of foundations and appurtenant structures is also very often used. Owing to the complexity of problems that have to be solved during their design, construction, and service, embankment dams fall within the most complex engineering structures. Thus, embankment dams should satisfy the following basic conditions:

- Slopes should have inclinations by means of which it is possible to secure the stability of the dam and its foundation under the loads of all possible forces and influences, in the course of construction and service periods;
- Deformations in the dam and its foundation, as well as in the individual constitutional components, should be kept within certain acceptable limits in order to preserve the proper functioning of the structure;
- Loss of water, owing to seepage through the body of the dam and its foundation, should be within acceptable limits, while infiltrating water should not cause seepage deformations or erosion; hydraulic gradients, seepage pressure, and velocities in the dam's body and beneath it, should be within permissible limits for the relevant materials;
- The crest of the dam should be sufficiently heightened above the maximum level of stored water so as to eliminate the possibility of water overflowing the dam, and attention should be paid to the possible height of waves, to the settlement of the embankment and the foundation following construction, as well as to other factors;
- It is necessary that the slopes and the crest of the dam be appropriately lined in order to provide protection against the action of waves, ice, or weathering influences;
- The prevention of water penetration along the circumference of the water-conveying elements carried out through the body of the dam.

Figure 6.1 represents a view of an embankment dam with its general basic elements, and denoted elements, which are found in each embankment dam. The *crest* (1) is the highest horizontal surface of the dam; and the *horizontal axis* (2) is a line of symmetry

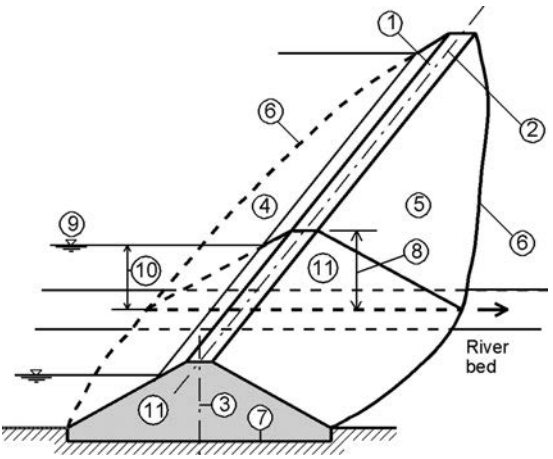

Figure 6.1 View of an embankment dam along with its basic elements.

of the crest in ground plan, whereas the *vertical axis* (3) is a normal, drawn through the middle of the crest in the cross-section of the dam. The *upstream slope* (4) is the face, i.e. the side of the dam that is turned towards the water, while the *downstream slope* (5) is the opposite unimmersed side.

The *abutments* of a dam are the surfaces of the valley, to the right and to the left of the river bed, upon which the dam is supported; the *contours* (6) are the lines along which are connected the slopes of the dam and the ground; and the *foundation* (7) is the ground upon which the dam is supported. The *body* of a dam is the volume that is confined within the surface of the foundation, within the slopes, as well as within the crest; its *height* (8) is the distance from the bottom of the excavation for the foundation in the riverbed to the crest of the dam. The *level of headwater* (9) is the level of water in the impounding reservoir, while the *height of headwater* (10) is the difference between the level of water in the riverbed before construction of the dam and the maximum level of the water in the storage lake. The *cross-section* (11) is any vertical section, which is perpendicular to the longitudinal axis of the dam.

The classification of embankment dams is determined in several ways. In accordance with the *kind of material* of which they are constructed, dams can be divided into: (1) *Earth dams*, the larger part of whose body (over 50%) is constructed from fine-grained earth materials – clay, loam, sand, or sandy-gravel materials; (2) *earth–rock dams,* whose basic body volume is constructed from coarse-grained gravel or rock materials, while water impermeability is provided by means of a waterproof element made of fine-grained earth material; (3) *rockfill dams*, whose body, similar to the previous kind of dam, is constructed from coarse-grained material, while water impermeability is achieved by means of an element made of artificial material.

According to the *structure*, embankment dams can be: (1) *Homogeneous*, which does not require any special waterproof element – only earth dams can be considered in

this group; (2) *zoned*, whose body can be divided into two or more zones, constructed from different local materials – this group usually encompasses earth–rock dams, but earth dams and rockfill dams can also be considered, provided they contain zones of different fine-grained or coarse-grained local materials; and (3) *embankment dams having a waterproof element of some artificial material;* this group usually consists of rockfill dams, and sometimes earth dams, as well.

According to *the position of the waterproof element* it is possible to distinguish dams that have a: (a) *facing,* when the upstream slope is lined with a waterproof element; or (b) *core,* in which case the waterproof element is positioned inside the body of the dam. If the core has been constructed from some artificial material, sometimes it is called a *diaphragm wall.* The core and the diaphragm wall can be vertical and set up along the axis of the dam, or else can be inclined towards the upstream face.

According to the *method of construction,* embankment dams can be divided into two groups: (1) those made by *the conventional method* of using material from borrow pits, its spreading and compacting in an appropriate way; and (2) those made by means of controlled and *checked mining* of the nearby hill massif. The latter method can be considered and applied in highly specific conditions, and is therefore rarely found in practice. For more details, the reader is referred to textbook references (Danilevsky, 1992; Nedriga et al., 1986).

With regards to their *purpose,* embankment dams (same as concrete) are divided into: (1) dams intended for raising the level of water in a river; (2) dams forming impounding reservoirs with water; and (3) dams forming space for deposition of waste material from industrial and mining processes. This last type of dam, known as a *tailings dam,* has a number of specific qualities, dictated by the kind of waste material, the nature of the specific industrial process, local conditions of the dam site, etc. These will briefly be reviewed in the last clause of this chapter.

The International Commission on Large Dams (ICOLD) divides dams according to their size – either large or small. In the group of *large dams* are dams that measure higher than 15 metres. This group also encompasses dams having a height between 10 and 15 metres, provided they fulfil at least one of the following conditions: (a) the length of dam's crest should not be smaller than 500 m; (b) the volume of the impounding reservoir, formed by the dam should not be smaller than 1 million m^3; (c) the maximum quantity of flood water which could be evacuated from the reservoir should not be smaller than 2000 m^3/s; (d) the conditions for founding the dam are particularly difficult; and (e) the dam has an unusual construction.

Regarding dam height, there is not an official classification. According to experience from the practice of design and construction, it seems logical to divide the embankment dams into *low dams,* having a height up to 30 m; *medium dams,* having a height $H = 30–80$ m; *high dams* having a height $H = 80–150$ m; and *particularly high dams,* having a height *of* $H > 150$ m.

With regard to the condition for passing floodwaters, embankment dams as a rule are constructed as *no spillway dams,* having special evacuation elements, constructed outside the body of the dam. In some particular cases, there might be constructed spillway elements over the dam, or else a permeable rockfill dam could be constructed (in cases when it serves only for retention of the flood flow wave).

Embankment dams possess a number of exceptional properties, which promote them as the dominant type of dam. The most significant among them are:

1. Applicability of this type of dam on dam sites having the most different shapes, both in wide valleys and in narrow river gorges with relatively steep sides;
2. Adaptability to a broad variation of conditions in the foundation, which can be built from high-quality solid hard and strong rock, down to soft and compressible or relatively permeable earth;
3. Use of natural materials, by reducing to a minimum the need for the procurement and transport of considerable quantities of processed, and consequently, expensive material;
4. Possibility of satisfying the design requirements in different ways, by the use of earth materials, gravel and crushed stone, as well as their optimum zoning into the body of the dam, adapted to local conditions and requirements;
5. Possibility of the use of waterproof elements from artificial materials at the dam sites, where local cohesive earth material is not available, or such a waterproof element has been imposed by other conditions;
6. High mechanization of the process of the execution of works by achieving maximum effectiveness.

Deficiencies of embankment dams, in relation to concrete dams, are not numerous. The most important among them is their incomparably larger susceptibility to damage and failure with water overflowing the crest, as well as their susceptibility to the influences of concentrated seepage paths, and internal erosion through the body of the dam and foundation.

In the practice of building large embankment dams, the most frequent application is that of earth–rock dams, schematically shown in Figure 1.1b–d. In the case of this type of dam, the watertight core made of cohesive earth material is pinned by means of supporting elements of coarse-grained, highly water-permeable material (crushed stone or gravel), through which water, percolated through the core, drains freely.

For the prevention of internal erosion, filtering layers are inserted between the cohesive material and the supporting elements. For those earth–rock dams that contain a vertical core, numerous large and extremely high dams have been erected.

An inclined position of the core is also extensively used. This position enables a smaller part of the water-permeable material in the dam's body to be immersed in water, while at certain dam sites it is also possible to achieve other advantages in relation to the vertical position. For example, the core can be constructed using a smaller quantity of material; the core and filtering layers, completely or partially, can be incorporated following the construction of the downstream supporting element; that is to say, a part of it, to generate conditions for a simpler overbuilding of the dam, i.e. its stage construction, etc. In certain cases, a vertical position of the core is more favourable, so that each separate case must be carefully analysed. These problems will be discussed in detail in Chapter 11.

Rockfill dams are characterised by the fact that their body is constructed from coarse-grained material – tipped rockfill or gravel – while waterproofing is secured by means of a special element made of artificial material, and not of earth, as is the case with earth–rock dams. From here results the basic difference in the way these two

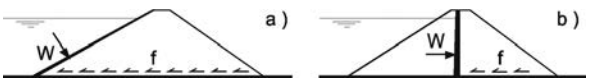

Figure 6.2 Influence of the position of the waterproof element on the stability of a dam.

basic kinds of embankment dams operate. Namely, owing to the absence of cohesive earth material, it does not lead to an occurrence of pore pressure in the body of a rockfill dam, and this in turn, makes conditions for construction and service much more favourable. Hence, they represent an alternative to earth–rock dams whenever, in the vicinity of the dam site, there is no cohesive material for the construction of a core, as well as in some other cases (Tančev, 1981, 1982).

It has been shown that rockfill dams can be classified in two ways: (1) According to the *position of the waterproof element,* and (2) according to the *material* from which the waterproof element has been made. According to the first, it is possible to distinguish: (a) rockfill dams with a *facing,* in which case the upstream slope of the dam is lined with a waterproof element; or (b) rockfill dams with a *core* (or *diaphragm wall*), which is constructed inside the body of the dam.

In practice, the solution involving a facing is being much more often used, which will be more understandable when the advantages and deficiencies of the first and the second solutions are analysed. Rockfill dams that have a facing possess the following advantages in relation to those that have a core:

1. Their degree of safety against slipping along the foundation is greater, because the whole body of the dam is dry, while the mass resisting the pressure of water is maximum (Fig. 6.2), in which case the force of the hydrostatic pressure of water from the impounding reservoir is inclined downwards, which is most favourable from the viewpoint of stability;
2. The construction of the body of a dam having a facing is performed independently of the facing, which is executed at the end, over a previously formed slope;
3. The facing is easily accessible for inspection, repairs, and possible reinforcement (i.e. strengthening);
4. The facing can also have a secondary function – slope protection against waves and other external influences;
5. Dams with a facing are simpler for heightening, because the embankment is extended only towards the downstream face, while the facing is extended upwards.

Facings have certain deficiencies, which in fact have imposed consideration for the application of cores inside the body of the dam. The basic deficiencies of facings are: (1) exposure to external influences (impact of waves and ice, temperature variations, etc.); the consequence could be damaging and faster aging of the facing made from artificial material; (2) a relatively complicated and long joint between the facing and the foundation, which is especially important when a deep grout curtain below the waterproof element is also constructed.

In contemporary practice, in relation to the material from which the waterproof element is made, reinforced concrete, asphalt concrete and geosynthetic facings are

most often used in rockfill dams, as well as asphalt cores. From time to time rockfill dams with geosynthetic and grout core are constructed, while steel facings and cores, as well as concrete cores, practically are abandoned. In that way, one can distinguish *concrete faced rockfill dams* (CFRD), asphalt concrete, steel and geosynthetic facings, as well as appropriate kinds of rockfill dams with an internal core. Over the last two decades the most popular rockfill dam with facing has been the CFRD, and with core the *asphaltic concrete core dams* (ACCD). The most frequently used rockfill dams have been analysed in Chapters 12, 13 and 14.

6.2 HISTORICAL DEVELOPMENT OF EMBANKMENT DAMS

The beginning of dam construction is marked with the dam Sad el-Kafara, built in Egypt in the period of the third or the fourth dynasty, between 2950 and 2750 BC. This dam formed an impounding reservoir for water, which served the needs of an alabaster quarry at a distance of 3 km. It was 12 m high and 106 m long. Even though its width was enormous (Fig. 6.3), owing to its poor structure the dam failed in the early years of its service, most likely due to water overflowing the crest. The end parts of the dam (abutments) stand visible even today (Smith, 1971; Schnitter, 1994).

In ancient times, other dams had also been constructed. In the middle of the third millennium BC, north of Baghdad, the Nimrud dam had been built, probably an earth dam, by means of which the course of the River Tigris had been diverted. The dam failed in 1200 BC, and so afterwards, the Tigris returned to its former river channel.

Another known dam from a later period is Sad el-Arim, located on the River Marib in Yemen. It is an earth dam, originally 4 m high, which was later heightened to 7 m (500 BC) and provided a spillway at one of the ends. The cross-section was triangular, with inclinations of the slopes 1:1, having an upstream slope lined with stone, placed in mortar. The Sad el-Arim dam formed an impounding reservoir with water that was used for irrigation. It failed in the 6th century of the new era, following a long period before that in which it had not been used or maintained.

Among a number of other mainly small earth dams and masonry dams built in Eastern Arabia, it is worth noting the one that had been constructed near Adra, which could be considered as a herald or forerunner of today's embankment dams having a stiff diaphragm. It consisted of a thin wall, constructed in stone material with lime mortar, supported by earth and rock.

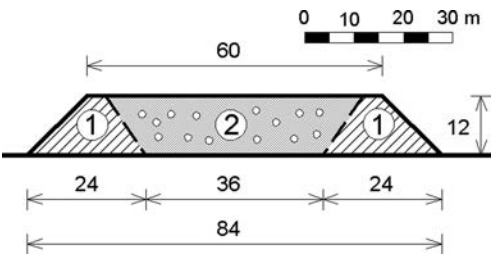

Figure 6.3 Sad el-Kafara dam, cross-section. (1) Placed arranged stone; (2) gravel borrowed from the bottom of the valley and stone from the adjacent hills.

In the period before the new era, embankment dams had also been built in India and Ceylon (Sri Lanka). Data on the oldest earth dam in Ceylon go back to the year 504 BC. One of the ancient Ceylon reservoirs, known as Padavil, had been formed by means of an embankment 21.4 m high and as much as 18 km long. Its crest was 8 m wide, the foundation 61 m wide, and the overall earthworks had reached, for that period, the tremendous quantity of 13 million m^3.

Among the monumental works that were built in the period of the Roman Empire, dams hold a particular place. The Cornalvo dam, Figure 6.4, built in the second century, exhibits the orientation of Roman engineers to build solid, hard, and firm structures. That dam is 20 m high, 200 m long, with an inclination of the upstream slope 1:1.5 and an inclination of the downstream slope 1:3 (Fig. 6.4). Inside the dam, stone walls were built, both longitudinal and transverse ones, which divided the dam into boxes, filled with clay and stone, while at the end the whole structure is covered with earth. The slopes are protected with masonry stone lining (Smith, 1971; Nonveiller, 1983).

In feudal Europe a number of dams were constructed in Germany, Austria, France, Great Britain, Italy, by using local material; however, they brought no progress in this field, as compared to dams built in previous periods.

The industrial revolution, which first spread over Great Britain and then through other European countries as well as North America, imposed the necessity of more intensive building of dams. In this way, towards the end of the 18th and the beginning of the 19th centuries, a number of dams were built in Great Britain and France, which served as water supply to the lower navigation channels, which were of great importance to industry. The largest among them is the Todd Brook dam (Great Britain), 21 m high. The first half of the 19th century was characterized by the construction of early embankment dams in Europe and the USA, which were intended for water supply.

In the second half of the 19th century, a number of smaller, so-called "rockfill dams", were built in the USA. They provided water for the needs of the mining industry in some distant regions in California in which there was an abundant quantity of stone, and where miners were skilful in its use. The first rockfill dams were constructed with a waterproofing element in the form of a wooden facing, which was later on improved with waterproofing material based on bitumen. Metal facings have replaced wood, which did not find a broad application. Later on, concrete facings and diaphragm walls appeared, and they dominated the scene up to the 1930s.

The study of the historical development of dams built of local material imposes the conclusion that, including the first quarter of the 20th century, their design and construction mainly represented empirical experience and trade. As a consequence of

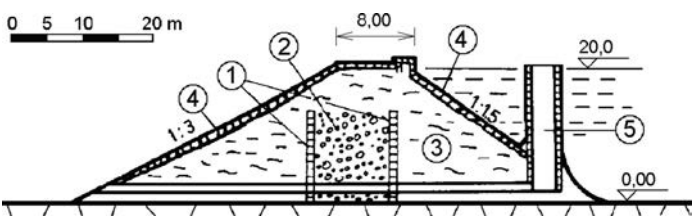

Figure 6.4 Cornalvo Dam, Spain, II century (after Nonveiller, 1983). (1) Stone walls; (2) filling of stone and clay; (3) earth; (4) stone lining; (5) water intake tower.

that, in the course of the 19th and at the beginning of the 20th centuries, failure of a number of dams took place in the industrial countries of Europe and North America, in some cases having disastrous consequences. In that not so glorious period in the history of dam construction with local materials, begins the creation of a theoretical basis for significant progress in the field.

First of all Darcy, in l856, announced the Law for flowing through porous sandy conditions, and then Forheimer, in 1886, indicated that water pressure distribution in a seepage environment takes place in accordance with Laplace's differential equation. Much more time has been necessary for these fundamental discoveries to find important application in dams built of local materials; that is to say, it was necessary to wait for the appearance of another new science – soil mechanics, whose foundation was established by Karl Terzaghi in the early 1920s. At the same time, an analytical study of slope stability also commenced in Sweden.

A further swift development of soil mechanics has made it possible to understand, in addition to seepage, the problems of consolidation, settlement, and others, associated with earth embankments. In that manner, the way has been opened towards the construction of large dams, since earth, that seemingly simple and yet essentially very complex material, no longer carries so many uncertainties as has been the case until then. The progress in the field of embankment dam construction has been also assisted by the manufacture of plants and equipment for carrying out large engineering projects, as well as by the development of numerical methods for static and dynamic analysis, methods for surveillance, etc.

6.3 DIMENSIONS OF THE BASIC ELEMENTS OF EMBANKMENT DAMS

In designing embankment dams, it is necessary to select a stable and, at the same time, economical cross-section. Dimensions of the cross-section depend on the type of the dam, its height, the kind of material in its foundation, as well as on the conditions of their construction and service. The crest and the slopes form the contour of the dam.

The width of the crest can be determined by means of empirical formulae, as a function of the dam's height. For example, the following expression is used in Japan:

$$b = 3.6\sqrt[3]{H} - 3 \tag{6.1}$$

where b = width of the crest in metres, and H = height of the dam, also, in metres. For low dams (15–20 m), USBR recommends the formula:

$$b = 0.2H + 3 \tag{6.2}$$

The following empirical expression can also be used:

$$b = 1 + A\sqrt{H} \tag{6.3}$$

in which $A = 1.1{-}1.65$.

The values of crest width gained by formulae 6.1 to 6.3 usually are greater than is necessary, and should be considered as a first approximation. The smallest width

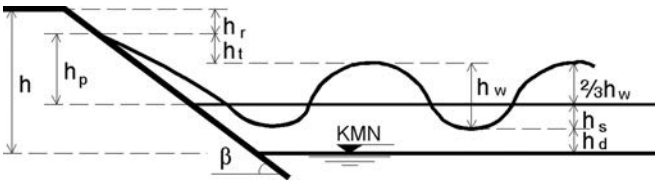

Figure 6.5 Diagram for calculation of the heightening of the dam's crest.

of the crest for small dams can be 3–4 m, while for large dams it is 5–6 m. If there is a road or a railway line passing along the crest, then the width of the crest is determined by the category of the road or railway line. In such cases it usually reaches 10–12 m.

In seismically active areas, the crest should be wider, because practice has shown that during an earthquake, largest deformations occur in the zone of the crest's edges. The Oroville dam (USA), 235 m high, has a crest 18.3 m wide, while the highest embankment dam in the world, Nurek (Tajikistan), 300 m high, has a crest 20 m wide.

The crest of the dam must be heightened with regards to the maximum static level of water in the impounding reservoir in order to prevent the possibility of water overflowing the dam. Such *a freeboard h* is calculated using the formula:

$$h = h_d + h_s + \frac{2}{3}h_w + h_t + h_r \tag{6.4}$$

where h_d = wind set-up, i.e. increase of the water level owing to its push towards the dam under the effect of the wind; h_s = increase of the water level due to occurrence of oscillations of the reservoir surface, i.e. seiches; h_w = wave height; h_t = wave run-up, i.e. height of the ascending wave up the slope; and h_r = reserve heightening. The term $^2/_3 h_w$ represents the rise of the wave above the static water level (Fig. 6.5).

The wind set-up can be calculated using the well-known Zuider Zee formula:

$$h_d = \frac{V^2 L \cos\theta}{63{,}000D} \tag{6.5}$$

where V = the sustained wind velocity in km/h; L = fetch, i.e. effective length of the blowing front of the wind in km; θ = angle between the direction of wind and the water surface; and D = mean depth of the impounding reservoir along the length L, in m.

It is clear from the expression that more significant values of h_d are obtained for impounding reservoirs of greater length, but small depth. In the case of deep reservoirs with a relatively small area of the water table, h_d can be neglected.

Seiches represent gradual variations of the level and they appear in the impounding reservoirs as a consequence of changes of the barometric pressure, alternating action of the wind, no uniform inflow and outflow, etc. Seiches last from several minutes up to several hours. In the case of large storage lakes, the member h_s could have a noticeable value. Since there are no methods for the calculation of h_s, its value is assumed or neglected, i.e. is inserted into the reserve.

For calculation of the wave height, methods have been outlined in the item on the determination of forces due to waves (Chapter 4). The height of the wave h_w can be replaced with the so-called *significant* height of the wave h_{ws}, which represents the average height of one third of all the highest waves that appear in observations in the course of 13% of the time duration of waves at a constant velocity of wind. On the basis of measurements of the real velocities of wind and the corresponding height of waves on three lakes in the USA, performed in the fifties and following a detailed analysis of the obtained results, it has been established that the significant height of waves can be determined with a high accuracy from the expression for waves in the open sea (Saville et al., 1962):

$$h_{ws} = 0.005 V^{1.06} L^{0.47} \tag{6.6}$$

where V is taken in km/h, L in km, while h_{ws} is obtained in metres.

In accordance with those investigations, the length of the significant wave can be obtained from the expression:

$$l_{ws} = 0.17 V^{0.88} L^{0.56} \tag{6.7}$$

With such parameters obtained from the diagram in Figure 6.6 for a certain inclination of the dam's slope (Fig. 6.6a for smooth slope facing, like concrete or asphaltic-concrete lining, Fig. 6.6b for rough and very permeable slope facing, like rip-rap), it is possible to obtain the value h_p/h_{ws}, in which h_p is the height of the wave above static level, along with the height of ascension of a wave up a slope. In other words:

$$h_p = \frac{2}{3} h_w + h_t \tag{6.8}$$

The value of ascension of a wave up a slope, besides depending on the length and height of the wave and the inclination of the slope, also depends on the roughness of the slope surface, as well as its permeability. There are empirical formulae, which also contain the last two parameters, but they yield only approximate results owing to the impossibility of the parameters being precisely determined. One of them is the formula of Junkovsky, which we often use:

$$h_p = 3.2 R h_w \tan \beta \tag{6.9}$$

where R is a coefficient dependent upon the kind of protection of the slope – for concrete and asphalt concrete it amounts to 0.9–1; for placed stone, 0.75–0.80; while for rockfill, it is 0.55–0.60.

Reserve heightening is assumed and usually ranges from 0.5 to 1.0 m. Within itself, it should contain everything that is not included in the previous terms of expression (6.4) and above all, the possibility of settlement of the embankment during an earthquake as a consequence of additional compaction, and the danger of occurrence of high waves caused by a strong tremor.

Maximum possible attention should be paid to proper determination of the freeboard and to the necessity for a complete and correct design of the dam, in order

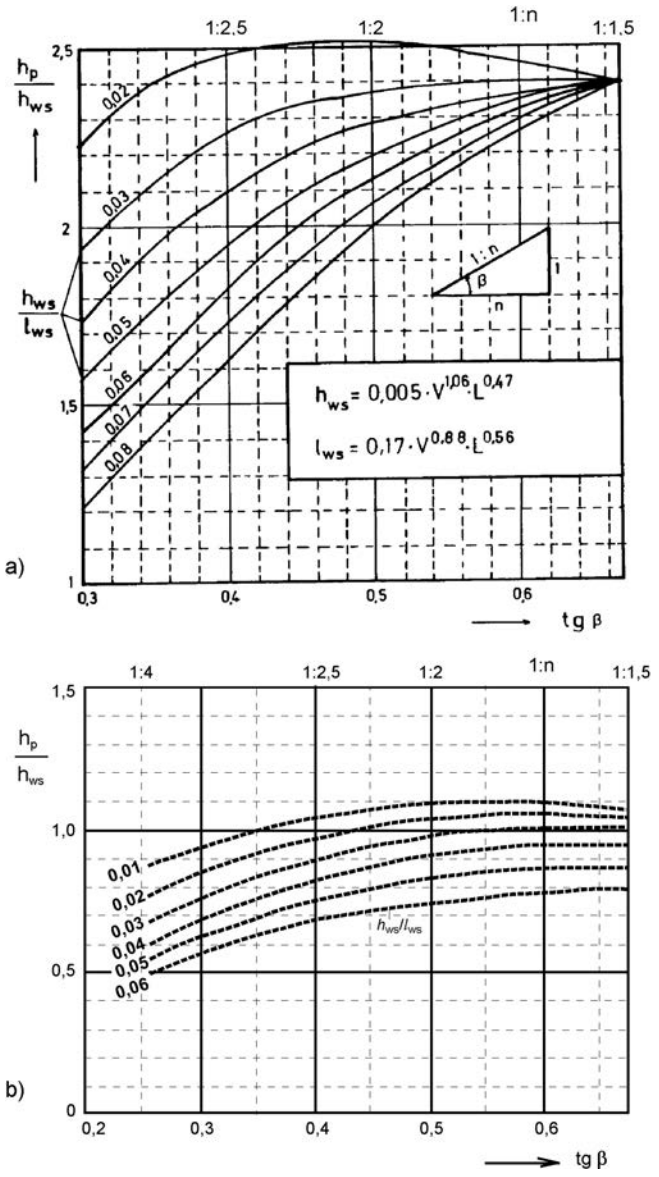

Figure 6.6 Diagram for determination of the ascension of a wave up a slope (after Saville et al., 1962). (a) For smooth slope facing, like concrete or asphaltic-concrete lining (b) for rough and very permeable slope facing, like rip-rap.

to reduce to a minimum the hazard of water overflowing the dam. From the example of a recent disaster in Rumania, we shall illustrate the mechanism of failure of an embankment dam during uncontrolled water overflowing the crest (Diacon et al., 1992).

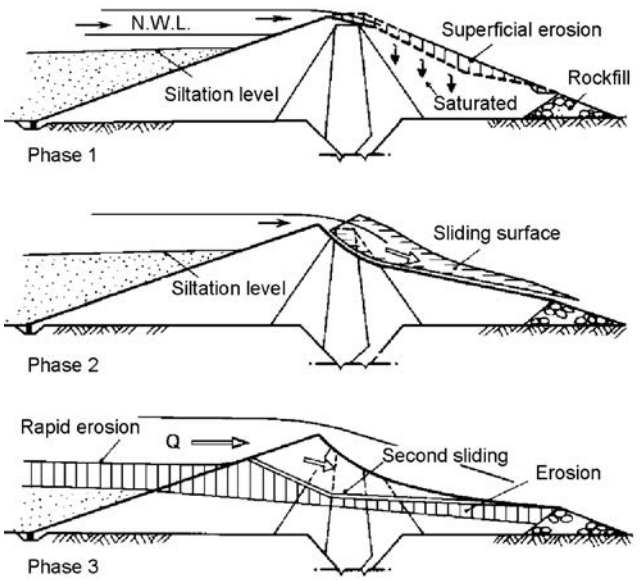

Figure 6.7 Failure mechanism of the Belchi dam (after Diacon et al., 1992).

The Belchi dam (Rumania) was completed in 1962 in order to form an impounding reservoir of $12.7 \times 10^6 m^3$ intended for water supply. Later on, a small hydroelectric plant with a power of 1.1 MW was installed. The dam was of an earth type, with a central clay core and 18 m high. It was extended on both sides of the central concrete overflowing part, having a total length of 415 m. The reservoir, prior to the disaster, was 75% filled with deposit.

On the night of July 28th, 1991, at a water level in the impounding reservoir of 40 cm below normal, a catastrophically heavy rainfall of more than $100\ l/m^2$ fell within the catchment area. At the same time, a number of unfortunate circumstances also occurred, which is a frequent case in such disasters. Namely, the hydroelectric plant had been out of use because of some defect and, at an attempt by the operator to open one of the two segmental gates of the controlled spillway, a breakdown of electric power took place. The operator and his assistant tried manually to lower the two gate flaps (the spillway had four bays two of which were provided with segmental gates, the remaining two with flap gates). However, the operation was very difficult and the success limited due to the abrupt outbreak of water, which had begun to flood the gates very rapidly. Only four hours after commencement of the rainfall, water overflowed the embankment dam; and 2.5 hours later, the first sliding of a part of the dam took place (phase 2, Fig. 6.7). Two and a half hours after that, a second sliding took place (phase 3, Fig. 6.7). The consequences were disastrous: 17 casualties, 350 houses either destroyed or heavily damaged. There were also consequences in relation to adjacent roads, bridges, telecommunications, and electric transmission lines. The unusually heavy rainfalls caused significant damage in the whole area of Bacau, where the Belchi dam is located, so that total casualties were 78 persons; nineteen people were reported missing. Since the Belchi dam failure the reservoir has been abandoned for a long period

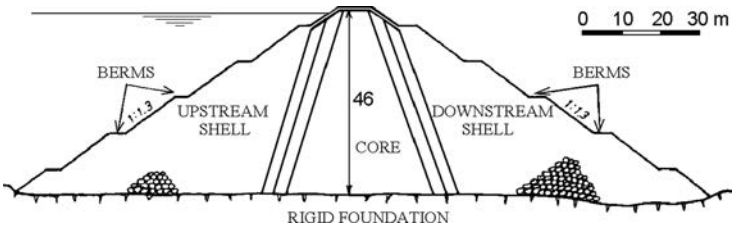

Figure 6.8 Typical cross-section of the Ice House dam, California.

of time during which the mechanical equipment was spoilt and deteriorated. Alternatives were analyzed for the reservoir restoration immediately after the failure, and some innovative proposals have also been advanced recently (Asman and Bratianu, 2013).

Dam slope inclinations at the beginning of a design are assumed on the basis of experience with similar dams, followed by theoretical analyses of their stability (Chapter 8), and afterwards, if necessary, appropriate corrections are made. In order to obtain the most economical solution, the dam should have a minimum volume. That is why slope inclinations should be as steep as possible, bearing in mind that one should satisfy the conditions of stability, as well as the possibilities for as easy a construction as possible.

Generally speaking, the slope inclinations of embankment dams depend on the strength of the foundation and that of the material anticipated for construction of the dam. Earth–rock and rockfill dams, founded on bedrock, usually have slope inclinations of 1:1.5 to 1:1.8 (1 vertically:1.8 horizontally). On weaker foundations, the inclinations will be more moderate. In the case of earth dams, slope inclinations, in addition to the above-cited basic factors, depend also upon the height of the dam, as well as on the grain size of the filling material. The higher the dam and the finer the material built into its body, the more moderate the anticipated slope. Most often slope inclinations of earth dams range from 1:2 for sandy gravel, up to 1:4 for clay; however, they can be also much more moderate in the case of founding on a weak foundation. In the cases of rockfill dams with waterproof element made from artificial material, i.e. when there is no pore water pressure in the dam body, the height does not practically influence inclinations of the slope.

The shape of the dam site can also influence slope inclinations. In damming narrow valleys, the slopes could well be somewhat steeper, because the steep banks of the valley, being relatively close to each other, provide the dam with additional stability. Such an effect can be expected at dam sites with a tight riverbed and inclinations of the valley banks of 1:3 or more.

In the case of slopes at rockfill dams, it is most economical for the inclination to be equal to the angle of repose of the rockfill material, because the construction of a more moderate slope requires additional work, which increases the cost of the structure. Since it is usually necessary to construct a slope with a more moderate inclination than the angle of repose, often the monotonous flat surface of the upstream and downstream slope is interrupted by means of horizontal surfaces, named *berms*. Between them, the slope has the angle of repose of the rock material, as in the example that is shown in Figure 6.8. Berms can be beneficial if the placement of the material is carried out in

layers of considerable thickness, when there is an aggravated construction of the slope with a more moderate inclination than the angle of repose of the rock material. Berms are being dispensed with lately, because by means of developed powerful plants and equipment there is an elimination of the above-cited difficulties in the construction of dams. However, in the case of earth dams, berms on the downstream face, along with a drain channel for drainage and grass planting of the surface, are most often an essential measure for effective protection against the erosive action of rainfall.

For any assigned factor of safety against shearing, the smallest volume of the dam embankment is obtained when slopes are steeper in their upper part, while more moderate in their lower part near the foundation. This is particularly so in the case of a higher dam, founded on a weaker foundation. The example of the Shefia dam (Algeria) is also interesting, where the slopes have been carried out in the form of continuous curves. The inclination of the downstream slope varies from 1:1 at the crest, up to 1:3 at the bottom.

6.4 CHOICE OF THE DAM SITE

Location for construction of a dam and formation of an impounding reservoir must satisfy a considerable number of functional and technical requirements. The functional suitability of the dam site depends, in the first place, on the equilibrium between its natural physical characteristics and its influence on the future impounding reservoir. Technical suitability is governed by the existence of a site (or sites) for the dam, the presence of materials needed for dam construction, on water impermeability and stability of the ground at the future reservoir, on the possibilities of using existing communications, and on the construction of access roads, etc. Hydrological, geological and geotechnical characteristics of the entire catchment area and of the dam site are the main elements for determining the technical suitability of the site for the planned impounding reservoir. To this there also must be added evaluations of the influence that the planned hydraulic scheme will have on the environment, caused by its construction and service.

Before choosing the dam site, studies are conducted to verify the justification for the construction of an impounding reservoir; its available storage capacity is also defined. One should necessarily consider several possible sites on a certain watercourse and then the choice of the dam site takes place, which makes it possible to achieve the assigned water utilization tasks and to provide a technically justifiable and economical solution. At the same time, all aspects that are encompassed within the first stage of the design are reviewed – investigations, taking into account not only the dam site, but also the entire impounding reservoir, as well as its broader area. An important part of this stage is a reconnaissance and investigations of the ground, which could extend over a long period of time (see the diagram in Fig. 5.3), having as its main objective the gathering of accurate topographic, geological, and hydrological data.

At the beginning, one must use existing maps and surveys, which will inevitably be followed by more detailed surveying and investigations. At this stage, as an addition to traditional air surveys, in recent time using modern techniques it is also possible to produce airplane photographs, on the basis of whose interpretation an experienced

geologist will draw out valuable information on the geology of the possible dam site as well as of the probability of the presence of local construction materials.

Lately, there is yet another possibility at our disposal. Most countries of the world utilize satellite photographs, which give a broad view of the region, and which is of interest for the sitting of the works. Such a broad view can give indications of the geological relationships of the area, their boundaries, and faults. Hydrological studies at this stage are directed towards determination of the rainfall and the characteristics of the surface water runoff, as well as an assessment of the data on floods that have happened in the analysed period. In parallel, the necessities and possibilities for the utilization of water are perceived.

As a concluding part of the investigations and analyses performed at this stage, it is necessary to work out *a feasibility study.* This gathers and interprets all available information, data and surveys and it also gives the early recommendations in relation to the technical and economical value of the anticipated hydraulic scheme along with a dam and an impounding reservoir. Possible variants of site locations, and the height and type of dam are also proposed.

Furthermore, comparisons of possible solutions in relation to cost, time of construction, conditions of service, etc. are carried out. This study gives recommendations for further, more detailed investigations, which would verify the recommended positioning of the structures within the hydraulic scheme; that is to say, the proposed dam site. In making a choice of dam site, one should also analyse different types of not only embankment dams but also concrete dams, which may be taken into consideration for the specific ground conditions.

Further on, the next stages of the investigation and design follow, in such a way and sequence as they are quoted and described in Chapter 5. At these stages, at a known volume of the impounding reservoir and defined dam type, it is possible to make only minor movements of the axis of the dam site, that is to say, defining its micro-location, in order to carry out a full adaptation of the local ground conditions. At that time, one must once again take into consideration and analyse a number of factors, the most important being (Tančev, 1992):

1. Engineering-geological and topographical conditions at the spot of the dam site, as well as regarding the storage space as a whole. As for topographical conditions, in most cases the narrowest spots are the most favourable because they provide the smallest volume for the dam. If conditions of the foundation in the narrowest profile are not the most favourable, then it is possible to have a more justifiable choice of a wider dam site with a better foundation.
2. Deposits of local materials for building the dam, which are in sufficient quantities in the vicinity of the dam site.
3. Possibilities of a rational and harmonious composition of all structures within the hydraulic scheme, in which particular attention should be paid to expensive spillway structures.
4. Possibilities of a safe and economical evacuation of water in the course of construction of the hydraulic scheme.
5. Faults and discontinuities in rock masses, through which it would be possible to lead to the circulation of water beneath the dam or sideways of it.

When choosing the dam site, one should take into consideration that the longitudinal axis of an embankment dam should not necessarily be in a straight line, but can also be broken or curved, if that would help the dam to achieve having a smaller volume, or else to obtain a more rational solution for some of its appurtenant structures.

6.5 MATERIALS FOR CONSTRUCTION OF EMBANKMENT DAMS

Conditions that should be fulfilled by local materials for the construction of embankment dams depend on the type of dam, its location, and the role of the material in the cross-section of the dam, as well as on the method of dam execution. At the same time, one should take into consideration the physical and mechanical characteristics of the local materials, climatic conditions of the locality on which the construction methods depend, the locations of the borrow pits, and the ways of their use, transport and incorporation of the materials.

There are different classifications of the soil material, but the one proposed by Casagrande (1948) and adopted in 1952 by USBR and USCE is widely used. This classification of cohesive soils is based on the grain size distribution, the liquid limit and the plasticity index (Fig. 6.9 and Table 6.1). The system also includes coarse materials (Table 6.1). This classification system helps to estimate the range of the properties and of the permeability of soils. Thus, it is a powerful tool in the hands of experienced geotechnical engineers.

The A-line separates clays from silts (Fig. 6.9), and only organic clays (OL and OH) are found below the A-line, i.e. on the silt side. They are not suitable as construction materials in dam engineering. The complete system includes 15 group symbols (Table 6.1). It covers all types of soil which are suitable in dam engineering, and it is important that the number of symbols can be extended using double symbols, like SC-PL, SP-SC, CL-ML.

For a correct choice of the structure of a dam and methods of its construction, we can in practice use all local materials, with the exception of earth materials containing inadmissible quantities of organic matter and water-soluble salts. For the construction of earth dams, we can use natural cohesive and non-cohesive earth materials that do not

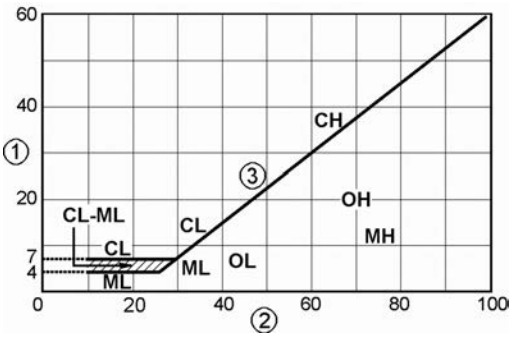

Figure 6.9 Chart for classification of cohesive soils (Unified Soil Classification Chart, adapted from Kutzner, 1997). (1) Plasticity index, (2) liquid limit (%), (3) A-line.

Table 6.1 Group symbols and typical names of soils (part of the Unified Soil Classification Chart, USBR, 1984).

Group symbols	*Typical names and laboratory classification criteria*
GW	Well graded gravels, gravel-sand mixtures; little or no fines. C_U greater than 4.
GP	Poorly graded gravels, gravel-sand mixtures; little or no fines. Not meeting all gradation requirements for GW.
GM	Silty gravels, poorly graded gravel-sand-silt mixtures. Atterberg limits below A-line, or PI less than 4.
GC	Clayey gravels, poorly graded gravel-sand-clay mixtures. Atterberg limits above A-line with PI greater than 7.
SW	Well graded sands, gravelly sands; little or no fines. C_U greater than 6.
SP	Poorly graded sands, gravelly sands; little or no fines. Not meeting all gradation requirements for SW.
SM	Silty sands, poorly graded sand-silt mixtures. Atterberg limits below A-line, or PI less than 4.
SC	Clayey sands, poorly graded sand-clay mixtures. Atterberg limits above A-line with PI greater than 7.
ML	Inorganic silts and very fine sands, rock flour, silty or clayey fine sands with slight plasticity.
CL	Inorganic clays of low to medium plasticity, gravelly clays, sandy clays, silty clays, lean clays
OL	Organic silts and organic silt-clays of low plasticity.
MH	Inorganic silts, micaceous or diatomaceous fine sandy or silty soils, plastic silts.
CH	Inorganic clays of high plasticity, fat clays.
OH	Organic clays of medium to high plasticity.
PT	Peat and other highly organic soils.

Note: Atterberg limits = liquid limit (LL) and plastic limit (PL); PI = Plasticity index (LL minus PL); C_U = Coefficient of uniformity d_{60}/d_{10}.

contain water-soluble chlorides or sulphate–chloride salts (more than 5% of the mass), sulphate salts (not more than 2%), and insoluble organic matter (not more than 5%). Figure 6.10 schematically presents the use of local materials for embankment dams, along with their basic physical and mechanical characteristics.

Water-impermeable earth elements (core, facing, upstream apron, vertical teeth) are made from low water-permeable materials, with a permeability coefficient of $k \leq 10^{-5}$cm/s. The best material for this purpose is clay with moisture close to the optimum or somewhat higher. The use of very wet or dried clay makes construction much more complicated and more expensive. In some cases, in the construction of water-impermeable elements, it is also possible to use an artificial mixture of clayey, sandy and gravel earth, made up on the basis of experimental investigations.

The shells of the earth–rock and the body of rockfill dams can be made from natural coarse-grained material – alluvial gravel which is, after Casagrande, the best "rock-fill", but usually crushed stone of igneous, sedimentary or metamorphic rocks have to be excavated from quarries. For the assessment of the quality of local coarse-grained materials, its petrographic composition, physical and mechanical properties and chemical composition are essential (Vallejo, 1995). Strong and durable rock fragments of the size of gravel and cobbles should be used, which do not experience crushing of grains during their transport and during tipping of the material from a height. The

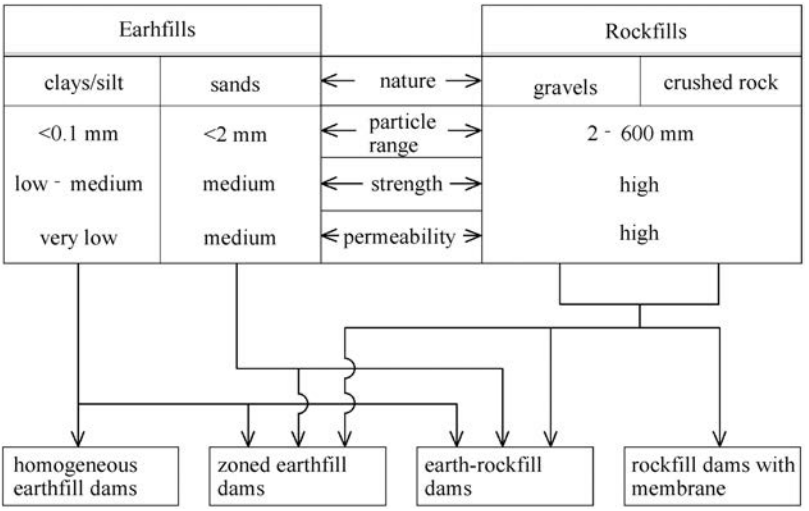

Figure 6.10 Use of local materials for embankment dams (after Novak et al., 2001).

rockfill material must be well graded, and excellent material for dam construction has the following grain size distribution:

- not more than 5% below 5 mm;
- not more than 30% below 20 mm;
- maximum particle size 600 to 1000 mm, depending on the rock strength and the tendency towards particle breakage; the maximum dimensions of the grains depend also on the methods of construction, as well as the available plant and equipment.

The ratio of the biggest to the smallest dimension of the grain should not be greater than 3–4, while grain size composition should be homogeneous, in order to prevent disintegration of the material during its filling and also in order to obtain as high compactness after placement as possible. The maximum size of grains should not be larger than ½–$^1/_3$ of the thickness of the compacted layer. The parts of the dam's body, which are permanently or occasionally under water, should be constructed of materials that are stable in water, that is to say materials having a minimum 0.9 coefficient of softening for igneous and metamorphic rocks and 0.8 for sedimentary rocks. It is often possible to use materials not only from quarries, but also from the sites of the excavations for subsoil parts of the structures within the hydraulic scheme. In so doing, it is necessary to provide a selective distribution of the materials in the cross-section of the dam. The finer and weaker materials are placed in the internal zones, while the coarse-grained and strong materials in the external ones (Stephenson, 1979). The permeability of competent rockfill material should be high, that means at least 10^{-2} m/s. Thus, it is free-draining and, therefore, no problems arise with pore pressure, both under static and dynamic loading. Generally speaking, the rockfill has high shear

strength, which may be reduced by submerging in water, by breakdown at high stresses and due to latent fractures in the rock fabric.

When such ideal rockfill material is lacking, a lot of dams have been built of rockfill material with non-ideal properties. It is a task and a challenge for the designer to adapt his design to the properties of available materials and to make use of them with the aim of achieving safety over the lifetime of the structure. More examples of rockfill dams made of different types of rockfill are discussed in appropriate chapters of this book.

For the construction of the transitional zones, filter zones and subsoil drains, sand, sandy gravel, gravel and stone gritting material is used in certain fractions (Khor & Woo, 1989). The materials should be resistant to the mechanical action of water and, in the case of need, frost resistant. The grain size composition of the materials for particular transitional or filter zones is determined by means of calculations, starting from the condition that the seepage resistance in the contact of the adjacent materials should not be endangered. If the grain size composition of the available natural materials does not comply with requirements, then it is necessary to carry out its improvement by sorting, washing up, adding up various fractions of another material, or else we can use crushed and separated material. Such material is usually 2–3 times more expensive than the natural material which is placed in the dam body or in the waterproofing elements (Singh & Varshney, 1995).

For the protection of dam slopes against the action of waves and weathering effects, stone from igneous, metamorphic, or sedimentary rocks, which satisfy the requirements in relation to grain size, strength, and frost resistance, can be used. Unsorted stone is most often used (for economy), below which one or two transitional layers of gravel or sandy gravel are placed, which depends upon the kind of material from which the slope has been constructed.

In the case of cohesive materials that are placed in the dam's body, it is particularly important to obtain good compaction of the layers, which depends on moisture of material, and the plant and equipment used, as well as on the work spent on compaction. The relationship of the moisture, density of compacted material, and work done is tested by means of the Proctor compaction test, with which it is possible to obtain the optimum moisture; that is to say, the moisture at which maximum volume weight of the compacted material is achieved at a defined compacting effort. The laboratory compaction test is a basis for technical specifications for field compaction, and for quality control of compacted material in the embankment. In compacting sand, the moisture has a rather low influence upon compaction.

Tests for direct shearing and triaxial investigations are used for the determination of strength characteristics of earth materials for which standard methods and apparatus have been developed, as described in detail in the textbook references on soil mechanics.

Much more complex and less investigated is the testing of strength characteristics of stone material used for filling, containing coarse grains, and having a diameter of even several tens of centimetres. In Croatia, some thirty-five years ago, by means of instruments for direct shearing, tests were carried out on samples having a thickness of 80 cm and cross-sections of from 1.0 to 1.5 m^2; however, owing to no uniform deformations and no homogeneous stress state, uncertain results were obtained.

An important move forward in this area was made at the commencement of construction of the El Infiernillo dam (Mexico), in 1960, when special equipment for

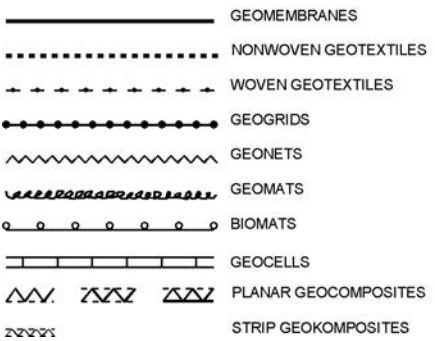

Figure 6.11 Symbols denoting geosynthetic materials.

testing samples of crushed rockfill was designed and manufactured. At the same time, various investigations were carried out, the most important being the one-dimensional compression test, which is carried out in an oedometer with a diameter of 50 cm and a height of 55 cm, with maximum possible axial stress of 3200 kN/m^2. The three-axial test on samples having large dimensions – 1.0 m in diameter, with confining pressures of up to 2.5 MPa – also have been performed (Marsal, 1973). To obtain sufficiently accurate test results, it is recommended that the smallest sample diameter of modeled rockfill material be 500 mm. Modeling to smaller sizes might omit the effect of particle edge crushing at high stresses, leading to increased shear strength of the modeled material in comparison to the original material.

The rockfill materials are, as a rule, large-grain-sized and cannot be handled in the laboratory. The grain size distribution of graded rockfill material as a whole must be simulated by particle mixtures which are reasonable in size for testing in a laboratory. The maximum particle size must be limited to 1/5 of the sample diameter of well graded material and about 1/10 of the sample diameter of poorly graded material. For the production of graded materials appropriate for testing, more details can be found in the literature, for example Kutzner, 1997.

Sometimes, "soft" rockfill material is available instead of material consisting of strong rock fragments. Such material may contain also sand, silt and clay. Consequently, such mixed material is not free-draining, and the shear strength is not as high as that of pure rockfill material. It is common practice in dam engineering, according to the saturated unconfined compression strength of the original rock, for rockfill material to be classified into *hard* (with saturated unconfined compression strength greater than 80 MPa), *medium strength* (30–80 MPa) and *soft* (less than 30 MPa). Soft rockfill materials are also used for dam construction, provided problems related to pore-water pressure elimination or decreasing are considered. Evretou Dam (Cyprus) is a typical example of this kind of large embankment dam. It is described in Chapter 11.

In addition to natural local materials, for certain structural elements during the construction of embankment dams, artificial materials are also used such as concrete, asphalt, geosynthetics, etc. Concrete is a well-known material, and the most important data on this material can be found in Chapters 16 and 18. Basic knowledge for asphaltic materials that are used in embankment dams is set out in Chapters 13 and 14.

Table 6.2 Uses of geosynthetic materials in embankment dams.

Diagram	*Use*	*Function*	*Spec. Requirements*	*Geosynthetic*
Fig. 6.11a	Horizontal drainage for reducing pore pressure	Separation, seepage, drainage	High resistance to pressure, high permeability	Geocomposites
Fig. 6.11b	Seepage, drainage	Seepage, drainage	High permeability, elasticity	Vertical striplike drainage
Fig. 6.11c	Drainage for lowering the seepage line downstream	Separation, seepage, drainage	High resistance to pressure, high permeability	Geocomposites
Fig. 6.11d	Drainage behind diaphragm for collecting and detecting infiltration water	Separation, seepage, drainage	High resistance to pressure, high permeability	Geocomposites
Fig. 6.11e Fig. 6.11f	Drainage below facing for preventing uplift at abrupt lowering of water level	Separation, seepage, drainage	High resistance to pressure, high permeability	Geocomposites
Fig. 6.11g	Drainage of infiltrating water through concrete	Drainage, seepage	Good mechanical properties, small openings	Geocomposites
Fig. 6.11h	Separation of earth materials at a zoned dam	Separation, seepage	Resistance, good tensile strength, good conductivity	Geotextile (woven or non-woven, geomesh
Fig. 6.11i	Reinforcing the slopes for strengthening	Reinforcement of earth	High tensile strength, friction	Geogrids, woven geotextile
Fig. 6.11j	Reinforcing the foundation for reducing the settlement	Soil stabilization	High tensile strength, friction and/or retaining	Geogrids, woven geotextile, geocells
Fig. 6.11m	Reinforcing the foundation for the case of locally unstable layer	Effect of membrane	As the previous case	Geogrids, woven geotextile
Fig. 6.11n	Stabilization of clay facing	Reinforcing	As the previous case	Geogrids
Fig. 6.11o	Impermeable facing	Water impermeability	Mechanical resistance	Geomembranes
Fig. 6.11p	Impermeable blanket	Water impermeability	Mechanical resistance	Geomembranes
Fig. 6.11q	Vertical low permeable element	Water impermeability	Vertical joints	Geomembranes
Fig. 6.11r Fig. 6.11s	Diaphragm–straight or zigzag one	Water impermeability	Mechanical resistance, good friction	Geomembranes
Fig. 6.11t	Heightening of a dam	Water impermeability	Mechanical resistance	Geomembranes
Fig. 6.11u	Bedding for protective layer on the slope	Separation, protection	Good mechanical and UV resistance	Non-woven geotextile, geomesh
Fig. 6.11v	Stabilization of a layer of gravel on the slope	Reinforcing connectibility	High tensile strength,	Geogrids
Fig. 6.11w Fig. 6.11x	Slope protection with long sacks filled with concrete or gravel	Retaining, seepage, separation	High tensile strength, openings appropriate for concrete or gravel	Woven geotextile, (concrete), geogrids (concrete), geogrids
Fig. 6.11y Fig. 6.11z	Protection of the downstream face (erosion)	Control of erosion	Good connectibility, perm. earth cover	Geomats, biomats, biocells

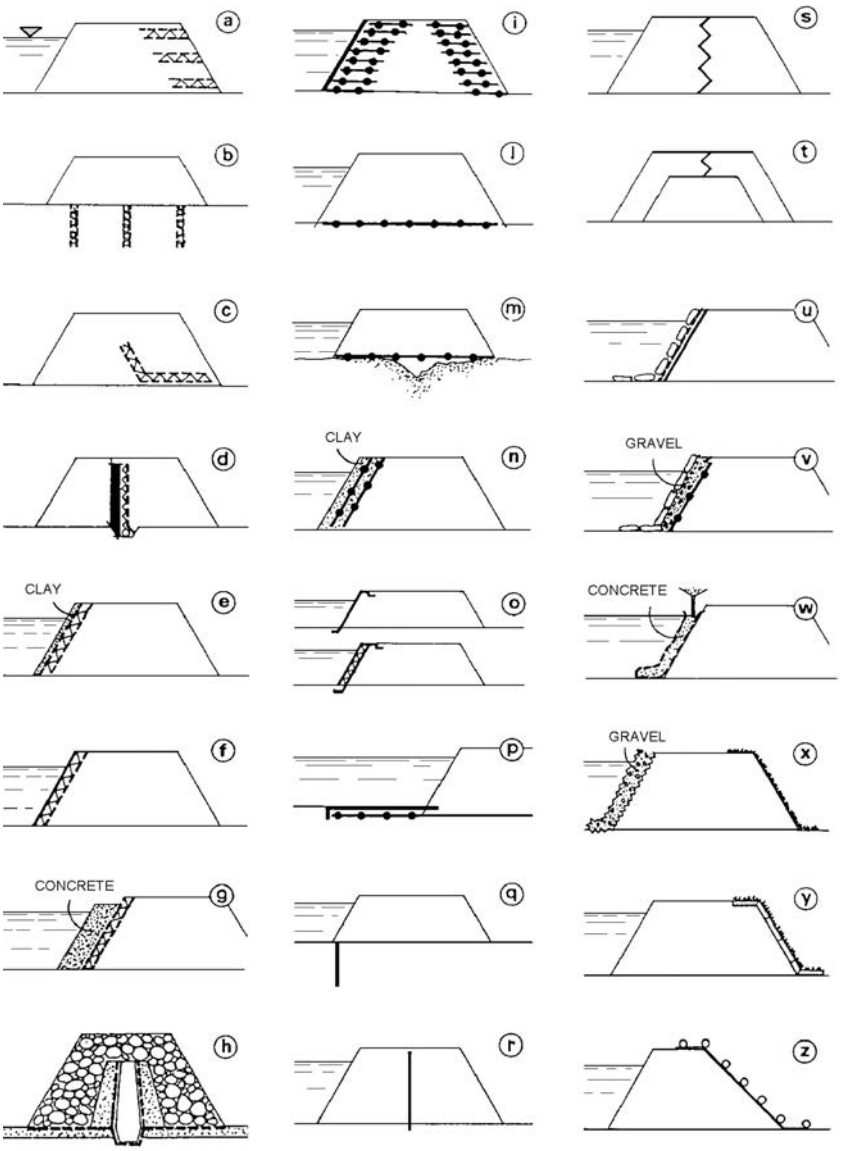

Figure 6.12 Uses of geosynthetic materials for embankment dams (after Cambiaghi & Rimoldi, 1991).

Here we shall dwell for a while on the subject of a relatively new material, *geosynthetics*, which finds increasingly wide use in practice. The first geosynthetics material – *geotextile* – was used more than fifty years ago in the well-known Delta-Project in the Netherlands. Towards the end of the seventies, *geomembranes* were developed – a new material, and in many situations an effective water-impermeable material. Later on, other kinds of geosynthetics appeared, so that today in civil

engineering a wide range of these products is used, mainly for the following objectives: *filtering, subsoil drains, separation of layers, protection of earth layers against damage, as waterproofing elements, for preventing erosion, for reinforcement and stabilization of earth, for reinforcing asphalt layers, for faster consolidation of thick layers by means of accelerated drainage* (Cambiaghi & Rimoldi, 1991; Giroud, 1989; Eadie & McGregor, 1988; Fell et al., 1992; Pilarczyk, 2000; Radchenko & Semenkov, 1993, ICOLD 2010). Figure 6.11 presents the international markings for geosynthetic materials, which are most often used in civil engineering. The application of geosynthetic materials in embankment dams, which has been more and more intensified in the last twenty years, is schematically represented in Figure 6.12, along with a description in Table 6.2.

6.6 CHOICE OF TYPE OF EMBANKMENT DAM

In designing hydraulic schemes including an embankment dam, one of the most important and most responsible tasks is the choice of the type of the dam, upon which to the greatest extent depend the economy of the hydraulic scheme, the speed of construction as well as the conditions for use. Two main factors dictate the choice of an optimum type of dam for a given dam site: *the technical justification of the solution* and *the cost*. In some instances the possibilities that are available are extremely limited, so that the choice of the type of dam is a simple matter; however in most cases it is possible to use a number of types – not only embankment ones, but also concrete dams. In such cases, extensive studies are more or less essential, through which, by comparing the possible variants, it is possible to come to an optimum solution. In the further presentation of the material, the subsequent chapters will also deal with the conditions for the applicability of particular types of embankment dams. In continuation, those conditions will be summarized and amended (Tančev, 1982, 1992; Bridle, 1988).

The use of homogeneous earth dams is limited to small (as well as low and medium height) dams at locations in whose immediate vicinity there are sufficient quantities of low-water-permeable earth material. In more numerous cases, when in the construction of large earth, earth–rock and rockfill dams, a water-impermeable element is also constructed in the form of a core, facing, or diaphragm wall made of cohesive earth material or of artificial material, the following factors influence the choice of waterproof element:

1) *Presence of local materials in the vicinity of the dam site*. The presence or absence of earth material in the vicinity of the dam site is of decisive importance in choosing the type of embankment dam. If there is no earth material at an economical distance, it is normal to consider a rockfill dam with a watertight element made of artificial material.

   Uniformity of the available earth material can also influence the choice of dam type. For instance, if the borrow pit is rich in, and yields two kinds of, earth material, then a zoned earth dam could be constructed, along with vertical and horizontal drainage, in which the material having a lower content of fine particles would be placed downstream of the vertical drainage.

Rock is a very suitable material for the construction of a dam body. That is why if it is available at an economically justifiable distance, it has a significant influence upon the choice and type of embankment dam. This is especially the case if there exist conditions for the utilization of rock material from the excavation for the foundation, as well as from the execution of appurtenant hydraulic structures.

The availability of filtering material also plays a significant role. Owing to the strict conditions that are required for filtering zones, it is often the case that the material must be brought from a considerable distance (even from as much as 50 km), or else in the case of very large dams, the necessity may arise for installing plants for separation and production of aggregate with specific properties. In the case of existence of special difficulties for providing appropriate filtering material, priority could be given to rockfill dams with a waterproof element made from artificial material.

2) *Climatic conditions in the area of construction*. In rainy regions and in general in areas with a short construction season, embankment dams with a facing have an advantage, the facing being built following completion of the dam's body. In the course of filling there would be no breakdowns as is the case with earth cores, the construction of which requires favourable climatic conditions, as well as optimum moisture of the material. From that point of view, characteristic are examples of dams constructed on high mountain grounds, having an asphalt facing, or else a diaphragm wall.

3) *Geological conditions in the foundation*. Embankment dams can be constructed on various foundations. Hard and sound rock in the foundation is an ideal condition for the construction of a rockfill dam with a reinforced concrete facing. In such a case, the slopes can be constructed with a maximum inclination, since there is no danger of forming a plane of slippage in the foundation. In such a way the main advantage of a facing comes to the fore – a complete utilization of strength at shearing of the rock material in dam's body, which means savings in the volume of the dam; whereas an earth core would require more moderate slopes. In more adverse geological conditions, in addition to losing the above described advantage of facings, the problem of a longer and more complicated joint between the facing and the foundation is also emphasized. In such a case, the solution with a core made of local material is imposed.

When making the choice of a dam type, one should take into consideration that the theoretical value of the maximum stress in foundation that is caused by an earth–rock dam, that is to say by a rockfill dam 100 m high, amounts to 1.8–2.1 MN/m^2. This is lower in relation to any type of a concrete dam (a gravity concrete dam, 100 m high, causes stress having a maximum intensity of 3.2–4 MN/m^2, a buttress dam 5.5–7.5 MN/m^2, while an arch dam even up to 7.5–10 MN/m^2).

4) *Topographical conditions at the dam site*. If a narrower site has been chosen for the dam, the topography of the ground could be of primary significance. If the upstream end is a long and excessively broken line, then it is very likely that the variant with a facing will be eliminated owing to the expensive foundation, especially if a deep grout curtain is also to be constructed.

In connection with the conditions cited under 3 and 4, it is important to emphasize that the deposit in the dammed profile also influences the choice of dam type.

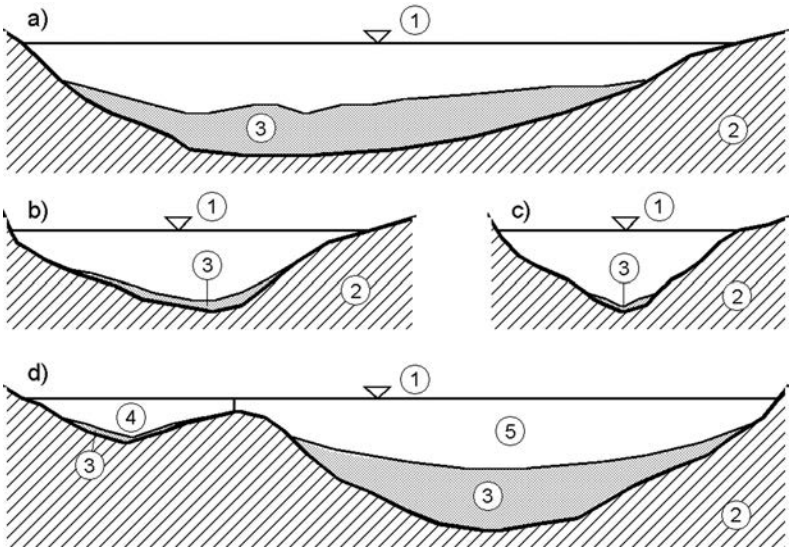

Figure 6.13 Influence of the sediment thickness and the profile form. (1) Crest of the dam; (2) sound rock; (3) sediment; (4) concrete part; (5) embankment part.

That influence, in connection with the shape of the dam site where a foundation of sound rock is concerned, is illustrated in Figure 6.13. In the case of a wide dam site, with a thick layer of deposit that is 5 to 10 metres or more, Figure 6.13a would be more apt when it does not pay to remove the large quantity of deposit material and when deformations to be expected in it would be significant; then, an earth dam would have the advantage.

A well-compacted layer of sediment with a favourable grain size composition could also sustain another type of embankment dam; that is to say, an earth–rock dam or a rockfill dam. In the case where the sound rock is at a small depth below the sediment material, and the dam site has a significant or moderate width such as in Figure 6.13b, a rockfill dam or an earth–rock dam have the advantage, when there is suitable stone material, or a cohesive earth material. When such materials are not available, then the choice will be between a gravity concrete dam and a buttress dam.

A narrow dam site on sound rock with a thin layer of sediment is illustrated in Figure 6.13c. Those are typical conditions for the application of an arch concrete dam. Economic analyses could give an advantage to one of the alternatives – an earth–rock dam, or a rockfill dam.

A location plan, illustrated in Figure 6.13d, with a thick layer of sediment at one part of the dam site, and a thin layer at the other part, may suggest a combined type of dam: an embankment dam at the part having a thick layer of sediment, and a gravity concrete dam (completely or partially overflowing), at the other part.

5) *Influence on the environment*. In principle, different types of embankment dams have similar effects on the environment. An exception is the borrow area for local materials, especially for cohesive soil, which very often is located near a village. The excavation of large quantities of earthen material can strongly affect the environment. In addition, the long transportation of such material also can have negative consequences for the environment. Such conditions can impose the solution of a dam with an artificial waterproof element, despite the availability of cohesive material.
6) *Transport conditions in the area of construction*. A good linking of the area of construction with industrially developed areas, especially by means of a railway line or waterway, enables relatively cheap transport of artificial materials. That imposes a consideration of the alternative with a facing or a core (diaphragm wall) made of artificial materials.
7) *Qualification and technical fitness of construction companies*. The qualification of the work force and how well equipped it is, as well as the possibilities of a supply of special plants and equipment, could contribute to resolving the dilemma as to the type of waterproofing element. Concrete facings and diaphragm walls are complicated to execute, while asphalt ones are simple; they, however, require special plants and equipment. Plants and equipment for the execution of earth works is most widespread in construction companies.
8) *Period of construction*. The time limit for construction could give an advantage to facings and, possibly, to cores made of artificial material. The advantage is especially emphasized in the case of long embankments, as well as embankments enclosing large storage reservoirs.
9) *Height of dam*. In the case of particularly high dams, experience with cores made of local materials are so favourable that, for heights greater than 150 m, this type is dominant in practice, together with the reinforced concrete facing dams.
10) *Function and regime of work of the impounding reservoir*. By using facings or cores made of artificial materials, it is possible to accomplish high water impermeability ($k = 10^{-9}$ up to 10^{-12} cm/s). That is significant for hydraulic storage lake basins in which water is more expensive; therefore, losses due to seepage should be reduced to the lowest possible measure. If the storage lake is often emptied, that could be an advantage for the facings because of their accessibility for inspection.
11) *Possible deformations and occurrences of fissures*. During the construction period, and especially during the service period, deformations occur at embankment dams, whose size and direction depend on a number of factors, among others on the type and position of the waterproofing element and composition and size of transitional zones. Possible deformations should be as much and as precisely anticipated as possible even when choosing the waterproofing element, in order to avoid unforeseeable problems during the service period. In general, deformations are manifested in three forms: (1) *settlement* (vertical displacement); (2) *deflection* (displacement perpendicular to the axis of the dam); and (3) *lateral displacement*.

Vertical settlement begins even during the dam's construction. It becomes intensified during the early years of the service period and most often continues in the course of some ten years. It usually reaches a total value of up to 1% of the dam

height; however, there are cases in which it could be considerably larger. That is why it should be as precisely assessed as possible for each specific case, because in the contrary case, it could lead to an incorrect choice of waterproofing element.

12) *Stability during an earthquake*. Embankment dams, if they have been well designed and constructed, are also safe in relation to the action of strong earthquakes. That has been confirmed by experience with a number of such structures, carried out in seismically active areas – Japan, California, Turkey, Tajikistan, etc.

During an earthquake, there is additional settlement of the embankment in the body of the dam, as well as deformations in its slopes, in which the lower parts are usually elevated. In the case of earth–rock dams, there are two factors which are unfavourable during the action of an earthquake: (1) the zones of different material behave differently during the tremor and so this leads to an interaction in the contact surface; (2) pore pressure occurs in noncohesive materials that are waterlogged, such as sand and gravel, as in the case of fine sand liquefaction, that is to say a losing of its load-bearing capacity (see Chapter 9 for more details on this matter).

These occurrences do not appear in rockfill dams having a facing made of artificial material. In the case of possible fissuring of the facing, the consequences could be more troublesome than during occurrence of fissures in the core. That is why, whichever type of dam is to be built within a tremor area, it is necessary that all of its elements be appropriately dimensioned for the action of seismic forces.

13) *Stage construction*. It is often economically justifiable to construct the dam in two or more stages. This is most often the case with dams that are intended for water supply, irrigation and hydraulic power engineering, when requirements in the early years of service could be satisfied with a lower dam; that is to say, with a smaller storage lake. If staged construction has been anticipated, then the advantage goes to rockfill dams with a rather inclined core, and earth dams and rockfill dams with a facing. There are also cases where a combined waterproofing element is used during staged construction.

6.7 TAILINGS DAMS

6.7.1 Definition and general features

Tailings dams, as defined in Chapter 1, are used for forming space for depositing waste material that originates from certain industrial or mining processes. Tailings are the fine particle residues which arise from the processing of various materials. The majority are produced by the processing of minerals to recover the economically valuable minerals. Their fine particle size may be the natural size of the waste fraction or, more commonly, it is caused by crushing and grinding of rock to fine sizes. Then, the material of value may be removed by flotation or chemical processes. The remaining fine grained materials rejected at the end of the process as worthless slurry are the tailings which have to be removed from the processing plant. In general the water content in the slurry is high enough to enable the tailings to flow away from the plant along channels or to be pumped through pipelines to sites suitable for their disposal.

The most economical solution to tailings disposal should be a balance between the cost of transportation, the cost of the site and the impact to the environment.

Because in the most cases the tailings have little or no economic value, they have to be disposed of safely as wastes, with the minimum impact to the environment. Possible methods are: economic utilization, discharge to rivers or the sea, underground disposal, dry disposal to land, and, most commonly, tailings impoundment structures. The latter method involves the construction of a retaining structure (dam), with the necessary associated elements, like inlet and spillway structures, drainages, filters and so on. The objective of the dam is to form a space for retention of the slurry and to allow the tailings to settle, thus enabling discharge or recycling of the slurry water and permanent retention of the tailings.

The ultimate aim of any tailings disposal scheme is that the tailings can safely be left in a condition that will required no maintenance to ensure their stability and thus are restored to a suitable subsequent land use and vegetation cover. Tailings dams have a number of features in common with water retention dams, but their purpose, construction techniques and operational conditions are different. In particular, the main differences are (ICOLD Bul.106):

- Tailings dams are designed to be abandoned and not operated.
- Construction is usually performed simultaneously with their operation.
- As a rule, they do not impound water for purposes other than sedimentation, reclamation and mill operation.
- In general, water retention is only incidental to their operation for the ultimate purpose of solid waste disposal; however, in some "closed circuit" schemes, where no discharge of water downstream is permitted for environmental reasons, some water storage may be required.

6.7.2 Classification of tailings dams

There are two main types of tailings dam:

– A conventional dam, as is used in water retaining hydraulic schemes, and
– A dam constructed by special technology, using the waste itself, originating from an industrial or mining process.

A tailings dam, when it is constructed as an ordinary water retaining dam – a concrete dam or an embankment dam – practically does not differ from dams used for the retention or storage of water. This type of structure is constructed where the storage space is to be utilized for both tailings and free water during the whole operational period, from the start of disposal of the tailings to the cessation of the use of the site. Necessary appurtenant structures for proper functioning of the scheme should be included. The main disadvantage of the application of a conventional dam as a tailings dam is the high cost of its construction.

Special technology of construction has been developed in cases when the waste itself, originating from an industrial or mining process, is used as a construction material. The application of this method is suitable and economical if the waste material contains a minimum 30–40% of sand. The use of tailings material is generally the

most economical construction method, but it has also some disadvantages, like: high susceptibility to internal piping, highly erodible surfaces, and high susceptibility of the fine tailings to frost action. Also, loose and saturated tailings are subject to liquefaction under earthquake shocks (see Chapter 9, section 9.3 and section 9.5, clause 9.5.4). During construction of the tailings dam, two major ways to improve these qualities are: use of coarse fractions of tailings and good compaction. The sand fractions, after being separated from the slimes, may be easy to compact using vibratory compactors. By compaction of this coarse fraction of the tailings, the end result is a dense mass of strong material that has greatly increased resistance to liquefaction.

6.7.3 Methods of construction of tailings dams

There are three methods of construction using tailings as construction materials for a tailings dam, depending upon the course, i.e. direction, in which the dam crest is displaced in its base plan, in the course of the process of the dam's growth (Thomas, 1976; ICOLD, 1989, 1996):

- Upstream method (Fig. 6.14a);
- Downstream method (Fig. 6.14b);
- Centerline method (Fig. 6.14c).

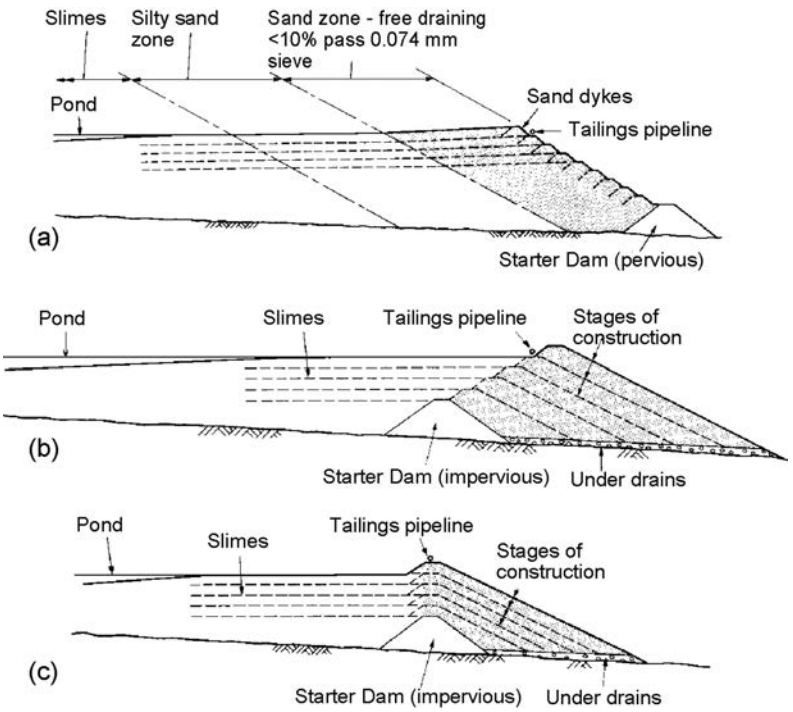

Figure 6.14 Tailings dams (after Thomas, 1976). (a) Upstream method; (b) downstream method; (c) central method.

All three methods anticipate first of all construction of an initial dam, which provides a starting space with sufficient volume for the commencement of sedimentation of the waste material; that is to say, space for the retention of water. The starter dam is similar to conventional dams, it should be capable of passing seepage water and the downstream portion should be resistant to piping.

In the case of the upstream method (Fig. 6.14a), the starter dam is located at the end of the forthcoming embankment, formed by means of the material laid down. Horizontal drainage zones may be installed during starter dam embankment construction to help maintain low pore pressure within the embankment.

The industrial (or mining) waste is transported through a pipeline, which is led over the crest of the starter dam and is provided with outlets (spigots), at intervals of $\approx$15 m, through which the material is discharged peripherally, usually from several outlets at the same time. Once the level of the deposited material has reached the crest of the initial dam, the process of construction of the dam commences from waste materials, upon which is placed the line of outlets from the pipeline. The waste material is discharged towards the downward face and is stockpiled by means of sedimentation. This deposition results in a dike and wide beach area composed of coarse material. The beach becomes the foundation of the next dike. In some applications, the dikes are mechanically placed and the discharge is used to build the beach only (in addition, slimes may be used to coat the upstream face of the dike to reduce permeability). These dikes can be built with borrow fill, or beach sand tailings can be excavated from the beach and placed by either dragline or bulldozer. Either way, some type of mechanical compaction of the dike is typically conducted before the next stage of the dam is constructed. This process leads to the formation of a slope, in which case the finer sand and silt is deposited further and further away towards the upstream face along with the flow of the mass towards the initial space. As a result, the density, strength, and permeability of the deposited solid material decline with the increase of the distance from the outlets. Once advancement reaches the upper end of the sand dike, a new dike is built and the process is repeated. The pipeline is progressively elevated with the construction of new increments of sand dikes.

Most often, instead of ordinary outlets, the tailings separation process employs hydraulic devices called cyclones (Fig. 6.15). They divide the waste mass into coarse and fine fractions. Thus, the whole process is carried out faster and more efficiently, so that the finer material is taken away further upstream behind the zone of sand.

The upstream construction method is the oldest and most economical method, but a single very important criterion for its application is that the tailings beach must form a competent foundation for the support of the next dike. After Vick (1990), as a general rule, the discharge should contain no less than 40 to 60% sand, which is limiting factor for the application of the upstream method. Other limiting factors for the application of this method could be: grain size distribution of the tailings, phreatic surface control, water storage capacity, seismic liquefaction susceptibility and the rate of dam raising. Tailings embankments constructed using the upstream method generally have a low relative density with a high water saturation. This combination can result in liquefaction of the tailings embankment in the event of earthquake. Therefore, upstream construction is not appropriate in areas with a potential for high seismic activity.

The downstream method is so named because subsequent stages of dike construction are supported on top of the downstream slope of the previous section, shifting

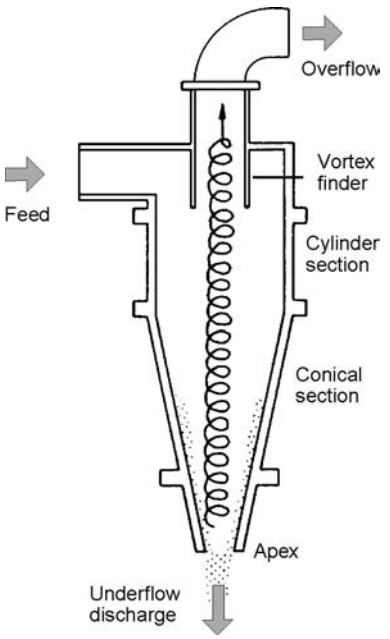

Figure 6.15 Diagram of a cyclone (after Fell et al., 1992).

the centerline of the top of the dam downstream as the dam stages are progressively raised. In this case the starter dam is located at the upstream toe of the forthcoming embankment. As in upstream construction, downstream construction also begins with a starter dam constructed of compacted borrow materials, however, this starter dam may be constructed of pervious sands and gravels or with predominantly silts and clays to minimize seepage through the dam. If low permeability materials are used in the starter dam, internal drains will need to be incorporated in the design. The sand, separated from the waste material, is laid downstream of the initial dam and advances progressively in presented stages (Fig. 6.14b). Drainage below the deposited embankment has an assignment lower down the seepage line. Other drain types can also be incorporated into the design. For example, an inclined chimney drain near the upstream face of the dam (5, Fig. 6.16a), and connected to a blanket drain (4) at the dam base, may be installed with each successive raising of the embankment. Cyclones are always being led along the last crest, discharging the coarser material downstream in thin layers, and the finer material (silt) upstream. For this kind of construction, mechanical compaction of the sand is often carried out. Due to the ability to incorporate drains into the design, this method of construction is well-suited to conditions where large volumes of water may be stored along with the tailings solids. One can conclude that the design requirements for the downstream method of construction of tailings dams are similar to those for conventional water storage dams.

The downstream method of construction provides a rather higher degree of stability comparing to the upstream construction method due to the ability and ease of compaction, the incorporation of phreatic surface control measures and the fact that

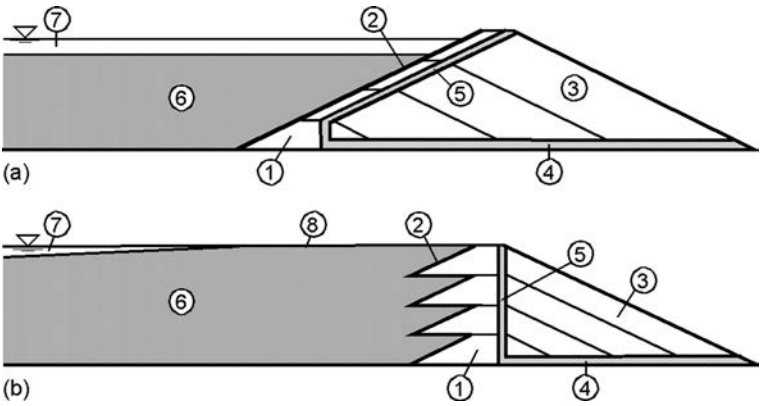

Figure 6.16 Downstream (a) and centerline (b) method of construction of tailings dams. (1) Starter dam; (2) impervious zone; (3) sand dam, constructed in stages; (4) base drainage layer; (5) chimney drain, constructed in stages; (6) slimes; (7) pond (or pool, area of supernatant liquid in the impoundment); (8) beach.

the dam raises are not structurally dependent upon the tailings deposits for foundation strength. A main disadvantage of this method is the large volume of fill material required to raise the dam. The increased volume of fill required can significantly increase the cost of this method of construction if the tailings from the mill cannot provide a sufficient volume of sand. Embankments constructed with downstream raises also cover a relatively large area, which can be a major disadvantage if available space is limited (Vick, 1990).

The centerline method (Fig. 6.14c) is a variation of the downstream method, noticing that here the crest of the dam remains in the same position in the plan, so that the upstream limit of the sand zone is practically vertical. As in both upstream and downstream construction methods, in the centerline method the construction of the embankment also begins with a starter dam and tailings are discharged from the crest of the dam to form a beach. The centerline of the embankment is maintained as fill and progressive raises are placed on both the beach and downstream face. The tailings placed on the downstream slope should be compacted to prevent shear failure. The centerline method of construction provides some of the advantages over the other two methods while mitigating some of the disadvantages.

As in the downstream method, drainage zones can be incorporated into the construction (4 and 5, Fig. 6.16b). A wide beach is not mandatory and this method is amenable for use with tailings that contain a relatively low percentage of sand. Thus, the dam raises may be added faster than in the upstream or downstream methods. Coarse gradation of the tailings is necessary if rapid drainage is required to provide support for construction equipment. Although this embankment dam type is not amenable to permanent storage of large volumes of water, shorter storage of water due to heavy precipitation events or mill shutdown will not adversely affect the stability of the dam.

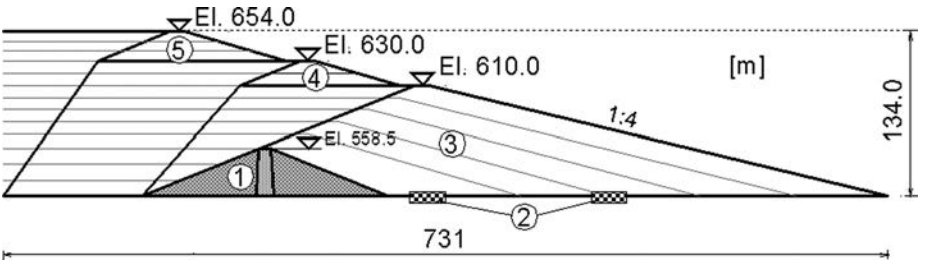

Figure 6.17 The cross-section of *Topolnica* tailings dam, R. Macedonia, constructed using the combined method. (1) Starter dam; (2) longitudinal base drainages; (3) first phase sand dam, constructed in stages using the downstream method; (4) second phase sand dam, constructed in stages using the upstream method; (5) third phase sand dam, constructed in stages using the upstream method.

Figure 6.18 Topolnica tailings dam, R. Macedonia (2012).

A tailings embankment dam, constructed using the centerline method, properly compacted and provided with good internal drainage, should be resistant to earthquakes. Even in the event that the slimes placed against the upstream slope liquefy, the central and downstream portions of the dam, if they are well compacted and have good drainage characteristics, may remain stable.

At the highest tailings dam in Macedonia, *Topolnica*, raised in the frame of the copper and gold mine *Buchim*, a combined method of construction was applied (Fig. 6.17). In the first phase the dam was constructed using the downstream method up to elevation of 610 m, when the downstream dam toe has almost reached the peripheral houses of the village Topolnica. Then, in the second and third phase (up to elevations of 630 and 654 m, respectively), the construction was continued using the upstream method. Currently, the third phase is in progress and the dam height reached 120 m

(the final height is planned to be 134 m (Fig. 6.17). Figure 6.18 shows the dam crest at an elevation some 14 m lower than the final one, with the beach upstream and a part of the downstream slope cultivated for prevention of aeolian erosion.

In the case of tailings dams, as in other dams, it is necessary to solve a number of problems. One of the most important problems is the accumulation and discharge of water. Namely, water comes along with the waste material, in an approximate ratio "water:waste material = 2:1". Moreover, consideration must also be taken of the natural inflow of the catchment area, which in some cases, could be quite significant. These factors have a vital influence on the choice of dam site and determination of the volume of reservoir space.

Another important aspect associated with this type of dam, already mentioned several times in this section, is the danger of the occurrence of *liquefaction* during an earthquake. This phenomenon, in former worldwide practice, has led to a number of disasters. Section 9.3 of Chapter 9 deals with the question of liquefaction.

More details on embankment dams intended for forming space for deposition of waste material can be found in textbooks (Vick, 1990; Fell et al., 1992), or magazines (Penman, 2003). ICOLD Bulletins: 45, 74, 97, 98, 101, 103, 104, 106 and 121 all deal with different aspects of tailings dams.

Chapter 7

Seepage through embankment dams

7.1 KINDS OF SEEPAGE THROUGH THE EMBANKMENT DAM BODY

In the case of embankment dams, seepage takes place through the body of earthfill dams, as well as through the waterproof element of earth–rock dams. We can distinguish permissible kinds of seepage, which are not dangerous for the structure if appropriate measures have been taken, and impermissible ones, which are dangerous for the stability of the dam as a whole or for its particular elements. Permissible kinds of seepage are:

1. *Stationary seepage flow* through the body of earthfill dams and the earth foundation (Fig. 7.1a) or the waterproof element (for instance, the core) of earth–rock dams (Fig. 7.1b), as determined by permanent boundary conditions (3) and (4) (unchangeable in the course of time).
2. *Non-stationary seepage flow with a variable boundary in the course of time, but with a constant volume of the porous medium.* Such a case appears, for example, in a sudden water drawdown in the impounding reservoir, from position (I) into position (II) (Fig. 7.2) when draining begins to take place from the pores of the poorly water-permeable material, at a change of the original highest seepage line in the course of time (Fig. 7.2a, b). In water-permeable material (2) with a sudden water drawdown in the reservoir, in practice simultaneous water drainage occurs.

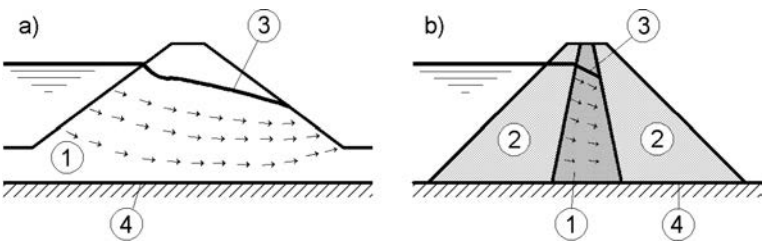

Figure 7.1 Stationary seepage flows through an earthfill dam (a), and through the core of an earth–rock dam (b). (1) Poorly water-permeable material; (2) water-permeable material; (3) upper boundary; (4) lower boundary of seepage flow.

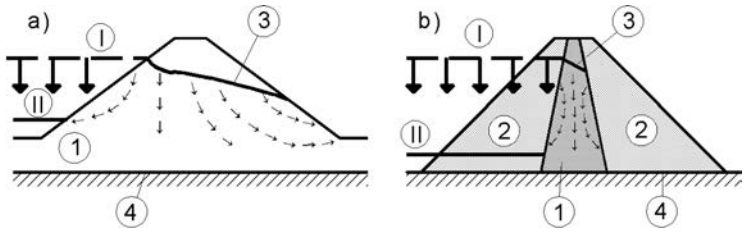

Figure 7.2 Non-stationary seepage flow in a sudden water drawdown. (1) Poorly water-permeable material; (2) water-permeable material; (3) original seepage line, variable in the course of time.

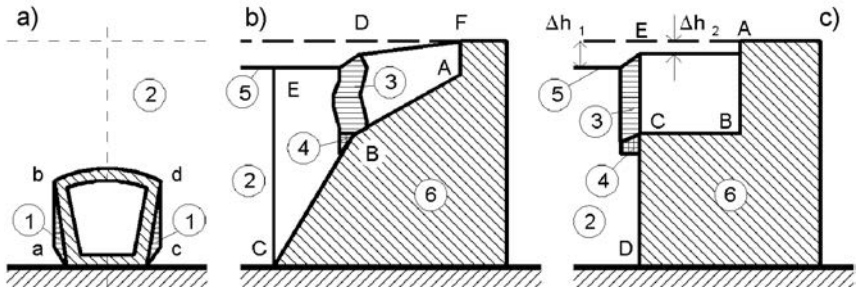

Figure 7.3 Forming of paths of concentrated seepage. (1) Fissures following settlement of the embankment (2); (3) incoherent soil; (4) seepage path; (5) surface of the settled embankment; (6) concrete wall.

3. *Non-stationary seepage flow in the case of a variable volume of the porous medium in the course of time.* The volume of the porous medium can vary in the course of time due to compaction of the clayey soil under the effect of loading or by compaction of incoherent sandy soil following the derangement of its structure, for instance, with some dynamic loading.

Earthfill dams are most often damaged or fail as a consequence of the creation of paths of concentrated seepage, originating immediately after construction. This could occur due to incorrect or negligent construction, because of errors in the design, or incorrect assessment of particular local conditions. Concentrated paths of seepage can also occur during service conditions of the dam owing to excess deformations of earth masses and the concrete structures that are connected with them.

Characteristic examples for the occurrence of impermissible seepage are:

1. *Incorrectly designed external contour of a concrete water-conveying structure in the dam body* (Fig. 7.3a). The external sides of the pipeline *ab* and *cd*, if they are inclined inwards, overhang above the embankment. Following settlement of the embankment (in the course of time) along the sides *ab* and *cd*, fissures will be formed (1) which represent ideal paths for the occurrence of concentrated seepage.

2. *Poorly designed joint of dam embankment with longitudinal concrete wall* (Fig. 7.3b). Side *AB* is relatively slightly inclined, while side *BC* is relatively steep. Earth massif *ABDF* during settlement comes across a friction resistance along surface *AB*, while massif *BCED* slides along the steep surface *BC*, as a result of which, in zone *DB*, it may lead to occurrence of a dangerous zone of poorly compacted earth – a potential path for concentrated seepage. Similarly, in the example shown in Figure 7.3c, in which it is evident that, owing to differential settlements to the left and to the right of line *DE*, it will lead to shearing of the earth material in zone *CE*. As a consequence, it can lead to formation of a concentrated seepage path.
3. *Incorrectly designed spillway structure over the dam*, in which case, following settlement of the embankment, a dangerous zone can occur immediately below the foundation of the concrete structure.

In Chapter 3 *mechanical erosion* was mentioned as one of the consequences of the seepage process through the body of embankment dams and through the foundations of both embankment and concrete dams. The mechanical erosion can initiate *piping*. Some characteristic examples for the occurrence of piping due to irregular contact of the fill material and concrete structures were given on the previous page.

In the case of a central core earth-rock dam there are mainly three processes which can initiate piping: *backward erosion*, *concentrated leak* and *mechanical suffusion*. *Backward erosion* is initiated at the exit point of seepage and the erosion gradually progresses backward forming *a pipe*. *Concentrated leak* initiates a crack or a loose soil zone emanating from the source of water to an exit point. Erosion gradually continues along the walls of the erosion hole intensifying the concentrated leak. *Suffusion* is the process whereby the fine particles of the soil wash out or erode through the voids formed by the coarser particles. This can be prevented if the soil has a sound grain-size distribution, with sufficient small voids. If suffusion takes place, then soil is called *internally instable*. The soil is *internally stable* if the seepage flow does not erode particles. Possible models for development of failure by piping at an earth-rock dam with a central core are presented in Figure 7.4A and B (adopted from Foster, 1999).

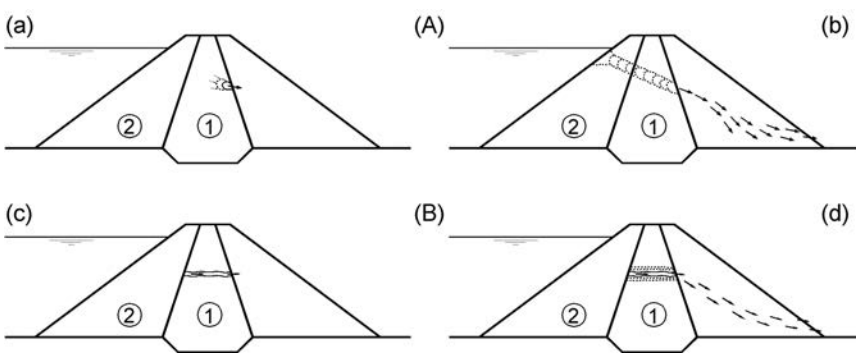

Figure 7.4 Possible models for development of failure by piping at an earth-rock dam with central core. (A) Backward erosion piping; (B) concentrated leak piping; (1) low-permeable earth material; (2) highly-permeable material.

Figure 7.4A shows the existence of leakage on the downstream core side and initiation of backward erosion piping (a). Then the backward erosion continues and progresses to form a pipe (b), leading to the formation of a breach mechanism. Figure 7.4B shows the model of concentrated leak piping. Firstly, the erosion is initiated through the crack or hole in the core (c), then the erosion continues, enlarging the hole as well as the concentrated leakage (d), with as a final consequence formation of a breach mechanism. Depending on the type of foundation, in some cases piping can also occur through the foundation and from the embankment into the foundation. Measures for prevention of the internal erosion are described in section 7.3.

7.2 SEEPAGE LINE AND HYDRODYNAMIC NET IN EMBANKMENT DAMS

In order for it to be possible to analyse the seepage in the body of an embankment dam, first of all it is necessary to determine the position of the seepage line following the establishment of the stationary flow, which represents an upper boundary line of motion. There are a number of methods for its determination, but the method of Arthur Casagrande is most often used, which will be shown in the example of a homogeneous earthfill dam (Fig. 7.5). Casagrande approximates the seepage line with a parabola whose focus is at point A. If m denotes the distance from the upstream end of the dam to the projection on the horizontal of the point of contact between the water and the dam, then the intersecting point of the theoretical parabola and the water level is 0.3 m away from point B. The equation of the parabola in polar coordinates is as follows:

$$\rho = \frac{y_0}{1 - \cos\theta} \tag{7.1}$$

where ρ = radial distance from the focus to an arbitrary point on the parabola, θ = the angle that is formed between the radial line and the axis of the parabola, in this case the x axis.

Parameter y_0 can be determined graphically if we draw a circular arch with a radius $R = AB_2$ and a centre at A, to the x axis, as has been shown on the diagram. Now, one can also obtain other points of the parabola by replacing $\theta = \alpha$, D ($\theta = 90$ deg), and E ($\theta = 180$ deg). In order to obtain the actual seepage line, it is necessary to carry out certain adjustments to the entrance and the exit part. Namely, the beginning of the seepage line must be at point B, at a right angle in relation to the slope of the dam, since it is the intersection of a flow line of motion and an equipotential line. Immediately afterwards, the seepage line tangentially connects with the theoretical parabola and goes on along it. On the downstream slope, it comes out not at point C_0, but somewhat lower, at C, at which the abandonment of the theoretical parabola and the joint with the dam slope is done tangentially. The distance Δa, according to the markings on Figure 7.5, depends on the angle α and can be determined by means of the value $c = \Delta a/(a + \Delta a)$ and by using the expression (7.1) when replacing $\theta = \alpha$ and $\rho = a + \Delta a$, so that it will be:

$$a + \Delta a = \frac{y_0}{1 - \cos\alpha} \tag{7.2}$$

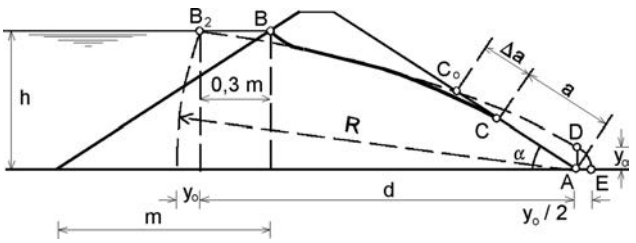

Figure 7.5 Determination of a seepage line.

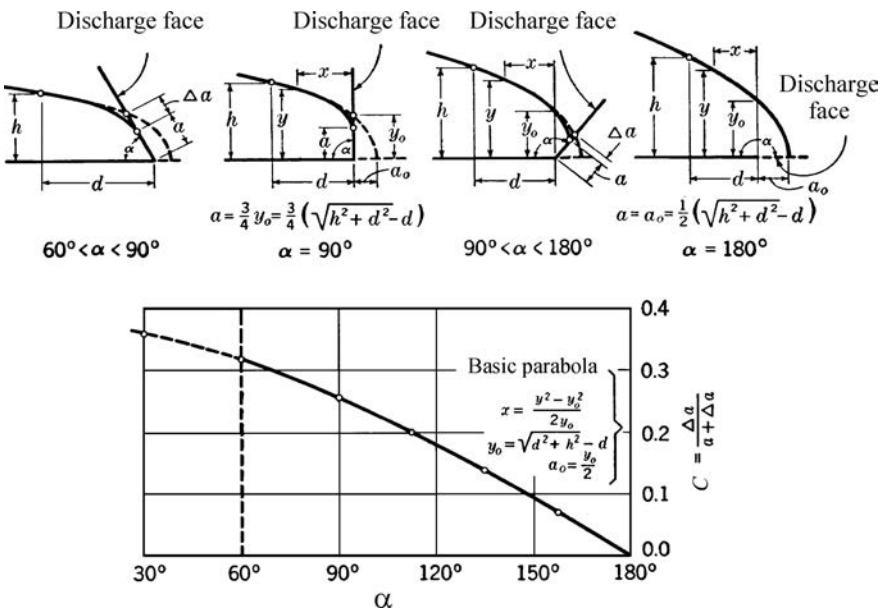

Figure 7.6 Diagram for determination of Δa (after Creager et al., 1955).

Figure 7.6 gives different schemes at the end of the seepage line, depending on the type of drainage at the end part and intermediate part of the earthfill dam (see Chapter 10). If it concerns an earth–rock dam, then the seepage line can be determined in the same way, of course only through the core. However, if it concerns a thin core, when $B/H < ½$, then the seepage line, owing to the short path on the downstream side of the core, moves down a little and can be drawn only by means of the entrance point and the exit point, obtained from the expression:

$$h_0 = \frac{0.65b}{1 - \tan\left(\frac{\pi}{2} - \alpha\right)} \tag{7.3}$$

according to the designations in Figure 7.7.

When boundary conditions are known, the hydrodynamic net through the body of an earthfill dam or through the core of an earth–rock dam for a stationary seepage

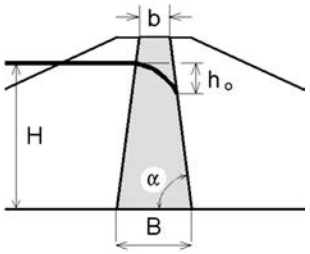

Figure 7.7 Seepage line in the case of a thin core.

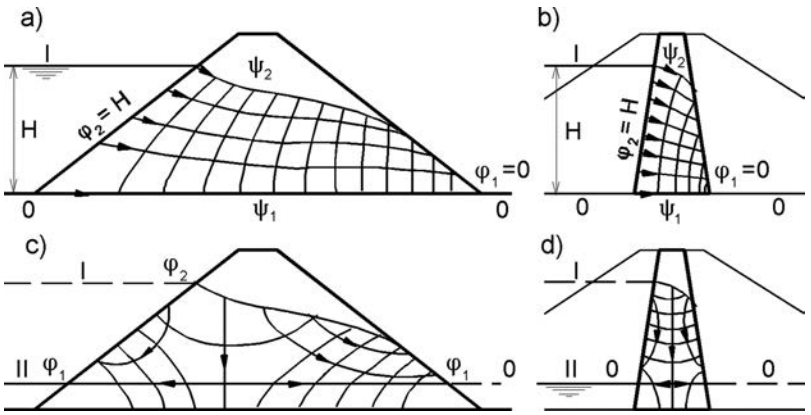

Figure 7.8 Hydrodynamic net through a homogeneous dam and through the core of an earth–rock dam.

flow can be drawn relatively easy, while adhering to the principles and rules laid out in section 3.5, as presented in Figures 7.8a and b. In the case of a non-stationary seepage flow, flow boundaries vary in the course of time, and so does the flow net or pattern. Figures 7.8c and 7.8d present hydrodynamic nets for the first moment, following the sudden drawdown of the water level from position I into position II.

In contemporary practice, the solution of problems connected with seepage through embankment dams is considerably facilitated, thanks to the application of the numerical methods (Kalkani, 1989), in the first place the finite element method. There are a number of software products in the world based on this method. Well-known software products dealing with seepage problems are the software packages SEEP/W (GEO-SLOPE, Canada), DIANA (TNO Company, The Netherlands), SVFlux (SoilVision Systems, Canada), among others. By means of these software packages it is possible to solve the simplest to the most complex stationary and non-stationary problems (taking into consideration anisotropy, nonhomogeneity, unlimited spreading of strata, etc.). The program automatically generates the seepage line, so that the methods for its determination for different kinds of embankment dams will appertain to the history. Working with these programs is relatively easy, since there is a possibility of automatic generation of the finite element mesh, clear assigning of the input

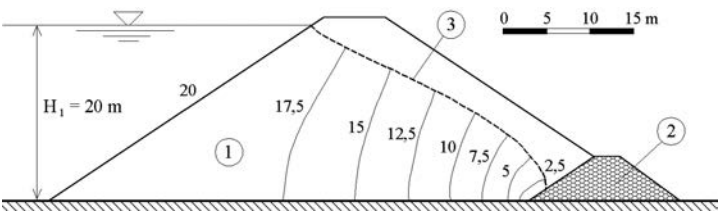

Figure 7.9 Equipotential lines (in metres) for a homogeneous dam on an impervious foundation for a stationary seepage flow, obtained by means of the finite element method using SEEP/W. (1) Dam's body of poorly permeable earth material; (2) drainage prism; (3) seepage line.

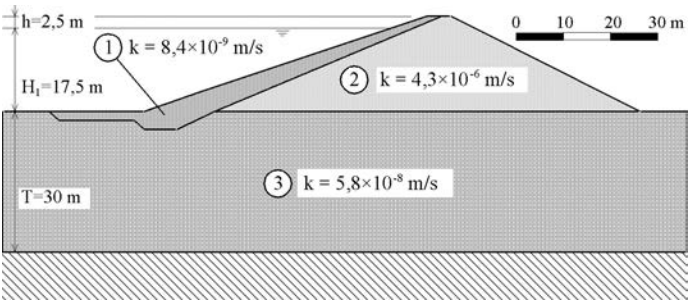

Figure 7.10 Cross-section of an analysed non-homogeneous dam.

parameters as well as an abundant analytical and graphical presentation of numerous output values. Of particular significance is the fact that the mentioned software packages can work together with other software packages (for analysis of stability, state of stresses-deformations, for transport of polluted materials, etc.), so that data obtained by the analysis of the seepage are automatically read into them as input.

As an illustration of solving the problems of seepage by using the above-mentioned programs, we will first of all quote a relatively simple example of stationary seepage flow through a homogeneous earthfill dam with a drainage prism founded on an impermeable foundation (Fig. 7.9). At a known geometry of the dam, water level, and coefficient of permeability of the poorly permeable material in the dam's body, the program generates the seepage line (3), and calculates the potential in the nodes of finite elements. Figure 7.9 shows the equipotential lines at an equidistance of 2.5 m, for a reference plane that coincides with the dam's foundation.

A more complex example of seepage under conditions of material non-homogeneity is presented in Figure 7.10. The dam, 20 m high, is constructed of permeable sandy material (2). It is founded on a relatively impermeable earth stratum (3), 30 m thick. As an impermeable element there has been anticipated a facing made of clay material (1), less permeable than the earth material in the foundation, which is extended in an upstream horizontal blanket for lengthening the path of seepage in the foundation.

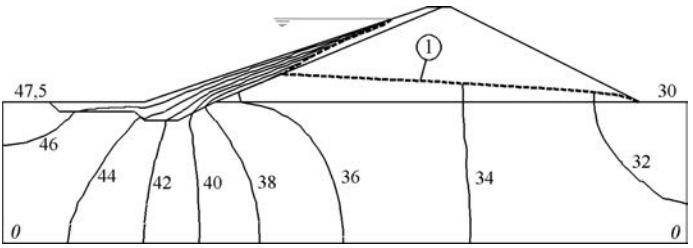

Figure 7.11 Equipotential lines (in metres) for the state of a filled reservoir (reference plane 0–0). (1) Seepage line.

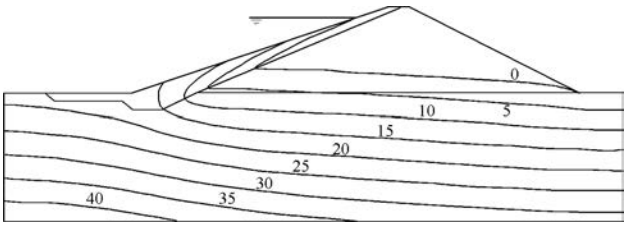

Figure 7.12 Contour lines of pore pressure for a filled reservoir (in metres).

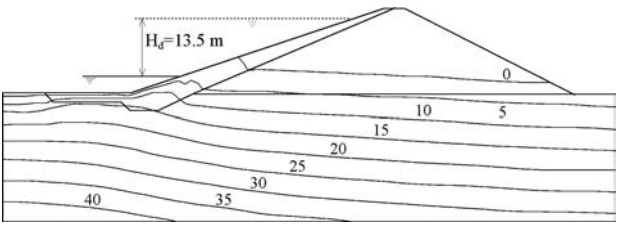

Figure 7.13 Contour lines of pore pressure for a sudden drawdown of water level (in metres).

With the application of software for seepage analyses, the complex problem can be successfully solved, seepage can clearly be perceived, and valuable data are obtained, essential for further analysis. For example, Figure 7.11 shows the equipotential lines for a state of established seepage flow for a filled reservoir. Owing to the great difference between permeability of materials in the dam's body and its facing, the seepage line (1) through the facing suddenly goes down, while through the dam's body it is not much raised above the foundation, with an exit at the downstream end. The equipotential lines are most densely concentrated in the most poorly impermeable material (in the facing), from which they extend continuously into the more permeable foundation.

Figure 7.12 presents the contour lines of pore pressure for the state of a filled reservoir, while Figure 7.13 does the same for a non-stationary seepage flow, following the drawdown of water level for 13.5 m (pressures are given in metres). Lowering of

the water level has been simulated in 10 increments, for a period of 11.5 days. From the above figures it is evident that, even with such a sudden drawdown of water level, pore pressure in the facing is dissipated to a great extent.

7.3 MEASURES AGAINST THE HARMFUL EFFECT OF SEEPAGE

One of the main objectives in designing and constructing earthfill dams consists of creating conditions under which the formation of concentrated seepage paths will be prevented and the danger of the occurrence of impermissible seepage deformations will be eliminated. In that respect, of the greatest importance is the action against local seepage rising, as well as internal erosion.

7.3.1 Action against local seepage rising

Local seepage rising through earth material can be caused by the effect of the force of uplift pressure F_w and the seepage force F_t, which are determined by means of the formulae (3.2) and (3.3). The basic measure for action against local rising of poorly water-permeable material is its loading with a layer of a cross-grained material – gravel or stone. Let us consider an earth layer, which is under the effect of vertical seepage forces F_t, and directed upwards (Fig. 7.14). In order to prevent rising of the earth volume $ABCD$, under the action of seepage forces, it should be loaded with a layer of coarse-grained material with a thickness y, determined by means of the equation:

$$\frac{1}{k_s}(y \cdot \gamma_k + d \cdot \gamma') = d \cdot F_t \tag{7.4}$$

where γ_k = unit weight of the coarse-grained material in a dry or submerged condition; d = thickness of the earth layer liable to rising; γ' = unit weight of the earth material in a submerged condition; and k_s = safety coefficient.

Another means of action against local seepage rising is the execution of drainage. Let us assume that the earthfill dam has been carried out on a relatively thin layer of clay, below which there is a layer of coarse-grained sand (relatively permeable material; Fig. 7.15). Let us analyse the loss of pressure along flow line $ABCD$. The loss of pressure at section BC through the permeable sand can be neglected, so that the loss of pressure will take place only on sections AB and CD. In each of them, there will be a loss of pressure equal to $0.5/H$, since pressure on the structure is equal to the loss of pressure along the entire length of any flow line, from the headwater to the tail water. In this way, the water level in the piezometers (1) and (2) will in practice be equal.

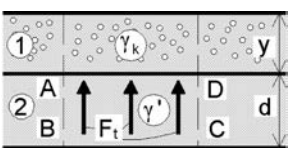

Figure 7.14 Measures against seepage rising. (1) Coarse-grained material; (2) earth material.

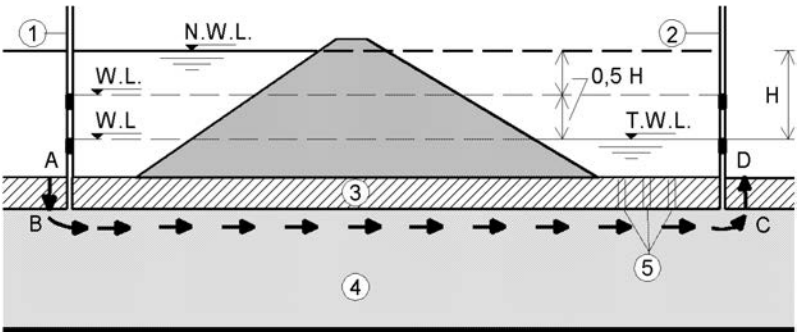

Figure 7.15 Action against seepage rising. (1), (2) Piezometers; (3) layer of clay; (4) sand; (5) drainage.

The thin clay layer in the tail water zone can be raised under pressure of seepage water (to the amount of $0.5H$). In order to prevent the occurrence of such a seepage deformation it is sufficient, in the area immediately downstream of the dam, to carry out vertical drainage (5). Having installed such drainage, there will be practically no loss of pressure on section *CD* of the flow line, while the water level in piezometer (2), as well as in piezometer (1), will go down to the level of the tail water. Total loss of pressure, equal to H, will take place on length *AB* of the examined flow line.

7.3.2 Action against internal erosion

What are called *inverse filters* (Fig. 7.16) are constructed as a protective measure against internal erosion. They consist of a combination of layers of earth or stone material with different grain size distributions. These filters are constructed at earthfill dams and at earth–rock dams, with the objective of preventing erosion of the earth material in the embankment and the foundation, which could occur under the effect of seepage forces in the dam's body, and the foundation. If these filters do not function satisfactorily, it may lead to a failure of the dam owing to erosion. That is why these filters are also called *critical filters*. This clause will consider construction and requirements regarding these filters.

More moderate are the requirements for the filters that are constructed upstream of the earth core in the case of earthfill dams and earth–rock dams, as well as below the protective layer of rock-filling across the slope of earthfill dams. These filters are called *non-critical filters* because, in quite a number of cases, their possible insufficient effective functioning does not endanger the stability of the dam.

The size of particles and grains of the material in particular layers increases in the direction of flow of seepage water. Filter layers are always constructed of water permeable material and must satisfy the following basic requirements:

1. Particles of the basic material, which is protected by means of the filters, must not penetrate into the pores of the first (adjacent) filtering layer; an exception would be only a small part of the particles, whose extraction cannot cause a more significant settlement of the basic layer;

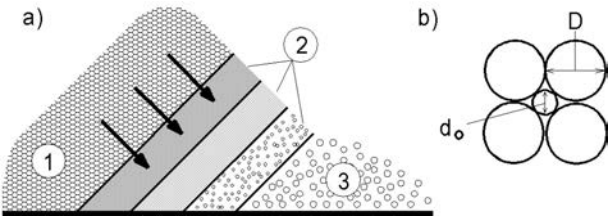

Figure 7.16 Schematic presentation of a filter (a) and a scheme for calculation of the filter (b). (1) Basic material; (2) filtering layers; (3) drainage.

2. Particles of any filtering layer must not penetrate into the pores of the next layer;
3. Particles of the last filtering layer must not penetrate among grains of the drainage that it touches;
4. Filtering layers must not lead to colmatation, i.e. deposition of sediments through the introduction of particles of the layer that is being protected; and
5. Filters must facilitate internal drainage of the seepage water, preventing an occurrence of increased pore pressure into the dam or the foundation.

For the first function, the filters should have sufficiently small pores in order to prevent the passage of particles from the core and to block the particles continuously, across the entire area of seepage, without local discontinuities.

Material for filters is obtained from borrow pits, as natural material, or else is obtained in particular fraction by means of crushing and/or by means of screening of local material. In designing the filters, it is necessary to determine the number and thickness of layers, as well as the required grain size distribution of each filter. The number of filtering layers, most often, ranges from 1 to 3. The thickness δ of the filtering layers depends on the conditions and methods of construction of the works and on the magnitude of the expected settlement of the filter foundation in the service period of the structure.

If there is not an anticipated settlement of the foundation, then the filters that are constructed between the basic low water-permeable material and the drainage should have a thickness of 20 cm, while it should be 50 cm for construction in water. If there is a possibility of settlement of the foundation, the thickness of the filtering layers significantly increases. The filters between the water impermeable element and the coarse-grained material in the body of earth–rock dams are most often made with a thickness of 3 to 4 m in order to enable unobstructed mechanized construction, even though for the performance of their function a thickness of 1.5 m would be sufficient.

The most important objective in designing filter protection is determination of the grain size distribution of particular filters, so that they should be able to fulfill the assigned tasks. The current practice in designing filters is mainly based on extension of the well-known concept proposed by Terzaghi. Its simple empirical criterion is conceived to meet the requirements in relation to water-permeability, and it has the following form:

$$d_{15}^{f} < 4; \quad \frac{d_{15}^{f}}{d_{15}^{0}} > 4 \tag{7.5}$$

where d_{15} and d_{85} are the diameters of the grains, of which 15%, or 85% respectively, are finer material, appropriate to the filtering and the basic material, depending on the index f or on 0. Terzaghi's criterion does not define the grain size distribution of the filtering material for a specific basic material. Therefore, sandy-gravel material that satisfies the criteria (7.5) can have a different grain size distribution and the following situation can occur: its permeability may differ a little from that of the basic material. Such a case has been noted at the well-known Teton dam (USA), whose failure has been a subject of detailed analyses. In addition to that, in the case of sandy-gravel materials with a wide grading which meet the criteria (7.5), there is a danger of the occurrence of discontinuities, which could lead to the occurrence of transverse fissures.

Authoritative institutions and experts have been trying to improve Terzaghi's rules, aiming also at establishing criteria for a more precise defining of the grain size distribution of filtering material. In contemporary practice, in designing filters, it is normal to distinguish two cases: (1) when a layer of incoherent material is protected, in which case we achieve a composite action of two adjacent materials, or else the last filtering layer is made composite with the drainage; and (2) when the cohesive material is made composite with the first filtering layer.

In the first case it is a question of non-cohesive materials and consideration can be given in the following way: let us assume that particles of the material, from some filtering layer or from the drainage, have the form of a sphere with a diameter D (Fig. 7.16b). Taking into consideration the stated conditions that filters have to meet, it is evident that the diameter $d$of the particles of basic material, which is being protected by the adjacent filter, should be such that the particles would not be able to get through pores with a diameter d_0, that have been formed among the grains of the filtering layer with a diameter D. The ratio D/d, that ensures geometric impassability of pores among coarse particles for fine particles with a diameter d, depends on the following factors: (1) A portion of the particles in reality do not have a spherical but an irregular form; (2) within the layers, grains have different sizes; and (3) in front of each relatively coarser pore, a vault of finer particles is formed.

The ratio $D/d = \xi$ is called *the interlayer coefficient* and, according to recommendations from textbook references, it should satisfy the following condition:

$$\xi \leq 10 \tag{7.6}$$

while simultaneously having met the condition of uniformity:

$$\eta \leq \frac{d_{60}}{d_{10}} \leq 10 \tag{7.7}$$

where d_{60} and d_{10} are diameters of the particles of the material, with a participation of 60%, or 10%, of the total mass.

If the seepage takes place from above downwards (Fig. 7.17a), then for ξ it is possible to permit even a larger value since, in such a case, there is additional resistance to the extraction of the particles of the finer-grain layer, exhibited by their mass. In the cases of smaller gradients of the pressure, such as in the case (b), the filter could also be left out (Sutherland, 1988).

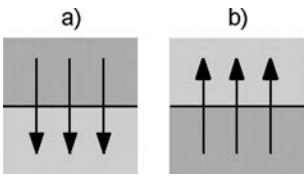

Figure 7.17 Different seepage directions.

In the latter case, when the cohesive basic material is being protected by means of a filter, the interlayer coefficient can be much greater than 10. For this purpose, as well as for filters protecting loose material, the USBR (USBR, 1977) method is widely used. Accordingly, it is:

$$d^f_{15} = (12 \div 40)d^0_{15}; \quad d^f_{50} = (12 \div 58)d^0_{50} \tag{7.8}$$

Two couples of points can be obtained in this way. By using them, it is possible to draw boundary lines of the grain size distribution of the filtering layer, while adhering to the following additional conditions: (1) Through a sieve of 0.074 mm, there must not pass more than 5% of the material in the filtering layer; (2) $d^f_{15} \leq d^0_{85}$; (3) the coarsest grains of the filter should not be larger than 70 mm in order to prevent segregation of the material; and (4) lines of the grain size distribution of the filter material should be approximately parallel to the line of the basic material.

The first member of the basic criterion (7.8) according to this method and the additional criterion (1), given above, make the filter more water-permeable than the basic material; the other criteria should make the filter effective in preventing erosion of the basic material.

If there is need of a second filter layer, then the boundary lines of its grain size distribution, for an assumed curve of the material in the first filter layer, can be determined by means of expressions analogous to equation (7.8):

$$d^{f_2}_{15} = (12 \div 40)d^{f_1}_{15}; \quad d^{f_2}_{50} = (12 \div 58)d^{f_1}_{50} \tag{7.9}$$

Experience with the application of this method indicates that it cannot be strictly applied for basic materials with very high clay content. Some authors (Fell et al., 1992) recommend when applying the USBR method, to ignore the criterion (4), and employ the rule of the US Corps of Engineers for the coefficient of uniformity:

$$\eta = \frac{d^f_{60}}{d^f_{10}} \leq 20 \tag{7.10}$$

Many incidents with embankment dams related to improper filter protection occurred up to the 1970s. Therefore, during the 1970s and 1980s prominent engineers investigated the problem of filter design, trying to improve the existing criteria, as well as develop new ones.

In 1967 a sink-hole appeared in the crest of Balderhead Dam (United Kingdom). The dam was designed in the late 1950s, and construction was completed in 1965. The reservoir was filled in February 1966 and remained full until April 1967, when a large sink-hole appeared in the crest. As an urgent measure, the reservoir was drawn down about 9 m when another sink-hole appeared. Study of the incident indicated that hydraulic fracturing of the broadly graded gravel-sand-silt-clay core and loss of core material by internal erosion into the filter had occurred. The fundamental purpose of the filter, to prevent the loss of the fine-grained core material even if cracking occurs, was not achieved at this dam. The problem was thoroughly investigated and a large number laboratory tests were performed, because at the time the Cow Green dam, belonging to the same owner and with similar embankment material properties, had just started construction. There was an urgent need to provide a filter that would prevent the loss of material even if a crack were to occur. As a result of the series of laboratory tests performed by Dr. Vaughan, criteria for so called "perfect" filter were given (Vaughan and Soares, 1982): *"The design principle adopted was to define a 'perfect' filter as one which will retain the smallest particles that can arise during erosion even if they arrive at the filter interface after complete segregation, unaccompanied by larger particles which would allow self-filtering to occur. At first sight, this principle appears to be impractical for clays, since a filter with sufficiently fine pores to retain the smallest clay mineral particles would itself be so fine grained as to be cohesive and subject to cracking in the same way as the core which it is supposed to protect. However, the combination of seepage water and clay chemistry is such that flocculation occurs, as is usually the case, then the finest particles which can arise are clay flocs".*

Well-known dam engineer J. Sherard expressed great interest in cracking, hydraulic fracture, and piping in embankment dams (Sherard, 1973, 1985). Especially important is his research work conducted in the Lincoln, Nebraska soil mechanics laboratory of the United States Department of Agriculture, over a four-year period (1981–1985), with results published in several papers. He stated that there is clear evidence that the impervious core of an embankment dam can crack and that a "critical" filter is required downstream of the core that will prevent the movement of soil particles from the core through the filter and, thus, will seal a concentrated leak. After extensive laboratory investigations, the "no erosion filter" test was devised, see Figure 7.18 (Sherard and Dunnigan, 1985). The investigations of Sherard and Dunnigan led to the following main recommendations:

1. For soils containing gravel, the filter should be designed on the grading of that part of the soil finer than 4.76 mm.
2. For fine silts and clays containing >85% (by weight) of particles finer than the 75 μm sieve, the allowable filter for design should have $d_{15}^{f} \leq 9d_{85}^{0}$.
3. For impervious soils – sandy silts and clays and silty and clayey sands – with 40 to 85% (by weight, of the portion finer than the 4.76 mm sieve) finer than 75 μm sieve, the allowable filter for design should satisfy the condition $d_{15}^{f} \leq 0.7$ mm.
4. For silty and clayey sand and gravels with ≤15% (by weight, of the portion finer than the 4.76 mm sieve) finer than the 75 μm sieve, the allowable filter for design should have:

$$d_{15}^{f} \leq 4\, d_{85}^{0} \tag{7.11}$$

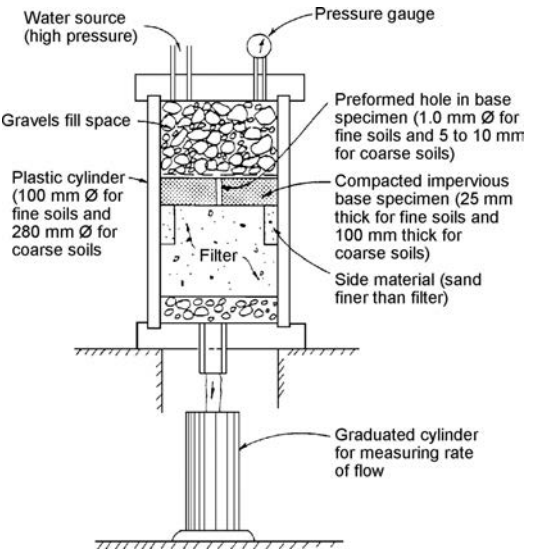

Figure 7.18 "No erosion filter" test apparatus (after Sherard and Dunnigan, 1985).

where d^0_{85} relates to the overall material, including gravels (Sherard and Dunnigan, 1985; Fell et al., 1992).

Practice shows that the recommendations of Sherard and Dunnigan should be accepted, along with the addition that filtering layers should not contain >5% particles finer than 75 μm sieve. If a high permeability of filter is required (as for drainage), this limit should be 2%. The coefficient of uniformity η should not exceed a value of 20. For large and very significant works, laboratory investigations of the filter should be performed by using water with the same chemical composition as that expected for the seepage water, in order to prove its effectiveness.

Foster and Fell have investigated filters in new and in existing dams (Foster and Fell, 2001). They collected and evaluated the detailed test results from different authors and performed additional tests to confirm previous work and to investigate continuing erosion. In summary, Foster and Fell support the test results obtained by Sherard and confirm their recommended criteria. Their work also confirmed that there is a significant margin of safety between the no-erosion and excessive erosion requirements for most soils. That is, even if some erosion occurs, the filters will eventually seal.

There have been attempts to set up even more complex criteria, which would take into consideration susceptibility of the material to erosion, expressed through *critical shearing stress* (Arulanandan & Perry, 1983). Based on statistical processing of data from laboratory investigations and results from a physical model for transport of earth material, a proposal has been put forward for the following improved criterion (Honjo & Veneziano, 1989), which can be applied for loose basic material:

$$\frac{d^f_{15}}{d^0_{85}} \leq 5.5 - 0.5\frac{d^0_{95}}{d^0_{75}} \quad \text{for} \quad \frac{d^0_{95}}{d^0_{75}} \leq 7 \tag{7.12}$$

where the ratio d_{95}^0/d_{75}^0 is called an *index of self-healing*, since with it is bound up the ability of earth material to form a layer that is susceptible to passable self-healing.

Vaughan and Bridle have continued their investigations and have published an update on the "perfect" filter (Vaughan & Bridle, 2005). On the basis of many different tested filters, the permeability of the 'perfect filter' had the following relationship to the floc or particle size it would trap:

$$k = 6.7 \cdot 10^{-6} \delta_R^{1.52} \tag{7.13}$$

where δ_R = size of smallest particle or floc retained in microns (10^{-6} mm), k = permeability of filter (m/s). Equation (7.13) is used to design filters for new dams. The smallest floc or particle size can be determined and a filter of the required permeability must be provided.

For use in existing dams, the following equation is proposed:

$$\delta_R = 2.54 \cdot 10^3 k^{0.658} \tag{7.14}$$

Equation (7.14) is for use in existing dams to give an indication of their vulnerability or otherwise to internal erosion. The permeability of the existing filter, or of non-cohesive fill downstream of the core, if no filter is present, is measured and the equation gives an indication of the particle or floc size that it could trap. Comparing this to the floc particle size present in the core shows whether erosion could occur and how much of the core may be lost.

The following observations and conclusions are made by the above-cited authors:

- The actual permeability of the filter in most cases is substantially lower than the required permeability. This implies that the gradation sizes below the D_{15} contain a substantial percentage of cohesionless silt, such that the permeability is reduced by silt-sized particles within the voids of the sands and gravels.
- The actual D_{15} size of the filter for Ardingly Dam is considerably larger than the calculated D_{15} size of the uniform filter. For the two projects in Cyprus, the actual D_{15} size is 7 to 10 times larger than the calculated D_{15} size of the uniform filter, yet the resulting permeability of the filter is below that required. This implies that a well-graded filter with ample percentages of fine sand and coarse cohesionless silt was used.
- The floc size for Cow Green Dam in the UK and for Dhypotamus Dam in Cyprus is 6 microns. The required permeability of the filter, 0.010 cm/s, and the resulting D_{15} size of a uniformly graded filter, 0.10 mm, are the same. The actual D_{15}, however, for these two dams is quite different, 0.10 mm for Cow Green and 1.00 mm for Dhypotamus. This is because the total grading curves of these two filters, both yielding the required permeability, are quite different.
- The crusher-run limestone filter (not designed according to "perfect" filter concepts) used at Balderhead Dam is included for comparison. The filter was segregated; permeability and the D_{15} size varied widely from one location to another allowing the fines from the core to wash through the filter.

Generally, the 'perfect filter' concept was estimated as a conservative one. However it does seem appropriate that for widely graded soils, as was the case at *Balderhead*

Dam, particularly those of glacial origin, consideration be given to adopting conservative filter designs, possibly checking the implications of using the 'perfect filter' concept.

An important property of a good filter is low susceptibility to segregation. Separation of a graded soil material into finer and coarser zones might occur upon placement of material by down-slope discharge during dumping and spreading operations. The larger particles have a tendency to accumulate at the bottom. Generally, all broadly graded materials that do not have sufficient fines to provide some degree of cohesion may segregate during the placement. Presence of a coarse zone in the filter larger than is necessary can increase the risk of loss of fines from the core by internal erosion. Therefore, it is especially important to restrict the maximum particle size included in a filter (Mattsson et al., 2008). Some authors warn that the issue of segregation is a critical uncertainty in filter design in dam engineering (Milligan, 2003). In practice, it is not easy to avoid segregation during the placement of filters.

Kenney and Westland (1993) performed segregation tests to study the process of segregation in different granular soils. Main conclusions were that: (1) all dry soils consisting of sands and gravels will readily segregate; (2) the patterns of segregation are repeatable in repeated tests and the amount of segregation might be predictable; (3) water effectively prevents segregation of finer soils (e.g. sands) while it has no influence on the segregation behaviour for coarser soils (e.g. gravels). Water in unsaturated soils reduces segregation because the sorting mechanism is suppressed by the increased effective stresses caused by the capillary tensions acting at points of contact between wetted particles. Soils with a high content of small particles are most strongly influenced by these effects of capillary stresses.

Milligan (2003) concludes that much of the uncertainty related to appropriate filter design and placement may be largely resolved by specifying the use of wide, narrowly graded, sand-rich filters, of a gradation finer than the limit suggested in Fig. 7.19 and placed wet in thin lifts.

In the case of non-critical filters, requirements regarding the grain size distribution are much more moderate. Thus, for the upstream filter layer in earth–rock dams, in the greatest number of cases it is possible to employ a mixture of sand, gravel, and

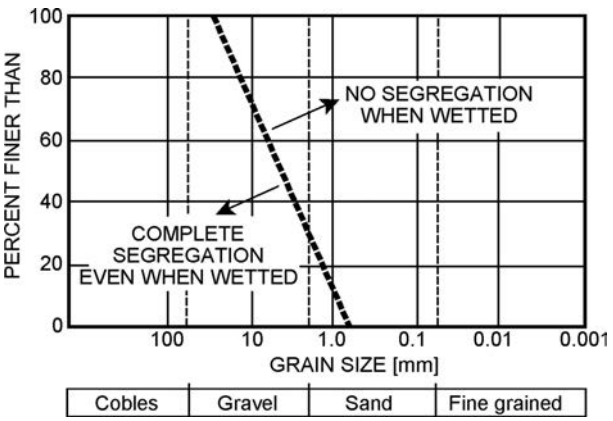

Figure 7.19 Approximate gradation limit for preventing segregation by wetting (after Milligan, 2003).

stone, with a maximum grain of 150 mm. This would make a transition between the fine-grain material in the core and the stone in the retaining elements. A similar filter can be also used below the protective layer of tipped rock-filling at the upstream slope.

In designing filters, *geotextile* is increasingly being used – water permeable fabric (most often synthetic), which is used in a combination with earth and rock materials in order to improve their properties and possibilities, or to cut costs. A wide range of geotextile materials are available that are suitable for application in the construction of filter layers. They differ with regard to the type of polymer used for their manufacture, the kind of fibre present, and the way the fabric has been manufactured.

According to intensity of application, the following materials are used for geotextile manufacture: polypropylene, polyester, polyamide (nylon), polyethylene, etc. Fibres of these materials are processed in different ways, so that geotextile is obtained in different forms and with different textures (Fell et al., 1992).

In the application of geotextile as a filter, its ability to retain particles with certain dimensions should be taken into consideration, as well as its water permeability. Worldwide practice has not adopted a strict standard for the size of particles geotextile should retain, or let pass through, or how they are determined. Yet, textbook references mention a geotextile letting through 0%, 2%, or 5%, of earth material.

An important property of geotextile is its ability to let water pass through. This property is called *permittivity* ψ and it is defined by means of the expression:

$$\psi = \frac{k_n}{t} \tag{7.15}$$

where ψ = permittivity; k_n = cross plane permeability of geotextile; and t = geotextile thickness at normal pressure on the geotextile.

By applying Darcy's law, it follows:

$$q = Aki = k_n \frac{\Delta h}{t} A \tag{7.16}$$

i.e.

$$\psi = \frac{k_n}{t} = \frac{q}{\Delta h\, A} \tag{7.17}$$

where q = flow rate; Δh = head loss across the geotextile; and A = area of flow through the geotextile.

Permittivity in geotextiles depends on normal stresses acting upon them; that is to say, the ability of geotextile to let water pass through is lowered if it has been created under conditions of the action of high pressure, which has to be taken into consideration in its design. Also, the filling up of the geotextile with fine earth particles has an influence on its permittivity.

In some cases, the geotextile can be used to transmit water along its plane, when it has the role of drainage. In such a case, it is a question of *transmissivity* (θ) of the geotextile and is given by (Fell et al., 1992):

$$\theta = k_p t = \frac{qL}{\Delta h\, W} \tag{7.18}$$

where k_p = permeability in the plane of the fabric; t = thickness of the fabric; L = length of the fabric; q = flow rate in the plane of the fabric; W = fabric width; and Δh = head lost.

On transmissivity, there also is an influence from the magnitude of normal stresses.

As for filters made of local material, here also are used different methods and criteria for their design. Their application permits drawing the following concise conclusions:

- Function of the filter should be clearly defined, taking into consideration hydraulic conditions, as well as the nature of the contact being protected.
- For a loose basic earth layer for seepage in one direction: (1) the geotextile should retain particles with a diameter d_{15} of the basic layer; (2) if the basic layer is not well graded, then a geotextile should be used with smaller openings; (3) particular attention should be paid to the case of a uniform basic layer, when a small error can lead to a situation in which all the particles are finer than the geotextile openings; (4) the case of non-uniform curve of the grain size distribution of the basic material requires individual investigation and a conservative approach in the design.
- For seepage with a variable direction, or at a turbulent flow in loose basic material, it is necessary to apply much more rigorous criteria.
- For a cohesive basic material, without a continuous concentrated flow through fissures or similar defects, geotextile with fine pores, in any case, will be a satisfactory solution.
- If there is danger of the occurrence of a continuous flow through fissures or through other openings in a cohesive earth material, the application of geotextile as filter protection is highly questionable.

7.4 CALCULATIONS OF THE CASUAL SEEPAGE STRENGTH OF EARTHFILL DAMS

Figure 7.20a shows a schematic presentation of the cross-section of an earthfill dam with drainage. L denotes the mean distance from the headwater to the drainage (that can also be the distance to the tail water, if there is no drainage). In order to prevent a disturbance of casual seepage strength of the dam's body and its foundation, the length L should satisfy the following condition:

$$J_k = J_{kd} \tag{7.19}$$

where J_k = piezometric gradient, at which it does not lead to a disturbance of casual seepage strength, equal to A, the mean gradient for a considered seepage area; J_{kd} = a permissible value of J_k, obtained by means of a statistical analysis of already constructed contemporary dams working normally. In calculating the casual seepage strength according to the formula (7.19), the dam's body is separately considered, and its foundation is separately considered. In Figure 7. 20a, both areas are separated by line AB.

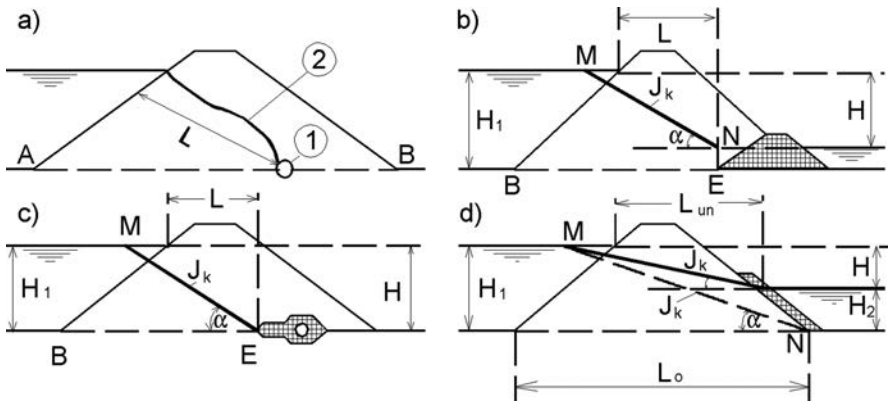

Figure 7.20 Schemes for calculation of casual seepage strength (after Chugaev, 1985). (1) Drainage; (2) seepage line.

The value of J_k for the dam's body in the case of a homogeneous earthfill dam with a downstream drainage prism (Fig. 7.20b) or drainage incorporating a pipe (Fig. 7.20c), is determined according to the formula:

$$J_k = \tan\alpha = \frac{H}{L + 0.4H_1} \tag{7.20}$$

where α = angle of inclination of the seepage line MN (assumed as a straight line) regarding the horizon; H = pressure on the dam; H_1 = depth of headwater; and L = horizontal distance from contact of the headwater with the dam to the beginning of the drainage.

If drainage is laid on the downstream slope, as shown in Figure 7.20d, or if there is no drainage, then the value of J_k is calculated according to the formula:

$$J_k = \tan\alpha = \frac{H}{L_{un} + 0.4H_1 + 0.4H_2} \tag{7.21}$$

where L_{un} = horizontal distance between the contacts of headwater and tail water with the dam; and H_2 = depth of tail water. If $H_2 = 0$, the seepage line is represented by the straight line MN.

In the case of a dam with a core or facing, the following formula can be used:

$$J_k = \frac{H'}{\delta} \tag{7.22}$$

where δ = mean thickness of the core or the facing; and H' = pressure on the core or the facing, obtained by means of approximate seepage calculations. If $H_2 = 0$, it can be assumed that $H' = H_1$.

Table 7.1 Permissible piezometric gradients (J_{kd}) at which there is no disturbance of casual seepage strength of the casual seepage strength of the body of earthfill dams (after Chugaev 1985).

Materials in dam's body	J_{kd}
Compacted clay	1.50–1.95
Loam	1.05–1.35
Medium-grained sand	0.70–1.00
Clayey sand	0.55–0.85
Fine-grained sand	0.45–0.75

Table 7.2 Permissible piezometric gradients (J_{kd}) at which there is no disturbance of casual seepage strength of earth foundations below dams (after Chugaev 1985).

Materials in dam's foundation	J_{kd}
Clay	0.70–1.08
Loam	0.35–0.54
Coarse sand	0.32–0.48
Medium-coarse sand	0.22–0.34
Fine-grained sand	0.18–0.26

Determination of J_k for the dam's foundation in the case of a dam without a blanket and plug, and with a laid drainage (Fig. 7.20d), is performed with the formula:

$$L_k = \frac{H}{L_0 + 0.88\,T_r} \tag{7.23}$$

where L_0 = width of dam in its foundation; and T_r = design depth of the earth layer below the dam – if this depth is undetermined, it can be assumed that $T_r = 0.5L_0$.

If there is another type of drainage (instead of that which is laid on the downstream slope), instead of L_0 in formula (7.23) the length BE is to be used (Figs. 7.20b and c). If there is a horizontal blanket or a vertical plug, i.e. stopper, then J_k is calculated by means of the same formula; however, L_0 is enlarged, for the length of the blanket, i.e. for twice the depth of the concrete cut-off.

Values of the permissible piezometric gradient J_{kd}, obtained by means of statistical processing of data of already constructed dams, are given in Table 7.1 and Table 7.2 (after R.R. Chugaev). These values vary, depending on the importance of the dam (Chugaev, 1985).

If, for a designed structure, $J_k > J_{kd}$ has been obtained, it will be necessary to carry out changes by means of which the length of seepage would be lengthened. In some cases, particularly when inadmissible gradients occur in the earth foundation, possibilities for solving the problem can be very limited, while the solution may be very expensive.

This page intentionally left blank

Chapter 8

Static stability of embankment dams

8.1 INTRODUCTION

The modern era of construction of embankment dams has imposed an essential need for the development of methods for determination of the static stability of these complex structures, which would make possible the design of a safe and economical dam structure. Calculation of stability of embankment dams is divided into *classical* and *contemporary* methods.

According to classical methods, which commenced their development in the early decades of the twentieth century, the analysis of the cross-section of embankment dams consists of examination of their stability through consideration of forces that act on the assumed plane of slippage of an earth wedge, as well as calculation of the resistance against shearing, developed across the anticipated plane of slippage.

Dam stability is expressed through a coefficient of safety against the sliding of the slopes. Methods of this group are called 'limit equilibrium' methods. Their common deficiency is the fact that they do not take into consideration deformations occurring both in the embankment and in the foundation.

The coefficient of safety gives only one datum – safety of slopes against land sliding, while for obtaining an economical and safe solution it is necessary with sufficient accuracy to anticipate the distribution of stresses and deformations which will develop at particular points in the embankment and the foundation. In this, defining the state of stresses or deformations in the dam's body and the foundation underneath is an extremely complex problem with many unknown values, because of which a need is imposed for making numerous assumptions and simplifications. Although the beginnings of attempts for solving this problem date back to the early thirties, a satisfactory solution was found only in the course of the last twenty years, thanks to the development and the application of the Finite Elements Method – the most powerful numerical method in the hands of engineers.

8.2 CLASSICAL METHODS

In practice, for an analysis of the stability of embankment dams, classical methods still have a noticeable application, by means of which one can determine the stability of an earth wedge, with an anticipated surface of sliding. Classical methods date from the second decade of the 20th century and had originally been developed for analysis of

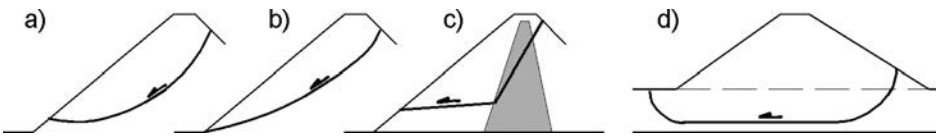

Figure 8.1 Different shapes of sliding surfaces.

the stability of original slopes during the execution of side cuts through them, intended for the construction of railway lines and roadways. Later on, they have been gradually adjusted to the specific requirements that have been imposed by embankment dams. The reader, who has a greater interest in these problems, has at his disposal special textbooks (Chowdhury, 1978; Nonveiller, 1987), appropriate chapters of textbooks (Eisenstein & Naylor, 1986; Nonveiller, 1979; Sherard et al., 1963; Sing & Sharma, 1976; Taylor, 1948), as well as numerous papers in professional journals (Abadjiev, 1994; Baker & Gorber, 1978; Christian et al., 1994; Chugh, 1981; Collins et al., 1988; Di Prisco et al., 1995; Drescher & Christopoulos, 1988; Katsuhiko & Keiichi, 1985; Leshchinsky, 1990; Low, 1989; Oka & Wu, 1990; Sarma, 1973, 1979; Stephenson, 1978; U.S.B.R, 2011; and Wright et al., 1973).

The most often applied form of a surface of sliding is the rotational surface of sliding which, in a cross-section, could be a circular line (Fig. 8.1a) or a curve of another form (b). The surface of sliding can also be a broken plane (c), or else a combination of a rotational and a plane surface (d).

Generally speaking, circular land sliding appears in homogeneous earth media, while rotational land sliding appears along a curve that is different from a circle, in a non-homogeneous medium.

Land sliding along a broken plane or combined land sliding appears when the dam has been constructed with zones with clearly different properties, or else when the uppermost stratum of the foundation consists of non-rock material. In this group of methods, also known by the name limit equilibrium methods, the necessary shear strength, the potential element of sliding, limited by the surface of sliding and the contour of the dam, in a state of limit equilibrium, is compared with the available shear strength of the local material. In this way, one can obtain a mean factor of safety along the surface of sliding.

In order to determine the surface of sliding, which has the smallest factor of safety, it is necessary to examine quite a number of surfaces of sliding in different positions. The problem is most often dealt with as a two-dimensional one, by which one obtains more conservative results regarding the space treatment of the problem. In continuation, there will briefly be presented only the method of slices and the method of wedge.

8.2.1 Method of slices

In this method the potential surface of sliding is assumed to be cylindrical; that is to say, circular in cross-section, with a center O and a radius R (Fig. 8.2). The earth mass ABCD over the assumed surface of sliding ABC by means of vertical planes is divided

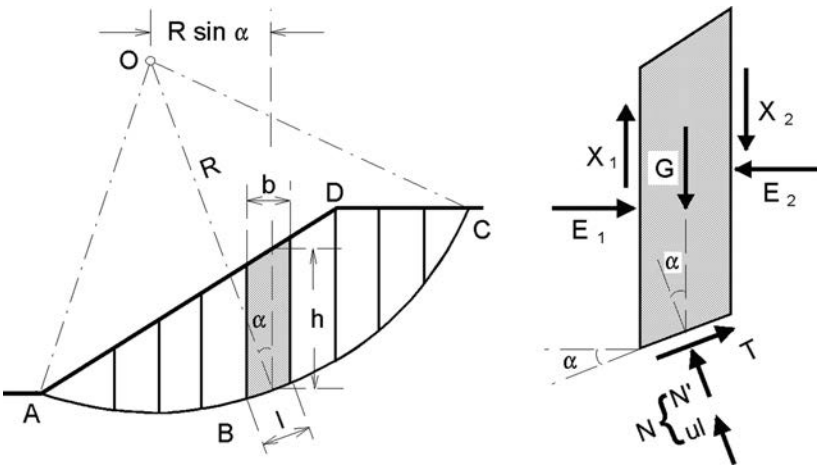

Figure 8.2 Method of slices.

into slices (usually 8–12 units) with a width b. It is assumed that the basis of each slice is a straight line.

In any slice the base forms an angle α with the horizontal, while the height, measured along the middle of the slice, is h. The factor of safety against sliding of the block ABCD (F_s) is defined as a ratio of the available shear strength τ_f and the shear strength τ_m, that should be mobilized in order to retain a state of limit equilibrium that is:

$$F_s = \frac{\tau_f}{\tau_m} \tag{8.1}$$

The safety factor is taken to be equal for each slice, assuming that between the slices there must act reciprocal forces.

The following forces act on each slice on a unit length normal to the cross-section:

- Total weight of the slice, $G = \gamma bh$ (if it is under water, the unit weight will be taken in a saturated condition);
- Total normal force on the base N; in general, this force has two components: the effective normal force N' and a water force ul, where u is pore water pressure at the center of gravity of the base, while l is the length of the base;
- Shear force on the base, $T = \tau_m l$;
- Total normal forces on the sides, E_1 and E_2;
- Shear forces on the sides, X_1 and X_2;
- Any other external forces.

The problem is statically indeterminate. In order to come to a solution, certain assumptions for the forces between slices E and X must be made, so that the value of the factor of safety is approximate.

The sum of moments due to shear forces T, acting along the arch ABC, regarding point O, for the case of an equilibrium, must be equal to the moment due to the weight

of earth mass *ABCD*. For an arbitrary slice, the lever arm of weight *G* is *R* sin α, so it will be:

$$\Sigma T \cdot R = \sigma G \cdot R \cdot \sin\alpha \tag{8.2}$$

Since:

$$T = \tau_m \, l = \frac{\tau_f}{F_s} l \tag{8.3}$$

it will be:

$$\sum \frac{\tau_f}{F_s} l = \Sigma G \cdot \sin\alpha \tag{8.4}$$

and

$$F_s = \frac{\sigma \tau_f \, l}{\Sigma G \cdot \sin\alpha} \tag{8.5}$$

For an analysis with effective stresses it will be:

$$F_s = \frac{(c' + \sigma' \tan\varphi')}{\Sigma G \cdot \sin\alpha} = \frac{(c' \, L_a + \tan\varphi' \Sigma N)}{\Sigma G \cdot \sin\alpha} \tag{8.6}$$

where L_a is the length of the arch *ABC*. For an assumed surface of sliding, the value of F_s will depend on the way in which the force N' has been determined, for which there are a number of solutions. In the continuation, two such solutions will be described.

8.2.1.1 Felenius' solution (Swedish method)

This is one of the oldest methods. It is characterized by the fact that for each slice we assume that the forces at contacts, i.e. interfaces with adjacent slices, are equal to zero. The normal force is found separately for each slice from the expression:

$$N' = G\cos\alpha - ul \tag{8.7}$$

so that the factor of safety will be:

$$F_s = \frac{c' \, L_a + \tan\varphi' \Sigma \, (G\cos\alpha - ul)}{\Sigma G \cdot \sin\alpha} \tag{8.8}$$

Values of components *G* sin α and *G* cos α can be determined for each slice by measuring from the drawing (graphically) or by calculations. This method gives lower values for the safety factor, as compared to the more accurate methods by 5–20%.

8.2.1.2 Modified Bishop's method

In this method, discovered in 1952, it is assumed that the resultant forces in the sides of slices are horizontal; that is:

$$X_1 - X_2 = 0 \tag{8.9}$$

At equilibrium in the base of each slice, the shear force is:

$$T = \frac{1}{F_s}(c'l + N' \tan \varphi') \tag{8.10}$$

By projecting all the forces acting on the slice in the vertical direction, we obtain:

$$G = N' \cos \alpha + ul \cos \alpha + \frac{c'l}{F_s} \sin \alpha + \frac{N'}{F_s} \tan \varphi' \sin \alpha \tag{8.11}$$

and hence:

$$N' = \frac{G - \frac{c'l}{F_s} \sin \alpha - ul \cos \alpha}{\cos \alpha + \frac{\tan \varphi' \sin \alpha}{F_s}} \tag{8.12}$$

If we carry out a replacement $l = b \sec \alpha$ from the equation (8.6), following certain rearrangements, we obtain:

$$F_s = \frac{1}{\Sigma G \sin \alpha} \sum \left\{ [c'b + (G - ub) \tan \varphi'] \frac{\sec \alpha}{1 + \frac{\tan \alpha \tan \varphi'}{F_s}} \right\} \tag{8.13}$$

For practical reasons it is good that the pore water pressure should be expressed relative to the total pressure of the embankment by means of the non-dimensional coefficient of pore water pressure r_u:

$$r_u = \frac{u}{\gamma h} \tag{8.14}$$

Then for each:

$$r_u = \frac{u}{\frac{G}{b}} \tag{8.15}$$

Now, equation (8.13) will be:

$$F_s = \frac{1}{\Sigma G \sin \alpha} \sum \left\{ [c'b + G(1 - r_u) \tan \varphi'] \frac{\sec \alpha}{1 + \frac{\tan \alpha \tan \varphi'}{F_s}} \right\} \tag{8.16}$$

Since in the last equation the safety factor is not given in an explicit form, the solution is obtained by means of successive approximations. This method is suitable for programming, in which one can bring into the program the more complex geometry of the dam, with more layers having different properties. This method is more accurate than the Swedish one, while the disregard of the safety factor does not exceed 7%.

8.2.2 Wedge method

In this method, which originated in the USA in the early forties, it is assumed that the surface of sliding is a broken plane which, along with the contour of the dam and the

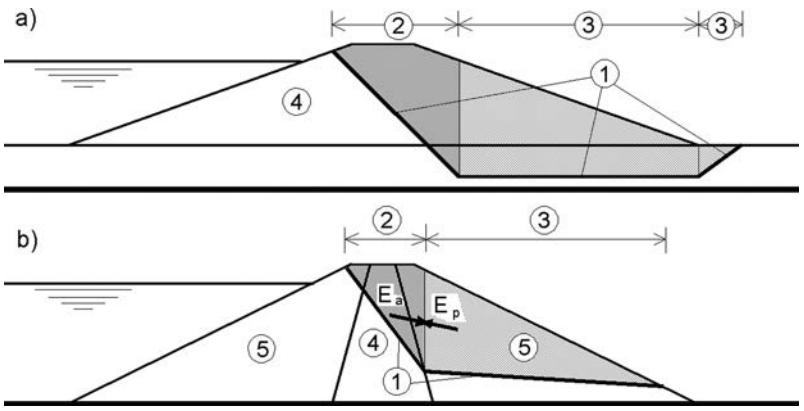

Figure 8.3 Cases of application of the wedge method. (a) Earthfill dams on a thin horizontal stratum of weak soil; (b) earth–rock dams founded on rock. (1) Anticipated plane of sliding; (2) active wedge; (3) passive wedge; (4) fine-grained cohesive earth material; (5) coarse-grained material.

vertical lines, drawn in the breaking, i.e. turning, points on the surface, divides the potential mass of sliding into two or three large blocks or wedges. The upper one is called the *active* wedge, while the lower one is called the *passive* wedge. In a case of the existence of three wedges, the two lower ones are called *passive* wedges. This method yields good results and is suitable for application in the following two cases:

1. When an earthfill dam is founded on a thin horizontal stratum of weak earth material, which represents the uppermost layer of the foundation (Fig. 8.3a);
2. When it is a question of an earth–rock dam, founded on rock (Fig. 8.3b).

In the first case, failure would most likely occur as a consequence of movement across the weak horizontal layer in the foundation; while in the second case, it can be expected that the surface of failure passing through the non-cohesive material in the shells will be close to a plane.

In order to determine the safety factor against sliding along an anticipated surface, what is considered is a state of equilibrium of the potential body, i.e. the element of sliding under the action of external and internal forces. The wedges set apart from the body and their equilibrium condition are analyzed. The force E (Fig. 8.3b) acts in the contact between the wedges, which is called the *active force of earth pressure*, or the *passive force of earth pressure*, depending on which wedge it belongs to.

In a general case, this force regarding the horizontal, forms an angle $\delta = (1/2 - 2/3)\varphi$, and if the contact surface is in the vicinity of the dam's crest, then it is assumed that it is horizontal. Following separation from the base, the reaction of soil R acts on the contact surface of the wedge, with a direction forming an angle φ to the normal of the contact surface. In this way, only the intensities of forces E and R are unknown for each wedge, so that they can be determined from the two conditions for equilibrium in a plane.

In order for the potential body, i.e. element of sliding, to be in a state of limit equilibrium, it must be $E_a = E_p$, where E_a and E_p are the forces of active and passive earth pressure, respectively.

The safety factor in this method is defined by the following expressions:

$$F_s = \frac{\tan \varphi}{\tan \varphi_d}; \qquad F_s = \frac{c}{c_d} \tag{8.17}$$

where φ and c are parameters of the shear strength of the material along the plane of sliding, while φ_d and c_d are appropriate parameters, necessary for the body to be in a state of limit equilibrium. Owing to the static indeterminacy of the problem, here also the safety factor is determined by means of assuming its value and by a gradual approach to the solution. Of course, in this model it is necessary as well to examine the stability of a great number of different planes of sliding in order to find the one that has the minimum safety factor.

8.2.3 States in which stability of embankment dams is examined

For embankment dams, it is necessary to examine the stability of both the upstream slope and the downstream slope, for the most adverse conditions of loading. When it is a question of an earthfill dam or an earth–rock dam, for the upstream slope, the state immediately following construction of the dam is critical, as well as of a rapid draw down of the reservoir level. This is because the pore pressure that water causes in the poorly water-permeable earth materials cannot be pushed out of the pores within a short time period. For the downstream slope, the most dangerous states are those immediately after construction and with a full reservoir with established stationary seepage flow.

8.2.3.1 State immediately following construction

Cohesive earth materials are placed in the embankment dam's body by means of compaction at optimum moisture (or somewhat larger than the optimum pressure), as a consequence of which 80–90% of the pores are filled with water, while the rest are filled with air. Loading that is imposed due to the advancement of the embankment and due to the means for compaction which, in the course of construction, is permanently increasing, exerts pressure upon the fluid water–air, causing pore pressure in the fine-grained poorly permeable material. The magnitude of pore water pressure depends on many factors – moisture during the placing of the material, compressibility and water permeability of the material being placed, advancement of the construction, and possibilities of dissipation of pore water pressure through drainage constructions.

There are several methods for anticipation of pore water pressure in the state immediately following construction; however, accuracy and reliability with all of them are limited because of the impossibility of really encompassing all of the relevant factors. The most frequently used method is the one that is based on parameters determined by means of a triaxial test. For an analyzed state, pore water pressure u,at some point of the earth layer, will be:

$$u = u_0 + \Delta u \tag{8.18}$$

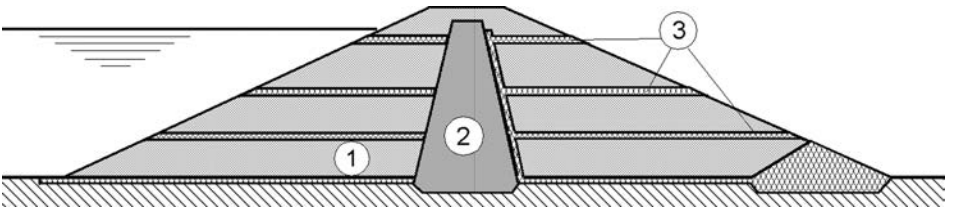

Figure 8.4 Earthfill dam with horizontal drainage layers. (1) Semi-permeable material; (2) impermeable material; (3) drainage layers (after Craig, 1978).

where u_0 is initial value of the pore water pressure, while Δu is the change of pore water pressure due to an increase of loading in undrained conditions. In terms of the change in total major principal stress, pore water pressure will be:

$$u = u_0 + \overline{B}\,\Delta\sigma_1 \tag{8.19}$$

where $\overline{B}$ is coefficient of the pore water pressure. The problem of pore water pressure and the coefficient $\overline{B}$ are brought up in detail in the general and specialized textbook references on soil mechanics. Thus, it follows that:

$$r_u = \frac{u_0}{\gamma h} + \overline{B}\frac{\Delta\sigma_1}{\gamma h} \tag{8.20}$$

The increase in total major principal stress is approximately equal to the pressure due to the filling material along the potential plane of sliding; thus, it will be:

$$r_u = \frac{u_0}{\gamma h} + \overline{B} \tag{8.21}$$

Since the earth material during compaction is partly saturated with water, initial pore water pressure u_0 is negative. The real value of u_0 depends on the amount of water during placement of material – the higher it is, the closer the value of u_0 to zero. The value of the coefficient $\overline{B}$, as well, depends on the amount of water – the value of $\overline{B}$ increases with the increase of water. For the upper limit of saturation with water it will be:

$$r_u = \overline{B} \tag{8.22}$$

The value of $\overline{B}$ must correspond to the state of stresses in the dam's body. The expressions (8.21) and (8.22) have been obtained on the assumption that, in the course of the dam's construction, there is no dissipation of the pore water pressure.

If the value of r_u, obtained according to the described way, is unacceptably high, then the dissipation of pore water pressure can be expedited by means of horizontal drainage layers incorporated into the dam's body and interconnected by means of a vertical drainage. A typical example is shown in Figure 8.4, in which an effective solution is obtained if the permeability of the drainage layers is 10^5 times larger than the permeability of the material in the dam's body.

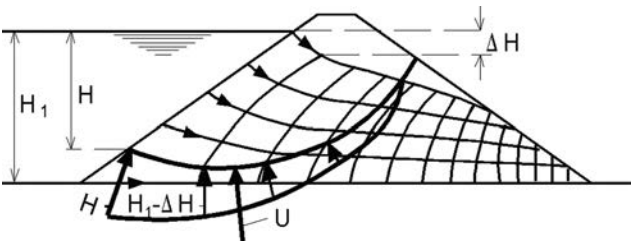

Figure 8.5 Determination of pore water pressure by means of a flow net pattern (full reservoir).

The critical state occurring immediately after the construction of the dam lasts for only a short time period, because in the course of time, a continuous dissipation of the pore water pressure occurs. In this case, it is permissible to have a relatively low value of safety factor amounting to 1.2–1.3. If unsure of the accuracy of the geomechanical parameters of the earth materials, then a higher safety factor can be assumed.

8.2.3.2 State of a full reservoir with established stationary seepage flow

After the filling of the reservoir and following the passage of a certain period of time, stationary seepage flow is established through the earthfill dam or through the water-impermeable element made of earth material, so that the material that is below the seepage line is completely saturated with water. The problem, in any case, is analyzed by means of effective parameters of the shear strength ϕ' and c'', while pore water pressure can best be determined by means of a flow net pattern, as shown in Figure 8.5.

If we use the modified Bishop's method, r_u reaches a value of up to 0.45 for homogeneous earthfill dams without drainage while, depending on the type of drainage, it can fall down to 0.20. The safety factor in this state, which is normal in service conditions, should be at least 1.5.

By way of illustration, Figure 8.6 indicates the changes of pore water pressure in the core of the Talbingo earth–rock dam (Australia), obtained from measurements. Drawing (a) shows the lines of equal pore water pressures at the end of construction (October 1970), while (b) shows those immediately after the filling of the reservoir, in effect, prior to the commencement of seepage through the core.

Hydrostatic pressure, acting on the upstream slope of the core, represents an additional load, due to an increase in pore water pressure. This state also is dangerous and should be carefully analyzed. This has been lately made possible through application of the finite elements method (see subsection 8.3.7) by means of which there has been made possible input of complex data into the calculations of all the influences.

In the course of time, and with the commencement of seepage, there comes about a lowering of the pore water pressure (c, November 1980), right through to the establishment of the stationary seepage flow (d) (Adikari & Parkin, 1982).

8.2.3.3 State at a rapid draw down of water level

Once a stationary seepage flow has been established through the dam (or through the core) made of earth material, a rapid draw down of water level in the reservoir would

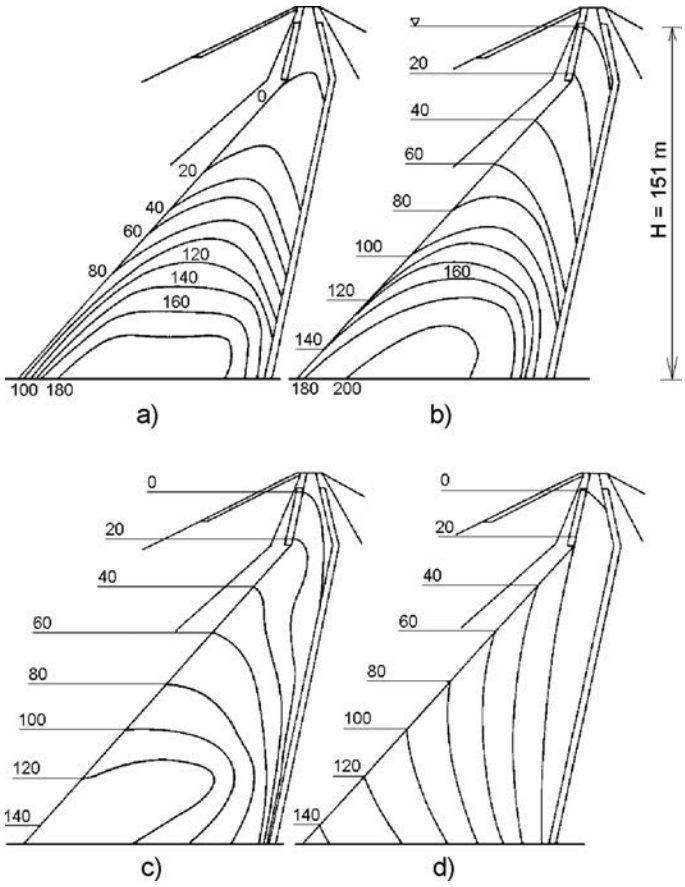

Figure 8.6 Distribution of pore water pressure in the core of the Talbingo dam (Australia) (in metres).

cause a change in the distribution of pore water pressure. If permeability of the earth material is low, then water-lowering, i.e. a draw down of water level within several months can be considered fast, as compared to the time which is necessary for the dissipation of the pore water pressure, so that the change of pore water pressure can be deemed as being carried out in undrained conditions.

According to Bishop and Bierum, the pore water pressure prior to a rapid draw down of the water level, at a point P of the potential plane of sliding, is given by the expression (Fig. 8.7):

$$u_0 = \gamma_w(h + h_w - h') \tag{8.23}$$

where h' is a loss of pressure on the seepage path from the upstream slope to point P.

Here again, it is possible to assume that the total major principal stress at P is equal to the pressure of the embankment. Change in stress σ_1 can take place due to a

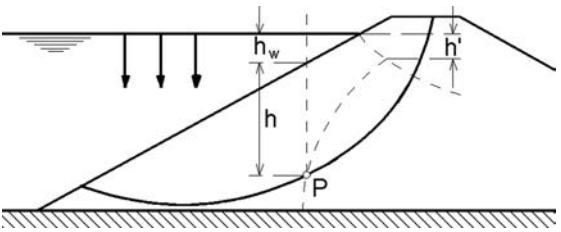

Figure 8.7 State at a rapid draw down of the water level in an earth dam (after Craig, 1978).

change in the water level above the slope along the vertical passing through P. For a draw down of the water level which is larger than the depth h_w it will be:

$$\Delta\sigma_1 = -\gamma_w h_w \tag{8.24}$$

In that case, the change in pore water pressure will be:

$$\Delta u = \overline{B}\,\Delta\sigma_1 = -\overline{B}\,\gamma_w\,h_w \tag{8.25}$$

Hence, the pore water pressure at point P, immediately after a draw down of the water level, is:

$$u = u_0 + \Delta u = \gamma_w[h + h_w(1 - \overline{B}) - h'] \tag{8.26}$$

Therefore:

$$r_u = \frac{u}{\gamma_{sat}\,h} = \frac{\gamma_w}{\gamma_{sat}}\left[1 + \frac{h_w}{h}(1 - \overline{B}) - \frac{h'}{h}\right] \tag{8.27}$$

For a decrease in total normal stress, the value of $\overline{B}$ is somewhat above 1. The value of r_u for this state most frequently ranges from 0.3 to 0.4, while the safety factor can go down to 1.2.

Immediately after a draw down of the water level in the reservoir, a picture of the previously established seepage flow changes, and so do the forces due to pore water pressure. To what extent the newly-occurred pore water pressure will have an influence on the stability of the upstream slope of an embankment dam depends on: (a) the extent of the draw down of the water level; (b) the speed of change of the water level; (c) the construction, i.e. geometry, of the dam; (d) permeability of the embankment and the foundation. Some aspects of the cited points have already been presented in Chapter 7, and Figure 8.8 illustrates new aspects, which will be brought out in the continuation (Fell et al., 1992).

Above all, in such analyses one regularly makes an assumption that the draw down of the water level to a certain depth is carried out instantaneously. That is a conservative approach, which is in the interest of safety. In the cases shown in Figure 8.8, it is assumed that the reservoir is being emptied to the bottom, which should not necessarily be the most dangerous case.

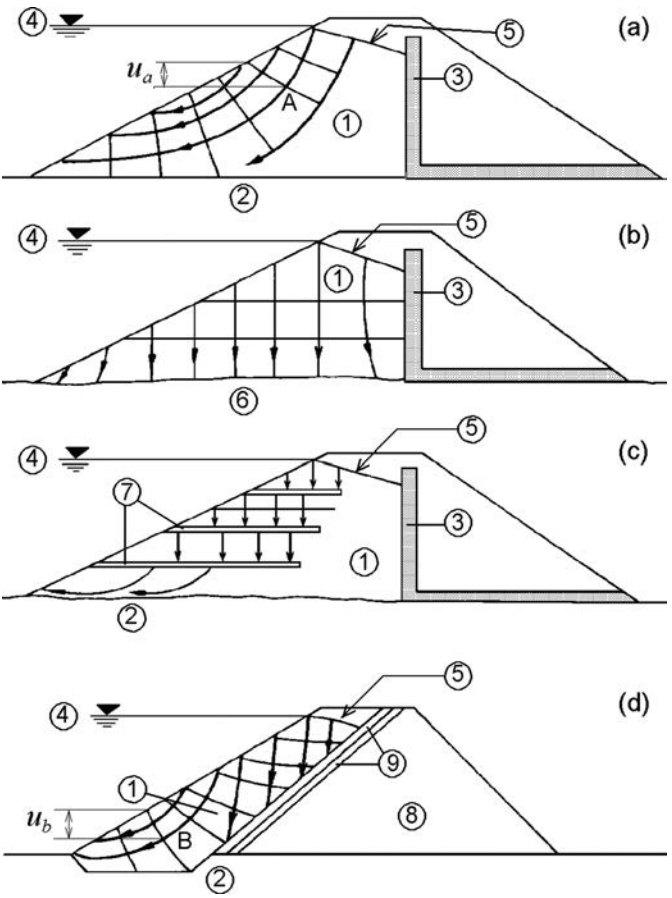

Figure 8.8 Flow net at a rapid draw down of a reservoir (Fell et al., 1992). (1) Poorly permeable material; (2) poorly permeable foundation; (3) drainage stack; (4) water level prior to draw down of water level; (5) seepage line prior to a draw down of the water level; (6) permeable foundation; (7) horizontal drainage layers; (8) water-permeable material; (9) filter layers.

In example (a), an earthfill dam is constructed on a foundation with a low permeability in relation to that of the embankment, so that the seepage flow, following a rapid draw down of the reservoir, will be directed to the upstream slope, along whose length the pore water pressure now is equal to zero. In this case, in the upstream part of the dam, relatively significant pore water pressures occur (for example u_a at point A), in contrast to (b), in which, due to the higher permeability of the foundation in relation to the dam's body, the seepage flow is directed downwards, so that the equipotential lines are almost horizontal, which results in a pore water pressure approximately equal to zero. In (c), horizontal drainage layers have been included in the upstream part of the earthfill dam, towards which the water runs in a vertical flow so that, owing to the low permeability of the foundation, the pore water pressure appears only in the lowermost zone.

In the case of an earth–rock dam with a facing made of cohesive earth material, (Fig. 8.8d), direction of the seepage flow is dictated by the permeable filter layers and the embankment made of coarse material downstream, and so, as a consequence, there occur low pore water pressures in the upper half of the facing. It is recommended that the reader should once again return to this subsection, following the study of the role and construction of drainages in Chapter 10.

8.2.4 Stability of rockfill dams

In contrast to earthfill dams and earth–rock dams, rockfill dams do not have the problem of pore water pressure, so that the analysis of stability of slopes is carried out relatively simply through effective stresses. In practice, results obtained by classical methods for this type of dam are useless. Namely, slopes of dams made of rock material are not expected to slide along a surface with a certain form, which could be anticipated in advance, and it is quite probable that it would be circular-cylindrical. What's more, the downstream slope of a rockfill dam with a facing, constructed even with the angle of repose of the rock material equal to 1:1.2–1:1.4, that is to say, the angle of inclination β is near or equal to the angle of internal friction φ, has no reason for not being stable, either under the action of only the weight of the dam itself, or in service conditions (Fell et al., 1992). Such steep inclinations, however, can be employed only in areas in which seismic activity is not expected or else, unlikely. It should be emphasized that in the shallow zones near the dam slopes the normal stresses are rather low. Thus, the friction angle φ of the rockfill has the highest values in these zones. Consequently, the rockfill in the zones below the slopes have very high shear resistance.

On the contrary, inclinations of a downstream slope at earth-rock dams with central core in some cases would have to be more moderate; for example, 1:1.6–1:1.7. Under conditions of possible significant seismic activity also on the upstream slope, lined with a reinforced concrete facing, it would be compulsory to anticipate similar inclinations.

In the case of rockfill dams with asphalt facing, the inclination of the upstream slope is usually dictated by its convenience for construction and is most often adopted as 1:1.7. In seismically active regions, it can be modified to 1:1.8–1:1.9, as is most often the practice in Japan (see Chapters 11, 12, and 13).

For assessment of the stability of rockfill dams, *deformations*, which occur in the dam's body, are of crucial importance, on which in the first place depends the safety of the thin water-impermeable element, and through this, indirectly, of the entire structure. Of importance are also stresses by means of which it is possible to evaluate the stability of separate, particularly loaded zones in the dam's body. These objectives can be achieved in an efficient way only with the application of contemporary numerical methods, which will be considered in the next section.

Of the material that has been set out in this subsection, it clearly follows that, in the application of the limit equilibrium method, a circular-cylindrical (or similar) surface of sliding cannot pass completely through an embankment made of rock material. As a consequence of this statement, in the case of earth–rock dams, we distinguish a *critical* and a *non-critical* surface of sliding (Fig. 8.9). The latter surface should not be taken into consideration in an analysis of stability, regardless of the fact that it yields a lower safety factor than the former, because such sliding is not physically possible. The

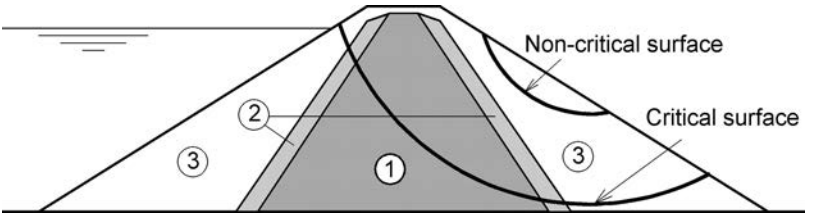

Figure 8.9 Critical and non-critical surface of sliding. (1) Cohesive material; (2) transitional layers; (3) rock material.

eminent rockfill dam specialists Cooke and Sherard (1987) state: *"... rockfills cannot fail along a plane or circular surface, whenever dumped or compacted, if the external slopes are 1.3(H):1.0(V) or 1.4(H):1.0(V) that are the usual slopes in CFRDs, because the friction angle of the rockfills are at least 45°, that is already a guarantee of stability. Rockfills are materials of high shear strength, and are dry, what means they do not have water in the voids to generate pore pressures as is the case of compacted soils. If the foundation is in rock, there is no risk of failure through the foundation."*

8.3 ADVANCED METHODS

In the early thirties of this century, the first serious attempts were made to solve the problem of determining the stress-deformation state in a dam's body and foundation, on the basis of which it would be possible also to determine the stability of the dam with sufficient accuracy.

At first the theory of elasticity was used, and later on, plasticity; all those developed methods, however, had serious deficiencies, which mainly were reflected in the fact that with their use it was impossible to insert into the calculations the irregular geometry of the construction and foundation, complex conditions of loading, and the complex behaviour of the earth materials (Tančev, 1989).

8.3.1 Application of the Finite Element Method

The above-cited deficiencies, which have prevented the efficient application of theories of elasticity and plasticity for analysis of embankment dams, have been bridged over with the development of the Finite Element Method (FEM), which soon following its formulation in the late fifties, became a powerful means in the hands of engineers for solving problems in mechanics.

The method turned out to be both universal and sufficiently flexible, so that even during the first decade of its application it was extended to a number of problems in geotechnics and hydraulic engineering. As is known, by means of the method of finite differences, which was an extensively used numerical method till the appearance of FEM, differentials were approximated with finite differences; that is to say, a mathematical approximation of the problem is carried out. On the other hand, by means of FEM, we perform a physical approximation of the continuum, which is replaced with a system consisting of a number of elements with finite dimensions, interconnected at

nodal points. Thus, instead of treating the problem as a whole, the solution is obtained in a number of consecutive steps, going from the parts to the whole. Properties of individual elements are chosen so that the majority of elements behave in the same manner as the original continuum. In that way, by means of FEM, the problem is reduced to a numerical solving of algebraic equations and, since their number is usually considerable, the solution must be reached by means of a computer. That is why both the appearance and the development of FEM came together with the significant improvement of the electronic computers.

FEM makes possible a determination of the stresses and deformations in the considered continuum, which can have an arbitrary geometry and materials and whose properties vary in particular zones. If, at the same time, we also add the possibility of simulation of complex loading, then it becomes evident why FEM has found such a wide application in the analysis of embankment dams (Tančev, 1989).

FEM has been elaborated in detail in a number of monographs and papers (Cheung & Yeo, 1979; Desai, 1979; Poceski, 1992; and Zienkiewicz, 1977). In the following, a concise presentation of the basic steps is presented, through which one comes to a solution of the problem by the application of this contemporary numerical method.

Step One: Discretisation of the considered area.
By means of the first step we can carry out a division of the continuum into a number of small bodies, i.e. figures, which are called finite elements, and which are *interconnected* at nodal points. The joints between any elements are called *nodal lines* or *nodal surfaces*. Depending on the kind of the problem being solved, we calculate certain unknown quantities, such as, displacements at nodal points, stresses, or certain other values.

As to the type of element by means of which discretisation is carried out, what is essential is the kind of problem being considered. In the case of one-dimensional problems, a linear or curved linear element is used, while in the case of two-dimensional problems, triangular and quadrilateral elements are most often used. In the case of three-dimensional problems, the tetrahedron and hexahedron are most often used. The number and size of elements depend on the type of element employed, the kind of problem, as well as on the geometry of the examined continuum.

Step Two: Choice of approximation function.
In this step we assume the form for solving the unknown quantities in the element, which most often is a polynomial of different degree. If u denotes the unknown quantities, then the interpolation function in the kind of polynomial can be expressed in the following way:

$$u = N_1 u_1 + N_2 u_2 + N_3 u_3 + \cdots, N_r u_r \tag{8.28}$$

where $u_1, u_2, u_3, \ldots, u_r$ = values of unknown quantities at nodal points, for example, displacements; $N_1, N_2, N_3, \ldots, N_r$ = interpolation functions.

In the formulation of the problem by using the FEM, the concept of *isoparametric elements* is often used, which also implies expressing both the displacement and the change of geometry of the element by means of the very same interpolation function N_i. In a matrix form, displacements at some point of the element can be expressed as:

$$\{u\} = [N]\{q\} \tag{8.29}$$

where $[N]$ = matrix of the interpolation functions; and $\{q\}$ = vector of forces.

By using the isoparametric concept, the coordinates of some point in the element can be expressed by the same function N_i:

$$\{x\} = [N]\{x_n\} \tag{8.30}$$

where $\{x_n\}$ contains the coordinates of the nodal points.

Step Three: Defining the constitutive law among the unknown quantities.
This step defines the law, according to which the unknown quantities depend upon one another. For instance, if those are stresses and strains, then their relationship can be expressed in a matrix form as:

$$\{\sigma\} = [D]\{\varepsilon\} \tag{8.31}$$

where $[D]$ is a matrix by means of which we define the properties of the material in the element.

In the case of a two-dimensional analysis of dams, when a cross-section is examined in the x–y plane, it is assumed that the component of displacements in the direction of the z-axis is negligible because of the considerable thickness of the structure. Such a treatment of the problem is called a *plane state of deformations*, in which case it is:

$$\left.\begin{matrix}\varepsilon_z \\ \gamma_{yz} \\ \gamma_{zx}\end{matrix}\right\} = 0 \tag{8.32}$$

Using Hooke's law in this case, we obtain:

$$\sigma_z = \nu(\sigma_x + \sigma_y) \tag{8.33}$$

that is:

$$\begin{aligned}\varepsilon_x &= \frac{1}{E}\left[\sigma_x(1-\nu^2) - \nu\sigma_y(1+\nu)\right] \\ \varepsilon_x &= \frac{1}{E}\left[\sigma_y(1-\nu^2) - \nu\sigma_x(1+\nu)\right] \\ \gamma_{xy} &= \frac{2(1+\nu)}{E}\tau_{xy}\end{aligned} \tag{8.34}$$

Solving the above equations for stresses and expressing them in a matrix form, we obtain:

$$\{\sigma\sigma\} = \left\{\begin{matrix}\sigma_x \\ \sigma_y \\ \tau_{xy}\end{matrix}\right\} = [D]\{\varepsilon\} \tag{8.35}$$

where:

$$[D] = \frac{E}{(1-\nu)(1-2\nu)} \begin{bmatrix} (1-\nu) & \nu & 0 \\ \nu & (1-\nu) & 0 \\ 0 & 0 & \frac{(1-2\nu)}{2} \end{bmatrix} \tag{8.36}$$

Step Four: Derivation of equations describing behaviour of the element.
Referring to well-known laws and principles, one can obtain the equations in a general form, which define behaviour of all finite elements in the discretised body. There are a number of procedures for the derivation of these equations, among them the most widespread being the energy method and the method of weighted residuals. With the energy method, many methods and variational principles are known; for example, the principle of stationary potential and complementary energy, and mixed and hybrid formulations. The method of weighted residuals is based on minimizing the remains, once the approximate solution is replaced in the differential equations, by means of which the problem is defined.

Application of any of the above-mentioned methods leads to equations that describe the behaviour of the element, which, in a general form, can be presented in the following:

$$[k]\{q\} = \{Q\} \tag{8.37}$$

where $[k]$ = element property matrix, that is to say, *stiffness matrix* in the displacement problem, and permeability matrix for the seepage problem; $\{q\}$ = vector of unknown quantities in the element nodes, for instance, of displacements; and $\{Q\}$ = vector of forces in the nodes of the element.

In formulating problems in mechanics, by using FEM, three different methods are used: displacement (or stiffness), stress (or equilibrium), and mixed. In the first method, displacement in an element is assumed as an unknown quantity and equations describing behaviour of the element are derived by the variational procedure based on the principle of *minimum potential energy*; while in the stress method, stresses are primary unknown quantities and, in this case, we use the principle of *minimum complementary energy*. In the case of the mixed method, both stresses and displacements are taken as unknown quantities, while special variational principles are used for derivation of the equations for the element.

In the analysis of embankment dams in which deformations are of primary importance, the displacements method is always used.

Step Five: Addition of the element equations in order to obtain general equations.
In order to obtain equations that will define the behaviour of the entire body, which consists of finite elements, it is necessary to add up the matrix equations of all of the elements. This addition, which is usually called a *direct stiffness* method, is carried out in such a manner as to satisfy the basic physical condition – that the structure remains continuous, i.e. to satisfy the condition for compatibility of displacements in the nodes belonging to two or more elements. As a result of this procedure, one can obtain an expression for the stiffness of the entire discretised body in the following form:

$$[K]\{r\} = \{R\} \tag{8.38}$$

where $[K]$ = total stiffness matrix; $\{r\}$ = total vector of displacements in nodes; and $\{R\}$ = total vector of forces in nodes.

Most often equations for stiffness of elements are formed in relation to the local coordinate system, so that it is necessary for them to be transformed into the general coordinate system, prior to their addition and formation of the expression (8.38). Also, in this step it is necessary to prescribe and introduce boundary conditions.

Step Six: Calculation of the primary and secondary unknown quantities.
In this step, we perform at first calculations for the primary unknown quantities; for instance, displacement, if the method of displacements has been used, by solving linear or non-linear simultaneous algebraic equations given with expression (8.38). For a solution, the Gaussian method of elimination is used or various iteration methods.

Finally, through primary quantities one can perform calculations for the secondary quantities, with the application of the relationship as defined in Step Two.

8.3.2 Specific properties of the application of the Finite Element Method (FEM) for analysis of embankment dams

For thirty years, substantial practice in the application of FEM in an analysis of embankment dams, in addition to the general regulations and principles connected with the choice of the type of finite element, density of elements mesh, execution of the numerical process, etc., clear regulations have crystallized, the application of which guarantees provision of a complete and real picture of deformations, stresses, and stability of the dam. The basic ones are as follows:

- Choice of a constitutive law expressing, inasmuch as objectively possible, the relationship between stresses and strains of materials in the dam's body and its foundation (if it is deformable);
- Input parameters, by means of which we represent the properties of materials in the dam's body and its foundation, should be accurately determined through field and laboratory investigations and testing, which are appropriate for a given material and which are compatible with a chosen constitutive law between stresses and strains (Vaughan, 1994);
- Simulation of the dam's construction, filling of the reservoir, and variations of loading during the service period;
- Influence of water should be introduced in a complex manner, with a simulation of: the effect of pore water during the execution of layers of cohesive materials, filling up of the reservoir in a number of increments, influence of water before and after establishing a stationary seepage flow through cohesive materials, process of consolidation, etc.;
- Contacts between any materials with different deformational characteristics, require employment of what are called *joint elements*, by means of which it is possible to determine differential displacements in different materials; thus, obtaining a real picture of stresses in the contact, i.e. the interface.

8.3.3 Choice of constitutive law

Constitutive laws of the stress–strains relationship for materials in the dam's body and its foundation can be obtained from the theory of elasticity or from the theory of plasticity. In practice various models are used for expressing the interdependence between stresses and strains of different earth and rock materials, which are used for the construction of embankment dams. It is very likely that stresses and deformations calculated according to the theory of elasticity will essentially differ from those that have been calculated by means of the theory of plasticity. That is why it is very important to distinctively differentiate between the elastic and plastic behaviour of earth materials.

Figure 8.10 gives a graphic representation of a number of types of possible constitutive dependencies, which can result from different compression tests carried out on cylindrical samples. Deformations of ideally elastic material completely recover during unloading; that is to say, energy applied to the material, after closing the loading cycle, is zero. Further more deformations of ideally elastic material depend on the change increment of stresses, while being independent of the instantaneous state stress–strain. Figure 8.10 (1) shows a *linearly elastic* model, which in fact is a special case of a *non-linearly elastic* model (2).

When deformations, or part of them, do not recover following unloading (3), then the non-recoverable deformations are called *plastic deformations*, while the material demonstrates a *plastic* behaviour.

In the case of ideally plastic material, in contrast to an ideally elastic material, deformations are dependent on the current state of stresses, while the direction of the vector of increment of deformations is independent on the direction of the increment of stresses. With such materials, the energy used in loading decreases in the material. That results in creating plastic deformations (Atkinson, 1973).

Drawing (4) presents *rigid plastic* behaviour, in which there are no elastic or recoverable deformations. Often, with the same material and with lower stresses,

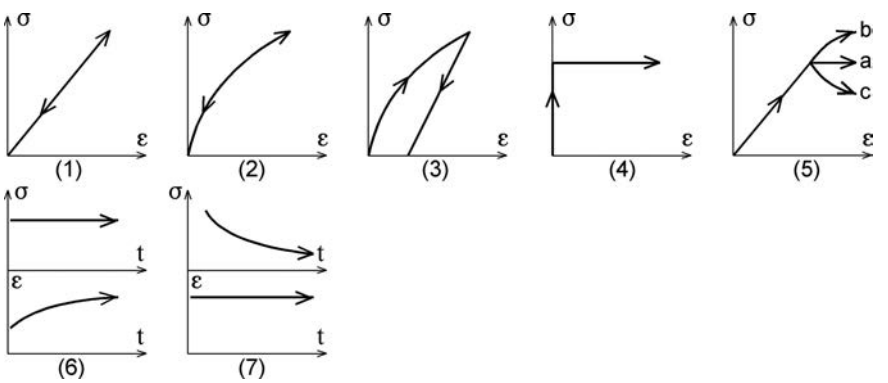

Figure 8.10 Types of stress–strain behaviour: (1) linearly elastic; (2) non-linearly elastic; (3) non-elastic, or plastic; (4) rigid, perfectly plastic; (5) elastoplastic: (a) perfectly plastic; (b) strain hardening; (c) strain softening; (6) visocoelastic creep at constant stress; (7) viscoelastic relaxation at constant strain.

recoverable deformations appear, while with higher stresses non-recoverable deformations appear. That leads to *elastoplastic* behaviour (5). In this, once a certain level of normal stress has been reached, we distinguish three cases of plastic behaviour: (a) *perfectly plastic* behaviour, when deformations in the plastic region do not exhibit any influence on the stress it causes; (b) *strain hardening;* and (c) *strain softening.*

In the five cases described above, changes of deformations and stresses come into existence simultaneously; that is to say, the deformation change comes only at a change of stresses. If there comes about an increase of deformations in the course of time, at a constant stress (6), or a decrease of stresses in the course of time at a constant deformation (7), then we have *viscous* or *viscoelastic* behaviour of the material.

Linearly viscoelastic is material for which the relationship between stresses and deformations within a given time interval is linear. In other words, if a load is applied in a certain time interval t, a certain deformation will appear, while if the same load is applied twice in the same time interval t, then the appeared deformation will be twice as much. Between stresses and deformations on the one hand, and time on the other hand, the relationship is almost never linear.

In the description in Step Three of solving the problems with FEM, we dealt with the *linearly elastic* stress–strain relationship in plane problems. Since, in certain cases and phases of design it is also possible to use the linearly–elastic relationship, and some methods of performing non-linear analysis use certain linear parameters, in the continuation there will be quoted the constants and parameters that appear in linearly elastic analysis, as well as the relationships among them.

1. *Young's modulus*, or the *modulus of elasticity E*, expresses the relationship between the axial stress and deformations in the test of compression or tension, so:

$$\sigma_x = E\varepsilon_x \tag{8.39}$$

2. *Poisson's ratio* ν is the ratio of the axial strain and the transverse normal strain in the test of compression or tension, i.e.:

$$\varepsilon_y = \varepsilon_z = \nu\varepsilon_x \tag{8.40}$$

3. *Shear modulus G*, which represents the ratio between the shear stress and the shear strain:

$$\tau_{xy} = G\gamma_{xy} \tag{8.41}$$

4. *Bulk modulus* K_b, which relates volumetric strain to the average or octahedral stress:

$$\sigma_{oct} = K_b\varepsilon_{vol} \tag{8.42}$$

5. *Lamé's constants* λ and μ. These relate stresses and strains, as follows:

$$\sigma_x = \lambda\varepsilon_{vol} = 2\mu\varepsilon_x \tag{8.43}$$

as well as in a similar expression for σ_y and σ_z.

6. *Constrained modulus M*, which relates axial strain to axial stress when the other two axial strains are held to zero:

$$\sigma_x = M\varepsilon_x. \tag{8.44}$$

The following relationships exist between the above-mentioned constants:

$$G = \mu = \frac{E}{2(1+\nu)}; \qquad K_b = \frac{E}{3(1-2\nu)} = \lambda + \frac{2}{3}\mu;$$
$$\lambda = \frac{\nu E}{(1+\nu)(1-2\nu)}; \quad M = \frac{(1-\nu)E}{(1+\nu)(1-2\nu)} \tag{8.45}$$

In elastic analyses, the stress–strain relationship, in considering problems as a plane strain, is represented by expressions (8.31) through (8.36). For a three-dimensional treatment of the problem, appropriate expressions are given in a number of books, for example (Desai et al., 1977; Fadeev, 1987).

Earth materials, as well as coarser graded materials, are not linear, so that the laws describing their behaviour are much more complicated as compared to the simple relationships described in the previous text. That is why, for obtaining a realistic picture of a dam's behaviour, it is necessary to apply non-linear stress-strain relationships to all the materials in its body (Doležalová, 1994; Finn & Miller, 1976). There are numerous methods that are used for expressing non-linearity in embankment filling materials, which can be divided into three groups: (1) Representing a given curve for stress-strain with a broken, i.e. packed, line, close to it, or by means of a mathematical function; (2) application of the theory of elasticity; (3) application of the theory of plasticity.

The representation of the curve stress-strain with a piecewise line implies the application of a *bilinear*, or *multilinear*, model that has been used during the initial period of the application of FEM. In the last 35 years for the analysis of embankment dams, *the hyperbolic relationship* has found its widest application, in which the stress–strain curve is represented by means of a mathematical function in the form of a hyperbola, Figure 8.11. This method is based on Hooke's Law with elastic parameters, determined in each element on the basis of the actual instantaneous state of stresses. The method was formulated by Duncan and Cheng in 1970, taking into consideration the conclusion of Kondner 1963, according to which the stress-strain curve, obtained through

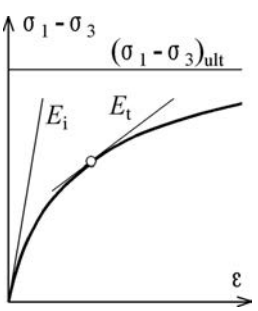

Figure 8.11 Hyperbolic relationship.

data from the triaxial compression test, for a number of earth materials is very close to a hyperbola. They formulated that relationship in the form (Duncan & Cheng, 1970):

$$(\sigma_1 - \sigma_3) = \frac{\varepsilon}{\frac{1}{E_i} + \frac{\varepsilon}{(\sigma_1 - \sigma_3)_{ult}}} \tag{8.46}$$

where $(\sigma_1 - \sigma_3)$ = deviator of stresses, $(\sigma_1 - \sigma_3)_{ult}$ = asymptote value of the difference of principal stresses at considerable axial strain, ε = axial strain, and E_i = initial tangent modulus (Fig. 8.11).

The asymptote value $(\sigma_1 - \sigma_3)_{ult}$ has been defined in relation to the real value of the difference of principal stresses at failure $(\sigma_1 - \sigma_3)_f$, and the relationship R_f as:

$$R_f = \frac{(\sigma_1 - \sigma_3)_f}{(\sigma_1 - \sigma_3)_{ult}} \tag{8.47}$$

Since compressive strength is reached before the curve becomes asymptote, R_f most often ranges within the limits 0.70–0.95. The initial tangent modulus can be calculated from an expression proposed by Janbu (1963):

$$E = Kp_a \left(\frac{\sigma_3}{p_a}\right)^n \tag{8.48}$$

where p_a = atmospheric pressure introduced into the expression in order to make K and n non-dimensional; K = modulus for expressing the stiffness of material; and n = exponent for expressing sensitivity of E_i due to changes in σ_3.

The deviator of stresses, at failure, is a function of the minor-stress σ_3 and one of the possibilities for its expressing, for applying the rectilinear *Mohr–Coulomb's* envelope, is given in this form:

$$(\sigma_1 - \sigma_3)_f = \frac{2c\cos\varphi + 2\sigma_3 \sin\varphi}{1 - \sin\varphi} \tag{8.49}$$

where φ = angle of internal friction, obtained from the true envelope of failure; c = cohesion. However, Mohr-Coulomb's envelope of failure is not always linear, i.e. the angle of internal friction φ is not constant, but can vary with a change of stresses. One such approach, proposed by Duncan (Boscardin et al., 1990; Stark et al., 1994), assumes φ to vary, depending on σ_3:

$$\varphi = \varphi_0 - \Delta\varphi \log\left(\frac{\sigma_3}{p_a}\right) \tag{8.50}$$

where φ_0 = value of φ at $\sigma_3 = p_a$; and $\Delta\varphi$ = reduction of φ, obtained for $\sigma_3 = 10p_a$.

If equation (8.46) is differentiated with regard to ε, and if equations (8.47), (8.48), (8.49), and (8.50) are replaced in the obtained expression, we come to the following expression for the tangent modulus of elasticity E_t, i.e. for the instantaneous

actual inclination of the hyperbola, by means of which is presented the stress–strain relationship, Figure 8.11:

$$E_t = \left[1 - \frac{R_f(1-\sin\varphi)(\sigma_1-\sigma_3)}{2c\cos\varphi + 2\sigma_3\sin\varphi}\right]^2 Kp_a\left(\frac{\sigma_3}{p_a}\right)^n \tag{8.51}$$

In this way the parameters describing Young's modulus, based on a hyperbolic relationship, are K, n, c, φ (or φ_0) and R_f.

For a complete determination of material stiffness, the other parameter of elasticity is also necessary. On the basis of investigations on a number of kinds of clay and sand, Kulhawy and Duncan propose the following expression for the tangent relationship of Poisson's ratio υ:

$$\nu_t = \frac{G - F\log\left(\dfrac{\sigma_3}{p_a}\right)}{\left\{1 - \dfrac{D(\sigma_1-\sigma_3)}{Kp_a\left(\dfrac{\sigma_3}{p_a}\right)^n\left[1 - \dfrac{R_f(1-\sin\varphi)(\sigma_1-\sigma_3)}{2c\ \cos\varphi + 2\sigma_3\sin\varphi}\right]}\right\}^2} \tag{8.52}$$

where G = initial value ν_i at pressure p_a (=103 kN/m^2); F = coefficient defining the change of ν_i with the change of lateral pressure σ_3; and D = coefficient expressing the change of ν_i, depending on the strain. The coefficients G, F and D are determined experimentally. At unloading, the tangent modulus is calculated from the expression:

$$E_{tr} = K_r p_a\left(\frac{\sigma_3}{p_a}\right)^n \tag{8.53}$$

where the modulus K_r has a higher value than K (for the very same material). When there is a lack of data obtained from laboratory investigations, it is usually assumed that $K_r = 1.25\,K$.

Parameters entering the hyperbolic relationship, through which one can determine the value of the tangent modulus E_t with expression (8.51), are obtained with a trial compression test, which for earth materials, is standard and broadly widespread.

During the last 40 years, in practice there have also been introduced triaxial tests for gravel and rock materials in an especially constructed apparatus with large dimensions, which is one of the reasons for the popularity of the hyperbolic relationship in spite of certain deficiencies that it has. The most significant deficiency of the method is the impossibility of accurate defining of the deviator of stresses, at which it comes to failure, as well as the uncertainty of data for high values of the relationship σ_1/σ_3 (for example >4).

Another important parameter, necessary for the application of Hooke's law in a generalized form, is the volumetric modulus B, which is defined as:

$$B = \frac{\Delta\sigma_m}{\Delta\varepsilon_{vol}} \tag{8.54}$$

where $\Delta\sigma_m$ is a variation of the mean normal stress, while $\Delta\varepsilon_{vol}$ is the change of the volumetric strain. For the conventional triaxial compression test with constant

Table 8.1 Approximate values for parameters of the hyperbolic relationship.

Parameter	*Clay*	*Sand*	*Gravel and stone*
K	100–300	400–600	800–2000
n	0.50–0.75	0.3–0.4	0.3
R_f	0.75–1	0.75–0.95	0.70–0.90

lateral pressure and with initial state with hydrostatic stress, equation (8.54) can be expressed as:

$$B = \frac{\sigma_1 - \sigma_3}{3\varepsilon_{vol}} \tag{8.55}$$

which represents a secant modulus, dependent on the data determining it. Duncan offers a method for selection of points obtained with investigations, which would be representative of given materials (Boscardin et al., 1990). The volumetric modulus can be defined as a function of σ_3 by means of the exponential law:

$$B = K_b p_a \left(\frac{\sigma_3}{p_a}\right)^m \tag{8.56}$$

where K_b is bulk modulus, while m is the exponent of the bulk modulus.

In some instances Poisson's ratio is varied depending on the tangent modulus of elasticity and the volumetric modulus, through the expression (Najmaii & Haj-Hasani, 1992):

$$\nu = 0.5 - \frac{E_t}{6B} \tag{8.57}$$

The approximate values for parameters entering into expressions of the hyperbolic relationship are given in Table 8.1.

In the hyperbolic relationship, as well as in a number of other constitutive models, Mohr–Coulomb's criterion for failure is used (8.49). A simple and conservative criterion, it can be used for cohesive and non-cohesive materials. In practice other criteria are also used, of which a great many have been formulated on the basis of Mohr–Coulomb's criterion (Griffiths, 1990).

Of constitutive laws that are based on the generalized Hooke's Law, (8.31)–(8.36), and (8.39)–(8.45), one can say that they represent a lower order of models, based on the theory of elasticity. In geotechnics it is possible to use elastic constitutive laws of a higher order, called *hyperelastic* and *hypoelastic* models. These models are defined with a large number of parameters, so that their practical application is very difficult and irrational (Desai & Christian, 1977).

Earth materials, like graded non-cohesive materials, generally speaking are *elastic-plastic*. Namely, deformations of these materials are a result of slippage among the particles, as well as elastic deformations of the individual particles (Desai & Christian,

1977; Hardin, 1983). The constitutive relationships described so far are called *deformation relationships* because, by means of their assistance, it is possible to directly present the stress–strain relationship, even in a case when they are expressed in the form of an instantaneous or tangent modulus.

On the other hand, relationships emerging from the *theory of plasticity* are usually *incremental ones*, i.e. both stresses and deformations are fully expressed through their incremental or differential behaviour. Here, it is not possible to establish a relationship between total stress and total deformation directly, without knowing the loading path.

The behaviour of some material, described by the theory of pure plasticity, is defined by means of the criterion of deformation f_f, which is a function of the stresses, deformations, and other parameters, so that *when* $f < 0$, the material is elastic, while when $f_f = 0$, the material is in a plastic state. The function f_f is never greater than 0.

The criterion of Tresca is well known in the theory of plasticity, according to which plastic creep comes into existence when the maximum shear stress reaches the shear strength. In an algebraic form, for a plane-strain approach it is:

$$f_f = \left(\frac{\sigma_x - \sigma_y}{2}\right)^2 + \tau_{xy}^2 - k^2 = 0 \tag{8.58}$$

where k is the shear strength.

A central concept in the theory of plasticity is the *theory of plastic potential* and the *associated law of creep*. According to these laws, when material is in a plastic state, the differential increments of deformations are proportional to the external normals on the surface of creep or, in other words, *the increments of deformations are proportional to the gradient of the surface of creep*. Following certain derivations, (whose listing would exceed the concept of this book), we come to an incremental stress–strain relationship in a matrix form, ready for application (Desai & Christian, 1977; Fadeev, 1987).

Another also often used criterion for creep is the one of Von Mises:

$$f_f = k^2 - J_2 \tag{8.59}$$

where J_2 is the second invariant of the deviator of tensor of stresses,

$$J_2 = \frac{1}{6}\sqrt{(\sigma_1 - \sigma_2)^2 + (\sigma_2 - \sigma_3)^2 + (\sigma_1 - \sigma_3)^2} \tag{8.60}$$

so that principal stress σ_2 also enters into the criterion, which facilitates the mathematical procedure (in relation to the previous case). The application of this criterion leads to an equation called the Prandtl-Reuss equation, which can be used directly in two-dimensional or three-dimensional applications.

Criteria for plastic creep that also takes into consideration friction of material have been developed by Drucker and Prager, based on the generalized form of Mohr–Coulomb's Law:

$$f_f = \sqrt{J_2} - \alpha J_1 \tag{8.61}$$

where $J_1 = \sigma_1 + \sigma_2 + \sigma_3$ is the first invariant of the tensor of stresses, while α and k are parameters of the material, for a plane-strain method, given with the expressions:

$$\alpha = \frac{\tan\varphi}{\sqrt{9 + 12\tan^2\varphi}}; \qquad k = \frac{3c}{\sqrt{9 + 12\tan^2\varphi}} \tag{8.62}$$

Drucker–Prager's expression (8.61) is called by some authors the *extended Von Mises' criterion*. It is widely used for a description of the shear strength of earth and rock materials in three-dimensional analyses, even though opinions exist that the tried and true Mohr–Coulomb's Law

$$\tau = c + \sigma_n \tan\varphi \tag{8.63}$$

agrees better with experimental data (Desai & Christian, 1977; Desai et al., 1981). The quoted elastic-plastic models fall into the group of models with *an open plane of deforming* and are appropriate for materials with relatively small volume deformations such as compacted sand and well-graded rock material. For normally consolidated clay, where we can expect larger volume deformations, more suitable are the models with *a closed plane of deforming*, as is the *critical state model* or *cap model* (Desai & Christian, 1977).

The literature also lists other different models, with an ambition as truly as possible to present the behaviour of earth and rock materials (Ivanov, 1985; Fadeev, 1987; Burland, 1990; Chandler, 1990; Clough & Zienkiewicz, 1987; Desai & Christian, 1977; Desai et al., 1981; Desai & Salami, 1987; Eisenstein & Naylor, 1986; Nonveiller, 1979; Sheng et al., 2008; Zeping Xu, 2009; Alonso & Cardoso, 2010; Alonso & Gens, 2011). Some of them are very complex, so that they treat the earth material as a *three-phase* one. Namely, during placement and compaction of a layer of filling material, the voids among individual grains and particles are partially filled with air. *Dungar*, in order to represent the behaviour of partially saturated earth material, approximates that the pore air pressure is equal to the atmospheric one, while the pore water pressure is below the atmospheric pressure because of the *capillary suction* in the fine earth pore. The pressure of suction is dependent on the size of particles of the material and is noticeable in clays and coarser earth materials containing admixtures of clay. The finer and the more plastic clay is and the lower the content of water is during compaction, the greater the capillary suction is. The initial capillary suction in a newly carried out clay embankment is usually 1.4 to 2.8 atmospheres below the atmospheric pressure and it can be measured with special laboratory equipment. With embankment construction advancement, the pressure in the lower layers causes a reduction of volume of the compressible air bubbles which, possibly, can burst and disperse and dissolve in the pore water. In that way, the quantity of free air is decreased, and as a consequence of this there is an increase in the degree of saturation with water, causing a reduction in the capillary suction. Dungar develops an elastic-plastic model by taking into consideration the capillary suction (Dungar, 1988b) and he deems that in order to obtain correct results in the analyses of embankment dams by means of FEM, such an approach is essential. Alonso et al. develop a similar model, in which they assume two independent variables of stresses – an increase of total stress above the air pressure and suction (subpressure in the water phase) (Alonso et al., 1990).

Later on such a model was developed by Pietruszczak & Pande (1996), analyzing two kinds of earth materials. In the first one, the air bubbles are much smaller than the average dimensions of solid particles, while in the second one, larger air bubbles have been inserted into the saturated earth skeleton. The mathematical formulation encompasses average ratio pores: bubbles as an independent parameter of the material. During the last 15 years further progress has been made in the field of understanding and modeling of the behaviour of unsaturated soils and the reader is refered to the literature dealing with this complex subject (Fredlund et al., 1995; Fredlund, 2006; Rampino et al., 2000; Alonso & Pinyol, 2008; Sheng et al., 2008; Alonso & Cardoso, 2010; Alonso & Gens, 2011).

From the previous review of these problems, it is self-evident that the choice of an appropriate constitutive law, which will truly present the behaviour of material, is a complicated task. It must be pointed out that the way to obtain a valuable and effective constitutive law for a given material consists of five steps:

1. Mathematical formulation of the model;
2. Identification of input parameters;
3. Determination of the parameters by an appropriate test;
4. Verification of the model in relation to laboratory tests and physical conditions;
5. Verification and assessment of the model in relation to boundary conditions.

All the quoted steps are important; however, the third one – determination of the input parameters by an appropriate test – deserves special attention. Namely, this step has a decisive role in arriving at true results, since even the most complex model is in vain if the input parameters are not a true reflection of the behaviour of the materials in the dam's body.

In the former practice for obtaining parameters for properties of the materials, the most frequently used test was the triaxial test, which gives a rather true picture of the space loading state of the earth and graded materials. Lately, the *multiaxial apparatus* is also used, by means of which cubical earth samples are tested having dimensions $10 \times 10 \times 10$ cm, with different directions of loading and its simulation – hydrostatic compression, conventional triaxial compression, conventional triaxial tension, reduced triaxial tension, and simple shearing (Desai et al., 1981).

We have already mentioned several times that, in the case of graded materials, obtaining the parameters for the strength characteristics is more complex than for cohesive materials, for which standard equipment for testing was constructed long ago. Proceeding from the assumption that in the case of graded media (sand, gravel, and crushed stone) the forces during loading are being transferred through the contacts between the grains, there also have been developed numerical models for monotonous cyclic loading of graded materials.

One such model was developed by means of the *Discrete Elements Method*, for which the authors (Ng & Dobry, 1994) deem that it is an effective addition to laboratory experiments and that it is suitable for application with graded materials. This method encompasses micromechanical phenomena among the grains of the material, which are correlated with the macroscopic response of the medium, so that the method deserves attention and further study.

We have already emphasized the complexity of the choice for appropriate constitutive model for materials for embankment dam analysis. Generally, the choice of stress-strain constitutive model used in the analysis should be balanced between simplicity and accuracy. Also the choice of constitutive model depends on the purpose of the modelling. If the purpose of the analysis is to analyze stresses and the trend of deformations then more simplistic models could be suitable, depending on the relative stiffness between different embankment materials. If more accurate modelling of the primary values at embankment dams – deformations – is required then a more complex stress-strain model should be applied. Based on the relatively rich practice, one can conclude that elastic stress-strain models, like linear elastic, multi-linear elastic or hyperbolic models, are appropriate where the soils are not stressed to failure, but that these models are not suitable for modelling undrained behaviour or problems where local failure occurs. For these situations (e.g. for wet placed earthfill cores of thin to medium width in zoned embankments) the use of models that incorporate plasticity theory is recommended (Duncan, 1966).

8.3.4 Simulation for dam construction in layers

Clough et al. (1967) showed the validity and importance of simulation for dam construction in layers in the first known scientific paper on analysis of embankment dams using FEM. With the example of a 30.5 m high hypothetical earthfill dam (Fig. 8.12a), discretised with triangular elements (b), it has been shown that the way one simulates a dam's construction has a decisive influence on the vertical deformations in its body.

Namely, if we imagine that the dam has been constructed instantaneously (in one layer), then the maximum settlement will occur at the crest of the dam (Fig. 8.13a). A completely different picture is obtained if the construction has been simulated in 10 layers (Fig. 8.13b), in which case we obtain a real picture, with a maximum settlement in the intermediate part of the dam and, in absolute value, twice smaller in comparison with the previous case.

In simulating construction in layers, it is also possible to simulate construction of the concrete elements and auxiliary dams, which are incorporated into the dam's body. Figure 8.14 shows the lines of uniform settlements at the 230 m high Oroville dam (USA), caused by its own weight. A nonlinear analysis has been carried out in three phases. The first one simulates construction of the concrete block below the core in nine layers, while the second phase represents construction of the 122 m high cofferdam, also in nine layers. Finally, the third phase simulates construction of the main embankment in 12 layers. The foundation has been treated as being rigid.

The greatest value of the settlement appears in the core, in the middle of dam's height and it amounts to 140 cm. Moving towards the transitional zones and shells, the settlement rapidly decreases. Another zone with relatively high values of settlement appears in the vicinity of core's center in the upstream cofferdam. Comparison of calculated settlements with measured ones shows that they do not deviate much – at 85% of the installed apparatus, the difference is within the limits of 25% (Kulhawy & Duncan, 1972).

The Gradec earth-rock dam, planned to be built on the River Vardar in its lower course, (Fig. 8.15), has been analyzed at the Faculty of Civil Engineering in Skopje, by

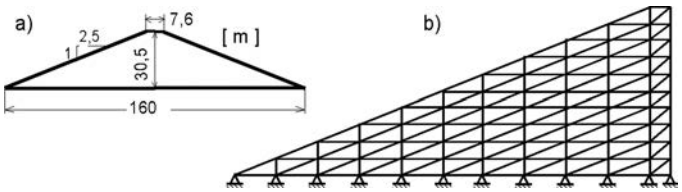

Figure 8.12 Dimensions of cross-section of the analyzed dam (a), and discretisation with finite elements (after Clough et al., 1967).

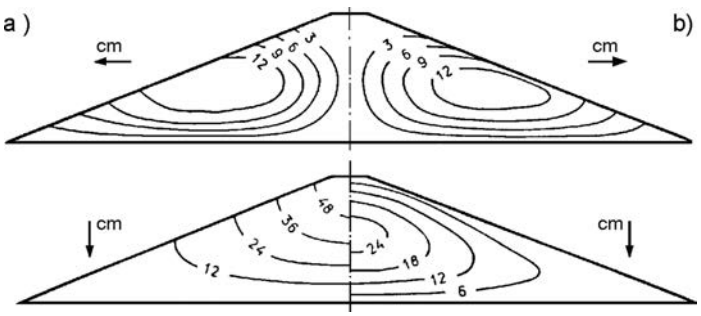

Figure 8.13 Horizontal and vertical displacements in the body of a hypothetical earthfill dam. (a) Construction of embankment in one layer; (b) construction in 10 layers.

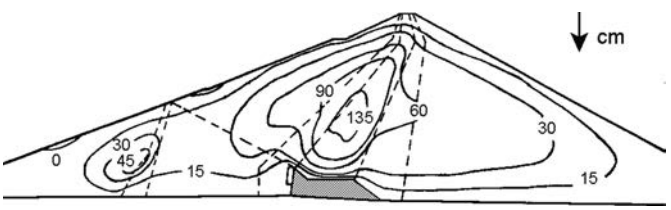

Figure 8.14 Lines of equal settlements for the Oroville dam (USA) obtained by means of FEM, and caused by its own weight.

the application of a complex nonlinear model, using the expressions (8.51)–(8.53) of the hyperbolic relationship (Tancev et al., 1991).

The method of analysis has been carried out in the following manner:

1. The dam has been discretised with parabolic isoparametric elements with eight nodal points, so that there are also encompassed a part of the foundation upstream and downstream, as well as below the dam, up to the rock. Discretisation has been carried out so as to encompass all of the different materials in the body and foundation by means of particular elements, and it is made possible a simulation

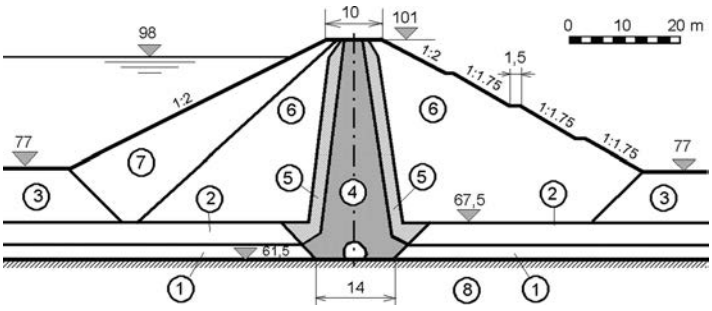

Figure 8.15 Cross-section of the Gradec dam (design). (1) Decomposed diabase in foundation; (2) layer of gravel in foundation; (3) river sediment – sand; (4) clay core; (5) filter layers; (6) shells of gravel; (7) rock fill; (8) rock in foundation – diabase.

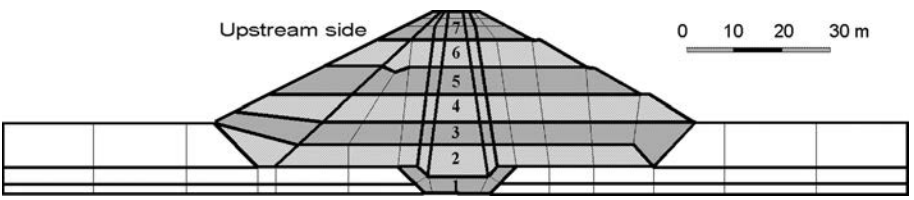

Figure 8.16 Gradec dam, simulation for construction in layers.

of dam's construction with a structural height of 39.5 m in seven layers, starting from the lowermost layer of the core, in contact with the foundation (Fig. 8.16).

2. There are assigned parameters for the physical-mechanical properties of all materials, taking into consideration that the nonlinearly dependent *modulus of elasticity* and *Poisson's ratio* receive certain initial values E_0 and v_0.
3. The first layer has been placed and for the action of all forces (in this case, only the weight of the material) with the values of E_0 and v_0 displacements in nodes have been calculated and, through them, the stresses σ_x, σ_y and τ_{xy}, from the expressions for a planar state of deformations. The total principal stresses σ_1 and σ_3, which E and v depend on, have been calculated by means of the well-known expression:

$$\sigma_{1,3} = \frac{\sigma_x + \sigma_y}{2} \pm \sqrt{\left(\frac{\sigma_x - \sigma_y}{2}\right)^2 + \tau_{xy}^2} \tag{8.64}$$

4. Values of E_0 and v_0 are worked out by means of an iteration process, as long as the condition:

$$\frac{|E_{ti} - E_{ti+1}|}{E_{ti}} \leq 0.1 \tag{8.65}$$

is fulfilled for all elements.

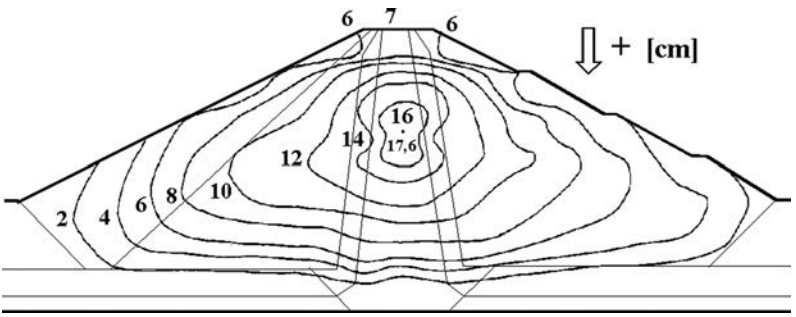

Figure 8.17 Gradec dam, contour lines of vertical displacements caused by the weight of the dam itself.

5. The next layer is then added, i.e. the following loading case is applied, and afterwards the entire process is repeated, taking into consideration that for the newly placed layer we enter the calculations with the initial assigned values E_0 and υ_0, while for the 'old' elements we start with the values of E_t and υ_t, that have been obtained in the last iteration cycle of loading.
6. Whether the element is loaded or unloaded, one can judge according to the value of the mobilized shear strength, calculated in its centroid by means of the expression:

$$m = \frac{\tau_{max}}{\tau_f} \tag{8.66}$$

where $\tau_{max} = \frac{1}{2}(\sigma_1 - \sigma_3)$, while τ_f is obtained through the expression (8.49), which represents a criterion for failure. If the mobilized strength is increased in relation to the previous loading case, the element is loaded and the expression (8.51) is valid; on the contrary, the expression (8.53) is valid.

Maximum settlement appears in the middle of the dam, at a height $\approx 0.6H$ and it amounts to 17.6 cm (Fig. 8.17). This analysis is more realistic than the previously presented two analyses, in which at the placement of each new layer, it has been assumed that deformations in the upper edge are zero. Another result of such an improved analysis is also the settlement of the crest (7 cm), caused by the weight of the dam itself (in the previous cases, it amounted to zero). Figure 8.17 clearly indicates that for such a dam – with small height and relatively slight slopes – in the parts upstream and downstream from the dam's ends on a non-rock foundation, practically, settlements do not occur. The same observation is also valid for horizontal displacements.

In textbook references and periodicals there are examples of analyses of embankment dams with a simulation of construction in layers (Cathie & Dungar, 1978). In some cases, a simulation is also made for the excavation in a dam's foundation (by assigning the weight of material as a force acting upward) in order to obtain a

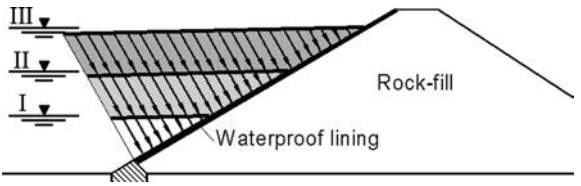

Figure 8.18 Simulation of the force of hydrostatic pressure on the dam facing.

more realistic initial state prior to the placement of the first layer of the embankment (Belloni & Tanzini, 1992; Desai & Christian, 1977).

8.3.5 Simulation for filling the reservoir and the effect of water

Water with its complex effects, considerably complicates the question of the determination of the stress–strain state in embankment dams, so that it is not by accident that the initial five years of the application of FEM for the analysis of these complex structures have boiled down to an analysis of the construction of dams in layers.

An increase of water in the reservoir should be added gradually, in several increments, by taking into consideration all accompanying effects. We shall try in the continuation to illustrate them on several characteristic kinds of embankment dams.

8.3.5.1 Rockfill dams with impermeable facing

Simply, the effect of water exhibits itself in rockfill dams with a water-impermeable facing when it reduces itself to the action of a force due to hydrostatic pressure on the facing, being applied in several increments (for instance, three, Fig. 8.18). The consequences of water action in this type of embankment dam are clearly perceived and are reduced to the following: (1) In the body of the dam there occur additional settlements and horizontal displacements toward the downstream face; (2) the facing is being deformed; and (3) there come about changes in the state of stresses, which have a beneficial reflection on the dam's stability.

As an illustration of the first consequence, Figure 8.19 indicates diagrams for contour lines of horizontal (a) and vertical (b) displacements, caused only due to the effect of water, for a hypothetical rockfill dam with asphaltic facing, 80 m high, analyzed by the author (Tančev, 1989) by means of the model already described in the example for the Gradec dam.

The greatest settlement appears on the facing and it amounts ≈4 cm, while Figure 8.19 shows that settlements appear only below the facing, predominantly in the lower part of the dam. In the zone of the crest, immediately below it, as well as in the upper part of downstream face, there comes about a slight rising with a maximum value of 0.4 cm. The maximum horizontal displacement caused by water, as well, occurs in the facing, somewhat lower than the middle part and it amounts to ≈6 cm.

Toward the downstream face, the magnitude of horizontal displacements progressively decreases, while in the dam's crest there comes about a displacement of 2 cm.

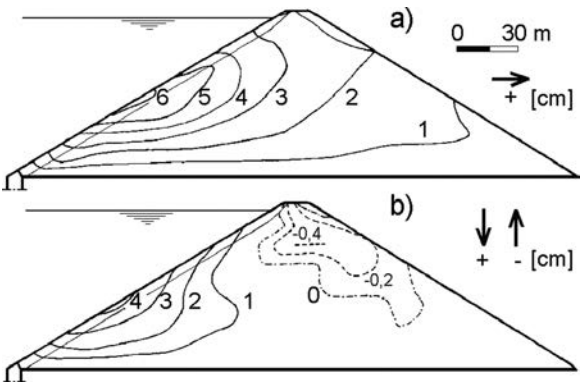

Figure 8.19 Horizontal (a) and vertical (b) displacements caused by the hydrostatic pressure.

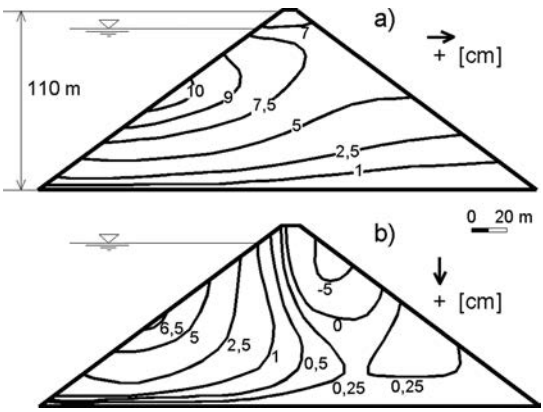

Figure 8.20 Horizontal (a) and vertical (b) displacements in the body of the rockfill dam, Cethana dam (Australia), with a reinforced concrete facing, due to the effect of hydrostatic pressure on the facing, calculated with a nonlinear model of FEM (after Khalid et al., 1992).

Obtained displacements are relatively small for a dam of such a height. This is due to the stiff rock material in the dam's body ($\gamma = 22.5\,\text{kN/m}^3$, $\varphi = 45°$, $K = 1500$).

Analysis by this method, carried out on the first modern dam, Cethana dam, in Australia, with a reinforced concrete facing, gives similar results, Figure 8.20 (Khalid et al., 1992). Deformations in this case are somewhat greater. This is due to the greater height of the dam (110 m), steeper inclinations of slopes, as well as differences in the main physical and mechanical characteristics of the rock material ($\gamma = 20\,\text{kN/m}^3$, $\varphi = 39°$, $K = 2500$).

The second effect, deformation of the facing, will be illustrated in the same examples. The asphalt-concrete facing, 25 cm thick at crest and 35 cm thick in the foundation, in the analyses of the author (Tančev, 1989), is deformed as it is shown in

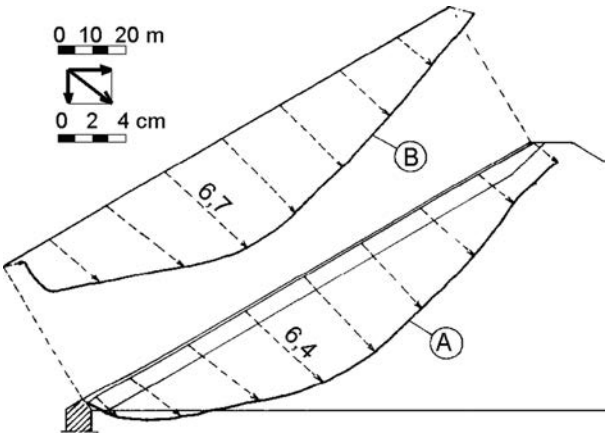

Figure 8.21 Deformation of the lower (A), and upper edge (B), of asphalt–concrete facing.

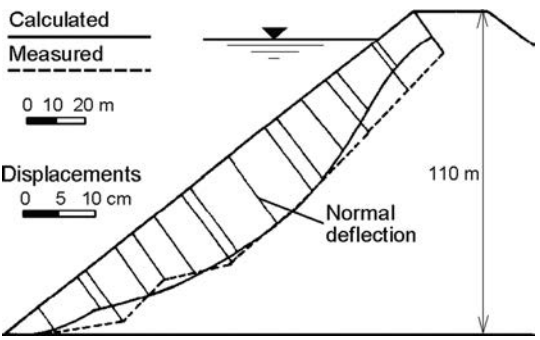

Figure 8.22 Normal deflection of facing for Cethana dam after filling the reservoir (after Khalid et al., 1992).

Figure 8.21. The maximum displacement is recorded approximately below the middle of the facing.

Deformation of the reinforced concrete facing of the Cethana dam, 3 cm thick at the crest and 5 cm thick in the foundation, calculated by means of FEM, is shown with a solid line in Figure 8.22, and is related to the upper edge. The diagram has a pattern similar to that in the case of an asphalt–concrete facing. The maximum summary displacement of the facing here again is approximately in the middle of the facing and amounts to $\approx$11.5 cm.

In the same figure, with a dashed line, is shown a diagram of summary displacements of the facing, drawn on the basis of measurement data, recorded immediately after the first filling of the reservoir (8 December 1971). There is evident a good agreement of the results of calculations and measurements. The considerable measured displacements in the upper part are due to the time-dependent deformations which are maximum in the highest part of the embankment, occurring in the course of the filling

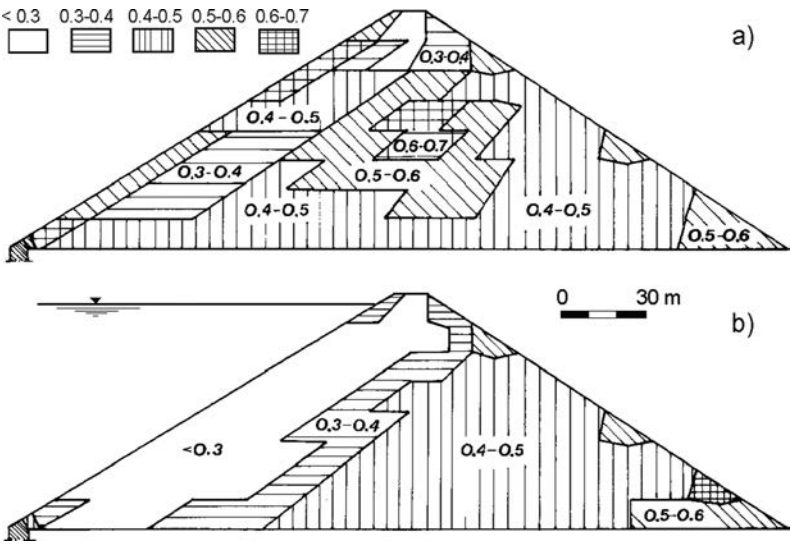

Figure 8.23 Diagrams for mobilized shear strength for a dam with asphalt–concrete facing, 80 m high.

of reservoir, and which have not been covered in the analysis. More attention will be devoted to this important phenomenon later in this chapter.

The above-obtained data for deformations of facings in rockfill dams give valuable understandings for the assessment of the stability of the water-impermeable element, as well as for its rational design. The development of numerical methods for analysis of dams is one of the reasons for the development of dams with a reinforced concrete facing in the last 35 years.

The third consequence for the action of water in dams with a facing – improvement of the stability of the dam – is paradoxical at first sight, but it is true. Namely, the fact that the filling material in its body does not come in contact with water is rather favorable for the dam. Furthermore, the vertical component of the hydrostatic pressure on the facing, in fact increases the weight of the dam. Within the gravity type of dam, to which embankment dams belong, it is favorable and makes a contribution to improving the dam's stability. If we add here the fact that the horizontal component of the force of water increases the normal horizontal stresses in the dam's body, which also increases the shear strength, it is no wonder that dams with a facing have greater stability when the reservoir is full. This is illustrated in Figure 8.23, with diagrams for the mobilized shear strength of a dam with asphalt-concrete facing, obtained by the analyses of the author (Tančev, 1989).

The diagrams have been obtained with the values for the mobilized shear strength, calculated at the center of gravity of each element by means of the expression (8.66). Figure 8.23a shows that, prior to the filling of the reservoir, the greatest values for the mobilized strength are obtained in the central part of the dam, as well as in some local zones below the facing. Even so, the maximum loaded elements mobilize less than

70% of the available strength. Loading with water 'unloads' the upstream and central part of the dam, while in the downstream part practically there is no influence (b).

In the case of a full reservoir, the zone immediately to the downstream end is maximally loaded; however, here, as well, the mobilized strength hardly exceeds the value of 60%. Here, it is significant that the reciprocal value for the mobilized shear strength represents a *coefficient of safety against shearing*. In this way, by means of the mobilized strength, the dam's stability in each of its local zones is represented, and also as a whole.

8.3.5.2 Embankment dams with an internal core

In the case of earth–rockfill dams with a central core and rockfill dams with a core made from artificial material, the effect of water is manifested rather differently compared with the case of rockfill dams with upstream water barrier. Analyses of first filling generally consider the main water barrier element to be impermeable during first filling and the water load to act on the upstream face of this zone. Water penetrates through the water-permeable material into the upstream shell, submerges it, and causes the following effects[1]:

1. Softening of the saturated non-cohesive granular material in the upstream shell, Figure 8.24a; the consequence is additional settlement and some horizontal deformations.
2. Buoyant uplift on upstream shell, saturated in water (Fig. 8.24b); the result is decrease of effective stresses in the permeable rockfill zone upstream of the core, which can cause deformations upward and upstream, but are likely to be very small due to the rather high tangent modulus on unloading and reloading of gravels and rockfills compared to their modulus during loading.
3. Action of a force due to hydrostatic pressure on the upstream side of the core of impermeable material, Fig. 8.24c, resulting in a net increase in the total stresses within and downstream of the core. The resultant deformation is downstream and downward.
4. Seepage of water into the core, with an established stationary seepage flow; seepage forces will cause additional deformations.

The first effect is very important and has a complex action that is exhibited with additional settlements in the embankment, horizontal displacements, as well as a change in the state of stresses, which sometimes can lead to an occurrence of fissures in the core. This effect is simply presented in Figure 8.24a, through causing additional settlement. The phenomenon of softening of non-cohesive materials can clearly be seen from the two curves representing the stress–strain relationship, obtained through triaxial testing of the material of the shell of the Oroville dam (USA), Fig. 8.25, (Eisenstein & Naylor, 1986). The curve of the wet material apparently gives lower strength characteristics for equal stresses, which can also be seen from the numerical values of the most important parameters entering the hyperbolic relationship: for the dry state: $\varphi = 46.3°$;

[1]We assume that the foundation is practically non-deformable and impermeable, which is the case for most large earth-rockfill and especially rockfill dams with an artificial waterproof barrier.

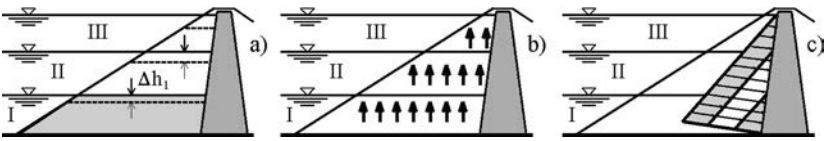

Figure 8.24 Simulation of the effect of water. (a) Effect of softening of non-cohesive granular material saturated with water; (b) buoyant uplift on upstream shell; (c) hydrostatic pressure on the upstream side of the core prior to establishing the seepage flow through it.

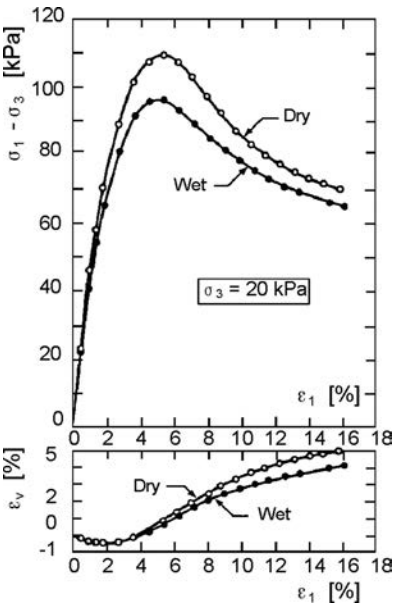

Figure 8.25 Stress-strain relationship showing the softening of non-cohesive material (after Eisenstein & Naylor, 1986).

$K = 2030$; $n = 0.34$; $R_f = 0.86$; for the wet state: $\varphi = 44.8°$; $K = 1690$; $n = 0.30$; $R_f = 0.85$.

With the analyses of rockfill dams with asphalt–concrete cores (vertical or inclined) (Tančev, 1989), the phenomenon of softening of non-cohesive material is introduced in a rather simpler way. With a number of numerical trials it is determined that, for the specific material, the effect can be approximately simulated in such a way so that the submerged elements are loaded in the centroid by a force equal to 4% of the weight of the fill over the centroid of the appropriate element (Fig. 8.26a).

Each stage of application of water is simulated in two increments: in the first, the cited effect of softening, while in the second, the next two effects of filling the reservoir – alleviation of the submerged material through assigning forces, directed upward, as well as the action of the force of the hydrostatic pressure on the core wall (Fig. 8.26b).

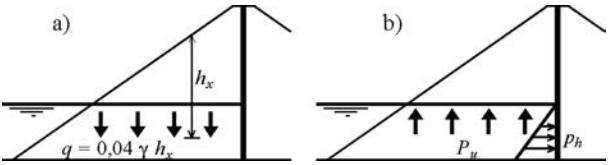

Figure 8.26 The effects of the water on the upstream shell and to the core wall during the reservoir filling.

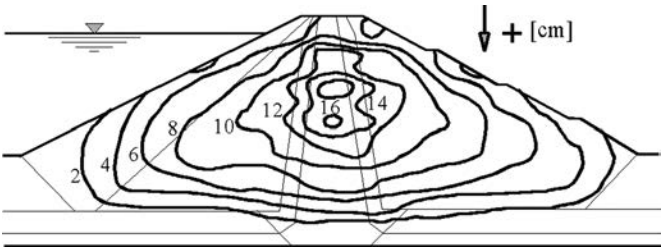

Figure 8.27 Contours of vertical displacements at Gradec dam.

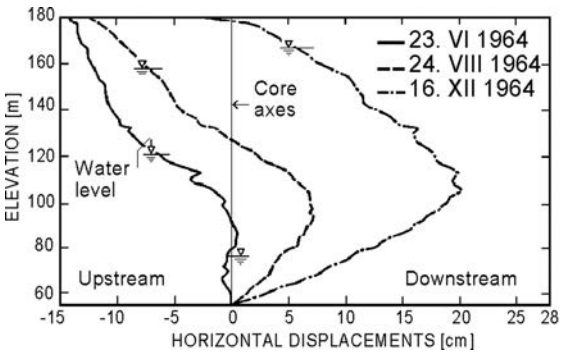

Figure 8.28 Horizontal displacements of core's vertical axis of the El Infiernillo dam (Mexico).

Obviously, simulation of the last two effects is relatively simple. Their appropriate presentation is given in Figure 8.24b and c, also for the case of an earth–rock dam.

An analogous procedure has been employed in the analysis of the above-mentioned Gradec earth–rock dam, for which the contour lines of the vertical displacements are shown in Figure 8.27 (Tančev et al., 1991). It is noticeable that the effect of first filling of the reservoir on the settlements is relatively small. This is due to the small height and good strength characteristics of the material anticipated for placement (compared with Fig. 8.17).

Results from observations of the horizontal displacement of the core's axis of the El Infiernillo dam (Mexico), at the first filling of the reservoir, can serve as an example of the complexity of the above listed effects of the water (Fig. 8.28); (Eisenstein & Naylor, 1986). For more on the El Infiernillo dam, see Chapter 11.

With regards to the vertical line of the axis, from the commencement of filling of the With regards to the vertical line of the axis, from the commencement of filling of the reservoir until the level reaches approximately half of its depth, the core dislocates towards the *upstream* face, especially its upper part. During this phase the weight of the unsubmerged material in the shell is relatively high and it dictates deformations due to the softening of material below it. With a further increase of level, the core shifts toward the downstream face, while with a full reservoir, all points are already shifted downstream except for the joint with the rock, which is rigid, and the crest, which is still shifted a little towards the downstream face. Of course, such "movement" of the core is a result of simultaneous action of the first three described effects. It is deemed that it is, to the greatest extent, due to the first effect.

Bulging out of the diagram of displacements, which is at its maximum when the reservoir is full and is located somewhat below the middle of the height is, of course, due to softening of the material and to the effect of the force of hydrostatic pressure on the core, prior to establishing stationary seepage flow in it. Similar behaviour has been recorded at other dams. The true simulation of this effect in the analyses with FEM is a very complex question, initiated in 1972 (Eisenstein & Naylor, 1986), and then for some time disregarded. Over the last 20 years further scientific research was performed resulting in appreciable progress, which will be described later in this chapter.

The fourth effect of filling the reservoir, *formation of stationary seepage* flow through the core (or through the entire dam, if it has been constructed of cohesive earth material), is characterized by the development of pore water pressure in the part of the core below the seepage line. The simulation of this phenomenon is carried out by introducing the forces of pore water pressure, obtained by an analysis of the seepage, performed with the same mesh of finite elements as for the analysis of the state stress–strain, which makes possible the most accurate transfer of the forces of seepage into the nodes (Li & Desai, 1983).

Observations on constructed dams, abundantly accommodated with instruments for occultation, indicate some displacements in the dam's body following the establishment of a stationary seepage flow. Here it must be admitted that it is very difficult (if not impossible) to distinguish a clear boundary between the state following the first filling of the reservoir and the state of established stationary seepage flow since, in practice, the process of seepage begins (to a smaller or greater extent) with the commencement of the raising of the water level.

In this stage, from an engineering viewpoint, it is very important that the analysis using FEM enables accurate comprehension of the state of stresses in the dam's body. Namely, on the distribution of stresses in the dam's body, and in its particular elements, there are influences from many factors – the construction and geometry of the dam, and shape and characteristics of the foundation, etc. In the case of embankment dams regularly, to a smaller or greater extent, there comes about a *transfer of forces* from one structural element to another, or else inside, within a certain structural element (Kulhawy & Gurtowski, 1976).

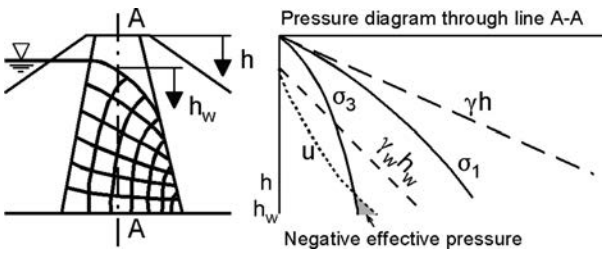

Figure 8.29 Indication of potential danger of hydraulic fracturing.

A consequence of the transfer of forces is the unloading of certain structural elements (or parts of an element) and overloading of others. That, in the end, can result in the occurrence of *hydraulic fracturing*. Hydraulic fracturing is manifested with fissuring of the cohesive material, when in some zone the force of the hydrostatic pressure or of pore water pressure exceeds the value of the total normal stress, that is to say, the effective normal stress. The diagram in Figure 8.29 indicates the lines of total earth pressure (γh), and total major principal stress (σ_1), which has smaller values than γh because of the transfer of forces, the total minor principal stress σ_3, the anticipated hydrostatic pressure along the axis A–A ($\gamma_w h_w$) and the pore water pressure u.

The most frequent reason for hydraulic fracturing is non-uniform settlement of the different materials, when the more deformable materials are 'hanging' on the stiffer ones and give over to them a part of their stresses. Furthermore, in cases when there is distinct unevenness in the foundation below the cohesive material, differentiated settlements of the homogeneous material occurs. This important and interesting phenomenon from an engineering-technical aspect will be dealt with in more detail in Chapter 11.

Although it had been known earlier, this phenomenon has been straightened out with the development of FEM, which alone is a precise and complete defining of the stress state in the dam's body possible. Figure 8.29 (shaded zone) indicates negative effective pressure and within that area there are conditions for the occurrence of a fissure, i.e. hydraulic fracturing. It is deemed that this on its own is not sufficient for fracturing the core since it is necessary to have a coincidence with yet another drawback – nonhomogeneity of the material in the same zone. One well-known expert in the field of embankment dams, Penman, considers that hydraulic fracturing can take place when the value of pore water pressure is between the values of the total major principal stress σ_1 and the total minor principal stress σ_3. Also this question, in order to be completely cleared up, requires further investigations. Worldwide there are records of a number of cases of damage and failure of earth dams and earth–rock dams as a consequence of hydraulic fracturing and progressive erosion through the occurred fissure. Among them is also the well-known failure of the Teton dam (USA), in 1976.

Other factors that can affect the embankment deformation during first filling and in the service period include so-called collapse settlement, time-dependent deformations, such as creep and earthfill consolidation, and differential settlement of the foundation (when the dam is founded on deformable foundations).

8.3.6 Collapse settlement

In section 8.3.5.2 of this chapter the effects of the water at embankment dams with an internal core during the reservoir impounding were briefly discussed. As a consequence of reservoir impounding, softening of the saturated non-cohesive granular material in the upstream shell occurs which leads to additional settlement. This additional settlement is caused by so-called collapse compression of the embankment material, which is an important component of the modelling of embankment dams with internal core as waterproof element. Mostly, the effects of collapse compression are most noted for the upstream dam shoulder on initial impoundment, but there are also events of collapse compression in the downstream shoulder following wetting due to rainfall, leakage or tail-water impoundment. For real analysis of embankment dams it is necessary to incorporate collapse compression into constitutive models, but it adds further complexity and uncertainty in the definition of material parameters, because the collapse compression depends on more factors, like: compacted density, stress conditions, material properties, and other factors. Evidence of collapse compression during first reservoir filling includes differential settlement across the dam crest with greater settlement of the upstream shoulder, crest spreading, and longitudinal crest cracking in some case studies (Hunter & Fell, 2003).

The susceptibility of a rockfill to collapse compression is dependent on a number of factors, like rock type, method of placement (layer thickness, roller type, number of passes), moisture content at placement, grain size distribution, particle shape (angular or rounded), degree of weathering of the rock, effective stress level, etc. In most cases the amount of collapse compression and its effect on the overall deformation behaviour of the dam is rather limited, while in some cases it is very large. A wide range of investigations was performed, especially in the last two decades, to clarify these important questions. Case study and laboratory test data indicate that the potential for magnitude of collapse compression is: greater for dry-placed rockfills, decreases with increasing compactive effort, and increases with increasing stress level (Nobari and Duncan 1972a; Marsal 1973; Alonso and Oldecop 2000). Dumped rockfill is particularly susceptible to collapse compression as evidenced by the very large deformations observed at different dams, including Tikvesh dam (R. Macedonia). The case study of observed large deformations at 105 m-high earth-rock dam Tikvesh during the first reservoir filling and in the service period is given in Chapter 11.

The deformation to a reduction in compressive strength of the rockfill on saturation, mainly in the outer surface of the particles, leading to failure at the highly stressed point contacts in an angular rockfill mass, has been analyzed by Terzagi (1960). Rock types that are generally more susceptible to collapse compression due to greater strength reduction of the substance strength on saturation are sedimentary rocks (sandstones to mudrocks), limestones, and metamorphic rocks from sedimentary parent rocks, while the igneous rocks are less susceptible. Earthfills are much less susceptible to collapse compression, mainly due to the high compactive effort used during the construction and placement at optimum moisture contents.

The phenomenon of softening of non-cohesive materials in this chapter practically was initiated in Figure 8.25, through the two curves representing the stress–strain relationship in dry and wet states, obtained by triaxial testing of the material of the shell of the Oroville dam (USA). Laboratory compression curves for a rockfill sample in dry and wet states are shown in Figure 8.30 (Nobari and Duncan 1972a).

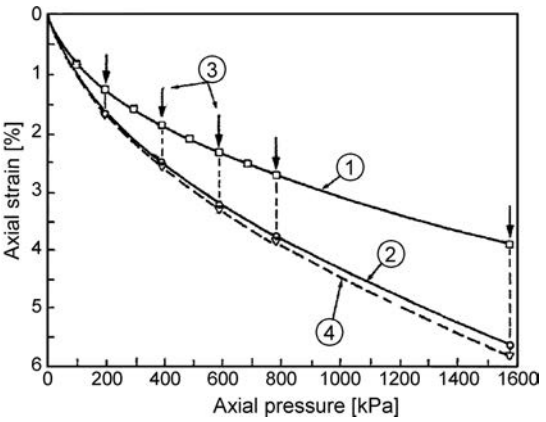

Figure 8.30 Compression curves for dry and wet states and collapse compression from the dry to wet state for gravel in the oedometer test (after Nobari & Duncan 1972a). (1) Initially dry; (2) initially wet; (3) water added; (4) initially dry, then water added.

Collapse effects in rockfill dam behaviour were first introduced into finite element analysis by Nobari and Duncan (1972a). The idea is to measure collapse strains by performing dry and wet oedometer and triaxial tests on rockfill samples (Fig. 8.30). The calculation starts by performing the finite element method using the set of material parameters corresponding to dry conditions; then collapse is numerically simulated in two stages. In the first stage the stress change due to saturation (at constant strain) is determined on the basis of the experimental data. In the second stage nodal forces that restore equilibrium are applied. The computed strains reproduce the collapse strains. This procedure was accepted and applied for different constitutive models by other authors (Eisenstein & Naylor, 1986; Veiga Pinto, 1983; Justo & Saura, 1983; Naylor et al., 1989; Soriano et al., 1990).

Collapse compression on wetting occurs for the dry rockfill when the stress state is above the normal compression line for wetted or saturated rockfill, and the collapse strain is equivalent to the difference in strain between the dry and wetted states at a given confining stress. Alonso and Oldecop (2000) showed that collapse deformations of similar magnitude to that occurring on sample flooding were obtained by imposing 100% relative humidity on a rockfill sample, indicating that flooding or wetting of the voids between the rock particles was not required for collapse deformation. They concluded that *any situation leading to a change in moisture content in the rock pores is enough to cause collapse deformation*, which is consistent with the observation of collapse deformations induced by flooding, such as on reservoir filling, or rainfall (Hunter & Fell, 2003).

Some weathered compacted rockfills are susceptible to very large settlements due to collapse compression when wetted, presumably if they are placed with limited quantities of water. At Ataturk dam the settlement of the upstream weathered rockfill was potentially very large as indicated by the very large post construction settlement of the crest (4% at almost 7 years after construction).The best known such example is

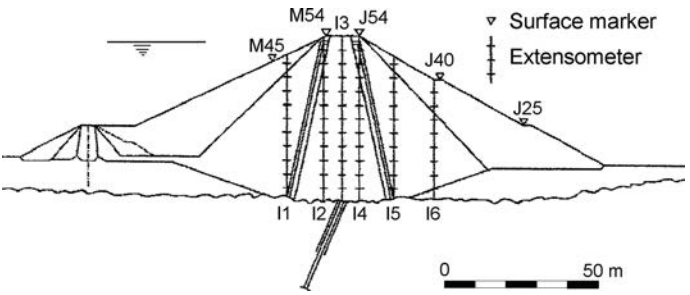

Figure 8.31 Beliche dam, central cross-section, showing the position of extensometers and surface settlement markers (after Naylor et al., 1997).

Beliche Dam, an earth-rock dam with rockfill shoulders and a central clay core, which experienced large collapse settlements due to reservoir impounding and direct action of rainfall. At this dam, vertical strains of up to 2.1% were measured upon first filling within the "lightly compacted" rockfill of weathered schists and greywackes. Beliche Dam has attracted wide attention from researchers working in the field of embankment dams. The reason for the long-lasting interest probably lies in the availability of a set of large-scale laboratory tests on the rockfill materials, as well as a comprehensive set of field monitoring data, which covers the construction and impoundment, and several years of dam operation. Since the first unexpected reservoir filling in 1984, further papers dealing with both laboratory and field behaviour of rockfill materials and the evolution of numerical techniques for analysis of Beliche dam have been published. Of particular interest are the papers published by Naylor et al. (1986, 1997) and by Alonso et al. (2005).

In their very illustrative and thorough paper, Alonso et al. (2005) described the development and improvement of the applied model for numerical analysis. Also, they interpreted laboratory test results of large scale rockfill under dry and flooded conditions, with identification of material parameters. Using their very sophisticated numerical model, they simulated the complete history of dam construction, impoundment and rainfall by means of a coupled flow–deformation model.

Beliche Dam is a 54 m high earth-rock dam, with a moderately curved shape in plan, located in the Algarve, Portugal. The dam core is vertical, supported by rockfill dam shells. A central dam cross-section, showing the position of extensometers and surface settlement markers is given in Figure 8.31. The core is made of low-plasticity clay. Two zones are distinguished on each shell: an inner one, made of lightly compacted fractured schists, and a harder outer one, made of compacted greywacke. Both schists and greywackes are known as relatively soft rocks, and large deformations may be expected. Construction started in 1984. When the dam was built to a height of 47 m (January–February 1986) the reservoir level rose to an unexpected temporary elevation of 29 m over foundation level due to heavy rains. Significant vertical displacements of the upstream shell were recorded in extensometer I1, located within the upstream inner shell. Maximum accumulated settlement, in excess of 0.80 m, was recorded at mid-height of the dam. The extensometer I6 (Fig. 18.31), located in the downstream shell,

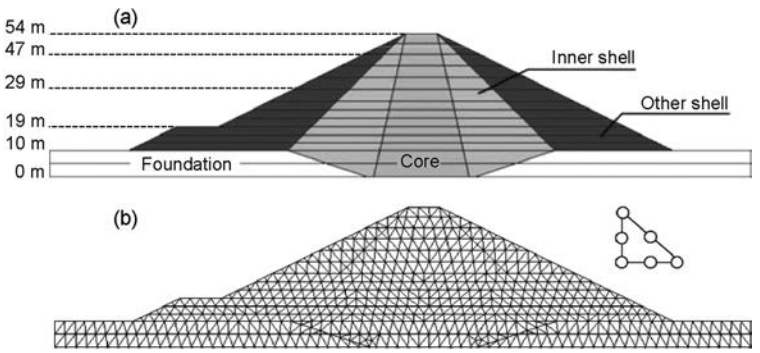

Figure 8.32 Beliche dam. (a) Geometry of dam for model calculations; (b) discretised model using quadratic triangles (Alonso et al., 2005).

despite not being affected by the impoundment, reached similar settlements. The dam was completed in March 1986, and then it was subjected to rainfall and reservoir level evolution. Observed settlements and horizontal displacements of the surface markers were in correlation with the rainfall intensity in the extreme rainfall periods during the first five years of the dam's operation.

The complete phenomenon was thoroughly investigated and analyzed by the authors. A coupled flow–deformation analysis of the history of construction, impoundment and the operational phase of Beliche Dam was done. Special attention was given to the role of rainfall, during both construction and subsequent phases. Model calculations are compared with field measurements. In the paper, first, the elastoplastic models used for the description of dam body materials is introduced, paying special attention to the rockfill material model and to the physical nature of model parameters. The results of oedometer and triaxial tests performed at the Laboratorio Nacional d'Engenheria Civil of Lisbon (LNEC) are back-analyzed in order to derive model parameters. Hydraulic parameters have been approximated on the basis of known identification data. Details of the coupled flow-mechanical analysis performed are also given. Spatial distributions of some measured variables at some specific times (vertical and horizontal displacements, stresses) are obtained and compared with measurements. Also, calculated time records of settlements and horizontal displacements are compared with actual measurements. Obtained stress paths at some specific points within the dam are given, with the purpose of understanding the deformation phenomena observed in the structure. An analysis was first conducted using the parameters derived directly from laboratory tests. This case represents the base case. Additional cases, modifying both the rockfill compressibility, to account for scale effects, and the rockfill permeability were also performed.

Two different constitutive models were used to describe the behaviour of a low-plasticity clay in the core, and the rockfill shoulders. For the clay core, the "Barcelona Basic Model" (BBM), proposed by Alonso et al. (1990) was adopted. The applied model for the rockfill shoulders is an extension of the compressibility model developed by Oldecop and Alonso (2001). Volumetric compressibility of rockfill for triaxial

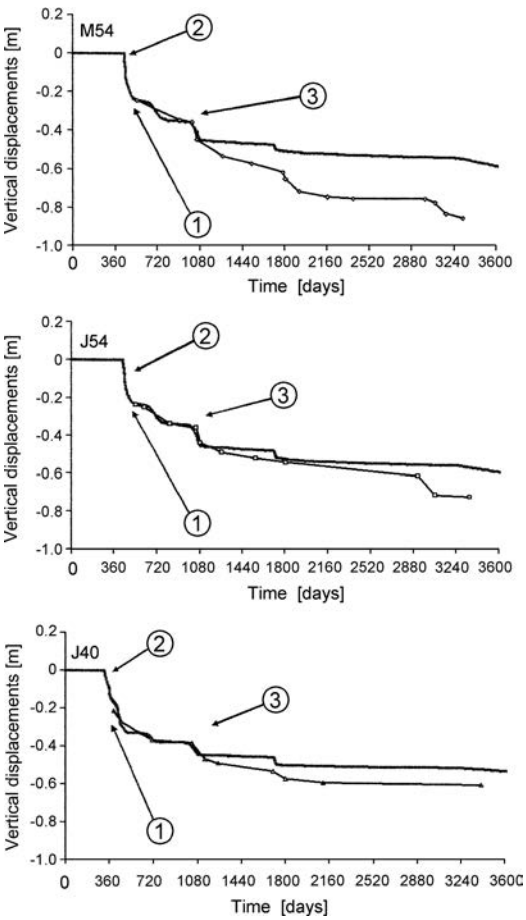

Figure 8.33 Evolution of vertical displacements of surface markers M54, J54 and J40 – comparison of measured and calculated values for base case (after Alonso et al., 2005). (1) Measurements start; (2) settlements due to dam construction and reservoir impoundment; (3) settlements due to rains (in the rain period).

conditions is assumed to have two components, whose origins are *a particle rearrangement* and *a particle breakage phenomenon*. The second is highly dependent on the prevailing relative humidity (or, alternatively, the total suction) at the rockfill particles. The analysis of the dam was performed with the finite element code CODE_BRIGHT, developed at the Department of Geotechnical Engineering of Universitat Politècnica de Catalunya, Barcelona.

Rockfill materials for the inner and outer shell zones were tested in a large-diameter oedometer (D = 500 mm) and triaxial (D = 300 mm) cells. The gradation of the material tested was scaled down by making the specimen cumulative grain size distributions parallel to the gradation curve of the in situ rockfill material. Tests were performed on a dry material. At some stage during the triaxial tests, specimens were flooded,

although the applied vertical strain rate was maintained during the sample inundation and subsequent straining.

The reader is referred to the source paper (Alonso et al., 2005) for details of above listed and very briefly described items, connected with the field measurements, laboratory investigations, parameter preparation, model formulation, etc.

Dam construction and reservoir impounding was envisaged to experience the following stages:

(A) Construction to elevation 29 m, $t = 0$–180 days.
(B) Construction to elevation 47 m, $t = 180$–360 days
(C) Impounding of the reservoir to elevation 29 m, $t = 360$–420 days
(D) Completion of construction to elevation 55 m, $t = 420$–450 days
(E) Impounding of reservoir to elevation 49 m, $t = 450$–1500 days
(F) Water level maintained in reservoir at elevation 49 m, $t = 1500$–3240 days
(G) Water level decreased in reservoir to level 20 m, $t = 3240$–3600 days

The initial time adopted in the simulation performed, $t = 0$, corresponds to the beginning of dam construction. A relatively high initial suction, $s = 20$ MPa, was assumed at the time of rockfill placement. It corresponds to a relative humidity of 85%. In relatively weak rockfill made of schists and greywackes, yielding starts at very low stresses, owing to the onset of particle breakage, and therefore quite a low initial yield stress was assumed for the inner and outer rockfill shells.

In the Figure 8.32 the geometry of the Beliche dam for model calculations is illustrated (a), as well as the discretised model using quadratic triangles (b). A base case was defined on the basis of the material parameters derived from the laboratory tests performed. For illustration of the various obtained results, the evolution in time of vertical displacements at surface marker points M54, J54 and J40 (see Fig. 8.31) for the base case is given in Figure 8.33. M54 and J54 are located at the upstream and downstream edges of the clay core, whereas J40 is a point above mid-height in the downstream shoulder. At appropriate moments in time sudden settlements caused by the reservoir filling (2), as well as originated of rains (3) can be seen from the lines of the vertical displacements. The best agreement between measured (line with points) and calculated values of the settlement is found at the point J54, located on the downstream dam slope, while for the point M54 calculated settlements are rather underestimated.

At the end of our brief presentation of the very worthy paper of Alonso et al. (2005), we reproduce a short fragment of the authors' conclusions: *"…Numerical models developed within the framework of effective stress analysis require some ad hoc computational devices to handle the development of strains as a consequence of suction or relative humidity changes, both in the core and in the rockfill shoulders. They may be useful to reproduce stress and deformation states at a given stage of dam construction and operation, even if the representation of material behaviour is inconsistent with physical phenomena. However, they lack the possibility of handling environmental factors, such as a weather regime. The Beliche Dam case highlighted the relevant effects of climate, which are directly responsible for the behaviour of the downstream shoulder. Ideally, the constitutive models used require suction controlled testing for the determination of material parameters".*

Roosta and Alizadeh (2012) detail some simulations that have been conducted to model collapse settlement and non-linear stress-strain behaviour of rockfill material observed in tested specimens. For simulation of collapse settlement, a technique is presented in which initial stresses in each element are decreased by a stress release coefficient and also mechanical parameters of rockfill is changed from dry to wet parameters. A stress-dependent coefficient for stress reduction is extracted from laboratory tests and shows how initial stresses decrease with wetting of rockfill material. Some other valid equations are also used for definition of mechanical parameters in the Strain-Hardening/Softening model of the software FLAC. Large scale triaxial tests were carried out on conglomerate rockfill samples from the borrow area of the 176 m high Gotvand embankment dam to investigate its mechanical properties. The analytical curves of collapse settlement tests well fitted to experimental results and the nonlinearity of stress-strain constitutive law is accurately followed by the rockfill material in laboratory tests.

In this chapter considerable space and great attention was devoted to the question of so-called collapse settlement at rockfill dams with internal core, i.e. at embankment dams with submerged upstream shell. This is in accordance with the author's opinion that it is impossible to perform a valuable static analysis of embankment dams without introducing this phenomenon into the model.

8.3.7 Simulation of behaviour at the interfaces of different materials

The body of embankment dams contains structural elements, constructed in different materials, so that in these structures there comes about contact of the materials with different deformable properties. Under the action of forces, elastic and plastic deformations appear in the contacts. The conventional application of FEM, owing to the compatibility of the joints of the elements, prevents comprehension of this phenomenon. In order for it to be possible to analyze the problems of interaction of the interface between different materials, which has its reflection on the entire behaviour of the dam structure, it is necessary in the analyses to introduce what is called a *joint element*, which enables differentiated displacement of various materials across the contact surface.

The first joint element was developed by Goodman et al. (1968) for the presentation of joints in rock masses. This element has been for a long time very popular in rock mechanics, while later on other somewhat modified elements, have been developed for the same purpose (Day & Potts, 1994; Ghaboussi, et al., 1973; Xiurun, 1981). The joint element has a significant application in solving the problems of concrete retaining walls. On the application of the joint element for embankment dams, textbook references and periodicals have only scarce data. It is only known that some twenty five years ago, it has been used by Sharma et al., – in the analysis of the Tehri dam, in India (a 260 m high earth–rock dam, not yet completed) (Sharma et al., 1976, 1979).

With Kokalanov, the author of this book (Kokalanov & Tančev, 1988, 1989; Tančev & Kokalanov, 1988, 1989, 1995), has formulated a parabolic isoparametric joint element by applying the assumptions for the joint elements derived until then in the world, and has employed it for an analysis of rockfill dams with asphalt–concrete,

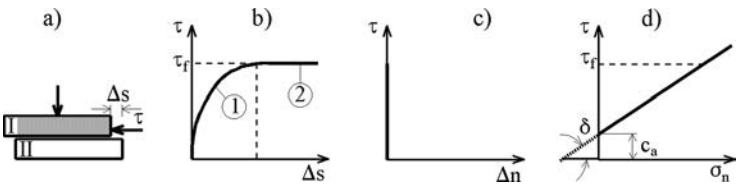

Figure 8.34 Behaviour of an interface.

water-impermeable elements. The element utilized is without thickness and has six nodal points.

Interfaces of different materials in embankment dams, in principle, act as compressed ones, i.e. there is no expansion of the interface in a transverse direction, but only relative displacement along the contact. Behaviour of the interface between two bodies of different material is schematically presented in Figure 8.34. Shear stress τ causes relative displacement of bodies 1 and 2 for a value Δs, in which one can distinguish two cases:

1. *No slip in the interface.* This case arises when the following condition is fulfilled:

$$\tau < \tau_f = c_a + \sigma_n \tan\delta \tag{8.67}$$

where τ = interface shear stress, τ_f = interface shear strength, c_a = adhesion in the interface, σ_n = normal stress, and δ = angle of friction. In this, *elastic shear deformations* appear in the interface, represented by the part of the curve designated as (1) in Figure 8.34b.

Properties of the joint element are determined by tangential stiffness K_s and normal stiffness K_n. When only elastic deformations of shearing appear in the interface, then K_n has the role of the modulus of elasticity E, while K_s has the role of the modulus of distortion G; thus, the following relations are valid:

$$\sigma_n = K_n \Delta n; \qquad \tau = K_s \Delta s \tag{8.68}$$

where Δn and Δs are the average normal and the average tangential relative displacement along the interface. Theoretical behaviour of the interface has been presented in Figure 8.34b and c, i.e. first of all elastic shear deformations (1) appear in the interface, and when the shear strength τ_f has been reached, plastic deformation will take place (2). In this, there are no deformations in the normal direction (Fig. 8.34c), which is simulated so that K_n is assigned a very high value, many times higher than the modulus of elasticity in the adjacent elements.

Behaviour of the interface, as the well as the Behaviour of adjacent materials, is most often nonlinear; that is to say, the elastic deformations (1) in Figure 8.34b are nonlinear. For expressing this nonlinearity, the same as for the basic material, a hyperbolic relationship has been formulated, from which it is possible to obtain

the tangent stiffness K_s for a certain level of τ as tangent to the hyperbola, from the expression:

$$K_{st} = K_I \gamma_w \left(\frac{\sigma_n}{p_a}\right)^n \left(1 - \frac{R'_f \tau}{c_a + \sigma_n \tan\delta}\right)^2 \tag{8.69}$$

where K_I = dimensionless stiffness number, γ_w = unit weight of water expressed in the same units as K_{st}, while the parameters n and R'_f have an analogous meaning, as the appropriate parameters in the hyperbolic relationship for the properties of materials. Along with K_I, c_a and δ are determined with a series of direct shear tests on the interface.

2. *Slip in the interface*. This takes place when the shear stress reaches the shear strength of the interface, i.e. when it will be:

$$\tau \geq \tau_f = c_a + \sigma_n \tan\delta \tag{8.70}$$

The stiffness K_s has in this case the value zero (for practical reasons, some symbolically small value is assumed) and the adjacent layers displace along the interface, irrespective of each other.

If in the case when tension occurs at the interface, when it loses its stiffness not only in the tangential direction but also in the normal direction, then both K_s and K_n are assigned a symbolically small value.

The above described joint element is incorporated into the computer program for nonlinear and inelastic analysis with the application of the hyperbolic constitutive law. There have also been conducted extensive analyses on three kinds of rockfill dams with asphalt–concrete water-impermeable elements (Tančev, 1989). In the following, a concise description is given of the role and influence of the joint element in the analyses (Tančev & Kokalanov, 1995).

Discretisation of the cross-section of the first analyzed dam – with an asphalt–concrete facing – is presented in Figure 8.35 (some results of the analyses of this dam, 80 m high, have already been presented in this section). Altogether, 109 elements have been employed, of which 17 are joint elements, which are represented by a dashed line in the figure. Construction of the dam is simulated in layers, each 10 m thick. The asphaltic facing has been placed along the slope upon a previously constructed and compacted embankment in one layer. Then, water pressure has been assigned in three increments, as has been described earlier in this textbook. The input parameters for properties of materials and interfaces have been assumed according to typical values given in the textbook references (Tančev, 1989; and Tančev & Kokalanov, 1995).

Prior to analyses with joint elements, the dam was analyzed without their application. Generally speaking, displacements in the dam's body, obtained in accordance with both methods, differ little. In the contact rock material – rigid foundation, in which joint elements have been introduced, insignificant elastic horizontal displacements appear with a value in mm (Fig. 8.36). Here, the joint elements make possible a realistic presentation of the behaviour of the contact asphalt–concrete – concrete cut-off at the upstream end of the dam, which is in close connection with the possibility of obtaining a clear and true picture of the stress-deformation state in the entire water-impermeable element.

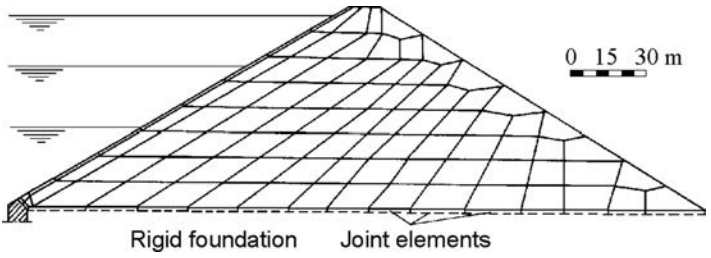

Figure 8.35 Discretisation of a rockfill dam with asphalt–concrete facing.

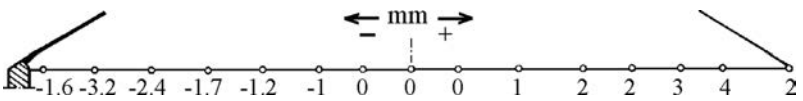

Figure 8.36 Horizontal displacements in the contact rock material – rigid foundation.

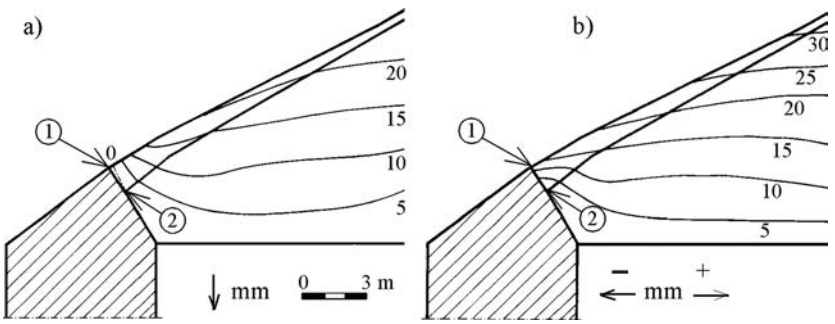

Figure 8.37 Contour lines of vertical (a), and horizontal (b) displacement at the contact asphalt–concrete facing – concrete cut-off.

The contour lines of vertical and horizontal displacements, after the filling of the reservoir in the mentioned zone of the contact facing – concrete cut-off, are presented in Figure 8.37. Tension appears in the joint element under the lowest part of the facing (1 m thick in that part). Because of that, the facing in that zone is being separated from the concrete cut-off and is becoming deformed independently, so as a consequence point 1 elevates 2.5 mm and shifts towards the downstream face by 12.7 mm. At the same time, the lower point, 2, remains in its original position. The other points of the lowest, strengthened part of the facing, displace downward and towards the downstream face. Of course, the interface, which works in this way, requires special construction in order to remain water-impermeable (placement of seals, treatment of the interface with special materials, etc.).

Application of joint elements enables us to obtain a realistic picture, not only of deformations, but also of stresses. Figure 8.38 presents diagrams of normal stresses σ_x

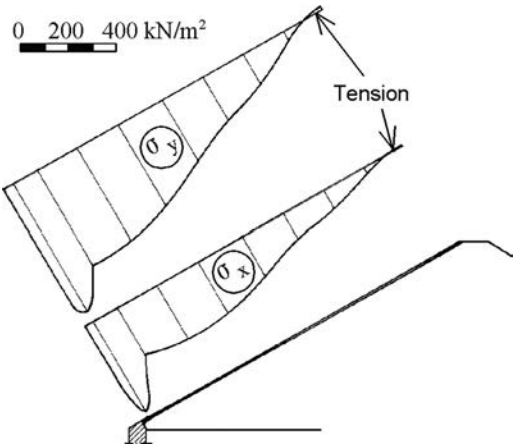

Figure 8.38 Diagram of normal stresses at the upper edge of facing.

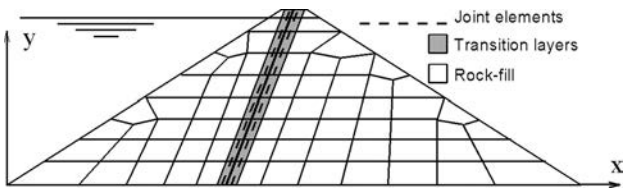

Figure 8.39 Discretisation of a dam with an asphaltic core.

and σ_y, at the upper edge of the facing. Conventional analysis, as a consequence of the compatibility of interfaces, gives tensile stress for σ_x equal to 500 kN/m^2 at the lowest point (1, Fig. 8.37). The opposite takes place in the analysis with joint elements, in which, as is to be expected, compression appears at the cited point (Fig. 8.38). Tension appears only at the upper end of the facing, near the dam's crest, however, with a value smaller than 20 kN/m^2.

There is yet another benefit in the above-described analysis with application of joint elements: savings in computer time. Namely, the number of iterations for each increment of loading has been decreased from 5–7 in conventional analysis, to 3–5 in analysis with joint elements.

In the case of a rockfill dam with an asphaltic diaphragm (core), 80 m high, joint elements have also been used in the interfaces diaphragm – transition zones (Fig. 8.39). The contour lines of vertical and horizontal displacements in the dam's body are represented in Figure 8.40. There is obvious discontinuous behaviour in the interfaces of the asphaltic diaphragm with the filling material. As a consequence of the possibility of differentiated displacement of the materials in the contacts, the transfer of forces from one material into another is presented more realistically.

We can conclude that, in certain situations, correct and complete analysis of embankment dams, with the application of the powerful numerical method of finite

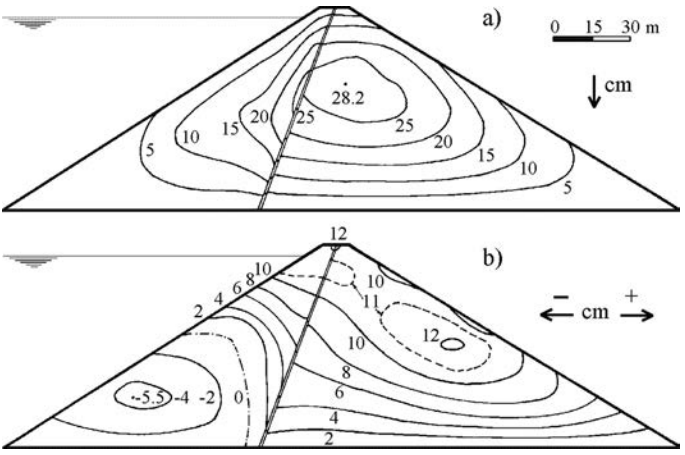

Figure 8.40 Contour lines of the vertical and horizontal displacements of a dam with an asphaltic core.

elements, can be carried out only with a compulsory application of joint elements in the contacts of materials with clearly different deformable characteristics.

8.3.8 Analysis of consolidation

Cohesive, poorly permeable earth materials, which are placed in the body of earthfill dams and earth–rock dams have one important specific quality which, in order to perform a correct and complete static analysis, must be taken into consideration. Namely, it is well known that cohesive materials are placed at *optimum moisture* (or close to it), so that, following compaction of the layer, due to the poor permeability of the material, the greater part of the pores are filled with water. At an increase of loading, for instance with the placement of a new earth layer, there comes about an occurrence of an *increase in pore water pressure* in the previously placed layer, since the water needs time to be extruded from pores, and so, in the initial period of change in loading, the water takes on an entire new pressure. In the course of time, an extrusion of water from pores takes place, an occurrence that is followed by *dissipation* of the increased pore water pressure and additional displacements in the layer, i.e. a process of *consolidation* takes place. A number of methods have been developed in soil mechanics for the calculation of consolidation, but difficulties appear in their practical realization.

In the static analysis of earthfill dams and earth–rock dams using FEM, the calculations of consolidation must be fitted into the analysis of deformations and stresses by using the same mesh of finite elements, that is to say the analysis of pore water pressure must become an integral part of the entire analysis (Lewis & Schrefler, 1998). A nonlinear incremental analysis with FEM, combined with analysis of pore water pressure, by means of which we successively obtain the instantaneous (undrained) and time-dependent (drained) deformations, has been developed by *Eisenstein* and *Law* (1977) and they apply it in analysing the cross-section of the Mica dam, in Canada, (more on this significant 243 m high dam, along with a sketch of the cross-section, can be found

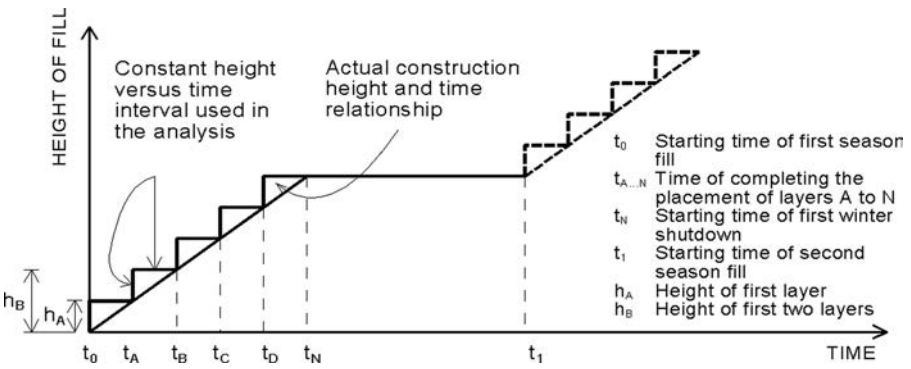

Figure 8.41 Time schedule diagram for progress of construction (after Eisenstein & Law, 1977).

in Chapter 11). The authors assume isotropic permeability of the core's material and two-dimensional consolidation with a movable upper boundary, for which conditions the following governing differential equation is valid:

$$C_v\left(\frac{\partial^2 u}{\partial x^2}+\frac{\partial^2 u}{\partial y^2}\right)=\frac{\partial u}{\partial t}-\overline{B}\frac{\partial \sigma_1}{\partial t} \tag{8.71}$$

where C_v = coefficient of consolidation of earth material; u = pore water pressure; $\overline{B}\sigma_1$ = pore pressure coefficient; and t = time variable. The pore pressure coefficient in the analyses has been taken from the results of oedometer tests, since the authors considered that in the dam's core, laterally compressed, the ratio σ_1/σ_3 is approximately constant. For these reasons it is justifiable also for the value of C_v to be taken from an oedometer test.

The entire analysis is carried out according to the following procedure:

1. Establish a time schedule for progress of the works during dam construction and assume a layout scheme for the execution of layers, which will be applied in the analysis, as is shown in Figure 8.41.
2. Layer A is put into position (parallelly, all materials of the shells and the core) and for the action of the weight of the material itself is performed the analysis through total stresses, so as to obtain displacements in the layer, under the assumption of its immediate construction. Then, calculate pore water pressure in the core for undrained conditions: $u_0 = \overline{B}\sigma_1$.
3. An assumption is made that the obtained total stress, in the time from the commencement of construction of the layer t_0 until its completion t_A, is constant, which is not quite true, but could be accepted if the period $(t_0 - t_A)$ is relatively short. The same assumption is made during the construction of each consecutive layer. Now, by means of equation (8.71), determine the pore water pressure u_{tA} in each element of the core at the moment t_A and, through the effective values of normal stresses in the core $(\sigma_{jA} - u_{tA})$ and total stresses in the shells (σ_{pA}), and determine the time (or consolidation) displacements in all nodes of the first layer

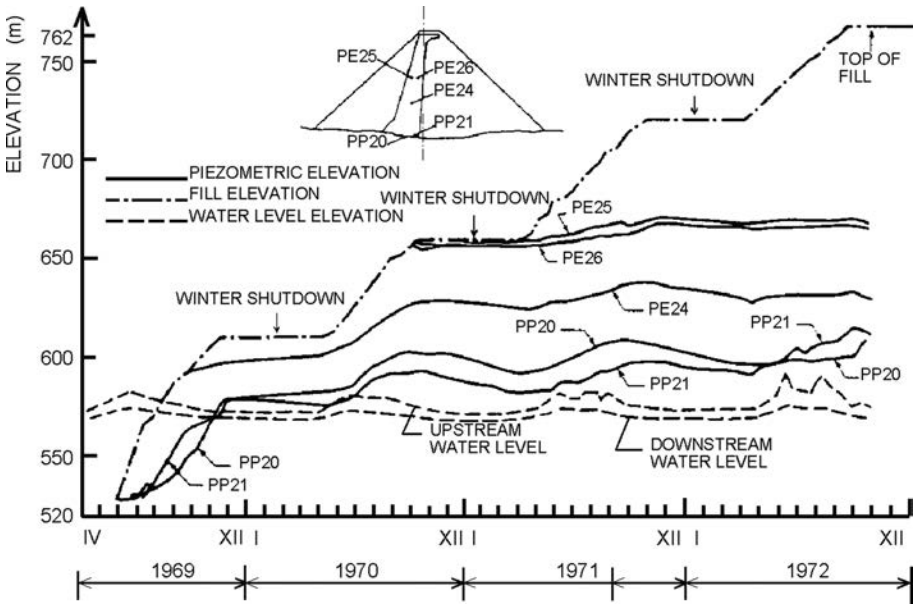

Figure 8.42 Relationship between progress of the embankment, the piezometer level, and the time of construction of the Mica dam (after Eisenstein & Law, 1977).

(in the core, but also in the shells, since the changes in the core also reflect in the adjacent zones).

4. Proceed with addition of the moments and time displacements in all nodes of the first layer, which yields the state of deformations at the moment of time of the construction of the first layer t_A.
5. The second layer is put into position and then an analysis is made for undrained conditions under the action of its weight, as if the layer were carried out instantaneously. In this way one can obtain new instantaneous displacements in the entire embankment (in both layers). Then, follow the calculation of changes of total stresses $\Delta\sigma$ in all nodes.
6. If t_B is the time for the completion of construction of the second layer, then the calculated changes of total stresses are considered to be constant in the time interval $t_B - t_A$. Having obtained such known changes to total stresses, one can determine the changes of pore water pressures in the core $(u_{tB} - u_{tA})$ for the time interval $t_B - t_A$. Now, conditions have been created for calculation of the consolidation displacements in the two constructed layers, originating due to the change of stresses in the core, whose effective value now is $\sigma_{jAB} - (u_{tB} - u_{tA})$.
7. Perform an addition of the consolidation and instantaneous displacements and so obtain the total deformations following the completion of construction of the second layer of the dam's body.
8. The procedure from point 5 to 7 is repeated for each subsequent layer.

Parameters for material in the core for performing analyses for the Mica dam according to the described procedure have been determined on the basis of oedometer tests by applying high pressure, amended with an isotropic compression test. Since the dam has been abundantly provided with instruments for oscultation, it is possible to make a comparison of the calculated values *vis-à-vis* the measured values. In continuation, there will be presented only a small number of the possible comparisons. First of all, for obtaining an impression of the pace and conditions for the dam's construction, Figure 8.48 shows the diagram of the progress of the works on the dam's construction over time, along with the level movement in several piezometers (marked on the sketch) and water level.

Figure 8.43 presents diagrams of the observed pore water pressure and the calculated pore water pressure in several piezometers. Agreement of results is good, while the larger discrepancies at the piezometer PP21 are due to the fact that the lower part of the core had been exposed to the effect of wetting from water both upstream and downstream, which had not been taken into consideration in the analyses.

Figure 8.44 gives a comparison of the calculated settlements with the observed settlements at two points in the core's foundation – one of them in the center of the core (a), while the other one close to the interface with the shell (b). In the first case, there is an extraordinary coincidence of results, while in the second case there is a certain discrepancy, which is probably due to the influence of the close interface of different materials in the core and the shell. Namely, high shear stresses develop in the lower zone of the interface, which influence the accuracy of the measuring instruments.

At the end of this review it must be pointed out that the analysis for the Mica dam was carried out *post mortem*, i.e. following the completion of construction. That has made possible accurate simulation of the time procedure for the execution, as well as an appropriate choice of input parameters. Finally, it has led to a very good agreement of the calculated and measured values of pore water pressure and displacements. If the analysis had been carried out at the initial stage of design, which is the normal procedure, it would have been difficult to predict the time schedule of construction for such a large embankment dam with a high degree of accuracy.

Extensive analyses, taking consolidation into consideration, have also been carried out at the El Infiernillo dam, some 30 years after its completion, in order to check the possibilities of the existing different software for the analysis of deformations and stresses for dams, taking into consideration the process of consolidation (ICOLD, 1994a). This 148 m high earth–rock dam had been built for 15 months, with a very regular progress of the works of some 10 m a month. Then there followed a consolidation period of 5 months prior to the filling of the reservoir, which was carried out over 6 months.

Analyses with FEM were carried out with a simulation of three phases: (a) phase of construction, followed by 5-month consolidation period; (b) filling of the reservoir (for six months); and (c) consolidation while obtaining a stationary seepage flow through the core, with establishment of constant values of pore water pressure and effective stresses after the consolidation period in which a stationary seepage flow had been established.

Of the numerous presented results (ICOLD, 1994a), Figure 8.45 represents the contour lines of pore water pressure for the three described states (a), (b), and (c), obtained with the analyses performed by Ozanam and Tardieu, of the well-known

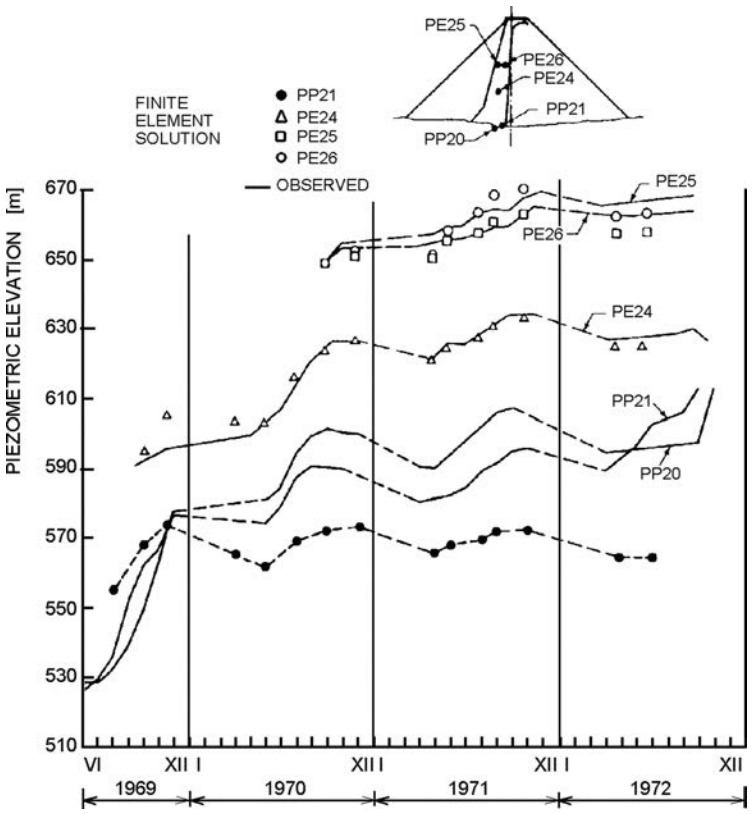

Figure 8.43 Observed and calculated pore water pressures for several piezometers at the Mica dam.

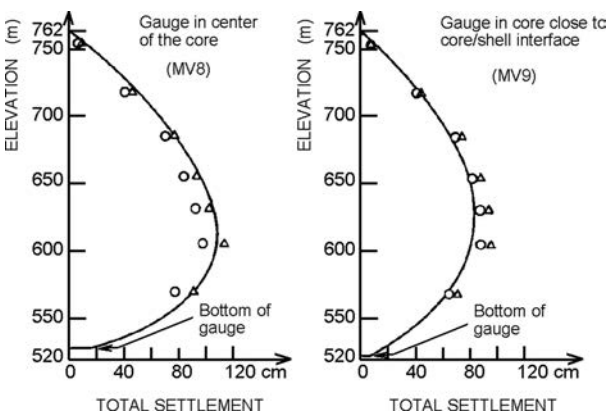

Figure 8.44 Comparison of calculated and observed settlements for two gauge stations in the core of the Mica dam.

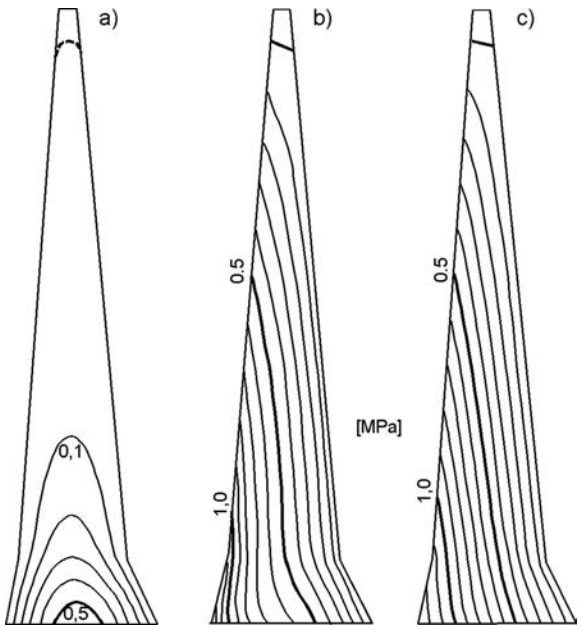

Figure 8.45 Calculated pore water pressure in the core of El Infiernillo dam. (a) After construction and a consolidation period of five months; (b) after filling the reservoir; (c) after the consolidation period in which a stationary seepage flow had been established.

French consulting company Coyne et Bellier, by applying the GEFDYN program for static and dynamic analysis. This program contains substantial possibilities, among others its application for various constitutive models for behaviour of materials, treatment of cohesive materials as a two-phase or three-phase medium (completely or partially saturated with water), etc. In this specific case, Mohr–Coulomb's two-dimensional failure criterion has been employed, along with the assumption that the core is 100% saturated with water and also with the application of a jointed analysis (the composition solid mass–fluid is analyzed in continuous steps).

If we compare these diagrams with the appropriate diagrams of measured pore water pressures in the core of the Talbingo dam, Figure 8.6, we will see that in this case the pore water pressure for the state following construction is considerably smaller than that after the filling of the reservoir. Results of the analyses for El Infiernillo dam should be taken with great reserve, even though they have been carried out in a recent period of time (1994), with participation of well-known companies, due to certain omissions that were made. For instance, in some of the models, a powerful finite element has not been used, and there has been no simulation of the rather important effect of 'softening' of non-cohesive materials saturated in water, etc. As a matter of fact, the survey results and comments there on were not compared with the results from measurements. How such a comparison looks can be seen in Figure 8.46. It is evident that measured values of horizontal displacements in the core's axis are much smaller than the calculated values in those seven analyses, and also the shape of the diagram is

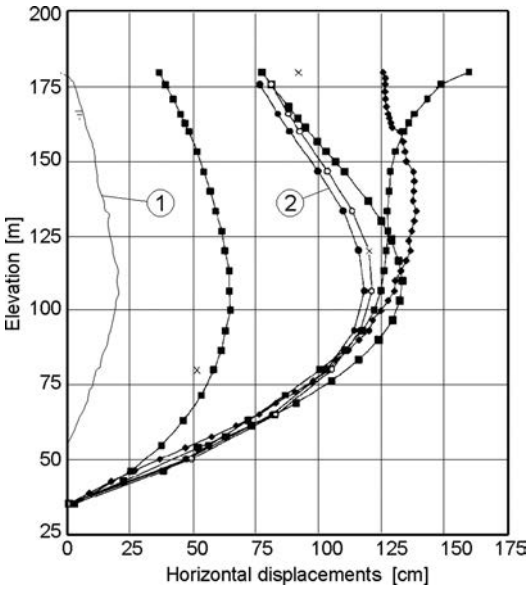

Figure 8.46 Comparison of results of numerical analyses for horizontal displacements in the core's axis of the El Infiernillo dam after the filling of the reservoir, with values measured by means of an inclinometer. (1) Measured, (2) calculated displacement with GEFDYN.

different – the horizontal displacement near the crest is still negative (also, see diagram in Figure 8.25, along with accompanying text). The fact that the highest section of the dam has not been encompassed within the measurements does not substantially influence such an evaluation – the differences are still, too large.

It can be concluded that the question of the application of FEM for the analyses of stresses and deformations for large embankment dams, with inclusion also of the process of consolidation, has not been finally solved. Further investigation is required in order to ascertain the most appropriate constitutive models for particular materials, and to solve different technical details in connection with the realization of the analyses that have influence the accuracy and reliability of results. It is significant that the software for this purpose has a fast development and there are several more programs that are being used in a number of countries, but there are no analyses carried out with them =resented in textbook references and periodicals.

Within the interpretation in this subsection, the discussion has been exclusively about consolidation deformations that occur as a result of a change in pore water pressure, causing change of the effective stresses. Such a consolidation is called *primary consolidation* and it takes place until complete drainage of all water from the pores of poorly permeable material has occurred or until constant values for pore water pressure have been established, similar to the case with the stationary seepage flow through earth material.

Numerous tests have shown that deformation of the earth material goes on afterwards, most often with a lower intensity. This phenomenon is called *secondary consolidation* and is due to the internal redistribution of certain particles in the earth

medium, which causes a change in the total stress σ. For an equal increment of change of the total stress ($\sigma_i - \sigma_{i-1}$), the relative deformation ε_t can be represented with the following expression:

$$\varepsilon_t = \varepsilon_1 + \frac{C_a}{1 + e_0} \log \frac{t}{t_1} \tag{8.72}$$

where t = time, ε_1 = deformation in the initial time t_1, and C_a = coefficient of secondary compressibility, which can be obtained with an oedometer test or a triaxial test with a sufficiently long time duration. Expression (8.72) is valid for cohesive earth materials.

Secondary consolidation most often results in small displacements. In the analyses of earthfill dams and earth–rock dams with FEM it should be taken into consideration if it is ascertained that it can cause significant deformations. Assessment depends on the kinds of material used, construction of the dam, anticipated time schedule for construction, and the extent of preliminary investigation works, etc.

8.3.9 Creep of materials in the body of embankment dams

In the case of earth and rock materials, as well as other materials that are used for the construction of embankment dams (concrete, asphalt, etc.), there is a relationship between stresses and deformations, as well as among *stresses, time*, and *deformations*. It means that materials exhibit *viscous* behaviour, a phenomenon which is dealt with by a special scientific discipline – *rheology*. This behaviour has already been presented in Figure 8.10 (6, and 7), and is also illustrated in Figure 8.47, from which it arises that even low stresses, provided they last for a long time, can lead to considerable deformations. Deformations so caused are called *creep of the material*.

For defining the above cited relations, various models are used in rheology by means of which it is possible to present the viscous properties of materials – from the simplest *Newton's body*, through the more complex *Kelvin–Voigt's, Maxwell's, Burger's, Bingham's* model up to some other, much more complex models, obtained by combining a number of simpler models. More or less complex differential equations originate from them, by means of which we can express the speed of deformation regarding the time (Desai & Christian, 1977; Nonveiller, 1979).

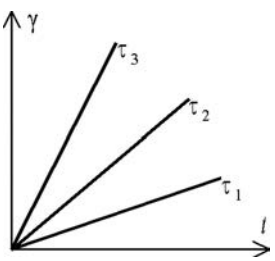

Figure 8.47 Creep of the material.

In the textbook references additional proposals can be found with empirical relations to calculate time-dependent deformations, mainly vertical ones (settlements). A few of them will be mentioned and briefly described.

ICOLD (1993) derived a general equation for the vertical strain of rockfill in terms of vertical stress, rockfill modulus and creep strain parameters:

$$e = \frac{\sigma}{E_M} + \sigma \frac{t}{\theta + \lambda t} \tag{8.73}$$

where e = relative strain, σ = vertical stress [MPa], E_M = modulus of instantaneous strain of the rockfill [MPa], t = time (in years), and θ and λ are the empirical parameters describing creep strain (in MPa per year, and MPa, respectively). The equation is based on the assumption of a linear relationship between stress and strain of coarse rockfill and non-linear relationship between strain and time. Derivations are given for the settlement at a specific elevation in the dam body and period of time after start of construction, settlement at the end of construction and settlement post-construction.

Sowers et al. (1965) proposed the following logarithmic relationship between crest settlement and time to describe the post-construction crest settlement for rockfill dams:

$$\Delta H = \alpha(\log t_2 - \log t_1) \tag{8.74}$$

where ΔH = crest settlement as a percentage of dam height, t_1 and t_2 are time in months from the date when construction was half completed, and α = slope of the crest settlement-time curve (in units of settlement as a percentage of dam height per log cycle of time, time in months).

Equation (8.74) was derived from a database of 14 rockfill dams (mix of concrete face rockfill, central core earth and rockfill, and sloping core rockfill dams) with rockfill ranging from sluiced and compacted to dumped and poorly sluiced. It was found that the coefficient α was dependent on the method of placement of rockfill and ranged from 0.2% per log cycle of time for compacted and well sluiced rockfills up to 0.7% per log cycle of time.

To obtain input parameters for different materials in the dam's body, and to introduce the creep phenomenon into the already complex model for analysis with FEM, is not at all a simple matter. In the textbook references, this model is found in the analysis of the *Cethana* rockfill dam with reinforced concrete facing (Khalid et al., 1990; Khalid, 1992), which was already discussed in this chapter. For rock material at a constant stress σ_0, relative deformation $\varepsilon(t)$ during time t from the commencement of the action of the constant stress, are expressed as:

$$\varepsilon(t) = \sigma_0 \left[\frac{1}{E} + F_K \log(t + 1) \right] \tag{8.75}$$

where σ_0 = constant stress; E = immediate tangent modulus of elasticity; F_K = a constant of creep, obtained as a quotient of the logarithmic gradient of creep due to a long-term oedometer test and the constant stress used in the test; t = time (in days) from the application of a constant load; and $\varepsilon(t)$ = total relative deformation, which represents the sum of the elastic deformation and the deformation due to creep in time t (in days), caused by constant stress.

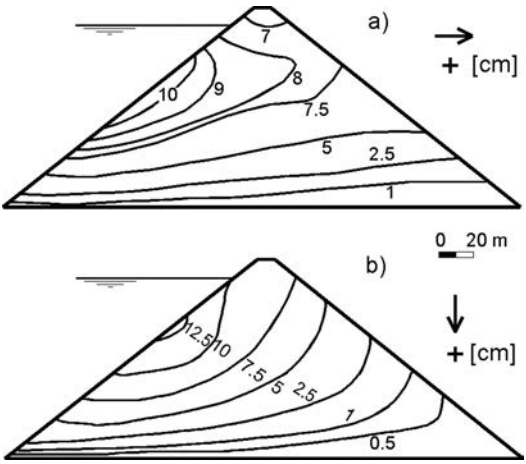

Figure 8.48 Contour lines of horizontal (a), and vertical displacements (b) in the rockfill Cethana dam (after Khalid et al., 1990).

Rock material, however, is nonlinear. It is being placed in the dam's body in layers, and the reservoir is being filled gradually, so that the state of stresses changes in the course of time. Because of that, equation (8.75) requires modification. In the analysis of the Cethana dam, the authors performed a number of modifications, whose presentation would exceed the purpose of this book. For the sake of illustration, Figure 8.48 shows the contour lines of the horizontal (a), and vertical (b) displacements in the dam's body, caused by the filling of the reservoir, taking into consideration creep, calculated by a modified method.

If we make a comparison with the analogous diagrams in which creep has not been taken into consideration (Fig. 8.20), then it will be seen that, when considering horizontal displacements, there is no essential difference, while vertical creep is considerable – it approximately doubles the values obtained due to the action of the hydrostatic pressure. The filling of the reservoir lasted for a short period of time – from the 4th of February until the 25th of April l971, while creep was calculated for the period from the 4th of February until the 8th of December, 1971. The authors do not present the appropriate diagrams, obtained with measurements. However, from comparisons of the calculated deflection of the facing, taking creep into consideration, it becomes clear that creep has been overestimated in the calculations (Fig. 8.49).

In any case, the question of creep of materials in the body of dams deserves more attention. With its successful solution, it will be possible to carry out a simulation of a dam's behaviour over a longer period of time. Good illustrations of the importance of creep are the diagrams of horizontal displacements of the core's axis of the El Infiernillo dam, Figure 8.56, extended from Figure 8.28 (Wilson, 1973). After the filling of the reservoir, an appropriate curve was obtained on the 16th of December, 1964, which is well known to us also from Figures 8.28 and 8.52. Following a period of a little over a year, on the 22nd of January, 1966, at practically permanent water level in the reservoir, the horizontal displacements further increase, so that the dam's crest for

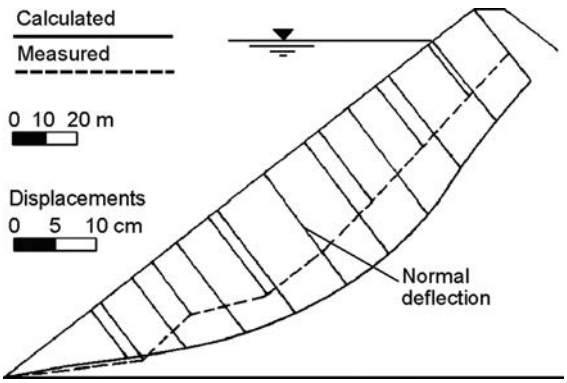

Figure 8.49 Comparison of the measured deflection of facing for the Cethana dam with calculated deflection, taking creep into consideration (after Khalid et al., 1990).

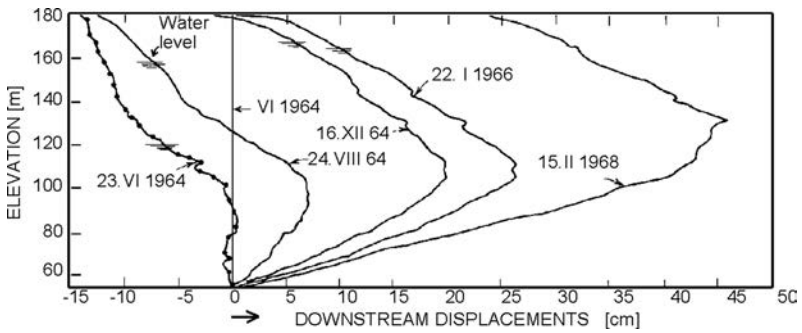

Figure 8.50 Horizontal displacements of the core's axis of the El Infiernillo dam (after Wilson, 1973).

the first time shifts towards the downstream face, and the maximum displacement increases from 20 to 27 cm which is, mainly, due to creep. Two years later, on the 15th of February, 1968, the maximum horizontal displacement moves higher and reaches 46 cm, which is, of course, due to creep and, partially, to the variations of water level.

From the text in this section we saw that, generally speaking, creep can be defined as a slow deformation of soil under constant effective stress. But more precisely, one can distinguish three types of creep, namely:

- *Primary creep*, or deformation at a decreasing rate with time under constant stress conditions, usually classed as "normal" type deformation behaviour.
- *Secondary creep*, or *secondary consolidation* (see section 8.3.8); this is due to the internal redistribution of certain particles in the earth medium, which causes a change in the total stress σ, and most often results in small displacements.

- *Tertiary creep* (or *creep to failure*) is creep whose rate increases with time and is an indication of the onset of failure.

It is obvious that the third type of creep is of the greatest importance. In many embankment dams, creep is responsible for the majority of post-construction displacements which in turn may produce cracking of the impervious element. Thus, the research works to develop more sophisticated methods for prediction of the creep rate and magnitude is fully justified. Two such recent works will be mentioned.

Justo et al. (2002) used two different viscoelastic rheological models to quantify the creep of granular materials, reaching a relatively good agreement between measured and calculated settlements. They gained identical results with two rheological models expressing the creep as a function of the fundamental parameters: initial or elasticity modulus, E_0, creep ratio, R_c and creep time T_{cr}. Firstly, these parameters are preliminarily estimated, then they must be corrected by *in situ* testing and field settlement measurements during and after construction. This is due to scale effects, the fact that the field density and particle breakage are difficult to reproduce in the laboratory, and, most importantly, the influence of collapse and weathering of granular materials, especially in soft rockfill.

The elasticity modulus E_0 has been estimated from 60 cm diameter plate loading tests, and then corrected by equations derived by the authors. The creep time T_{cr} has been estimated from settlement measurements after construction through equations derived by the authors. The creep ratio, $R_c = E_0/E_f$ (where E_f = final modulus) has been estimated from settlement measurements upon construction completion by applying the author's equations.

The proposed method allows calculation of the wait-time needed before constructing the impervious face of an embankment dam, so that the remaining settlement will not be significant enough to cause cracking. The method has been applied to the faced rockfill dam Martin Gonzalo (see also Chapter 13). The comparison of the measured and calculated settlements at different dates up to 580 days after construction shows a very good agreement.

All approaches described briefly above have a common deficiency: they are purely phenomenological, and hence they do not provide insight into the nature of the observed time-dependent behaviour of rockfill. Oldecop and Alonso (2007) took an important step forward in exploring the fundamental phenomena that may be involved in the rockfill straining process. They developed a conceptual model able to explain the features of the observed time-dependent behaviour of rockfill, as observed in large-diameter suction-controlled oedometer tests. One-dimensional compression tests were carried out on specimens of a crushed slate with a maximum particle size of 40 mm. The relative humidity within the specimen was controlled by means of a vapour equilibrium technique, making it possible to gradually change the specimens' water content and suction during the test. It was found that the compressibility index λ is not only a function of stress σ and total suction ψ, but also of the selected reference time t^r, that means:

$$\lambda(\sigma, \psi, t^r) = \frac{d\varepsilon_{(\psi, t^r = \text{constant})}}{d(\ln \sigma)} \tag{8.76}$$

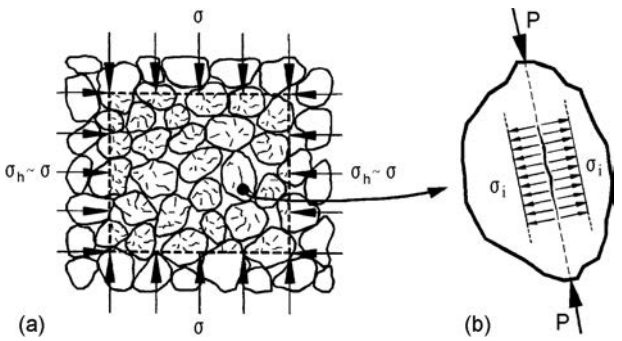

Figure 8.51 (a) Rockfill element formed by rock particles containing macro- and micro-cracks and flaws; (b) rock particle subjected to contact loads (after Oldecop & Alonso, 2007).

Then, a logarithmic function was fitted to the long-term part of these records. In this way, a time-dependent compressibility index was computed, which is formally identical to the secondary compressibility index usually adopted in modelling secondary soil consolidation:

$$\lambda^t = \frac{d\varepsilon}{d(\ln t)} \tag{8.77}$$

where $d\varepsilon$ = strain increment, t = time elapsed since the application of the last load increment.

The authors proposed a micromechanical conceptual model to explain the features of rockfill compressibility following the hypothesis that, in the first stages of compression (isotropic or 1-D compression), rockfill deforms mainly because of particle rearrangement involving interparticle sliding and rotation. As compression proceeds, the void ratio decreases, and at some point the granular structure becomes blocked, and further strain increment can occur only in the case of breakage of rock particles. In the proposed model, a rockfill element (Fig. 8.51a), integrated by a certain number of rock particles containing cracks, is subjected to a compressive stress state. Under the combined action of the applied stresses and water, cracks propagate at a certain velocity given by the rate of a chemical reaction at the crack tip, known as *stress corrosion*. Crack propagation eventually leads to the breakage of rock particles and to the consequent rearrangement of the granular structure in order to reach a new equilibrium configuration. Each of these rearrangements involves a macroscopic strain increment. Hence, upon blockage of the granular structure, the straining process of rockfill becomes controlled by the stress corrosion phenomenon. As stress corrosion causes the cracks to propagate at a finite velocity, and its value depends on the water energy, a dependence of rockfill deformations on time and relative humidity is expected. Adopting simplified geometry and loading conditions for the rock particles (cracked discs under a diametrically opposed concentrated loading), it was found that, in a first stage, the crack propagates slowly. At some critical time the velocity of propagation increases rapidly, and a sudden breakage takes place. The time to breakage may

change by many orders of magnitude for relatively small changes in the initial crack length. This result provides an explanation for the apparently never-ending process of settlement accumulation observed in rockfill structures (Oldecop & Alonso, 2007).

8.3.10 Three-dimensional analysis

8.3.10.1 General considerations

In most cases, embankment dams are constructed at wide dam sites at which with sufficient accuracy it is possible to employ two-dimensional analysis. Lefebvre, Duncan, and Wilson, in their classic paper (Lefebvre et al., 1973) examine the accuracy that is obtained by the two-dimensional analysis of stresses and deformations for embankment dams in valleys with a V-shape, comparing obtained results with results from a three-dimensional analysis.

In the two-dimensional analysis a quadrilateral element with arbitrary geometry has been used, while as a basic three-dimensional element an isoparametric element with eight nodal points has been used. Basically, it has been assumed that the change of displacements takes place linearly, and in the mesh there have been taken additional degrees of freedom, which, to a large extent, tops up the accuracy of the problem's treatment. The analysis has been carried out for a homogeneous dam and for three different inclinations of slopes of the valley – 1:1, 1:3, and 1:6 (1 – vertically, 6 – horizontally). The examined dam is 49 m high, it has slope inclinations of 1:2.5. Linearly elastic behaviour of the material has been assumed, with $E = 9850\,\text{kN/m}^2$, $\nu = 0.4$, and a unit weight of $\gamma = 19.6\,\text{kN/m}^3$. The incremental method has been used in both analyses, in which layers are successively being added one over another in eight layers. The comparison has been made so that, for the common points in the highest, central cross-section, the stresses and deformations, obtained with a two-dimensional analysis, are expressed as a percentage of the appropriate values, obtained with a three-dimensional analysis.

On the basis of the obtained data, the authors conclude that, for inclinations of slopes of the river valley of 1:3 and slighter, a two-dimensional analysis of the maximum cross-section yields acceptable accuracy for stresses and displacements, while for inclinations steeper than 1:3 the inaccuracy increases owing to the fast change of the cross-section along the dam. In such cases, it would be necessary to employ the rather more expensive three-dimensional analysis.

Conclusions presented in the last quoted paper have been considered as a "law" for a long time, in spite of the fact that the analysis, upon which they have been based, has a number of deficiencies, of which the chief ones are the execution of a linearly-elastic analysis, and examination of a homogeneous dam which is relatively low in height.

Raskazov et al., (1987) cite examples from analyses carried out in the former USSR. They show that, even for a coefficient of a dam site of $L{:}H = 5.3$, the coefficient of safety, obtained with a three-dimensional analysis, is 25% greater than the appropriate coefficient, calculated according to two-dimensional analysis. For a coefficient of a dam site of 2.5 in the three-dimensional analysis, F_s had increased from 1.7 to 2.2. These investigations relate to an earth–rock dam with a central core, with a height of 123 m.

Other three-dimensional analyses were also carried out in the former USSR. They are significant since there have been constructed a number of large dams on narrow

dam sites, among them also the two highest embankment dams in the world – Rogun (under construction) and Nurek (see Chapter 11) (Krizanovskij, 1982; Rasskazov & Beljakov, 1982).

The Rogun earth–rock dam, 335 m high, has an irregular S-shape in its layout plan, and it has been analyzed with a three-dimensional FEM, along with the upstream cofferdam. The analysis simulates the stages of dam construction, taking into consideration creep of material. However, only a small part of the obtained results has been presented, without a more detailed review of the method and techniques used in performing the analysis (Hunba, 1993).

With the rapid advancement of computer technology (dramatically increased speed and capacity, possibilities of automatic processing of extensive input and output data), three-dimensional analysis of embankment dams becomes much more accessible. By means of extensive parametric analyses it will be necessary to come to a safer criterion for the ratio L:H, in which three-dimensional analysis will be compulsory. In front of researchers there is a task with a model which will be able to simulate all necessary effects (non-linearity of materials, stage construction, complex effects of water, as they have been described in the subsections on two-dimensional analysis, and the behaviour of contacts between different materials, collapse settlement, consolidation, and creep), to create a parametric three-dimensional analysis by means of which it will be possible to enrich our knowledge of the behaviour and stability of different types of embankment dams. Especially valuable would be analyses by means of which it would be possible to determine the influence of steep abutments on the dam's stability and on the hazards of hydraulic fracturing in poorly permeable materials in the dam's body. Also, it is only by means of a complex three-dimensional analysis that we can judge the benefit or harm arising from curvature in the longitudinal axis of the dam in its layout plan, and the radius of curvature to which we can possibly improve the dam's behaviour, as well as other questions to which theory and practice have not given completely satisfactory answers, as yet. Some recent case studies of three-dimensional FEM analysis of different types of rockfill dams will be presented.

8.3.10.2 Analysis of a CFRD: case study of Hongjiadu Dam (China)

Hongjiadu CFRD, $H = 179.5$, is located in the Guizhou Province, Southwest China. The crest length is $L = 427.8$ m, the ratio $L{:}H = 427.8{:}179.5 = 2.38$, and the factor of valley shape is $A/H^2 = 2.32$. Thus, the dam is located in a narrow valley. The width of the dam crest is 11 m and the crest elevation is 1148 m.a.s.l. The upstream and downstream slopes are $1.4H{:}1V$. The river valley has a very unsymmetrical V shape. The abutment mountain height is over 300 m. From upstream to downstream, the left abutment has two cliffs with a height of about 100 m. In between the cliffs, there is a gentle mudstone slope 80 m to 120 m wide. The slope of the right abutment is about 25° to 40°. A typical dam cross-section is shown in Figure 8.52.

As a constitutive model of the rockfill material Duncan-Chang's hyperbola, non-linear elastic incremental model was applied. The parameters used in the analysis come from large scale laboratory triaxial tests, and are given in Table 8.2.

The horizontal end vertical displacements in the dam cross-section for the stage after construction are shown in Figure 8.53 by contour lines. The maximum horizontal

Table 8.2 Parameters for the hyperbolic constitutive law.

Material	γ_d [kN/m^3]	K	K_{ur}	n	R_f	K_b	m [°]	φ [°]	$\Delta\varphi$
2B	22.05	1100	2250	0.40	0.865	680	0.21	52	10
3A	21.90	1050	2150	0.43	0.867	620	0.24	53	9
3B	21.81	1000	2050	0.47	0.870	600	0.40	53	9
3C	21.20	850	1750	0.36	0.290	580	0.30	52	10

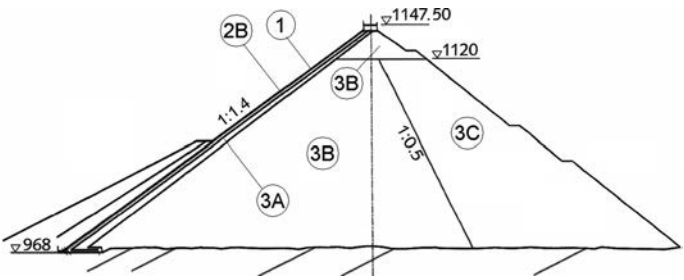

Figure 8.52 Typical cross-section of Hongjiadu Dam (after Cruz et al., 2009). (1) Concrete face slab; (3A, 2B, 3B and 3C) – see Table 8.2.

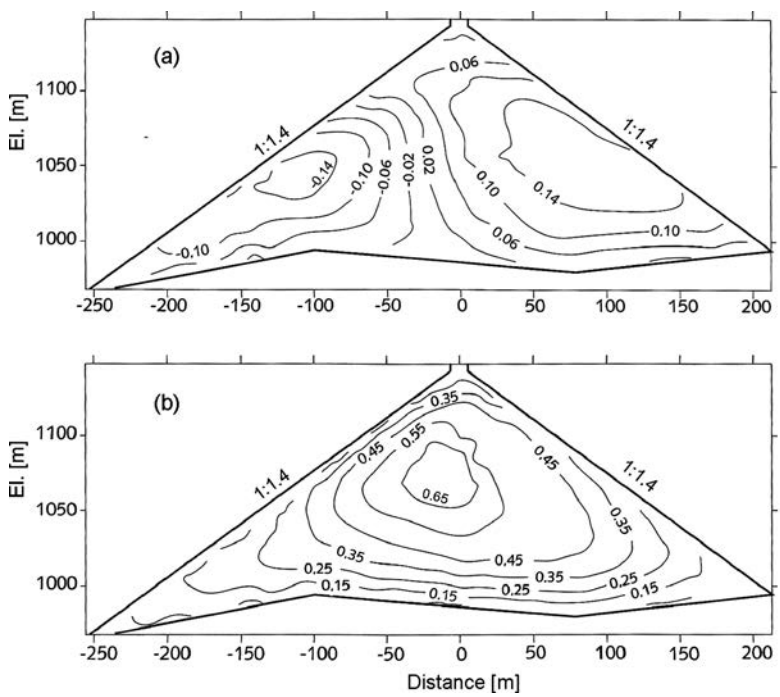

Figure 8.53 The counter lines in [m] of equal displacements in the dam cross-section for the stage after dam construction (after Cruz et al., 2009). (a) Horizontal, + towards downstream, – towards upstream; (b) vertical (settlement).

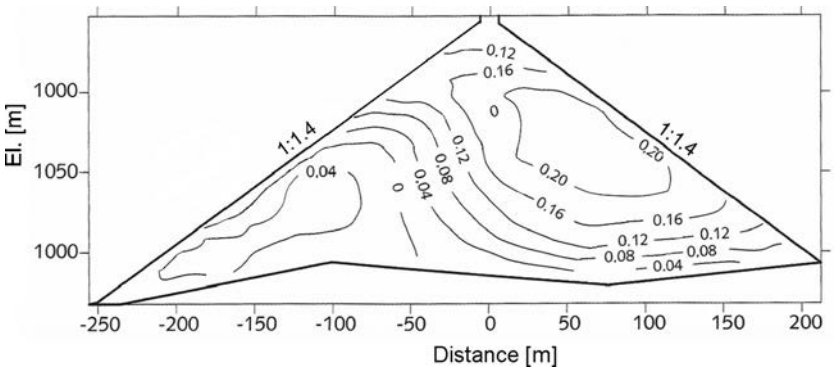

Figure 8.54 The counter lines in [m] of equal horizontal displacements in the dam cross-section for the stage after first reservoir filling (after Cruz et al., 2009). + Toward downstream.

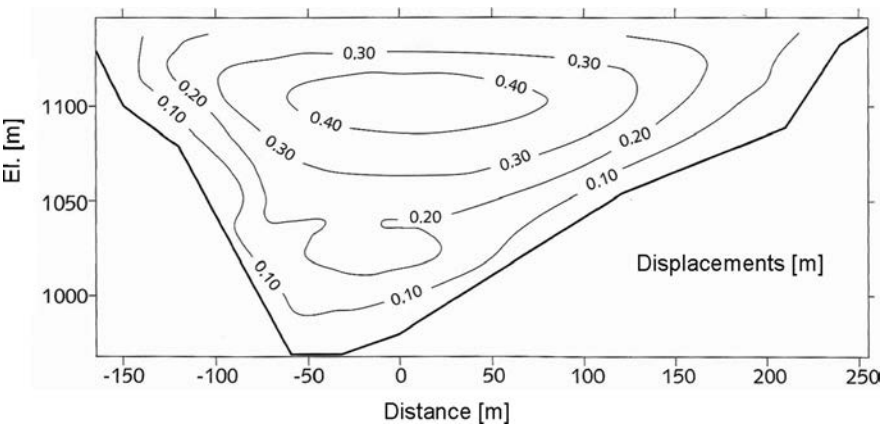

Figure 8.55 The displacements of the concrete slab after first reservoir filling in the direction normal to the slab, in [m] (after Cruz et al., 2009).

displacements at the upstream and downstream ends are 0.14 and 0.16 m respectively (a), while the maximum settlement is 0.78 m (0.44% of the dam height), located at about middle height of the dam. The distribution and the magnitude of both horizontal and vertical displacements are usual for a dam of this type and size.

After reservoir filling, the distribution of horizontal displacements on the dam cross-section undergoes an obvious change, as a result of the influence of the horizontal hydrostatic pressure on the waterproof dam face (Fig. 8.54). All dam points are moved to downstream direction. In this stage the maximum horizontal displacement is directed downstream and has a value of 0.24 m, and is located approximately in the middle of the dam height, near the downstream slope. The maximum settlement of dam body increases slightly and reaches a value of 0.81 m.

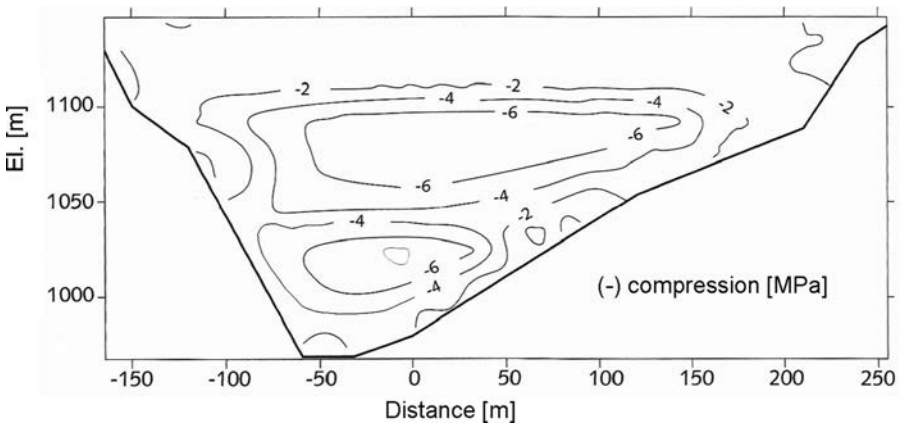

Figure 8.56 The counters of equal normal stresses along the upstream slope (concrete slab) after reservoir filling (after Cruz et al., 2009).

The displacements of the concrete slab after first reservoir filling in the direction normal to the slab are shown in Figure 8.55. The maximum normal displacement of the concrete slab is located at the upper part of the slab, on the riverbed section. From this position to the abutment, normal displacements gradually reduce. On the left, steeper bank, the gradient of the normal slab displacement is relatively large.

The counters of equal normal stresses along the upstream slope (concrete slab) after reservoir filling are shown in Figure 8.56. From the slab stress distribution after reservoir impounding, it is clear that the larger position of the concrete slab is subjected to compression. The tensile stresses are mainly developed along the perimeter and crest. The maximum compression stress along the slope is of the order of 7 MPa. Along the upstream slope, tensile stresses have occurred on the top of the slab.

Numerical research indicates that the most effective method of deformation control of CFRDs is rockfill zoning and compaction. Rational arrangement of rockfill zoning and suitable control of rockfill compaction specifications will play an important role in improving the working conditions of the face slab and the safety of the dam.

Numerical analyses show that the compaction density of rockfill material, the sequence of rockfill construction, and the material properties of the downstream 3C zone will have a significant impact on the stress and deformation of the dam and face slab. For high CFRDs, the rockfill material in upstream and downstream zones should not exhibit a great difference in the modules and densities. Considering the special topographical conditions of the Hongjiadu CFRD and in order to eliminate adverse impacts of the differential deformation between upstream and downstream rockfills, the same compaction density of upstream and downstream rockfills was required in the construction. Besides, near the steep abutment a special compaction zone with higher density was demanded with the purpose of reducing the differential deformation of rockfill along the dam axis direction (Cruz et al., 2009).

8.3.10.3 Analysis of an earth-rock dam: case study of Kozyak Dam (R. Macedonia)

The dam is of earth-rock type, 114 m high above the terrain, with rockfill shells (limestone), transition zones (sand), and an inclined clay core (see the dam layout, cross-section and a photo in Figs 11.26–11.28, Chapter 11). The core and transition zones are founded on the base rock (limestone), and the shells on the river deposit. The dam crest is at an elevation of 471.1 m.a.s.l., the normal water level is 459 m.a.s.l., while the maximum water level is 466 m.a.s.l. The volume of 100 million m^3 between elevations 459 and 466 is reserved for flood water storage. The dam was constructed in the period September 1997–March 2000, while the first reservoir filling was performed from May 2003 (water level 362 m.a.s.l.) till June 2004 (water level 452 m.a.s.l.).

In the second half of 2004 the Faculty of Civil Engineering, Skopje, made a study of deformation-stress state of the dam, taking into account: (a) the constructed geometry of the dam body, (b) geotechnical parameters of the materials gained from control tests in the construction period, (c) the real loads during the dam construction, and (d) the regime of the first reservoir filling and fluctuation of the water level at the beginning of the service period. The main aim of the analyses was to gain data of deformation-stress state of the dam body, following the history of the behaviour of the structure by means of numerical experiments. These data, finally, would serve for comparison with the measured results and their verification.

Kozyak Dam was analyzed by means of both two- and three-dimensional model. The two-dimensional analyses were performed using the commercial software SIGMA/W, SEEP/W and SLOPE/W, while for three-dimensional analyses SOFiSTiK program for determination of the deformation-stress state was used, and SEEP-3D for seepage analyses. The necessity of application of a very complex three-dimensional model which is time consuming and requires much more effort than a two-dimensional one, was imposed by the steep dam site sides: the left 1:1.5 (Ver:Hor), and the right 1:1. In such cases appreciable influence of the three dimensional effects is to be expected (Dodeva et al., 2002).

The used computer software SOFiSTiK for three-dimensional deformation-stress analyses is based on the finite element method. It has a wide range of possibilities for simulation of embankment dam behaviour and inclusion in the analyses of additional necessary phenomena, important for real simulation of the embankment dam behaviour.

The discretization of the dam body was done in such a way that all different zones of materials were included. The rock foundation was treated as rigid. The dam construction process was simulated in 11 increments, while the mathematical model has included four basic groups of materials: a clay core, transition zones, rockfill shells, and arranged stone on the upstream slope (see Fig. 11.27, Chapter 11). Each group was further divided in two sub-groups: one which could be submerged during the service period, and another which would be dry. The finite element mesh was generated automatically, using "brick" or "tetrahedron" elements. Figure 8.57 shows the general view of the dam body, divided in 11 horizontal layers for simulation of the incremental construction. An important characteristic of the software package SOFiSTiK is the possibility to model the contacts between materials with different deformability with

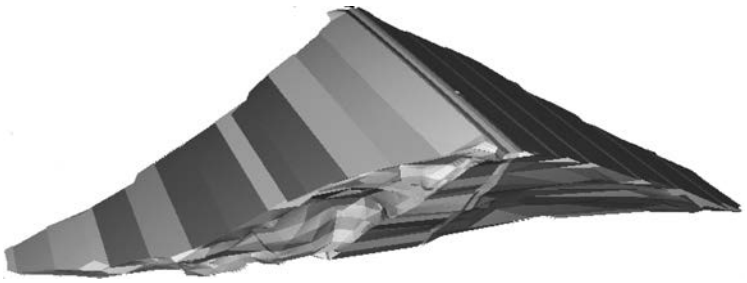

Figure 8.57 General view of the dam body, divided into 11 horizontal layers for simulation of the incremental construction process.

special contact springs. They enable differential movements in the contacts and real simulations of the dam behaviour, without occurrence of false tensile stresses. Using this useful opportunity the whole contact *dam body – rigid foundation* was modeled. Practically, without this opportunity, the real analysis would be impossible, especially in those cases, where the dam site sides are rather steep.

For the purpose of the analyses the dam body was discretized as it was constructed – practically without modifications. The same is valid for the base – it was taken from the digital record, with lots of irregularities in the shape. The consequence was a very large number of finite elements (mainly tetrahedrons) and nodes, which testifies to the complexity of the numerical solution and possible difficulties during the execution of different load cases.

The choice of the parameters for the materials is one of the most important questions in the geostatic analyses of embankment dams. Keeping in mind that previously performed two-dimensional analyses have shown that there are no appreciable differences in the results gained by non-linear analyses, compared with those gained by linear ones, it was decided to apply a linear constitutive stress-strain relationship for the embankment dam materials. In favor of this decision goes the fact that the execution of the analysis for one case loading, using a strong computer for that time – takes about 20 hours! That means the non-linear constitutive laws for the materials would make the analyses hardly feasible. In Table 8.3 the properties of the materials used in the analyses are given.

As was mentioned above, the contact *rigid foundation – deformable dam embankment materials* was modeled with contact springs, which enable differential displacements in the joint. Interfaces of different materials in embankment dams, in principle, act as compressed ones, i.e. there is no expansion of the interface in the normal direction, but only relative displacement along the contact. Therefore, the behaviour of the springs is described by two parameters: normal stiffness K_n and tangential stiffness K_s. For K_n very high value was assigned, while K_s was determined experimentally, by specially arranged laboratory direct shear test.

From the large number of results obtained by three-dimensional analyses, only a part of deformations, which are of primary importance at embankment dams, are analyzed. The aim of this consideration is to gain a general picture of the predicted dam

Table 8.3 Geotechnical parameters of the materials applied in the numerical analyses of the Kozyak dam.

Material zone	*Unit measure*	*Clay core*	*Sand transition*	*Rockfill shells*	*Gravel river dep.*	*Formula*
γ_s	kN/m^3	26.3	26.7	26.7	26.7	specific weight
γ_d	kN/m^3	15.5	21.7	21.3	21.6	dray volumetric weight
n		0.411	0.187	0.202	0.191	$n = 1-\gamma_d/\gamma_s$
e		0.697	0.230	0.254	0.236	$e = n/(1-n)$
w_s	%	26.0	8.5	9.3	8.7	$w_z = e\cdot(\gamma_w/\gamma_s)\cdot 100$
w_{opt}	%	25.6	8.5			$w_{opt} < w_z$
w	%	25.6	5.3	2.1	6.0	natural wet
γ_s	kN/m^3	19.5	23.5	23.3	23.5	$\gamma_s = \gamma\cdot(1-n)\cdot(1+w_s/100)$
γ	kN/m^3	19.5	22.9	21.7	22.9	$\gamma = \gamma_s\cdot(1-n)\cdot(1+w/100)$
γ'	kN/m^3	9.7	13.7	13.5	13.7	$\gamma' = \gamma_s - \gamma_w$
φ	°	18.6	40.0	38.3	40.0	angle of internal friction
c	kN/m^2	67.0	0.0	0.0	0.0	cohesion
k	m/s	3.0E–10	7.0E–02	9.0E–02	3.0E–03	permeability coefficient
E	kN/m^2	25,000	40,000	60,000	50,000	elasticity modulus
ν		0.40	0.35	0.30	0.35	Poisson number

behaviour after the construction process, as well as after the first reservoir filling, and, also, to illustrate the possibilities of the applied three-dimensional model of analysis.

The displacements in the dam body are shown graphically, with the lines of equal displacements in three directions:

- *x-direction*, i.e. horizontal displacements normal to the longitudinal crest axes (transversal direction); (+) means displacement towards downstream, (–) displacement towards upstream;
- *y-direction*, i.e. longitudinal displacements in the same direction with the longitudinal dam axes (longitudinal direction); (+) means displacement from right to left abutment, and (–) from left to right abutment;
- *z-direction*, i.e. vertical displacements; (+) means settlement, and (–) upraise.

Figure 8.58 shows the main dam cross-section with the lines of equal horizontal displacements, and Figure 8.59 the appropriate values of vertical displacements.

In the case of horizontal displacements in the transversal direction (x), the zero-line almost coincides with the inclined core axis (Fig. 8.58), and the maximum values are located in the middle parts of the shells, approximately at 40% of the dam height, which is typical for embankment dams. The maximum value is slightly above 20 cm, and it is smaller compared with the appropriate value gained by the two-dimensional model. This is due to clear influence of the space-effect.

For the analyzed dam cross-section, located in the middle part of the dam, the horizontal displacements in the longitudinal directions are rather small (max. 5–6 cm), and they are not shown here[2].

[2] Actually, these displacements would be zero in the case of symmetrical longitudinal dam section (both geometrical and material).

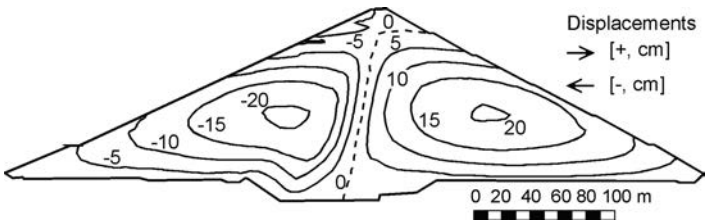

Figure 8.58 Lines of equal horizontal displacements after the dam construction, in [cm] (Tančev et al., 2007).

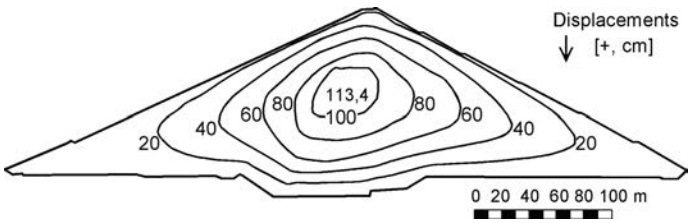

Figure 8.59 Lines of equal vertical displacements after the dam construction, in [cm]; maximum value 113.4 cm (Tančev et al., 2007).

The lines of equal vertical displacements have a regular shape for such a structure, with maximum value in the middle part of the dam core, located approximately at 60% of the dam's height (Fig. 8.59). The maximum settlement has a value of 113 cm, and it agrees very well with the measured one. The corresponding value gained by two-dimensional analyses was 131 cm. That means that the space effect, i.e. the influence of the steep dam site sides, again plays a remarkable role.

Figure 8.60a shows the longitudinal dam section through the inclined central clay core plane, with the lines of equal horizontal displacements parallel to the longitudinal dam axis (y-axis)[3]. The direction of the displacements is from abutments towards the middle part of the dam, where a zero displacement line is formed. Maximum values are below 20 cm, and appear approximately at the middle of the dam height.

The appropriate lines of equal vertical displacements are shown on the Figure 8.60b. Noticeable is the concentration of the maximum settlements in the middle, highest dam part. Of course, again appears the same maximum values of the settlement (113.4 cm), as in the Figure 8.59.

At earth-rock dams with a central core (vertical or slightly inclined), the first reservoir filling causes different and complex effects, described in section 8.3.5.2 and graphically presented on Figure 8.24. At Kozyak dam analysis the effects of the water were simulated folowing the same procedure as was described in the above cited section and applied at an hipothetical dam with asphaltic core (Fig. 8.26), and at Gradec dam

[3]Appropriate diagrams of horizontal displacements in x-direction are not shown, because after the dam construction they have values near the zero.

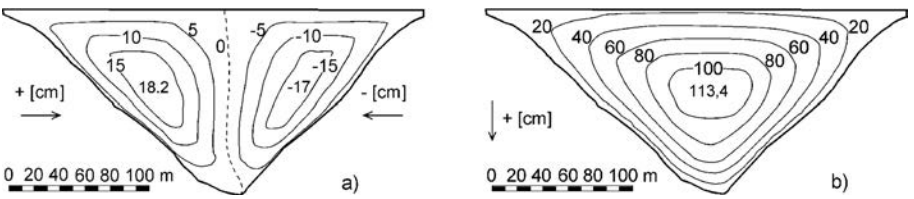

Figure 8.60 Longitudinal dam section through the inclined central clay core plane: a) lines of equal horizontal displacements parallel to the longitudinal dam axis (*y*), b) lines of equal vertical displacements, i.e. settlements (*z*) (Tančev et al., 2007).

Table 8.4 Applied parameters of the non-cohesive submerged materials (in bold).

Material Zone	*Unit measure*	*Clay core*	*Sand transitions*	*Rockfill shells*	*Gravel river dep.*	*Parameter*
φ	°	18.6	40.0	38.3	40.0	angle of internal friction
φ	°	18.6	**38.5**	**37.0**	**38.5**	**angle of internal friction**
E	kN/m^2	25,000	40,000	60,000	50,000	elasticity modulus
E	kN/m^2	25,000	**35,000**	**53,000**	**44,000**	**elasticity modulus**

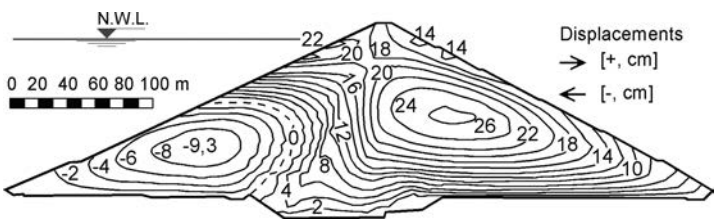

Figure 8.61 Main dam cross-section, lines of equal cumulative horizontal displacements in *x*-direction after the first reservoir filling (water elevation 460 m.a.s.l.) (Tančev et al., 2007).

(Fig. 8.27). New parameters were assigned to the non-cohesive submerged materials, based on the data given in the literature, because, for the purpose of Kozyak dam appropriate investigations were not carried out. The new values of these parameters are given in Table 8.4 in bold (in order to be distinguished of the corresponding parameters in dry condition).

The reservoir filling was simulated in more stages. Also the case of draw-down of the water level from elevation 460 m.a.s.l. to 430 m.a.s.l. was analyzed. Figure 8.61 shows the lines of equal cumulative horizontal displacements (in *x*-direction) in the main dam cross-section, for the stage of full reservoir (water level 460 m.a.s.l.). This drawing gives a clear demonstration of the effect of the first reservoir filling. Namely, comparing with the stage just after construction of the dam (Fig. 8.58), the points in the dam body are displaced to downstream. As a consequence, the absolute value of

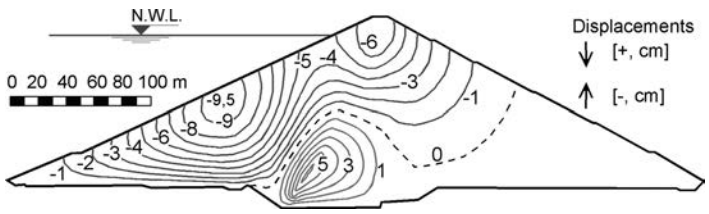

Figure 8.62 Main dam cross-section – lines of equal partial vertical displacements (z-direction), caused by the first reservoir filling (water elevation 460 m.a.s.l.), relatively to the stage just after dam construction (Tančev et al., 2007).

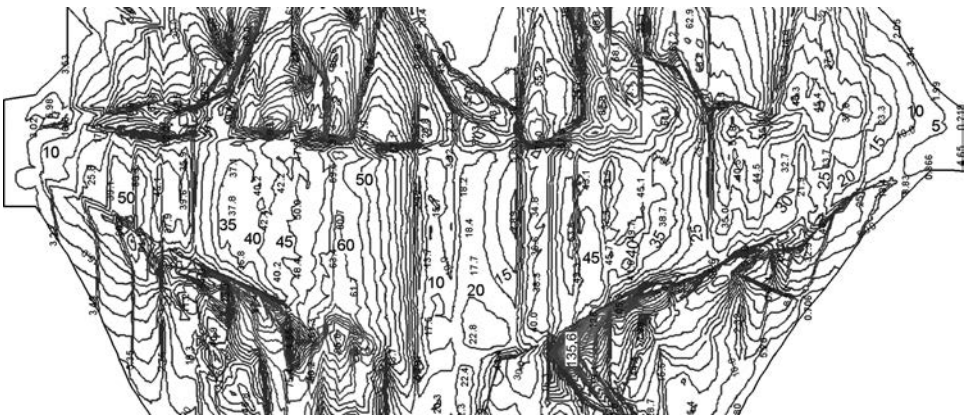

Figure 8.63 Contact *dam body – rock foundation* (a horizontal projection), with the lines of equal total displacements in the contact, caused by the influence of dam self-weight during the construction process; equidistance 5 mm, maximum displacement 135.6 mm (Tančev et al., 2007).

the maximum displacement in the upstream shell is diminished, while the maximum value for whole cross-section, located in the middle of downstream shell, is decreased to 26.5 cm, Figure 8.61 (in the previous case the corresponding value is slightly higher than 20 cm, Fig. 8.58).

The water loads cause rather complex effects concerning the vertical displacements in the dam body. In our case, additional settlement appears in the lowest part of the clay core, which is clearly visible from the diagram of the partial vertical displacements, Figure 8.62. The maximum value of the additional settlement is 6.2 cm. In the same time, the other parts of the central and upstream dam body portions are moved upward, with the maximum value of 9.5 cm, reached just below the upstream slope, in the middle part of the upstream shell.

For a real analysis and simulation of the dam behaviour and to obtain data for the displacements in the joint of the clay core with the rock foundation, contact springs are introduced in the whole contact *dam body – rock foundation*. Without these special elements, which enable differential movements in the contact, a real analysis would be

impossible. The applied spring element, as well as other joint elements, is known from the literature, as well as from section 8.3.7 of this Chapter.

Figure 8.63 presents the horizontal projection of the dam base, with equal lines of the calculated total displacements in the contact, for the stage just after dam construction, with the assumption that the foundation is rigid (non-deformable). Due to the fact that during the dam construction the vertical deformations (settlements) are predominant, it is clear that the presented deformations mainly are in the $y-z$ plane, i.e. they are directed mainly downward, from the steep abutments to the lower dam parts. In the Figure 8.63 one can see zones where larger values of displacements are concentrated. One of the reasons for that is the presence of remarkable discontinuities in the contact *dam body – rigid foundation*. Such zones are also the contacts of the core with the adjacent transition layers, because the core is buried in the rock foundation. The maximum value of the displacements in the joint *dam body – rock foundation* appears in the upstream contact *core – transition layer*, located in the lowest part of the right dam side, and is equal to 13.6 cm (Fig. 8.63). Based on the shown figure, taking into account the geometry of the contact surface, as well as the properties of the materials in the contact *clay core – rock foundation*, one can conclude that the values of displacements are relatively low, but they enable relaxation of the deformable dam material, and they prevent the occurrence of false extension stresses in the dam body.

The reservoir filling (to the elevation 460 m.a.s.l) causes lower partial displacements in the contact, (of the order of 1/3 of those caused by the dam construction), and they are not shown here.

8.3.10.4 Analysis of rockfill dam with asphaltic concrete core: Knezhevo dam (Republic of Macedonia, 2010, H = 80 m)

In the first half of 2010 Knezhevo dam was completed, the first rockfill dam with asphaltic conrete core in Macedonia. Description of the dam and appurtenant structures is given in Chapter 14, section 14.1.3.2, where also are given a layout of the hydraulic scheme (Fig. 14.24), and a typical dam cross-section (Fig. 14.25). For the purpose of the as-built design, the dam was analyzed in 2010 by means of both two- and three-dimensional model. Taking into account that the dam site is narrow ($L{:}H = 280{:}80 = 3.5$) the application of three dimensional model was considered as obligated one. The same software and similar analyzing procedure as at previously presented case study of Kozyak dam, was also applied at Knezhevo dam.

The discretization of the dam body was done in such a way that all different zones of materials were included. The rock foundation was treated as rigid. The dam construction process was simulated in 10 increments, while the mathematical model has included five basic groups of materials: an asphaltic cocncrete core, fine transition zones, coarse transition zones, rockfill shells, and arranged stone on both upstream and downstream slopes. In the longitudinal direction the dam was divided in 12 vertical segments, each long 20–25 m. The finite element mesh was generated automatically, using "brick" or "tetrahedron" elements. To enable differential movements in the contacts between materials with different deformation properties the whole contact dam body – rigid foundation, as well as the contact asphaltic core – fine transitions, were modeled by special plane contact elements.

Table 8.5 Parameters of the materials for the hyperbolic constitutive law.

Material	γ [kN/m^3]	γ_s [kN/m^3]	φ [°]	c [kPa]	K	K_s	K_{ur}	n	R_f	ν
Rockfill	21.5	23.0	37	0	1100	900	$\times 2(K,K_s)$	0.38	0.78	0.30
Coarse trans.	21.5	23.0	39	0	1200	1000	$\times 2(K,K_s)$	0.36	0.80	0.30
Fine trans.	21.5	23.0	39	0	1200	1000	$\times 2(K,K_s)$	0.36	0.80	0.30
Asphalt	24.5	24.5	35	150	1300	1300	$\times 2(K,K_s)$	0.20	0.83	0.25
Alluvium	20.0	22.0	35	0	1000	800	$\times 2(K,K_s)$	0.40	0.85	0.35

Note: γ_s and K_s are unit weight and modulus in saturated conditions.

Similar as it was done at Kozyak dam, the Knezhevo dam body was discretized as it was constructed – practically without any modifications. The same is valid for the base – it was taken from the digital record, with the irregularities in the shape. The consequence was very large number of finite elements (mainly tetrahedrons) and nodes, which talks of the complexity of the numerical solution and possible difficulties during the execution of different load cases.

FEM numerical analyses were performed using the hyperbolic constitutive law. The parameters for all materials in the dam body are shown in the Table 8.5. They were extracted from the triaxial tests performed before and during the dam construction in apparatus with diameter 150 mm and height of 300 mm. Results from large scale direct shear test were also used. For the asphalt concrete standard triaxial tests were performed.

Large quantity of output results were obtained by three-dimensional analyses and only a part of them are presented and discussed.

The displacements in the dam body are shown graphically, with the lines of equal displacements in three directions:

- *x-direction*, i.e. horizontal displacements normal to the longitudinal crest axes (transversal direction); (+) means displacement towards upstream, (−) displacement towards downstream;
- *y-direction*, i.e. longitudinal displacements in the same direction with the longitudinal dam axes (longitudinal direction); (+) means displacement from right to left abutment, and (−) from left to right abutment;
- *z-direction*, i.e. vertical displacements; (+) means settlement, and (−) upraise.

Figure 8.64 shows the main dam cross-section with the lines of equal horizontal displacements in transversal direction, and Figure 8.65 shows the distribution of horizontal displacements in the same cross-section, but in longitudinal direction.

In the case of horizontal displacements in the transversal direction (x), the maximum values are located in the shells near the slopes, approximately at one third of the dam height. The maximum value in the upstream shell is 10 cm, while in the downstream shell it is 10% smaller due to a certain asymmetry of the dam cross-section. The horizontal displacements in the longitudinal directions have small values (up to

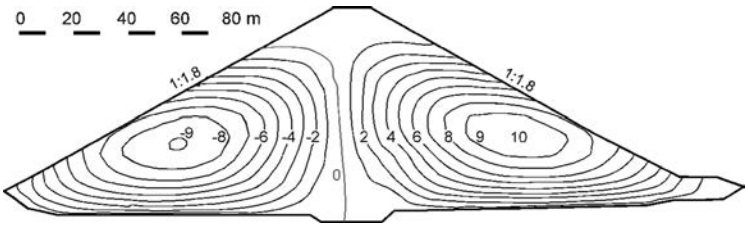

Figure 8.64 Lines of equal horizontal displacements in transversal (x) direction after the dam construction, in [cm]; equidistance: 1 cm; maximum values: x = (-9 to 10) cm; (−) displacements to downstream side, (+) displacements to upstream side.

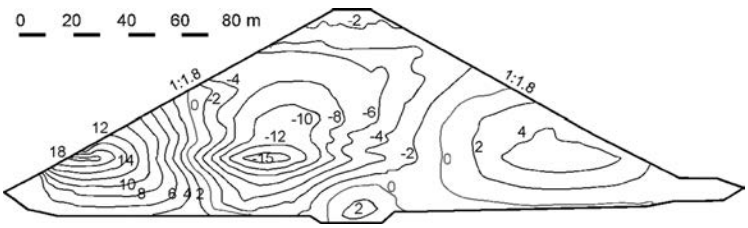

Figure 8.65 Lines of equal horizontal displacements in longitudinal (y) direction after the dam construction, in [mm]; equidistance: 2 mm; maximum values: x = (-15 to 18) cm; (−) displacements from left to right abutment; (+) displacements from right to left abutment.

18 mm), caused by the spatial dam body asymmetry in the longitudinal direction, and related to the central dam cross-section.

The appropriate values of vertical displacements have a regular distribution and intensity for such structure, with maximum value of 41.7 cm in the middle part of the dam core, located approximately at 60% of the dam height. Corresponding value gained by two-dimensional analyses was 56.1 cm. This means that the space effect, i.e. the *influence* of the steep dam site sides, plays a remarkable role.

Figure 8.66 shows the longitudinal dam section through the central vertical asphaltic concrete core plane, with the lines of equal horizontal displacements normal to the longitudinal dam axis, i.e. in x-direction. As can be seen from the contour lines the displacements are relatively small. In the right side they reach a value of 2.7 cm (in the upstream direction), while in the left side they hardly reach a value of 1 cm (directed towards downstream). Such a distribution and direction of x-horizontal displacements is imposed by the irregular spatial dam shape.

In the Figure 8.67 contour lines of the horizontal displacements in the longitudinal plane section in y-direction are shown. The displacements have a direction from abutments towards the middle part of the dam, where a zero displacement line is formed. Maximum values are around 6 cm, almost identical on the left and right side, and appear approximately at 70% of the dam height, close to the abutments.

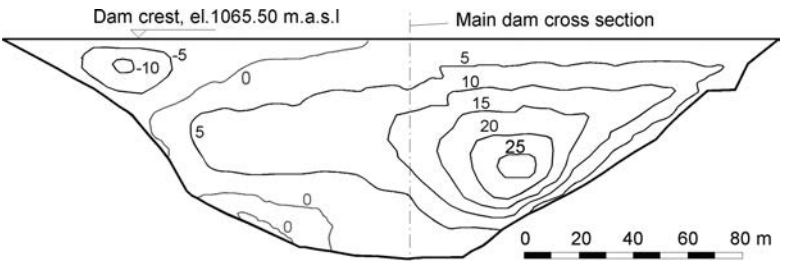

Figure 8.66 Longitudinal dam section through the central vertical asphaltic concrete core plane, with the lines of equal horizontal displacements in *x*-direction (after the dam construction).

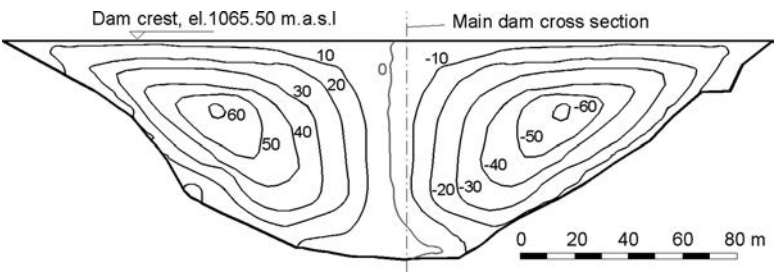

Figure 8.67 Longitudinal dam section through the central vertical asphaltic concrete core plane, with the lines of equal horizontal displacements in *y*-direction (after the dam construction), in [mm]; equidistance: 1 cm; maximal values: $y = (-6.1 \text{ to } 6.0)$ cm; [−] displacement from right to left; [+] displacement from left to right.

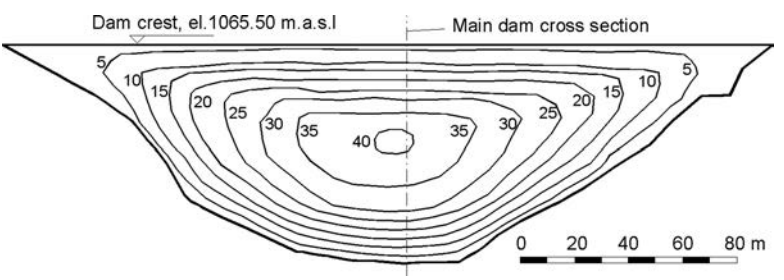

Figure 8.68 Longitudinal dam section through the central vertical asphaltic concrete core plane, with the lines of equal vertical displacements in z-direction (after the dam construction), in [cm]; equidistance: 5 cm; maximal values: $z = 40.6$ cm; [+] settlement.

The contour lines of the vertical displacements in the longitudinal dam section are shown in Figure 8.68. Their distribution is typical for an embankment dam. The maximum value of 40.6 cm is slightly lower than corresponding value appeared in the central dam cross-section due to the fact that the highest settlement after dam construction

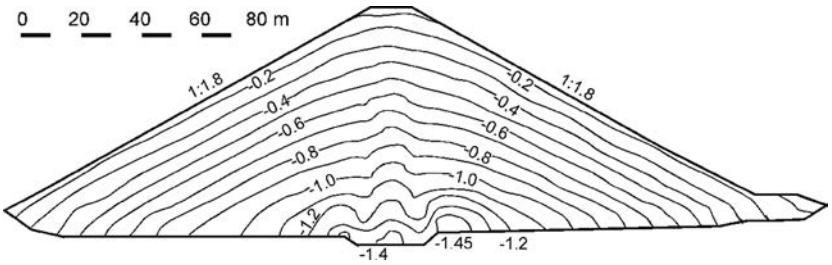

Figure 8.69 Contour lines of the major normal stress σ_1 in the central dam cross-section after the dam construction; maximum value: $\sigma_1 = 1.45$ MPa; (+) compression; equidistance: 0.1 Mpa.

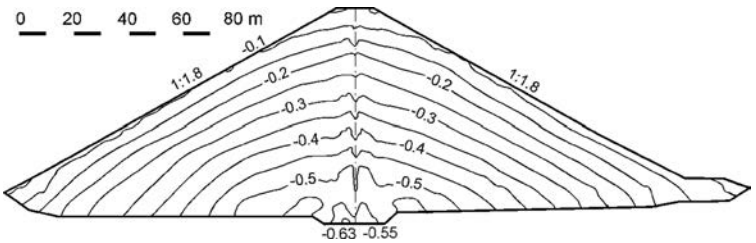

Figure 8.70 Contour lines of the normal stress σ_2 in the central dam cross-section after the dam construction; maximum value: $\sigma_2 = 0.63$ MPa; (+) compression; equidistance: 0.05 Mpa.

appears at some short distance downstream of the vertical central longitudinal dam plane section.

Figure 8.69 shows the contour lines of the major normal stress σ_1 in the central dam cross-section after the dam construction. Only compressive stresses appear reaching the maximum value of 1.45 MPa. Their intensity and distribution are customary for an embankment dam of this type and dimensions. Due to some differences in the dam material properties applied in the central dam part, slight load transfer between the transition zones (dacit) and rockfill shells (shist) can be seen. Similar can be said for the normal stresses σ_2 (Fig. 8.70), and σ_3 (Fig. 8.71). Moderate load transfer between the asphalt core and the adjacent transition zones can be noted at σ_2 contour lines. Maximum value of the minor stress σ_3 is 0.56 MPa and the ratio σ_1/σ_3 in the central, vital and the most loaded part of the dam body, is mainly between $^1/_2$–$^2/_3$, which is customary for triaxial loading condition.

Data for the strains in every node of the discretized dam body can be obtained using the values for the stresses and displacements. In this context, of the highest importance are the data for the crucial element in the dam body – the waterproof asphaltic concrete core. Figure 8.72a shows the diagram of axial strains along the vertical axis of the asphaltic concrete core, for state after the dam construction. From the diagram it can be seen that maximal values of the strains are higher in the bottom 20 m of the core and they reach 1.7% (compressive strain). The asphalt in the core, investigated with triaxial tests, reaches the highest strength at axial strains in the limits of 3% up to

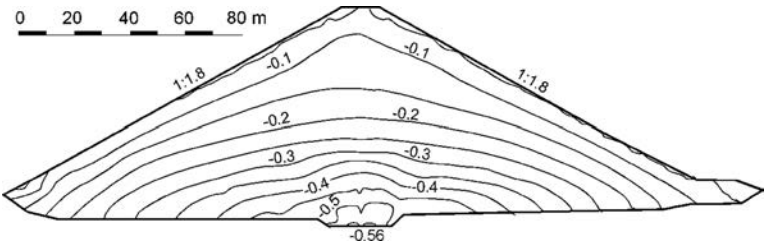

Figure 8.71 Contour lines of the minor normal stress σ_3 in the central dam cross-section after the dam construction; maximum value: $\sigma_3 = 0.56$ MPa; (+) compression; equidistance: 0.05 MPa.

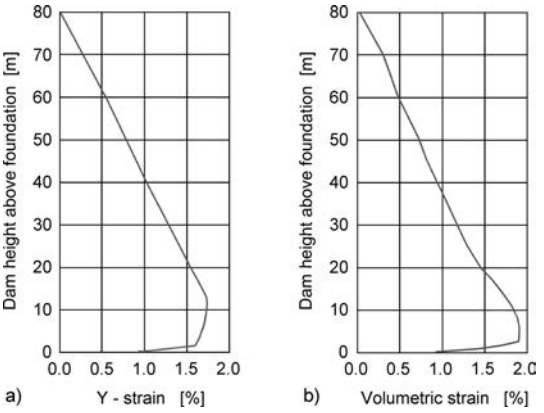

Figure 8.72 a) Diagram of the strains along the vertical axis of the asphaltic-concrete core (axial strains), for state after the construction of the dam; (+) compressive strain. b) Diagram of the vertical volumetric strains of the asphaltic concrete core, for state after the construction of the dam; (+) shrinkage.

4%, which means that in this case the stresses are far below the material strength. In the laboratory of STRABAG (Köln, Germany), it has been established that in a case of a homogeneous rockfill dam 150 m high, the relative vertical contraction (strain) of the asphaltic concrete core amounts to 7% (see also Chapter 14, section 14.1.1). At asphaltic concrete used in the hydraulic engineering, from especial importance are the volumetric strains, because, in order not to disturb the watertightness, eventual increasing of the volume can be allowed only with high restrictive value. From the diagram on Figure 8.72b it can be seen that volumetric strains (shrinkage) reach maximal value of 1.9%, also a moderate value for that kind of material.

An important characteristic of the asphalt core rockfill dams is that during the reservoir filling, as well as during the whole dam service life, the hydrostatic pressure of the reservoir water loads the waterproof element, with intensity depending on the water level. Also, other complex effects of the water, described in section 8.3.5.2 and graphically presented in Figure 8.24 should be applied in the analysis. At Knezhevo dam analysis the effects of the water were simulated following the same procedure

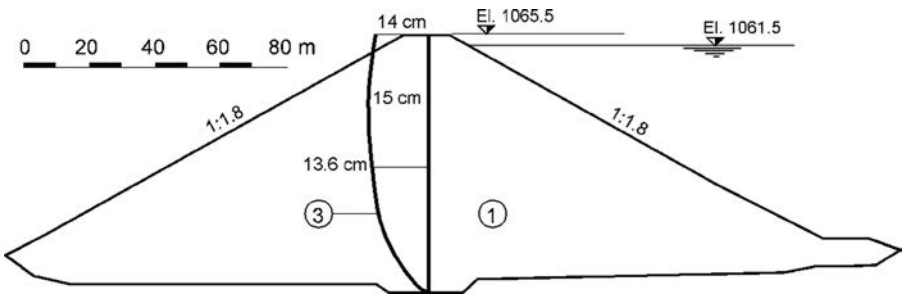

Figure 8.73 Horizontal displacements of the asphaltic concrete core as a result of the reservoir filling. (1) Position of the core after the dam construction; (2) position of the core after the reservoir filling.

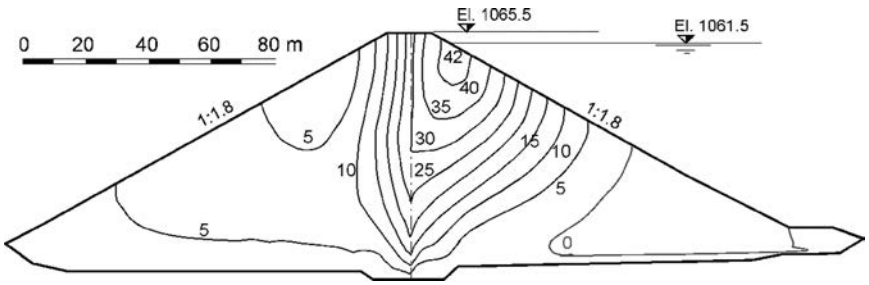

Figure 8.74 Partial contour lines of vertical displacements caused only by the water (in z-direction) after the reservoir filling; [+] settlement, [−] raising, in mm, equidistance 5 mm.

as was described in the above cited section and applied at a hypothetical dam with asphaltic core (Fig. 8.26), using the corresponding material parameters assigned to the non-cohesive submerged (saturated) materials (Table 8.5). The reservoir filling was simulated in four stages.

Figure 8.73 shows the horizontal displacements of the asphaltic concrete core caused by the reservoir filling. Mainly due to the force of the hydrostatic pressure the axis of the core moves downstream, with maximal value 15 cm, reached in the upper part. At the crest, the corresponding value is 14 cm. Comparison of the horizontal core displacements of Knezhevo dam with two other such dams is given in Chapter 14, Figure 14.31.

The complex effect of the water on the vertical displacements can be seen in Figure 8.74, where the partial contour lines of vertical displacements caused only by the water are shown. Settlements in the upstream shell can be noted, with a maximum value of 4.2 cm, located in the upper part of the dam slope. In the dry downstream shell due to transfer of pressure from the core to the rockfill additional settlements appear just near the core, with small magnitude of 2.5 cm.

The differential displacements dam base – rigid foundation are gained by means of installed special contact plane elements in the model. The calculated displacement

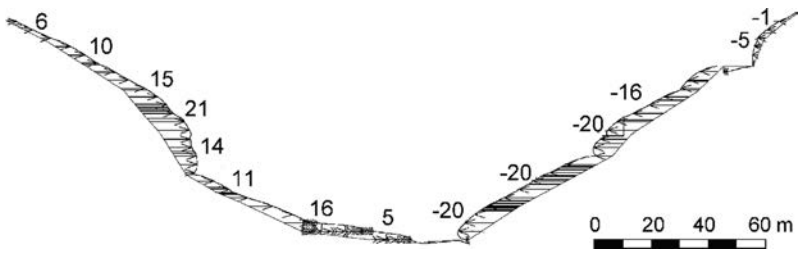

Figure 8.75 Horizontal displacements in *y*-direction in the contact of the longitudinal core axis with the concrete foundation slab after the dam construction, in [mm]; [+] displacements towards the right side, [−] displacements towards the left side; range of the calculated values: −20 to +21 mm.

in the contacts of rockfill materials with the base rock have values up to 6 cm and they are not of any interest for the evaluation of the dam behaviour. Much more important is the fact that the used model enables to calculate the displacements in the contact asphalt core – rigid concrete slab, anchored in the rock. The horizontal displacement in the contact asphalt core – concrete slab in *x*-direction, originated of dam body construction, are small, with an order of magnitude to 7 mm. The reservoir filling causes displacements in the contact towards downstream, as a consequence of the influence of the hydrostatic force. The maximal value, as it can be expected, is located in the central part of the dam longitudinal section and amounts to 17 mm. The maximal horizontal displacements in *y*-direction after the dam construction amount to 21 mm and are located in the steeper parts of the abutments, Figure 8.75. The reservoir filling, practically does not affect values gained by the dam construction simulation. Similar can be said for the vertical displacements. They have the extreme value of $z_{max} = 28$ mm, calculated for the simulation of the dam body construction in 10 layers.

The author has not any evidence that the questione of the diferential displacements of the contact asphalt core – concrete foundation has been mentioned in the literature. Thus, there are no data for comparison. But, keeping in mined that in the contact zone with the concrete slab the asphalt core is widened from 60 cm to 120 cm, it is certain that the calculated displacements in the contact are harmless.

This page intentionally left blank

Chapter 9

Dynamic stability of embankment dams

9.1 EFFECT OF EARTHQUAKES ON EMBANKMENT DAMS

Earthquakes induce an additional load on embankment dams. Under certain conditions, the seismic effect represents a major risk for large dams. It imposes a need during the analysis – in order to obtain a realistic solution – in addition to the static conditions existing before the earthquake, to also take into consideration the state of additional load during an earthquake. Earthquake load is of short duration, cyclic and involves motion in both horizontal and vertical directions. Earthquakes can affect embankment dams by causing any of the following consequences:

- Sliding, or the instability of both the upstream and downstream slopes. As a final consequence, sliding can lead to total failure of a dam;
- Deformations, i.e. vertical and horizontal displacements of the embankment, followed by developed cracks, especially exhibited in the zone of the dam's crest;
- Reduction of freeboard as a result of considerable crest settlement caused by additional compaction of the embankment due to ground motion, which may, in a worst case scenario, result in overtopping of the dam;
- Differential movement in the contacts of the dam's body, abutments and embankments – the concrete parts – which would increase the hazard of contact seepage and the formation of privileged seepage paths along contact surfaces;
- Liquefaction, or loss of shear strength in zones of the embankment or its foundation, due to increase in pore pressures which, in a worst case, may lead to failure of a dam (De Alba et al., 1988; Seid-Karbasi & Byrne, 2004);
- Differential movement in a possible fault passing through a dam's foundation below its body;
- Overtopping of the dam by flood waves due to earthquake-induced landslides into the reservoir from the valley sides;
- Damage to appurtenant hydraulic structures, both general and specific, as well as to the equipment, including damage caused by landslides and rockfalls in very steep valleys (as happened in 2008, during the Wenchuan earthquake in China).

The potential hazard of an earthquake inducing some of the quoted consequences depends on: the seismicity of the ground in the zone in which the dam is sited, the geological structure and topographic conditions in the dam site, and the type, construction and size of the dam (Chopra, 1967; Finn, 1991; Wieland, 2011).

Analyses of the behaviour of embankment dams that have been affected by strong earthquakes, throw a rather clear light on their behaviour in such unfavourable load conditions. In that respect, of particular importance is the study of the behaviour of earth dams near the San Andreas fault during the 1906 San Francisco earthquake. At that time, at a distance up to 50 km from the fault, there were 33 earth dams, of which 15 were at a distance smaller than 8 km from the fault. There is no doubt that the earthquake, with a magnitude of 8.25 on the Richter scale, caused strong shocks on all of the mentioned dams, within a time duration longer than 1 minute.

In accordance with the latest investigations, peak acceleration in all dams has been larger than 0.35 g, while in the 15 dams closest to the fault, peak acceleration exceeded 0.6 g. However, none of these older dams was seriously damaged, nor was any sliding of slopes observed.

The main feature of most of these dams is that they had been constructed of clayey earth over bedrock or over a clayey foundation. Only two of them had been constructed largely of sand, which, evidently, had not been saturated with water during the earthquake. Accordingly, it can be concluded that dams that have been built of clayey earth offer a high resistance to earthquakes.

This conclusion was also confirmed during the earthquake in Ojika (Japan) in 1939, when 12 dams failed, while 40 other dams suffered sliding of slopes. Most of the damaged and failed dams had been constructed of sandy material; there were no records of failures of dams made of clayey material, not even in the immediate vicinity of the epicentre. Indeed, even at a large distance from the epicentre, dams made of sand failed.

Another important phenomenon which was recorded during this earthquake is that, of all the failed dams, only a small number actually failed during the ground shaking period. The greater part of the dams failed from 2 to 24 hours following the shaking, most likely as a consequence of the erosive effect of seepage jets through cracks in the embankment, which originated during the ground motion.

Other earthquakes have also had similar consequences. For example, in 1971, during the San Fernando, California earthquake, slope sliding of the hydraulic fill occurred in the Upper and Lower San Fernando dams, which were constructed with shells of sand. Meanwhile, 25 earth dams constructed with compaction in thin layers and exposed to acceleration of from 0.2 to 0.4 g, exhibited excellent resistance (Seed, 1979).

A summary of investigations into the behaviour of embankment dams during an earthquake includes the following major conclusions:

- Dams raised by hydraulic fill methods have proven to be very unreliable because of the effects of shocks induced by strong earthquakes. Only hydraulic fill dams constructed with very slight slopes upon bedrock foundation can sustain moderate earthquake shocks with acceleration up to 0.2 g and a magnitude of 6.5 on the Richter scale.
- Generally speaking, each well-constructed embankment dam on a hard foundation can sustain a moderate earthquake with a peak acceleration of 0.2 g, without harmful consequences.
- Dams that have been built of constructed clayey material over a clayey and bedrock foundation can sustain strong earthquake movement with peak acceleration within the limits 0.35 to 0.8 g, at a magnitude of 8.25, without considerable damage.

- Rockfill dams containing a dry dam body, if they have been well designed and constructed, can sustain strong earthquakes, suffering deformations within acceptable limits.
- Embankment dams that have failed because of earthquakes were constructed mainly of sandy material, saturated with water during the earthquake, or built on a saturated sandy foundation.
- In cases where dams are well-constructed (see above sections), where an earthquake shock would not be expected to cause a maximum acceleration larger than 0.2 g, time and money should not be spent on dynamic analysis. Instead, attention should be focused on dams containing large zones of incoherent material (especially, sand), which during ground motion and while being saturated with water, can lose a large or small part of its strength. Also, careful analyses should be performed on embankment dams at which it is possible to expect an earthquake shock that would cause acceleration larger than 0.2 g.
- For dams constructed using saturated incoherent earth material, and those exposed to earthquakes, the primary reason damage occurs is the increased pore pressure in the embankment, and the possible loss of load-bearing capacity – a phenomenon known as liquefaction – which could occur as a result of such increased pore pressure. These complex phenomena cannot be encompassed and anticipated by means of pseudo-static analyses, so it is necessary to apply much more complex methods.

The above-described favourable behaviour of clay in relation to sandy material in the body of embankment dams during earthquakes has also been confirmed in laboratory tests involving cyclic loading. The kinds of clay used for the construction of dams do not exhibit considerable changes in pore pressure during cyclic loading, which corresponds to that caused by an earthquake. At the same time, the strength of the material changes little during such tests. Similar behaviour is exhibited by samples of very dense sandy gravel tested with cyclic loading in undrained conditions. Inversely, for loose to moderately compacted saturated sands, an increase in pore pressure caused by laboratory cyclic loading can cause a significant reduction in strength and lead to large deformations.

Particular interest is aroused by the perceived fact that during the Ojika earthquake, the failure of the dam occurred a certain time after the earth stopped shaking. This could be due to the progressive development of the erosive process through fissures caused by the earthquake. It could also be a result of the time necessary to reach a redistribution of pore pressure in order to achieve conditions for failure. In any case, dam stability during the post-earthquake period is a factor that must be considered while assessing the stability of embankment dams during earthquakes.

9.2 ASSESSMENT OF DESIGN EARTHQUAKE

9.2.1 Strength, attenuation, and amplification of earthquakes

During an earthquake, energy is released. The quantitative value, which radiates from the epicentre of an earthquake is recorded with seismographs and is called

the *magnitude* of the earthquake. There are two expressions, i.e. measures, for the magnitude. The local magnitude amounts to:

$$M_L = \log A \tag{9.1}$$

where, A = maximum seismic wave amplitude (in thousandths of a millimetre), recorded by a standard seismograph, at a distance of 100 km from the earthquake epicentre. The other expression is:

$$M_L = \log A - F(\Delta) + k \tag{9.2}$$

where $F(\Delta)$ is a distance correction, while k = scaling constant. This allows calculation of M_L at various distances from the epicentre of an earthquake.

Body wave magnitude M_b is:

$$M_b = \log V + 2.3 \log \Delta \tag{9.3}$$

where V is the maximum ground velocity in microns/sec, recorded by the seismograph, while Δ is the distance from the epicentre.

Earthquakes with a magnitude of less than 3 usually do not cause any felt effect, while those with a magnitude less than 5 will usually not cause any damage. The maximum-recorded magnitude is 8.9. The scale is not linear – each increased step on the magnitude scale represents a thirty-fold increase in energy released by the earthquake in comparison with the previous one. Thus, an earthquake measuring a magnitude of 5 releases 900 times the energy of a magnitude 3 earthquake. The magnitude, epicentral location, and hypocentre (focal depth) of an earthquake are determined using a seismograph (for more details see chapter on monitoring of embankment dams).

Earthquake intensity is a quantitative value based on the responses of objects and people to the earthquake. Intensity depends on distance from the earthquake epicentre, ground conditions, and topography; thus, there will be a range of intensity values for any earthquake. The most commonly used scale for the determination of earthquake intensity is the *Modified Mercalli Scale,* which has XII degrees.

Of interest where dams are concerned, is the range from VII to IX degrees, since an earthquake weaker than VII degrees does not represent a danger for a dam that has been well designed to withstand static loads, while to dimension a dam for an earthquake stronger than IX degrees is extremely irrational. Table 9.1 represents the part of the Mercalli Scale in the range from VI to X degrees, with a description of the effects caused by an earthquake of relevant strength (Fell et al., 1992; Newmark & Rosenblueth, 1971).

In the design of dams, the horizontal and vertical *acceleration,* which is induced by an earthquake at the base of the dam, is usually required. Information on acceleration is best obtained from an accelerograph, installed at the dam site. Records of other places with similar geological structure should also be maintained. Typical accelerograph records can be seen in Figures 9.11, 9.17, and 9.23 and 9.27 below. Acceleration is most often expressed in relation to acceleration due to gravity, for example 0.15 g. The response of the dam is dependent on the amplitude of ground acceleration, duration of the ground motion, and frequency of cycling. There are no unique relationships between magnitude, intensity, and acceleration, as quoted values

Table 9.1 Modified Mercalli Scale (1956 version), range from VI to X degrees.

Intensity	*Effects*
VI	Felt by all, many of whom are frightened and run outdoors. Causes persons to walk unsteadily; windows, dishes, and glassware broken. Knick-knacks, books, etc. fall off shelves, pictures fall off walls, and furniture moves or is overturned. Weak plaster and masonry D crack, small bells set to ringing (church, school), and trees and bushes shake visibly, or are heard to rustle – CFR.
VII	Difficult to stand. Noticed by drivers of motorcars. Hanging objects quiver, furniture breaks. Damage to masonry D, including cracks, weak chimneys break at roofline. Plaster, loose bricks, stones, tiles, cornices (also unbraced parapets and architectural ornaments – CFR), fall. Some cracks in masonry C. Waves on ponds, water turbid with mud. Small slides and caving in along sand or gravel banks. Large bells set to ringing. Damage to concrete irrigation ditches.
VIII	Steering of motorcars affected. Damage to, and partial collapse of, masonry C. Some damage to masonry B, none to masonry A. Stucco and some masonry walls collapse. Chimneys, factory stacks, monuments, towers, and elevated tanks twist and fall. Framed houses move on foundations, if not bolted down, panel walls are thrown out. Decayed piling breaks off. Branches break from trees. Changes occur in flow or temperature of springs and wells. Cracks develop in wet ground and on steep slopes.
IX	General panic. Masonry D is destroyed; masonry C suffers heavy damage, sometimes with complete collapse; masonry B suffers serious damage. (General damage to foundations – CFR). Framed structures, if not bolted, shift off of foundations. Frames crack. Serious damage to reservoirs, underground pipes break. Conspicuous cracks appear in ground. In alluvial areas, sand and mud are ejected, earthquake fountains, and sand craters.
X	Most masonry and frame structures are destroyed along with their foundations. Some well-built wooden structures and bridges are destroyed. Serious damage to dams, dikes, and embankments. Large landslides, water overflows banks of canals, rivers, lakes, etc. Sand and mud shift horizontally on beachheads and flatland. Rails bend slightly.

Note: *Masonry A:* Good workmanship, mortar and design; reinforced, especially laterally, and bound together by using steel, concrete, etc.; designed to resist lateral forces. *Masonry B:* Good workmanship and mortar, reinforced, but not designed to resist lateral forces. *Masonry C:* Ordinary workmanship and mortar; no extreme weaknesses such as non-tied-in corners, but masonry is neither reinforced nor designed against horizontal forces. *Masonry D:* Weak materials, such as adobe; poor mortar; low standards of workmanship; weak horizontally. *CFR* indicates additions to classification system by Richter (1958).

depend on energy released by the earthquake, the source mechanism of the earthquake, geological conditions in the space affected by the earthquake, distance from the epicentre, and geological conditions and topography at the dam site. Figure 9.1 represents an approximation diagram for the relationship between magnitude, released energy, epicentral intensity, and acceleration, for a dam site with a hard foundation, not affected by local ground topography. Acceleration and intensity in the diagram relate to the epicentre of the earthquake.

The effect of an earthquake is attenuated with an increase of the distance from the epicentre. On the basis of recorded earthquakes and performed measurements, several formulae have been derived for ground acceleration at the anticipated dam site. One of them is the formula by Esteva and Rozenbluet (1969):

$$A = 2000\, e^{0.8M} R^{-2} \tag{9.4}$$

where, A = peak acceleration as % of acceleration due to gravity g, R = focal distance (distance from epicentre) in km, and M = earthquake magnitude.

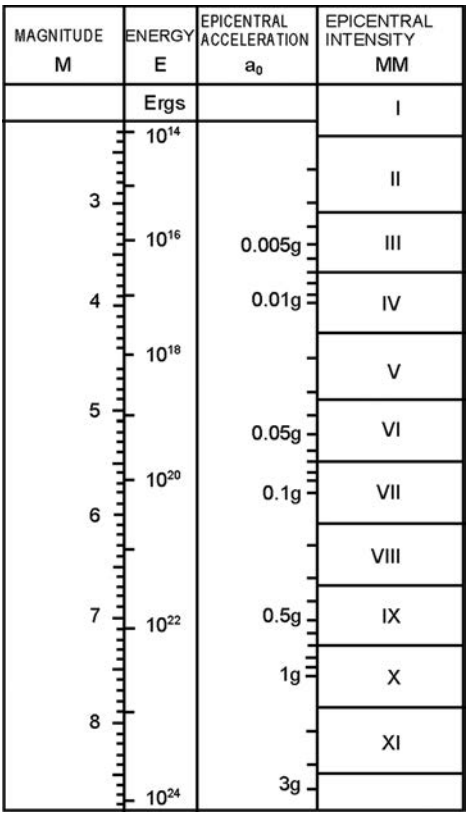

Figure 9.1 Approximate correlation between magnitude, released energy, epicentral intensity, and acceleration (after Fell *et al.*, 1992).

Hunt (1984) gave the following relationship for earthquake intensity:

$$I_s = C_1 + C_2 I_0 - C_3 \ln(R + C) \tag{9.5}$$

where I_s = intensity at the site anticipated for dam construction, according to the Modified Mercalli Scale; R = focal distance (distance from the epicentre) in km; C, C_1, C_2 and C_3 = constants; and $\ln(R + C)$ = error term for correction (Fell et al., 1992).

The above quoted equations allow us to estimate the intensity and peak acceleration in the bedrock of a dam site. Dam sites on rigid ground with a thick layer of incoherent earth material will have similar peak acceleration to that in the bedrock. Dam sites located on soft or medium soft clay or on a shallow layer of incoherent soil, experience peak acceleration in the foundation that can significantly deviate from that in the bedrock. In such cases, according to some authors, upon an acceleration of less than 0.1 g, earthquake amplification may occur, while upon an acceleration larger than 0.3 g, peak acceleration may be decreased due to dissipation of energy. The 1985

Mexico earthquake, a good example, is well known. Bedrock accelerations reached 0.03 g, with peak accelerations of 0.17 g recorded on the surface of soft soil areas.

Ground topography, as well, has an influence on accelerations. An accelerograph sited on a ridge high on a dam abutment, is likely to record significantly higher accelerations than one sited at the river channel. Later on, we shall see what results are obtained from the comparison of accelerations, from calculations on the dam's crest, in the lower zones, and down to the foundation.

9.2.2 Design earthquake

An important issue in the seismic analysis of dams is the selection of the *design earthquake*. Two main kinds of design earthquakes that are recommended in analyses are: *Operating Basis Earthquake (OBE)* and *Maximum Credible Earthquake (MCE)*.

OBE is an earthquake that is liable to occur at least once during the expected operation life of a dam, which is 100 years or more. It has a probability of occurrence of about 50% during a service life of 100 years. The return period is taken as 145 years. In practice, there are no strictly defined conditions that have to be fulfilled by an embankment dam exposed to OBE. Generally, no structural damage (cracks, deformations, leakage etc.) which affects the operation of the dam and the reservoir is permitted. Minor, repairable damage, is accepted. The objective of an analysis with OBE is to evaluate the displacements in the dam's body given the effect of such an earthquake, where such displacements should be within acceptable limits, while the stability of the dam should not be called into question. Appurtenant structures and hydro-mechanical equipment should also remain in operational condition, without distortions.

The OBE ground motion parameters are usually estimated by means of probabilistic analysis of earthquakes recorded in the vicinity of the dam site. ICOLD recommends the Cornell–McGuire method, which consists of the following procedure (Fell et al., 1992):

- Obtain records of the earthquake's magnitude, location of the epicentre, and depth;
- Determine attenuation laws of the earthquake, in order to evaluate peak acceleration at the dam site for each recorded earthquake. This can be based on recorded accelerograms or on the basis of known equations for attenuation of earthquake movement combined with distance from the epicentre;
- Draw evaluated peak accelerations for the recording period and extrapolate the required return period for OBE.

Figure 9.2 shows the results of such an analysis. In this case, there were no accelerograph records, so published attenuation equations have been used. A wide scatter of results is apparent and is because the formulae published later predicted larger accelerations. The significance of possessing accurate historical data for the evaluation of earthquakes is stressed increasingly of late.

The MCE is the event that produces the largest ground motion expected at the dam site on the basis of the seismic history and the seismotectonic setup in the region. It is estimated based on deterministic earthquake scenarios. According to ICOLD (2010) the ground motion parameters of the MCE shall be taken as the 84 percentiles (mean plus one standard deviation).

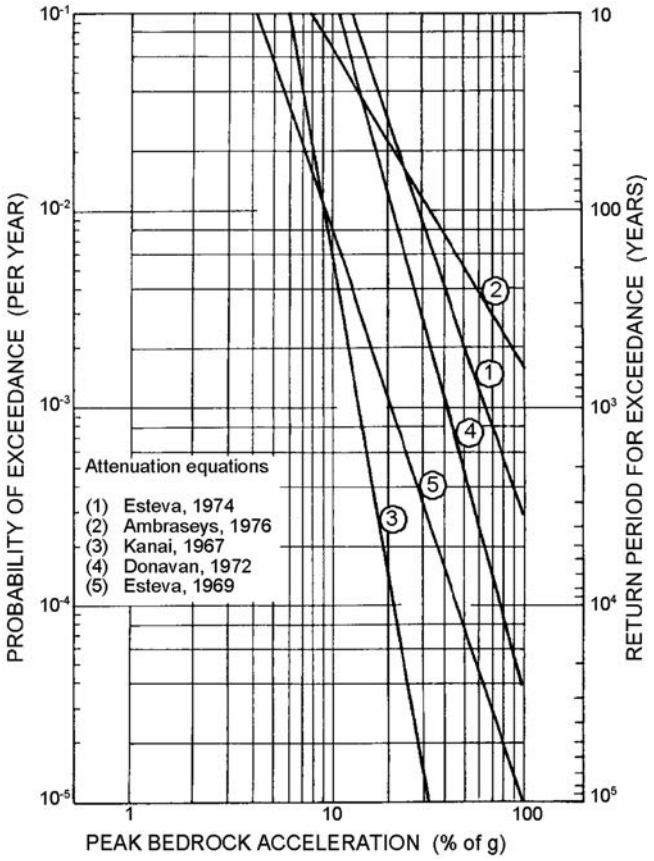

Figure 9.2 Peak bedrock acceleration versus probability of exceedance in an embankment dam.

Maximum Credible Earthquake (MCE) represents the strongest earthquake that can be conceived to occur at a dam site on the basis of the seismic history and the seismotectonic setup in the region, taking also into consideration active faults in the vicinity. An embankment dam should be designed in such a manner that MCE should not cause:

1. Failure of the dam due to liquefaction of a certain layer in the dam's body or foundation;
2. Failure of the dam due to large displacement of a surface by sliding, in one of the slopes or in the foundation;
3. Loss of freeboard due to settlement or deformation of crest;
4. Development of uncontrolled leakage of water through cracks or at interfaces with concrete structures or abutment rocks;
5. Spillways and other appurtenant structures to be damaged to the extent that the functionality and safety of the dam would be endangered.

Estimation of MCE is similar to the estimation of probable maximum precipitation in hydrology and is better performed using a deterministic rather than a probabilistic approach (84 percentile values of ground motion parameters shall be used). Such a procedure will involve the following:

- Identification of major faults within the vicinity of the dam site, which can encompass an area of up to several hundred kilometres;
- Assessment to determine whether the faults are active or potentially active by considering whether recent earthquakes have been recorded along the fault. For this purpose, geomorphologic studies may be necessary (for instance, trenching across faults to identify the age of the displacement);
- Assessment of MCE in each identified fault. This may be determined by considering the length of the fault but also from the general seismicity of the area. Previously monitored earthquakes indicate that the magnitude of an earthquake increases with the length of the fault;
- Assessment of maximum acceleration at the dam site, resulting from the MCE for each of the faults and determination of the most critical earthquake. Taken into consideration should be the duration of the earthquake and the period of oscillations, which are dependent on the magnitude of the earthquake. The effect of an earthquake on a dam is also dependent on these factors, as well as on peak accelerations, and often, more than one earthquake may have to be used in the analysis.

In the event that it is not practicable to estimate the MCE from the above procedure, a probabilistic approach may be used, but with caution. In such a case, it would be necessary to figure in a return period of 0.01%.

When a dynamic analysis is to be performed for OBE or MCE, an appropriate seismogram of the earthquake must be produced, using calculated peak acceleration based on records of earthquakes that have happened at sites with similar geological conditions. The different design earthquake ground motions are characterized by the following seismic parameters:

- Peak ground acceleration (PGA) of horizontal and vertical earthquake components.
- Acceleration response spectra of horizontal and vertical earthquake components typically for 5% damping, i.e. uniform hazard spectra for OBE obtained from the probabilistic seismic hazard analysis (mean values) and 84 percentile values of acceleration spectra for MCE obtained from the deterministic analysis using different attenuation models.
- Spectrum-compatible acceleration time histories for the horizontal and vertical components of the MCE ground motion determined either from a random process or by scaling of recorded earthquake ground motions. The artificially generated acceleration time histories of the horizontal and vertical earthquake components shall be stochastically independent.

In addition, the following design earthquakes for the seismic design of the dam and different appurtenant structures in the frame of a hydraulic scheme can be met:

- *Maximum Design Earthquake (MDE)*. For large dams the return period of the MDE is taken as 10,000 years. For dams with small or limited damage potential shorter return periods can be specified. The MDE ground motion parameters are estimated based on a probabilistic seismic hazard analysis (PSHA).
- *Safety Evaluation Earthquake (SEE)*. In the revised Bulletin 72 (ICOLD, 2010), the SEE replaces the term Maximum Design Earthquake (MDE) used in the first edition of this bulletin. The Safety Evaluation Earthquake (SEE) is the maximum level of ground motion for which the dam should be designed or analyzed. For dams whose failure would present a great social hazard the SEE will normally be characterized by a level of motion equal to that expected at the dam site from the occurrence of a deterministically-evaluated maximum credible earthquake or of the probabilistically-evaluated earthquake ground motion with a very long return period, for example 10,000 years. Deterministically-evaluated earthquakes may be more appropriate in locations with relatively frequent earthquakes that occur on well-identified sources, for example near plate boundaries. This is an earthquake ground motion which a dam must be able to resist without uncontrolled release of the reservoir. Structural damage (cracks, deformations, leakage etc.) is accepted as long as the stability of the dam is ensured and no large quantities of water are released from the reservoir causing flooding in the downstream region of the dam. The SEE is the governing earthquake ground motion for the safety assessment and seismic design of the dam and safety-relevant components, which have to be functioning after the SEE. Where there is not a great risk to human life the SEE may be chosen to have a lower return period depending on the consequences of dam failure.
- *Design Basis Earthquake (DBE)*. The DBE with a return period of 475 years is the reference design earthquake for appurtenant structures. The DBE ground motion parameters are estimated based on a PSHA. The mean values of the ground motion parameters of the DBE can be taken.
- *Construction Earthquake (CE)*. This used for the design of temporary structures such as coffer dams and takes into account the service life of the temporary structure. There are different methods to calculate this design earthquake. For the temporary diversion facilities the return period of the CE may be taken as that of the design flood of the river diversion.

9.3 LIQUEFACTION

One of the most critical issues relating to the effect of earthquakes on embankment dams is whether *liquefaction* in the dam's body and/or its foundation may occur. If so, then the primary concern becomes: what would the consequences be? The phenomenon of liquefaction occurs *in incoherent saturated earth material when there are excessive deformations and displacements as a result of transient or repeated dynamic loading.* This phenomenon is accompanied by an *increase in pore pressure* and partial or total *loss of shear strength*, which speaks clearly of the hazards liquefaction conceals relating

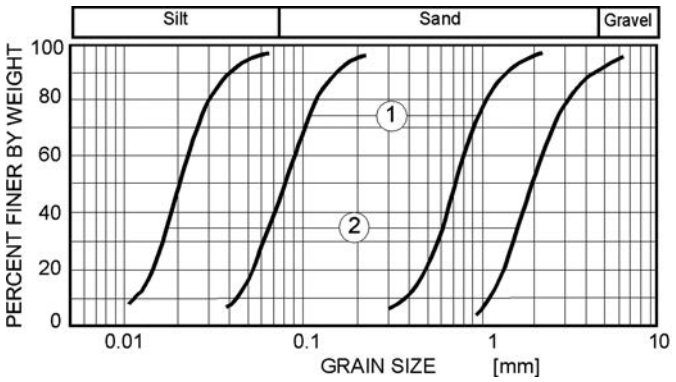

Figure 9.3 Limit curves of granulometric composition for natural earth materials susceptible to liquefaction. (1) Limits for most liquefiable material; (2) limits for potentially liquefiable material.

to the stability of embankment dams (Fell et al., 1992; Mansouri et al., 1983; Roth et al., 1991; Yegian et al., 1994; Youd & Bennett, 1983).

Saturated, silty and gravelly sands are susceptible to liquefaction. Figure 9.3 presents the limits in the gradation curves of natural earth materials susceptible to liquefaction (Fell et al., 1992).

Many researchers in the world in order to explain the phenomenon of liquefaction, have performed extensive laboratory testing. Summarized in brief, the most important conclusions of those investigations are the following (Alarcon-Guzman et al., 1988; Arulanandan et al., 1983; Berrill & Davis, 1985; Boulanger & Seed, 1995; Charlie et al., 1995; Finn et al., 1991; Georgiannou et al., 1990; Goh, 1994; Hryciw et al., 1990; Ishihara, 1996; Konrad, 1990a,b; Konrad & Watts, 1995; Lee & Foo, 1990; Martin & Clough, 1994; Seed, 1987; Stark & Olson, 1995; Takahi et al., 1991; Vaid & Thomas, 1995; Zeghal & Elgamal, 1994):

1. Cyclic loading causes densification of dry, granular (earth) materials by particle rearrangement. If the earth material is saturated and not allowed to drain during cyclic loading, a decrease in volume cannot occur; therefore, as a reaction to the tendency for the volume decrease, there is a counteraction of an increase in pore pressure and a decrease in effective stresses. Pore pressures build up gradually with the number of cycles of loading and, only if pore pressures build up to equal the total stress σ (the effective stress $\sigma' = 0$), does the initial liquefaction condition occur.
2. The number of cycles necessary to reach the $\sigma' = 0$ condition depends on the relative density and magnitude of the cyclic stress compared to the initial stress τ_c/σ'_v, where τ_c is cyclic shear stress, while σ'_v is vertical stress. Loose sand is more susceptible to liquefaction than dense sand. There are also indications that cyclic shear strains must exceed a threshold value (about 0.01%) before any pore pressure build-up can occur (Fig. 9.4).

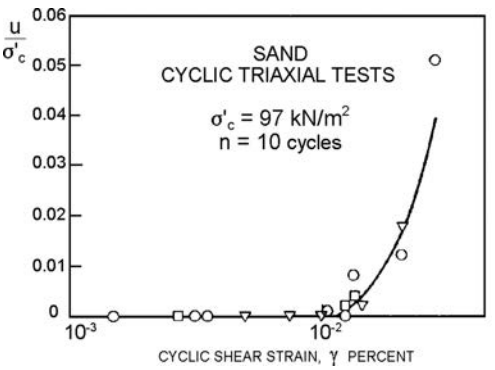

Figure 9.4 Illustration of the initial strain required to cause generation of excess pore water pressures (after Fell et al., 1992).

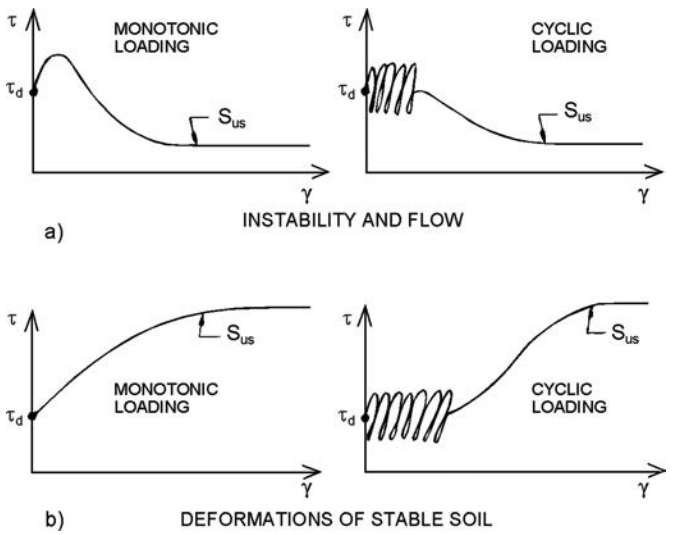

Figure 9.5 Unstable (a) and stable (b) behaviour under static and cyclic loading (Fell et al., 1992). τ = shear stress; τ_d = static (driving) shear stress; γ = shear strain; S_{us} = undrained steady state strength.

3. Earth materials, during liquefaction still exhibit a residual undrained strength, even if the $\sigma' = 0$ condition develops during cycling. Once cycling stops, the soil will still retain a certain shear strength so that, e.g. for medium dense and dense sands, the undrained steady state strength is not affected during large strains, as is shown in Figure 9.5b. And if, for loose sand, the cyclic loading strains exceed the monotonic (static) shear strength, the remaining shear strength may not be sufficient to sustain the static loading τ_d leading to further strain and loss of shear strength until S_{us} is reached (Fig. 9.5.a). This can result in *flow failure,* a condition where the earth mass deforms continually under the effect of shear stresses equal to the static shear stresses acting upon it. At this point, slope instability or failure

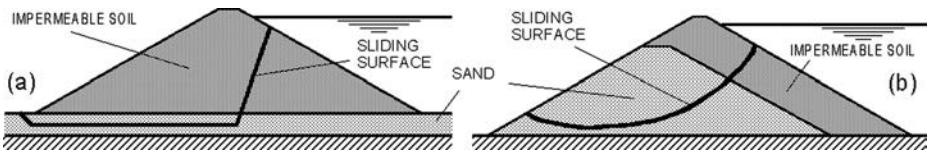

Figure 9.6 Cases potentially susceptible to liquefaction.

may occur followed by loss of the entire load-bearing capacity. Figure 9.6 schematically presents situations wherein the static shearing force (τ_d) acts and, if there occur conditions of the type shown in Figure 9.5a, then flow failure will follow.

4. Initial stress conditions affect the liquefaction potential. Experiments have shown that the presence of an initial (or static) shear stress in the earth sample increases the cyclic stress ratio required to increase pore pressure, e.g. to reach the $\sigma' = 0$ condition, when compared to tests without initial shear stresses. Hence, the worst condition is the horizontal (or nearly horizontal) saturated ground layer. That effect has been studied using a model dam that experiences shaking in a centrifuge.

The evaluation of the susceptibility of the earth material to liquefaction is complex and there are on-going worldwide efforts that hope to define the most accurate methods possible, even though, at present, there are a number of methods being used, those being mainly empirical and semi-empirical. When a horizontal ground layer is the issue, the simplest and most often applied is the semi-empirical method, developed by Bolton Seed and his co-researchers. The semi-empirical method is based on the peak acceleration induced by the credible earthquake, on earth pressure, magnitude of the credible earthquake, fines content of the soil (% passing 75 μm), and other factors (Seed et al., 1983).

9.4 ANALYSIS OF STABILITY AND DEFORMATIONS IN EMBANKMENT DAMS INDUCED BY EARTHQUAKES

The seismic effect often causes large, sometimes major, risk when considering the design of a large dam. For a quality and realistic analysis of the behaviour of a dam during an earthquake, it is necessary first to, as accurately as possible, determine the static conditions that exist prior to an earthquake, as well as the state of loading during an earthquake. Methods for static analysis of embankment dams, both classic and contemporary, are described in Chapter 8.

The designer of a dam, depending on the method selected for analysis of earthquake conditions, will have previously selected the appropriate method for analysis of the static state, which will best fit into the dynamic analysis. What follows is a concise review of the best-known methods for analysis of embankment dams during earthquakes.

9.4.1 Pseudo-static method

Until some 30 years ago, this method was standard when assessment of the safety of embankment dams during earthquakes came into question. The pseudo-static method

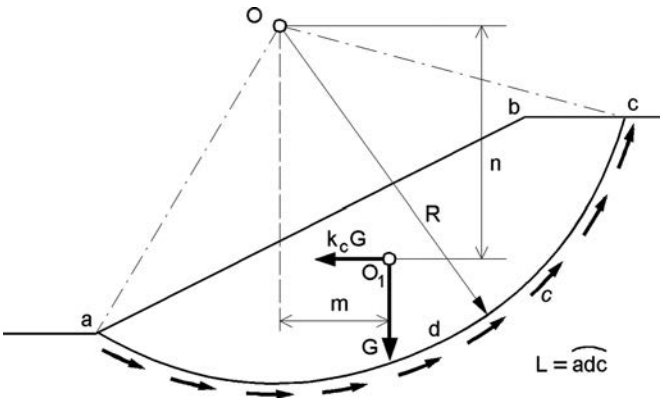

Figure 9.7 Conventional method for stability analysis of dam slope (after Terzaghi, 1950).

is based on the classical method of limit equilibrium, in which the effect of an earthquake on a potential sliding mass is represented with an equivalent static horizontal force, determined as a product of the coefficient of seismicity k_c and the weight of the potential sliding mass. If an earth embankment without water is involved, a simplified scheme of the method is presented in Figure 9.7.

Forces G and $k_c \cdot G$ pass through the centroid of gravity O_1 of the slice *abed*. The force, due to seismic effect $k_c \cdot G$ acts relating to O at a lever arm n and it increases the moment that has a tendency to cause rotation of the slice *abc* around point O. In that way, an earthquake decreases the coefficient of safety of the slope against sliding, from k_s to k'_s:

$$k'_s = \frac{c \cdot L \cdot R}{G \cdot m + k_c \cdot n \cdot G} \tag{9.6}$$

Equation (9.6) is based on the assumption that horizontal acceleration acts permanently and in one direction, which considerably simplifies consideration of the problem. Because of that, the accuracy of such an analysis is limited. Theoretically, value $k'_s = 1$ could mean sliding, but in practice, the slope may remain stable as well at $k'_s < 1$, depending on the character of the material from which the slope is formed.

In spite of the small l accuracy it yields, this method has been employed for the evaluation of seismic stability of thousands of dams, by using relatively low values for the coefficient of seismicity. For example, a typical range of values in the USA has been 0.05–0.15 (even for an area such as California, which is known for its strong earthquakes). In Japan, values smaller than 0.2 have been used. Similar values are also customary in other countries with credible seismic activity. Typical values, used for the analysis of certain dams, are shown in Table 9.2.

Such confidence in this extremely simple method is due to the fact that relatively few embankment dams have suffered during earthquakes, and even in the case of those dams that have suffered, an explanation exists regarding the age of the dams and/or their inadequate methods of construction. Following the failure of two dams

Table 9.2 Typical values of k_c and $k'_{s\,min}$ used in practice.

Dam	*Country*	k_c (*horizontal*)	$k'_{s\,min}$
1. Aviemore	New Zealand	0.1	1.5
2. Bersemisnoi	Canada	0.1	1.25
3. Digma	Chile	0.1	1.15
4. Globochica	Macedonia	0.1	1.0
5. Karamauri	Turkey	0.1	1.2
6. Kisenyama	Japan	0.12	1.15
7. Mica	Canada	0.1	1.25
8. Misakubo	Japan	0.12	–
9. Netzahualcoyote	Mexico	0.15	1.36
10. Oroville	USA	0.1	1.2
11. Paloma	Chile	0.12–0.2	1.25–1.1
12. Ramganga	India	0.12	1.2
13. Terkan	Turkey	0.15	1.2
14. Yeso	Chile	0.12	1.5

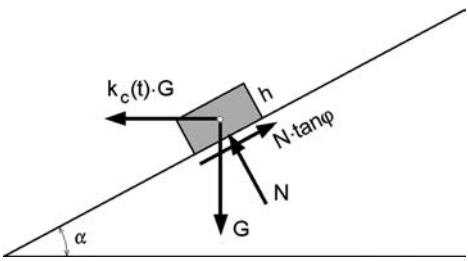

Figure 9.8 Forces on a sliding block.

(Upper and Lower San Fernando) in the 1971 California earthquake, confidence in this method was lost resulting in extensive research work begun to develop more accurate and complex evaluation methods.

This method is still being used, however, in preliminary stages of design, but with higher values for k_c. For instance, in the USA a value equal to 1/2 of the predicted acceleration in the foundation, is used. Furthermore, it is recommended that the strength of the filling materials be reduced by 20%; the permissible safety factor is 1.0 (Seed, 1979).

9.4.2 Pseudo-static methods with a non-uniform coefficient of acceleration

By means of numerous analyses and monitoring of the behaviour of dams during earthquakes, it has been determined that acceleration is amplified from the dam's base upward, resulting accelerations at the dam crest that may be several times greater than at the base. If such variable and amplified acceleration is used in the analysis by means of the method of limit equilibrium, one may obtain a more realistic picture of a dam's coefficient of safety.

Thus, pseudo-static methods have evolved, which analysis encompasses a *non-uniform coefficient of acceleration.* Also, in this case, we consider only one immediate

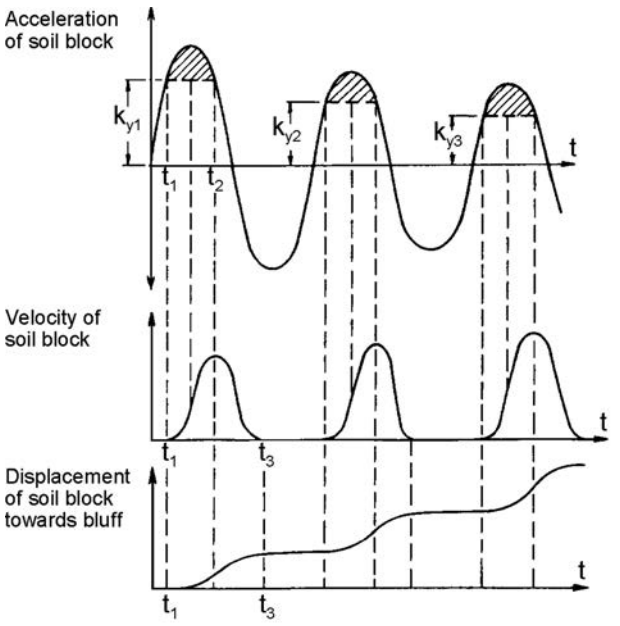

Figure 9.9 Integration of effective accelerations relating to time for determination of velocities and displacements.

state, so that the following question arises: what does $k'_s < 1$ indicate for the stability of a dam? Theoretically, it would mean instability of the dam; while practically, for a real assessment, it is necessary to know the values of the possible permanent deformations.

Newmark (1965) developed a simple method for evaluation of deformations, which would be a result of the cumulative earthquake period, when acceleration exceeds the critical one, above which the occurrence of permanent deformations may result. Newmark assumed that during an earthquake, displacements would be initiated along the slope of an embankment dam when inertial forces of the potential sliding mass would be sufficiently large to exceed the resistance of the material, while displacements would stop because of a reversed direction of inertial forces. Therefore, by determining the acceleration at which inertial forces become sufficiently large to cause commencement of displacement (Fig. 9.8), and integrating the effective acceleration of the sliding mass, which exceeds critical acceleration as a function of time (Fig. 9.9), it is possible to assess velocities and final displacements of the sliding mass (Fell et al., 1992; Seed, 1979).

The major deficiency of this method – as well as of all pseudo-static methods – is that it does not take into consideration the dependence of the behaviour of filling materials on the state of stresses, and that pore pressure, which can occur during cyclic loading, is neglected. Furthermore, the assumption of a stiff sliding wedge is too great a simplification for constructions exhibiting dynamic properties. That is why this method is applicable only for dams constructed in materials whose strength does not essentially decrease under cyclic loading. Those materials would be clay, dry sand, and some very well compacted incoherent materials.

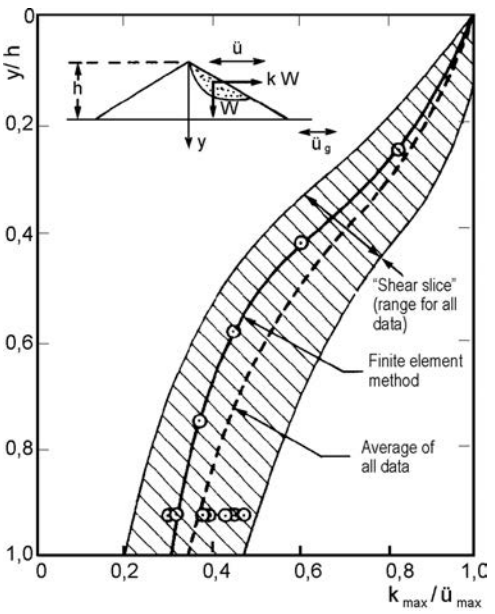

Figure 9.10 Variation of seismic coefficient k_{max} with depth of the base of the potential slide block.

Seed deems that for embankment dams, for which acceleration at the crest does not exceed 0.75 g, deformations calculated according to Newmark's method are usually small. Yet, this is valid only for dams that are not too high.

Through extensive investigations of the dynamic response of embankment dams, it has been concluded that effective peak acceleration of the potential sliding mass decreases with an increase of the depth of the surface of sliding in the embankment. In this way, the value of the effective peak acceleration k_{max} at different depths of the embankment, with sufficient accuracy, can be ascertained using the curves shown in Figure 9.10, given by Makdisi and Seed in 1978.[1]. Once these values have been determined, together with the value of acceleration caused by movement of the soil mass k_y, then by means of double integration, it is a relatively simple operation to determine displacements that will develop for a specific earthquake. Such analyses, for an earthquake of approximately 6.5 magnitude, have been performed by a number of authors, resulting in an extraordinarily accurate concensus results.

Newmark's method, in spite of all its deficiencies and limitations relating to the material on which it can be applied, represents a great step forward in the philosophy of assessing the behaviour of embankment dams during earthquakes. For specific materials and conditions, this method, which is based on an assessment of the value of displacements, represents quite an appropriate procedure.

[1]Later on in section 9.4.4, an explanation will be offered on how the acceleration in the body of an embankment dam can be most efficiently and accurately determined using pure response dynamic analysis by means of the Finite Element Method.

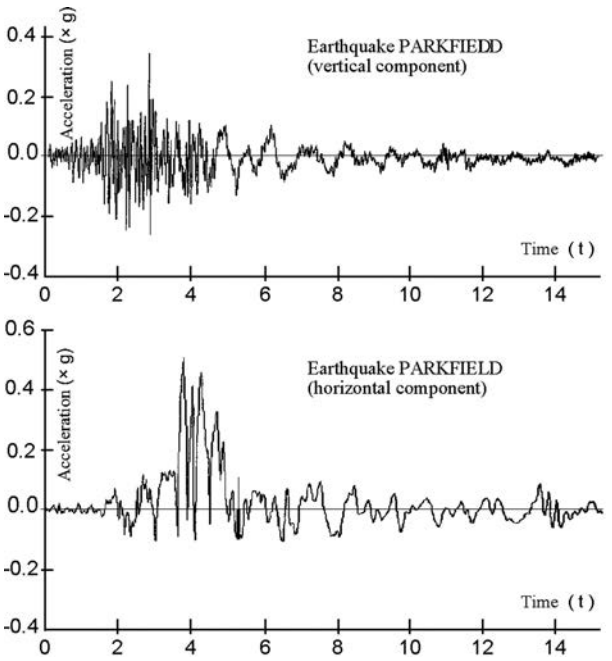

Figure 9.11 Accelerograms of the Parkfield earthquake, used in dynamic analysis for the Gradec dam.

By using the results of the pure dynamic analysis in a Finite Element Method static analysis, it is possible to determine the permanent displacements in a dam's body following an improved pseudo-static method. The author of this book, along with his co-operators, has applied this procedure in the static analysis[2] and in the dynamic analysis of the embankment parts of the Gradec dam (Tancev et al., 1991). With pure dynamic analysis using FEM, and application of the accelerogram of the Parkfield earthquake, adapted to the conditions of the Gradec dam site (Fig. 9.11), accelerations in the dam's body were determined.

The contour lines of accelerations caused by the horizontal component of an earthquake in the time instant $t = 3.8$ s, when acceleration has a maximum value, are presented in Figure 9.12. The figure indicates relative accelerations – in order to obtain absolute accelerations, it is necessary to add to them a ground acceleration of 0.53 g. These obtained absolute accelerations, reduced by the coefficient of damping 4, which is usual for embankment structures, are assigned in the centroids of the finite elements, changing the value along the height – from 0.25 g near the crest, to 0.05 near the ground. By applying a horizontal inertial force in the centroid of each element, directed toward the downward face, a pseudo-static nonlinear analysis has been carried out as a continuation of the incremental static analysis, performed in the case of a full reservoir.

[2]Also, see Chapter 8, where a cross-section of the dam is presented, along with discretisation with finite elements and other details.

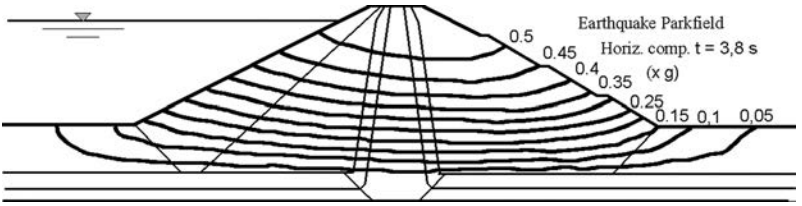

Figure 9.12 Contour lines of relative horizontal accelerations for the Gradec dam, obtained with FEM dynamic analysis.

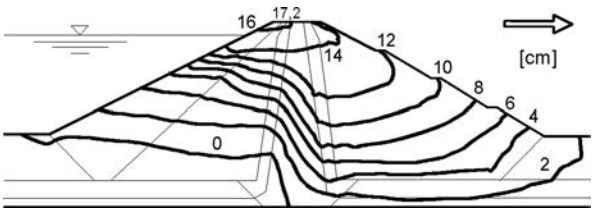

Figure 9.13 Contour lines of horizontal displacements for the Gradec dam, induced by the Parkfield earthquake.

Horizontal displacements in the main cross-section of the Gradec dam, obtained according to the analysis described above, are shown through the contour line in Figure 9.13. The distribution of displacements is quite logical in that, maximum displacement appears at the crest and its value of 17.2 cm coincides with the type and height of the dam (24 m from the ground, 39.5 m from the core foundation). The character of the earthquake, and selected peak acceleration of the base, which is in a logical correlation with other analysed dams throughout the world, also makes sense.

Figure 9.14 shows diagrams of the normal stresses (a) and (b), as well as of shear stresses (c), in the time instant with peak acceleration in the accelerogram of the Parkfield earthquake, obtained with pure FEM dynamic analysis of the Gradec dam. Here, tensile stresses appear; however, they last only for a moment, and then the picture abruptly changes. So, the obtained data can serve as a basis for an assessment of stability by means of methods against sliding of slopes and determination of permanent deformations.

Here, briefly, we shall also mention the *semi-empirical method*, as well as that of Makdisi and Seed, in which seismic effects are estimated through a correlation of the properties of the given dam in comparison with those for similar dams, where the response and permanent deformations have been previously monitored or established. This method suffers from similar deficiencies to those of the pseudo-static method, and can only be used to a limited extent for determination of a certain level of induced displacements from an earthquake (Makdisi & Seed, 1978, 1979).

9.4.3 Equivalent linear method

Realizing the deficiencies and limitations in the application of the pseudo-static method, as well as difficulties in determining the limit state at which there comes about

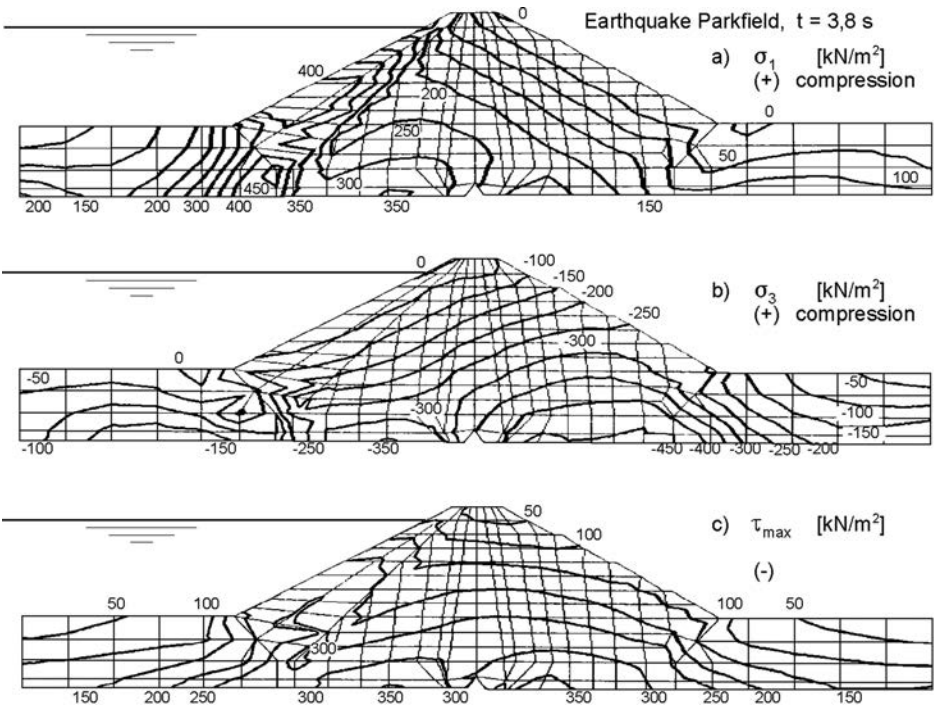

Figure 9.14 Diagrams obtained with pure dynamic analysis for the Gradec dam.

a separation of the earth block from the embankment in most of the saturated incoherent materials, Seed (1966) developed an alternative *equivalent linear method*. Later on, on several occasions, this method was improved by the author and his co-workers by introducing (in particular stages) calculations by means of the Finite Element Method, as well as by introducing results from updated methods for testing materials.

In this model, in order to determine the earthquake response, the dam construction is idealized as an equivalent elastic system. In the latest version of the method, the nonlinear effects of permanent deformation and induced pore pressure are calculated with further, separate analyses, by means of the Finite Element Method. The equivalent linear method has been widely used for seismic analysis of new or existing embankment dams. The basic idea of the method is to reach equivalent properties of the materials used in an elastic analysis, with the properties of the materials obtained from laboratory testing (Seed, 1979).

In the realization of this method, we usually introduce only the cyclic test for materials; consequently for that reason, as well as for others, a number of problems arise. Equivalent material stiffness is dependent on the history of deformations, so that an iterative procedure has to be carried out, resulting in the material stiffness obtaining more accurate data, calculated in the previous iteration cycle.

The results of the equivalent linear analysis do not yield direct data for nonlinear behaviour. These may be extracted by means of the magnitude of calculated equivalent

cyclic deformations, along with relevant results from investigations of those deformations. It is possible to obtain and introduce permanent values of induced pore pressure easily, while permanent deformations can be obtained only by means of some kind of integration technique which is based on permanent axial deformations, observed in cyclic triaxial tests – a method which is open to discussion and review.

The equivalent linear method gained great publicity owing to its efficient application in the analyses of sliding that took place in 1971 in the earthquake at the Lower and Upper San Fernando (California) dams. These hydraulic fill dams have a low relative density, at which liquefaction has taken place, which, in the analyses by this method after the failure, was clearly demonstrated. Yet, the examinations mentioned in the previous paragraph indicate difficulties in its execution and in the interpretation of its results.

9.4.4 Pure nonlinear response method

The *pure nonlinear method* is a powerful tool in the hands of contemporary structural hydraulic engineers of embankment dams. An analysis by this method requires that the material be represented by an elastic-plastic or other nonlinear model. Then, the equations of motion for undamped systems are solved in the time domain, with a full calculation of nonlinearity, along with advancement of the solution, as follows.

$$[M]\{\ddot{u}\} + [K]\{u\} = -\{m\}\ddot{y}(t) \tag{9.7}$$

in which $\{u\}$ and $\{\ddot{u}\}$ = the nodal point displacement and acceleration vectors, respectively; $[M]$ and $\{K\}$ = the mass and stiffness matrices; and $\ddot{y}(t)$ = the given input acceleration time history. Viscous damping is incorporated in the formulation of the complex shear modulus expression. The computer program solves equation (9.7) in the frequency domain.

The calculation of natural period is made with solution of the eigenvalue problem:

$$[K] = w^2\{M\} \tag{9.8}$$

in which $[K]$, $\{M\}$ and w represent stiffness matrix, mass vector, and natural circular frequency, respectively. The formulation of the stiffness matrix is based upon shear moduli which correspond to the average shear strain experienced during the duration of base motion.

This method is based on the possibility of nonlinear behaviour of different materials being mathematically modelled, depending on their deformations. The mathematical model is incorporated into the relevant program so that a joint analysis is carried out. In this way, with unique parameters the full equations of motion are solved, as well as time-dependent effective stresses, and the appearance of pore pressure, along with the permanent (plastic) history of deformation. If we assume that this model appropriately represents the behaviour of the materials and that the equations have been correctly solved, then the solution obtained by means of this method will give an accurate representation of the nonlinear response of an embankment dam. Also, a checkup of possible liquefaction can implicitly be inserted into the method.

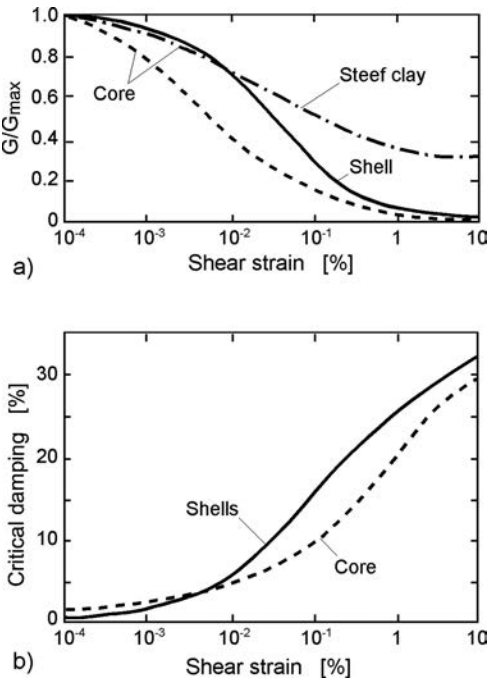

Figure 9.15 The moduli reduction (a) and dumping curves (b) for Oroville Dam soils (after Mejia et al., 1982).

One of the early applications of this method at an important dam, using the numerical finite element method, was that on the earth-rock Oroville dam[3] (Vrymoed, 1981). In that analysis the shear moduli values for the core material were determined by the use of the undrained strength, while the shear modulus for the shell material, which has a predominant influence in the response analyses, was computed by the following relationship:

$$G_{\max} = K_{2\max} 1000 \sqrt{\sigma'_{\mathrm{m}}} \tag{9.9}$$

where $G_{\max}$ = the shear modulus, in pounds per square foot, at small shear strains (10^{-4}%); $K_{2\max}$ = the shear modulus parameter at small shear strains (10^{-4}%); and σ'_{m} = the mean effective confining pressure, in pounds per square foot, computed using the results from the static FEM analysis.

In view of the available data reported in the literature, a $K_{2\max}$ value of 205 was adopted as a reasonable one for the Oroville dam shell material. A procedure, using adjusted soil properties, has been applied to take into account the three-dimensional response of an earth-rock dam using two-dimensional finite element techniques. Dynamic characteristics observed during seismic activity which occurred in 1975

[3]See also Chapter 8, section 8.3.5, and Chapter 11, section 11.3.

within close proximity to the dam were also employed in the constructed dynamic FEM model of Oroville dam. Based on the good agreement between the observed and computed motions produced by two seismic events the author concluded that the model was appropriate. One year later a truly three-dimensional dynamic analysis of Oroville Dam was presented (Mejia et al., 1982). Shear moduli for the shell materials were computed again from equation (9.9). The moduli reduction and dumping curves used for both the core and the shell materials are shown in Figure 9.15. The authors concluded that a $K_{2\max}$ value of 170 is representative of the *in situ* dynamic characteristics of the Oroville gravels and cobbles. They received a reasonable agreement between these values and laboratory-measured values on scaled samples, as well as between the computed and the recorded response of the dam.

Joint analyses with a pure nonlinear response method are carried out with the application of the numerical Finite Element Method. Bearing in mind the fact that the degree of saturation and the kind of draining of filling materials have an important role in relating to the stress-deformation state, those phenomena, also including modelling of partially saturated earth materials (Dungar, 1988a; Lewis & Schrefler, 1998), must be included in the analyses in an appropriate way. For filling materials it is said that they are either drained or undrained, depending on the time necessary to arrive at the time span of the applied load. The core of an earth–rock dam has low permeability and it may take several years before pore pressure reaches equilibrium state, if it does at all. Coarser grade earth can reach equilibrium within several months, while crushed stone can require only a fraction of a minute. Under earthquake conditions, the quoted classification must be revised since in such a case the load-action time is of the order of seconds. That is why, the upstream shell in earth–rock dams and rockfill dams with a diaphragm often falls in the category *saturated* and *undrained*.

To illustrate the capacity of the pure nonlinear response method, the procedure concerning the analysis of the 200 m high earth–rock Conwap dam (Philippines), and a small part of the results, will be presented. An analysis of this dam was carried out by using the *EFESYS* computer program (Dungar, 1988a), which allows zones of different materials to have different conditions of draining for given loading cases. In other words, draining conditions can be varied from one case to another case of loading. For example, the clay core in the stage of static analysis may be treated as undrained in a simulation of dam construction performed in layers. Therefore, drained conditions would be taken as the established stationary seepage flow, by assuming pore pressure as seepage pressure, while seepage forces would be added to the forces due to weight, in order to define total loading of the construction.

During the stage of seismic loading, the seepage pressure at stationary flow is taken as an *initial pressure*. On the basis of the undrained behaviour of the material, one may then calculate changes in pore pressure caused by dynamic loading. The basic constitutive model for the behaviour of materials is the elastic–plastic one, but only as an additional possibility. It is possible to take into consideration the effect due to nonlinear elasticity of the materials. Also, it is possible in the analysis, to treat materials as partially saturated with water.

Analyses were performed according to the plain strain procedure of the Finite Element Method. The dam's section was discretised with 200 eight-nodal elements by encompassing the body of the dam, which lies on sound rock, as well as on the fluid from the upstream face (Fig. 9.16). The author of the model developed an efficient

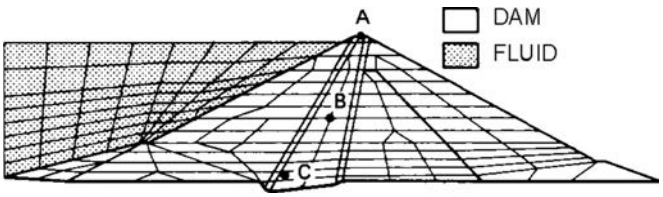

Figure 9.16 Discretisation of the cross-section for the Conwap earth–rock dam.

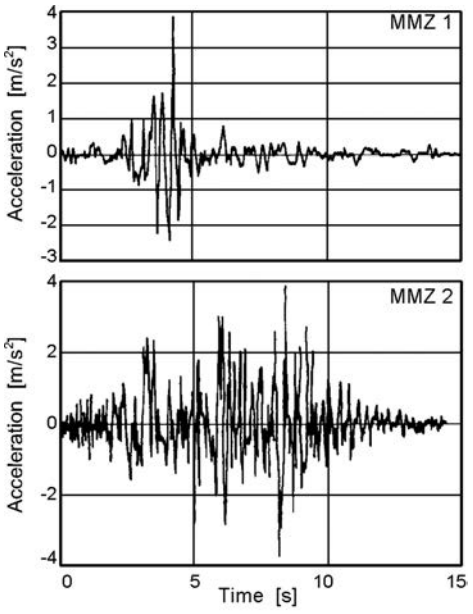

Figure 9.17 Accelerograms for maximum credible earthquake, used for the Conwap dam.

method of connecting the fluid with the structure, wherein the domain of the fluid is considered as non-compressible (Dungar, 1988a). A maximum credible earthquake (MCE) is assumed, with a peak acceleration of 3.9 m/s^2, which corresponds to an earthquake of magnitude 7 according to the Richter scale, at a distance of 50–150 km from the dam.

Two records have been selected for examination – MCE1 and MCE2 (Fig. 9.17) where the horizontal components of acceleration are shown. The first record is dated 1966, with a magnitude of 6.5 and a peak acceleration of 3.6 m/s^2, while the second one, dated February, 1971 (the San Fernando earthquake), presents a magnitude of 6.6 and maximum acceleration of 12.5 m/s^2. The records have been converted using a new scale, so that maximum acceleration is 3.9 m/s^2. As can be seen from the records, MCE1 contains only a few pulsations that bounce away, while MCE2 contains a number of larger pulsations, which last for a longer period of time.

The history of emerged deformations in the course of time is illustrated in Figure 9.18 for points *A* and *B* (Fig. 9.16). Presented are appropriate horizontal displacements for the two earthquakes in the initial 20 seconds of the response time of the dam. The horizontal displacements (positive ones are towards the downstream face) are mainly affected by the quasi-resonance of the horizontal mode of vibrations, along with the nonlinear effect, both of which are mainly directed towards the upstream face.

The vertical displacements (negative ones mean settlement) show a strong tendency to nonlinear directed settlement, with a weak effect of quasi-resonance of the vertical mode of vibration. The excitation of vertical vibration with an applied horizontal earthquake is due to the plastic behaviour of the materials in the dam's body, wherein the response in the vertical direction joins the horizontal motion through the nonlinear model of the materials. At the same time, the diagrams in Figure 9.18 graphically indicate that, even at equal peak acceleration, two different earthquakes can cause a significant difference in their permanent displacements. Namely, a permanent crest settlement of 55 cm is obtained due to the earthquake MCE1, whereas a settlement of 135 cm is due to MCE2. This illustrates the known fact that peak acceleration may not be the only criterion in selecting the design earthquake.

The history of horizontal normal, vertical normal, and shear stresses, in relation to time, is indicated for point *C* (Fig. 9.16), and in diagrams in Figure 9.19 for the two earthquakes. The same figure also shows a diagram of variations in pore pressure, occurrence of increased pore pressure, and its dissipation in the course of the earthquake.

Figure 9.20 presents the contour lines of total vertical displacements caused by all influences, taken in the analysis: the self-weight in simulating the construction in layers, filling the impounding reservoir, and establishing a stationary seepage flow, as well as the influence of MCE2, graphically presented in Figure 9.21. These results facilitate clear comprehension of the dam's behaviour under static and dynamic conditions. They also help in constructing the section (for instance, determination of the freeboard of the dam's crest, etc.).

This program also enables pursuance of the dam's stability under dynamic excitation. In the case of the Conwap dam, a coefficient of safety 1 against the occurrence of uncontrolled plastic displacements was obtained, i.e. in situations critical for stability, the displacements have been within acceptable limits for conditions of MCE.

Other known models for dynamic analysis of embankment dams have also been developed throughout the world. Many of them have been adjusted according to the needs for assessing the dynamic stability of tailing dams, which characteristic is susceptibility to liquefaction (Jeyapalan et al., 1983a, 1983b; Seid-Karbasi & Byrne, 2004).

The *GEFDYN* program is also well known, and is largely used in the USA, France, and in other countries. It has also been used in analyzing the well-known El Infiernillo dam (Mexico). The static analysis of this dam with the same model has been dealt with in Chapter 8, while the dam's cross-section is shown and described in Chapter 11. The dam, since its completion in 1964, has experienced several earthquakes, of which the most severe one was in 1979. In addition to the already presented main capabilities of the models for nonlinear pure response dynamic analysis, this model also enables a simulation of post-earthquake consolidation of pore pressure in the zones of coherent material (ICOLD, 1994d). As it has been seen from the chapter on static analysis of

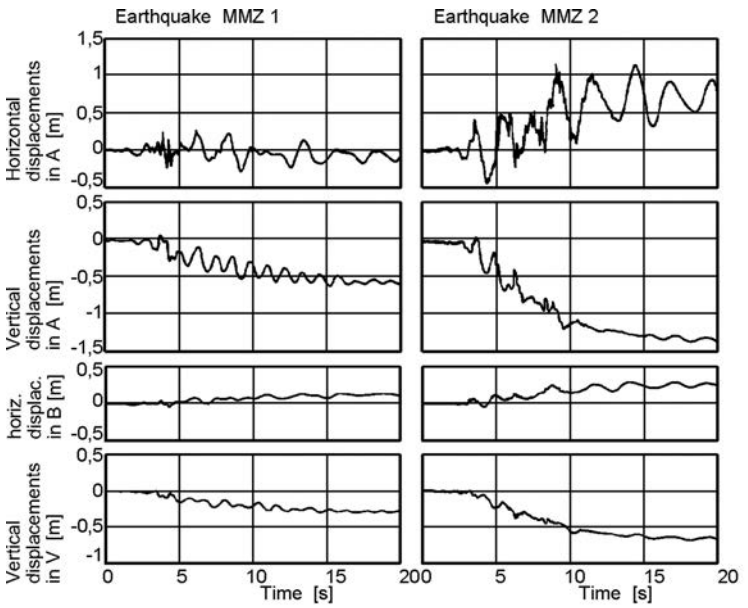

Figure 9.18 History of displacements at points A and B of the two earthquakes.

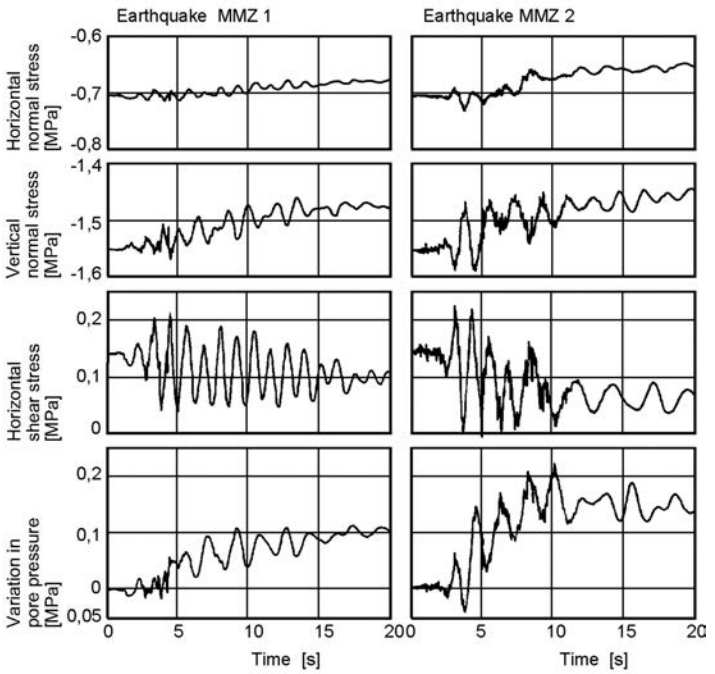

Figure 9.19 History of stresses and pore pressure at point C.

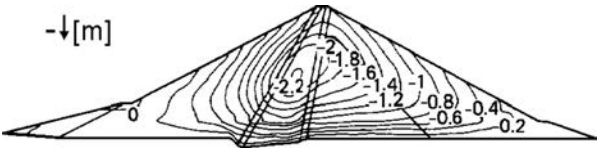

Figure 9.20 Contour lines of vertical displacements for the Conwap dam.

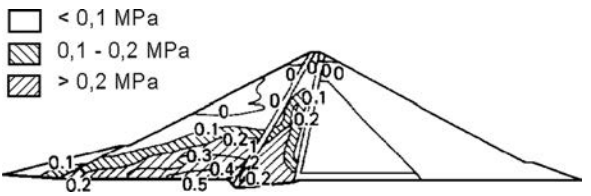

Figure 9.21 Pore pressure caused by MCE2, for the Conwap dam.

embankment dams, the results obtained with this and some other models, by means of which the El Infiernillo dam has been analyzed do not agree with *in situ* measurements and because of that it follows that much further work in the development of such models, needs to be done.

Also significant are dynamic analyses performed in the former USSR on the highest embankment dams in the world – Nurek and Rogun, in Tajikistan, seismically a very active area (Goljdin & Rasskazov, 1987; Ljather et al., 1984; Savinov, et al., 1986). The results and knowledge obtained from these analyses are very useful; however, no sufficient data for the technique of their modelling and execution were presented.

In addition to earth dams and earth–rock dams, lately published have been results from analyses of rockfill dams with water-impermeable elements made of artificial material – asphaltic core (Valstad et al., 1991; Akhtarpour & Khodai, 2009; Feizi-Khankandi et al., 2008, 2009; Nejad et al., 2010; Akhtarpour et al., 2011) and reinforced concrete facing (Uddin & Gazetas, 1995; Matsumoto et al., 2000). The Finite Element Method was also established in this field, making it possible to obtain a clear impression of the behaviour of the thin impervious element under conditions of complex loading with earthquakes. Different questions regarding seismic stability of asphaltic concrete core dams are discussed in Chapter 14, section 14.3.

Along with the development of numerical methods and computer technology, conditions have been created for the development and application of three-dimensional methods for dynamic analysis of embankment dams. The model applied at Oroville Dam was already mentioned (Mejia et al., 1982), other were developed later on (Meijia & Seed, 1983; Dakoulas & Gazetas, 1987; Abdel-Ghaffar & Elgamal, 1987; Elgamal & Abdel-Ghaffar, 1987; Griffiths & Prevost, 1988; Boulanger et al., 1995). Similarly to the case of static analysis, dynamic three-dimensional analysis is also particularly useful and needed if it is a case of a dam in a narrow dam site, in which there is a significant influence of valley sides, i.e. dam abutments, on the stability of the dam. Here, in addition, the question of the interaction of the steep dam abutments,

i.e. valley sides, with the dam's base is also interesting, for the simulation of which it is necessary to introduce special spatial joint elements. When taking the third dimension into consideration, the problem of dynamic analysis of embankment dams becomes extremely clumsy and complex, especially for performing a nonlinear analysis. Yet, similar to the case of static analysis, it is certain that sooner or later three-dimensional analysis will be introduced into everyday practice.

9.5 CASE STUDIES OF RECENT ACTUAL EVENTS

Over the past years several dams have been strongly shaken by earthquakes with an epicentre relatively close to the dam site. All these dams have been well instrumented and the gained results of the dams' response to the shakes are of great importance for the evaluation of the dam behaviour under such exceptional loading. Two case studies of dams affected by the Iwate-Miyagi earthquake (M = 6.9 on the Richter scale)[4] occurred on 14 June 2008 in Japan, and the Sechuan earthquake (M = 7.2) which occurred on 14 June 2008 in China, are presented in following sections.

9.5.1 Case study of Aratozawa dam (Japan, 2008)

The Iwate-Miyagi Nairiku earthquake (M = 7.2) occurred at 08h 43' on 14 June 2008 in Iwate Prefecture (Japan), with a focal depth of 8 km. Several dams in the vicinity of the earthquake were strongly shaken by the main shock, as well as by many aftershocks. Among them was the Aratozawa dam, a 74.4 m-high earth-rock structure, located only 15 km from the epicentre of the main shock. At the time of the main shock, the reservoir water level was at elevation 268.48 m, the high water level being at el. 274.4. During the earthquake extensive landslides occurred upstream of the dam, and a substantial volume of soil collapsed into the reservoir, resulting in a sudden 2.4 m rise of the reservoir water level, equivalent to an increase in water volume of 1.5×10^6 m^3.

During the main shock, strong motion accelerometers installed at the Aratozawa dam registered a peak acceleration of 10.24 m/s^2 at the bottom gallery. Despite such a high acceleration, the dam remained in a safe and stable condition, with little impact on the reservoir functions. At the dam, the earthquake motion acceleration was recorded not only during the main shock, but also during weaker earthquakes before and after the main event. Ohmachi (2011) has analyzed the earthquake response characteristics of the dam during the main shock, especially from the point of view of strain-dependent nonlinearity. The records from three earthquake events in 1996 are used to estimate linear and initial characteristics at low strain before the main shock, and the records from 185 events after the main shock have been used to evaluate the long-term decay process of the nonlinearity produced by the main shock.

Figure 9.22 shows the cross-section and the longitudinal section of the Aratozawa dam. The earth-rock dam consists of core, filters, transitions, inner rockfill, and outer

[4]Or 7.2, using the Japanese Meteorological Agency scale (JMA). Since the 1970s the USA and other countries have used the so-called Moment magnitude scale, which has similar values as the Richter scale.

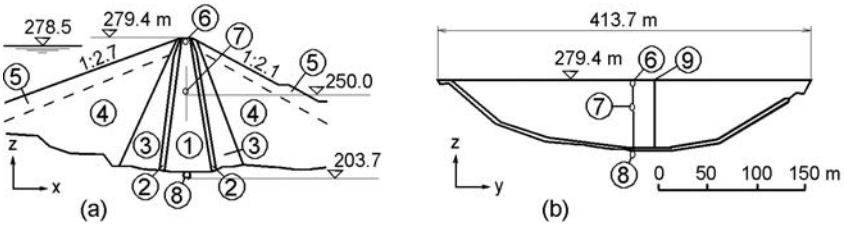

Figure 9.22 Cross-section (a) and longitudinal section (b) of the Aratozawa dam; the vibration components in the stream, dam-axis and vertical directions are referred to as *x*-, *y*- and *z*-components, respectively; the positive directions of those components are also indicated with arrows (after Ohmachi, 2011). (1) Earth core; (2) filters; (3) transitions; (4) inner rockfill; (5) outer rockfill; (6, 7, 8) strong motion accelerometers on dam crest, in the mid-dam and in the gallery, respectively; (9) settlement gauge.

rockfill. The dam has a crest length of 413.7 m, and a crest width of 10 m. The construction of the embankment dam body was finished in 1991, but the whole scheme was completed in 1998. As a result of the main shock of the 2008 earthquake, the dam underwent major permanent displacements. According to the measurements, the top settlement gauge (at el. 275 m), showed settlement of 37.9 cm as a result of the main shock. In addition, minor cracks in the asphalt pavement were observed at the right bank corner of the crest (Ohmachi, 2011).

Three-component strong motion accelerometers are installed in the dam body at three locations: on the dam crest, mid-core and in the bottom gallery (Fig. 9.22). The acceleration time histories in x (stream) direction of the main shock and the peak accelerations observed during the main shock of the 2008 event are shown in Figure 9.23. It can be seen that the peak acceleration at the bottom gallery was the largest (it was also the case in directions y and z). This seems unusual, because earthquake acceleration is usually highest at the dam crest, because of the amplification effects of the dam body. From the figure it can be concluded that the time history recorded at the gallery is full of short period components, mostly attenuated at the dam crest and mid-core. One or two large pulses of longer period have been recorded at the beginning of the strong earthquake motion in all the time histories. The acceleration time histories were sampled at 100 Hz with a frequency range of 0.1–30 Hz.

The seismic wave velocity between a pair of the accelerometers was estimated from the Fourier phase spectra of the acceleration time histories. When a seismic wave observed at seismometer A is propagated to seismometer B, the arrival time at seismometer B is delayed from that at seismometer A by $\Delta t = l/v$, where l is the distance between the two seismometers and v is the wave velocity. With Fourier phase θ_A at accelerometer A and θ_B at accelerometer B, the phase difference $\theta = \theta_B - \theta_A$ is expressed as $\theta = 2\pi l/\lambda$, where λ is the wave length expressed as $\lambda = vT$ with period T. Accordingly, with frequency $f = 1/T$, it is obtained $\theta = 2\pi lf/v$. Hence, when the phase difference θ is plotted against the frequency f, the velocity v can be estimated from the slope of the plots. Thus, the seismic wave velocity during the main shock was estimated from Fourier phases of the acceleration time histories. The obtained

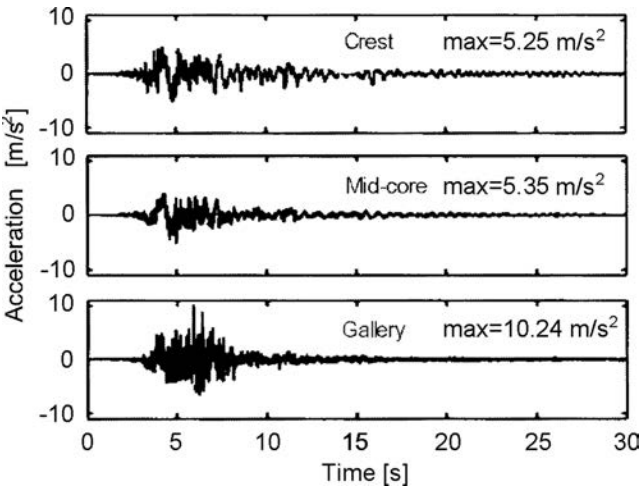

Figure 9.23 Accelerations time histories of the main shock in *x* (stream) direction (after Ohmachi, 2011).

velocities for the three measuring points in the dam axis were in the range of 130 to 550 m/s in *x*-direction, and in the range of 200 to 550 m/s in *y*-direction.

The acceleration time histories of the transverse (*x*) direction (Fig. 9.23) and in longitudinal (*y*) direction were integrated twice to obtain displacement histories. All the trajectories of horizontal displacements were almost identical during the first 4 seconds, but during the following 2 seconds the horizontal displacement of the dam body was amplified at the dam crest in both *x* and *y* directions, and had an elliptical trajectory. From the displacement time histories, relative displacements between the two ends of each section were obtained and divided by the distance between a pair of installations, so that the mean shear strain of each was calculated. The time history of the mean shear strain of the *x*-component of section *gallery-dam crest* during the main shock is shown in Figure 9.24, where the thick line is an envelope of the mean shear strain at any given time. The maximum absolute shear strain is 1.5×10^{-3}.

From the obtained results the shear modulus ratio G/G_0 for both horizontal components at the three measuring sections were estimated and summarized with six thin lines (Fig. 9.25). It can be noted that with the increase in the shear strain to more than 10^{-4}, the shear modulus ratio G/G_0 shows a sudden decrease, which is consistent with previously published studies. Regardless of the depth of the section and horizontal direction, the sudden decrease takes place in a similar manner until the ratio G/G_0 reaches its minimum value.

Regarding the minimum values of the ratio G/G_0, the higher the section is, the smaller the minimum value becomes. At the end of intense ground motion input at the gallery, the shear modulus ratio G/G_0 began to increase gradually with the decrease in the shear strain towards the end of the main shock. In Figure 9.25, the six thin lines associated with the gradual increase of the three sections and two components are almost parallel to each other. As a result of the parallel increase in the ratio G/G_0,

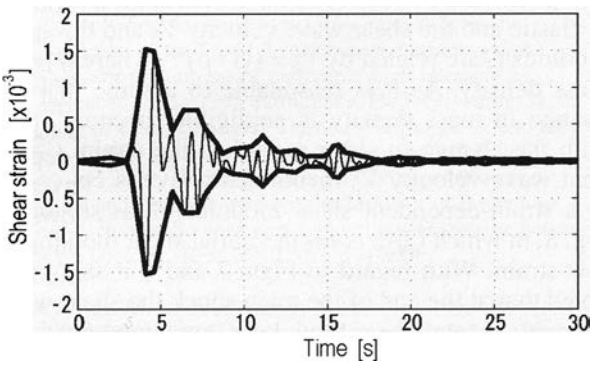

Figure 9.24 The time history of the mean shear strain of the *x*-component of section *gallery-dam crest* during the main shock (after Ohmachi, 2011).

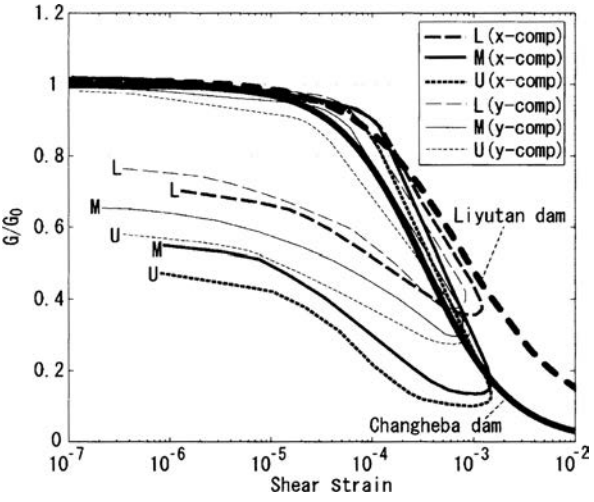

Figure 9.25 Strain-dependent shear modulus of the Aratazawa dam, the Changheba dam and the Liyutan dam (Ohmachi, 2011).

the modulus *G* in the core became anisotropic during the increasing process, including the final state. It is preferable that the strain-dependent shear modulus during the main shock is compared with data from laboratory tests using the same soil. However, since such data were not available for the Aratozawa dam, it has been compared with core material shear moduli of the Changheba dam (240 m-high rockfill dam), and the Liyutan dam (96 m-high earthfill dam). The six thin lines associated with the shear modulus evaluated for the Aratozawa dam lie between the two broad lines associated with the shear moduli of the other two dams, and seem compatible with each other at least within the strain range observed during the main shock.

From the presented case study the following main conclusions have been drawn (Ohmachi, 2011):

- During the main shock of the 2008 earthquake, the acceleration of the transverse component (in x-direction) exceeded 10 m/s^2 at the gallery, which is almost twice the maximum value reached at the dam crest (5.3 m/s^2). Similar kind of attenuation in the acceleration response was observed in all three components (in x-, y-, and z-direction), which is rather unusual.
- The intense shaking of the main shock induced large shear strains (higher than 10^{-3}) in the transverse direction, and a little less than 10^{-3} in the longitudinal (y) direction.
- Due to the large strains in the horizontal directions, the shear modulus G exhibited a remarkable decrease comparing to the initial shear modulus G_0: by 90% in the upper part and 60% in the lower part of the core, respectively.
- As a result of the decrease in G, the shear wave velocity V in the dam core was significantly reduced, which led to the attenuation of the earthquake response of the dam.
- Towards the end of the main shock, the modulus G in the dam core showed a gradual increase, but remained below G_0 and was anisotropic.
- The decreased shear wave velocity continued to recover and the anisotropy decreased with the passage of time after the main shock, and the full recovery of the wave velocity to the initial one of isotropy was found to take almost one year.

The data obtained by the measurements at Aratozawa Dam during the 2008 earthquake, as well as the results and conclusions of the cited case-study would be very useful for the design and analysis of other earth-rock dams.

9.5.2 Case study of Zipingpu dam (China, 2008)

The Sichuan province, located in the southwestern part of China, is an area rich in water resources and in particular hydropower resources. Actually, it is the most important hydropower energy base in China. Many dams and hydropower projects have been constructed or are currently under construction in this area. On 12 May 2008, at 14:28 hrs, Wenchuan County in Sichuan province was hit by a very strong earthquake of magnitude 8.0 (Richter scale). More than 60,000 people were killed, and enormous damage was inflicted.

There are four major dams, higher than 100 m, near the epicentre of the Wenchuan earthquake: the Zipingpu concrete faced rockfill dam ($H = 156$ m); the Shapai roller-compacted concrete dam ($H = 132$ m), the Bikou central core earth-rock dam ($H = 102$ m); and the Baozhushi concrete gravity dam ($H = 132$ m). The highest is the Zipingpu dam, located 17 km from the earthquake epicentre.

The Zipingpu CFRD is located some 60 km northwest of Chengdu, the capital of Sichuan province. The main purposes of the project are water supply and electricity power generation. The total storage capacity of the reservoir is 1.1×10^9 m^3 and the installed capacity of the hydro power plant is 760 MW. The Zipingpu dam was completed in 2006 and represented the latest CFRD technology applied in China. As has

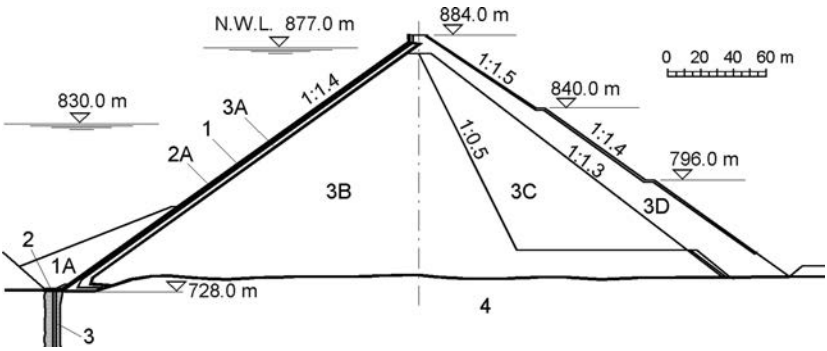

Figure 9.26 Typical cross-section of Zipingpu dam (after Zeping, 2009). (1) Concrete slab; (2) plinth; (3) grout curtain; (4) rock foundation; (1A, 2A, 3A, 3B, 3C, 3D) different zones of the rockfill dam (for details of the different zones of the concrete faced rockfill dams see Chapter 12).

already been mentioned, the dam is 156 high, with inclination of the upstream slope of 1:1.4. The downstream slope is designed with two different inclinations to ensure the stability of the dam crest during the earthquake: the upper part of the slope is 1:1.5 and the lower part is 1:1.4. A typical dam section is shown in Figure 9.26.

According to the original earthquake intensity map, the basic earthquake intensity of the dam site area is VII. The designed earthquake intensity was VIII (Chinese scale), with a peak ground acceleration of 0.26 g. Figure 9.27 shows the accelerogram recorded at the centre of dam crest during the earthquake. It can be seen that acceleration at the crest reached 2 g. Considering the normal amplification factor, the ground acceleration should be larger than 0.5 g, which is far beyond the peak ground acceleration value adopted for the design.

A careful inspection of the dam immediately after the earthquake found that Zipingpu dam was structurally stable and safe. However, the dam did sustain various forms of damage during the quake, including rupture of the face slab and concrete spalling of the parapet wall. The dam was well instrumented for monitoring purposes, and although some instruments were damaged by the earthquake, most of the instruments remained in good operational condition, and they have provided valuable information concerning the performance of the dam during and after the earthquake.

Significant deformations caused by the earthquake occurred on the dam. Immediately after the main quake, settlement of the dam crest in the riverbed section was identified, even by eye. The maximum measured settlement was located in the central cross-section with a value of 68.4 cm. After the main shock, numerous aftershocks occurred, and the dam body continued to settle, but the rate of settlement decreased rapidly. Five days after the main shock the maximum settlement of the dam crest reached 74.4 cm. On the tenth day after the main shock the crest settlement had basically stabilized. The maximum displacement of the crest in the downstream direction was 20 cm. In the direction of the dam crest axis (longitudinal direction), the rockfill in the abutment areas tended to move towards the centre of the river, reaching the value of 22.6 cm (in the left abutment).

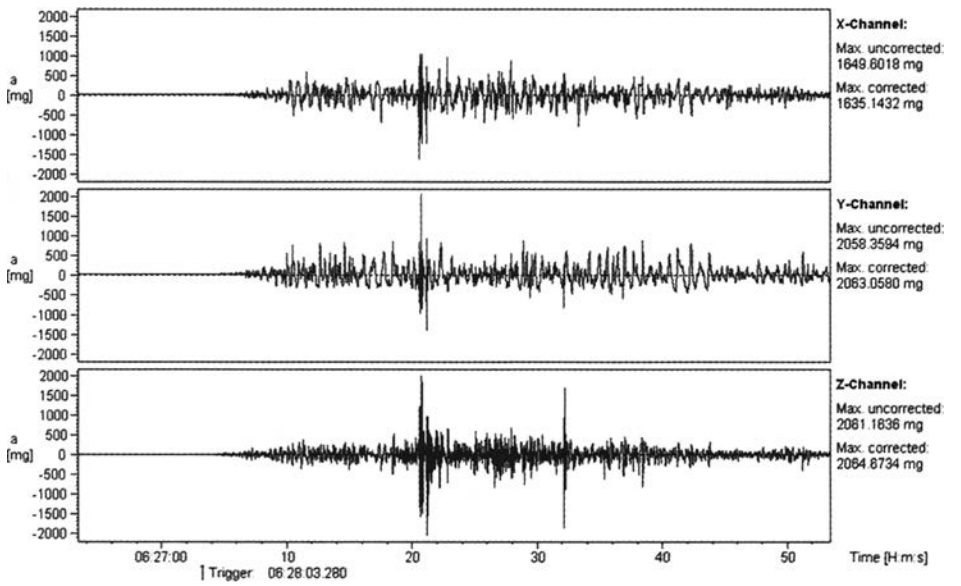

Figure 9.27 Accelerogram recorded at the centre of the dam crest (after Zeping, 2009).

Settlement caused by the earthquake was also registered within the dam body. It was higher at higher elevations, with values of: 10.6 cm, 32.2 cm and 81 cm at elevations of 760 m, 820 m, and 850 m, respectively (measurements were taken in the axis of the central dam cross-section).

The downstream part of the dam body experienced relatively larger horizontal displacement compared with the central part. At elevations of 766 m, 795 m, 824 m and 854 m, the observed horizontal displacement towards the downstream direction was 7 cm, 16.7 cm, 26 cm and 27.4 cm, respectively.

The most sensitive element of CFRDs – the waterproof reinforced concrete facing slab–experienced some damage during the earthquake, including cracks and ruptures of the slab (Fig. 9.28). The main damages were:

- At el. 845 m, where the construction joint of the second and third stage face slab is located, the slabs were overlapped. The height of the overlap was 15–17 cm and the reinforcement across the joint has become bent into a "Z" shape.
- Along the vertical joint of the face slab 5 and 6 (at the left abutment) and face slab 23 and 24 (in the riverbed), the slabs were ruptured by the action of large compressive stress along the dam axis.
- Large areas of the upper part of the slab were separated from the rockfill. The maximum value of the gap between the face slab and rockfill at the top of the third stage face slab at the left abutment was 23 cm. The corresponding value of the gap at the top of the second stage face slab at the right abutment was 7 cm. This conclusion is based on investigation works involving drilling.

Figure 9.28 An illustration of the damage to a reinforced concrete slab of the Zipingpu dam in horizontal direction.

- Many cracks and ruptures appeared on the parapet wall. Near the abutment, the originally closed joints were opened. In riverbed section, the parapet wall was ruptured by major compressive stress.

As a result of the earthquake relatively large displacements appeared in the perimeter joints. A part of the installed instruments were damaged. At some points, the displacements exceeded the measuring range of the instruments. The measured displacements of the perimeter joint at the left abutment (elevation 833 m) were: 9.3 cm of settlement, 5.8 cm of joint opening displacement and 1.3 cm of shear displacement. As a comparison, the displacements at the same position, measured before the earthquake, were: 1.6 cm (settlement), 1.2 cm (opening) and 0.5 cm (shear).

During the earthquake the reservoir level was low (elevation 830 m, see Fig. 9.26) and its volume was 0.3×10^9 m^3, while under normal operation conditions the reservoir volume is 1.1×10^9 m^3. The leakage observation of the dam is shown in Figure 9.29. It can be seen that the leakage has been closely related to the reservoir level. Before the earthquake, the leakage measured at the dam was 10.38 *l*/s (10 May). Since the earthquake, the leakage has increased to 19 *l*/s. During the first two days following the earthquake, the seepage water was turbid, but subsequently it became clear.

Zipingpu dam was successfully repaired and six months after the earthquake it was once again in operational condition.

As a rule, the CFRDs have been considered inherently resistant to seismic loading, mainly due to following reasons: (a) the rockfill is dry; therefore earthquake shaking cannot generate excess pore water pressures and shear strength degradation, and (b) the reservoir water pressure acts externally on the upstream waterproof face and hence the entire rockfill mass acts to provide stability.

The presented case study of the behaviour of a high CFRD subjected to very strong earthquakes have confirmed the stability of this type of dam under such extreme

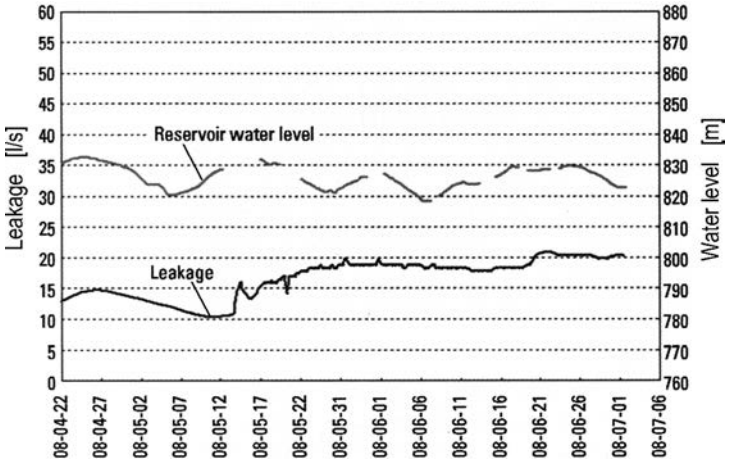

Figure 9.29 Leakage measured in a certain period before and after the earthquake on 12 May 2008 (after Zeping, 2009).

loading. However, there are certain features with these dams, which should not be overlooked, like: crack development in the concrete face slab, vulnerability of perimeter joint and possible large settlement in the rockfill.

To improve the performance and the seismic safety of the CFRDs, Wieland (2010) has recommended the following design measures: flatter slopes (to reduce seismic deformations); generous freeboard (accounts for seismic deformations and impulse waves in the reservoir); wider crest (improves safety of crest region of dam and increases resistance against overtopping from impulse waves); proper material selection in dam body with proper zoning (rockfill shall allow free draining of water leaking through the concrete face); provision of geogrid and other techniques for strengthening the upper part of the downstream slope; provision of a bottom outlet (to lower the reservoir if the concrete face or waterproofing system is damaged); concrete slab panel with smaller width to account for non-uniform deformations of the concrete face; arrangement of reinforcement of the face slab to improve its load bearing behaviour in-plane and out-of-plane and to improve its ductility; arrangement of proper joint system including horizontal joints and selection of the joint width to account for the reversible nature of the seismic response; water-proofing system of face slab and the plinth joint to account for static and seismic joint movements, and well compacted rockfill.

Chapter 10

Earthfill dams

10.1 CLASSIFICATION AND CONSTRUCTION OF EARTHFILL DAMS

Earthfill dams are a form of embankment dam of which more than half the cross-sections are constructed of earth material. According to their structure, earthfill dams are divided into the following basic categories:

Homogeneous dams, which are constructed of one kind of low-permeable earth material (Fig. 10.1a);
Zoned earthfill dams, a cross-section of which is filled with different materials which are arranged in such manner so that water-permeability increases towards the downstream face (Fig. 10.1b), or the most impermeable material is placed in the central part (Fig. 10.1c).
Dams with an upstream facing of low-permeability earth material, with or without a horizontal blanket (Fig. 10.1d, e);
Dams with a core of low-permeability earth material, usually positioned centrally, with or without a horizontal blanket (Fig. 10.1f, g); and
Earthfill dams with a water-impermeable element of artificial material (concrete, reinforced concrete, asphalt, steel, geosynthetics, etc.), carried out as an upstream facing (Fig. 10.1h), or an internal diaphragm wall (Fig. 10.1i).

In addition to the elements quoted in the schematic presentation, earth dams also contain other structural members that contribute to their regular and safe operation. Thus, in the body of homogeneous dams it is compulsory to arrange drainage in order to decline the seepage line and to capture seepage water (3 in Fig. 10.2).

Protective construction is carried out to secure the local strength of the earth material of slopes. The upstream slope is protected against mechanical action of waves and ice, while the downstream slope is protected against atmospheric rainfall and snowfall, as well as against tailwater, if any. In the dam foundation a *cutoff trench* (4) is frequently constructed, which cuts the soil foundation to a certain depth in order to reduce water-permeability and to achieve a better joint between dam and foundation. Sometimes, berms are constructed, a practice which was elaborated on in the clause on elements of embankment dams (Chapter 6).

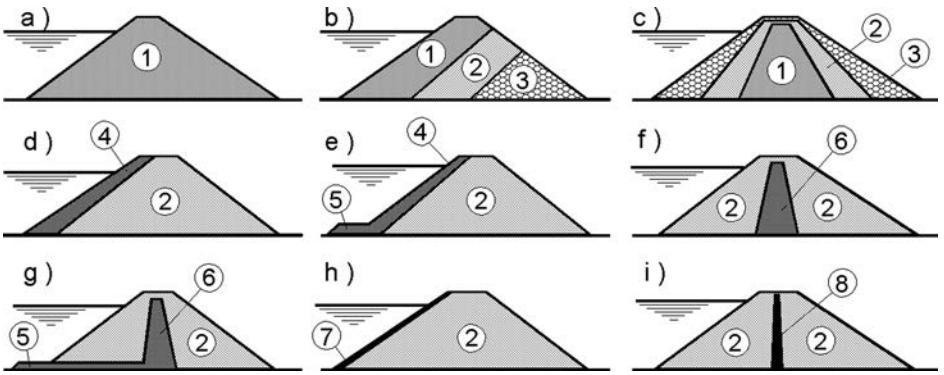

Figure 10.1 Schematic presentation of the basic types of earthfill dam. (1) Loam; (2) sand; (3) gravel; (4) earth facing; (5) blanket; (6) earth core; (7) facing of artificial material; (8) diaphragm wall of artificial material.

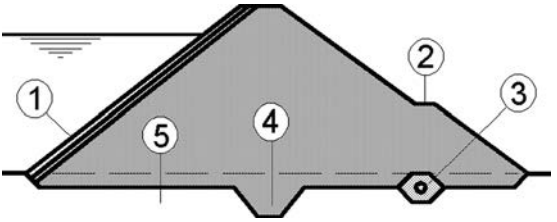

Figure 10.2 Cross-section of an earthfill dam. (1) Slope protection; (2) berm; (3) drainage; (4) cutoff trench; (5) non-rock foundation.

In most types of earthfill dams, a considerable part of the dam's body is subjected to the permanent influence of seepage flow, which imposes the need for careful construction and compaction in order to avoid the danger of creating concentrated seepage paths. Owing to the presence of water, overall conditions for static performance of an earthfill dam are aggravated, so that they are built, mainly, of small to medium height. Earthfill dams are more rarely constructed on a rock foundation, as compared to the other two types of embankment dams. For some time now, a number of small dams and impounding reservoirs have been constructed on a non-rock foundation; thus, rapidly increasing the representation of small dams.

10.2 STRUCTURAL DETAILS FOR EARTHFILL DAMS

Crest structure. The dam crest is structurally formed depending on the kind and category of the roadway passing over it. Footways are usually constructed at either end, separated from the crest edges by means of a guardrail, which is mounted on posts (Fig. 10.3). In the case of impassable dams, it is sufficient to protect the crest through the planting of grass.

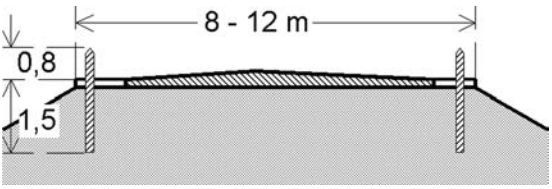

Figure 10.3 Detail of a dam's crest.

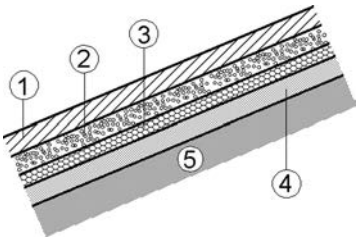

Figure 10.4 Scheme for protective lining. (1) Lining layer; (2) drainage layer; (3) filter layer; (4) protective layer; (5) the dam's body.

10.2.1 Slope protection

Dam slopes are protected with linings which have to be resistant to wave effects and the washout owing to the external water (Tørum, 1994), seepage flow running out of the dam, mechanical effects due to ice, rainfall waters, the effect of wind, fissuration of the clay materials during the winter period or in summer, when the part of the dam which is over the water, because of drying up, can fissurate, etc.

In general, the protective lining consists of the following elements (Fig. 10.4):

1. *Lining layer,* which protects the slope against external mechanical effects;
2. *Drainage layer;*
3. *Filter layer,* which is constructed of material that is finer than that of the drainage;
4. *Protective layer,* which is located between the embankment's clay material and the filtering layer and is constructed of sand or coarser earth material with strength characteristics at least equal to the material in the dam's body of which the slope has been formed. It is customary for the drainage, filter, and protective layers to share a common name – *a base*. Depending on specific conditions, individual base layers may be eliminated.

The following kinds of protective linings are constructed for the upstream slope:

(1) *Rockfill.* Protection with rockfill is simple and, at the same time, very effective and safe because it cannot be damaged during deformation of the dam's body. This type of lining consists of a layer of rockfill placed over one or more filter layers. Thickness of the filter layers should not be less than 15 cm. Rockfill linings are used for a height of waves up to 2.5 m. Rock for this purpose should have a compressive strength of 50 MPa, be resistant to ice, and have a unit weight of $\gamma > 24\,\mathrm{kN/m^3}$.

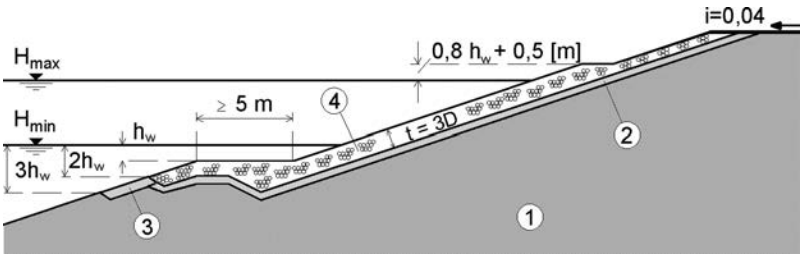

Figure 10.5 Slope protection with rockfill. (1) The dam's body; (2) filter layer; (3) layer of gravel (30 cm); (4) rockfill.

In order to be stable during wave action, individual pieces of rock should have a certain minimum weight, which, for slope inclinations $m = 1$–3, can be calculated by means of the following formula (according to Russian regulations):

$$Q = \frac{\mu \gamma_r h_w^2 \lambda_w}{\left(\frac{\gamma_r}{\gamma_w} - 1\right)^3 \sqrt{1 + m^3}} \tag{10.1}$$

where Q is the weight of stones; μ is the coefficient which is 0.025 for rockfill; if concrete blocks are used, then $\mu = 0.021$; γ_r, γ_w are unit weight of stone, resp. of water; and h_w, λ_w are the height and length of waves respectively.

Transition from weight of the stone pieces to the diameter of spherical pieces D may be performed by means of the formula:

$$D = \sqrt[3]{\frac{Q}{0.524\gamma_r}} \tag{10.2}$$

D can approximately be calculated from the expression:

$$D = \varepsilon h_w \tag{10.3}$$

where the coefficient $\varepsilon = 0.25$–0.35, in which the greater value relates to a relatively small unit weight of stone (up to 25 kN/m^2).

In the rockfill layer, more than 50% of the pieces should have the minimum calculated weight. The thickness of the lining should be minimally (2.5–3.0)D. Figure 10.5 illustrates an example of slope protection with rockfill, which is not present down to the end of the dam, but ends higher than that. If protection extends to the toe of the dam, then the composite construction with the foundation may be constructed as shown in Figure 10.6.

Instead of using rockfill, the protective lining may also be constructed in the form of stone paving, with a layer thickness of 20–25 cm and the weight of individual stones 20–40 kg. This construction has given satisfactory results for a height of waves up to 1 m. In spite of savings in material, stone paving is rarely used today as it requires the employment of an expensive labour force.

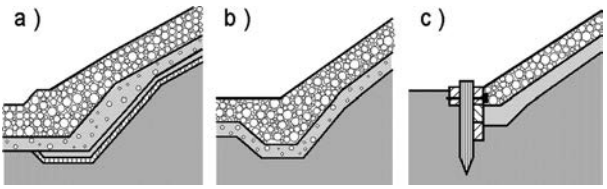

Figure 10.6 Composite construction between the rockfill protection and foundation. (a) With a rockfill prism; (b) with stone backing; (c) with stakes (or sheet piling).

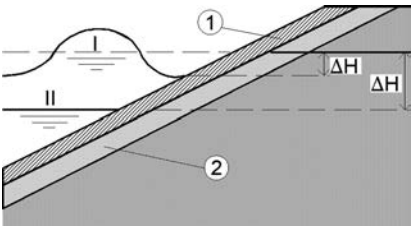

Figure 10.7 Uplift below the concrete slabs. (1) Concrete slab; (2) continuous drainage layer.

(2) *Concrete and reinforced concrete slabs*. These are constructed as monolithic or prefabricated slabs.

Concreting directly upon the slope is done using monolithic concrete slabs, 15 to 50 cm thick. During their execution, they are divided into bays with dimensions of 5×5 up to 20×20 m (even larger ones, in rare cases), separated with temperature-deformation joints, with compulsory protruding of reinforcement through the joints. Joints may be of a small width and non-filled (water-permeable), or filled. Below the slabs, it is necessary to construct either a continuous drainage layer (protected with filter layers, Fig. 10.7), or strip drainage, also protected with filter layers (Fig. 10.8).

If there are no seepage openings in the slabs and in the existence of a continuous drainage layer, unfavourable conditions may occur consisting of a rapid drawdown of the water level or during entailing of the wave along the slope (Fig. 10.7). In such a case, the water level in the drainage layer can be higher than the reservoir level by the value of ΔH, so that the uplift caused by the water, which is in the voids of the drainage layer, can cause failure of the slabs.

The slab strength is examined according to the maximum bending moment caused by the dynamic action of waves (a slab on an elastic foundation is analysed), according to which the reinforcement is consequently determined, which usually amounts to 0.4–0.6%. The thickness of the monolithic slabs δ_p is determined from the condition against rising upward of the slab, under the effect of uplift, and it amounts to:

$$\delta_p = 0.07 k_s h_w \frac{\gamma_w}{\gamma_c - \gamma_w} \frac{\sqrt{m^2 + 1}}{m} \sqrt[3]{\frac{\lambda_w}{B}} \tag{10.4}$$

where B is the length of slab along the normal of the contact of water and dam slope, while k_s is the coefficient of safety, equal to 1.25–1.50.

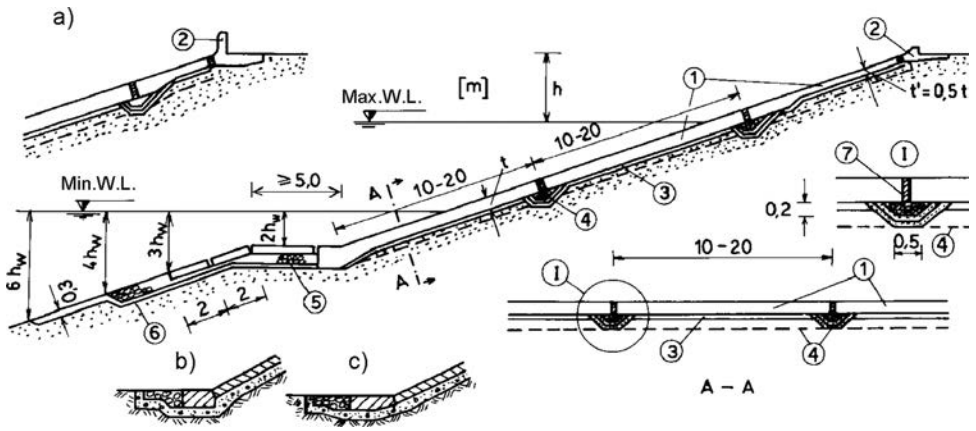

Figure 10.8 Protection of upstream slope with concrete slabs. (a) Alternative for crest shaping; (b, c) possible solutions for the joint between the concrete protection and the base. (1) Concrete slabs; (2) parapet; (3) layer of compacted gravel 10 cm thick; (4) strip drainage underneath the joint; (5) stone gritting material; (6) gravel 20 cm; (7) bituminized boards, $\delta = 2.5$ cm.

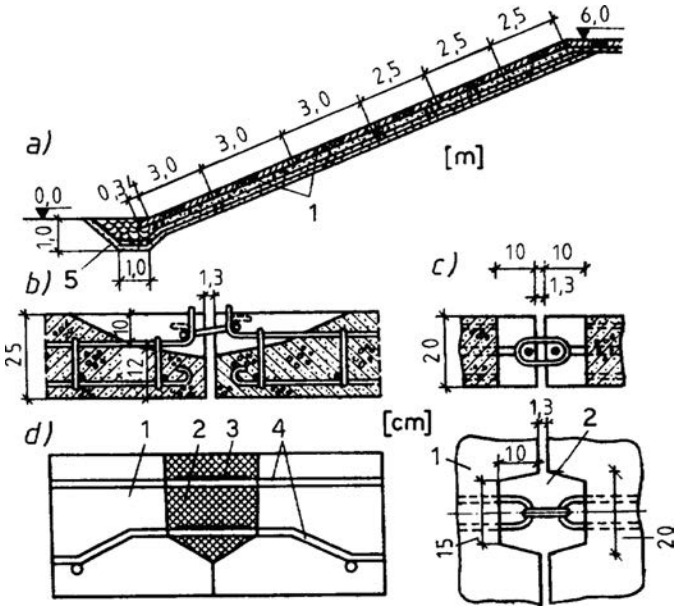

Figure 10.9 Protective construction with prefabricated reinforced concrete slabs. (a) Section through construction; (b) hinge connection of slabs; (c) connecting of the slabs with special dowel reinforcing bars; (d) concreting of joints of small slabs. (1) Slabs; (2) joint infilling with asphalt mass; (3) weld; (4) steel reinforcement; (5) retaining prism.

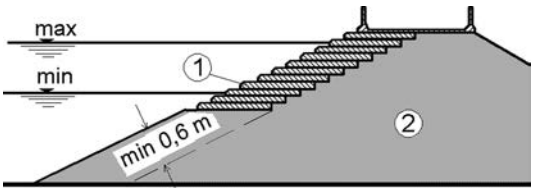

Figure 10.10 Protection with a mixture of sandy gravel, cement and water. (1) Protective lining; (2) the dam's body.

Prefabricated slabs are manufactured at a thickness of 8–20 cm with dimensions of 1.5 × 1.5 m up to 5 × 5 m, depending on the availability of plant and equipment for their lifting. The slabs are laid on a continuous filter layer with a hinge connection between them. During placement, the prefabricated slabs can be connected, i.e. assembled, into larger units (10 × 10 m up to 20 × 20 m) by concreting of the joints, so that prefabricated monolithic slabs are obtained (Fig. 10.9d). Filling them with asphalt mass closes the joints between the larger slabs, so that the protective construction gains certain elasticity, necessary for adaptation to possible deformations that can appear as a result of settlement of the structure (Grishin et al., 1979).

Monolithic slabs have a wider application than prefabricated slabs, even though they are more susceptible to settlement of the embankment below the slopes. A number of factors influence selection of the type of lining structure, the term for completion of the works, as well as the capabilities of the contractor.

(3) *Asphalt lining.* Asphalt protective linings find more and more expanding application in the world owing to their suitable deformation characteristics, complete mechanization of the construction process, absence of joints, etc. In contrast to facings, linings play the role of a water-impermeable element; protective asphalt linings can also be water-permeable.

They are used for waves up to 3.0 m high, and also successfully perform under conditions where an ice cover of up to 1 m thick forms on the storage lake. If the asphalt linings are made water-impermeable, they may require a base of drainage and filter layer in order to prevent uplift. Thickness of asphalt layers ranges from 5–10 cm, and, depending on base conditions, can contain one, two or more layers (Zdanov, 1984).

(4) *Other forms of protection.* In the USA, protection is often used consisting of a mixture of sandy gravel and additives of 7–14% cement and water, implemented in layers with a thickness of around 15 cm, compacted with rollers (Fig. 10.10). The thickness of such a lining, normal to the slope, should be a minimum of 0.6 m and is used for heights of waves up to 2.5 m. Disadvantages of such a construction are the danger of uplift, the possibility of fissuring at freezing, as well as relatively high cost (Golzé, 1977).

Several dams in the Czech Republic have protective linings composed of a mixture of sand and bitumen (18–23% in relation to the mass), with a thickness of 60–80 cm, which has proved efficient and economical (Rozanov, 1983).

In some cases it is more economical to construct rather slight slopes, while dropping the protective construction. This is the case when it is proven that protective

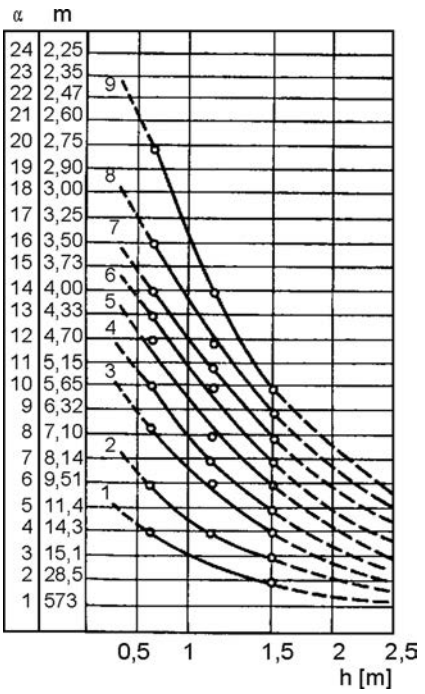

Figure 10.11 Graph for determination of inclination of a stable upstream slope. (1) Clay; (2) loess; (3) loam; (4) fine sand; (5) medium-grained sand; (6) loam with stones; (7) coarse sand; (8) gravel; (9) coarse gravel (dotted lines are extrapolated).

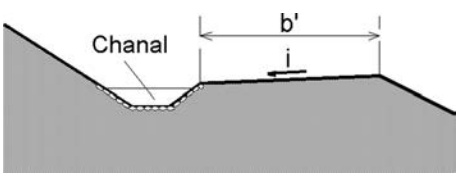

Figure 10.12 Berm.

linings of rockfill, concrete slabs, etc., appear to be too expensive. By means of the graph in Figure 10.11, which was obtained on the basis of observation data of the effects of waves on earth banks, it is possible to determine the slope inclination of a certain material for a given height of waves, at which the slope will be stable without protection. By multiplying that inclination by a certain coefficient of safety (1.2–1.4), one can obtain a practical datum for the design of low dams (Grishin et al., 1979).

The downstream berm is most often protected by means of grassing, where a layer of topsoil 20–30 cm thick is put into position across the surface. Sometimes protection is achieved with a layer of gravel (10 cm), along with compulsory interception and runoff of surface waters. If berms are constructed (Fig. 10.12), the width b′ should not

be less than 1.5 m, while a small channel for the gathering and run-off of atmospheric waters is created at the internal edge. The channel can be lined with stone, and in today's practice, concrete lining is more frequently used. The channel falls from the middle towards the ends in order to be able to run off the water to the perimeter channels in the contact between the dam and slopes at the dam site, which, afterwards, evacuate the water downwards of the dam.

10.2.2 Water-impermeable elements

From the former presentations it is evident that special water-impermeable elements for earthfill dams are constructed only in particular cases, aiming at: (1) Reducing the quantity of seepage water through the dam (Brauns et al., 1988); (2) Reducing the piezometric gradient of seepage flow in the dam's body and thus increasing the normal and casual seepage strength; (3) Lowering the seepage line through the dam and thus increasing the stability of the downstream slope and of the dam as a whole.

Construction of a water-impermeable element is essential if the material in the dam is susceptible to erosion, or if there are contacts of different materials of which the dam's body has been made. The following water-impermeable elements are used for earthfill dams:

(1) *Facing and blanket of clayey materials.* Facings (in combination with a cutoff trench and blanket) are most frequently constructed of impermeable elements for earthfill dams, especially low dams. In contrast to the internal core, the facing has the advantage of being constructed at the end on the slope of the dam's body, which facilitates and speeds up the construction.

Thickness of the earth facing is determined as a constant, or increases towards the lower end (Fig. 10.13). Minimum thickness at the top should be $\delta_v = 0.8–1.0$ m, while at the foundation $\delta_{n\,min} = H/J_k$, where J_k is the piezometric gradient, at which the casual seepage strength of the facing has been preserved. For clayey materials, $J_k = 6–10$ (Chugaev, 1985).

The top of the facing should be constructed at such a level that, following settlement of the dam, it will not be lower than the maximum water level. The facing is made as a composite construction with the foundation by means of a cutoff trench, the depth of which depends on the quality of the foundation. On the upper side it is covered with a protective layer, most often of local material (sand or gravel). In the case of considerable permeability of the foundation, the facing is extended in front of the dam to form a blanket (2, Fig. 10.13), which contributes to a decline in the seepage line of the dam behind the facing. In this, the filtration path is lengthened while the facing uplift after reservoir water-level declining, is decreased. The length of the blanket is determined by the conditions for preserving the casual seepage strength of the dam's foundation. The thickness of the blanket should be such that the piezometric gradient of the vertical seepage flow in it is not greater than 12 to 15. The minimum structural thickness of the earth blanket amounts to 0.7 m.

If the upstream part of the dam's body is made of coarse-grained earth material, then below the facing there should be a transition layer with a granulometric composition determined by means of the filter rules. An analogous procedure is also used for the blanket.

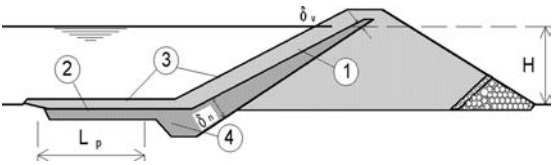

Figure 10.13 Dam with (1) Earth facing; (2) blanket; (3) protective layer; (4) cutoff trench.

(2) *Asphalt facings*. These facings fall into the order of the safest and the most prospective water-impermeable elements; however, they are rarely used for earthfill dams, owing to the danger of uplift during a rapid drawdown of the reservoir water level. However, their application is widespread in rockfill dams.

(3) *Facings of geomembrane*. In world practice, during the last 30 years, *geomembranes* have been widely used as a water-impermeable facing for dams which, as a rule, are not higher than 30–35 m. The term 'geomembrane' in hydraulic engineering denotes an elastic water-impermeable material, with a thickness of 0.5 to several mm, made from synthetic polymers (chemical compounds with a high molecular mass). In addition to the common ones, *reinforced* geomembranes are also used, which have an increased strength. A geomembrane is considered to be reinforced if the material that has been used for reinforcing is uniformly distributed across its entire surface. The reinforcement can be constructed with a non-woven or woven geotextile of polyester, polypropylene, or a geogrid of polyester and glass fibres.

Geomembranes are usually manufactured in a factory in the form of rolls. Their placement is most often carried out in two stages. The base is placed first, which is manufactured in a factory or at the construction site, and then the geomembrane. It is not unusual for geomembranes to be constructed along with geotextile, which serves as a base for the grout element. In this way, the geomembrane and geotextile can simply be consecutively fitted on the spot, or be factory jointed, the latter being a *combined* or *composite* geomembrane. These geomembranes are stronger and more resistant to damage. The geotextile embedded in them acts as a drainage layer and lowers the possibility of the occurrence of pore pressure below the facing. Quality of geomembranes must strictly be controlled. In accordance with international practice, tests are divided into three groups:

1. Control tests of the constituent materials during manufacture of the geomembrane in the factory;
2. Acceptance tests of the geomembrane yielding results which, in practice, are its identity card. Basically, included are tests of the individual components (chemical analyses, spectral analyses with infrared rays, etc.), determination of the rheological properties (relative elongation, resistance to exfoliation) and thermal properties;
3. Tests for the working characteristics of the geomembrane – water-permeability, elongation, friction, rupture, resistance to notching, resistance to impact (dynamic resistance), defoliation of joints, resistance to shearing along layers.

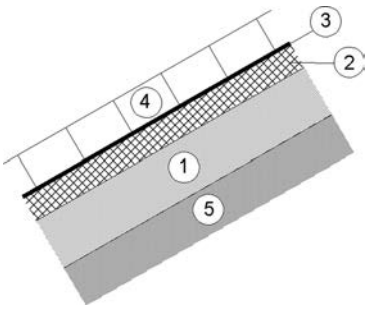

Figure 10.14 Facing with geomembrane. (1) Load-bearing layer; (2) base layer; (3) geomembrane; (4) protective layer; (5) the dam's body.

In addition, geomembranes are subjected to further tests in order to determine the influence of the working environment upon it. These test for the effects on the geomembrane by an aggressive environment, chemical matter and ozone, ultraviolet rays, radiation, various microorganisms, and high temperatures.

Like every other artificial material, geomembranes are also susceptible to ageing, which is manifested in an alteration of their properties in the course of time under the effect of the environment (Giroud, 1989). Data on ageing are obtained by means of accelerated laboratory testing, according to which the specified quality is guaranteed for 50–60 years. The observation of constructed dams indicates that, after 20–30 years of service, quality of the geomembranes is quite satisfactory. In this, one should take into consideration that the quality of geomembranes, manufactured 30 years ago, was lower than today's quality.

In the application of geomembranes as facing for earthfill dams, attention should be paid to the danger of uplift pressure below the facing, so that it is necessary to examine the slope stability under all possible conditions of use. Slope inclinations range within the following approximate limits: for clay 1:(2.5–3.5); for loam and sandy clay 1:(2–3); and for sand 1:2.

As a rule, the facing structure, with the geomembrane as an impermeable element, consists of the following elements (Fig. 10.14):

(1) *Load-bearing layer*, which is constructed of material that is coarser than the material in the body of the earthfill dam (5), with granulometric composition determined according to the filter rules.

(2) *Base layer*, which serves at the same time as a drainage, for which purpose earth material with a coefficient of permeability of $k = 10^{-2}$–10^{-3} m/s is used. Thickness of the base layer depends on the dam's height. The joint of the base with the load-bearing layer is treated with herbicides in order to prevent plant damage to the facing. This layer can also be constructed of geotextile placed directly on the load-bearing layer.

(3) *Geomembrane*, which type and thickness are selected in such a manner that they correspond to all local conditions and requirements. Rolls are laid from the crest downwards and are interjoined by means of welding, gluing, vulcanisation, hot air, or hot bitumen. It is advantageous if the strips run from the crest to the plinth of the slope – horizontal joints are undesirable since they are susceptible to elongation in the

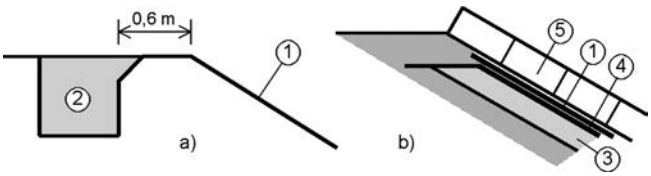

Figure 10.15 Anchored (a) and unanchored (b) geomembrane in the crest. (1) Geomembrane; (2) earth filling; (3) drainage layer (base layer); (4) geomembrane only in the upper part, separated from (1); (5) protective layer.

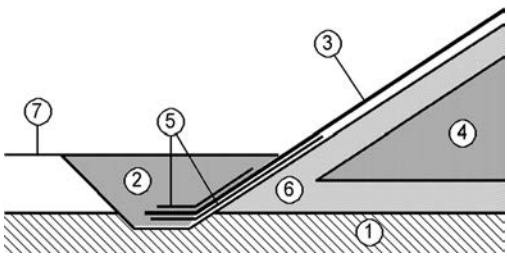

Figure 10.16 Anchoring of the slope in the dam's toe. (1) Water-impermeable foundation; (2) compacted earthfill; (3) geomembrane; (4) the dam's body; (5) geotextile; (6) drainage layer (base layer); (7) ground line.

process of fitting and operation. A protective layer of sand (no thinner than 50 cm, with grains 1–6 mm) is laid over the membrane, porous asphalt, or prefabricated concrete slabs. In light of this, attention should be paid to the influence of this layer on the geomembrane during construction and service conditions (danger of elongation, impracticability for revision and overhaul, etc.). Examples of constructed earthfill dams exist that contain geomembranes without a protective layer, where the facing is usually fixed by means of concrete beams at defined spacings, from the crest downwards along the slope. In such cases, the geomembrane is usually made of a polyvinyl chloride.

The joint of the geomembrane with the dam's crest can be made with anchoring (Fig. 10.15a) or without anchoring (Fig. 10.15b), details are as shown in sketches.

The method of geomembrane anchoring in the toe of the slope is shown in Figure 10.16. If a concrete plinth is laid, then the possible ways of joining are shown in Figure 10.17.

As an illustration of the application of geomembranes in earthfill dams, Figure 10.18 presents a cross-section of the Valence d'Alby Dam, 15 m high and constructed in France in 1989. The geomembrane of this modern dam is made of polymer on a base of bitumen and is 4 mm thick. Strips are joined by means of hot air. A thick layer of sand was laid as protection (Radchenko & Semenkov, 1993).

(4) *Earth cores*. These are made of the same material as earth facings. An earth core is usually positioned vertically (Fig. 10.19a), with the axis coinciding with the dam's axis, and in some infrequent cases, it is inclined towards the upstream face (Fig. 10.19b). In contrast to rockfill dams, the core position in earthfill dams does not

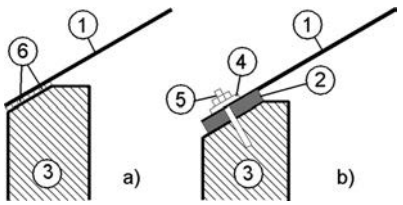

Figure 10.17 Joint of geomembrane with concrete plinth (a) with gluing; (b) with anchoring. (1) Geomembrane; (2) layer of elastic material; (3) concrete plinth; (4) steel plate; (5) bolt; (6) glued joint.

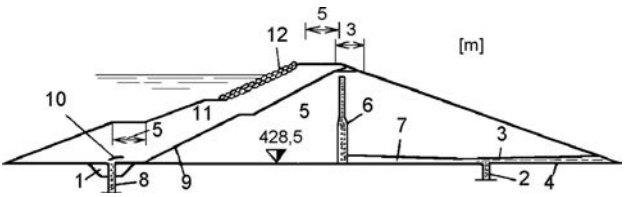

Figure 10.18 Valence d'Alby Dam (France). (1) Trench around concrete cutoff; (2) drainage trench; (3) drainage; (4) drainage pipe; (5) upstream shell; (6) vertical drainage; (7) drainage offtake; (8) concrete cutoff; (9) geomembrane; (10) additional cover membrane; (11) protective layer of sand; (12) rockfill.

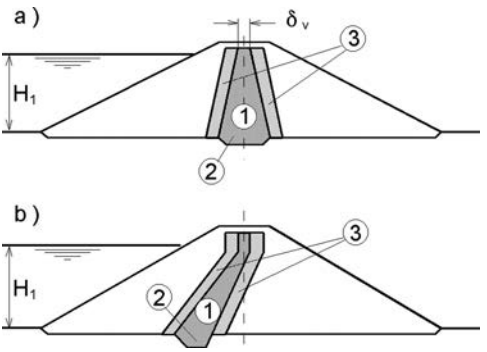

Figure 10.19 Earthfill dam with vertical (a) and sloping (b) core. (1) Core; (2) cutoff; (3) transition layers.

affect the inclination of the dam's downstream slope. At the same time, principles set out in the chapter on earth–rock dams will be valid for core dimensions, joint with foundation, anticipation of transition layers in the contacts with the material of the dam's body, and other details.

(5) *Grout cores*. Grout cores are constructed by means of pressure intrusion of grout mixture into the pores of the earth material. At a coefficient of seepage of the

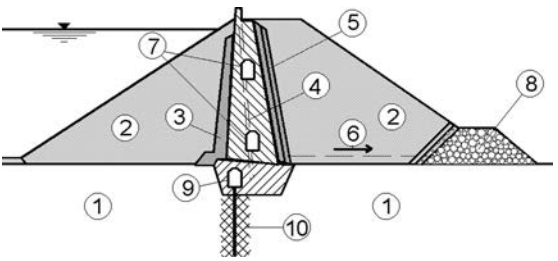

Figure 10.20 Dam with concrete diaphragm wall. (1) Bedrock; (2) earth material; (3) clay; (4) drainage pipes; (5) drainage layer; (6) water offtake; (7) drainage and inspection galleries; (8) downstream drainage; (9) grouting gallery; (10) grout curtain.

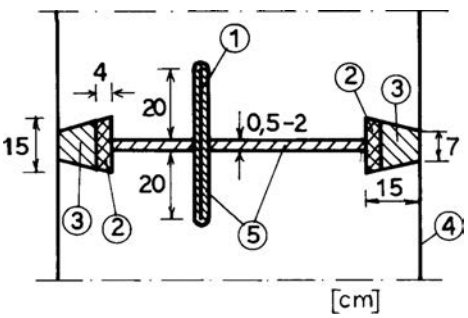

Figure 10.21 Example of filling of vertical deformation joint of concrete diaphragm wall. (1) Steel sheet, 2–4 mm thick; (2) resin infilling; (3) concrete plug; (4) downstream face of diaphragm wall; (5) asphalt mastic infilling.

material in the dam's body greater than 0.1 cm/s, a clay–cement solution is used as the grouting mixture, with the quantity of cement a minimum of 20% (by weight), while at $k < 0.1$ cm/s, clay–silicate solution can be used. Thickness of the grout core is increased downwards and amounts to approximately 1/8–1/10 of the dam's height. Grout cores are relatively new, water-impermeable elements and have a limited application in cases where there is no clayey material in the vicinity of the dam site, as well as in regions with severe climatic conditions.

(6) *Concrete diaphragm walls.* These are made out of concrete with a minimum grade of 20 MPa. In a cross-section, the axis usually passes through the upstream edge of the dam's crest (Fig. 10.20). Thickness of the diaphragm at the crest amounts to 0.5–0.7 m, while inclination of the faces ranges around 20:1. To accepting deformations, the diaphragm wall is divided by means of vertical joints, which are filled in an appropriate manner (Fig. 10.21). In the joint with the foundation, the diaphragm wall is connected with a joint, which allows small displacements of the diaphragm wall (Fig. 10.22). For the improvement of water-impermeability of the upstream face, a clay layer (3, Fig. 10.20) may be constructed on the diaphragm wall, or some other

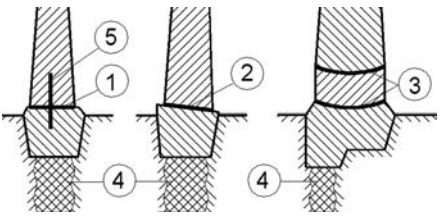

Figure 10.22 Alternative solutions at the joint between the concrete diaphragm wall and foundation. (1) Horizontal joint; (2) inclined joint; (3) cylindrical joint; (4) grout curtain; (5) steel sheet.

form of waterproofing. For catchment and control of water, which would possibly percolate through the diaphragm wall, a drainage layer of coarse-grained material (5) is constructed on the downstream face of the diaphragm wall. Higher diaphragm walls are provided with vertical drainage in the form of pipes, as well as with horizontal drainage and inspection galleries (4, 7). Thus, the concrete diaphragm wall becomes a complex structure with relatively large dimensions (Chugaev, 1985).

In addition to concrete diaphragm walls, reinforced concrete diaphragm walls are sometimes, though rarely, constructed. These are characterised by a considerably smaller thickness and can be monolithic or prefabricated-monolithic diaphragm walls.

(7) *Asphalt diaphragm walls*. This form of water-impermeable element appeared later than facings, and has been used during the last 30 years. The idea is to retain the positive features offered by the asphalt–concrete as a very suitable material for the construction of the water-impermeable body for embankment dams, while simultaneously avoiding the deficiencies caused by the position of the facing on the upstream dam's sloping.

The main advantages that are obtained with the relocation of the facing from the upstream slope to the interior of the dam are:

1. The diaphragm wall in the dam's body is not subjected to external influences, especially to significant temperature variations, to which the asphalt is very sensitive; and
2. The diaphragm wall is jointed in a simpler way with the foundation, and the joint is less exposed to damage due to settlement, while the foundation has a shorter length.

The main advantages of asphalt–concrete diaphragm walls, along with their high degree of impermeability, and manufacture of plant and equipment for simple placement of the asphalt mass, have led to their more intensive application. Among some 40 known dams with this form of impermeable element, there are also a few earthfill ones. Since most of them are rockfill dams, the asphalt diaphragm walls will be considered in more detail in the chapter on rockfill dams.

(8) *Other forms of diaphragm walls*. Membrane diaphragm walls are constructed as sloping or vertical ones. Jointing and the field of applications are similar to the

facings of geomembrane, but a disadvantage is their more difficult execution and inaccessibility for revision and repairs.

Metal diaphragm walls can be carried out as a sheet piling barrier, or else as a barrier formed of welded steel sheet. The joints must be closed and, owing to their limited duration and expensive anti-corrosion protection, are rarely employed.

10.2.3 Drainages

Drainages are carried out in the body and foundation of earthfill dams for the fulfilment of the following objectives:

1. Acceptance and drainage of seepage water towards the downstream face in order to avoid seepage deformations in the dam's body and the foundation underneath;
2. Reduction of the zone in which the seepage flow acts, which increases the stability of the downstream slope;
3. Decline in the seepage line and, thus, elimination of the danger of freezing of the earth material; and
4. Acceleration of the process of consolidation of clayey materials and reduction of pore pressure in individual zones of the dam and its foundation.

As a rule, drainages consist of an intake part and an offlet part. The intake part usually consists of layers of sand, gravel, or a stone gritting material, set out according to the filter rules. The offlet part is made of more water-permeable material (for example, rockfill), or there are drain pipes. In some instances, both the intake and the offlet parts may be constructed of the same material (for example, coarse-grained sand).

Drainages in the downstream toe of a dam are constructed of earth and rock materials with the necessary quality for such purposes. Concrete or asbestos–cement pipes are used for drainage pipesand are either perforated or contain non-sealed joints. Perforations and open joints must be protected with filter layers. The following types of drainages are constructed in the downstream end:

(1) *Drainage prism* (Fig. 10.23a) is constructed of rockfill, with filter protection. The top of the prism should have a freeboard value of d_0, over the level of the tailwater, amounting to a minimum of 0.5–1.0 m. Width of the prism at its top depends on the method of execution, but should not be less than 1.0 m. Inclination of the internal slope of the prism should be equal to the angle of repose of the material in the filter layer. The drainage prism should be designed in such a manner so that the seepage line should drop for a value a below the downstream slope, which satisfies the condition:

$$a \geq h_{\mathrm{m}} + h_{\mathrm{cr}} \tag{10.5}$$

where h_{m} is the maximum depth of soil freezing in certain region, and h_{cr} is the height of maximum capillary rising for a given earth material.

(2) *Retained drainage* (Fig. 10.23b) is used when there is no suitable material for prism construction in the vicinity of the dam site. Retained drainage does not lower the water table line in the dam's body; however, it does prevent any lifting of the earth material on the downstream slope. Thickness of the retained drainage should be not less than $(2.5–3.0)D + \delta_{\mathrm{f}}$, where D is the average diameter of the stone material, and

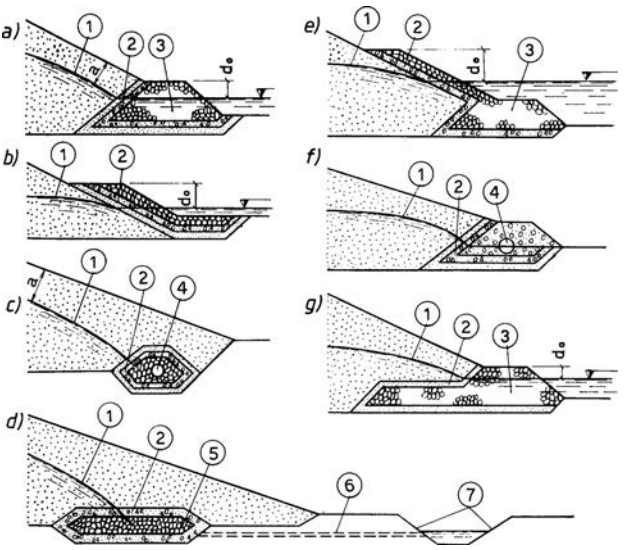

Figure 10.23 Drainage constructions at the downstream end of dam. (1) Seepage line; (2) filter layers; (3) prism; (4) pipe; (5) drainage strip; (6) offtake pipe; (7) drainage channel.

δ_f is the thickness of the filter layer. Values of a and d_0 are determined similarly as for the drainage prism.

(3) *Pipe drainage* (Fig. 10.23c) is accomplished with perforated concrete, asbestos–cement or plastic pipes, laid parallel to the end of the dam, with a certain inclination. Pipe diameter is determined by hydraulic calculations, but is assumed to be not less than 20 cm. Flow velocity should ideally be within the limits $0.25 \leq V \geq 0.75$. The value of a is determined according to the formula (10.5).

Inspection wells are carried out along the pipe drainage at each 50–200 m and the pipe should be protected with filter layers. Width of the drainage, along with the filter, must satisfy the condition $b \geq 0.5q/k$, where k is the coefficient of permeability of the earth material in the dam's body, while q is the seepage water quantity per unit length of the dam (where the foundation is impermeable). Sometimes, this drainage construction is executed without a pipe, using only coarse-grained rock material and, in such a case, it is called a *horizontal longitudinal drainage strip*.

(4) *Horizontal drainage* (Fig. 10.23d) is accomplished in the form of a flat drainage layer, made of coarse-grained material, protected with a filter. It is used for considerable declining of the seepage line. An offtake pipe (6) and a drainage channel (7) are used for water runoff. Horizontal drainage strips are made with a minimum thickness, i.e. depth, of 1 m.

(5) *Combined drainages* (Fig. 10.23e, f and g) represent a combination of the previously described drainage constructions, which increases their efficiency.

Drainages in the dam's body in the form of horizontal, vertical or sloping strips (Fig. 10.24) are constructed for improvement of slope stability in earthfill dams (constructed of low-permeable material), for reducing the zone in which seepage takes

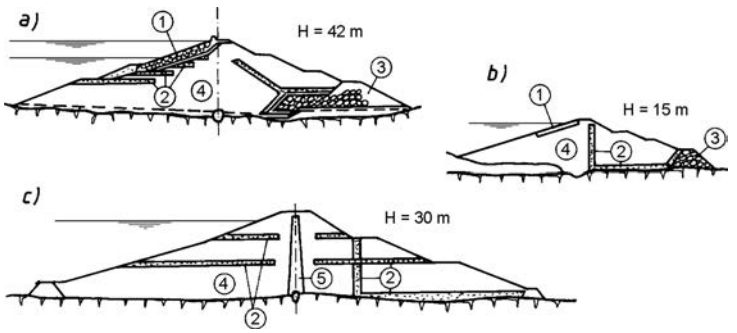

Figure 10.24 Drainage strips in the body of earthfill dams. (1) Slope protection; (2) drainage strips; (3) drainage prism; (4) the dam's body, made of low-permeable material; (5) clay core.

place, for reducing the pore pressure, and for acceleration of the consolidation process, as well as for preventing seepage deformations in the fissures of dams made of clay materials. Vertical drainage strips are particularly effective in anisotropic soil conditions, when horizontal permeability is considerably greater than the vertical.

The construction of the example (b), Figure 10.24, is especially frequently used, in which the vertical drainage can also be slightly inclined. The position of the vertical drainage element is chosen from the condition that ensures dam stability, as well as a sufficiently long path of the seepage water in the upstream, low-permeable material, in order to prevent high hydraulic gradients of the flow.

Like every drainage construction, this one should be properly dimensioned and carried out in order to be capable of correct fulfilment of its function, as in Figure 10.25a, where the drainage intercepts all the seepage water and the seepage line passes inside, into the drainage (Cedergren, 1973). If the drainage is of insufficient capacity, an unfavourable situation would occur such as in case (b), in which the shaded zone of the downstream shell, will be under the influence of pore pressure, and this can endanger the stability of the downstream slope.

The rate of flow of the horizontal drainage, without pressure occurring in it, can be determined from the expression given by Cedergren (Fell et al., 1992):

$$q = \frac{k_{\mathrm{h}} d^2}{2L_{\mathrm{h}}} \tag{10.6}$$

where q is the rate of flow of the horizontal drainage per 1 m of drain width; k_{h} is the coefficient of seepage of drainage material; d is the thickness of drainage layer; and L_{h} is the length of horizontal drainage (Fig. 10.26).

The rate of flow q_{v} of the vertical drainage almost never represents a critical element, and so its thickness is regularly governed by structural restrictions. Its rate of flow can be checked with the expression:

$$q_{\mathrm{v}} = \frac{k_{\mathrm{v}} h_{\mathrm{v}} t}{L} \tag{10.7}$$

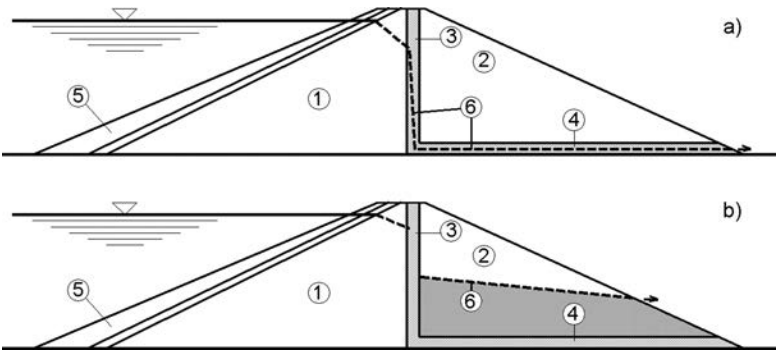

Figure 10.25 Earthfill dam with properly (a) and improperly (b) dimensioned internal drainage, and combined vertical and horizontal parts. (1) Low-permeable earth embankment; (2) downstream zone, less permeable than drainage; (3) vertical part; (4) horizontal part of the drainage construction; (5) zone of rockfill; (6) seepage line.

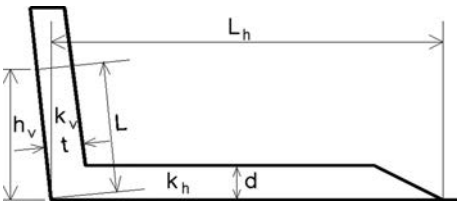

Figure 10.26 Scheme for calculation of combined drainage.

where k_v is the permeability of a vertical drain with a height (up to the water) of h_v, while L and t are shown in Figure 10.26.

In the examples shown in Figure 10.24, drainage strips have a thickness of 1 m, which is a typical value for these constructions. Thickness of vertical and horizontal drainage layers of up to 2 m may be found. Water from the banks also pours down towards the downstream side of the dam's toe, so the finishing part of the horizontal drainage layer should be reinforced with a drainage prism.

(6) *Pressure-relief wells*. In the case of dams with low-pervious earth material foundations, which rest on a layer of pervious material, there is a danger of development of uplift force below the dam. In addition to the horizontal drainage layer in the downstream part below the dam, vertical drainages constructed in the form of wells (Fig. 10.27) or trenches filled with sand, are very helpful for reducing uplift pressure. In the USA, pressure-relief wells with internal perforated pipes are often used, having a diameter of 15 cm (6 inches), which is much more efficient than pressure-relief wells filled with gravel (USBR, 1977a).

Different types of pipes have successfully been tried, and most frequently wooden ones have been used which, in conditions of permanent saturation with water, have proved to be more durable than others. More recently, metal pipes have been used, galvanized or saturated in bitumen insulation mass.

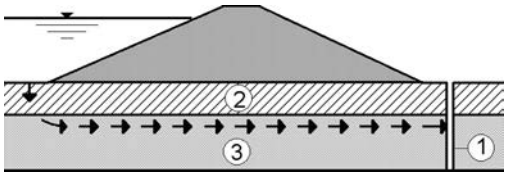

Figure 10.27 Application of vertical wells, trenches, or boreholes (1) for reducing of the uplift pressure; (2) impervious layer; (3) pervious layer.

A system of pressure-relief wells should primarily fulfil the following requirements:

1. Wells should extend into the pervious layer to such a depth as to enable a reduction of pressure, so that total thickness of the impervious layer and drained material is sufficient to ensure stability under the influence of the remaining pressure. It is usually sufficient that the depth of the well be equal to the dam's height. Wells can also extend through the entire pervious layer.
2. Wells should be positioned sufficiently close to each other as to be able to capture the seepage water and to reduce the uplift pressure among the wells to an acceptable level. They are usually positioned at a mutual spacing of 15 to 30 m, and, when the need arises, additional in-between wells may be added later.
3. Wells should be designed in such a manner as to exhibit minimum resistance to infiltration of the seepage water, without a danger of their being thrown out of service due to blockage or pipe corrosion.

Figure 10.28 illustrates a type of pressure-relief well, employed for reducing seepage uplift in the Red Willow Dam in Nebraska, USA. The pipe, with a diameter of around 10 cm, is made of stainless steel (14) and is surrounded by at least 15 cm of compacted filter material (13), and closed at the upper-side with an impervious mixture of clay and silt (10) in order to prevent water from rising along the outside of the pipe. The inspection well (1), consisting of a precast concrete pipe with a diameter of 106 cm, enables easy control over the operation of the well and provides working space for maintenance. Water, that has drained into the well, is taken away through a pipe (7), having a diameter of 20 cm, into collection drainage, constructed lengthwise at the downstream end of the dam.

Figure 10.29 illustrates the pressure-relief well used in the alluvium underneath the embankments at the Mississippi River. The well consists of a screen, wooden riser pipe, gravel filter, sand backfill, and a concrete backfill seal near the ground surface. Inside diameter of the wooden pipe is approximately 20 cm and pipe openings are accomplished in the form of notches, with dimensions of 0.5×8.3 cm. The bottom of the pipe is closed off with a wooden plug (USBR, 1977a).

Pressure-relief wells, as well as other drainage systems, have certain limitations and disadvantages. When the quantity of seepage water is significant, it may be necessary to construct a number of wells, which may prove irrational. In such a case, it is possible to use an upstream blanket to reduce the quantity of seepage water.

The main disadvantages of pressure-relief wells are: (1) they reduce the mean seepage path and increase the quantity of seepage water; (2) their design and construction

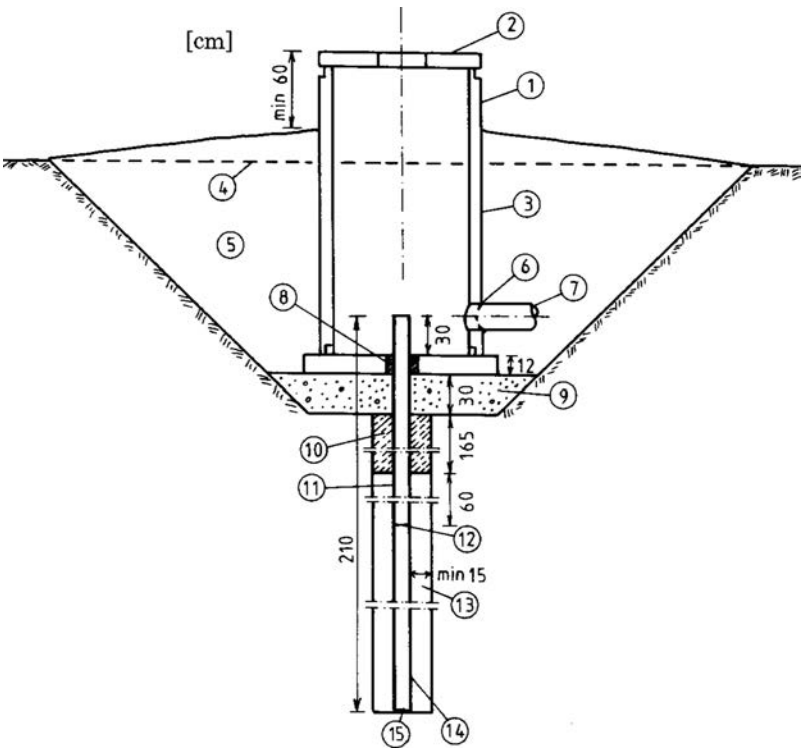

Figure 10.28 Pressure-relief well with steel pipe and inspection well (after USBR, 1977a). (1) Inspection well; (2) cover; (3) pre-cast concrete; (4) existing ground surface; (5) back fill; (6) rubberized sealing compound; (7) outflow pipe (2% slope); (8) rubberized sealing compound; (9) sand and gravel; (10) clay and silt seal; (11) steel riser pipe; (12) top of well screen; (13) pack material; (14) stainless steel well screen 10 cm; (15) plug.

require special knowledge, experience, and equipment; (3) they require permanent control and maintenance in the course of use. Therefore, pressure-relief wells are recommended mainly in cases when it is unreasonable to use other forms of drainage constructions.

Drainage plays a very important role in ensuring the stability and proper functioning of an earthfill dam. All stages in the realization of drainage, regardless of form – selection of type, structure, and execution – must be carried out with maximum care, attention, and profoundness. Numerous examples exist where errors were made during the design and construction of drainages for earthfill dams, which, as a consequence, have had considerable difficulties and complications during operation of the structure, resulting in the investment of considerable funds for remedial measures such as the construction of additional drainage.

Mavrovo dam is an interesting example – it was the first embankment dam built in Macedonia (construction commenced in 1948, during which time powerful plants and equipment were not available; the hydraulic scheme was commissioned for use

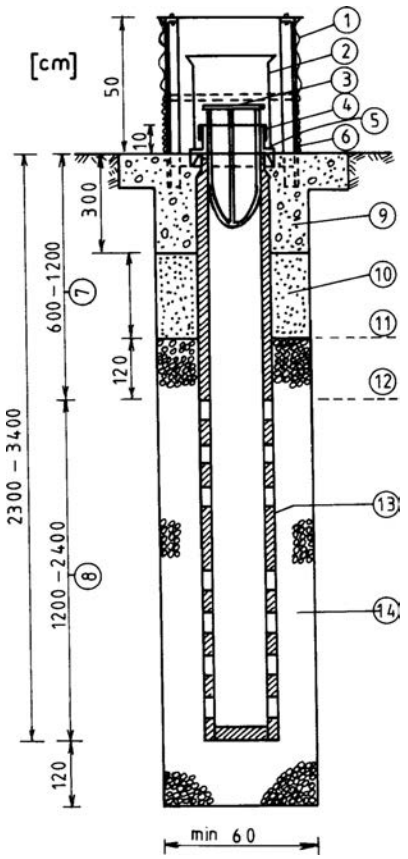

Figure 10.29 Pressure-relief well with a wooden pipe (after USBR, 1977a). (1) Corrugated metal well guard; (2) plastic standpipe; (3) check valve; (4) rubber gasket; (5) cast-iron tenon; (6) wire mesh; (7) wood riser pipe; (8) wood screen with slots; (9) concrete backfill; (10) sand backfill; (11) top of gravel filter; (12) top of well screen; (13) blank pipe through very fine sand strata; (14) gravel filter.

10 years later). This dam is located at the beginning of the craggy part of the Mavrovo River, i.e. immediately close to its way out from the Mavrovo Plain, at 25 km from Gostivar. It impounds a storage capacity of 357 millions m^3. The Mavrovo dam is the most important and the largest structure within the above-mentioned hydraulic scheme, and is intended for the production of electric energy. According to its construction, it is an earthfill zoned dam, (Figs. 10.30, 10.31), with the following basic dimensions:

1. Maximum height of dam above ground	56.0 m
2. Structural height (from core foundation to crest)	62.0 m
3. Crest width	6.0 m
4. Dam width at its foundation	286.0 m
5. Length of crest	210.0 m

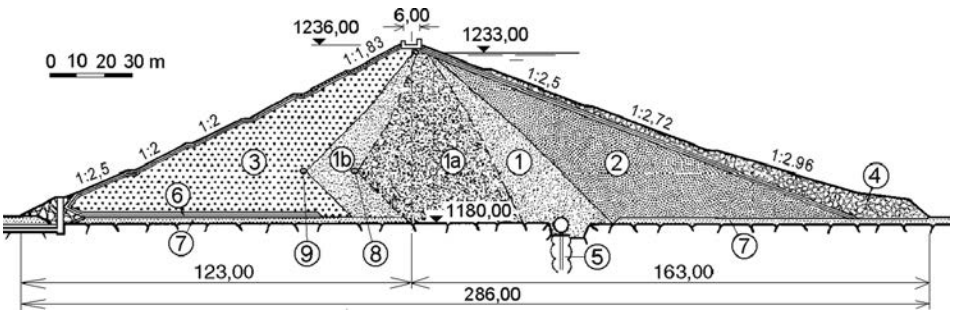

Figure 10.30 Cross-section of the *Mavrovo* dam. (1, 1a, 1b) Clay and weathered schist; (2) upstream shell of schist; (3) downstream shell of coarse schist; (4) facing of crushed rock; (5) grout curtain; (6) horizontal drainage blanket; (7) sediment of alluvial gravel; (8, 9) longitudinal horizontal drainages.

6. Slope inclinations:
   – upstream 1:2.50 1:2.96
   – downstream 1:1.83 1:2.50
7. Elevation of dam's crest 1236 mwl
8. Elevation of maximum water level in storage lake 1233 mwl

The dam's body consists of different materials, which are located according to their purpose (Fig. 10.30). Low-pervious earth materials have been built into the central part, as follows:

- clay and weathered schist, zone (1), with a foundation embedded 5.0 m into the rock, in which a control-inspection gallery is constructed;
- zone (1a), downwards of the core, approximately centrally positioned, is also made of clay and weathered schist, with the lowest permeability coefficient;
- zone (1b), with identical composition and properties as zone (1a). Shells are constructed of: upstream shell of schist (2), protected on the surface against wave effects by means of a lining of crushed stone, with a downstream shell of coarse-grained schist (3).

At the contact between the downstream abutment and the rock foundation of volcanic tuff, a horizontal drainage filter layer of fine sand and coarse gravel (6) has been constructed. Below the upstream and downstream shell, as well as below zone (1b), the layer of sediment of alluvium gravel (7) remains. The foundation at the dam site consists of volcanic andesite and dacite tuff. There is a grout curtain below the dam and in its abutments.

In the course of the dam's construction, material in the downstream shell (3) had a lower water-permeability than that anticipated in the design. In order to enable – in such aggravated conditions – the seepage line to decline towards the beginning of the horizontal drainage, i.e. not to emerge out of zone (1b), two additional horizontal drainages (8) and (9) were constructed, parallel to the longitudinal dam axis.

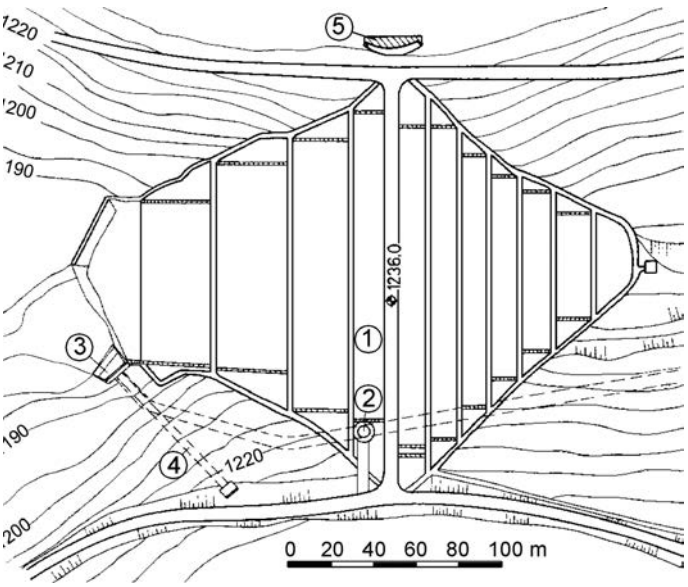

Figure 10.31 Layout plan of the Mavrovo dam. (1) The dam's body; (2) gate chamber; (3) water-intake structure; (4) sloping ramp; (5) observation platform.

10.3 PREPARATION OF THE FOUNDATION AND THE JOINT BETWEEN EARTHFILL DAMS AND THE FOUNDATION

In the foundation zone, prior to placement of the dam's embankment, it is necessary to prepare the ground. The extent of these preparations depends on the type of earthfill dam, its height, the hazard it causes, topography of the dam site, strength, permeability, and compressibility of the soil or that of the rock in the foundation.

Preparation of the foundation below the impervious earth embankment essentially differs from preparation of the part of foundation that carries the 'ballast,' i.e. the load-bearing material. The latter foundation is called a *general foundation*, in contrast to the former, whose preparations require the application of more rigorous criteria, since, within must be kept or maintained, the continuity of impermeability of both the overground and underground parts of the dam.

The purpose for the preparation of the *general foundation* is to remove weak and compressible material in order to ensure a foundation with appropriate strength, capable of carrying the embankment. If the foundation is bedrock, then it will always be much stronger than the embankment and it will not govern or dictate the dam's stability. Also, water-permeability in most cases is not a critical factor for the general foundation.

In the joint zone of the water-impervious element, i.e. between the dam material and the foundation, the preparation should achieve the following: removal of highly-pervious and erodible material below the line of the general foundation in order to ensure a foundation that is low-pervious and resistant to erosion. In the case of earthfill

dams, this target is most frequently achieved with the construction of a cutoff trench of low-pervious earth material, as well as with more complex operations, in cases when the pervious and erodible material extends to a considerable depth.

10.3.1 Preparation of the general foundation

In the zone of the general dam foundation, the ground should be properly cleared of top soil, roots, plants and it is also necessary to remove the passages pierced by underground burrowing animals. In the case of rock foundations, the top fissured and weathered layer of the rock is removed, as well as individual rock boulders. If there exist local tectonic faults in the form of wide and deep fractures, measures for their clearing out and filling are adequately taken. If there is occurrence of unsuitably oriented (dipped) weak rock strata, which would affect the dam's stability, it is necessary to go about their removal, while in more difficult cases modifications to the design should also be made, in order to achieve adaptation to the newfound conditions of the foundation. Following the clearing out, earth foundations are levelled, and they can be compacted with smooth-drum rollers or by means of sheepsfoot rollers. It often happens in the upper part of the foundation a relatively thin layer of earth material with weaker strength characteristics than those of the material in the dam's body is met with. It is usually justifiable to remove such a layer, while on account of that somewhat steeper slopes can be anticipated. The final treatment of the foundation surface often requires cleaning up by air jetting or by means of a mixture of air and water (Singh & Varshney, 1995).

10.3.2 Preparation of the foundation when using a dam cutoff trench

A frequent method for jointing the water-impervious element (or zone) of the earthfill dam with the foundation is the construction of a cutoff trench, as is shown in the example in Figure 10.32a. For a non-rock foundation, first of all one should perform a treatment the same as that for the general foundation, followed by excavation for the cutoff trench. Depending on *in situ* conditions, it is possible to carry out modification of the cutoff trench construction (deepening and widening, etc.). If pervious layers below the cutoff trench appear, which are susceptible to erosion, the downstream inclined face of the cutoff trench is laid over a filter layer, designed for controlling erosion. In some extreme cases, it may be necessary to cover the slope with pneumatically-applied mortar (Fell et al., 1992). Loose and dry material should be removed by means of light plant and equipment or, if that is not possible, by means of air jetting. The foundation of the cutoff trench should be wetted and compacted prior to the placement of the first layer of the embankment.

For a rock foundation, in the zone of the cutoff trench rock with open joints and other fractures must be removed, which lead to greater permeability. It is necessary to remove the rock with joints that are potentially susceptible to erosion. The rock surface must be properly cleaned up (often manually) and any remaining fissures and fractures should be filled with cement–sand grout injections, pneumatically placed mortar, or concrete. Rolling of the pit bottom is not allowed by any means since this may destroy the structure of the surface rock. Sometimes, it is necessary to use wetting

of the surface immediately prior to the placement of the earth embankment in order to maintain necessary moisture.

10.3.3 Joint of the earthfill dam and the foundation

The joint between the earthfill dam and its foundation should be properly planned, designed, and constructed, in order to be able to provide a compact, low-pervious, and stable joint between the embankment and the natural ground. Therefore, it is necessary to differentiate three basic cases:

The impervious layer begins at the ground surface. For a clay foundation upon which a homogeneous earthfill dam has been constructed, it is sufficient that the joint to be executed with a cutoff trench, as shown in Figure 10.32a. If the earthfill dam has a core or facing made of coherent earth material, then the cutoff trench is constructed in contact with the water-impervious element and the foundation. Also, in cases of sound and firm rock, or for rocks with minor damage close to the surface, the joint can be constructed with a cutoff trench.

For rock foundations, when the surface parts are regularly fissured i.e. fractured, it is often necessary to perform additional work to improve water-impermeability, which consists of construction of grout curtains. In such a case, earthfill dams are regularly constructed with a water-impervious element in the form of a core or facing, while the grout curtain is carried out below the impervious element. Figures 10.32b and c illustrate joints of dams with a core and fractured rock foundation. The joint can be constructed with a concrete slab (b), which serves as a base for grouting, or with a concrete gallery (c), from which grouting is carried out. The thickness of the grout curtain, which in fact represents a continuation of the core, is determined so that the transverse gradients of pressure in it should not be greater than 20. The concrete slab ensures a proper contact between the core and the foundation and serves as a base for grouting, prevents the grouting mixture (squeezed under pressure into the boreholes) from exiting through the fractures onto the rock surface.

The impervious layer is at an inaccessible depth. In such a case, the foundation cannot be jointed directly with the impervious layer, so that cutoff trenches are carried out as in Figure 10.32a. Below the facings or cores, it is possible to construct suspended barriers (low-pervious elements) in the form of sheet piling or a concrete wall (Fig. 10.32d, e), which considerably, and to a sufficient degree, lengthens the path of seepage water below the dam, thus providing acceptable gradients of the seepage flow.

The impervious layer is at accessible depth. In this case, it is usually rational to joint the dam's body with the impervious layer, especially when the pervious layer is more water-pervious than the dam's body. If the highly water-pervious layer is cut off in this manner, the suspended barrier (low-pervious element) should be extended also in the dam's body, up to the crest. Otherwise, the seepage path of the water would be very short – *abc* in Figure 10.32f – on which section considerable seepage deformations could be expected. Such a barrier could be constructed in the form of a concrete or asphalt diaphragm wall, or else in the form of a clay core (Fig. 10.32g), constructed in an open cut pit or as a concrete diaphragm wall and executed in a trench with vertical sides (Fig. 10.32h). The barrier is kept stable by means of shoring or by means of bentonite suspension, which is more economical and more practical, and would fill

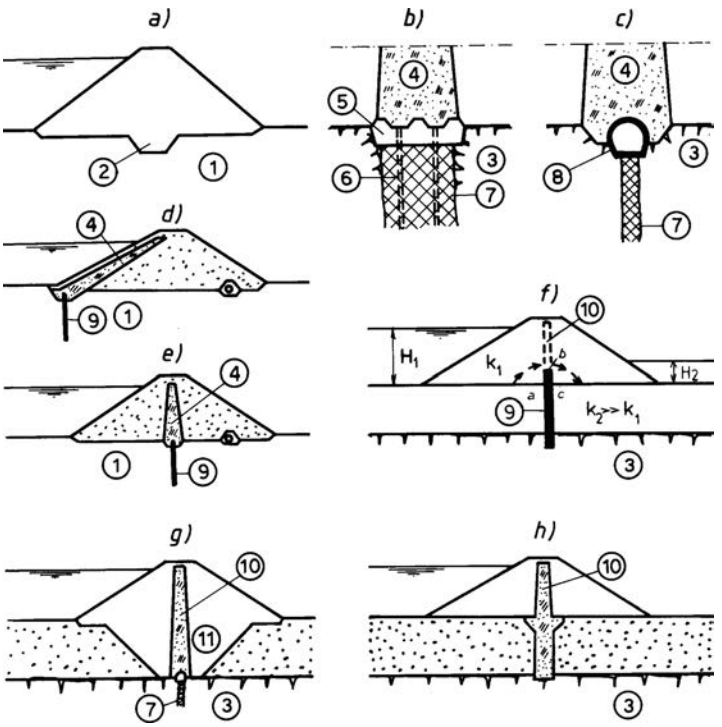

Figure 10.32 Joint between an earthfill dam and its foundation. (1) Impervious earth foundation; (2) cut-off trench; (3) rock; (4) core (or facing); (5) concrete slab; (6) grout hole; (7) grout curtain; (8) grouting gallery; (9) sheet piling barrier (or concrete wall); (10) core or diaphragm wall; (11) construction pit.

the excavated trench. The pervious layer can also be cut off with steel sheet piling, with a diaphragm wall of clay-cement or grout.

Even though in the practice of earthfill dam construction all of the above-mentioned ways of jointing are met with, the joint with a cutoff trench has the most frequent application. That is why more attention will be paid to the details of its construction. Consider the example of an earthfill dam with a wide central core made of coherent earth material, Figure 10.33.

The width of the cutoff trench depends on the kind and quality of the foundation at the level of founding of the cutoff trench, size and hazard that the dam causes, as well as the type of dam. For a rock foundation, cutoff trench width would depend on the quality of rock. For example, for a low-pervious, non-erodible rock, the ratio b/H can be only 0.25 (however, there are cases where it is $b/H = 0.1$). On more pervious, erodible rock, the ratio b/H is usually >0.5 and can be assumed to be up to 1. The minimum width can be 3 m, the width of the machinery needed for excavation and placement.

For a non-rock foundation it is customary to assume $b/H = 1$, in order to obtain lower gradients of seepage flow for tough conditions in the foundation. Width of the

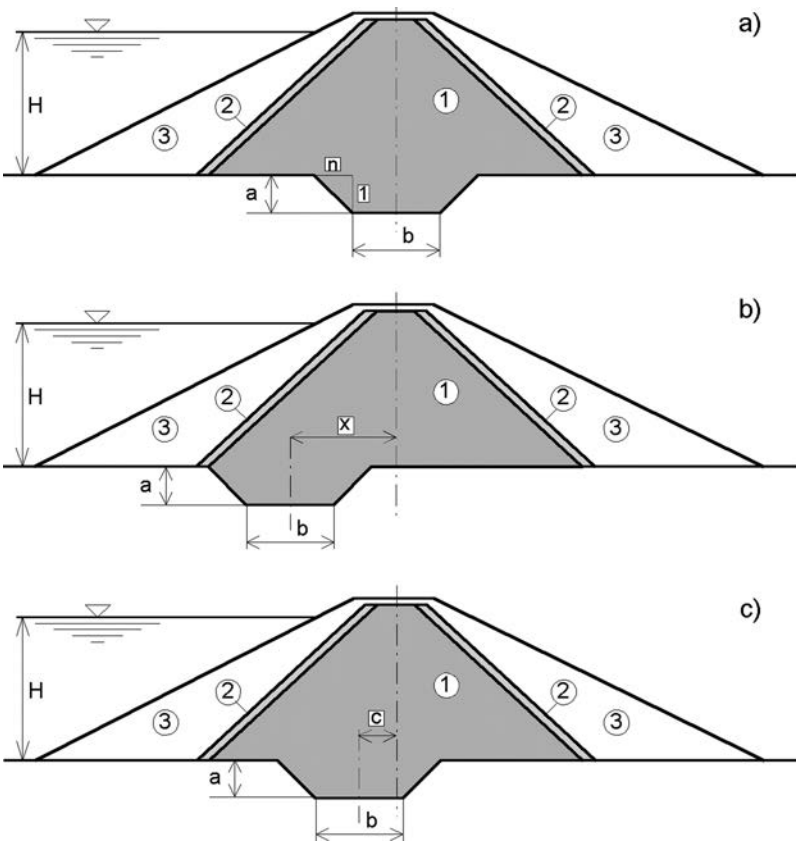

Figure 10.33 Construction of cutoff trench underneath a wide core (after Fell et al., 1992). (1) Coherent earth material; (2) filter layers; (3) rockfill.

cutoff trench can be fixed, but can also be varied lengthwise, becoming narrower in the bank abutments towards the ends of the dam, where there is a smaller dam height.

Depth of the cutoff trench *a* depends on the quality of the foundation, that is to say, on the necessary length of the seepage path that has to be provided. Of course, if the required depth is too great from the viewpoint of engineering feasibility and practicability and/or economy, then such a solution will be abandoned and another one searched for. It is important to consider that the cutoff trench depth is never adopted as a fixed value but only as an approximate one, which will be definitely determined and fixed following the gradual excavation, and after direct insight into the foundation quality.

Slope inclinations of the cutoff trench (1:*n*, Fig. 10.33a) should not be steeper than 1:0.5 in order for it to be possible to achieve proper compactness in the contact with the filling material. On the other hand, slope inclinations should be sufficiently slight as to avoid the phenomenon of 'hanging' of the filling material, which leads to the danger of hydraulic fracture. The stability of the excavation may also influence

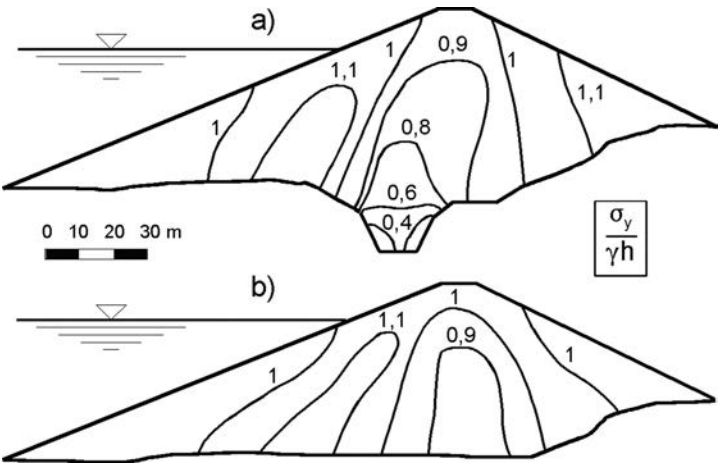

Figure 10.34 Transfer of vertical stresses from the dam's body into the foundation in the zone of a cutoff trench of the Teton earthfill dam. (a) Section with cutoff trench; (b) section without cutoff trench.

the inclinations of the cutoff trench slopes, which depend on the kind and condition of material in the foundation, as well as the presence of underground water. For a non-rock foundation, slopes can have inclinations of 1:1, and even up to 1:1.5.

The cutoff trench position in relation to the dam axis is an issue that also deserves attention. From the viewpoint of construction, it is best when the axis of the cutoff trench coincides with the dam axis (Fig. 10.33a), since, in such a case, the cutoff trench is constructed in alignment, but only if the axis of the dam is not curved. However, the cutoff trench often retreats towards the upstream face and can commence even at the upstream edge of the core, or of the dam, if it is homogeneous (Fig. 10.33b), which is governed by local topographic and geological conditions in the foundation. In such a case, the cutoff trench is curved and construction is aggravated. A compromise solution is presented in case (c), where the axis of the cutoff trench is located at a certain fixed distance c from the axis of the dam.

Finally, it should be noted that the structure of the cutoff trench (position, width, depth and inclination of sides) should be very carefully planned and constructed. Otherwise, it may lead to irregularities in the operation of the dam, or even its failure. In this respect, the Teton dam (USA) is an edifying example. This dam failed in 1976 during the first filling of the reservoir, as a consequence of progressive erosion occurring in the lower part of the dam. The reason for the occurrence of progressive erosion resulted from a number of omissions and defaults in the design and construction, one of them being an inappropriately designed cutoff trench below one part of the dam (Fig. 10.34a). Namely, the cutoff trench was narrow in one zone, with steep faces, and located in the central part of the section. An analysis of the state of stresses clearly indicates this as one of the main reasons that led to the disaster.

Figure 10.34 shows contour lines of the ratio between vertical normal stress σ_y and total earth pressure γh, for a section with cutoff trench (a), and without cutoff

trench (b). Drawing (a) clearly indicates the great reduction of vertical normal stress in the zone of the cutoff trench, occurring due to an enormous transfer of forces from the filling material into the steep rocky sides, upon which the deformable material of the cutoff trench has been 'hung.' As a consequence of this and other unfavourable circumstances, a hydraulic fracture occurred during the first filling of the storage lake, which resulted in failure of the dam. Details of this example are given in a number of references (see Eisenstein & Naylor, 1986; Jansen, 1988; Nonveiller, 1983).

For treatment of surfaces of the banks upon which the water-impervious material of the earthfill dam is founded, details are also given in the chapter on earth–rock dams. The principles laid out there are, generally, valid for earthfill dams – especially larger ones.

Chapter 11

Earth–rock dams

11.1 CONSTRUCTION OF EARTH–ROCK DAMS

When it is a question of large dams, earth–rock ones are the most frequently constructed dams. They are constructed on rock foundation (with rare exceptions at lower dams), with a construction that is schematically presented in Figure 11.1. The shells (1) are made of coarse-graded material – gravel or rockfill, with slope inclinations which, depending on the material and foundation, most often range within limits of 1:1.5 to 1:2.2.

Water-impermeability is provided by means of a relatively thin *core* of coherent earth material (2), with a crest width 3–4 m (for structural reasons), while at the base it is usually 0.2–1 times the dam height, which depends on the water-impermeability and deformability of the used earth material. *Filter*, i.e. *transition layers* (1–3) are carried out between the *shells* and core, and they have the following purposes: (1) To provide gradual transition between materials in the shells and the core, which have an extremely different granulometric composition and thus enable execution of the interface; (2) To prevent mechanical erosion, i.e. the removal of fine particles from the core into the downstream shell, due to seepage through the core at a full reservoir, and from the core into both the downstream and upstream shells at a rapid drawdown of the reservoir, in the process of consolidation of the coherent material; the above removal of fine particles from the core could lead to its distortion, while their insertion among the grains of the coarser material in the shells could worsen its strength characteristics; (3) To give a possibility of self-remedy of a possible fissure occurring in the core; namely, under water pressure, material of the adjacent filter layer is squeezed into such fissures, and thus there could come about considerable reduction of the concentrated seepage through the fissure and prevention of its progressive widening.

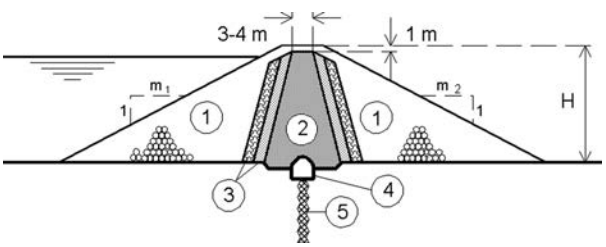

Figure 11.1 Schematic presentation of an earth–rock dam.

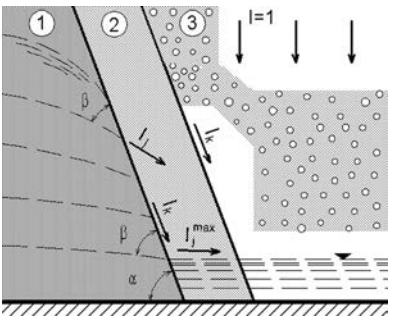

Figure 11.2 Design hydraulic gradient of seepage. (1) Core; (2) filter layer; (3) downstream shell.

Filter layers should be designed according to the rules that have been discussed in the chapter on earthfill dams. There is an additional condition that has to be fulfilled in order to consider the earth material of the filter layer as non-suffusional one (Moyseev & Moyseev, 1977):

$$\frac{D_3}{D_{17}} = (0.32 + 0.01\eta)\ \sqrt[6]{\eta} - \frac{\eta}{1-n} \tag{11.1}$$

where, $\eta = D_{60}/D_{10}$ is the uniformity coefficient, n, the porosity, and D_3 and D_{17} are the diameters of the fractions that are contained in the material less than 3% and 17%.

The thickness of the first filter layer in large earth–rock dams should be determined not only from the conditions of seepage and for structural reasons, but also taking into consideration possible horizontal deformations of the core.

The design hydraulic gradient of seepage I_j in the core in front of the contact with the filter layer (Fig. 11.2) can be calculated using the expression (Moyseev & Moyseev, 1977):

$$I_j = \frac{\sin\alpha}{\cos\beta} \tag{11.2}$$

where the angle β is taken from the hydrodynamic net.

The gradient I^{max} is assumed in practice for the core and it is obtained for $\beta = \alpha$, i.e.:

$$I_j^{max} = \tan\alpha \tag{11.3}$$

Below the core, a *grouting gallery* is almost regularly constructed, through which it is possible to make water-impermeable grout curtain below the dam, in the rock foundation. The core is embedded 1–2 m into the rock, in order to provide a better joint and to lengthen the path of the contact seepage.

The construction of earth–rock dams is relatively simple, as is their operation. Drainage is not necessary, because its role is played by the downstream shell (together

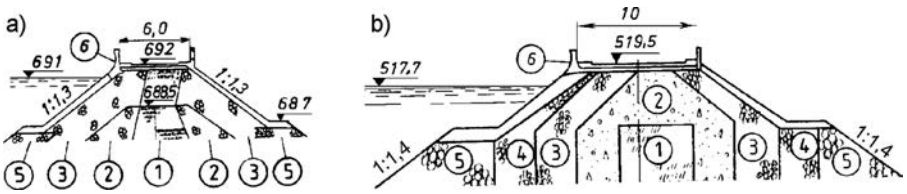

Figure 11.3 Crest of Globochica dam (a) and Kalimanci dam (b), Macedonia. (1) Core; (2) filter layer I; (3) filter layer II; (4) filter layer III; (5) rockfill; (6) reinforced concrete wall.

Figure 11.4 The crest of Globochica dam (Macedonia).

with the appropriate filter layers). Particular protection for the slopes and the crest is usually not necessary and so it comes down to possible rockfilling of coarser rock material across the upstream slope. All of this, together with the safety and practically unlimited durability (without a need for special maintenance and repair), is a reason for the great popularity of this type of dam.

In constructing the dam crest it is necessary to take care in order to have a protective layer over the core of coarse-grained material of sufficient thickness. In the upstream edge, a wall is also often constructed (Figs. 11.3, 11.4), which is dimensioned for impact wave action, by means of which it is possible to decrease dam height. Since it is a question of a stiff construction, a wall can be built in cases when considerable deformations of the crest are not expected.

Table 11.1 Earth–rock dams higher than 200 m (* under construction).

Dam	State	Constructed (year)	Height (m)	Volume of dam $m^3 \times 10^3$	Volume of reservoir $m^3 \times 10^6$
1. Rogun*	Tajikistan	(?)	335	75,900	13,300
2. Nurek	Tajikistan	1980	300	58,000	10,500
3. Chicoazen (Manuel Torres)	Mexico	1980	261	15,370	1613
4. Tehri	India	2006	261	22,750	2600
5. Alberto Lleras (Guavio)	Colombia	1989	243	17,755	787
6. Mica	Canada	1973	242	32,111	24,700
7. La Esmeralda	Colombia	1976	237	11,400	760
9. Oroville	USA	1968	230	59,635	4297
10. Irape	Brazil	2006	208	10,300	
11. Keban	Turkey	1974	207	15,586	30,600

Construction of rockfill shells is carried out in two ways: (1) By filling and compacting using vibratory rollers (5–10) t in layers with thicknesses 1–3 m, by wetting with water (100–300 l/m^3); and (2) By filling in thick layers (4–5 m and more) without compaction, but by using washing out with hydromonitors, with the use of 2–4 m^3 of water per 1 m^3 of rock.

Gravel is built in by means of compaction, as well as stone, in layers of thickness 0.5–1 m. The coherent material in the water-impermeable core is built-in, same as for earthfill dams, in layers with thicknesses 15–25 cm, at optimum (or somewhat greater) moisture, at favourable weather conditions. This circumstance tends to retard construction, since the shells are constructed simultaneously with the core, so that at locations with a short construction season, earth–rock dams become non-economical.

Thanks to the above-quoted advantages of this type of dam, they made it possible to achieve the greatest heights, which can also be seen from the survey of earth–rock dams higher than 200 m (Table 11.1).

An important structural characteristic of earth–rock dams is the position of the core in the dam's body. In that respect, we can distinguish three cases: (1) A core that is vertical, usually positioned centrally regarding the dam; (2) A core that is very much inclined towards the upstream face; and (3) A core that is slightly inclined.

11.2 EARTH–ROCK DAMS WITH VERTICAL CORE

Vertical core is most often used because of the following advantages in relation to the sloping core: (1) The zone with the weakest material (core) is a maximum distance from the slopes, which makes an influence on their stability; (2) Contact between the core and foundation is shorter, which is particularly important if a grout curtain is constructed; (3) Pressure in the contact core-foundation is higher, which decreases the possibility for contact seepage; (4) It is possible to undertake remedial measures for possibly occurring fissures in the core, by means of grouting from crest; (5) In the case when a grouting gallery has not been constructed, it is possible to perform additional

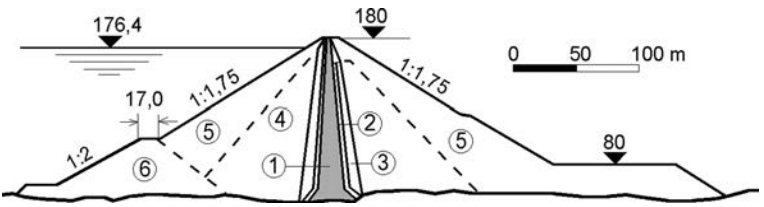

Figure 11.5 El Infiernillo dam (Mexico). (1) Clay core; (2, 3) first and second filter layer, with particle size 0.1–10 and 5–150 mm; (4) compacted fill of small stones; (5) rockfill; (6) cofferdam, incorporated into the body of the main dam.

grouting in the foundation below the core, by means of boring through the coherent material; and (6) Thickness of the vertical core is somewhat larger than the thickness of the sloping core, for the same quantity of used earth material.

Modern earth–rock dams with vertical core were intensively built, starting from the sixties of this century, when there were built several very significant dams with exceptionally thin cores. For example, El Infiernillo dam (Mexico), completed in 1964, 148 m high, has a clay core with a thickness of some $0.2H$ (Fig. 11.5), compacted in layers of 15 cm each by means of specially designed sheepsfoot roller, at moisture 2–6% larger than the optimum one. For better contact with foundation, the core is widened in its lowest part. Filter layers of sand are added, in layers of 30 cm each, with water sprinkling and compaction with four passes of a 3-ton vibratory roller. Both the upstream and downstream shell is divided into two zones. The largest grains of the internal zone reach 45 cm, placed in layers of 60 cm each, while fill from the external face has larger grains and is placed in layers of 2 m. El Infiernillo dam is sited in a seismically active zone in the vicinity of the Pacific coast. Since its completion, the dam has experienced a number of earthquakes, of which one was very strong – in 1979. Being a modern engineered and constructed dam, it has sustained the earthquakes well. And yet, deformations have occurred in its body, which cannot be neglected in comparison with those that developed during construction, due to the first filling of the reservoir and owing to the normal operation of the dam (Goljdin & Rasskazov, 1987; Golzé, 1977, Moyseev & Moyseev, 1977).

Another known dam with a thin central core is Gepatch (Austria), also completed in 1964 (Fig. 11.6). It is 153 m high, has a core that is only $0.15H$ wide in its foundation. The rockfill body was constructed in layers of 2 m each, compacted with four passes of an 8.7-ton vibratory roller. The core is divided into two zones – the first one made of clay and debris (1), and the second one of similar material plus an addition of 1% bentonite (2). This mixture, which is not frequently used, improves the material properties in the core; that is to say, its water-impermeability and resistance against mechanical erosion are increased. The cost of such a core is higher; however, the possibility for improvement of its properties by addition of bentonite should always be considered in cases of a shortage of appropriate coherent material, since a higher cost could be compensated by increased safety (Borovoy et al., 1976).

In the above-cited examples, the inclinations of both upstream and downstream slopes were equal, which is customary for this type of dam. Sometimes, as shown

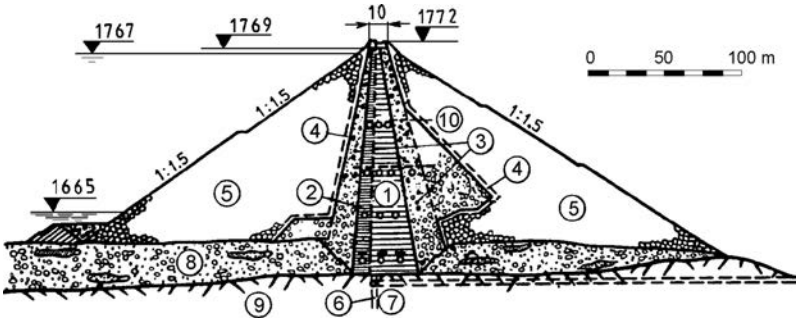

Figure 11.6 Gepatch dam (Austria). (1) Core of clay and debris; (2) upstream core zone with addition of 1% bentonite; (3) transition zones; (4) stone chippings; (5) rockfill; (6) grout curtain; (7) grouting gallery and access to it; (8) alluvial sediment; (9) foundation gneiss; (10) ceramic filters, $d = 3$ cm.

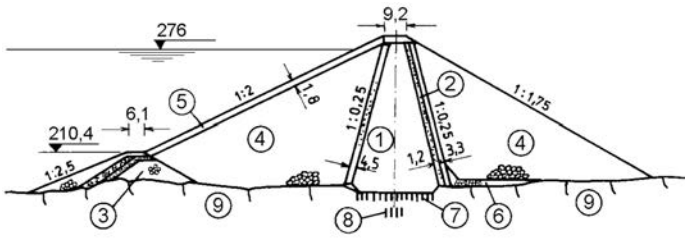

Figure 11.7 Llyn Brianne dam (UK), $H = 90$ m. (1) Clay core; (2) transition layer; (3) cofferdam; (4) shells of schist with flaky shape of grains; (5) protection of coarse stones; (6) drainage layer; (7) surface grouting; (8) grout curtain; (9) schistose claystone.

in Figure 11.7, the upstream slope is constructed with a slighter inclination, which is governed by local conditions and must be supported with appropriate calculations (Rozanov, 1983).

Figure 11.8 presents a dam that has been constructed in a number of zones of different materials in which the central wide core consists of several zones of impermeable and semi-permeable earth material, while the shells have been constructed of zones of gravel with stone gritting material and rockfill. A number of berms have been made on both slopes, which contribute to warping of the entire inclination, because the rockfill has been placed in thick layers with the angle of repose. Such construction of the dam was governed by the quantities of available local materials in the vicinity of the dam site (Creager et al., 1955; Sherard et al., 1963).

The highest earth–rock dam constructed so far–Nurek (Tajikistan), $H = 300$ m – belongs to the group of earth–rock dams with a central core. The core is made of loam, with inclinations of the faces 1:0.25, and is founded on concrete block in which there is accommodated a gallery for consolidation grouting and for deep grouting (Fig. 11.9). Basically, this dam's body is constructed of alluvial and coarse gravel with a thick surface layer of coarse stones. The Nurek dam was constructed on the River Vahsh in Tajikistan, a well-known seismically active area in which earthquakes of

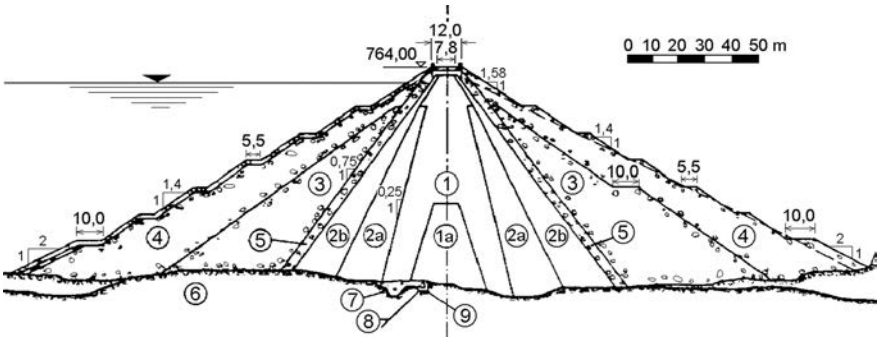

Figure 11.8 Las Pircuitas dam, Argentina (after Creager et al., 1955). (1, 1a) Impermeable earth material; (2a) semi-permeable earth material; (2b) permeable earth material; (3) gravel and stone gritting material; (4) rockfill; (5) filter layer; (6) rock; (7) concrete; (8) grout curtain; (9) grouting and drainage gallery.

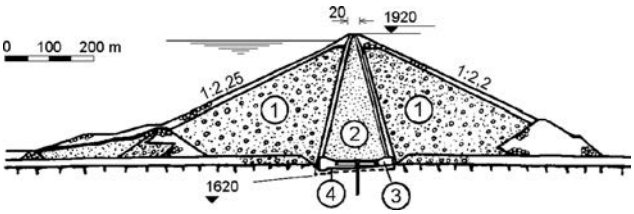

Figure 11.9 Nurek dam (Tajikistan), 300 m high. (1) Sandy gravel; (2) loam; (3) concrete block with grouting gallery; (4) consolidation grouting up to 20 m.

intensities reaching 8–9 degrees according to the Mercalli scale, take place. On the same watercourse but 70 km upstream, the construction of an even higher earth–rock dam Rogun has been started, with a designed height of 335 m[1].

11.3 EARTH–ROCK DAMS WITH A SLOPING CORE

Earth–rock dams with a core that is very inclined towards the upstream face, have the following advantages in relation to dams with a vertical core: (1) A smaller part of the dam's body is under water; (2) The downstream shell can be constructed as a whole, even then the core, which is significant for areas with a short construction season; (3) Filter layers between core and shells can be thinner and are easier to construct; (4) Grouting can be performed parallel to the construction of the downstream shell, which forms the greater part of the volume of the dam; (5) Pore pressure, immediately following the rapid drawdown of water level in the case of very inclined core, is

[1]The *Rogun* dam was to be completed in 1991; however, owing to the events in the region, the construction has been delayed and the completion of the entire hydraulic scheme is uncertain.

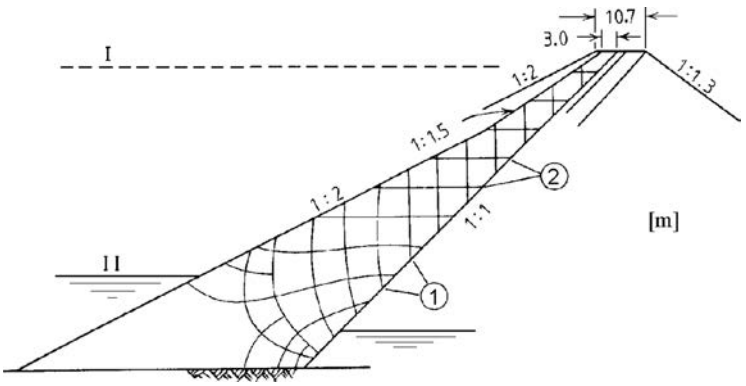

Figure 11.10 Flow net in case of a highly inclined core, immediately after rapid drawdown of water level (after Sherard et al., 1963). (I) Level at full reservoir; (II) level at rapid drawdown of reservoir. (1) flow lines; (2) equipotentials.

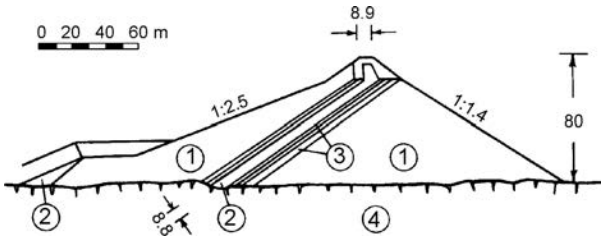

Figure 11.11 Nantahala dam (USA). (1) Rockfill; (2) clay core; (3) transition zones; (4) rock foundation.

practically zero, which can be seen from the shape of the equipotentials in the example in Figure 11.10 (Sherard et al., 1963).

On the basis of the above-cited advantages of the two types of earth–rock dams, it is not generally possible to give advantage to any of them, but the assessment should be made on the basis of the specific local conditions for each individual case. We would make mention of the fact that the volume of the two types of earth–rock dams is approximately equal, since, in the case of the sloping core, the upstream slope is made slighter, while the downstream slope steeper in relation to a dam with a vertical core.

One of the first known dams with a highly inclined core is Nantahala, in the USA (Fig. 11.11), built at the beginning of the forties of the previous century. Owing to the small quantities of available coherent material, the core was constructed with a small thickness, and calculated so as to provide satisfactory water-impermeability. After nine years in operation, the vertical settlement at the crest has reached 66 cm, with the greatest horizontal displacement being 31 cm. The elastic core has easily adapted itself to such deformations, at which the seepage water quantity has remained relatively small, 4.67 m^3/day (Golzé, 1977).

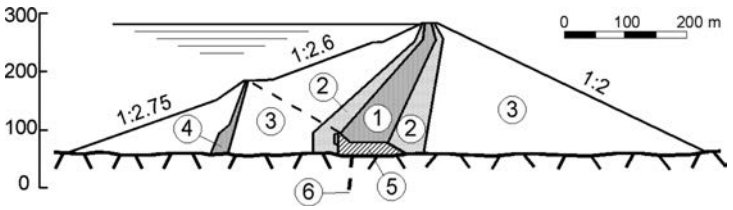

Figure 11.12 Oroville dam (USA). (1) Core; (2) transition zones; (3) shells of gravel and round stones; (4) core of the cofferdam; (5) concrete block; (6) grout curtain.

During the last two or three decades, earth–rock dams with slightly sloping cores became popular, by means of which endeavours have been made to remove some of the disadvantages of dams with highly sloped cores, while, at the same time, to keep their advantages. One of the most significant dams of this type is Oroville dam (California, USA), completed in 1967. The material for filling of this dam's body and the transition layers – 59 millions m^3 – consisted of sand, gravel, and round stones, what remained leftover from the excavation, washing out, and separation of the alluvial sediments that had been carried out by gold-diggers in the course of the fifties at the end of the nineteenth century and the beginning of twentieth century. As a result of this treatment, the finer particles of gravel had been separated and stockpiled further away, so that there had been a possibility for a separate extraction of the gravel and round stones for placement into the shells of the dam, as well as the sand used for construction of the transition zones. Figure 11.12 shows a cross-section of the dam along with three zones of different material. The core, with an inclination of the upstream slope of 1:0.9 and downstream slope 1:0.5, consists of clayey sand and gravel placed in layers of 25 cm each, in a compacted state. In the body of this 235 m high dam, a 91 m high cofferdam was also incorporated, under whose protection the remaining part of the dam was constructed. The core is founded on a thick concrete foundation block, which had also served as a base for grouting (Moyseev, 1977; Golzé, 1977).

Large dams, with a slightly sloping core, were also built in Macedonia. One of them, Turiya (Fig. 11.13), was constructed in the sixties in the vicinity of Strumica. The embankment is 80 m high and is made of a thick layer of alluvial sediment (7). The clay core is founded on wells of clay–concrete (6), which has a lower stiffness than concrete, which makes it possible to adapt to deformations. The mix of clay and concrete is so designed as to correspond to the requirements set up with the seismic analysis – to be water-impermeable at least the same as the core, and to be able to be built-in by means of pumps, which also governed its composition: dry mass:water = 2:1 and clay:cement = 3:1. It has an achieved strength of the incorporated clay–concrete greater than 1500 kN/m^2. It can be noted that the upstream slope is steeper than the downstream one, because a bigger part of the downstream shell was constructed of gravel, and also because there is ballast material filled at the upstream end (YCOLD, 1970, 1971).

Another embankment dam, but with slightly sloping core, was built in Macedonia between 1964 and 1968. This was the Tikvesh dam, with a height of 104.5 m (the structural height is 113.5 m), the highest embankment dam not only in Macedonia,

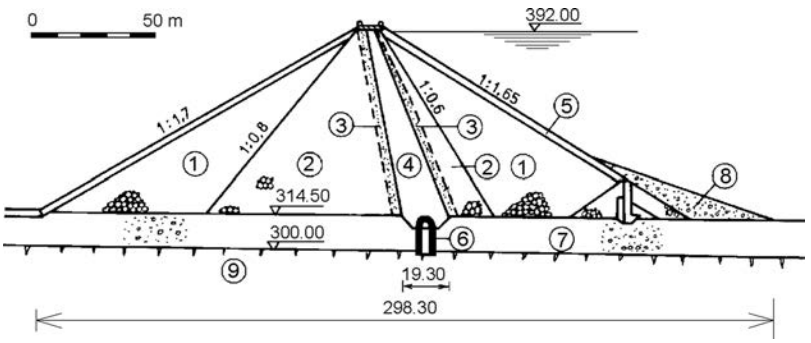

Figure 11.13 Turiya dam (Macedonia). (1) Rockfill; (2) gravel; (3) filter layers; (4) clay; (5) protection of coarse stones; (6) clay-concrete; (7) alluvial sediment; (8) ballast of river sediment; (9) layered schists and gneisses.

but also within the territory of the entire former Yugoslavia. It dams the river Crna Reka in the vicinity of Kavadarci and enables storing of 475×10^6 m^3 water, aimed at facilitating irrigation of the Tikvesh Field (18,300 ha), as well as for more than 200 GWh mean annual electricity production (Figs. 11.14, 11.15). The foundation at the dam site consists of various kinds of schists, while in the riverbed amphibolites can be found. The rock mass, mainly, is non-homogeneous and anisotropic. The dam has been built of sericite-quartzite schists, obtained from the quarry at a distance of 1–1.5 km. At this dam probably for the last time in Europe was applied the construction of the dam body with dumped rockfill, without compaction with rollers. The stone is dumped in layers of 5 m each, and compacted only with hydromonitors, with an angle of repose of the slopes, so that a berm is formed between each of the layers in order to achieve the necessary average inclination of slopes of 1:1.7. The thin clay core (2) is slightly inclined and is compacted in layers of 20 cm each by means of sheepsfoot rollers and compactors. It is joined with the foundation through a grouting gallery, which rests on a massive concrete block (9), cutting the alluvial deposit (10) in the river bed (Fig. 11.15). Two filter layers (3, 4) were placed on each dam side between the core and dam shells. The upstream rockfill cofferdam (7) with clay screen (8) was incorporated in the main dam body. A three-row grout curtain is constructed from the gallery, which is described and presented in Chapter 2, section 4. The dam site is rather narrow, with a ratio dam length:dam height = 3.4. The crest dam axis is slightly curved in its layout. The whole hydraulic scheme (the dam and appurtenant structures), was built from August 1964 to March 1968.

Tikvesh dam was equipped with measuring instruments in accordance with the prevailing practice of the 1960s, when it was designed and built. With the installed instruments and devices, almost all in good order during the first reservoir filling and the beginning of the service period of the hydraulic scheme, it was possible to register the necessary data for evaluation of the dam's behaviour.

As a consequence of the relatively fast dam construction, as well as the method of compaction of the shells – in thick layers of 5 m each, with hydromonitors – relatively large dam crest settlements have occurred during the reservoir filling and the

Figure 11.14 Tikvesh dam (Macedonia), with reservoir water level at 15 m below normal.

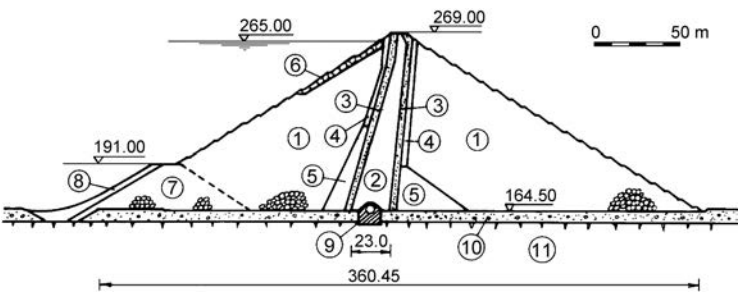

Figure 11.15 Tikvesh dam (Macedonia). (1) Rockfill; (2) clay core; (3) filter layer I; (4) filter layer II; (5) stone chippings; (6) coarse stones; (7) cofferdam of rockfill; (8) clay screen of cofferdam; (9) grouting gallery; (10) river sediment; (11) rock foundation.

first decade of service, exceeding the value of 220 cm in the highest dam cross-section. This phenomenon can be clearly seen in Figures 11.16 and 11.17. Namely, the dam and appurtenant hydraulic structures were finished at the end of November 1967, and in March 1968 the first reservoir filling started. From Figures 11.16 one can see that in the longitudinal section the dam crest was built with a "camber" (see the "as-built" line at 29.11.1967). Namely, at the highest (central) cross-section, the dam crest elevation was raised to 270.85 m a.s.l., instead of to the designed level of 269.00 m a.s.l., in order to compensate the predicted settlement. Some 15 years later, the line of dam crest was at a much lower position almost over the whole dam length (3.6.1982, Fig. 11.16), with the dam crest at an elevation of 268.68 m a.s.l. in the central dam cross-section. Because the left bank of the dam site is steeper than the right one, consequently, the settlements in the left dam side are larger than in the right one (see

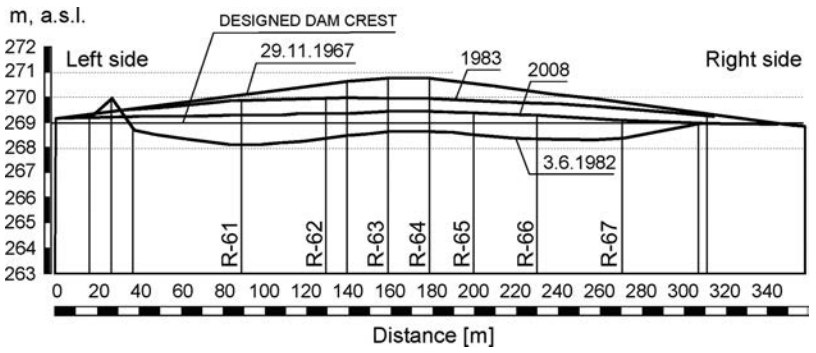

Figure 11.16 Tikvesh dam, longitudinal dam section with the vertical variations of the dam crest from November1967 to June 1982; R-61 to R-67: measuring points located on the dam crest.

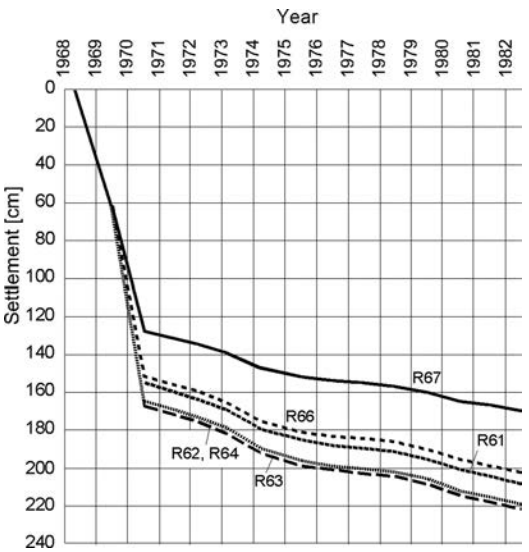

Figure 11.17 Tikvesh dam, settlement of characteristic measuring points on the dam crest during the first reservoir filling and the beginning service period.

the line at 3.6.1982). This is also clear from Figure 11.17, where the settlements of characteristic measuring points on the dam crest during the first reservoir filling and the beginning service period are shown. The reservoir closure was done at the end of March 1968, and in October 1968 the power plant was put in service. A very large degree of settlement was registered from the beginning of the reservoir filling (March 1968) to June 1970, with average values from 58 cm per year (measuring point R-67 on the right side), to 80 cm per year, or 1.5% of the dam height for somewhat more than two years (March 1968-June 1970, measuring point R-63 and R-64 at the central dam cross-sections). From Figures 11.17 and 11.18 it is clear that the starting point of the largest rate of settlement corresponds with the highest water level in the

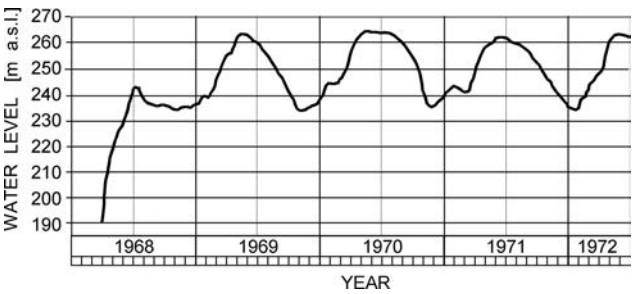

Figure 11.18 Tikvesh dam, variations of the water level in the reservoir during the first filling and first three years of service period.

reservoir (≈263 m a.s.l.), reached during the first reservoir filling (June 1969). Then, in November 1969 the water level dropped to a minimum level of ≈233 m a.s.l., before again reaching its peak (≈264 m a.s.l.) in May–June 1970. At this moment the very large rate of settlements stopped. Over the next service period of 12 years (June 1970–June 1982) the tendency of large crest settlement continued, but at a lower rate of approximately 3.3–4.5 cm per year (Fig. 11.17). At the same time, the fluctuations of the reservoir water level were rather regular with a minimum level of 233–235 m a.s.l. in late autumn or early winter, and peaks in May–July (Fig. 11.18, only the period to June 1972 is shown) (Tančev and Milevski, 2009).

As a main consequence of this occurrence, the dam crest was at a lower level than was designed (269.00 m a.s.l.), almost across the whole dam length, reaching the lowest level of 268.00 m a.s.l. at point R-61 (Fig. 11.16). The crest in the highest dam cross-section, located between points R-63 and R-64, in June 1982, is shown with full lines in Figure 11.20. Due to larger camber, the crest in this section is at a higher level, compared with the cross-sections with a lower height (for example R-61 and R-66, Fig. 11.16).

Parallel with the appearance of large settlement, also unusual horizontal movements have appeared at different measuring points on the dam surface. The largest values are registered in the central cross-section, on the downstream slope, at a level of 267 m a.s.l., just below the dam crest (Fig. 11.19). Horizontal movements with a very large rate of 100 cm per year started in the middle of 1968, when the water level in the reservoir reached ≈242 m a.s.l. After the middle of 1969, up to the end 1979, the rate gradually decreased. Then, from 1980 up to now, the rate became almost constant, at ≈1.7 cm per year. But, the total maximum horizontal movement in the whole service period has reached a considerable value of more than 200 cm. This is, without a doubt, closely connected to the large registered crest settlement.

To improve the unfavourable situation caused by the very large crest settlement, i.e. to eliminate the danger of dam overtopping, in 1983 the dam crest was rebuilt up to 1.9 m above the existing level (1982, Fig. 11.16), with the prediction that in the future the rate of the crest settlement will be in the range of up to 2 cm per year. Figure 11.20 shows the highest dam cross-section before the reconstruction (June

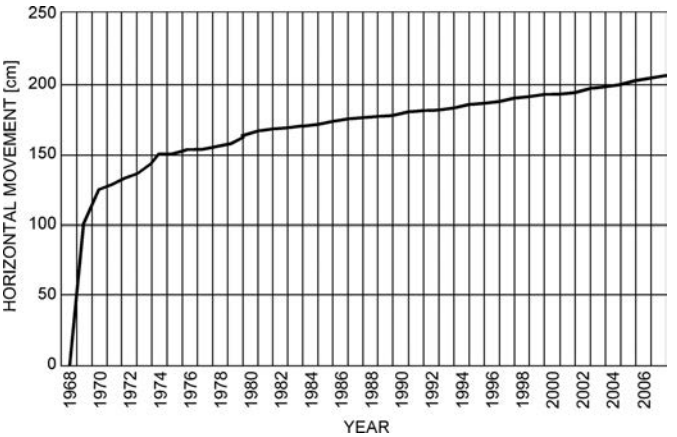

Figure 11.19 Tikvesh dam, horizontal displacements of a measuring point on the downstream slope at a level of 267 m a.s.l., in the central dam cross-section, during the first reservoir filling and the service period.

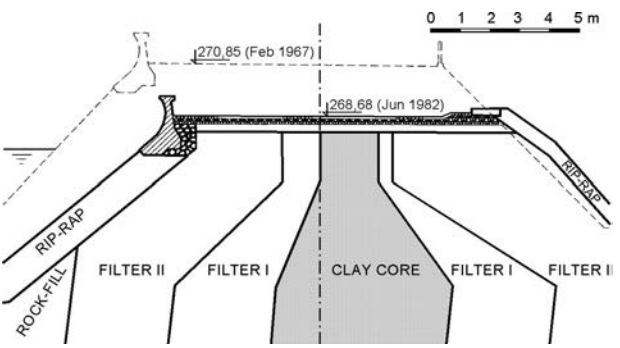

Figure 11.20 Tikvesh dam, typical cross-section with an "as built" dam crest (dashed line, February 1967), and settled position (June 1982).

1982), while Figure 11.21 shows the same cross-section after the reconstruction, performed in 1983. At this cross-section the dam crest was raised to 270 m a.s.l., i.e. 1.0 m above the original design. The reconstruction was done in such a way, that the old parapet wall was left in place, while a new one was built at higher level. This can be also seen from Figure 11.22.

In the next service period (from 1984 to 2008) the measured settlements of the points on the crest were with rather lower rate comparing with the previous period – from 1.2 to 1.7 cm per year (Fig. 11.23). That means the prediction of 2.0 cm per year, made before the reconstruction of the dam crest, was on the side of the safety. But, from course of the lines shown on Figure 11.23, it is clear that the settlement will continue, despite during the service period of 40 years it reached the rather high total value of about 2.5% of the dam height.

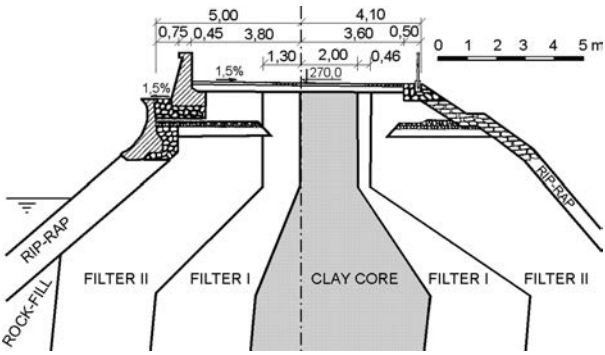

Figure 11.21 The crest of Tikvesh dam after the reconstruction in 1983 (the highest dam cross-section).

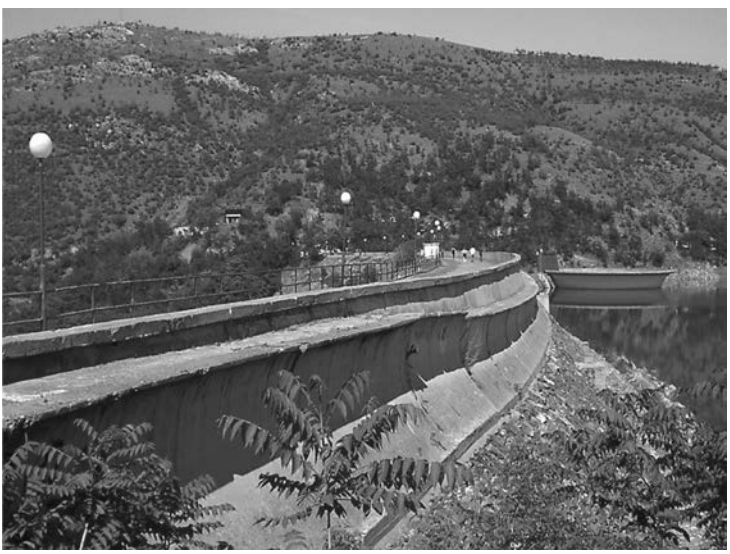

Figure 11.22 Tikvesh dam crest today, with both new and deformed old crest parapet wall.

Figure 11.24 shows the measured settlements at six embankment dams in R. Macedonia, and at three abroad, during the first nine years of their use life. Tikvesh Dam demonstrates the largest settlement and the only dam that comes close is Salt Springs (built 1931), a reinforced concrete faced rockfill dam, also built by dumping of rockfill, without compaction with rollers. At the other dams in Republic of Macedonia much lower values of settlements have been measured (1–5, Fig. 11.24). In the case of the highest dam Kozyak (R. Macedonia, commissioned in 2004), extremely small settlements were registered, mainly due to sound compaction of the clay core and limestone shells in thin layers.

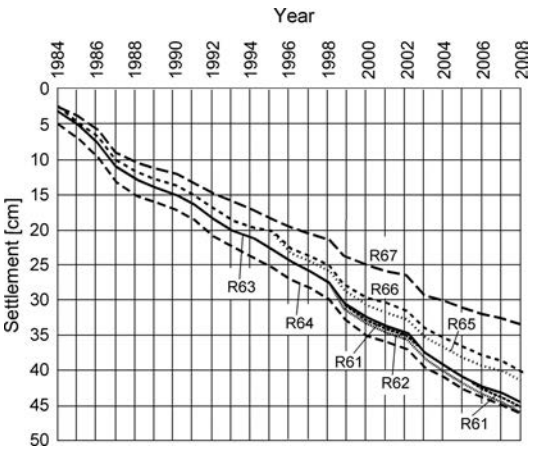

Figure 11.23 Tikvesh dam, settlement of characteristic measuring points on the dam crest after the reconstruction in 1983.

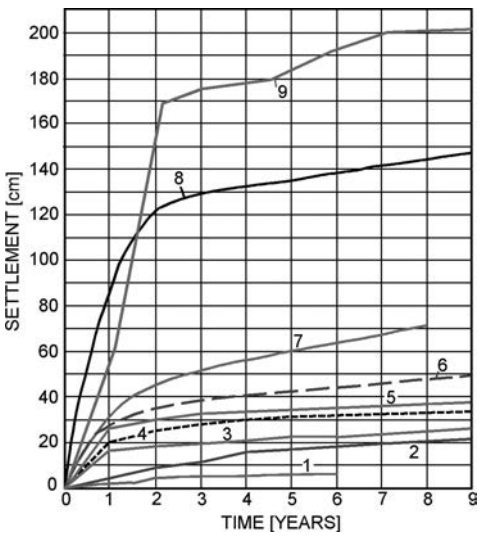

Figure 11.24 Settlement of dam crest at some embankment dams. (1) Kozyak, $H = 114$ m; (2) Mavrovo, 54 m; (3) Turiya, 77,5 m; (4) Globochica, 82,5 m; (5) Shpilje, 101 m; (6) Bou Hanifia, Algeria, 70 m; (7) Nantahala, USA, 88 m; (8) Salt Springs, USA, 100 m; (9) Tikvesh, 104 m.

The case study of the Tikvesh dam has confirmed that the placement of the rock-fill in thick layers and its compaction using only hydro-monitors is not an efficient construction method. But, despite such a large settlement of 1.5% of the dam height occurring in the central dam cross-section during the first reservoir filling, thanks to the rather large "camber" of the dam crest, provided during the construction, there

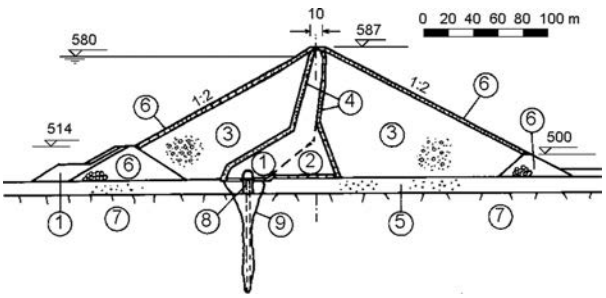

Figure 11.25 Cross-section of Shpilje dam (Macedonia). (1) Clay core; (2) clayey gravel; (3) gravel; (4) filter layers; (5) river sediment; (6) coarse rockfill; (7) limestone; (8) caisson diaphragm wall with grouting gallery; (9) grout curtain.

was no danger of overtopping of the dam. The dam was successfully repaired without any permanent consequences.

Two significant embankment dams, each with a slightly sloping core, were built on the river Crn Drim – Globochica ($H = 82.5$ m) and Shpilje. Shpilje dam, located immediately before the discharge of the River Radika into the river Crn Drim, was constructed between 1966 and 1969. With its height of 101 m above the ground, it impounds a storage space of 520×10^6 m^3. The dam was constructed of gravel with a clay core (Fig. 11.25). The foundation of the dam site has a complex geological structure. Basically, limestone and marly schists are present, while in the riverbed, alluvial sediments reach a depth of 12 m. Because of tectonic damage conditions, materials in the foundations of these dams are moderately to high water-permeable.

Each dam's body is filled with coarse gravel, which was present in the riverbed of Radika in enormous quantities. The core is executed with additions of sand and gravel, used from a borrow pit at a distance of about 1 km. The filter layers were made of sand transported some 2.5 km.

Gravel is compacted in layers of 1 m each in loose condition, by means of vibratory rollers, with 6–8 passes and by addition of 50–100 litres of water per m^3. Filter layers, 3.5 m wide, have been filled in layers of 0.5 m and compacted also by means of vibratory rollers. The core was constructed in layers of 25 cm each, using compaction with sheepsfoot rollers.

Dam site was selected as the most convenient one from a viewpoint of ground topography. The core structure is characteristic, because of its broken form. In the upper part it is slightly inclined, while the lower part is very much inclined in order to achieve a good joint with the caisson diaphragm wall, below which – in an optimum position, determined by means of investigations – the grout curtain is located. To decrease both the hydraulic gradient of seepage as well as the danger of fissures, the lower, broken part of the core was widened towards the downstream face with a wedge of clayey gravel.

Along its banks, i.e. dam abutments, the dam foundation lies on surface-cleaned rock, while the sediment material in the riverbed is cut off with a concrete diaphragm wall 6 m thick in its greatest part, worked out as a caisson type under conditions of

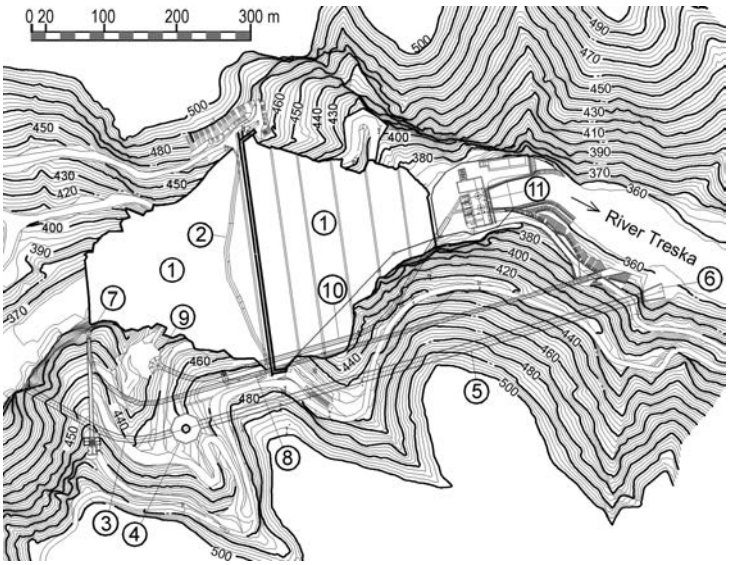

Figure 11.26 Layout of the hydraulic scheme with Kozyak Dam. (1) Dam body; (2) grouting gallery; (3) diversion tunnel; (4) morning glory (shaft) spillway; (5) spillway tunnel; (6) flip bucket; (7) intake structure of the bottom outlet; (8) bottom outlet tunnel; (9) intake structure of the power plant; (10) water supply tunnel for the power plant; (11) tail raise channel.

an unprotected construction pit. The diaphragm wall was constructed by sinking four caisson blocks, each 12 m long with free space, in between 0.8–1 m, and then filled with sediment. At the downstream face, this interspace is closed by means of Larssen sheet piles and by grouting with a clay-cement mixture. The diaphragm wall is embedded 1–3 m into the foundation rock. Through a grouting gallery, which is placed on a caisson diaphragm wall in the riverbed, a grout curtain 100–145 m deep was constructed.

In the summer of 2004 the highest dam in Macedonia was commissioned – Kozyak Dam, on the river Treska, a tributary of the river Vardar, some 16 km upstream from the existing dam Matka. This is a key-structure in the multipurpose scheme whose main task is flood protection with retention storage of 100×10^6 m^3. Also it will serve for electricity production (152×10^6 kWh per year) and water-supply. Figure 11.26 shows the layout of the dam with appurtenant hydraulic structures. The construction of the hydraulic scheme started in 1994. The dam was constructed in the period September 1997–March 2000, while the first reservoir filling was performed from May 2003 (water level 362 m.a.s.l.) till June 2004 (water level 452 m.a.s.l.).

The Kozyak Dam is an earth–rock dam with a structural height of 130 m, and with a height above the terrain of 114 m (Figs. 11.27, 11.28). The dam site is narrow, with valley slopes of 1:1 and 1:1.5 respectively. The dam body is built from rockfill (limestone), taken from the quarry near the dam, and compacted in layers of 80 cm. The waterproof element is in the form of a slightly inclined clay core. The transition zones and the core are founded on the base rock (limestone), while the shells are placed

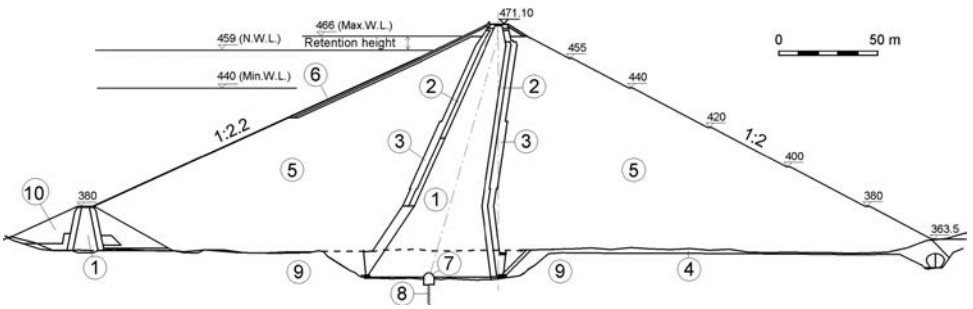

Figure 11.27 Main cross-section of Kozyak Dam. (1) Clay core; (2) first transition zone; (3) second transition zone; (4) river deposit; (5) rockfill shells (limestone); (6) arranged slope protective stones; (7) grouting gallery; (8) grout curtain; (9) rock foundation (limestone); (10) gravel in the upstream cofferdam.

Figure 11.28 Upstream view of Kozyak dam before the dam closure in 2003.

on the river deposit. The dam slope inclinations are rather gentle (1:2.2 upstream and 1:2 downstream) because the dam is located above the city of Skopje, a region with high seismicity. The clay was transported from distance of 15 km. For transition layers, separated material from the river Treska was used, but an additional quantity of material was transported from a distance of 40 km away.

The dam is instrumented with all necessary measuring devices. After the dam construction and the first reservoir filling, the dam behaviour is estimated as normal. The intensity of measured values of both vertical and horizontal displacements is very

low and confirms that the dam body is very well compacted. In the first years of service the main attention has been paid to the filtration through the foundation. Namely, the limestone in the foundation and in the abutments has some irregularities, and, despite intensive grouting works performed during the construction of the scheme, additional grouting works have been done after the first reservoir filling, and even more are planned.

11.4 EARTH–ROCK DAMS OF 'SOFT' ROCKS

The formerly described dams were constructed of rockfill whose properties correspond to the requirements described in Chapter 6, section 5. However, ever-increasing needs for water in certain situations impose the employment of soft rockfill, which, according to recent comprehension, has been deemed useless for earth–rock dams. From a geotechnical aspect, the term *soft rockfill* implies material that has been obtained from weak rocks, that breaks during handling. At that, a considerable quantity of stone chippings is obtained, which fills the voids into placed layers. As a result, placed material has low permeability and matches to earth embankment, not to rockfill, whose grains are characterized with large strength and voids between grains. Soft rockfill is used lately for Evretou dam, Cyprus, built between 1984 and 1986, with its first filling of the reservoir in the winter of 1986–87.

The dam, which is 72 m high, with a vertical core (Fig. 11.29), has shells of weak limestone that has been softened under influence of water. This material has been used as a result of shortage of other material and also due to the fact that, over alluvial foundation resting on marl, other type of dam with the required height cannot be constructed. The compressive strength of test samples has ranged from 24 to 30 MN/m^2. Three borrow pits of materials have been investigated, of which two have been selected for use, with materials denoted class *B*, i.e. class *C*. During the construction of a trial embankment it has been stated that the quality of material from borrow pits varies more than it has been anticipated. Owing to this, certain alterations

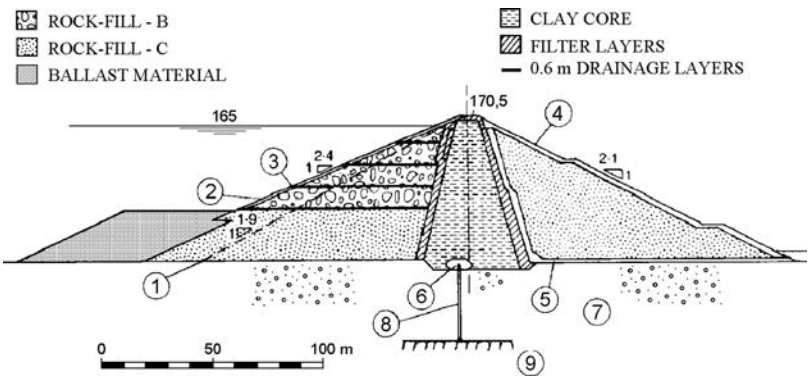

Figure 11.29 Cross-section of Evretou dam (after Brown, 1988). (1) Slope, anticipated in design; (2) layer of selected rockfill; (3) horizontal drainage layers; (4) lining of rockfill, class B; (5) drainage of gravel; (6) plastic clay; (7) alluvial deposit; (8) diaphragm wall; (9) marl.

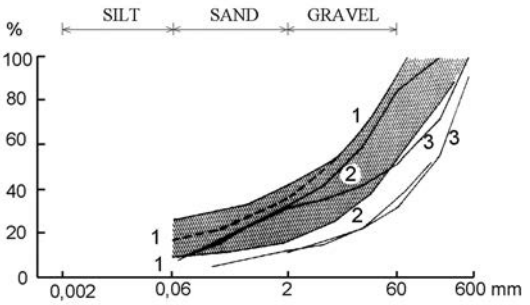

Figure 11.30 Comparison of the granulometric composition for used soft rockfill in three dams (after Brown, 1988). (1) Weak limestone – Evretou; (2) sandstone – Mangrove Creek; (3) sandstone – Scamonden.

of dam's cross-section have been carried out. Better material (class *B*) has been placed into the upper part of the upstream shell, while instead of significant warping of the upstream slope, the worst material from the borrow pits has been placed into the toe. In the remaining part of the shells, material of class *C* has been incorporated, with a curve of granulometric composition within the hatched area (Fig. 11.30). The curves indicate that on an average some 25% of the material passes through the sieve 2 mm, while 15% of the material passes sieve 0.06 mm, which means that the material contains an unusual quantity of fine particles originated with crushing of the material. As a consequence of crushing of the grains, during compaction of the material, a tendency has occurred for the fine particles to emerge on the surface of the layer. When they have emerged in considerable quantity, they have been removed and replaced with coarser material. In order to prevent washing out of these particles at greater hydraulic gradients, an upstream filter layer is carried out, even though the customary filter rules had indicated that it had not been necessary. Behind the downstream filter layer it is constructed drainage in the form of a chimney and a horizontal blanket below the downstream shell, with a task: at possible concentrated seepage through a fissure in the core – not to allow saturation of the soft rockfill in the downstream shell, which would endanger the slope stability (Brown, 1988).

In addition to the above-mentioned measures, in the course of construction there have also been anticipated the following measures, assessed as indispensable in order to enable use of soft rockfill:

- Thickness of the layers is reduced to 0.5m for material of class C, i.e. 0.7 m for material class B;
- During spreading of material, water was added (1% by volume) by means of sprinkling, to enable better compaction of the layer;
- For reducing pore pressure at rapid drawdown of water level, in the upper part of the upstream shell there have been constructed horizontal drainage layers of thicknesses 0.6 m each, spaced at vertical distances of 10 m, made of selected gravel;

- The upstream slope is lined with a layer of rockfill (2 m), while the downstream slope is lined with material of class B;
- In the upstream shell, hydraulic piezometers have been incorporated for controlling the work of the horizontal drainage layers.

The dam also has particular conditions for founding, since it lies on a layer of alluvial deposit with a thickness up to 40 m. This layer is completely cut off by means of a diaphragm wall of bentonite, constructed in a narrow foundation pit, kept in a stable state during construction by means of suspension. In the upper end, the diaphragm wall is surrounded with a cap of plastic clay, while in the lower end it reaches marly rock.

In the course of dam construction and filling of the reservoir, considerable displacements were observed (vertical displacements have reached 29 cm, while horizontal ones achieved 5.3 cm), as well as irregularities in the dam's operation. It can be concluded that soft sedimentary rock can be used for construction of earth–rock dams, provided we anticipate appropriate measures and structural solutions.

11.5 FISSURES IN THE CORE OF EARTH–ROCK DAMS

11.5.1 Kinds of fissures and causes for their occurrence

One of the most important issues in the assessment of the construction of earth–rock dams is the degree of safety against the occurrence of fissures in the core (Sherard, 1973). The problem is aggravated with the fact that this phenomenon cannot be visually observed, but only consequences can be perceived – damage, even a failure of the dam, which is often erroneously attributed to other causes. The analysis of results from observations on already constructed dams enable to perceive the basic causes for generation of fissures in the core, which can be stated in two main groups: (1) *Non-uniform deformations* of the dam as a whole, in its individual structural members or in the foundation; (2) *Hydraulic fracture*.

A number of factors make influence on the degree of danger for occurrence of fissures: *topographic conditions* in the zone of dam site, *geological conditions* in the foundation, *structural particularities* of the dam, properties of built-in materials, rate of construction progress and filling of the reservoir, intensity and duration of possible seismic effects, atmospheric influences etc. (Khan, 1983). Fissures generated in the core, can be classified in the following way:

1. According to their location and geometry – surface fissures, internal fissures, transverse fissures (parallel to the river course), longitudinal fissures (parallel to dam axis), narrow ($\delta < 1$ mm), wide ($1 < \delta \leq 5$ mm) and open fissures ($\delta > 5$ mm);
2. According to the influence that causes them, fissures may originate during static action of the mass of the filling material, from water pressure from the upstream face, dynamic or seismic forces, or due to atmospheric influences in the surface part (freezing and thawing, drying, etc.);
3. According to the character of origination, fissures may originate due to tension (usually at the crown), due to shearing (most frequently in the vicinity of the contact core-foundation), or due to seepage erosion in the contact core-filter;

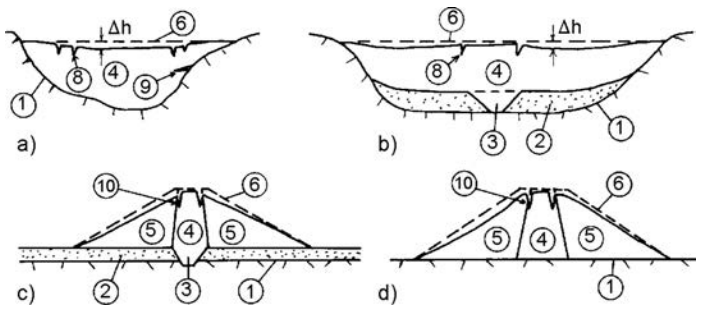

Figure 11.31 Scheme of spots of occurrence of fissures owing to non-uniform deformations. (1) Rock; (2) incoherent sediment; (3) cutoff trench of well- compacted material; (4) core of well-compacted material; (5) shells; (6) contour of the dam before settlement; (7) after settlement; (8) vertical transverse fissures; (9) horizontal transverse fissures; (10) longitudinal fissures.

4. According to the potential danger – fissures may create concentrated paths of seepage through the core; dangerous fissures, which do not pass through the entire thickness of the core, occur near the crest or else are hidden in the interior; however, under additional influences, these could be extended and become very dangerous; less dangerous, small and shallow fissures in the upper zone, which can be repaired simply and at a low cost.

Figure 11.31 shows the schemes for cases when it comes to fissures most frequently caused by non-uniform settlements. Vertical longitudinal fissures are due to the non-uniform settlements at a narrow dam site with steep banks, i.e. abutments (a). In other words, due to a different settlement of the loose, deposited material and well-compacted core (b). Horizontal longitudinal fissure (9) in drawing (a) is due to the sudden change in the inclination of the bank, i.e. dam abutment. In the cases of drawings (c) and (d), longitudinal vertical fissures occur in the contacts core-shells in the vicinity of the crest due to non-uniform settlement. The first case is caused by significant settlement of the incoherent deposit material, while the second case is caused by those of the shells. It is important to point out that when there exist conditions for occurrence of fissures, it is more unfavourable if the core is constructed of low-plasticity earth material, especially if compacting has been performed with moisture, which is lower than the optimum.

Fissures can occur in the core near the crest at the first filling of the reservoir and due to the variations of water level in the course of dam service. Generally speaking, under the effect of water the lower part of the vertical or slightly sloping core, shifts towards the downstream face, while the upper one shifts towards the upstream face, which create conditions for occurrence of tensile zones that usually result in fissuring. Let us follow through that process on the example of Gepatch dam, on the basis of results from measurements at the first filling of the reservoir and in the course of the first seven years of operation. Figure 11.32a presents the crest of the dam with points A, B, C and D on the surface, whose displacements are recorded twice a year, at low

water level and high water level. From the lines of displacements (Fig. 11.32b) it can be seen that the main direction of movement of points A, B and C is towards the upstream face, meaning in the opposite direction of the loading action of water. Only point C, which lies on the downstream slope, is shifted towards the downstream face so that the centre line (zero line) of horizontal displacements lies somewhat downstream from the crest of the dam. Thus, expansion has occurred between points A and B (4.8%) and B and C (3.7%), while contraction has occurred between points A and D (–1.25%), which leads to a number of longitudinal fissures (2); however, without a harmful effect. The vertical settlement of dam's crest reached 2 m or 1.3% of dam height, at which the plastic properties of the material in the core have had a favourable effect in preventing considerable damage (Borovoy, 1976).

A number of other examples of dams are known for which longitudinal fissures at the crest have been recorded. For example, at Cooger dam (USA), completed in 1963, 158 m high, 480 m long, with a loam core, transition zones of gravelly earth and shells of rockfill, there have occurred longitudinal fissures at the crest, in the contact of the core and the upstream filter layer. Fissures have opened up to 1.8 cm, while the upstream edge of the crest settled 30 cm more than that of the downstream edge. Analogous fissures also occurred at Round Butt dam (USA, 1964), $H = 132$ m, $L = 420$ m, with a slightly sloping core (Ayrapetyan, 1979).

Observations on already constructed dams show that, under earthquake effects, in the vicinity of the dam, fissures and fractures are formed of different directions and depths. Most widespread are longitudinal fissures in the core and in the contacts of the core with adjacent zones, but they can also occur in the lower parts of the core and in the shells. In the case of dams that are built in a seismically active area, it is necessary to undertake particular measures for preventing fissures. The crest, where the greatest deformations occur, should be wider, like the transition zones, which, in addition, should also have similar deformable properties with the core.

Regarding earth–rock dams, *internal longitudinal* fissures are more dangerous. The most frequent cause for their occurrence is layers in the foundation, which are susceptible to deformation. In this, the rapid drawdown of the reservoir under such conditions is a particularly good stimulator for longitudinal internal fissures.

Another cause for the occurrence of fissures in the core that is in practice and theoretically verified, is the *hydraulic fracture*. This only originates at a full reservoir if in a certain point of the core or in its contact with the foundation, the value of normal stress becomes smaller than the value of hydrostatic pressure (head) γH. This takes place due to the transfer of stresses in the contacts of materials with different deformable properties: when the 'softer' material 'is hanging' from the stiffer one and causes a transfer of part of the stresses, unloading itself. This phenomenon is analysed and cleared up in a later period, thanks to the results from observations on already-constructed dams, as well as the analyses by means of the Finite Element Method, which was discussed in Chapter 8. It is assumed that, due to hydraulic fracture, fissures have occurred in a number of dams, but these have been without significant consequences, either because of the small water pressure above the fissure, or due to the successful self-healing by means of the filter layer. There are cases when it has been necessary to undertake expensive remedial measures (grouting, additional diaphragm wall); for example, at dams Boulderhead (G. Britain, $H = 50$ m) and Niteyuvet (Norway, $H = 90$ m), both of them with a thin central core. Professional literature pays significant attention to the

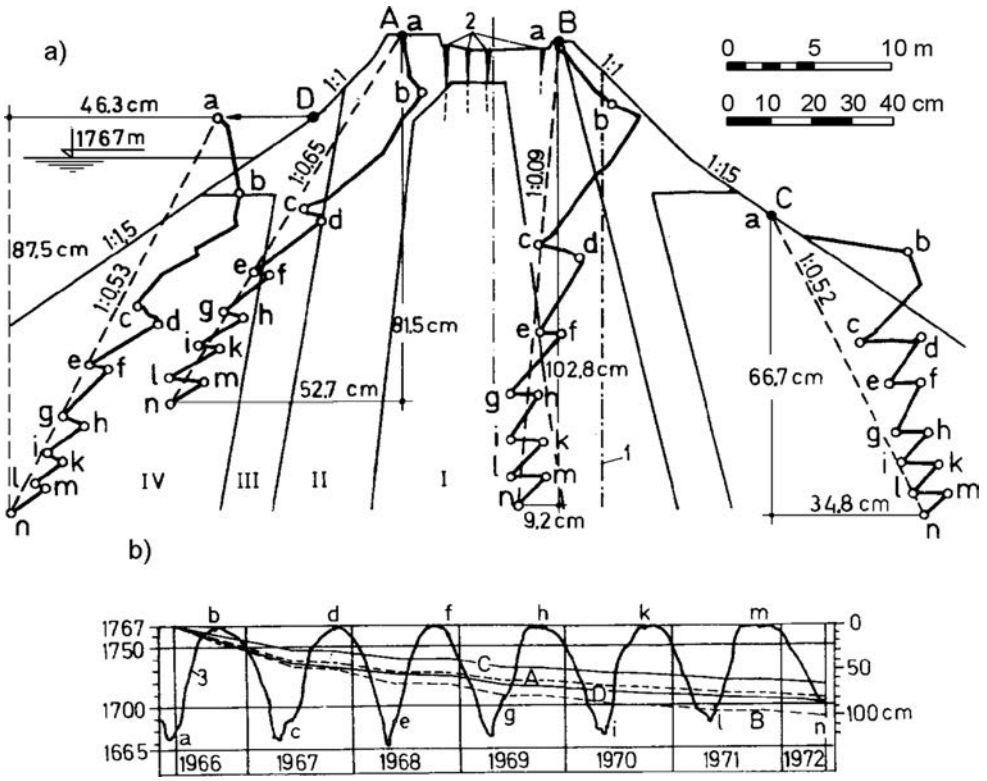

Figure 11.32 Crest deformations in a major cross-section of Gepatch dam. (a) (I) Core with sandy loam, in the upstream part enriched with 1% bentonite; (II) and (III) transition zones; (IV) rockfill; (a–n) displacements of surface points A, B, C and D in the course of time. (1) centre line of horizontal displacements; (2) longitudinal fissures; (b) (a–n) variations of water level in the course of time; (3) line of water level variations; (A, B, C and D) curves of settlement in points A, B, C and D.

occurrences of transfer of forces between materials with different deformable properties and hydraulic fracture (Kulhawy & Gurtowski, 1976; Nonveiller, 1983; Sherard, 1986; Squier, 1970; Tančev, 1989). However, further work is needed for a complete understanding of this mechanism, particularly with the application of complex three-dimensional numerical analyses.

11.5.2 Measures for preventing the occurrence of fissures

Internal fissures may be recorded indirectly through instruments for measuring stresses and deformations, but can also be indicated through the occurrence of muddy seepage water. For a timely reaction, it is clear what the significance is of a regular and permanent monitoring of the dam – through built-in instruments and visual observations. Regarding the monitoring by means of built-in instruments, it must be emphasized that there are not yet special instruments and devices for direct recording of fissures, so that additional work and efforts should be made for the invention of the same.

Because of the individual character of each dam site and of each dam, it is difficult to give general or common rules for the design and construction of dams, which will be safe against the occurrence of fissures in the core. That is why, in each specific case, it is necessary to analyse cautiously the possibilities for occurrence of fissures caused by the described phenomena, in order to undertake the most appropriate and precautionary measures. Yet, on the basis of presented material, as well as experience from world practice, we draw the following recommendations:

1. Pay particular attention to the selection of earth material of which the core of the earth–rock dam is to be constructed. For that purpose, it is necessary to perform profound investigative works for determination of physical-mechanical and chemical properties of materials anticipated for incorporation. The use earth materials originated with airing out of granites is not recommended, as well as materials whose fine particles contain a considerable percentage of sodium cations. Such material is susceptible to erosion.
2. Perform static and dynamic analysis by means of modern methods with whose aid, among other things, will also be evaluated the danger of fissures in the core. Conclusions will be drawn as to the need of modification, i.e. improvement of the foundation, construction of the dam and the regime for the first filling of the reservoir.
3. During execution of the core, pay particular attention to the method of compaction of layers, the uniformity of the granulometric composition and moisture, which must not be lower than optimum. This is particularly significant if low-plasticity material is to be built-in.
4. Carry out appropriate treatment of the foundation (Reinius, 1988), in order to provide uniform change of the slopes of banks, i.e. dam abutments (Russian regulations specify the change of inclination to be carried out at an angle of 10%).
5. Transition zones (filter layers), which can perform self-healing of an occurred fissure, should be properly selected and designed with appropriate dimensions and granulometric composition.
6. The rate of construction progress of the embankment should be adjusted to the characteristic of the earth material, with a possibility to come to certain dissipation of pore pressure in the course of construction.
7. Perform rigorous control of works during the preparation of the foundation, as well as during dam construction.
8. Assess properly the seismicity in the region of the dam and the influence of a possible earthquake on the dam.
9. Build in appropriate instruments, by means of which it will be possible to keep under observation deformations and stresses in the dam's body during its construction, the first filling of the reservoir, and the service period.
10. Anticipate an appropriate regime of the first filling of the reservoir in order to avoid the danger of hydraulic fracture.
11. Avoid grouting of the foundation through the core, since, under the effect of grouting pressure, fissures may occur in the embankment, through which the grouting mixture may penetrate into the transition zones (filters), deranging their structure.

When an internal fissure occurs, it is necessary to undertake measures for its more accurate siting and repair. Minor fissures are often self-healed by squeezing of the material from the upstream transition layer (the filter) into the core fissure, under the effect of water pressure. Non-healed fissures indicate that they are 'alive' through constant or progressive seepage. They require compulsory investigation and remedy. The first measure is to drawdown the water level of the reservoir in order to prevent erosion of the material. Then, investigations may be performed by digging a well, shaft, or by boring and pulling out undisturbed cores. Stated fissures may be filled with a clay suspension, prepared on the crest and squeezed by pump at low pressure. In more difficult cases, we may undertake more radical measures, such as execution of grouting core (Ortokoyskaya dam, Russia, $H = 53$ m), or placement of a facing of polymer sheets (Terzaghi dam, Canada, $H = 61$ m). There are cases of repairing, i.e. improvement by means of execution of additional asphalt facing.

Mica dam (Canada), whose design and construction commenced in 1967, will be described in continuation; consideration was taken for the danger of occurrence of fissures and a series of measures were taken for its elimination (Eisenstein & Law, 1977; Teyteljbaum et al., 1975).

Mica dam is 242 m high, with very steep banks, i.e. valley sides at the dam site (Fig. 11.33a, b). The foundation of this dam is rocky, composed of mica schists and granitic gneisses, with a not very thick layer of deposit that was removed from the construction foundation pit below the core. The core was constructed of clayey moraine materials (glacial deposits), while the shells were made of sandy gravel. Triaxial tests at high stresses have indicated that deformation characteristics of these two materials are not very much different, while, as well, the available rock material has been considerably more deformable, so that it has been used only in the end zones, under the

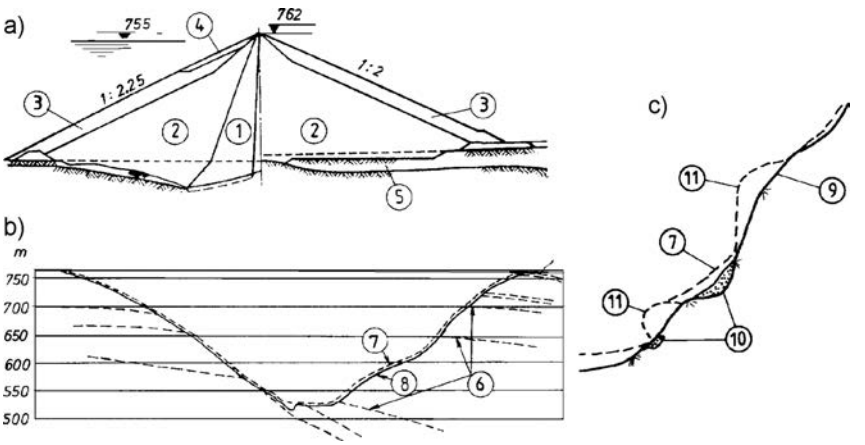

Figure 11.33 Cross-section (a) and longitudinal section (b) of Mica dam, along with a detail for treatment of the foundation (c). (1) Core of moraine material; (2) shells of sandy gravel; (3) sandy gravel and rockfill; (4) protection of the upstream slope; (5) alluvial deposit in the riverbed; (6) boundaries of layers in the foundation; (7) line of natural ground in the canyon; (8) line of core founding; (9) excavation up to sound rock; (10) concrete filling; (11) irregularities of the surface – corrected.

slopes. The moraine material has been given advantage in relation to the alternative plastic clay, owing to its good impermeability, high shear strength, good compatibility at moisture which is close to the natural one, favourable behaviour in relation to dissipation of pore pressure, low compressibility, and excellent ability for self-healing of any possibly occurring fissures.

The longitudinal axis of the dam is slightly curved, with the convex side towards the water. The core is slightly sloped towards the upstream face, but sufficiently to enable the downstream shell to be partially constructed prior to the core, so that the intensive settlement was to have occurred before construction of the appropriate part of the core. In the lower part, the core is widened towards the upstream face in order to enable an increase of the hydraulic gradient of seepage water. The upper part of the core and the dam's crest as well, gradually widen at the banks towards the ends of the dam, each at a length of 168 m, in which zone tensile stresses could be expected, and as a consequence of the above, longitudinal fissures.

Material in the shells is compacted very cautiously in layers of 30 cm each in order to keep additional settlement to a minimum. The foundation below the core is also carefully prepared, with thorough cleaning, easing and levelling of sharp breaks, while at some spots here and there, filling with concrete has been performed, Figure 11.33c. During the construction process, an especially rigorous control was maintained on the granulometric composition of materials, moisture, and compactness.

Maru dam (or Poiana Marului) in Romania is an interesting example of a dam at which during construction errors were removed in the execution of the contact clay core – foundation, threatening to bring to anomalies in the dam's operation and to an occurrence of fissures. The earth–rock dam, with a central slightly sloping core, has a maximum height of 130 m, length of crest 408 m and a volume of 5.3×10^6 m^3. It represents a major water-retaining structure in the hydroelectric power system *Bistra-Poiana Marului* (Fig. 11.34; Stematiu et al., 1991).

The dam site has a trapezium form, with inclination of the left bank 30°, and of the right bank 40°. The shells and the core are founded on firm rock – granite, granitic gneiss and feldspar. The shells are constructed of granite, while the core is constructed of material which consists of clay, silty clay and clayey sand, with a high content of fine fractions below 0.005 mm (20 – 40%) and a coefficient of permeability 10^{-5}–10^{-7} cm/s, drawn from a borrow pit 12 km distant from the dam site. The natural moisture of the clayey material (≈22%) was close to optimal.

In August 1989 the dam was constructed up to an elevation of 587 m, which means 87 m above the level of founding, and it was commissioned for partial operation following the construction up to an elevation of 575 m.

The joint core-foundation has been made of clay with rather high plasticity (so-called *contact clay*), which is capable of adapting to the settlements of the core without danger of occurrence of fissures, which is particularly important where the steep right bank is concerned. The technical conditions for construction have anticipated that the clay, with increased plasticity in the contact zone, should be compacted at moisture $w = w_{opt} + (2–3)\%$. This measure has been rigorously carried out in the beginning of construction, but the laboratory tests carried out in the summer of 1988 have indicated that the contact clay placed in the period June–August, had a lower moisture after placement than had been specified. This has related to a 14 m thick embankment, situated in the intermediate third of dam's section, between

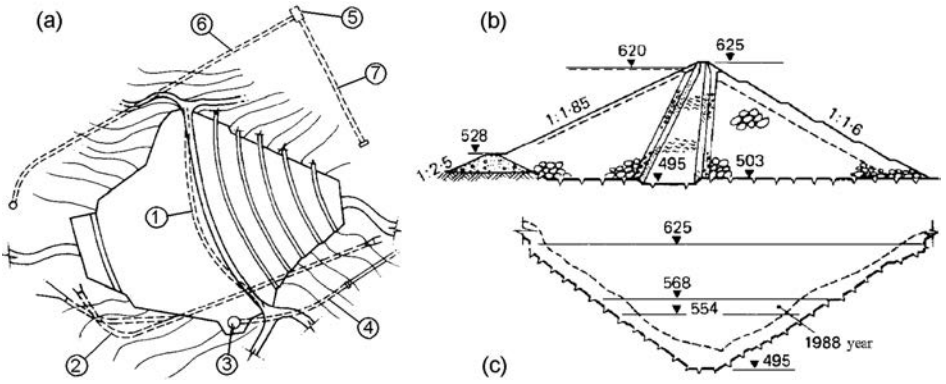

Figure 11.34 Layout plan (a), cross-section (b) and longitudinal section (c) of Maru dam (after Stematiu et al., 1991). (1) Grouting gallery; (2) diversion tunnel and bottom outlet; (3) shaft spillway, 668 m^3/s; (4) overflow tunnel; (5) underground hydroelectric power station, 80 MW; (6) main headrace tunnel; (7) access gallery.

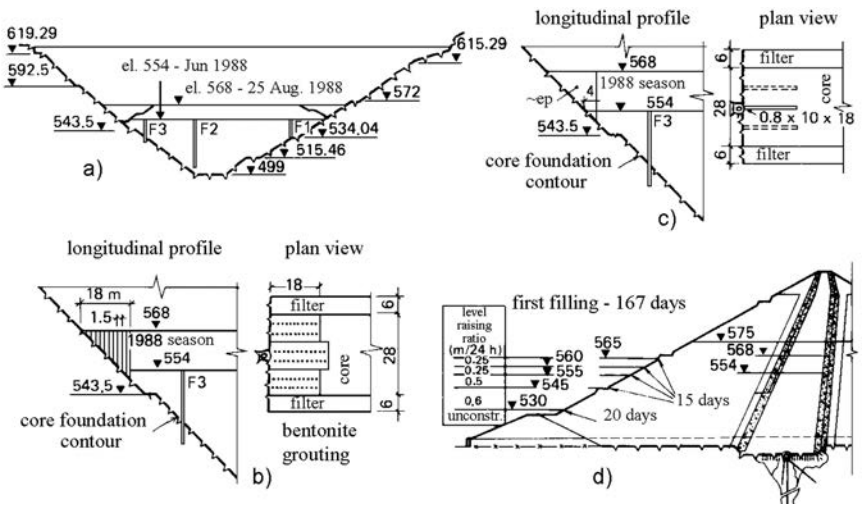

Figure 11.35 Proposed measures for problem solving (after Stematiu et al., 1991). (a) Removal of embankment, carried out in 1988; (b) grouting with bentonite; (c) execution of foundation wall of bentonite; (d) change in the regime for reservoir filling.

elevations of 554 m and 568 m, Figure 11.35. Two reasons for this omission have been stated: insufficient attention during moistening of the material during construction and exceptionally hot and dry weather.

Right in the quoted zone, built up of clay lacking in moisture, maximum settlements have been expected under the influence of self-weight. The shortage of moisture in the contact clay brings a decrease in plasticity and, as a consequence, an increase in

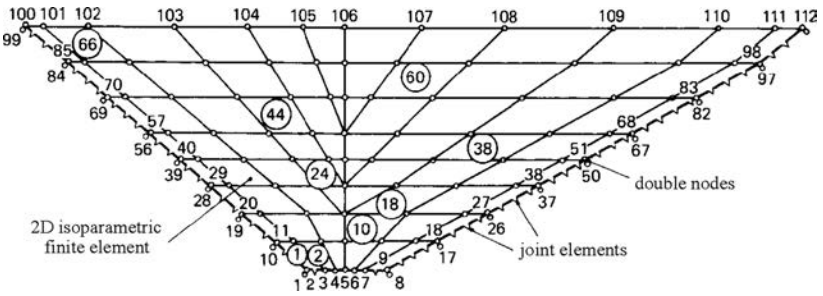

Figure 11.36 Discretization of the analysed section.

the potential risk of occurrence of fissures. Another consequence could be an increase in the values of parameters of shear strength (cohesion and angle of internal friction), which would lead to additional loading of those zones and appropriate unloading of the lower layers. Those local decreases of normal stresses in the contact zone would increase the danger of hydraulic fracture.

For preventing possible serious consequences, the following possible measures have been analysed:

1. Removal of the embankment that was constructed in 1988 in the vicinity of the banks and its replacement with contact clay, which corresponds to the specified requirements. This solution would be very expensive and would lead to considerable delay of works.
2. Grouting of the contact zone with liquid bentonite. This solution is cheaper than the previous one, but it contains uncertainties about the positioning of the grouting material and in connection with the danger of occurrence of hydraulic fracture during grouting.
3. Execution of a foundation wall of bentonite, founded in the bank, in the zone of influence of the contact clay. This solution provides greater safety than the previous one, however at rather higher cost.
4. Change of the regime of filling the reservoir by decreasing the velocity of increase of water level in the zone between the bottom level and top level of the embankment, constructed in 1988. Seepage through the core should commence at the first filling, which would compensate the shortage of moisture in the appropriate zone; the water level should rise accordingly.

In order to quantify the unfavourable effects of the defective contact layer, a number of analyses were performed. By means of geomechanical laboratory tests on many samples of the built-in material, variations were established of the geomechanical parameters through a mathematical model, based on FEM, which determined the state of stresses during construction of the dam, with and without modified parameters in the contact clay in the critical zone. Two-dimensional FEM analysis was performed, and the longitudinal section along the axis of the core was discretized by means of linear quadrangle isoparametric elements (Fig. 11.36).

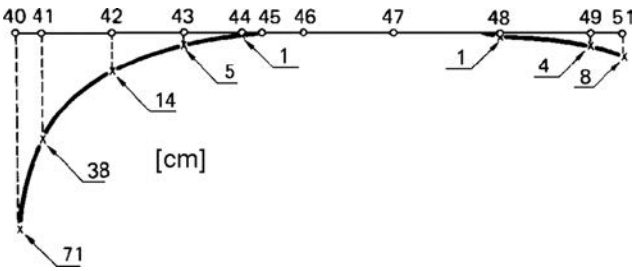

Figure 11.37 Settlements in the cross-section at the 554 m level, caused by the embankment placed above the level of 568 m.

Construction was simulated in eight layers, five of which relate to the completed works until the end of August, 1988. Behaviour of the contact core-foundation in the dam abutments was simulated with 16 joint elements, jointed to the basic net by means of double nodes.

Comparison of the data obtained from measurements during construction of the contact zone and those that have been theoretically obtained, brings some interesting comprehension and conclusions, of which the most important ones briefly follow:

- Contour lines of the vertical displacements have regular shape, with maximum values in the central part of the section. Between the two cases (theoretical solution – observations) certain differences have been recorded, even though, in general, the method of deforming and obtained values is very similar.
- The embankment, placed over an elevation of 658 m, caused the maximum settlement in the zone of the steeper bank, and a smaller one in the zone of the bank with a slighter inclination. To illustrate, Figure 11.37 shows the settlements of the embankment placed above the elevation of 658 m that have occurred at an elevation of 554 m. There is evident a difference between the settlements at the steeper bank in relation to those of the more slightly inclined bank (numbers 40–51 refer to the nodes denoted in Fig. 11.36). Also, Figure 11.37 clearly shows the zone in which the new embankment has no influence.
- Actual shear displacements in the zone of the steeper bank, constructed of contact clay with lower moisture, have been five to six times lower than those constructed of clay with normal moisture.
- Appropriate shear stresses in the contact points clay-foundation have been twice, i.e. 1.5 times greater, and that is why the effective stresses, directly below the zone of influence of the new embankment, have been greatly reduced because of the effect of 'hanging.' The final consequence of such a situation could be the occurrence of a hydraulic fracture at the first filling of the reservoir. Therefore, a shortage of moisture in the contact clay placed in the season of 1988, in an extreme situation may lead to a danger of occurrence of hydraulic fracture, without exhibiting the reduction of the global stability of the dam.
- Physical and mechanical characteristics of the contact clay induce direct influence on displacements and stresses in the dam's body, especially in the zone of

the steeper bank. This clearly indicates the necessity of strict application of the specified technical requirements.

- Reduction of stresses in the zone of the steeper bank between elevations 545 and 555 m, along with local changes in the interaction clay embankment – bank, impose special requirements for observation of displacements in the quoted critical zone.

Finally, on the basis of all of these analyses and investigations, it was decided that placement of the embankment should continue. At that, a condition was specified for decreasing the speed of filling the reservoir to a degree that would enable in the critical zone, self-correction of moisture contents in the contact clay. The example in a pictorial way presents the invisible traps, which may appear during execution of the contact core – steep bank. If these situations are not discovered in time, hydraulic fracture and fissures in the water-impermeable element may occur.

Therefore, the proper execution of the contact dam–foundation is of great importance. With that, the assumptions and rules for these problems, set out in Chapter 10, are also valid for earth–rock dams, but in are emphasized even more, taking into consideration that earth–rock dams are constructed with significant heights. For more details about the treatment of the foundation in the contact core–foundation, the reader is referred to the textbook references (Fell et al., 1992; Golzé, 1977; Nonveiller, 1983).

11.6 DESIGNING EARTH–ROCK DAMS IN SEISMICALLY ACTIVE AREAS

The basic assumptions of dynamic analysis of embankment dams have been brought out in Chapter 9. We have seen that methods for execution of such analysis are permanently developing and improving, becoming more complex and more and more accurate. With their proper application, and with increasingly greater accuracy, it is possible to determine stability, as well as the state of stresses-deformations in dam's body at simulating the effect of an earthquake with appropriate strength and characteristics (Kikusawa & Hasegawa, 1985; Kikusawa, 1990; Ohmachi, 1994; Seed, 1973; Seed et al., 1978).

Even so, and in such advanced stage, the methods of analysis are not yet capable of enabling explicit evaluation of the stability of the complex construction of an embankment dam. Even with the most sophisticated method of analysis, we only perform a checkup of the stability and the state of stresses-deformations for the assumed cross-section of the dam. That is why, particular attention should be paid to the design of dam's body that will be adopted for analysis. A number of experts in the field of embankment dams attribute greater significance to the proper selection of the dam site, materials in dam's body, their configuration and dimensions of structural elements. At that, when it is a question of a dam site located in a seismically active area, it is recommended, in designing the dam, to undertake defensive measures, which will with great certainty guarantee its safety (Abdel-Ghaffar & Scott, 1979a). Then, the dynamic analysis should only confirm the proper selection of the structure and possibly suggest only minor adjustments.

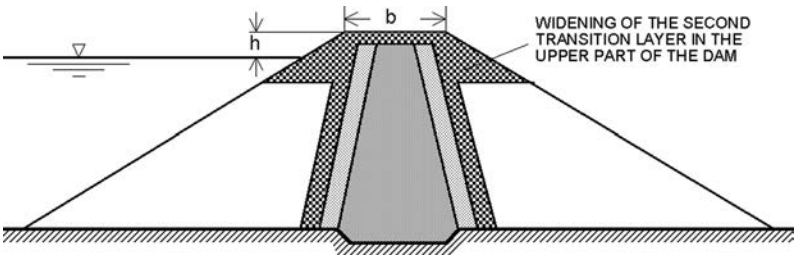

Figure 11.38 Improvement of earth–rock dam cross-section for seismic conditions.

These are the most important defensive measures to which it is necessary to pay attention to in the design of an embankment dam in a seismically active area:

- Advantage should always be given to a dam site with sound rock in the foundation.
- Avoid dam sites if there is an active fault in its foundation.
- A possible existing layer of deposit in the foundation, for which there are indications that it could be susceptible to liquefaction, should compulsorily be removed in the zone below the dam's body. No materials which are susceptible to liquefaction should be placed into a dam's body.
- The core should be constructed with a greater thickness in order to decrease the hazard of possible fissure, and it should be widened at contact with the rock. Avoid use of low-plasticity clay as material for the core.
- Filter zones, i.e. transition zones, should be constructed with greater thickness (3–4 m), with proper compaction and of material that is not susceptible to exfoliation and fissuring.
- Upstream of the core, a well-graded filter layer should be placed, which will be capable, under the influence of water pressure, of enabling the sealing of fissures in the core.
- Width of the crest b (Fig. 11.38) should be assumed larger than is customary, since it is very much subjected to deformations during earthquakes.
- Rock material in the shells should be made with good compaction and in thinner layers. Material with good draining properties should be placed in the upstream shell, so that as small excess pore pressure as possible will occur in it during an earthquake.
- Anticipate sufficiently large freeboard h, Figure 11.38 because during an earthquake it comes to additional compaction of the embankment and thus also to instantaneous settlement (Jansen, 1990).
- Construct the second filter (transition) layer on both sides of the core of well-graded material (stone chippings, gravel), with a high shear strength. These layers in the upper part should be widened to the entire section (Fig. 11.38). Thus, a strong compact zone would be formed in the highest part of the dam, which, during earthquakes, is subjected to maximum accelerations and in which most of the wedges, which are potentially susceptible to sliding, are sited. The extension of this zone could reach a depth below normal water level, equal to the freeboard

h. Of course, the upstream slope in the cited zone of the dam would be protected against the erosion effect of waves by means of a special construction of dumped rockfill.

- Analyse the possibility for the execution of a special construction of dam crest, which would make possible minor accidental overtopping without harmful consequences.
- Avoid the use of controlled spillway structures, since deformations caused by earthquakes could throw out of service the hydromechanical equipment.

The above quoted measures, together with other possible measures imposed by local conditions of the dam site and the construction of the hydraulic scheme as a whole, would reduce to minimum the hazard of damage during earthquakes.

Chapter 12

Rockfill dams with reinforced concrete facing

12.1 DEFINITION, FIELD OF APPLICATION AND CONSTRUCTION

Rockfill dams with reinforced concrete facing are constructed of rockfill or gravel, while water-impermeability is provided by reinforced concrete facing, by means of which the upstream dam's slope is lined. The reinforced concrete facing is the most frequently used water-impermeable element in rockfill dams, Figure 12.1. Throughout the world, it has particularly been used up until World War Two, and following some hold-up, it has been experiencing a real renaissance during the last four decades, more precisely since 1970 (ASCE, 1987; Cooke, 1984, 1987, 1991, 1992, 2000a; Cruz et al., 2009). From Figure 12.1 the domination of concrete faced rockfill dams (CFRDs)[1] is clearly visible, compared with the alternatives: rockfill dams with asphaltic core and asphaltic lining, especially in the period 1991–2012.

Rockfill dams are an alternative to earth–rock dams and, in relation to them, they have the following advantages:

1. No part of dam's body is submerged in water, so that the weight of built-in material, along with the weight of water above facing, is utilized to maximum.
2. No coherent materials are built into dam's body, therefore, complex problems with pore pressure do not occur, which are unavoidable in the case of earth–rock dams.
3. Construction of dam's body is simpler and faster, because it is carried out irrespective of the facing which is executed at the end, over previously formed slope, while in the case of high and especially high dams this is achieved in two, resp. in three stages.
4. Facing is easily accessible for inspection, repairs and possible strengthening.
5. Facing can also have a secondary function – protection of the slope against waves and other external influences.
6. Heightening is more simply achieved in these dams, since in such a case the embankment is extended only towards the downstream face, while the facing is extended upwards.

[1]The commonly used name of this dam type is *concrete faced rockfill dam,* abbreviated to "CFRD" or "CFRDs" for plural.

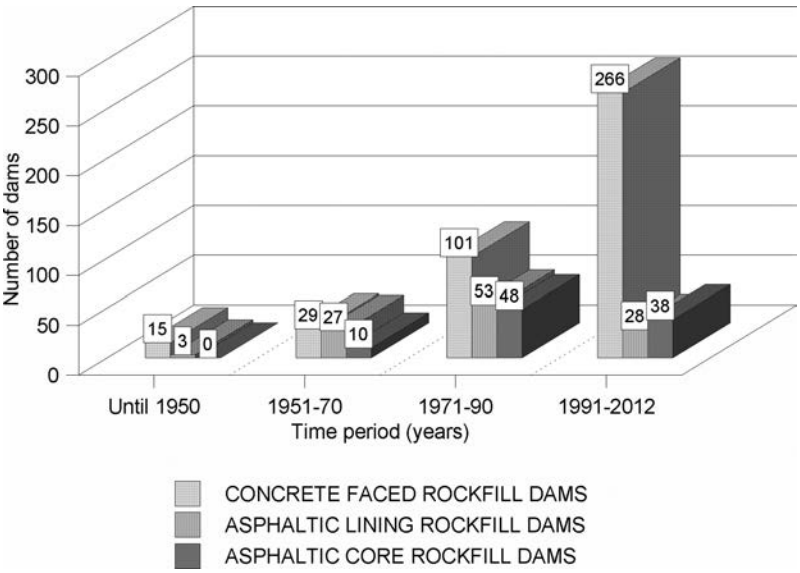

Figure 12.1 Number of rockfill dams with artificial sealing constructed in different time periods.

7. Rockfill dams are usually considerably cheaper than earth–rock dams, owing to their steep slopes. They have smaller overall volume than earth–rock dams; however, the volume of the rockfill material is approximately equal in both cases. We can consider that total cost of the rockfill embankment is approximately equal for the two kinds of dams, since the expenses for better compaction of the embankment for rockfill dams are compensated with a broader working front and independence of weather conditions, owing to the independent construction of the embankment from that of the facing. On the other hand, total cost of the earth core together with filter layers is almost always greater than the cost of the reinforced concrete facing, and is drastically greater at shortage of earth materials in the vicinity of dam site. The smaller width of dam's base (due to steeper slopes) results in shorter water-conveying structures (tunnels, pipelines, spillways), which also contributes to a lower overall cost. This is particularly significant in the construction of large hydroelectric plants and in a need for a flood discharge of large quantities of water in the course of construction and service of the hydraulic scheme. Time for construction of rockfill dams is shorter, which also influences the cost.
8. Seepage of water in rockfill dams either appears as a consequence of penetration through the facing or through the rock foundation. In both cases there is no earth material in dam's body which would be eroded under the effect of seepage flow; that is why the seepage through the body of earth–rock dams with facing has considerably less unfavourable effect in relation to that in earth–rock dams. It does not endanger the stability of the dam, but it is only a question of loss of water (Casinader & Rome, 1988).

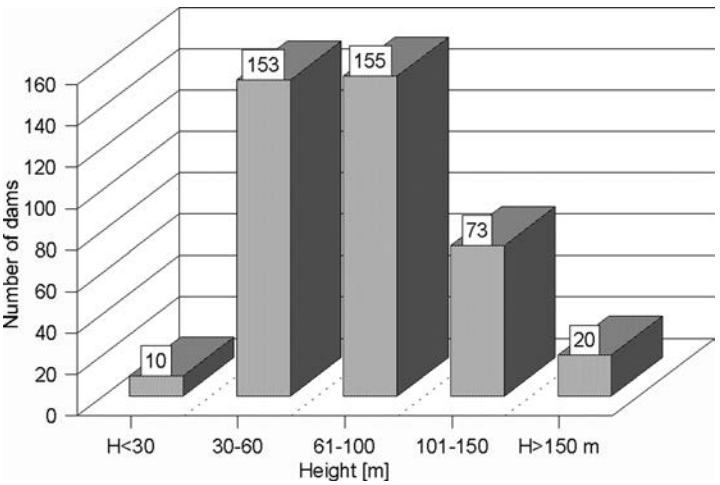

Figure 12.2 Number of CFRDs grouped by height.

Rockfill dams with facing also have other advantages, which will be considered in appropriate parts of the textbook. They also have certain disadvantages in relation to the earth–rock dams, of which the following are basic ones: (1) The construction of the facing is relatively complex work and it requires skilled workers; (2) Maintenance of the facing is necessary during the post-construction period; (3) The facing is exposed to external influences; (4)In some cases, the joint of the facing and foundation can be a complicated and long one, and that can be of significant importance when below it a deep grout curtain is constructed.

Dams with reinforced concrete facings can reach considerable heights (Fig. 12.2), almost like earth–rock dams, which are a significant advantage in relation to dams with asphalt–concrete facing at which, because of difficulties during construction, the height is practically limited to some 90–100 metres. In recent years several CFRDs higher than 200 m have been constructed, including the highest one – *Shuibuya* in China, $H = 233$ m. Two factors have played a decisive role in the return of popularity of CFRDs and their massive use over the last two decades:

- This type of dam, contemporaneously constructed, is very favourable from all technical viewpoints;
- Most often, this is the cheapest type of dam to build.

These dams are used for the creation of reservoirs with varying purposes and sizes: from small irrigation systems, via large reservoirs on water-abundant rivers, up to pumped-storage plants. The facing should satisfy two basic conditions:

1. It should be sufficiently water-impermeable;
2. It should be stable in different conditions existing in the course of construction and operation of the dam.

The first requirement is not difficult to satisfy, in spite of the fact that concrete facing is not that much impermeable as is the asphalt–concrete one (Casinader & Rome, 1988). Here, it should be pointed out that under considerable penetration of water, the problem can simply be solved by adding sandy silt into the reservoir, which has the ability to seal, i.e. close cracks or large pores in the concrete facing, and that has been employed in practice. The second requirement implies a certain ability for adaptation of the facing to deformations, which would occur in dam's body below the facing. Reinforced concrete facing does not have the ability to follow larger deformations in dam's body without damage, but can only bridge some of them or adapt to the smaller ones. That is why, the body of such dams should be constructed by filling in thinner layers, with compulsory compaction. Below the facing, a leveling layer is always anticipated which can be carried out in the form of dry stone masonry or of well-compacted selected coarse rockfill or stone chippings, i.e. gritting material. Dry sub-facing masonry is not employed in modern practice, since it requires engagement of an expensive work force for the placement of the coarse stone blocks, as well as a construction of leveling concrete layer below the facing with a thickness of about 15 cm. This cannot be compensated with a somewhat smaller volume of the dam, owing to the possibility for the upstream slope to be steeper. The thickness of dry stone masonry, applied in the very early period of the building of CFRDs, in the upper part amounts to 0.5–1.5 m, while it expands downwards and reaches up to 8% of the dam's height.

The sub-facing layer of selected and sorted rockfill or stone chippings, which is nowadays almost regularly used, has a thickness of minimum 3 m horizontal, in order to ensure unobstructed work for the plant and equipment for spreading and compacting. A contemporary tendency is that this layer should contain more gritting material, so that it should be semi-permeable in order to be able, at possible cracking of the facing, to slow down the flow of penetrating water.

Reinforced concrete facings are constructed of concrete with a compressive strength of 20 MPa at 28 days, taking into consideration that water impermeability and durability are more important for the concrete. To add pozzolan it is customary in modern practice, while the maximum aggregate grain usually does not exceed 38 mm. The usual reinforcement percentage of 0.5% in both directions for modern dams, with well-compacted embankment, is lowered to 0.4% and even 0.3%, which is deemed as a substantive advancement, which not only makes the dam cheaper, but also speeds up construction. In certain zones, reinforcing can be increased even up to 1%.

According to the construction, three basic kinds of reinforced concrete facings can be distinguished: *stiff*, *semi-stiff*, and *elastic*. *Stiff* facings consist of one layer of reinforced concrete. In early applications, these have been constructed only for lower dams, with compulsory sub-facing dry stone masonry, in order to minimize the deformations. They have been cut in only by means of temperature joints.

One-layer facings are exceptionally used in contemporary practice, without a sub-facing layer of dry stone masonry. The rockfill in a dam's body is zoned according to the grain size and is maximally compacted by placement in thin layers, so that the subsequent deformations would be as small as possible. Besides, the joints, which are executed in the vertical direction, are paid particular attention in order to remain water-impermeable also at certain differentiated displacements of the reinforced concrete slabs.

Semi-stiff facings, which are a kind of historical example, consist of one layer. They are divided into sections by means of transverse and longitudinal temperature-deformation joints at every 4–15 m. They are constructed on a leveling concrete layer, i.e. bedding, coated with a bitumen-based mixture, which enables the facing to deform irrespective of a dam's body. In order to prevent slipping of concrete slabs across the bituminous coat, they are anchored into the sub-facing layer and are also firmly jointed with the foundation by means of a concrete cutoff. In the upper part of the facing, the slab thickness amounts to 0.25–0.30 m, while in the lower part it is 0.40–0.50 m.

Elastic reinforced concrete facings also belong to history. They consist of a number of layers of reinforced concrete slabs with bituminous coating between them as well as between them and the first layer of slabs and the sub-facing layer. The slabs have up to 10 m long sides and they are placed so as to cover the joints of the layer below. This structure is not used in contemporary practice.

The older dams with a reinforced concrete facing have shown various deficiencies in their service, of which the considerable loss of water and significant funds for permanent repairs and reconstructions have been the most important ones. However, the safety, static and dynamic stability has not been endangered in any of these dams. A brief description of some of these older dams will be given in continuation, which have played a significant role in the evolution of dams with reinforced concrete facing and have contributed for their today's rapid development (Cooke, 1992).

- *Meadow Lake, California, USA, 1903*. A 23 m high dam, with slope inclinations of 1:0.5 and 1:0.75, one of the first such dams constructed in California, without mechanical compaction. A load-bearing layer of dry stone masonry has been carried out below the facing. This dam is one of the typical examples proving the high shear strength possessed by the rockfill.
- *Bucks Creek, California, USA, 1928*. The facing of this 40 m high dam is monolithic, with reinforcement protruding through the control joints. Neither cracks nor water penetrations have been noticed in the course of its service.
- *McKay, California, USA, 1925*. A 49 m high dam, with similar properties as the previous one. It is significant because of the continuous execution of the concrete slabs (from the foundation to the crest); such experience has not been sufficiently noticed and it was used again in 1967.
- *Salt Springs, California, USA, 1931*. A 100 m high dam with rectangular slabs, separated with compressible joints. During its service life, joint opening and considerable water penetration have taken place. Some subsequent dams with similar construction and height, have exhibited identical behaviour. In this way it has been shown that high rockfill dams, carried out without compaction, in spite of their static stability, are not a good solution because of the high penetration of water and high expenses for maintenance.
- *Coqoti, Chile, 1940*. An 85 m high dam, one of the 17 rockfill dams with reinforced concrete facing, built in Chile in the thirties. This type of dam has been selected as one, which is resistant to earthquakes. The upstream slope had an inclination of 1:1.4. The sub-facing layer, in contrast to the then usual practice, has been carried out of sandy gravel. The strong earthquake of 1943 has caused a crest settlement of 40 cm, without damage to the facing.

- *Lower Beas River No. 1, California, USA, 1943*. A 75 m high dam with identical construction like Salt Springs. There has not been any damage of its facing, nor appreciable water penetration, which leads to the conclusion that the high compressibility of the uncompacted rockfill can be compatible for a dam with smaller height, but not for a 100 m high dam.
- *Quioch, Scotland, 1956*. A 38 m high dam with which it begins a transition from the application of uncompacted to compacted rockfill. The layers with thicknesses of 0.6 m, have been compacted by means of a 3.5-ton static smooth roller. The settlement during filling of the reservoir amounted to negligible 3 cm.
- *Sassière, France, 1959*. This 39 m high dam has a body of uncompacted rockfill; for the first time it has been used a construction of a 3 m wide sub-facing layer made of finer compacted rockfill, as well as a constant thickness of the facing of 30 cm along the entire height which, later on, has been accepted as a standard for dams with heights up to 40 m.
- *New Exchequer, California, USA, 1966*. A 150 m high dam at which it has been kept the old construction of rectangular slabs with joints and with one central waterstop. The main advancement in this dam has been the application of an incorporated plug in the form of a reinforced concrete foundation, instead of the former rough method of forming a construction pit by means of mining and filling with concrete. The rockfill in dam's body is zoned and it consisted of compacted layers with thicknesses of 0.5 and 1.2 m, up to the biggest zone that has been built in layers of 3–20 m. The sub-facing layer had a gradation of 5–25 cm, which has resulted in a loose and segregated surface. Significant damages of the facing and high water penetrations (4 m^3/s) have occurred in the course of its service. A satisfactory rehabilitation was carried out in 1987. That was the last high dam with a reinforced concrete facing, which contained uncompacted zones of rockfill.
- *Piedras, Spain, 1970*. This 40 m high dam has been made of compacted rockfill with slope inclinations of 1:1.3; it has slabs that had been carried out continuously, instead of by then customary rectangular ones, which practice has been accepted and used afterwards. The slabs have been placed in a chess like pattern, and not one next to another. When only the alternative slabs have been executed, a great flood has taken place. The water has risen up to 2/3 of dam's height. The quantity of penetrated water has been rather large, while its discharge has been quiet, without destruction of the embankment. This has demonstrated that the compacted rockfill is safe during water flowing through it, which has also been demonstrated in similar situations in such other dams, for instance, during the construction of the modern Cethana dam.
- *Pindari, Australia, 1970*. It has the same construction as Piedras dam, only that the thickness of the slabs has been increased in order to enable subsequent heightening of the dam from 46 to 85 m (accomplished in the period 1992–1994). This a commencement of the era of construction of reinforced concrete facings in a number of stages, and not only after completely carried out the embankment. After 20 years of service, the settlement of dam's crest, with a height of 46 m, has been 7.5 cm. The traditional formula for the thickness of facing ($d = 0.3 + 0.0067H$), has been changed for this dam into $d = 0.3 + 0.003H$, which has been accepted in subsequent dams.

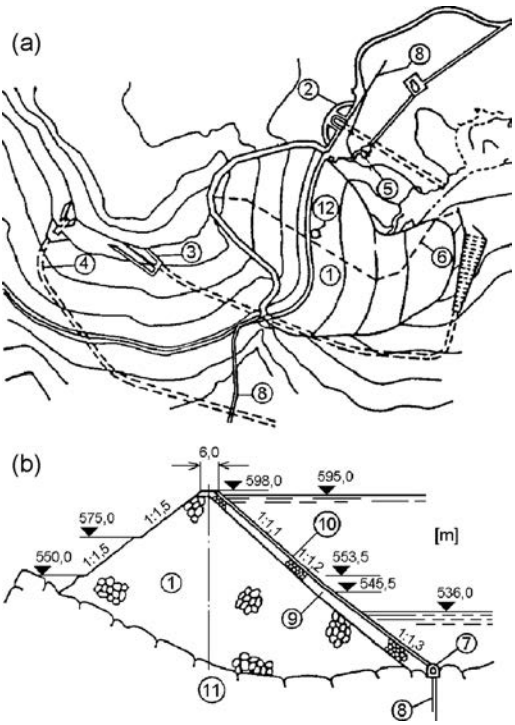

Figure 12.3 Layout plan (a) and cross-section (b) of Rama dam. (1) Dam's body; (2) spillway; (3) diversion tunnel; (4) derivation (supply) tunnel; (5) observation station; (6) drainage gallery; (7) grouting gallery; (8) Grout curtain; (9) sub-facing layer; (10) reinforced concrete facing ($d = 30$–90 cm); (11) limestone in foundation; (12) measuring manhole.

In this group we can also place the biggest rockfill dam with a reinforced concrete facing, constructed in former Yugoslavia, Rama, in Kovachevo Field (Bosnia and Herzegovina), Figure 12.3. It is 103 m high, and its axis has a S-shape in plan, for more appropriate adjustment to the ground conditions. The reinforced concrete facing is connected with a concrete grouting gallery by means of an elastic and water-impermeable joint. Rama dam has been carried out in complex geological conditions, over permeable limestone, so that a deep grout curtain (195 m) is carried out below the gallery, cut into the banks. The overall area of the grout curtain is 86,500 m^2 while the cement consumption is 41.5 kg/m^2. A drainage gallery is extended along the river bed, in which measurements are made for the water filtrated through the facing as well as deformations of the foundation which, only under the influence of the dam's weight, have reached 52 cm at the end of construction (Nonveiller, 1983).

The dam with a reinforced concrete facing has been selected following a detailed analysis and comparison of possible alternatives, when a decisive influence has been played by the factor that by means of this type of dam, due to the steeper slopes, it is possible to do savings in dam's volume regarding a corresponding earth–rock dam as well as savings in time needed for construction under conditions of frequent rainfalls

existing in the area of the dam. The facing consists of slabs with dimensions 13 × 13 m, with joints closed, i.e. sealed with profiled rubber strips 23 cm wide. The joints are 30–50 mm wide and are filled with elastic synthetic material and with asphalt mastic. Steel reinforcement amounting to 60 kg/m^3 has been used. The dam's body of rockfill is constructed in layers of 2 m each along with 250 l/m^3 watering and compaction with 8–10 passes of a 10.5-ton vibratory roller. The sub-facing layer is constructed of coarse rock pieces, placed by means of a crane, which provides stability of the steep slope, carried out at a greater angle than the angle of repose of the rockfill. Prior to the construction of the facing, the surface of the sub-facing layer is levelled with concrete. The facing is connected with the lining of the concrete gallery by means of 3 m high contour slabs at elevations higher than 545.5 mwl, which are doubled at the lower elevations. Such a construction enables the facing to follow the deformations of the dam and to adapt to the local slope deformations. The settlement of the dam after its construction amounted to 0.55% of its height, while following the filling of reservoir at a height of 77.5 m the settlement increased to 0.77%. The entire dam with a volume of 1.45 millions of m^3 rockfill and 20,500 m^3 reinforced concrete was completed within three years. After more than 40 years of service, there is a plan for the dam facing to be covered by geomembrane with the main aim of improving impermeability and protecting the concrete against ageing.

12.2 MODERN DAMS WITH REINFORCED CONCRETE FACING

Modern rockfill dams with reinforced concrete facing have occurred in the last four decades as a result of the progress in the technology of their construction and design, which is reflected in the following: (1) New methods of construction which ensure proper compactness of the embankment and, thus, low subsequent settlements; (2) Execution of the reinforced concrete slabs of the facing by using climbing formwork, i.e. slipform, which enables construction of the facing of high dams in a number of stages, simultaneously with the advancement of the embankment; (3) New constructions of joints which, along with the progress in concrete technology, enable execution of concrete construction with high water-impermeability and durability (Beach et al., 1991; Cooke, 1991, 1992, 2000; Keming et al., 1992; Cruz et al., 2009).

The following elements are contained within the reinforced concrete facing in modern constructions (Fig. 12.4): (1) Plinth, or concrete foundation, in the upstream toe of the dam; (2) Perimeter joint; (3) Initial slabs with irregular form; (4) Slabs of the facing with vertical spreading; (7) Parapet at the crest of the dam (Schewe, 1990). All these elements of a CFRD are more or less important for a proper working of the dam and they will be discussed in the following sections. But we will start the discussion with the rockfill dam body, as the main structure of the entire system, responsible for the stability on the whole.

12.2.1 Rockfill dam body

As a rule, the concrete faced rockfill dams are built on rock foundation. The preparation of the foundation as a base for rockfill embankment of CFRDs is similar to

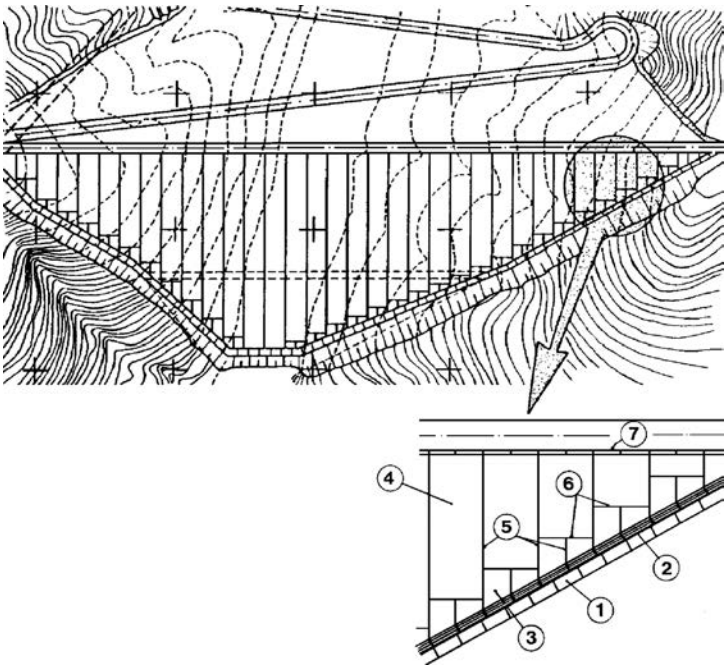

Figure 12.4 Layout plan of modern construction of reinforced concrete facing with a detail containing denoted elements of the facing. (1) Concrete plinth (toe slab); (2) perimeter joint; (3) initial facing slabs with irregular form; (4) slabs of facing with vertical spreading; (5, 6); joints (7) parapet wall at the crest of the dam.

that for other types of rockfill dam. Generally speaking, the criteria for foundation treatment of CFRDs below the downstream dam slope are fewer than those for the clay core rockfill dams, taking into account that for the CFRDs the water load of the reservoir is taken into the rock foundation upstream from the dam axis. Alluvial gravel deposits in the riverbed, except sand, are commonly left in place except for a short distance downstream from the toe slab (plinth), as in some examples described in section 12.4. The treatment of the foundation below the upstream dam slope, especially in the vicinity of the dam toe, should be done more thoroughly.

Another important aspect is the zoning of the dam body, because for CFRDs there are appreciable differences between the loading of the upstream and downstream shell. The basic concept of zoning given by Cooke and Sherard (1987), with some modifications, is widely accepted in practice (Fig. 12.5):

- Zone 1A – silt, a low cohesion impervious soil material.
- Zone 1B – random material to confine zone 1A.
- Zone 2B – transition zone or (filter) from processed rock, placed directly under the concrete facing.
- Zone 3A – transition selected small rock placed in same layer thickness as zone 2B.

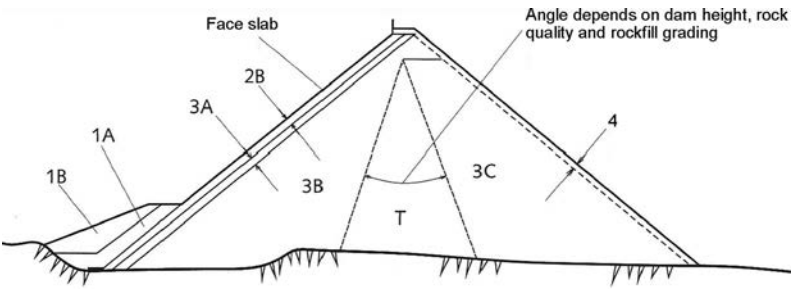

Figure 12.5 Zone designations for CFRD of sound rockfill (after Cooke & Sherard, 1987).

- Zone 3B – main upstream quarry run rockfill, up to 1 m layers, located downstream of zone 3A.
- T – central rockfill zone, placed between 3B and 3C zones.
- Zone 3C – downstream quarry run rockfill, placed after T or 3B zones, about 1.5 to 2.0 m layers.
- Zone 3D – material placed close to the downstream slope.
- Zone 4 – protection material of downstream slope.

The purpose of zone 1A is to cover the perimeter joint and slab in the lower elevation with impervious soil which would seal any cracks or joint openings. For stability, zone 1A is covered by waste material, zone 1B. Zones 1A and 1B are not necessary and they are used only if a problem appears.

The primary purpose of the thin zone 2B of finer rock directly under the slab is to provide even and firm support for the concrete slab. In recent practice this zone made with select grading provides a semi-impervious barrier, preventing any large leakage path developing through a crack in the concrete slab or in a waterstop.

An important improvement which insures an excellent support for the concrete slabs of the facing was applied at Itá dam, in Brazil in 1999. An extruded concrete wall was built along the slope of zone 2B, preventing erosion and eliminating the need for other, not so effective, measures for slope stabilization like asphalt emulsion spray, and similar. It is also an excellent support for the face slabs. The extruded concrete wall is made from lean concrete, with cement content up to 75 kg per m^3 concrete, with details shown on Figure 12.6. Bond-breaker products between the curb surface and the concrete slab have been suggested to reduce the shearing forces transmitted at the interface. Of course, the application of the curb does not eliminate zone 2B, necessary for flow control in the case of leakage. Since the Itá dam, the extruded concrete curb has been widely used throughout the world.

Zone 3B should be made from high quality rockfill, well compacted, because most of the water load passes into the foundation through the upstream shell. Therefore, it should be placed in layers no thicker than 1 m, with good compaction by vibratory rollers. The downstream zone 3C takes negligible water load. Its compressibility has little influence on the settlement of the face slab and it can be placed in layers with thickness up to 2 m. Thus, the maximum size rocks can be placed in this zone.

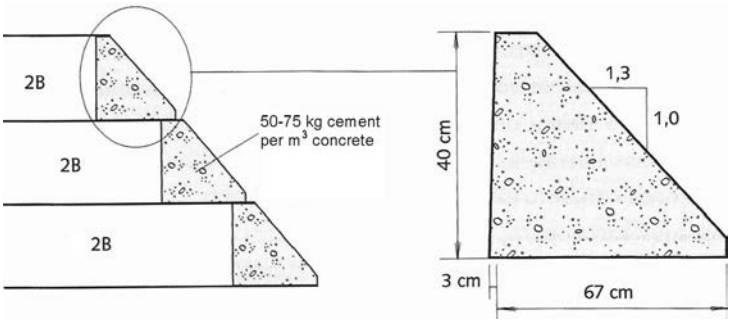

Figure 12.6 Curb detail (after Cruz et al., 2009).

The specifications for layer thickness and compaction equipment are stronger for the highest CFRDs, like Campos Novos ($H = 202$ m), and Shuibuya ($H = 233$ m). To enable better compaction and to minimize the post construction settlement, the addition of at least 200 l/m^3 water to rockfill has become a common practice. The downstream face of the CFRDs is made of selected large rock blocks, guided by batter boards or laser beams to provide an aesthetically pleasing surface. The discussion regarding the dam body zoning will continue in the descriptions of examples of modern CFRDs later on in this chapter.

12.2.2 Concrete plinth

The *concrete plinth* in the upstream toe of the dam provides water-impermeable joint between slabs of the facing and the grouting element in the foundation, which can be either grout curtain or diaphragm wall. Two types of plinths are employed: in the form of a slab or in the form of a wall, i.e. cutoff, which can contain a gallery.

The plinth in the form of a slab is used in sound, non erodible fresh rock in the foundation, with low permeability, when the excavation is limited to the surface zone. In such a case, the rock in the foundation can easily be grouted from the slab whose stability, if necessary, can be provided by anchoring into the rock (Cooke, 2000). Careful excavation of the surface rock foundation is used to minimize fracturing of the rock surface on which the toe slab is placed. Air or air-water cleanup, just prior to placing concrete, is required to obtain a bonded contact of the concrete to the foundation. The plinth, the name most commonly used for the toe slab, plays a very important role in the performance of CFRDs controlling the flow through the foundation, because at the upstream side is the reservoir and behind the plinth there are permeable rockfill zones (Cooke & Sherard, 1987; Cruz et al., 2009).

The width of the slab, founded on firm rock, is taken as 4–5% of the height of the water column above it, but it should not be smaller than 2 m, resp. 3 m for dams higher than 40 m. It means the hydraulic gradient H:B (height of the water:width of the plinth) is equal to 18–20. An extended width of the plinth of 6–8.5% is used for lower quality rock, lowering the hydraulic gradient to 10. In the case of weaker rock in the foundation, say with a compressive strength less than 30–40 MPa, a cutoff wall should be applied.

It is a common practice today that the extension of the plinth is made under the dam so that the external width is limited to 3–4 m. Whenever the rock is sound, but fractured, an internal filter behind the plinth is necessary.

The thickness of the slab, from the aspect of stability, taking into consideration water pressure, would sufficiently be 0.3–0.5 m. In many cases it is assumed to be higher in order to withstand the pressure of grouting, but it rarely exceeds 1 m. There are lots of examples where the toe slab thickness is equal to the face slab thickness. In checking the stability of the slab, it is necessary to consider the pressure of water from the upper, front and bottom side, as well as the pressure due to dam's embankment from the back side. The upstream pressure from the bottom side is assumed to be decreasing linearly from a full water pressure of the upstream side up to zero in the downstream end of the slab. Since the perimeter joint separates the foundation slab from the facing, so that there is no interaction between them, there is no force of thrust that the facing would transfer to the slab. That is why, in normal cases, the foundation slab has sufficient stability against slipping, through friction with the foundation (Franco & Pena, 1988).

Regarding the layout, the plinth is laid out as a series of straight lines with the angle points selected to suit the foundation conditions and topography (1, Fig. 12.4). The reference line for the excavation usually is at the bottom of the plinth, in the plane of the bottom of the face slab.

The toe slab requires reinforcing of 0.3% in both directions (Fig. 12.7), thereby providing uniform distribution of temperature stresses and also reduces to a minimum the width of possible cracks, caused by bending. The reinforcement is placed from the upper side of the slab, at a distance 10–15 cm from the upper edge. Distribution reinforcement also extends through control structural joints of the slab, on which no waterstops are used if the foundation consists of a firm, non-deformable rock, where settlement cannot be expected. The arrangement of control structural joints need not be the same as in the slabs of the facing, but it only depends on the conditions of construction (Schewe, 1990).

The anchors connecting the foundation slab with the rock should take on a part of the pressure due to grouting. Reinforcing bars with diameter 25–35 mm are placed at mutual spacing 1–1.5 m in both directions – transversely and longitudinally. By means of a hook, anchors are fastened to the main reinforcement.

When the conditions in the foundation are less favourable and when a relatively deep excavation is required in order to reach sound rock or, else, when it is necessary to lengthen the seepage path through the permeable rock, a concrete cutoff wall is employed as a foundation to the facing; which cutoff wall can also contain a gallery. In such a case, the concrete foundation can be considered as a slab placed in a vertical position. A simple concrete cutoff wall will be used if it is intended to cut the foundation to sound rock or, else, to lengthen the seepage path, and a gallery is anticipated in the cutoff wall if, as an addition to the grout curtain, a drainage system is necessary, and also when an efficient observation system is required, with measurement of seepage below plinth and through the perimeter joint as well as for oscultation of the behaviour of the facing as a whole. The height of the cutoff wall depends on the depth, which it should reach in order to perform the function, and that of the gallery – on the required internal dimensions, dependent on the intention, i.e. the purpose. The thickness of the cutoff wall is determined depending on the external forces, such as water pressure and earth pressure. Possibly needed reinforcement is determined considering the plinth as

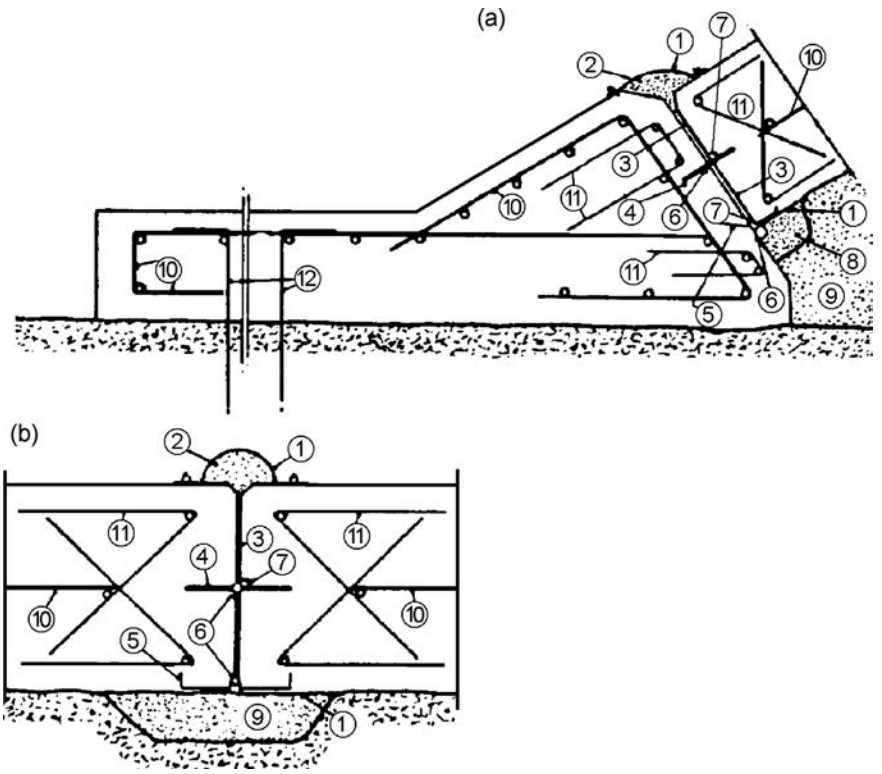

Figure 12.7 Toe slab (plinth) and perimeter joint at the bottom of the valley (a), and at banks (b). (1) Geomembrane cover on waterstop; (2) waterstop of asphalt mastic; (3) filter; (4) waterstop in the central part of slab; (5) waterstop at the bottom; (6) neoprene tube; (7) special filter; (8) shim of sand asphalt; (9) stone chippings; (10) reinforcement; (11) distribution reinforcement; (12) anchors.

a structural element in which, under the influence of the working loads, cracks must not occur. If the concrete cutoff wall is not completely embedded, then it is necessary to check up its stability against slipping and turning over for the condition of a full reservoir, and in a number of sections, since in addition to the external forces, influences are also made by the self-weight and the shape of the cutoff wall which usually varies along the length of the facing's perimeter.

Using the toe slab (plinth) as a grout cap, both consolidation and deep grouting is performed. The grouting under the plinth has the purpose of reducing the flow through the rock foundation. Therefore, the identification of more permeable layers within the rock foundation is a basic requirement to the specifications in regard of depth and grout pressures to be applied. The traditional 3 lines of grouting, with a deeper central line in the range from 1/3H to 2/3H (H – the water head above the plinth) should be considered only as a basis for the design. The consolidation grouting below the plinth is of special importance for this type of dam because of the relatively short seepage path through the rock directly under the toe slab. It should be carried to depths sufficient to

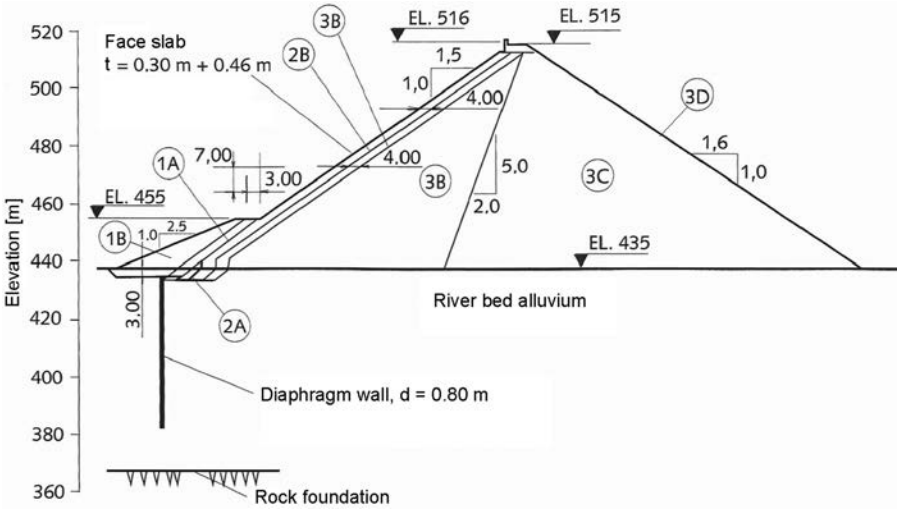

Figure 12.8 Cross-section of Puclaro Dam, with diaphragm wall below the plinth (adapted from Cruz et al., 2009).

penetrate any surface zone of open fissures or higher permeability. At Alto Anchicaya Dam (Colombia), 5 lines of grouting were necessary to improve the sedimentary rock of the foundation below the plinth (Cruz et al., 2009).

There are some examples of CFRDs built on relatively deep alluvium materials, mostly compacted gravel. As a rule, they were provided with a diaphragm wall built below the plinth, as at Puclaro Dam (Fig. 12.8).

12.2.3 Concrete face slabs

The slabs of the facing lie on a *basic sub-facing layer,* which also represents a constituent part of the facing. It is a zone of a fine-grained filling material, most often stone chippings, intended to provide well-compacted, homogeneous and firm base to the slabs. In a usual execution of horizontal layers, the thickness of the sub-facing layer amounts to minimum 3 m, and most often 4–5 m, while placement is carried out in layers with a thickness 0.4–0.5 m, along with compacting by means of vibratory rollers. Sherard recommends that the material in the sub-facing layer should contain 40% particles finer than 4.76 mm in order to prevent segregation in placing the layer. The same author has demonstrated that this layer, executed with appropriately graded material, holds the penetration of water in the occurrence of a crack in the facing or in damaging of any of the joints. Sherard (1985) and ICOLD (1989) recommend the grading curves of the material in the sub-facing layer given in Table 12.1, in order for it to successfully serve its intention. Apparently the two propositions do not differ essentially. It is considered that well-compacted material with a grain size composition within the cited limits does not erode during heavier rainfall and has a coefficient of permeability 10^{-6} m/s.

Table 12.1 Desirable grain size composition of the material in the sub-facing layer.

Size (mm)	*Sherard (1985) % finer*	*ICOLD (1989) % finer*
75	90–100	90–100
37	70–95	70–100
19	55–80	55–80
4.76	35–55	35–55
0.6	8–30	8–30
0.075	2–12	5–15

If it turns out that the surface of the sub-facing layer is still not able to withstand the plant and equipment for the construction of the facing without damaging or, else, is unstable during heavy rainfall, it is stabilized in one of the following methods, applied in practice:

- Spraying with bituminous emulsion or with some other means based on bitumen or tar, able to penetrate into the layer of stone chippings forming, at the same time, a bound stable surface layer. The method is used in a number of older dams, but also in modern dams.
- The execution of a stabilizing asphalt layer which is used with the closed grading of the sub-facing layer, at which the materials that are applied by spraying, do not penetrate sufficiently deep into the layer (4–5 cm).
- Execution of a stabilizing layer of shot-crete. For cases of larger areas this has proved to be a method more expensive than the previous ones. The surface layer thus formed, is stiffer, however, from a technical viewpoint it gives a satisfactory solution.
- Construction of an extruded concrete wall (Fig. 12.6). Since its first application at Itá dam (Brazil) this method has become very popular and widely used in practice. It is an excellent support for the face slabs.

In order to perform their function, *the concrete slabs* of the facing should be durable, flexible and water-impermeable. In terms of the compressive strength, concrete grade 20 MPa is sufficient, while for better impermeability concrete grade 30 MPa is recommended. Aggregate for concrete preparation should not contain grains coarser than 38 mm, and addition of pozzolan has proved to be beneficial in practice. The concrete's strength has been specified for either 28 or 90 days in order to take advantage of the pozzolan action over time. At the recently constructed CFRDs a 60 to 90 day compressive strength of 20–25 MPa was specified. Air entrainment, addictives and slump rates (ranging from 3 to 8 cm) must be specified for slip forming concrete. Slump control represents a key factor for face slab pouring and quality control. Both slip forming speed and concrete quality must be controlled by slump management. At batching plants, sand moisture content and concrete water consumption must be controlled in order to ensure that slumps range from 3 to 8 cm (Cruz et al., 2009).

The thickness of facing slabs on the early dams built of dumped rockfill was traditionally $0.3 + 0.0067H$ [m]. For the CFRD with compacted rockfill and a compacted

upstream face, the thickness increment was decreased to $0.003H$, and even to $0.002H$ or less. Based on the satisfactory performance of these slabs, there is a general trend toward application of thinner slabs. The minimum thickness of 0.3 m is necessary for covering of the reinforcement, construction of appropriate joints and reducing to minimum the cracks due to shrinkage of concrete. With lower dams, let say below 70 m, this minimum thickness could be kept along the entire height of the facing. The maximum hydraulic gradient on the slab should not be higher than 200–220. At two very high dams in Brazil, commissioned around 2005, Campos Novos ($H = 202$ m) and Barra Grande (185 m), the slab thickness was taken as: $0.30 + 0.0020H$, for $H < 100$ m, and $0.0050H$, for $H > 100$ m. Thus, The slab thickness at the base was around 100 cm.

The facing slabs are reinforced. The main role of the reinforcement is similar to that of the foundation slab – to ensure uniform distribution of the temperature stresses and to reduce to a minimum the danger of cracks occurring. In the practice of construction of CFRDs in the period 1980–1990 the usual quantity of placed reinforcement was 0.3% of the cross-section in both directions of the broader central zone which is compressed and 0.4% around the perimeter and into the initial slabs. In the case of very high dams the quantity of reinforcement was determined in accordance with the distribution of stresses and according to strains determined by means of the analyses performed by numerical methods, mainly by FEM, and the usual quantity was 0.4% in both directions, and in certain zones it increased by up to 1%.

During last 20–25 years more very high CFRDs have been constructed. Some of these important examples demonstrated the tendency to generate high stresses close to the abutments. The use of 0.5% reinforcing in the area of 25–30 m perpendicular to the plinth alignment became a common practice as it had yielded good results. Furthermore, at Tianshengqiao 1 Dam (China, $H = 178$ m) a double reinforcement was adopted in the 3rd stretch of the slab (Cruz et al., 2009).

The slabs under working loads are subjected to horizontal pressure. That is why the vertical joints are tightened, i.e. contracted, especially those near the banks and it is customary for the horizontal reinforcement to be conducted through the vertical joints, which reduces the danger of cracks opening. In many cases a copper waterstop is still built-in near the bottom on mortar bedding, (Fig. 12.9a), even in cases when reinforcement passes through the vertical joint, although, in fact, it is unnecessary. If the reinforcement does not pass through the joint, then the waterstop is a compulsory requirement and it should best be a double type of waterstop, as shown in Figure 12.9b. The reinforcement always passes through the horizontal joints, so that it is not usual to carry out waterstops, as shown in Figure 12.9d.

The reinforcement in the slabs of the facing is usually placed in the form of reinforcement wire mesh in the middle of the slab or somewhat higher, which ensures flexibility of the slab, its bending strength in both directions and capability to adjust to small differentiated settlements of the foundation.

In the case of older dams, slabs have been constructed at the end, following the entire completion of the embankment of dam's body, in the form of rectangular slabs, separated from each other, not only by means of vertical, but also with horizontal joints. Significant advancement has also been achieved in the modern dams, by establishing a method for construction of monolithic slabs, without horizontal joints. Thereby, not only structural improvement has been achieved, but also construction has been speeded up, while costs are cut down.

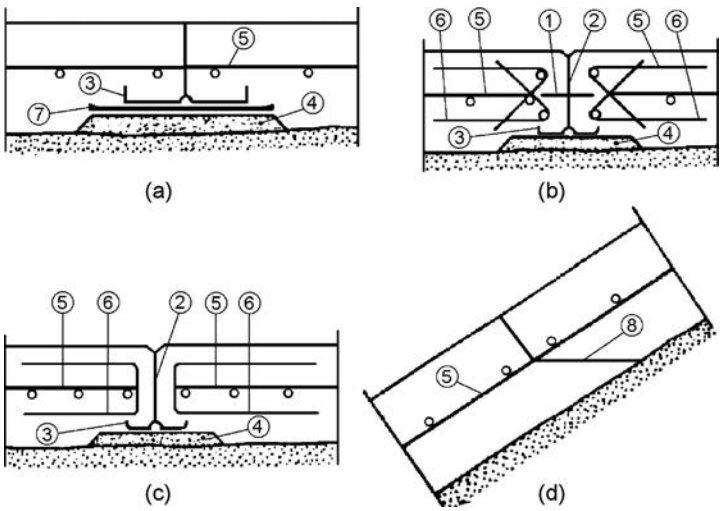

Figure 12.9 Slabs of the facing with reinforcement and control structural joints. (a) Vertical joint with reinforcement through it; (b) vertical joint without reinforcement through it, with a double waterstop; (c) same as in case (b), but with only one waterstop; (d) horizontal joint. (1) central waterstop; (2) bituminous coating; (3) waterstop at bottom; (4) mortar bedding; (5) main reinforcement through the slab; (6) additional reinforcement; (7) bituminous felt; (8) broken joint.

Generally accepted slab width in the case of modern dams is 12–18 m. That enables rational placement of reinforcement meshes and suitable employment of the slipping equipment during placement (see also section 12.1.4). That width is also rational from the aspect of concrete production, which should be synchronized with the progress of construction, and it is considered to be effective if it amounts to 2–3 m/h.

The slabs for modern facings are carried out gradually, i.e. by stages, without a need first of all to carry out the entire embankment. That eases the protection of the construction pit and has a positive influence on the time for construction of works and the cost. The contractor of the works is allowed to determine the number of stages and the level, which will be reached in a certain stage. The design specifies the control structural joints, with reinforcement passing through the joints, between slabs carried out in different stages.

The first stage-by-stage construction has been applied for the Alto Anchicaya dam (Columbia, 1974, $H = 140$ m), and then for Golillas dam (Columbia, 1978, 125 m). The positive experiences with these dams have made the stage-by-stage construction to become a standard construction method for all high dams. Figure 12.10 shows the development of the stage-by-stage construction of facings through examples of six significant dams that have been carried out in Latin America in the last 35–40 years.

In the first example, Alto Anchicaya dam (a), the 15 m wide slabs have been carried out in two stages. Even though three types of joints are employed, they all contain waterstops in the middle, made of natural rubber. Copper waterstops have not been carried out and the mortar toe between slabs is eliminated. The reinforcement has been

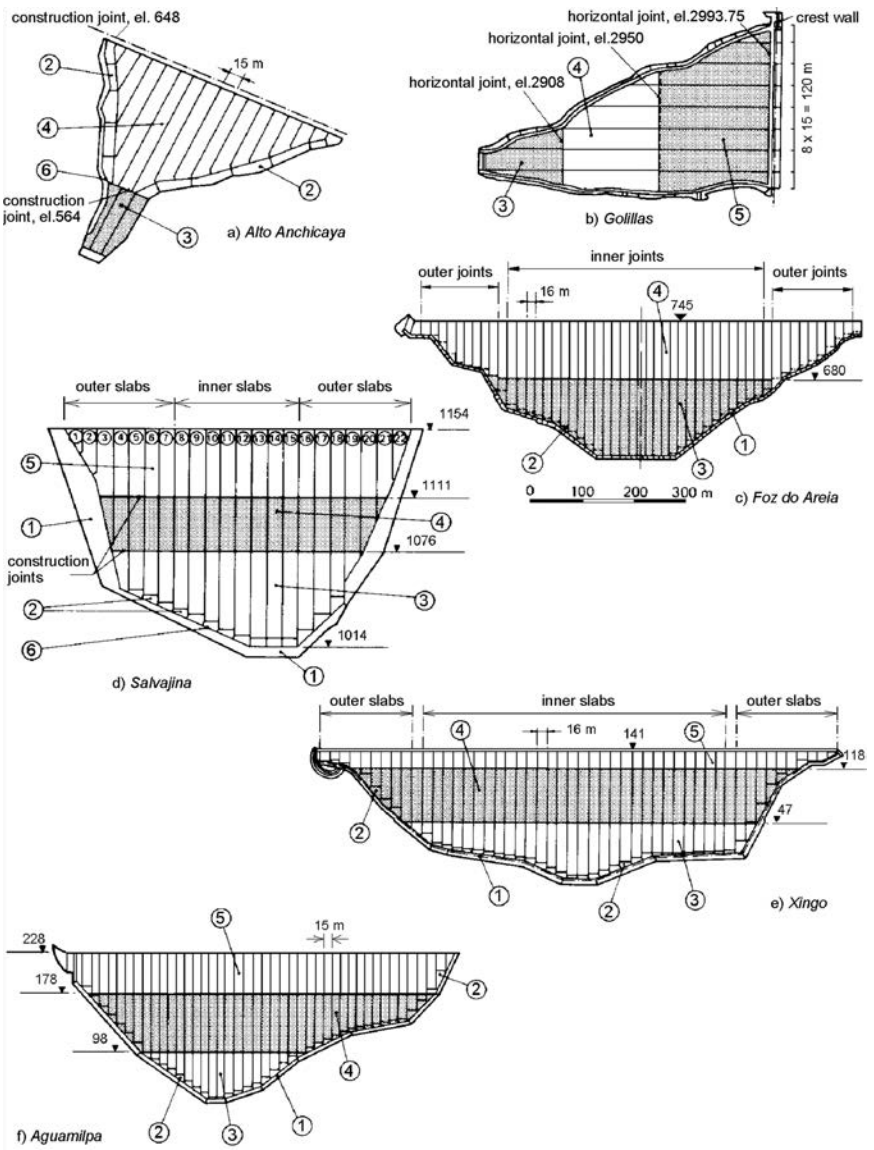

Figure 12.10 Development of stage-by-stage construction of reinforced concrete facings. (1) Plinth; (2) starter slabs; (3) first stage; (4) second stage; (5) third stage; (6) perimeter joint.

placed on the spot owing to the low cost of the work force as well as difficulties for operation of the mechanical devices along the slope of the sub-facing layer, which has not been particularly stabilized. During concrete placement, relatively simple slipform has been used, that has been completely worked out on the construction site. The concrete mix has been poured from mixers into three metal silos, and from there it has been distributed before the slipform (Marulanda et al., 1991).

Golillas dam (b) is also built in Columbia, immediately after Alto Anchicaya dam. It is characteristic that the dam has been carried out on an extremely narrow dam site. As a consequence of this, the surface of the facing is small and consists of only eight main slabs. The slabs have been executed in three stages, with control structural joints at appropriate elevations. The surface of the sub-facing layer is stabilized with a thin layer of shot-crete that has facilitated the placement of reinforcement.

Foz do Areia dam has been built in Brazil in the period 1976–1980 on the basis of experiences of Australian and Columbian dams and by developing a new concept, which afterwards has been massively accepted and employed. Being the highest dam of this type in service (160 m), it has had a strong influence on the further development of dams with reinforced concrete facing. The main slabs have been carried out in two stages (c). The simultaneous construction of both the slabs and the embankment has brought to savings of 8 months in the construction period of the dam with such a large volume – 14 millions m^3. The sub-facing layer has been progressively stabilized with a mixture of asphalt emulsion and sand. The placement of reinforcement in the slabs has been performed by means of a semi-mechanized process: the steel reinforcing bars have been moved down by means of a small vehicle with rubber wheels, operated from the crest by means of a winch, while the main reinforcement mesh has been prepared on the spot due to the relatively cheap work force. On an average 300 t of reinforcement per month have been placed into the structure. All in all, in the example of this grandiose dam, excellent performances have been obtained, while the construction of the facing slabs has not slowed down the construction of the dam as a whole.

Salvajina dam (Columbia) has been built in the period 1982–1984 and it is 148 m high. The shape of the dam site and the varying quality of the material in the foundation, have imposed construction of a plinth with usual geometry in the lower parts and wider plinth at the intermediate and high elevations (Fig. 12.10d). Similarly to Golillas dam, the execution of the slabs has been carried out in three stages, which, in addition to other advantages, has also enabled earlier commencement of the reservoir filling. Here also, improvement, i.e. strengthening of the sub-facing layer has been performed by means of shot-crete. The entire process of the execution of the facing is carried out by a mechanized way, while the quantity of reinforcement has experienced further reduction in relation to the previous dams. Another interesting aspect has been the installation of a machine on the crest of the dam, which had been continuously producing copper waterstops with U-section from rolls of copper sheet.

At Xingo dam (Brazil), with construction commenced in 1987 and completed in 1994, it has been anticipated that the slabs of the facing should be constructed in three stages (Fig. 12.10e). The sub-facing layer has been stabilized with asphalt material, since it is graded in such a manner that segregation is reduced to minimum, but it is not resistant to erosion during heavy rainfalls. In the case of the peripheral slabs, the central PVC waterstop is eliminated, while the copper waterstop at the bottom and the external treatment with mastic have been retained. The placement of reinforcement has been realized by means of a special dolly by means of which prepared mesh of 11×16 m is transported, operated from the crest by means of a hoist. Same type of slipform has been used as for dams Foz do Areia and Segredo. Finally, Figure 12.10f presents the facing of the 187 m high Aguamilpa dam (Mexico), at which the 15 m wide slabs are also carried out in three stages.

12.2.4 Joints for reinforced concrete facing slabs

For a successful work of the concrete facing, a necessary condition is its joint deformation with the shell, i.e. the compatibility with the displacements of the rockfill, when there will not be derangement of the impermeability. In order to achieve this, it is necessary between the slabs to anticipate joints with perfect structure and execution (Bayat & Choi, 1988; Filho, 1995). Displacements of joints depend exclusively on deformations of the rockfill and, under the effect of loading of water, they have a direction, which is normal to the facing. Observations on constructed facings indicate that the facing displaces maximum at approximate height of 40% of dam's height. In that, the whole facing displaces downstream with a tendency to have compression stresses over the entire surface, except for the zone at the crest and at the contact with the concrete plinth, which can be seen from the lines of equal deformations at the facing of the 160 m high dam Foz do Areia (Brazil), Figure 12.11 (Pinto & Mori, 1988).

Displacements of the joints are directly connected with the above-described effect. Vertical joints close in the central part, and they open near the base. For the above-quoted dam, the maximum joints opening amounted to 3 cm, while the relative displacements have taken place in the plane of the facing, that is to say it has not come at differentiated displacements in the adjacent slabs, thanks to the uniform variation of the deformations in the rockfill.

The vertical or temperature joints are positioned at each 12–18 m, same as the width of the slabs in modern dams. They extend across the entire length of the slope – from the crest to the foundation. As a rule, the displacements, which are parallel with the longitudinal axis of the dam, are quite small, so that the temperature joints should be as much elastic as is necessary to take on the temperature deformations. On the other hand, the deformation joints must be more elastic in order to follow to a maximum possible extend the displacements in the embankment below them, at the same time remaining water-impermeable. Customary materials are used for sealing the joints – metal sheets (copper ones or made of special stainless steel), rubber waterstops with various profiles and various compounds based on bitumen. Figure 12.12 shows the construction of deformation joints and temperature joints in these dams.

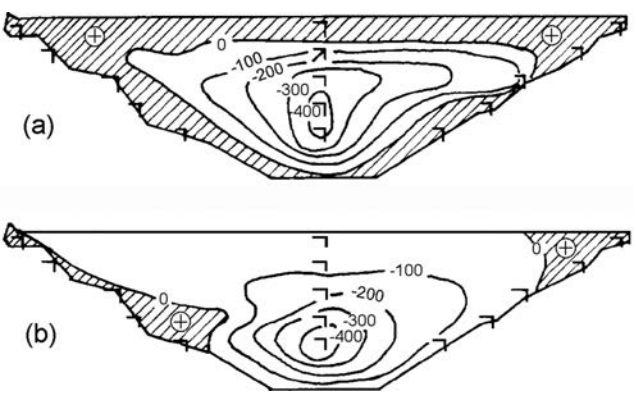

Figure 12.11 Lines of equal deformations in the longitudinal section of the facing of Foz do Areia dam (Pinto & Mori, 1988). (a) In the direction of the slope; (b) in the horizontal direction; (−) contraction; (+) expansion.

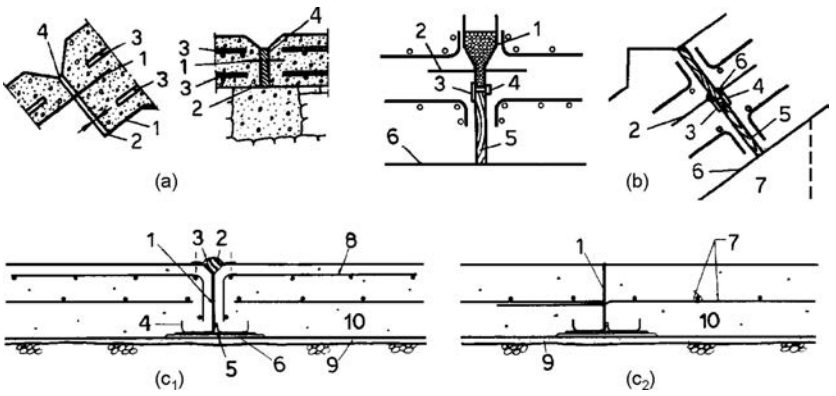

Figure 12.12 Joints in reinforced concrete facings. (a) Quioch dam: (1) Copper sheet; (2) bitumen; (3) reinforcement; (4) boards, (b) Naradela dam: (1) Cast rubber; (2) metal sheet; (3) bituminous waterproof paper; (4) clamp for fixing of waterproof paper; (5) wood; (6) coating with asphalt mastic; (7) concrete girder; (c) New Spicer Meadow dam: (c_1) Vertical temperature joint; (c_2) vertical control structural joint: (1) Bituminous coating on the joint; (2) plastic membrane 3.2 mm, fixed at the ends by means of plates and bolts; (3) sealing compound; (4) copper sheet; (5) bituminous felt of 6.5 mm or PVC strip; (6) mortar bedding; (7) reinforcement in the facing; (8) additional reinforcement in the joint; (9) shot-crete, minimum 2.5 cm; (10) reinforced concrete facing.

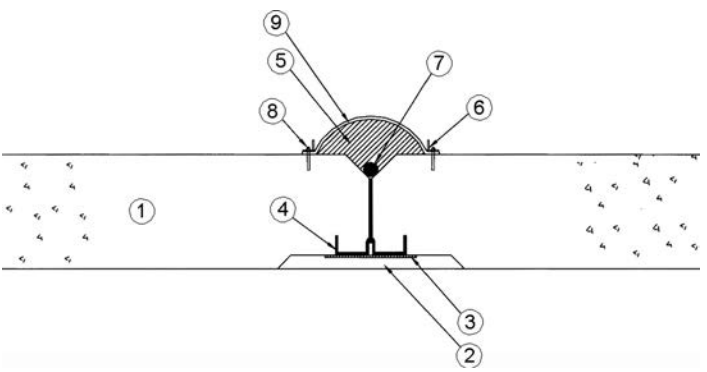

Figure 12.13 Typical special waterstop structure of vertical compression/tension slab joint used at some very high Chinese CFRDs. (1) Face slab; (2) cement mortar; (3) rubber cushion; (4) "W" shape copper waterstop; (5) mastic, called GB filler; (6) rubber rod; (7) "L" steel profile; (8) expansion bolts; (9) resistant cover material manufactured with EPDM.

China is a country with an extremely rich dam construction practice, and it is understandable that Chinese engineers have developed innovations and made improvements to different dam elements. Figure 12.13 shows a special type of waterstop structure of vertical compression/tension slab joint developed by the China Institute of Water Resources and Hydropower Research (IWHR).

12.2.5 Perimeter joint

With reinforced concrete facing the greatest displacements occur in the joint between the facing and the concrete plinth that is to say in the perimeter joint, because the concrete plinth is fixed into the rock and the facing practically floats over the embankment. The perimeter joint always opens and offsets moderately when the reservoir is filled and is a potential source of leakage if not well designed, inspected, and constructed. For dams of low to moderate height ($H < 75$ m), the joint movement has commonly been only a few millimetres, while for higher dams, the joint openings and displacements have been in the order of several centimetres.

At perimeter joint we distinguish three components of motion: opening, normal to the joint (3, Fig. 12.14), displacement normal to the facing (4) and tangential displacement, parallel with the joint (5).

In order for the perimeter joint to be able to "work" under such conditions and at the same time to remain water-impermeable, it requires at least a double waterstop, as is the case in Cethana dam (Australia, $H = 110$ m; Fig. 12.15), where the embankment has been placed and compacted in an exceptionally quality manner.

Later on a more complex construction was carried out in 1980 for the higher dam Foz do Areia where in addition to a double waterstop, a "reservoir" of asphalt mastic was added (Fig. 12.16). The two waterstops of different material and of different shape should reduce to a minimum the prospects for forming an opening, in case if one of the waterstops has been damaged. The asphalt mastic is anticipated as a reserve material, which, with penetration into the joint under the water pressure, would enable self-healing, provided, yet, it comes to considerable penetration of water. The sandy

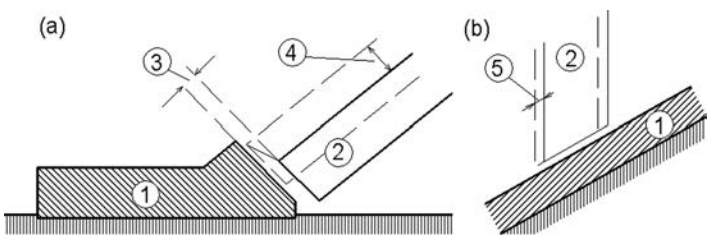

Figure 12.14 Displacement of the perimeter joint (after Pinto & Mori, 1988). (a) Cross-section; (b) longitudinal section. (1) Concrete plinth; (2) Concrete slab.

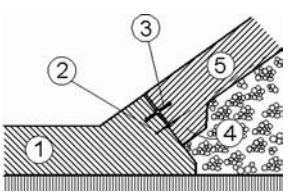

Figure 12.15 Perimeter joint at Cethana dam. (1) Concrete plinth; (2) waterstop of copper sheet; (3) rubber waterstop; (4) concrete bedding; (5) slab of the facing.

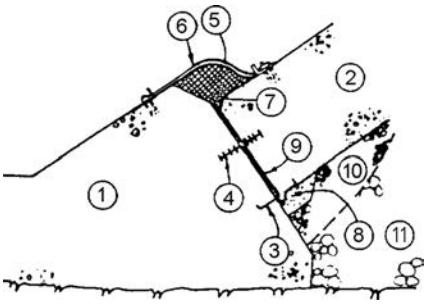

Figure 12.16 The perimeter joint at Foz do Areia dam, Brazil (after Pinto & Mori, 1988). (1) Concrete plinth; (2) facing slab; (3) copper waterstop; (4) PVC waterstop; (5) mastic; (6) PVC cover; (7) neoprene tube Ø 50 mm; (8) sand asphalt; (9) timber sawdust; (10) stone chippings; (11) rockfill.

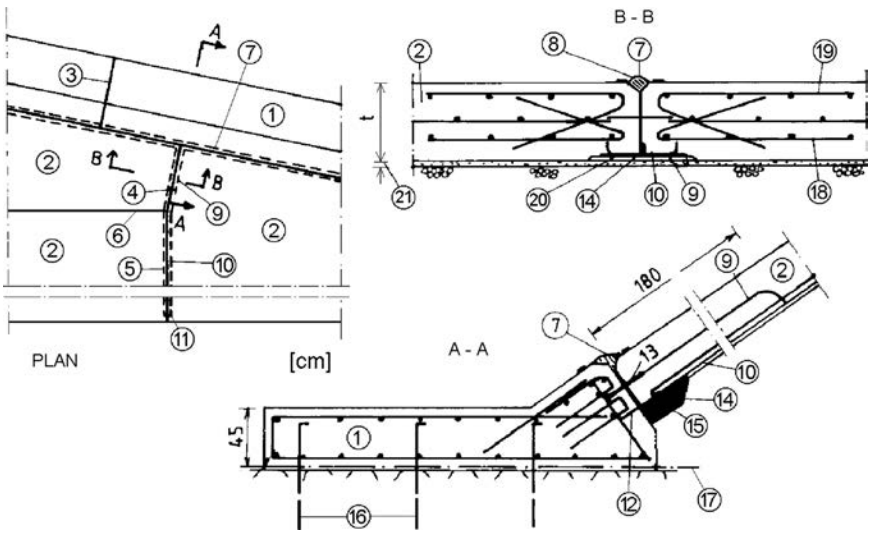

Figure 12.17 Details of the joint between the facing and the plinth of New Spicer Meadow dam. (1) Reinforced concrete plinth; (2) reinforced concrete facing; (3) control structural joint; (4) end of strengthened joint (section B–B); (5) vertical deformation joint; (6) horizontal control structural joint; (7) plastic membrane over sealing compound (8); (9) copper sheet, type II and III (10); (11) end of copper sheet type II, at elevation 2017 mwl; (12) copper sheet, type I; (13) PVC waterstop; (14) bituminous felt of 6.5 mm or PVC strip; (15) sand asphalt; (16) anchor bolts, Ø 2.5 cm; (17) theoretical line of the foundation; (18) main reinforcement; (19) additional reinforcement; (20) mortar bedding; (21) shot-crete, minimum 2.5 cm.

asphalt serves as bedding for the copper waterstop and it prevents the effluence of the mastic. The tube of synthetic neoprene would help in closing a bigger opening, in case of a significant widening of the joint. A part of the concrete plinth and the perimeter joint, in which the pressure of water is bigger than 112 m, is covered with

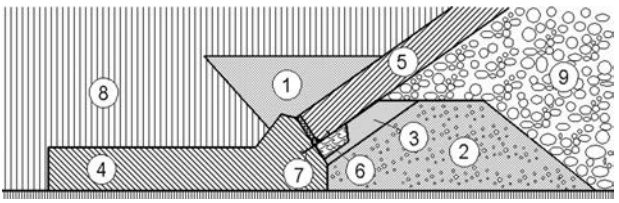

Figure 12.18 Proposed construction of peripheral joint (after Pinto & Mori, 1988). (1) Fine sand; (2) filter material; (3) same as (2), enriched with 5% cement; (4) toe slab; (5) concrete slab of the facing; (6) bedding of sandy asphalt; (7) waterstop of copper sheet; (8) earth embankment; (9) transition sub-facing layer.

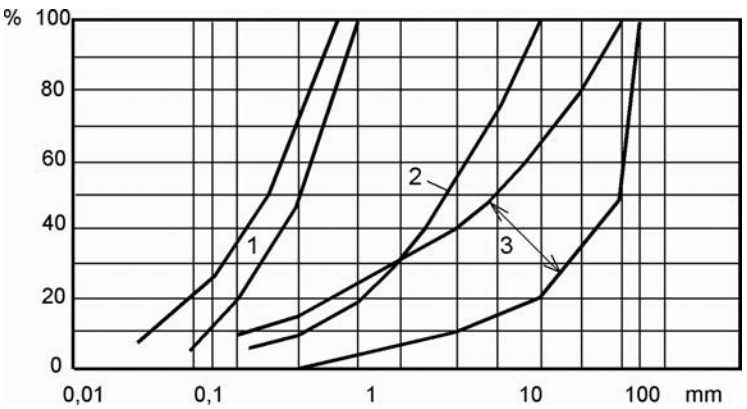

Figure 12.19 Curves of grain size distribution of the fine sand (1), filter material (2) and transition sub-facing layer (3) (after Pinto & Mori, 1988).

earth embankment, as another additional obstacle to the penetration of water, more specifically in the zone of the joint in which maximum displacements are expected. The perimeter joint of this dam turned out to be safe in service, so that a construction with a triple sealing is carried out in many other new dams, among the others New Spicer Meadow dam (USA), for which details of the joint between the facing and the plinth in both layout plan and sections, are shown in Figure 12.17.

The designers of the Foz do Areia dam have performed additional laboratory tests in order to clarify the role and the endurance of individual sealing elements. For a joint of 1.2 cm, the PVC waterstop has performed very effectively as long as there have been no displacements. A 2.5 cm opening of the joint has caused breaking of the waterstop and significant penetration of water, which has increased over the course of time. It means that the asphalt mastic has not been efficient in relation to the expected self-healing, most likely owing to the high cohesion. On the basis of further investigations, the construction presented in Figure 12.18 has been proposed as the most efficient one, which has a constructed wedge of fine sand (1) instead of a reservoir with asphalt mastic. Below the joint, in addition to the bedding of sandy asphalt (6), filter layers

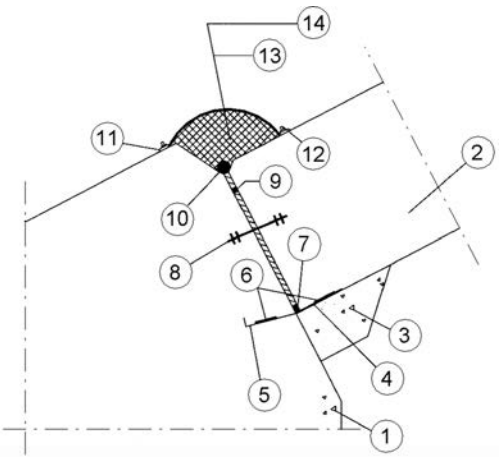

Figure 12.20 Typical waterstop structure of perimeter joint developed by IWHR and used at some Chinese CFRDs. (1) Plinth; (2) face slab; (3) cement mortar; (4) PVC cushion; (5) "F" shape copper waterstop; (6) GB sealant; (7) foam plastic) (8) rubber waterstop; (9) timber; (10) rubber rod; (11) flat steel; (12) expansion bolts; (13) GF filer (mastic); (14) GB-EPDM cover.

(2) and (3) have been anticipated of materials with a grain size distribution as shown in Figure 12.19. The fine sand without cohesion, with a coefficient of permeability $k \approx 10^{-4}$ cm/s, in combination with the filter layers, during laboratory tests had been efficiently closing, i.e. sealing for joint openings of 3 cm (Pinto & Mori, 1988; Pinto et al., 1988; Montañez-Cartaxo, 1992).

In that way, by means of laboratory tests it has been proved that with fine sand, which is built-in above the perimeter joint of the reinforced concrete facing, we can successfully prevent penetration of water at displacement of the slabs. The designers deem that in combination with a filter layer below the slabs, it is very likely that the fine sand would prevent penetration of water even in the case of a very high dam.

Figure 12.20 shows a typical waterstop structure of perimeter joint developed by IWHR and used at some Chinese CFRDs. The similarity with the solution at Foz do Areia dam is evident.

12.2.6 Parapet wall and camber

It is usual practice for the facing in the upper end to end up with a parapet wall (Fig. 12.21), located at the upstream edge of a dam's crest. Three objectives are obtained with the parapet which is elevated over the dam's crest: (1) The parapet provides a firm and stable ending of the facing; (2) Savings are achieved on the embankment of the dam, since the crest is at a lower elevation; (3) Freeboard is reduced, because due to the shape of the wall, the wave run-up is smaller. The parapet, in fact, represents a cantilevered retaining wall, connected with the slabs of the facing by means of a flexible joint, with a base slab placed on the sub-facing layer on the upper side, fixed with the embankment of the crest (Schewe, 1990).

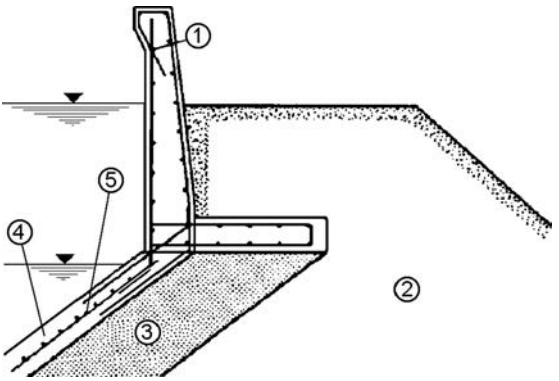

Figure 12.21 Parapet wall at the upper end of facing. (1) Parapet wall; (2) dam embankment; (3) sub-facing layer; (4) slabs of the facing; (5) reinforcement.

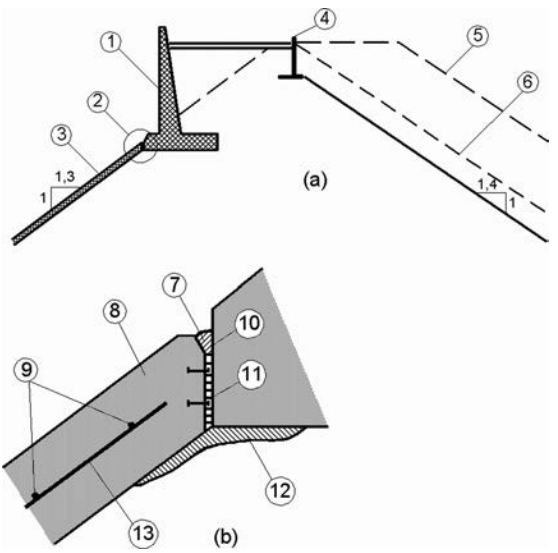

Figure 12.22 Detail of dam's crest (according to ICOLD 1989). (a) Detail of the crest; (b) detail of the joint. (1) parapet wall; (2) detail b; (3, 8) concrete slab; (4) downstream parapet wall; (5) additional embankment there were no wall; (6) additional embankment without downstream wall; (7) asphalt mastic; (9) horizontal reinforcement; (10) coating; (11) joint filling; (12) mortar bedding; (13) sloping reinforcement.

The base of the parapet wall is placed above the elevation of the normal water level in the reservoir. The wall would best be connected with the slabs of the facing by means of an elastic joint, as shown in Figure 12.22, in accordance with the recommendations of ICOLD. The joint should be vertical and not normal to the plane of slabs, in order to enable proper adaptation to differentiated settlements (Fell et al., 1992).

The camber, or the heightening of the dam crest for compensation of the post construction settlement, has to take into consideration the amount of the expected rockfill creep. For modern CFRDs a large amount of time settlement is not expected, because the dam body is well compacted and it is separated from the reservoir by the watertight facing. Appreciable settlement can cause a strong earthquake, but the probability of occurrence of such event is very small.

12.3 CONSTRUCTION OF THE REINFORCED CONCRETE FACING

The construction of a reinforced concrete facing for moderately high dams begins when the embankment will be carried out up to the full height, while dam's crest is a basis for the performance of all activities about the construction, except for the plinth and the initial slabs in the river valley. In the case of modern high dams, the facing is carried out stage-by-stage, i.e. in two or three stages, which has already been considered in section 12.2.3.

Construction of the plinth in the river valley can be performed before, during or after the construction of the embankment part of the dam. In order to save time, the plinth would best be carried out parallel with the construction of the embankment. The construction of the plinth covers the following main activities: (1) Excavation of a trench up to sound rock, resp. to the anticipated depth of foundation; (2) Building-in of a binding layer of concrete; (3) Installation of fit-up formwork by means of which it is possible to cast a section of the plinth which is up to 20 m long; (4) Drilling of anchor holes and placing of anchors; (5)Placement of waterstops and fit-up mesh reinforcement; (6) Casting and curing of concrete; (7) Release, i.e. striking of the formwork and (8) Grouting of the foundation.

Prior to the construction of the concrete slabs of the facing, the surface of the sub-facing layer is treated by one of the methods described in section 12.2.3. Thus the base, upon which concrete will be placed, becomes more stable and it is also prevented infiltration of concrete laitance into the sub-facing layer. This operation is carried out by means of a mobile platform on rubber wheels, operated and provided with materials from the crest or from the temporary crest in the case of stage-by-stage construction. The extruded curbs are constructed parallel to the embankment layers by means of special formwork and other appropriate equipment.

The following preliminary works, preceding concrete slab casting, are to be considered: placement of waterstops at the bottom and execution of mortar bedding, construction of foundation blocks and girders for the rails of the slipform, placement of fit-up formwork for the irregular initial slabs around the perimeter, placement of reinforcement and waterstops. The materials (rails and reinforcement) are transported by means of rail transporters, operated from the crest, as it is shown in Figures 12.23 and 12.24. Concrete casting is carried out separately for the initial slabs and for the long monolithic strip like slabs. Since the initial slabs have irregular shape, they are concreted in a classical way by means of fit-up formwork. And the monolithic slabs which are, in fact, the main elements of the facing, are concreted by means of slipform, operated from the crest and precisely lead along on rails, in strips which are as wide as is the width of the slabs (Fig. 12.24 presents the equipment used for slab concreting, 10 m wide). The equipment has been so constructed as to be able to adapt to the

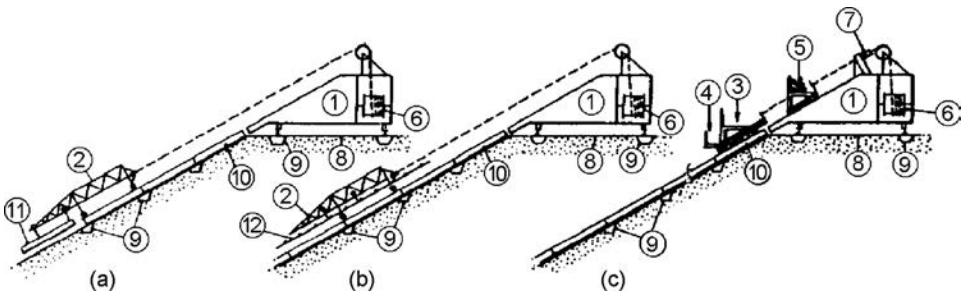

Figure 12.23 Transportation equipment for the construction of concrete facing. (a) Transportation of rails, (b) of reinforcement and (c) of slipform: (1) Rail transporter on the crest; (2) transporter for rails and reinforcement; (3) slipform; (4) working platform; (5) platform for delivery of concrete; (6) pulley for lifting; (7) hydraulic hoist; (8) crest of dam; (9) supports for rails; (10) mounted rails; (11) rails for slipform; (12) fit-up reinforcement mesh.

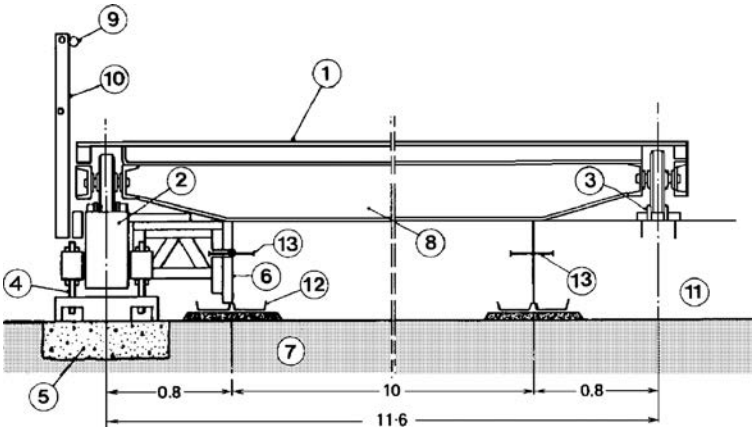

Figure 12.24 Layout of equipment for the construction of the slabs of facing. (1) Slipform – basic frame; (2) rail beam; (3) rail; (4) screw for centring the rail; (5) concrete plinth block; (6) lateral formwork; (7) mortar bedding; (8) regulating guide; (9) cable in protective tube; (10) railing; (11) cast slab; (12) waterstop at bottom; (13) intermediate waterstop.

width of the slabs. During concreting of the strip, one rail is laid along the adjacent, already concreted slab, while the other one on a rail beam, which is supported on the sub-facing layer, Figure 12.24, Figure 12.25. The size of the section being concreted is planned in such a manner as to enable optimum utilization of the formwork, and the negative effects of concrete shrinkage and those due to hot weather to be reduced to minimum (Beach et al., 1991; Schewe, 1990).

The method of placement of reinforcement depends on the required speed of advancement of works and the cost of the skilled work force in the country where

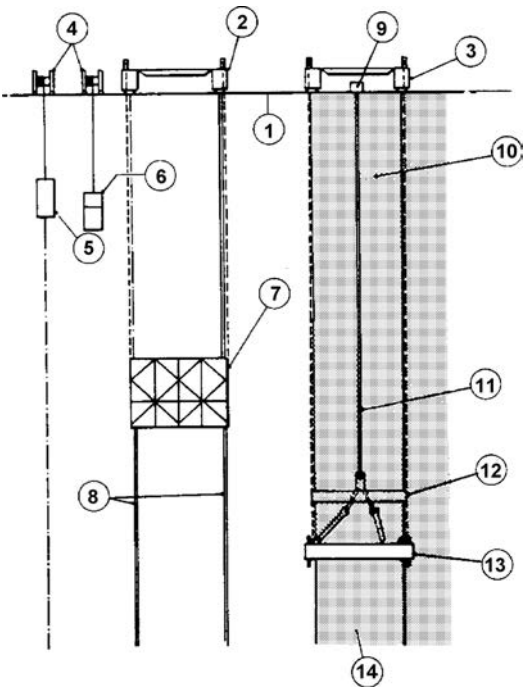

Figure 12.25 Section through the climbing formwork (slipform). (1) Dam's crest; (2) rail transporter on the crest; (3) rail transporter of slipform; (4) hoist for lifting; (5) rail transporter for the execution of mortar bedding; (6) transporter for access to the slabs of the facing; (7) transporter for rails and reinforcement; (8) installed rails for the slipform; (9) concrete pump; (10) reinforcement mesh; (11) pipe for concrete delivery; (12) platform; (13) slipform; (14) concreted slab.

the dam is carried out. Construction works must not be delayed due to placement of the reinforcement. It must have been placed in due time prior to casting of the concrete. During the execution of the concrete works, concrete is poured into silos, located on the top of the embankment of appropriate stage, from where it is distributed before the formwork. In this way, concreting of the slabs advances with a speed of 2–3 m/h. The manufacture of concrete is usually limited by the capacity for transportation of the concrete mix. Normally are produced 13–22 m^3/h (for modern dams the maximum amounts to 50–60 m^3/h). In that way, in the case of modern dams (Foz do Areia, Segredo etc.) it has been possible for the facing to advance by 13,000 m^2 a month, by spending 1–1.5 hour per worker per m^2 (Materon et al., 1992).

For illustration of the construction phase of the CFRD, Figure 12.26 shows Siah Bishe Lower dam (Iran, $H = 128$ m), during the final stage of facing slabs construction, in 2009. The dam, which is a part of a pumped storage scheme, was commissioned in 2012. The second dam of the scheme, Siah Bishe Higher, $H = 100$ m, is also of the CFRD type.

Figure 12.26 Siah Bishe Lower dam (Iran, $H = 128$ m), during the final stage of facing slabs construction, in 2009 (courtesy Mr. Lotfali Modarres).

12.4 EXAMPLES OF MODERN CFRDs

Since the first modern dam with a reinforced concrete facing, Cethana, was constructed in 1971, considerable progress has been made in the field of design and construction of very high CFRDs. Recently, the height of 200 m was exceeded. The plot in Figure 12.27 illustrates the evolution of this dam type during the last 40 years. Next, some important CFRDs, constructed in different sequences of this period, will be described.

12.4.1 Examples from the period 1971–1980

12.4.1.1 Cethana dam (1971)

The first modern dam with a reinforced concrete facing is Cethana dam (Australia), completed in 1971. It is 110 m high, with slope inclinations 1:1.3, Figure 12.28. In the course of design and construction of this dam, there has been a complete utilization of the lessons, knowledge and experiences of till then constructed dams, and original improvements have also been carried out. The major improvement is the execution of the embankment by means of finer grains of rockfill. The sub-facing layer also encompasses fine particles, which helps providing a firm and even semi-permeable zone. Other improvements are: incorporation of two waterstops in the joints, stabilization of the surface zone of the sub-facing layer by means of spraying with bituminous emulsion, already exercised continuous execution of the slabs from the foundation to the crest, as well as a division of the rockfill embankment in three zones. Dam's body

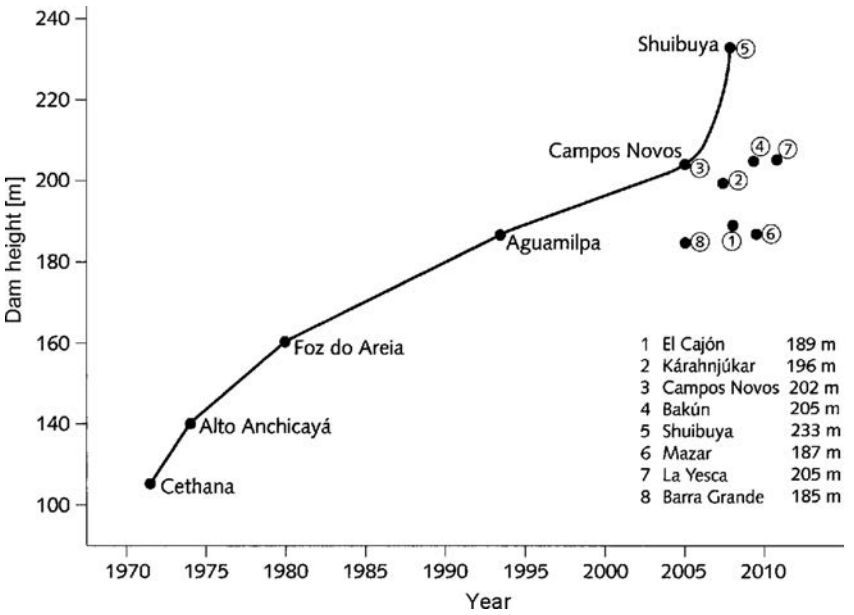

Figure 12.27 CFRD height evolution after 1970.

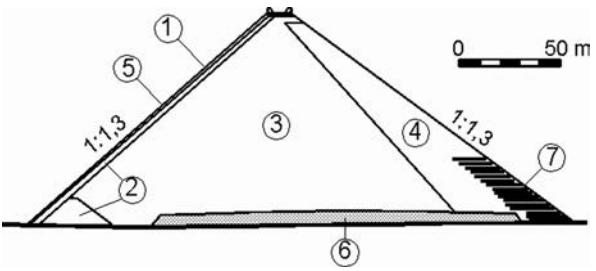

Figure 12.28 Cethana dam (Australia). (1) Reinforced concrete facing; (2) hard, well-graded rockfill, grains up to 610 mm, placed in layers of 45 cm each; (3) same as (2), however placed in layers of 90 cm each; (4) rockfill, grains up to 900 mm, compacted in layers of 135 cm each; (5) sub-facing base of rockfill, grains up to 225 mm; (6) river channel; (7) protective steel mesh.

has been carried out of hard quartzite with a maximum grain size 610 mm, in layers of ≈90 cm each, compacted with four passes of a 9-ton vibratory roller and with simultaneous sprinkling with water in quantities of minimum 15% of the volume of embankment. As a base to the facing, it is constructed a 3 m thick layer of especially selected material with a maximum grain size 225 mm, compacted in layers of ≈45 cm each, with a greater number of passes. During the compaction and in order to prevent damaging, the layers have been stabilized with bituminous emulsion (Fell et al., 1992).

The reinforced concrete facing has been carried out by means of slipform, in monolithic slabs 12.2 m wide, with expansion joints. At the periphery there are also inserted transverse inter-joints in order to prevent cracking of the slab in the zones of possible horizontal tensile stresses. The main joints are closed with wooden laths, while the inter-joints are not closed at all. The reinforcing amounts to 0.5% in both directions, while it is higher in the zones of jointing with the plinth. The thickness of the facing amounts to $0.30 + 0.002H$ m. After clearing and stripping of the foundation, the plinth has a surface joint with the rock. The minimum width has amounted 3 m. The plinth is anchored into the base in order to be able to withstand the pressure of the consolidation grouting. The dam is abundantly provided with instruments which, in the course of construction and after filling of the reservoir, have recorded small deformations in dam's body and normal work of the facing (compressive stresses, maximum deflection 13 mm, maximum opening of the joints 11.5 mm, seepage water quantity 0.035 m^3/s).

12.4.1.2 Alto Anchicaya dam (1974)

After Cethana dam, another significant dam with a reinforced concrete facing has been constructed – Alto Anchicaya (1974), even 140 m high, Figure 12.29. Yet, it has been an initial period for the construction of such high dams with the new construction technology, and it did not pass without serious problems. During the first filling of the reservoir, it has been recorded a penetration of water in a quantity of 2 m^3/s. The reservoir has been emptied, causes established and removed by means of appropriate rehabilitation. The dislocation of the perimeter joint, under the effect of the hydrostatic

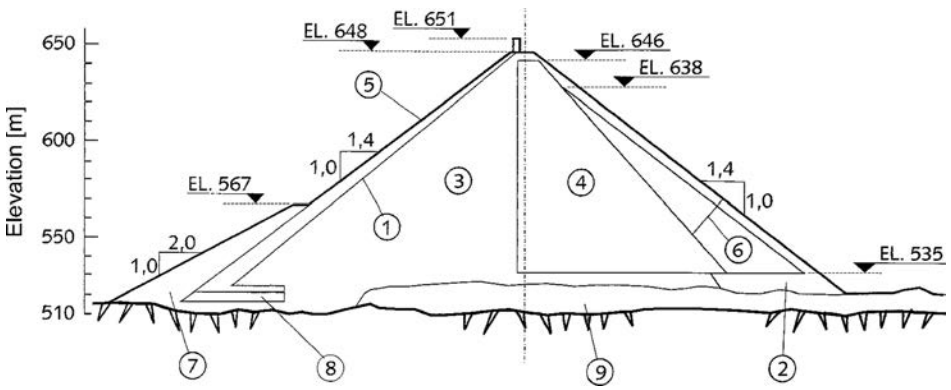

Figure 12.29 Cross-section of Alto Anchicayá dam (Colombia). (1) Zone 2B, compacted in 50 cm layers with vibratory roller 10 t, 4 passes horizontally and 8 in the upslope direction; (2) drain, placed in layers of 1 m each, compacted with vibratory roller 10 t; (3) zone 3B compacted in layers of 60 cm with vibratory roller 10 t, 4 passes, water 200 l/m^3; (4) zone 3C fine rockfill, compacted in layers of 60 cm with vibratory roller 10 t, 4 passes, water 200 l/m^3; (5) face concrete slabs, $t = 0.30 + 0.003H$ [m]; (6) zone 3D, over sizes rockfill, vibratory roller 10 t, 4 passes; (7) zone 1, clayed silt, compacted with usual construction equipment; (8) sand and coarse filter, compacted with 2 passes of 10 t vibratory roller; (9) dens natural river bed gravel.

pressure, has been significant – 10 cm, while the single waterstop (rubber) has been damaged. It has been established that during execution of works, there has not been taken special care for the compaction of the material behind the plinth. The rehabilitation of the perimeter joint has been successfully carried out with a surface cover of rubberised asphalt (Marulanda et al., 1991).

12.4.1.3 Foz do Areia dam (1981)

Foz do Areia dam (Brazil) was completed in 1981. With its 160 m height – it is not only the highest such dam till then, but it also had the biggest reservoir. The analyses have shown that this type of dam is the most economical for the given hydroelectric plant. Total rockfill placed into dam's body, comes from excavations for the works. Having the experiences of Alto Anchicaya dam, particular attention has been paid to the perimeter joint, as well as to the gradation of the material, the compaction and the control in the zone of the plinth. The perimeter joint has three waterstops (see Fig. 12.16). The sub-facing layer contains grains of maximum diameter 6 cm, and the reinforcing of the slab is rationally carried out. After 10 years of service, the settlements are within specified limits, (Mori & Pinto, 1988), while seepage has reached only 70 l/s.

12.4.2 Examples from the period 1982–2000

12.4.2.1 New Spicer Meadow dam (USA)

In the USA, at the end of 1989 construction of the 79.3 m high New Spicer Meadow dam was completed, sited at over 2000 m height above sea level (Fig. 12.30). The dam with facing has been selected following the comparison with other possible solutions, above all, with earth–rock and concrete gravity dams, in relation to which it has proved to be more economical. It is founded on a foundation of granodiorite, of which material the dam's body is also carried out, with slope inclinations 1:1.4. Some 2 million m^3 of rock material have been built in, zoned as shown on the drawing.

The facing is constructed of concrete with concrete grade 25 MN/m^2, with a maximum aggregate grain of 38 mm, on previously leveled surface, with a layer of shot-crete, with a thickness of minimum 2.5 cm. Thickness of the facing varies according to the

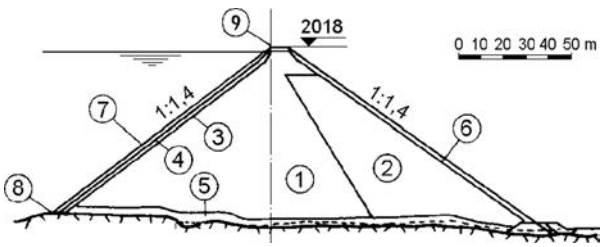

Figure 12.30 New Spicer Meadow dam (USA). (1) Rockfill compacted in layers of 90 cm; (2) rockfill, compacted in layers of 1.5 m; (3) transition layer, coarse stone chippings, compacted in layers of 45 cm; (4) sub-facing layer of stone chippings, layers of 45 cm; (5) drainage layer of compacted rockfill; (6) treatment of the downstream slope; (7) reinforced concrete facing; (8) reinforced concrete plinth; (9) parapet wall 1.8 m.

expression $d = 0.3 + 0.003H$ m, where H is the depth of the section below the normal water level. Low-alkali Portland cement with addition of 15% pozzolan has been used as a binding agent. The facing is reinforced in two directions, with minimum reinforcement 0.4% of the section of the facing, and with horizontal reinforcement increased to 0.5% in the lowermost slabs. The reinforced concrete plinth at the end of the facing has a variable thickness, in order to adapt more appropriately to the ground, without too large excavation, while in the same time it also serves as a base for grouting. Consolidation grouting has been carried out in the rock to a depth of 3 m, with a pressure of 140 kN/m^2. A grout curtain has been carried out by means of a line of boreholes spaced at 3 m, up to a depth of $0.33H$. The facing is divided into slabs with vertical deformation joints and control structural joints, spaced at 18 m apart (Fig. 12.12c) and with two horizontal control joints – one of them above the joint with the plinth, and the other one in the central part.

12.4.2.2 Segredo dam (Brazil)

In 1992 in Brazil was completed Segredo dam, 145 m high, constructed on the basis of principles of Foz do Areia dam, with certain improvements and rationalizations. The upstream slope is steeper – 1:1.3 (1:1.4 at Foz do Areia), the reinforcement in the central zone of the facing has been decreased to 0.3%, the maximum grain in the subfacing layer has been reduced from 15 cm to 10 cm, and parallel with the perimeter joint it has been inserted 3 m wide zone of fine filter material, with particularly carefully performed compaction. The fine filter layer should reduce the penetration of water at possible yielding of waterstops of the perimeter joint. By this change, the central waterstop has been dropped. The reinforcement through the plinth is continuous, with control structural joints without waterstops. Measuring of the penetrating water has not been anticipated, since the construction of such dams has already been proved as very safe one (Blinder et al., 1992; Neidert & Toniatti, 1991).

12.4.2.3 Aguamilpa dam (Mexico)

In the course of 1994 the highest dam with a reinforced concrete facing at that time was completed – Aguamilpa, in Mexico (187 m). It is constructed according to the most modern principles. It is interesting to point out that the layer of alluvial deposit is not removed from below the dam, except in the zone from 90 m behind the foundation of the facing, while gravel has been exploited from the river bed and placed in great quantities in the lower part of the dam. Especially detailed analyses and tests have been made in the selection of waterstops for the perimeter joint, for the construction of which it has been used the concept shown in Figure 12.18.

12.4.2.4 Xingo dam (Brazil)

Another very large dam, Xingo, 140 m high (Figs. 12.31–33), was completed in Brazil in 1994. Regarding the construction it is very similar to Segredo dam. The rockfill into the dam abutments is placed at a depth of 20 m under the water prior to diversion of the river. In that way, a larger part of the rock excavation entered directly the dam's body. Another specific characteristic of this dam is the execution of a zone of roller compacted concrete (RCC) at the downstream slope, to ensure firm overflowing

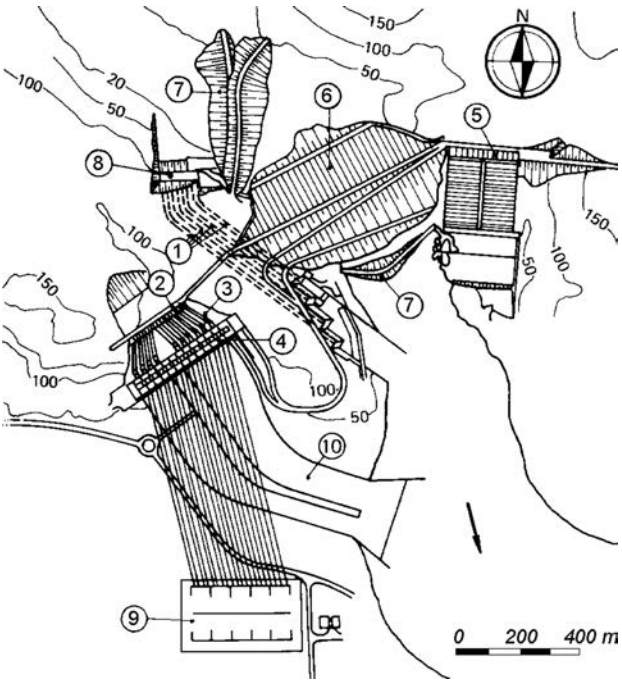

Figure 12.31 Layout plan of Xingo dam, with appurtenant structures. (1) Diversion tunnels; (2) intake for the hydroelectric power plant; (3) penstocks; (4) powerhouse; (5) spillway; (6) dam; (7) cofferdam; (8) intake for diversion of the river; (9) substation; (10) tailrace channel.

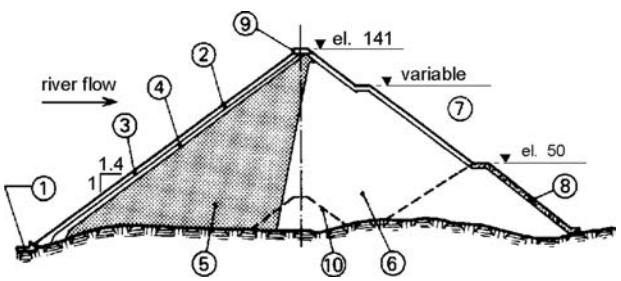

Figure 12.32 Xingo dam cross-section. (1) Concrete plinth; (2) face slab; (3) zone I; (4) zone II; (5) rockfill zone III; (6) rockfill zone IV; (7) zone V; (8) roller compacted concrete; (9) parapet; (10) central cofferdam.

surface for the case of submersion of the constructed part of the dam in the course of construction stage one, owing to river's abundance with water. For these reasons, the protection of the construction foundation pit is very complex. It consists of a 50 m high cofferdam and even four tunnels with diameters of 16 m, by means of which it is possible to divert water of a return period of 30 years. In order to accept possible

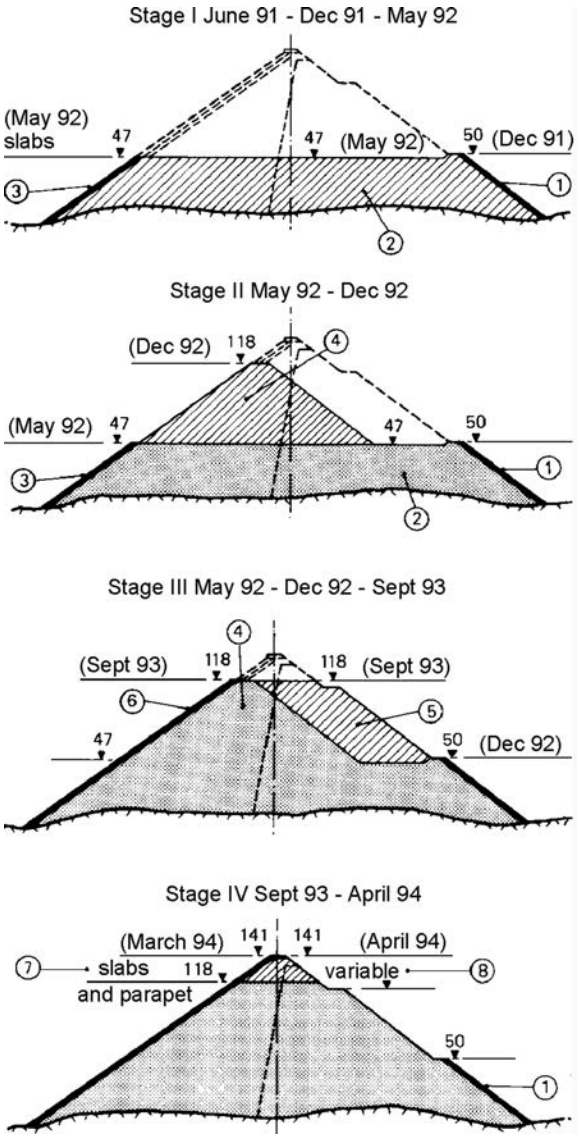

Figure 12.33 Construction of the body and facing of Xingo dam, in stages. (1) Roller compacted concrete; (2) rockfill up to elevation 47 m; (3) slabs of the facing – stage I; (4) rockfill up to elevation 118 m; (5) rockfill – downstream, up to elevation 118 m; (6) slabs of the facing – stage II; (7) slabs and parapet wall – stage III; (8) rockfill up to elevation 141 m.

200-year water, the lower part of the downstream face of the dam is strengthened up to the height of the cofferdam by means of RCC lining.

As it is seen from Figure 12.32, the rockfill material in dam's body is divided into five zones. The sub-facing layer (zone I) is made of separated stone chippings

with maximum grain size of 10 cm, compacted in layers of 40 cm with six passes of a 10-ton vibratory roller. Zone II contains maximum grain of 40 cm, and it is compacted in the same way as the previous one. The zone III has a maximum grain of 1 m, and it is compacted with four passes of a 10-ton vibratory roller in layers of 1 m, with addition of water. Zone IV contains blocks up to 2 m diameter, is placed same as the previous zone, but in layers of 2 m thickness, without addition of water. Zone V represents a mechanically formed layer of coarse rock with a thickness of 1 m, for the protection of the downstream slope. The RCC is carried out in layers of 40 cm, compacted with eight passes of a 9-ton vibratory roller (Materon et al., 1992). See Chapter 18 on details for RCC.

Figure 12.33 presents planned stage-by-stage construction of the dam by seasons. The first season is planned for the first dry season. Having passed the first flooding season, the dam is heightened in the second dry season up to a level, which could accommodate diversion of possible 1000-year water. The RCC – 4 m wide, is heightened along with the advancement of the embankment. The lining of RCC is anchored into the embankment by means of reinforcing steel bars. At each 1.2 m heightening of the embankment, there come three layers of 0.4 m RCC. Steel tubes are embedded into the RCC to serve as drainage. In the course of the first stage of construction, the dam was flooded in March 1992, however, for that purpose planned construction has properly endured the impact. The river Sao Francisco has an average annual discharge of 2900 m^3/s at the dam site Xingo.

At the end of the 1990s a CFRD around 180 m high – Tianshengqiao I ($H = 178$ m) – was also completed in China. Thus, we can conclude that the last decade of the 20th century was a decade of successful construction of 180 m-high CFRDs, mainly with very satisfactory behaviour.

12.4.3 First decade of XXI century

The very high CFRDs successfully designed and constructed in the last decade of the 20th century have encouraged dam engineers to design and construct even higher embankment dams of this type. As a result several other very high dams have been constructed during the first decade of the 21st century: Barra Grande ($H = 185$ m), Campos Novos (202 m), El Cajón (189 m), Sanbaxi (186 m), Kárahnjúkar (196 m), Mazar (170 m), Bakun (205 m), culminating with the Shuibuya dam in China, with a height of 233 m. But some problematic events observed at the Barra Grande dam in September 2005, the Campos Novos dam in October 2005, and the Mohale dam in February 2006, when extensive rupture of the concrete face occurred under compression, have drawn attention to one characteristic of CFRDs which had until then gone unnoticed: the high compressive strains which can be imposed on the face slab mainly because of an adverse combination of dam height, low rockfill deformation modulus, and unfavourable valley shape. The understanding of this phenomenon and of the agents involved and the appraisal of their influence on the design of very high CFRD dams has been of great importance to advance the design and construction of this popular dam type (Pinto, 2007, 2008).

The tendency of concrete faced rockfill dams to deform, mostly normal to the face, as a result of reservoir loading, with a clear component towards the centre of the valley, has been known since the times of the early dumped rockfill dams.

At modern dams, well compacted and with face slabs concreted by means of slipform, containing only vertical joints, occurrence of an accident caused by high compressive stress was reported at the Tianshengqiao I dam in September 2003. The upper reach of one joint showed signs of concrete spalling along a band, about 1 m wide, with an average depth of 0.24 m into the slab. The reservoir had been at NWL 780 m, earlier (in 2000), and the accident occurred at a lower reservoir level (el. 753 m), after the third annual drawdown from el. 775 m. The spalling extended down to a few metres below the water level. Repair works consisted of concrete filling. In May 2004, the spalling recurred, extending down to el. 710 m. The previous repair work was crushed, and the damage was extended to the bottom of the slab. Repair works included the insertion of a 2 cm-thick rubber plate in the joint to allow for some closing movement. No damage occurred when the reservoir level was subsequently increased. The extension of the event was limited to the upper portion of one vertical joint. Although resulting from horizontal compressive stresses at the concrete face caused by rockfill deformation, that early accident was mostly attributed to stress concentration effects, and did not result in a noticeable increase in leakage through the dam (Pinto, 2008).

12.4.3.1 Barra Grande dam (2005)

In 2005 the construction of the Barra Grande dam and powerplant was finished in Brazil, located in the Pelotas River. The construction pit was protected by the diversion system, which comprised two cofferdams (one located upstream, 66 m high, and one downstream, 25 m high), and two tunnels (15 m wide and 17 high, with a length from 816 m to 921 m). The diversion design flood was 7500 m^3/s, with an annual probability of occurrence of 1:50.

The dam is 185 m high, with a crest 10 m wide and 665 m long. It is located in a very narrow valley, with a ratio between crest length and dam height 3.65. The abutments have an average inclination close to 45°. The valley shape ratio $A/H^2 = 3.16$ (A – area of the upstream facing). The dam body is built from basalt with total volume of embankment about 12 million m^3, placed and compacted on sound rock foundation.

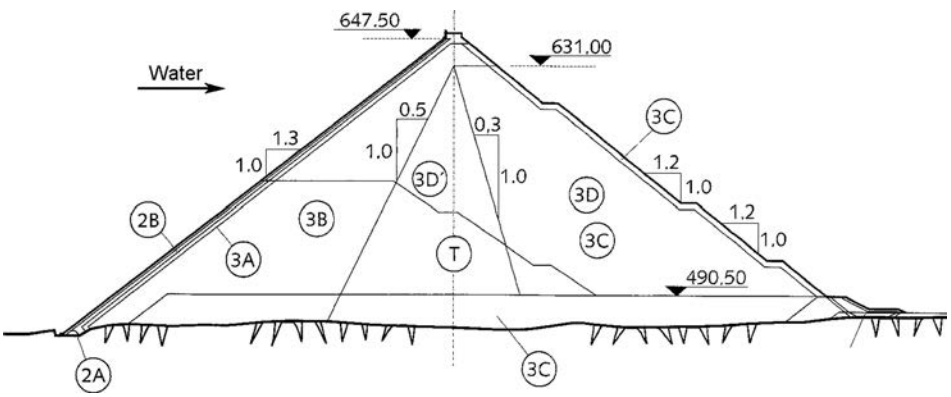

Figure 12.34 Cross-section of Barra Grande dam (Brazil) (After Cruz et al., 2009).

Table 12.2 Barra Grande dam materials and other data (zones are designated in Fig. 12.34).

Zone	*Material*	*Classification*	*Placing*	*Compaction*	*Unconfined compressive strength*
2A	Fine transition under perimeter joint	Sound basalt $\varnothing_{max} = 25$ mm	50 cm layers	9 t vibratory roller	
2B	Fine transition	Dense basalt $\varnothing_{max} = 100$ mm	50 cm layers	9 t vibratory roller	
3A	Fine rockfill	Dense basalt $\varnothing_{max} = 500$ mm	50 cm layers	9 t vibratory roller	
3B	Upstream rockfill	Min. 70% of dense basalt or riodacite $\varnothing_{max} = 1.0$ m	1.0 m layers	9 t vibratory roller, 6 passes, water 200 l/m^3	70% over 50 MPa
3C	Downstream rockfill and river bed	$\varnothing_{max} = 1.6$ m	1.6 m layers	12 t vibratory roller, 4 passes	70% over 40 MPa
3D	Downstream rockfill	$\varnothing_{max} = 1.6$ m	1.6 m layers	12 t vibratory roller, 4 passes	70% over 25 MPa
3D′T	Central zone rockfill	Min. 70% of dense basalt or riodacite $\varnothing_{max} = 1.0$ m	1.0 m layers	12 t vibratory roller, 6 passes, water 200 l/m^3	70% over 25 MPa

The rockfill in the dam body followed the classical zoning for CFRD, more careful grading and compaction were concentrated in the upstream third of the dam. Data about the dam body zones and materials, their placement, methods of compaction and compressive strength are given in Table 12.2. The unconfined compression tests of the basalt rock showed that the strength was over 90 MPa. The average void ratio of the upstream built in zones was 0.24 and average unit weight was 22.1 kN/m^3, while the downstream third of the dam section showed an average unit weight of 20.2 kN/m^3. For protection of the processed transition and bedding for the upstream slab, an extruded curb concrete was poured with an average cement ratio of 50 kg/m^3.

The face slab with a total area of about 108,000 m^2 was built in 16 m wide strips, separated by vertical joints. The thickness of the concrete face slabs t varied from 0.30 m at the crest to about 1.00 m at the base, according to the following formulas: $t = 0.30 + 0.002H$ (for $H \leq 100$ m), and $t = 0.005H$ (for H > 100 m).

Double reinforcements were adopted in the first 20 m of the slabs above the plinth, with a rate of 0.5% in both directions. In this zone, the reinforcement was shared in the two slabs' surfaces, top and bottom, being 60% on the upper face and 40% on the lower face. Reinforcement of 0.3% of concrete in the horizontal direction and 0.4% in the vertical direction were provided in the central zone of the concrete face.

All vertical joints are protected by copper joint seals at the base of the slab. In the tensile region, near the abutments, the joints are covered with a mastic-filled

PVC membrane. The perimeter joint between the plinth and face slabs was protected by a copper waterstop and a surface sealant (mastic) covered with a PVC membrane. The foundation treatment included consolidation grouting and curtain grouting under the plinth.

The reservoir filling started in the beginning of July 2005, and the water level reached elevation 617.50 m.a.s.l. on September 5th 2005, sixty-three days after diversion closure. Due to the occurrence of heavy rains filling speed in this period was about 2.15 m per day. On September 19th 2005, the flow meter collecting the water leakage through the dam recorded 220 l/s. Three days later, on September 22nd, when the water in the reservoir reached an elevation of 634 m, which means about 93% of the maximum head, the leakage increased to 400 l/s. Then a failure was observed along the compression joint between two central face slabs, and the leakage increased to 1300 l/s.

An underwater investigation by divers and a robot (used in offshore works) showed that the failure reached a depth of about 100 m. The reservoir was lowered to elevation 630 m and the concrete slabs and the joint above the water level were repaired. Filling of the reservoir restarted in November, 2005. Then, a maximum leakage of 1284 l/s was measured. Maximum registered face deflection was 56 cm for a transverse rockfill modulus of 94 MPa. The interpenetration of the slabs was of the order of 12 cm. In March 2006 the placing of clay-silt material in the reservoir started with the aim of sealing the joint and the damaged concrete of the slabs under water. This initial placing reduced the infiltration flows to about 800 l/s. In July 2006, after the increase in percolation, additional clay-silt material was placed. Thus, the total amount of placed clay-silt material reached 22,000 m^3. This treatment reduced the leakage to 500 l/s, but later on it once again increased to order of 935 l/s. A new campaign to reduce the leakage by dropping soil material over the crest was carried out in June 2007. Recognizing the existence of a transverse crack, 13,000 m^3 of clayish soil was again thrown from the dam crest not only over the central vertical joint, but closer to the abutments as well. The effect was positive, and the leakage dropped to about 800 l/s. But as the reservoir level fluctuated about 5 m, the leakage returned to around 1000 l/s. Brazilian experts deem this leakage acceptable, considering the dam dimensions and reservoir head and when compared to other similar dams in operation around the world. Further treatment was not undertaken. It is assumed that the failure was caused by high compressive stresses in the transversal and longitudinal directions of the central face slabs.

Settlements at Barra Grande dam are being measured by Swedish box settlement devices, placed across the dam at four levels, and by magnetic settlement gauges placed in three vertical sections. Maximum displacement of the slab until 2009 reached 71 cm near the dam crest. Based on the results of the monitoring instrumentation and the observation of the dam for 20 months after the filling of the reservoir, its behaviour was evaluated as safe and within the usual range observed in other concrete face rockfill dams.

12.4.3.2 Campos Novos dam (2006)

In 2006, one year after Barra Grande dam was commissioned, another very large CFRD was finished nearby: the Campos Novos dam, on the Canoas River, 21 km

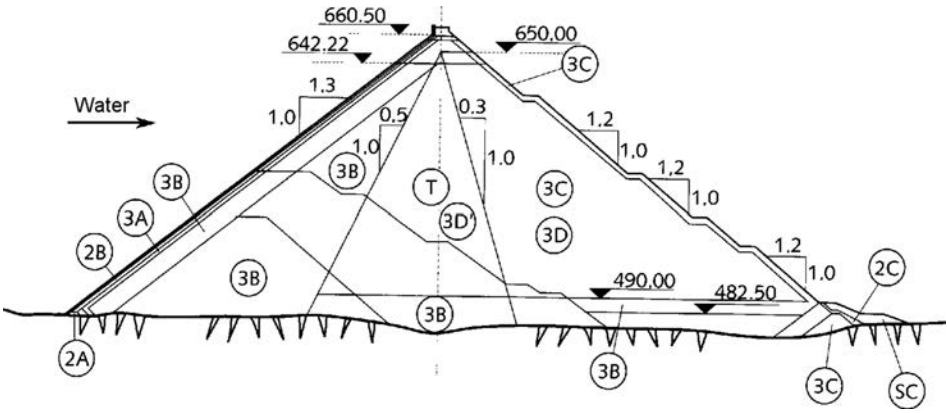

Figure 12.35 Cross-section of Campos Novos dam, Brazil, 2006 (After Cruz et al., 2009).

upstream from where it joins the Pelotas River in the State of Santa Catarina, around 380 km from Florianopolis. The hydraulic scheme, designed for electricity production, is very complex, and basically consists of a concrete-faced rockfill dam, 202 m high (the highest in the world until 2008), a river diversion through two tunnels provided with control structures for closing, the surface spillway on the right bank with four large gates, 17.4 by 20 m, a concrete gravity intake followed by three power tunnels and a powerhouse equipped with three vertical axis Francis hydro-generating units, with a total capacity of 880 MW.

The river diversion works began with the construction of two tunnels on the right bank. Auxiliary cofferdams were built in the outlet and inlet regions of the tunnels to protect the tunnel excavation works and the concrete pouring of the diversion intake structure.

In order to protect the dam construction pit, two cofferdams were built, one upstream and the other downstream from the dam axis, both with a rockfill section with an impervious clay zone. The main upstream cofferdam was built with its crest at elevation 516 m, providing protection against floods at up to 20-year recurrence intervals. The downstream cofferdam, with a crest at elevation 489 m, is incorporated in the body of the main dam. Its section consists of a rockfill embankment and an impervious earthfill zone.

The Campos Novos dam is 590 m long. Thus, the L:H ratio is 2.92, which, together with a valley shape ratio A:$H^2 = 2.6 < 3$, is a clear indication that the dam site is very narrow, with steep abutments. The total rockfill volume from excavating basalt rock was 12.5 million m^3, placed and compacted over a sound rock foundation. The upstream shell has a slope of 1(V):1.3(H), while the downstream shell has an average slope of 1(V):1.4(H). For the dam body, the zoning experiences of other CFRDs were followed. Figure 12.35 shows the dam cross-section, while in Table 12.3 some data and brief explanations are given.

The materials 3B and 3D′, placed in the third upstream and the central region of the dam body, compacted in 1.0 m thick layers and watered at a ratio of 200 l/m^3, had

Table 12.3 Campos Novos dam materials and other data (zones are designated in Fig. 12.35)

Zone	*Material*	*Classification*	*Placing*	*Compaction*	*Unconfined compressive strength*
2A	Fine filter	$\varnothing_{max} = 25$ mm	50 cm layers	12 t vibratory roller	
2B	Fine transition	Sound proc. basalt $\varnothing_{max} = 100$ mm	50 cm layers	12 t vibratory roller, 6 passes	
3A	Coarse transition	Sound basalt $\varnothing_{max} < 500$ mm	50 cm layers	12 t vibratory roller, 6 passes	
3B	Upstream rockfill	Min. 70% of sound basalt or riodacite $\varnothing_{max} = 100$ cm	1.0 m layers	12 t vibratory roller, 6 passes, water 200 l/m^3	At least 70% above 50 MPa
3C	Downstream rockfill	$\varnothing_{max} = 160$ cm	1.6 m layers	12 t vibratory roller, 6 passes	At least 70% above 40 MPa
3D	Downstream rockfill	$\varnothing_{max} = 160$ cm	1.6 m layers	12 t vibratory roller, 6 passes	At least 70% above 25 MPa
3D'T	Central rockfill	Min. 70% sound basalt or dense riodacite $\varnothing_{max} = 1.0$ m	1.0 m layers	12 t vibratory roller, 6 passes, water 200 l/m^3	At least 70% above 25 MPa
SC	Soil	Saprolitic soil	Dumped		
2C	Soil	Saprolitic soil	40 cm layers	Compacted by usual equipment	

an average void ratio of 0.22 and density = 21.4 kN/m^3. The unconfined compression tests indicated that the strength of the rockfill was higher than 75 MPa. The third downstream, 3C and 3D, made from rockfill compacted in layers of 1.6 m, without addition of water, had a density of 20.2 kN/m^3. The transitions under the slabs – materials 2B and 3A – were compacted in 0.50 m layers and reached void ratios of 0.20. For protecting the processed transition and bedding for concreting the upstream face an extruded concrete facing was done, concomitantly with the transitions, at an average cement rate of 75 kg/m^3. The facings slabs are 16 m wide, covering a total area of around 105,000 m^2, with thicknesses varying from 0.30 to 1.00 m, adopting the same equations used at the Barra Grande dam.

The vertical joints are protected by copper waterstops and are placed at the slab base, and in the region of tension (abutments) the joints are coated with a PVC cover with filler. The perimeter joints of the plinth are also in copper and a PVC cover with filler.

A major challenge in building the Campos Novos HPP was the creation of access routes to carry out the diversion works, since the canyon where the plant was built was completely inaccessible, with almost perpendicular slopes, and it was only possible to reach the river bank after five months of construction work. Another basic point in planning the works was to be able to divert the river, having previously built the plinth

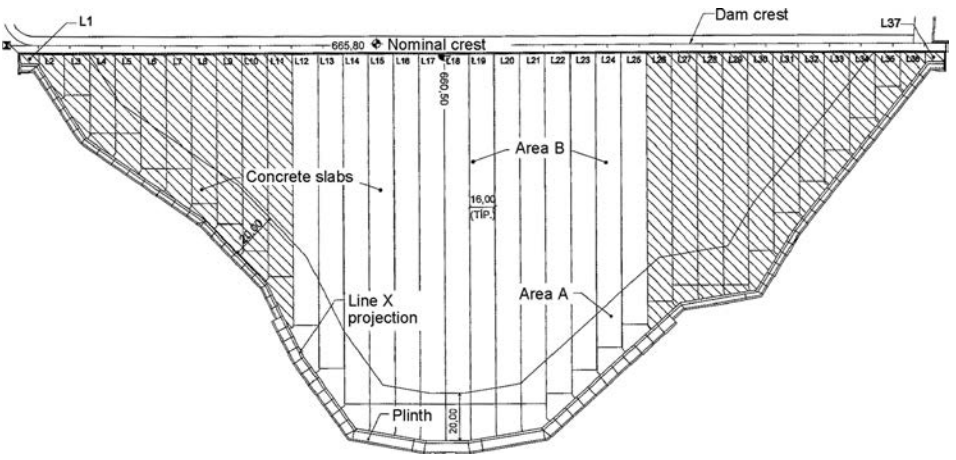

Figure 12.36 Longitudinal section of the Campos Novos dam, Brazil, 2006 (After CBDS, 2009).

on the two abutments. This condition was necessary, bearing in mind that the diversion would be at the end of the rainy season (October 2002) and it was also necessary to reach the elevation of the first stage of the dam (around 100 meters high) before the end of the dry season (April 2003), over a six-month period or so.

The rockfill for the dam body was carried out in three stages and the face slabs were concreted in two stages. First the rockfill was raised upstream to an elevation of 570 m and the concrete slabs to an elevation of 568 m. This heightening corresponds to approximately 52% of the final height of the dam and to the recurrence interval against floods of 1:500 years. Next, the downstream rockfill was raised to 570 m elevation and later complemented to an elevation of 660 m. After completion of the rockfill, the second stage of slab concreting began and was concluded in February 2005, around eight months before starting to fill the reservoir.

The rockfill of the dam was compacted using 12-ton vibrating rollers. The average production of compacted rockfill was 700,000 m^3/month, while the 16 m wide slab strips were carried out at an average speed of 2.9 m/hour. The complementation of the dam crest after concluding the face slabs was made by placing precast parapet walls upstream and downstream, and later filling the spaces between them with in situ concrete in the case of the upstream wall.

At the end of the construction period, the obtained average values of the deformability modules were as follows: upstream zone rockfill – $E = 60$ MPa; central zone rockfill – $E = 50$ MPa; downstream zone rockfill – $E = 30$ MPa.

The reservoir filling began on 10 October 2005. When the reservoir was filled to an elevation of 642 m, around 90% of its maximum depth, only one week after diversion tunnel closure, it was observed that the compression joint between slabs 16 and 17 of the face slabs had broken. This had been preceded by an increase in leakage from 30 l/s to 450 l/s, observed at the toe of the dam. The crack and the leakage remained stationary for five days. Then, the spalling process extended quickly to the top of the vertical joint in the contact with the base of the parapet wall, and the leakage increased

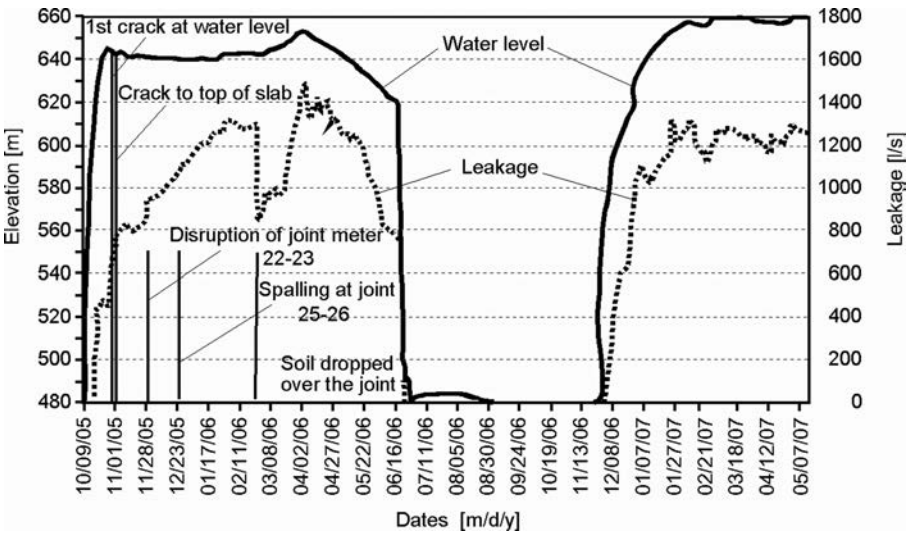

Figure 12.37 Campos Novos dam: reservoir elevation and leakage versus time (after Pinto, 2008).

in the following two weeks, reaching a value of 800 l/s. That was a first indication that the rupture of the concrete had progressed from a lower level towards the top of the dam. Although the reservoir level remained nearly constant (640 to 645 m), the leakage increased systematically in the following 60 days to reach about 1400 l/s, which was again an indication that the phenomenon was still active.

There were two other lines of evidence on the evolution of the process during that time interval: (1) the sudden interruption of the response of a joint meter at mid height of joint 22/23, about 50 m to the left of joint 16–17; and, (2) the limited spalling which took place at the top of joint 25–26 a few days later, as shown on the plot in Figure 12.37. After the loose concrete pieces had been removed, it became clear that the slabs had been crushed in compression, the intensity of the phenomenon visible by the interpenetration of the two slabs of about 12 to 15 cm. The horizontal reinforcing steel in the centre of the slab collapsed by buckling (CBDB, 2009; Pinto, 2008).

Analyses using three-dimensional finite element modelling had been carried out prior to the first filling of the reservoir with the objective of predicting deformations in the rockfill embankment and the dam face. However, the FEM studies were not able to represent what was observed in practice, that is, movement in the longitudinal plane of the dam with opposite directions of the abutments to the valley, which was almost annulled in the central section, concentrating the stresses in the joint between central slabs 16 and 17. At the beginning stage of the accident the instrumentation in the dam indicated that the transversal deformations of the rockfill embankment were as expected. The longitudinal deformations evaluated by the superficial marks placed on the crest of the dam and on the downstream slope indicated maximum settlements of about 30 cm and predominantly horizontal displacements in the direction of the abutments to the centre of the valley, with a maximum value of around 14 cm in both directions (vectors of the horizontal directions are shown in Fig. 12.38). This tendency

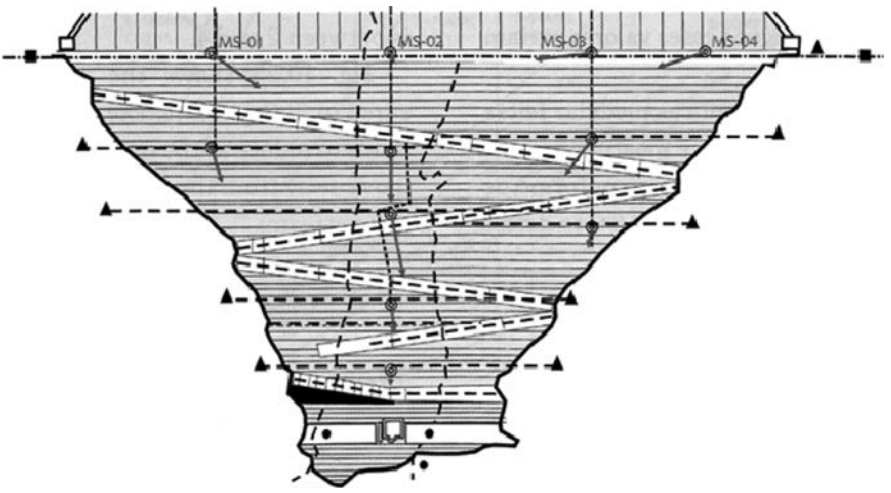

Figure 12.38 Campos Novos dam: vectors of horizontal displacements of the surface marks on the crest and on the downstream side (26 April 2006), Cruz et al., 2009.

for longitudinal movement directly influenced the behaviour of the compression slabs, as there was no space between the slabs to absorb the displacements in this direction (Xavier et al., 2008).

An underwater investigation was performed with divers and a robot, by which it was discovered that the failure extended to a depth of more than 100 m. No movement of material in suspension that could reveal suction effects near the cracks was detected. The leakage appeared to be distributed along the joint. No evidences were identified to suggest another type of incident than the crushing of the face slab by horizontal compressive stresses along the central vertical joint. This phenomenon also occurred at the Barra Grande dam, observed one month earlier, and at the Mohale dam in Lesotho, four months later.

The concrete and joint above the water level were repaired and below the water level clay-silt material of about 8000 m^3 was dumped to seal the joint and the damaged concrete of the slabs. This initial dumping was partially successful, reducing the seepage flow from 1.3 m^3/s to around 0.8 m^3/s. As the reservoir level rose to an elevation of 655 m over the next month, there was an increase in leakage to a peak of 1500 l/s. Two months later, in June 2006, eight months after the accident, the reservoir had to be drawn down rapidly because of an unrelated problem with one of the diversion tunnels. The lowering of the water in the reservoir revealed a 300 m-long transverse crack across the valley at about ⅓ of the dam height. The vertical joint rupture first identified above the reservoir level was seen to extend to the bottom of the valley, not continuously along one single joint, but migrating across the slabs to three successive neighbouring joints as it progressed downwards. The configuration of the cracks and the degree of damage in their crossing zone are an indication that the failure began at that central point of maximum deflection normal to the face, and irradiated both in the vertical and transversal directions, see Figure 12.39 (Pinto, 2008).

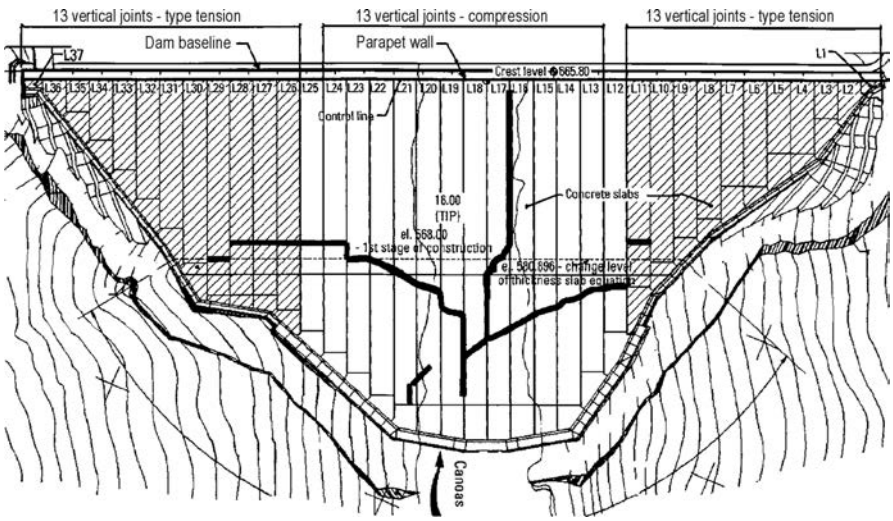

Figure 12.39 Map of the fissures (after Xavier et al., 2008).

Prior to re-filling the reservoir, the damaged slab strips and joints were fully recovered, and the cracks were repaired within four months. Although the embankment had undergone almost all reservoir head during the first filling, and therefore had mobilized most of its deformation, four soft vertical joints, each 50 mm wide, were provided in the central compression region of the face, in order to permit horizontal displacements between slabs and thus prevent high stress levels. The joint concrete between slabs 16 to 20 was cut, leaving an opening of 5 cm, which was filled with mastic and lined with EPDM elastomer layer.Then, at the end of November 2006, the reservoir refilling started. Figure 12.37 shows the filling and emptying processes and the infiltration flows. The maximum operating level (660 m.a.s.l.) was reached in February 2007, and the scheme has been operating normally since then. Leakage at that reservoir level has been stabilized at about 1200 l/s. The joints closed a total of 60 mm during reservoir refilling, and contributed positively to the uneventful operation. Maximum deflection of the slab was much less than during first filling, the rockfill proving to be four times stiffer at reloading (Sobrinho et al., 2007, Pinto, 2008, Xavier et al., 2008).

The initial plan for monitoring the Campos Novas dam was the installation of two main instrumentation sections, which were placed at Cross-section 13 + 10 m (riverbed) and stake 21 + 10 m (left bank), containing 28 settlement cells and four magnetic settlement meters to help determine the deformability modules of the different zones in the rockfill. The upstream face was instrumented with electrolevel sections in the central region and on the right bank, with triorthogonal joint meters between the plinth and slab and with joint meters between slabs, plus surface benchmarks placed at the top of the dam.

After recovering the affected slabs of the dam face, new instruments were installed in the concrete face to monitor the performance of the repaired stretches during refilling

of the reservoir. Overall, more than thirty new instruments were installed, with special mention to 13 joint meters to monitor the closure of the central joints between central slabs 16 to 20, seven concrete stress meters to assess the stress levels which they would undergo again and an extra row with ten electro-levels placed in the right abutment of the dam to assess the deflections of the face in this abutment (Pinto, 2008, CBDB, 2009).

The displacements measured in the rockfill embankment and in the concrete face through settlement cells, electrolevels and joint meters were less than 35% of what they had been during first reservoir filling, as a result of the pre-settlement of the rockfill embankment as a whole. The settlements undergone by the dam in the second impounding of the reservoir are gradually dropping with a tendency to reach stabilization, as is typical of similar rockfill dams. Slow deformation (creep) in the central part of the dam was 6 mm/month on average between April 2007 and April 2008. Fifteen months after its second filling, the dam behaviour was fully satisfactory (CBDB, 2009).

Experiences with the Campos Novos, Barra Grande and Mohale dams were very instructive. The phenomenon of high compressive stresses in the central zone of the concrete face was understood and more design provisions are being made to prevent similar accidents. After 2006 several CFRDs higher than 180 m have been successfully built and used in the first years of their service period, confirming the reliability of very high dams of this type.

12.4.3.3 Kárahnjúkar Dam (Island)

Kárahnjúkar Dam (Island), the highest CFRD in Europe ($H = 196$ m), was completed in 2007, and the reservoir was filled to the normal water level in the same year. The dam site has an asymmetric shape and a 45 m deep canyon with vertical walls at its base. In the deep canyon the dam was supported by a toe wall made from roller compacted concrete (RCC), see Figure 12.40. To overcome possible difficulties due to asymmetric dam site shape and the deep toe wall, soft central vertical joints were designed. For the same reason, in the original project a higher percentage of reinforcement was planned than was usually used worldwide in CFRD practice.

The dam was at an advanced stage of construction at the end of 2005 when ruptures in the central joints were being reported. To overcome the problem and to avoid further difficulties the following main adaptations have been implemented:

- Compaction in 40 cm layers between elevations 584 m and 625 m.
- Placement of a 3 mm bond breaker film over the extruded curb.
- Increasing the thickness of the ten central slabs by 10 cm, above el. 535 m, with a transition between the old and new slabs.
- Reduction of the mortar pad and elimination of the top V notch to increase the contact area between the slabs.
- Use of spacers of 15 mm between compression joints, and 25 mm between the joints in the parapet wall.
- Improvement of the anti-spalling reinforcement (Fig. 12.41).
- Raising up of the non-cohesive material placed over the slab to el. 540 m, (1) in Figure 12.40.

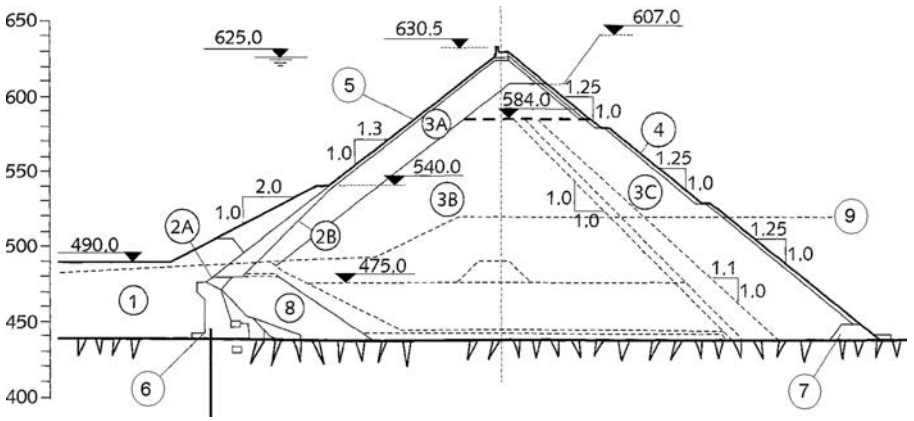

Figure 12.40 Cross-section of Kárahnjúkar Dam (Island, $H = 196$ m, 2007). (1) Glacial silt, fine sand, compacted in 50 cm layers; (2A) fine filter, compacted with vibratory plate and water in 20 cm layers; (2B) transition, maximum grain size 7.5 cm, compacted in 40 cm layers; (3A) pillow lava, compacted in 40 cm layers; (3B) sandy gravel and pillow lava, compacted in 40, 60 and 80 cm layers, with water in summer, without water in winter; (3C) durable free drainage basalt, compacted in 160 cm layers; (4) selected durable stones, placed by backhoe; (5) concrete slabs; (6) RCC toe wall (7) downstream cofferdam; (8) natural gravel, compacted in 40 cm layers; (9) river canyon edge.

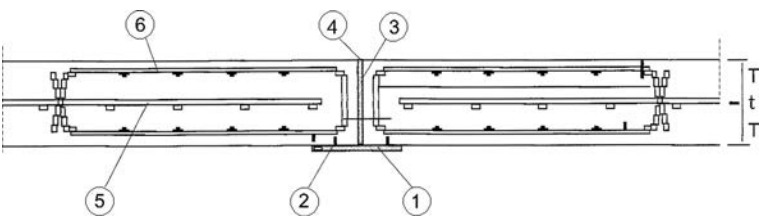

Figure 12.41 Modified design of face slab joint at central compression zone, Kárahnjúkar Dam (after Perez et al., 2007). (1) Mortar pad; (2) copper waterstop (3) filler; (4) no V notch; (5) central rebar; (6) anti-spalling rebar.

The performance of the dam after the filling of the reservoir at the end of 2007, and after emptying and refilling in 2008, has been excellent, with low settlements and leakage below 200 l/s, which is considered normal in glacial areas.

12.4.3.4 El Cajón dam (Mexico)

Another important CFRD, with reservoir filled to normal level at the end of 2007, is the El Cajón dam, in Mexico, on the Santiago River, upstream of Aguamilpa's reservoir. El Cajón is the second modern CFRD built in Mexico. The main structures in the frame of the hydraulic scheme (some of which can be seen in the photo, Fig. 12.43) are: a 188 m-high dam, a surface gated controlled spillway having a concrete-lined chute with a flip bucket designed for a maximum discharge 14,864 m^3/s, the diversion works of two 14 m diameter tunnels (734 m long and 811 m long respectively) with a

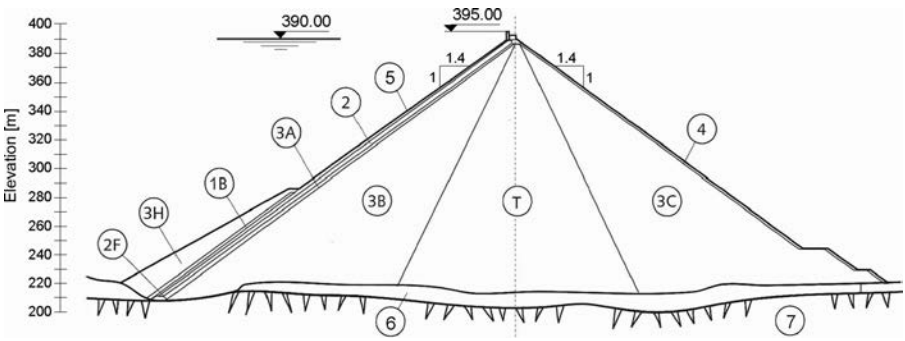

Figure 12.42 Cross-section of El Cajón dam (Mexico, $H = 188$ m, 2007). (1B) Compacted by dozer in 30 cm layers; (2F) compacted in 30 cm layers with 10 t vibratory roller, 6 passes; (2B) compacted in 30 cm layers with 10 t vibratory roller, 8 passes; (3A) compacted in 30 cm layers with 10 t vibratory roller, 8 passes; (3B) compacted in 80 cm layers with 12 t vibratory roller, 6 passes, with water >200 l/m^3; (T) compacted in 100 cm layers with 12 t vibratory roller, 6 passes, with water >200 l/m^3; (3C) compacted in 140 cm layers with 12 t vibratory roller, 6 passes, with water >200 l/m^3; (3H) compacted in 40 cm by dozer; (4) slope protection, placed by backhoe; (5) concrete slabs (6) river deposit; (7) rock foundation.

48 m high upstream cofferdam, an underground powerplant with a separate concrete intake structure for each of two 375 MW Francis turbine units, and two steel-lined power tunnels (each with a diameter of 9.5 m). The reservoir capacity is 2.4×10 m^9, and the expected average power generation from the plant is 1200 GWh per year (Mendez et al. 2007).

The dam is 550 m long at the crest, with a rather low ratio $L{:}H = 550{:}188 = 2.93$, and a valley shape factor $A{:}H^2 = 113{,}300{:}188^2 = 3.21$. The dam slopes have an inclination of 1:1.4. Almost 11 million m^3 of volcanic rock was quarried on site and placed in the dam body over 24 months. The dam has a typical cross-section for a modern CFRD, comprising several types of selected rockfill material (Fig. 12.42). The placement of the embankment was done in six phases with the aim of achieving the construction of staged slabs and coping with the floods during construction with the minimum volume of rockfill (details of construction of the dam body and facing slabs in phases are given by Mendez et al., 2007). Once the embankment had been completed, work on the parapet wall, from el. 392 m to el. 397.5 m, began. The wall was built with cast-in-place concrete, using conventional steel forms, from mid-August to 15 November 2006, which is the date of the official completion of the dam.

The transition 2B was built with well graded processed material with a maximum grain size of 7.5 mm. The 3A material was also processed with a maximum size of 150 mm, well graded and compacted in a similar way as 2B. Materials of zones 2B, T and 3C were built of ignimbrite, a rock with a relatively low specific gravity, properly compacted (see the caption under Fig. 12.42). The compressibility moduli were rather high: for zone 3B 110 MPa, for T 125 MPa, and for 3C 75 MPa. The quantity of water used during construction of these zones, compacted by 10–12 t rollers with transmitted pressures over 5 t per meter on the vibratory cylinder, was higher than originally specified 200 l/m^3, with a good effect.

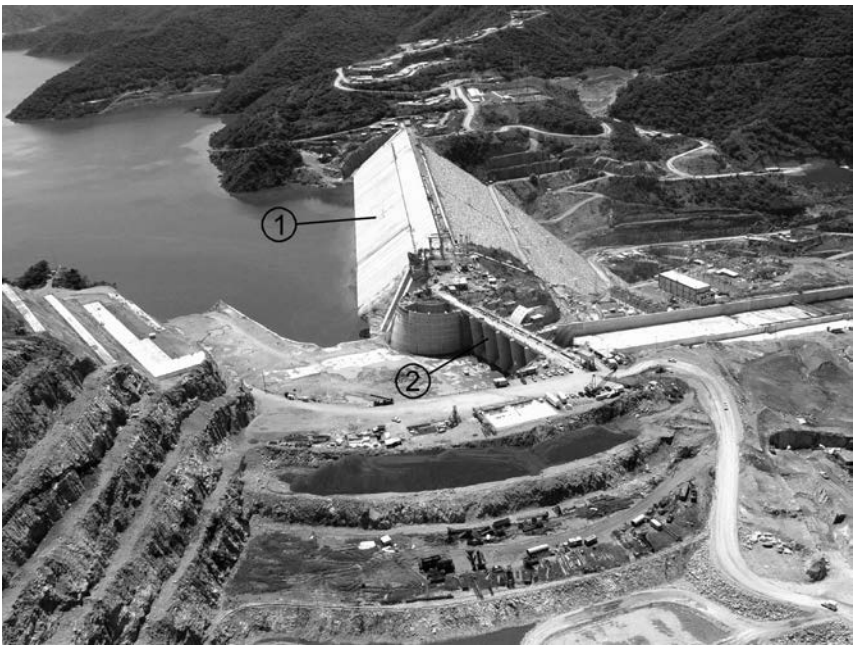

Figure 12.43 El Cajón dam at final construction stage. (1) Upstream dam face; (2) controlled spillway.

The concrete face slab has a total area of 113,300 m^2, and the slab thickness is: 0.30–0.50 m (for depth below the crest 0–100 m); 0.50–0.80 m (for depth below the crest >100 m);

The slab was built in strips 15 m wide, in four stages, with a production of 3–5.5 m per hour. The maximum face deflection after the first reservoir filling occurs at el. 310 m, at about 0.54 of the dam height and was 17.5 cm, which was less than half of what was predicted in the design stage.

The dam was supplied with an extensive array of instruments both on the concrete slab and inside the dam body, to emphasize the need for long-term monitoring, taking into account face crack incidents that had already been recorded at some recent high CFRD dams.

Movement of the concrete face slabs relative to the plinth is measured in three directions, using normal, parallel and perpendicular joint-meters. After the first filling, at nearly full reservoir, the maximum displacements of the perimeter joint were in accordance with the predicted movements and much lower than the deformation capacity of the used waterstops. The registered values are: vertical displacement (settlement): 24.4 mm; opening movement: 8.8 mm; shear displacement: 3.4 mm.

The joints between the face slabs are well supplied with electrical joint movement detectors located near the abutments, as well as with mechanical one-dimensional joint movement detectors to monitor the behaviour of the compression joints in the middle part of the facing. At around 95% of the normal water head, the registered maximum opening was 9 mm, while the compression movements were less than 1 mm.

The performance of the El Cajón dam could be evaluated as excellent for such a high dam in a narrow valley, mainly due to the well compacted rockfill, with high compressibility modulus, which reduces the slab displacements and compression stresses.

12.4.3.5 Shuibuya dam (China)

The highest CFRD in operation in the world is Shuibuya dam (China), completed in 2008 on the Qingjian River, tributary of the Yangtze, in the Hubei province, Central China. Its main features and behavioural data should be the key reference for discussions on future planned extra high CFRD dams.

Main characteristics of the Shuibuya dam are: $H = 233$ m; $L = 660$ m; $L/H = 2.83$; $A/H^2 = 2.21$ (very narrow dam site); type of rockfill material – limestone, dam slope inclination (upstream and downstream) 1:1.4, dam body volume $= 15.7 \times 10^6$ m^3, face surface area $= 139{,}000$ m^2 (Pinto, 2009; Cruz et al., 2009). Figure 12.44 shows the characteristic dam cross-section, with the position of different zones of material, with the appropriate explanations given in the caption. We will add that an extruded concrete curb, 40 cm high, was also constructed at the upstream dam face, for the stabilization of the fill surface and to serve as a support of the concrete face slab. The compaction of the dam body was quite rigorous, as can be seen from some data given in the caption of the Figure 12.44.

Other features of the dam are:

- Concrete: 278 to 307 kg/m^3 cement (20 per cent fly ash), air entraining (0.015–0.020%), and water reducing (0.5 per cent) agents, polyacrylonitrite fiber 0.8 kg/m^3.

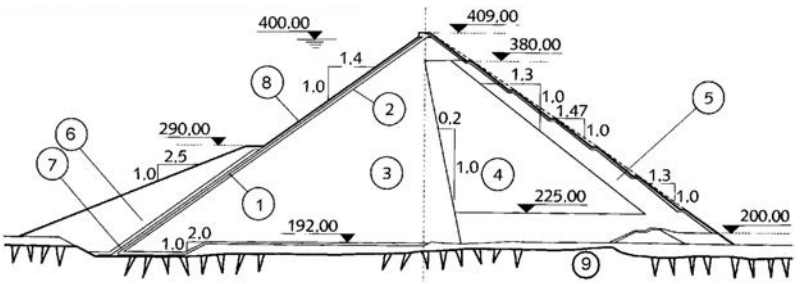

Figure 12.44 Cross-section of Shuibuya dam (China), the highest CFRD in the world, $H = 233$ m (after Cruz et al., 2009). (1) Zone 2B, filter, processed limestone, $\gamma_d = 22.5$ kN/m^2, compacted in 40 cm layers by 8 passes of a 18 t vibratory roller, and water; (2) zone 3A, transition, processed limestone, $\gamma_d = 22.0$ kN/m^2, compacted in 40 cm layers by 8 passes of a 18 t vibratory roller, and 15% water; (3) zone 3B, limestone, blasting, excavation, $\gamma_d = 21.8$ kN/m^2, compacted in 80 cm layers by 8 passes of a 25 t vibratory roller, and 15% water; (4) zone 3C, limestone, blasting, excavation, $\gamma_d = 21.5$ kN/m^2, $\varnothing_{max} = 800$ mm, compacted in 80 cm layers by 8 passes of a 25 t vibratory roller, and 10% water; (5) zone 3D, limestone, blasting, excavation, $\gamma_d = 21.5$ kN/m^2, $\varnothing_{max} = 800$ mm, compacted in 120 cm layers by 8 passes of a 25 t vibratory roller; (6) zone 1B, soil, placed by construction equipment; (7) soil, placed by construction equipment; (8) facing slab; (9) rock foundation.

- Steel fibre: 0.7 kg/m^3 above el. 340 m, average slump 7 cm, average strength 40 MPa.
- Reinforcing: single matt, 0.4% vertical, 0.35% horizontal, double matt along the region of perimeter joint, horizontal, and construction joints.
- Plinth: external slab for grouting, internal slab under the rockfill for seepage control length.
- Vertical joints: thin isolation filler for soft contact, copper waterstop at bottom, flexible membrane at top.
- Perimeter joint: three defence lines, bottom copper waterstop, top wave rubber waterstop, self healing GB elastoplastic filler covered with GB-EPDM membrane; middle copper waterstop below el. 350 m.
- Upstream earthfill: 89 m high, 15 m wide at crest el. 265 m, 1:2.5 face slope.

Keeping in mind the three accidents had happened recently before the completion of Shuibuya dam, special care was taken to reduce the chances of the concrete face cracking. The concrete was cast after most of the rockfill creep had taken place, which was less than 5 mm per month. Fibers were incorporated in the concrete in order to reduce the fissures frequency on the facing slab. The concrete curb face was cut along the vertical joint alignment of the face slab, to reduce any potentially harmful effects of stresses in the concrete slab. Also, an asphalt emulsion was placed over the curb surface to break the bond with the concrete face. Careful curing procedures were followed. A horizontal joint was added to the concrete face at about two-thirds of the dam height (el. 332 m). The joint includes wooden plank filler. The longitudinal steel reinforcing is continuous through the joint, and two waterstops are provided, at the bottom and top of the slab, as for the vertical joints.

An important aspect of this dam is the use of a special type of waterstop, along with mastic (called GB), developed by the China Institute of Water Resources and Hydropower Research (IWHR), as shown in Figure 12.13. This mastic is protected by a band of a resistant material manufactured with EPDM elastomer. All joints (either tension or compression) are protected with this same mastic. After the performance of the Campos Novos and Barra Grande dams, at Shuibuya dam compressive materials were included in the central compression joints to avoid the stress concentration. Close to the abutments the number of joints was increased dividing the slab width by means of intermediate joints.

Shuibuya Dam was completed in 2008, and in April of that same year the reservoir was nearly full (only 9 m below its normal level). The behaviour of the dam has been excellent since the first filling, with illustrative monitoring data as follows: a) maximum rockfill settlement: 214 cm (end of construction), and 247 cm (after the reservoir filling); b) rockfill modulus at the central dam section: 120 MPa (estimated – end of construction); c) maximum deflection normal to face slab: 57.3 cm (reservoir at el. 390 m); d) maximum seepage flow: 40 l/s.

After the success with the 233 m-high Shuibuya Dam, a number of sites for dams up to 300 m high are reported to be under study in China. The CFRD dam is one of the dam types under consideration together with various alternative dam types. Perhaps the height of Nurek dam, described in Chapter 11, will soon be reached by a CFRD?

12.5 CONCRETE FACINGS OF NON-CONVENTIONAL CONCRETE

Historically, the era of embankment dams with waterproof upstream lining began as early as 1660, with La Granjilla Dam, in Spain, on the Rio Aulencia, west of Madrid. It was an embankment dam made of soil, rockfill and stone masonry, with an impervious face of mortar and lime. The upstream dam slope was 1:0.16 (V:H), while the downstream slope was 1:1. The dam was 13 m-high, closing the reservoir with a capacity of 345,000 m^3 (Smith, 1992). Then, at the turn of the 20th century, began the era of embankment dams with facings made of conventional reinforced concrete, with the first such dams being constructed in the USA.

An attempt to modify the construction of the reinforced concrete facings, applying non-conventional concrete, was made in the middle of the 1950s in Australia, where two dams were constructed with facings of shot-crete. The mixture was composed of sand and cement in the ratio 3:1 (by volume) and it was applied around the placed reinforcement over the sub-facing layer of placed rockfill. The inclination of the upstream dam slope had been steep – 1:1.25 (same as for the downstream one). In the case of the first dam (Corella, $H = 23$ m), the sub-facing layer was 60 cm thick, and the layer of shot-crete 5–10 cm. In the other dam (Leihard, $H = 26.5$ m) the appropriate thicknesses were 75 cm and 7.5–12.5 cm, respectively. In spite of the relatively sound behaviour of these dams over the course of numerous decades of service, this kind of facing has not found broader application (Truscott & Traves, 1988).

Prestressed concrete, in spite of its positive properties – high load-bearing capacity at small cross-sectional dimensions of the construction – so far has not found more significant applications in dams. At one part of Skalka dam, in former Czechoslovakia, 17 m high (Fig. 12.45), a facing of prestressed concrete has been constructed, which is much more flexible and better takes on bending deformations than ordinary reinforced concrete facing. The slabs extend along the entire height of the dam, so that they have a length of 32 m, and they are relatively narrow – 3.25 m in width, while their thickness is 20 cm. The slabs are placed on a sub-facing layer, which consists of 95 cm gravel and 5 cm sand. The joints of the slabs are filled with foam rubber, and sealing is carried out with rubber waterstops (Borovoy, 1976). Although the experiment with Skalka dam has been successful, in practice the facings of prestressed concrete have not found further application, most probably owing to the complicated construction procedures.

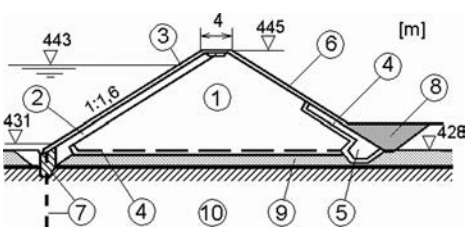

Figure 12.45 Skalka dam. (1) Rockfill; (2) compacted gravel – 95 cm and sand 5 cm; (3) prestressed concrete facing – 20 cm; (4) filter layer; (5) selected rockfill; (6) top soil; (7) concrete cutoff with grout curtain; (8) earth filling; (9) alluvial deposit; (10) rock foundation.

This page intentionally left blank

Chapter 13

Rockfill dams with asphaltic concrete and other types of facings

13.1 ROCKFILL DAMS WITH ASPHALTIC CONCRETE FACING

13.1.1 General characteristics

In the period between 1950 and 1990, in addition to reinforced concrete facings, asphaltic concrete facings also found a wide application in the world practice of construction of rockfill dams, as watertight elements (Schmid & Frohnauer, 2001). Textbook references denote more than 200 such dams. The main advantages of asphaltic concrete facings, in relation to reinforced concrete facings, are as follows:

- Asphaltic concrete produced for application in hydraulic engineering, is almost completely watertight;
- From a structural point of view, it is very simple because it is constructed as a monolithic unit, without joints;
- Asphaltic concrete linings, i.e. facings, have plastic properties and so are capable of following the deformations of the slope, without the occurrence of significant cracks; besides, there has been proved the ability of asphaltic concrete of self-healing (self-repair) under the effects of water pressure;
- Mechanization of the entire construction process considerably facilitates the decrease in workforce and material resources, as well as time necessary for construction.

Asphaltic concrete facing also has disadvantages in relation to reinforced concrete facing:

- The height of dams with asphaltic concrete facing is limited mainly due to constructional reasons: the asphaltic concrete layers are constructed in strips starting from the dam toe toward the crest, with equipment attached to stationary and to movable, devices on the dam's crest; these operations would be risky for dams higher than 90 m; there are only three such dams higher than 80 m, Figure 13.1.
- Asphaltic concrete is a thermoplastic material; that is to say, it changes its properties with changes in temperature, so that at high temperatures it becomes soft, while at low temperatures it becomes rigid;
- Asphaltic concrete that is exposed to light and ultraviolet rays, has the property of ageing, i.e. it loses certain properties in the course of time (Charles & Penman,

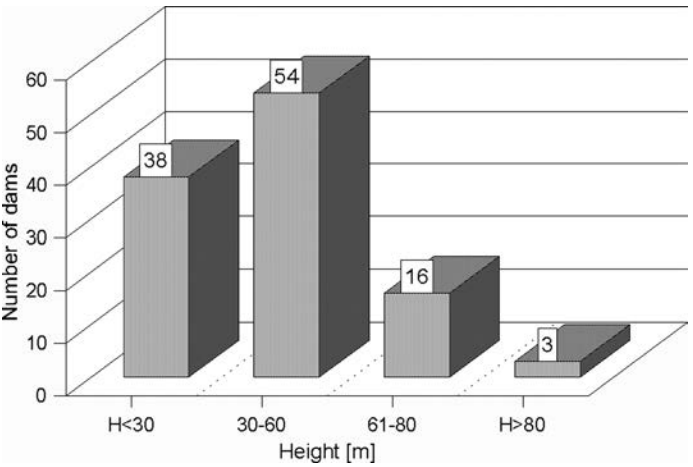

Figure 13.1 Number of asphaltic facing rockfill dams by height.

1988; Fabian & Ditter, 1988; GSCLD, 1988; Hasegawa & Kikusawa, 1988; Smith et al., 1988; Van Asbeck, 1962). This disadvantage is the main reason why the application of this dam type has rapidly decreased since 1990 (see Fig. 12.1, Chapter 12).

Yet, the last two disadvantages can, to a great extent, be eased with proper selection of the constituent elements and proper composition of the asphaltic mixture. During designing, dimensioning, and acceptance of the construction of the asphaltic concrete facing, it is necessary to take into consideration that it should satisfy the following requirements: (1) To be stable against flow across the slope during construction at high temperatures following the completion of construction process and during service, i.e. operation conditions; (2) To be watertight; (3) To be sufficiently elastic and resistant to the occurrence of cracks at low temperatures; (4) To be able to adapt to deformations that are expected to originate in the slope, without derangement of the basic function – watertightness; (5) To be resistant to mechanical effects of waves and ice.

These kinds of dams were extensively investigated in the period from 1960 to 1990. The reader can find details for the construction, and static and dynamic stability in abundant textbook references on that subject (Belloni et al., 1988; Fabian & Ditter, 1988; Gonzales & Rodriguez, 1988; GSCLD, 1988; Haas, et al., 1988; Hasegawa & Kikusawa, 1988; ICOLD, 1982; ICOLD, 1999; Ishii & Kamili, 1988; Le Bel, 1981; Routh, 1988; Schenk, 1988; Smith et al., 1988; Tanĕev, 1981, 1989; Tschernutter, 1988; Weinhold & Haug, 1988; Yang & Ding, 1988).

13.1.2 Composition and characteristics of hydraulic asphaltic concrete

Asphaltic concrete is a mixture of mineral material with various sizes of grains – stone chippings in various fractions, sand, filler (stone flour) – with bitumen. The mixture,

prepared in special equipment at a temperature that depends on the type of bitumen, reaches its monolithism, strength, and stability regarding the external influences after the placement and compaction in layers of certain thickness. The selection and quantitative participation of the constituent components of asphaltic concrete is dictated by the role they play in providing watertightness, strength, and long duration, as well as other service characteristics of the placed layer.

Stone chippings form the skeleton of the asphaltic concrete, which facilitates resistance to external loadings. Sand has the task to fill the pores among grains of the skeleton, while at the same time increasing its stability and forming together the mineral skeleton of the asphaltic concrete. Besides, sand decreased the need for other, more expensive components of the asphaltic concrete – bitumen and filler. Bitumen represents the basic binder, vital for binding the grains of the mineral skeleton into a monolithic complex, able to resist the external influences. Filler, with its enormous specific surface (250–300 m^2/kg), attracts to itself the bitumen, transforming its quantity from a space to a surface state. At the same time, the filler plays the role of structural addition, which considerably increases the adhesion and ability for binding the bitumen, at the same time decreasing its thermal sensitivity.

In that way, the asphaltic concrete, according to its structure, represents a multicomponent conglomerate in which the individual grains, cemented in a monolithic unity, form its skeleton. The structure of asphaltic concrete is characterized with the size, form, quantitative ratio of grains of different sizes, with the properties of the mineral filling, structure, composition, and properties of binder, as well as with the nature of mutual actions between it and the grains of the mineral mixture. The character of the structure of asphaltic concrete, also determines, to a great extent, its properties.

The asphaltic concrete used in hydraulic engineering, according to its composition and structure, is very similar to asphaltic concrete, which is used for the construction of roadway pavement. The difference between these two congenial materials results from the fact that they work in different conditions. While the pavement asphaltic concrete layers take on the dynamic loads due to movement of vehicles, the main function of the hydraulic asphaltic concrete is to provide watertightness of the hydraulic structure, as well as to adapt to deformations of the embankment of the dam's body. That is why in the latter case, there are increased requirements in relation to elasticity and resistance to occurrence of cracks, while some other criteria are eased – friction and resistance to wear, i.e. abrasion etc.

In addition to the asphaltic concrete in the construction of facings, two more kinds of asphaltic mixtures are used – porous asphalt and asphaltic mastic.

Porous asphalt is made of the same components as asphaltic concrete; however, with different structure. First of all, it is characterised with a lower participation of the fines and the binder, which, in the end, brings to it a watertight asphalt layer of high porosity – 10–20% in relation to the entire volume. In the case of the asphaltic facings, it is used for the execution of a drainage layer for so-called *sandwich constructions* and as a binding layer (binder) between the lowermost asphaltic concrete layer and the sub-facing leveling or stabilizing course.

Asphaltic mastic is a mixture of bitumen with filler, with a usual ratio of 40:60. It is usually applied in a thin layer (2 mm) over the asphaltic concrete surface and it serves as protection of the asphaltic concrete layer, as well as for improving its watertightness. Since it contains a considerable quantity of bitumen and is applied in a thin layer that

cools down fast, the asphalt mastic is difficult to place, so it is often replaced with various ready-made industrial products which, in the form of coatings, are simply applied in a cold state.

Asphalt, depending on the state and conditions of deformations in it, appears as an *elastic-viscous-plastic material*. Within the state of stresses – deformations, the asphaltic concrete exhibits a variety of complex properties: elasticity, plasticity, creep, relaxation of stresses, and superposition of deformations at multiple repetitions of loadings, etc. Depending on the exhibited property, it is possible to apply the theories of elasticity or plasticity. However, the properties of asphaltic concrete can most completely be determined by applying the methods of *rheology* – a scientific discipline that represents part of a relatively new field of science – *physical-chemical mechanics*. Rheology deals with general laws and rules of forming and developing of the deformations, depending on time.

Defining of the properties of hydraulic asphaltic concrete is very difficult in the presented manner and it requires special apparatus. That has led to the introduction of practical conditional indicators, which present the physical and mechanical properties of the hydraulic asphaltic concrete, of which the most important ones are as follows (Tanĕev, 1981):

Strength limit is determined by subjecting cylindrical test specimens to pressure at temperature of 0, 20 and 50°C and velocity of motion of the press at 3 mm/min.

Thermal stability is characterised by the ratio of the limit of compressive strength at 20°C (*R*20) to the limit of compressive strength at 50°C, which is called *the coefficient of thermal stability* (K_t).

Stability in water is characterised by the coefficient of stability (resistance) in water – the ratio of the limit of compressive strength of water-saturated test specimens – and that of dry test specimens at 20°C:

$$K_w = \frac{R_w}{R_{20}} \tag{13.1}$$

and also by water absorption and by swelling in %, regarding the volume at saturation of the asphaltic concrete in water in vacuum.

Density is achieved with careful selection of the aggregate gradation and by using an increased quantity of filler and bitumen (as compared to pavement asphaltic concrete). With the density of the asphaltic concrete closely are related its water stability, watertightness, resistance to corrosion, deformability, etc. The built-in layer of asphaltic concrete should contain less than 4% free voids (by volume) in order to be watertight enough, while at high temperatures porosity should be less than 3%, when a coefficient of permeability less than 10^{-7} cm/s is obtained. In the asphaltic concrete layer there must also be preserved a certain minimum of free voids, which serve as spare space for expansion of the bitumen during the summer period (or else there would be cropping at the surface).

Thermal stability defines the stability of the asphaltic concrete facing of the slope against creeping under the effect of self weight at high temperatures which, in summer, can reach 60–70°C, at the surface.

Table 13.1 Properties and requirements for asphalt materials.

Properties of asphalt and requirements it should fulfil	*Asphaltic concrete*		*Porous asphalt*
	Normal	*Upgraded*	
1. Limit of compressive strength			
at 20°C (R_{20}), minimum [kN/m^2]	25	30	15
at 50°C (R_{50}), minimum [kN/m^2]	12	15	5
2. Coefficient of thermal stability $K_t = R20^{wsat}/R_{50}^{wsat}$, maximum	3	2.5	4
3. Coefficient of water stability under vacuum $K_v = R_2^{wsat}/R_{50}$, minimum	0.85	0.90	0.75
4. Coefficient of elasticity, $K_e = R_0/R_{20}$	2–3	2–4	2–4
5. Free voids [%]	1–3	1–2.5	6–20
6. Water absorption under vacuum, % by volume, max	2	1.5	5–18
7. Swelling under vacuum [%], maximum	1	0.5	–
8. Thickness of bituminous film at the surface of the mineral part [μ]	1–1.8	1–1.5	2–4
9. Adhesion of bitumen to the surface of the mineral material, %, min.	85	90	90
10. Water stability after 6 months of keeping the test specimens in water at normal temperature:			
– coefficient of water stability, min	0.8	0.85	0.75
– water absorption, % by volume, maximum	3	2	–
– swelling, % by volume, maximum	1.5	1	–

Ageing. Tests on already constructed asphaltic concrete facings in dams have shown that the asphaltic concrete ages, which is exhibited through increase of its rigidity. That process takes place slowly and is limited to the surface part. In well-compacted layers, with free voids below 3%, as well as with facings protected with coating or with another lining, the ageing of the asphaltic concrete has smaller influence.

Frost resistance. By means of investigations constructed at 150 cycles of freezing and thawing, it has been shown that there is no necessity for special requirements in terms of frost resistance in cases when asphaltic concrete satisfies the requirements regarding water stability and porosity.

Chemical resistance is sufficiently high and is defined by the chemical resistance of the used bitumen and mineral aggregate. Under conditions of alkaline and sulphate aggressiveness of the water, it is necessary to use mineral material of limestone or dolomite, while in acid medium – quartz, granite, diabase, and other acid-resistant materials.

Table 13.1 gives the properties and requirements that asphaltic concrete and porous asphalt should fulfill in terms of physical and mechanical properties, worked out on the basis of different standards and regulations, as well as results from investigations and the specified conditions for the construction of a lot of dams with asphaltic facing in the world. For lower dams, as well as for simple operation conditions,

so-called *normal asphaltic concrete* has been used, while in the case of higher dams and for tough operation conditions (high external temperature or frequent variation of water level in the reservoir), upgraded asphaltic concrete will be used with compulsory fulfilment of the requirements listed under 8, 9, and 10, as well.

13.1.3 Construction of the asphaltic concrete facings

In order to be able to meet the requirements that are cited in the previous clause, the facing should be properly constructed and dimensioned. In addition, beside the theoretical considerations and analyses, there is also extensive experimental testing, as well as utilization of the experiences from the abundant world practice. The asphaltic facings consist of the following basic elements: *(A) Base below the asphaltic concrete facing; (B) Asphaltic concrete lining; (C) Surface treatment;* and *(D) Protective layer* (in particular cases).

13.1.3.1 Base below the asphaltic concrete lining

The asphaltic concrete lining lies on the surface of the upstream slope and it transfers the external influences upon it. Besides, upon it the base takes on itself the plant and equipment, as well as workers, during construction of the facing. That is why it requires preliminary treatment. The facing can be constructed even at very steep slopes. In such a case, sub-facing masonry is compulsory to construct, and, because of that, in modern practice, this construction has been abandoned. For a successful and safe construction of the facing, the slope inclination must not be higher than 1:1.5, while a limit is recommended to assume 1:1.7. In Japan, due to high seismic activity, even slighter inclinations are regularly used.

In the case of the rockfill dams, the layer below the facing with a thickness of 2–4 m, should be constructed of crushed rock with grains no larger than 200 mm, in order to fill the voids among the coarse blocks and also to form a compact base. Above this layer come stone chippings with a grain size less than 70 mm, with a thickness of 15–30 cm, which serves for levelling of the surface under the facing. This layer is compacted with rollers in order to obtain a compact surface of the base, as well as to reduce the additional settlements to the least possible measure. The practice shows that, at slope inclinations steeper than 1:2, and thus, prepared base, it is still not able to take on, without damage, the weight of the pave-finisher during the placement of the first asphalt layer. That is why the layer of stone chippings is most often stabilized with bituminous emulsion or, even better, with special materials based on bitumen, able to penetrate even several centimetres, thus forming a sufficiently firmly stabilizing layer upon which equipment can freely work. Depending on the type of stone chippings, grain size distribution, and degree of stability to which it is aimed, a 3–6 l/m^2 binder is usually proportioned.

13.1.3.2 Asphaltic concrete lining

Asphaltic concrete lining is the most important part of the facing. The majority of requirements that facing has to fulfill depend precisely on the characteristics and dimensions of layers of the lining. On the other hand, the asphaltic concrete layers fall within the most expensive elements in the case of dams with a facing, so that the design of

the lining should satisfy not only the technical requirements and safety, but also offer the most economical possible solution.

According to the number of layers, linings can have *one layer, two layers* or be *multi-layered*. According to the type of asphalt mixture from which they have been constructed, layers are divided into *watertight* (asphaltic concrete) and *porous,* or *drainage* types.

The basic function of the lining is to make the facing watertight, in which many other requirements must also be fulfilled, which have already been considered. In order to provide for watertightness, a relatively small thickness of dense asphaltic concrete layer is sufficient. For low protective embankments, a simple lining can be used, consisting of an asphaltic concrete layer with a thickness of 8 cm, constructed over bituminous stabilization, (Fig. 13.2a). In the case of small dams and embankments enclosing hydraulic storage basins, somewhat more complex construction is used, which also contains a layer of porous asphalt below the asphaltic concrete lining, called a *binding layer* or *binder,* Figure 13.2b.

Binder contains a percentage of free voids more than 5%, usually within 10–20%, and approximately twice less quantity of bitumen and filler than the asphaltic concrete, which are the most expensive constituent parts of the asphalt mass. Thus, the layer of porous asphalt is considerably cheaper then the asphaltic concrete one, and within the asphaltic lining, it makes replacement in all capacities, except for ensuring watertightness.

In the case of dams higher than 20 m, linings consist of several layers. With some old dams, such as El Grib and Bou Hanifiia, constructed in Algeria before World War II, there was used a construction with a very steep facing of two asphaltic concrete layers over a drainage layer of porous concrete, protected from the upper side with slabs, made also of porous concrete (Van Asbeck, 1962). A last example of such an out-of-date construction is the facing of Radoyna dam within the system of water power plants Kokin Brod – Bistrica (Serbia), on the River Uvac. This dam, with a maximum height of 43 m (Fig. 13.3), encloses a reservoir for the hydro-electric power station Bistrica with a gross storage capacity of 7.6×10^6 m^3. Construction started in 1953 and, according to the design, there should have been constructed a reinforced concrete facing over dry sub-facing stone masonry. However, once the embankment

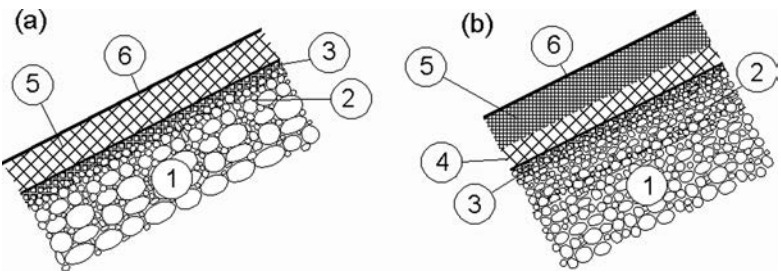

Figure 13.2 Facing for low protective embankment (a) and for small dams and pumped storage reservoir basins (b). (1) Rockfill; (2) stone chippings; (3) bituminous stabilization; (4) porous asphalt; (5) asphaltic concrete; (6) surface treatment.

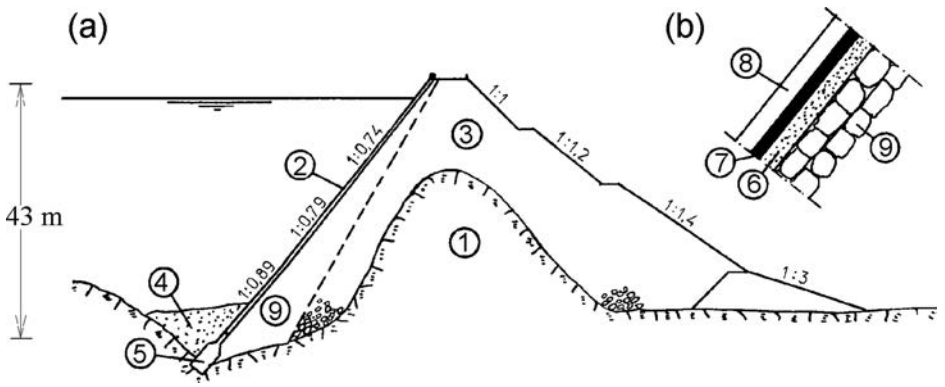

Figure 13.3 Radoyna dam, cross-section (a) and detail of facing (b). (1) Rock; (2) facing; (3) rockfill; (4) clay backfill; (5) concrete cutoff; (6) porous concrete; (7) asphaltic concrete 2 × 4.5 cm; (8) reinforced concrete 15 cm; (9) dry stone masonry.

has been constructed, and owing to doubts on the quality of the employed rockfill material – limestone, it has been decided to carry out an asphalt concrete facing which would adapt to possible considerable deformations.

The facing was constructed in the period July–November 1959. The slope was constructed with dry stone masonry, so a relatively smooth surface has been obtained. Along the dam's toe and just below the crest, at first there has been placed a leveling layer of concrete; that is to say, for confirming dimensions according to the new and old design. Over this layer and over the remaining manually placed rock, there has been applied a layer of porous concrete across the entire surface of the slope. It serves as bedding for the layers of asphaltic concrete and as a filter for the seepage of water through the asphaltic concrete. The levelling layer is made of concrete grade 16 MPa, in bays of 6 × 6 m, i.e. 6 × 4 m in both belts of 10 metres above the toe and below the crest of the dam, with joints of 6 cm. Over it there has been placed a layer of porous concrete with grains within 8–15 mm, 15 cm thick. First of all, posts are placed 6 m apart, made of concrete grade 16 MPa, which, later on, served as guides for the application of the porous concrete. For porous concrete there have been used 170 kg cement per m^3, while tamping has been performed manually, since vibrators had separated the cement from aggregate.

Asphaltic concrete lining has consisted of two layers, each 4.5 cm. Construction has been commended to the Slovenia Ceste Company from Ljubljana, which, for this purpose, worked out projects and drawings and also produced special plant and equipment, which is adjusted for work along the slope, inclined at an angle of 50–55°. This entirely new plant and equipment consisted of a pave-finisher for spreading the asphalt mass, a vibratory roller for its compaction, and a movable train on rails, along with hoists for lifting and lowering of the pave-finisher and the vibratory roller. On the train, there has also been a command spot for an electrical operator who operates the overall plant and equipment.

Asphaltic concrete mixture has been determined by means of extensive laboratory tests performed in the institute for testing of materials and structures in Ljubljana and, together with the built-in layer, it has had to fulfill the following requirements:

- To remain without deformations on inclination of 1:0.8 at a temperature from −10°C to +50°C during the stages of construction and operation;
- To be sufficiently plastic in order to be able to follow up the deformations without forming of cracks;
- To be watertight under a pressure of 5 bars;
- To have minimum shearing strength of 2 N/cm^2;
- To be easily workable, and, at the same time, not to flow along the slope with an inclination of 1:0.8;
- To possess conditions for self-healing.

The mineral mixture that fulfils these requirements consisted of stone chippings – limestone up to 20 mm, filler, and hydrated lime, which makes a better contribution for closing of voids. To such determined mineral aggregate, there have been added 8.6% binder, consisting of 92% bitumen with penetration from 50 to 75, and 8% natural asphalt, whose role has been to make the bitumen more rigid.

Asphalt mixture has been prepared in the asphalt plant of capacity 10 to 12 tons per hour, 2 km away from the construction site. Besides this, there has been mounted a crushing plant for the preparation of rock aggregate for the asphaltic concrete in all necessary fractions. The hot asphalt mixture has been transported by means of tipping trucks to a wooden silo at the beginning of dam's crest. From here, parallel with the rails of a standard gauge track, there has also been set up a narrow gauge track for operation of ordinary transportation wagons, which have been loaded with asphalt mixture from the silo, transported to the train and then, by means of a hoist and on sloping rails, they have been drawn out on it. Here the asphalt mixture has been put in another wagon, by means of which it has been transported to the silo of the pave-finisher. Such an organisation has been conducted in order to avoid dragging of the pave-finisher to the top at each filling with asphalt mixture, which would mean wasting a lot of time, since the speed of the pave-finisher has been only 4 m/min.

Asphaltic concrete lining on the upper side is protected with a layer of reinforced concrete, with a thickness of 12 cm, constructed without expansion joints and without breaks in the reinforcement. There is double reinforcement, in two layers, spaced at a distance of 7 cm, composed of steel bars Ø10 mm, forming squares with a side of 12 cm. Concreting is constructed by means of slipform. Concrete has been prepared at the two ends of the dam and transported along the dam's crest, from where it has been taken down the slope through pipes attached to the reinforcement. Compaction has been performed by means of electrical vibrators, while concreting has been performed in a quality manner within less than a month.

During 1960, the dam was handed over to operation. Seepage water through the facing is negligible. On the facing, until now, there has not been recorded any damage. For this reason, certainly the very small settlement of the dam has also made a contribution, which, in the part of the greatest height, amounted to only 10 mm. This is certainly due to the long period of construction of dam's body made of rockfill, which period was retarded from 1953 to 1958.

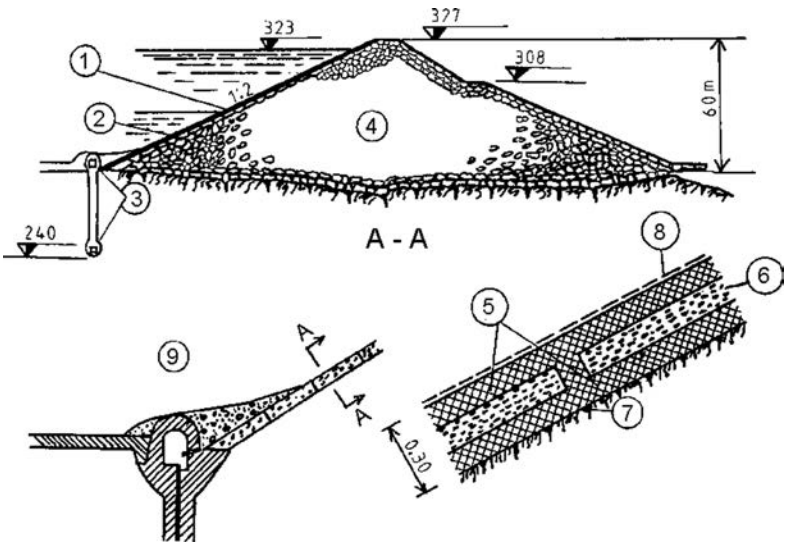

Figure 13.4 Henne dam (Germany). (1) Three-layered asphaltic facing; (2) selected rockfill; (3) drainage gallery; (4) rockfill; (5) asphaltic concrete 2 × 10 cm; (6) porous asphalt 10 cm; (7) base course of stone chippings, 15 cm thick; (8) surface finishing treatment; (9) joint of the facing and the concrete gallery.

In practice, *the sandwich construction* is often used at which among the watertight asphaltic concrete layers there is a layer of porous asphalt, which enables drainage of the seepage water as well as control of its quantity (Tanĕev, 1981, Garcia, 1988). The porous layer is of thickness 10–12 cm and it makes a contribution to the overall stability and strength of the facing, as well as the watertight layers, but its cost is considerably lower. One of the first applications of this type of facing is recorded at Henne dam (Germany), 67 m high, Figure 13.4. The lining consists of three layers of 10 cm each – two asphaltic concrete layers and one porous layer in between, which has been divided into a number of sections with separate run-off of the seepage water in order to facilitate easier locating of possible crack in the upper asphaltic concrete layer. This construction has turned out to be successful in the course of service. The facing has not required overhaul, even though the settlement of the dam has reached 30 cm, while the facing has been exposed to the action of waves 2.5 m high and ice with a thickness of 50 cm.

Another type of lining, which has often been used in the USA, is the homogeneous multilayer asphaltic concrete lining, without a drainage layer of porous asphalt. An example of such construction is Homestake dam, Figure 13.5, completed in 1966, 76 m high. This dam was constructed at a high altitude (over 3000 m), so by dropping the porous layer, there has been eliminated the danger to come about freezing of possibly remained water in it at a rapid drawdown of the water level in the reservoir. The lining has been constructed of two layers in the upper part of the facing, three layers in the intermediate part and four layers at the joint with the concrete foundation. Each layer

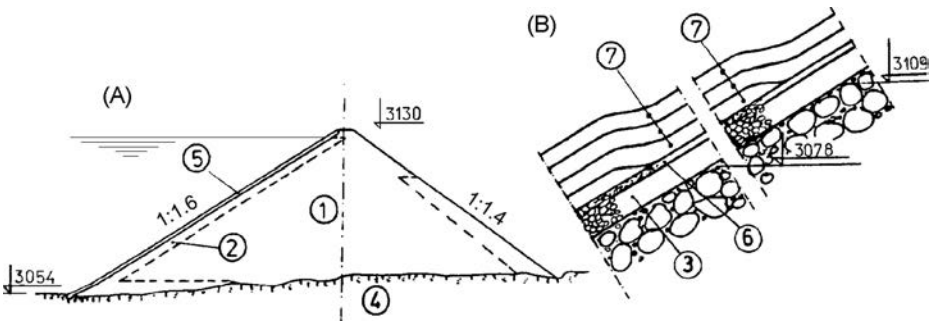

Figure 13.5 Homestake dam (USA), cross-section (A) and detail of the facing (B) (after Golzé, 1977). (1) Rockfill, zone I, ≈91 cm maximum size of rock; (2) rockfill, zone II, ≈45 cm maximum size; (3) base course, zone III, ≈7.6 cm maximum size; (4) rock foundation; (5) asphaltic concrete face; (6) stabilizing course; (7) asphaltic concrete courses.

is of a thickness 9 cm, so that the overall thickness of the asphaltic concrete lining varies from 18 to 36 cm. This kind of construction works without damages in fierce climatic conditions (Golzé, 1977).

13.1.3.3 Surface finishing treatment

Even though the asphaltic concrete layers are designed so as to be watertight and stable at maximum possible temperature, there is still a widespread practice for the surface of the facing to be treated with a finishing coat, which can have two functions: (1) to completely close the surface of the facing; (2) to lower the maximum temperature in the uppermost asphaltic concrete layer.

For the first purpose, they most often use asphalt mastic or some of the special agents, i.e. compounds for coating that are based on bitumen and are produced under various trademarks.

For lowering the temperature in the uppermost asphaltic concrete layer in areas of hot climate, it is most simple to perform painting of the asphalt surface with white paint, which reflects the solar rays. From tests and measurements of French engineers, it comes out that the white paint decreases the temperature in the centre of the uppermost asphaltic concrete layer by 16% (see Fig. 4.15).

13.1.3.4 Protection against mechanical damage

During the action of waves higher than 3 m and thickness of ice greater than 1 m, and at a rate of variation of the water level greater than 50 cm/day, the design thickness of the asphaltic lining becomes so large that it is irrational. In such cases, they apply a protective lining of reinforced concrete slabs, prefabricated or cast-in-place. The thickness of this protective lining is obtained by calculations and ranges from 10 to 20 cm.

13.1.4 Joint of the lining with a gallery or concrete cutoff in dam's toe

Asphaltic concrete facing in the upstream toe ends up with a gallery or with a concrete cutoff, which represents foundation of the facing. The concrete cutoff could be embedded deeply up to sound strata in the foundation, or else embedded to a narrow depth to serve as a grouting cap. Since this foundation is rigidly jointed with the foundation, it is necessary to carry out a successful joint which would enable synchronized work of the stiff concrete and flexible asphaltic concrete at the settlement of the embankment due to dam's self-weight during filling of the reservoir and later on, during operation of the works (Le Bel, 1981).

In practice, various methods have been used for jointing of the facing and the foundation. Also, model tests have been constructed, and obtained results have been checked and compared with theoretical calculations of the vertical displacements in the asphaltic lining at the joint under water pressure. In that way, it is possible to draw apparent rules for the design of this important structural element.

At the joint of the asphaltic concrete lining with the cement-concrete construction in the foundation of the facing, the settlement below the lining must be quite limited. Such a requirement would be met ideally if the concrete wall did not elevate beyond the rock in the foundation, while the asphaltic lining is of slight inclination before the joint (Fig. 13.6a).

For the construction that elevates from the rock of the foundation (Fig. 13.6b), the wall must also be constructed with a slight inclination. In that way, the differences of the settlements in the zone of the joint are small and the deformation of the asphaltic lining takes place on a long, even, and sloping surface.

Figure 13.6c presents the joint in the concrete cutoff of Bigge dam (Germany). The height of the embankment over the concrete wall is small, as compared to the construction under (b). When wall inclination is smaller than 45°, it is assumed that there would not come about an earth pressure below the lining, directed upward, as a consequence of spreading of the forces due to embankment at the bottom of the dam. In a general case, we should avoid the level of the underground water in dam's body

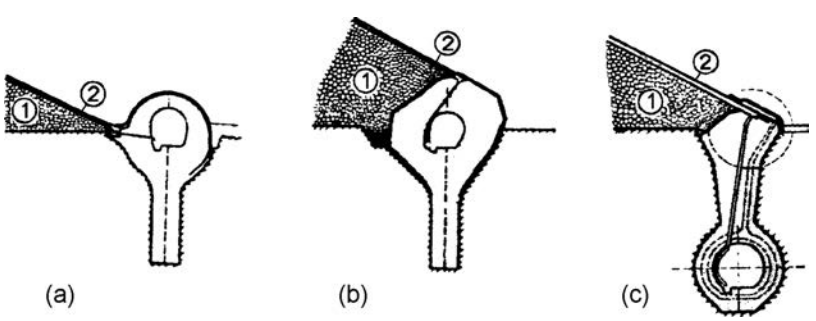

Figure 13.6 Various joints of the asphaltic facing with the foundation. (a) Joint at Henne dam, 1955; (b) Genkel, 1952; (c) Bigge, 1965, all in Germany. (1) Rockfill; (2) asphaltic lining.

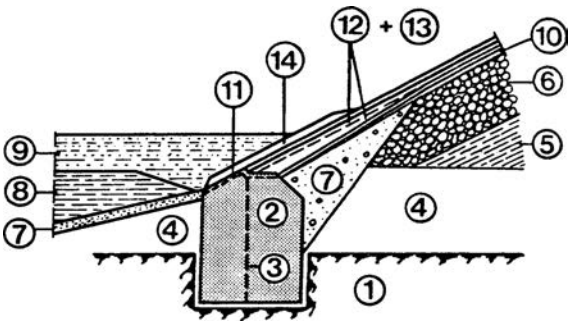

Figure 13.7 Joint of the facing and the foundation at Nidda dam (Germany, 1972). (1) Rock; (2) concrete wall; (3) waterstop; (4) natural ground; (5) rockfill; (6) sub-facing layer of crushed rock; (7) graded gravel; (8) gravel; (9) clay; (10) bituminous levelling layer; (11) coating of bituminous emulsion; (12,13) asphaltic concrete; (14) asphaltic concrete protective layer.

to be higher than the joint of the structure, in which way the asphaltic lining is not subjected to the uplift action.

The joint under (a) has the inconvenient feature of being difficult for execution. Namely, the gallery, since it is elevated, obstructs the work of the plant and equipment during the placement of the asphalt layers, so that a large area must be placed manually. The case under (c) is very convenient regarding construction.

Experimental and theoretical investigations have shown, and practice has confirmed, that layers of the lining in the zone of the joint should be reinforced and at significant expected deformations, should be jointed with the concrete construction by means of an expansion joint. From the upper side, the joint should be protected with a cover layer of reinforced concrete or metal sheeting, in order to prevent contamination and filling-in with extraneous material.

It is very often that the asphaltic concrete lining in the zone of the joint expands in the form of a wedge, which takes on the enlarged stresses in this most loaded part of the facing and the function of an elastic safety fender, i.e. buffer stop. In the case of Nidda dam (Germany; Fig. 13.7), the wedge is constructed with well-graded gravel (7) and is positioned between the sub-facing drainage layer (6) and the natural foundation (4). Gravel has been applied in thin layers together with proper compaction. The joint is constructed without an expansion joint, while from the upper side it is covered with an asphaltic concrete protective layer (14). Originally planned and constructed, the joint works successfully and without damage.

Similar joint construction of the facing and the foundation, which contains a gallery, has been constructed in Sainte Cecile D'Andorge dam, built in France in 1972 (Fig. 13.8); the difference is that here the wedge is formed by expanding of the layer of porous asphalt (1) from 10 to 40 cm into the joint with the concrete construction. From the upper side, the joint is protected with shot-crete (8).

In the case of the 62 m high Salagou dam (France; Fig. 13.9), the joint of the facing with the concrete gallery is executed similarly to Henne dam (Fig. 13.4). The asphaltic concrete wedge (2) is constructed towards the upper side of the facing, while

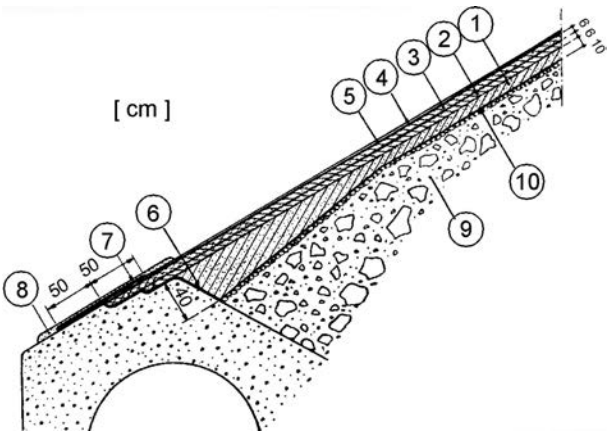

Figure 13.8 Joint of the facing and the concrete gallery at Sainte Cecile D'Andorge dam (after Thomas, 1976). (1) Drainage asphalt layer; (2,3) asphaltic concrete; (4) mastic; (5) light paint; (6) binding coat; (7) reinforcement; (8) shot-crete; (9) crushed rock 0–200 mm; (10) aggregate 15–45 mm.

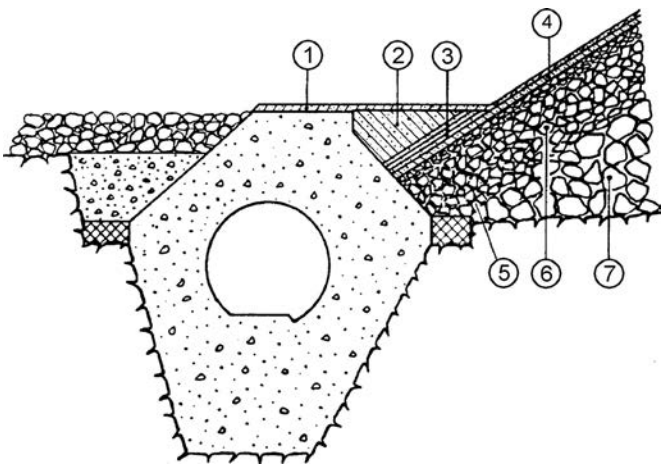

Figure 13.9 Joint of the facing with the concrete gallery at Salagou dam (after Thomas, 1976). (1) Protective asphaltic concrete layer; (2) asphaltic concrete; (3) three layers of asphaltic concrete; (4) asphaltic concrete lining; (5) course stabilized with bituminous mastic; (6) rockfill 80–250 mm; (7) rockfill.

as a protection of the joint, over the wedge there comes a horizontal asphaltic concrete layer (1).

The German Association of Soil Mechanics and Foundation Engineering has issued recommendations for construction of the joints of asphaltic concrete linings in hydraulic engineering on the basis of detailed preliminary studies. Also worked out

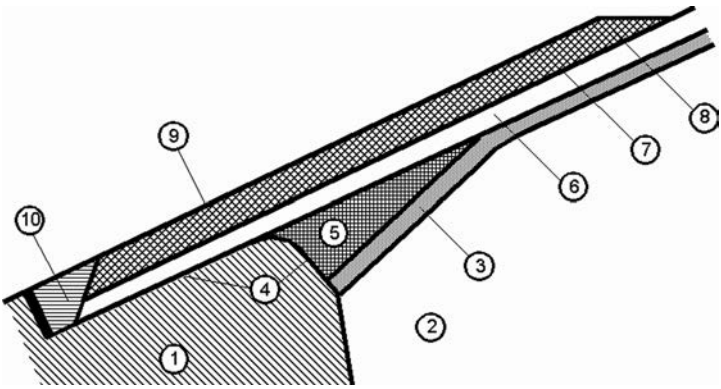

Figure 13.10 Joint without expansion connection (German Association of Soil Mechanics and Foundation Engineering). (1) Concrete; (2) compacted rockfill; (3) asphaltic leveling layer; (4) coating; (5) asphaltic concrete wedge; (6) asphaltic concrete layer; (7) geotextile; (8) asphaltic concrete protective layer; (9) mastic; (10) sealing compound.

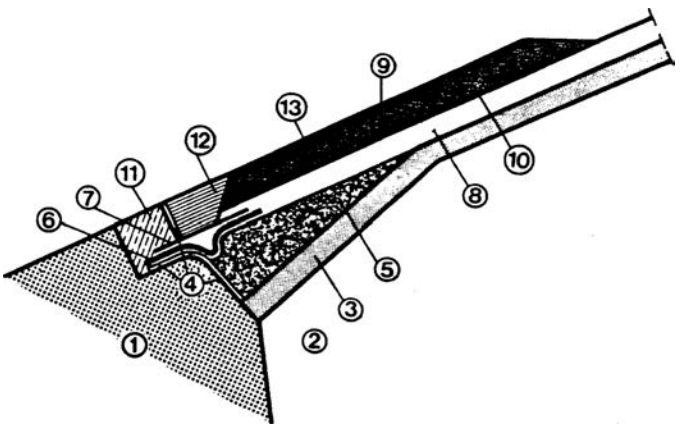

Figure 13.11 Joint with expansion connection (German Association of Soil Mechanics and Foundation Engineering). (1) Concrete; (2) compacted rockfill; (3) asphalt leveling layer; (4) binding coating; (5) asphaltic concrete wedge; (6) expansion joint; (7) copper cover sheet; (8) watertight asphaltic concrete; (9) geotextile; (10) asphaltic concrete protective layer; (11) cement-concrete; (12) sealing compound; (13) mastic.

are designs for joints – Figures 13.10 and 13.11. In accordance with these recommendations, for all joint constructions, there have to be taken into consideration and analysed the following factors (Idel, 1979):

- Rigid cement-concrete structures should have joints spaced at a distance from 2 to maximum 24 metres, in order to prevent occurrence of cracks in the joint;

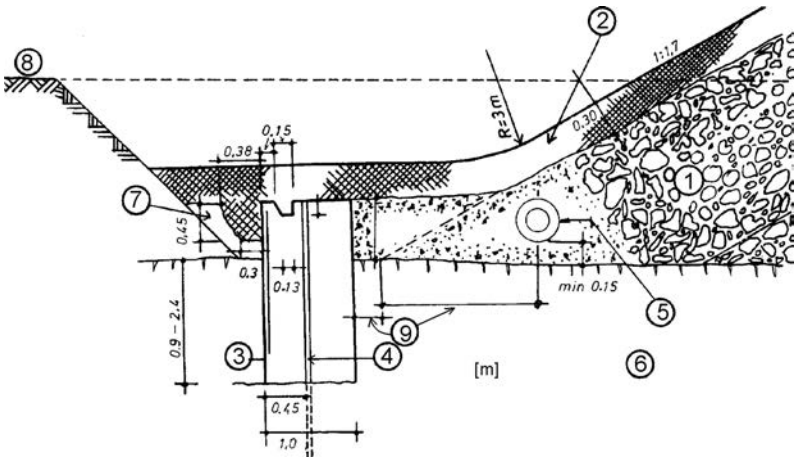

Figure 13.12 Joint of the facing and the concrete foundation at Montgomery dam, USA (after USBR, 1977b). (1) Drainage layer of tipped rock; (2) asphaltic concrete lining; (3) concrete cutoff; (4) grouting pipe; (5) drainage pipe; (6) rock; (7) filling; (8) ground; (9) variable distance.

- Control structural joints between the concrete blocks should be covered with overlapping copper sheets, and fixed with mastic;
- If significant displacements are expected along the blocks of the concrete cutoff trench, then the asphaltic concrete lining must be reinforced with textiles (fabrics), and protected with one or two additional asphaltic concrete layers. Figure 13.10 presents a joint for expected small settlements and displacements according to the design recommendations of the above German Association. The concrete surface in the zone of the joint is first sprayed with bituminous emulsion, and then the asphaltic concrete wedge and the first asphaltic concrete layer are constructed. The space between the concrete and the asphaltic concrete in the butt joint is filled with a wedge-like element made of sealing compound, which makes it highly plastic and elastic.

For more rigorous requirements in relation to settlements and displacements, the joint shown in Figure 13.11 is recommended, which is reinforced with an expansion joint containing copper sheeting; it protects the joint from filling in with extraneous matter.

The joint is often constructed by curving the lower part of the lining, which, at the same time, passes over the concrete wall with very slight inclination. In this manner is constructed the joint of the facing and the concrete foundation for Montgomery dam (USA; Fig. 13.12). This construction is somewhat more expensive; however, the foundation is moved away from dam's body, which reduces to a minimum the mutually harmful effect.

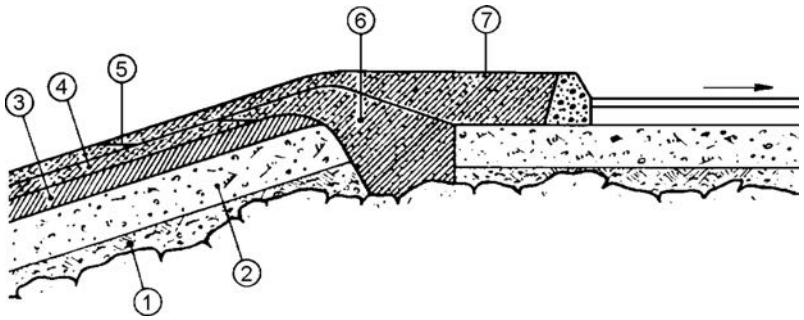

Figure 13.13 Joint of the facing into the crest of Vallon D'Ol (France). (1) Earth bedding below the facing; (2) layer of compacted gravel; (3) binding layer of porous asphalt, 10 cm; (4) asphaltic concrete layers 2 × 6 cm; (5) coating of liquid bitumen; (6) asphaltic concrete cover layer; (7) asphaltic concrete sidewalk pavement.

13.1.5 Joint of the facing with dam's crest

The joint of the facing with dam's crest, too, must be technically properly constructed in order to avoid cracks due to deformations in the crest, as well as possible penetration of water between the asphalt layers and into the drainage layer, which could be very dangerous at a rapid drawdown of the water level in the storage lake.

Figure 13.13 presents perfectly visualised and executed joint at the crest of Vallon D'Ol dam (France), constructed with three-layered asphaltic lining. Right at the joint, the asphaltic concrete layers are reinforced and constructed in such a manner so that, between the layers and in the drainage layer, water penetration would be impossible.

Figure 13.14 presents a possible solution of a joint *sandwich construction* of the lining with the parapet wall, which is extended towards the lining and covers the whole edge of the crest. The end of the drainage layer is completely isolated against penetration of water.

13.2 ROCKFILL DAMS WITH STEEL FACING

Steel facings are rarely used owing to the relatively complicated construction procedure and the necessity of profound anti-corrosive protection. Otherwise, a properly designed and executed steel facing is elastic, able to adapt to differentiated settlements, resistant to seismic influences, and operate satisfactorily in different service conditions. We usually employ special stainless steel or structural steel with well-made anti-corrosive protection. Two types of protection are mainly used in practice: thin coating (0.2 mm) of vinyl-acrylic mixture and elastomer coating of bituminous rubber (about 2 mm). The protection has to be renewed each ten years. The thickness of the plate ranges from 4 to 10 mm, while the jointing in the recent practice is exclusively performed by welding. In order to facilitate dilatation of the plate, there are anticipated joints which are spaced 4–16 m apart, usually in the form of omega (Ω), which can be either concave or convex (see examples that follow).

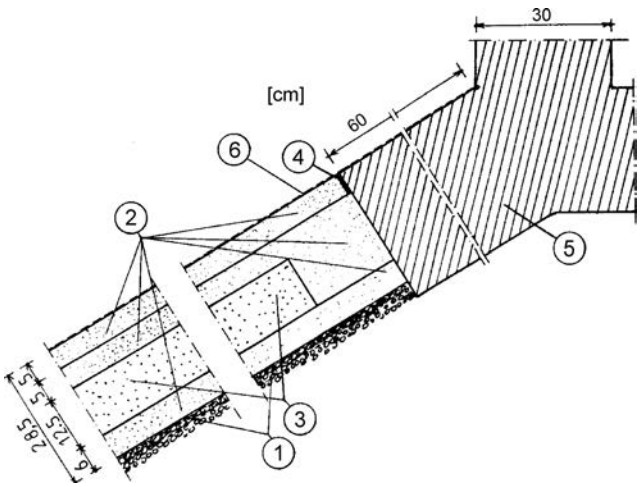

Figure 13.14 Joint of *sandwich construction* of the lining along with concrete parapet wall. (1) Bituminous stabilisation; (2) watertight asphaltic concrete; (3) drainage layer of porous asphalt; (4) joint sealed with mastic; (5) concrete mole extended towards the facing along the slope of dam; (6) finishing coat.

The conditions for the application of steel facings are similar as for the other types of facings made of artificial materials, and their particular advantage in relation to the earth cores is in conditions of short construction season, when for fast construction there are needed conditions for independent execution of the facing from that of the dam's body.

Steel facings, like reinforced concrete ones, can be constructed on a bedding of sub-facing stone masonry, as is shown in Figure 13.15, or on particularly selected layers of filling material, as is shown in Figure 13.16.

The first case is illustrated in the example of the 40.7 m high facing of Lago Verde dam (Italy), built in 1967, at a considerable height above sea level. The inclination of the upstream slope of this dam, upon the facing rests, is very steep (1:0.9), which has been facilitated by means of sub-facing masonry. Drawings present details of the construction and the facing, constructed with concave omega-joints. In order to prevent the danger of damaging of the facing due to ice, there has been installed a system for blowing air, by means of which the water has been prevented from freezing near the facing. In the practice of operation of the dam, this system has proved to be efficient (INCOLD, 1988).

Figure 13.16 presents the cross-section of Lagartijo dam (Venezuela), together with details of the steel facing, built for only 60 days. Namely, in the course of 1958 there occurred a great shortage of water for the capital city of Caracas. The only efficient solution for solving the problem was the construction of a 25 m high and 122 m long dam that was to be designed and constructed within a few months. In the vicinity of dam site, there has been clay in large quantities; however, the designers have feared that a clay core could not be constructed in a quality manner within the short and rainy available period. That has been a reason for adopting the solution of a rockfill dam

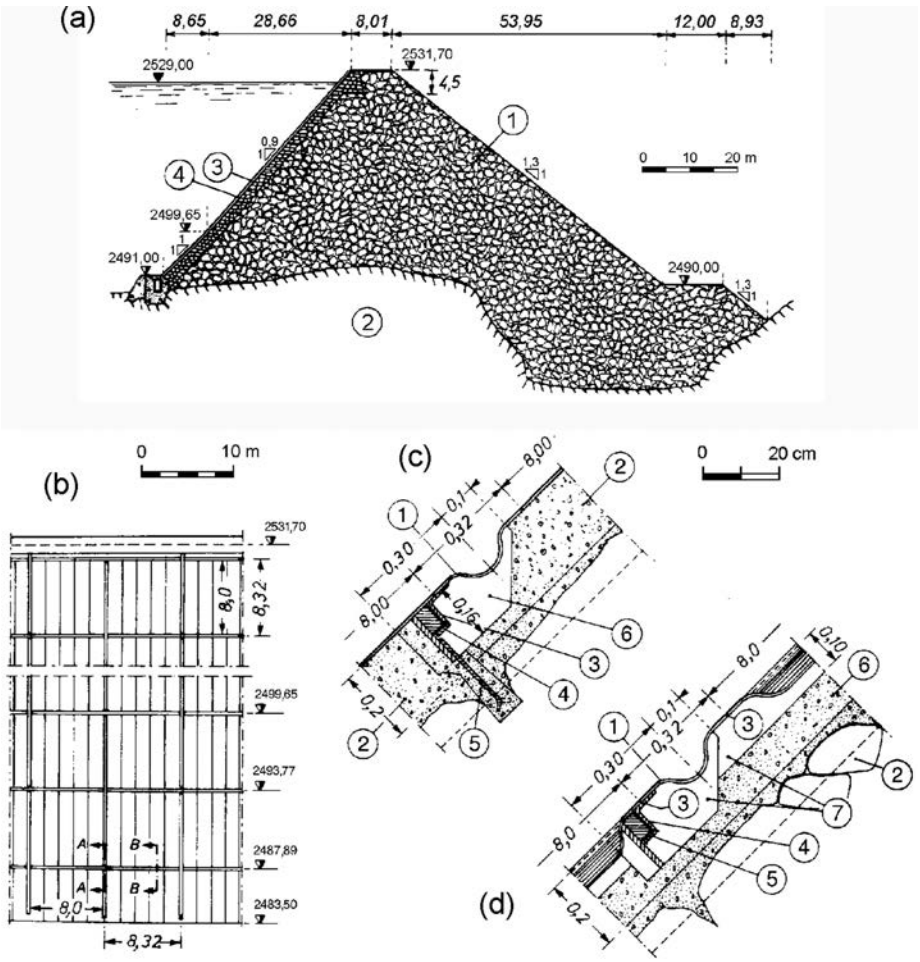

Figure 13.15 Lago Verde dam, with steel facing (after INCOLD, 1988). (a) Cross-section: (1) rockfill; (2) diorite; (3) steel facing; (4) dry sub-facing masonry; (b) elevation of facing; (c) section B–B: (1) joint of concave omega-plate, 4 mm thick; (2) porous concrete; (3) steel angle; (4) steel plate; (5) anchor; (6) groove; (d) section A–A: (1) joint; (2) dry masonry; (3) welded joint; (4) angle bar; (5) plate; (6) porous concrete; (7) groove.

with steel facing, which has been successfully constructed within the anticipated short period. The constituent elements of the facing have been factory-manufactured in the course of construction of dam's body made of rockfill. The facing is laid over two well-compacted layers of selected material, over a slope of inclination 1:1.5. Convex joints have been used, which can be seen from the details in the figure. Non-rock strata below the dam are cut-in with a concrete diaphragm wall, executed below the foundation of the facing (Sherard et al., 1963).

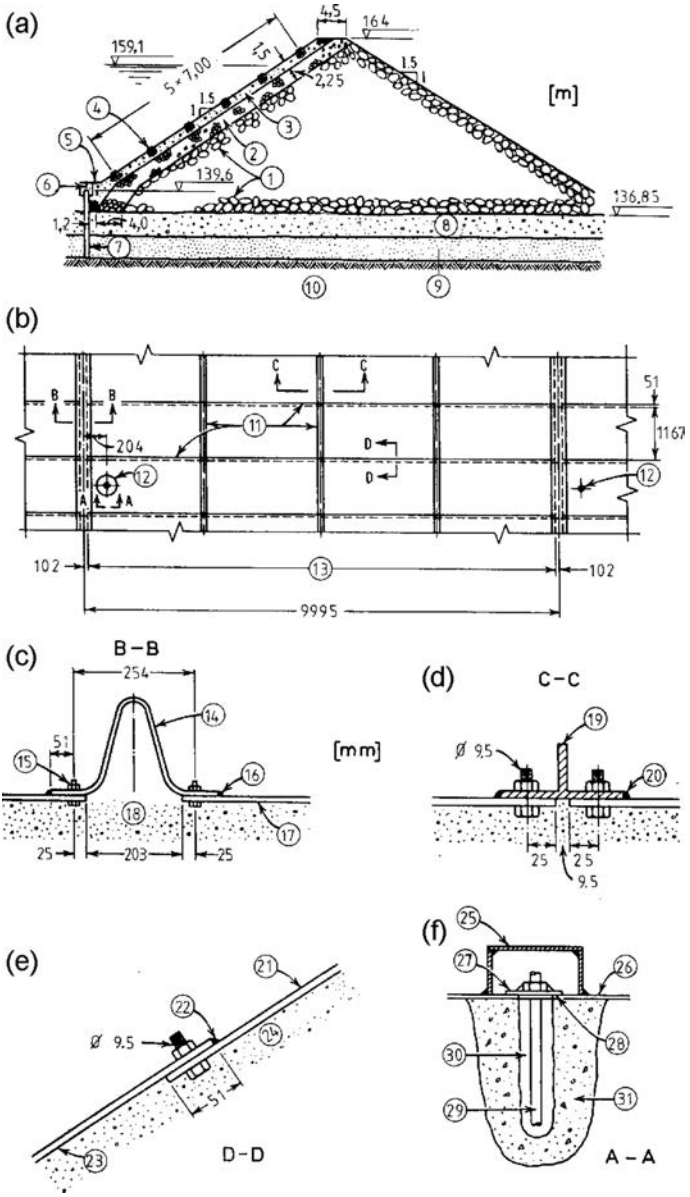

Figure 13.16 Lagartijo dam (Venezuela) with steel facing (after Sherard et al, 1963). (a) Cross-section; (b) part of the plan of the facing; (c) expansion joint; (d) joint along the slope; (e) horizontal joint; (f) anchor. (1) Dam's body of coarse and clean rockfill; (2) well-graded and compacted rockfill; (3) compacted gravel and stone chippings; (4) plate of 6.35 mm (1/4″); (5) expansion joint; (6) steel plate; (7) concrete diaphragm wall; (8) gravel; (9) silt; (10) rock; (11) plate 1219 × 6.35 × 2438 mm; (12) anchor; (13) four plates of 2438 mm with a spacing between them of 9.5 mm; (14) plate 6.35 × 660 mm; (15) bolt of 9.5 mm; (16) continuous weld; (17) plate of 6.35 mm; (18) sand; (19) T-section of 100 mm; (20) continuous weld; (21) plate 1219 × 6.35 × 2438 mm; (22) continuous weld; (23) plate as 21; (24) sand; (25) watertight box 200 × 200 × 100 mm; (26) steel facing; (27) plate of 12.7 mm; (28) opening 41 × 82 mm; (29) anchor bolt 38 × 711 mm; (30) grouted; (31) concrete.

13.3 ROCKFILL DAMS WITH FACING OF GEOMEMBRANE

13.3.1 General

The facing of various kinds of geomembranes is a modern type of a facing, which is often used with earth dams, and during the last 30 years or so it is also finding application in the rockfill dams. All that has been said for this watertight construction in Chapter 10 for earthfill dams is also valid here. In continuation, we shall highlight certain differences when it is a question of the application of geomembranes for rockfill dams in relation to earthfill dams.

First of all, there is a difference in the construction of the load-bearing layer. In the case of a rockfill dam, it must consist of several layers, most often three, in order for a fine-grained surface to be created for the bedding by means of gradual transition from the coarse-aggregate material in dam's body. Usually, first of all a layer of stone chippings (80–150 mm) is constructed, with a minimum thickness of 60 cm. Above it comes a layer of gravel (grains up to 30 mm), of a thickness 20–30 cm, and then what follows is a layer of sand (1–6 mm). Bedding is applied over such a composed load-bearing layer. For the purpose of the bedding, there are used the same materials as with the earthfill dams, with the only difference that here, the bedding in most cases has no need to play the role of drainage, since the body of rockfill dams is water-permeable and so drains well.

There is yet another difference, which has its reflex, mainly, on the method of construction of the geomembrane. Namely, the inclination of the upstream slope in rockfill dams ranges from 1:1.5 to 1:2. Steeper inclination is not constructed (regardless of the fact of whether it is possible to be constructed, taking into consideration the stability of the dam) in order not to aggravate the conditions for the execution of the geomembrane.

13.3.2 Examples of rockfill dams with geomembrane facing

The application of geomembranes as facing for rockfill dams dates back to the end of the fifties (Contrada Sabeta, Italy, 1959, $H = 32.5$ m, Dobchina, Czechia, 1960, $H = 10$ m), with positive experiences. For illustration of the structure, construction, and performance of rockfill dams with geomembrane facings, we quote several characteristic examples from modern world practice.

13.3.2.1 Codolle dam (France, 1983)

Codolle dam was built in France in 1983, is 28 m high, and the inclination of its slopes is 1:1.7. The load-bearing construction consists of 2 m thick layer of well-compacted sand and gravel, with a size of grains 25–120 mm, upon which there comes a layer of 15 cm thick gravel ($d = 25$–50 mm). Bedding is 5 cm thick and is constructed of asphalt, prepared with cold bituminous emulsion, with mineral aggregate of 6–12 mm. Above this layer comes geotextile, as a direct bedding of the geomembrane of polyvinyl chloride (PVC), 2 mm thick, joined by means of hot air. A layer of geotextile (400 g/m^2) is laid over the geomembrane, as bedding for the protective concrete slabs (Fig. 13.17; Radchenko & Semenkov, 1993).

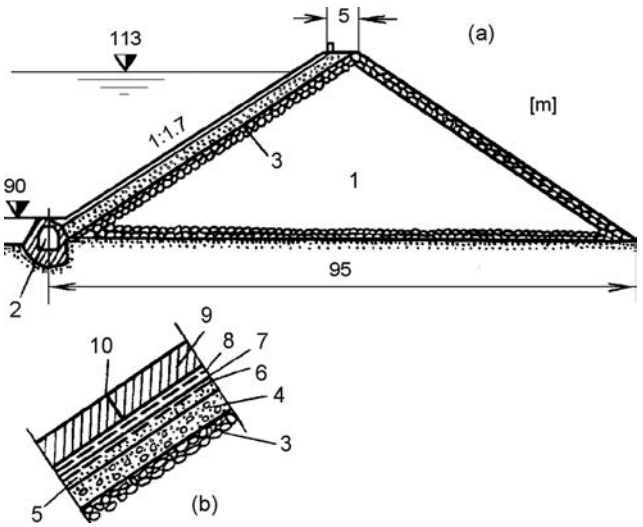

Figure 13.17 Codolle dam (France). (a) Cross-section of the dam; (b) detail of facing with the geomembrane. (1) Rock-fill 0–1000 mm; (2) gallery; (3) compacted sand and gravel, 2 m; (4) gravel, 15 cm; (5) bedding of cold asphalt, 5 cm; (6) base of geotextile; (7) geomembrane of polyvinyl chloride, 2 mm; (8) geotextile; (9) concrete slabs 4.5 × 5 m, d = 14 cm; (10) joint.

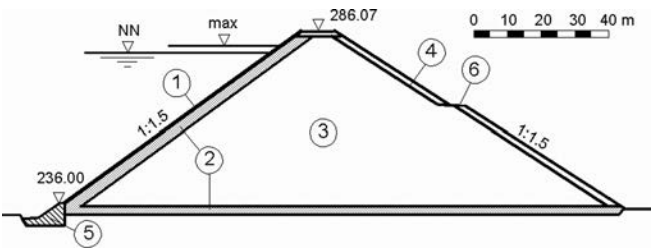

Figure 13.18 Martin Gonzalo dam, Spain (after Justo et al., 1988). (1) Facing with geomembrane; (2) load-bearing, i.e. drainage layer; (3) compacted crushed rock; (4) coarse rockfill; (5) concrete foundation; (6) berm.

13.3.2.2 Martin Gonzalo (Spain, 1986)

Another interesting example is Martin Gonzalo dam, 54 m high, constructed in Cordoba, Spain, in 1986 (Fig. 13.18). Originally, it was designed with a reinforced concrete facing, but in the course of construction of dam's body, by means of oedometer tests of crushed rock, it has been established that there is a three-fold lower modulus of deformation than the established one with preliminary investigations. Newly conducted analyses with the application of the Finite Element Method have indicated that, in such a case, the reinforced concrete facing would experience unacceptable deformations (>30 cm).

Following numerous analyses and consultations, it has been decided that the reinforced concrete facing should be replaced with a synthetic membrane, reinforced with synthetic fibres, and cast on the spot, directly over the bedding of geotextile impregnated with watertight polymer in liquid state. As a bedding of the watertight element of the facing there has been constructed a layer of asphalt-cement mortar in cold treatment, composed on the basis of extensive laboratory tests. Namely, this layer should have sufficient stability against shearing along the slope and to ensure proper connection with the geomembrane. Placement of this layer was done in strips 3 m wide, without expansion joints. Above such prepared bedding, geomembrane has been cast *in situ,* with a special machine operated from the crest, in strips 3.1–3.2 m wide. The strips have been overlapped by 20 cm in order to achieve a continuous watertight surface. Dam's body was completed at the end of April 1986, while the membrane was completed at the end of September, the same year (Justo et al., 1988).

Filling of the reservoir began in June 1987, and soon afterwards there was recorded a seepage of 6–8 l/s, which is acceptable, as well as a 25 cm settlement of the crest, which has confirmed the bad quality of the rockfill. There has also been demonstrated the justifiability for changing the type of the watertight element. In November of the same year, following ample rainfalls, the water level reached half the height of the dam, when suddenly seepage water increased to 5.79 m^3. The reservoir was immediately emptied and it was apparent that the upstream slope had suffered great deformations due to which a large crack has occurred in the plastic facing. The situation has been repaired by removal of the plastic facing along with the base – and execution of asphaltic concrete facing, by utilizing the existing concrete foundation – a solution that has been the most appropriate for the size and type of the dam (Flemme et al., 1990).

13.3.2.3 Bovilla dam (Albania, 1996)

The highest rockfill dam with geomembrane facing built up to now is Bovilla dam, in Albania, Figure 13.19. The 91 m high dam is located in a narrow gorge cut through a ridge of limestone rock just downstream from a tectonic contact with a schist formation. The limestone is heavily karstified. The dam is located in a seismic region. As above described Martin Gonzalo dam, Bovilla dam was also originally designed with a reinforced concrete facing. The 0.6 m thick reinforced facing slabs were to be installed over a grid of vertical and horizontal reinforced concrete beams. The reinforcing of the concrete elements, as well as the copper and PVC waterstops, was quite complex.

After construction began, original design was altered to include a PVC membrane as the only watertight element. To eliminate gullying by rainwater, and to provide a uniform draining support to the PVC liner, a 40 cm thick layer of gravel, stabilized with a low-cement concrete to hold the gravel together, was installed over the fill. This transition layer, having a permeability of $k > 1$ cm/s, was placed in 2 m high strips as the fill was being raised, starting from top of the fill, and then smoothed and compacted with a vibratory plate mounted on the arm of an excavator.

The material selected for the liner of Bovilla dam was a composite membrane consisting of a 3 mm thick PVC geomembrane heat-coupled to a 700 g/m^2 polypropylene geotextile. The choice of a PVC geocomposite was dictated by the benefits provided by a geotextile backing when intimately connected to the geomembrane, in reducing the

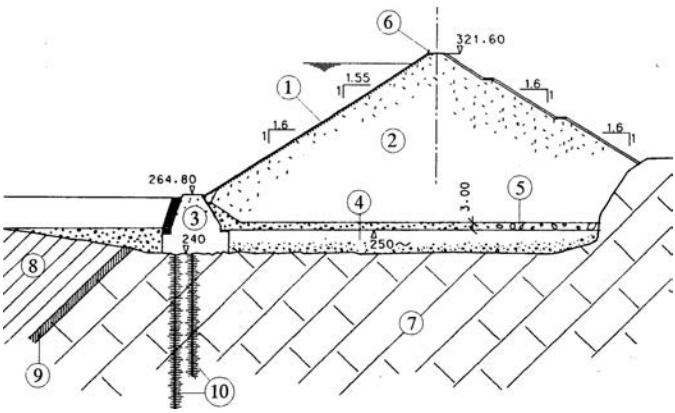

Figure 13.19 Bovilla dam, cross-section (after CARPI 1996). (1) Geosynthetic waterproofing system; (2) rockfill; (3) concrete block; (4) river deposit; (5) drainage layer; (6) crest wall; (7) karstified limestone (8) schist; (9) fault; (10) grout curtain.

coefficient of thermal expansion, in preventing the formation of wrinkles, high friction coefficient (<38° on used transition layer), and in providing extra anti-puncture protection (Scuero et al., 1999).

The geocomposite was installed after the transition layer had been completed. Due to construction of the perimeter plinth, installation started with the central part in May 1966, while the right and the left parts were placed after grouting from the perimeter beam had been completed. The geocomposite was supplied in 2.05 m wide rolls, custom-made in the factory to avoid horizontal seams, to expedite installation and to minimize waste. Rolls in the central part of the dam were 115 m long and manufactured in one single element, approximately 1000 kg of weight. Rolls were placed on the crest of the dam, temporarily fastened with bolts and nuts over the concrete beam at crest, and hence unrolled down to the upstream toe. Adjacent sheets overlapped 10 cm along their longitudinal edges. All longitudinal seams between sheets were made by the double track hot air seaming method, and air pressure tested. Installation of the membrane was completed in October 1996.

The liner has been protected with cast-in-place, unreinforced concrete slabs, 30 cm thick in the lower part of the face, and 20 cm thick in the upper 50 m (Fig. 13.20). Each slab was 6 m long and 3 m wide. An 800 g/m^2 polypropylene geotextile was placed over the PVC membrane to protect it from possible damage during concreting of the slabs. The slabs are keyed along all sides to block them.

The concrete protective (or ballasted) slabs were very carefully designed and constructed. A detail of the slab layout is shown in Figure 13.21a. Special attention was paid to the both vertical and horizontal joints between the slabs. They are open, vertical joints are continuous and horizontal joints are staggered. The horizontal joints have the purpose of allowing angular deformations, so that the slabs can adapt to the deformations of the dam. A single layer of geotextile is inserted in all horizontal joints to ease angular movements (Figure 13.21b). The vertical joints have the purpose of relieving uplift at drawdown, so they must have sufficient permeability to ensure that

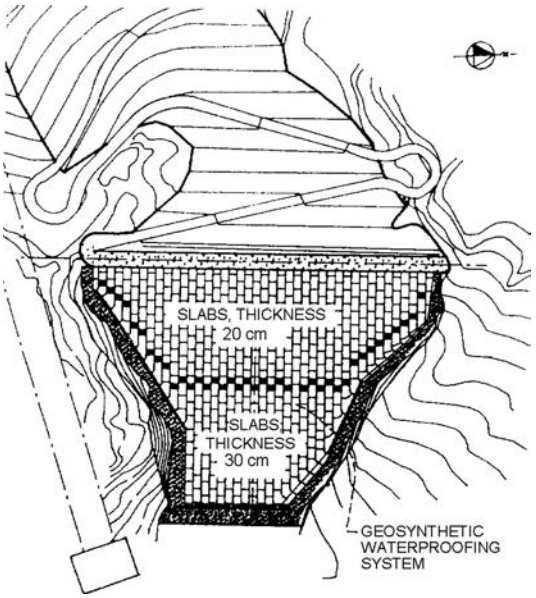

Figure 13.20 Bovilla dam, layout (after CARPI, 1996).

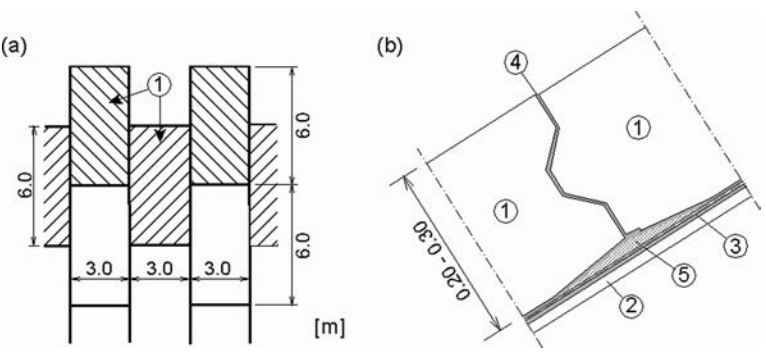

Figure 13.21 Bovilla dam. (a) Layout of the protective slabs; (b) horizontal joint between albs (after CARPI, 1996 and Sembenelli P. and Sembenelli G., 2013). (1) Concrete slabs; (2) lean concrete base layer; (3) waterproof element – geocomposite; (4) single-layer geotextile; (5) foamed polystyrene wedge.

there is a free-draining space under the slabs. Three layers of geotextile are placed along all vertical joints to provide relief from uplift pressures (Figure 13.22). All slabs' edges are appropriately shaped and provided with a foamed polystyrene wedge (Fig. 13.21b and 13.22). This measure is expected to prevent the edge of the slabs damaging the waterproofing geocomposite in the case of relative rotation to each other during service (Scuero & Vaschetti, 2011; Sembenelli & Sembenelli, 2013).

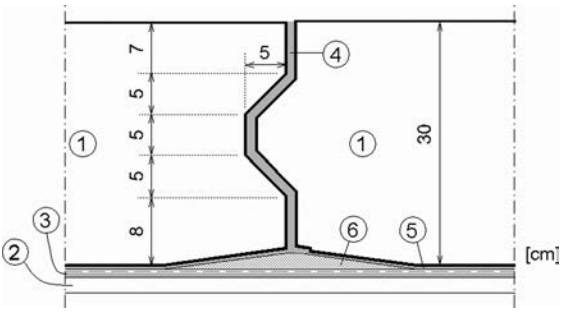

Figure 13.22 Bovilla dam, vertical joint between slabs (after Sembenelli & Sembenelli, 2013). (1) Concrete slabs; (2) lean concrete base layer; (3) waterproof element – geocomposite; (4) triple-layer geotextile; (5) single-layer geotextile; (6) foamed polystyrene wedge.

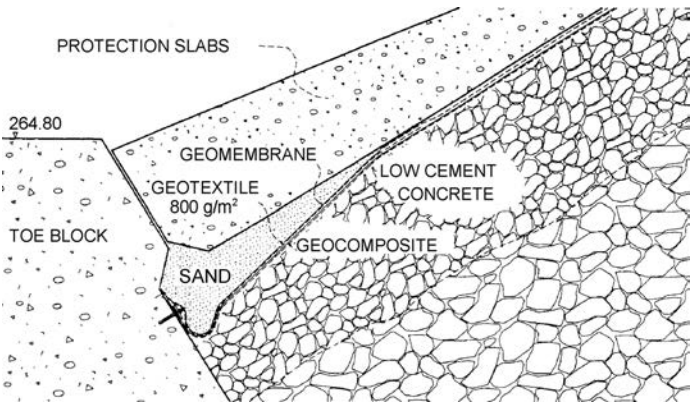

Figure 13.23 Connection of the geomembrane with the plinth (after CARPI, 1996).

At plinth connection, the subgrade is shaped thus to allow the geomembrane to make a large 180° open fold where it is tied into the concrete plinth (Fig. 13.23). The fold is covered with filter material so that the geomembrane is free to use its elongation properties to withstand the expected face settlements. The perimeter anchorage had to allow for sharp differential settlements of the fill and of the peripheral anchorage line. For this purpose, an extra length of geocomposite was provided along the perimeter beam, sandwiched between anti-grip sheets of 0.2 mm membrane and nonwoven geotextile. A strip of PVC geomembrane was used to form the peripheral connection along the block toe and the side beam. The connection was mechanical, made by an 8 mm thick stainless steel flat profile secured by 10 mm bolts embedded in the concrete at 0.15 m spacing.

The cost of the waterproofing system, including transition (bedding) layer, geosynthetics system, peripheral seal, and concrete cover was in the order of 160 US$/m^2. It was about half of the cost of the originally designed concrete facing. After more than 15 years of service, the dam as a whole, as well as the wateproofing system, work properly, and are in a very good condition (CARPI, 1996; Scuero & Vaschetti, 2011).

13.3.2.4 Loshana dam (Republic of Macedonia, 2002)

At the end of 2002 Loshana dam was finished, the first rockfill dam with geosynthetic lining in the Republic of Macedonia. With a height of 41 m, it forms a reservoir with a storage capacity of 1×10^6 m^3, for the water supply of the town of Delchevo. The foundation is of granite, as well as the rockfill dam body. The material was excavated from the future reservoir area. The decision to apply geosynthetic lining was imposed by the lack of suitable cohesive soil material in the dam site vicinity. Firstly, a reinforced concrete plinth in the upstream toe was constructed, with the purpose of supporting the lining and to serve as a base for grouting. A filter layer was provided below the lining (2 m thick in normal direction to the lining) and above the foundation (1 m thick), see Figures 13.24 and 13.25.

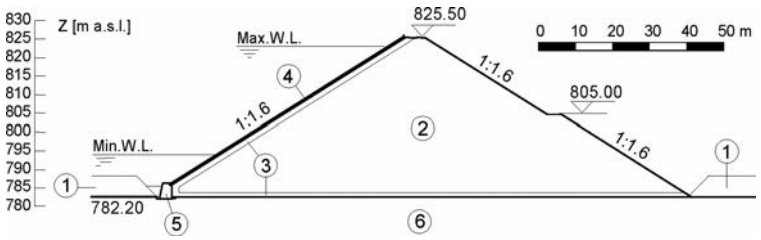

Figure 13.24 Cross-section of Loshana dam (Republic of Macedonia, $H = 41$ m). (1) River deposit; (2) rockfill; (3) filter layer; (4) geosynthetic lining; (5) concrete plinth; (6) rock foundation.

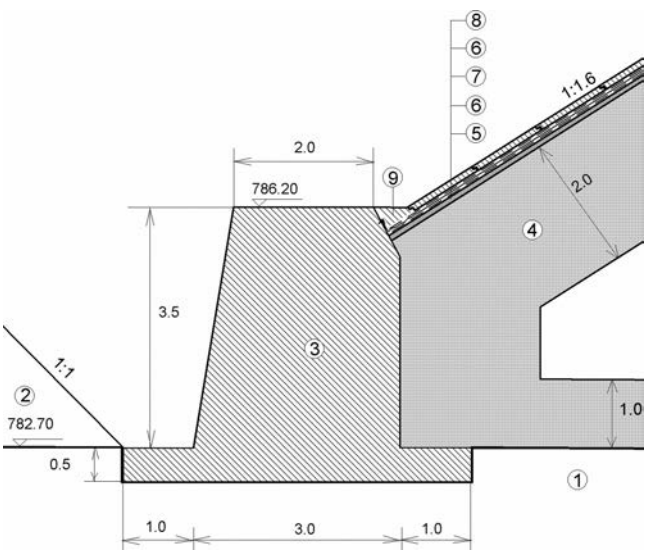

Figure 13.25 Connection of the geosynthetic lining with the reinforced concrete plinth. (1) Rock foundation; (2) river deposit: (3) reinforced concrete plinth; (4) filter layer; (5) lean concrete, d = 7 cm; (6) geotextile, 500 gr/m^2; (7) PVC geomembrane, 2.5 mm; (8) precast reinforced concrete slabs, d = 10 cm; (9) concrete plug.

The lining consists of the following elements (Fig. 13.25): 1) supporting layer of lean concrete with cement content of 65 kg/m^3, with maximum grain-size of 12 mm, 7 cm thick; 2) geotextile, 500 gr/m^2; 3) PVC geomembrane, d = 2.5 mm; 4) geotextile, 500 gr/m^2; 4)protective precast reinforced concrete slabs 1 × 1 m, d = 10 cm. The joint between the geomembrane and the concrete plinth was made with special care. Above the geomembrane along the whole length of the joint a strip of special non-oxidizing steel, 40 mm wide and 6 mm thick, was placed. The steel strip, together with the geomembrane, was fixed to the plinth by means of special screw-bolts, Ø10 mm, at a distance of 15 cm. The watertightness was improved by special putty placed between the geomembrane and the concrete below the entire length of the steel strip. The protective concrete slabs were produced in the contractor's factory of precast elements located in Delchevo, 16 km from the dam-site and were placed by means of a crane. The total covered area was ≈9000 m^2 and the effective time of construction of the lining, including placement of the precast concrete slabs, was 3 months. Geosynthetic material was produced in Belgium and Spain and the placement was done by a firm from Croatia. The dam is provided with a side-channel spillway and with a bottom outlet formed by a steel pipe Ø800 mm covered with reinforced concrete.

13.3.2.5 Exposed geomembrane: Sar Cheshmeh dam (Iran) and Runcu dam (Romania)

Although the solution of geomembrane facing covered by concrete slabs seems very safe and stable because the waterproofing element is protected and well ballasted, there are some important negative aspects to all ballasted solutions. The main negative aspects are:

- The risk of damage to the composite during the application of the ballast layer.
- The difficulty of locating eventual leaks once the reservoir is impounded.
- The complexity and length of repairs, if required.
- The ballasted layer is costly.

On the contrary, exposed facings allow easy inspections and relatively simple repairs. The objection to exposed solutions has been the faster aging rate, but improvements in polymer production and the positive records accumulating from geomembrane liners long in service, are downplaying this aspect. Exposed solutions are nowadays more and more reliable as the polymer industry can produce high resistance and slow aging composites (Sembenelli & Sembenelli, 2013). An important aspect of the application of exposed solutions is the necessity to anchor the geomembrane reliably in the dam body. The geomembrane has a customary watertight peripheral anchorage, but it must also be safely anchored against uplift by fast sudden drawdown of water level in the reservoir and waves. The concept of the application of the exposed geomembrane is to provide watertightness to the dam by a totally deformable system. The waterproofing liner and its face anchorage system are made from the same material, a geocomposite, incorporating the impervious element (a PVC geomembrane) and a multi-functional layer, geotextile, coupled to the geomembrane in the factory.

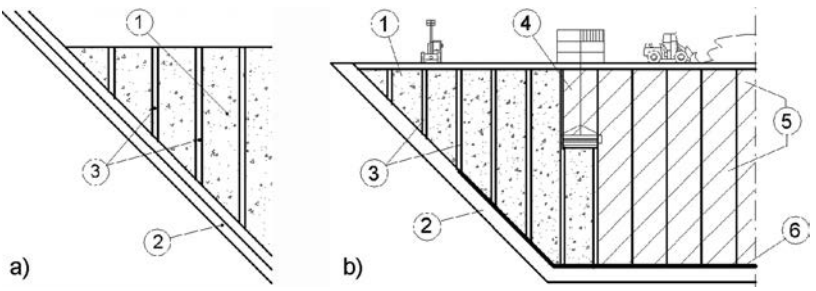

Figure 13.26 Scheme of face anchorage (a) and scheme of the placement of PVC sheets (b) (after Vaschetti & Scuero, 2009). (1) Base/anchorage layer; (2) concrete plinth; (3) PVC anchor strips; (4) PVC geocomposite sheets; (5) geocomposite sheets welded to anchor strips; (6) watertight perimeter seal.

This solution contains the following elements and layering (Vaschetti & Scuero, 2009; Scuero & Vaschetti, 2011):

- Dam body, zoning is not strictly required, a single fill material can be used.
- Filter (drainage) layer, as in other embankment dams, but of reduced thickness.
- Base/anchorage layer, a single layer forming the transition between the dam body and the watertight system, incorporating the anchorage system for the waterproofing liner, and it can also work as drainage layer.
- Waterproofing liner – PVC geocomposite.

The face anchorage system is integrated in the dam in the form of flexible PVC wings, about 50 cm wide, placed on the base layer and anchored to it by the ballasting action of the fill (Figure 13.26a). Part of the wings is left protruding from the upstream face of the dam, so as to form continuous 50 cm wide PVC anchor strips placed vertically on the dam upstream side. Spacing between anchor strips depends on service loads, the most severe one generally being that of wind (Vaschetti & Scuero, 2009).

The base layer for the waterproofing geocomposite can be gravel compacted with a vibratory plate mounted on the arm of an excavator, and stabilized with lean concrete layer, or other types of stabilization, used for CFRDs (see Chapter 12) and asphaltic concrete facings (in this chapter, section 13.1.3.1). A novel solution by use of so called extruded lean concrete curbs will be described later on in this chapter.

The PVC geocomposite sheets are deployed over the base layer (Fig. 13.26b), and anchored to the embedded PVC strips by heat welding. Adjacent PVC geocomposite sheets are joined by watertight vertical welds, creating a continuous watertight liner over the entire upstream face of the dam. At the peripheries, the geocomposite is anchored by a concrete foundation (plinth) in a similar manner as the ballasted solution. Perimeter seals are designed to be able to accommodate the differential movements and settlements typical at these locations.

Being prefabricated in the controlled environment of a factory under ISO procedures all components of the waterproofing system (PVC liner and anchor wings, components of the perimeter seal) have pre-established and constant properties that

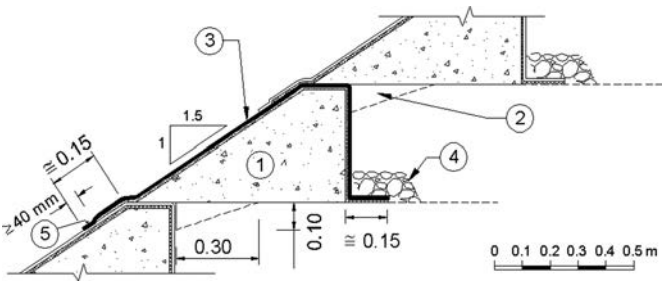

Figure 13.27 Forming the extruded curbs, details of the PVC geomembrane wings placed over the curbs at Sar Cheshmeh tailings dam (after Vaschetti & Scuero, 2009). (1) Porous concrete curb; (2) Interlock keys between curbs, 4 m long, centered between two anchor strips; (3) anchor strips w = 50 cm, PVC geocomposite Sibelon CNT 4400; (4) temporary ballast (concrete, gravel, sand, steel bar, etc.; (5) heat weld, ≥40 mm.

are verified upon arrival of materials on site and are not altered by weather conditions upon installation. Joints and perimeter seals are verified for watertightness with standard methods. Hence the characteristics and the quality of the waterproofing system are pre-established and constant throughout installation. The impervious liner and its anchorage system are capable of following the deformation of the dam and of accommodating all possible differential movements that may occur during service, because all components of the waterproofing system are fully deformable.

An alternative, novel solution for the basic layer under the geosynthetic waterproofing element, made by extruded lean concrete curbs, was applied at the 75 m high Sar Cheshmeh tailings dam in Iran (2007). The existing dam, designed and constructed in the late 1970s, has an impervious clay core. The upgrading project includes strengthening and raising of the main embankment and a saddle dam in four stages, for a total of 40 m of heightening. An upstream exposed geomembrane was adopted on the basis of it being a more stable, efficient and buildable arrangement, and preferable from a construction, performance and cost perspective (Vaschetti & Scuero, 2009).

The base layer of the raised dam consists of the extruded curbs (1, Fig. 13.27), known from the application to CFRDs (see Chapter 12, section 12.2.1, Fig. 12.6), allow the construction of a fairly regular slope in a short time, not erodible by rainwater. The slope formed in this way can be steep and has constant characteristics. The curbs are extruded along the edge of the rising fill to work as containment to the rockfill and as a smooth, pervious bedding to the composite. To avoid lateral displacements caused by the pressure of the fill and by the horizontal stresses as result of compaction while the embankment is being raised, the curbs are cast so that they interlock with each other. In tandem with the construction of the curbs, geosynthetic anchor wings have been placed, (3), Figure 13.27. Composite strips are mounted at regular intervals over each curb and welded at the overlaps to form continuous anchorage lines on the face of the dam, (5), Figure 13.27. Then, they were blocked by the next, upper curb. A distance of 12 m was maintained between strips (it depends on the weight of the liner and design wind forces).

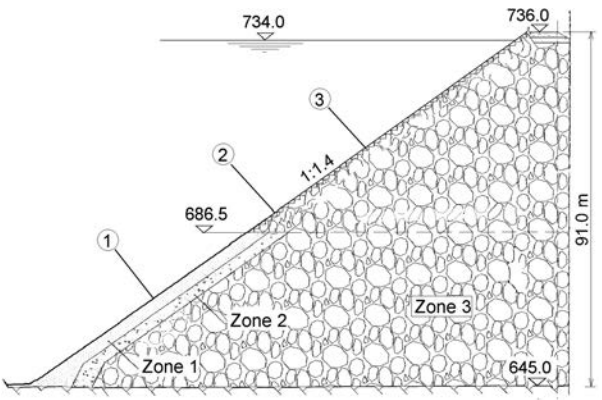

Figure 13.28 Upstream part of Runcu dam, Romania (Scuero & Vaschetti, 2011). (1) Geocomposite placed on lean concrete base layer; (2) geocomposite placed on curbs; (porose concrete curbs as a base for the waterproofing system.

The waterproofing liner and the anchor strips are made of the same material, Sibelon CNT 4400, consists of a PVC geomembrane 3 mm thick laminated during fabrication to a 500 g/m^2 geotextile. Installation of the waterproofing system was staged to follow the construction of the dam, so that the waterproofing system was completed practically concurrent with completion of civil works. The PVC geocomposite sheets, temporarily fastened at the crest, were deployed over the curbs and then fastened to two adjacent anchor strips by heat-welding. The high friction at the interface geotextile/curbs facilitated placement of the geocomposite and increased stability with respect to sliding.

Runcu dam (Romania) is a 91 m high rockfill dam under construction, planned to be completed in 2014. When completed, Runcu will be the highest embankment dam in the world with an exposed geomembrane facing as the only waterproofing element. The dam, which will be used to form a reservoir for water supply and irrigation, was originally designed as a CFRD. When construction of the dam had already started, the designer modified the design, incorporating an exposed geomembrane instead of the concrete facing. The reasons for changing the design were related to the particularly long construction time required, and to the high cost. Very costly elements were three different zones of granular material made on-site as support for the concrete slabs.

The dam body is a homogeneous rockfill (Zone 3: 600–800 mm), Figure 13.28, placed in 1.5 m thick compacted lifts with quite steep (1:1.4) upstream face. In the original design a Zone 2 (5–250 mm) layer is placed on the fill, followed by a Zone 1 (5–90 mm) layer; the plan was to cover both layers, each about 5 m thick, by a porous concrete layer before placement of the concrete slabs.

The dam is constructed in phases, a first phase up to an elevation of 681 m, a second phase up to 710 m that will allow partial operation of the dam to a water level of +700 m, and the third phase up to a crest elevation of 736 m. When the design was changed, the rockfill had already been constructed up to an elevation of 681 m, with a 20 cm thick layer of sand and gravel placed on top of Zone 1. The design of the new

waterproofing system was accommodated to the existing situation. Up to elevation 686.50 m the dam was constructed according to the original design. From elevation 686.50 m up to the crest, the Zone 1 and Zone 2 layers were eliminated and the face of the embankment was to be formed by porous concrete curbs extruded by a curb extruder, as was done also at the Sar Cheshmeh tailings dam (Iran).

The design concept for the face anchorage system of the waterproofing liner is the same for the whole dam, i.e. it is made by welding the PVC waterproofing liner to PVC anchor strips embedded in the dam, except for the already constructed lower section, where there are no curbs (from the plinth to elevation 686.50 m).

In the bottom section vertical trenches spaced about 6 m apart will be excavated in the existing surface where a 0.20 m layer of porous concrete is placed on the sand and gravel. Concrete beams, about 0.40×0.40 m, will be cast in situ, partially embedded in the porous concrete and wrapped in a PVC geocomposite. The waterproofing PVC liner will be anchored to the vertical beams by heat-welding it to the PVC geocomposite wrapping the beams. The concept is similar to that adopted at the Sar Cheshmeh dam, but instead of being embedded in the curbs the PVC strips are wrapped around the concrete beams. From an elevation of 686.50 m to the crest, the upstream face is formed by porous concrete curbs, in which PVC anchor strips will be embedded, in the same configuration as that adopted at the Sar Cheshmeh dam.

The waterproofing liner of all three sections is a PVC geocomposite, with different thickness depending on the water head: in the bottom section it is Sibelon CNT 5250, a 3.5 mm thick impervious PVC geomembrane laminated during fabrication to a 700 g/m^2 geotextile; in the middle section it is Sibelon CNT 5050, a 3.5 mm thick impervious PVC geomembrane laminated during fabrication to a 500 g/m^2 geotextile; and, in the top section it is Sibelon CNT 3750, a 2.5 mm thick impervious PVC geomembrane laminated during fabrication to a 500 g/m^2 geotextile.

The perimeter seal on the plinth will be of a mechanical type, with stainless steel batten strips fastened to the concrete with chemical anchors. Top anchorage at the crest will be mechanical by stainless steel batten strips nailed to the L-shaped conventional concrete parapet and wave wall.

Chapter 14

Rockfill dams with internal non-earth core

14.1 ROCKFILL DAMS WITH ASPHALTIC CONCRETE CORE

14.1.1 Function, conditions of work and materials

Since the development and rapid increase in the application of asphaltic concrete facings for embankment dams in the fifties of the last century, consideration has been given to the application of asphaltic concrete core inside dam's body. The idea has been to retain the basic positive features offered by asphalt concrete as a very suitable material for construction of the watertight element in embankment dams, while at the same time also avoiding the deficiencies caused by the exposed position of the facing at the upstream slope of the dam. The main advantages, which are obtained with the dislocation of the waterproof element from the upstream slope towards the interior of the dam body, are as follows:

1. Waterproof element in dam's body is not exposed to external influences, especially to significant temperature variations, to which asphalt is rather sensitive;
2. Asphaltic concrete core is jointed with the foundation in a simpler manner, the joint is less exposed to danger of damage due to differential settlement, while the foundation is of smaller length; if there is need of a grout curtain, the smaller foundation length is especially handy.

The above major advantages of the asphaltic concrete cores, along with their high degree of watertightness, high deformability, and chemical inertness, resulted in their more extensive application, especially in the last 30-35 years, following the engineering and fabrication of machinery for the simple placement and compaction of the asphalt mixture. Among more than 90 large dams of this type built so far, the highest ones are Storglomvatn (1997, Norway), $H = 128$ m, and Yele (2006, China), $H = 125$ m. Also, of particular importance are two dams in Hong Kong over 100 m high, as well as Finstertal dam (1979, Austria), 98 m high. The distribution of the large asphaltic concrete core dams (ACCD)[1] by height is shown in Figure 14.1, while the number of ACCDs constructed in different time periods was shown in Figure 12.1 (Chapter 12).

[1]The most frequently used name for this type of dam is: Asphaltic concrete core dam, with the acronym ACCD. In the literature one also encounters the term "Dam with asphaltic concrete wall", as well as "Dam with central bituminous concrete membrane".

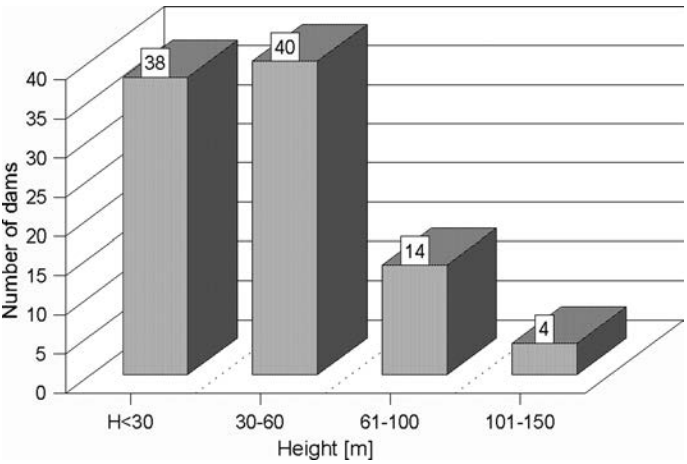

Figure 14.1 Distribution of the large asphaltic concrete core dams (ACCD) by height.

There are just a few dams of this type higher than 100 m, but there are more in the beginning stage of construction, or under design, all over world.

In most cases, asphaltic concrete cores are employed as watertight elements for dams when there is a shortage of appropriate local material. There are cases when they have turned up to be more acceptable even when there has been the presence of local earth material as a consequence of other technical and economic factors such as unfavourable climatic conditions which shorten the construction season, and a shorter period of construction, which enables earlier commissioning of the structure into operation, etc.

For the application of the asphalt asphaltic concrete cores for such high and significant structures, great contributions have been made by the knowledge obtained from observations of the behaviour of a great number of embankment dams with different watertight elements, which have been performed extensively during the last thirty years. These observations have given precious data on deformations of the embankment dams, so that now during the design process, we can have a relatively clear picture for the state in which there will be both the watertight element and the dam as a whole during operation. Also, in Germany, in the laboratory of Strabag-Bau (Cologne), there have been conducted extensive laboratory tests on the asphalt materials for the construction of asphaltic concrete cores, which have indicated that their application is feasible for dams even up to 150 m high (Moiseev et al., 1988; Obrezkov, 1993; Schober, 1988; Tančev, 1984).

The basic function of the asphaltic concrete core is to provide watertightness. Besides, it should be stable and deformable, thereby being able to take on the stresses caused by the weight of the dam, and hydrostatic pressure, as well as other influences, without damage and derangement of the basic function. Deformability, also, enables the asphaltic concrete core to adapt to the settlements and horizontal deformations of dam's body, without damage. In order to fulfill the above functions, the asphaltic

Figure 14.2 Stress conditions in the interiors of a dam's body.

concrete core should be properly dimensioned and designed, the asphalt mixture should be well composed, and placement should be appropriately done.

In the interior of dam's body, the asphaltic concrete core is subjected to vertical and horizontal stresses – σ_v and σ_h (Fig. 14.2). The state of stresses and deformations in asphaltic concrete cores depends to the greatest extent on the filled material in the dam's body. The greatest transformations of stresses in the asphaltic concrete cores occur in the case of rigid embankments. That is why it is necessary to find material for the execution of the embankment around the asphaltic concrete core with such a grain size distribution, that, following its compaction, the contraction of the asphaltic concrete would be within the limits of allowable circumferential stresses. So, for instance, it has been established that in a case of a homogeneous rockfill dam 150 m high, the relative vertical contraction (strain) of the asphaltic concrete core amounts to 7%, while for a dam of the same height filled with gravel, it amounts to only 0.8%. The horizontal stresses along the axis of asphaltic concrete core are approximately the same for both cited cases.

The asphaltic concrete core best fulfills its function if it is of a composition that will enable adaptation to the deformations of dam's body. Very rigid asphaltic concrete would be subjected to the effect of high vertical stresses as well as lateral pressure, which it could not take on without derangement of the basic function – watertightness. Very plastic asphaltic concrete would be subjected to the danger of damage and failure due to the water pressure. That is why, the selection and proper composition of the asphaltic concrete mixture, which will correspond to the particular conditions of work of the asphaltic concrete core, is also of the primary importance for the safety and the proper functioning of the structure.

In terms of the composition, properties, and quality of employed components, the grain size distribution of the mixture, as well as the physical and mechanical properties of the asphaltic concrete mixture, there is no essential difference with the asphaltic concrete cores in relation to the facings constructed outside, at the upstream slope of the dam. Some significant difference could be present in the type of bitumen used. Namely, the asphaltic concrete core is not exposed to considerable temperature variations. Depending on the area in which they are constructed and the height above sea level, they range from 4 to 20°C. That is why softer bitumen may also be used for asphaltic concrete cores, with a penetration from 80 to 200, which eases composition of the mixture, which would correspond to all specified requirements.

The asphaltic concrete core is separated from the embankment in a dam's body by means of transition zones 1–2 m thick, made of mineral aggregate with a maximum grain of 100 mm. It is recommended that the upstream transition zone would be enriched with a finer fraction, which would help in self-healing of a possibly occurring crack in the asphaltic concrete core.

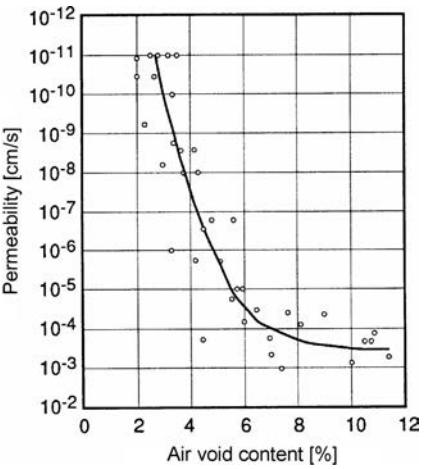

Figure 14.3 Permeability of asphaltic concrete as a function of air voids content (after Kjærnsli et al., 1966).

In designing the asphaltic concrete core, it is recommended to enter the analyses with a coefficient of permeability 10^{-9} m/s. Practice shows that this value is easily achieved and is even smaller. Figure 14.3 shows the permeability of asphaltic concrete as a function of air voids content. The permeability of 10^{-9} m/s is achieved at a void ratio of 3%, which is a widely accepted criterion for compaction of asphaltic concrete. So, for example, in the case of the Megget dam (Fig. 14.12), the seepage flow amounts to $q = 1.6$ l/s, for an area of the asphaltic concrete core $F = 20{,}000\,\text{m}^2$, in the case of Finstertal (Fig. 14.5.), $q = 2.5$ l/s ($F = 37{,}000\,\text{m}^2$), and in the case of Storvatn (Norway) $q = 10$ l/s ($F = 79{,}000\,\text{m}^2$).

The datum on the seepage water quantity for this type of dam, as well as for all dams with a watertight element made of artificial material, is very important. For its safe determination, it is indispensable to satisfactorily solve the separation of the filtrated water in the joint of the asphaltic concrete core with the banks, as well as in the foundation of the river channel, and also to perform special intake of the atmospheric water, penetrated into the downstream shell.

14.1.2 Structure of the asphaltic concrete cores

Asphaltic concrete cores can be vertical or slightly inclined towards the upstream face, usually at an inclination of 1:0.4. The advantages and disadvantages of the first and the second solutions are similar as in the case of the earth–rock dams with a vertical and an inclined earth core.

Thickness of the asphaltic concrete core depends on the height of the dam and in the upper part it ranges from 30 to 80 cm, while at the foundation it is from 40 to 120 cm. The change in thickness can be performed in a staggered manner (in 2–4 intervals) or continuously. The continuous variation of the thickness creates difficulties during execution of the works and it also makes the dam more expensive. Some investigations

indicate that a staggered variation in thickness leads to a complex stress state at the places of change; therefore, it is recommended that the asphaltic concrete core have a constant thickness along the entire height. For dams higher than 30 m, it can amount to 50–100 cm, depending on the pressure upon the core.

14.1.2.1 Application of poured asphalt

In the modern practice, the asphaltic concrete core is constructed by applying the asphalt mixture with a machine in layers of 20 to 25 cm thick and subsequent compaction. With the small number of dams, the asphalt core, instead of asphaltic concrete, is constructed of poured asphalt, by means of steel formwork, which draws out upwards along with the advancement of the embankment. One example is the Lastioulles Sud dam (Fig. 14.4), in which pieces of coarse rock (up to 35 cm) have been manually placed into the hot mixture of poured asphalt. Hard, firm basalt has been used for filling the dam. The asphalt core is buried into the bedrock, with a cut-off trench 2.5 m deep, in whose continuation there has been constructed a bituminous grout curtain. The asphalt core is sloped at an inclination of 1:0.4 towards the steep upstream slope and it encompasses 17,600 m^3 asphaltic concrete.

Poured asphalt has also been used in one of the first dams with an asphaltic core, Rotgueldensee (Austria, Fig. 14.5). In this case, a 1.2 m thick asphalt wall has been formed of a skeleton of rocks, with interspaces grouted with rich asphaltic mixture. The asphalt core has been founded in rock (gneiss), at a depth of 1.5 m. The zone of the dam of rockfill ($d_{max} = 70$ cm) has been constructed in layers of 1 m each, compacted

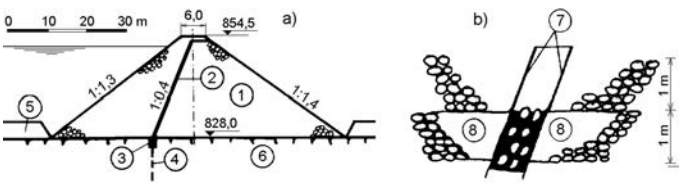

Figure 14.4 Lastioulles Sud dam (France). (1) Rockfill; (2) asphaltic core; (3) asphaltic cutoff trench; (4) bituminous grout curtain; (5) sediment; (6) bedrock (granite); (7) steel formwork drawing out upwards; (8) compacted schist.

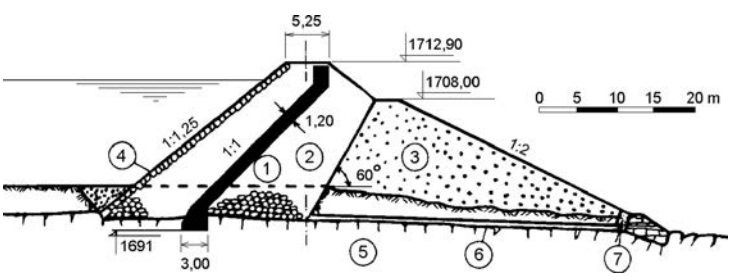

Figure 14.5 Rotgueldensee dam (Austria). (1) Asphaltic core wall; (2) rockfill, arranged in layers; (3) embankment; (4) rock blocks; (5) bedrock; (6) drainage pipe ϕ60 cm; (7) filter.

with an 8-ton vibratory roller. Sides towards the core have been constructed with stones manually arranged in layers, while the voids are greatly reduced, so that filter layers have been avoided, which would have prevented impressing of the asphaltic mixture into the rockfill. The stones that have composed the skeleton of the asphalt wall have had dimensions of 10 to 40 cm. The dam was completed in 1957, and in the course of its longtime operation has proved to be completely watertight. This method is almost abandoned today (it is applied only for small dams), since it was decided that it hides a risk of uncontrolled seepage through the core wall (Tančev, 1984; Van Asbeck, 1962).

14.1.2.2 Application of mechanically placed asphaltic concrete

The first dam with a mechanically placed asphaltic concrete core is Dhünn (Germany), constructed in 1962 (Fig. 14.6). The dam is 35.5 m high. The asphaltic concrete core is vertical, positioned centrally. Its thickness decreases from the bottom towards the crest from 0.70 to 0.60 and to 0.50 metres. For controlling the behaviour of the asphaltic concrete core and the dam as a whole, a vertical manhole has been constructed. During filling of the reservoir, there has been recorded a total vertical settlement of 115 mm and horizontal displacements of 40 mm at the crest and 75 mm in the middle of the asphaltic concrete core. After emptying of the storage lake, deformations have almost vanished, which means that they have been elastic (Schenk, 1988; Renner, 1994).

One of the most significant dams with an asphaltic concrete core is Finstertal (Fig. 14.7 and 14.8), which is one of several such dams built in the mountainous regions of Austria, with a maximum height of the asphaltic concrete core of 92 m. Dam site is located at the exit of a natural glacial lake. A relatively narrow hill, in the form of the letter S, cuts the valley, and the dam has been constructed on top of it, with the same shape as in plan (S). It has a volume of 4.4×10^6 m^3. The asphaltic concrete core constructed at an inclination of 1:0.4 has a surface of 36,000 m^2 and a volume of 24,000 m^3. The position of the dam and the asphaltic concrete core are so selected as to ensure foundation of the watertight element into the very rocky hill, while the inclination of the asphaltic concrete core facilitates a steeper inclination of the downstream slope, thus also achieving savings in the overall volume of the dam. The thickness of the diaphragm is 50 cm from the crest up to 20 m depth, 60 cm at a depth from 20 to 50 m, and 70 cm at a depth of 50 m and lower (Pircher & Schwab,

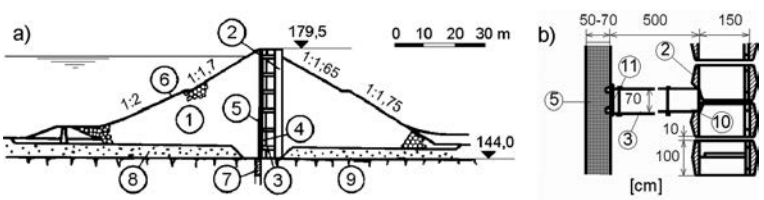

Figure 14.6 Dhünn dam (Germany). (1) Rockfill; (2) reinforced concrete inspection manhole (Swedish well); (3) pipes for instruments for observation of the asphaltic concrete core; (4) filter layer; (5) asphaltic concrete core; (6) stone lining; (7) concrete cutoff and grout curtain; (8) alluvial deposit; (9) bedrock; (10) benchmark for measuring the vertical deformations; (11) benchmark for measuring the horizontal deformations.

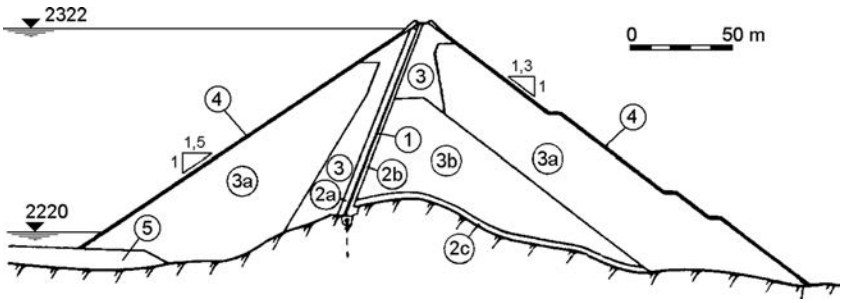

Figure 14.7 Finstertal dam (Austria) (after Pircher & Schwab, 1988). (1) Asphaltic concrete core; (2a) upstream filter layer, up to 100 mm grain size; (2b, c) Drainage layer, rock material, up to 700 mm; (3, 3a) rockfill up to 700 mm; (3b) moraine material, up to 700 mm; (4) protective lining; (5) deposited moraine material.

Figure 14.8 Finstertal dam and reservoir (Austria).

1988). The dam is very well equipped with sophisticated instruments for surveillance and measurements. Even the variations of the core thickness can be measured. The dam's behaviour after the commissioning has been excellent. As a result of the first reservoir filling in 1980, the horizontal displacement of the top of the core was 14 cm.

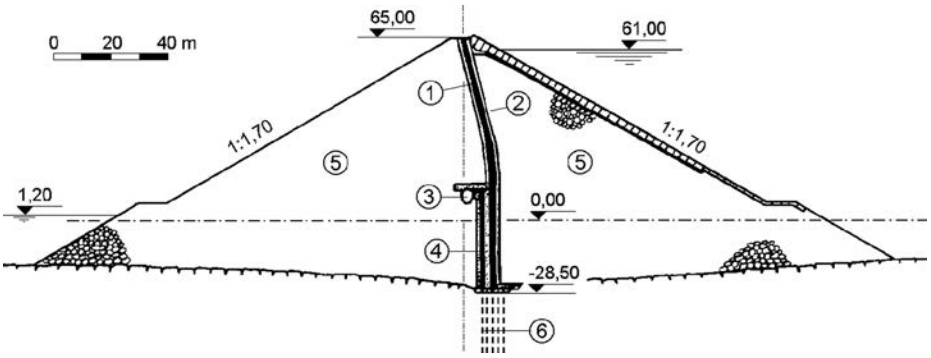

Figure 14.9 High Island (western) dam. (1) Asphaltic concrete core; (2) filter layer; (3) inspection gallery; (4) auxiliary asphaltic concrete core; (5) rockfill; (6) grout curtain.

After 30 years of service with a lot of variations of the reservoir level, only 19 cm were measured. It confirms that the values of the rockfill elasticity modulus are much higher for unloading and reloading conditions, comparing with the one for first loading conditions.

Towards the middle of the last decade two rockfill dams were completed in Hong Kong, one called eastern High Island, 110 m high, and another western High Island dam, 101 m high, provided with an asphaltic concrete core with a thickness from 0.80–1.20 m (Fig. 14.9). Placement of asphaltic concrete has been carried out in layers of 20 cm each by means of a special machine, which, during the placement, heats the previous layer. The asphaltic concrete cores have been founded on concrete slabs below sea level. In order to facilitate the control of seepage, another (smaller) secondary asphaltic concrete core has been constructed, spaced at a distance of 2.80 m from the main one, towards the sea, as well as an inspection gallery, positioned 8 m above the sea level. Both asphaltic concrete cores near the gallery are jointed by mean of an asphalt blanket. The overall structure has been so constructed that only possible filtrated water through the main asphaltic concrete core can penetrate through the drainage pipe into the gallery. These two dams, taking into consideration their height and difficult conditions of work, confirm the significant possibilities for the asphalt cores (Tančev, 1984, 1985).

14.1.2.3 Norwegian practice

Characteristic and instructive is the application of the asphaltic concrete cores in the embankment dams in Norway. At 70% of more than 170 large embankment dams, a core made of moraine material has been constructed. At places where no appropriate moraine material had been available or where it had not been located at economically justifiable distances, watertight elements of artificial materials were used. In the case of rockfill dams, the asphaltic concrete cores have usually been considered as an attractive solution, by means of which excellent results have been achieved. Namely, it has been

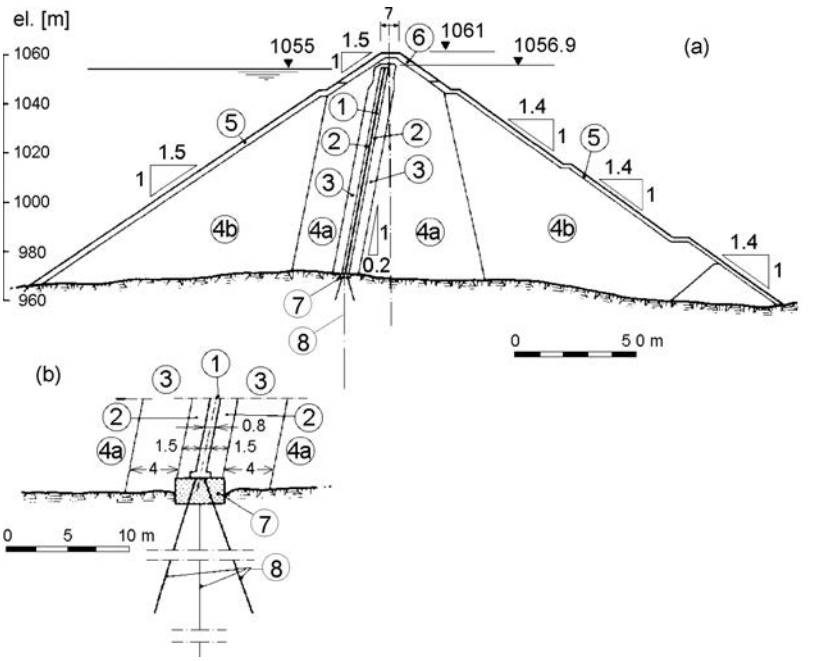

Figure 14.10 Cross-section of Storvatn dam (a) and detail of foundation of asphaltic concrete core (b) (after Arnevik et al., 1988). (1) Asphaltic concrete diaphragm; (2) transition zone (crushed rock 0–60 mm); (3) transition zone (crushed rock 0–200 mm); (4a) quarried rock 0–400 mm; (4b) quarried rock 0–800 mm; (5) slope protection (large blocks); (6) crown cap; (7) concrete sill; (8) grout curtain.

used in twelve large dams, of which Storglomvatn (1997) is the highest ($H = 128$ m) (Arnevik et al., 1988; Hoeg, 1992; World Atlas, 2012).

One of the characteristic Norwegian rockfill dams with an asphaltic concrete core is Storvatn dam, 90 m high, with a core 50–100 cm thick, at an inclination 1:0.2 (Fig. 14.10), and constructed in the period 1981–1987. As at other such Norwegian dams, here too high construction technology, rigorous control of quality and placement of materials were the norm. The asphaltic concrete (total 49,000 m^3) has been compacted at a temperature of 160–180°C and has immediately been receiving lateral support from the adjacent transition zones. The construction of the asphaltic concrete core, filter zones and the transition zones has taken place simultaneously, with equal thickness of the layers of 0.2 m (Arnevik et al., 1988).

A special construction machine (Fig. 14.11) has simultaneously constructed both the asphaltic concrete core and the adjacent materials on both sides, pouring the asphaltic concrete mixture just before the crushed rock of the transition zones. At the front side, the machine has been equipped with a powerful vacuum cleaner (1), which sucks in the dust and water of the surface of the already constructed asphaltic concrete layer. Behind the vacuum cleaner, the built-in infrared heater (2) has facilitated drying of the remaining surface moisture, and it has also heated the lower layer

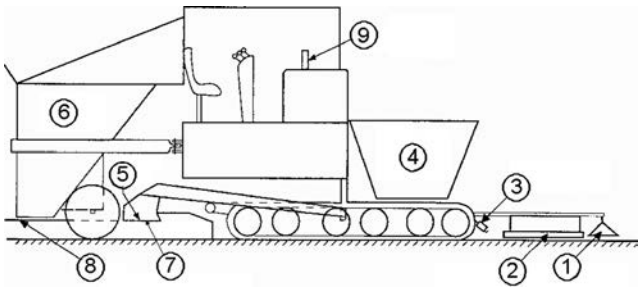

Figure 14.11 Machine for simultaneous placement of both the asphaltic concrete material and the adjacent transition layers. (1) Vacuum cleaner; (2) infrared heater; (3) TV-camera; (4) hopper for asphaltic concrete; (5) asphalt screed; (6) filter material; (7) asphalt funnel; (8) laser controlled screed; (9) TV-monitor.

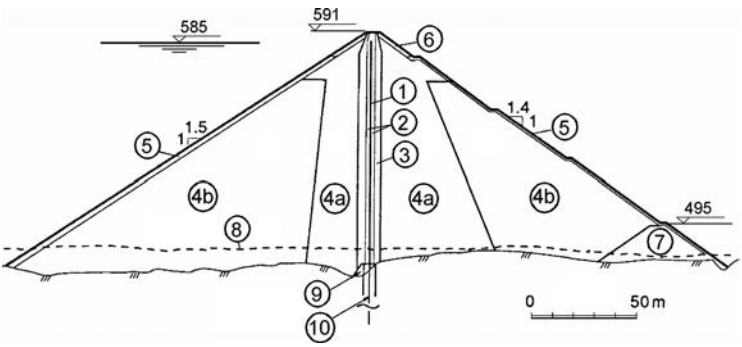

Figure 14.12 Cross-section of Storglomvatn dam, $H = 128$ m (Norway, 1997). (1) Asphaltic concrete core; (2) transition layers, crushed rock 0–60 mm; (3) coarse transition layer, crushed rock 0–200 mm; (4a) quarried rock 0–400 mm; (4b) quarried rock 0–800 mm; (5) slope protection, selected large blocks $>0.5\ m^3$, individually places by backhoe; (6) crown cap, selected large blocks $>1\ m^3$, individually places by backhoe; (7) toe drain, selected large blocks $>0.5\ m^3$, dumped in lifts up to 4 m; (8) top alluvium; (9) concrete sill; (10) grout curtain.

in order to provide a solid and homogeneous joint with the next layer. By means of the same machine, there has been performed initial compaction of the layers, while control of the evenness and horizontality of the layers has been automatic, by means of a laser device. The final compactness has been achieved by means of vibratory rollers, which have been following the machine for placing (Arnevik et al., 1988; Hoeg, 1992).

In 1997 in Norway the construction of the Storglomvatn dam finished on schedule, in four seasons, the highest ACCD in the world ($H = 128$ m), following a similar procedure as at the previously described Storvatn dam. The Storglomvatn dam is located at the latitude of the Arctic Circle where the effective construction season lasts from 1 July to the end of October. During the rest of the year the site is inaccessible due to snow (Hoeg, 1993). The Storglomvatn dam reservoir is Norway's biggest, with 3.5 billion m^3. A typical dam cross-section is shown in Figure 14.12. The alluvial overburden to bedrock, to a depth of up to 20 m, has been excavated. The core has

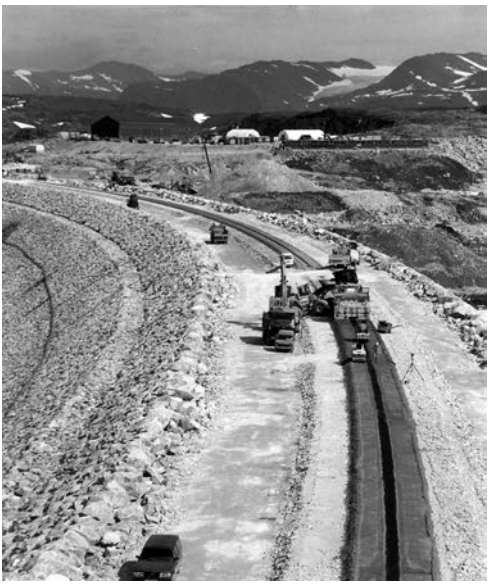

Figure 14.13 Storglomvatn dam, during construction (courtesy Mr. Helge Saxegaard).

been made of soft asphalt, rich with bitumen. Core width at the bottom is 95 cm decreasing gradually to 50 cm, which is maintained for the upper 50 meters. The dam zoning with necessary descriptions are given in the figure. Figure 14.13 shows the dam during construction. Total dam volume is 5.2 million m^3, while the asphalt core volume is 22,500 m^3.

The latest Norwegian design of the placement machine, used at most of the recently built dams, is the same as one schematically shown in Figure 14.11 with small modification. The machine is a hydraulically driven crawler paver, and the widths of the core and transition zone screeds are adjusted according to the design specifications. The level of the screeds is automatically controlled by a rotating laser (8) which ensures a horizontal base for the next layer. The precise center line is marked for each layer and fixed by a thin metal string. A video camera (3) mounted in front of the machine and a television monitor (9) inside the cab enable the operator to steer the machine with precision following the course of the string. In front, the machine is equipped with a gas-fired infrared heater (2) and a heavy duty vacuum cleaner (2) which removes dust and moisture. The heater dries and heats the surface before the next layer is placed, if required. No tack coat is applied between the asphalt concrete layers as subsequent core sampling has proved that the joint is tight and hardly detectable. Progress of the machine is adjusted in accordance with the plant and transport facilities, but is normally 1–3 m/min.

The asphalt concrete is compacted at a temperature of 150–160°C depending on the type (viscosity) of bitumen used, and is given immediate lateral support from adjacent transition zones on either side of the core. Placement of the core wall transition zones occurs simultaneously with equal layer thickness, usually limited to 20 cm

Figure 14.14 General view of the dam construction site, Mora de Rubielos dam, Spain, 2005.

(after compaction) but there are cases where the thickness is 25 cm, like at the Foz do Chapeco dam (Brazil, $H = 49$ m), commissioned in 2010. Compaction is achieved by three vibratory rollers following the placing unit. The rollers operate in a coordinated manner, side by side, to avoid lateral displacement of the hot asphalt concrete. The construction procedure, performed by modern Norwegian equipment is illustrated in Figures 14.14 to 14.17. The photos were taken during the construction of the Mora de Rubielos dam in 2005 (Spain, $H = 36$ m).

Figure 14.14 gives a general view of the dam site, with the construction equipment and different zones of materials in the dam body, and a part of the plinth on the abutment. The Mora de Rubielos dam has been built mainly from gravel, separated from the outer rockfill by filters. The dam body contains 89,000 m^3 of gravel, 70,000 m^3 of rockfill, 18,000 m^3 of filter material (crushed stone) and 1700 m^3 of asphaltic concrete. The dam was constructed between April and September 2005. Figure 14.15 shows the synchronized compaction of the transition layers of both sides of the asphaltic concrete core by two vibratory rollers of appropriate width, while Figure 14.16 depicts the next operation – compaction of the asphaltic concrete core by a small vibratory roller.

Figure 14.17 shows the framework prepared for hand-placement of the asphaltic concrete in the end of the core (near an abutment), inaccessible for the placement machine due to its large dimensions. Also one can see the widening of the core just near the abutment. A part of the concrete plinth is covered with 1 cm thick asphalt mastic, which allows for a better connection between concrete and asphalt concrete layers. Before the placement of the mastic the concrete surface must be clean and

Figure 14.15 Synchronized compaction of the transition layers of both sides of the asphaltic core.

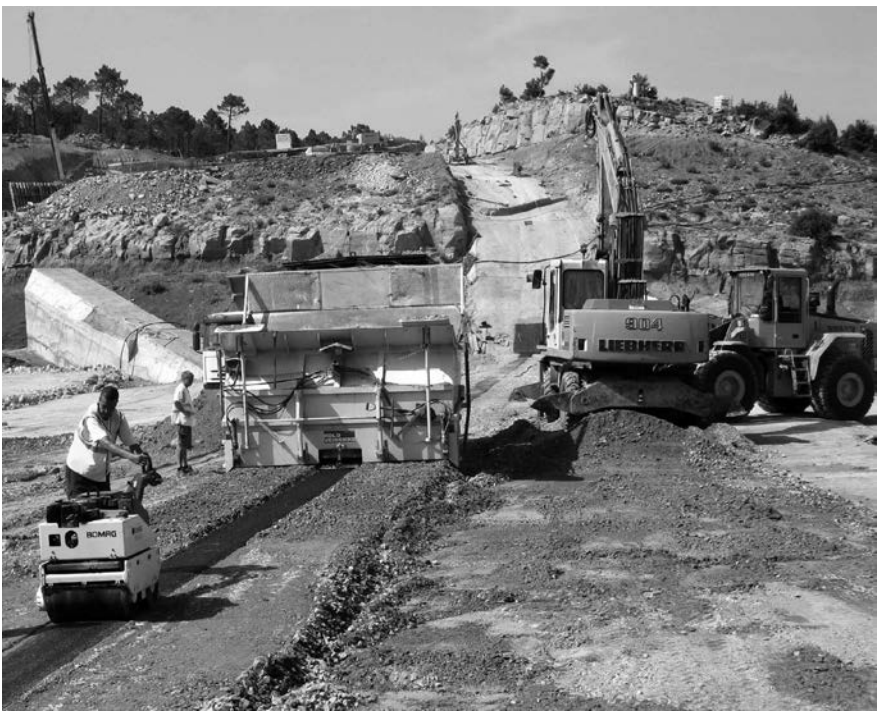

Figure 14.16 Compaction of the asphaltic concrete core by small vibratory roller.

Figure 14.17 Framework prepared for hand-placement of the asphaltic concrete in the end of the core (near an abutment), inaccessible for the placement machine.

dry and may have to be sandblasted and/or washed with hydrochloric acid to promote good adhesion (bond) between concrete and asphalt mastic. The concrete surface must be heated prior to the application of mastic to a temperature of 150°C. The mastic strip along the plinth is at least 50 cm wider than the base of the asphaltic core. If the plinth contains construction joints, then the mastic fills the space around the joints. In such a case, the waterstops in the joints must be made of material that can withstand the heat coming from the hot mastic.

14.1.2.4 Application of soft rockfill

In Austria, in 1990, Feistritzbach dam was completed which is, after Finstertal dam, the highest rockfill dam with an asphaltic concrete core in that country with very long and rich dam construction practice. The 85 m high dam has a central vertical asphaltic concrete core, slightly inclined in the upper part. The layout plan of the dam and appurtenant structures is shown in Figure 14.18, while the cross-section and the longitudinal section are shown in Figure 14.19. The purpose of the hydraulic scheme, within whose framework this dam has been constructed, is energy production. It is located in the vicinity of the border between Austria and Slovenia, which has

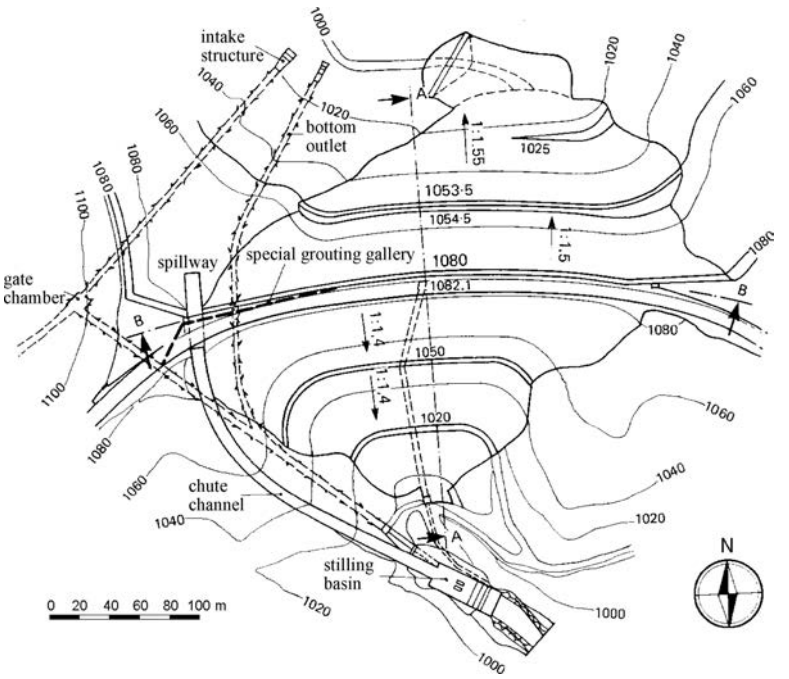

Figure 14.18 Layout plan of Feistritzbach (Austria) (Nackler & Tschernutter, 1992).

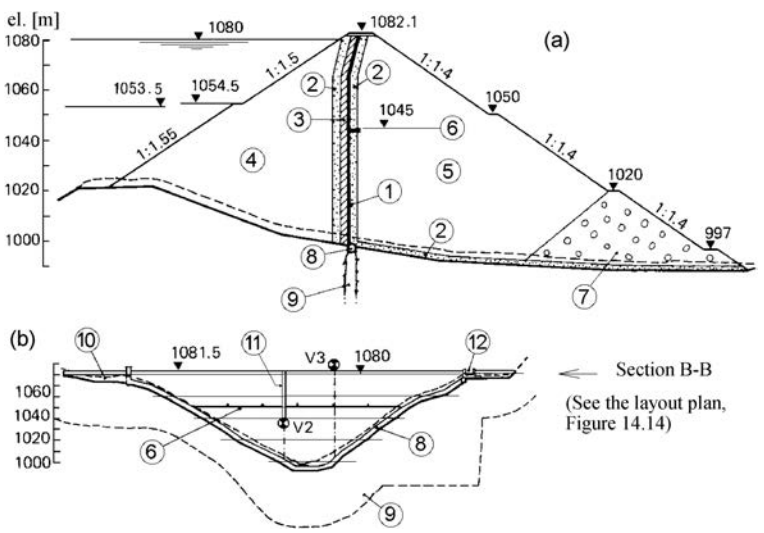

Figure 14.19 Cross-section (a) and longitudinal section (b) of the Feistritzbach dam (after Nackler & Tschernutter, 1992). (1) Asphaltic concrete core; (2) filter; (3) fine-graded zone; (4) upstream shell; (5) downstream shell; (6) horizontal seepage section; (7) drainage; (8) grouting gallery; (9) grout curtain; (10) concrete concrete wall; (11) observation manhole (Swedish well); (12) Spillway.

participated in its financing with 20%, in order to obtain appropriate quantity of electric power.

The design has anticipated the shells of the dam to be constructed of compacted rockfill. In the course of construction, individual rock lots have turned up to be weak since they have been crushed in fine parts during mining operations, tipping as well as during compaction. As a consequence, a good part of the material could have been classified as soft rock. Yet, it has been possible to separate sufficient quantity of sound and hard firm material for the filter and other zones, which are subjected to the greatest stresses. That is why, better and stronger rock, with poorly expressed tendency to crushing, has been placed in the upstream shell, while soft rock has been used for the construction of the downstream shell. Material has been placed in layers of 60 cm each, with a maximum grain size of 40 cm. Compaction has been realized with three to four passes of a vibratory roller, without the addition of water, in which there has regularly been achieved the required density of 22.5 kN/m^3 (Nackler & Tschernutter, 1992).

Soft rockfill, besides its negative features, also has one positive effect: it causes both horizontal and vertical earth pressure, representing excellent support for the membrane and for the adjacent transition zones. As a consequence, in practice, there has not been noticed expansion of the asphaltic concrete core during construction.

For the execution of the drainage prism, stone of good quality has been used, placed in layers with maximum thickness of 130 cm, the largest grain being 100 cm. Over the entire contact of the downstream shell, along the foundation there is constructed a filter layer, in order to prevent the washing out of the fine particles from the embankment across the base of the dam. This zone, 1.5 m wide, has been constructed in layers of 50 cm each, of material with a maximum grain size 60 mm. Material of the same gradation has also been used for the protection of the zone of fine material in front of the asphaltic concrete core, built-in in layers of 20 cm each, within a zone 2 m wide. Especially rigorous geotechnical criteria have been applied for the downstream filter, behind the asphaltic concrete core, which has implied limitation of the dimensions of the maximum grain, good quality of the stone, low level of foliation, limitation of the contents of fine particles (finer than 2 mm) to a maximum of 5%. This 1.5 m wide zone has been constructed in layers of 20 cm each, in only one operation, together with the asphaltic concrete core and the zone of fine material in front of the asphaltic concrete core, by applying special material. The final compaction of this very important zone has been performed by means of 1.2-ton vibratory roller, at which there has been achieved unit weight in wet conditions of 24.5 kN/m^3, along with 16% voids.

There has been an unusual construction of a zone of fine material in front of the asphaltic concrete core (3, Fig. 14.19) that had been anticipated, since in the vicinity of dam site there had been impermeable, partially coherent material. Tests have indicated that this material has got similar strength characteristics as the material in the downstream filter, so that it does not represent any problem in relation to the stability. As it has been already mentioned, it has been carried out within one integral operation with the asphaltic concrete core, in a zone 1.5 m wide, in layers of 20 cm thick.

The upstream slope is protected against the effects of waves by means of a layer of rockfill with a thickness of 1.5 m and with grains with $D_{max} = 70$ cm, while $D_{50\%} = 30$ cm and by limitation regarding the percentage of fine particles.

Asphaltic concrete core is carried out with a width of 70, 60 and 50 cm, in layers of 20 cm thickness, within one integral construction operation along with the adjacent zones, and with the application of a special pave-finisher. In the upper top 15 m, the asphaltic concrete core is inclined, in accordance with the analyses conducted by means of the Finite Element Method, which have indicated that in that manner there is an increase of the lateral earth pressure on the asphaltic concrete core, which, in that way, gets better support. The asphaltic core is widened in the contact with the concrete foundation, while the material has been manually placed. The concrete surface prior to the placement of the asphaltic concrete mixture has been carefully cleaned and coated twice with asphalt mastic. The components from which the asphaltic concrete mixture is composed, have been subjected to strict criteria and control during construction which, along with automated and well-visualized construction, has resulted in a final product – an asphaltic concrete core, which, on the basis of undistracted samples taken out at the end of construction, has been proven to be absolutely watertight.

Because some of the available rock turned out to be severely weathered and crumbled badly during processing, the embankment settled at least three to four times as much as originally calculated in the design stage. The dam settlement in the central part during construction and first impoundment of the reservoir reached a maximum of about 1.0% of the dam height. The value of total settlement increased to 1.5% of the total dam height during the first 15 years of service. Such high settlement is unusual for modern rockfill dams, but the asphaltic concrete core followed all deformations of the embankment without cracking and with unchanged watertightness.

In the investigation phase of the project realization the preliminary triaxial tests gave values of the angle of internal friction between 39° and 44°, depending on the magnitude of the normal stress and the applied σ_3 values (up to 10 N/cm^2). The large scale direct shear tests with a shear surface of 1×1 m showed a significantly lower angle of internal friction ($\sigma_1 = 20$–100 N/cm^2, $\varphi = 34°$, $c = 5$ N/cm^2). Further triaxial laboratory tests on soft and partly crumbled rock gave for low σ_3 values a substantial cohesion (between 3 and 7.3 N/cm^2), which had not been found during the test on solid rock material. The angle of internal friction of the weathered soft rock decreased to 34°–41°. Also, the crumbled soft rock had a lower modulus of deformation and it had a tendency to higher settlements.

During the whole construction period settlements and deformations were observed by several horizontal and vertical plate gauges, clinometers and extensometers. Measurements on the asphaltic core and in the transitions gave only minor lateral strains. There was practically no widening of the core during dam construction and reservoir water fluctuation. The settlements of the dam body during the construction (up to December 1990) are shown by line (1) in Figure 14.20, and those measured at the beginning of the first reservoir filling by line (2), when they reached the value of 81 cm. At that time displacements in the direction of the dam axis as well as ones transverse to the axis had not exceeded a few centimetres. Minor settlement differences were measured between the upstream and downstream shell, which can be seen in Figure 14.20 (Tschernutter, 2009).

At the end of the first reservoir impounding, line (3), the settlements in the upstream shell increased to about 95 cm, while the maximum settlement in the downstream shell increased to just 82 cm. During the 15-year service period (up to 2006),

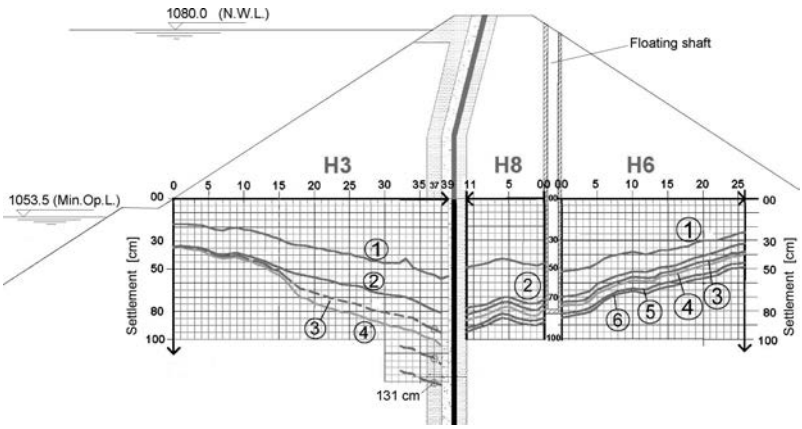

Figure 14.20 Settlement of the Feistritzbach dam after the construction, first reservoir filling and 15 years service (after Tschernutter, 2009). (1) End of construction; (2) beginning of the first reservoir impounding; (3) end of the first impounding; (4) after the first drawdown; (5) measured in 1996; (6) measured in 2006.

there was a further increase of the settlements in the downstream shell, but at a slower rate, lines (4), (5) and (6) in Figure 14.20, reaching the maximum value of about 95 cm. During the same time the upstream shell settled up to a value of 131 cm, which is a clear demonstration of the saturation effects, discussed in Chapter 8.

The settlements of the asphaltic concrete were measured by special devices, and they are fairly even with the settlements in the 13 m wide zone between the core and the floating shaft. This is an indication that the shell of the dam forces its deformation on the asphaltic core. The floating inspection shaft (Swedish well) is 40 m deep and enables the deformations of the embankment fill and the core to be measured, including the variations of asphaltic concrete core thickness. According to the measured values up to 2006, the increase of the thickness of the dam core was less than 1 cm.

Earth pressure cells for measuring both horizontal and vertical pressures were mainly installed in the downstream transition, near the asphaltic core. By determining horizontal and vertical earth pressures occurring in the vicinity of the core it is possible to obtain deformation moduli by back calculation for the downstream transition zone. The time-dependent change of the horizontal and vertical earth pressure as well as the ratio of both values just downstream of the core, show an increase of the vertical earth pressure over the entire dam height and only a slight increase of the horizontal earth pressures in the lower third of the dam height. The ratio of horizontal to vertical earth pressure increased primarily in the lower dam area and improved the support of the waterproof element.

It can be concluded that despite the much lower quality of the rockfill material built on the dam body, resulting in rather higher values of the settlements compared with the expected ones, the dam, and in particular the asphaltic concrete core, has performed well for more than 15 years of service.

14.1.3 Recent examples

In the first decade of the 21st century ACCDs have been built or are planned in almost all continents: Europe, North America, South America, Asia and Africa. China is currently building several dams of this type, including the 170 m-high Quxue dam, the highest so far.

14.1.3.1 Yele dam (China, 2006, H = 125 m)

An important example of such a dam was finished in China, in 2006 – Yele dam, located in the Sichuan province. The project includes a rockfill dam 125 m high, a diversion tunnel 7.2 km long, and an underground power house. The reservoir capacity is 298 million m^3, and the installed capacity of the power station is 240 MW, with two 120 MW Pelton turbine units. The average annual energy output is 647 kWh. The dam site is located at rather high altitude (dam crest elevation is 2654.5 m), and the winter lasts six to seven months. The average annual temperature is 7°C, and there are 215 rainy days per year on average. The construction of the project commenced at the end of 2000. In January of 2005, the reservoir started impounding. Two units began to generate power by the end of that year. In August 2006, the whole project was completed.

The dam is located on an extremely complex foundation in a region of high seismicity. There is a quartz diorite rock base under an alluvial overburden of 35–60 m on the left bank, a 55–160 m overburden on the river bed, and more than 220 m of overburden on the right bank (Fig. 14.21). The embedded depth of the relatively impervious stratum exceeds 200 m. Considering the difficult geological foundation conditions with an irregular and compressible overburden, as well as the high regional seismicity, only an embankment type dam was considered feasible.

Three alternatives were examined for the impervious barrier in a rockfill dam: (1) earth core (ECRD), (2) upstream concrete facing (CFRD), and (3) asphalt concrete core (ACCD). To choose the most suitable among these alternatives emphasis was placed on costs, severe weather conditions during construction, earthquake resistance, and compatibility with the geological conditions which might cause significant

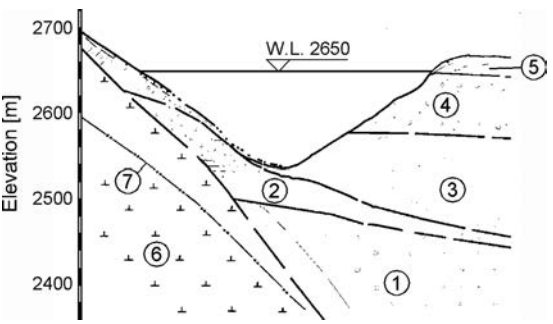

Figure 14.21 Geological cross-section of the Yele dam foundation (adapted from Wang and Höeg, 2010). (1) Gravel with thin sand layers; (2) stony, hard cohesive soils; (3) gravel layers alternated with loamy soil layers; (4) gravel; (5) loamy soil, sandy loamy soil with carbonized plant fragments; (6) quartz diorite bedrock; (7) crevice/lineament.

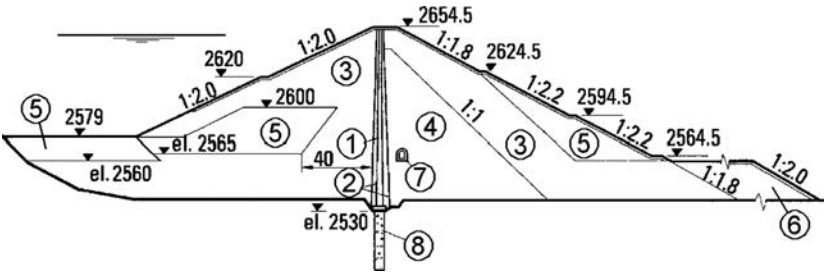

Figure 14.22 Cross-section of the Yele dam. (after Wang and Höeg, 2010). (1) Asphalt core; (2) transition zone; (3) rockfill I; (4) specially well compacted rockfill II; (5) natural gravel or rockfill III; (6) toe berm, 22 m in thickness and 215 m in length; (7) observation gallery for field instrumentation; (8) concrete cutoff wall.

differential settlements across the valley. After all aspects had been considered, the ACCD alternative was decided to be the most suitable (Wang and Höeg, 2010).

The dam is 125 high, 411 m long with a 300 m long extension over the right bank, with a total dam volume of 6.6×10^6 m^3. The asphaltic concrete core is 120 m high, and has a variable thickness of 0.6 m at the top to 1.2 m at the bottom, with a total asphalt volume of 32,000 m^3. The asphaltic core is confined by upstream and downstream transition layers. The dam body consists of the downstream main rockfill zone, and the upstream and downstream secondary rockfill zone. The typical dam cross-section is shown in Figure 14.22.

Due to the high seismicity at the site, the rockfill dam is designed with relatively gentle slopes. The upstream dam slope is 1:2 (V:H), with a 4 m-wide berm and a 150 m-wide platform at an elevation of 2579 m between the main dam and the upstream cofferdam. The downstream dam slope above 2624.50 m is 1:1.8, and below it is 1:2.2, with three 4 m-wide berms. To improve the slope stability in the event of a strong earthquake, a horizontal geo-grid was applied on the 30 m thick top part of the dam body. The downstream toe zone is covered by a 300 m-wide sand and gravel blanket.

The asphaltic core is founded on concrete plinth 3 m thick. Under the plinth there is a concrete cutoff wall of 54,100 m^2 in area, as well as a grout curtain of 48,200 m in total length. On the right abutment, the cutoff contains two parts: the upper wall and lower wall, connected by a reinforced concrete gallery. The maximum depth of the single wall is 84 m, Figure 14.23.

An extensive field monitoring program has been implemented for Yele Dam, and the recorded results are back-analyzed and compared to those of other high rockfill dams with an asphalt core. Based on the field measurements, the back-analyses, the tests on the properties of the asphalt concrete and the joint between the core and the plinth, it is concluded that the asphalt core of the Yele Dam performs very well.

The very strong Wenchuan earthquake in May 2008, with its epicentre 258 km away, caused an additional crest settlement of only 15 mm and had insignificant effects on the dam. There are no indications of any leakage through the core or at the joint between the asphalt core and the concrete plinth above the foundation cut-off wall.

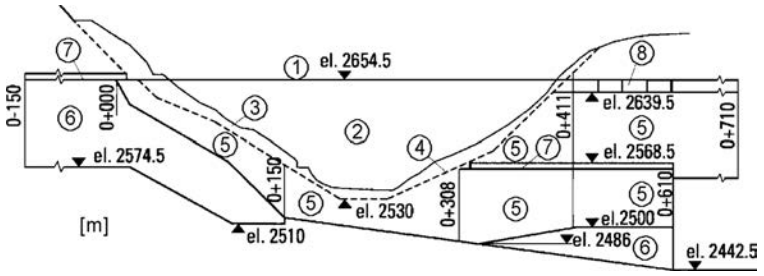

Figure 14.23 Water barriers in the Yele dam foundation (after Wang and Höeg, 2010) (1) Dam crest; (2) asphalt core; (3) ground surface; (4) excavation line; (5) concrete cutoff wall; (6) grout curtain; (7) construction gallery used for construction of grout curtain and concrete cut-off wall; (8) concrete core wall.

However, as anticipated at this geologically very difficult site, there is some leakage under the dam in spite of the extensive use of deep cut-off walls and curtain grouting. During the floods of 2006, the water level in the reservoir reached 2642.6 m, the leakage through dam body and foundation was about 140 l/s, and the bypass seepage flow on the right bank was about 120 l/s. In early 2008 the leakage amounted to about 260 l/s, and in November 2008, when the reservoir was at full supply level (el. 2650 m), the leakage increased to 277 l/s. Continuous surveillance is taking place to study and control the development of this under-seepage.

14.1.3.2 Knezhevo dam (Republic of Macedonia, 2010, H = 80 m)

In 2010 the Knezhevo dam was completed, the first rockfill dam with asphaltic concrete core in Macedonia. The dam is a key structure in the frame of the hydro-system Zletovica, located in the north-east part of the Republic of Macedonia, planned to fulfill the following purposes: water supply of the population and the industry in several municipalities, irrigation of 3000 ha of agricultural land, electricity production, and retention of the flood waters. For the initial design of the dam, made in 1996, an earth-rock dam with clay core was proposed. In 2005 the design was reviewed and one of the first findings was the very questionable availability of clay for the dam core. Namely, the borrow area was located 22 km away from dam site, at an altitude 600 m lower than the dam site, on 10 hectares of cultivated land, with high acquisition cost. The loss of such valued agricultural land could provoke serious social problems. It was therefore proposed to replace this type of dam by another type and another study was carried out for the choice of an alternative dam. Besides an earth-rock dam, three other alternatives were analysed: a concrete face rockfill dam, an asphaltic concrete rockfill dam and a roller compacted concrete dam. Finally, the asphaltic concrete core rockfill dam was chosen as the best solution from a technical, economic and environmental point of view. The layout of the hydraulic scheme is shown in Figure 14.24. Besides the dam, the scheme contains a diversion tunnel, 300 m long, rearranged in bottom outlet in the second stage, and a shaft spillway. Both cofferdams (upstream and downstream) are incorporated in the main dam body (Tanchev et al., 2009; 2011).

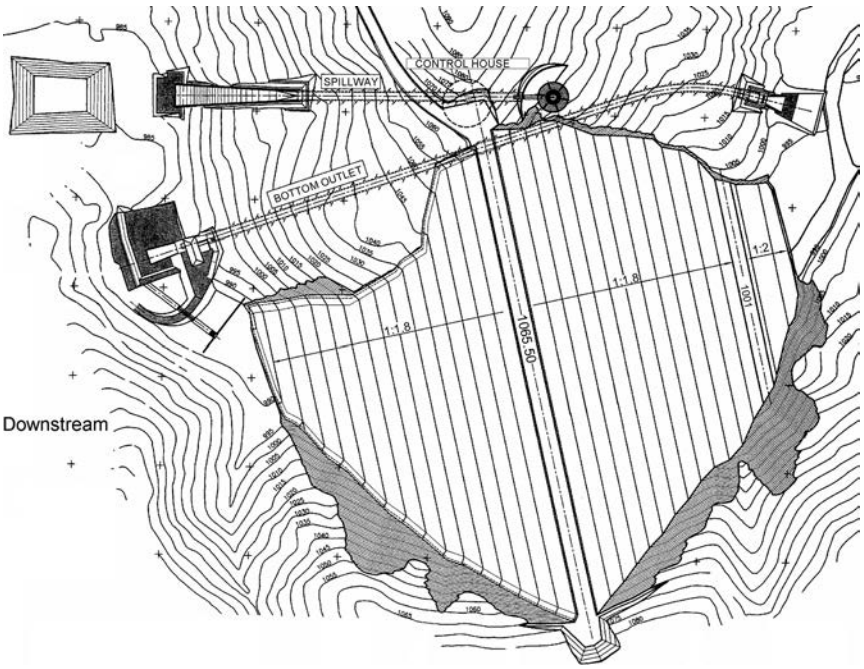

Figure 14.24 Layout of the hydraulic scheme of Knezhevo (2010, Republic of Macedonia).

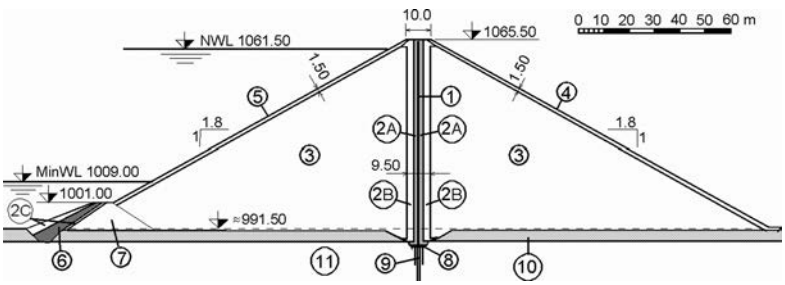

Figure 14.25 Typical cross-section of the Knezhevo dam in the river bed. (1) Asphaltic concrete core; (2A) fine transition zones, crushed andesite, 0–60 mm; (2B)coarse transition zones, crushed andesite, 0–250 mm; (2C) filter in the cofferdam; (3) rockfill – schist, stones up to 650 mm; (4) downstream protection, large blocks; (5) rip rap, andesite, blocks up to 800 mm; (6) clay core in the cofferdam; (7) rockfill in the upstream cofferdam; (8) reinforced concrete plinth; (9) grout curtain; (10) river alluvium; (11) rock foundation.

The typical dam cross-section in the river bed is shown in Figure 14.25. It was chosen using the experiences from the part of the already constructed dams of this type in the world and taking into consideration the availability and the characteristics of the local materials. In the following, the elements and the characteristics of the dam are briefly described:

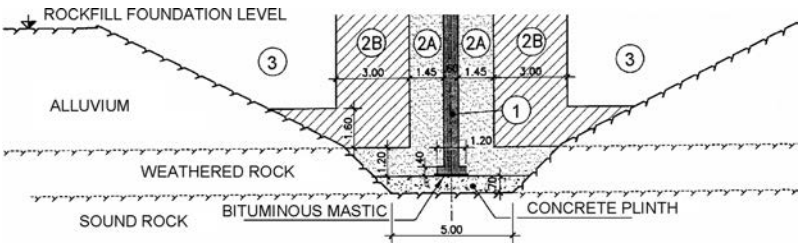

Figure 14.26 Knezhevo dam, core foundation detail in the river bed. (1) Asphaltic concrete core; (2A) fine transition zones, crushed andesite, 0–60 mm; (2B) coarse transition zones, crushed andesite, 0–250 mm; (3) rockfill – schist, stones up to 650 mm.

- The dam body is made of excavated random rockfill from the proposed borrow area for the schist, located 2 km downstream of the dam site. The rockfill was compacted in 80 cm thick layers. In accordance with the examples drawn from practice and the calculation for the static and seismic stability, an inclination ratio of the upstream and the downstream slope of 1:1.8 (V:H) was adopted to.
- The watertightness of the dam is ensured by central vertical asphaltic concrete core, with a constant width of 60 cm; upstream and downstream of the core are foreseen appropriate filter (transition) zones made of fine grained crushed andesite, each 1.45 m wide, maximum grain size 60 mm; between these filter layers and the rockfill shoulder there are transition zones of coarse crushed rock at the upstream and the downstream side, 3 m wide, maximum grain size 250 mm. For both zones 2A and 2B crushed andesite is used, from the quarry located 13 km downstream of the dam site. The thickness of the layers of both asphalt and transition material during the placement is 20 cm (compacted). A current state-of-the-art running core placing machine utilized, which allows the placing of the hot asphalt for the core together with its adjacent fine transitions, which play the role of support. The required in-situ void content of asphalt layer after the compaction should be $\leq 3\%$. In principle, two layers of asphaltic concrete ($2 \times 20 = 40$ cm) may be placed in 24 hours, but it is possible to place three, or even four layers in exceptional cases.
- As a base of the asphaltic core serves a reinforced concrete slab (plinth), located centrally under the core, founded on sound rock. The interface between concrete plinth and base of asphaltic core is covered with a 20 mm thick layer of asphalt mastic. The concrete surface must be clean and dry and may have to be sandblasted and/or washed with hydrochloric acid to promote good adhesion (bond) between concrete and mastic. To insure better connection, a widening is made of the bottom part of the core to 120 cm, Figure 14.26 and 14.27. The plinth is concreted without contraction joints and it is reinforced with a continuous mesh of steel bars (Ø 25 mm 25 cm apart, in two directions). Below elevation 1030 m.a.s.l. the width of the slab is 5 m and the thickness 70 cm, while above elevation 1030 m.a.s.l. the width is decreased to 4 m and the thickness to 50 cm.
- The bottom concrete slab also serves as a base for performing of the grouting works (consolidation grouting and carrying out of the waterproof grout curtain). For securing of the safety of the slab, it is anchored in the base.

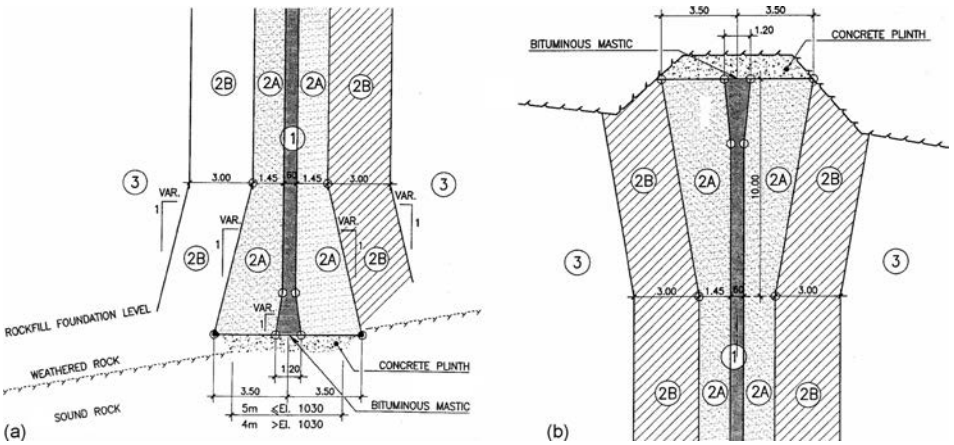

Figure 14.27 Knezhevo dam, core foundation detail in the banks; (a) vertical section; (b) horizontal section. (1) Asphaltic concrete core; (2A) fine transition zones, crushed andesite, 0–60 mm; (2B) coarse transition zones, crushed andesite, 0–250 mm; (3) rockfill – schist, stones up to 650 mm.

- The upstream slope is protected from variation of the reservoir water level and erosion from the waves with 1.5 m thick rip-rap lining, made of firm stone.
- The downstream slope is also protected from thermal effects, atmospherics, etc., with downstream protection from firm rock, also 1.5 m thick.
- The dam crest has a width of 10 m, and it is located at level 1065.5 m.a.s.l., 5 m above the normal water level that is at elevation 1061.5 m.a.s.l. The freeboard of 2 m above the maximal water level at elevation 1063.5 m.a.s.l., is taken.
- On the crest of the dam is included an 8 m wide road (with stone-cubes lining), that will enable private access to the left shore.
- The total volume of the 80 m high dam is more than 1,500,000 m^3, and the volume of asphaltic concrete core about 8500 m^3.
- The upstream cofferdam that serves for diversion of the river during the construction of the dam is integrated in the upstream end of the shell of the main dam, with crest elevation at 1001 m.a.s.l., apropos it has 11 m maximal height above the alluvial foundation. The watertightness is secured with sloping clay core, that cuts the alluvial layer and it is founded in the layer beneath it, composed of weathered rock. Filter/transition layers are located on the two sides of the clay core with upstream slope of 2.5H:1V.

The dam body construction started in September 2008 and was completed at the end of December 2009, with a break of three month during the 2008/2009 winter. The asphalt plant was located at the site. The asphalt mineral aggregate (limestone) was transported from a quarry 130 km far from the site. The bitumen content was 7% by weight and bitumen type was B80/90 (penetration 80–90). Contemporary Norwegian

Figure 14.28 Knezhevo dam, compaction of the just placed transition and asphaltic concrete layers.

Figure 14.29 Knezhevo dam, light snow is not a serious obstacle for the placement of asphaltic concrete layers as long as the air temperature is not lower than 5°C.

equipment was used for asphalt placement and compaction, as was described in subsection 14.1.2.3 (Norwegian practice). Figures 14.28, 14.29 and 14.30 illustrate the construction process of the asphaltic concrete core with adjacent transition layers.

The monitoring system of the Knezhevo dam has been classically designed with the aim of controlling the behaviour of the dam during the construction stage, impounding

Figure 14.30 Knezhevo dam, placement of the last asphaltic concrete layer.

of the reservoir and during its service period. Different instruments have been installed for measurement of displacements, pressure in the foundation, seepage discharge through the dam body and foundation, etc. A so-called DSM system (displacement system of measurement) was installed in a dam in Macedonia for the first time. This system contains devices installed in two dam cross-sections, placed at two different elevations, allowing measurement of the internal settlements of the rockfill in the dam body. The results of the settlement gained during the construction of the dam accorded well with the values calculated in the basic design. Two inclinometers were installed between the transition layers downstream of the asphalt core for registration of the internal horizontal displacements.

Also for the first time in Macedonia, an optical fibre cable was installed at the Knezhevo dam, just downstream of the waterproof element, with the aim to register any change in temperature, which is more or less constant inside the dam body. Therefore, any sudden change of the temperature means a leakage. The temperature reading allows indirect detecting of leakage through the core (see Chapter 15), but this method enables not only the detection of a leakage, but also determination of its location.

Although the Knezhevo dam was completed during the first half of 2010, it was not yet commissioned at the time of writing due to some unsolved problems in the hydro-system as a whole. Thus, the measured values cannot yet be compared with the calculated ones. Especially interesting would be to see how would the real horizontal displacements of the asphaltic core after the first reservoir filling match with the values gained by FEM. In the early 1980s the author of this book analyzed a hypothetical rockfill dam with an inclined asphaltic concrete core using two-dimensional FEM with

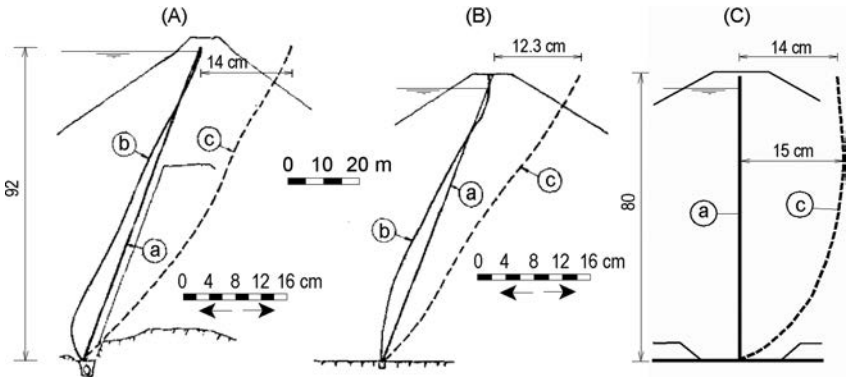

Figure 14.31 Horizontal displacements of the core after first reservoir filling at Finstertal dam (A, measured values), at a hypothetical dam 80 m high (B, calculated by 2D FEM), and at Knezhevo dam (C, calculated by 3D FEM). (a) Designed position of the core axis; (b) position of the core axis after the dam construction; (c) position of the core axis after the first reservoir filling.

hyperbolic constitutive relation. The dam material properties were similar with those of Finstertal dam. Very good agreement with measured values at Finstertal dam was gained, Figure 14.31A and B, of course, taking into account the difference in the height. Knezhevo dam was analyzed by application of three-dimensional FEM model (see Chapter 8, section 8.3.5.2), and the expected horizontal displacements of the asphaltic concrete core are shown in Figure 14.31C.

14.1.4 Joint of asphaltic concrete core with the foundation and lateral concrete structures

In the case of dams with an asphaltic concrete core, the joint of the watertight element is not as complex as it is in the case of dams with asphaltic facing (Chapter 13). Yet, it is deserving of more attention. Most often the joint between asphalt core and the impermeable layer of the foundation, is carried out with concrete structure, so that the asphaltic concrete core would obtain a homogeneous foundation. This concrete foundation can be with or without inspection gallery. In past practice both methods were represented in almost equal measure. The possibilities for permanent inspection, control of seepage in individual sections along the length of the central line, as well as the possibility for additional grouting, are the main advantages of the control, i.e. inspection gallery which, in some countries – as, for example, in Austria – make it a compulsory element.

Figure 14.32 presents typical solutions for foundation below asphaltic concrete core without a control, i.e. inspection gallery. In this, there are some particularities in the construction, which are common with the solution containing a gallery. The lower end of the asphaltic concrete core is widened, in order to lengthen the seepage path along the joint with the foundation. The surface of the foundation is covered with a layer of asphalt mastic of 2 cm, which covers the surface unevenness

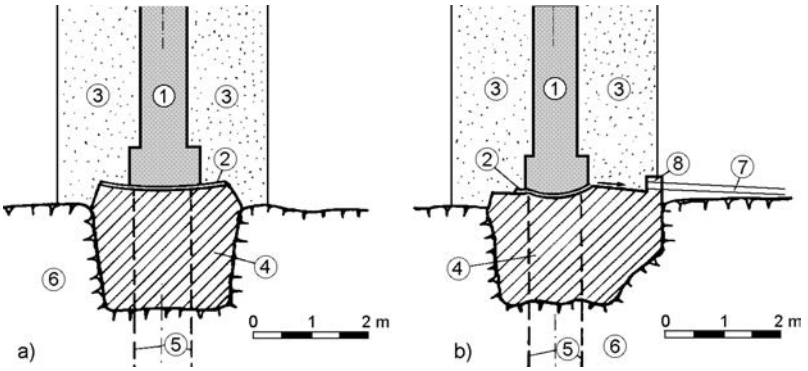

Figure 14.32 Joint of the asphaltic concrete core with concrete foundation (plinth) without a gallery. (a) Without control of seepage; (b) with control of seepage. (1) Asphaltic concrete core; (2) asphalt mastic; (3) transition zone; (4) concrete foundation; (5) grout curtain; (6) bedrock; (7) drainage pipe; (8) concrete wall.

and ensures watertightness. It also gives an opportunity for sliding of the asphaltic concrete core at possible horizontal displacements, which are small in the base of the asphaltic concrete core.

Figure 14.32a presents a solution without control of seepage, which can be employed for lower dams. However, even with the solution without a gallery, it is possible to ensure control of seepage, as for example, in the case presented in Figure 14.32b. The foundation is widened towards the downstream side, on the concrete surface there is constructed waterproofing and a small wall at the end, which directs the possibly filtrated water towards the drainage pipe, which then drains it towards the downstream toe of the dam where is measured.

In the case of the Dhünn dam that has been previously described, there has been achieved control of seepage without widening of the foundation. At the valley thalweg, a collector has been constructed, out of which water is drained towards the downstream toe of the dam (Fig. 14.33).

The conveniences offered by the control gallery bring about its frequent use, especially with the large dams. Typical example for a joint construction at vertical asphaltic concrete core with control (inspection) gallery is Megget dam in Scotland, constructed in the period 1978–1980 (Fig. 14.34). By means of low transverse walls, the gallery has been divided into a great number of sections, each being provided with a drainage pipe, so that it has been facilitated precise locating of the zone in which water has possibly penetrated (Gallacher, 1988).

Figure 14.35 presents the joint of the asphaltic concrete core with the inspection gallery (1) at Finstertal dam, which has already been considered. The upper edge of the control gallery has two recesses – the first one to accommodate the toe of the asphaltic concrete core, and a second one to collect the possibly filtrated water through the asphaltic concrete core of a certain section. This is separated from the adjacent section by means of a small concrete overflow wall (3), and through the inlet (5) to bring it into the gallery, where it is measured (Fig. 14.36). During observations of this type of dam,

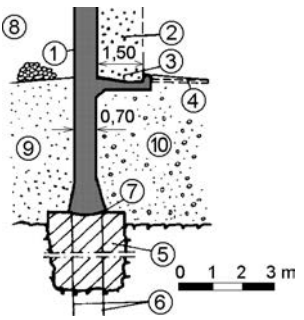

Figure 14.33 Joint of the asphaltic concrete core with the foundation of Dhünn dam. (1) Asphaltic concrete core; (2) transition zone; (3) collector; (4) drainage pipe; (5) concrete foundation (plinth); (6) grout curtain; (7) asphalt mastic; (8) rockfill; (9) compacted (dense) clay; (10) river gravel.

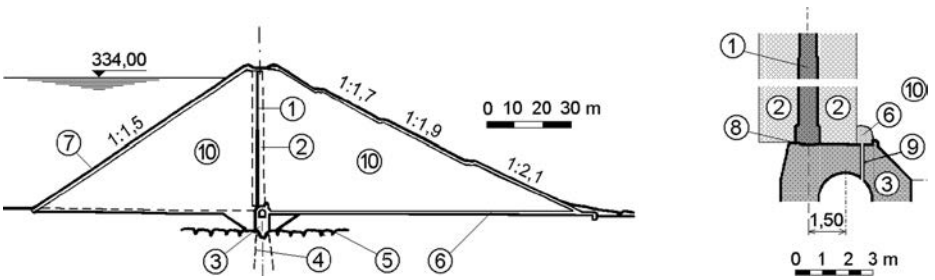

Figure 14.34 Megget dam (Scotland) with detail of the joint of the asphaltic concrete core and the foundation (after Gallacher, 1988). (1) Asphaltic concrete core; (2) transition zone; (3) inspection gallery; (4) grout curtain; (5) firm rock; (6) filter material; (7) stone lining; (8) asphaltic mastic; (9) drainage pipe; (10) gravel embankment.

the precise identification of the seepage is of utmost importance. That is why, with this dam, the atmospheric water, penetrated into the downstream part of the dam, as well as the water filtrated through the rocky foundation, are especially intercepted by means of a concrete directing wall (4) and with inlet pipe (6) and, also are measured in the control gallery.

The asphaltic core of Mora de Rubielos dam (2005, Spain), is founded on a gallery in the lower part (the upper part is founded on a plinth, see Figs. 14.14 to 14.16). The contact of the vertical asphaltic core with the gallery is similar to the solution at Megget dam (Fig. 14.37). Of course, the core is founded on the upstream gallery wall.

The two dams in Hong Kong are particularly significant and interesting. In the lower zone there has been constructed an unusual combination of a double asphaltic concrete core, founded over a concrete slab, with control of seepage in a gallery, positioned in dam's body, at a higher level than the foundation – approximately, 8 m above sea level. The foundation slab, upon which the asphaltic concrete cores have been founded, is 12 metres wide. That width has been needed for construction of six

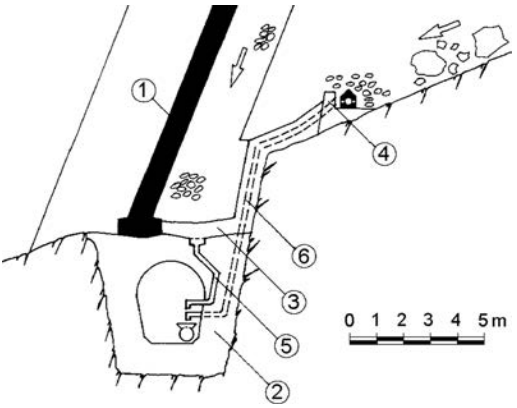

Figure 14.35 Joint of the asphaltic concrete core with the control gallery, Finstertal dam (ANCOLD, 1991). (1) Control gallery; (2) asphaltic concrete core; (3) concrete overflowing wall; (4) concrete directing wall with a drain; (5) drain pipe for water filtrated through certain section of the asphaltic concrete core; (6) outlet of infiltrated atmospheric water and water penetrated through rock foundation.

Figure 14.36 One of the seepage measuring points in the gallery of Finstertal dam (photograph taken in September 2010).

rows for the grout curtain. Maximum length of slabs amounts to 10 m, while they have been mutually interconnected by means of expansion joints, sealed with asphalt mastic.

As has already been described, dams have been founded below sea level, so that in the area of the foundation, water gets in from everywhere. The secondary (smaller) asphaltic concrete core (Fig. 14.38) is constructed at a distance of 2.80 m from the main one and is intended to prevent seepage from the downstream side and to make possible control of seepage of the upstream side. The two asphaltic concrete cores are jointed with the control gallery by means of an asphalt blanket. The joints between the blanket and the gallery are compressed. Filtrated water can enter the gallery through

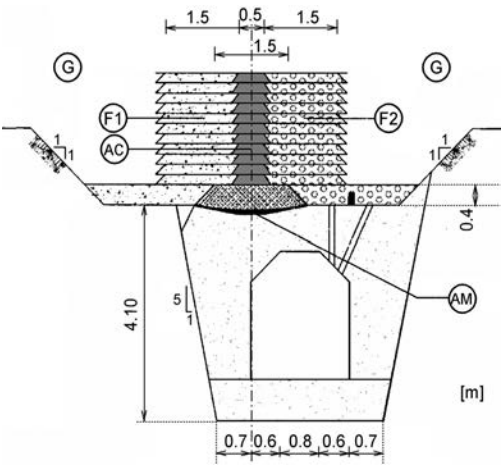

Figure 14.37 Joint of the asphaltic concrete core with the control gallery, Mora de Rubielos dam (2005, Spain). (AC) Asphalt concrete core; (F1) upstream filter layer; (F2) downstream filter layer; (G) gravel in the dam shells; (AM) asphalt mastic.

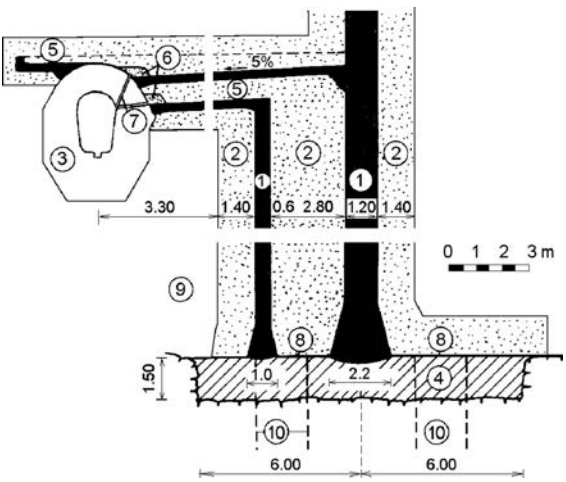

Figure 14.38 Joint of the asphaltic concrete core with the foundation, High Island dams (Hong Kong). (1) Asphaltic concrete core; (2) transition zone; (3) control gallery; (4) concrete foundation slab; (5) upper and lower asphaltic concrete blanket; (6) filter material; (7) upper and lower drainage pipe; (8) asphaltic mastic; (9) rockfill; (10) grout curtain.

drainage pipes positioned above the upper and lower blanket. By means of transverse walls spaced at 60 m, the space between the two asphaltic concrete cores below the gallery is divided into sections in order to obtain easier locating of possible defects.

Sometimes there occurs a need to carry out a joint between the asphaltic concrete core and a concrete lateral wall or some other concrete structure. Legadadi dam

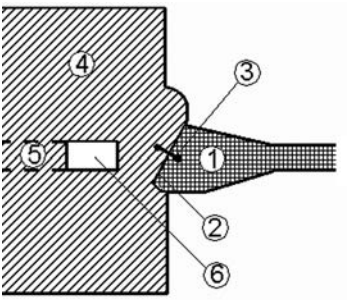

Figure 14.39 Joint of the asphaltic concrete core and the lateral wall, Legadadi dam (Ethiopia). (1) Asphaltic concrete core; (2) asphalt mastic; (3) rubber waterstop; (4) concrete buttress; (5) control gallery; (6) control manhole.

(Ethiopia) contains a constructed joint of an asphaltic concrete core with the adjacent buttress of a concrete dam, Figure 14.39. Namely, a part of the buttress concrete dam has been constructed as a rockfill dam with asphaltic concrete core, because of unfavourable geological conditions on the ground of one section. The asphaltic concrete core in the zone of the joint is thickened, while the contact with the concrete structural element is inclined and broken, aiming at increasing its length, which reduces the danger of contact seepage. The coating of asphalt mastic (2) is a customary measure at the contacts concrete-asphaltic concrete, as well as the control manhole and gallery (6 and 5 in the sketch). The joint as it is shown in the sketch, should be watertight and without waterstop (3), which has been incorporated as an additional safety measure (Tančev, 1985). The joint between the asphaltic core and roller compacted concrete part of the combined dam Foz do Chapecó (Brazil), completed in 2010, was solved in similar fashion, without a waterstop. The RCC wall at the joint was inclined at a ratio 3(V):1(H) (Saxegaard, 2012).

14.2 OTHER TYPES OF NON-EARTH CORES

14.2.1 Concrete core walls

The application, construction, and characteristics of concrete core walls have already been considered in the chapter on earthfill dams. In the case of rockfill dams, they have been relatively often used in the first three decades of the twentieth century mainly for dams of lower height. In the next 50 years, they have been abandoned because, in a great number of cases, there have come about heavy damage to the watertight element and loss of its functionality due to the impossibility for it to adapt to the significant deformations of the uncompacted rockfill, as well as owing to the transfer of stresses from the embankment into the concrete wall. These would be caused by the exceptionally different deformation characteristics of the two materials. Similar to the case of the concrete facings, the new structure and construction technology of dam's body of rockfill, placed in thinner layers and compacted by means of vibratory rollers, creates the possibility to reconsider this partly forgotten watertight element,

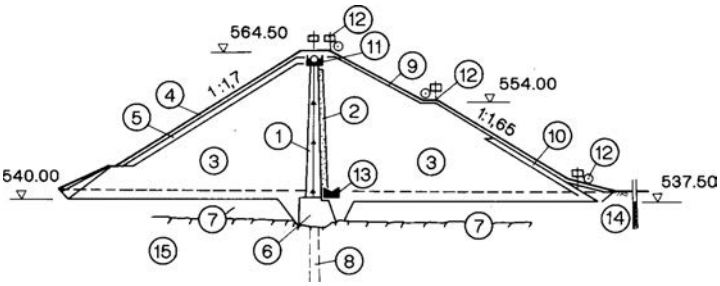

Figure 14.40 Cross-section of Falkenstein dam (Girod et al., 1994). (1) Reinforced concrete internal wall; (2) filter layer 0.8 m; (3) shells of phyllite schist; (4) coarse rockfill for the slope protection, 0.8 m; (5) transition layer, 0.6 m; (6) concrete foundation; (7) river gravel; (8) two-row grout curtain; (9) grassed protected layer, 0.2 m; (10) transition layer, 0.8 m; (11) plumb-line well; (12) measuring points for aligning and leveling; (13) measuring system for seepage waters; (14) observation for the underground water level; (15) phyllite, damaged at surface.

constructed of artificial material with broadest application in civil engineering. In spite of that, one should be extremely careful and cognizant in selecting the materials for the construction of dam's body since, even at the best construction practices, there may occur significant horizontal deformations, which could endanger the stability of concrete wall and, thereby, the dam as a whole.

In that respect, the example of the Falkenstein dam (Saxony, Germany), completed in 1974, is a rather informative one. The dam, 27 m high, is provided with a central reinforced concrete wall (Fig. 14.40). From the commencement of reservoir filling, the dam (along with the concrete wall) has been continuously shifting towards the downstream side. Displacements have increased at normal water level and they have intensified in the course of time, followed by an increased seepage through the concrete wall. Detailed investigations and analyses have immediately been performed, aimed at determining the causes for such a state and for assessment whether further deformations could bring to doubt the stability of the dam. Within the investigations, data have been used from the abundant monitoring network, while the analyses have been performed according to the Finite Element Method.

Reinforced concrete internal wall is 2 m thick at the base, constricting continuously towards the crest up to 1 m. At the downstream side there has been constructed a filter layer (2) for the drainage of seepage waters. By means of vertical joints, the concrete wall has been divided into sections, 5–10 m long. The joints are closed with copper sheets. The joint with the foundation has been constructed with a concrete block (6), divided into sections identically with the concrete wall. The block is horizontal in the riverbed, while it is benched (stepped) into the bank (Fig. 14.41). In order to enable differentiated horizontal displacements between the concrete wall and the foundation, a specially designed joint has been constructed. The concrete block, in addition to the role of a foundation for the concrete wall, also serves as bedding for the execution of the grout curtain, with a maximum depth of 20 m. At the upstream face of the concrete wall, there has been constructed a complex structure which serves for intake

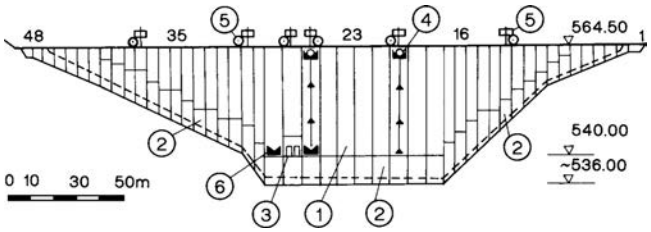

Figure 14.41 Longitudinal section of Falkenstein dam (Girod et al., 1994). (1) Reinforced concrete wall; (2) concrete block (foundation); (3) access to the complex structure for overflowing of water; (4) plumb line well; (5) measuring points for aligning and leveling; (6) drainage pipes for seepage water.

of water, as well as for evacuation of floodwaters. It is reached through the access communications (3) (Fig. 14.41). Phyllite schists have been placed in the dam shells in layers of 80 cm, each compacted with 6 passes of vibratory rollers. The behaviour of reinforced concrete internal wall, as well as that of the dam as a whole, has been monitored through an advanced system of monitoring. The horizontal displacements measured following the first filling of the reservoir and after 19 years of operation (1993) have been relatively significant and they were of a continuing character, which causes justifiable suspicion that could be open to doubts concerning the stability of the concrete wall and that of the dam, as a whole.

Additional laboratory tests of the phyllite schist incorporated into the shells of the dam, with oedometer and triaxial tests, conducted in 1990, have indicated that they have unfavourable deformation characteristics, when it is a question of this type of construction. With the newly obtained parameters, there has been performed an analysis by means of the Finite Element Method, applying jointing elements in the contacts between concrete and adjacent materials. The model for static analysis has reproduced the former history of the stress-deformations state by extrapolation also regarding a future period. Finally, the complex analyses have shown that the present and future (expected or anticipated) deformations do not call into question the stability of the dam, but only reduce it up to a certain degree (Girod et al., 1994).

Later on, interest was aroused by the news, introduced in Austria at the beginning of the 1990s, that the first rockfill dam with concrete wall had been constructed there. According to the latest construction technology, which anticipates additional sliding, bituminous layers lower friction that occurs between the concrete wall and the adjacent layers – transition layer and the drainage layer, respectively. This technology was applied in 1981–1982, during the construction of the Bockhartsee dam in Austria (Schober, 1991; ANCOLD, 1991), but it has not found further application.

14.2.2 Grout and plastic concrete walls (cores)

Of the other types of internal cores made of artificial materials, owing to the favourable properties in certain conditions, the *plastic* and *grout* concrete walls (cores) could be prospective.

The advantage of an internal core made of plastic mass, in relation to the appropriate construction in the form of facing, described in Chapters 10 and 13, is that it is not subjected to external influences, to which the delicate construction is sensitive, so it is usually necessary to provide specific protective construction.

The grout core walls have a significant advantage in the fact that they are constructed once dam's body has already been completed, and in case of need of a repair, it is possible to perform additional grouting, without emptying the reservoir. Yet, this construction is justified only in certain specific conditions and cases.

An interesting example is *Atbashinskaya* dam built in 1972 at the river Atbashi in the Kyrgyz Republic (formerly USSR), 79 m high, where a combined core wall has been constructed – one plastic and one grout (Fig. 14.42). Polyethylene strip, with a thickness of 0.6 mm, is placed in the upper 44 m of the dam, while in the lower part, in which there exist considerable pressures that the polyethylene strip cannot sustain, a grout core wall has been executed. The joint between them has been realized through a concrete grouting gallery, from which there have been constructed the grout curtain in the foundation, as well as grout core wall. The contact of the plastic core wall with steep banks of the canyon has been constructed by means of concrete equalizing and aligning slabs, anchored into the rock (Grishin et al., 1979; Rozanov, 1983).

From both sides (upstream and downstream) geotextile has been attached to the core wall, also with a thickness of 0.6 mm. The construction of the plastic core wall is between two layers of sand, with a maximum particle size of 5 mm.

The grout concrete wall, 22 m deep and 20 m wide, has been constructed of seven rows of boreholes, spaced 3.5 m apart, with distance between boreholes in a row of 1 m. Cement – bentonite solution has been used for grouting (cement 350–475 kg, bentonite 59–82 kg, and water 826–853 1 per 1 m^3 solution), injected under pressure of 0.5 to 3 MPa. Besides, in the centre of the concrete wall there have been constructed two additional boreholes, through which aluminium-silicate solution has been injected. Calculations have shown that by such unusual construction of the watertight element, by means of which the originally anticipated loam facing has been replaced, the cost of the dam has been significantly reduced.

Recently an internal geomembrane was installed as impervious core at the Gibe III cofferdam in Ethiopia, in the context of a hydraulic scheme with one of the largest hydropower plants in Africa. The project includes a 240 m high RCC dam and an upstream 50 m high rockfill cofferdam of around 500,000 m^3, made of river gravel, basalt and trachyte. The construction of the cofferdam had to be completed during the short, six-month period of the dry season, when the average river flow is 200 m^3/s. Of decisive importance in selecting a central geomembrane core were the following factors: short construction period, simplicity, lack of clay suitable for an impervious earth core and safety (Scuero and Vaschetti, 2011).

The impervious core, placed in a zigzag procedure during construction of the cofferdam embankment, consists of a flexible PVC geomembrane, sandwiched between two anti-puncture layers consisting of a high tenacity needle-punched geotextile. The geotextile is produced from 100% virgin polypropylene fibres, with a mass of 1200 g/m^2. Its function is to protect the geomembrane against possible damage during the placement of the upstream and downstream cofferdam fills. Two 50 cm thick sandy filter layers, with maximum grain size of 50 mm, were placed respectively at the

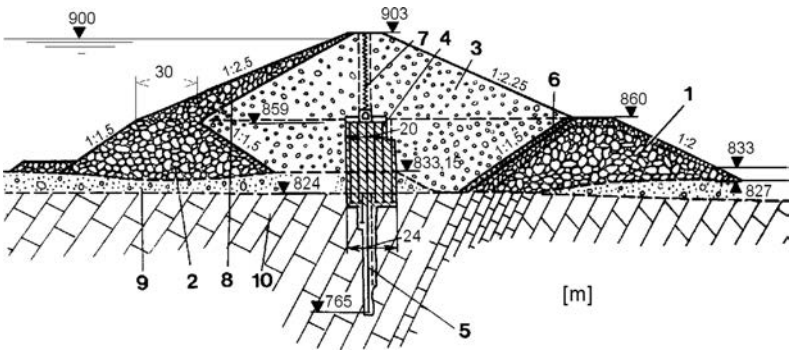

Figure 14.42 *Atbashinskaya* dam (Kyrgyz Republic) (after Grishin et al., 1979). (1) Rockfill; (2) rockfill into water; (3) gravel embankment; (4) grout concrete wall in the dam; (5) grout curtain in the foundation; (6) transition zone; (7) polyethylene concrete wall in sand; (8) rockfill; (9) alluvial deposit; (10) marbled limestone.

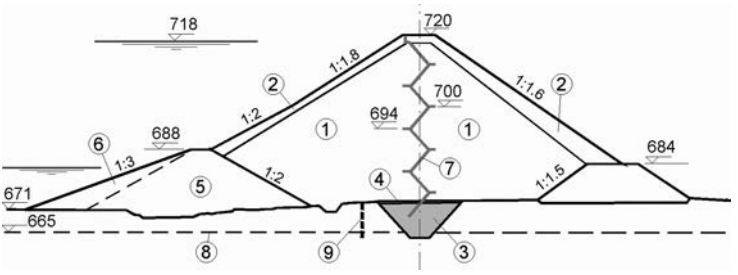

Figure 14.43 Typical cross-section of Gibe III upstream cofferdam (after Scuero and Vaschetti, 2011). (1) Basalt and trachyte; (2) selected rockfill; (3) clay cut-off; (4) filter layer; (5) pre-cofferdam made of gravel; (6) sandy clay; (7) internal zigzag waterproof element of geosynthetic; (8) bed rock below the river deposit; (9) relief wells.

upstream and downstream side to separate the waterproof element from the coarse embankment material.

The construction of the cofferdam was preceded by the construction of an approximately 20 m high pre-cofferdam, incorporated into the final cofferdam, to divert the Omo River into the diversion tunnels and to dry out the cofferdam foundation. In this way the cofferdam cut-off could be realized in clay (on which the geomembrane is encased), which waterproofs the riverbed alluvium and the shoulders colluvium.

The geomembrane was installed from the bottom cut-off up to the crest, in a zigzag pattern, so as to follow the step by step the construction of the embankment (Figs. 14.43 and 14.44). The waterproofing system thus creates a continuous impervious barrier running all along the longitudinal axis of the dam, from the bottom cut-off up to the crest. The first section of the cofferdam body is downstream directed and has a height of 6 m. The next sections follow one upstream and one downstream directed and have a constant height of 12 m.

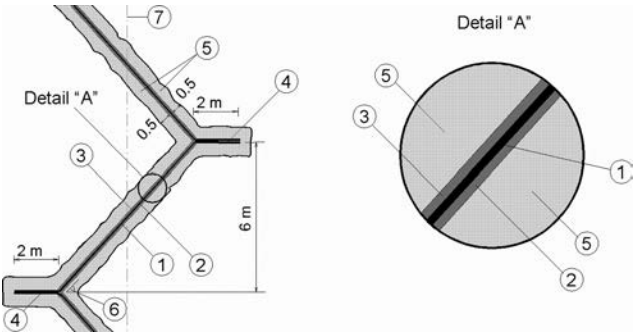

Figure 14.44 Detail of the impervious core of Gibe III upstream cofferdam (after Scuero and Vaschetti, 2011). (1) Geomembrane, 3.5 mm thick; (2) non-woven geotextile, lower layer, 1200 g/m^2; (3) non-woven geotextile, upper layer, 1200 g/m^2; (4) geomembrane, overlapping welded junction; (5) sandy filter layers, 0.50 m thick, $d_{max} = 50$ mm; (6) natural slope angle, $\approx 45°$; (7) cofferdam axis.

The impervious element of the core was a flexible impervious 3.5 mm thick PVC geomembrane, resistant to deterioration under the alkali environment of damp concrete, and to degradation from organic and bacterial growth. The zigzag path of the waterproofing system was selected to provide sufficient material which can easily absorb any future deformation of the dam body caused by possible settlements. Furthermore the properties of the PVC geomembrane material, the anti-puncture properties of the geotextiles and the size of the aggregates composing the filter layers in contact with the waterproofing system should avoid any puncture or damage of the geomembrane.

The bottom anchorage was made by embedding the geomembrane in the 6 to 8 m deep clay cut-off and by backfilling with the same impervious earth material. At the two abutments, due to the difficulty of excavating the cut-off with the same depth due to the presence of surfacing rocks in the river bed, the geometry was slightly modified during construction, adapting the thickness of the clay layer below and above the geomembrane. The top anchorage of the geomembrane was made with steel anchor and plates fixed to the reinforced concrete crest wall.

When the 5 m of the temporary crest of the first section of the cofferdam body had been finished where the waterproofing system was to be installed, the surface was inspected, and deviations were corrected. The first anti-puncture geotextile was placed on the sandy filter layer. The geotextile was supplied in rolls 5.9 m wide and 42 m long, which were cut in sheets of sufficient length to cover the entire inclined slope and extend 2 m on the flat temporary crest. The geotextile sheets were placed vertically from the top to the bottom of the slope, with an overlap between adjacent sheets to allow joining by manual thermo-fusion seaming. At the toe of the first slope, the geotextile was placed in the cut-off. When the placement of anti-puncture geotextile was well advanced, the geomembrane, supplied in rolls 2.10 m wide and 12.5 m long, so that each roll could easily cover the entire inclined slope and extend 2 m on the flat temporary crest and 2 m more at the bottom of the slope, was placed on top of it. After

the placement geomembrane sheets were temporarily ballasted on the temporary crest with sand bags, and then completely unrolled down the slope. Adjoining sheets were joined by thermo-fusion seaming at the overlap. The seams, continuous for the entire length of the sheets, were executed by an automatic machine performing a double track seam, 100% tested with air in pressure.

In the areas where the geomembrane had been installed, welded and checked, a final joint inspection was carried out to verify that no defects were present before placement of the next section of the fill. Due to the fact that the cofferdam body was constructed by horizontal lifts of fill material, the placement of the protective geotextile on top of the PVC geomembrane had to be done with sheets placed horizontally from the bottom toward crest, following the placement of the lifts. The protective geotextile stops at top of the slope. The geomembrane placed on the temporary flat crest section 2 m wide was protected with stronger material to avoid major potential damages during the construction of upper part of the new section. After placing the second anti-puncture geotextile on top of the geomembrane, construction of the second section of the fill started, directed at the opposite side. The construction of the dam body proceeded by alternate sections, both upstream and downstream directed. The crest of each section is thus also the bottom of the section above it, and in this flat area the geomembrane lining the lower section is impermeably connected to the geomembrane lining the section above it. In the flat area at the crest of each section of the fill, the geomembrane lining the upper section overlaps the geomembrane lining of the section below it, over a width of about 2 m. Corresponding to this 2 m wide overlap area, the connection of the two sheets of geomembrane is made by means of a double track seam executed with automatic machine and tested as already described. The execution of this horizontal longitudinal connection seam, parallel to the axis of the dam, is made at the same time as the installation of the geomembrane sheets over the inclined slope of the upper section. Before the execution of this seam the protection placed to avoid damages on the geomembrane was removed, the area was cleaned, the integrity of the geomembrane was checked and, if needed, damages were repaired. The procedures described were repeated for each step of the construction of the dam body sections from the bottom of the cofferdam (elevation 670 m) up to the crest (elevation 720 m), where the upper edge of the geomembrane was mechanically fastened to the reinforced concrete crest wall (Scuero and Vaschetti, 2011).

14.3 STABILITY OF EARTH–ROCK DAMS WITH ASPHALTIC CONCRETE CORE

Regarding the conditions in which the static stability of earth–rock dams with concrete walls is accomplished, it is apparent that they are less favourable in comparison with dams with facing, because here the upstream shell is immersed in water. However, taking into consideration the materials of which rockfill dams are constructed as well as the fact that there is no pore pressure in any zone of the dam, it is clear that the static conditions of work of rockfill dams with concrete wall are more favourable in relation to the appropriate conditions existing in earth–rock dams. The author has performed detailed analyses of rockfill dams with asphaltic concrete watertight elements. For the applied methods and for the most important obtained results, there has already been

discussion in short in Chapter 8. For more detailed acquaintance with these problems, the reader is referred to the textbook references (Kokalanov & Tančev, 1988; Tančev, 1984, 1985, 1989; Tančev & Kokalanov, 1988, 1995; Le Coroller et al., 1988).

There is a question that is almost regularly asked when making comparison between the earth-rock dams and rockfill dams: what is the stability of the thin watertight element in case of an earthquake, and how significant is the hazard of its cracking during a strong earthquake? For clarification of this question, significant are the analyses performed for Storvatn dam (Norway) with asphaltic concrete wall, the construction of which has been described in this chapter (see Fig. 14.10). The dam has been built in a region where an earthquake of moderate intensity is possible, while the analyses have been performed for a *design* earthquake with a return period of 200 years and a *maximum* earthquake with a return period of 10,000 years (see Chapter 9).

Valstad et al. (1991) have, first of all, checked the stability of slopes by means of a simple pseudo-static method assuming that the slopes are infinite. That method is based on consideration of a shallow mass of the embankment in the direction parallel to the slope. The safety coefficient against sliding of that mass, *F*, is expressed in explicit form, particularly for the *upstream slope*:

$$F = \frac{(\gamma' - \gamma_s k_c \tan\beta)\tan\varphi'}{\gamma' \tan\beta + \gamma_s k_c} \tag{14.1}$$

and also for the downstream slope:

$$F = \frac{(1 - k_c \tan\beta)\tan\varphi'}{\tan\beta + k_c} \tag{14.2}$$

where, γ' and γ_s are unit weight of the filling material in submerged, i.e. saturated condition; β is the angle between the slope and the horizon; φ is the angle of internal friction of the filling material, and k_c is the coefficient of seismicity.

The above-quoted method is recommended by Seed for cases when the material in a dam's body is well-drained even when it is not subjected to significant reduction of the strength against shearing at cyclic loading (not larger than 15%). Precisely such is the case with the filling material in dam's body of Storvatn dam. With that pseudo-static analysis, it is required a coefficient of safety larger than 1.15, while for the anticipated mean intensity of the earthquake it is assumed $k_c = 0.1$, while $k_c = 0.15$ for high seismicity. Analyses have shown that the slopes of the selected inclination have sufficient safety for moderate seismicity, such as there exists in the region of the dam. At high seismicity, the inclination of the upstream slope should be modified from 1:1.5 to 1:1.85, while for the downstream slope, from 1:1.4 to 1:1.5.

The quoted dam has also been analysed with Newmark's dynamic method, modified by Makdisi and Seed (1978). The applied dynamic properties of the materials are illustrated in Table 14.1.

For rockfill into dam's body, dynamic shearing modulus *G* is taken, depending on effective shearing deformations, according to the curve shown in Figure 14.45, with participation also of an initial modulus G_0, dependent on the average effective normal stress. The earthquake Taft from 1952 has been selected as a characteristic one, with a

Table 14.1 Dynamic properties of materials in the body of Storvatn dam.

Zone (Fig. 14.10)	State	γ [kN/m^3]	Dynamic modulus, G [MPa]	Remarks
1	(asphalt)	24.50	$G_{dyn} = 4500$	constant modulus
2	wet	21.50	$G_o = 97.4\ p_a\ (\sigma'_m/p_a)^{1/2}$	modulus dependent on
	saturated	23.60	where:	deformations (Fig. 14.45)
3	wet	21.50	σ'_m = average effective stress	
	saturated	23.65	p_a = atmospheric pressure	
4	wet	20.50		
	saturated	22.50		
5	wet	20.50		
	saturated	22.50		

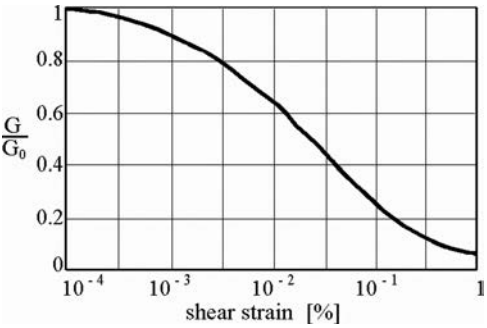

Figure 14.45 Dependence of the dynamic shearing modulus on deformations (after Valstad et al., 1991).

magnitude of 7.6. The horizontal component of the accelerogram has been scaled for the maximum acceleration of 0.5 g, with a vertical component of 0.32 g.

There have been performed a number of analyses – with influence of a horizontal component of acceleration and with a joint influence of both the horizontal and the vertical component. For illustration, Figure 14.46 presents contour lines of the maximum horizontal acceleration for the first case. The drawing shows a noticeable concentration of the maximum horizontal accelerations in the upper zone of the dam.

According to well-known methodology (see Chapter 9), there have been calculated the permanent deformations of the potential sliding blocks (Fig. 14.47). Analyses have shown that, from the aspect of stability and deformations, the upstream side is more critical, especially its upper part. The biggest permanent displacement (for the assumed magnitude of 7.6) has been calculated for a block cutting the concrete wall at the elevation of the maximum water level and it has amounted 1.3 m that is more than the thickness of concrete wall, which varies from 0.5 m at the crest up to 0.8 m at the base. In accordance with the procedure of Makdisi and Seed, there have been evaluated the permanent displacements also for a magnitude of 8.25 (for the same maximum acceleration of 0.5 g). In this case, the values of the permanent deformations have reached 3.0 m – considerably more than the thickness of the concrete wall.

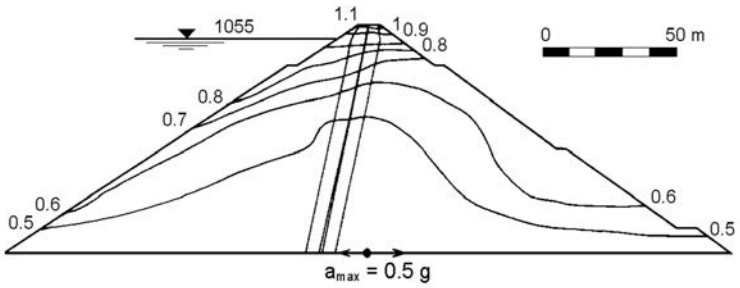

Figure 14.46 Maximum horizontal acceleration for the horizontal input component, Storvatn dam (after Valstad et al., 1991).

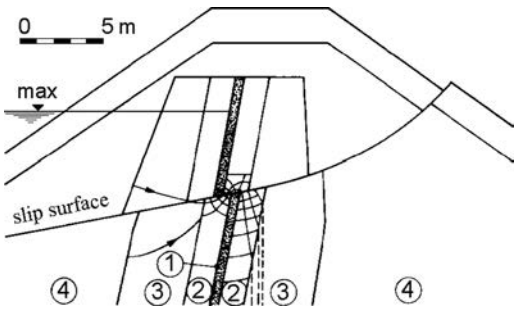

Figure 14.47 Permanent displacement of block with breaking of the concrete wall, forming of opening, and hydrodynamic flow net around opening (Valstad et al., 1991). (1) Asphaltic concrete; (2) crushed stone (0–40 mm); (3) well-graded rockfill embankment (0–200 mm); (4) rockfill.

It is clear from the presentation that, for the assessment of the value of acceptable permanent deformations, of fundamental importance is their influence on the asphaltic concrete waterproof core. Namely, if the value of the permanent deformation is smaller than the thickness of concrete wall, then the parts of the concrete wall above and below the place of sliding, will still remain in contact. Taking into consideration that significant deformations occur in the uppermost zone of the dam, where water pressure is low and, in such a case, the concrete wall performs its function, in spite of the weakened section. Another case occurs when deformation will exceed thickness of concrete wall that is to say, when it will split and it will create an opening between its two parts through which water will penetrate. Now, for an appraisal of future behaviour of the dam, the quantity of penetrated water is important, and that depends on the width of opening, its depth below the water level and on the permeability of the zone, immediately adjacent to the concrete wall. That material, in this specific case, has had $k = 10^{-5}$ m/s. The quantity of penetrated water has been calculated by means of a flow net (Fig. 14.47), and for various depths of opening and different width it is presented in Figure 14.48.

The maximum deformation of 3 m has been calculated for the maximum water level, which means that, through the opening caused by it, there would not come about

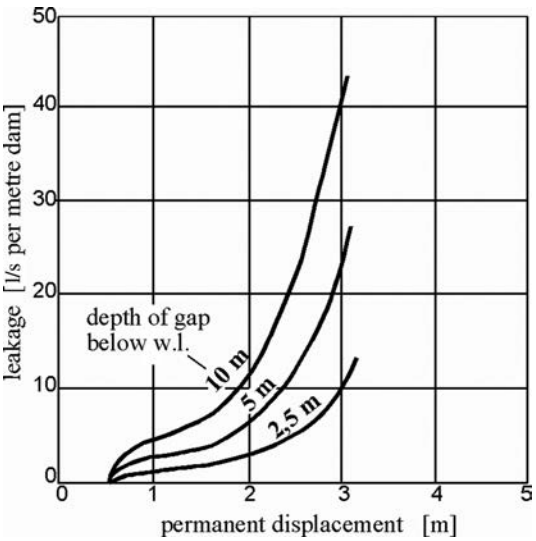

Figure 14.48 Water penetration through opening in concrete wall (Valstad et al., 1991).

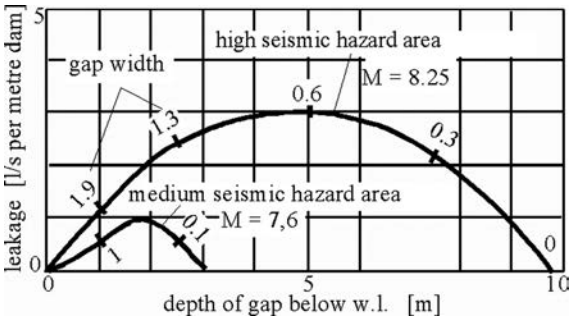

Figure 14.49 Water penetration through opening in concrete wall, caused by earthquake (Valstad et al., 1991).

water flowing. Going downwards, there is a reduction in the size of deformations, and an increase in water pressure. Figure 14.49 presents the dependence of the quantity of penetrated water depending on depth of penetration and the width of the crack in the asphaltic concrete core for a region with medium, i.e. with high seismicity. At the most adverse combination of these two values, there has been calculated the largest quantity of penetrating water, which, for a very strong earthquake ($M = 8.25$) amounts to 3 l/s per 1 m of dam's length (Fig. 14.49). That seepage does not endanger the stability of the dam in the zone of penetration, having in mind the kind of material adjacent to the concrete wall, as well as in the entire dam's body. However, if the crack widens over the entire length of the dam, then governing quantity would be the quantity of water, which has to be taken away through the downstream end of the dam. In this specific

case, that would be considerable, since Storvatn dam is very long (1460 m). Therefore, when such a dam would have to be constructed in a region of high seismicity (not moderate, as it is in this specific case), then the slope inclinations could not be so steep (1:1.5, resp. 1:1.4).

Finally, in such an analyses, it is necessary to take into consideration that, during maximum earthquake vibration, there may occur a number of cracks, i.e. openings along the height of asphaltic concrete core wall; this imposes a need of especially careful analysis.

Above-described analysis confirms the knowledge and comprehension that dams with asphaltic concrete core, if properly designed, are safe against earthquakes, in spite of the small thickness of the watertight element. This is particularly manifested when dam's body is constructed of rock material, at which it does not come at a reduction of the shearing strength at cyclic loading and in cases when consideration has been taken for transition zones to be constructed with well-graded crushed stone.

Over the last decade several experimental studies have been described in the literature, carried out to investigate the behaviour of hydraulic asphalt material subjected to cyclic loads simulating earthquake shaking. Nakamura et al. (2004) carried out cyclic tension tests to simulate the tension conditions which may arise in an upstream asphalt concrete facing of a dam subjected to seismic loads. They also studied the use of an additive to the bitumen to increase the ductility and resistance to cracking. Recently, Feizi-Khankandi et al. (2009) reported the results of cyclic triaxial tests to derive material parameters for the seismic analysis of the Garmrood asphaltic core embankment dam in Iran.

Wang and Höeg studied the effects of cyclic loading on the stress-strain-strength behaviour and permeability of asphalt concrete for different temperature and static and cyclic stress conditions. Cyclic and residual strains were recorded for the various static and cyclic stress combinations and temperatures. In a supplementary series of tests, the effects of a number of load cycles was investigated by using thousands of load cycles. The post-cyclic stress-strain-strength behaviour and permeability were compared with that of specimens not subjected to previous cyclic loading, to study any degradation effects caused by the cyclic loading. The most important conclusions are:

- The cyclic stress versus cyclic strain relationship was found to be nearly linear for all the conditions tested, although the cyclic shear stresses imposed on some of the specimens corresponded to severe earthquake shaking.
- The cyclic modulus versus mean static stress showed an approximately linear relationship in a logarithmic diagram.
- The test temperature had a significant effect on the value of the cyclic modulus, for example: at 1 MPa mean sustained stress, the cyclic modulus at 20°C was approximately 900 MPa, at 9°C it was 1900 MPa, and at 3.5°C about 2500 MPa.
- The damping ratio was found to be between 0.07 and 0.30, depending on stress state and temperature level.
- The number of load cycles (up to 6000) had no significant effects on the magnitude of induced cyclic strain, but there was an accumulation of residual (plastic) strains, primarily caused by the sustained static stress on the specimens.
- The cyclic loading had an insignificant degrading effect on the post-cyclic stress-strain-strength behaviour and watertightness of the asphalt concrete.

Based on the results, the authors concluded that the asphalt core of an embankment dam in a seismic region can withstand very severe seismic shaking without cracking and losing impermeability. They believe that the earthquake resistance of the dam will rather depend on proper design and zoning of the embankment itself, considering the available fill materials, the foundation conditions, and the seismicity at the site (Wang and Höeg, 2010).

In the literature there is only one case dealing with the effects of an actual earthquake on an asphaltic concrete embankment dam. The eight installed strong motion seismographs recorded the response of Yele dam to the very strong Wenchuan earthquake in May 2008, the epicentre of which lay about 258 km away. The shake caused an additional crest settlement of only 15 mm and had insignificant effects on the dam, and there are no indications of any leakage through the asphaltic core (Hao and He, 2008).

Chapter 15

Monitoring and surveillance of embankment dams

15.1 TASK AND PURPOSE OF MONITORING

In the course of construction and particularly during the service period, it is necessary to perform continuous monitoring, i.e. observation, and surveillance of the embankment dam in order to have permanent insight into the condition and behaviour of the structure, enabling timely anticipation of any possible threat to its safety. *Monitoring* is carried out by means of measurements and keeping track of seepage phenomena, displacements and stresses both in the dam's body and in the foundation. In the case of dams impounding exceptionally large storage reservoirs, as well as those which are located in seismically active areas, it is necessary to keep track of the seismic activity before, during and after forming the reservoir. *Surveillance* means a continuing examination of the condition of a dam and its appurtenant structures and the review of operation, maintenance and monitoring procedures and results in order to determine whether a hazardous trend is developing or appears likely to develop (Penman et al., 1999; Singh & Varshney, 1995).

Through keeping track of the behaviour of the dam there is a control on whether the individual elements work and behave properly, as has been anticipated in the design, or else whether it is obligatory to undertake measures for improving their work (D'Appolonia, 1990). By means of observation and surveillance it is also possible to discover any errors that have been made in the design or during construction, which with timely intervention could be removed if because of them the safety of the dam and its environment has been called into question. These observations of the dam can be divided into two general kinds: control observations and special observations.

Control observations are obligatory and they must be treated in detail in the design, paying attention to the valid standards. They have the task of providing systematic control of the behaviour and condition of the dam from the commencement of construction, as well as in the course of its service period. They encompass already cited measurements and, for that purpose, both in the dam's body and its foundation there are built-in appropriate measuring instruments to an extent that depends on the size, importance, and construction of the works (Dobrinin et al., 1994; Hanna, 1985).

By means of special observations we can perform a check-up of certain assumptions and applied methods for which at this moment there is no safe theoretical or experimental basis. In that way it is possible to obtain a picture of the temperature regime of individual structural elements, to examine the accuracy of the approximate

numerical methods by means of which there has been determined the state of stresses-deformations in the dam's body and its foundation, to confirm the efficiency of new kinds and constructions of watertight elements and drainages, as well as to solve a series of other questions which can only be efficiently investigated in natural conditions, that is to say on a model scaled 1:1 (Karasawa, et al., 1994; Hrabowski & Rzadkowki, 1988). By means of special observations it is also possible to appraise the work and effectiveness of various measuring instruments with the same function and also to elaborate schemes for their most rational distribution. Therefore, special observations are carried out for scientific purposes and in accordance with an especially worked out programme.

Parallel with the monitoring by means of instruments, it is also necessary to perform a visual control. Thus we can swiftly discover any particularly dangerous defects and appearances in the dam, such as significant settlements or displacements, sliding, cracks, considerable amounts of seepage water, etc. (Heigerth et al., 1994).

The frequency of measurements is determined in the design and depends on a number of factors. In the course of the dam's construction, the first filling of the reservoir and during initial period of operation they must be more frequent (Basmaci, 1991). By stabilizing individual processes – reduction of settlements, dissipation of pore pressure and the like – the interval between measurements is increased, for instance from 1 to 30 days in the period of construction, at 2 to 12 months during the later period of service.

15.2 MONITORING OF PORE PRESSURE AND SEEPAGE

Pore pressure is measured in the dam's body, in its abutments, and the foundation by means of piezometers which, depending on their purpose, can have different structures and certain specialities in connection with their incorporation.

Piezometers in the foundation, dam abutments, and dam body are placed in previously made boreholes. Sometimes, in the embankment, they are built in parallel with the construction. They should be so located as to give full information on the intensity and space distribution of pore pressure. For that purpose, there are placed several rows of piezometers transversely to the dam, starting somewhere from the upstream edge of the crest, down to the downstream toe. Additional piezometers are set up at the contacts of the embankment and the concrete constructions.

There are two basic types of piezometers: (1) *hydraulic* piezometers, where the water pressure is obtained directly by measuring the water level or the pressure into the tube; and (2) *electrical* piezometers, where the pressure is measured with electrical-acoustic or electric-resistant pressure gauges (manometers). Lately, *pneumatic electric* piezometers are also used.

15.2.1 Hydraulic piezometers

Hydraulic piezometers, depending on their purpose, can have various constructions. They all consist of three basic parts: (1) a *water inlet part*, with a filter, which protects the piezometer from penetration of deposit; (2) a *piezometer tube*; and (3) an

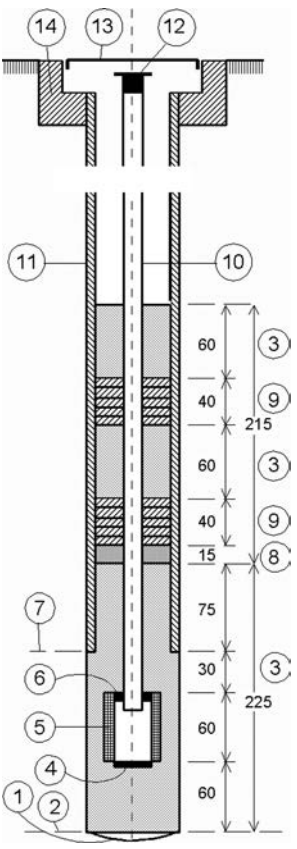

Figure 15.1 Casagrande piezometer set up in a prepared borehole (not to scale). (1) Bottom of cleaned borehole; (2) limit of boring; (3) sand filling; (4) rubber waterstop; (5) porous tube, 60 cm long, internal diameter 2.5 cm, external diameter 3.8 cm; (6) waterstop of soft rubber; (7) after placement of the porous tube with waterstops, the steel tube is elevated up to here; (8) well-graded sand; (9) plugs of compacted bentonite; (10) plastic tube, external diameter 13 mm; (11) steel tube ø 50 mm; (12) Valve; (13) cover; (14) concrete block.

upper part, with protective devices. We further differentiate between *open* and *closed* hydraulic piezometers.

The simplest kind of open piezometer can be in the form of an ordinary plastic or galvanized steel tube Ø40–60 mm, perforated at the lower end, in which the water level is measured from above, by lowering a mechanical or electric 'whistle', which whistles in contact with water. This is used for water-permeable materials, for instance sand, for measuring the pore water pressure.

For fine-grained, poorly permeable earth materials, a *Casagrande open piezometer* (Fig. 15.1) is very often used, which is set up in a borehole in the foundation or into the dam's embankment. The internal plastic tube emerges at the surface and, if the pressure of pore water in the tube is lower than the level of embankment surface, then the height of water in the piezometer (pore pressure) is measured by means of an ordinary electric

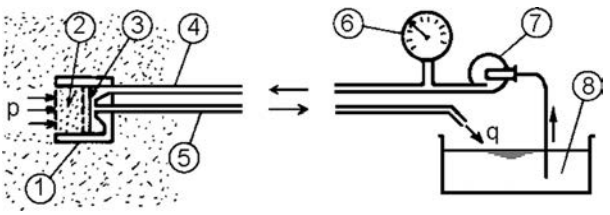

Figure 15.2 Scheme of the Gletzl type of closed hydraulic piezometer. (1) Plastic box; (2) porous ceramic tile; (3) elastic membrane; (4) supply pipe; (5) offtake pipe; (6) manometer (pressure gauge); (7) pump for circulation of oil; (8) oil vessel.

whistle. If the pressure is above the level of embankment, then the pressure is measured after extending the tube above the level of the embankment. During the incorporation of the piezometer, it is particularly important to provide good sealing around the central tube, since flowing of water into that space would derange the hydrodynamic equilibrium of the system and so the results would be useless (Nonveiller, 1983).

The main deficiency of this piezometer is that there is a need for a certain discharge of water to or from the piezometer tube, in order for it to adapt to the changes of the pore pressure. As a consequence of this, there comes about a certain time-lag in recording the changes of the pore pressure, especially if they take place quickly.

In order to avoid the deficiencies of the open piezometer, there has been constructed a *closed hydraulic piezometer,* which has had a wide application in dams in the USA and Great Britain. One newer such construction is the piezometer according to the Gletzl system (Fig. 15.2). Within a plastic box, incorporated into a hole excavated into the coherent material, there is placed a porous ceramic tile. Through the porous tile, the pore pressure into the box acts upon an elastic membrane. On the other side, the membrane acts upon a valve by means of which the supply tube for measuring pressure is separated from the offtake tube. Upon the supply tube there have been mounted a manometer (pressure gauge) and a pump, which can draw oil from a special vessel. When pore pressure acts on the membrane, the pump increases the pressure on the valve as long as there is oil dripping through the offtake tube. The pressure which is necessary to open the valve of the non-loaded box, represents a constant of the box, Δp. If the pressure measured on the manometer (pressure gauge) is $p_{\max}$, then the pore pressure will be $p = p_{\max} - \Delta p$. This piezometer, with careful working, is safe and accurate; however, the entire installation is complex and sensitive, while the measurement takes a long time (Nonveiller, 1983).

Another type of closed piezometer is *Bishop's piezometer.* It relates to poorly permeable and non-saturated earth material so that by using it, one can determine both the negative and the positive pore pressure in compacted earth material. Both hydraulic supplies, set up in a trench (2, Fig. 15.3) are permanently filled with water and can be conducted at large distances (>200 m) to a suitable location of a housing with instrumentation, where the pore pressure is measured by means of a transducer, or by means of a mercury pressure gauge (manometer) (4), provided with a unit for a reading. At certain intervals, it is necessary to perform de-aeration in order to remove the air, which is captured in the supplies or which penetrates from the embankment

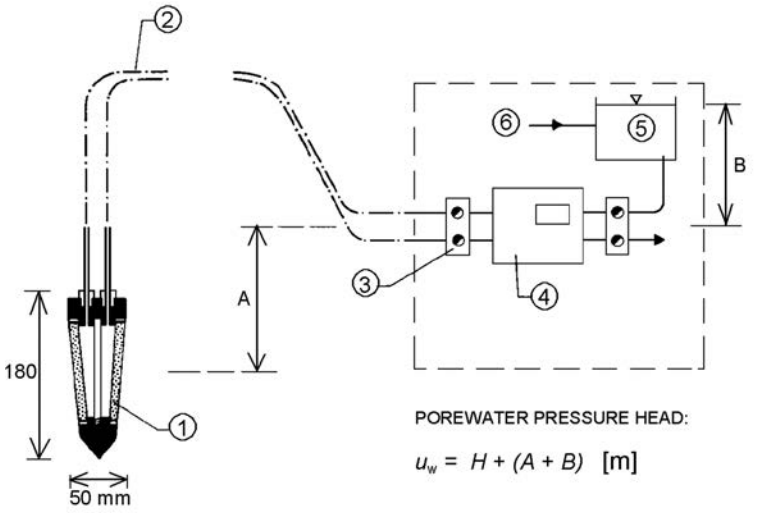

Figure 15.3 Bishop's piezometer. (1) Ceramic inlet element with fine pores; (2) twin leads laid in trench; (3) piezometer valve manifold; (4) pressure transducer and readout unit head *H*, (m); (5) header tank; (6) de-aired water.

or from the pore fluid. The need for de-aeration decreases with the application of a special inlet ceramic element, with fine pores (1). Bishop's piezometer has proved to be efficient, accurate, and durable, so that it has been widely used and incorporated into embankments for measuring of the pore pressure in the course of construction (Fell et al., 1992; Novak et al., 2001; Sing & Sharma, 1976).

15.2.2 Electric piezometers

Electric piezometers possess a number of advantages in comparison to hydraulic ones – there is no need of an inflow or discharge of water in order to record the pressure. There are no problems with the water circulation around the tube nor is there an occurrence of air bubbles in the tubes. This is especially evident in measuring the pore pressure with very impermeable clays. The first electric piezometers were used in the USA in the mid-thirties. They operated in such a manner that by means of air pressure there is balancing of the pore pressure disconnecting the electric contact. Later on a piezometer was used in which deflection has been measured by an electric manner; that deflection is caused by the pore pressure onto a sensitive diaphragm. Since 1955 there has been used on a massive scale a piezometer with a vibrating wire, where the changes of pore pressure are transferred onto the diaphragm or onto a piston, causing changes in the tension, as well as the frequency of vibration of a thin steel wire (Fig. 15.4). The wire (1) by means of a magnet (2) is allowed to vibrate, while the measurement of frequency enables very precise recording of the pore pressure. The main advantage of this type of electric piezometer in comparison to the older types is that readings do

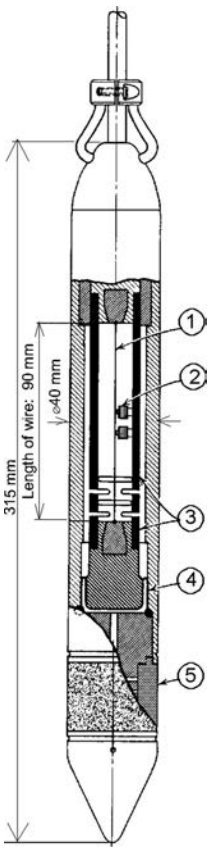

Figure 15.4 Telemac electric piezometer system (Sherard et al., 1963). (1) Vibrating wire; (2) magnets; (3) compressible steel tube; (4) flexible diaphragm; (5) porous stone.

not depend on the electrical resistance of cables, which is variable due to variations in temperature (Sherard et al., 1963).

The pneumatic electric piezometer works with the action of a known and controlled counter-pressure (gas or liquid), which balances the pore pressure acting on the diaphragm. This balancing is recorded by a deflection of the diaphragm, which allows the gas or liquid to reach the flow indicator. The working principle of this contemporary type of piezometer is shown in Figure 15.5. The piezometer tube is connected with two other tubes. Gas or liquid is supplied through one of them (2), and thereby opens the sensitive diaphragm (4) when their pressure equalizes with the hydrostatic pressure at the other side of the diaphragm. After the diaphragm opens, the gas or liquid goes out through the other, outlet tube (3). The applied pressure, required for opening the diaphragm, is taken as a measure of the pore pressure in the piezometer (Novak et al., 2001).

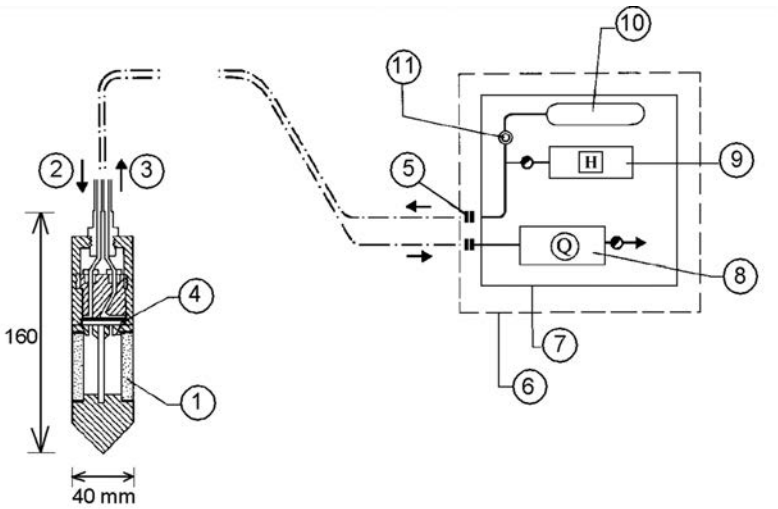

Figure 15.5 Pneumatic piezometer (after Novak et al., 1990). (1) Ceramic inlet element with fine pores; (2) supply of gas under pressure; (3) outlet of gas under pressure; (4) pressure of pore water, resp. gas, on a flexible diaphragm which closes or opens the entrance into the outlet line; (5) snap couplings; (6) terminal chamber; (7) portable measuring unit; (8) flow indicator; (9) transducer and gas pressure readout; (10) N_2 gas pressure bottle; (11) variable reducing valve.

15.2.3 Monitoring of seepage

Observation of seepage through the dam's body and foundation abutments is very important in order to obtain a clear picture of the operation of the dam as a whole, as well as its particular elements, above all, the watertight elements and drainage. In that respect, it is necessary to pursue the level of the seepage line, and the quantity of seepage water, as well as its turbidity and chemical composition.

The elevating of the level of seepage line above the anticipated one in the design is an indication of derangement of the normal operation of the structure – either due to the filling of drainages with deposit, or due to the occurrence of concentrated paths of seepage. The position of the seepage line is established by means of piezometers, located at an appropriate cross-section.

The quantity of seepage water, as well, is an interesting datum, which indicates the regularity of the dam's operation as a whole or that of the watertight element. Measurement is most frequently constructed by means of a calibrated triangular overflow, located behind the downstream toe of the dam, once there is intercepted and gathered the water from different seepage places. If it is a question of a small quantity, water can be directed into a tube, from which it is collected and measured in a measuring cylinder. It is particularly important for the seepage to be carefully followed during the first filling of the reservoir.

If a control or grouting gallery has been constructed under the dam, then it is a very suitable place for tracking seepage through the dam's body and foundation.

Details in that respect have been given within the presentation of individual types of embankment dams.

Visual monitoring is particularly important in pursuing the seepage phenomena. It helps to determine the turbidity of water, which is a dangerous sign, since it indicates erosion of fine particles of coherent material, taken out of the dam's body or the foundation, so that it is possible to notice and take into account the appearance of springs at the downstream side. Springs usually appear during the first filling of the reservoir owing to insufficient impermeability of the natural foundation or that of the grout curtain however, they can appear even later, such as at the Shpilje dam (Macedonia), at which there have been constructed additional grouting works in the foundation, some 15 years following the commencement of the dam's operation.

While measuring the quantity of seepage water, it is necessary from time to time to take water for chemical analysis, by means of which we can determine the concentration of salts, dissolved from the material in the dam's body or in the foundation.

Should there be a need, the installed piezometers can also be used for measuring the velocity and direction of the seepage flow, by releasing color or radioactive isotopes.

15.2.3.1 Detection of the seepage by means of fiber-optic cable

During the last 15–20 years a new method for detection of leakage has been developed and used, based on the measurements of the temperature distribution in the observed soil medium. The installed system contains a fiber-optic cable as a sensor and the temperature can be measured along the entire length of the cable. The technology of distributed fiber-optic temperature sensing offers the possibility to measure the temperature along fiber-optic cables of a few kilometres in length, continuously and with high accuracy. The method is based on the fact that the optical properties of the fiber are dependent on the ambient temperature. A highly developed measuring technique enables the analysis and evaluation of property changes with the result of a reliable temperature distribution along the fiber.

In embankment dams and their foundation, the internal temperature field is dependent on the flow field. Temperature gradients can exist in the form of permanent or seasonal temperature differences, or in the form of significant temperature variations at the probable source of seepage. If leakage is present, temperature anomalies will be transported into the structure by means of convection and will propagate throughout the earthen body, distorting the temperature field. Distributed fiber-optic temperature measurements allow for a detection of the anomaly, locating quite precisely the area affected by leakage. Another approach to interpret temperature measurements is the so-called *active method* or *heat pulse method*. This approach is based on the thermal response of the surrounding cables to the additional heat and can indicate whether the cable is within a moist, a partially saturated or fully saturated medium, and whether seepage flow is present or not. By applying an electrical voltage to the electric conductors integrated in a hybrid fiber-optic cable, the cable is heated up. The temperature increase in the cable depends on the thermal capacity and conductivity of the surrounding soil material (Fig. 15.6). In the case of presence of seepage water the conductive heat transport is superposed by the more effective convective heat transport. Thus, the heat input from the cable is dissipated more quickly. Consequently, the sections with

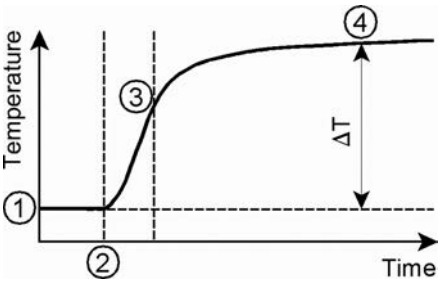

Figure 15.6 Temperature increase inside the cable (after Goltz et al., 2011). (1) Reference temperature; (2) start heating; (3) influenced by the cable design and immediate surrounding material; (4) influenced by the type of the heat transport.

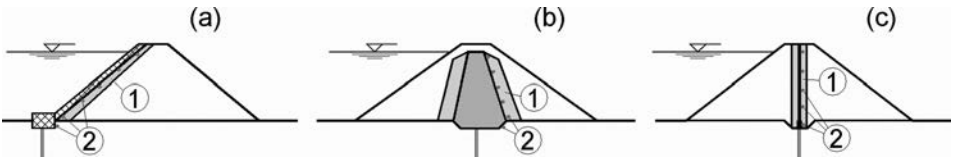

Figure 15.7 Application of a fiber-optic temperature measuring system at embankment dams. (a) Dam with waterproof facing; (b) dam with an internal earth core; (c) dam with an internal artificial core. (1) Filter zone; (2) fiber-optic cable.

seepage show distinct anomalies in temperature increase. Therefore the analysis of the measurement data includes the evaluation of the temperature difference between the heated stage and a reference stage before heating. The reader can find details of the relatively new fiber-optic temperature measurement method for seepage detection in the literature (Johansson, 1997; Aufleger et al., 2005; Johansson and Sjödahl, 2007; Aufleger et al., 2007; Dornstädter & Heinemann, 2010; Dornstädter, 2013).

A fiber-optic temperature measuring system can be applied at new dams, as well as at existing ones. The most common application for existing dams is installation of the fiber-optic cable in the dam toe, below a refurbished surface sealing or in existent standpipes. In the case of new embankment dams the cable can be installed during the construction at locations where the monitoring will give the most useful information. Such places are: behind the waterproof facing (Fig. 15.7a), or behind the internal dam core, made of natural (Fig. 15.7b) or artificial material (Fig. 15.7c).

In case (a), the optic cable is located in a zone with relatively low stresses and deformations, while in cases (b) and (c) it is installed in the middle part of the dam, where the cable is exposed to lateral pressure due to the deformations and the stresses in the dam body, as well as to possible tensile forces. Therefore, in cases (b) and (c) measures for protection of the optic cable should be undertaken. To evaluate the influence of deformations and stresses on the results of the measurements, laboratory tests have been carried out in which realistic loads on the cable have been simulated. Such tests have been performed at the hydraulic laboratory of Innsbruck University (Fig. 15.8). The laboratory tests for determination of the effects of pressure perpendicular to the

Figure 15.8 An installation for testing of fiber-optic cable for the purpose of seepage detection in the hydraulic laboratory of Innsbruck University (September, 2010).

fiber-optic cable axis on the results of the measurements have been performed on the cable installed in a 3.78 long, 0.6 m wide and 0.6 m high reinforced steel box, using different bedding materials. The load was applied force controlled using a fatigue testing machine with a capacity of 1600 kN, that guaranteed constant loading during the different load steps. In addition to the fiber-optic temperature measurements, conventional temperature sensors were used to record the temperature in the steel box, as well as the air temperature for the duration of the tests. Thus it was possible to check if the thermal boundary conditions remained constant. If changes in the ambient temperature occurred it was possible to consider their influence for the evaluation of the fiber-optic temperature measurement data. After installation of the cable in the soil material it took a certain time until stationary thermal conditions were reached, which were necessary to start the tests. Before applying the load, reference measurements were conducted for about 10 minutes. The load was applied in load steps of 125 kN. Each load step took 6 minutes. After completion of the final load step the sample was unloaded. The tests were carried out with a standard hybrid fiber-optic cable 12.9 mm in diameter, with 4 fibers and 6 conductors (Fig. 15.9). Sand, gravel and sand-gravel mixes, both natural and processed material, were used as bedding materials for the tests. To investigate the influence of particle shape both natural and processed materials were used (Goltz et al., 2011).

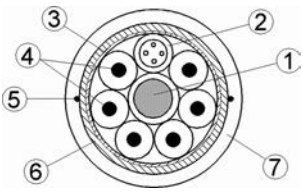

Figure 15.9 Fiber-optic cable used for laboratory tests (after Goltz et al., 2011). (1) Central strength member; (2) loose tube; (3) water absorbent tape; (4) Cu wire, 1.5 mm^2; (5) rip cord; (6) armour; (7) HDPE outer jacket.

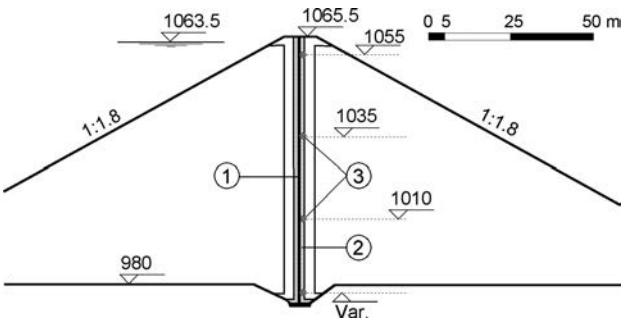

Figure 15.10 Typical cross-section of Knezhevo dam – allocation of the fiber-optic cable. (1) Asphaltic concrete core; (2) downstream transition zone (2A); (3) fiber-optic cable.

The results of the laboratory tests show that pressure perpendicular to the cable axis can have significant influence on the measuring results of fiber-optic temperature monitoring. Based on the results it was recommended to use well-graded bedding material and to limit the maximum particle size to 16 mm. One of the conclusions was that, bearing in mind these recommendations, installation of fiber-optic cable in dams with a height of up to 85 m should not cause problems regarding the reliability and accuracy of the measurements. As a result of the applied loads in some tests damages to the cable sheath occurred and high optical losses led to distortion of the measurement data. However, the applied loads did not cause the rupture of the optical fiber in any of the tests. By analyzing both the raw data (optical losses) and the temperature data, temperature anomalies caused by mechanical loading can be detected.

A fiber-optic measuring system was applied in the asphaltic concrete core rockfill dam Knezhevo (R. Macedonia, see also Chapter 14). The cable was placed in the filter (transition) zone, just downstream from the asphaltic core (Fig. 15.10). According to the specification, the maximum grain size for the first filter zone material varied from 25 to 60 mm. To avoid damaging the cable during compaction of the filter material, uniform sand with a maximum grain size of 2 to 5 mm was used as cushion material around the cable. All necessary facilities such as measuring hut, reference section and power supply are located on the right bank above the dam crest. The cable used for

the leakage detection system is a standard outdoor fiber-optic hybrid cable, similar to the one shown in Figure 15.9. The external diameter is 17.0 mm. The element used for the measurements is a mobile unit and only on-site during measuring periods.

To evaluate the change of seepage conditions in the dam due to impounding of the reservoir and during operation of the dam, reference measurements before filling the reservoir were performed. The reference measurements were carried out when partial impounding of the reservoir was started (14-07-2010). In most parts of the dam the results of the reference measurement showed no anomalies. Only at the lowest part of the dam did temperature differences indicate that the material around the cable was saturated or that minor percolation was occurring. In general, the variations of the temperature differences are mainly caused by different thermal conductivities of the surrounding soil material. The thermal conductivity of a soil depends among other things on mineralogical composition, the bulk density and the water content.

A leakage simulation test was also carried out to check for proper operation of the installed system. For this purpose a water tank was placed at the dam crest. The amount of seepage was adjusted to approximately 0.15 l/s to prove the sensitivity of system. Water was infiltrated at two different points. The infiltration at the first location was started at 9:45 h and lasted for about 3 hours. Since it was assumed that the infiltrating water flows along the slope, infiltration was started at a second point at 13:30 h. This infiltration lasted for about 5 hours. Significant anomalies were recorded at the right slope between el. 1025 and el. 1050 m, caused by the infiltration at the first point. The anomaly increases with continuing infiltration. Anomaly was also recorded by infiltration at the second point. The anomalies intensify during the measurements. Both time characteristics and position suggest that the anomalies are caused by the increase of water level due to impounding of the reservoir (Goltz et al., 2011).

Since the reference measurements were carried out at the beginning of the partial impoundment, the results will serve as guide values to assess changes of the seepage conditions during the first complete reservoir filling, as well as in the service period. The results of the leakage simulation test prove the proper operation of the system and the suitability of the system to detect small changes in the seepage behavior of the dam.

An alternative geophysical technique to track map and monitor leakage through dams, called *Controlled Source Audio Frequency Domain Magnetics*, is described by Hughes, 2010. This technique was used to locate leakage and to propose remedial works at a rockfill dam in Sri Lanka.

15.3 MONITORING OF DISPLACEMENTS

For the assessment of the behaviour and operation of embankment dams, of great importance are displacements, i.e. deformations, occurring both at the surface and in the interior of the dam in the course of its construction and service. In the case of low dams, only surface displacements are monitored, while in the case of medium and high dams, it is obligatory to measure deformations in the interior of the dam, as well. This is particularly important for dams with watertight elements made of artificial materials, where permissible deformations are more rigorously limited and they are of decisive importance for the operation of the watertight element.

15.3.1 Measurement of displacements at the surface of the dam

For measuring the displacements of particular points at the surface of the dam, abutments and banks of the river valley, geodetic methods are employed. For that purpose, there is formed a micro-trigonometrical network, i.e. skeleton of posts along with spots for setting up instruments by means of which the bench marks outside the dam's body and its surface, located at easily accessible places – at the crest, berms and downstream toe – are visible. Bench marks are also installed on the appurtenant concrete structures, within the dam – spillway structures, the outlet structure of the bottom outlet, etc. All permanent points must be set up on a concrete foundation, with a depth which is larger than the depth of freezing (minimum 80 cm; Fig. 15.11). The points of the micro-trigonometrical network should be sufficiently distant from the dam in order not to lead to deformations due to the weight of the dam and the water in the storage lake. For greater safety, these points should be interconnected, with permanent points (bench marks) at some more distant stable places. In locating the points of the micro-trigonometrical network, it is advisable to consult an experienced surveying engineer.

Vertical displacements are measured by leveling, i.e. using an elevation network, while horizontal displacements are measured using a trigonometrical approach, with an accuracy of ±3 mm, which is sufficient for a control of the dam's behaviour and for comparison with anticipated displacements. The number and arrangement of the benchmarks depend on the structure of the dam, its size, and the layout plan of the appurtenant structures.

The first, or *zero measurement,* is performed at the completion of construction works, immediately after the placement of benchmarks and so it determines the position of the benchmarks. During the first filling of the reservoir and during the initial period, measurements are performed more frequently, and, later on, usually once a year.

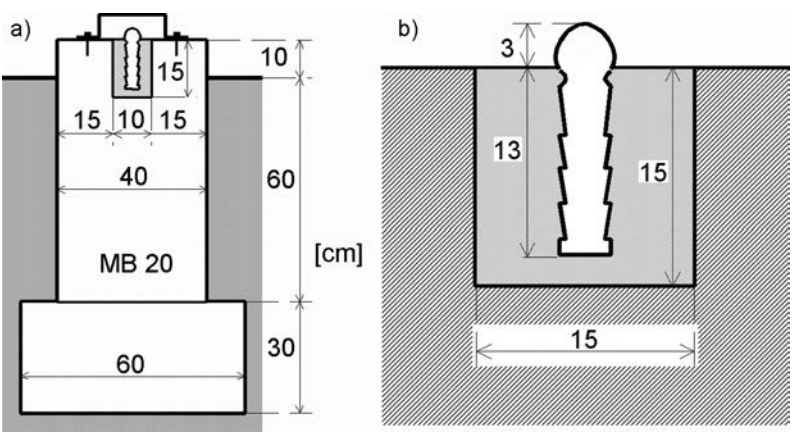

Figure 15.11 Post with a benchmark at the surface of the dam and a benchmark incorporated into the concrete construction.

15.3.2 Measuring displacements in the interior of the dam

Bench marks and measuring instruments are placed within the body of medium-high and high dams, which help in keeping track of deformations in the embankment in the course of construction and, later on, during the service period. According to their purpose, two types of these instruments are mainly incorporated: (a) for measuring vertical displacements; (b) for measuring horizontal displacements. Some of the instruments may be used for both purposes, while others are used to determine the spatial vector of displacements.

15.3.2.1 Measuring vertical displacements

For measuring vertical displacements, there is most often used a mechanical device (Fig. 15.12a), which consists of jointed vertical tubes with an internal diameter of 51 mm and 38 mm (1). At the narrower tube with a link (2), there are transversely attached steel U-sections (3), 180 cm long, and a steel plate at both ends. The steel sections are set up in excavated ditches parallel with the advancement of the embankment, at a mutual spacing of 150 cm (there are examples when they are built-in at even larger distances). The incorporation of the entire device is presented in Figure 15.12a. In a borehole, with a diameter of a minimum of 10 cm (4), and a depth of about 2.5 m, made in the foundation, there is placed a larger tube (5), into which there is inserted and attached a narrower tube (6), along with a U-section, with which it forms a cross, so that the U-section should lean well on the leveled base. Further on, there is again incorporated a larger tube, and within it there is a narrower tube with a cross, as there is advancement of the embankment construction. Attention should be paid to the fact that the material, which is built in around the device, should be well compacted (approximately equal to that in the more distant zones), in order to obtain realistic results for the settlements.

The vertical settlement of the measuring points in each segment are measured with a specially constructed torpedo, which is lowered into the tube on a steel measuring tape. There are various constructions of torpedoes. Figure 15.12b presents a torpedo with vanes, i.e. wings, which protrude through two openings and are inserted when the torpedo passes through the narrower tubes, and then reopen when the torpedo exits. In getting out of the narrower tube, the steel tape is tightened up, while the vanes are fastened to the bottom edge of the narrower tube. In that way, it is possible to measure the distance from the top of the system (16). By moving the torpedo down, the position of all measuring points from the top to the bottom are measured. To pull the torpedo out, it is suddenly hit from the bottom of the tube, and afterwards it is automatically drawn through the vanes on the lower movable part of the torpedo and closes them (Nonveiller, 1983).

The above-described device is suitable only for embankments made of fine-grained material, even though it can also be used for an embankment of rockfill, if constructed in layers thinner than 2 m. Other devices are used for measuring the vertical displacements for dams made of rockfill. One of the older types is what is called the *Swedish well*, which consists of a vertical pipe of large diameter, made of reinforced concrete elements (Fig. 15.13; Sherard et al., 1963). Pipes are installed in pits during the construction of the embankment and are, first, separated with wooden wedges at distances greater than the anticipated settlements. With the advancement of the embankment

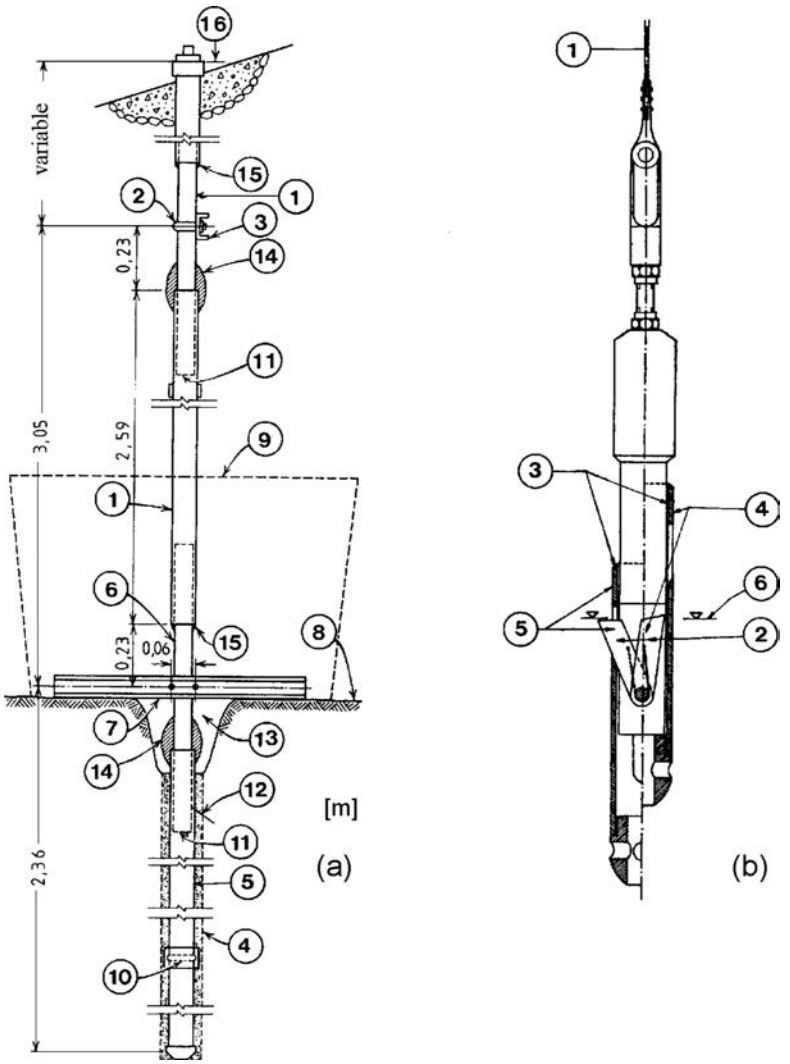

Figure 15.12 Cross-arm measuring device. (a) Mechanical device for measurement of vertical displacements in the dam's body: (1) tube, 38 and 51 mm; (2) link; (3) U-section (cross arm), 75 mm; borehole, min 10 cm; (5) wider tube, 51 mm; (6) narrower tube, 38 mm; (7) U-section; (8) foundation; (9) excavation; (10) slab for blocking of the torpedo; (11) measuring points; (12) grouted; (13) manually compacted filling; (14) hemp tow, fixed with jute cloth; (15) hemp tow; (16) top of the system. (b) Torpedo for determination of the position of measuring points: (1) measuring tape; (2) vanes (wings); (3) sleeve; (4) closed position; (5) open position; (6) Level of measuring point – zero on the measuring tape.

construction, the wedges are knocked out so that the individual pipes are not interconnected one with another and are held by means of the pressure on the adjacent filled material. In that case, the pipes are free to displace along with embankment construction, and, through the incorporated measuring bars, it is possible to determine both

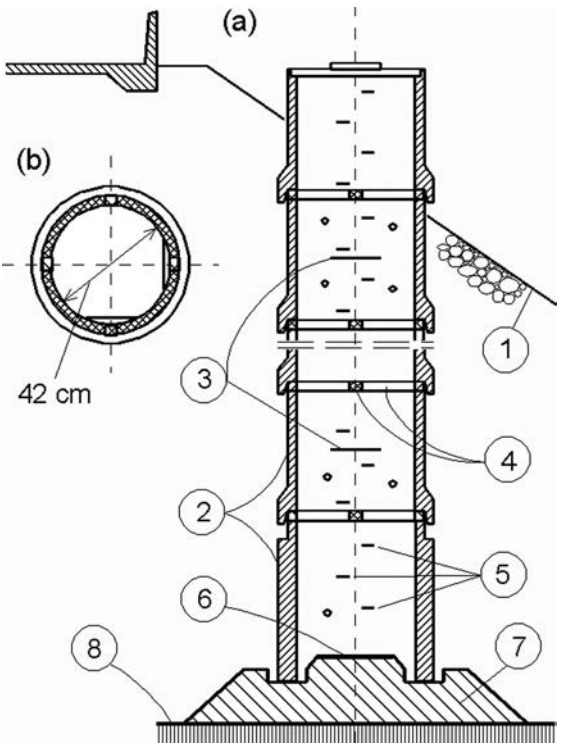

Figure 15.13 Swedish well (Sherard, 1963). (a) Longitudinal section; (b) cross-section. (1) Embankment slope; (2) reinforced concrete pipes; (3) measuring bars; (4) wood blocks; (5) ladder rungs; (6) brass plate; (7) concrete; (8) rock.

vertical displacements and displacements in the other two directions. Of the examples given in this book, this Swedish well has been employed in the Dhünn dam (Fig. 14.6); however, with a somewhat different structure and with a larger diameter (1.5 m), since it also serves as an inspection manhole for the pursuance of the work of the diaphragm.

The Swedish well is an expensive unit and its placement, particularly measurements, is not that simple. Much more practical is the measurement of vertical displacements with hydraulic elevation benchmarks placed during construction in the zones of non-coherent material. Such a benchmark is schematically presented in Figure 15.14 (Nonveiller, 1983). It consists of a firm box with a cover (1), in which there is an overflow tube, whose upper edge represents a level of the benchmark. The interior of the box must be open towards the atmosphere and also must have an opening for draining the overflowing water. The overflow tube of the benchmark is connected by means of a plastic hose to the measuring spot, located downstream, at a lower spot. The measuring spot consists of a closed vessel with water, with a manometer and an indicator of the water level. By compressing the air, the pressure in the vessel is increased, as long as the manometer pressure is normalised, corresponding to the height of the water column of the water level in the vessel up to the level at the edge

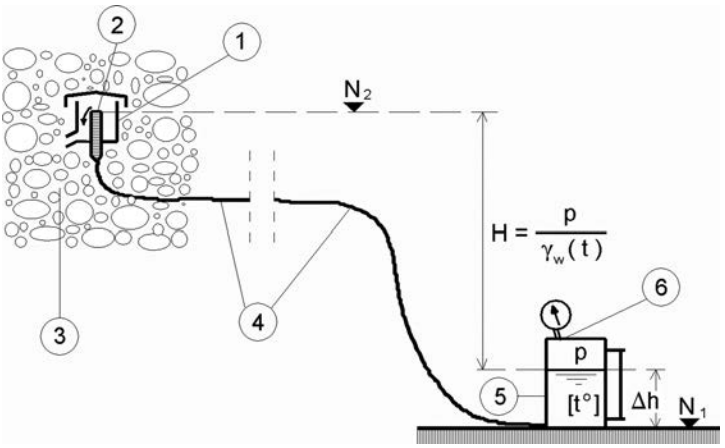

Figure 15.14 Hydraulic elevation benchmark with measuring device. (1) Closed concrete box with a drain; (2) overflow tube; (3) compacted embankment; (4) jointing pipe; (5) tank with water under pressure, calibrated glass for measuring the level, and a manometer; (6) outlet connection for a pump with compressing of the air.

of the overflow tube. With these data, starting from a known level, N_1, it is possible to calculate the level of the benchmark N_2 at the moment of measuring, by means of the expression:

$$N_2 = N_1 + \Delta h + \frac{p}{\rho g} \tag{15.1}$$

The result can be obtained within an accuracy of several millimetres if we also insert a correction for the density of the water, depending on the temperature.

Vertical displacements in the interior of embankment dams can also be measured with a telescopic device, primarily for recording horizontal displacements, as described in the next sub-section.

15.3.2.2 Measuring horizontal displacements

For determination of horizontal displacements, measuring devices are placed at various elevations in the dam's body. The principle of the placement and work of these devices will be explained using the example of the *Scamonden* earth–rock dam which, when it was constructed (some 25 years ago), was the highest dam in Great Britain. In the main cross-section of the dam there are incorporated four rows of measuring devices, which extend from the downstream slope to the core, (Fig. 15.15). They commence with a reinforced concrete housing for instruments at the dam's slope (A, B, C, D), of which the lowest one (A) is the main one and larger than the others. From the housings, along with the advancement of the embankment construction, in excavated ditches there are placed rigid PVC tubes (66 mm internal diameter, 76 mm external diameter) with a gradient of about 1:40 towards the external side (Penman, 1971).

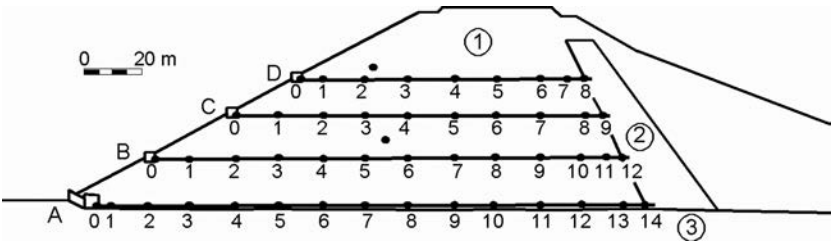

Figure 15.15 Main cross-section of Scamonden dam, with four rows of measuring devices. (1) Rockfill; (2) clay core; (3) foundation of schist.

The tubes have telescopic joints at each 3 m, provided with rubber sealing rings, so that they can take on linear displacements of 75 mm. At each 15 m on the tube, there are drawn on square steel plates with a central opening which have an area of 300 mm^2 and a thickness of 5 mm, protected against corrosion by means of bituminous coatings. Within the housing for instruments, the tube is connected with an end steel plate, placed into the wall (1, Fig. 15.16a), while at the upstream end it terminates with a special part, with a factory-built valve, set up at least 3 m upstream from the last plate, in order for the measuring instrument with its motive motor to be able to pass behind the plate. The ditch for laying the tubes is 1 m deep and there is gravel at the bottom with grains from 3 to 10 mm. The same material is used for filling in the ditch on its sides and above the tubes (Penman et al., 1971).

The instrument for measuring horizontal displacements, i.e. the spacing between plates along the tubes, consists of a torpedo (Fig. 15.16c), on which there is wound a reel of enamelled copper wire, connected with a special coaxial cable with a housing for instruments (when the torpedo is inside the tube). The torpedo moves by means of a winch and wire through the tube, and when the induction coil passes alongside the steel plate, the inductivity changes and, by means of the steel measuring tape attached to the torpedo, it is possible to determine the position of the plate. In that way, the horizontal displacements of all steel plates may be measured. The torpedo is pulled through the tube by means of a tubular motor, which operates by compressed air.

By means of a similar torpedo (Fig. 15.16d), it is also possible to measure vertical displacements of the plates. For that purpose, the torpedo along the axis has been provided with a jet nozzle of 2 mm, jointed with the instrumentation housing through a nylon tube of 6 mm, connected with a transparent vertical tube (2, Fig. 15.16e). Water, which is added in the vertical tube, can overflow through the jet nozzle, from where it is free to go out of the torpedo through radial openings and to return into the instrumentation housing through a PVC hose. In performing the test, the torpedo is set up at the upstream end of the tube with a tubular motor, where the entire length of the connecting tube is washed out with a double quantity of de-aired water in relation to its volume, obtained by means of a piezometer apparatus for de-aeration. Then the vertical tube is filled with water prior to turning off the de-aired water, and also the time of lowering the water into the vertical tube up to the achievement of equilibrium is recorded. Since the most distant plates can be above the instrumentation housing, in such a case, for measuring the level at those points, it is necessary to use a pump

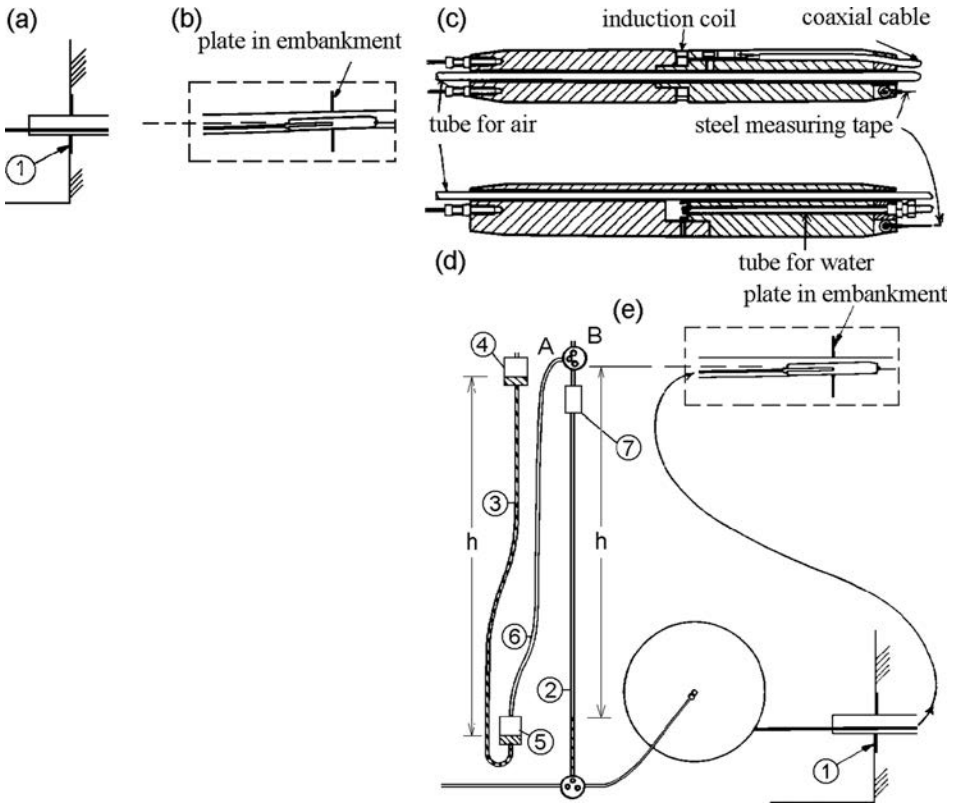

Figure 15.16 Devices for measuring horizontal and vertical displacements (after Penman, 1971). (a) Housing for instruments; (b) torpedo in tube; (c) torpedo for measuring horizontal displacements; (d) torpedo for measuring vertical displacements; (e) schematic presentation of device for measuring vertical displacements.

in order to maintain the level below the cover of the housing. That pump consists of a water column in a vertical hose (3) in the vicinity of the vertical tube, with an open tank for water at the top (4) and a closed container at the bottom (5), connected with a tube for air (6) with a container (7) at the top of the vertical tube, as has been shown in Figure 15.16e. The vertical water column (3) causes air pressure, which lowers the water level in the vertical tube (2) exactly to the vertical height of the column of the level of the water table in the container at the bottom, up to the water level in the upper tank. Next, the torpedo sets out back and at each passing of a plate, the water level in the vertical tube should rise by 0.5 m; thus, we can determine the elevation position of the plate. Following the determination of the elevation of the plates, when the water level in the tube is near the bottom, the air from the pump is let off by the valve A, while the upper part of the tube opens towards the atmosphere with valve B, in order to prepare the system for the forthcoming measurements. The elevation of all

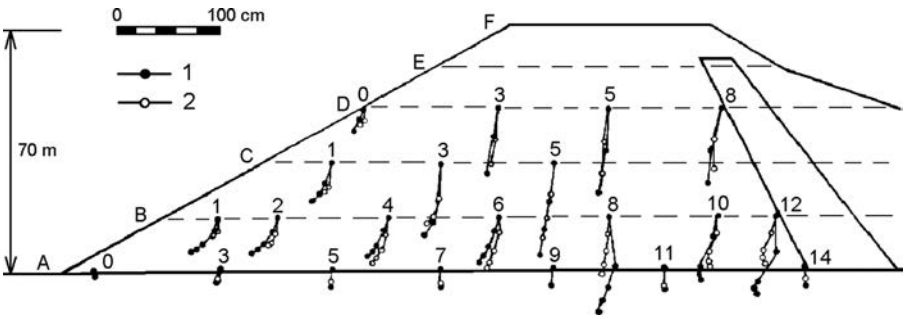

Figure 15.17 Observed and calculated displacements, occurring in the course of construction of the Scamonden dam. (1) Measured displacements; (2) anticipated displacements.

plates is determined in relation to the level of the reference plate (1), incorporated into the wall of the end housing.

The coaxial cable, steel measuring tape, and nylon air hose are accommodated in three cylinders with a frame for winding. The cable and air hose are set up at the ends of the main axis and they turn by means of a device for adjustment, so that the tension is approximately equal in all three directions. When the levels of plates are measured, the cylinder with a coaxial cable is replaced by a cylinder with a nylon hose, filled with de-aerated water for the application on the overflowing device.

The accuracy of measurements by means of the described device is ± 3 mm. The entire installation should be well conceived and planned, as well as precisely constructed, since additional repairs or corrections will not be possible. Displacements of the instrumentation housing, in relation to which are determined displacements of the steel plates around tubes, are controlled and are determined by means of geodetic methods through posts, located in a stable surrounding ground.

By way of illustration, Figure 15.17 presents both measured and anticipated (by means of the Finite Element Method) displacements in the Scamonden dam, which appeared in the course of dam construction.

For measuring horizontal displacements, devices which are called *inclinometers* are employed. They consist of a lining of elastic tube, with a diameter of about 10 cm (1, Fig. 15.18), most often made of aluminium, with four rectilinear grooves (3) on the internal side, installed in the embankment in a vertical position. A probe (2) with wheels (4) is lowered through the tube, and the wheels move along two opposite grooves. The probe contains a sensor in the form of an electrical circuit, which can record deviations of the tube, normally to the vertical, occurring due to deflection caused by horizontal deformations of the embankment. Passing through the tube, the sensor of the probe identifies and records its deflection as a change in the inclination from one point to another and, since it is connected to an energy source, it transmits an electrical signal, which is recorded at the outlet unit that then prints the measured data and, by those means, it is possible to determine the angle between the axis of the probe and the vertical. Measured values of the angle of inclination and depth of the probe are used for the calculation of the horizontal deviations of the tube from the exact vertical, as is shown in Figure 15.18c. The probe also moves down through the

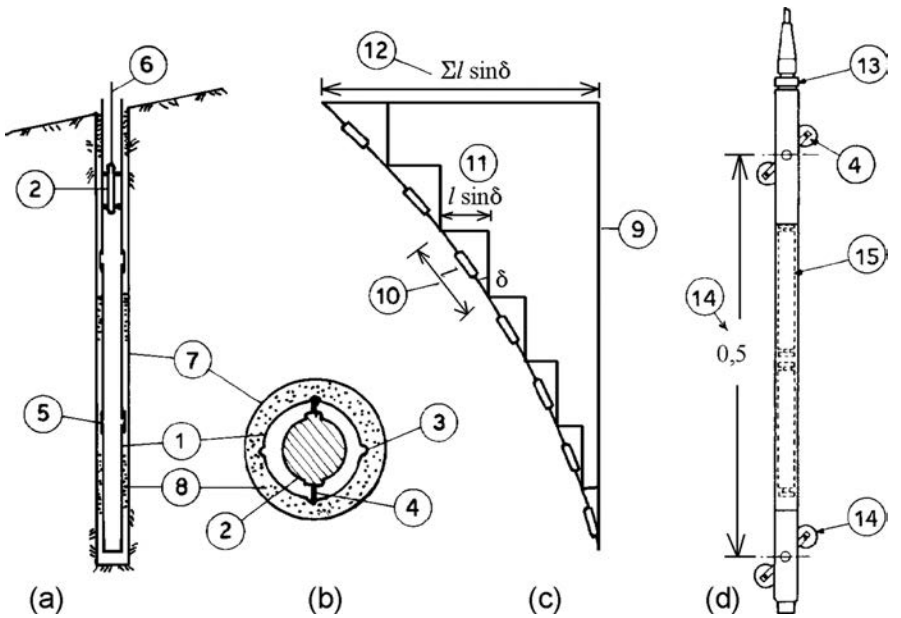

Figure 15.18 Inclinometer. (a) Vertical section; (b) horizontal section; (c) calculation of displacements; (d) probe with servo-accelerators. (1) Elastic tube; (2) probe with sensor; (3) groove; (4) wheels; (5) joints; (6) cable; (7) borehole; (8) grouted or filled with sand; (9) initial vertical profile; (10) distance between two subsequent readings; (11) displacement; (12) cumulative displacement; (13) plug; (14) measuring length, 50 cm; (15) servo-accelerator.

other two grooves, so that measurements are performed in two normal planes. The bottom of the tube is usually fixed into the bedrock and it serves as a reference point for the measured cumulative change of the inclination.

There are many types of inclinometers and they operate according to the described principle, while differences exist in the different constructions of the probe. During the sixties, the initial period of application, the most popular was *Wilson's* inclinometer, in which the probe worked on the principle of Wheatstone's bridge. Today, the most popular method for measuring is the one which utilizes the application of two servo-accelerators, located inside of the probe (Fig. 15.18d)–(Golzé, 1977; Hanna, 1985).

Inclinometers are also used both with coherent and incoherent materials in the dam's *Inclinometers* are also used both with coherent and incoherent materials in the dam's body. In the case of coherent materials, they are most often incorporated at the completion of construction, in a borehole with a diameter of 15.0 cm, in which tubes are lowered and connected with joints (5). The space between the tubes and the wall of the borehole in the zone of the rock is grouted, while in the zone of the embankment, it can be filled with sand. In the case of coarse-grained materials, parallel with the embankment construction, pipes 2 m long are built in, by which they are protected from damage by means of an embankment around them in the form of a cone. Inclinometers are accurate instruments. In order to utilize their performances to the maximum, it

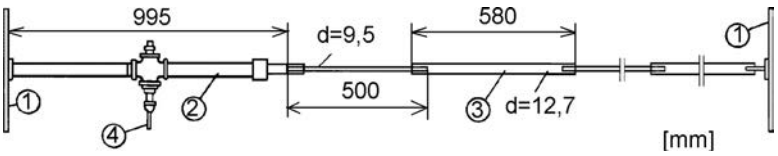

Figure 15.19 Extensometer. (1) Plates; (2) linear potentiometer; (3) movable tubes; (4) cable.

is necessary to pay greater attention and preciseness during installation and use. In practice, they are most frequently used for measurements which are connected with the slope sliding, in the case of earth dams, as well as for research purposes.

Extensometers are used for determination of the relative deformations between two points. Figure 15.19 presents such a device, used in the El Infiernillo dam. It consists of two steel plates, with dimensions 500 × 450 × 8 mm, set up at a mutual spacing of 4–5 m, of a system of movable tubes, with a diameter of 9.5 mm and 12.7 mm, and also of a linear potentiometer and a cable that goes outwards. The device measures displacement of the plates, and thus, also the relative deformations of the filling material between the plates. Measurements can be constructed in any arbitrary direction, with an appropriate incorporation of the instrument (Nichiporovich, 1973).

15.4 MEASUREMENTS OF STRESSES

Measurement of stresses in the body of an embankment dam is of minor significance in relation to determination of deformations. Exceptions to this are the contact zones between the filling material and the rigid constructions (concrete retaining walls, diaphragm walls, galleries, pipelines, etc.). Furthermore, the measurement of pressures is connected with a number of difficulties, because of which results obtained are of uncertain accuracy. The greatest problem lies in the fact that results depend on the stiffness of the cell of the measuring instrument. If it is greater than the stiffness of the surrounding filling material, then there will be obtained values which are higher than the real ones, and if it is smaller the results will be underestimated.

In an ideal case, the measuring cell should have the same stiffness as the filling material, which, in practice is difficult to attain. This problem can be moderated and eased if we use a cylindrical cell with high stiffness, and with a low value of the thickness versus diameter ratio. Moreover, a good cell should also fulfill other requirements: it must be non-sensitive to the effect of temperature variations, impermeable to dampness, firm and durable, and simple to install, etc.

In practice, there have been used a number of different constructions of instruments for measuring stresses, most of which can be used not only for embankment dams, but also for concrete dams. One such steel cell is represented in Figure 15.20. It has a diameter of 175, and a thickness of 35.4 mm, and it functions on the principle of Wheatstone's bridge. It can be used for measuring pressures up to 30 N/cm^2. The upper plate (1) is sufficiently thick so as to reduce to a minimum the deflection under loading. The space below it is filled with mercury (2), which transfers the pressure of the embankment from the plate to the diaphragm (3), 0.75 mm thick. The deflection of

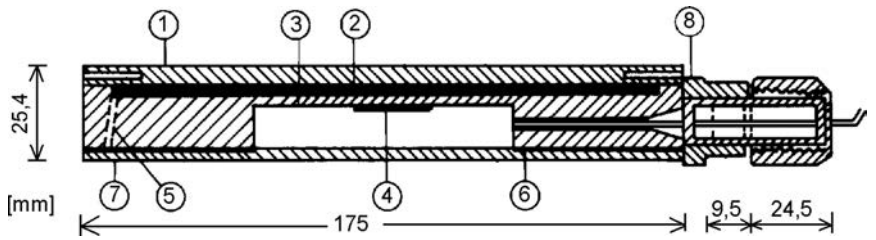

Figure 15.20 Cell for measurement of stresses. (1) Upper plate; (2) space filled with mercury; (3) diaphragm, 0,75 mm thick; (4) measuring plate; (5) opening for mercury filling; (6) rubber waterstop; (7) lower plate; (8) welded.

the diaphragm is measured by four electric measuring stations of polyester (4), stuck on the bottom side of the diaphragm. The measuring stations are thin wires in which the deflection of the diaphragm causes a change of the resistance and that is recorded on the indicator of the Witson's bridge (Sing & Sharma, 1976).

This apparatus is simple; however, the accuracy of results decreases owing to temperature variations, as well as due to the change of the resistance of the connecting cable, which must often be folded during mounting.

15.5 SEISMIC MEASUREMENTS

Tremors of the soil, caused by an earthquake, are transferred to the dam and so they cause additional loadings and deformations. In order to enable further development and perfection of methods for dynamic calculation of embankment dams, it is necessary to collect and analyse data on the response of dams to tremors. In order to assess the effects of earthquakes on the dam, it is essential to obtain measurements of the acceleration, displacements, and relative velocity of the response to different places in the dam and surrounding ground. For that purpose there are set up appropriate seismic instruments – *accelerographs for strong earthquakes, recording instruments (recorders) of the structure response*, and *seismoscopes*.

Accelerographs for strong earthquakes have three electromagnetic torsional swinging pendulums, called *peak detectors*, each of them with a natural period of vibrations of 1/20 s. Two of them correspond to the horizontal components of the earth's acceleration in mutually normal directions, while the third one (normal) corresponds to the vertical component. Each swinging pendulum is provided with a mirror, which, through a lens reflects the light beam from an appropriately set up light source to a roller, at which the beam is recorded on photography paper. The instrument is activated when the acceleration is larger than 0.05 g, when it produces records called *accelerograms*, only in the case of strong earthquakes.

A seismoscope is used as an addition to the accelerograph for strong earthquakes and it serves for the determination of displacements, relative velocities, and accelerations of the structure subjected to an earthquake. *The response recorders* of the structure are simplified instruments for direct measuring of the maximum dynamic

response of the structure, which has the same dynamic characteristics (damping and natural period) as the measuring instrument.

As a minimum it is necessary to install one seismic instrument at the dam's crest, another one in the downstream toe and one more on the natural foundation, however it is desirable to have more of the – especially if it is a question of a high dam (Abdel-Ghaffar & Scott, 1979a).

15.6 GENERAL PRINCIPLES ON THE SELECTION AND POSITIONING LAYOUT OF MEASURING INSTRUMENTS

The selection of the type, number, and arrangement, i.e. positioning layout, of measuring instruments that are to be installed in the dam and the appurtenant structures depends on the nature of the required information, their purpose, the size and kind of hydraulic scheme, its structural particularities, and geological conditions of dam site, etc. An insufficient number of instruments, or else their improper positioning layout in the structures, will not enable the collection of high quality information, while too many instruments will appreciate the construction and service of the works. That is why the number and positioning of instruments should be optimum, with a minimum of incorporated devices to obtain maximum useful information. Measuring instruments should be set up in the zones of the greatest anticipated deformations and stresses. For that purpose, very helpful are the results of already performed observations on similar dams, and especially the results of numerical analyses.

In principle, the main cross-section of the dam should be provided in detail with measuring instruments, and at least two more sections should be provided with more significant devices. In modern practice, we come across a number of dams which are abundantly provided with instruments for monitoring. One of them is the 162 m high Talbingo earth–rock dam (Australia), built in the period 1968–1970. The maximum level of the reservoir was reached at the beginning of 1972. The main cross-section, with its six zones of different materials and the built-in instruments for observation, is shown in Figure 15.21. The inclined clay core has been compacted into layers of 15 cm each. The filter and transition layers (2A, 2B) have been compacted into layers of 50 cm each and are more rigid than the core, while the zones of rockfill contain blocks of a diameter up to 1 m and are compacted in layers of from 1 to 2 m. The foundation consists of rock of volcanic origin.

For pursuance of behaviour, there have been installed instruments for measuring the settlements and horizontal displacements in all zones, and in the foundation; total heads, as well as pore pressures (Figs. 15.21 and 15.22) have also been measured. Readings commenced immediately after the installation of the appropriate instrument, that have been performed periodically in the course of the dam's construction, as well as in the course of the filling of the reservoir. After the first filling, the intensity of readings depends on the conditions of operation of the works. In general, they are constructed every six months. In the course of design, the maximum cross-section is analysed by means of the Finite Element Method, with a complex nonlinear model, in which there have also been inserted forces due to pore pressure, as well as its dissipation in the course of time. The results of measured and calculated displacements and pressures mainly indicate a good mutual agreement; however, owing to the complex conditions

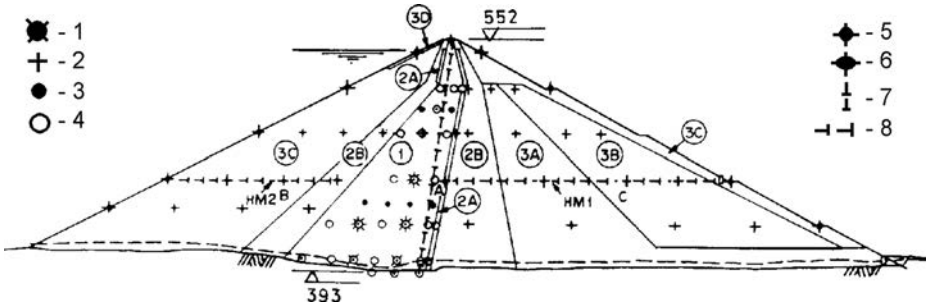

Figure 15.21 Main cross-section of Talbingo dam (after Adikari & Parkin, 1982). (1) Cells for measurement of pressure; (2) station for hydrostatic measurement of settlements; (3) electric piezometer; (4) hydraulic piezometer; (5) measuring points on slopes; (6) measuring points on crest; (7) electric measurement of horizontal displacements.

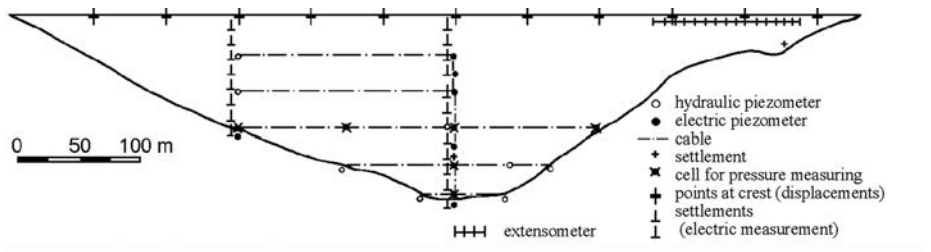

Figure 15.22 Longitudinal profile of Talbingo dam, with positioning layout of measuring instruments (after Adikari & Parkin, 1982).

for placement of the material with different moisture in the core, differences in dissipation of pore pressure in various zones of the core, and variation of the properties of the material in a certain zone, there inevitably come about certain deviations. By way of illustration, Figure 15.23 presents diagrams of measured and anticipated pore pressures in the core at the completion of the construction process (in October, 1970) and after the first filling of the reservoir (January, 1972). In the first case (a), results agree well in the central part of the core, while the greatest deviations appear near the downstream filter layer, where a certain dissipation of the pore pressure has already taken place. In the lower part of the core there have been measured higher pore pressures than those anticipated, which is probably due to the fact that the material placed in the core had higher moisture than the optimum one. After the filling of the reservoir, there came about an increase of the pore pressure owing to the water loading at the upstream side of the core (Fig. 15.23b; Adikari & Parkin, 1982).

The rockfill dam with asphalt-concrete facing (Tataragi, Japan), 64.5 m high, is located in a seismically active area, and is provided with exceptionally abundant equipment for surveillance (Fig. 15.24). Taking into consideration the type of dam and its location, as primary measurements there have been established the measurements of

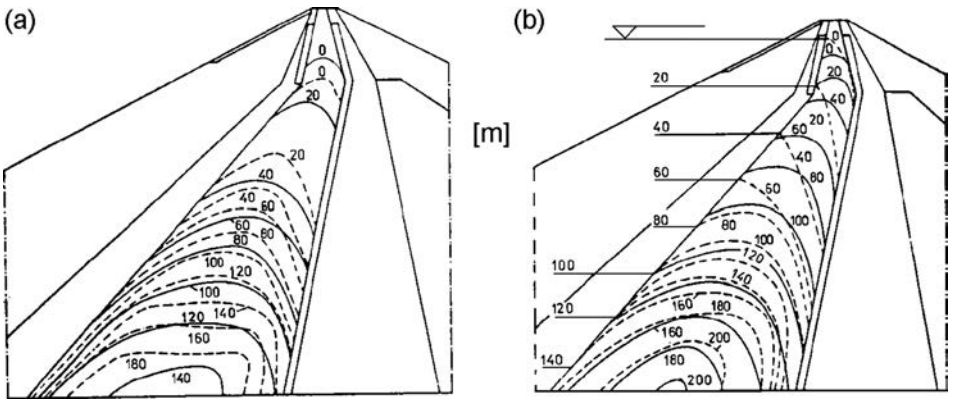

Figure 15.23 Measured (- – - -) and anticipated (–) pore pressures in the Talbingo dam (after Adikari & Parkin, 1982).

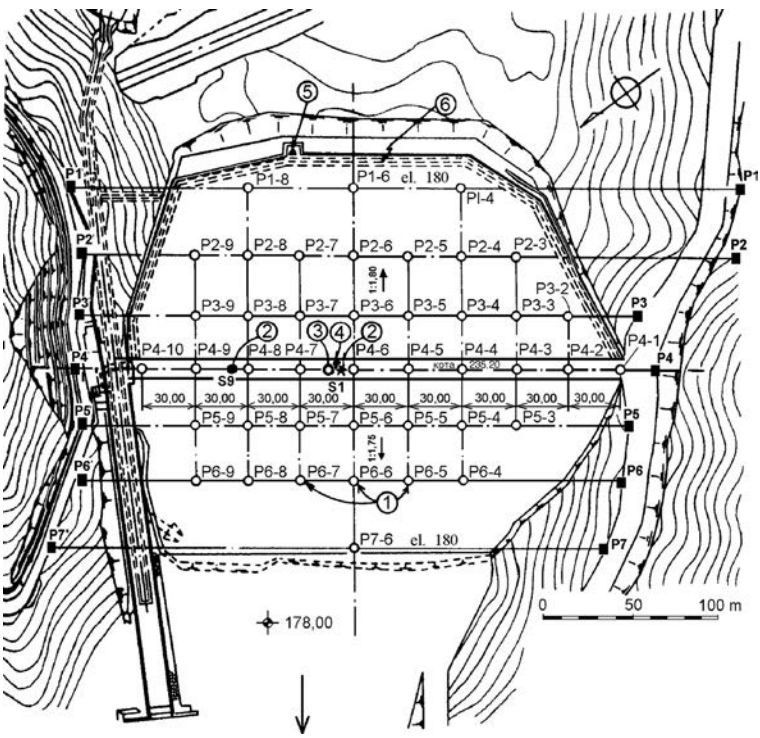

Figure 15.24 Layout plan of Tataragi dam, with instrumentation for monitoring (after Daicho, 1988). (1) Benchmarks at the surface; (2, 3, 4) instruments for dynamic observation – accelerograph, vibrograph and starter; (5) measuring device for seepage; (6) inspection gallery.

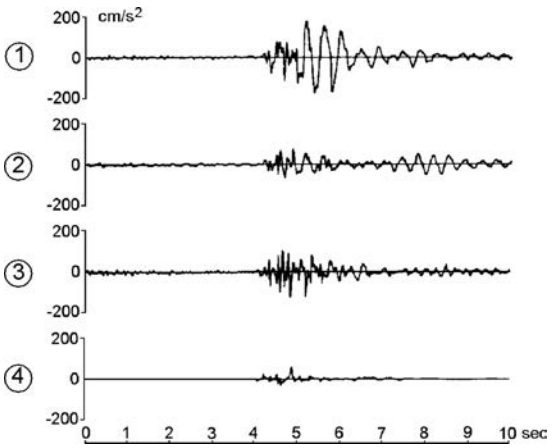

Figure 15.25 Records of the strongest tremor recorded during the service period of the Tataragi dam, Japan (after Daicho, 1988).

displacements and seepage through the facing, as well as dynamic measurements. The following diagram shows an illustration of the anticipated observations:

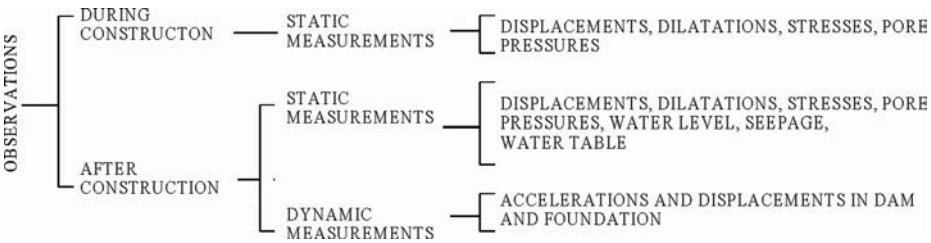

During construction (1971–1973), and operation (1974–1986), there has been recorded normal behaviour of the dam, taking into consideration that seepage through the asphalt-concrete facing has not been recorded at all. The seismic devices, in the course of the cited service period, have recorded 128 tremors, of which one, with an epicentre 30 km distant from the dam, caused damage in the vicinity. The records of the accelerations in the midpoint of the dam's crest and its foundation are given in Figure 15.25. The maximum acceleration in the upstream – downstream direction (1) amounts to 178.3 cm/s^2; in the direction of the crest axis (2) 77.9; in a vertical direction (3) 120.8, and in the foundation 64.3 cm/s^2 (4) (Daicho, 1988).

This page intentionally left blank

Part 3

Concrete dams

This page intentionally left blank

Chapter 16

Gravity dams on rock foundations

16.1 GRAVITY DAMS IN GENERAL

Gravity dams are very often used and, in quite a number of cases, they are in competition with embankment dams. Their name comes from the Latin word *gravitas*, which means *weight*, since they resist the action of the basic force – the horizontal static pressure of water – by means of their self-weight, which creates a force of resistance against sliding across the foundation.

Gravity dams, constructed in stone masonry, were built even in ancient times, most often in Egypt, Greece, and the Roman Empire (Smith, 1971; Vogel, 2001). They have lasted for millennia. In most cases, those dams consisted of masonry caissons, their interior filled with "opus insertum", that is to say, with masonry consisting of pieces (waste) of rock. The ancient Romans produced concrete using as a binder a mixture of lime and pozzolan that was applied to some of the dams constructed of perfectly-shaped rock blocks, for filling the interspace of the upstream face. Such dams have been exceptionally safe and resistant, thanks to the coarse rock blocks at the upstream surface. The construction of masonry dams continued later on, and was particularly intensified after the industrial revolution. Numerous solid, aesthetically nice-shaped gravity masonry dams, with a cross-section similar to the one which is used today, were built at the end of the 19th century. At the same time, there appeared the era of gravity concrete dams, which, up to the appearance of soil mechanics, had no competition in terms of economy and safety, with the exception of narrow dam sites with sound rock in the foundation, where thin arch dams had the mastery over other dams. A particularly important event in the history of gravity dams is the construction of the dam Boulder (or Hoover), in the USA, before World War II, when great progress was achieved in the manufacture and placement of mass concrete. However, in the subsequent period, embankment dams took the mastery. New revolutionary advancement in the case of gravity dams was made in the last decades of the 20th century, with the commencement of the application of economical roller-compacted concrete.

Concrete gravity dams have achieved impressive heights (see Table 16.1), and a number of grandiose works have been built, such as the dam, Grand Coolee (USA), completed in 1942. This was the first massive structure that was constructed by man and which, according to its volume, is larger than the Cheops pyramid (Grishin et al., 1979; Creager et al., 1955; USBR, 1976; USCOLD, 1988; Golzé, 1977).

Table 16.1 Concrete gravity dams higher than 200 m.

Dam	*Country*	*Built (year)*	*High (m)*	*Volume of dam ($m^3 \times 10^3$)*	*Volume of reservoir ($m^3 \times 10^6$)*
1. Grande Dixens	Switzerland	1961	285	6000	401
2. Sayano-Shushenska	Russia	1990	242	8435	31,300
3. Bhakra	India	1963	226	4130	9621
4. Hoover	USA	1936	223	2845	34,852
5. Dworshak	USA	1973	219	4931	4278
6. Longtan*	China	2009	217	7458	27,270
7. Toktogul	Kyrgyzstan	1978	215	3345	19,500
8. Guangzhao*	China	2008	201	2870	3245

*Roller-compacted concrete dam.

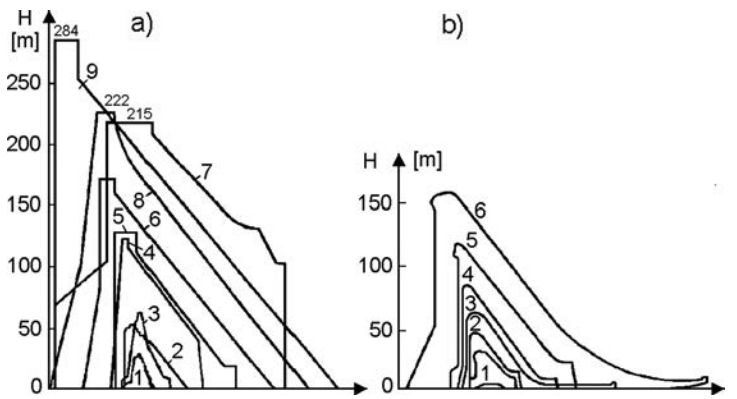

Figure 16.1 Cross-sections of some gravity dams. (a) Non-overflow dams: (1) Grobois (1838); (2) Puentes (1791); (3) Furens (1866); (4) Chambon (1934); (5) Bratskaya (1965); (6) Grand Coolee (1942); (7) Toktogul (1978); (8) Hoover (1935); (9) Grande Dixens (1961). (b) Overflow dams: (1) Tsimlanskaya (1951); (2) Dneprovskaya (1932); (3) Noris (1935) (4) Grand Coolee (1942); (5) Krasnoyarskaya (1970); (6) Shasta (1944).

From a structural viewpoint, gravity dams are divided into non-overflow and overflow dams (Fig. 16.1a, b). They are most often constructed as a combination of overflow and non-overflow parts, in which the overflow part is in the middle, in the zone of the riverbed.

Regarding the material from which they are constructed, they can be stone gravity dams or concrete gravity dams. The first, constructed as dry masonry or with the application of a binder, has been abandoned for a long time, since they require the engagement of expensive labour, so that modern mass gravity dams are constructed exclusively in concrete.

In relation to the way of placing of concrete, gravity dams can be made of *conventional mass concrete*, placed in blocks with internal vibration, or made of *roller-compacted concrete*, placed in thin horizontal layers, compacted by means of heavy

vibratory rollers. In this chapter general issues of gravity dams are discussed, as well as specific questions related to gravity dams made from massive (conventional) concrete. Chapter 18 deals with roller-compacted gravity dams, introduced in the practice since 1980 and now very popular. Practically, all gravity dams constructed in the last three decades around the world are roller-compacted concrete dams.

An important division of gravity dams has been constructed in relation to the material from which the foundation has been composed, which has an essential influence on the dimensions and structural characteristics of the dam's body. In that respect, we distinguish dams on *rock foundation* and on *non-rock* (*soil*) *foundation*. This chapter deals with gravity dams on rock foundations, made of mass, conventional concrete; however, Sections 16.2 through to 16.6, encompass general questions which also relate to the next two chapters, 17 and 18. Questions specific to concrete gravity dams on a soil foundation are analyzed in Chapter 17.

16.2 MASS CONCRETE FOR DAMS

16.2.1 General

Looking at the surface only, concrete is simple, but from a physical and chemical viewpoint, it is a very complex construction material. Its positive features are in the adaptability of the form, the application of widespread mineral materials and, in the developed countries, its low unit cost.

Mass concrete, placed in dams, is not subjected to very significant compressive stresses such as appear in most other large structures. The volume of the dam's body is relatively large, so that concrete should be manufactured, transported, and placed in large daily quantities. That is why a few other properties are ranked equally with the strength, such as indicators of quality and suitability for a certain application, i.e. function. The required characteristics of mass concrete, which is used for dams, can be summarized as follows: (a) satisfactory density and strength; (b) durability; (c) low thermal change of volume; (d) resistance to cracking; (e) low permeability, (f) workability; and (g) economy. All of these characteristics depend on one another to a small or great extent. For example, strength, impermeability, and durability are closely associated with a dense, well-composed concrete mixture. In a similar manner, less direct relationships can be established between other properties; for instance, between constancy of volume and resistance against cracks.

The technology of concrete is a wide-spread discipline with abundant textbook references. This chapter gives a short introduction to the problems, with an emphasis on those elements for the technology of concrete which relate directly to dam construction (USBR, 1976; Golzé, 1977; JCOLD, 2000; Novak et al., 2001).

16.2.2 Constituent elements of mass concrete

Mass concrete contains primary and secondary constituent elements. The primary constituent elements of concrete are: cement, mineral aggregate, and water. The secondary elements, which are used in mass concrete for dams, are pozzolan and other, selected additives.

Cement. The hydration of ordinary Portland cement is strictly exothermal. As a result, there comes about a rise in temperature and a release of heat in significant quantities, which is undesirable and unacceptable due to the problems that are caused by slow dissipation of heat and the occurrence of cracks. That is why it is better to use low-thermal or modified Portland cement. Thermal problems can also be eased by the application of Portland cement enriched with pozzolan. If there is a shortage of special cement, a partial replacement of the cement with ash pulverized fuel may be helpful. A widespread measure is also the cooling down of the concrete or of its constituent components (see further, section 16.6).

Mineral aggregate. Coarse-grained and fine-grained aggregate are cheap and firm filling for the concrete mixture. The optimum value of the maximum diameter of aggregate grains is considered to be 75–100 mm, with round or irregular grains of natural gravel or crushed stone aggregate. Within the zone of fine aggregate (according to American and British regulations, <4.67 mm) natural sand is considered to be better in relation to crushed, fine particles of rock. The aggregate should be clean and without any signs of surface erosion. A continuous, well-graded particle size distribution curve of the granulometric composition of the aggregate, composed of various fractions, ensures generation of maximum density of the placed concrete mixture, and thereby also the most favorable in terms of other physical and mechanical characteristics.

Water. The water which is used for the preparation of concrete must be chemically unpolluted, including organic pollution. Generally speaking, one can adopt as a rule that the water should meet the requirements for consumption.

Pozzolan. Pozzolan is a silicate-aluminium substance that reacts chemically with the calcium hydroxide in the cement, forming additional binding components. We distinguish natural and artificial pozzolan. If there is pozzolan, it usually substitutes 25–50% of the cement. The use of pozzolan usually reduces the hydrating heat and it lengthens the time for increase of the concrete's strength. The strength after a long time period increases to some extent, certain aspects of durability can be upgraded, and the cost of the concrete is somewhat cut down, however the utilization of pozzolan must be pursued with a strict control of quality.

Admixtures. Various admixtures can be used for improving the properties of concrete. The most frequently employed is an admixture of generating air bubbles in the mixture in a quantity of 2% to 6% of the volume per minute, thus considerably improving the durability of concrete during long-term cycles of freezing and thawing; the need for water in the fresh concrete is also reduced and workability is improved. Sometimes, special admixtures are used for reducing the need for water, which reduces it by 7–9%. They also influence the extension of the setting time of the concrete at high external temperatures.

16.2.3 Parameters of concrete mixture

The following are the parameters on which, in principle, there depend properties of manufactured concrete by the application of certain kinds of aggregate and cement: quantity of cement (C, kg/m^3), quantity of water (W, kg/m^3) and the water:cement ratio (by weight). Possibly, the use of pozzolan and/or admixtures can have a certain influence.

Required primary characteristics – density, strength, durability, and water-impermeability – first of all, depend on the quantity of the cement and the water:cement ratio. Increasing the quantity of cement and reducing the water:cement ratio upgrade them. However, thermal characteristics, such as constancy of volume, are improved by decreasing the content of the cement in the mixture. Economy is also directly dependent on minimizing the quantity of cement. Such a controversial influence on certain elements imposes the indispensable need to achieve equilibrium with the variation of parameters within certain limits. It can be stated that, in selecting the appropriate concrete mixture, the control of thermal characteristics is dominant, as well as the low cost along with achieving sufficient strength and durability.

The properties of a placed, well-compacted mixture depend on the attainment of maximum density through effective compaction. The capability of obtaining dense placed concrete depends on the properties of the fresh mixture, primarily on its *workability*, which means that again a decisive role is played by the proportions of the constituent components, and most of all the water:cement ratio. Workability is defined as the amount of useful internal work that results full compaction, in other words it is the ease of flow of fresh concrete and the ease of dealing with it in transporting, placing and compacting without segregation. There are many factors that affect the workability of fresh concrete, but the most important is the water content in the mix. Three tests on workability are used in the concrete laboratory:

- *The slump test*. This test measure the slump in a frustum cone shaped concrete mix, the slump that occurs is classified as: *zero slumps*, if the slump is equal to zero, which means very stiff mixes; *true slump*, if the slump is above 0 to 12.5 cm (the higher slump value indicates higher workability); *shear slump*, if the mix cone sheared into two parts (one half of the cone slides down an inclined plane); *collapse*, if the slump is between 15 and 21 cm. For high strength concrete the slump should to be less than 5 cm, for reinforced concrete the slump value is ranged from 5 to 10 cm.
- *Compaction factor test*. This method is based on using the inverse approach of the workability definition, i.e. it measures the degree of compaction done by a standard work, which results from falling through the hoppers. This test is more sensitive to low workable mixes than to high workable ones. The compacting factor is measured by the density ratio, i.e. the ratio of the density of the mix obtained by the mix to the density of the mix fully compacted. The largest value that can be obtained for the compaction factor value is 1. As the nearest the compaction factor is to 1, more workable the mix is.
- *VEBE test*. It is based on measuring the time (called VEBE time) needed to transfer the shape of a concrete mix from a frustum cone to a cylinder (these shapes are standardized by the apparatus of this test), by vibrating and compacting the mix. The more VEBE time needed the less workable the mix is. This method is very useful for stiff mixes.

Thus, attainment of a satisfactory concrete mixture is a question of balancing the conflicting requirements and conditions. Orientational proportions of the mixture and concrete properties, crystallized from the substantial practice, are shown in Table 16.2.

Table 16.2 Characteristics of mass concrete for dams (after Novak et al., 2001).

Characteristics	*Concrete mixture*	
	Hearting	*Facing*
Cement + pozzolan [kg/m^3]	150–230	250–320
Pozzolan/(cement + pozzolan)[%]	20–35	0–25
Water/cement ratio	0.50–0.70	0.45–0.65
Compressive strength at 90 days, σ_c [MN/m^2]	18–30	25–40
Tensile strength:compressive strength σ_t/σ_c	0.10–0.15	0.07–0.10
Unit weight, γ_b [kN/m^3]	23–25	
Modulus of elasticity, E [GN/m^2]	30–45	
Poisson's ratio	0.15–0.22	
Shrinkage (% at one year)	0.02–0.05	
Coefficient of thermal expansion [$\times 10^{-6}$ °C]	9–12	

Of course, in each specific case, it is necessary to compose a mixture which is based on experimental investigations.

16.2.4 Fabrication and placing of concrete

Dams are structures with large dimensions and their body contains significant quantities of concrete. In order for such a structure to be able to be constructed within a reasonable period of time, it is necessary to ensure high daily production, transportation, and placement of the concrete mixture. That requires careful planning and execution of a central plant for the production of concrete, along with all necessary capacities for supply and storage of the constituent components. The concrete plant should be so adjusted as to meet all variable requirements during execution of the works, all in accordance with the anticipated construction progress of work on particular blocks, as well as global advancement of the works.

Depending on the size of the structure, as well as the ground topography, an appropriate method is planned for transportation of the concrete mixture to the spot of placing. Concrete is poured in a minimum of two layers and is compacted by means of vibrators. The entire planning of the execution of the concrete works is an operation of vital importance, associated with the efficiency and economy of the dam construction, while at the same time it is exceptionally difficult. Details for planning of works, for production, placing, and compaction of concrete can be found in textbook references.

16.3 CROSS-SECTION OF GRAVITY DAMS

16.3.1 Cross-sections in general

Early concrete gravity dams, such as Puentes (1791) and Grobois (1838) had a trapezoidal shape, with a noticeable width in relation to the height (Fig. 16.1; Grishin et al., 1979). With the development of methods for dimensioning, more economical sections

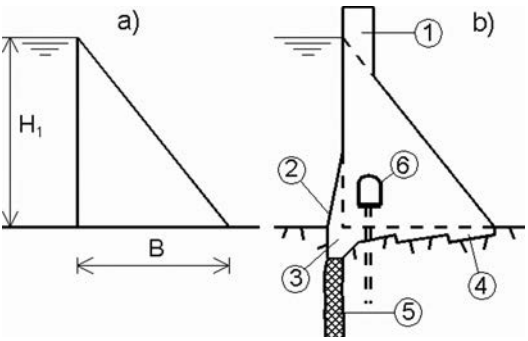

Figure 16.2 Triangular cross-section of a dam. (a) Theoretical; (b) practical, with additions: (1) Shaping of crest; (2) sloping of the upstream face; (3) cutoff trench; (4) indented (toothed) foundation; (5) grout curtain; (6) drainage gallery.

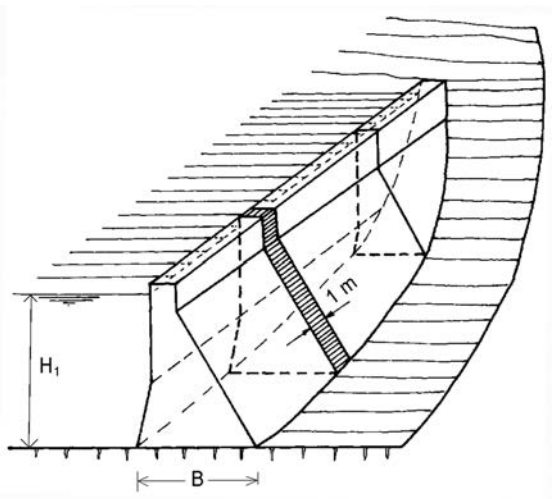

Figure 16.3 Axonometric view of part of a concrete gravity dam.

have emerged later on, while the triangular section has proved to be the most economical one, along with some corrections resulting from the conditions of work at the dam (Fig. 16.2). We will add that the upstream edge of the gravity dam base is called *a heel*, while the downstream edge of the dam is called *a toe*.

Dimensions of the cross-section of a dam are obtained by means of static analysis, most often under the assumption that there exists a plane state of stresses and deformations. This implies that a two-dimensional analysis is performed, along with consideration of the cross-section of the structure with a unit length, parallel with the longitudinal axis (Fig. 16.3).

Chapter 4 considered the forces acting upon dams and, in a particular case, forces acting upon concrete gravity dams, as illustrated in Figure 4.1. Various combinations

of forces are possible in the analysis of dams, including the combination at an empty reservoir.

The combination of vertical and horizontal static forces that are assumed to be acting upon the gravity dam will be balanced with an equivalent opposite reactive resultant R, derived from the vertical reaction and from the reactive horizontal resistance of the foundation. Those conditions of the most essential importance for stability are, in fact, the general conditions for equilibrium of structures:

$$\Sigma H = 0; \quad \Sigma V = 0; \quad \Sigma M = 0 \tag{16.1}$$

In expressions (16.1), ΣH and ΣV denote the sum of all active and reactive horizontal and vertical forces, while ΣM represents the sum of bending moments due to those forces in relation to an arbitrary point. The first two cases in the expression (16.1) state that translatory motion of the dam is not possible, while the third one prevents any rotary movement, for example overturning. Besides, it is also necessary to analyse certain conditions, which arise from distribution of stresses, conditioned by the bending moments acting on the dam. In that way, the stability of a gravity dam depends on the previous criteria. The profile of the dam, for different possible loading conditions, must have an acceptable safety in relation to:

(a) *rotation and overturning*;
(b) *translation and sliding*;
(c) *exceeding the permissible stresses and failure of the material.*

The overall stability of the dam depends on criteria (a) and (b). Both criteria must be satisfied in relation to all profiles, i.e. cross-sections, over any horizontal plane and foundation. In this, criterion (b) often appears to be a critical one. The criterion (c) – keeping stresses within allowable limits – must be satisfied both for the concrete in the dam and for the rock in the foundation.

16.3.2 Theoretical cross-section

First of all, let us consider the theoretical cross-section of a concrete gravity dam in the form of a triangle (Fig. 16.4) with a unit length, a width of the foundation B, and height H. The sides are inclined, so that the horizontal projections of the upstream and downstream slope, respectively are nB and $(1 - n)\ B$, where $n < 1$. It is assumed that the following forces act upon the dam: self-weight G, horizontal force of hydrostatic pressure W_1, weight of water W_2 and the force of seepage uplift below the dam U in the form of a triangle with a height $\alpha_1 H$. It is assumed that the water reaches the top of the triangle, while the action of water from the downstream face is neglected.

For the presented loading scheme, it is evident that the result of all forces R^F due to the effect of the horizontal force W_1 will be downstream of the central point C. At an empty reservoir, the force of self-weight is the only effect; that is to say; the result is equal to the force G and it acts upstream of the central point C. Since concrete can take on only compressive stresses, it is clear that the result of forces, even at the most adverse conditions of loading, must not go outside the core (middle third) of the section, whose end points for a rectangular cross-section (width of the base $B \times 1$) are at a distance

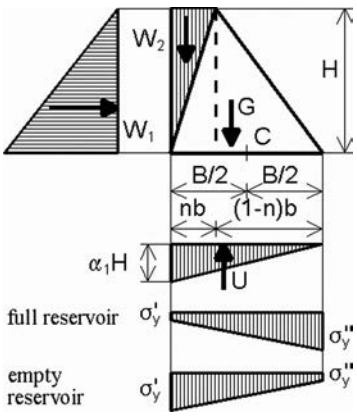

Figure 16.4 Forces and stresses for a dam with a triangular section.

$B/3$ from the edges of the dam. The normal edge stresses in the lowermost horizontal section (as in any other horizontal section) can be calculated from the expression for eccentric pressure:

$$\sigma = \frac{V}{B}\left(1 \pm \frac{6\,e}{B}\right) \tag{16.2}$$

where V is the sum of vertical forces, and e is the eccentricity of the force V; that is to say, its distance from the center, C. Diagrams of normal stresses in the most loaded section, for a full and empty reservoir that have been obtained in this way, are presented in Figure 16.4.

The triangular cross-section will be the most economical one is the width B has the minimum value when the following two requirements are satisfied: (1) there should be no tensile stresses in the cross-section; (2) the dam should be stable against sliding across the foundation.

The first requirement, for the most economical cross-section of the dam, will be met if the normal stress at the upstream edge is equal to zero ($\sigma'_v = 0$); that is to say, when the resultant forces act on the downstream edge of the core of the cross-section. That requirement can be expressed by the equalization to zero of the sum of all bending moments in relation to the point S_2 (downstream edge of the core, i.e. the middle third, of the cross-section), from where, after sorting-out, we can obtain:

$$B = \frac{H}{\sqrt{\dfrac{\gamma_b}{\gamma_w}(1-n) + n(2-n) - \alpha_1}} \tag{16.3}$$

where γ_b is the unit weight of concrete.

The minimum value of B would be obtained for the maximum value of the denominator of the fraction in the expression (16.3). By means of differentiation in relation to n of the sub-root expression and equalizing it to zero, it follows:

$$\frac{\partial\left[\frac{\gamma_b}{\gamma_w}(1-n)+n(2-n)-\alpha_1\right]}{\partial n}=-\frac{\gamma_b}{\gamma_w}+2-2n=0 \tag{16.4}$$

that is to say,

$$n=\frac{2-\frac{\gamma_b}{\gamma_w}}{2} \tag{16.5}$$

Taking into consideration that the value of γ_b/γ_w can be assumed to be 2.4, it follows that $n=-0.2$, which means that the upstream face, in order to obtain the most economical solution, should have an inverse inclination. And, since such a profile, i.e. cross-section, which is hanging over the ground, is inconvenient for execution, it can be concluded that from the aspect of economy, and for fulfilling the first requirement, the most favorable cross-section of the dam is a right-angled triangle with a vertical upstream face.

The second requirement – stability of the dam against sliding across the foundation – can be represented by means of the expression:

$$k_s\,W_1=f\cdot W \tag{16.6}$$

where f is the coefficient of friction of the dam across the foundation, and k_s is the coefficient of safety. Since $W_1=\gamma_{wH}^2/2$, and $V=(BH/2)(\gamma_b+\gamma_w n-\alpha_1\gamma_w)$, it will be:

$$k_s\gamma_w\frac{H^2}{2}=f\frac{BH}{2}(\gamma_b+\gamma_w n-\alpha_1\,\gamma_w) \tag{16.7}$$

from where:

$$B=k_s\frac{H}{f\left(\frac{\gamma_b}{\gamma_w}+n-\alpha_1\right)} \tag{16.8}$$

For example, in the case of a rock foundation, for $n=0$; $f=0.7$; $\gamma_b/\gamma_w=2.4$; $\alpha_1=0.5$ and $k_s=1$ (which means, a case of limited equilibrium) it follows:

$$B=\frac{H}{0.7(2.2+0-0.5)}=\frac{H}{1.33}\approx 0.75H$$

If there is no seepage force of uplift ($\alpha_1=0$), it will be:

$$B=\frac{H}{0.7\times 2.4}\approx 0.6H$$

In the case of a soil, i.e. non-rock, foundation, the coefficient f decreases to 0.4–0.5 for sand and down to 0.2–0.3 for clay. Consequently, the width B becomes much greater in relation to the required one for satisfying the requirement that tensile stresses should not occur.

16.3.3 Practical cross-section

Under real conditions, there are also other forces acting on the dam, and not only the forces due to water and due to self-weight (Fig. 4.1). That imposes the necessity of modifying the triangular cross-section. Thus, the seismic forces and forces due to sediment and ice can require an inclination of the upstream slope – fully or partially (2, Fig. 16.2b). The necessity for providing freeboard is a condition for overbuilding (1) which, in some instances, can impose the need of warping the downstream slope.

Endeavours are to be made so that sloping of the upstream face should be as small as possible, since, by means of warping of the inclination, there is an increase of the maximum principal stresses at the points of the slope. Thus, owing to the effect of the listed additional forces, and because of the necessity for widening of the foundation and the stability or reducing of the stresses in the foundation, it is almost always essential to provide a certain inclination. The optimum height of the inclination of the upstream slope can be determined by means of the level where the line of attack of the mass of the crest (the hatched part in Fig. 16.5) intersects the straight line joining the contact of water with the dam, and the point which is distant from its projection on the base for one third of the width, as has been shown in Figure 16.5.

The execution of a spillway over the dam requires lowering the crest level in the zone of the overflowing part, in order to ensure an overflowing height H_0 (Fig. 16.6), as well as its particular shape. The overflowing crest (1) can be positioned at the elevation of the normal level, so that, in the case of a raising of the water level in the reservoir, water automatically overflows the crest. Another case occurs when the overflowing crest is positioned lower than the normal level, where it is necessary for the spillway to be provided with gates for regulating the level of the water, as well as the overflowing water quantity.

The crest and downstream face of the mass overflow dam are shaped according to the form of the overflow current. If, along the entire length of movement under the

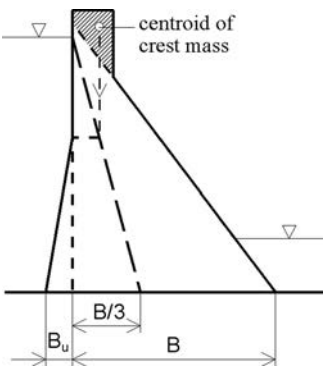

Figure 16.5 Sloping of the upstream face.

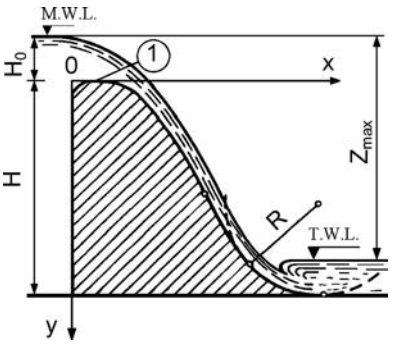

Figure 16.6 Vacuumless overflow profile, curvilinearly jointed with the stilling basin.

Table 16.3 Data for drawing a vacuum-less profile.

N°	x	y	N°	x	y	N°	x	y	N°	X	y
1	0.0	0.126	11	1.0	0.256	21	2.0	1.235	31	3.0	2.824
2	0.1	0.036	12	1.1	0.321	22	2.1	1.369	32	3.1	3.013
3	0.2	0.007	13	1.2	0.394	23	2.2	1.508	33	3.2	3.207
4	0.3	0.000	14	1.3	0.475	24	2.3	1.653	34	3.3	3.405
5	0.4	0.006	15	1.4	0.564	25	2.4	1.894	35	3.4	3.609
6	0.5	0.025	16	1.5	0.661	26	2.5	1.960	36	3.5	3.818
7	0.6	0.060	17	1.6	0.764	27	2.6	2.122	37	3.6	4.031
8	0.7	0.100	18	1.7	0.873	28	2.7	2.289	38	3.7	3.249
9	0.8	0.146	19	1.8	0.987	29	2.8	2.462	39	3.8	*4.471*
10	0.9	0.198	20	1.9	1.108	30	2.9	2.640	40	3.9	4.698

water current, pressure is maintained, which is equal to or greater than atmospheric, then such a dam is called an overflow dam with a *vacuumless profile*. On the other hand, if under the overflow current there has been generated a vacuum, then such a dam is called a dam with a *vacuum profile*. The area of the cross-section of the vacuum dam is 15–25% smaller in relation to the vacuum-less dam, while the coefficient of discharge is 7–15% greater. In the case of vacuum profiles, due to the entrance of air below the water current, there occur vibrations, which decrease the stability of the dam; there is also the possibility of the occurrence of cavitational erosion. That is why this profile is recommended only for lower pressures.

Drawing the vacuumless profile can be performed according to the data given by Kreager-Officeroff, (Table 16.3 and Fig. 16.6), by means of which it is possible to determine the coordinates x and y of the overflow profile at a height of the overflow, i.e. discharge, of 1 m. For obtaining the real coordinates, the tabulated value of x and y should be multiplied by the real height of the overflow. The construction of the vacuumless profile is constructed so that, first of all, a triangular profile is drawn with the required width B (Fig. 16.7a), and then, according to the data from Table 16.3, the vacuumless profile P is drawn. The joint of the dam with the absorption basin

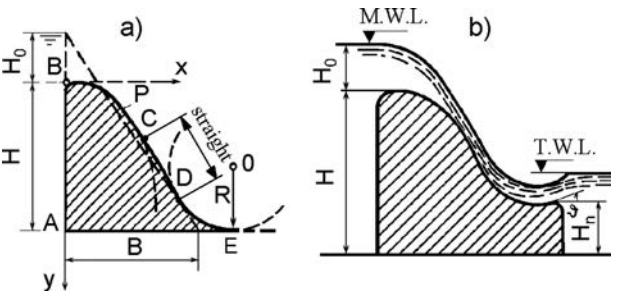

Figure 16.7 Structure of a vacuumless profile (a) and a dam with vacuumless profile ending with a sill bucket (b).

(stilling pool) is most often constructed by means of a circular curve with a radius R, so that such a curve touches the downstream slope at point D and the base of the dam at point E. The point D is obtained when, from a certain point C, according to which the theoretically obtained profile becomes steep, there is drawn a tangent up to the section with the theoretical profile. For high dams on rock foundations and an overflow height up to 5 m, the radius of curvature is obtained from the expression:

$$R = (0.25 \div 0.5)(H_0 + Z_{\max}) \tag{16.9}$$

where $Z_{\max}$ is the distance between the maximum level of the headwater and tailwater (Butakov, 1995).

In cases where the overflow water can safely be discharged directly into the river channel without the construction of a stilling basin, the dam ends up with a sill bucket through which the overflow water can be thrown away a certain distance from the structure (Fig. 16.7b). The path of that overflow water depends on the energy of the water current at the end of the sill bucket, as well as on the angle at which the overflow water leaves the sill bucket. The angle ν, which the end of the sill bucket closes with the horizontal, usually ranges from 20 to 45°, and a value of 30° is recommended. The radius of curvature of the sill bucket R should not be smaller than five depths of the water. In dimensioning this type of massive dam, in addition to other forces, it is necessary to take into consideration the hydrodynamic force on the sill bucket.

When an overflow dam is provided with gates (both operational and overhaul) it is necessary to carry out a rectilinear part, with a length that depends on the dimensions and type of gate. In such a case, the profile is constructed up to the intersection with an x-axis, and afterwards there is left the necessary horizontal part. We then proceed with the construction of the contour with a y-axis shifted into the position y' (Fig. 16.8).

16.4 DIMENSIONING OF CONCRETE GRAVITY DAMS

The first gravity dams were constructed as vertical masonry walls. Then, to enhance the dam stability and to reduce its volume, the downstream face was sloped. But high gravity dams failed despite this improvement. However, the investigations of the

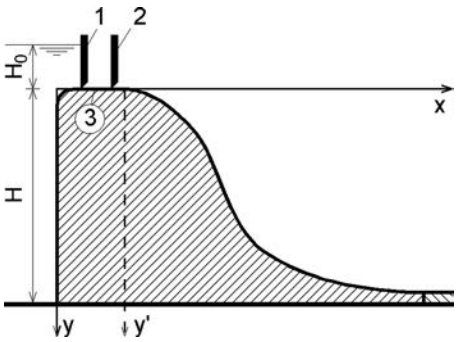

Figure 16.8 Overflow dam with gates (schematically). (1) Overhaul gate; (2) operational gate; (3) rectilinear part.

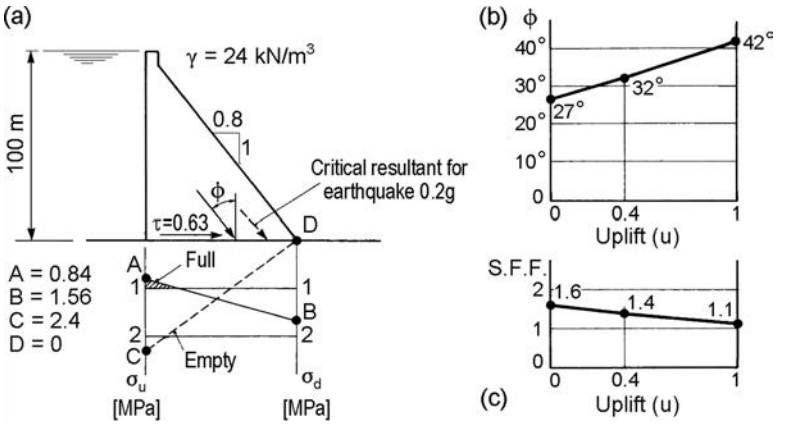

Figure 16.9 Gravity dam stresses and stability (after Londe & Pino, 1992).

failures led to the discovery at the end of 19th century of the effect of uplift forces. Two design criteria were then proposed, which are still used today:

$$\sigma_u - \gamma_w H > \sigma_t; \quad \text{Maurice Lévy condition, and} \tag{16.10}$$

$$\frac{d\sigma_u}{da} > 0; \quad \text{Oscar Hoffman condition} \tag{16.11}$$

where: σ_u = total vertical upstream stress; γ_w = unit weight of water; H = height of reservoir water; σ_t = uniaxial tensile strength of concrete; a = length of crack measured from the upstream face.

These conditions led to the usual optimum gravity dam profile on rock foundation, with a vertical (or almost vertical) upstream face and a downstream face inclined to approximately 0.8:1 (H:V). As an introduction of the dimensioning of the gravity dams, a rough analysis of a typical 100 m-high gravity dam will be given (Londe & Pino, 1992). In Figure 16.9a the stresses at the base of such a typical gravity dam are shown

(all stresses in this consideration are proportional to dam height). Point A shows that a compressive stress of only 0.84 MPa develops at the heel of the dam, calling for a tensile strength of 0.16 MPa to satisfy Lévy's condition. The Hoffman condition is just satisfied with no safety margin. However, much greater tensile strength is required in the event of an earthquake, should cracking be considered detrimental to safety. For example, assuming an earthquake acceleration of 0.2 g, tensile stresses in the range 1 to 2 MPa (depending on the rigidity of the foundation, the recording interval of the time history, and so on) would occur at the heel, giving rise to a serious risk of cracking. Another important fact is that the gravity dam develops stresses at its foundation that vary considerably between empty and full reservoir conditions, that is, during impounding or drawdown operations. The comparison of line AB with line CD in Figure 16a illustrates this behaviour.

As far as shear strength is concerned, a mean shear stress $t = 0.63$ MPa is obtained. However, the most significant criterion is the angle ϕ, measuring the inclination of the resultant to the vertical. This inclination depends on the uplift assumption. Figure 16.9b gives ϕ in terms of the uplift u ($u = 0$ meaning no uplift, $u = 1$ full triangular uplift, $u = 0.4$ uplift reduction to 40 percent of full triangular uplift). The values of ϕ indicate that a reasonably good rock foundation is necessary (with ϕ no less than 32°), particularly when considering that $u = 0$ (no uplift) is not realistic because of the impossibility of controlling completely the seepage flow under the dam. Conversely, even with the usual assumption that $u = 0.4$, it may happen that, with time, the grout and drainage curtains deteriorate to the point that $u = 1$ would apply. For years, gravity dams were designed with a resultant 37° ($\tan \phi = 0.75$), requiring extensive drainage.

Another criterion which has been widely used, although it is questionable, is the Shear Friction Factor (S.F.F.), for which an assumption is made for the friction angle and the cohesion of the foundation rock (see also Section 16.7.1). In Figure 16.9c, the set $\phi = 30°$ and $c = 0.3$ MPa was chosen. It corresponds to a rock mass of moderate strength. For $u = 0.4$, one obtains S.F.F = 1.4 which could hardly be considered as adequate; in the event of $u = 1$, the value would be as low as SFF 1.1 (Londe & Pino, 1992).

The above-described example of a hypothetical dam 100 m in height, gives an idea regarding the gravity dam dimensions, as well as regarding significant limitations imposed by the foundation quality and the possibility to control the uplift forces.

Assuming the cross-section, using the assumptions of the previous sections, the dimensioning of concrete gravity dams is performed and, afterwards, a check-up is carried out of stresses in the dam's body and its foundation, as well as the stability, for three states:

1. *State of full reservoir*, in service conditions, when the dam is subjected to all possible forces with the most adverse possible effect. This is the basic state.
2. *State following the construction of the dam*, when forces due to water do not yet exist, while there act forces due to self-weight and seismic forces due to the concrete mass, directed in the most adverse direction and course.
3. *Overhaul state*, when repairs are carried out in a certain part of the dam.

The primary regime of loading of gravity dams on a rock foundation is fixed. There are few possibilities for deviation from the standard practical cross-section (Fig. 16.2b),

with a downstream face 1:0.75. That is why, in the designing of small gravity dams on a rock foundation, such geometry can be changed, along with a checking-up of stresses and minimum necessary modifications, if they are essential.

In the case of more significant, i.e. larger, dams, an original profile has to be defined in order to enable a satisfying of the specific requirements. For that purpose, it is possible to use two elementary methods – the method of layers and the method of full profile, which fall within what is called *gravitational method*. These methods are based on a determination of the width of the cross-section of the dam under the conditions that normal tensile stresses should not appear. In contemporary practice, high dams are dimensioned by the trial loads method or, even more frequently, by the Finite Element Method, which enables a complete comprehension of the state stresses-deformations in the dam's body and the foundation, with a possibility of true simulation of the boundary conditions.

16.4.1 Elementary methods

16.4.1.1 Method of layers

With this method the cross-section of the dam is divided into horizontal layers with a height, i.e. thickness, of from 5 to 10 metres (I to V, Fig. 16.10) and then the width of each layer is determined from the condition at full of the reservoir, the result of forces acting at the downstream edge of the core (middle third) of the cross-section. In that way, since all forces and lever arms can be expressed through the unknown width of layer B_n, the following equation is obtained:

$$f(B_n) = 0 \tag{16.12}$$

By solving the above, the width of layer B_n is obtained. Normal edge stresses are obtained from the well-known expression (16.2), and then diagrams of σ_y are drawn, as is shown in Figure 16.10. If in an empty reservoir there appear tensile stresses in the downstream edge of the layer, it is necessary to perform a slight sloping of the upstream face and to repeat the calculations.

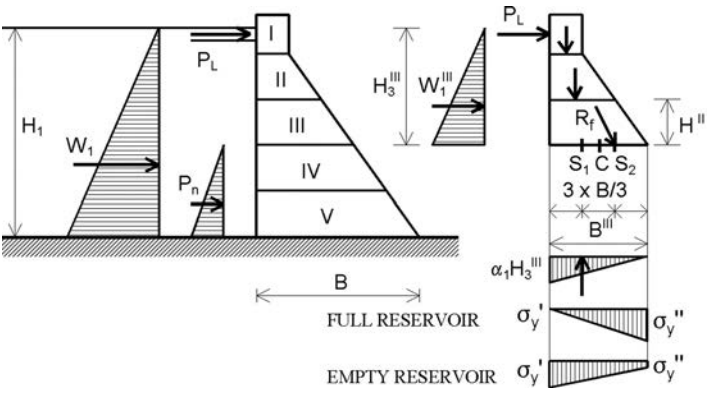

Figure 16.10 Dimensioning of gravity dam according to the method of layers.

16.4.1.2 Full profile method

With this method there is a consideration of the entire cross-section of the dam (Fig. 16.11) under the action of all forces, including the inertial forces due to the mass of water and concrete. All the forces are expressed through the unknown quantities x and y, in which $B = x + y$. The most economical width of the dam, with a fulfilled condition that, in the lowermost (most loaded) part only compressive stresses would appear, is obtained from the condition that, at a full reservoir, the result of forces R_f should act at the downstream edge of the core (middle third) of the cross-section S_2, while at an empty reservoir (R_e) it should act at the upstream edge S_1 (Fig. 16.11). In that way, two equations are

$$\begin{aligned} f_f &= (x, y) = 0 \\ f_e &= (x, y) = 0 \end{aligned} \tag{16.13}$$

whose solutions, as a system, we obtain the unknown quantities x and y. The indices f and e denote a full and empty reservoir, respectively. For such a defined cross-section, we perform a check-up of normal stresses also for the higher sections.

16.4.2 Modern methods

Simplifications and many approximations, on which elementary methods are based, make them less and less applicable, with the increase of the dam's height. This is especially emphasized in narrow dam sites with steep abutments. With the increase of the height, there comes about an increasingly greater interaction between the adjacent blocks, which results in a transfer of forces and a more complex response of the structure. Such an interaction increases the filling of joints (by grouting or with another method), and it is much more emphasized with the possible non-uniform deformations of the foundation. In such cases, it is indispensable to apply more sophisticated

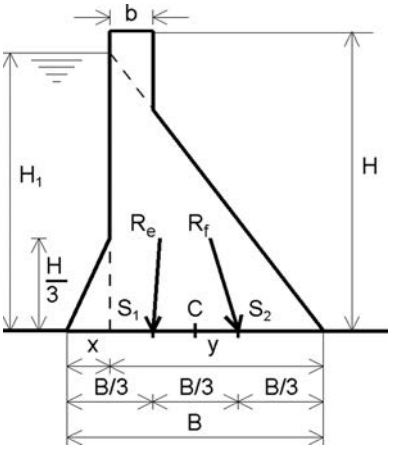

Figure 16.11 Dam dimensioning according to the full profile method.

methods, two of which are used in practice – the *trial loads method* and *the finite element method*.

In the *trial loads method,* which will also be dealt with in Chapter 20, and which is devoted to arch dams, an assumption is made that the dam is divided by horizontal and vertical planes into horizontal beams and vertical cantilevers, upon which the loads are distributed, so that the deflection of the beams and cantilevers is equal at each joint point of all beams and cantilevers. This method is particularly suitable when, as a consequence of steep banks, a considerable rotation is expected in the vertical cantilevers. At the same time, as a result of interaction among the cantilevers, there appear torsional moments. Also, there also comes about a certain transfer of the load of the water into the steep banks. This causes a redistribution of stresses. Thus, the loads will be taken as a combination of the action of the cantilevers, horizontal beams, and the rotation, i.e. torsion (USBR, 1976, 1977).

The analysis according to this method for gravity dams is carried out by dividing the dam into sections of vertical and horizontal longitudinal elements, each with a unit thickness, interconnected at the intersecting points. Thus, the loads are distributed proportionally to the elements, depending on their structural character and then the deformation in each intersection point is determined. For a proper distribution of loads, in which at all intersecting points there will be satisfied the condition:

$$\delta_{\text{cantilever}} = \delta_{\text{beam}} = \delta_{\text{torsion}} \tag{16.14}$$

It is necessary to carry out a procedure of an iterative solution of a complex field of equations. The analysis by this method, which appeared before World War II, yields good results. It is rather complex; however with the development of the computer technology it has become much more accessible. Yet, lately it has made room for the much more powerful and more flexible Finite Element Method.

The *Finite Element Method*, as has already been explained in Chapter 8, represents the most efficient method for an analysis and dimensioning of dams. In the analysis of concrete gravity dams, the flexibility and power of the FEM can be comprehended in its capability of encompassing the irregular geometry of the dam, insertion of the foundation with different layers of materials, taking into consideration secondary loadings, as well as the temperature effect, anticipation of the effect of cracks, openings of joints in the dam and the foundation, etc.

In the case of concrete dams a dilemma is imposed in an aggravated form: should a two-dimensional or a three-dimensional analysis be performed? The two-dimensional analysis, treating the problems as a plane state of stresses, is rational and cheaper than the three-dimensional one. However, in the case of steep banks, i.e. abutments, the three-dimensional effect cannot be neglected. Figure 16.12 shows the influence of the ratio $\beta = L/H$ on the lateral stress σ_2 in two sections (a–a and f–f). From the diagrams, it can be seen that the ratio L/H has a considerable influence on the lateral stress σ_2. In the future, taking into consideration the fast development of personal computers, which enable relatively cheap analysis, it is possible to expect the higher concrete gravity dams to be dealt with exclusively by the three-dimensional method, even for a dam of a significant length (Clough & Zienkiewicz, 1987). The development of numerous commercial software packages for three-dimensional analysis in the last decades has verified the validity of this statement.

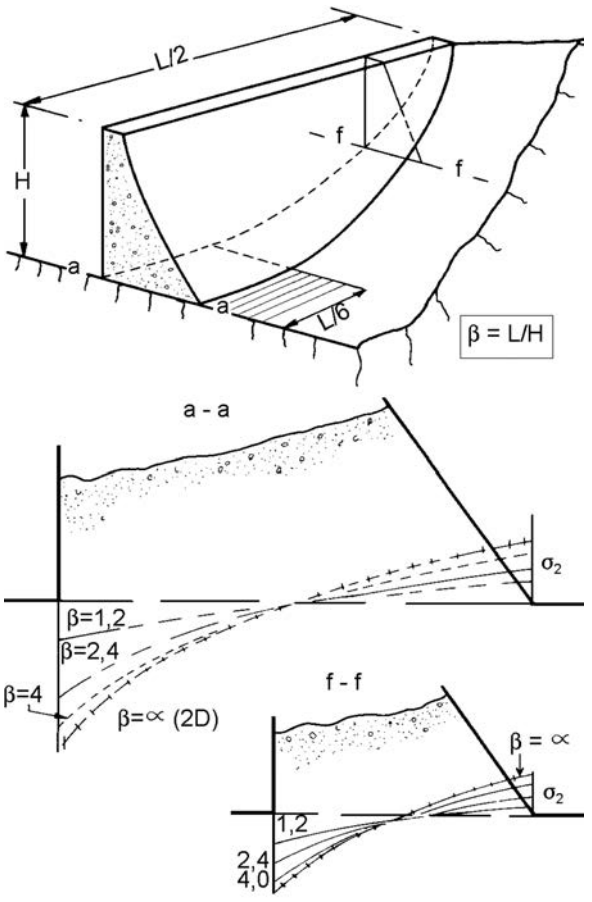

Figure 16.12 Three-dimensional effect in a concrete gravity dam ($\beta = 8$ represents a two-dimensional analysis).

By way of illustration of part of the capabilities and results that are obtained by analysis with FEM, there are presented the vertical displacements at the surface on the foundation under the effect of the self-weight of the dam (I) and the self-weight, together with the hydrostatic pressure of water (II) (Fig. 16.13) – in the case of a 16 m high dam on a rock foundation. The cross-section of the dam has been weakened by a gallery, upon which a possible crack in the concrete has been simulated. The foundation is encompassed to a depth as great as is the height of the dam, with a width upstream and downstream of the dam of twice the height of the dam. The numbers from 49 to 63 denote the points at the surface on the foundation of the dam displaced under the effect of loading – displacements are shown in a very enlarged scale (Clough & Zienkiewicz, 1987).

The application of FEM in the process of dimensioning of gravity dams in contemporary practice is obligatory. At the disposal of dam engineers are various widely spread

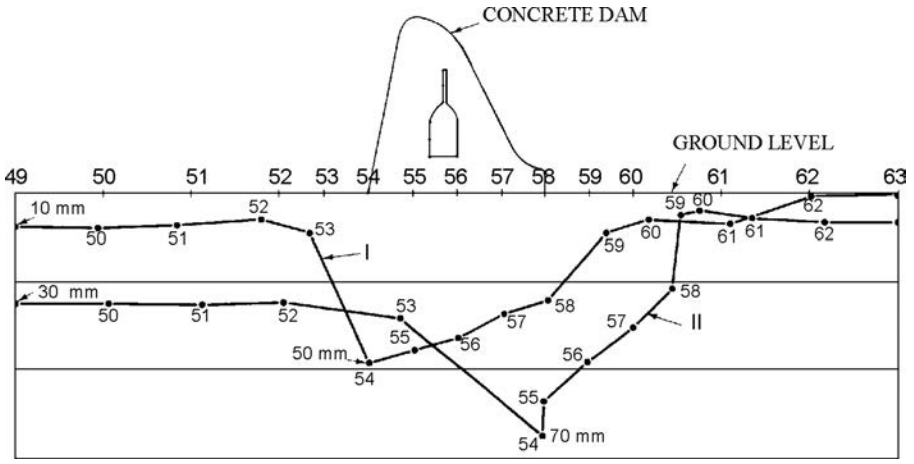

Figure 16.13 Vertical displacements at the surface of the foundation of a concrete dam, calculated by the Finite Element Method.

general software packages for structural analysis, as well as modules especially aimed at concrete dam analysis. Most of them contain features enabling powerful analyses to be performed, including: coupled thermo-stress analysis, Young hardening concrete behaviour, time temperature and maturity dependency, discrete and smeared crack analysis, dedicated post-processing of crack patterns, etc. Various material models are also available, like: linear, nonlinear and hyper elasticity; Mohr-Coulomb and Drucker-Prager; multi-directional fixed crack model; total strain crack models; models for joints; viscoelasticity; shrinkage; linear elastic and plastic reinforcements, etc. The software packages have large manuals explaining the theory and applications in detail. The dam engineer can design the dam cross-section with all necessary elements, and then he can choose the method of analysis and appropriate constitutive laws. The computer will perform the analyses and will offer an output with large quantity of results like stresses, deformations, temperature variations and stability. But a wise engineer comprehends well that calculations are just the basis for further, sounder engineering judgment.

16.5 DETERMINATION OF STRESSES

For checking the obtained dimensions of a concrete gravity dam and for the assessment of its operation, it is necessary to calculate the stresses in its body. In every good analysis, it is necessary to determine:

1. Vertical normal stresses σ_y, on horizontal planes;
2. Horizontal and vertical shear stresses τ_{xy} and τ_{yx};
3. Horizontal normal stresses σ_x, on vertical planes;
4. Principal stresses σ_1 and σ_3 by direction and magnitude.

The determination of stresses can be carried out in a relatively simple way with the gravitational method or by methods based on the theory of elasticity. The Finite

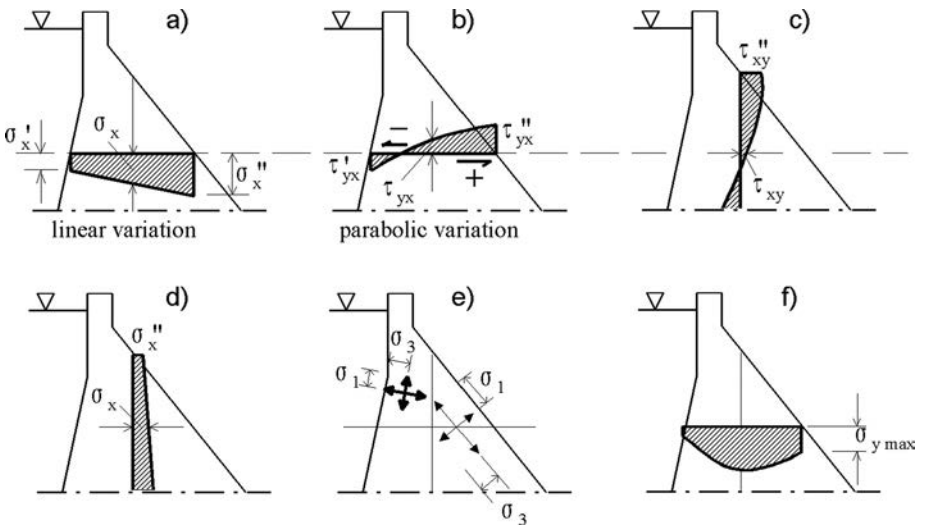

Figure 16.14 Schematic presentation of distribution of stresses in the dam's body.

Element Method, briefly described in the previous sub-section, obtains the best and most abundant results.

16.5.1 Determination of stresses by the gravitational method

The gravitational method for the analysis of stresses is simple and is based on assumptions from the theory of elasticity. This method assumes that the 'trapezium law' is valid; that is to say, it assumes that normal stresses vary linearly between the upstream and the downstream face in all horizontal planes. More rigorous analyses show that this assumption is not valid in the zone close to the foundation owing to the concentration of stresses at the ends of dam. This method is suitable for dams dimensioned with elementary methods, i.e. those in which there has not been anticipated monolithization of the joints between blocks.

Figure 16.14a-d presents diagrams for: normal stresses σ_y, over a horizontal plane (a), shear stresses over a horizontal plane, τ_{yx} (b), shear stresses on a vertical plane, τ_{xy} (c) and normal stresses on a vertical plane, σ_x (d), all of them obtained by means of the gravitational method of analysis. There is a noticeable distribution of normal stresses across the plane. Diagrams (e) and (f) present the principal stresses at various points and normal stresses at the horizontal plane σ_y, with nonlinear distribution, obtained by the powerful Finite Element Method (Novak et al., 2001).

Vertical normal stress σ_y in an arbitrary plane, according to this method, is determined by the expression for eccentric stresses for beams, along with certain modifications:

$$\sigma_y = \frac{\sigma V}{A} \pm \frac{\sigma M \cdot x'}{I} \tag{16.15}$$

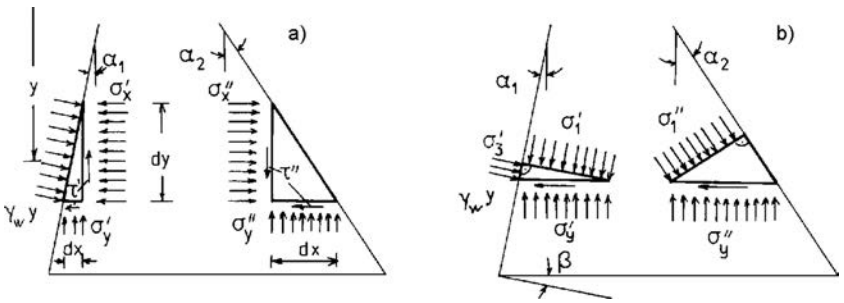

Figure 16.15 Scheme for determination of stresses upon slopes of a dam.

where ΣV is the vertical resultant force acting over the considered plane, A is the area of the plane on which the forces act (in a two-dimensional analysis $A = B \times 1$, ΣM is the sum of bending moments determined in relation to the centroid of the plane, x' is the distance from the neutral axis on the plane up to the point in which the stress σ_y is calculated, and I is the moment of inertia of the plane in relation to the centroid.

Maximum, and minimum stress, respectively, are obtained at the end of the dam from the expression (16.2), originating from the expression (16.15).

The normal horizontal stresses σ_x and the shear stresses $\tau_{xy} = \tau_{yx} = \tau$, can be determined from the conditions for equilibrium of the elementary triangles with cathetus dx and dy, extracted from the slopes in the cross-section of the dam (Fig. 16.15a).

Let us examine, as an example, the triangle extracted from the upstream face. At its sides with infinitesimal dimensions, there act the normal stresses σ_x and σ_y, the shear stress $\tau = \tau_{xy} = \tau_{yx}$, and hydrostatic pressure at a depth γ, equal to $\gamma_w \gamma$. If we apply the condition for equilibrium, the projection of all forces acting on the triangle over y-axis equal to zero, then we obtain:

$$\gamma_w y \frac{dx}{\sin \alpha_1} \sin \alpha_1 - \tau' dy - \sigma'_y dx = 0 \tag{16.16}$$

Following the substitution $dy = dx\ ctg\ \alpha_1$ and organizing the expression, it follows:

$$\tau = (\gamma_w y - \sigma'_y) \tan \alpha_1 \tag{16.17}$$

Examining the equilibrium with the projection of all forces over the x-axis, by analogy we obtain the expression for calculation of the normal horizontal stress:

$$\sigma'_x = \gamma_w y - (\gamma_w y - \sigma'_y) \tan^2 \alpha_1 \tag{16.18}$$

In the same way, the downstream slope is obtained:

$$\tau'' = \sigma''_y \tan\ \alpha_2 \tag{16.19}$$

$$\sigma''_x = \sigma''_y \tan^2 \alpha_2 \tag{16.20}$$

With known edge stresses, one can easily determine the stresses in the interior of the dam's body, with an assumption of their linear distribution between the ends, which can be accepted for rough engineering calculations, since the real distribution of stresses is curvilinear.

For determination of the strength characteristics of concrete in the dam's body, the principal stresses and maximum shear stresses are the governing ones. The principal axes are rotated in relation to the x–y coordinate system for an angle β, (Fig. 16.15b), which can be calculated by means of the expression:

$$2\beta = -\frac{2\tau}{\sigma_x - \sigma_y} \tag{16.21}$$

in which the minus sign denotes that the axes are rotated clockwise. Principal stresses are calculated by the well-known expression:

$$\sigma_{1,3} = \frac{1}{2}(\sigma_x + \sigma_y) \pm \frac{1}{2}\sqrt{(\sigma_x - \sigma_y)^2 + 4\tau} \tag{16.22}$$

Maximum shear stresses appear for axes, rotated in relation to the principal ones, at an angle of 45° and are calculated from the expression:

$$\tau_{max} = \pm\frac{1}{2}(\sigma_1 - \sigma_3) \tag{16.23}$$

In the case of gravity dams, for the point at the external sides of the dam, the principal axes are set up in such a manner that one of them coincides with the external face of the dam, while the other one is perpendicular to it. Namely, across the surface of the external faces of the dam, the shear stresses are zero, which means that they are the principal axes for one of the principal stresses. In addition to the formula (16.22), the magnitude of the principal stresses in the external faces of the dam can also be determined from the conditions for equilibrium of elementary right-angle triangles, whose cathetus coincides with the principal axes (Fig. 16.15b).

The principal stress σ'_1, which acts perpendicular to the upstream face of the dam, is obviously equal to the hydrostatic pressure:

$$\sigma'_1 = \gamma_w y \tag{16.24}$$

By projecting along the y-axis of all forces acting on the triangle in the upstream face, one obtains:

$$\gamma_w y\,dx \sin\alpha_1 \sin\alpha_1 + \sigma'_3 dx \cos\alpha_1 \cos\alpha_1 - \sigma'_y dx = 0 \tag{16.25}$$

from where the second principal stress σ_3 will be:

$$\sigma'_3 = \frac{\sigma'_y - \gamma_w y \sin^2\alpha_1}{\cos^2\alpha_1} = \sigma'_y\left(1 + \tan^2\alpha_1\right) - \gamma_w y \tan^2\alpha_1 \tag{16.26}$$

By analogy, from the downstream face, it will be:

$$\sigma_1'' dx \cos\alpha_2 \cos\alpha_2 - \sigma_y'' dx = 0 \tag{16.27}$$

from where:

$$\sigma_1'' = \frac{\sigma_y''}{\cos^2\alpha_2} = \sigma_y''(1 + \tan^2\alpha_2) \tag{16.28}$$

The second principal stress is $\sigma_3'' = 0$, if there is no water at the downstream face.

For the case of an empty reservoir, all of the quoted formulae may be used, by inserting $\gamma_w = 0$.

16.5.2 Calculation of stresses by using the theory of elasticity

The application of the theory of elasticity enables calculation of stresses not only along the faces of the dam, but also in the interior of the cross-section. In this case too, the problem is dealt with as a plane problem. Let us examine the case when, on the dam, there act forces due to self-weight and the hydrostatic pressure of the water. For simplification, the cross-section of the dam will be treated as a triangle, with an assumption that water reaches the top, i.e. the vertex, of the triangle, while the force due to seepage uplift will be neglected. In accordance with the theory of elasticity, stresses at a certain point of such a section with an infinite height (Fig. 16.16) are expressed as linear functions of the coordinates:

$$\begin{aligned} \sigma_x &= a_1 x + b_1 y \\ \sigma_y &= a_2 x + b_2 y \\ \tau &= a_3 x + b_3 y \end{aligned} \tag{16.29}$$

The coefficients of these equations are obtained by the analysis of stresses within the boundaries of the dam, and they amount to:

$$\begin{aligned} a_1 &= \frac{\gamma_b}{(m_1+m_2)^2} m_1 m_2 (m_2 - m_1) + \frac{\gamma_w}{(m_1+m_2)^2} m_1 m_2 (m_1 m_2 - m_2^2 - 2) \\ b_1 &= \frac{\gamma_b}{(m_1+m_2)^2} 2 m_1^2 m_2^1 - \frac{\gamma_w}{(m_1+m_2)^2} m_2^2 (2 m_1^2 m_2 - 3 m_1 - m_2) \\ a_2 &= \frac{\gamma_b}{(m_1+m_2)^2} (m_2 - m_1) - \frac{\gamma_w}{(m_1+m_2)^2} (m_1^2 + 3 m_1 m_2 - 2) \\ b_2 &= \frac{\gamma_b}{(m_1+m_2)^2} (m_1^2 + m_2^2) - \frac{\gamma_w}{(m_1+m_2)^2} (m_2 - m_1 - 2 m_2^2 m_1) \\ a_3 &= \gamma_b - b_2; \quad b_3 = -a_1 \end{aligned} \tag{16.30}$$

where $m_1 = \tan\alpha_1$, and $m_2 = \tan\alpha_2$.

The principal normal and maximum shear stresses are calculated from the expressions (16.22) and (16.23).

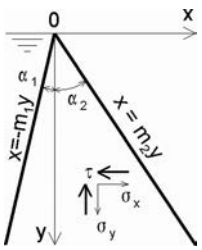

Figure 16.16 Scheme for calculation of stresses using the theory of elasticity.

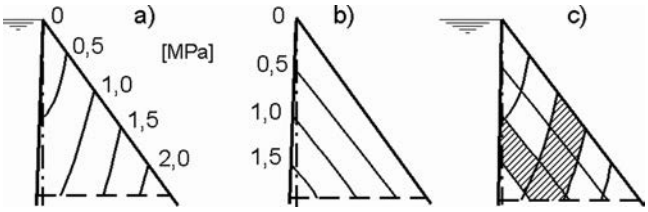

Figure 16.17 Isostates of principal stresses 1.

Stresses in the faces of the dam are obtained from the equations (16.29) and (16.30), substituting $x = -m_1 y$ for the upstream slope, and $x = m_2 y$ for the downstream slope. For example, stresses σ'_y and σ''_y in such a case will be calculated with the expressions:

$$\sigma'_y = a_2 x + b_2 y = (-a_2 m_1 + b_2) y \tag{16.31}$$

$$\sigma''_y = a_2 x + b_2 y = (a_2 m_2 + b_2) y \tag{16.32}$$

The state of stresses in the dam's body can be pictorially presented by means of lines of equal stresses – isostates, as well as with curves indicating the direction of the action of stresses – trajectories of stresses.

The isostates of any of the stresses can be drawn according to the equations (16.29) and (16.30). For example, for a constant value $\sigma = \text{const.}$, and from the equation $\sigma_x = a_1 x + b_1 y = \text{const.}$, for different values of the abscissa x, there are obtained appropriate values of the ordinate y. By connecting the thus obtained coordinates, we obtain a line along whose length the horizontal normal stress σ_x is of a constant value.

Figure 16.17 presents the isostates of the principal stresses σ_1 in the dam for the case of a full reservoir (a) and an empty reservoir (b), obtained according to the theory of elasticity (Grishin et al., 1979).

If the curves for both cases are presented in one drawing (c), then one can simply separate the zones in the dam's body in which there is the possibility of an occurrence of stresses within certain limits. For example, in the hatched zone there can occur compressive stresses within the limits from 1.0 to 1.5 MPa. In that way, it is possible to define the zones in the dam's body in which concrete of appropriate grade will be placed.

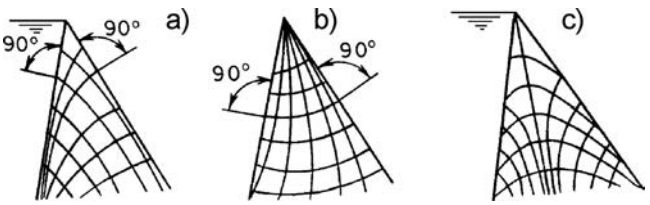

Figure 16.18 Trajectories of principal stresses (a, b) and maximum shear stresses (c).

Trajectories of the principal stresses are determined by means of the angle β, calculated at various points with the expression (16.21).

Figure 16.18 presents the trajectories of the greatest and the smallest principal stresses for a full (a) and empty (b) reservoir, as well as the trajectories of maximum shear stresses for a full reservoir. The trajectories of the principal stresses, σ_1 and σ_3, are mutually perpendicular, which results from the features of these stresses, while the trajectories of the maximum shear stresses form an angle of 45° with the trajectories of the principal stresses.

In the theory of elasticity, there have also been given methods for calculation of stresses due to the effect of a uniformly distributed load along the slope of the dam, due to the concentrated forces and moment; however, they will not be discussed here.

16.5.3 Calculation of stresses by using the Finite Element Method

The most efficient method for calculation of stresses at dams without any doubt is the finite element method. The fundamentals of the method are presented in Chapter 8, while a short description of its application in concrete gravity dams is given in section 16.42. For illustration of the calculation of the stresses in the dam body and in the foundation, just a small part of the result of a two-dimensional analysis of dam *Veles*, R. Macedonia (under design) will be presented.

Veles dam on river Vardar is designed as a concrete gravity dam with an overflow section in the middle. The dam height from the foundation is 64 m. The dam will form a reservoir with a total volume of 189×10^6 m^3. The dam is a key-structure of the hydraulic scheme with a main purpose of electricity production. The typical cross-section through the overflow part of the dam, together with part of the foundation, is shown in Figure 16.19.

To perform the analysis the following steps have been undertaken: (1) choice of constitutional laws and material parameters; (2) discretization of the dam cross-section; and (3) simulation of the dam construction process and reservoir filling.

The constitutive law for the concrete was adopted according to EC 2, concrete type 30. The stress-strain relation is shown in Figure 16.20 and is given by the following equation:

$$\begin{aligned} \sigma_c &= f_{cd}\left[1-\left(1-\frac{\varepsilon_c}{\varepsilon_{c2}}\right)^n\right] \quad \text{for } 0 \le \varepsilon_c \le \varepsilon_{c2} \\ \sigma_c &= f_{cd} \quad \text{for } \varepsilon_{c2} \le \varepsilon_c \le \varepsilon_{cu2}f \end{aligned} \tag{16.33}$$

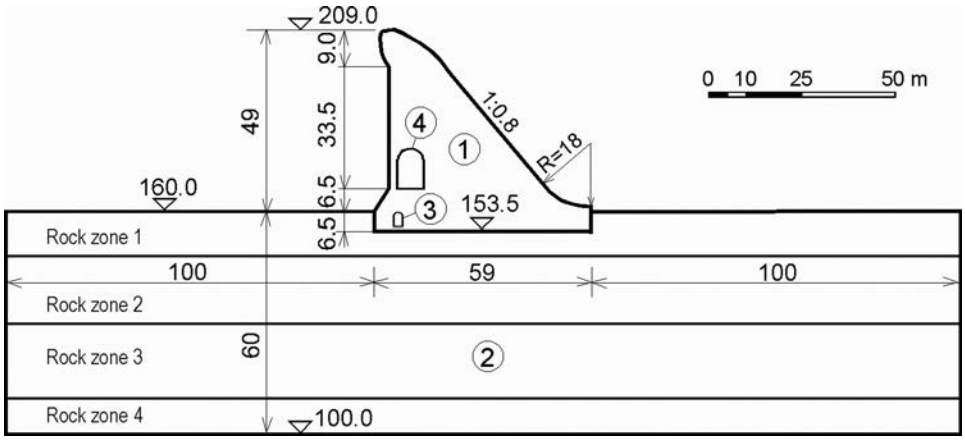

Figure 16.19 Cross-section through the overflow part of the Veles dam, together with part of the foundation (Mitovski, 2013). (1) Dam body; (2) rock foundation; (3) grouting gallery; (4) control gallery.

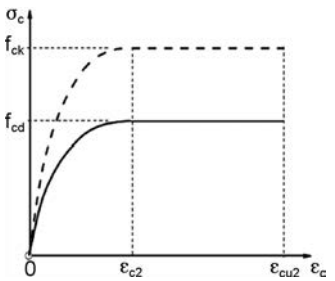

Figure 16.20 Stress-strain constitutive law for concrete.

Table 16.4 Parameters for the materials used in the analyses.

Material	*Elasticity modulus [N/mm²]*	*Poisson coefficient*	*Unit weight [kN/m³]*	*Nominal strength [N/mm²]*	*Coefficient of thermal expansion [$\times 10^{-6}$]*
Concrete	31,939	0.20	24	30	1.0
Rock foundation:					
Zone 1	4	0.25	26.3		
Zone 2	5	0.25	26.7		
Zone 3	8	0.25	26.7		
Zone 4	10	0.25	26.7		

where: f_{cd} = compression strength; n – exponent; ε_{c2} = strain at maximum strength; and ε_{cu2} = ultimate strain.

The parameters for the materials used in the analyses, including the schist foundation divided into four zones, are given in Table 16.4.

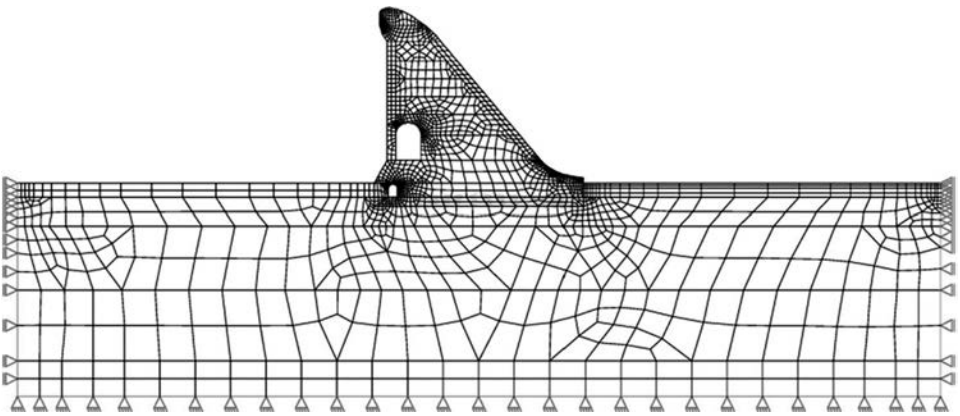

Figure 16.21 Finite element mesh of the dam and part of the foundation (1961 elements, 2172 nodal points, and 41 spring elements in the contact dam body – foundation) (Mitovski, 2013).

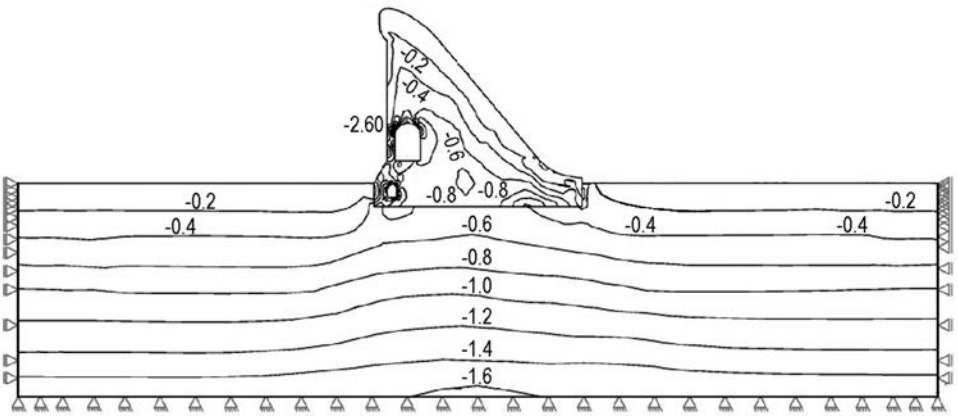

Figure 16.22 Lines of equal major normal stresses $\sigma_1 = (0.05 \div -2.60)$ MPa, where $(-)$ means compression; equidistance: 0.2 MPa (Mitovski, 2013).

The discretization of the dam and schist foundation, shown in Figure 16.21, was arranged so as to include four different zones of the foundation and to enable the simulation of the dam construction stages. In the contact dam body – rock foundation special spring elements were applied to enable differential movement in the contact. The mesh is denser in the sensitive areas near the openings where concentrated stresses are expected.

Figure 16.22 shows the lines of equal major normal stresses σ_1 in the dam cross-section for the reservoir full condition. The stresses have an expected distribution and intensity for a gravity dam around 50 m high. But a concentration of stresses is visible in the zone of the control gallery, where σ_1 reaches the value of -2.60 MPa. Above the grouting gallery tension stress appears, but with limited intensity.

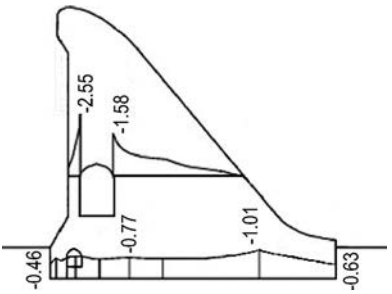

Figure 16.23 Vertical stresses σ_y in the contact dam body – foundation, and for a section through the control gallery for the stage of full reservoir (Mitovski 2013).

Vertical normal stresses σ_y in horizontal sections in the contact dam body – foundation, and through the control gallery for the stage of full reservoir are presented in Figure 16.23. In the later section, located in the top part of the vertical gallery walls there is a concentration of normal stresses near the opening. Maximum value of −2.55 MPa was calculated in the contact point of the straight and curved part of the gallery on the upstream side.

16.5.4 Influence of temperature changes, shrinkage and expansion of concrete on stresses in dams

The state of stresses in the dam's body of concrete dams does not depend only on the action of the external forces, but also on the volumetric deformations in the concrete, which arise from temperature changes and due to shrinkage of the concrete.

There are distinguished two types of temperature appearances in concrete dams, which arise from the properties of concrete: (1) during construction, there comes about a heating of the concrete due to the exothermic process for 15–25°C followed by its non-uniform cooling, because of which there occur compressive stresses, as well as tensile stresses; (2) in the period of the service life of the dam, there occur temperature stresses owing to oscillation in the temperature of the water and air which surround the dam.

First of all let us discuss the first appearance. We consider 1 m^3 of concrete placed in a block, which is in the interior of the dam. The examined concrete mixture possesses a certain initial temperature. The chemical reaction of hydration of the cement, which originates during setting and hardening of concrete, is an exothermic one – that is to say, releasing heat performs it. Because of that, there comes about a heating of the concrete in the initial period. Then there comes about a cooling of the external surfaces of the massive structure, which, as a consequence, yields a non-uniform distribution of the temperature, and this causes noticeable thermal stresses in the concrete, which can cause dangerous cracks through which there also easily comes destructive seepage. Because of that, thermal cracks are a major problem during construction and service, i.e. the operation, of mass concrete dams. In the course of time, in the central part of the

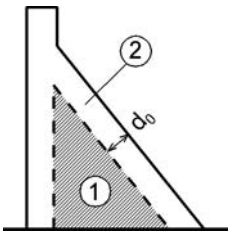

Figure 16.24 Internal region of the dam (1) and active zone (2).

dam (1, Fig. 16.24), there will be established a constant multi-year mean temperature T_{mean}, which is characteristic of the region in which the dam has been built.

Let us now also examine the second appearance. In the external parts of a concrete gravity dam (2, Fig. 16.24), the temperature in the course of service, i.e. operation, will vary depending on the temperature of the surrounding medium. The active zone (2) is of a thickness $d = 2–5$ m. Possible cracks, occurring in this zone, expand during the winter period.

A similar effect to the temperature changes, but to a smaller extent, is also caused by both shrinkage and swelling of the concrete. In this, volumetric deformations are manifested as: (1) reduction of the volume of the concrete as a result of physical and chemical reactions during its hardening; (2) reduction or increase in the concrete volume with the reduction or increase of its moisture in the course of construction, as well as later on, during the period of service. This occurrence also takes place only in the zone of the surface layer (2–4 m), since in the central zone the moisture, like the temperature, is constant in the course of the period of service. For reducing the harmful influences caused by the described appearances, and for preventing the appearance of cracks, the deposition of concrete into the dam is constructed in blocks of limited dimensions, so that, in the dam, there are formed temporary joints in the contacts between the blocks, which have a lower strength than concrete.

16.5.5 Permissible stresses and cracks

Stresses in concrete gravity dams occurring under the effect of primary loads are very low and they rarely exceed 2–3 MN/m^2, with the exception of very high structures. The factor of safety F_c, in relation to the permissible compressive stress in the concrete has not been specified. The criterion $F_c = 3$ is often used. USBR specifies values for F_c, depending on the combination of loads, Table 16.5. This table also presents appropriate factors of safety F_r for the rock in the foundation.

In the case of concrete gravity dams, also of interest is the analysis of the danger of the occurrence of cracks and the limits of their tolerance. It can be assumed that there will occur a horizontal crack at the upstream face when σ_{yu} (calculated without uplift), falls below the specified minimum value (Novak et al., 2001):

$$\sigma_{yu\,min} = \frac{k_d \gamma_w y - \sigma_t}{F_t} \tag{16.34}$$

Table 16.5 Permissible compressive stresses (after USBR 1976).

	Minimum factor of safety for compressive strength	
Combination of loads	F_c (concrete)	F_r *(rock)*
Normal	3.0	4.0
Exceptional	2.0	2.7
Extreme	1.0	1.3

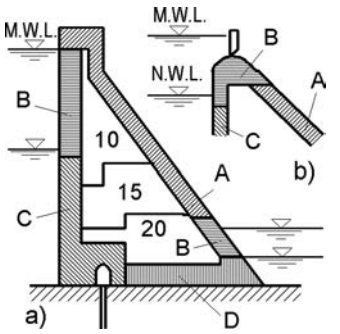

Figure 16.25 Schemes for zoning of concrete.

where k_d is the drainage factor ($k_d = 0.4$ for an effective drainage, $k_d = 1$ when there is no drainage); σ_t is the tensile strength of the concrete through a horizontal jointing surface; y is the depth below the water level; and F_t is the safety factor, dependent on the loading combinations (its value is 3.0, 2.0 and 1.0, like F_c in Table 16.5).

Normally, cracks are permitted only for an extreme combination of loading. It is assumed that the crack can be extended to the point where it is $\sigma_y = p_w$, where p_w is the water pressure. In such a case, the stability and stresses are reassessed for a section without a crack, while the dam is deemed to be safe if the stresses remain within the specified limits and if the stability against sliding has not been endangered.

16.6 GENERAL STRUCTURAL FEATURES OF GRAVITY DAMS

Zoning of the cross-section. The cross-section of gravity dams is constructed in zones of different characteristics (Fig. 16.25). In each zone, the concrete should satisfy the strength requirements, defined by the state of stresses. In the peripheral zones the concrete is also subjected to the influence of external factors – variations in the temperature of the air, seepage of water, erosion of overflow surfaces – so that the concrete, depending on its exposure to external influences, should also satisfy other requirements. Thus, for instance, in the zone which is always exposed to atmospheric influences, of which the most important are the temperature influences of the air (A, Fig. 16.25a), it is necessary to place concrete which is resistant to ice up to a depth not less than the depth of freezing of the concrete.

In the case of overflow dams discharge water flows with a high velocity along the downstream face; therefore; the concrete should be resistant to abrasion, as well as to the effect of cavitation if there is a danger of this happening (zone A, Fig. 16.25b). In zones in which there is a variation of water level (of the upstream and downstream face – zone B), the concrete must be resistant to water and ice, as well as water-impermeable. In zone C, which is permanently under water, it is necessary to place concrete, which is impermeable and stable in water. In zone D, the requirements in terms of impermeability can be modified, i.e. eased.

These cited limits of different zones are always encompassed within a division of the profile into zones. In doing so, the width of any one zone must not be less than 2 m (Grishin et al., 1979; Chugaev, 1985).

Improving the temperature regime. In order to improve the temperature regime of massive concrete works and to avoid cracks, the following measures may be undertaken (USBR, 1976; Golzé, 1977):

1. Maximum possible decrease in the hydration heat with proportioning minimum quantity of cement, sufficient only to obtain sufficiently hard, impermeable, and durable concrete, by using low thermal cement or by applying a mixture of cement and pozzolan, which reduces the generation of heat;
2. Placement of concrete with low temperature, if possible much lower than that of the environment, with artificial cooling of the constituent component of the concrete;
3. Artificial cooling of the placed concrete by means of circulation of cold water: (a) through a system of built-in pipes; (b) through a system of openings, drilled from galleries; or (c) through open vertical joints;
4. Continuous cooling of the surfaces of newly placed concrete up to a certain age by introducing water or by means of an artificially cooled formwork, which is not removed for a certain period.

The first three measures are most often used, because the fourth one depends on the time interval during the execution of the concrete blocks and their size. They are mainly used at the upper horizontal surface.

The second measure – precooling of the constituent component of concrete – is an economical and effective measure. In some cases, it may be sufficient to store the coarse aggregate in the shade and spray it with cold water. In other cases, it would also be necessary to perform cooling of the water used for preparation of the concrete mix to a temperature from 0 to 5°C. Another good method is the addition of pieces of ice into the concrete mixture. The coarse aggregate can be cooled down to a temperature of about 2°C by keeping it for a certain time in a large reservoir with cooled down water or by blowing in cooled air during its transportation on a rubber belt, which can also be employed for sand. By means of the quoted methods, it is possible to achieve a temperature of placement of the concrete of 10°C, while its considerable lowering would require a progressive increase of costs.

By means of the third method – artificial cooling of the placed concrete – two aims may be achieved: (1) lowering the temperature, raised by the development of hydrating heat; (2) lowering the temperature of the concrete in order to open the joints, which is necessary for performing their grouting; that is to say, for achieving what is called the *temperature of grouting the joints*. This is most frequently achieved by means

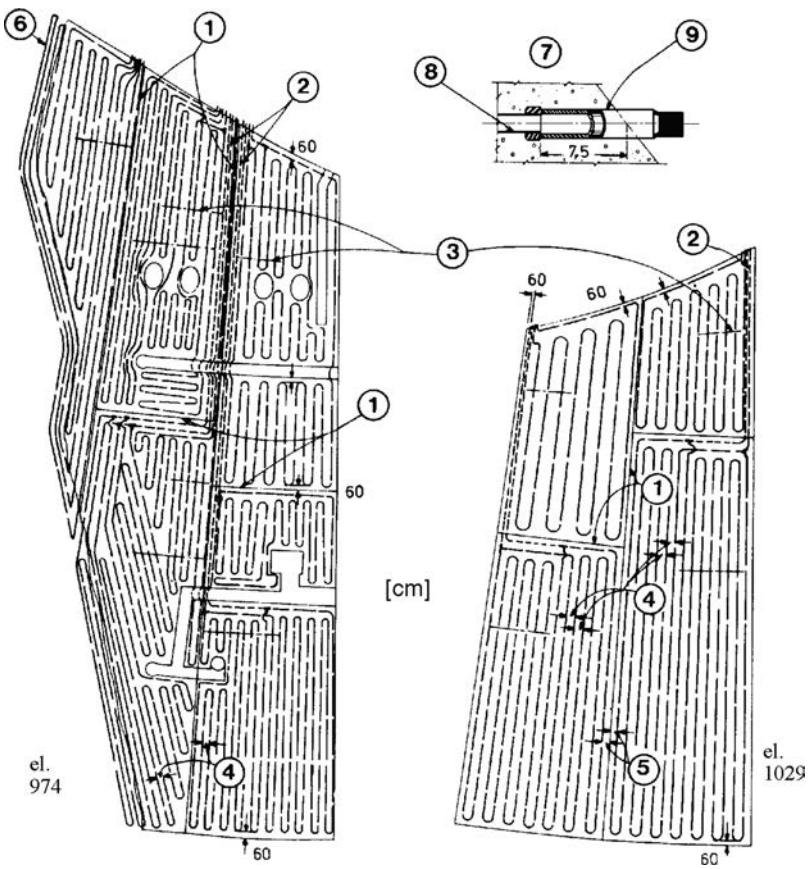

Figure 16.26 Layout of the cooling system in the Glen Canyon dam (USBR, 1976; Golzé, 1977). (1) Joints; (2) supply pipes; (3) thermal joint with wires; (4) specified distance, s = 1.20–1.80 m; (5) distances equal to (1/4–3/4) s; (6) pipe penetrating 60 cm into the rock; (7) detail of downstream slope; (8) thin-walled pipe of 25 mm diameter; (9) lining, which after cooling (or grouting, i.e. sealing of joints), is removed and the opening is filled.

of a system of built-in pipes in the dam's body. A typical layout of such a system is shown in Figure 16.26, constructed within the Glen Canyon (USA) arch-gravity dam (the problems of cooling the concrete and the construction of the joints are, mainly, common to various types of concrete dams and, in the greater part, are dealt with in this section). The system consists of pipes, which are spirally set up on the surface of each concrete block after hardening of the concrete. The spirals are formed by means of interconnecting metal thin-walled pipes. The supply and off take of water to the spirals is carried out by means of pipes, which are set up at the downstream face of the dam (sometimes manholes, galleries and vertical pipes in the dam's body are also used).

Spirals employ pipes of 25 mm in which the velocity of the cooling water should not be less than 0.3 m/s. Water is pumped, although there are also examples of gravitational systems. If artificially cooled water is used, then warm water returns into the system for

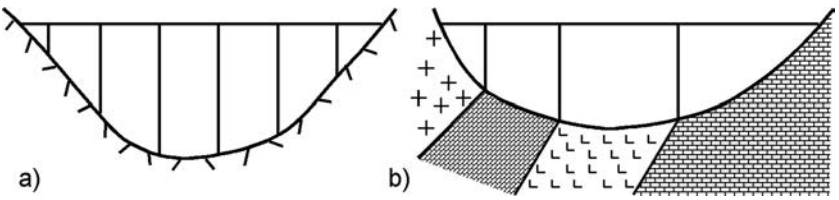

Figure 16.27 Permanent cross-joints in the dam. (a) Temperature joints; and (b) structural joints.

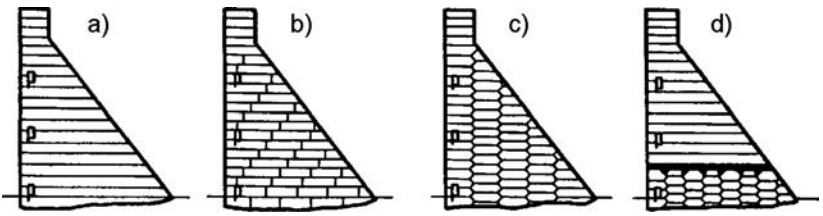

Figure 16.28 Division of dam into blocks during concreting.

reuse. It is necessary to avoid river water containing sediment, because of the danger of blocking the system. This method for controlling the temperature is effective, but is expensive. That is why it is necessary to perform a profound study of the conditions for its application, depending on the structure of the dam, composition of concrete, method of execution, and local conditions (USBR, 1976; Golzé, 1977).

For avoiding vertical cracks, which are very dangerous, and which originate due to tensile stresses during the winter period, when concrete shrinks owing to low temperatures, the dam is divided into sections with permanent vertical temperature joints, Figure 16.27a.

Along with the temperature joints, vertical structural joints are also made (Fig. 16.27b) in order to avoid cracks due to non-uniform settlement, caused by different degrees of stiffness of particular minerals forming the foundation of the dam.

Vertical joints are indispensable in the mass concrete, and sometimes transverse joints, spaced at 15 to 20 m, are also used. If the dam is very thick in its foundation (>40 m), then longitudinal joints spaced at 20 m are also beneficial.

Dam concreting by blocks. During concreting, the dam is divided into blocks according to one of the following schemes (Fig. 16.28, Grishin et al., 1979; Teleshev, 1982):

(a) *Sectional scheme,* with long blocks when the whole section of the dam, between the cross structural joints, is concreted in one block;
(b) By *covering the vertical joints between the blocks,* so that they are spaced one from another by 1/3–1/2 of the height of the blocks;
(c) In the form of *columns,* so that vertical joints are formed which, in the end, are cemented or concreted;
(d) By combining the quoted schemes.

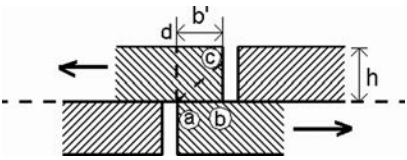

Figure 16.29 Sliding in the horizontal joint I-I caused by temperature deformations.

In the case of a sectional scheme, blocks are constructed of a small height (0.7–1.5 m), in order to create a favorable thermal regime, so that the difference between the internal and the external temperatures of the concrete, in the course of construction and operation, should not be greater than 17 to 20°C. In the contrary situation, cracks can appear in the blocks. This method has been successfully used in the Toktogul dam (Kirghizistan).

The method of covering the vertical joints between blocks is used with dams up to 50 m high. The length of the blocks amounts to 9–12 m, their height is 2–4 m, and in the vicinity of the foundation 1–2 m. With this scheme, for sliding along a horizontal joint I-I (Fig. 16.29), caused by temperature deformations, in the zone of the area ab with a length of b', a force of friction develops which can cause failure at the angle of the block along the surface ac, or breaking of the block across the surface ad. Because of that, it is necessary to endeavour to make the surface of the block as smooth as possible.

This scheme, according to which blocks up to 15 m long and 3 m high are constructed in the form of a column, one over another, allows greater speed in execution, since the individual blocks are independent of one another. In the course of construction, the blocks have a larger cooling surface, while the cementing of the joints between the vertical blocks is easier, as compared to the other schemes. This scheme facilitates simple and economical step-by-step construction and operation of the dam, which can be seen in the examples of the Bratskaya dam (Russia) and the Grande Dixens (Switzerland) (Fig. 16.30, Grishin et al., 1979).

Joints in the body of gravity dams. The following types of joints are differentiated in the body of gravity dams: (1) *deformation joints* (also called structural *joints* or permanent joints), which are kept in the process of the dam's operation, dividing its body into separate structural sections; (2) *temporary joints*, in the form of a cut or notch, which are cemented after hardening and cooling down of the concrete; (3) *working* or *functional joints*, which divide the dam into blocks during concreting, dividing the structural sections, separated with permanent (deformation) joints.

Permanent deformation joints (temperature and structural ones) have been mentioned in a previous section. As a rule, they are set up at equal distances (7–20 m) along the length of the dam, depending on the climatic conditions and temperature regime of the dam in its service period (Fig. 16.31). The arrangement of joints is coordinated with the division into blocks for concreting, as well as with the position of the openings in the dam, which must not be cut off. Temperature joints expand from 1 to 10 mm, in which the joint closes at maximum temperature, while it is completely open at minimum temperatures. The width of opening of joints, for dams on a soil

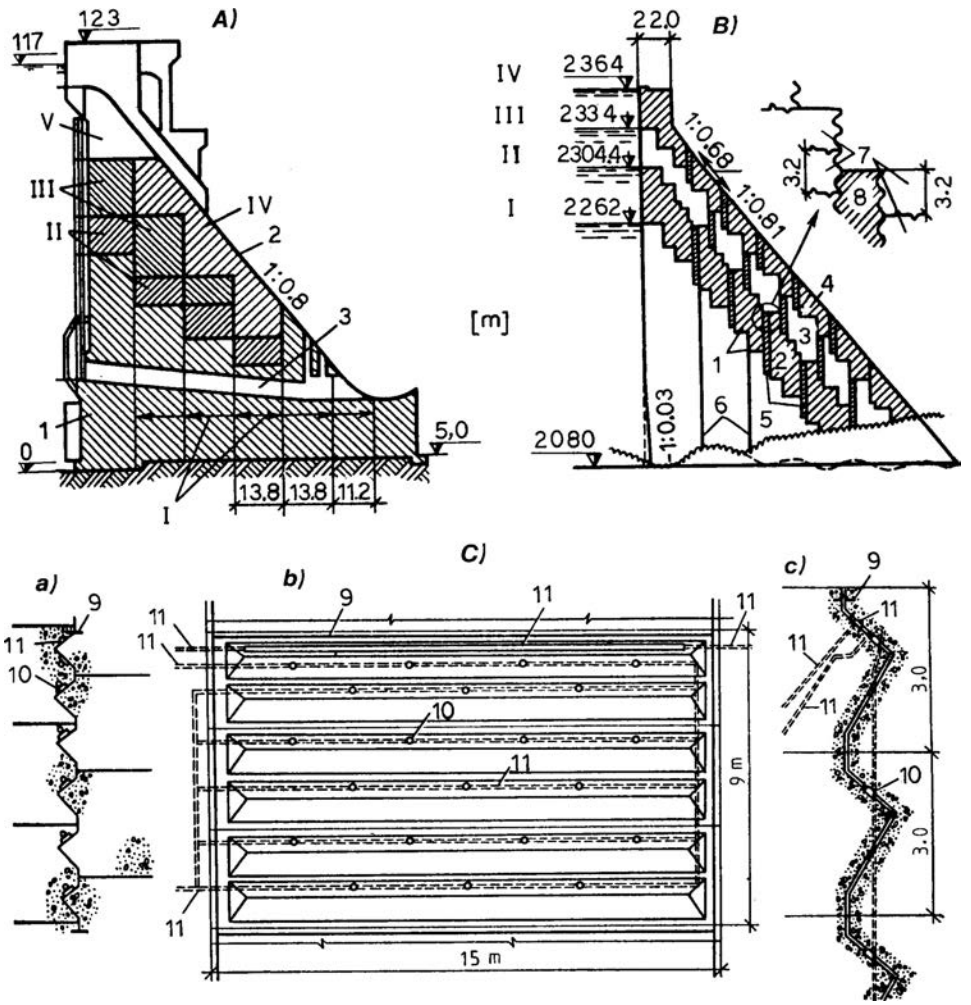

Figure 16.30 Concreting of blocks forming columns in the Bratskaya (A), and Grande Dixens dams (B), as well as structure of a temporary joint for the Bratskaya dam (C). (a) Vertical section along staggered joint; (b) view of the joint; (c) detail (I–V) stages of construction; (1–4) Profiles of the dam during certain construction stages; (5) vertical joints between blocks; (6) joints in the first construction stage; (7) block of concreting; (8) filling with concrete; (9) external closing of the joint; (10) outlets for cement solution; (11) supply and off-take pipes for cement solution, or air.

(non-rock) foundation, is larger (up to 20 mm), because the deformations of sections are considerably greater owing to settlement of the foundation.

In most cases flat or straight joints are employed (Fig. 16.32a), with which individual sections of the dam work and deform independently of one another. More rarely, what are called *hinge joints* are used (Fig. 16.32b), in which a transfer of shear stresses

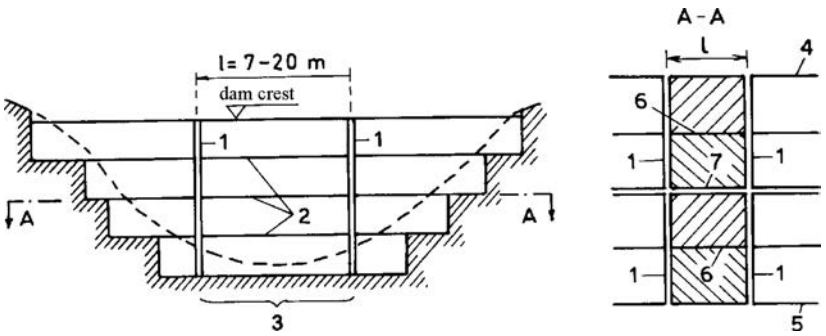

Figure 16.31 Types of joints (longitudinal section of dam at downstream face). (1) Permanent continuous joints; (2) horizontal working joints; (3) structural section; (4, 5) upstream and downstream faces of the dam; (6) vertical working joints; (7) temporary vertical deformation joint.

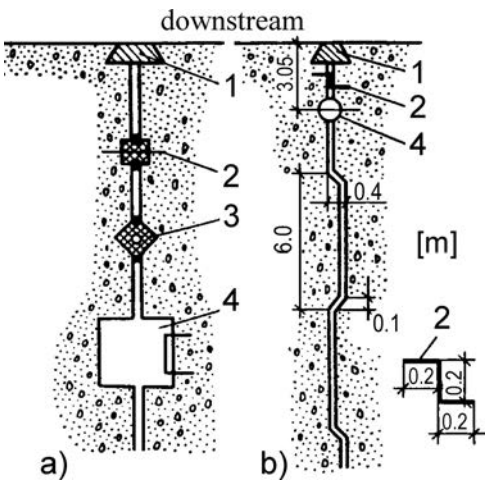

Figure 16.32 Horizontal section through joint of a dam on rock foundation. (a) Straight joint; (b) hinge joint. (1) Contour closing of joint; (2) basic closing; (3) additional basic closing; (4) drainage and inspection manhole.

from one section into another occurs. This, in a way, unloads the more loaded sections. With this type of joint, there is an aggravated off-take of water, which penetrates through the seal or waterstop, and, in addition, concrete cracks are possible in breaks and folds. The joint should be water-impermeable during any possible deformation of the relevant section of the structure. For that purpose, blocking is performed, which should also protect the joint against the effect of waves and ice, as well as pollution. This blocking is constructed along the sides of the dam, as well as in the interior along the contours of the openings (Grishin et al., 1979).

The position of the seals and/or waterstops is given schematically in Figure 16.33, with contour sealing elements on the external surfaces of the dam, as well as on the

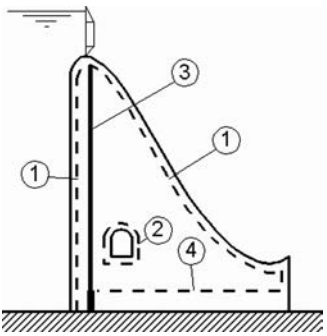

Figure 16.33 Layout of seals and/or waterstops in permanent joints. (1) Contour external seals and/or waterstops; (2) contour internal elements; (3) basic internal elements; (4) additional elements.

surfaces of openings inside the dam, and with the internal basic seal, i.e. waterstop. The contour sealing elements have the basic task of protecting the joint against the effect of ice, waves, and various forms of pollution; thus, also providing a certain water-impermeability of the joint. The basic seal, i.e. waterstop, has to provide complete water-impermeability, which is, for dams on a rock foundation, vertical (3, Fig. 16.33). The water-impermeability of the openings is provided by means of a contour sealing, i.e. waterstop, around them. The sealing or water stopping elements must be elastic and remain watertight during all kinds of deformations in the relevant section of the dam. This is particularly significant for dams on a soil (non-rock) foundation, the deformations of which are different and relatively greater in comparison with those found in dams on a rock foundation.

External contour seals and waterstops (Fig. 16.34) are wedges constructed in the form of concrete, reinforced concrete, or wooden battens or plugs, rubber or steel strips, which are incorporated into niches on a surface that has previously been coated with bitumen or with asphalt mastic. On the downstream face, such a seal or waterstop protects the joint only against pollution, and that enables the application of simpler means.

Wooden wedges may be employed only in those parts of the dam, which are permanently in water, while concrete ones are employed in parts of the dam that come into contact with earth filling. Wide joints in dams on soil foundations may also be closed with reinforced concrete slabs.

In areas with a moderate or warm climate, a solution is sometimes employed by coating the joint surface with mastic and sloping of the edges, in which case the basic internal closing of the joint must be performed with a metal sheet or with a rubber strip. In the same way, there are also performed the internal contour seals, i.e. waterstops, in the joints of the inspection galleries and other openings in the interior of the dam.

In the case of rock foundations, the basic internal seals and waterstops are constructed in the form of metal, rubber, and plastic waterstops and asphalt wedges. They are set up at a distance of from 1.5 to 2 m from the upstream face of the dam.

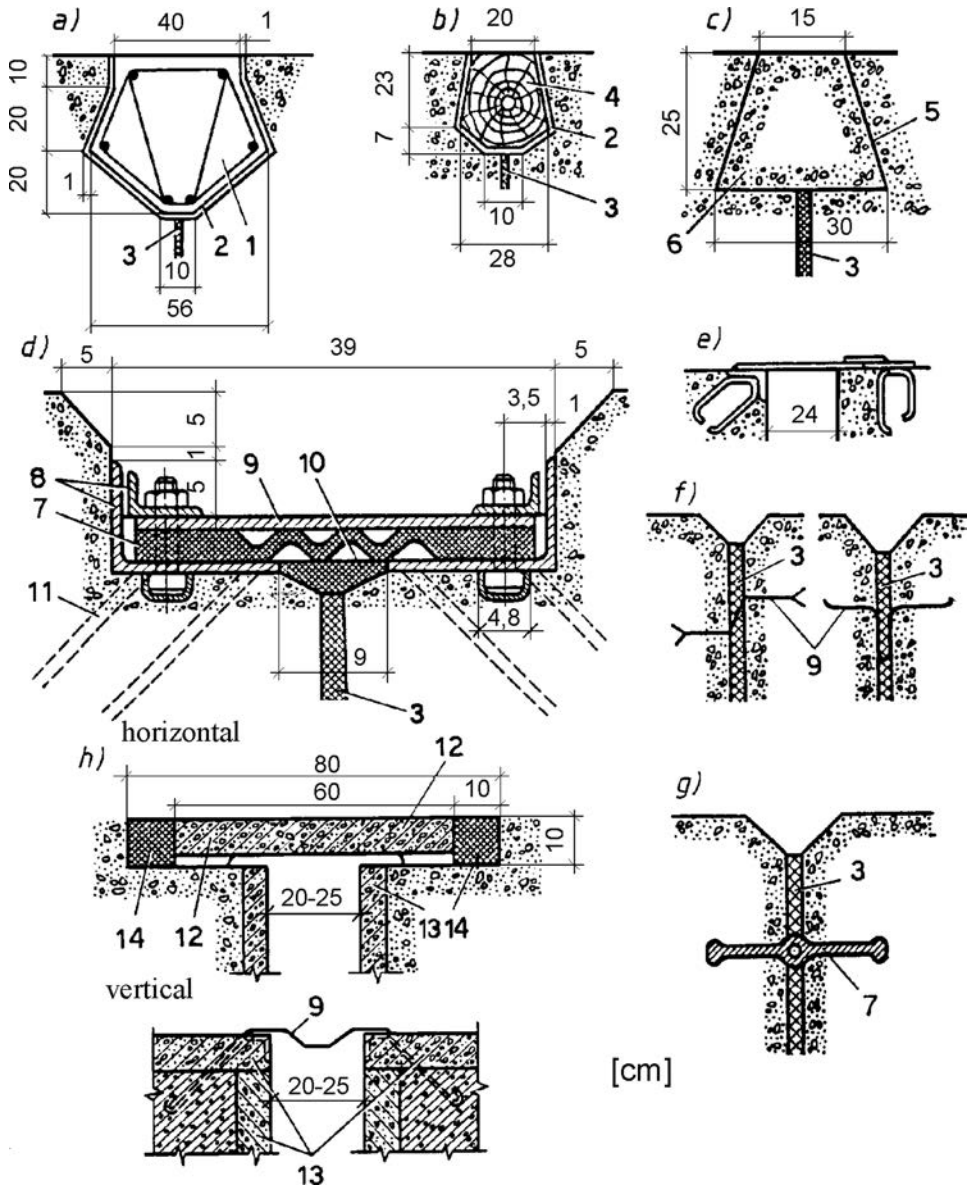

Figure 16.34 Contour basic closing of joints. (a) Reinforced concrete beam; (b) wooden beam; (c) concrete plug; (d) rubber seal; (e) steel plate; (f, g) coating on the joint surface and internal basic waterstop with metal or rubber strip; (h) contour closing in case of soil (non-rock) foundations: (1, 4) Beam; (2) bitumen; (3) joints; (5) bituminous coating; (6) plug; (7) rubber strip; (8) steel angles; (9) steel plate; (10) slag mixture; (11) anchors; (12) reinforced concrete slab; (13) lining slabs; (14) asphalt mastic.

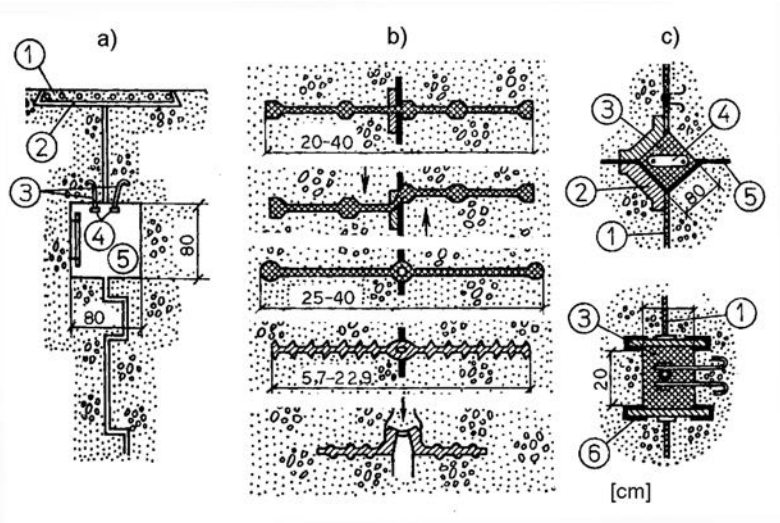

Figure 16.35 Basic internal seals and waterstops in dams on rock foundations. (a): (1) Reinforced concrete slab; (2) bituminous base; (3) anchors; (4) copper sheet; (5) manhole; (b) rubber waterstop; (c) asphalt wedge – big and small: (1) joint; (2) reinforced concrete channel; (3) asphalt mastic; (4) electric heater; (5) metal sheet; (6) seal.

Metal waterstops are manufactured in copper or stainless steel. In addition to the types shown in Figure 16.34f, it is also necessary to mention waterstops that are set up in inspection manholes (Fig. 16.35a).

Rubber moulded strips (Fig. 16.35b) are employed for narrow, i.e. tight, joints and are set up so that, under the effect of hydrostatic pressure, the rubber works, mainly, under compression, and to a smaller extent, in tension. Increasingly, a greater application of poly-vinyl-chloride (PVC) waterstops in the form of strips is being employed. The strips are placed analogously to the rubber ones (Grishin et al., 1979; Chugaev, 1985).

Asphalt wedges are made in the form of vertical openings in the concrete, which are filled with asphalt mixture. They are provided with devices for heating the asphalt by means of electric current, hot air, or vapor in order to make it possible to perform addition (or replacement) of asphalt that flows out over the course of time. In order to prevent such flowing out, metal sheets may be incorporated.

Of all types of basic seals, metal waterstops are the safest. Rubber and plastic elements possess good water-impermeability, but less durability.

Within the composition of the construction of permanent joints, there usually falls also the inspection manhole, positioned closely behind the seal or waterstop and serving for control of its functioning, for draining of possible penetrated water and, in case of need, for overhaul or replacement of seals or waterstops (Figs. 16.32–16.35a).

Cementing of temporary joints is carried out with an application of cement grout through a system of built-in pipes, at low temperature, when the joints are open; in case of need, it is possible to perform artificial cooling of the concrete blocks in order

to reach the temperature of the grouting of the joints. The opening of the joint can be determined with the formula:

$$\delta = \frac{\Delta l_1 + \Delta l_2}{2} \tag{16.35}$$

where Δl_1 and Δl_2 are linear temperature deformations of two adjacent blocks during cooling, equal to:

$$\begin{aligned} \Delta l &= \alpha[(t_b - t_0) + k(t_{max} - t_b)] \qquad t_b \geq t_0 \\ \Delta l &= \alpha k(t_{max} - t_b) \qquad\qquad\qquad\quad t_b < t_0 \end{aligned} \tag{16.36}$$

where t_b is the temperature of concrete mixture at placing; t_0 is the temperature of grouting the joints; t_{max} is the maximum temperature in the block; α is the coefficient of linear temperature deformation; and k is the coefficient depending on the thermal-stressed state in the block, ranging from 0.25 to 0.60.

The temperature of grouting is determined from the expression:

$$t_0 = t_s + \frac{\sigma_{gr}}{E\alpha k} \tag{16.37}$$

where t_s is the temperature of concrete during service period of dam; σ_{gr} is the stresses occurring in the concrete due to grouting; and E is Young's modulus.

In the practice of building concrete dams, the temperature of grouting the joints usually ranges from 5 to 12°C.

Drainage in the dam's body. For reducing the seepage uplift and the mechanical and physical-chemical effect of the seepage water, drainage is constructed in the dam's body. It consists of a system of vertical (sometimes also horizontal) openings with a circular cross-section, set up in the vicinity of the upstream face. Vertical drains have a diameter of 15–30 cm, and the water penetrating into them is collected into longitudinal galleries, which are constructed at height distances from 20–30 m (Fig. 16.36). These galleries also serve for inspection. From these galleries, water is drained downstream through transverse drain openings. Water, which has filtrated into the dam's foundation, is also drained into the lowermost gallery. Drainage openings are made with the incorporation – in the dam's body – of pipes of porous concrete and steel, whose external side is coated with used or other mineral oil in order to enable their pulling out and upwards along with the advancement of the concreting.

From the lowermost drainage gallery, that is to say, from the inspection gallery (see below), there are drilled drainage holes in the foundation with a diameter most often of from 75 to 100 mm, mutually spaced at 3–5 m. The efficiency of drainage in the foundation, as well as in the dam's body, depends on its geometry, i.e. on the diameter of the drill holes, and on their mutual spacing, as well as on their distance from the upstream edge of the dam. There are diagrams in the textbook references, from which it is possible to approximately evaluate the efficiency of the drainage system, as a function of the quoted parameters.

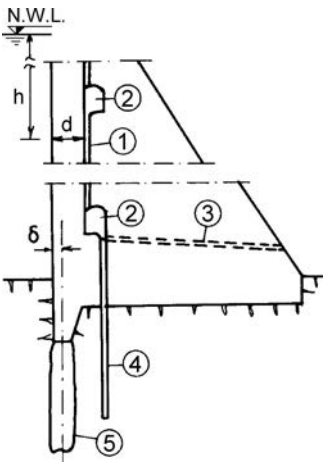

Figure 16.36 Drainage of the dam's body and foundation. (1) Drainage of dam; (2) gallery; (3) outlet opening; (4) drainage into foundation; (5) grout curtain.

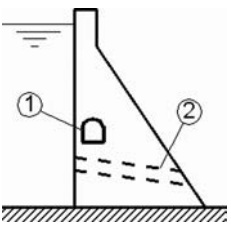

Figure 16.37 Openings in the dam's body. (1) Longitudinal gallery; (2) opening for discharge.

Distance d from the upstream face of the dam to the drainage in a certain horizontal section can roughly be determined with the expression:

$$d = (0.05 \div 0.07)h \tag{16.38}$$

where h is the distance of the considered section from the water level. The distance between drains amounts to 3–4 m.

Inspection galleries. For visual surveillance of the behaviour of the dam's interior (seepage, occurrence of cracks), as well as for installation of various measuring instruments, there are constructed special horizontal or inclined galleries (Fig. 16.37), as well as vertical manholes. The galleries have minimum dimensions of 2×1.2 m. They are usually 2–3 m wide and over 3 m high. Sometimes, the lowermost inspection gallery can also serve for the execution of a grout curtain below the dam. The entrance into the horizontal galleries is either through manholes (inclined or vertical) from the crest, or directly from the banks. As well as with an appropriate access, the gallery must also be provided with devices for ventilation and lighting.

Other openings can also be left in the dam's body, for instance, for bottom outlet or a large opening for accommodating a hydroelectric power station. The cross-section

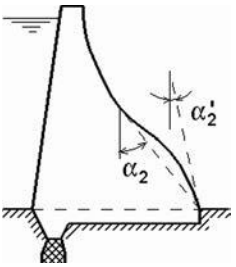

Figure 16.38 Improvement of the stress condition by curving the downstream dam side.

of the dam may be weakened with openings by 1/4. Openings derange the continuity of the construction and so there comes about a concentration of stresses along their edges, which should be taken into consideration in the dimensioning of the dam.

Shaping the downstream slopes. The downstream slope of gravity dams on a rock foundation is most frequently constructed as a straight-line slope, with an inclination of 1:0.65–1:0.85. In the case of high dams, for a full reservoir, at the downstream end of the dam, there can appear, mainly, normal compressive stress, which exceeds the concrete strength. In such a case, a solution that involves a curving of the slope towards the external side (Fig. 16.38) may turn out to be a rational one, and, for the calculation of the principal stresses, the angle α_2' will be the ruling one (instead of α_2), which the tangent to the curve forms with the vertical. Thus, smaller principal stresses will be obtained, since their value depends on the tangent of the angle α_2.

16.7 STABILITY OF GRAVITY DAMS ON ROCK FOUNDATION

Concrete gravity dams on a rock foundation have certain specific qualities, which originate from the features of the foundation upon which they are built. Namely, owing to the high values of parameters f and c – the coefficient of friction and the specific force of adhesion – upon which depends resistance against sliding, this type of dam has a smaller volume and, thus, is cheaper than dams built on a soil foundation.

The basic elements of the stability of concrete gravity dams have been elaborated in Section 16.3. Generally speaking, the stability of a gravity dam on a rock foundation can be disturbed owing to the following reasons: (1) *sliding across the foundation* or *along cracks in the foundation* at unallowable stresses of shearing and tension; (2) *overturning of the dam* when losing contact with the foundation; (3) *failure of the concrete in the dam's body or destroying of the rock mass of the foundation* under the effect of the developed high stresses (Grishin et al., 1979; Orehov, 1990; Novak et al., 2001).

The third effect cannot take place if there is proper designing of the dam, when, for all states of loading, the stresses in the dam's body and its foundation range within permissible limits.

Stability against overturning can be expressed by means of the factor of safety F_{ovt}, against overturning around the downstream end of the dam as a ratio of the passive and active moments ΣM_{pas}, and ΣM_{act}, respectively:

$$F_{ovt} = \frac{\Sigma M_{pas}}{\Sigma M_{act}} \tag{16.39}$$

Active forces cause active moments – such as hydrostatic pressure of water – while passive moments are caused by the weight of the dam. Therefore, in the appropriate sums there appear moments with the same sign. It is significant that uplift is an active force (its moment, in relation to the downstream end of the dam, has the same sign as the moment due to hydrostatic pressure), and it acts unfavorably in relation to the stability of the dam. The stability against overturning of the dam around the downstream end of the dam for a full reservoir need not be checked if there are no tensile stresses in the upstream face. Namely, overturning of the entire dam, without deranging its particular parts, is quite unreal to expect, so that the stability against overturning is closely connected with the state of stresses. F_{ovt} must be bigger than 1.5; in practice, with other conditions for stability fulfilled, this coefficient usually ranges about 2.

16.7.1 Dam sliding and shearing across foundation

Stability against sliding and shearing through a certain section through the dam across the foundation or along cracks in the foundation is of utmost importance. That is why it needs to be examined with special attention (Volpe, et al., 1991; Oberti, 1991). In this, different cases are possible, for example: sliding through the massive section, through the horizontal structural joint, across the horizontal foundation of the dam (Fig. 16.39a), over an inclined foundation (b), along an indented, i.e. toothed, foundation (c), along a crack in the foundation (abd, Fig. 16.39d) or over a privileged weak layer (dc, Fig. 16.39e). The resistance against sliding and shearing, which can be mobilized over the surface of sliding, is expressed through two parameters: c and $f = \tan\varphi$. Cohesion c represents the unit strength against shearing of concrete or rock under conditions of zero normal stresses. The coefficient of friction $f = \tan\varphi$ represents resistance to friction, where φ is the angle of internal friction (there is a noticeable analogy with the corresponding parameters in soil mechanics).

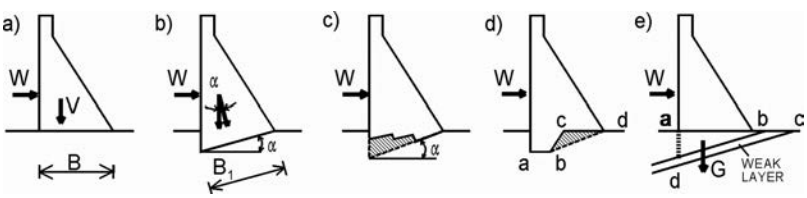

Figure 16.39 Schemes for calculation of stability against sliding.

With respect to analysis and design, stability against sliding and shearing across the foundation is expressed with the coefficient of safety k_s, with the formula:

$$k_s = \frac{S}{\Sigma W} \tag{16.40}$$

where S is the maximum resistance against shearing which can be mobilized, while ΣW is the sum of the horizontal forces acting on the dam. For a horizontal plane of sliding (Fig. 16.39a), it will be:

$$S = \Sigma V \tan \varphi + cA_h \tag{16.41}$$

where ΣV is the sum of all vertical forces, while A_h is the area of contact surface of sliding; in this case, for a two-dimensional analysis, $A_h = B \times 1$. Substituting in the equation (16.40), one obtains:

$$k_s = \frac{\Sigma V \tan \varphi + cB}{\Sigma W} \tag{16.42}$$

If the surface of sliding is inclined at an angle α in relation to the horizontal (Fig. 16.40), then it will be:

$$S = \Sigma V \tan(\varphi + \alpha) + \frac{cB}{\cos \alpha \, (1 - \tan \varphi \tan \alpha)} \tag{16.43}$$

Under certain conditions, it may be justifiable also to include the force of the passive wedge P_p in the resistance (Fig. 16.41). Then the expression for the coefficient of safety will be:

$$k_s = \frac{S + P_p}{\Sigma W} \tag{16.44}$$

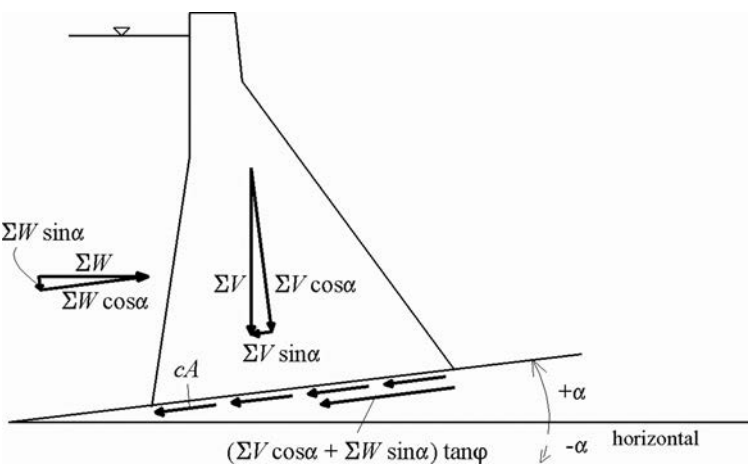

Figure 16.40 (after Novak et al., 2001).

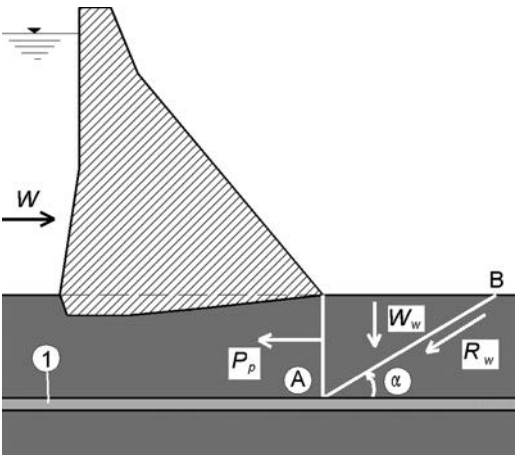

Figure 16.41 Thin weak layer in the foundation (1) and resistance of a passive wedge (after Novak et al., 2001).

where

$$P_p = W_w \tan(\varphi + \alpha) + \frac{c\, B_{AB}}{\cos\alpha\,(1 - \tan\varphi \tan\alpha)} \tag{16.45}$$

in which W_w is the weight of the passive wedge, while B_{AB} is the additional length of sliding, as is shown in the figure. If, in the foundation, there is a privileged layer with low strength against shearing, as shown in Figure 16.36, then it is recommended to include $S = 0$ in the expression (16.44).

For a usual combination of loadings, it is recommended to adopt $k_s = 4$ in the zone of the foundation, while $k_s = 3$ in the dam's body and in the contact with foundation. For exceptional loading, the engineer should evaluate which coefficient of safety is rational, taking into consideration the significance and size of the structure. It is customary, in including the seismic forces, for higher dams to perform a reduction of k_s by 33%.

Of great importance is the question of proper selection of the parameters of strength against sliding, i.e. against shearing. The most authentic results will be achieved if we enter calculations with values of the strength characteristics of concrete and rock in the foundation f and c, determined by appropriate field geotechnical investigations. In the case of lack of data from experimental investigations, in the initial stages of design for the parameters f and c, we can use the approximate values given in Table 16.6. We can take for concrete, $f = 1$–1.5; and $c = 150$–350 kPa, while through the horizontal structural joint,/has the same value as in the concrete, and $c = 80$–250 kPa.

The formula (16.43) can also be used when there is constructed an indented, i.e. toothed, dam foundation, inclined at an angle $\propto$ to the horizontal (Fig. 16.39c). By means of such a solution, the resistance against sliding increases (as in the case

Table 16.6 Parameters of sliding for different rock foundations

	Parameters of sliding							
	Over contact Concrete-rock		*Over cracks in rock, filled with particles with diameter*					
			0.5 mm		*2–20 mm*		*>20 mm*	
Kind of rock in foundation	*f*	*C [kPa]*	*f*	*C [kPa]*	*f*	*C [kPa]*	*f*	*C [kPa]*
1. Rock masses in large blocks, layered, slab type minerals with compressive strength P > 40 MPa, practically non-eroded	0.95	400	0.80	150	0.70	100	0.55	50
2. Same as item 1, but with certain cracks, low erosion-prone ground	0.85	300	0.80	150	0.70	100	0.55	50
3. Highly fissured rocks, P ≈ 40 MPa, semi-rock foundation low eroded; P = 20–40 MPa	0.75	200	0.70	100	0.65	60	0.45	20
4. Semi-rock foundations, slab-type, moderately and highly fissured; P = 2.5–20 MPa	0.70	100	0.65	50	0.50	30	0.45	20

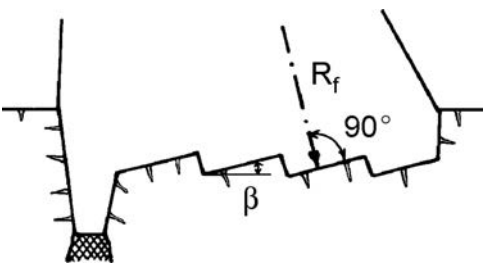

Figure 16.42 Teeth in the foundation part of a dam.

under b); however, there are also savings both in concrete and rock excavation in the amount as shown by the hatched part.

Shaping of the foundation part of the dam with teeth is often used as a structural solution aimed at improving the joint with the foundation, as well as increasing the resistance against sliding. Teeth are made only when the foundation consists of firm and sound rock, so that their number should not be very large (4–6 are usually sufficient), in order not to complicate construction and also not to create conditions for cracks in the foundation part of the dam. The angle β should amount to 10–15° (Fig. 16.42), so that the resultant force (for a full reservoir) would be approximately normal to the bottom of teeth.

In checking the danger of sliding of the dam along a crack in the rock (*abd*, Fig. 16.39d), or over a weak layer (*dc*, Fig. 16.39e), to the sum of vertical forces there has to be added the weight of rock *G* of a volume *bcd*, or *adc*.

Stability against sliding has lately (since 1980) also been treated in another way – by applying the method of limit equilibrium. In accordance with that approach, we follow the logic of soil mechanics, and the factor of safety k_{se}, is expressed as a ratio of the strength against shearing τ_f, and the average shearing stress τ across the possible surface of sliding, i.e.:

$$k_{se} = \frac{\tau_f}{\tau} \tag{16.46}$$

Further, τ_f can be expressed through Mohr-Coulomb's criterion for failure, so that it follows:

$$k_{se} = \frac{\sigma_n \tan \varphi + c}{\tau} \tag{16.47}$$

where σ_n is the stress acting normal to the plane of sliding.

Taking into consideration Figure 16.40, in which a flat surface of sliding is illustrated, by using appropriate substitutions in the equation (16.45) it follows:

$$k_{se} = \frac{(\Sigma V \cos \alpha + \Sigma W \sin \alpha) \tan \varphi + cB}{\Sigma W \cos \alpha - \Sigma V \sin \alpha} \tag{16.48}$$

It is not difficult to see that, for a horizontal plane of sliding ($\alpha = 0$), the last equation changes into (16.40); that is to say, in such a case, $k_s = k_{se}$. The equation (16.48) can further be developed for the application to a surface of sliding, composed of broken or folded planes, in case of a complex foundation. It is recommended that the minimum factor of safety for the approach, according to the method of limit equilibrium, should be $k_s = 2$ for normal loading, i.e. 1.3 for the application of exceptional loads.

16.8 HOLLOW GRAVITY DAMS

Mass gravity dams are relatively simple regarding their structure and construction; however, they also have certain deficiencies. These are summarized in the continuation: (1) a large volume of material in the dam's body, including expensive cement, which leads to the high cost of gravity dams, as compared to other types of dams; (2) reduced monolithism, due to the vital execution of temperature and deformation joints; (3) insufficient clearness for the state of stresses in the zone of the foundation; (4) a high value of the seepage uplift, with an insufficiently clear definition of the diagram of its action; (5) incomplete utilization of the concrete strength, which is especially expressed in the case of dams lower than 100 m, in order to reduce the influence of some of these deficiencies – especially of the first and the fourth ones – *hollow gravity dams* are introduced (Fig. 16.43).

The overall dimensions of these dams do not differ much in relation to mass dams, but on each side of the blocks an opening is made with a width approximately equal to $0.5e$ and height z, so that the volume of concrete in each block is reduced by $0.5 \cdot b_0 \cdot z \cdot e$. In practice, with this type of dam, joints between the blocks of the centre part are extended.

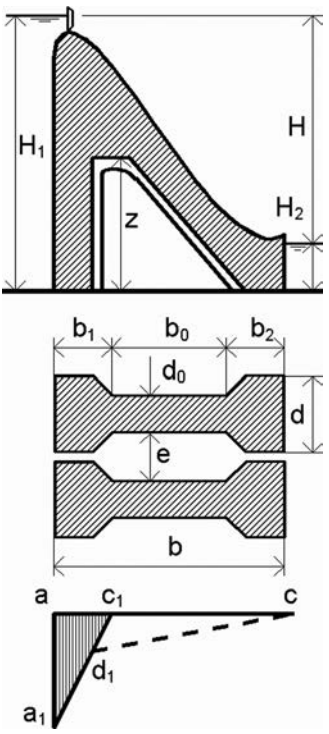

Figure 16.43 Hollow gravity dam. (a) Cross-section; (b) layout of two concrete blocks; (c) diagram of uplift pressure.

Diagram of seepage uplift, in this case, is represented by the hatched triangle c_1cd_1 in relation to a mass dam with a grout curtain and drainage. If U_m denotes the force of uplift for a mass dam, and U_{hol} denotes the force of uplift for a hollow dam, then the reduction of concrete in one block will be:

$$V_n = 0.5 \cdot b_0 \cdot z \cdot e \; = \; \frac{U_m - U_{hol}}{\gamma_w} \tag{16.49}$$

By means of the last expression, it is possible to obtain the dimensions of the openings z and e, i.e. we can determine the savings in concrete at the expense of the reduced uplift. In practice, the width ranges from 3 to 9 m, or $(0.50–0.40)d$, where d is the width of the block. The expansion of the joint begins at a distance of $(0.4–1)d$ from the upstream face. The width of the expanded joint at the Mamakanskaya dam (Russia); (Fig. 16.44), is 6 m, while the ratio e/d = 0.40 (Grishin et al., 1979).

Savings in concrete, in the case of hollow dams, amounts to 15% of the volume of a mass dam constructed under the same conditions; however, savings in cost are smaller, due to higher unit price of concrete, caused by the increased participation of the formwork and work force.

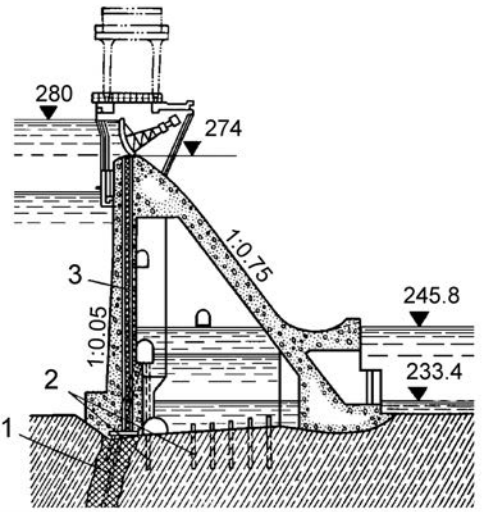

Figure 16.44 Mamakanskaya dam (Russia). (1) Grout curtain; (2) drainage of foundation; (3) drainage of the dam's body.

Static calculations for hollow dams, if the ratio *e/d* is small (0.1–0.2), are performed the same as for mass dams. For wider joints, we can use the methods for buttress dams (see Chapter 19).

In spite of the savings in concrete, hollow dams are not used very much because of some of their deficiencies, such as their higher unit cost of concrete, the need for construction of bridges across the wide joints for crossing into galleries, the necessity of covering the joints during the winter period of construction, in order that a lowering of the temperature in the concrete to an excessive extent, etc. does not occur.

The highest hollow dam in the world is the main dam in the context of the hydraulic scheme *Itaipu,* an extremely large project finished in 1982, shared between Brazil and Paraguay. The dam is 196 m high and 610 m long. In this case, the low cost labor had a decisive role in the choice of the dam type. The Itaipu scheme containes various types of dams, including buttressed, an the total length of all dams is more than 7 km. More data and drawings of this important scheme are given in Chapter 32.

Realization of hollow dams may also be achieved by leaving longitudinal openings, such as in the example of one design for such a dam, Austria (Fig. 16.45), in which case there is again a savings in concrete at the expense of reduction of the seepage uplift. In this, there comes about some changes in the state of stresses: normal stresses across the foundation are increased; however, for that reason, it is possible to achieve a more uniform distribution (with the result being to act closer to the centre), with an appropriate selection of the position of the lowest opening. With this type of dam, it is necessary to pay attention to the fact that there comes about a concentration of stresses around openings, which should be calculated in an appropriate way and, if necessary, taken on by means of reinforcement.

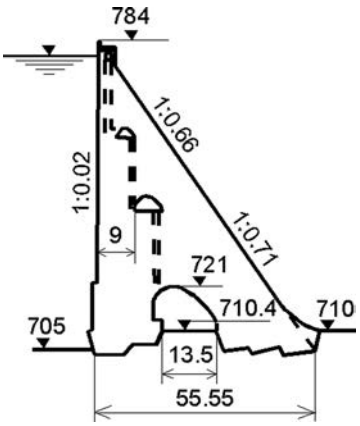

Figure 16.45 Hollow gravity dam with longitudinal openings.

In practice, there is known yet another way of reducing the quantity of concrete in the case of gravity dams. Namely, a decrease in the dam's width is possible, with its anchoring into the rock foundation (Chugaev, 1985; Golzé, 1977; Grishin et al., 1979; Novak et al., 2001; USBR, 1976). This method has turned out to be effective with dams 50–60 m high, in which a 30–40% savings in concrete is possible, with an overall savings in cost of 10–20%. However, the execution of such dams is more complicated.

This page intentionally left blank

Chapter 17

Gravity dams on soil foundations

17.1 FUNDAMENTALS OF GRAVITY DAMS ON SOIL FOUNDATION

Gravity dams on a soil (non-rock) foundation differ from those that are founded on rock by their expanded form of cross-section. In that way a greater weight of the dam has been provided, which should compensate for a 2–4 times smaller resistance of the foundation against sliding in relation to a rock foundation. Such an expanded form is also required due to the weaker strength characteristics of the soil foundation. For these reasons, the height of these dams is limited and usually does not exceed 40 m. This type of dams serves for slowing down of the watercourse aimed at creating conditions for water tapping, most often for the needs of amelioration and energetics, or else for increasing the depth of the river for the sake of providing conditions for navigation. They are usually built on rivers which are rich in water and are regularly carried out either as purely overflow dams, or else as combined dams – with an overflow and a non-overflow part. The overflow part can consist of one span or two or more individual spans if it is necessary to provide greater length for overflowing. Overflowing can take place freely, but more often there is a controlled overflow, when the overflowing spans are provided with gates, which open in case of need.

Structural schemes of this type of dam, especially the underground part and the foundation, are dictated by the engineering and geological features of the soil foundation which usually encompasses complex and different earth materials, which can be divided into two different groups: *cohesionless* or *incoherent materials* and *cohesive* or *coherent materials,* with characteristics as described in section 6.5.

The scheme of a concrete dam on a soil foundation can properly be selected only by the combined taking into consideration of three basic requirements: 1) the provision of dam stability against sliding while maintaining foundation stability; 2) obtaining the least value of uplift of seepage water for secured seepage stability of the foundation; 3) dissipation, of the energy of the overflow stream over the dam. The first two requirements are connected with the geological particularities of the foundation, while the third one is connected with the discharge of the overflow stream. When increasing the specific discharge, there is also an increase in the depth of the stilling basin for dissipation and stilling of the energy, and thus also the slab thickness in its base. A rational scheme of the dam must also satisfy the requirements for its minimum cost, so that the selection of the solution is carried out by analysis of a number of variants.

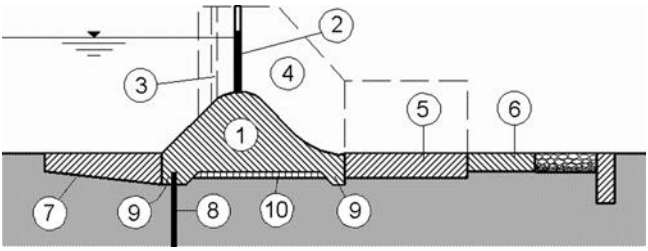

Figure 17.1 Schematic presentation of cross-section of a concrete dam on soil foundation.

Schematically, the constituent elements of an overflow concrete dam on a soil foundation are presented in Figure 17.1. The overflow part of the dam (1) is hydraulically dimensioned and shaped for a given quantity of overflow water which approximately should not exceed 40–50 m^3/s per metre of the width of the overflow part of the dam. It is placed on a flat foundation slab, with teeth at the upstream and downstream ends for a better joint with the foundation. The dimensions of the slab are determined as a consequence of the loads acting upon it, on the load-bearing capacity of the foundation, as well as on the over-all dimensions of the overflow and conditions for passing water through the overflow. Forces acting on the foundation slab should be distributed so that the coefficient of non-uniformity of stresses in the toe $a = \sigma_{max}/\sigma_{min}$ ranges within the following limits: for a clayey foundation $a < 2$, for a sandy foundation $a < 3$. The overflowing crest of the dam, with a pressure head greater than 15 m, is shaped in the form of an overflow with a vacuum-free practical profile. For a lower pressure head, there is usually applied an overflow with a broad crest.

Stresses in the foundation can be determined from the expression for eccentric compression. The coefficient of safety against sliding across the foundation in a general form can be expressed as:

$$k = \frac{\Sigma(N - U)}{\Sigma W} \tan \varphi \tag{17.1}$$

where N = vertical forces acting from above downwards; U = uplift forces acting from below upwards; W = horizontal forces; φ = angle of internal friction of material in the foundation.

For the regulation of water level, operational gates (2) are used and set up at the crest of the dam. The overhaul-accident gate (3) is placed at a distance of a minimum of 1.5 m away from the operational one, in order to provide space for execution of overhaul in case of a faulty condition of the operational gate.

Side or *training* walls (4) serve for separation of individual overflowing spans, as well as for bearing the gates and a possible bridge structure. In the stilling basin (5), dissipation is performed, as well as stilling of the energy of the overflow stream, while the riseberm (6) represents recuperation, i.e. reinforcement, of the ground immediate to the stilling basin.

For reducing the uplift water-pressure below the structure as well as ensuring seepage stability of the earth foundation, such a function is provided by the underground

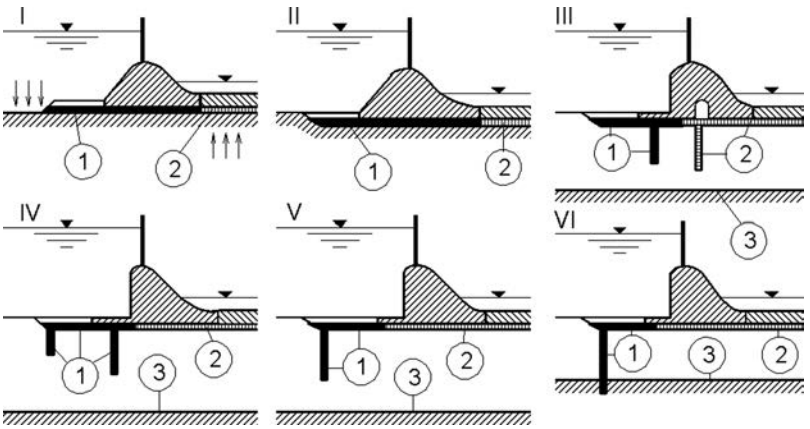

Figure 17.2 Schemes for overflow dams on soil foundation (after Grishin et al., 1979). (1) Impervious parts of the underground contour; (2) drainages; (3) water-impervious layer.

waterproof contour of the dam. Its basic elements are the *upstream blanket* (7), *sheet piling* (or *curtains*) (8), *cutoff walls (teeth)* (9) and *drainage construction* (10).

The role of the upstream blanket is to lengthen the path of seepage in the foundation of the dam. The sheet piling, curtains and cutoff walls are vertical waterproof elements for the effective reduction of the seepage uplift below the structure as well as for the reduction of the gradient of the underground flow.

17.2 SCHEMES FOR THE UNDERGROUND CONTOUR OF THE DAM

Schemes for the underground contour of the dam are formed depending on the kind of foundation and the requirement for the underground contour to ensure minimum seepage uplift as well as preservation of the seepage stability of the foundation. If the foundation is composed of relatively homogeneous cohesionless material, , while the impervious layer is at considerable depth, then jointing of that layer with the dam is useless, i.e. unsuitable. In such a case, the vertical waterproof elements do not reach the impervious layer and are called *hanging* or *suspended* elements.

Figure 17.2 presents possible schemes for the construction of the underground waterproof contour of the dam. The bold line denotes the impervious elements, while the hatched line denotes the pervious elements, i.e. drainages (Grishin et al., 1979).

Scheme I represents a flat underground contour without vertical elements. The foundation part is quite shallowly embedded into the foundation. *Scheme II* presents an embedded underground contour, which is much more often found in practice. The embedment usually amounts 1/3–1/5 of the total height of the dam. The drainage of the stilling basin is obligatory and can be extended across the entire foundation slab, even below the blanket. *Scheme III* presents an underground contour with upstream hanging sheet piling. This scheme is most often employed in practice. Drainage below the

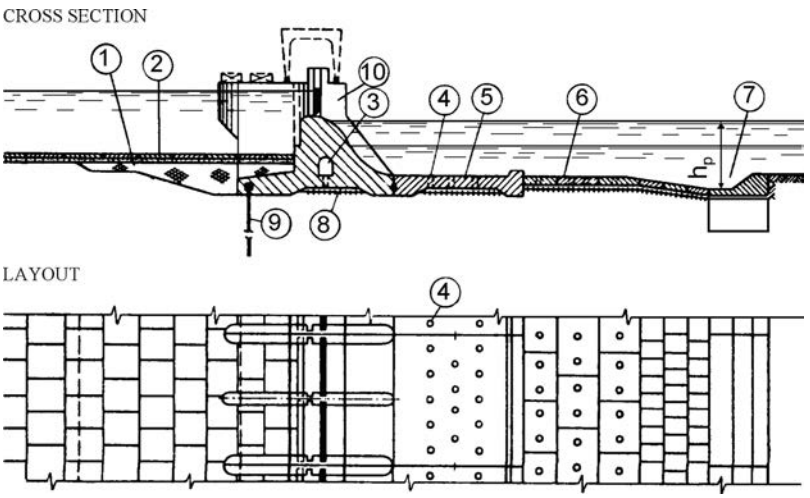

Figure 17.3 An overflow dam on sandy foundation with sheet piling at the upstream face. (1) Clay blanket; (2) protective concrete slabs over sand layer; (3) drainage gallery; (4) drainage openings; (5) stilling-basin slab; (6) concrete slabs for the protection of riseberms; (7) end of riseberm; (8) drainage with inverse filter; (9) steel sheet piling; (10) training wall.

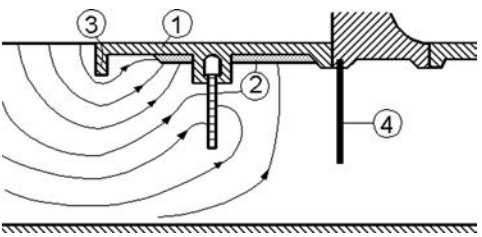

Figure 17.4 Action against chemically aggressive waters. (1) Blanket; (2) drainage; (3) cutoff wall; (4) sheet piling.

dam practically eliminates the uplift pressure. If the foundation contains interbeds of poorly water-permeable material, then vertical drainage is also beneficial. An example of such a type of dam is shown in Figure 17.3.

Scheme IV presents an underground contour with a double sheet piling. When the foundation slab of the dam is extended towards the upstream face, as shown in Figure 17.3, then it is rational to set up the sheet piling at the beginning of the blanket, as in *scheme V.* This scheme is also purposeful in cases when it is necessary to retain the seepage flow in front of the dam, for instance when there exist of seepage waters which would have an aggressive effect on concrete. In such a case a more complex scheme would be even more effective, with drainage below the blanket, which would intake chemically aggressive waters, as well as vertical waterproof elements before and after the drainage, Figure 17.4. As an addition to the presented measures against the effect

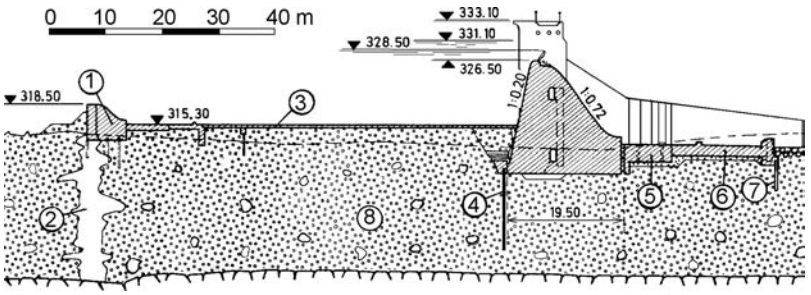

Figure 17.5 Jajce dam, Bosnia and Herzegovina (YCOLD, 1970). (1) Cofferdam; (2) grout curtain; (3) concrete blanket; (4) sheet piling made of Larssen piles; (5) slab in front of stilling basin; (6) stilling basin; (7) timber piling; (8) alluvial deposit.

of aggressive waters, there should also be included the application of special cements for the construction of the dam, especially in its foundation part.

When the depth to the impervious layer is not considerable, then *scheme VI* is used, in which the water-pervious layer is cut off by means of sheet piling, a diaphragm, or else with a grout curtain. This scheme, practically, prevents seepage below the dam and there are eliminated all of its harmful effects. This kind of scheme, in a somewhat more complex form, has been employed in the *Jajce* dam, built in 1954 in former Yugoslavia, on the River Vrbas (Bosnia and Herzegovina), Figure 17.5 (YCOLD 1971).

In founding the dam on a coherent clayey foundation, the construction of sheet piling and grout curtains, located at the upstream as well as the downstream ends of the dam, is uneconomical and irrational, since their permeability will not be much lower than that of the foundation. In such cases it is better to build vertical, not very deep, cutoff walls.

17.3 DETERMINATION OF BASIC DIMENSIONS OF UNDERGROUND CONTOUR

Optimum dimensions of the underground contour are determined by means of economic-technical comparisons of possible variants. For preliminary needs, the dimensions of individual elements in the above-designated schemes can be determined according to the following recommendations: 1) the width of the dam's foundation usually amounts to $(1.5–2.5)H$, where H is water-pressure. In this, it is possible to rationally set up the overflow and to provide stability of the dam; 2) in establishing the length of the impervious part, one should take into consideration that the horizontal water-impervious elements make a small influence in dissipating the energy of the seepage flow and for reducing the uplift pressure it is necessary to provide vertical waterproof elements. Besides, drainage is carried out below the dam and below the blanket. The above two cited measures cut short the length of the horizontal projection of the impervious part of the underground contour and also reduce the seepage flow; 3) the length of upstream blanket should range within the limits $(1 - 1.5)H$, and a maximum of up to $2.5H$; 4) The length of sheet piling below the blanket ranges within

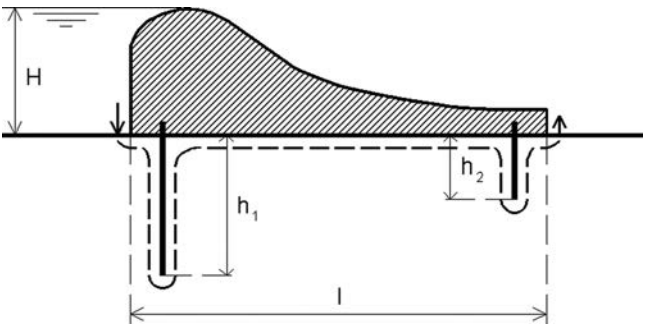

Figure 17.6 Designations referring to Lane's criterion.

Table 17.1 Lane's criterion.

Material in dam's foundation	*L:H*
Very fine sand or dust	8.5 – 7
Medium to coarse sand	6 – 5
Fine to coarse gravel	4 – 3
Gravel with coarse boulders	2.5
Clay with soft to medium consistency	3 – 2
Clay with semi-hard to hard consistency	1.8 – 1.6

the limits of (0.5–1.5)H. In the case of hanging sheet piling, the distance between two sheet pilings should not be smaller than the summary length of the sheet pilings. If the sheet piling is driven into the impervious layer, then the depth of driving amounts to 23 m.

In establishing the dimensions and the shape of the underground contour, in practice *Lane's* criterion is often used to begin with (*Lane*, 1935). It serves for the assessment of the danger of seepage erosion in the foundation below the dam, and it has been derived on the basis of statistical processing of data for the failure and damaging of a lot of dams on a soil foundation. Lane has drawn a conclusion that the danger of erosion in the foundation can be expressed with the critical ratio of the weighted length of seepage L versus the hydrostatic pressure H (Fig. 17.6):

$$L = \frac{1}{3}l + \Sigma 2h_{\mathrm{i}} \tag{17.2}$$

where l = horizontal distance between the points of inlet and outlet of the seepage water; h = vertical path of seepage at places of vertical water-impervious elements in the foundation.

The ratio L:H is competent and governing for the evaluation of the danger of erosion, which would occur when that ratio is smaller than the critical one, given in Table 17.1, depending on the material in the foundation.

If in a certain case Lane's criterion is not satisfied, we have at our disposal the above described measures for lengthening the seepage path – execution of horizontal upstream blanket, longer vertical waterproof elements, etc.

17.4 CONSTRUCTION OF ELEMENTS OF THE UNDERGROUND CONTOUR

Upstream blanket. In accordance with the degree of impermeability, the upstream blanket can be water-impervious or poorly water-permeable, with a coefficient of seepage of the order of 10^{-6} cm/s. The first one is applied with clayey foundations, while the second one with sand foundations. According to the structural solution, the blanket can be either elastic or rigid. Elastic blankets are made of clay, loam, asphalt, clay-concrete or synthetic materials; the earth blanket has a thickness in any section $t \geq \Delta H / J_{\text{perm}}$, where ΔH = the difference in pressure from the top and bottom side over the blanket, J_{perm} = permissible gradient of seepage through the blanket (for clay 6–8, for loam 4–5). The minimum thickness of the blanket at the upstream end should be 0.75 m, while at the dam 1–2 m. A layer of sand-gravel of $15 \div 20$ cm is carried out over the blanket, upon which is placed a protective concrete slab 20–30 cm, or stone paving in cement mortar, as a protection of the clayey material of the blanket against mechanical erosion at higher velocities in certain zones, upstream of the concrete cutoff wall (for instance, in front of the entrance of the bottom outlet and in front of overflowing spans with low crest). According to the investigations of *Uginchus,* the length of the poorly water-permeable blanket should be smaller than the limit length l_{ul}, given by the expression:

$$l_{\text{ul}} = 2\sqrt{\frac{k_0}{k_{\text{p}}} t\, T_{\text{p}}} \tag{17.3}$$

where k_0 and k_{p} are the coefficient of seepage of the blanket's bedding, t = mean thickness of blanket, T_{p} = distance of the impervious layer in the blanket's bedding. Uginchus has shown that for $l_{\text{p}} = l_{\text{ul}}$, $q_2 \approx 0$, $q_1 = q_{\text{ul}}$ (Fig. 17.7), so that it does not make sense to have any further increase of the length of the blanket, since in practice it does not have any influence on the reduction of seepage below the dam. In practice the water-impervious elastic upstream blankets can be performed of different constructions and types, most often asphalt ones, Figure 17.8B, (Grishin et al., 1979, Chugaev, 1985).

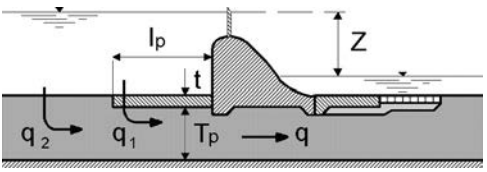

Figure 17.7 Limited effect of the upstream blanket.

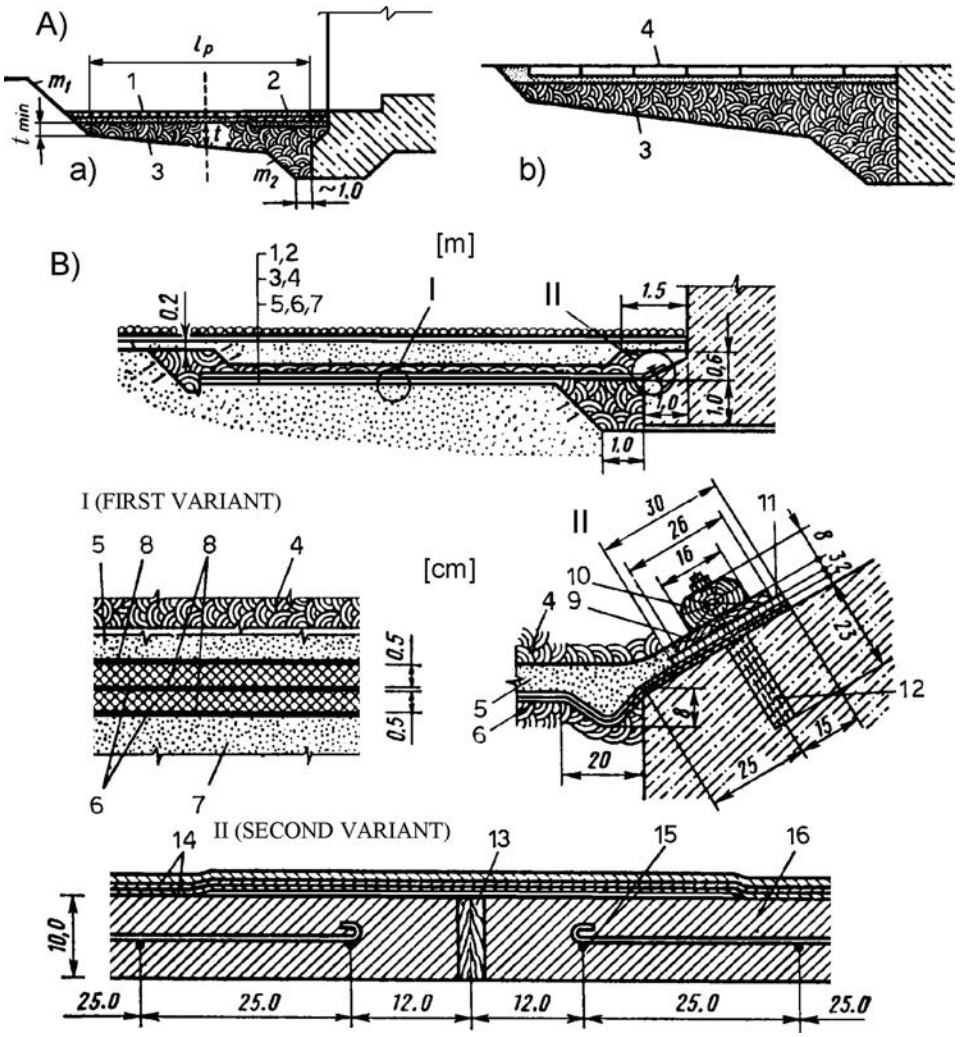

Figure 17.8 Elastic upstream blanket. (A) Clay blanket protected by placed stone (a), and protected by concrete slabs (b): (1) placed stone over a layer of gravel of 15 cm; (2) double layer of placed stone in cement mortar; (3) clay blanket; (4) concrete slabs $3 \times 3 \times 0.5$ m over a layer of gravel 15 cm. (B) Asphalt blanket over bedding of gravel: (1) placed stone or concrete slabs; (2) gravel 10 cm; (3) sand 60 cm; (4) clay 20 cm; (5) protective layer of sand 5 cm; (6) bituminous insulation; (7) load-bearing layer of asphalt material; (8) waterproof paper; (9) board; (10) beam; (11) porous material; (12) anchor bolt; (13) board coated with bitumen; (14) two layers of bituminous insulation; (15) reinforcement ϕ 6 mm; (16) concrete.

Rigid blankets are carried out on a compacted bedding, either concrete or reinforced concrete blankets, divided into slabs by means of joints, filled with waterproofing (Fig. 17.9.a). Occurrence of cracks is possible in the slabs, while at a pressure head greater than 10 m, multi-layer waterproofing is regularly carried out, most often

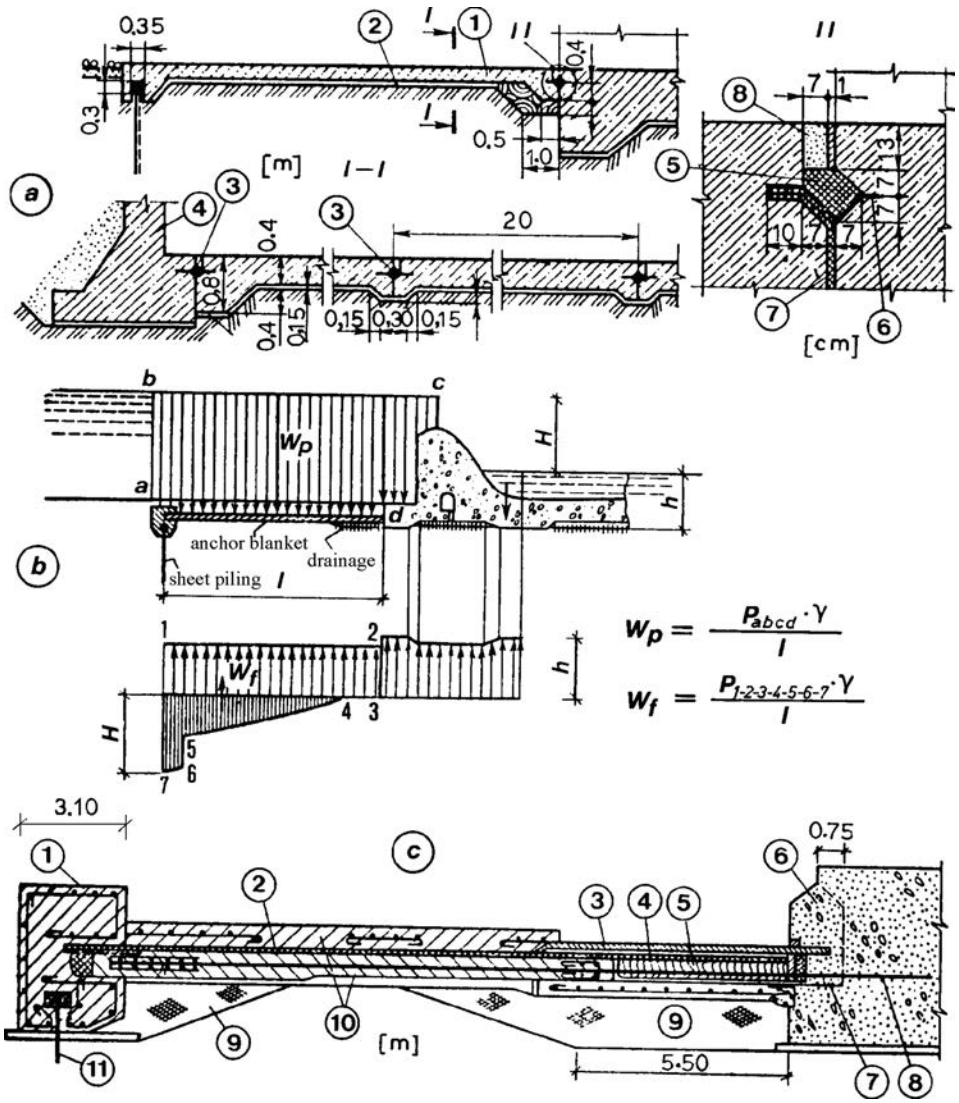

Figure 17.9 Rigid upstream blanket. (a) Reinforced concrete blanket over loam bedding: (1) reinforced concrete slab 40 cm; (2) concrete bedding 5 cm; (3) closing of the joint; (4) retaining wall; (5) asphalt mastic; (6) steel sheet; (7) bituminous waterproof paper; (8) cement mortar. (b) Scheme for dimensioning of *anchor* blanket, (c) Anchor blanket: (1) beam; (2) bituminous waterproof paper; (3) three rows of boards on waterproofing; (4) bitumen; (5) asphalt mastic. (6, 7) additional concreted part of the dam's body; (8) steel anchor; (9) clay; (10) reinforced concrete slab; (11) sheet piling.

based on bitumen. For a pressure head greater than 15 m, the construction of an anchor blanket is recommended (Fig. 17.9b and c). It is usually carried out in the form of a reinforced concrete slab, with a thickness of 0.4 to 0.7 m, with surface waterproofing of bituminous or polymer materials. The longitudinal reinforcement

enters the foundation slab of the dam. The force of sliding which is taken on by the anchor blanket can approximately be determined with the formula:

$$Q = \frac{(G + W_p - W_f)f + cL}{k_n} \tag{17.4}$$

where Q = force of sliding, G = weight of anchor blanket, along with the earth layer upon it (in submerged condition), W_f = seepage uplift from the bottom side, f = coefficient of friction of the blanket across the bedding, c = specific cohesion of the foundation below the blanket, l = length of blanket, k_n = coefficient of safety that ranges from 1.1 to 1.25, depending on the significance of the structure.

The force of sliding Q, calculated by means of the formula (17.4), represents the potential resistance which can be used together with the resistance against sliding of the dam's body for bringing under control the horizontal component of the resultant of all active forces acting on the dam. Because of that it is necessary to connect the blanket with the dam's body by means of anchor reinforcement bars, and that has led to the name *anchor blanket*.

Sheet piling. It can be: steel sheet piling, reinforced concrete sheet piling or, more rarely, timber sheet piling. Steel sheet piling is made out of flat or trough steel sheet elements. The first have the advantage of being simpler and cheaper elements. The reinforced concrete sheet pilings have a thickness of $10 \div 15$ cm, and a width of $50 \div 60$ cm. They can be carried out even in the case of gravel foundations, i.e. beddings. Sheet piling can be jointed with the concrete dam, or else with the blanket. Appropriate attention should be paid to the joint between the sheet piling and the dam, in order to ensure free deformation of the dam, independent of the sheet piling. During settlement, the mastic of the joint (Fig. 17.10) squeezes into the reserve empty openings, which are made at a distance of 4–5 m. The joint should be carried out conscientiously and thoroughly, since possible cracks in the asphalt mastic, and the penetration of water, would render the sheet piling ineffective as a waterproof element (Butakov 1995).

Concrete cutoff walls. If they are shallow, they are made in order to cut off the path of the dangerous contact seepage, while deep ones are carried out instead of sheet piling, in cases when the foundation does not allow its construction, or else in cases of particularly significant structures. As a rule, an upstream cutoff wall is constructed (either shallow or deep). A downstream cutoff wall below the dam is constructed in order to insulate the drainage below the dam from the downstream part of the structure and to obtain the possibility for separation of the water of that drainage, for example, for controlling its work. Concrete cutoff walls can be executed in open drained pits, by means of underwater concreting or by means of caissons, which are employed when the concrete cutoff wall goes up to the impervious layer. The depth of the concrete cutoff walls is determined on the basis of calculations of the seepage stability of the foundation. The depth d from the bottom of the cutoff wall up to the bottom of the filter below the stilling-basin slab (Fig. 17.11B) should be $d = (0.05\text{–}0.10)T$, but not larger than $(0.05 - 0.10)l_0$, where T is the depth of the impervious layer, while l_0 is the length of the horizontal projection of the underground contour. The length d_1 should be selected so that the part MN of the bottom of the dam rests on sufficiently strong and impervious soil. Only in cases when it is not possible to execute a ditch below the cutoff wall, is a dam without a cutoff wall constructed (Fig. 17.11C).

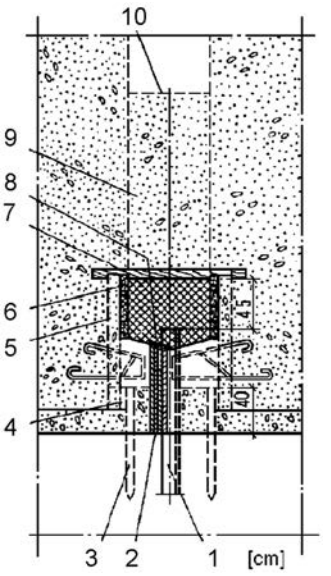

Figure 17.10 Joint of sheet piling with foundation slab. (1) Sheet piling; (2) filling; (3) wooden piles; (4) planks; (5) supports spaced at 1.0 m; (6) planks; (7) asphalt mastic; (8) oakum; (9) standby openings, left every 4 m; (10) level of asphalt mix in the openings.

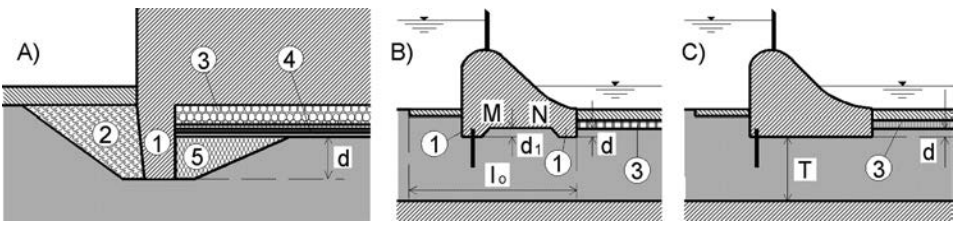

Figure 17.11 Construction and dimensions of concrete cutoff walls. (a) Construction of cutoff wall in a pit; (B) construction of shallow cutoff walls; (c) dam without cutoff walls: (1) Concrete cutoff wall; (2) clay-concrete; (3) drainage; (4) inverse filter; (5) filling of well-compacted earth.

17.5 CONSTRUCTION OF DAM BODY

Dividing into sections. Dams which are constructed on soil foundation should be divided into sections by means of joints and taking into consideration temperature deformations as well as deformations conditioned or stipulated by the expected non-uniform settlements of the works. Here we also distinguish permanent joints, which ensure independent displacements of individual sections of the dam both in a vertical and a horizontal direction, as well as temporary ones, by means of which the structure is divided into blocks for concreting in the construction process.

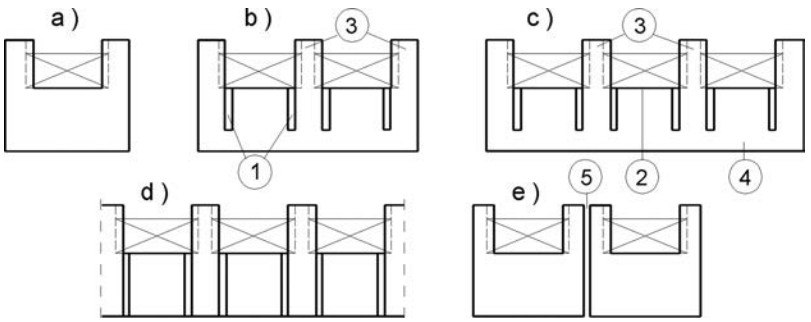

Figure 17.12 Dividing of dams into sections. (a) Dam with one span, (b) with two spans, (c) with three spans; (d) training walls separated from the overflow; (e) two parted sections. (1) Cut-joint; (2) overflow crest.

Typical schemes for dividing the dams using permanent deformation joints are shown in Figure 17.12. Dividing of the dam with full joints is carried out along the parting piers, i.e. training walls, for eliminating the possibility of non-uniform settlement of the parting piers or training walls, and also to avoid distortion of the gate. Depending on the degree of heterogeneousness, i.e. diversity of the foundation, such dividing with full joints is performed over one, two or three spans (Fig. 17.12a, b and c). The length of individual sections is assumed to be 40 to 60 m. In sections of two or more spans, for preventing considerable temperature stresses in the dam's body, next to the parting piers or training walls), there are carried out cut-joints, from the overflow crest to the foundation slab, Figure 17.12b and c. The execution of full joints between the parting piers or training walls and the overflowing part (Fig. 17.12d) is permitted in the case of low-deformable foundations.

The width between the temperature joints is the same as in temperature-deformation joints used for mass dams on a rock foundation, while deformation joints are carried out as flat vertical joints, 4 to 5 cm wide in the upper part, while 1–2 cm in the zone of the foundation slab. The width of the cut-joints amounts to 1–2 cm.

The arrangement of the basic and contour seals and waterstops at the deformation joints is presented in Figure 17.13a, at the example of the joint in a training wall, while regarding the temperature joints (b) at the example of a joint in the overflowing part of the dam. Vertical joints, both basic and contour ones, are carried out in the same way as in the case of mass dams on a rock foundation (see section 16.6, Fig. 16.28). Here particular attention should be paid to the horizontal seals and/or waterstops, which are carried out along the contact joint (c) and in the transition from a wider to a tighter joint (d). Illustration (e) gives an example of closing of the joint around inspection gallery, which is carried out when there is a danger of flooding by the tailwater. Here, also, as with joints in mass dams on a rock foundation, there are to be anticipated drainages and inspection manholes. The basic vertical closures should be carried out at a certain distance from the upstream face, and that depends on the mean monthly minimum temperature of the coldest month, ranging from 1 to 2.5 m.

Training walls. They serve for separating, i.e. parting the overflow front (width) into a number of parts, and can also serve as a support for the gates both for transit

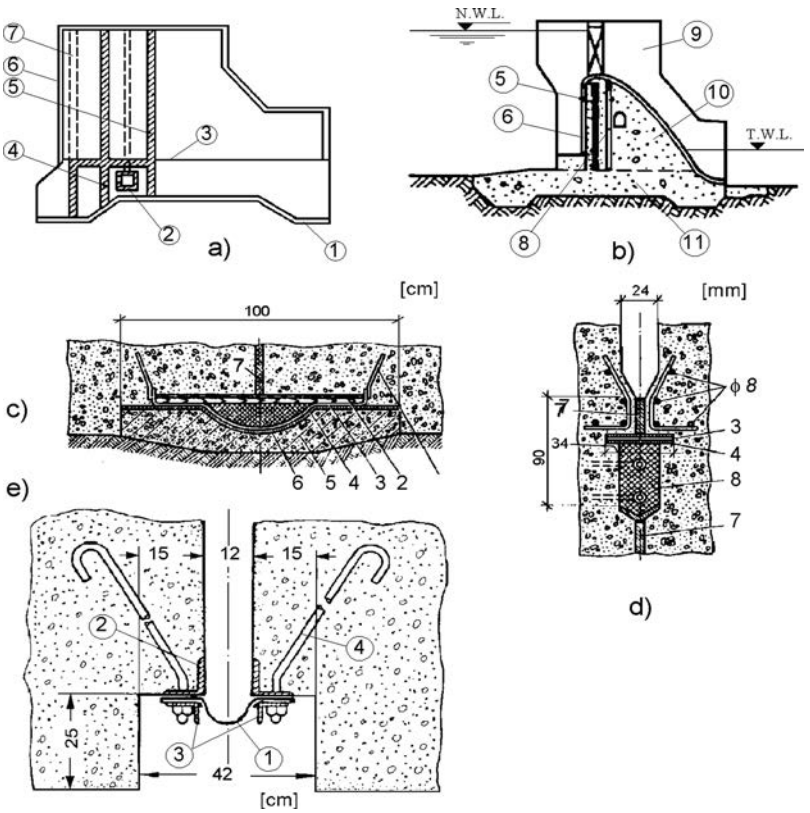

Figure 17.13 Arrangement for closing of joints in the training wall (a), overflow part (b), schemes for horizontal closing in the bottom (c), at a transition from a wide towards a narrow joint (d) and inspection gallery (e). (a, b): (1) Closing in the bottom; (2) internal contour closing; (3) boundary of a narrow and a wide joint; (4) closing in the narrow part of the joint; (5) basic closing in the wide part of the joint; (6) external contour closing; (7) opening; (8) inspection manhole; (9) training wall; (10) overflowing part of the dam; (11) foundation. (c, d): (1) Steel anchors; (2) boards, 2×20 cm; (3) steel plate, 4 mm thick; (4) bituminous waterproofing paper; (5) reinforced concrete block; (6) asphalt mastic; (7) filling of cold asphalt; (8) filling with bitumen-rich solution. (e): (1) Steel plate, $\delta = 8$ mm, $L = 650$ mm; (2) steel angles $100 \times 100 \times 10$ mm; (3) angles $75 \times 50 \times 8$ mm; (4) anchors 20 mm, $l = 70$ cm, spaced at 25 cm.

and service bridges; they also carry the stationary gears and mechanisms for lifting the gates.

The height of the training wall should be sufficient for carrying the gate into a lifted position, while its thickness and length are determined so that it can perform the cited functions and have space for niches and/or recesses for the retaining parts of the gate. Possible forms of the training walls in layout plan are shown in Figure 17.14. The forms b and c are more convenient, since they exhibit a smaller resistance to the flowing of water.

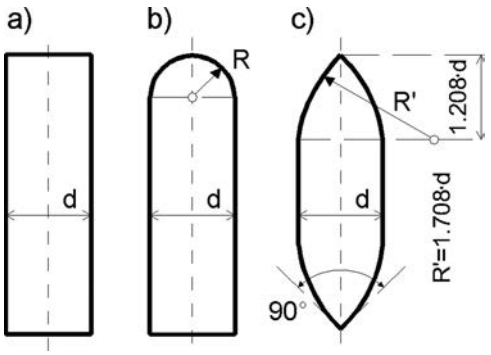

Figure 17.14 Forms of training walls.

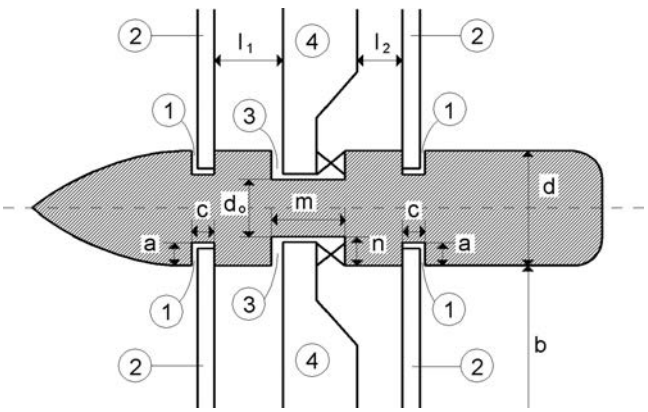

Figure 17.15 Layout plan of a training wall. (a) Niches and/or recesses for overhaul or accident gates (2); (3) recess for the operational gate (4).

Figure 17.15 presents a training wall with a recess for working gates (3) and for overhaul or for accident gates. When the level of water at the downstream side is always lower than the crest of the dam, then recesses (1) are not made downstream of the operational gate. There are also found particular cases when recesses (1) are not made at the upstream face either. Approximately, the dimensions of the recesses can be taken as $a = c = 0.5$ m; $n = c/2 = 0.7$–2 m; $m = (1/7$–$1/10)b = 2$–4 m, where b is a clear span between the training walls. The narrowest part is usually taken as $d_o \geq 1$–1.5 m (Grishin et al., 1979).

Figure 17.16 presents a longitudinal section of a training wall with a mobile crane and a plan of the wall, divided with a joint (Rozanov et al. 1985).

Stilling basin. This serves for dissipation of the energy of the overflowing stream as well as for ensuring a steady flow at the downstream face. The dimensions of the stilling basin are determined with the well-known calculations in hydraulics. The stilling basin is usually constructed in the form of a mass concrete slab. Special hard

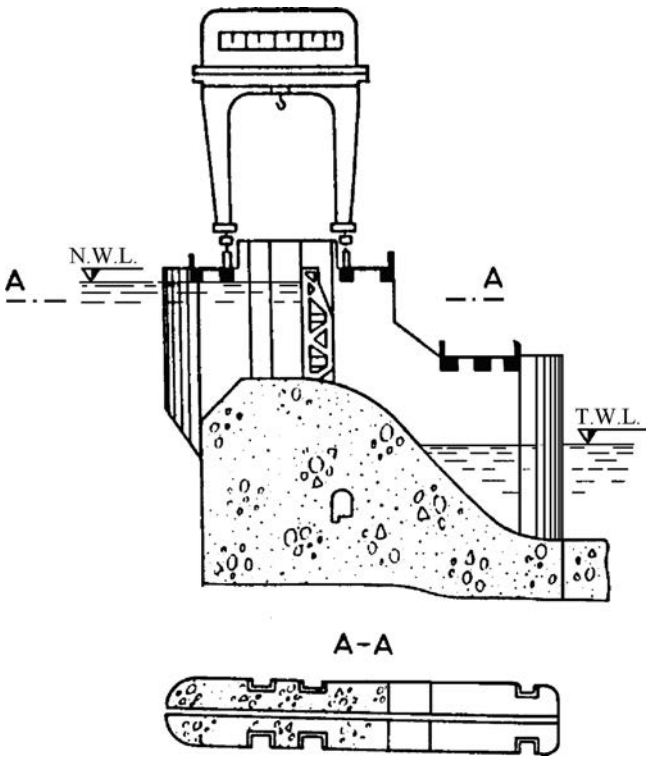

Figure 17.16 Longitudinal section and a plan of a training wall with a joint.

concretes, to which synthetic resins can also be added, are used against the abrasion effect of the sediment and the floating matter, as well as against damages at the surface due to cavitation. The thickness of the layer of the highly resistant material amounts to a minimum of 0.5 m. At the end of the stilling basin there is executed a foundation cutoff in order to provide a good connection with the riseberm.

Dimensioning of the stilling-basin slab is carried out by means of static calculations based on the scheme of forces as is shown in Figure 17.17, acting at a maximum discharge at 1 m of the width of the slab. From the above side there act: the force of weight of water W_g, defined with the drawn diagram, in which h_1 and h_2 are the conjugated depths of the hydraulic jump, while $\Delta h = (0.6–0.7)(h_2 - h_1)$; the force of weight of the slab of stilling basin $G = \gamma_b L_s d$. From the bottom side there acts the uplift force $U = W_b + W_p + W_d$, represented by the diagram 1–2–3–4, in which $W_b = \gamma_w L_s d$ is the force of water displaced by the slab, W_p is the force of uplift represented by the diagram 5–6–7–3–8–5, equivalent to W_g, while $W_d = 0.5\gamma_w \Delta h L_1$ represents the deficiency of pressure on the stilling-basin slab, occurring due to the whirl formed during the hydraulic jump. L_1 is the distance from the beginning of the slab to the drainage openings. Depending on the scheme of the underground contour, a seepage

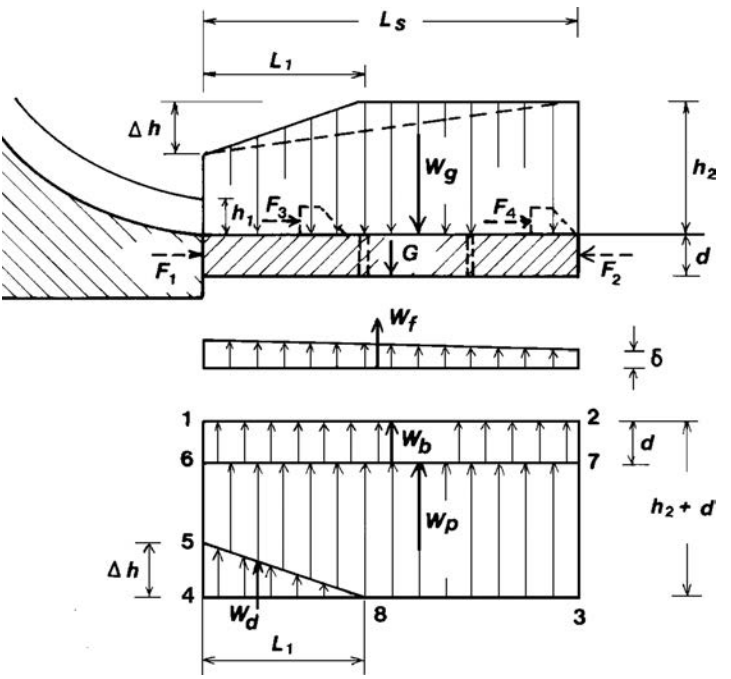

Figure 17.17 Scheme of forces for dimensioning the slab of stilling basin.

force W_e can also act, whose ordinate δ at the end of the slab is reduced owing to the resistance at seepage.

In this way, the coefficient of safety against rising to the surface of the stilling-basin slab can be given with the expression:

$$k_s = \frac{G'}{W_d + W_f} = \frac{(\gamma_b - \gamma_w) \cdot d \cdot L_s}{W_d + W_f} \geq 1.5\text{–}2.0 \tag{17.5}$$

from which is determined the thickness of the slab d.

With large and significant structures, it is also necessary to take into consideration the pulsation hydrodynamic force, directed vertically upwards. This force, at certain points, has considerable value, however due to discrepancy in phases, the mean pulsation pressure on the slab does not exceed 7% of the velocity pressure in the constricted section.

If across the surface of the slab there are set up transverse sills or crests or individual teeth, which will be dealt with in the continuation of the text, then it is necessary to check the safety of the slab against horizontal displacements. In such a case there will be taken into consideration the following horizontal forces, shown in Figure 17.17 with a broken line: F_1 = the horizontal force which is taken on by the stilling-basin slab at the upstream edge; F_2 = force of passive pressure at the downstream edge;

F_3 and F_4 are forces of horizontal hydrodynamic pressure on sills, crests or teeth, which are calculated by means of the expression (4.2).

The coefficient of safety against sliding of the slab will be:

$$k_{sl} = \frac{\Sigma V \cdot f}{\Sigma F} \geq 1.5 \tag{17.6}$$

where: ΣV = total vertical force; f = coefficient of friction between concrete and foundation, i.e. bedding, approximately taken as 0.4–0.6; ΣF = total horizontal force.

For preliminary, orientational calculations, the thickness of the slab can be determined according to the empirical formula proposed by *Dombrovsky*:

$$d = 0.15\, v_1 \sqrt{h_1} \tag{17.7}$$

in which v_1 and h_1 are the velocity, i.e. depth of water, in the constricted section, respectively (Chugaev, 1985).

In a number of mass overflow dams constructed on a soil foundation at a pressure head up to 25 m and specific discharge up to 45 m^3/s, the thickness of the stilling-basin slab amounts to 1–4 m.

The side walls of the stilling basin are carried out with a freeboard of a minimum of 0.5 m above the maximum depth of the water, most often as reinforced concrete walls with a width of 0.30 at the top up to 1–2 m in the base. If the side walls of the stilling basin also serve as retaining walls of the river banks, then they should be appropriately constructed and dimensioned, Figure 17.18.

At the beginning, at the end and in the middle of the slab of the stilling basin there can be executed teeth which contribute to better stilling of the flow as well as to a reduction in the dimensions of the stilling basin. The execution of drainage openings in the slab of the stilling basin is recommended only in exceptional cases, since, owing to the high velocities of flow and pulsations of the pressure, it is hard to ensure prevention of washing out of the drainage material through the openings.

For reducing the seepage uplift of the slabs of the stilling basin, below them is carried out a drainage layer with an inverse filter. Filtrated water is taken off the drainage through openings in the slabs, which also contribute to reducing the uplift, Figure 17.19 (Chugaev, 1985), or through the extension of the drainage below the riseberm.

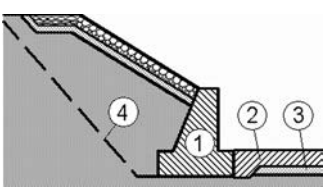

Figure 17.18 Mass stilling-basin wall (1); (2) stilling-basin slab; (3) drainage; (4) boundary of excavation.

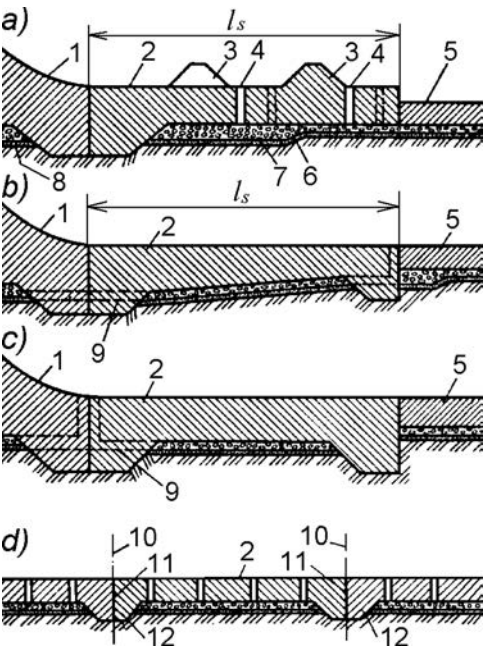

Figure 17.19 Structural scheme of the stilling-basin slab. (a, b, c) Longitudinal section of slab separated from the dam by means of a joint; (d) cross-section. (1) Dam; (2) stilling-basin slab; (3) teeth; (4) drainage openings; (5) riseberm; (6) drainage; (7) inverse filter; (8) drainage below the dam; (9) pipe for draining the water of the drainage below the dam; (10) axis of draining walls; (11) joint; (12) tooth.

Riseberm. This serves for further stilling of the flow downstream of the stilling basin. It can be horizontal, horizontal with an inclined part or inclined. The length of the riseberm is determined by means of model investigations. In a number of already constructed dams, the horizontal part ranges within the limits $(1–2)l_s$, where l_s is the length of the stilling basin.

From a structural viewpoint, the riseberm should be elastic, capable of adapting to possible deformations at the bottom without deranging the stability, while at the same time it should be sufficiently water-permeable to be able to offtake the seepage waters.

The simplest, yet at the same time the most effective construction satisfying the quoted requirements, is a riseberm made of coarse tipped rockfill, placed on filter layers, which prevents erosion of the soil, caused by the seepage water. The thickness of the layer of tipped rockfill can be determined from the expression:

$$d \geq 0.06V_r^2 \tag{17.8}$$

where V_r is the velocity of water at the surface of the riseberm in m/s; d ranges within the boundaries 0.5–1.5 m (Chugaev, 1985).

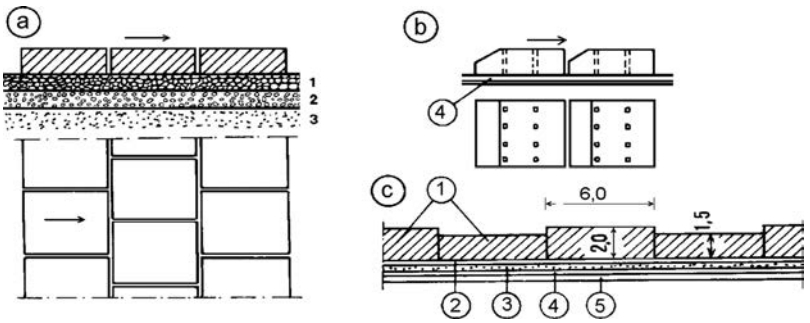

Figure 17.20 Construction of the riseberm. (a) Slabs; (b) perforated slabs with inclination: (1) crushed stone; (2) gravel; (3) sand; (4) inverse filter. (c) Slabs with different thickness: (1) concrete; (2) concrete levelling layer, 15 cm; (3) crushed stone, 30 cm; (4) gravel, 25 cm; (5) coarse sand, 25 cm.

In infrequent cases, a riseberm made of tipped rockfill is reinforced with timber waffle, i.e. a coffered construction of driven vertical beams mutually spaced at 2.5–4 m, to which there are attached horizontal beams both in the longitudinal and the transverse direction.

An effective, but more expensive, structure of a riseberm can be constructed by means of concrete slabs 0.5 to 1.0 m thick, with dimensions 2 to 20 m, placed over a two-layer or three-layer inverse filter (40 to 60 cm), separated by staggered longitudinal joints, Figure 17.20. The concrete grade for the slab can be 15 MPa. They usually require reinforcing with mesh reinforcement, both at the top and bottom. For reducing the influence of the hydrodynamic flow, in the slabs there are made openings and also the upstream sides are inclined. For better stilling of the flow, the slabs can have a different height, i.e. thickness. The thickness of the slabs as well as their stability are determined in the same way as for the slabs of the stilling basin from the condition of rising to the surface, overturning and sliding. The action of forces is examined for different schemes of opening of the gates. As a ruling or critical (design) case there is usually adopted the state of maximum discharge.

Dimensions of drainage openings in the slabs of the riseberm range from 0.25×0.25 to 1.0×1.0 m (or corresponding circular opening). Basically, the openings are set up at distances of 5 to 10 m.

In order to obtain a more economical solution, the length of the riseberm can be made somewhat smaller, but in such a case a special finishing structure is carried out (Fig. 17.21). Most often at the end a pit is executed along with reinforcing of the internal slope and the bottom (Fig. 17.21a). The depth of the pit can approximately be taken as:

$$h_j = \frac{k\,q}{V_{0\,\max}} \tag{17.9}$$

where k is a coefficient dependent on the length of the riseberm and can be taken for the first approximation $k = 1.3$; q is the specific discharge, while $v_{0\,\max}$ is the permissible

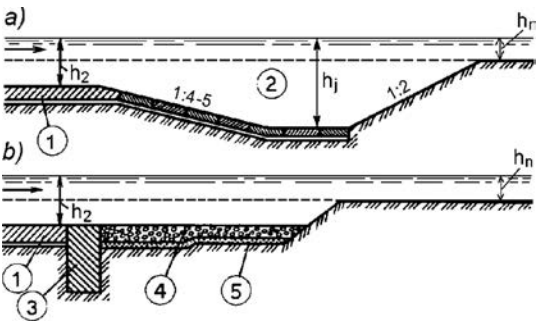

Figure 17.21 Finishing part of riseberm. (1) Riseberm; (2) pit; (3) concrete tooth wall; (4) tipped rock-fill; (5) sand.

velocity for the material in the foundation at uniform flow. The solution as shown in Figure 17.21b is also possible.

17.6 DIMENSIONING AND STABILITY OF GRAVITY DAMS ON SOIL FOUNDATION

For dimensioning gravity dams on a soil foundation there are used the same methods that have been elaborated in Chapter 16. There exist certain specialities in terms of the forces that are taken into consideration. The most dangerous state with this type of dam occurs for a static state with maximum water level, Figure 17.22, when the forces due to the hydrostatic pressure from the upstream and downstream face act on the dam. Furthermore, one should take into consideration the forces due to the uplift water-pressure across the bottom of the dam, expressed through diagrams, obtained by means of a hydrodynamic net. Depending on the construction of the dam, other forces can also be taken into consideration, for example, the horizontal force due to the pressure of the earth blanket, the force of the active earth pressure at the upstream tooth wall, the passive earth pressure at the downstream one, etc. Also consideration should be given to the forces of the static and dynamic pressure of ice, which have been dealt with in section 4.5.

In the case of overflow gravity dams it is characteristic that the static pressure of ice in its greatest part (or as a whole) is transferred to the training walls which are much more rigid than the gates. The gates can also be protected against the generation of ice. In such a case, the scheme for the transferring of static pressure due to ice on the dam looks like the one presented in Figure 17.23. The static force P_0^{l}, which is transferred to one training wall, is equal to $P_{\mathrm{l}} \times d$, where P_{l} is the pressure of ice per one metre of length of the dam, determined as for a non-overflow dam, while d is the thickness of the training wall. The force P_0^{l} cannot be greater than the limit value $P_{\mathrm{l\,max}}$, at which there comes about a crushing and squashing of the ice. That force can be obtained from the expression:

$$P_{\mathrm{l\,max}} = d \cdot \delta \cdot R_{\mathrm{j}} \tag{17.10}$$

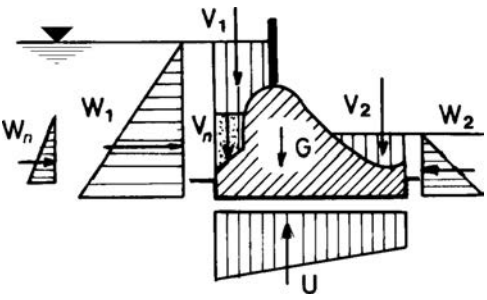

Figure 17.22 Schematic presentation of forces acting on a gravity dam on soil foundation.

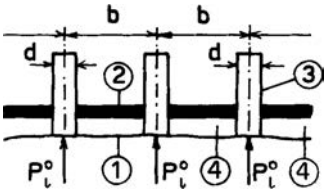

Figure 17.23 Pressure of ice on the dam. (1) Edge of ice; (2) gate; (3) training wall; (4) overflow spans.

where δ = thickness of ice in metres; $R_j = 450\,\text{kPa}$ = limit of compressive strength of ice (Grishin et al. 1979).

The most important checking that has to be performed for these dams is to determine the stability against sliding across the soil foundation, which, often, is not sufficiently high due to the force of uplift pressure and the lower value of the coefficient of friction. For alleviation of the calculation, we usually make a simplification of the cross-section of the dam, in which case the sheet pilings are not taken into consideration, nor the slab of the stilling basin, whose stability against sliding is regularly close to the limit one.

When the stability of dams on a soil foundation is analysed, it is assumed that the overflow part is not cut off from the training walls, so that we examine the structural section of the dam which consists of two semi-training walls and the corresponding part of the dam between them.

If the bottom of the dam is horizontal, and the earth in the foundation is homogeneous, then it is most likely that sliding would take place across the surface of the foundation and in such a case the calculations are performed in the same way as for dams on rock foundation.

Very frequent is the case when the most dangerous surface of sliding passes inside, into the foundation, that is to say when the dam slides along with a part of the foundation. Such sliding can occur in two cases: 1) in the case of a deep and rigid cutoff wall at the upstream end of the dam which, during sliding, drags along a certain volume of the foundation (Fig. 17.24); 2) in the case of non-homogeneity of the foundation,

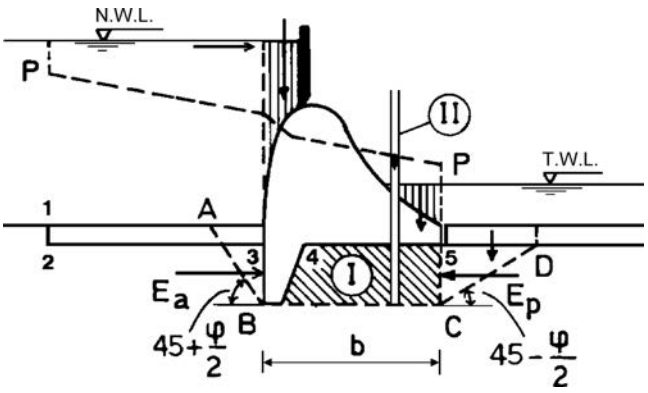

Figure 17.24 Scheme for stability against sliding across the horizontal plane BC. (I) Embraced earth material; (II) imaginary piezometer.

when the strength of the earth material at a certain depth is lower than that on the surface.

In the first case, it is assumed that the surface of possible sliding consists of three planes: *AB, BC* and *CD* (Fig. 17.24). The horizontal part *BC* is conditionally deemed as the bottom of the dam, in which case the earth above the surface of sliding *BC* is added to the dam's body. In such a case, the piezometer line *P-P*, which determines the uplift below the dam if drainage has not been carried out, refers to the conditional underground contour 1-2-3-B-C-5, while the unit weight of the caught earth material is taken in a saturated state. If there is drainage, the line *P-P* will refer to the real underground contour 1-2-3-B-4-5, while the unit weight of the caught volume of earth is taken in a submerged state. The coefficient of safety against sliding, in that case, will be as follows:

$$k_s = \frac{R}{W} \tag{17.11}$$

where W = sum of horizontal forces, including the active earth pressure E_a from the upstream side; R = limit force of the resistance against sliding:

$$R = V \tan \varphi + cB + mE_p \tag{17.12}$$

where V = sum of all active vertical forces acting on the dam, including here the caught earth; b = width of foundation of the dam; c and φ are the specific cohesion and the angle of internal friction of the material in the foundation; E_p = passive earth pressure; m = coefficient, dependent on the conditions of work of E_p (it can be taken 0.7).

So defined the coefficient of pressure should range within limits from 1.1 to 1.25. In the application of the above-described method, the following factors should be taken into consideration: a) if it is deemed that it is possible for there to come about a depositing of sediment in front of the dam, then it is necessary that the sediment also be taken into consideration; b) the force caused by the active pressure of the dam

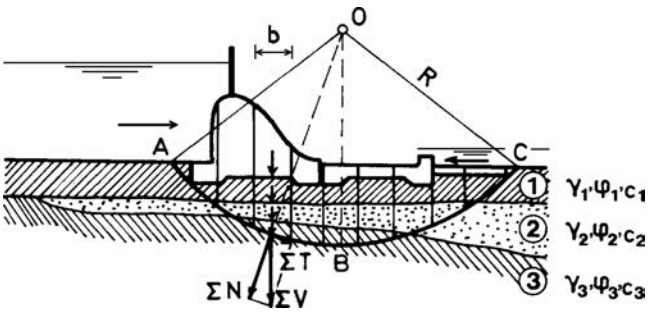

Figure 17.25 Scheme for calculation of the stability against sliding along a circular-cylindrical surface.

on a possible clay blanket, it is also necessary to take into consideration the vertical components of the seepage forces acting on the material of the blanket; c) the passive pressure E_p is taken into consideration only if there is anticipated a small deformation of sliding of the dam towards the downstream face; otherwise, it is neglected. In general, in calculations of this kind it is possible to neglect less significant forces and effects, if that works in favour of the safety.

In the second case, when it is a question of an incoherent foundation, the problem again can be reduced to the framework of the method of limit equilibrium, with the application, however, of the circular-cylindrical surfaces of sliding (this method can also be applied in the first case), Figure 17.25. A number of circular-cylindrical surfaces are assumed, in order to find out the critical one, with a minimum coefficient of safety. The calculation is performed in a similar way to that in the case of the determination of the stability of slopes for embankment dams.

This page intentionally left blank

Chapter 18

Roller-compacted concrete gravity dams

18.1 INTRODUCTION

As we have been able to see in the first, introductory chapter, an enormous number of dams have been built in the world, while the need for new such structures is still evident. Their high cost, as well as the influence on the environment, impose the need to work permanently on their advancement and rationalization of their structure and methods of construction. One can say that progress in the field of dam construction has been achieved when engineers will be able to construct faster – safer, higher, and cheaper dams. That can be achieved with the utilization of new materials, with new conceptions in the construction, as well as with more knowledge – both theoretical and practical.

Gravity concrete dams in the seventies were not able to withstand the competition of the much cheaper embankment dams, which can be illustrated and seen from the diagram in Figure 18.1 (USCOLD, 1988), in which has been presented the intensity of construction of mass concrete dams higher than 30 m by decades in the USA, from the end of the 19th century until 1985. The reason for this has been in the fast progress in the design and construction of earth-rock and rockfill dams with the application of powerful plant and equipment, capable of carrying out works of a tremendous extent. At the same time, gravity dams, being the greatest competitor to embankment dams, constructed of conventional concrete which is compacted by means of vibration, are constructed slowly and have a high unit cost, which cannot be compensated with the five to six times lower volume of the dam's body. Such a trend has been a challenge for builders of concrete dams to think about the possibilities of rationalizing the methods for constructing gravity dams. The most important obstacle to speeding up and making cheaper the construction of these important structures has been the joints between individual blocks of mass concrete. And, so the idea has been born of using highly productive plant and equipment for the execution of earthworks, i.e. for placing earth material with added cement, in order to construct a gravity concrete dam without joints. The concept of putting into place a mixture of earth and cement by the application of heavy plant and equipment was employed for the execution of bases for roads even in the early fifties, while for reinforcing the upstream slope of embankment dams – in the early sixties.

With this material, named roller-compacted concrete by its inventor John Lowe III, in the sixties, constructed the core of 70 m high embankment cofferdam for the

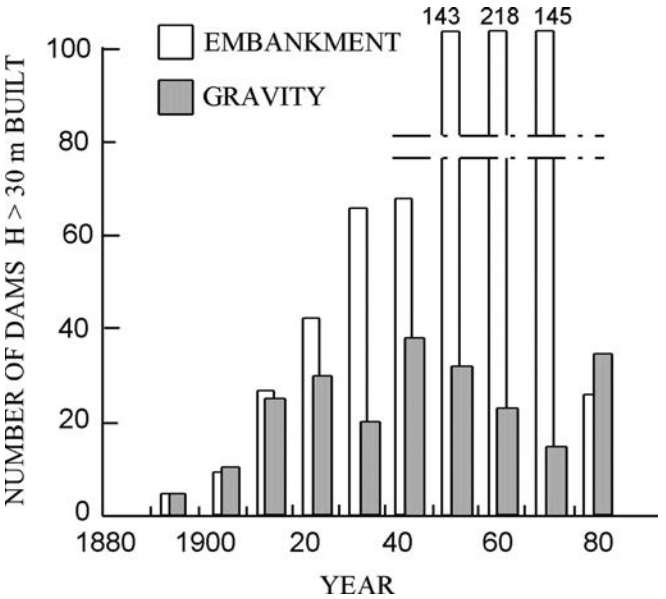

Figure 18.1 Intensity of construction of gravity and embankment dams in USA over decades.

Shimen dam in Taiwan, while later on there have been constructed reparation works on the Tarbella embankment dam in Pakistan. However, it has taken some more time for consideration of and experiments on the application of the roller-compacted concrete for gravity dams, in order to develop criteria for the composition of the mixture and the technology of construction with the application of heavy vibratory rollers for compaction. The first published proposal for the application of the roller-compacted concrete (RCC) for the complete execution of a gravity dam dates from 1970, while the idea was finally realized in 1980, when in Japan in accordance with the new technology was constructed the side spillway of the Shimajigawa dam with 170,000 m^3 placed roller-compacted concrete, while in the USA it commenced with the construction of seven dams of roller-compacted concrete. The first completed dam was the Willow Creek dam (1982, Heppner, Oregon), 52 m high, and 543 m long, with a 116 m-long uncontrolled overflow. The total volume of the dam amounts to 331,000 m^3, with about 300,000 m^3 RCC placed in five months, with the entire dam being built in one year from the awarding of the contract to completion. The upstream face is vertical and it has been formed by means of prefabricated concrete panels 1.2×5 m, $\approx$9 cm thick, anchored in roller-compacted concrete. The downstream face, with an inclination of 1:0.8, has been formed in a step-like fashion owing to its execution in horizontal layers, without particular treatment, while the crest of the overflow has been shaped by means of sprayed (gunite) concrete with a thickness of 60×90 cm. Following these early constructed dams, the method of construction has been developing fast. Dams of conventional concrete have gained a significant reputation in terms of

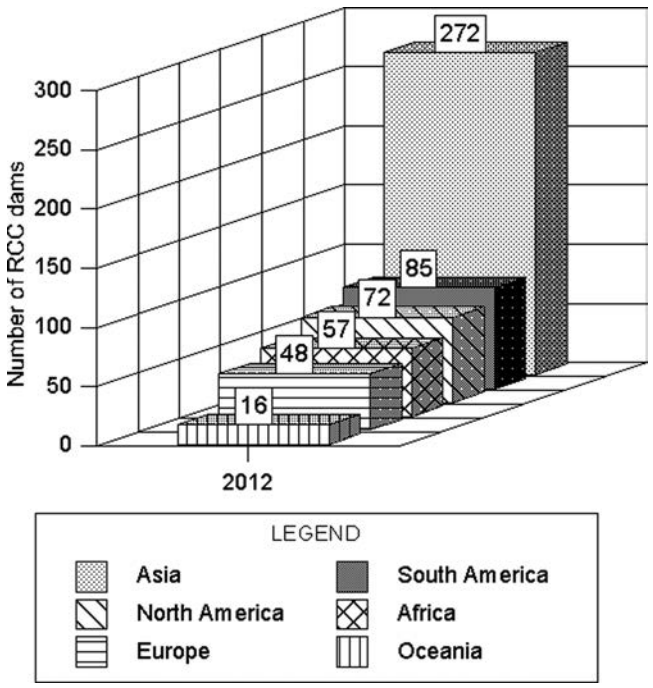

Figure 18.2 Dams of roller-compacted concrete (by continent).

safety, since they can withstand overflowing remarkably above the anticipated quantity of water according to the design, do not suffer from internal erosion, and have undergone strong earthquakes without recording failure. Nowadays, dams of roller-compacted concrete are built with identical features, so that they can completely replace the gravity dams of conventional, vibrated concrete, with remarkable savings in view of cost and time for construction. Therefore, the new material has been widely accepted worldwide.

In general, RCC uses a low-moisture concrete mix, with "zero slump". The mix is typically placed in a series of 30 cm-thick horizontal layers, with each layer compacted by roiling with heavy equipment, typically a 10 ton vibratory roller. One newer technique, referred to as the "slope layer method", uses a series of rapidly placed sloping layers to create a "lift", usually 2–3 m high. This new technique reduces the exposed area of each layer and the time required before the subsequent layer is placed. Placing the layers before the mix "sets" minimizes surface clean-up requirements and allows the "lift" of multiple layers to harden into a monolithic mass with virtually no seams.

Until now (2012), the literature lists 550 dams constructed of roller-compacted concrete that are higher than 15 m, in various parts of the world, in almost all continents (World Atlas, 2012). By continents, their distribution is shown in Figure 18.2,

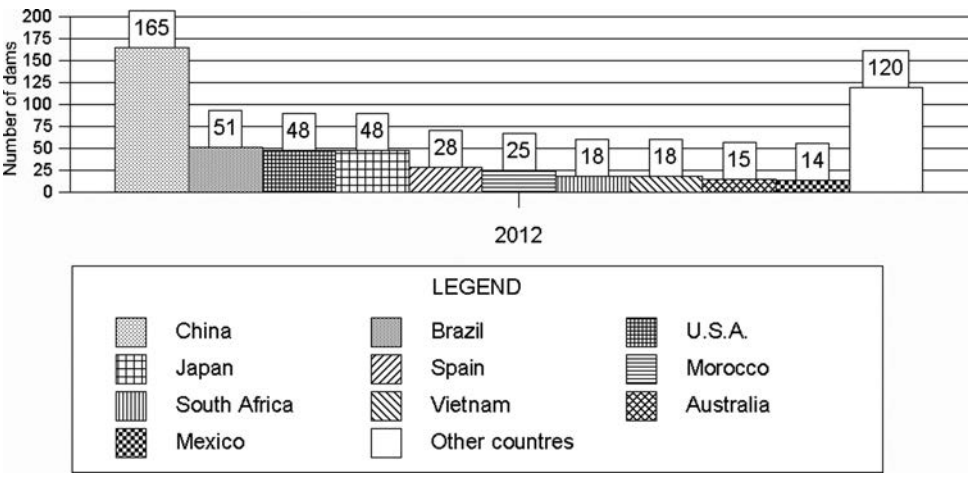

Figure 18.3 Distribution of roller-compacted concrete by country.

while their distribution by countries is shown in Figure 18.3. Although the United States initially had the greatest number of RCC dams, these are now more prevalent in countries such as China, Spain and Brazil. The greatest number of such dams has been built in Asia, mainly in China and Japan. China is well ahead of all other countries, with 165 RCC dams now either complete or under final stage of construction. Noteworthy is the rapid expansion of the popularity of RCC dams in Vietnam: after the success of Son La dam, Vietnam has started construction on a great number of RCC dams and from having only one completed RCC dam in 2006, six years later there are 18 either complete or under construction. As such, it is confirmed that once a country starts building RCC dams, they build more. In North America, more of RCC dams are located in the USA, but the trend in the United States has moved from using RCC dams primarily for new dams to using it more for rehabilitation and support or the buttressing of existing dams, for raising the height of existing dams, and for providing emergency spillway capacity over existing embankment dams (see Chapters 26 and 35). Spain takes the leadership in Europe, both in terms of the number of dams constructed and in terms of the achieved heights of these dams.

Figure 18.3 shows that the six leading countries for RCC dam construction are now China (165 RCC dams), Japan, Brazil and the USA (each with about 50 RCC dams), Spain with 28, and Morocco with 25. Four of the five leading countries in 1990 (one decade since the beginning of the RCC dams era) are still in the top six in 2012. The number of dams constructed in these six countries each year is shown in Figure 18.4, together with the total number of dams. It can be seen that since 1990, the total number has been increasing at a constant rate, although there has been a slight increase in that rate in the last few years (Dunstan, 2012).

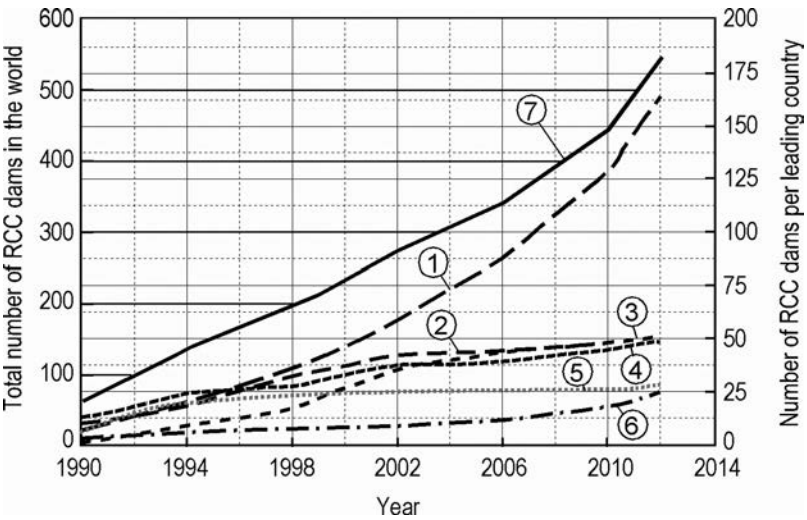

Figure 18.4 Number of RCC dams constructed each year in the six leading RCC dam constructing countries and total number of RCC dams (after Dunstan, 2012). (1) China; (2) Brazil; (3) USA; (4) Japan; (5) Spain; (6) Morocco; (7) total number of RCC dams.

18.2 CHARACTERISTICS OF ROLLER-COMPACTED CONCRETE

18.2.1 Roller-compacted concrete mixture, placement and properties

Dam engineers have always strived to design and construct safe, durable and economical structures. Based on the classic methods of embankment and concrete dam construction, the RCC technology has been developed combining the economical and rapid placement resulting from a high degree of mechanisation with the strength and durability of concrete. Therefore, instead, as a new material, roller-compacted concrete is often described as a concrete being transported, placed, spread and compacted using earth moving equipment in the certain RCC construction process. RCC is a concrete with no-slump consistency in its unhardened state, which has to support the heavy equipment while being compacted. The properties of hardened RCC can be similar to those of conventional vibratable mass concrete, but can also be designed with hardened properties outside the typical range for traditionally placed concrete (ICOLD 2003).

Roller-compacted concrete contains the same basic constituent components as mass concrete: *binder, water, sand, mineral aggregate* and possibly *admixtures*. As aggregate stone chippings is used with a maximum grain of 80 mm (twice less than the usual practice for mass concrete, in order to reduce problems with segregation). A coarse gradation will produce higher laboratory strengths but will also cause more strength variability, more placement problems, and lower-quality lift joints, as was a

case with some early RCC dams. The initial recommendation of the American Concrete Institute was to use a maximum aggregate size of 76 mm, but the current trend is to use a finer maximum aggregate size of 38 to 50 mm.

Grading and properties of sand play a particularly important role in obtaining high quality roller-compacted concrete, on which there depend the minimum required quantities of cement material and water, by means of which one would obtain maximum water-impermeability and density as well as high strength. As a general guide, about 50% of the all aggregate in the gradation should be finer than 9.5 mm, and 35–45% should be sand (finer than 4.75 mm). However, the main requirement for gradation is that it has smooth shape to the curve, with no gaps and a reasonable amount retained at each sieve size.

Earlier a common practice for RCC projects was to use multiple aggregate piles and size groups. This is an acceptable approach, but it results in more cost, equipment, handling, and mixing than using one or two aggregate sizes. Excellent control, without segregation, can be achieved with RCC aggregate using only one or two sizes, especially if the aggregate contains fines and is stockpiled damp. This simplifies the RCC operation, reduces cost, and substantially decreases the area required for storage, as well as the distance aggregates need to be transported back to the mixer when RCC is produced. If the stockpile is split into two size groups, the split should be made at 20 mm (Schrader, 2004).

Portland cement with pozzolan or pulverized fly ash (PFA) is the most often used cementitious materials at RCC. In general, the total quantity of the cementitious material in the RCC mixture is smaller than is the case with the conventional concrete, sometimes even below 100 kg/m^3 (cement and pozzolan or PFA together), so that the roller-compacted concrete is lean concrete. Water is proportioned in a minimum quantity, just as it is necessary to obtain a workable dry mixture, without cone slump; the machines for transportation, spreading and compaction will not sink into the already placed layers.

Roughly, RCC mixtures should be classified as having low or high cementitious contents. Both types of mixtures are common and have some advantages and disadvantages. High-cementitious content mixtures cost more because of the increased cementitious materials, specific requirements for cleaner and more carefully controlled aggregate, and typically greater cooling or thermal considerations. But low-cementitious content mixtures may require special lift joint treatment or other efforts to provide total watertightness.

The mixture must have a sufficiently cementitious paste in order to ensure its penetration into all the voids in the sand. A high ratio of mortar/paste is required for filling the entire space among the grains of the mineral aggregate, for which it is necessary to use a greater quantity of sand, in comparison with conventional concrete. For an optimum value of this ratio, maximum density of the material is obtained, which, sometimes, also reaches the higher possible values of conventional concrete, since it has a lower percentage of free voids (Serafim, 1988; Schrader & Namikas, 1988; Sterenberg, 1992). Many engineers, describing the RCC types, instead of "cementitious content" use the terms "high paste" and "low paste" to describe types of RCC. *Paste* includes all material finer than 75 microns: cement, slag, pozzolan (fly ash), aggregate fines, admixtures, water, and air. But all good RCC has 19–21% paste by volume, regardless of the cement or pozzolan content, although in an effort to make

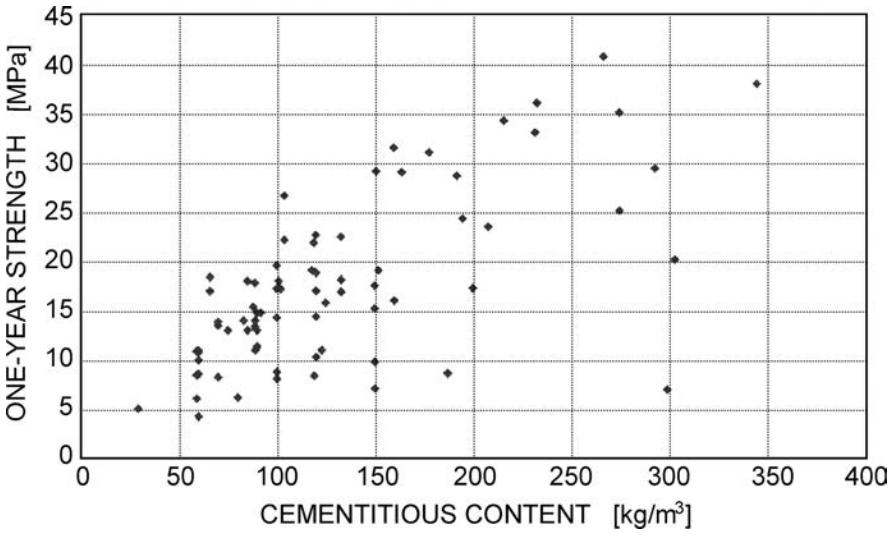

Figure 18.5 The relationship between the one-year strength of RCC vs. cementitious content (after Schrader, 2004).

more construction-friendly mixtures, the trend has been moving towards slightly higher paste contents of 20–22%. Mixtures with less paste tend to segregate, and mixes with more paste tend to produce less strength per kilogram of cementitious material. Therefore, RCC with less cement requires aggregate fines to provide adequate paste without excess water, while mixtures with more cement require cleaner aggregates. Generally speaking, more mass is not required for RCC dams with lean mixtures unless dams are higher than 100 m. In such a case, if higher-cementitious content mixtures with more strength are less expensive than adding more mass, stronger mixtures can be used only in zones where higher stresses occur. This has been the case with Miel 1 dam in Colombia ($H = 188$ m), where a combination of added mass with lower-cementitious content RCC and zoned areas of higher-cementitious content RCC for areas of high stress have been used to achieve an optimal design (Schrader, 2004).

The wide range of mixtures available for RCC material results in a similarly wide range of concrete strengths. For illustration, Figure 18.5 shows the relationship between the one-year strength of RCC vs. cementitious content. This data comes from average results of quality control tests of RCC in place at various dams, as well as the results of variations to mix designs tested by engineers trying to optimize the mix in various projects. For example, projects built with low-cementitious-content RCC usually also were evaluated with high-cementitious-content mixtures and mixtures using ash. Evidently, one-year strength of RCC varies widely with cementitious content, indicating that no single mix is best for all situations (Schrader, 2004).

For determination of the optimum moisture of the mixture, at which maximum density, i.e. compactness, is obtained, as well as for determination of the most suitable grain size distribution of the mineral aggregate, the Proctor compaction test is

used. Since there must not be a cone slump of the concrete, the workability of the roller-compacted concrete must be determined by means of other tests (for example, the VEBE-test), with the application of new apparatus that has to be sufficiently simple to make possible rapid obtaining of results in the course of the execution of the works.

Furthermore, RCC can also be classified as having high, low, or no pozzolan or fly ash content. Fly ash is the most commonly used, but manufactured and natural pozzolans are also used. Ground slag is also effective where available. A lot of RCC dams have a large portion of pozzolan, but there are also numerous examples where pozzolan was not applied. Each project should be evaluated with regard to available materials before deciding what is best, because some locations have no pozzolan, while others have readily available fly ash at low cost. Also, it should be mentioned that very high ash contents may results in unacceptably low density and lower strength, and extraordinary water demands.

The water content required for compaction of RCC is essentially fixed for any given aggregate type and gradation, regardless of cement content. Therefore, lower-cementitious-content mixtures have high ratios of water to cementitious materials. This ratio increases as cement content decreases. Consequently, higher water to cementitious materials ratios in RCC generally result in mixes with more strength per kg cementitious materials, if the increase results from decreasing cementitious material rather than from adding water.

It is difficult to determine what percent of added pozzolan or fly ash brings the greatest strength increase as a function of the RCC age. Experience on RCC dam construction shows a large variation in the strength gain of different types of mixtures. Some mixtures with high pozzolan percentages demonstrate substantial increases (300–500%) in strength at one year when compared to strength at 28 days (Fig. 18.6), but other mixtures with pozzolan have less long-term strength gain than mixtures containing only cement. In addition, some cement-only mixtures have had very low strength increase after 28 days, while other cement-only mixtures have had one-year strengths 125–250% of the 28-day strength (Fig. 18.6). In extreme cases, RCC mixtures without pozzolan have shown strength increases at one year of more than 350% over 28-day strength, and high-pozzolan mixtures have shown strength increases of as much as 500% (Fig. 18.6). The reason for such large variation in behaviors is not always the same and not always clear. It is usually related to the amount, particle size, and composition of aggregate fines, in combination with the chemical and physical properties of the cement and pozzolan available. Finally, in some cases strength actually increased more at one year by adding pozzolan, compared to adding the same weight of cement. In other cases, the strength decreased when pozzolan was added while the cement content was kept constant (Schrader, 2004).

For preparation of the mixture, it is possible to use ordinary or special mixers, while transportation is accomplished by means of large trucks or, even better, by means of conveyor belts. Spreading in layers, with typical thickness of 30 cm, in a strip of full length from bank to bank is achieved by means of large bulldozers and scrapers, while compaction is performed by means of heavy vibratory rollers.

From past, already abundant practice in the application of roller-compacted concrete, it is possible to conclude that the lean concrete mixture, thanks to the high quantity of pozzolan or PFA (even more than half of the volume of the binding agent,

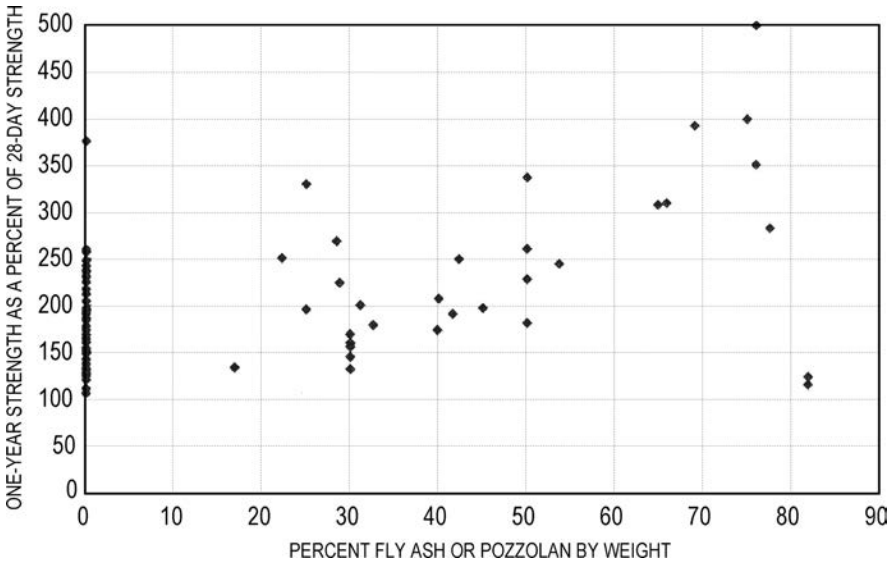

Figure 18.6 Experience in RCC dam construction shows a large variation in the strength gain of different types of mixes. For example, RCC mixes without pozzolan have shown strength increases at one year of more than 350 percent over 28-day strength. And high-pozzolan mixes have shown strength increases of as much as 500 percent (after Schrader, 2004).

i.e. binder), and to the low water/cement ratio, can be placed in layers and perfectly compacted with vibratory rollers, by means of which the body of the gravity dam can be constructed in continuous layers from one bank to another, without joints.

Shrinkage of roller-compacted concrete is minimal; however, thermal problems, owing to the generation of hydration heat of the cement material, are also present here (Zhu & Xu, 1995). As is known, there appear cracks in the concrete owing to the contraction caused by the cooling down of the concrete from the maximum temperature after its placement to its final mean temperature. The maximum temperature following deposition of the concrete depends on the released hydration heat of the concrete, as well as on the absorption of concrete heat by the environment in the process of hardening of the concrete. Roller-compacted concrete is more favorable in relation to the danger of cracks, as compared to conventional concrete, since the mixture is leaner and contains a high percentage of pozzolan or PFA, so that, owing to that, there is a lower generation of hydration heat. The higher percentage of pozzolan or PFA also brings about a slower attainment of the strength, a lower modulus of elasticity in the initial period and, thus, a higher creep over a longer time period. That makes a contribution to the adaptation regarding a part of the dilatations caused by temperature changes. That is why, in moderate climatic conditions, one should expect roller-compacted concrete not to crack considerably if it is poured in colder months and if consideration has been taken about the mixture temperature during deposition. In less favorable climatic conditions, there can come about cracks – longitudinal cracks are less probable, while

transverse ones can be expected, but they need not extend across the entire section of the dam. Hansen and Forbes (2012) give a thorough study of the thermal induced cracking performance of RCC dams. Based on nine case studies and the authors' rich experience, they drew the following main conclusions:

- Major thermal-related cracks are basically vertical, through the entire dam section, and may be of sufficient width to pass water at times. Because RCC dams invariably have a traditional gravity dam shape, these vertical cracks are not considered detrimental to the structural stability of the dam.
- Cracks in an RCC gravity dam may not have been caused solely by thermal induced tensile stresses. In some cases, reservoir induced horizontal movements in the foundation or differential settlements in a non-rock or low modulus rock foundation as well as concrete shrinkage due to loss of water may have contributed to the cracking.
- All transverse cracks do not initiate at the same time, nor are they of the same width. While a constant crack width is used in a simplified thermal analysis, measured crack widths can vary by a factor of more than 4 between the widest and narrowest crack width in a transverse joint. The first cracks observed tend to be the widest in the long run.
- The most common cause of greater than anticipated cracking than predicted by a thermal analysis is a delay of construction schedule that pushes RCC placement into the warmer summer months resulting in a higher peak temperature in the RCC mass than used in the analysis.
- Average crack spacing for stronger RCC tends to be greater than lower strength concrete due to its increased tensile strain capacity. Because the total length reduction needs to be accommodated by a lesser number of cracks, the average width is greater. These wider cracks are a greater problem if they pass water.
- The location of uncontrolled cracks tend to be at planes of reduced cross-section or stress concentrations such as: through the gallery entrance adit, in the centre and at times near the ends of the spillway notch, high in the dam near the abutments where there is greater foundation restraint together with a reduced section, protrusions of the foundation rock into the dam, adjacent to a conduit penetrating the dam, or near a change in the axis of the dam.
- Repair of wide uncontrolled cracks can be quite expensive, especially if the reservoir cannot be completely lowered for repairs.
- The cost for providing an equal reduction in RCC placing temperature is not constant. The use of chilled water or ice in the mixing water provides the lowest cooling cost per degree; the use of liquid nitrogen is considered expensive and may not provide sufficient cooling benefit in relation to its cost.
- Surface cracks due to a high thermal gradient between a hot interior and a cool surface may not initially penetrate far into the surface. However, they may turn into full section cracking as it is easier to propagate an existing crack than initiate a new one.
- While a complex computer thermal analysis can be quite accurate in predicting temperatures with time as the RCC is placed layer by layer, they are less accurate in predicting crack location and width.

The main recommendations given in this noteworthy work are:

- In order to reasonably control thermal-induced cracking in a RCC dam, the designer needs to consider both pre-cooling measures for the concrete and also the installation of transverse contraction joints.
- If the construction schedule will permit, producing aggregate in the winter and restricting RCC placement to nights and the cooler part of the day or year is invariably the most effective and least costly temperature control method.
- The limiting maximum placing temperature for the RCC should consider the annual average temperature at the site, the function of the dam, and the cost of extreme cooling measures, if too low a RCC placing limit is specified.
- Rather than specifying a strict maximum placing temperature for the RCC, consideration should be given to specifying a limiting average temperature over a 1 or 3 day period with a higher placing temperature allowed for a short period of time each day. In this manner, the contractor can better plan his cooling method and placement schedule with an eye towards cost reduction, without increasing cracking potential.
- Cooling should be pre-planned by the contractor for the worst case weather scenario especially with respect to cooling of aggregates. If additional cooling is required at the last moment, low cost cooling methods may no longer be available.
- Transverse joints should include a waterstop and drain, be relatively easy to install, not affect RCC placement to any great extent and use low cost materials to produce a weakened plane. Considerable care should be taken in installing waterstops. There are too many cases in all types of concrete dams of improperly installed waterstops leading to excessive leakage at the joint and costly repairs.
- Transverse joints should be strategically located and need not be spaced equally across the dam. Recently, quite a few designs have used an average spacing of about 20 m.
- Sealed or waterstopped joints in the facing concrete (where used) should also be part of the design to control drying shrinkage or initial thermal related surface cracking; these vertical face joint notches are usually spaced in the range of 3.7 to 4.9 m; surface cracks will usually initiate in the face joint and could propagate downstream later. The face joint notches should be either waterstopped or sealed; at times these will require resealing
- Crack inducers need not be placed in every lift in the full upstream – downstream direction to be effective. Placing the crack inducer in every other lift seems to work effectively; extending the inducer only a partial distance from both the upstream and downstream faces is not recommended, as it has been found the upstream – downstream propagation of the cracks do not actually meet up, with the result that the downstream initiated one is not sealed by a waterstop (Salto Caxias dam, Brazil, is a good example of this).
- An old graph showing typical adiabatic heat rise curves for up to 28 days for varying Type I and II Portland cements should not be used because newer cements produce more early heat than in the past due to finer grinding and the use of fly ash in the mixture produces a heat peak well past 28 days; this increased temperature peak may be offset by a heat loss to the atmosphere and other boundary conditions greater than the 25% assumed by some designers.

Generally speaking, the compressive strength of roller-compacted concrete is close to that of conventional concrete. The resistance against tensile strains is similar. If there is ensured a good bond between the horizontal layers, for which a required condition is for not more than eight hours to elapse between the applications of two adjacent layers, then it is possible to achieve good water-impermeability of the joints. In general, roller-compacted concrete has a somewhat higher water-permeability in relation to conventional concrete. If there elapses a longer time period between the placement of two consecutive layers, then between the old and the new layer it is necessary to deposit a 2 cm thick layer of mortar, which will ensure a good bond. For improving water-impermeability, other measures are also often undertaken, which will be elaborated hereinafter.

18.2.2 Lift joint bond

One of the significant differences between a conventional vibrated concrete (CVC) dam and a RCC dam is the number of horizontal construction lift joints. Placed in 30 cm lifts RCC contains 5–7 times more joints and potential planes of weakness for sliding or overturning failures to occur along, compared with formed CVC. Various approaches have been adopted in earlier RCC dams to achieve acceptable bond between lift joints, including minimizing deterioration by plant of the compacted lift surface, maintaining curing, preparation of the surface, final clean up and use of a bonding concrete, mortar bedding, or grout over all or part of the width of the lift. Another approach is the use of RCC mixes containing a high fly ash or pozzolan content, relying on the delayed hydration and cementation process of the fly ash or pozzolan to assist in the bonding process with the overlying lift.

In contemporary RCC dam construction practice the horizontal construction joints are classified as *hot joints* (no treatment needed), *cold joints* (treatment needed), and *warm joints* (any treatment if desired). Several criteria could be met for determining whether a joint could be considered hot, warm or cold. One of them is the so-called *Maturity Factor (MF)*, defined as:

$$MF = t \times T \tag{18.1}$$

where t = the mean hourly temperature, measured on the surface of the layers in degrees Centigrade; T = the time (in hours) which has lapsed between the placing of two successive layers.

In the beginning, the MF was fixed at between 150 and 250 [°C × h]. With these values it was necessary in many cases to divide the dam into blocks through form-worked joints, depending on the size of the facilities. In practice, this criterion was applied with flexibility. Every dam is a prototype that has an *MF* variable with time, according to the environmental conditions of temperature and relative humidity. So, experimental data obtained on the test section would provide a value of MF to be applied as a practical control for the constructive process. Depending on the cases, the MF varies between 80 and 300, which assumes an exposure time of the layer from 6 to 9 hours for concretes with not so high cementitious material content ($<120\,kg/m^3$). Treatment with mortar would be required in the case of time between layers above that marked.

In the case of RCC with very high cementitious material content (>200 kg/m^3) it is possible to have an exposure time of 24 hours. Some experts have recommended for RCC containing very high cementitious materials that the joints be treated as follows:

- An exposure time of less than 24 hours – *hot joint*; no treatment is required if the surface has not been damaged; simply remove the water and the detritus by a vacuum-equipped truck.
- An exposure time of between 24 and 48 hours, or with a favorable climate, up to 72 hours – *prepared or warm joint*; it is sufficient to rake the surface with a steel wire brush and remove the detritus by a vacuum-equipped truck, for instance.
- An exposure time of more than 72 hours, or with unfavorable climate 48 hours – *cold joint*; wash the surface with pressurized sand and/or water and complete the process as the previous case.

Since it is almost impossible to be able to place more than 1 or 2 RCC lifts per day, the initial and final set of the cement will have truly occurred before the next lift is placed, especially with un-retarded RCC mixes. As a consequence, the ability of the surface of the lower lift to develop full bond with the under surface of the overlying lift, is largely lost. Forbes (2008) reported that vertical cores taken through RCC lift joints commonly show 1 in 2 joints recovered broken, i.e. the bond was insufficient to overcome the torque applied by the coring bit. Direct tensile strengths of bonded joints has been shown to vary considerably, seldom are joints more than 1/3 of the parent RCC tensile strength, those using a bedding mortar may reach 2/3, but it is very unlikely that penetration of aggregate particles for the overlying lift will be seen to have penetrated the surface of the lower lift. Forbes has concluded that with this background experience it is now generally accepted that unless the overlying lift can be placed *within the initial set time* of the RCC then lift joint strengths must dominate the design and will determine the potential failure plane. Hence the RCC strength itself is of lesser importance (Forbes, 2008).

Two basic approaches have been introduced to overcome the above described problem:

- To heavily retard the hydration process by use of *a chemical admixture (retarder)*; and
- To significantly reduce the surface area of the placed lift by using *the method of sloping layers*.

Chemical retarders were first used in RCC in China for Jiangya Dam in 1997. Retardation extended initial set from 1.5–2.0 hours (unretarded) to 6–8 hours depending on summer/winter temperature. The placing process involved forming up a 3 m thick block using a form aligned on a transverse contraction joint, such that the area enclosed resulted in a 300 mm thick RCC layer with a volume equal or less than the volume of RCC that could be produced by the mixing plant in the retarded initial set time. In this way 10 layers of RCC would be placed all within the retarded initial set time of the RCC. A gap in the form and a sloped RCC ramp allowed access into the placement area. On completion of the lift the transverse form would be re-erected and the adjoining 3 m lift placed. The surface of the cold lift joint would be "greencut"

and a bedding mortar applied with the first RCC layer. The process was encumbered by the cost and time of setting up the transverse form and the cost of the retarding admixture, but this was offset by the time and cost saved in lift joint preparation. The main advantage of this method is that it simplifies the forming up of the downstream stepped face of the dam, which is complex when lift heights exceed the step height.

A further development of the procedure, still using lift heights of 1.2 m being equal to the downstream face step height, has been to eliminate the transverse form entirely, i.e. extending the access ramp of RCC to full width of the block between upstream and downstream faces. Ideally the ramp is located over the transverse contraction joints, wherever possible. The four layers of RCC are ramped down to the previous cold lift surface so as to finish off with a ramp slope of 4H:1V. The "feather edge" of the ramp is cut back during the preparation of the lower lift surface to a minimum thickness of 10 cm, and then covered entirely with bedding mortar at the start of placing the first layer in the adjoining lift. A disadvantage of this method is that the lift surface preparation in the adjoining block cannot be effectively undertaken until the lift has been completed (Forbes, 2008).

The placing rate, selection of plant and retarder dose rate is based on the maximum lift volume of the dam – which typically occurs at about one third of the dam height for uniformly sloping abutments. For this method placing rates for large dams of up to 10,000 m^3/day are usually necessary, as was the case at Yeywa Dam. For some projects that are set up for very high RCC placement rates, often using a high pozzolan or fly ash content in the RCC mix which, together with a retarding admixture, can achieve delayed initial set times of 18–24 hours, it is possible to place a single 30 cm lift over the full area of the dam within the delayed initial set time of the previously placed lift (Forbes, 2008).

The sloped layer method (SLM) of placing RCC was conceived during the construction of Jiangya Dam in late 1997 and adopted from about mid-height onwards. With this new method placing rates increased considerably and the project was thus completed on target as a direct result of this innovation. Since then the sloped layer method has been successfully used on many other dams. The procedure initially adopted for Jiangya Dam had been to place the RCC in blocks 3 m high as described above. By removing the transverse form and placing the 30 cm thick layers of RCC on a slope, in a direction parallel to the axis of the dam, from one abutment to the other between the formed upstream and downstream faces (Figure 18.7), the same 3 m lift could be built up as a continuous process across the entire dam without the need for the transverse form (Forbes, 2008).

The volume of RCC placed in the 30 cm thick sloping layer can be altered by simply changing the slope selected for the layers. For example, using say 3 m high forms, as were adopted at Jiangya Dam, with a RCC mixer output of 500 m^3 per hour, and initial set time of the un-retarded RCC of 2 hours, and a width between upstream and downstream faces of W, then S, denoting the slope (Fig. 18.7), will need to be:

$$S < \frac{2 \cdot 500}{W \cdot 3 \cdot 0.3} \quad \text{or approximately: } S < \frac{1000}{W} \tag{18.2}$$

Using the approximate formula (18.2), for example, at lower elevations, where the width W is say 100 m, then a slope of 1 on 10 is required. Later, when the width has

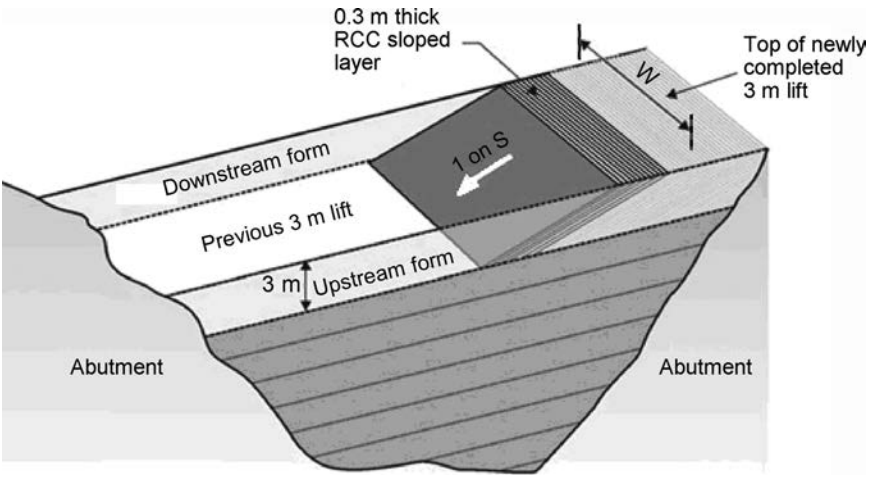

Figure 18.7 Schematic presentation of the Sloped Layer Method (after Forbes, 2008).

reduced to say 25 m at upper elevations nearer the crest, then a flatter slope of 1 on 40 might be adopted if the time between placing RCC layers of only 0.5 hours with a 1 on 10 slope is, for some reason, considered to be too short.

When using the SLM the need for final clean up and preparation of the lower lift surface, including application of bedding mortar, is restricted to a narrow strip along the toe of the sloped layer where it is in contact with the previous lift surface. For slopes of 1 on 10 the width of such a strip is about 3 m and for slopes of 1 on 40 it is about 13 m. The newly completed horizontal lift surface behind can be green-cut whilst the RCC is still young and the upstream and downstream face forms can be lifted; 5–10 days would be available to prepare for the start of the next 3 m lift. Form lifting and lift surface preparation are thus effectively removed from the "critical path". If the 30 cm thick sloping layers are placed within the initial set time of the RCC no surface preparation, clean up or bedding mortar is required prior to placing the next sloped layer. For 3 m high lifts this reduces the surface preparation required by 90%. It also reduces the number of lift joints (and potential failure surfaces through the RCC dam) by 90% (Forbes, 2008).

For inclined downstream faces the best arrangement appears to be to use vertical steps. If formwork is used then the step height would be equal to the lift height. At Jiangya Dam and also Kinta Dam ($H = 90$ m, Malaysia, 2006) where 3 m high lifts were used, precast concrete blocks were provided to form the 1 m and 0.6 m high steps on the downstream face respectively. Blocks are simply recovered from behind and added ahead of the advancing layers as the horizontal RCC steps were constructed and a base for the blocks to form the next step above became available. This stepped precast block "formwork" system would appear to be an ideal method where more than one step is required to match the selected lift height.

Cores of RCC extracted from Jiangya, and more recent Chinese dams using the sloped layer method, where a thin layer of bedding mortar has been applied on any layer

or lift joints older than the initial set time of the RCC, are at times being recovered in single, un-broken lengths up to 15 m long equal to the length of the core barrel. Typically more than 9 joints out of 10 are being recovered intact compared with 1 out of 2 for joints where the initial set time has been exceeded (Forbes, 2008).

Details of the slope layer method are given by Forbes (2008). He has summarized the following advantages of the FLM: achieves homogenous, monolithic RCC across lift joints; reduces the horizontal construction lift joints by up to 90%; initial and final lift joint preparation and form lifting taken off the critical path; reduces the area of young RCC exposed to rainfall or subject to freezing, reduces the potential for RCC to heat gain in hot ambient conditions; provides a low "notch" or channel over the RCC placement area allowing the works to be safely overtopped by floods with plant parked up above the flood reduces subsequent clean up work; proven increases in RCC placement rates of 30–50%. Forbes has also mentioned possible disadvantages of the SLM: downstream face requires either the use of high steps equal to the lift height or use of temporary pre-cast concrete blocks to form up the steps; increased loading on the vertical forms; "feather edges" running in an up-downstream direction at the top and bottom of the slope need to be properly dealt with; survey control of the RCC placing is a little more complex.

18.3 TYPES OF ROLLER-COMPACTED CONCRETE

In the past more than 30-year practice in which period more than 500 large dams of roller-compacted concrete have been constructed, different variants of roller-compacted concrete have been used, which can be classified into 4 major groups:

- *Lean and dry mixture*. Roller-compacted concrete of this type has less than 100 kg/m^3 cementitious material (Portland cement and pozzolan or PFA together), of which up to 40% can be pozzolan or PFA. It is placed in layers with a thickness of ≈30 cm. Aggregate with a high participation of fine particles is often used for this type of mixture. Characteristic examples from the early period of construction of RCC dams are the Willow Creek, Grindstone Canyon, and Monksville dams (USA), while more recent examples are Hassan II (Morocco) and Çindere (Turkey).
- *Rich and wet mixture*. Sometimes for this type of mixture the term *high-paste content RCC* is used. Concrete of this type is designed to contain a very low quantity of free voids and to obtain a good bond between layers, possibly without treatment of the surface while placing the following layer. As in the previous case, here too placement is performed in thin layers ≈30 cm thick. The quantity of cementitious material exceeds 150 kg/m^3, but the greater part, usually 50–80%, is pozzolan or PFA, so that the quantity of Portland cement is low. Characteristic examples are the Upper Stillwater (USA), Santa Eugenia (Spain), and Knellpoort (South Africa) dams (from the early construction period), and a lot of RCC dams constructed during the last two decades, like Platanovryssi (Greece), Ralco (Chile), Kinta (Malaysia), Son La (Vietnam), and Longtan, Guangzhao and Jin'anqiao (China).

Table 18.1 Classification of RCC for dams.

Type of the mixture	*Low-cementitious*	*High-cementitious*	*Medium-cementitious*	*RCD (used in Japan)*
Cementitious content (cement + pozzolan [kg/m^3])	<99	>150	100–149	120–130
Pozzolan content [% mass of cementitious material]	0–40	30–80	20–60	20–35
Compressive strength [MPa]	5–15	17.5–31.5	11–21	

Table 18.2 Average mixture proportions of the different design philosophies of RCC, based on data of constructed dams up to 2010 (after Dunstan, 2012).

Material Type of the mixture	*Cement (c) [kg/m^3]*	*Pozzolan (p) [kg/m^3]*	*Total (c+p) [kg/m^3]*	*Water (w) [kg/m^3]*	*w/(c+p) [ratio]*
Low-cementitious	68	11	79	123	1.55
High-cementitious	88	108	196	110	0.56
Medium-cementitious	77	40	117	116	0.99
RCD (used in Japan)	86	36	122	94	0.77
Hard-fill	60	13	73	135	1.86

- *Medium wet mixture*. This concrete contains between 100 and 150 kg/m^3 of cementitious material. It represents a transition between the first two types of roller-compacted concrete. With this type of RCC the whole range of cementitious content is covered. Examples are: Copperfield (Australia), Sahla (Morocco), Salto Caxias (Brazil), Al Wehdah (Jordan/Syria) and Feke II (Turkey).
- *Roller-compacted concrete used in Japan*. This type of concrete differs from the roller-compacted concrete used in other countries – where they have as a rule used a mixture that has fallen within one of the above three groups. It is rather different from them, and dams built using this material in Japan are called *roller-compacted dams (RCD)*. This concrete is placed in layers of about 30 cm, but the compaction is made in lifts up to 100 cm, while joints are cut in from the upstream to the downstream face of the dam. The upstream face is covered with a layer of conventional concrete 2 to 3 m thick, provided with seals, i.e. waterstops, and drains at all joints. The quantity of cementitious material ranges from 120 to 130 kg/m^3, of which 20–30% is pozzolan or PFA. Typical examples for this are the Shimajigawa, Tamagawa, Origawa, Ueno and Takizawa dams.

The above presented classification of RCC mixtures for dams is summarized in Table 18.1. As a supplement to Table 18.1, in Table 18.2 the average mixture proportions of the RCCs used in practice for each of the different design concepts are shown. In the table are included so-called *hard-fill dams*, which have approximately equal upstream and downstream slopes. Together with the *cemented sand and gravel (CSG)* dams, they might be described as a cement-stabilized rockfill dams. The concept

is to design a dam section somewhere between the gravity dam and the embankment dam, using a material with characteristics between concrete and soil. Hard-fill and CSG dams have been introduced during last 20 years, and are discussed in the last section of this chapter. It is characteristic that the average water content of the high-workability high-cementitious RCC (Loaded VeBe usually 8 to 20 s) is rather lower than the water content of the much less workable hard-fill and low-cementitious RCCs (Loaded VeBe usually 30 to 60 s). This is because of the high proportions of pozzolan (frequently fly ash). The average Portland cement content of all five average sets of mixture proportions is fairly similar (only ranging from 60 to 90 kg/m^3), while the average pozzolan content varies considerably (from about 10 to 110 kg/m^3).

Although the four various approaches to the composition and placement of the mixture of roller-compacted concrete described have many common elements, yet, each of them also contains in part its original philosophy. In the case of dams constructed of a lean mixture, there is incorporated a certain form of upstream membrane as a water-impermeable element. Between the layers of roller-compacted concrete there is often placed a thin bonding layer, especially in the vicinity of the upstream face, in order to improve the bond, i.e. joint between layers and also to reduce the seepage between layers of roller-compacted concrete.

Behind the philosophy of rich and wet mixture, there stands the assumption that mass (non-reinforced) concrete poured without joints across the surface, will almost certainly crack as a result of temperature changes. That is why it is considered that the interior of the dam will represent a water-impermeable barrier, while the surface layer will protect it against external influences. This type of concrete is considered to have layers that are closely jointed between themselves and that its water-impermeability will be almost the same as for conventional concrete. This immersion-vibrated concrete is used on the faces of the dam, and is provided to give an improved finish and to contain the waterstops at the upstream end of induced contraction joints.

18.4 TRENDS IN DEVELOPMENT OF DAMS MADE OF ROLLER-COMPACTED CONCRETE

Within the period of more than 30 years of construction of dams of roller-compacted concrete one can notice tendencies towards permanent development and improvement of this type of structure. Figure 18.8 presents the cumulative number of dams constructed of roller-compacted concrete until the end of 1996, i.e. in the first half of the period of application of this dam type up to now, according to the type of the concrete mixture. From the diagram, it can be seen that in the period till the end of 1986, which can be considered as the period of the first generation of dams made of roller-compacted concrete, of a total of 14 completed dams – five are of a lean mixture (low-cementitious), while only one can be classified among dams made of a rich and wet mixture (high-cementitious). In the following two years, 19 other dams were completed, of which only one is of a lean mixture, while nine have been constructed of a rich and wet mixture. In the subsequent period a more intensive construction of dams of roller-compacted concrete came about with expressed domination of the rich and wet mixture (high-cementitious). One of the reasons for this trend in development is certainly the fact that the richer and wetter mixture can be prepared and placed faster,

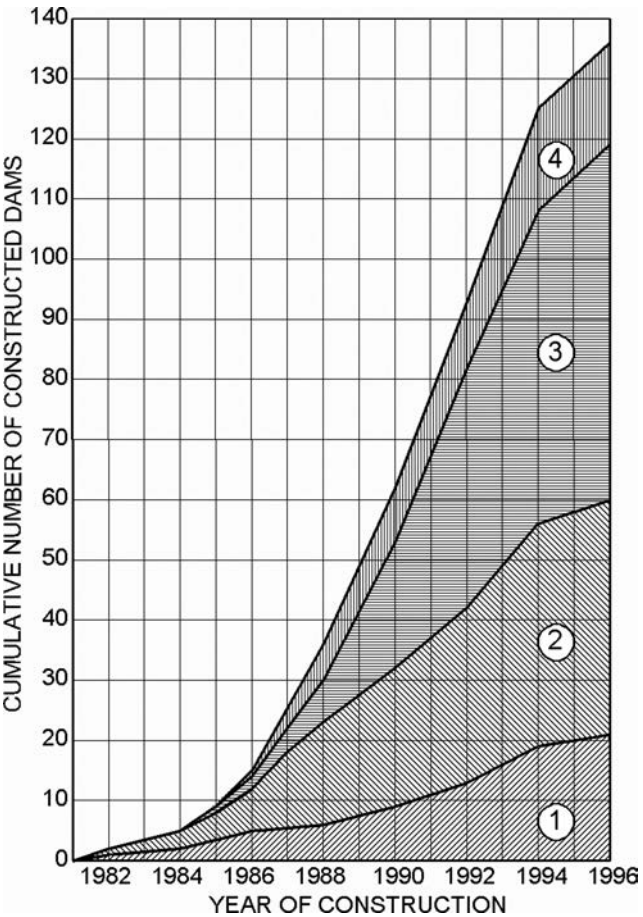

Figure 18.8 Dams of roller-compacted concrete constructed until 1996, classified in accordance with the type of roller-compacted concrete. (1) Dams of lean and dry mixture (low-cementitious); (2) dams of medium-wet mixture (medium-cementitious); (3) dam of rich and wet mixture (high-cementitious); (4) dams of roller-compacted concrete used in Japan (RCD).

although it has been noticed that workability, besides being influenced by the quantity of cementitious materials and contents of water, is also influenced by other factors, for instance, the contents of the fine particles.

Figure 18.9 shows the total number of dams constructed of roller-compacted concrete until the end of 2012, i.e. in the whole period of more than three decades of application of this dam type, according to the type of the concrete mixture. From the chart it can be seen that 255 out of total number of 550 constructed RCC dams (or 46.4%) are built of high-cementitious concrete mixture, at 125 dams (22.7%) medium-cementitious mixture was applied, 80 dams (14.5%) were constructed of a lean concrete mixture (low-cementitious), while the number of constructed RCDs was

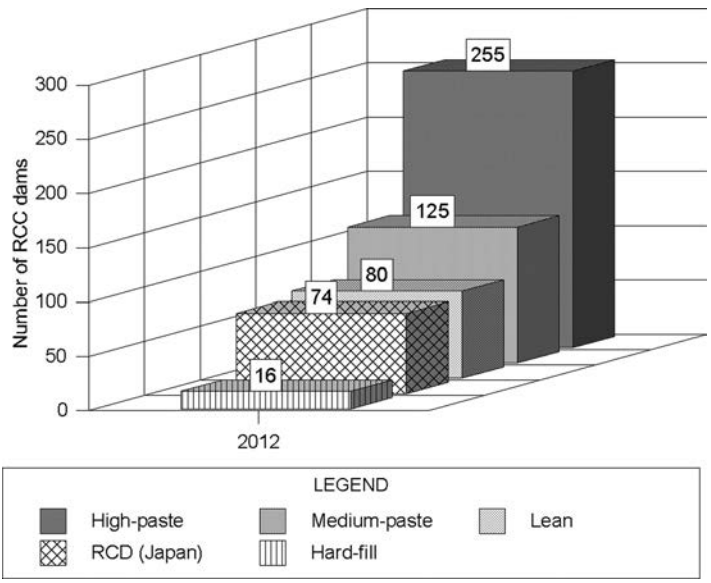

Figure 18.9 Dams of roller-compacted concrete constructed until 2012, classified in accordance with the type of roller-compacted concrete (source: World Atlas, 2012).

74 (13.5%). Similar proportions were established in 1996, when the total number of constructed RCC dams was 135, or less than ¼ of such dams constructed to the end of 2012. A major change that has taken place in the period 1996–2012 has been the increasing number of high-cementitious RCC dams, the percentage having increased from about 38% to 46.4%, with a corresponding decline in medium-cementitious RCC dams, which have decreased from about 35% to 22.7%. The chart also includes so-called *hard-fill and cemented sand and gravel (CSG) dams*, which have been introduced during last 20 years. But they are still relatively few in number (16), and make up less than 3 percent of the total RCC dams. However, the domination of the high-cementitious RCC dams is more evident if the volume of RCC that has been placed is considered: as much as 62.5% of all RCC placed to date has been high-cementitious RCC.

Improved properties of dams of roller-compacted concrete, attained partly through the abundant experience obtained, and partly with an increased quantity of cementitious materials, have brought about a greater confidence in this kind of structure, so that the more recently designed and constructed structures have a much greater height than the ones executed in the first generation. Up to the end of 1986, only one dam had been constructed with a height greater than 60 m (Shimajigawa), but then, in the subsequent two years, as many as eight dams were constructed, of which two – the Tamagawa and Upper Stillwater – are higher than 90 m. In the period from 1991 to 2001 24 RCC dams higher than 100 m were constructed all over the world, mainly in Japan and China (see Table 18.3). Two were higher than 150 m (Urayama 156 m,

Table 18.3 Roller-compacted concrete dams ≥100 m, constructed up to 2001.

Dam	*Country*	*Year of construction*	*Height [m]*	*Volume of RCC [$m^3 \times 10^3$]*	*Total volume of concrete [$m^3 \times 10^3$]*
1. Urayama	Japan	1995	156	1294	1860
2. Miagasse	Japan	1995	155	1537	2001
3. Boasusi	China	1995	132	450	2300
4. Shagai	China	1996	131	280	300
5. Jiangya	China	1999	131	1100	1340
6. Gassan	Japan	1998	123	731	1160
7. Porce II	Colombia	2000	123	1305	1445
8. Ueno	Japan	2000	120	269	720
9. Beni Haroun	Algeria	2000	118	1690	1900
10. Sakaigawa	Japan	1991	115	373	718
11. Mianhuatan	China	2001	115	540	640
12. Satzunaigawa	Japan	1995	114	536	760
13. Origawa	Japan	2000	114	406	695
14. Pangue	Chile	1995	113	740	780
15. Yantan	China	1992	111	626	905
16. Tomisato	Japan	1997	111	409	480
17. Dachaoshan	China	2000	111	757	1127
18. Capanda	Angola	1992	110	757	1154
19. Kazunogawa	Japan	1997	105	428	622
20. Sabigawa	Japan	1991	104	400	590
21. Kodama	Japan	1993	102	358	554
22. Shuikou	China	1992	101	600	1710
23. Tamagawa	Japan	1986	100	772	1150
24. Ryumon	Japan	1992	100	521	836
25. Trigomil	Mexico	1992	100	362	681

and Miagase 155 m). In the next 11 years another 77 RCC dams higher than 100 m were finished, or are in the advanced stage of construction (Figure 18.10). Nine are higher than 150 m, the highest finished reaching 217 m (Longtan, China, 2008). Currently in the advanced stage of construction is Gibe III dam (Ethiopia), designed to be 249 m high (Table 18.4). From the chart of the dams of roller-compacted concrete constructed up to 2001 and up to 2012, classified according to their height (Fig. 18.10), it can be seen that the group of 50 to 74 m is the dominant one. The chart also highlights the tendency after 2001 for constructing higher RCC dams compared to the first two decades of the application of this modern dam type.

A respectable role in the progress of the construction of roller-compacted concrete dams, besides their economy and possibility of fast construction, has also been played by the development of methods for analysis of such complex structures. Besides the usual methods for static and dynamic analysis by determination of state of stresses and deformations through the Finite Element Method, there have also been developed methods for thermal analysis by the application of the same numerical method. Those complex methods, until recently, hardly acceptable for everyday work, are now being applied, virtually obligatorily. Incremental analysis, in which temperature changes are taken into account, is considered both in the period of construction and in the period

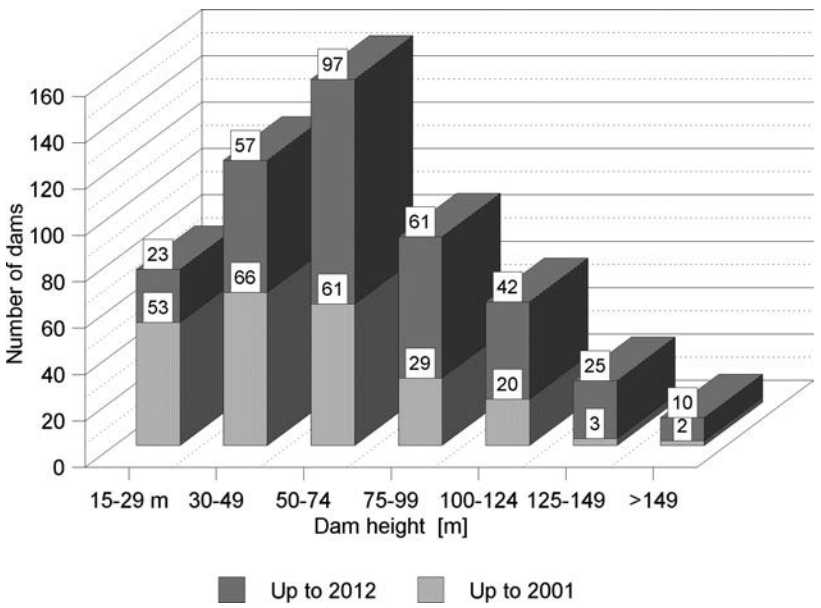

Figure 18.10 Dams of roller-compacted concrete constructed till 2001 and constructed or in the advanced stage of construction till 2012, grouped by their height.

Table 18.4 Roller-compacted concrete dams ≥150 m.

Dam	*Country*	*Year of construction*	*Height [m]*	*Volume of RCC [$m^3 \times 10^3$]*	*Total volume of concrete [$m^3 \times 10^3$]*	*Cementitious mat. [kg/m^3]*	
						Cement	*Pozzolan*
1. Gibe III	Ethiopia	(2015)	249	5900	6300	70–120	50–60
2. Longtan	China	2008	217	4952	7458	99	121
3. Guangzhao	China	2008	201	2420	2870	61	91
4. Miel I	Colombia	2002	188	1669	3920	85–160	0
5. Guandi	China	2012	168	2970	4710		
6. Guanyinyan	China	(2015)	168	6473	9364		
7. Wanjiakouzi	China	(2014)	161	–	–		
8. Jin'anqiao	China	2011	160	2400	1730	72	108
9. Urayama	Japan	1995	156	1294	1860	91	39
10. Shatuo	China	2009	156	1510	1980		
11. Miagasse	Japan	1995	155	1537	2001	91	39
12. Ralco	Chile	2003	155	1596	1640	133	57

of the first twenty years following construction. Special jointing elements also enter into the analysis, by means of which it is possible to simulate cracks in the dam's body, as well as an assessment of their sizes (Hollingworth & Geringer, 1992; Schrader & Namikas, 1988; Zhu & Xu, 1995; Hansen & Forbes, 2012).

18.5 IMPROVING THE WATER-IMPERMEABILITY OF DAMS MADE OF ROLLER-COMPACTED CONCRETE

Providing the water-impermeability of the body of dams made of roller-compacted concrete is a question to which, in the course of their more than 30-year development, there has been paid particular attention and, in that respect, time has brought permanent improvements and innovations. Dams of roller-compacted concrete, constructed according to the Japanese system in respect of water-impermeability, have turned out to be very successful. The wide wall of conventional concrete at the upstream face of the dam with the joints containing two seals, i.e. waterstops and a drainage opening, along with the joints cut into the roller-compacted concrete, result in a final construction, which is very similar to the gravity dam of conventional concrete. However, this complex method of construction, although efficient, results in losing one of the most important advantages of the roller-compacted concrete – fast construction, which is possible only with simple structures. Because of that, a number of attempts and a lot of efforts have been made to find a method for achieving water-impermeability for dams made of roller-compacted concrete, with, at the same time, the construction remaining as simple as possible and, thus, providing fast advancement during construction. Those attempts may be classified in the following way:

- *Execution of a monolithic thin upstream membrane of conventional concrete against formwork*. This method is the one most often used. The thickness of the membrane amounts 30 to 90 cm and, in some cases, within the membrane there are embedded exciters of cracks (Middle Fork, Arabie, Grindstone Canyon) in order to keep the location of occurred cracks under control. This construction leads to certain difficulties during construction due to the need for a minimum of two types of concrete to be prepared simultaneously and also due to the potential danger of the occurrence of cracks in the membrane. But despite these difficulties, this method for improvement of the water-tightness of the RCC dams is the most popular.
- *Execution of a bonding mortar course between layers of roller-compacted concrete*. These mortar courses are built-in either when there is an upstream membrane of conventional concrete or independently, for preventing or setting back seepage between the layers of the roller-compacted concrete (Copperfield, Craigbourne). This concept is endorsed by the theory according to which the weakness of the dams of roller-compacted concrete, in relation to their water-impermeability, are precisely those joints between individual layers.
- *Execution of a geomembrane behind prefabricated concrete panels at the upstream face*. This method has been used for the *Winchester* dam, and has also been proposed for the Urugua dam (Argentina). The Galesville dam encompasses a membrane that has been formed by means of spraying of a rubber mass upon the poured concrete surface, but it has not succeeded in bridging cracks on the surface of the concrete.
- *Execution of a layer of asphalt mastic behind the prefabricated concrete panels at the upstream face*. This kind of construction of water-impermeable membrane has been used for the Kengkou dam in China.

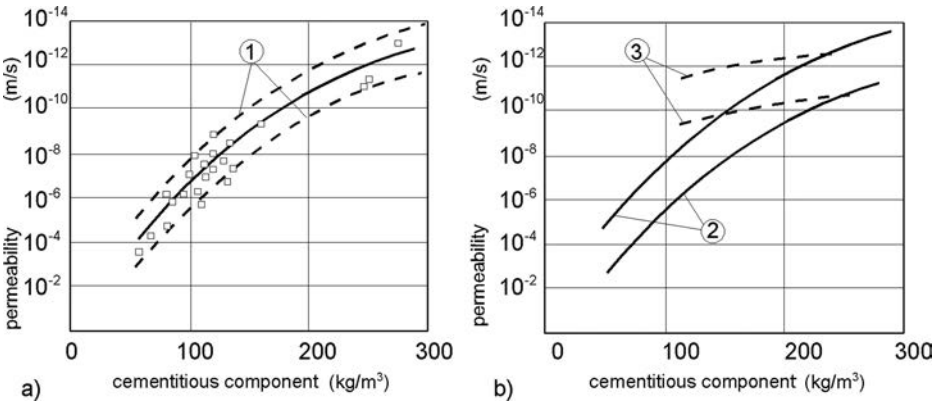

Figure 18.11 Ratio between water-permeability in situ and the content of binder for roller-compacted concrete (a) and comparison between the water-permeability of dams of roller-compacted concrete and of conventional concrete (b). (1) Boundary curves with a certainty of 95%; (2) dams of roller-compacted concrete; (3) dams of conventional concrete.

- *Placement of roller-compacted concrete with higher content of binder in the vicinity of the upstream face.* This method has been used for the *Santa* Eugenia dam (Spain) and Ain al Koreima dam (Morocco), and it was also implemented in a dam in South Africa. Of course, the higher content of cement improves the water-impermeability. This method, by means of which there is formed a wider barrier in front of the water, is probably more efficient than the execution of a thin partition of conventional concrete.
- *Construction of the entire dam's body of water-impermeable concrete.* The concept of the execution of roller-compacted concrete of a rich and wet mixture aims at obtaining concrete with a high density and with a good bond between the layers. The ratio between the coefficient of permeability and the content of the binder in roller-compacted concrete is shown by the diagram in Figure 18.11a, worked out on the basis of former investigations in designing and constructing dams of roller-compacted concrete. When those results are compared with a similar ratio for conventional, vibrated concrete (Fig. 18.11b), it can be noticed that, in order to achieve water-impermeability of the roller-compacted concrete of the same order as with conventional concrete, a minimum quantity of 150 kg/m^3 binder is necessary.
- *Additional closing of cracks across the upstream surface of the dam in order to achieve water-impermeability of the construction.* This concept has been employed in the Upper Stillwater dam, constructed in harsh climatic conditions, with variations of temperature of 60°C. The working regime of the reservoir that has been created at that dam is such that every winter the water level goes down. That is why it has been concluded that the most efficient method of keeping the cracks in the concrete under control is to allow their occurrence, and then to close them when the concrete cools down. This method seems efficient for the given conditions, especially if all expected cracks do not appear. In a similar way, the cracks

that have appeared across the surface of the upstream face of the Galesville dam have been successfully closed.

- *Application of Grout Enriched RCC for facing concrete (GERCC).* The main difference in the proportions of the ingredient materials of conventional internally vibratable concrete (CVC) and RCC is that CVC has a greater quantity of cement and water than RCC. By adding additional cement and water to unconsolidated, freshly spread RCC in the form of grout, such that it is reasonably distributed throughout the RCC, the RCC can be mobilized and the grout uniformly worked through the RCC during consolidation by a poker vibrator. This is the basic premise of grout enriched RCC (GERCC). For the GERCC process to "work", the applied grout needs to fully drain down into the spread RCC lift. To do this it is essential that the RCC is in a loose, "as spread" condition. Usually it is necessary to trim back by hand the low windrow left by the dozer blade that develops along the forms and to roughly level off the surface of the RCC to that expected of the 'final' GERCC surface before applying the grout. Also it can assist grout penetration and distribution if the RCC is hand 'rodded' using a length of 12 mm diameter reinforcing rod, say at regular 20–25 cm intervals, to full depth of the lift. During all stages up till the poker vibrator is inserted into the RCC, it is essential that the RCC remain in its loose state and no precompaction occurs, either by workers' feet, or by the vibratory drum roller getting any closer than about 1.5 m to the GERCC zone. The adjoining zone of RCC should only be compacted after the GERCC has been compacted. Exposed final GERCC top surfaces can be finished to a smooth level surface by first tamping with a long timber plank on edge, to level up the surface, after which it can then be wood-floated to final surface. GERCC lift surfaces may need to have any residual grout/laitance removed, according to the specification requirements for lift surface of the RCC. If the next lift is to be placed within a few hours the poker vibrator will re-penetrate the lower GERCC lift and the lift joint will "disappear", in which case there is no need to remove any laitance. The quantity of grout required can be determined by laboratory or field trials. About 8 litres/m/40 cm facing width for a 30 cm thick RCC lift has been found to be adequate where the parent RCC has a VeBe of 15–20 seconds (Forbes, 2008). By having the water: cement ratio of the grout equal to that of the RCC, similar compressive strengths will be achieved for the GERCC. Admixtures such as water reducers, set retarders, air entrainers and plasticisers can be added to the grout if necessary. The viscosity of the grout must be such that it will flow into the voids of the unconsolidated RCC lift, not pool on the surface. GERCC methods have been applied at more recent dams, including Miel I ($H = 188$ m, Colombia, 2002) and Ralco (155 m, Chile, 2003). Cores taken horizontally through the facing and into the parent RCC behind consistently show fully compacted GERCC, often with no clear indication of the transition to the RCC which appears monolithic with the GERCC. Likewise horizontal cores taken across lift joints have consistently shown excellent bond between GERCC lifts (Forbes, 2008).

  Details of the GERCC method are given by Forbes (2008), summarizing the following advantages of the method: provides a durable, impervious, high quality off-form finish for upstream and downstream facing to the body of the RCC dam; forms a homogeneous and monolithic mass with its adjacent parent RCC;

the entire procedure is simple, easily controlled and does not control the progress of RCC placing; no separate batching, mixing, transportation system is required, unlike with CVC; grout can be mixed by hand or by grout plant; tests on projects to date confirm the uniformity of GERCC is similar to the parent RCC; coefficients of variation as low as 10% have been achieved; ability to incorporate reinforcing steel, waterstops, pipe encasements etc; can be used between abutment rock and the RCC body to achieve good bond and filling of all rock cavities, irregularities etc; low cost, in the region of US$ 15/m^2 for a 40 cm thick facing. Requirements and limitations of GE-RCC include: quality control relies on inspection, an understanding of the requirements by those applying the grout and carrying out vibration, inspection and repair of any defective zones where evident upon stripping of the forms, and with simple procedures in place to regulate grout dose rates; lift joint treatment is necessary, as with any conventional concrete lift surface; achieving a toweled, level surface, say for exposed step surfaces, is not as easily achieved as with conventional concrete since it is less workable; where transverse joint waterstops are incorporated it may be necessary to locally widen/transition the adjacent facing width to facilitate the large RCC drum rollers negotiating around the waterstop installation.

- *Application of Grout Enriched Vibratable RCC (GEVR)*. This is a similar process as GE-RCC. The grout is placed directly on the previously compacted RCC lift. Then loose RCC is placed over the grout and internal vibration is used to draw the grout up into the RCC to produce the facing. The GEVR method is only used with very workable (low Vebe time) RCC mixes, which can possibly be consolidated by vibrators without the addition of grout to produce acceptable results. The field of application as well as the advantages and disadvantages of the GEVR method are similar to those of the GERCC method. GEVR was applied at Olivenhain dam (southern California, $H = 94$ m) to produce a smooth backing for an exposed geomembrane liner on the upstream face.

The application of different methods for improvement of the watertightness of the upstream facing of RCC dams up to 1990 and up to 2010 (in percentages) is shown in Fig. 18.12. Evidently, a predominantly used method is the placement of traditional facing concrete against formwork (1 in Figure 18.12), participating with more than 63% in 1990 and with more than 44% in 2010. In the first decade of the construction of RCC dams the only other methodology that was used in more than 10 percent of dams was that of precast concrete panels (5). The main changes that have taken place over the next 20 years were the decrease in application of the most popular method (1) and the increase of application of recently introduced methods (5): *grout-enriched vibratable RCC* (GEVR), in which the grout is spread on the top of the previous layer and vibrated upwards through the new layer, and *grout-enriched RCC* (GE-RCC), in which the grout is added on top of the new layer and vibrated downwards through the layer, that has completely changed the methodology of forming the upstream face of RCC dams. Dunstan (2012) believes that it is possible within a few years for GEVR/GE-RCC methods to become the most popular method of forming the face of an RCC dam. It is not so long ago that a number of dams were completed with RCC being directly compacted against the upstream formwork, thus raising confidence that the RCC can create an impermeable barrier in the dam, without any form of membrane.

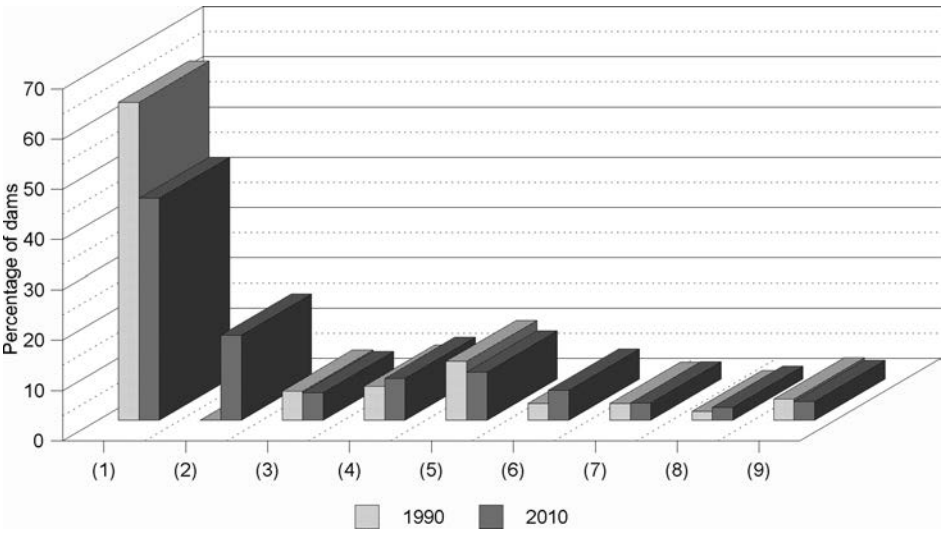

Figure 18.12 Methods used to improve the watertightness of the upstream facing of RCC dams up to 1990 and up to 2010 (after Dunstan, 2012). (1) Facing concrete against formwork (63.3% in 1990, 44.1% in 2010); (2) GEVR/GE-RCC against formwork (0%, 16.9%); (3) RCC against formwork (5.8%, 5.5%); (4) reinforced concrete before/after RCC (6.7%, 8.3%); (5) CVC/RCC against precast panels (11.7%, 9.6%); (6) precast panels with geomembrane (3.3%, 6.0%); (7) external geomembrane against CVC/RCC (3.3%, 3.4%); (8) slip-formed facing elements (1.7%, 2.5%); (9) others (4.2%, 3.7%).

Practically, this tendency was followed by the introduction of GEVR and GE-RCC methods.

It can be concluded that in the course of past practice various methods have crystallized for providing water-impermeability to dams made of roller-compacted concrete and, in every specific case, one should select the most appropriate method for the given conditions. In the description of the examples that follow, more attention will be paid to this important question.

18.6 COST OF DAMS MADE OF ROLLER-COMPACTED CONCRETE

Typical reasons for using RCC are the reduced cost and construction time it offers. Theoretically, savings can be dramatic, sometimes in excess of 50%. However, in reality, some projects lacking proper planning, equipment and supervision have not saved any construction time, and the potential cost savings have been lost. There are examples of RCC dams experiencing added costs because of design decisions of the engineer or owner that resulted in expensive or time-consuming options. Thus, each project must be evaluated on its own.

Although bid price data for various portions of the RCC are abundant, it is still difficult to obtain final actual cost data for roller-compacted concrete dams. From data on the cost of 20 RCC dams constructed during the first 15 years of the application of

Table 18.5 Assumed criteria for four types of dam of roller-compacted concrete.

	Downstream slope	*PC* (kg/m³)	*Fly ash* (kg/m³)	*Joints*	*Bonding course*	*Slope of the dam* upstream	downstream
(1)	1:0.85	75	25	no	partially	impermeable	untreated
(2)	1:0.8	80	40	no	yes	impermeable	untreated
(3)	1:0.725	50	150	no	no	formed with climbing formwork	
(4)	1:0.65	60	190	no	no	formed with climbing formwork	

Table 18.6 Assumed cost $.

Kind of material or work	*USA* $
Binder:	
Portland cement	87.5/t
Pozzolan or PFA	45/t
Roller-compacted concrete (without binder)	20/m³
Bonding course (across entire surface)	0.9/m³
Surfaces of the dam:	
Water-impermeable upstream face	80/m²
Surface treated with climbing formwork	40/m²
Untreated surface	20/m²

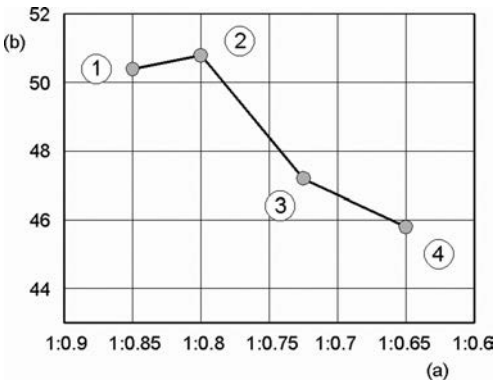

Figure 18.13 Cost per 1 m length of various dams of roller-compacted concrete, with a height of 60 m. *X*-axis (a): inclination of downstream slope; *Y*-axis (b): cost per 1 m length (USA × 10^3); numbers (1, 2, 3, 4) refer to numbers in the first column of Table 18.5.

this dam type, grouped in four categories according to their characteristics (see Table 18.5), with assumed average the costs of individual materials and works as shown in Table 18.6, a cost per 1 m length of a 60 m high dam has been obtained, graphically presented in Figure 18.13.

The results shown indicate that dams of rich roller-compacted concrete, in which the cost of material is higher, but the volume is the minimum, are the cheapest solution

for given conditions. Yet, even though this comparison shows that reducing the cost of material need not also mean the cheapest solution. That is why the designer, before coming to an optimum solution, the same as for every other hydraulic structure, should consider and examine the structure as a whole and in composition with other structures within the framework of the hydraulic complex, since roller-compacted concrete dams also depend on the conditions of the dam site, as much as other types of dams.

Bid tabulations from several RCC dam projects completed after 2003 show that the unit cost of in-place RCC ranges approximately from \$98 to \$186 per m^3. This unit cost includes cost of materials, mixing, transporting, placing and curing. It is based on reported bid prices of successful bidders.

The comparison of cost for dams made of roller-compacted concrete with the alternative solutions (dams of conventional concrete and embankment dams) is difficult to perform in general. However, performed comparisons with some carried out dams indicate that, depending on the local conditions, a roller-compacted concrete dam can achieve savings in cost from 20 to 40%, and in some exceptional cases even 60–70% are mentioned, which should, however, be taken with reserve. A significant influence can have the fact on the amount of savings of whether in the specific case a gain is accomplished through much faster construction and how large that gain is, as well as many other factors. In any case, for each dam site where construction of an embankment or gravity concrete dam can be considered, a dam made of roller-compacted concrete should also enter into the possible combinations (Andriolo, 1998; Dunstan & Santos, 2001; Giovagnoli et al., 1992).

In making comparisons, certain deficiencies of dams made of roller-compacted concrete should also be taken into consideration. Classic mass concrete has the great advantage of allowing relatively easy construction of all water-conveying and other structures in the dam's body (bottom outlet, water intake structures, supply pipelines, drainages, grouting and inspection galleries, system of cooling pipes, instrumentation for monitoring, etc.), which, in dams made of roller-compacted concrete, owing to the method of placement in continuous layers with the application of heavy plant and equipment, is rather aggravated. That is why, whenever it is possible, the appurtenant structures should be located outside the body of the dam made of roller-compacted concrete, which, of course, is reflected to a certain measure in the overall cost of the hydraulic complex. For certain methods of their execution in the dam's body consideration will be given in the description of individual examples of constructed dams.

18.7 EXAMPLES OF DAMS MADE OF ROLLER-COMPACTED CONCRETE

Dams of roller-compacted concrete caused considerable interest soon after their appearance. Quite a number of such dams have been described in periodicals, as well as in conference proceedings. In the continuation, as an illustration of the material presented in the previous six sections of this chapter, with a number of examples of designed and constructed dams in various parts of the world, there will be described the structure and construction of dams of roller-compacted concrete, with a review of certain particular questions and a summary of the characteristics of their construction in particular areas.

18.7.1 Examples of the early period of construction of RCC dams

18.7.1.1 Middle Fork dam (USA, 1984)

The Middle Fork dam, completed in 1984 (Fig. 18.14), 37.8 m high, was the second dam of roller-compacted concrete in the USA. It has a dual function: protection against flooding, as well as accumulation of water for industry. This type of dam was selected once it had been established that it is much less expensive than an earth-rock dam, for which the foundation had been almost completely prepared. The positive experiences gained from the recently completed Willow Creek dam (1982) have contributed to such a decision. In relation to the topography and geology (marlstone), the dam site is quite appropriate for a concrete gravity dam (USCOLD, 1988).

The dam is constructed completely of roller-compacted concrete, with the exception of the surface parts at the upstream and downstream faces, where there has been poured mass concrete 30–60 cm thick, placed with conventional formwork. Roller-compacted concrete has been placed in layers with a final thickness of 30 cm, at an inclination of 1:50 towards the downstream face. The construction of each layer encompassed five working operations. First, a mass concrete wall was made at the upstream face, 45 cm thick. Second, behind this wall bonding concrete was applied with a high content of sand and retarder, in a layer 3 m wide and 5 cm thick, which is intended for reducing the permeability of the layers. Third, from the downstream face there was constructed a 36 cm thick curb of conventional mass concrete, in order to limit the layer from that side, too. Fourth, roller-compacted concrete was also applied along the entire length and width of the dam, starting from the downstream face. In the fifth stage, the remaining space was filled with mass concrete as far as the downstream curb.

By means of this kind of construction and method of execution there has been achieved good water-impermeability of the dam, which has been important due to the danger of the freezing of the concrete below the downstream slope, owing to the considerable height above sea level. As an additional measure, a drainage pipe has also been built-in (22, Fig. 18.14), in order to cut off possible filtrated water; that is to say, to prevent its penetration in the vicinity of the slope. At 10 m away from the crest, the continuous construction was interrupted in order to enable realization of the drilling of a series of drainage openings at a mutual axial distance of 3 m up to the drainage gallery close to the foundation. Drainage openings have also been drilled through the gallery into the foundation, downstream of the grout curtain.

The optimum mixture of which the roller-compacted concrete has been prepared was obtained by means of profound laboratory investigations and, finally, it has had the following composition (per 1 m^3 of concrete):

- Coarse aggregate (marlstone) 774 kg
- Fine aggregate 1161 kg
- Portland cement 65 kg
- Water 94 kg

The control during construction consisted of checking the grain size distribution of the aggregate and the density, i.e. compactness, of placed layer with the application

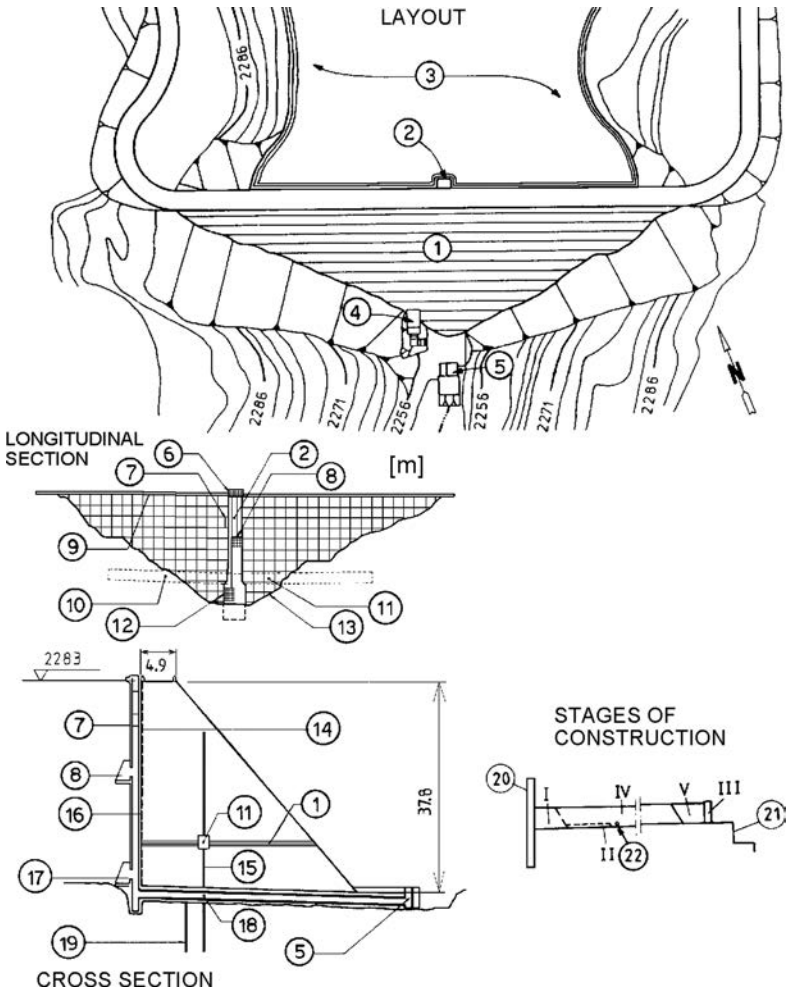

Figure 18.14 Middle Fork dam (USA). (1) The dam's body of roller-compacted concrete; (2) overflow and outlet structure-inlet structure; (3) normal level; (4) approach towards drainage gallery; (5) outlet structure; (6) higher overflow and (7) lower overflow; (8) discharge outlet; (9) concrete fence; (10) drainage tunnel; (11) drainage gallery; (12) discharge outlet in the course of construction; (13) layout plan of dam; (14) stoppage of concreting due to drilling; (15) drainage drill holes; (16) upstream face; (17) entrance for offtake of construction waters; (18) overflow and discharge outlet pipes; (19) grout curtain; (20) formwork at the upstream face; (21) step-like downstream slope; (22) drainage pipe. (I–V) Stages of construction.

of radioactive isotopes. For comparison of the achieved strength of placed roller-compacted concrete with the anticipated strength, which was established by laboratory test specimens, cores with a diameter of 15 cm were taken out from the placed layer. A part of the results obtained is presented in Table 18.7.

Table 18.7 Properties of roller-compacted concrete for Middle Fork dam.

Properties of roller-compacted concrete for Middle Fork dam	*Age (days)*	*Planned (1983)*	*Realized (1984)*
Unit weight in compacted state (kN/m^3)		21.6	21.0
Quantity of cement (kg/m^3)		65	61
Compressive strength (MN/m^2)	7	8.9	–
	28	11.6	10.2
	90		14.8
Tensile strength (MN/m^2)	7	0.62	–
	28	1.5	2.0
	90	2.0	2.4
Modulus of elasticity (MN/m^2)	28	6890	
Poisson's ratio	28	0.16	
Mean coefficient of permeability (cm/s)		9×10^{-6}	

Prior to commencement of the filling of the reservoir, there was performed a visual inspection of the dam and the gallery. As had been expected, fine cracks were found in the mass concrete, both at the upstream and the downstream faces, while in the roller-compacted concrete there were found no thermal cracks at all.

During the first filling of the reservoir (spring, 1985), there was recorded water seepage into the gallery in the quantity of 12.6 l/s, which increased to 31.6 l/s in one month, and then immediately started to decrease, while towards the middle of the summer it dropped to 6.3 l/s, at a permanent normal level in the reservoir. This seepage in its greatest extent was due to the penetration of water from the foundation through the drainage openings, and not through the dam's body. The drastic lowering of the seepage was a result of calcification of the seepage paths in the foundation. In the initial years of the dam's service, in the body of which within a record short time there have been placed 42,000 m^3 roller-compacted concrete and 3800 m^3 mass concrete, operated quite normally.

18.7.1.2 Copperfield dam (Australia, 1984)

The Copperfield dam (Australia) was completed in 1984 and its design and construction took only 10 months. In contrast to the Middle Fork dam, a part of this dam, at a length of 100 m, is an overflow part (the total length of the dam along its crest is 340 m), Figure 18.15. The dam is 40 high and within its body there have been placed 140,000 m^3 roller-compacted concrete and 16,800 m^3 conventional mass concrete (Forbes, 1988).

The upstream face is vertical, constructed by means of formwork, in conventional mass concrete. Contrary to the first example, here the conventional concrete has not been poured to the full depth of 30 cm, so that the upper part of the layer of roller-compacted concrete has been placed over the mass concrete and has remained exposed. In spite of certain segregation, at some 10 cm away from the interior, it has been quite all right.

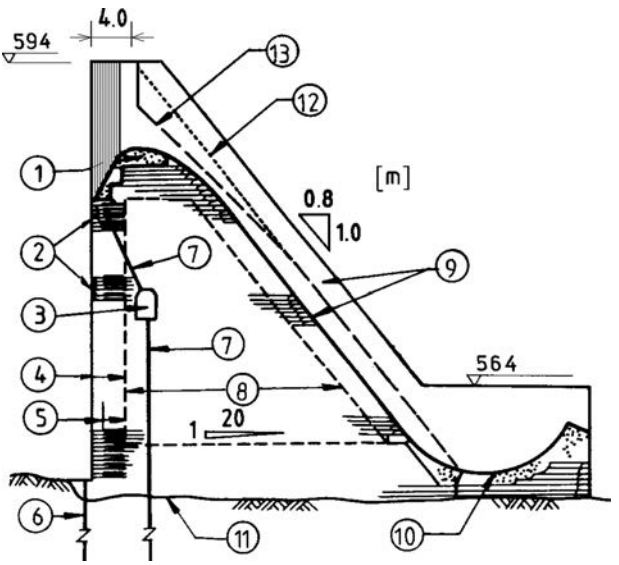

Figure 18.15 Cross-section of Copperfield dam (Australia). (1) Crest overflow made of mass concrete; (2) upstream surface of mass concrete; (3) drainage gallery; (4) roller-compacted concrete, type I; (5) bonding concrete between layers of roller-compacted concrete; (6) grouting curtain; (7) drainage drill holes; (8) roller-compacted concrete, type II; (9) lining of mass concrete; (10) reinforced concrete sill bucket; (11) foundation of granite; (12) originally anticipated slope at the non-overflow part of the dam; (13) executed slope – 1:0.9.

The downstream face has been designed with an inclination 1:0.8. Owing to certain difficulties in the construction of the upper part, some modifications have been performed. Namely, the aggregate of the roller-compacted concrete has been manufactured from rounded natural river gravel, with a low quantity of crushed material, so that the angle of repose of the material has been slighter. Due to that, in the upper half, the inclination of the downstream slope has been warped, i.e. eased to 1:0.9, while the four metres below the crest have been executed vertically, by means of formwork.

The overflow part of the dam consists of an appropriately shaped crest, a chute spillway, side walls and a sill bucket. The sill bucket has been completely constructed in reinforced conventional concrete, while the side walls and the 60 cm thick lining of the chute spillway have been constructed in ordinary (plain) concrete, but with additions enabling parallel execution of the layers of roller-compacted concrete, as well as a good mutual bond. The overflow crest, as well, has been constructed in conventional mass concrete, by means of steel formwork, while in the longitudinal direction there has been performed a division into sections of 10 m each.

The method of construction of the drainage gallery (3) is rather interesting in that it has been executed by mining, i.e. quarry excavation of sand and aggregate for roller-compacted concrete without cement, placed parallel with the roller-compacted concrete at the appropriate place. Drainage openings have been drilled from the gallery

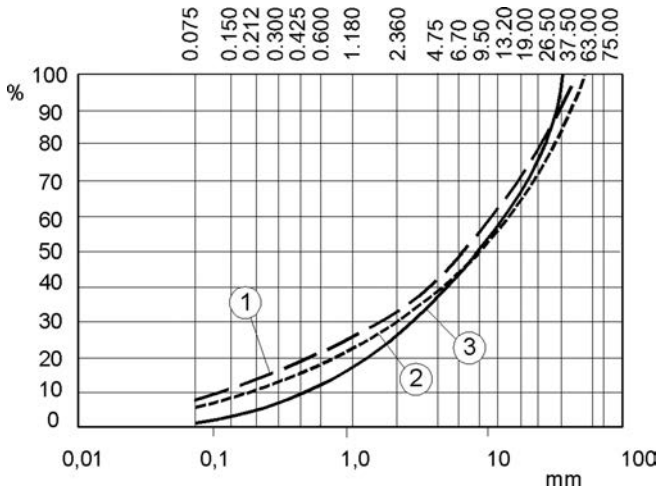

Figure 18.16 Grain size distribution of the aggregate for roller-compacted concrete for three dams in Australia. (1) Copperfield; (2) Craigburn; (3) Boucca.

through the roller-compacted concrete into the foundation of granite, aiming at reducing the uplift pressure. The upper drainage openings have been drilled from the crest to the gallery. Grouting of the foundation has been achieved through a foundation of roller-compacted concrete, prior to the drilling of the drainage openings.

Two types of mixtures have been employed for the dam's body. Type I, placed in the upstream part, as a binder contains 110 kg low-thermal cement per m^3, while type II has been used, for the internal part of the dam, 80 kg/m^3, plus 30 kg/m^3 pulverized fly ash. The aggregate has been produced from river gravel and it has been well-graded, with a maximum grain of 50 mm, (Fig. 18.16). Placement has been performed in layers of 30 cm (in a compacted state), at an inclination of 1:20 towards the downstream face. The compressive strength of the roller-compacted concrete at 90 days amounted on average to 15 MPa.

Similar to the previously described dam, here also the impermeability between layers has been improved by means of the insertion of bonding layers, i.e. courses, of ordinary concrete with an increased content of sand, 2 m wide, 4 m thick, which begin at 1 m from the upstream face.

There have been constructed three vertical transverse joints at the Copperfield dam: two joints at the ends of the overflow part and one joint at the main vertical change taking place in the foundation. The joints have been formed by means of PVC-slabs, placed vertically into the roller-compacted concrete before compaction. The closing of the joints has been performed with seals, i.e. waterstops, incorporated in the mass concrete from the upstream face.

Five months after the completion of the dam, the water level increased to 3 m below the normal, while the measured seepage amounted to 24 l/s. Four months later it had gone down to 10 l/s, while immediately afterwards, in the middle of the winter, a vertical transverse crack occurred approximately in the middle of the overflow part.

That led to an increase of the seepage to 16 l/s; however, due to the property of self-healing, which property is apparently possessed by the roller-compacted concrete, 18 months later, at almost normal level in the reservoir, the seepage water quantity had been reduced to only 5.5 l/s.

18.7.1.3 Two arch-gravity dams in South Africa (1988, 1989)

In South Africa, there have been constructed several gravity dams made of roller-compacted concrete (Hollingworth et al., 1988; Hollingworth & Geringer, 1992), while the Knellpoort dam (Fig. 18.17), completed in 1988, is the first arch-gravity dam in the world to have been constructed in roller-compacted concrete. It is 50 m high, 200 m long at the crest, and contains 59,000 m^3 of concrete. Following this dam, one more arch-gravity dam has been constructed, the Wolwedans, with a maximum height of 70 m, length at the crest of 270 m and volume of concrete 180,000 m^3 (Fig. 18.18).

It is characteristic of these two dams that there were undertaken measures for provocation of the occurrence of controlled cracks by means of the incorporation of exciters of cracks close to the upstream and downstream faces. From the upstream face, the exciters are built-in at distances spaced at 10 m, while at the downstream face opposite to them, in a radial direction. The exciters are combined with water-impermeable seals and/or waterstops, which at the same time serve as seals and waterstops for

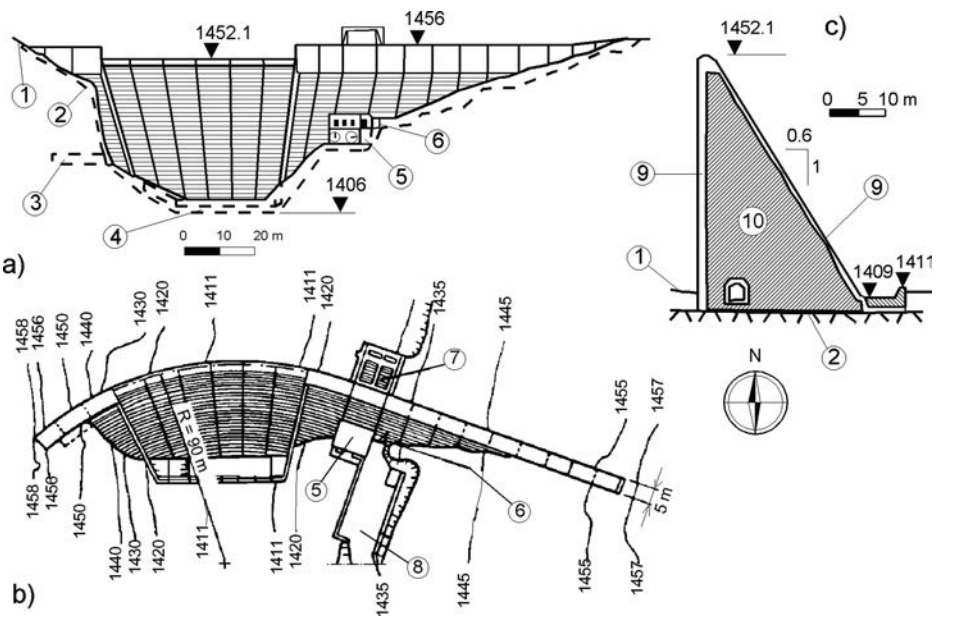

Figure 18.17 Layout plan and sections of Knellpoort dam. (1) Ground line; (2) bedrock line; (3) drainage tunnel; (4) concrete sill; (5) gate structure of the discharge outlet; (6) approach to the gallery; (7) intake tower for the discharge outlet; (8) parking lot; (9) surface layer of concrete.

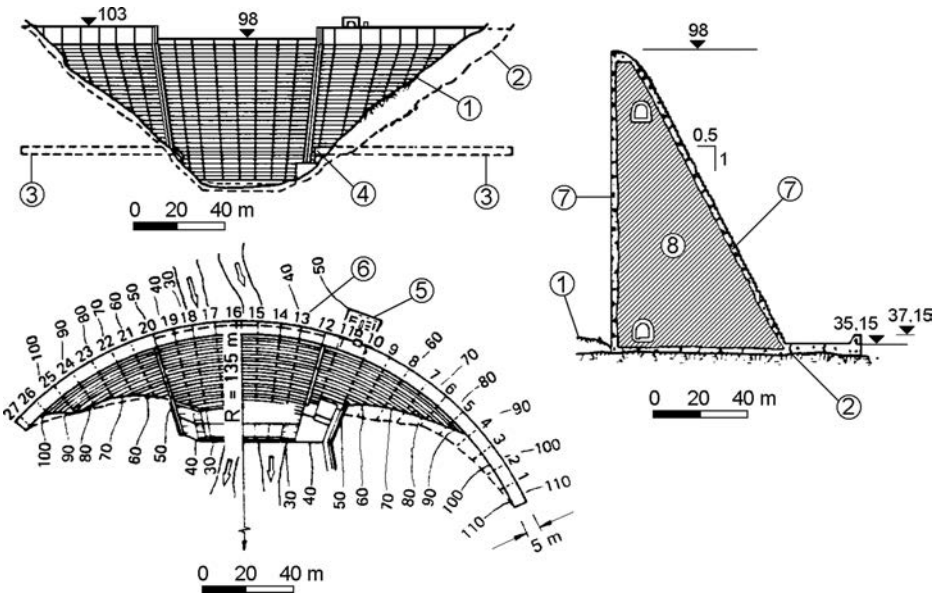

Figure 18.18 Layout plan and sections for Wolwedans dam. (1) Ground line; (2) bedrock line; (3) drainage tunnel; (4) gate structure of the discharge outlet; (5) inlet tower for the outlet; (6) number of induced cracks; (7) surface layer of concrete.

the grout mixture. In the case of the first dam, the exciters are constructed in the form of formed voids, while in the case of the second dam in the form of PVC-sheets (Fig. 18.19). Between the upstream and the downstream exciters, at 1 m elevation intervals there have been placed orientators, i.e. rectifiers of the cracks, whose task is to induce, i.e. initiate, every crack in a radial direction. Since discontinuity of the roller-compacted concrete is generated with these rectifiers, there have been undertaken measures for grouting these discontinuities and associated cracks.

For recording the size and expansion of cracks through the planes of the rectifiers of cracks, measuring stations for recording dilatations and temperature have been incorporated at a number of spots, which operate on the principle of vibrating wire. If cracks, which should be grouted, develop, their selective grouting has been planned in order to ensure continuous work of the partition as an arch. Grouting would be performed at low external temperature and at the lowest practical water level in the reservoir.

The two arch-gravity dams described have been constructed with the maximum possible simple form. The external radius is constant, so that the upstream face is vertical. The downstream face is step-like, which simplifies the construction and enables moving along the slope, but also serves as an efficient dissipater of the energy of the overflow stream, so that at the end there has been executed only a short stilling basin with a cutoff wall.

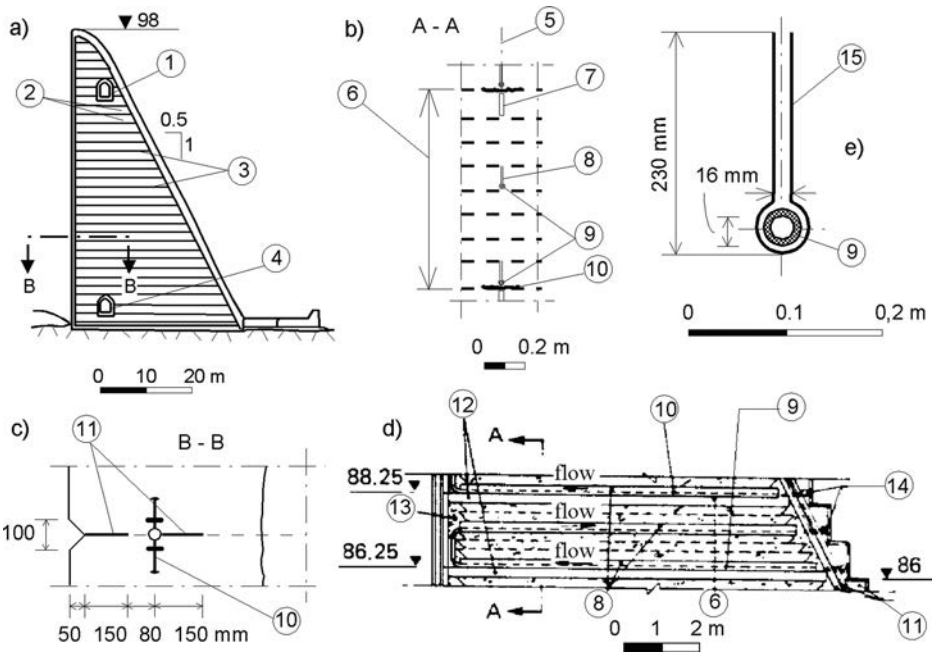

Figure 18.19 Details of exciters and rectifiers of cracks for the Wolwedans dam. (1) Monitoring gallery; (2) sections for grouting, 2 m high; (3) PVC waterstops, 250 mm, for limitation of the sections for grouting; (4) main drainage gallery; (5) vertical section of exciters of cracks; (6) eight layers of roller-compacted concrete, 250 mm each, forming one grouting section between waterstops; (7) dual PVC sheet of 250 microns, with a role of rectifier of cracks without a pipe; (8) rectifier of cracks (see also under e); (9) perforated pipes of 40 mm for supplying grouting mixture; (10) PVC waterstops of 250 mm; (11) exciters of cracks, 150 mm wide, 2 mm thick; (12) unit plastic exciters of cracks; (13) surface concrete; (14) galvanized steel pipes, 32 mm internal diameter, for supply of grouting mixture; (15) 250 microns thick PVC sheet.

The results of monitoring the size and spreading of cracks, recorded by the above-mentioned built-in instruments, will be decisive in making decisions whether to grout cracks or not.

For the two arch-gravity dams of roller-compacted concrete described, a rich mixture has been used, with a quantity of cementitious material of 180–200 kg/m^3, in order to achieve higher strength necessary for this type of dam (in comparison with gravity ones) and especially to achieve a good bond between the layers. The increase in the quantity of the binder has been achieved by the use of a greater participation of pozzolan (Table 18.8), so that the ratio Portland cement to pozzolan is 30:70, which reduces the development of hydration heat. The increased paste:mortar ratio leads to denser, water-impermeable concrete, much more workable and with a lower tendency to segregation. In that sense, there is also a contribution from the smaller maximum grain (53 mm).

Table 18.8 Mixture for roller-compacted concrete for dams Wolwedans and Knellpoort.

Mixture for roller-compacted concrete for two arch-gravity dams in South Africa	*Wolwedans*	*Knellpoort*
Compressive strength at 28 days (MPa)	23.7	18
Kind of coarse aggregate	quartzite	dolerite
Water:cement ratio	0.43	0.53
Portland cement (kg/m^3)	58	59
Pozzolan	136	136
Water (kg/m^3)	83	103
Coarse aggregate: (kg/m^3)		
38–53 mm	469	511
19–38 mm	625	707
4.75–19 mm	469	452
Sand (70% crushed, 30% ground sand) (kg/m^3)	640	703
Admixtures	no	No
Theoretical maximum density (kg/m^3)	2480	2671

The aggregate for the Knellpoort dam was edged and angular, while for the Wolwedans it was rounded. Both aggregates have turned out suitable for the preparation and placement of roller-compacted concrete, with the observation that the edged (angular) aggregate has led to greater strength of the concrete, while the rounded one has led to better workability, with insignificant segregation and a high final density, i.e. compactness, of the concrete.

18.7.1.4 New Victoria dam (Australia, 1991)

The largest dam of roller-compacted concrete that had been built in Australia up to 1991 was the New Victoria dam, with the function of forming a reservoir for the water supply of Perth (Wark & Mann 1992). It is located 300 m upstream of the old dam intended for the same purpose, built at the end of the 19th century. It has a structural height of 52 m (Fig. 18.20), a length of 285 m along the crest (together with a 130 m long central overflow section). The total volume of concrete in the dam is 134,500 m^3, of which 121,000 m^3 is roller-compacted concrete of rich mixture (cement + fly ash = 80 + 160 kg/m^3), while 13,500 m^3 is conventional concrete, incorporated at the external contours by means of a climbing formwork. The type of dam was selected once it had been established that it is the most economical one as compared to the other possible solutions – a concrete gravity dam made of conventional concrete or an embankment dam. Besides, the selected type of dam requires a one-year shorter period for construction, which is significant especially when the function of the dam is taken into consideration. The shorter period of construction also cuts down costs for deviation of the river, as well as the protection of the construction pit, owing to the lowering of the governing construction water.

Dams of roller-compacted concrete, constructed with a rich mixture, are deemed to be sufficiently water-impermeable, without undertaking additional measures. In order to increase durability of the structure, improve aesthetics of the dam and ensure

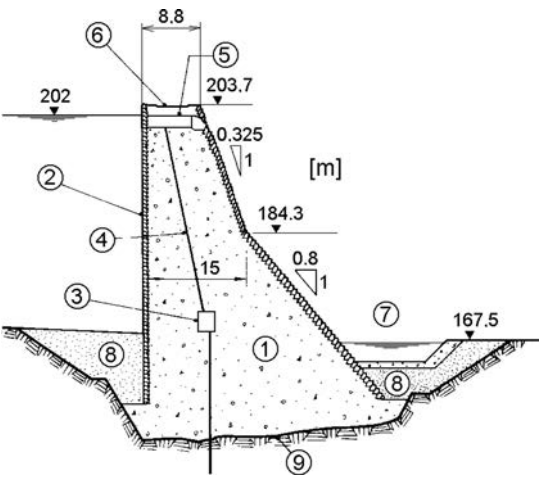

Figure 18.20 Typical cross-section of New Victoria dam, Australia (after (Wark & Mann 1992). (1) Roller-compacted concrete; (2) lining of conventional concrete; (3) main gallery; (4) drainage; (5) overflow crest; (6) roadway; (7) stilling basin; (8) earthfill; (9) foundation.

structural support during the construction of the layers of roller-compacted concrete, along the upstream and downstream faces of the dam there has been placed a layer of conventional concrete by means of a slipform. The downstream face has been shaped step-like, and it is deemed that there will be achieved a dissipation of the energy of the overflow stream, amounting to 70–80%. The crest in the non-overflow part is 8.8 m wide, which has been necessary for unobstructed accommodation of plant and equipment and efficient execution of the works.

Layers of roller-compacted concrete have been placed with a final thickness of 30 cm. Each layer has an inclination of 1:15 towards the upstream face, in order to provide drainage of the surface of every layer during construction, and also to improve the resistance against sliding in the joint between the layers of the constructed dam (this measure has also been taken with other dams, but with a slighter inclination – which can be seen in the cases of some of the previously described dams).

On the account of control, drainage, and monitoring, within the dam's body there have been constructed a number of galleries (Fig. 18.20 shows only the main one). They are located at 8 m from the upstream face, in order to leave appropriate space for the construction of works in the zone between the upstream edge and galleries. The walls of the galleries have been constructed either with slipform or with classic formwork, following the execution of the layers of roller-compacted concrete, while the ceiling has been made of flat prefabricated panels. Drainage openings have been drilled through the galleries, the same as from the main gallery to the foundation. The offtake of the bottom outlet has been concreted in a ditch in the foundation, prior to commencement of the execution of layers of roller-compacted concrete.

In the case of the New Victoria dam, we should once again notice the speed at which it is possible to construct these dams. The decision to build the dam was made

Table 18.9 Typical mixture of roller-compacted concrete for New Victoria dam.

Material	*[kg/m³]*
Coarse aggregate	1415
Fine aggregate (>4.75 mm)	740
Portland cement	80
Pulverized fly ash	160
Water	105

in February 1989, construction design and laboratory investigations for the mixture of roller-compacted concrete began to be realized in July of the same year, while the construction itself began in July 1990. Excavation of foundations and grouting works were completed in February 1991. The first of the 170 layers of roller-compacted concrete was placed on 11th of March, while the last one was placed on 18th August 1991, after 160 days. Filling of the reservoir began on 16th September the same year, somewhat more than a year after the commencement of the works.

The typical mixture from which roller-compacted concrete is prepared is given in Table 18.9. The specified curve of the grain size distribution has been accomplished by using three fractions of aggregate and one fraction of sand. The maximum grain of the aggregate has been 40 mm. In the course of the advancement of the works, and in correlation with the experiences gained, certain alterations in the proportions among individual components have been performed, aimed at reducing the danger of segregation, improving the workability of the mixture and increasing economy. Thermal analyses have anticipated that at a maximum temperature of deposition of the concrete mixture of 18°C, the maximum increase of the temperature in the dam would be about 18°C and would occur some five weeks following the placing of the concrete. The maximum measured temperature has amounted to 40°C, which means that the increase has been 22°C, and it has been recorded 8–10 weeks following the placement of concrete. Conditions dictated that the 121,000 m^3 of RCC had to be placed in the summer of 1991. With a specified maximum placing temperature of 18°C the RCC had to be cooled by 10°C. For cooling down of the concrete mixture of roller-compacted concrete and conventional concrete, the following measures were employed: (1) shading aggregate stockpiles, (2) sprinkling aggregate stockpiles for evaporative cooling, (3) chilled mix water at 4°C, (4) chilled water flowing down the conveyor feeding coarse aggregate up into the mixer holding bin, (5) injecting liquid nitrogen into the Portland cement while being transferred from the delivery trucks to the storage silos, and (6) liquid nitrogen being introduced into the mix at three conveyor transfer points after it came out of the continuous RCC mixing plant. Records from the contractor indicated the actual cost of cooling all the RCC, as well as 13,000 m^3 of conventional concrete, was A$ 6.80/m^3 or 10.5% additional cost to the RCC in place (Hansen and Forbes, 2012).

Five expansion joints have been anticipated in the dam's body at a maximum spacing of up to 75 m. Analyses have shown that reduction of this distance would not lead to any significant lowering of the thermal stresses. The position of the joints coincides

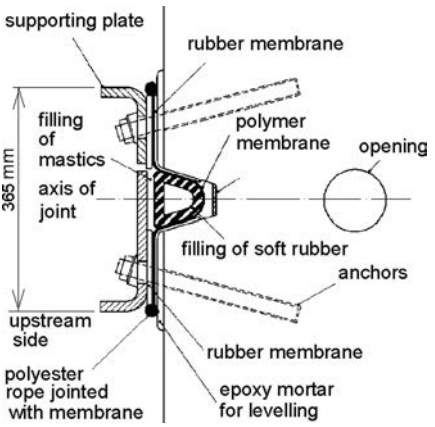

Figure 18.21 Plan of closing of a joint at the upstream face (New Victoria dam).

with sharp changes of the shape of the foundation in the longitudinal direction. Two uncontrolled cracks initially developed between the relatively long joint spacing. One was in line with the gallery entrance (adit) and another between the end of the gallery and the right abutment. Both cracks were subsequently grouted.

The five transverse joints in the dam's body have been induced with the use of galvanized steel plates, pressed inside 200 mm, embedded in each layer of roller-compacted concrete at appropriate spots. In that way, there has been formed a weakened plane through the entire section. The expansion joints at the upstream face have been closed by means of a system containing membranes and steel plates of stainless steel (Fig. 18.21). Membranes help in sealing around openings for bolts through polymer sealing membrane and in rectifying, i.e. setting right, points of unevenness on the surface. This kind of joint has been previously treated in laboratory conditions on a natural scale, at a pressure head of 94 m, with 50 cycles of opening and closing of 20 mm, in accordance with design requirements. In order to induce a joint through the surface elements, there have been formed openings with a diameter of 100 mm behind the waterstop. In the case of two joints, the opening is connected with the galleries by means of a pipe, thus, making possible monitoring of the behaviour of the waterstop. The most difficult work during the construction of these seals (waterstops) has been cutting and indenting then into the surface concrete elements, as well as their precise shaping, equalizing and levelling-off. That was necessary for the successful placement of the elements of the waterstop.

18.7.2 Examples from recent practice

18.7.2.1 Miel I dam (Colombia, 2002)

When it was finished in 2002, Miel I dam, with a height of 188 m, was the world's highest RCC dam. It has been built in Colombia in a narrow site located in a tropical region with high ambient temperatures (up to 38°C), and significant rainfall (more

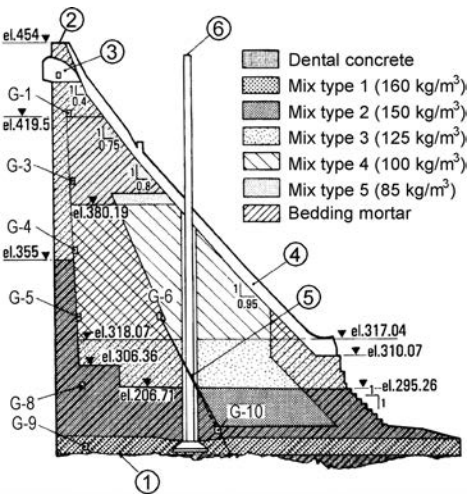

Figure 18.22 Cross-section through the axis of the spillway part of Miel I dam, Colombia (after Marulanda et al., 2002). (1) Foundation; (2) dam crest; (3) ogee spillway crest; (4) spillway channel; (5) longitudinal joint; (6) tower crane mast; G-1, G-3–G-6, G-8–G10: galleries.

than 4200 mm/year). The dam is the key structure of the Miel I hydroelectric project, aimed for electricity production of 1460 GWh/year in average, with installed capacity of 375 MW. The average flow of La Miel river is 84.3 m^3/s. The reservoir volume is 565×10^6 m^3, with a length of 22 km.

The RCC dam construction began in April 2000 and was completed after 26 months in June 2002. The total RCC volume of the dam is 1.75×10^6 m^3. RCC is placed in 0.3 m-thick lifts, using low to moderate cement content mixtures (85 to 160 kg/m^3) and no pozzolans. Bedding mortar was placed between the lifts in most of the dam body, and transverse contraction joints were supplied at a distance of 18.5 m. RCC placement has been done using conveyor belts, a tower crane and a crawler placer, with monthly rates of up to 120,000 m^3.

The dam is straight in plan, with an 8 m wide and 354 m long crest. The upstream dam face is vertical, while the downstream one is inclined and stepped, with a slope varying between 1H:1V at the heel and 0.4H:1V at the crest (Fig. 18.22).

The dam site foundation consists of massive and sound metamorphic and igneous rocks with a deformation modulus compatible with the RCC structure. The rocks are composed mainly of quartzite and gneiss, with a few andesitic and pegmatitic dikes. In other words, it was suitable for foundation of a concrete gravity dam. It was necessary to remove soils, weathered rock and loose blocks from the dam foundation. Impermeability of the foundation was achieved by a deep grout curtain and a series of consolidation and contact grout fans, to prevent leakage through the relief and tectonic joints.

Based on stress-strain dynamic structural analyses, five types of RCC mixtures were considered for the dam, as shown on the cross-section in Figure 18.22. In

Table 18.10 Properties of the applied RCC mixtures in the Miel I dam body (after Marulanda et al., 2002).

Mix type	*Cement content [kg/m³]*	*Mix volume [m³]*	*Percentage of dam volume*	*Compressive strength [MPa]*	*Tensile strength [MPa]*	*Modulus of elasticity [GPa]*
IA	160	29,930	1.7	21.0	2.32	42
I	150	255,480	14.6	21.0	2.32	42
2	125	438,100	25.1	16.5	2.00	36
3	100	709,800	40.7	13.5	1.54	29
4	85	311,450	17.9	10.0	1.30	26

Table 18.10 the cement contents and volumes of the placed different RCC mixtures, as well as the corresponding average design strengths and the modulus of elasticity at a 365-day age are given.

Aggregates for the RCC production were obtained by crushing rocks from underground excavations works and from a quarry. The materials from underground excavations were a combination of gneiss, and quartzdiorite, with minor proportions of schist and andesitic dikes. Quarried materials consisted mainly of quartzite and gneiss. The maximum aggregate size was 63 mm and the average fines content in the RCC mixture was 13% (including cement). The crushing plant installed for the production of aggregates for both RCC and conventional concrete, was located 650 m downstream of the dam site. It had a production capacity of 260 m^3/h, and it contained three parallel and independent production lines which fed four stockpiles of different aggregate sizes, including sand. The quarry was located on the left river bank, 1.3 km from the crushing plant. The quarried material of loose rock fragments was delivered to the crushing plant by 25 t dump-trucks at a rate close to 6000 m^3/day. The quarry produced a volume of 1,500,000 m^3 of material for RCC and conventional concrete mixes for the dam. The removed topsoil material reached 300,000 m^3.

For production of RCC and bedding mix, a mixing plant with a capacity of 600 m^3/h was set up. The plant featured four identical and independent batch mixers (three for the RCC and one for the bedding mix), each with a 150 t cement silo. Each mixer had a capacity of 2.67 m^3 of concrete per batch, and fed a 50 m-long extractor conveyor belt which discharged into a 35 m^3 holding hopper. A conveyor system for RCC delivery was set up between the concrete plant and the dam site. It consisted of eight conveyor segments, a tower crane and a crawler placer. The conveyor segments were 760 mm wide, 800 m long, and passed through a 340 m-long tunnel, built for this purpose. The RCC mix was delivered at a speed of 4 m/s with a nominal delivery rate of 400 m^3/h. The conveyor segment, extending from the right abutment to a platform built around the tower crane mast, pivoted about the abutment support, adjusting its angle according to the increase in dam height. The tower crane featured a 3.5 m-diameter steel tube and a 100 m-long arm, capable of carrying a maximum weight of 25 t at the arm end (Marulanda et al., 2002).

Before the placement of the concrete the abutments were carefully prepared. As the dam height increased, the abutments were cleaned of loose boulders and

soil ahead of the RCC placement. Dental concrete was placed as required in areas of abrupt geometry changes, or where RCC compaction with rollers would be difficult.

Surface preparation and cleaning of the old RCC layer before the placement of a new RCC layer was performed depending on the type of horizontal joint. In the normal cases, loose particles from the surface were removed, and the surface was kept moist. When the surface was exposed less than 36 hours, then the hardened paste was removed using an air-water jet, while when the surface was exposed for more than 36 hours, the hardened mortar was removed to expose aggregates using a high pressure air-water jet or wire brush. To achieve a close connection between the RCC layers the bedding mortar was placed. The bedding mortar was produced in the same batching plant as the RCC, and it was transported to the dam site in a mixer truck, which fed buckets. The buckets were lifted to the placing surface using the tower crane. Then, the mortar was spread using a rubber band attached to a tractor, and was covered by the new RCC layer within 20 minutes after the placement.

The RCC mix was placed using a crawler placer, and was spread in 0.33 m-thick layers (to obtain 0.3 m compacted lifts) using bulldozers equipped with a laser-guided automatic levelling system. Normally, the RCC lifts were compacted by six passes of a 12 t double-drum vibrating roller, while a small 2 t roller was used for reduced areas where the large roller could not operate. After compaction, RCC curing was done continuously using high-pressure hoses with nozzles to spray the hardened RCC surface.

To improve the dam water-impermeability, along the upstream vertical face of the dam and the RCC-abutment contact near the face grout-enriched vibrated RCC (GEVR) was placed (see section 18.5 for more details of the method). The main benefit of GEVR is the creation of a homogeneous barrier which prevents leakage through the discontinuities within the RCC lifts and joints The grout, with a water-cement ratio of 0.8:1.0, was added along a 0.4 m-wide strip in a volume of 10 liters per linear meter. To enhance the penetration of the grout into the RCC bed, a superplasticizer was added in the quantity of 0.8% of the cement weight. The grout was mixed on site and handled and poured manually. Compaction of the enriched RCC mixture was done using immersion vibrators and a vibrating plate. The placement rate of the GEVR mix varied between 80 and 100 m/hour.

In addition to the GEVR zone, an impervious PVC geomembrane on the upstream dam face was installed. Taking in mind that Miel I dam is very high (188 m) this double protection was considered necessary. Thus, 31,500 m^2 of upstream face was fully covered by an exposed PVC geomembrane. The PVC geomembrane, 2.5–3 mm thick, is anchored to the plinth and completely covers the upstream dam face. It is also anchored to galvanized steel shapes embedded into the GEVR face. Any leakage collected behind the membrane will be conveyed by a network of galvanized steel pipes to the drainage galleries inside the dam. A set of five service platforms hanging from a steel structure (bolted to the dam face) was used for installing the PVC geomembrane face. This operation was completely independently of, and parallel to, the RCC placement. The membrane is placed in standard 2.1 m-wide strips, and welded in situ. The membrane edges were embedded into the plinth and anchored to the dam's crest using stainless steel plates and bolts. Epoxy adhesives, resins and rubber bands were also used to guarantee watertightness.

Figure 18.23 Miel I dam. (a) PVC installation almost completed in lower section, and starting in the section above, where placement of the support geocomposite on the contraction joints is being performed from the travelling platform; (b) the PVC geocomposite, already installed in the lower sections allowed impounding the reservoir, while RCC placement and waterproofing works were ongoing above (Vaschetti and Scuero, 2009).

The waterproofing liner is a geocomposite, consisting of PVC geomembrane laminated to a 500 g/m^2 polypropylene non-woven geotextile. In the lowest part of the dam, from elevation 268 m to elevation 330 m, the PVC geomembrane is 3 mm thick, and from elevation 330 m to elevation 450 m it is 2.5 mm thick.

The attachment system for the PVC geocomposite on the dam face is made by parallel vertical tensioning profiles, placed at 3.70 m spacing. Where the water head is higher, from elevation 268 m to 358 m, the stainless steel profiles have a central reinforcement. The first component of the tensioning profile assembly was attached to the formworks, and embedded in the 0.3 m high RCC lifts.

A very important and rather complicated aspect of the face geomembrane waterproofing lining is the integrated face drainage system behind the geocomposite, which consists of:

- The face drainage layer created by the gap between the liner and the dam face, and by the geotextile laminated to the PVC geomembrane;
- The vertical conduits formed by the tensioning profiles;
- A peripheral collector embedded in the RCC and the transverse discharge pipes discharging into the gallery;
- A ventilation pipe assuring water flow at ambient pressure.

The drainage system is divided into four horizontal sections (compartments), each discharging in the gallery located at its bottom. Each horizontal compartment is in turn divided into vertical compartments with separate discharge. In total there are 45 separate compartments, achieving very accurate monitoring of the behaviour of the waterproofing system. In correspondence of the contraction joints, two layers of sacrificial geocomposite, of the same type used for the waterproofing liner, provide support to the liner on the joint (Fig. 18.23a). The PVC geocomposite was installed

in 6 horizontal sections, to allow early impounding while the dam was still under construction (Fig. 18.23b), and to follow at best the division of the drainage system into horizontal compartments. A movable railing system was used to install the PVC waterproofing system concurrently and independently of RCC activities. The railing system was attached to the dam face at first at approximately 90 m above foundation, and then moved to some 140 m above foundation. The travelling platforms, from which all activities were carried out, were suspended at the railing system.

Construction of the grouting plinth was made following placement of the RCC. A PVC geocomposite, placed over the completed RCC lifts and over the natural excavation rock, waterproofs the plinth. The liner waterproofing the plinth is watertight connected to the liner waterproofing the upstream face by a mechanical seal. The seal achieves watertightness by compressing the PVC geocomposite with 80 × 8 mm stainless steel batten strips on the concrete regularised with epoxy resin. Rubber gaskets and spice plates assure that compression is evenly distributed. This type of seal, tested at 2.4 MPa, is placed also at the crest, to counter water overtopping. The second component of the tensioning profile assembly, placed over the installed PVC geocomposite and connected to the first component, secures and tensions the PVC liner on the upstream face. Where the water head is higher, from elevation 268 m to 358 m, the profiles have a central reinforcement. The profiles are waterproofed with PVC cover strips (Vaschetti and Scuero, 2009).

Due to the severe local conditions at Miel I site the RCC mixture placing temperature did not have an upper limit. Therefore, to minimize thermal cracking, 17 transversal contraction joints were provided for in the dam body, spaced at 18.5 m intervals. Considering this set of joints, the only requirements for concrete temperature control of a given mix were related to the cement mixing temperature (60°C max.) and cement hydration heat. Transverse contraction joints were generated by driving 0.3 m × 2.4 m steel sheets into the newly compacted RCC lift, before it hardened, using a "joint inserter" consisting of a 2.45 m-long vibrating steel blade attached to a loader. After the steel sheet had been inserted, re-compaction of the RCC layer around the joint was carried out with two additional passes of the roller.

A single inclined longitudinal contraction joint was also provided for the lower third of the dam, parallel to the downstream face (5, Fig. 18.22). The purpose of this joint is to provide a weakness plane within the RCC mass for an eventual induced crack, and to prevent the spread of thermal cracking. If the joint opens, it can be grouted from the two galleries which intercept the joint plane (galleries G-6 and G-10, Fig. 18.22), allowing for a significant degree of RCC continuity and therefore, monolithic RCC behaviour. The longitudinal joint was formed stepwise, with strips of geo-grid placed at every lift (Marulanda et al., 2002).

Eight drainage and inspection galleries (2.5 m wide and 3 m high) have been designed within the dam body and the abutments, crossing the dam in the longitudinal direction (Figure 18.22). Six of these galleries (those located near the upstream face) were built for the purpose of grouting and drainage. All the galleries are also used for RCC inspection. Galleries G-6 and G-l0 would be used for grouting the longitudinal joint if necessary. The galleries inside the Miel I dam body were built using traditional formwork for the walls and precast 0.3 m-thick slabs for the ceiling. On

both sides of the galleries, RCC was placed and compacted against the formwork, on which the bedding mix had previously been placed. Construction of the galleries had no significant effect on the RCC placement speed, mainly because of the continuous RCC placement with the crawler placer, the arm of which placed RCC on the upstream side of the gallery being built while sitting on the downstream side. Also, while the formwork was erected, one or two partial lifts were placed on the downstream side of the dam, and therefore the placing rate was not actually affected. Finally, placement of precast panels for the gallery ceiling was typically done during the scheduled weekend recess and it therefore did not slow RCC placement down. RCC compaction in areas adjacent to gallery formworks was done using lighter equipment.

The downstream face steps (on the non-overflow part) were 0.6 m-high and were therefore completed in two stages (that is, two RCC lifts), using a formwork.

The central part of the Miel I dam is designed to serve as a spillway, having a discharge capacity of 12,800 m^3/s (the 10,000 year flood return period). The spillway is uncontrolled, with ogee crest 65 m wide. The spillway is enclosed by two converging 4 m-high walls on the downstream slope and ends in a 32 m-wide flip bucket. The spillway was constructed using total volume of conventional concrete of 17,200 m^3.

The Miel I dam was appropriately instrumented, keeping in mind its height. Instruments were installed within the dam body, as well as in the foundation, to record the RCC stress-strain behaviour, temperature development, pore-water pressures and joint displacements. These instruments consisted of 334 thermocouples, 23 load cells, 45 strain gauges, 117 contraction joint crack-meters, 10 longitudinal joint crack-meters and 64 piezometers, distributed in arrays at seven levels of the dam.

During the construction of the Miel I dam a strict control of all materials and works was performed. The RCC compaction achieved by the contractor as a percentage of the theoretical air-free density of the mix was verified repeatedly during every shift, using single-probe nuclear densimeters and correlated with laboratory and field tests, On average, one densometer record was taken for every 43 m^3 of compacted material. Likewise, RCC production and placing temperatures were recorded during each shift in several instances. Every shift took an RCC sample randomly at the batch plant to determine its wet gradation and moisture, and to evaluate the strength and deformation modulus. Approximately 22,000 cast specimens were obtained and tested during the construction. Furthermore, about 1000 m of RCC cores were extracted from the dam, and were tested in the laboratory for density, compressive and tensile strength, and modulus of deformation.

The construction of the Miel I RCC dam, with a total RCC volume of 1,745,000 m^3, was completed in a period of 26 months. The RCC placement volume averaged approximately 3000 m^3/day, with peaks of up to 7200 m^3/day. In the nine months between April and December 2001, monthly placement averaged about 100,000 m^3, with a maximum of nearly 120,000 m^3/month. The placement curve was very close to the scheduled one (Marulanda et al., 2002).

18.7.2.2 Olivenhain dam (USA, 2003)

Olivenhain RCC dam in California is a gravity dam 788 m long, with maximum height of 97 m. This is the highest RCC dam in USA and the first RCC dam built in the highly seismic state of California. Olivenhain dam is a key element of the Emergency Storage

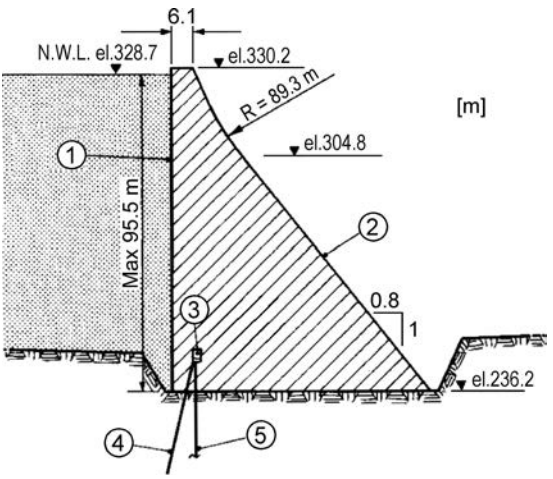

Figure 18.24 Cross-section of the Olivenhain dam (after Dunstan, 2002). (1) Exposed geomembrane liner; (2) downstream face; (3) foundation gallery; (4) grout curtain; (5) foundation drain.

Project (ESP) of the San Diego County Water Authority, owner of the dam. About 90% of water is brought to San Diego from hundreds of miles away, and the aqueducts cross several large active faults, including the San Andreas Fault. The ESP will provide water to the San Diego region in case of an interruption in water delivery deriving from an earthquake or drought. The project is located on a normally dry tributary of the Escondido Creek, some 40 km north of San Diego in southern California. The reservoir will be filled with imported water from the California State Water Project and the Colorado River.

The construction of the Olivenhain dam started in June 2001 and the dam was completed in July 2003. The RCC placement began in February 2002 and finished in October 2002, after eight months. Thus, taking into account that the volume of RCC is more than one million m^3, it is one of the fastest-placed RCC dams to date. Olivenhain is a relatively simple straight-gravity RCC dam (Figures 18.24 and 18.25). The upstream face is vertical, while the downstream face has a typical inclination for a gravity dam of 0.80H:1V. The dam site is irregular with a large valley to the left of the main valley, and a smaller recess near the top of the dam on the right abutment (Fig. 18.25). Owing to high seismic loads, special features of the Olivenhain dam design are the abutment shaping blocks (1, 2, Fig. 18.25) which have been used to fill these subsidiary valleys. The role of these blocks is to replace the poor foundations and to optimize the performance of the dam geometry under dynamic loading. The right abutment shaping block (RASB) was used for one of the full-scale trials and the first production RCC placement was in the left abutment shaping block (LASB). The cross-sections of the LASB (2), Figure 18.26, and RASB are wider than the main dam and the stresses, and thus the strength requirements, were lower.

The contractor undertook a supplementary trial mix programme in two stages in parallel with that being undertaken by the designer, to try to simplify the method of

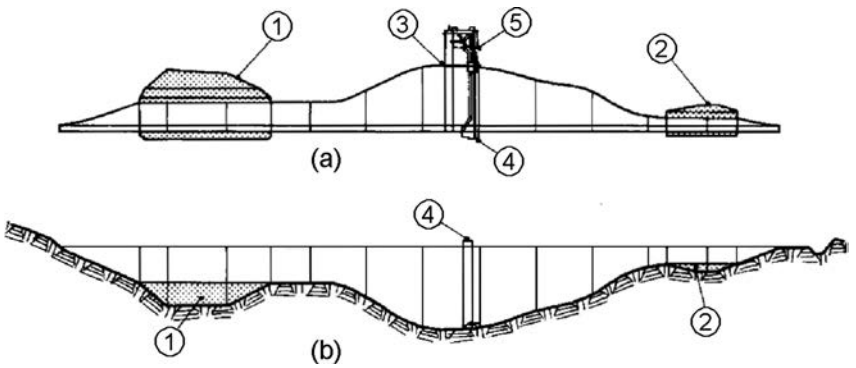

Figure 18.25 Plan (a) and longitudinal section (b) of the Olivenhain dam (after Dunstan, 2002). (1) Left abutment RCC foundation shaping block; (2) right abutment RCC foundation shaping block; (3) spillway; (4) intake-outlet tower; (5) intake-outlet conduit.

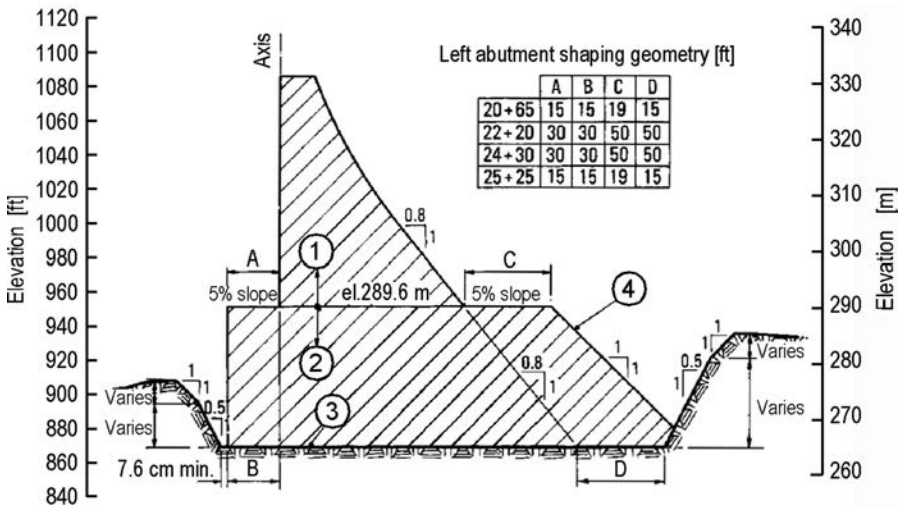

Figure 18.26 Cross-section of the Olivenhain dam through the left abutment shaping block (after Dunstan, 2002). (1) Dam body; (2) left abutment shaping block; (3) top of foundation rock (varies); (4) unformed RCC downstream face.

construction. One of the objectives of the programme was to improve the workability of the RCC so that it could be discharged into trucks, dumped from trucks, spread by a bulldozer and compacted by a vibratory roller without a trace of segregation. Without segregation the placement can progress at a fast rate, and the in-situ properties are improved, particularly at the joints. As the contractor was to submit a value-engineering proposal, any solution had to be economic, while meeting the original design criteria.

Table 18.11 Main features of Olivenhain dam (after Dunstan, 2002; Worl Atlas, 2012).

Dam type	*RCC straight gravity*
Max. height above foundation [m]	97
Crest length [m]	778
Crest width [m]	6.1
Crest level [el. m]	330.2
Normal water level (NWL) [el. m]	328.7
Total excavation volume [m^3]	535,000
Total concrete volume [m^3]	1,140,000
RCC volume [m^3]	1,070,000
Thickness of the compacted RCC layers [cm]	30
Cementitious content in RCC (cement + fly ash) [kg/m^3]	74 + 121
Type of upstream sealing	Geomembrane liner
Length of drilling for grouting and drainage [m]	26,000
Reservoir volume at NWL [$m^3 \times 10^6$]	30
Reservoir area at NWL [ha]	80

The aim of Stage I was to assess the performance of the materials and it started with the optimization of the gradation and of the workability. As a result, the fine aggregate proportion was reduced within the overall gradation to about 35%, which was equivalent to a loaded VeBe time of about 14–17 s. Then, the early-age performance of the cementitious materials (Type-TI Portland cement and a low-lime fly ash) was found to be rather poor. However, previous experience with RCCs containing high proportions of fly ash has shown that if the early-age performance of the cementitious materials is poor, the long-term strength development can be significant.

The aim of the Stage II was to refine the RCC mixture proportions. For this purpose eight mixes in all were tested, four for the RCC itself, two investigating the use of a retarder and two looking at the development of strength of grout enriched vibratable RCC (GEVR), which was proposed for use against the abutments as a replacement for a conventional interface concrete. Four RCC mixes were investigated containing different cementitious content: *Mix 10* (69 kg/m^3 Portland Cement + 128 kg/m^3 of fly ash), initially expected to be the RCC to be used in the main body of the dam, and was designed for a characteristic strength of 20.7 MPa at the design age of 365 days; *Mix 11* (74 + 121 kg/m^3, designed for a slightly higher strength of 22.8 MPa; *Mix 12* (59 + 133 kg/m^3), designed for a characteristic strength of 17.2 MPa and for use in the LASB; and *Mix 17* (82 + 115 kg/m^3), designed for a higher characteristic strength of 25.9 MPa.

Beside the laboratory test, a very large series of full-scale trials was conducted in three areas with the objective, as far as was possible, of using the RCC test fills as permanent structures to minimize waste of material. The first preliminary trial was placed downstream of the dam under a flow control structure, the second (largest) full-scale trial was in the RASB as a foundation replacement, and a third trial was run concurrently with the second and was constructed in the car park of the contractor's offices (the last trial contained the only RCC that was not used as part of the final

structures). A significant number of cores was extracted from the full-scale trials for testing in the laboratory. Some of the cores were accelerated by placing them in an oven for seven days prior to testing at 91 days (the age of test for all the cores). Although it was not known what age the accelerated cores would represent, it was considered that it would give a first indication of the strength at some time in the future. A critical objective of the trial placements was to identify the in-situ performance of the RCC at the lift joints. Four levels of joint treatment were investigated during the full-scale trials (Dunstan, 2002):

- A "hot joint", having little or no treatment other than keeping the joint clean (from the results of testing it was concluded that a hot joint was up to 16 hours old in the summer and up to 24 hours old in the winter. It was expected that the majority of the joints in the dam would be of this type).
- A "warm joint", which was cleaned with a vacuum truck and onto which a thin layer of grout was spread (the age of a warm joint was up to 39 hours in the summer and up to 59 hours in the winter).
- A "cold joint", which was swept with a road brush and vacuumed, and onto which a thin layer of grout was spread (the age of a cold joint was up to 61 hours in the summer and up to 82 hours in the winter).
- A "super-cold joint", for which an *exposed-aggregate* finish was produced and onto which a thin layer of grout was spread. The super cold joint treatment was to be used in excess of the exposure time for a cold joint.

More details of the test and the results are given by Dunstan (2002). It was concluded that the properties of the RCC achieved during the full-scale trial were satisfactory, and that *Mix 11* should be used in the main body of the dam. At the same time that the cores were being extracted from the full-scale trial, a trench was cut through the RASB trial using a diamond wire saw, so as to examine the profile of the lift joints physically. It was difficult to see the joints between the layers.

Before placement in the dam the RCC was pre-cooled by use of a *wet belt* and ice. The RCC was mixed in a pair of concrete plants each having two 6 m^3 twin-shaft batch mixers. Then the RCC was conveyed to the dam by a 900 mm wide conveyor with a capacity of about 640 m^3/h. At the end of the conveyor a "swinger" was located that loads 35 tonne CAT 769 dump trucks. The RCC was then transported to the point of placement, dumped from the trucks and spread by two CAT D6s. Two 10 tonne single-drum vibratory rollers were used to compact the RCC in approximately four passes. Two smaller (2 tonne) twin-drum vibratory rollers were used to compact the RCC in areas where the larger rollers were unable to work efficiently.

The RCC has been designed so that there was no segregation during the whole process from mixing to roller compaction, which allowed a rapid rate of placement. In addition, a retarding/water-reducing admixture was added which delays the initial set until 20 to 24 hours after mixing. This allowed the layers to be placed on top of each other before the initial set, which creates a strong bond between successive layers. To avoid high temperatures during the middle of the day the RCC was placed in two shifts: from 15 hrs to 1 hr and from 1 hr to 9 hrs. To control thermal cracking, a maximum placing temperature of 16.5°C was required in the lowest portion of the

dam, while in the middle of the dam the maximum permitted placing temperature was 19.5°C and towards the top of the dam 21°C.

The RCC was placed directly against vertical timber formwork on the upstream face of the dam. The finish was improved by the placement of a 50 cm wide layer of grout on the surface of the previous layer of RCC before spreading and roller compaction of the new layer. On the downstream face, the RCC was compacted directly against ~900 mm high stepped steel formwork (Dunstan, 2002).

Olivenhain dam is an example of the same exposed waterproof system adopted at Miel I dam, but with an addition of a geonet, placed between the dam face and the PVC geocomposite, to increase the drainage capacity. In the stability analysis, the exposed geomembrane liner and its face drainage system were considered two features that would tend to reduce the uplift pressure. The external geomembrane system received the highest score among the 11 considered alternatives. The main role of the drainage geonet installed on the RCC is to enhance discharge capabilities in the case of accidental damage of the impervious geomembrane. Under the pressure of the hydrostatic load the geonet will maintain high transmissivity, no water will be able to migrate through lift joints in the body of the dam, thus saturation levels and pore pressures in the dam will be lowered, with beneficial effects on the dam stability. The upstream face has been divided into 12 compartments, separated by a vertical watertight seal, to allow defining the area of the leak in case of damage of the geomembrane. The peripheral seals are of the same type adopted at Miel I dam. Waterproofing works were completed in 5 months; the cost of the exposed geocomposite system was about 5% of the US $124,959,204 contract (Vaschetti and Scuero, 2009).

Treatment of foundations included curtain grouting, consolidation grouting from the foundation surface, and stitch grouting at locations of potential preferential seepage pathways. GEVR was used against the abutments to develop a good bond between the RCC and the granodiorite rock foundation. Grout was spread against the abutment, then RCC was spread over the grout and the GEVR is then vibrated and finished with a vibrating plate.

It can be concluded that the method of construction applied at Olivenhain has been made very simple. As a consequence, the construction of the RCC dam was economical and it was done in a short time of only eight months.

The reservoir filling started on August 7, 2003. On June 16, 2004, with reservoir almost at full supply level, a 5.5 Richter scale earthquake occurred at 100 km from the dam. The blocks of the dam shook and moved, but no damage has been reported and watertightness of the dam has been totally maintained, fully meeting the design and safety requirements.

18.7.3 RCC dam construction practice in China

An enormous number of dams has been constructed in China (see Chapter 1). However, due to the country's isolation, it has not had a significant influence on the development of dam construction in the world; and yet, China has eagerly followed modern world trends. Thus, according to the number of dams of roller-compacted concrete constructed, China takes first place in the world (Fig. 18.3). Its experts became acquainted with the early Japanese and American experiences in the very beginning of the application of roller-compacted concrete. This resulted in the completion of their first dam

Table 18.12 Performance of the four highest RCC dams in China.

Dam	Height *[m]*	*Impounding time*	*Max displacement [mm]*		*Max seepage [l/s]*
			Along river	*Vertical*	
Longtan	192 (stage I)	September 2006	6.65	Very small	4.725 (dam foundation), uplift pressure reduction coefficient behind the curtain is less than 0.13
Guangzhao	201	December 2007	10.98	3	21.1 (dam foundation, uplift pressure coefficient behind the curtain is less than 0.13
Guandi	168	November 2011	<15	Very small	27.8 (dam body)
Jin'anqiao	160	November 2010	11.5	6	Foundation: uplift pressure reduction coefficient behind the curtain is less than 0.17; dam body: seepage pressure coefficient is less than 0.03

of this kind – the Kengkou dam ($H = 56.8$ m) – in 1986. Chinese mixtures for roller-compacted concrete in the early period of construction of RCC dams are characterized by a low quantity of cement and a high quantity of pulverized fly ash, in order to reduce the cost and the release of hydration heat. In most cases, the quantity of the water used amounted to less than 100 l/m^3 of the concrete. Sand is proportioned in a quantity of about 700 kg/m^3 of concrete, with a maximum aggregate grain size of 80 mm. From Table 18.3, it can be seen that up to 2001 seven dams higher than 100 m have been constructed in China, while Table 18.4 shows that up to now seven dams higher than 150 m (out of total number of 12 worldwide) are located in China. The substantial experience gained from previous practice has enabled the realization of daring plans (Chonggang, 1991; Polimon et al., 2012).

By the end of 2012 in China 165 RCC dams had been completed or were in the final stage of construction, of which 40 are higher than 100 m. RCC dams have now become one of the most competitive dam types in China. Table 18.12 gives some data of the four highest RCC dams completed in China. Most of high RCC dams have operated normally and some have demonstrated excellent behaviour (Polimon et al., 2012).

Along with the rapid increase of the number of RCC dams constructed, the associated construction technology has made great progress in China, based on accumulated experience and constant innovation. Examples are in mixture design optimization, temperature control and crack prevention, the development and application of digital dynamic monitoring systems, quick construction technologies, the use of RCC in severe conditions, and so on.

The world's highest RCC gravity dam projects, Longtan (217 m high, 192 m in the first stage 2006, completed to full height in 2009) and Guangzhao (201 m high, completed in 2009), were clear indication that RCC dams with heights of more than 200 m can be built.

Thus, the Longtan dam is now the highest finished RCC dam in the world. The main purpose of the Longtan project is electricity production with installed capacity of the underground powerhouse of 6300 MW. Other purposes of the project are flood control and navigation. This is one of the top-ten key projects of the Great Western Development Plan and the strategic projects of "Power transmission from west to east", and it is also the critical controlling project in the cascade development of Hongshui River. The project layout, besides the gravity dam (850 m long), includes: flood discharge structure arranged in the river-bed dam section (7 surface spillways and 2 bottom outlets), left-bank underground diversion power-generation system (9 units, 700 MW each), and right-bank navigation structure equipped with 2-steps vertical ship-lifts (the greatest in the world). The main data of the dam are given in Table 18.4. The construction period of the project started in July 2001, the first stage (dam height of 192 m) was completed in 2006, and the dam was entirely completed ($H = 217$ m) in 2009.

18.7.4 RCC dam construction practice in Spain

Spain is the greatest builder of dams of roller-compacted concrete in Europe, (Fig. 18.3). This is not at all surprising, when one considers that in Spain there have been constructed over 1250 dams so far, 72% of which are concrete dams. From this, it is understandable that the Spanish engineers have immediately accepted the new, economical concept of dam construction with the application of roller-compacted concrete dams. The first such dam was constructed in 1985, and between 1990 and 1994 a total of 14 RCC dams were built. Now there are 28 RCC dams in Spain (Figures18.3 and 18.4; 27 dams are in operation while one is under construction). The technology of application of roller-compacted concrete adopted in Spain is directed towards obtaining compact material, which will be produced and placed in the fastest and most economical way. Roller-compacted concrete is designed to be sufficiently water-impermeable, while the application of conventional concrete is limited to the following zones (Laá, 1992):

- Contact between the dam's foundation and the bedrock, with a thickness of 0.5–2 m;
- The downstream face of the overflow part;
- The upstream face, with a thickness >1 m (in some cases);
- The non-overflow downstream slope, with a thickness <1 m (in exceptional cases);
- Zones of water-conveying structures;
- Around inspection galleries (completely or partially);
- The uppermost part, with a thickness of 1 m, for forming a roadway along the crest.

The average percentage of RCC in the total concrete volume at Spanish dams is around 84%, with two main exceptions: the Urdalur and Los Canchales dams, with 62% and 45%, respectively. For that reason, the construction of these dams was quite complex (Ibañez de Aldecon et al., 2012; Lafuente and Pascual, 2012; Allende et al., 2012).

18.7.4.1 General principles for the design of the RCC dams in Spain

All RCC dams in Spain are gravity structures, straight in the plane, with a more or less standard cross-section, with slight changes to facilitate the new technology of continuous placing of the concrete. Figure 18.27 presents cross-sections of eleven characteristic Spanish dams, ordered chronologically, the basic data of which are given in Table 18.13.

Both the quality and geotechnical characteristics of the foundation affect the final design of the cross-section (for example at the Puebla de Cazalla and Rialb dams). The seismicity of the Iberian Peninsula generally has very little influence in this respect. The experience of constructing RCC dams in Spain over 30 years has demonstrated to engineers that the design of the dam body should be as simple as reasonably possible. It has not always been possible to have a simplified design. So in some cases, some of the inherent advantages of the RCC have been lost. Like other dams of roller-compacted concrete in Spain, the characteristic shown examples (Fig. 18.27 and Table 18.13) have been designed and constructed complying with the following basic principles (Laá, 1992; Alonso-Franco, 2003; Ibañez de Aldecon et al., 2012; Lafuente and Pascual, 2012; Allende, 2012):

- It is more advantageous, in terms of speed of construction and economy, to construct the whole dam section using only one high cementitious material content RCC (or so called very rich paste content RCC, where paste means cement with fly ash and water). Typical examples are Brena II and Puente de Santolea dams.
- One of the consequences of the application of RCC with very high cementitious materials content is that the differences between conventional concrete and the RCC have been gradually reduced, with the result that the main essence of each technology is the placement procedure.
- The dam crest width must be sufficient to allow for vehicles and machinery to drive across without any interference. An overall width of more than 8 m (usually 10 m) will facilitate construction.
- The upstream side, mainly, is vertical, with some possible sloping at the bottom part. The construction is by means of a slipform, anchored into the dam.
- The downstream face, in general, is step-like, with a step equal to a multiple of the layer thickness, which is more consistent with the construction process and facilitates the task of arranging the formwork. This has enabled the application of stepped spillways at many dams.
- Longitudinal inspection and drainage galleries are constructed in a minimum number and their construction should not interfere with the concreting work. Usually, at least one gallery is constructed lined with conventional concrete. If only one gallery is planned, attempts will be made to ensure that it is 'perimetric' to allow for the entire corrective foundation works, and grout and drainage curtain, to be constructed in a more rational way and with the greatest efficiency. These perimetric galleries have been implemented mainly by embedding them in a trench in the ground encased in the conventional concrete.
- The conduits for intakes, outlets and diversions are now concentrated in one block, with their valves and operating mechanisms located next to the downstream face, and their inlets, if possible, in a tower backing on to the upstream face.

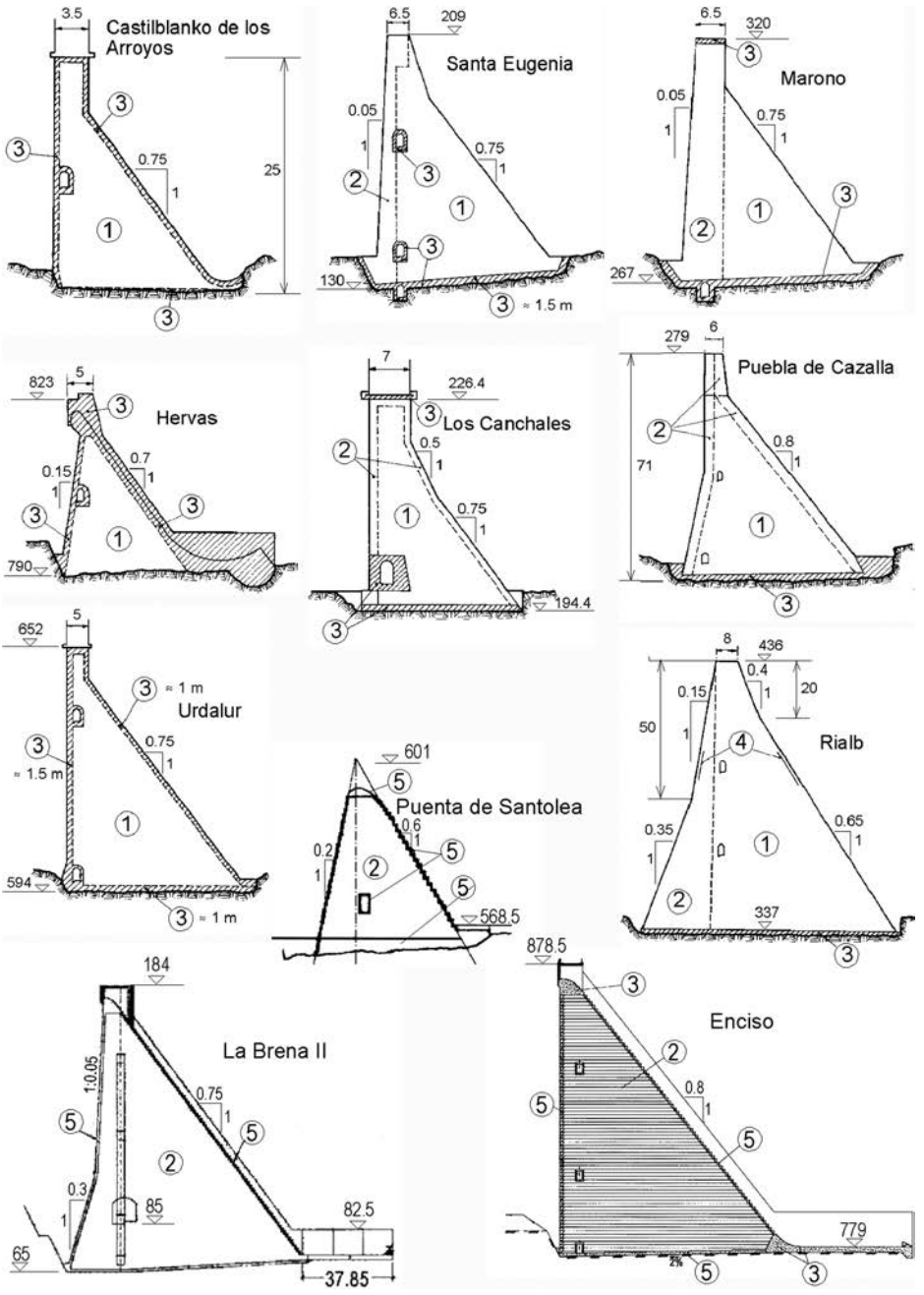

Figure 18.27 Some characteristic dams of roller-compacted concrete constructed in Spain, ordered chronologically (see also Table 18.13). (1) RCC; (2) RCC with higher cementitious material content; (3) conventional vibrated concrete; (4) conventional concrete with slipformed curb; (5) mortar enriched vibratable RCC (MEVR).

Table 18.13 Data on some characteristic roller-compacted concrete dams in Spain (cross-sections shown in Fig. 18.27).

Dam	Built (year)	Height (m)	Length (m)	Slopes (H:V)		RCC ($m^3 \times 10^3$)	CVC ($m^3 \times 10^3$)	Res. vol. ($m^3 \times 10^6$)
				Upstream.	Downstr.			
Castilblanco de los Arroyos	1985	25	124	0	0.75	14	6	0.82
Santa Eugenia	1988	83	280	0.05	0.75	225	29	13.6
Marono	1990	53	182	0.05	0.75	80	11	2.23
Hervas	1990	33	210	0.15	0.70	23.8	19	0.22
Los Canchales	1991	32	240	0	0.50–0.80	25	29	14
Puebla de Cazalla	1992	71	220	0–0.2	0.80	205	5	7.4
Urdalur	1993	58	396	0	0.75	160	48	5.4
Rialb	2000	99	630	0.15–0.35	0.40–0.65	980	36	402
La Brena II	2008	119	685	0.05–0.30	0.75	1438	200	823
Puenta de Santolea	2011	35	203	0.20	0.60	65	5	17.7
Enciso	U.C.	103	376	0	0.80	641	77	46.5

- Concrete works have made a progress of 200 m^3/h. Thus, at the Santa Eugenia dam, 250,000 m^3 of concrete were placed within 11 months.
- Layers are placed with a thickness of about 30 cm, in a continuous manner (without interruptions) three to ten at a time. In that way, joints have been achieved without special treatment – only by spraying with water. Compaction has been implemented for every layer separately, up to full compactness. In Spain, they have been analyzing the Japanese practice of laying and compacting several layers at the same time, which reduces the anisotropy in relation to water-permeability.
- The aggregates used at Spanish RCC dams have had practically identical characteristics to those used with conventional concrete. For the preparation of the RCC concrete mixture there is used rounded and crushed mineral aggregate of limestone or silicate origin, with a maximum grain of 80 mm (sometimes of 60 mm, and exceptionally of 100 mm). But since 2000, in accordance with the current trends, and contrary to the common practice of some years ago, the maximum size of crushed aggregate has been reduced to 50 mm, to reduce segregation, to increase the workability, and to ensure a good appearance for the faces of the dam body.
- The cementitious material used in Spain for roller compacted concretes has generally been a mixture of Portland cement and fly ash, class F (type silica-aluminous), with a content of the latter which is much larger than that of the cement (on average, 1.8 times higher). The cementitious material is proportioned in a quantity of 180–240 kg/m^3, of which 30–40% is Portland cement, while 60–70% fly ash. Rock powder filler, as another component of the RCC, to improve the filling of the voids, has been added during the construction of La Brena II dam (46 kg, 20% of the total of high quality limestone filler).
- To design the RCC mixtures concrete technology has generally been used. The result is a grading for the coarse aggregates with a minimum volume of voids,

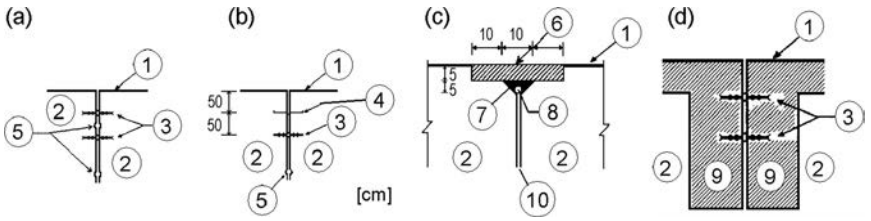

Figure 18.28 Some types of waterproofing of the vertical transversal joints used at RCC dams in Spain (after Ibanez de Aldecon et al., 2012). (1) Upstream face; (2) RCC; (3) waterstop; (4) cooper sheet; (5) molded conduit; (6) mortar; (7) mastic; (8) neoprene roller; (9) GEVR, MEVR; (10) sawn joint.

which subsequently would be filled with mortar. It was preferable to have a very well graded grain size distribution of the aggregates, and to measure the consistency of the concrete with the Modified Vebe apparatus.

- Usually the design age of the RCC has been 90 days but in the recent case of La Brena II dam, the time was 180 days. In addition, in recent cases the critical design criterion has been the use of the results of direct tensile strength of the jointed cores, instead of the compressive strength of cylinders.
- In the case of mixtures of this type (rich with cementitious materials), the generation of heat begins within 1 hour; that is to say, prior to the previous placed layer being covered by the next one. An increase of temperature of 14–18°C is recorded as an exothermal reaction, which keeps on for days.
- In order to avoid cracks caused by the differentiated shrinkage the RCC dams are divided into blocks through vertical joints which are made using conventional formwork or crack inductors. The locations of these joints are mainly based on a thermal study, to determine suitable distances, i.e. dimensions of the blocks, and the necessity of cooling the concrete. In the early period joints at all dams were made with formwork, at a mutual distance of 40 to 60 m. The blocks created allowed for the placing of formwork on the face of one of them, while the other was being concreted. The main disadvantage of this procedure was the difficulty of transferring the machines from one block to another. Subsequently, the blocks were made longer (100, 130 and 150 m), but in all cases, they have to be divided into intermediate sub-blocks, to avoid cracking as a result of hydraulic and thermal shrinkage. This division of the blocks was done by sawing the layer with a disc saw or, more frequently, inducing a crack on the layer by driving in a plate or sheet, with equipment which inserts, by vibration, a synthetic film or galvanized sheet. Vertical joints are extended across the entire section.
- Water-impermeability of the vertical transvers joints is achieved by incorporating one or more seals, i.e. waterstops next to the upstream face. Until 2000, one or two conduits were left molded in the joint (Fig. 18.28a and b), one of them connected to the inspection and drainage gallery. In contemporary practice the joint sealings do not differ from those used in conventional concrete dams (Figures 18.28a-d).
- For every Spanish RCC dam test sections have been done. Before starting the placement of the concrete in the dam, a full scale trial has been constructed, during

which the data obtained from the laboratory tests were corrected and optimized, as well as those imposed by the technical specifications of the project. On the test section, the conditions of placement have been tested, like: faces, thickness of layers, segregation, treatment of joints between layers, etc. In the case of La Brena II dam, a test section was constructed with 12 layers and an approximate volume of 3000 m^3. From the test section, cores were drilled to measure concrete densities, bond between layers and in situ permeability by filling boreholes with water.

It is interesting to notice that Spain has experience with the flooding of uncompleted constructions of dams made of roller-compacted concrete. Namely, in the course of construction in one rainy period in 1987/88, the Santa Eugenia dam was twice completely flooded without being damaged. The first time it had been raised to 21 m height, while the second time the construction height was 43 m.

18.7.4.2 Improvement of the watertightness

Until 2000, mainly the following two methods for improvement of the watertightness at RCC dam body were used in Spain:

- Construction of a zone in the upstream dam face of conventional high quality concrete with a minimum width of 1.5 m;
- Placement of a different type of RCC near the upstream dam face in a zone with a minimum width of 3 m, but increasing with the head of water; this higher-quality RCC contains more cementitious materials and a smaller maximum aggregate size.

At some dams, for example Puebla de Cazalla, a strip of bedding mortar, 80 cm wide, was placed between the layers near the upstream face. In practice during the last two decades there has been a tendency to use RCC with high cementitious material content in the whole dam body. In this way, it is possible to gain a durable and watertight structure, avoiding the placement of geomembrane on the upstream face.

Grout-enriched vibratable RCC (GEVR) was also used. At Brena II dam, the highest RCC dam in Spain, a modified GEVR method, called *mortar enriched vibratable RCC* (MEVR) was applied, with very good results. However, the latest tests carried out at the beginning of construction of the 102 m-high Enciso RCC dam, with a very workable and super-retarded mix, were very successful in showing the efficiency of the direct immersion vibration of RCC without any additional grout. Preliminary results of these tests indicate that a significant step forward has been made towards the improvement of the in-situ quality and the general behaviour of RCC dams. With this new, so-called Immersion Vibrated RCC (IVRCC) technology, it has been possible to design a concrete mix which can be consolidated either by traditional pokers or by vibratory rollers. The application of this innovative technique would further simplify the construction of concrete dams and would enhance the quality of the RCC (Allende et al., 2012; Ibanez de Aldecoa and Ortega, 2013).

18.7.5 RCC dam construction practice in Japan

As was shown in the introductory section of this chapter, Japan, with 48 finished dams, is one of the leading countries worldwide in the field of RCC dam construction. Also it was mentioned that the first dam of this type originated from Japan. From Table 18.3 one can see that up to 2001, of the 25 RCC dams higher than 100 m around the world, 13 have been constructed in Japan. Furthermore, during that time two of the world's highest RCC dams were located in Japan – Urayama (H = 156 m), and Miagasse (H = 155 m).

Roller-compacted concrete used in Japan is rather different from RCC used at dams in other countries. Therefore, dams built using this material in Japan are called *roller-compacted dams (RCD – Roller Compacted Dam concrete)*. RCD dams are distinguished from the other roller-compacted concrete (RCC) dams because there are some differences in their design and construction philosophies. This concrete is placed in layers of about 30 cm, but the compaction is made in lifts up to 100 cm. The quantity of cementitious materials ranges from 120 to 130 kg/m^3, of which 20–30% is pozzolan or PFA. For the first 15 years of construction of RCC dams such quantity of cementitious material was considered high. Later, the situation changed, and in contemporary practice predominantly RCC dams with high cementitious material content are constructed.

The philosophy of the RCD construction method is to keep the same performance as concrete dams constructed with the conventional concrete construction method, but with improved economy. Therefore, RCD is a construction method aimed to rationalize the dam construction works, while the required functions of RCD dams should be the same as that of conventional concrete gravity dams. To achieve this aim, the following technical measures have been applied:

- Transverse contraction joints are installed at every 15 m in order to prevent temperature cracks in the dam's body.
- High quality conventional concrete is placed at the upstream and the downstream dam surfaces in order to obtain watertightness and high durability.
- Lift joints (horizontal surfaces) are treated in the same way as at the conventional concrete dams in order to assure good bond and watertightness between the lifts.

Keeping in mind that RCC can be defined as concrete compacted by a roller, we can say that RCD is a kind of RCC. Actually, both have a common concept, technical know-how, machinery and procedure. A typical feature of RCD construction method is that the concrete is spread into several thin layers (usually three) by bulldozers, and then the thus formed multi-layer lift, usually 1 m thick, is compacted by vibratory rollers. Thin layer spreading of concrete is the key factor that makes thick lift placement possible. The reason of higher lift compaction in RCD is to reduce the number of weak planes between successive lifts, thus increasing the dam stability against earthquakes and other influences.

Tables 18.1 and 18.2, in which the main features of some types of concrete for dams are given, show the differences between these concrete types. Further, Figure 18.29 shows graphically the relationship between RCC and RCD concretes from the view of cementitious material contents and density or strength of concrete. From the

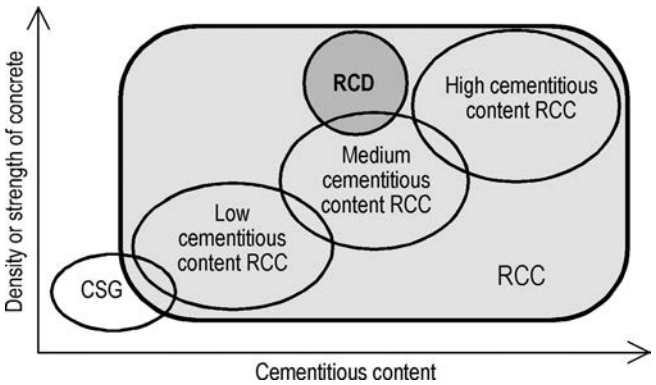

Figure 18.29 Conceptual position of RCC and RCD concrete from the view of the cementitious material contents and density or strength of concrete; CSG: Cemented Sand and Gravel, relatively new material for dams (after Nagataki et al., 2008).

graph it is not difficult to realize that RCD occupies an important position in RCC technology: one can say that RCD is a high grade version of RCC. The popularity of such high quality dam material in Japan is understandable, keeping in mind the high risk of earthquakes or floods in this country.

The unit cement content and unit water content in the RCD concrete mixture are much less than those in the conventional concrete for dams (see Table 18.2), because RCD concrete should be dry and lean. Dry concrete is required to allow the construction equipment to travel on fresh concrete, while lean concrete is required to minimize temperature rises which may cause cracks. At the same time, hardened RCD concrete should have the same properties as conventional concrete, to ensure construction of safe and watertight structures. Many efforts have been made by Japanese researchers and dam engineers to ensure that RCD concrete has all these properties. Also, the zoning of the dam cross-section has been carefully analyzed and carried out (Fig. 18.30).

In RCD dams, like conventional concrete dams, the concrete is classified into external concrete that is used at the surface of the dam (A1, A2, Fig. 18.30), foundation concrete (A3) that faces the bedrock, structural concrete (A4) that is used in and around structural elements, and internal RCD concrete (B1 and B2) that is used inside the dam body. Thus, RCD concrete volume is estimated excluding external, foundation and structural zones, and this volume is a key point in the adoption of RCD construction method. For the zones A1 to A4 high quality conventional concrete is applied to maintain watertightness, durability, structural stability etc.

Since RCD concrete is dry and lean concrete, it is more sensitive to rainfall than conventional concrete. If the rainfall is stronger than 2–4 mm/hour or in the case of danger that the concrete surface might be disturbed by the rain, the concrete placement is interrupted and a cold joint is provided.

In RCD dams it is difficult to use embedded pipe cooling. Therefore, the temperature control plan at the planning stage should be prepared to prevent temperature cracks. Moderate-heat Portland cement with fly ash is used and the unit cement content

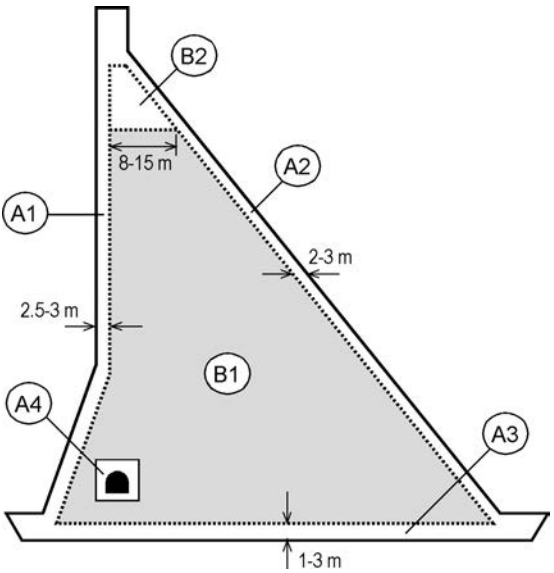

Figure 18.30 Cross-section of RCD dams with internal zoning (after Nagataki et al., 2008). (A1) Upstream external concrete zone; (A2) downstream external concrete; (A3) foundation concrete; (A4) structural concrete; (B1), (B2) internal RCD concrete zones.

is reduced to suppress the heat of hydration. Experiences have shown that temperature cracks can be prevented mostly when the transverse joints are placed about 15 meters apart. Through the term of concrete placing in most RCD dams the concrete is cured by ponding and water sprinkler. Further, in cold winter, the surfaces of RCD should be covered by heat insulators like urethane materials. In the summer season, at most RCD dams pre-cooling of concrete materials (mainly water and coarse aggregates) has been performed.

Various simplifications of inside structures have been implemented to speed up the RCD concrete works in Japan, like adoption of precast elements, rearrangement or shortcut of galleries to avoid duplication with concrete works, repositioning or bridging of temporary diversion channels, course and elevation change of conduits, and improvement of complicated structural works (Nagataki et al., 2008).

Japanese researchers and dam engineers intend to improve and rationalize the RCD technology at new dams of this type. At *Kasegawa dam* (2009, $H = 97$ m), one of the latest RCD dams, an improvement of RCD construction method was provided in order to place a lot of concrete rapidly above the middle dam elevation. The essential presuppositions of this new technology were:

- The thickness of a lift was from 75 cm to 100 cm to reduce horizontal joints which are prone to be the weaknesses in the case of earthquakes.
- Green cut and mortar spreading is implemented on every compacted face to attach layers completely, considering seismic characteristics in Japan.

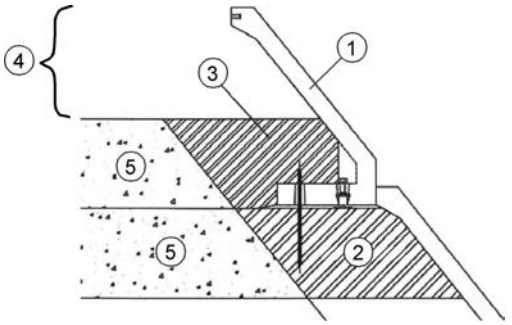

Figure 18.31 Cross-section of precast form (after Nagataki et al., 2008). (1) Precast form, h = 100 cm; (2) external concrete; (3) placed layer of the external concrete; (4) next layer of external concrete, h = 50 cm; (5) internal CSG concrete.

Under the above presupposition, in the conventional method of construction, external conventional concrete has been placed prior to internal RCD concrete placement. However, in the new method, internal RCD concrete was placed prior to external conventional concrete placement. As a result of the above methodological change, the following effects were gained:

- The internal RCD concrete and the external conventional concrete could be placed independently of each other, and the efficiency of concrete works has been greatly increased.
- The external conventional concrete has been compacted efficiently because of the firm binding between the internal RCD concrete and installed external forms.

In Japan, the concrete structures of pre-fabricated members have been developed to increase the safety and efficiency in construction works of RCD concrete dams. So far, it has been improved in light-weighting of members, holding of strength and watertightness at each segment junction, adhesion to the around concrete and concrete placing under precast floors. Recently, external precast forms for both the upstream and downstream dam side have been developed, and it was confirmed to be efficient in facilitating the concrete works. Such an example is shown in Figure 18.31.

In recent years, Information Technology (IT) for the quality management by use of the latest measuring equipment, and integrated information on design and construction is rapidly progressing. A full-scale real-time IT system is adopted in the already mentioned *Kasegawa dam* for quality and quantity management, concrete volume surveying, internal concrete temperature observation, three-dimensional drawings, and labor-saving measures. Construction management by IT for concrete dams is scheduled to be adopted at other RCD dams to increase the quality and efficiency of dam construction in Japan (Nagataki et al., 2008).

18.8 HARDFILL DAMS

18.8.1 Basic idea and concept

In the early 1980s roller-compacted concrete, as a new material, was successfully adapted in the existing shape of concrete gravity dams. Thus, RCC today is mainly used for building conventionally shaped gravity dams requiring high materials performance, such as good compressive, tensile and shear strengths, together with watertightness. Another approach to achieve technical progress is the adaptation of the shape of structures to new materials. Such an alternative consists of a new dam shape, called Faced Symmetrical Hardfill Dam (FSHD) and using low strength and pervious hard fill, was introduced in practice in the 1990s. The hard-fill material can be defined as RCC containing low cement content, with or without addition of pozzolan or fly ash, mixed with high water content, resulting in a high value of the water/cement ratio. The average used values (cement = 60 kg/m^3, pozzolan = 13 kg/m^3, water = 135 kg/m^3, and W/C ratio = 1.86) are given in Table 18.1 and can be compared with the corresponding values of the other RCC types. The hardfill can be defined as an intermediate material between embankment material and concrete, or as an embankment material which has very high cohesion and high resistance to erosion.

The basic idea of hardfill dams is well explained by Londe and Lino (1992). They analysed a hypothetical 100 m-high FSHD with 0.7H/1V upstream and downstream slopes. The stresses prevailing at the base of the dam are shown in Figure 18.32a. They compared this figure with Figure 16.9 (see Chapter 16) in which corresponding stresses at the base for a conventional gravity dam (CGD) of same height are given (the unit weight of the hardfill is slightly less than the RCC unit weight for a gravity dam to account for its overall lower quality). It is obvious that in the case of the symmetrical profile point A is well above Lévy's condition, represented here by the line at 1 MPa. The Hoffman condition is also adequately covered. The material requires no tensile strength and there is an ample margin of 0.4 MPa for resisting the nominal tensile

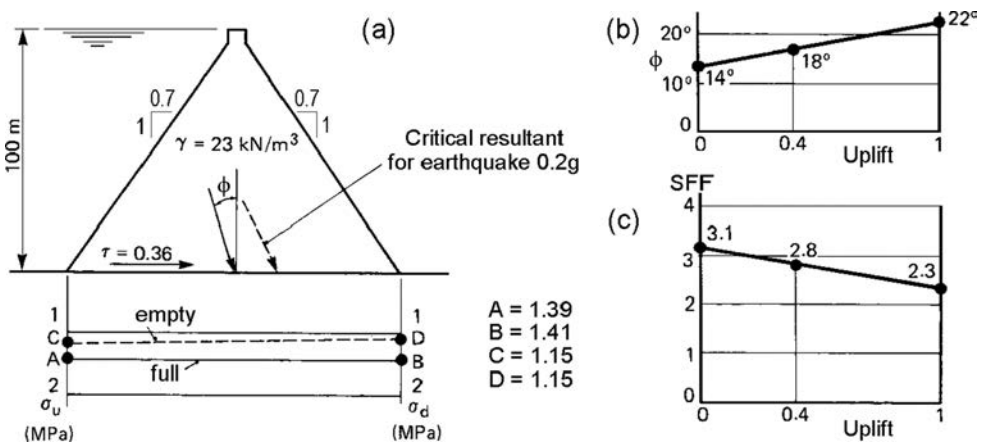

Figure 18.32 FSHD stability (after Londe & Lino, 1992).

stress resulting from an earthquake. In fact, an earthquake of acceleration 0.2g would not develop tensile stresses at all, which is vital at many dam sites in the world, where a conventional gravity profile is exposed to severe cracking at the heel. The maximum compression at the base is substantially less than in the gravity dam: 1.4 MPa, instead of 2.4 MPa.

Another significant difference between conventional gravity dams and FSHDs concerns shear stresses. At FSHDs the mean shear stress is reduced from 0.63 MPa to 0.36 MPa. The angle ϕ for different uplift assumptions varies from 14° to 22° (Fig. 18.32b) instead of 28° to 43° at conventional gravity dams. Therefore low strength rock foundations are acceptable for FSHDs, even when they contain tectonic shear planes. The shear friction factor is always higher than 2 (Fig. 18.32c), even for the low cohesion rock mass assumed here ($\phi = 30°$, $c = 0.3$ MPa).

Figure 18.33a and b give the variation of the shear friction factor (S.F.F.) and ϕ versus the slope of the faces, respectively, for values of uplift of 0, 0.4 and 1. The gravity dam values are marked with points for reference. Obviously, the values of S.F.F. are significantly higher and required values of ϕ rather lower for FSHDs than for CGDs.

A very important feature of the FSHD is that the vertical loading of the foundation is practically uniform and unchanged for all reservoir levels, which is not the case with the conventional gravity dam. This is particularly significant for low modulus rock foundations. Figure 18.34 shows the upstream (a) and downstream (b) total normal stresses versus hardfill dam slopes for empty and full reservoir conditions. The gravity dam stresses are marked with points for reference.

From Figures 18.33 and 18.34 it could be concluded that the FSHD with a 0.7 slopes inclination is far better in terms of safety than the conventional gravity dam. Where the foundation rock is weak, it allows this "cement-soil" dam to be built when a conventional gravity dam would not be acceptable. The engineering properties of hardfill could be much lower than those of RCC, which could be a compensation for the larger volume of the placed material. The ϕ value gives an indication of the friction angle required for horizontal joints between lifts; it does not have to exceed

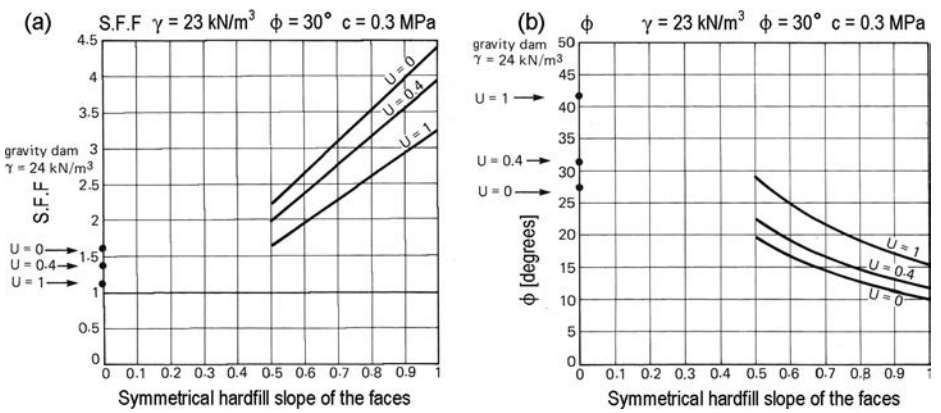

Figure 18.33 Shear friction factor S.F.F. (a), and angle of internal friction ϕ (b), versus the slope of the faces for the FSHD (after Londe & Lino, 1992).

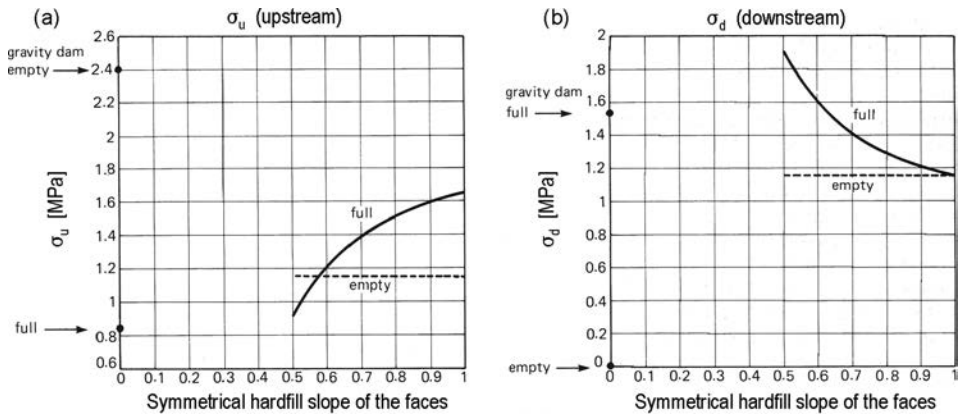

Figure 18.34 Total vertical stresses versus the slope of the faces at the base of a 100 m-high FSHD, for empty and full reservoir (after Londe & Lino, 1992). (a) Upstream side; (b) downstream side.

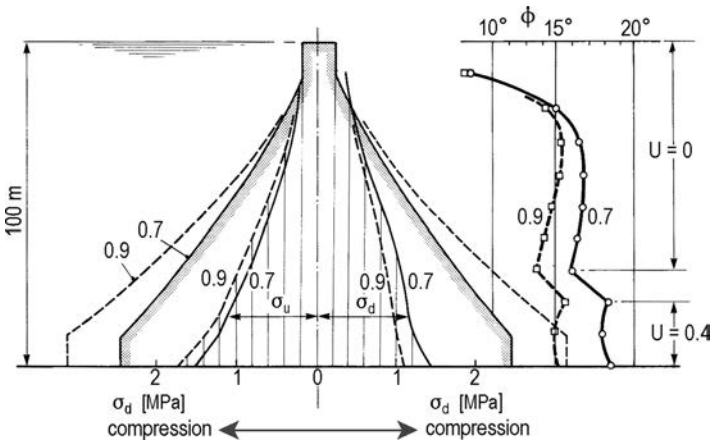

Figure 18.35 Total vertical stresses and angle ϕ in a 100 m-high parabolic FSHD (after Londe & Lino, 1992).

22° even with an extreme uplift assumption of $u = 1$, which could not actually prevail downstream of a facing.

Londe & Lino (1992) have also analysed an alternative FSHD section, consisting of parabolic instead of straight faces, so as to keep the volume increase as small as possible (comparing with a CGD). The total vertical stresses are still very moderate (Fig. 18.35). It is assumed here that the upstream facing fully controls seepage ($u = 0$) in the body of the dam, but that some seepage is present in the lower part of the dam because of imperfections in the foundation grout and drainage curtains ($u = 0.4$). The toes of the profile are cut vertically to reduce the area of excavation, which does not significantly affect the magnitude of the critical stresses.

18.8.2 Hardfill as a dam construction material

Hardfill is a new type of artificially cemented material for dam construction, produced by adding low content cementitious material and water to rock-based aggregate such as random alluvium or weak quarry rock with minimum processing. Broad gradation curves are acceptable and local segregation in the fill is not detrimental to the global low strength requirements. High fines content (up to 30%) is acceptable. Such material mixed with a simple device and placed using standard mechanization for earth works, is significantly cheaper than RCC. The mechanical properties of hardfill material are similar to that of rockfill material before being hardened, while the strength and deformation modulus of the hardened hardfill are much greater. The mechanical behaviour of hardfill material falls in an intermediate area between concrete and rockfill materials. This behaviour is governed, on the one hand, by the friction between the grains, and on the other hand, by the bonds between the grains due to cementation. Therefore hardfill can be considered as a cohesive-frictional material. It can be considered as a lean RCC material with linear elastic modulus from the concrete viewpoint, whereas it can be handled as a cemented rockfill material with nonlinear stress-strain relationship from the geotechnical viewpoint. The mechanical behavior of the material may not be properly described just from one perspective separately. The mechanical properties of hardfill material can be defined by performing large-scale triaxial shear tests on specimens at different ages. Thus an age-related constitutive model of hardfill could be developed, which can reflect the mechanical characteristics of both rockfill-like nonlinearity and concrete-like age relativity (Wu et al., 2011).

Practically, hardfill is a material derived from the RCC by relaxing the severe specifications which tend to make RCC performance as high as that of conventional concrete. The trapezoidal shape of the FSHD makes the best use of hardfill. The relaxations of the specifications lead to a material which is perfectly suitable for the low stresses prevailing in the FSHD. In the previous section it was shown that maximum compressive stress in a 100 m-high hardfill dam is lower than 1.5 MPa, which does not require unconfined compressive strength in excess of 4 to 6 MPa (for a safety factor in the range of 3 to 4). No tensile strength is required at all, because even in the event of a severe earthquake, there would be no tensile stresses in the symmetrical profile. Shear stresses are very low and not at all critical. This has two consequences (Londe & Lino, 1992):

- Unconfined compressive strength is the only requirement for hardfill.
- No costly treatment of the lift surface is required, even in the case of a "cold" lift, after an interruption in placement.

Another very significant property for a dam material is permeability. As was discussed in some of the previous sections of this chapter, low permeability is difficult and costly to achieve for a RCC dam body, mainly because of the high anisotropy resulting from placement in a large number of layers. Taking into account the relaxed requirements for the hardfill, it is clear that at FSHDs watertightness has to be provided by an upstream facing. Therefore, the more pervious the fill is, the better the dam will behave. Hardfill material has relatively high porosity (in the order of 15%), due to the low cement content, rendering the material rather pervious. In fact, high permeability

will usually be achieved as a consequence of the other properties, which also means that segregation can be tolerated.

Deformability is also an important property of dam materials. The conventional concrete and RCC generally are less deformable than the rock mass on which these are placed. In this case, the dam body behaves as a stiff solid supported by a more deformable medium, which may generate structural stresses and cause cracking. Thus, creating a low stiffness material is therefore favorable from a structural point of view. In hardfill low stiffness is a consequence of the limited unconfined strength of this material. In fact, the Young's modulus of hardfill greatly depends on the stiffness of the aggregates, their gradation curves, and the nature and content of fines. Hardfill stiffness can be expected to be significantly below 10 GPa.

Low cement content is one of the basic characteristic of hardfill. It is known that it is possible to achieve a 5 MPa (90 days' age) unconfined compressive strength with a cement content of only 50 kg/m^3. Regarding the thermal behaviour, a low cement content means a small temperature rise. One can expect an adiabatic temperature rise of about half the temperature rise of conventional RCC. Thermal stresses are roughly proportional to the adiabatic temperature rise and to Young's modulus. Thus, thermal stresses will be much lower than in typical RCC dams, making contraction joints unnecessary (Londe and Lino, 1992).

18.8.3 Design of hardfill dams

As was elaborated in section 18.8.1, the shape of the FSHD enables the use of hardfill materials. A typical hardfill dam cross-section is trapezoidal with slope of the faces in the range of 1:0.5 to 1:0.8 (V:H), see Figure 18.36. Because the hardfill material does not, by itself, offer the required watertightness an additional impervious element has to be provided (2, Fig. 18.36). For that purpose some of the methods used at RCC dams can be utilized, but in practice usually the conventional concrete face slab is applied, like at concrete faced rockfill dams (Chapter 12). The geomembrane lining, applied as a waterproof element at both embankment and concrete dams, also seems a reasonable and economical solution in the case of a hardfill dam. The watertight

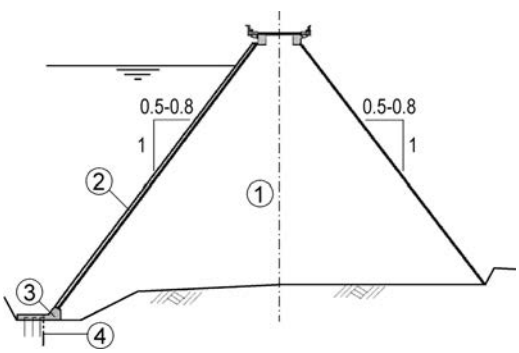

Figure 18.36 Cross-section of a typical hardfill dam. (1) Hardfill; (2) waterproof facing; (3) plinth; (4) grout curtain.

element at the upstream toe is connected to the plinth (3) through the perimeter joint, which is similar in shape and function to the plinth of CFRDs. A grout curtain (4) is usually constructed through the plinth. Thus the concrete slab, the plinth and the grout curtain form a continuous watertight barrier.

The upstream facing is an essential component of the FSHD. It is placed on the hardfill after completion of fill placement, that is, when cracking, if there is any, has had time to occur. Placement of the reinforced concrete facing uses the technology developed for the CFRD, that is, using slipforms. Reinforcement could be lighter, as the expected deformations are much smaller than in the case of a CFRD (ratio of 1 to 10 or even 1 to 100). This favorable condition also makes the treatment of the perimetral joints much easier. In this case the copper waterstop that is obvious for CFRDs is not required, since the SFHD body is practically not deformable.

Having the watertight barrier on the face of the dam, (in principle) leaves the whole dam body on the dry side, which is beneficial to structural stability. So the design of the dam must ensure that water is kept out of the dam body. But leakages through the watertight element, the perimeter joint and the grout curtain cannot be avoided. Water may also enter the dam body through the abutments during rainfall. So provisions should be made to direct the percolating water out of the dam body. The pervious nature of the hardfill dam material is favorable to that purpose and the shortcoming of medium permeability of the material is conveniently turned into an advantage. Drainage pipes may be embedded in the downstream zone of hardfill to ease the outflow of water. Nevertheless water pressure may develop in the dam body and that should be taken into consideration. There are practically three alternatives available to the designer: a) to design the dam assuming that internal pressures develop in the dam body with a linear distribution between the upstream and downstream faces, b) to provide drainage adjacent to the watertight element, and c) to provide drainage at some distance from the watertight element (Moutafis, 2009).

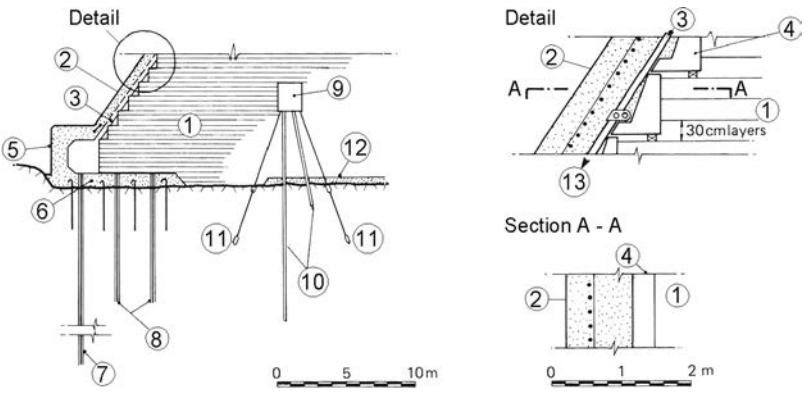

Figure 18.37 Upstream facing and galleries for the FHSD (after Londe & Lino, 1992). (1) Hardfill; (2) waterproof facing; (3) drains (perforated PVC pipes); (4) prefabricated element; (5) face drainage gallery; (6) grouting slab; (7) deep grout curtain; (8) consolidation grouting; (9) foundation drainage gallery; (10) drains; (11) electrical pore pressure cell; (12) porous concrete; (13) to the gallery.

Table 18.14 Data on some characteristic hardfill dams.

Dam	Country	Built (year)	Height (m)	Length (m)	Volume ($m^3 \times 10^3$) RCC	Volume ($m^3 \times 10^3$) Total	Slopes (H:V) Upstream.	Slopes (H:V) Downstr.	Cement* (kg/m^3)
Marathia	Greece	1993	28	265	31	48	0.50	0.50	55+15
Ano Mera	Greece	1997	32	170	49	64	0.50	0.50	55+15
Contraembalse De Monsión	Dominican Republic	1998	20	254	130	155	0.70	0.67	80
Steno	Greece	2003	32	170	69	70	0.70	0.70	55+5
Rio Rejo	Peru	2004	35						
Rio Grande	Peru	2005	46						
Çindere	Turkey	2005	107	280	1500	1680	0.70	0.70	50+20
Can Asujan	Philippines	2005	42	135	75	85	0.60	0.60	100
Beydag	Turkey	2008	96	800	2350	2650	0.35	0.80	60+30
Taum Sauk	USA	2010	49	2060	2448	2500	0.60	0.60	59+59
Lithaios	Greece	2010	32	526	160	220	0.80	0.80	50+10
Camilica III	Turkey	2010	52	800	153	219	0.70	0.70	88+37
Koris Yefiri	Greece	2011	42	121	170	190	0.80	0.80	50+10
Valsamiotis	Greece	2011	65	330	640	820	0.80	0.80	60
SafSaf	Algeria	2011	36	270			0.65	0.65	120
Tamaloot	Morocco	2012	61	320	380	415	0.50	0.70	60

*Cement + pozzolan or fly ash (if it is added).

Figure 18.37 gives an example of the arrangements used for a FSHD upstream facing. The upstream base gallery (5) is dimensioned to allow for easy inspection and maintenance of the drains (3) located behind the upstream facing, as well as drilling, grouting and maintenance of the foundation grout curtain (7). Several different approaches may be implemented for drainage of the underface of the upstream facing. Imperfect compaction of the hardfill at its contact with the facing is not detrimental. Figure 18.37 shows a possible arrangement using prefabricated concrete elements (4). An alternative is to drill drainage holes.

In the case of the Can Asujan dam (Philippines, 2005, see Table 18.14 for basic data) the upstream concrete facing, 40 cm thick, has been fully anchored to and supported throughout by the underlying hardfill so as not to structurally load the plinth. Namely, the reinforced concrete facing on the upstream face of a CFRD essentially rests on, and is supported by, the underlying rockfill. It will move and deflect as loadings come onto the rockfill. It is sealed against the peripheral plinth via a plinth joint, but the connection is one of sealing and not structural support. To achieve a similar behaviour the steeper upstream sloping face (1V:0.6H) of a FSHD had to be fully anchored to and supported throughout by the underlying hardfill. This was achieved by providing a grid of anchored bars into the pre-cast unit lifting holes. Further support to the face would have been achieved by the upstream backfill (Mason et al., 2008).

The downstream face of FSHD can support a spillway chute in a similar way to the common RCC design, either with a reinforced-concrete slab and ski-jump bucket, or with free flow on steps. The arrangement of the crest is given similar to the crests of CRFDs.

Hardfill material is hauled to the site by tracks, unloaded in piles and spread by bulldozers in horizontal layers and compacted by ordinary drum vibratory rollers. Layer thickness may vary from 0.30 to 0.50 m depending on the compaction equipment used.

18.8.4 Main features and field of application

The Faced Symmetrical Hardfill Dam is usually compared with a conventional roller-compacted concrete dam and with rockfill dams. The main advantages of the FSHD are:

- greatly improved stability, which means it can be built safely on weak foundations and in areas prone to strong earthquakes (compared with a RCC dam);
- low compressive and shear strength requirements (compared with a RCC dam);
- capability of water overtopping both during and after construction (compared with a rockfill dam);
- reduced cement requirements which result in reduced unit costs (compared with RCC dams);
- more relaxed specification for aggregates including grading requirements (compared with a RCC dam);
- little or no requirement for joint preparation between placed layers;
- since the dam body is not the watertight element, minor shrinkage or deformation cracks in the structure do not impair its functionality and therefore minor cracking of the dam body is acceptable; this eliminates the need for contraction joints.
- FSHD would be a better solution than a rockfill dam whenever hydraulic structures are large; with the FSHD approach the appurtenant hydraulic structures can more easily be incorporated into the dam itself, having shorter water conveying structures, resulting in time and cost savings.

The listed advantages of a FSHD and other features of this relatively new dam type determine to a large extent its main field of application. This dam type is especially favorable at sites with:

- lack of appropriate cohesive material for construction of natural waterproof element at a rockfill dam;
- possibility to obtain cheap aggregates from nearby borrow pits or quarries;
- weak foundation, unsuitable for classically shaped gravity dam;
- high seismicity;
- unfavorable hydrological conditions.

It is well known that the cost often plays a decisive role in the process of dam type choice. The volume of a FSHD is greater than that of a gravity dam, but the relaxation of RCC specifications may be sufficient to pay for the increased volume of the hardfill dam and for the dam facing. Thus, under the above listed dam site conditions the total cost of a FSHD may be lower than that of a conventional section RCC gravity dam.

To date, sixteen FSHDs have been constructed throughout the world. The heights of these FSHDs mainly range from 30 m to 60 m, the highest being the 107 m high

Çindere dam in Turkey. The main data on these dams, constructed in the period 1993–2012, are given in Table 18.14.

In Japan the FSHD is called the Cement Sand Gravel (CSG) dam, while in China the term Cemented Material Dam (CMD) is used. In these two countries, known as great builders of RCC dams, this new dam type is mainly applied for construction of small dams and cofferdams. The aim of the promotion of CMD in China has been to create safer and faster construction, with low investment costs and based on environmentally friendly technology.

Chapter 19

Buttress dams

19.1 DEFINITION, CLASSIFICATION, AND GENERAL CONCEPTIONS

Buttress dams consist of two principal structural elements: (1) a sloping upstream deck that supports the water, and (2) the buttresses or vertical walls that support the deck and transmit the load to the foundation. According to the structure of the dam deck, one can distinguish three basic types of buttress dams (Fig. 19.1): (a) buttress dams *with a massive head*, formed by means of flaring the buttress on the upstream face; (b) buttress dams *with a flat-slab deck*; and (c) buttress dams *with thin curved multiple-arch deck*. In addition to *the slabs and buttresses*, as additional structural elements, there can also be used *longitudinal beams* (5) for stiffening and bracing the buttresses. Sometimes there is also constructed a *foundation slab* (6) below the entire dam, provided with *drainage openings* (7) for eliminating the uplift pressure.

The mass of buttress dams is much smaller than the mass of gravity dams. Owing to that, the stability against sliding is ensured with the weight of water on the inclined deck, and on account of the decrease in the uplift water pressure. By way of illustration, this has been shown in Figure 19.2, with comparisons of the method of work of a concrete gravity dam (a), hollow dam (b) and the three basic types of buttress dams (c, d and e) (Chugaev, 1985; Grishin et al., 1979; Kudin, 1981).

A gravity dam is subjected to a great force due to the uplift pressure, U_a, while a hollow dam is subjected to a smaller one. In the case of buttress dams, savings in concrete are achieved not only by a drastic reduction (or complete elimination) of the uplift force, but also by sloping the upstream face, thus, utilizing the weight of water W_2. By increasing the inclination of the upstream face, we improve the utilization of the weight of water; that is to say, we increase the savings in concrete.

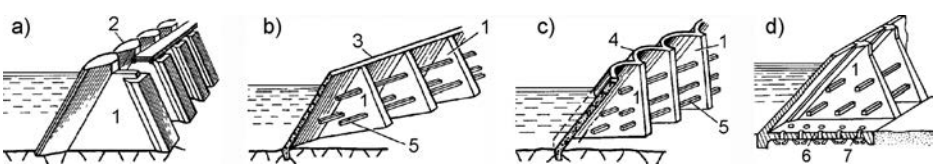

Figure 19.1 Types of buttress dams. (a) Massive-head type; (b) flat-slab type; (c) multiple-arch type; (d) with a foundation slab (6). (1) Buttresses; (2) massive head; (3) flat slab; (4) arch; (5) longitudinal stiffening beams; (7) drainage openings.

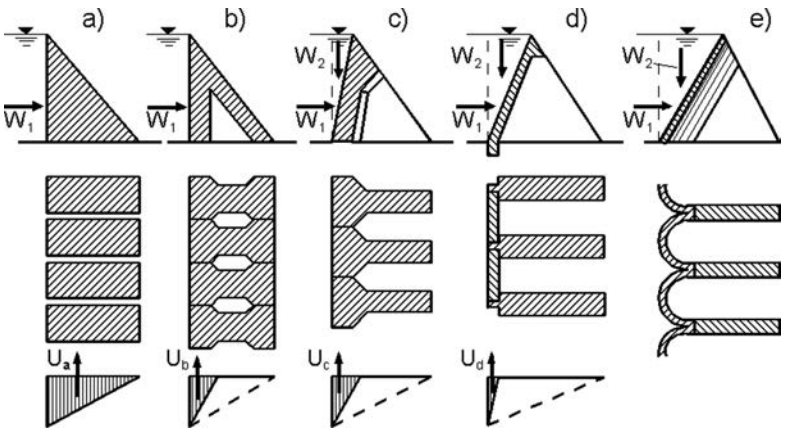

Figure 19.2 Comparison of the methods of work of concrete gravity dams and buttress dams. (a) Gravity dam; (b) hollow dam; (c) massive head buttress dam; (d) flat-slab buttress dam; (e) multiple-arch buttress dam.

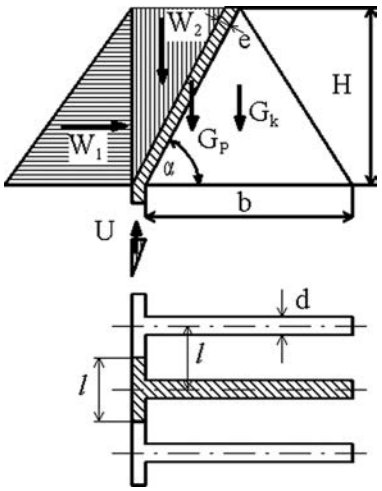

Figure 19.3 Forces acting on a buttress dam.

In increasing the inclination, there exists a certain limit at which the concrete dam deck must be replaced by a reinforced concrete one, in which case it is also possible to increase the span between the buttresses. Therefore, the inclination of the impermeable dam deck is an important feature influencing the construction of buttress dams.

The distance l between the buttresses and the angle of inclination of the dam barrier α can be determined from the condition for sliding stability of the dam (Fig. 19.3)

$$W_1 = \frac{(G_k + G_p + W_2 - U)f + c \cdot d \cdot b}{k_s} \tag{19.1}$$

where, G_k and G_p are the weights of the buttress and dam deck at a section with a length l. The bigger the span l and the smaller the angle α, the greater is the savings in concrete. In this, one should take into consideration that there is an increase of stresses both in the dam deck and the buttress itself, which imposes an increase of the reinforcement in the deck and in the requirements for the quality of the foundation.

The water pressure is transferred to the buttresses uniformly along their whole length, so that the requirements for the quality of the foundation are similar to those for gravity dams. Only in exceptional cases, buttress dams are constructed on a soil (non-rock) foundation. In such a case, they are of small height, while across the entire width and length there are constructed foundation slabs provided with drainage openings for the elimination of seepage uplift pressure (Fig. 19.1d).

In modern practice, buttress dams are constructed in a smaller number in relation to the other types of dams. In the first half of the 20th century they were very popular, especially in the USA, where within the period 1900–1980 there were constructed more than 1100 buttress dams higher than 10 m, which is more than the number of gravity dams (980) and arch dams (1080). The greatest number of buttress dams was built in the first half of the 20th century thanks to the cheap labor that is necessary for the construction of the thin elements of these dams. Their popularity has fallen down drastically since 1955, when there was significant enhancement of labor costs, while, on the other hand, there has been developed powerful plant and equipment for mass execution of both earth works and concrete works. In Macedonia only one buttress dam has been constructed – the Prilep multiple-arch dam, 38.5 m high.

19.2 MASSIVE-HEAD BUTTRESS DAMS

With this type of dam, the buttresses are flared at the upstream face and thereby a massive dam barrier is formed (Figs. 19.1a, 19.2c). They differ from hollow dams in that the cavities between the buttresses are considerably larger; they also have an inclined upstream face.

The buttresses can be *single buttresses* (Figs. 19.4a–e) or *twin buttresses* (f, g). Twin buttresses are more stable against lateral overturning, which is important in seismically-active areas.

The head, that is to say the upstream flare, of the buttress in a horizontal section, can be shaped in various ways, as is schematically presented in Figure 19.4. The *curvilinear* form (a, f) is the most perfect, in terms of the distribution of stresses, caused by water, and which are compressive stresses. The *polygonal* form (b, g) is easier for execution, but allows only small tensile stresses. In the case of flat heads (c–e) there inevitably comes about tensile stresses, which must be coped with by reinforcement. From the viewpoint of construction, they are the simplest ones (Grishin et al., 1979).

In constructing massive-head buttress dams it is necessary to select the inclination of the faces and the axial distance between the buttresses, starting from the conditions for stability and economy. For a height from 40 to 60 metres, as these dams are usually built, the span of the buttresses ranges from 10 to 20 m, in which greater heights go along with greater spans. In the case of twin buttresses, the span can reach as much as 26 metres. The inclination of the upstream face most often ranges within the limits 1:0.4 to 1:0.5 while the downstream one ranges from 1:0.45 to 0.60.

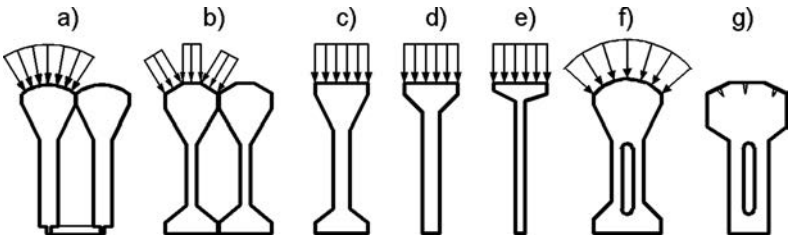

Figure 19.4 Various forms of buttresses and shaping of the flare in horizontal section.

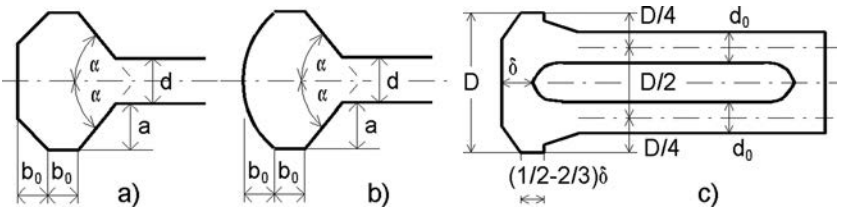

Figure 19.5 Dimensions of basic elements and the head of a single buttress (a, b) and twin buttress (c).

The thickness of the single buttresses depends on the pressure H (Fig. 19.3) and can be either permanent or can increase, going from above downwards, and it ranges within limits from 3.5 to 8 m. The thickness of the head on the external side up to the beginning of the buttress also depends on the pressure H and amounts to approximately $0.8l$ (l is the distance between axes of buttresses). On the downstream side, the buttresses can also be flared (Fig. 19.4b, c, f) or else a slab can be constructed upon them, if that has been imposed by a need for stability (seismicity of the ground, etc.) or else if the dam is an overflow dam.

The basic elements of a massive head are shown in Figure 19.5a–c. In engineering the section and the preliminary designing of the heads of single buttresses, the angle α is adopted from 30° to 45°. The ratio $e = b_0/a$ depends on the height of the dam H and for values of H up to 50 m it is adopted $e = 0.02$, while for $H = 50$–120 m, $e = 0.02$–0.37.

The relationships between the individual elements of the twin buttress are shown in Figure 19.5c. Values of 8 and d_0 depend on the height of the dam and the kind of foundation, as well as on the other structural elements of the dam. We can approximately take $d_0 = (1/5–1/6)\ D$, and $\delta = (1/3–1/4)D$.

The concrete in buttresses is subjected to changes of volume due to temperature variations and shrinkage of the concrete. Since the base of the dam is rigidly jointed with the foundation, there is a danger of crack occurrence in the concrete. By means of joints, we can eliminate the influence of temperature effects on the buttresses all along the length of the dam, as well as on the forces occurring as a result of possible differentiated settlement in the case of higher dams. The joints between massive heads must be water-impermeable, which imposes the need for appropriate sealing of the joints.

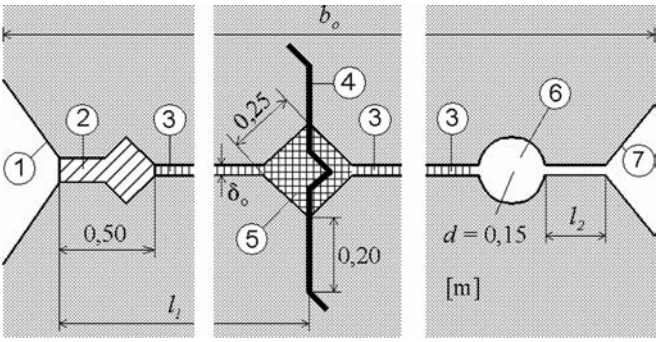

Figure 19.6 Example of sealing of a vertical deformation joint (horizontal section). (1) Upstream face of the dam; (2) concrete plug; (3) joint, closed, i.e. sealed, with bitumen; (4) waterstop of stainless steel; (5) asphalt mastic (or bitumen); (6) drainage; (7) downstream face.

Figure 19.6 presents an example of a vertical deformation joint with water-impermeable sealing. The length of the joint b_0 should be so determined as to provide sufficient space to perform sealing and to accommodate the drainage (6), as well as to enable the distances l_1 and l_2 to have sufficient length. The distance l_2 should be larger than the depth of freezing of the concrete at the downstream face. The distance *l1* from the upstream face to the water-impermeable sealing is determined according to the thickness of the active zone (see Fig. 16.18), in which the temperature significantly varies in the course of time. The width of the joint δ_0, over a rock foundation, when non-uniform settlements of the dam are not expected, is assumed to be 1 cm (Chugaev, 1985). Otherwise, the buttress dams can endure certain non-uniform settlements, since the buttresses are mutually separated.

Figure 19.7 presents the sealing of the joint for the Pantano d'Avio dam, whose plan and sections are given in Figure 19.10 (Chugaev, 1985).

Jointing of buttresses with the foundation is achieved through the concrete structure. Massive-head buttress dams are constructed on a rock foundation. If the rock is sound, firm, and hard, the founding of the buttresses can be performed without expanding (Fig. 19.8a). In the case of weaker rocks, it is necessary to perform some expansion in the foundation in order to reduce the normal edge stresses, which are transmitted to the foundation (Fig. 19.8b). If the required expansion is so large that the footings are joined to one another (Fig. 19.8c), then drainage openings are necessary for eliminating the uplift. This happens regularly in the case of twin buttresses on weaker rock. Details of such merged foundation footings, along with the drainage openings, are shown in Figure 19.8.d (cross-section and layout).

Should there be a need for a grout curtain, it is executed through a gallery below the massive head of the buttresses, while in the case of lower dams it is accomplished through the concrete foundation.

Zoning of concrete is also performed for buttress dams. Water-impermeable concrete is placed in the massive heads and downstream slab or frost-resistant concrete in the flares, while in the buttresses there is placed concrete corresponding to the strength requirements. Reinforcing is not necessary, except for parts of the structure in which

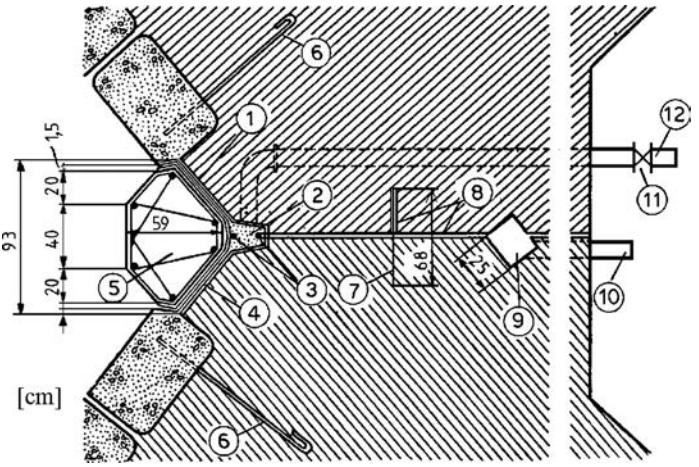

Figure 19.7 Sealing of joint for Pantano d'Avio dam, Italy. (1) Bituminous waterproofing paper in 3 layers; (2) plug of bitumen; (3) steel conductor for heating the bitumen; (4) leveling course of 1.5 cm thickness; (5) reinforced concrete prism; (6) anchor of diameter 20 mm; (7) zinc sheet, 2 mm; (8) surface coated with bitumen; (9) drainage manhole; (10) offtake pipe; (11) valve; (12) pipe for discharging of bitumen.

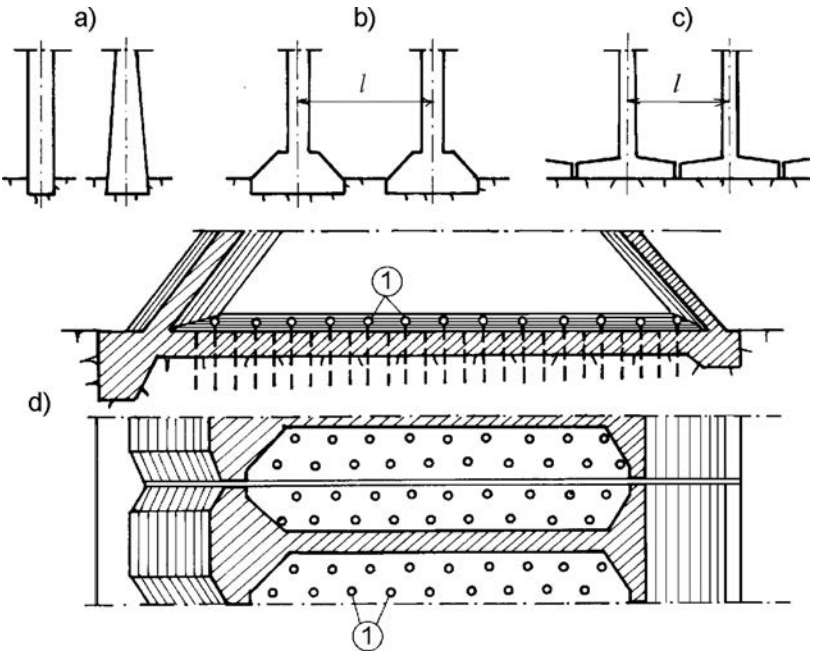

Figure 19.8 Founding of buttresses. (a) On sound, hard and firm rock; (b) on weaker rock; (c) with merged foundation footings; (d) detail of foundation with drainage openings (1).

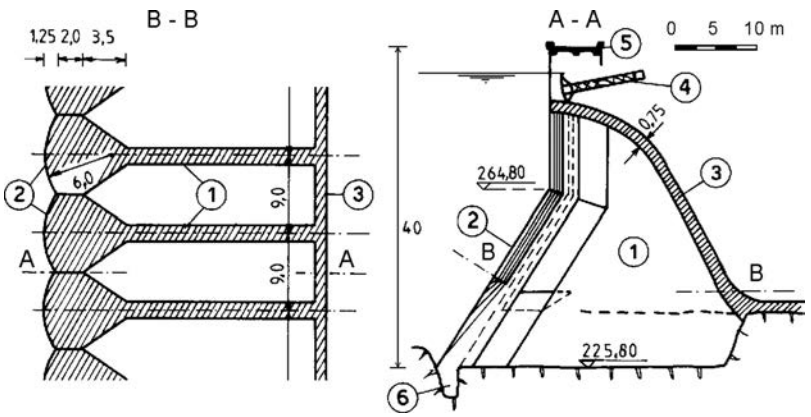

Figure 19.9 Venustiano Carranza dam (formerly, Don Martin dam), Mexico, 1927/28. (1) Buttresses; (2) upstream heads; (3) downstream slab; (4) gate; (5) bridge; (6) cut-off wall.

there have occurred tensile stresses, as, for example, in the downstream protective slab, in the cantilevers at the flat heads of buttresses, in the vicinity of possible openings through buttresses and the like.

Examinations of stability are performed similarly to those for gravity dams. In designing the buttresses, the problem is not treated as a plane problem, but the buttress is considered as a whole, as a spatial girder. By means of the theory of eccentric compression, one can find the vertical normal stresses at the most dangerous points in the buttress for the cases of both a full and an empty reservoir. Then, there are determined the total principal and maximum shear stresses, valid for determination of the grade of concrete. The upstream head of the buttresses is dimensioned according to more complex methods – for instance, by the application of the theory of elasticity, or else on the basis of results obtained from model investigations. During the last 15 years, the Finite Element Method has proved a powerful means for both the two-dimensional and three-dimensional analysis of buttress dams (Clough & Zienkiewicz, 1987; ICOLD, 1994b).

Figure 19.9 presents a plan and cross-section of an overflow dam with single buttresses, and with a rounded head – according to the system of the American engineer Noetzli[1]. The overflow surface is formed of a continuous slab passing through the crest and forming the downstream face of the dam.

Figure 19.10 presents the plan and sections of the Pantano d'Avio buttress dam (France), with twin buttresses, 60 m high.

[1]It is interesting to note that the American engineer Fred Noetzli developed the concept of a buttress dam with rounded head – in which the water pressure is directed towards the centre of the head in order to eliminate tensile stresses – that he proposed in 1925. The first construction of this type, however, was only carried out in the USA in 1975.

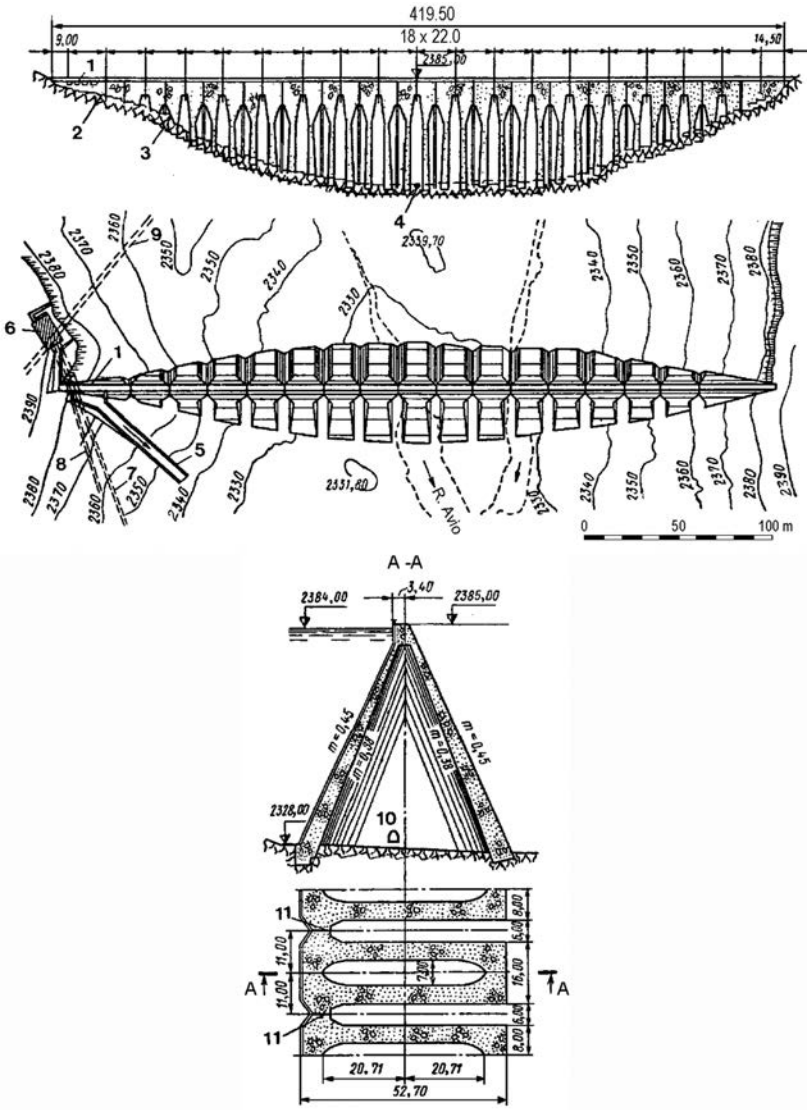

Figure 19.10 Pantano d'Avio buttress dam, Italy, with twin buttresses. (1) Spillway; (2) top of cutoff wall; (3) bottom of cutoff wall; (4) bottom outlet; (5) chute spillway; (6) office building and manhole; (7) tunnel of the outlet; (8) inclined gallery for communication with the gate chamber; (9) tunnel of the intake; (10) gallery in buttress; (11) joint with sealing (detail in Fig. 19.7).

19.3 FLAT-SLAB BUTTRESS DAMS

These dams, also known as the Ambursen type of dams, were popular at the beginning of the 20th century, mainly for smaller heights. Several such dams with a height greater

than 40 m are also known, among them the highest one being the Rodriguez dam (H = 76 m), built in Mexico. In the USA, more than 350 flat-slab buttress dams have been built, mainly before WWII (USCOLD, 1988). Most of them can be attributed to Nils Ambursen and his company. Ambursen dams had a simple structure – they consisted of reinforced concrete slabs inclined at an angle from 45° to 50°, freely supported on concrete buttresses with a trapezium form. Besides the low labour cost, in favour of the popularity of such split constructions was also their ability for adaptation to certain differentiated displacements in the foundation, especially those caused by seismic effects, under which conditions monolithic concrete constructions would fail. Another advantage of these structures is their easy adaptability to great variations in the topography of the dam site. These dams also have significant deficiencies:

- Their height is limited, because, with its increase, there comes about a non-proportional increase in the slab thickness and in the amount of reinforcement required;
- It is indispensable to perform a rigorous control of the quality of materials and their placement, in order to avoid the danger of accident and destruction of some of the thin structural elements.

The above-cited deficiencies, along with the significant increase in labor costs, are the reasons for which this type of dams is rarely met in contemporary practice. The best illustration of this is the fact that today in the USA there are in service only some 60 such dams, of which the last one was built in 1969.

The basic elements of flat-slab buttress dams are the buttresses, then the upstream slabs and beams for stiffening the buttresses, all illustrated in Figure 19.1. Differences in terms of the structural elements occur depending on whether the dam has been founded on a rock foundation or on a soil foundation, which is a scarcer case in practice. In the case of soil foundations, there also appears a foundation slab (Figs. 19.1d and 19.11d–f).

This type of dam can be constructed both as a non-overflow construction and an overflow construction. With overflow dams, a downstream overflow slab is made, by means of which an enclosed space is formed, which is sometimes filled with ballast material, as shown in Figure 19.11d. There is also another special type of such a dam, called an inverted dam, in which the impermeable slab is constructed at the downstream face, at the same time also playing the role of an overflow slab (Fig. 19.11f). In this, the spaces between the buttresses are filled with water.

The upstream and overflow slabs are freely supported on the flared buttresses (Fig. 19.12c), by which the whole divided, i.e. split, system is allowed to have a certain adaptation to deformations of the foundation, without the occurrence of additional stresses. The water-impermeability at the interfaces is provided by means of coating the flares of the buttresses, upon which are supported the slabs, with bituminous mastic.

Concrete buttresses are most often set up at axial distances $l = 4.5–5.5$ m (Fig. 19.12). The angle of inclination of the upstream face with the horizontal is $\alpha = 45–60°$, while that of the downstream face is $\beta = 60–85°$. The width of buttress at the bottom amounts to $B = (1–1.5)H$, while the thickness of buttresses at the top is

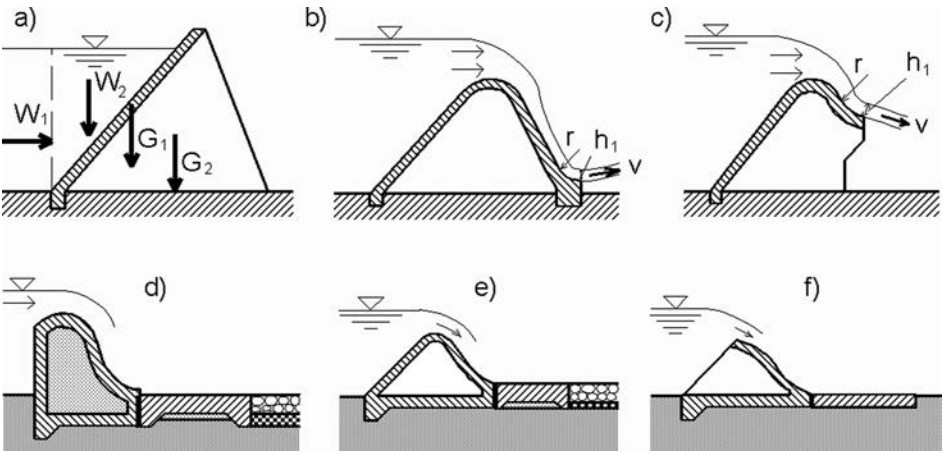

Figure 19.11 Flat-slab buttress dams. (a–c) On rock foundation; (d–f) on soil foundation.

assumed to be $d_v = 0.25–1.0$ m, and that at the bottom is computed according to the empirical formula:

$$d_{max} = 0.1\, H\, d_v \tag{19.2}$$

The flaring, i.e. widening of the buttress upon which the slabs rest, amounts to $a = (0.5–1.0)e$, where e is the thickness of the slabs. The value of δ can be either smaller or larger than e, and it is determined from the condition that the section m–n (and also other sections parallel to it) should be sufficiently resistant to the effect of shear stresses, caused by pressure of the slabs on the widening.

The parting reinforced concrete slabs at the crest have a thickness of $e = 0.2–0.3$ m, while the lower sections are dimensioned by means of static calculations, as slabs being simply supported at both ends.

In order to prevent longitudinal buckling of the relatively thin buttresses, which appears when $H/d > 15$, there are employed longitudinal stiffening beams at a mutual horizontal distance 4–8 m and a vertical distance 5–12 m. These beams are not rigidly jointed with the buttresses – one or two of the ends should freely enter the appropriate beds. The cross-section of the beams is calculated only for the action of their self-weight.

Sometimes curvilinear joints are constructed in the buttresses, and they coincide with the lines of the total major principal stress. This prevents the danger of cracks in the buttresses caused by temperature variations and shrinkage of the concrete, reduces the need for reinforcement and alleviates the construction of the buttress. Such a divided buttress acts and behaves as if it were composed of a number of 'columns,' of which each takes on a part of the pressure on the slab, transferring it to the foundation. Along the length of the joints, the 'columns' are interconnected with jointing wedges, aimed at providing compactness of the buttress. This system was used for the first time in the highest buttress dam with a flat-slab deck in the USA, the Moris Sheppard dam ($H = 57.6$ m), built in the period 1938–41 (Fig. 19.13). This dam is 498 m long, with an additional earth embankment, 337 m long.

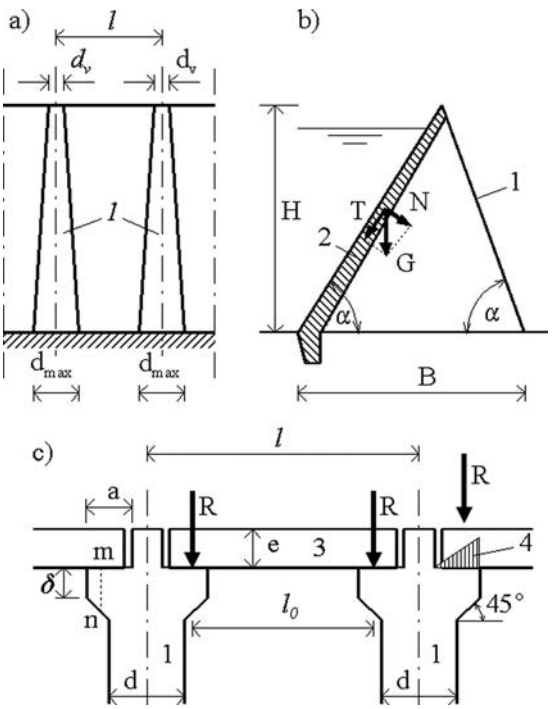

Figure 19.12 Schematic review of a flat-slab buttress dam. (a) Vertical section; (b) cross-section; (c) plan. (1) Buttress; (2) flat-slab deck; (3) reinforced concrete slab; (4) diagram of the reaction.

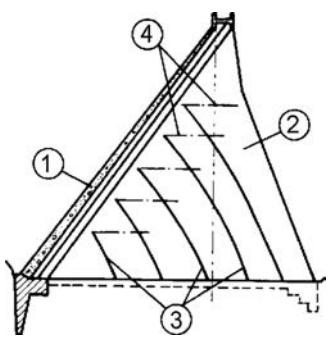

Figure 19.13 Morris Sheppard dam (USA). (1) Slab; (2) buttress; (3) expansion joints; (4) structural joints.

By way of illustration of the application of this type of dam, Figure 19.14 presents the layout, longitudinal and cross-section, as well as details of the Stoney Gorge dam, built in 1928 in California, USA (Golzé, 1977). The foundation consists of sedimentary rocks steeply descending in depth, with a number of smaller faults positioned perpendicular to the dam's axis. There were suspicions that these could lead to differentiated

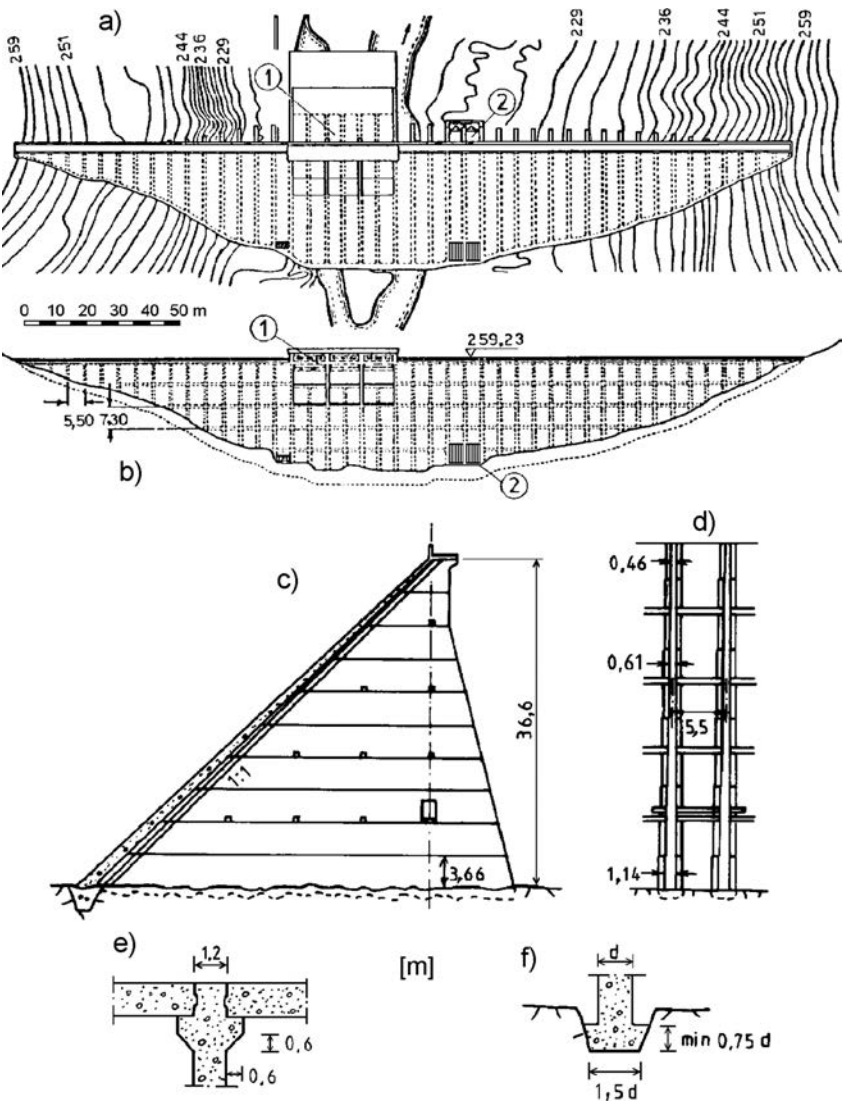

Figure 19.14 Stoney Gorge dam (after Golzé, 1977). (a) Layout; (b) longitudinal section; (c) cross-section; (d) elevation from the downstream face; (e) typical joint of a buttress with slabs; (f) foundation of buttress. (1) Controlled overflow; (2) bottom outlet.

displacements, which was decisive in selecting the type of dam. Slabs of the flat deck are separated from the buttresses; that is to say, they are simply supported on them, over a surface that has previously been coated with mastic. Both the slab and the buttresses are reinforced. At the outset, the buttresses were reinforced both in the vertical and diagonal direction, but once there have appeared cracks in the first buttress owing to shrinkage of concrete, horizontal reinforcement was also placed in the lower parts.

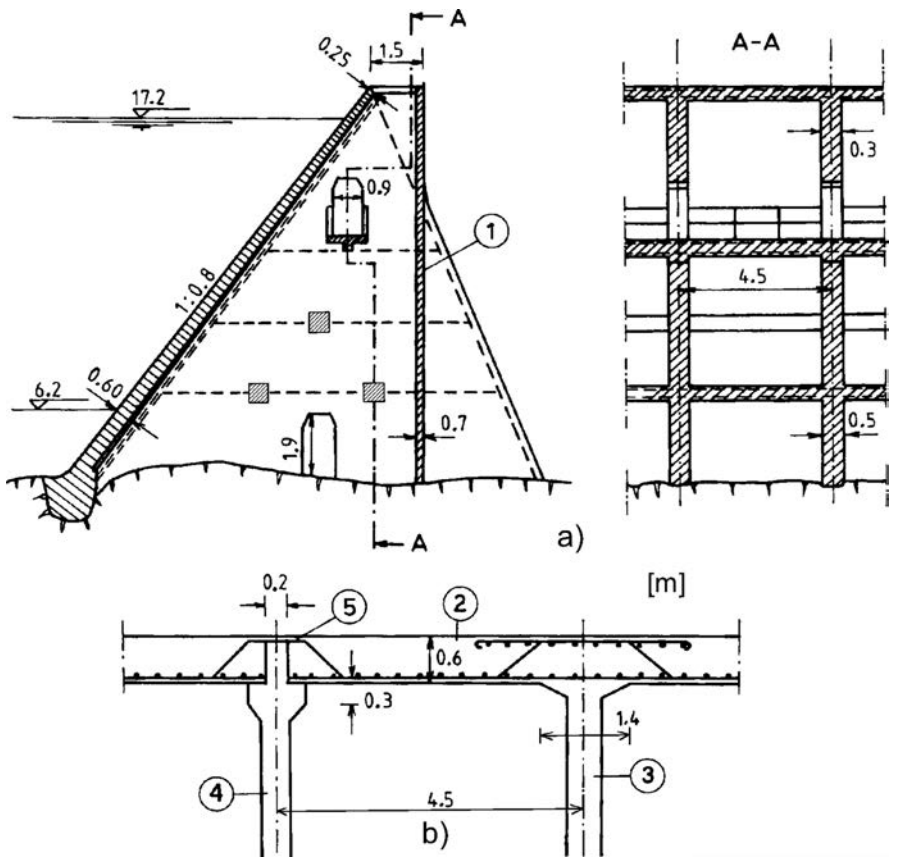

Figure 19.15 Fergental buttress flat-slab dam. (a) Cross-section and section A-A; (b) section of the cover slabs at a depth of 10 m. (1) Reinforced concrete wall aimed at reducing the cooling down of the space downstream of the upstream slabs; (2) external side of the slabs, coated with cement grout; (3) buttress, rigidly jointed with the slab; (4) every third buttress, separated from the slabs; (5) asphalt insulation.

Long-term observations have shown that the dam behaves satisfactorily. Cracks have been noticed in a number of buttresses, and these cracks have been deemed to be a consequence of temperature variations and shrinkage of concrete; however, it has been concluded that these cracks do not deserve particular attention. A new study, worked out in 1983, has shown that the dam corresponds to the modern seismic criteria; that is to say, it would withstand the anticipated dynamic loadings.

The construction of buttress dams has experienced various modifications aimed at their adaptation to specific conditions and requirements. Thus, for example, several such dams have been constructed in the harsh climatic conditions of Norway. They are closed with a reinforced concrete wall from the downstream face in order to reduce the cooling down of the slabs from the lower side. The construction of one of them, the Fergental dam, is shown in Figure 19.15.

19.4 MULTIPLE-ARCH BUTTRESS DAMS

With the use of buttress dams with a multiple-arch deck, it is possible to achieve greater savings in concrete than with any other buttress dam, in comparison with concrete gravity dams (up to 60%). The oldest known example of such a type of a dam is the Meer Allum dam, built at the beginning of the 19th century in India (Smith, 1971). It is 12 m high, and some 760 m long. It contains 21 semicircular arches with a span of 21 m at the ends and up to 45 m in the middle; details are given in Figure 19.16. The development of buttress dams with a multiple-arch deck went on in the course of the 19th century and the beginning of the 20th century, when they were built as thin, reinforced concrete constructions with a span of buttresses up to 25 m. Lately, there have been constructed concrete dams with spans of even over 50 m, with thick buttresses. Considered as a whole, multiple-arch buttress dams are constructed rarely, mainly due to their more difficult execution, as well as owing to their lower adaptation to non-uniform settlements; that is to say, because of the more rigorous requirements in relation to the quality of the foundation, as compared with other types of buttress dams. In the USA, there are in service only 35 such dams higher than 10 m, and they were built during the period from 1907 to 1961.

On the basis of experience gained from the construction of medium-high dams, in the initial phase of their designing we can assume individual dimensions in accordance with the following recommendations:

- Axial distance between buttresses: $l = 10$–25 m;
- Angle of inclination of the upstream slope with the horizontal: $\alpha = 50$–$60°$;
- Angle of inclination of the downstream slope of buttress: $\beta = 60$–$90°$;
- Thickness of buttress at the top: $e_c = (1.5\text{–}2.0)e_v$, where e_v is the thickness of the arch near the crest;
- Thickness of the buttress near the foundation, according to the empirical formula:

$$d_{max} = (0.07\text{–}1.1)Hd_v \tag{19.3}$$

- Width of the buttress at the foundation: $b_{max} = (1\text{–}1.5)H$;
- Thickness of the reinforced concrete arch at the top: $e_v = 0.25$–0.75 m (usually 0.30–0.40 m);
- Thickness of the concrete arch at the top: $e_v = 1.7$–2.0 m;
- Thickness of the arch at the foundation: $e_{max} = 0.6$–3.6 m (usually 1.3–2.0 m);
- Central angle of the arch: 160–180°.

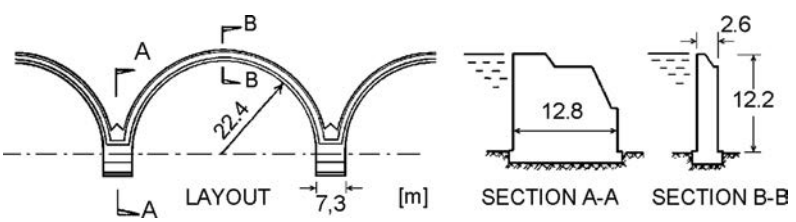

Figure 19.16 Meer Allum dam (India).

The basic task in designing multiple-arch buttress dams is for a given height to determine such a span between the buttresses, radius of curvature and a central angle of the arches at which the minimum cost of the dam would be achieved. In addition, the angles of inclination of the faces must enter into the analysis, on which is dependent the span of buttresses. The problem is solved by means of comparison of a number of possible variants.

As a rule, the arches are made with a constant radius and central angle. Going downwards, the thickness of the arches increases, while a cylindrical shape is retained on the internal side, aiming at simpler execution of the formwork. Arches are reinforced with double reinforcement. On the external side, they are covered with a layer of shotcrete, bitumen or epoxies and polyester coatings for achieving water-impermeability.

The buttresses have the same shape as in the case of dams with a flat-slab deck, in that here, they have a greater thickness owing to the greater span. They are stiffened by means of beams or ribs, as shown in Figure 19.17. The buttresses are often reinforced during construction with the use of wire-mesh reinforcement.

The joint between the arch and the buttress can be achieved in two ways: as a rigid joint (Fig. 19.18a), when the reinforcement of the arch enters the buttress and, alternatively, as a freely supported joint (Fig. 19.18b), when the arch leans freely on the side of the buttress *ab*. The first solution has a deficiency in that the construction cannot adapt to non-uniform settlements of the foundation, and temperature variations can also cause cracks. In the case of the second solution, the buttresses can be constructed independently of the arches.

In the case of non-reinforced or lightly reinforced dams, the joint between the arch and the buttress can be constructed with joints and waterstops, as it is the case with the Grandval dam (France; Fig. 19.18c). In the case of opening of the joints (for instance, owing to non-uniform settlement of buttresses), their sealing can be performed with grouting of cement grout through a system of built-in pipes (6).

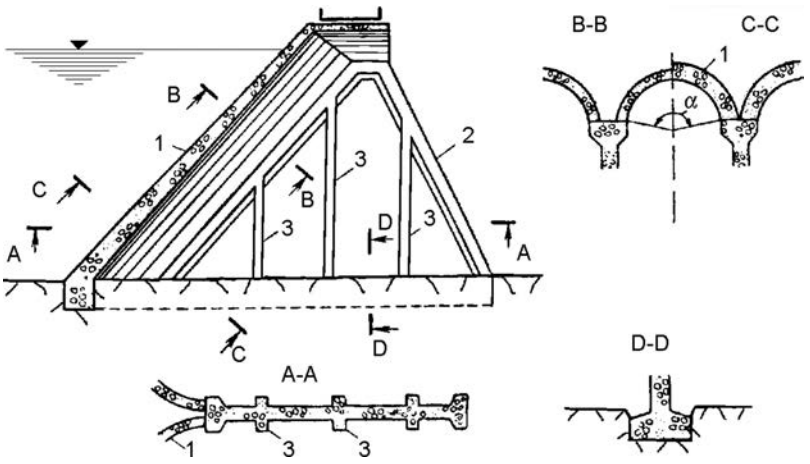

Figure 19.17 Buttress dam with multiple-arch deck and stiffening ribs. (1) Multiple-arch deck; (2) buttress; (3) stiffening ribs.

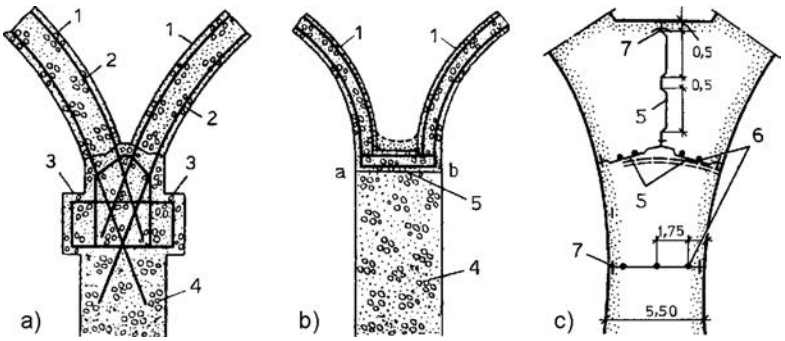

Figure 19.18 Joint of the arch with the buttress (horizontal section). (1) Arch; (2) reinforcement; (3) support for the formwork; (4) buttress; (5) joint; (6) grouting pipes; (7) waterstops.

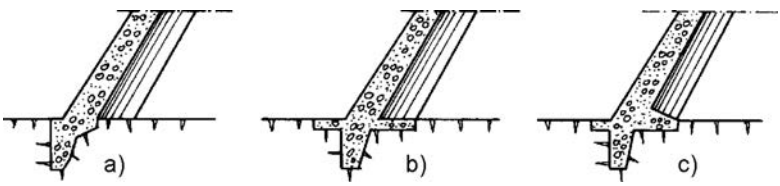

Figure 19.19 Different ways of jointing the arch with the rock foundation.

Figure 19.19 presents different ways of jointing the arch with the rock foundation, which, with this type of dam, is obligatory, because non-uniform settlement at the buttresses is not allowed. The construction of the joint depends on the type and condition of the rock. Along the contour of the arch, it is obligatory to execute a concrete cutoff wall, and in case of need, a grout curtain is also anticipated.

Static and dynamic dimensioning of arches and other structural elements is achieved according to the methods that are investigated in the theory of structures.

One of the characteristic multiple-arch buttress dams is the Bartlett dam, constructed in the period 1936–1939, with its 87 m the highest buttress dam in the USA, (Figs. 19.20–19.21). It consists of 10 inclined arches, supported by nine buttresses and two short gravity wings at the ends. The arches are cylindrical, semicircular in section, with a radius of 7.3 m. The thickness of the arches at the foundation amounts to 2.1 m and, towards the crest, it decreases to 0.6 m. The arches are inclined in relation to the vertical at an angle of 42°. The buttresses have twin walls, with cavities in between, while in the transverse direction they are stiffened by means of concrete diaphragms. In the lower part of the buttresses there have been constructed horizontal structural joints at maximum distances of 3 m. The buttresses are set up at distances of 18 m (centre-to-centre), while their thickness is variable, in which the variation is constructed according to inclined lines. Every buttress consists of two external concrete walls, separated by a vertical empty space (from foundation to crest) 2.4 m wide. The external concrete walls vary in thickness from 0.6 m at the crest to 2.1 m near

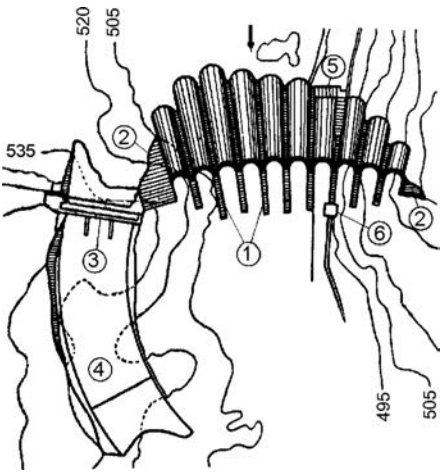

Figure 19.20 Bartlett Dam (USA), H = 87.5 m (layout). (1) Buttresses; (2) gravity blocks; (3) controlled overflow; (4) chute spillway; (5) bottom outlet; (6) gate chamber.

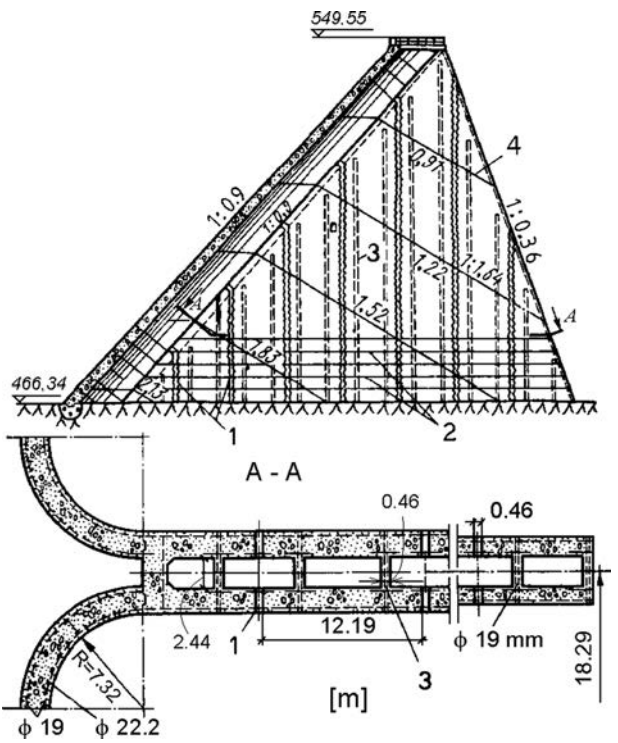

Figure 19.21 Bartlett Dam, longitudinal section. (1) Vertical toothed openings; (2) horizontal structural joints; (3) diaphragm in the cavity of the buttress; (4) limits of variation of buttress thickness.

the foundation. The buttresses contain vertical toothed openings, 46 cm wide, spaced at mutual distances of about 12 m, anticipated to enable shrinkage of the concrete of buttresses, after which they are filled with concrete. The buttresses, like the arches, are heavily reinforced. During construction, the dam has experienced two heavy floods, yet it has not suffered significant damage.

In the last twenty or so years, the Bartlett dam, as well as all other significant old dams in the USA, has been subjected to reexamination in order to determine: (1) what would be the situation of the dam at the possible arrival of the maximum probable flood; (2)whether the dam is stable for the effect of a maximum possible earthquake.

As a result of the conclusions from the analyses performed, the dam has been heightened by 6.6 m (in order to create larger retention storage), and there have also been performed certain modifications aiming at improving its stability for the effects of an extremely strong earthquake (Nuss et al., 1994).

Multiple-arch buttress dams are constructed, mainly, as non-overflow dams, because the execution of a spillway through the arches is rather complicated. In the case of smaller overflow quantities of water, the spillway and other water-conveying structures can be accommodated within the buttresses, as is the case with the example in Figure 19.22, in which the Grandval dam (France) has been presented, 80 m high, with spans between buttresses of 50 m (Grishin et al., 1979).

A very interesting example of a multiple-arch buttress dam is the Coolidge dam, USA, built in the course of 1927 and 1928. Prior to making a decision on the realization of this original project, six other possible types of dam were also analysed, and the solution was accepted as the most economical one (it has already been said that at those times the skilled work force, necessary for the execution of such complex constructions, was very inexpensive). The dam consists of three domes, resting on two buttresses and on the walls of the canyon, (Fig. 19.23).

The maximum height of the dam is 76.2 m, while the length along the crest is 178 m, without counting the two overflows at the ends. The domes are of varying thickness ranging from 1.20 m (at the crest) to 7.6 m. The thickness of the buttresses varies from 7.3 to 18.3 m and they are non-reinforced, except in the zone near the contour of the domes, while the domes are abundantly reinforced. In each buttress, there have been built two inclined expansion joints in order to enable expansion and contraction of the concrete during temperature variations. The joints are approximately parallel to the lines of the total minor principle stress.

Regarding the appurtenant structures within the hydraulic scheme, there have been constructed two free overflows with chute spillways, two intake structures in the form of a tower and the power house of the hydroelectric power station, accommodated in the intermediate dome.

The only buttress dam in Macedonia, the Prilep dam, was built in the vicinity of the town of the same name, on the River Oreovachka, in the period of March 1964–March 1966. The dam is 35 m high above ground, while the dam site, with granite bedrock, is wide, so that the length along the crest of the dam amounts to 408.5 m. Construction of various types of dams is possible at such a dam site. The clients decided in favor of a combined dam with a dominant central part of a buttress dam with a multiple-arch deck, 280 m long. It consists of 14 inclined cylindrical shells, resting on 13 buttresses and two blocks at the ends, (Figs. 19.24, 19.25, 19.26). The buttresses are spaced at a mutual axial distance of 20 m. They are of triangular form,

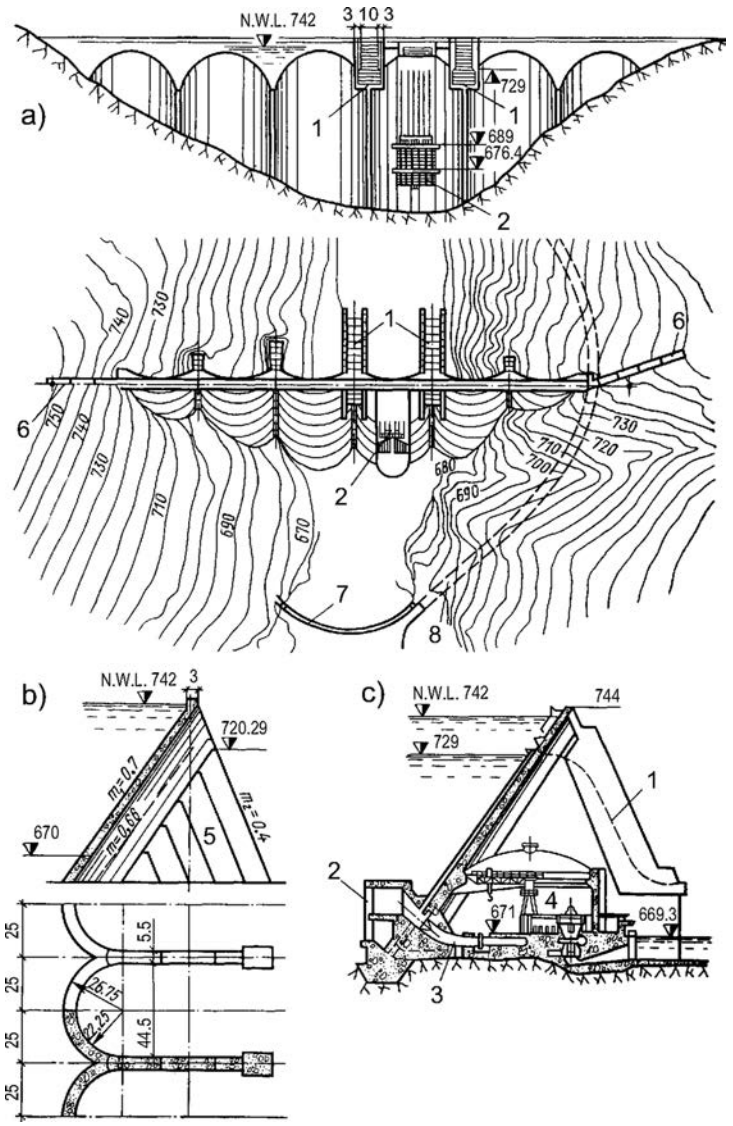

Figure 19.22 Grandval Dam (France). (a) Layout and view of the upstream face; (b) cross-section and layout of the dam; (c) section through the span with hydroelectric power station. (1) Spillway in the buttress; (2) trash rack; (3) penstock; (4) power house; (5) joints; (6) grout curtains in bank; (7) cofferdam; (8) diversion tunnel.

with an inclination of the upstream face of 1:0.85 and that of the downstream face 1:0.3 (Fig. 19.27). The thickness of buttresses at the crest amounts to 1.40 m and it increases downwards by 4 cm per each linear metre. At the upstream face, the buttresses are thickened to 2.80 m along the entire height, in order to ensure proper resting of

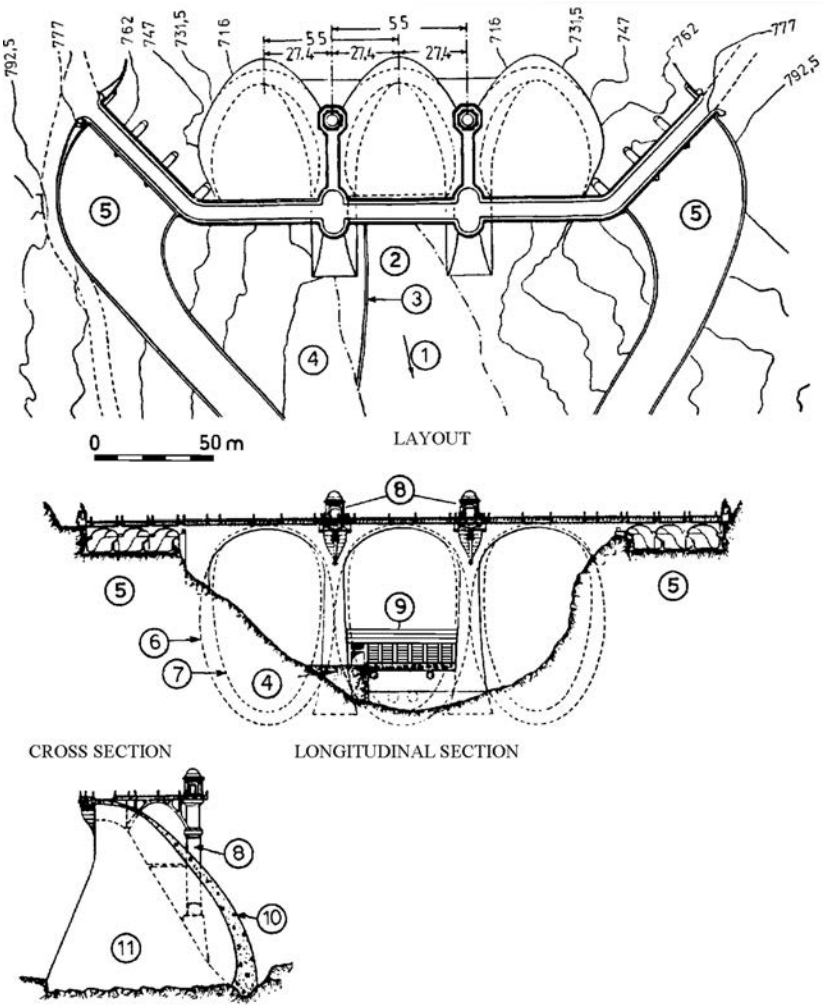

Figure 19.23 Coolidge Dam, USA (after Creager et al., 1955). (1) The river Jila; (2) minor river bed; (3) retaining wall; (4) earthfill; (5) spillway structure; (6) external contour of the dome; (7) internal contour of the dome; (8) intake towers; (9) machine building; (10) dome; (11) buttress.

the adjacent cylindrical shells. This part of the buttress has been constructed of higher quality concrete (30 MPa) in relation to the remainder (22 MPa). The buttresses have been reinforced during construction with 14 kg reinforcing steel per 1 m^3 concrete. In the longitudinal direction, the buttresses are stiffened with six beams and a bridge passing across the crest of the dam (YCOLD, 1970).

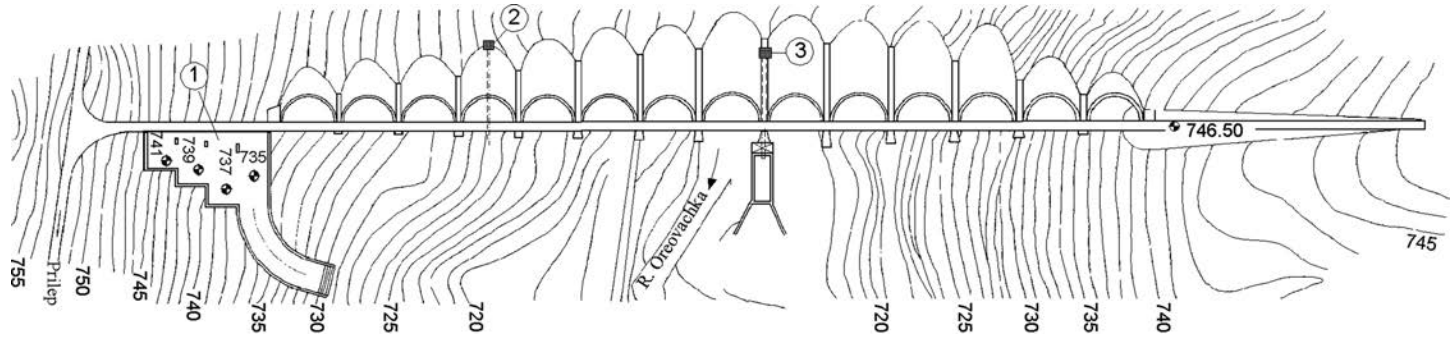

Figure 19.24 Prilep Dam, layout. (1) Overflow; (2) Intake; (3) Bottom outlet .

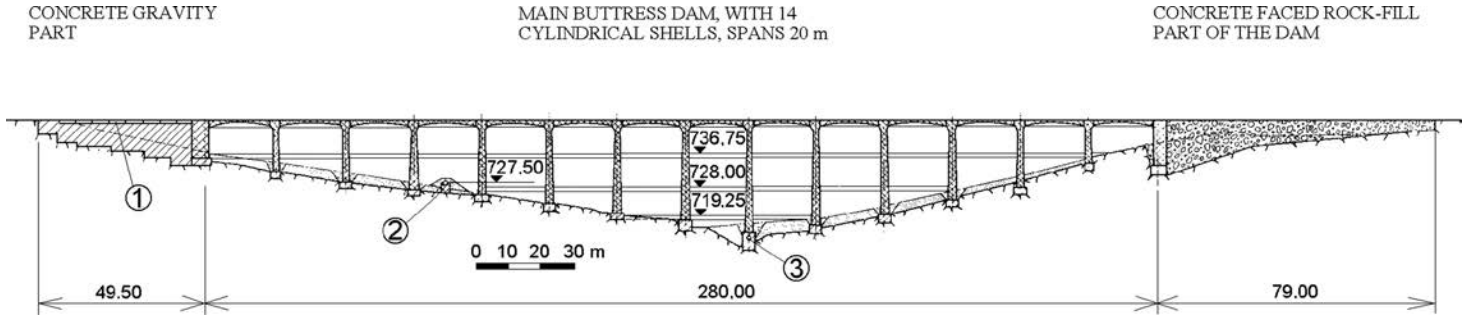

Figure 19.25 Prilep Dam, longitudinal section. (1) Overflow; (2) Intake; (3) Bottom outlet.

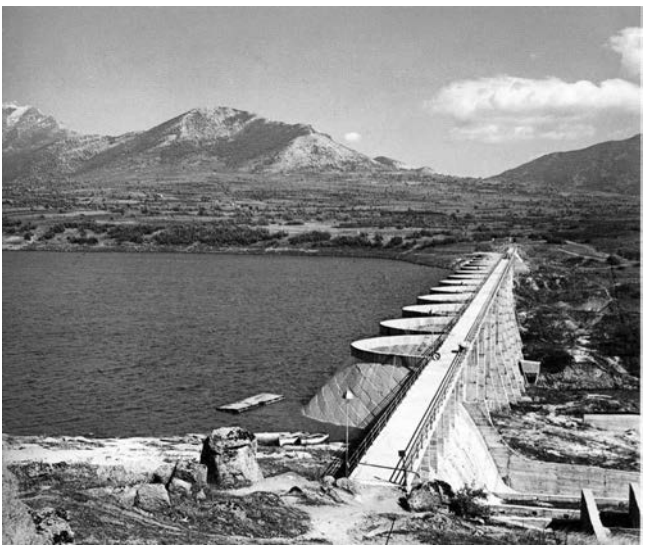

Figure 19.26 Prilep Dam, Macedonia.

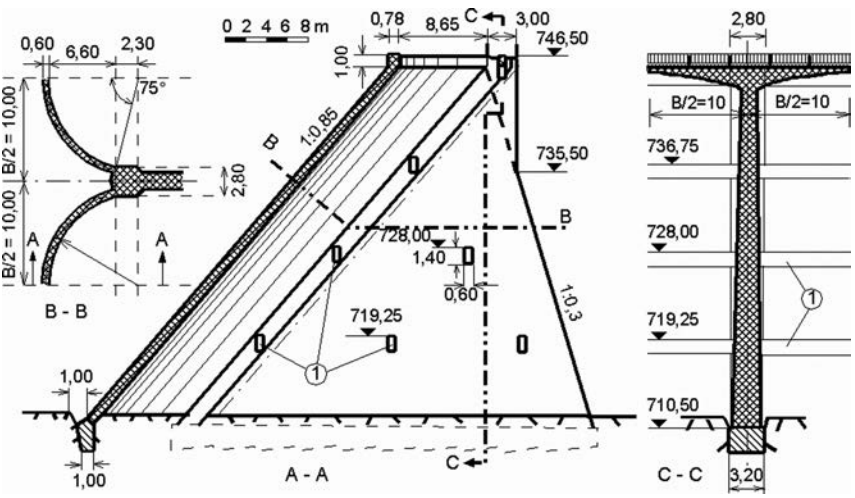

Figure 19.27 Cross-section (A-A) and details of Prilep buttress dam. (1) Longitudinal stiffening beams.

The cylindrical shells have the same inclination as the buttresses (1:0.85). They have a constant thickness along the entire height – 0.60 m. They have been designed with a central angle of 150° and a radius of 9.20 m. The execution has been in water-impermeable concrete (30 MPa) and reinforcement amounting to 45 kg/m3 concrete. The water-impermeability of the joint with the front part of the buttress has been ensured by means of a copper sheet 1 mm thick, with an unfolded width of

60 cm. Prior to filling the reservoir, at the upstream face of the dam, in order to improve the water-impermeability, there has been placed waterproofing of reinforced polyester.

At the right-hand side there has been executed a gravity concrete part, with a maximum height of 10 m, which has been shaped as an overfall spillway, which consists of eight overflowing spans, each of them 4.8 m wide. For the energy dissipation of the overflow stream, there has been anticipated a stilling basin with four canals with cascade positioning.

To the left the dam ends with an embankment part, 78 m long, with a maximum height of 14 m. A reinforced concrete facing 20 cm thick has been constructed to act as a water-impermeable element for this small embankment. The dam's body is constructed of tipped rockfill, with inclinations of the slopes 1:1 upstream and 1:1.2 downstream.

The concrete plant with a capacity of 8 m^3/hour has been located at the right-hand bank, 50 m away from the dam site. Altogether, 25,500 m^3 concrete have been poured in, which, in the buttresses by means of a movable timber formwork, while in the cylindrical shells by means of fixed formwork, resting on steel tubular scaffolding.

The dam forms a reservoir with an available storage capacity of 5 million m^3, intended for irrigation of tobacco fields. In the course of its 35-year service, it has been operating successfully. There are ideas for increasing the available storage capacity by heightening the dam.

19.5 CONDITIONS FOR APPLICATION OF BUTTRESS DAMS

Buttress dams can be constructed at dam sites with various forms, but they appear to be the most competitive at broad dam sites. Regarding their economy, they can compete with embankment dams. As an illustration to this, in addition to the previously described Prilep dam, we can use the highest buttress dam in the world, the multiple-arch Daniel Johnson dam, (Fig. 19.28), built in Canada. The dam is founded on granite and has a length of 1220 m. It consists of 13 sections with arch spans of 76.2 m and a central arch with a span of 116.5 m and a height of 215 m (Patokov et al., 1986).

In narrow dam sites with a good geology of the foundation, regarding the economy, buttress dams cannot compete with arch concrete dams. In principle, buttress dams are constructed on a rock foundation; however, in the case of smaller dam heights, soil foundations are also acceptable, in which case a foundation slab is constructed underneath the entire dam, with obligatory longitudinal beams or ribs for stiffening (struts or braces).

In relation to climatic conditions, buttress dams have practically no limitations. However, in regions where very low temperatures are expected, the interior of the dam should be protected by constructing an insulation wall between the buttresses from the downstream face (1, Fig. 19.15), which creates conditions for a favorable thermal regime.

Buttress dams can be constructed in seismically active regions; however, it is necessary to anticipate special structures, i.e. structural members, for safeguarding stability in the longitudinal direction, such as beams or ribs for stiffening. An exception in relation to the applicability of this type of dam in seismically-active areas are buttress dams with massive heads, construction of which is unfavorable for such conditions.

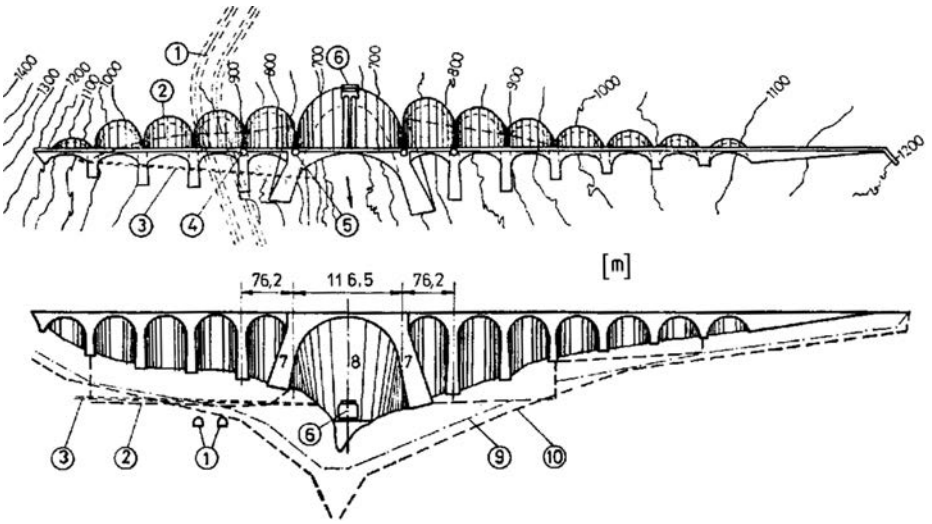

Figure 19.28 Daniel Johnson multiple-arch buttress dam (Canada). (a) Plan; (b) Elevation from the downstream face. (1) Headwater tunnels; (2) drainage gallery; (3) inspection gallery; (4) manhole for surveillance of deformations, without a lift; (5) with a lift; (6)inlet structure of the bottom outlet; (7) central buttress 25 to 40 m wide; (8) central arch with a thickness of 8 to 25 m; (9) bottom of the vertical drainage; (10) limit of the grout curtain.

One of the reasons for the relatively low representation of buttress dams, especially in Europe, is the widespread opinion that this type of dam, owing to the disassembled construction, is easily susceptible to intentional failure and, thus, is also disadvantageous in a case of war.

In contemporary practice of the construction of buttress dams, attempts are made to eliminate certain disadvantages of these dams (which have been discussed in the previous sections), in order for them to become more competitive in relation to other dams. So, for example, in order to prevent cracks, in the interior of the massive heads there are left longitudinal cavities for faster removal of the exothermal heat. There are also included surface cuts on the head (Fig. 19.4 g), which serve the same purpose. It is certainly that multiple-arch buttress dams have the best prospects, and with them, efforts are also being made for perfecting the construction. From a structural point of view, it is endeavoured to improve the deck by employing the construction of dome decks, as well as two-hinge and three-hinge arches, all in order to reduce rigidity.

Chapter 20

Arch dams

20.1 ARCH DAMS IN GENERAL – CLASSIFICATION

Arch dams are curved water-retaining structures, which work as a vault that takes on the loading from the upstream face and transfers it to the foundation; that is to say, onto the rock into which it is encastered, i.e. end-fixed (Fig. 20.1c). Arch dams, according to the way they function, differ essentially from gravity dams, which resist the horizontal forces, mainly, by means of their self-weight. The great French constructor of dams André Coyne writes: "*When you think well about it, then it is clear that it is much more rational for the stability of a structure to be provided by means of its suitable form rather than by its weight*" (Coyne, 1943).

The contours of the arch dam in a horizontal section usually have a circular form with a perpendicular joint of the ends with the bank. In cross-section, arch dams represent cantilevers, which can have different forms, usually with a curved upstream or downstream face, or else both faces, (Fig. 20.2). From the way of functioning of arch dams, it is evident that their cross-section will be of significantly smaller dimensions, as compared with gravity dams.

The basic parameters in the arch dams are: (1) *radius of curvature R* of the arch in plan; (2) *central angle* 2α of the appropriate horizontal section; (3) the ratio of the width of the dam site *L* to the height *H (L:H)* and (4) the ratio of the width of dam *B* to the height *H (B:H)*, i.e. *the slenderness* of the dam.

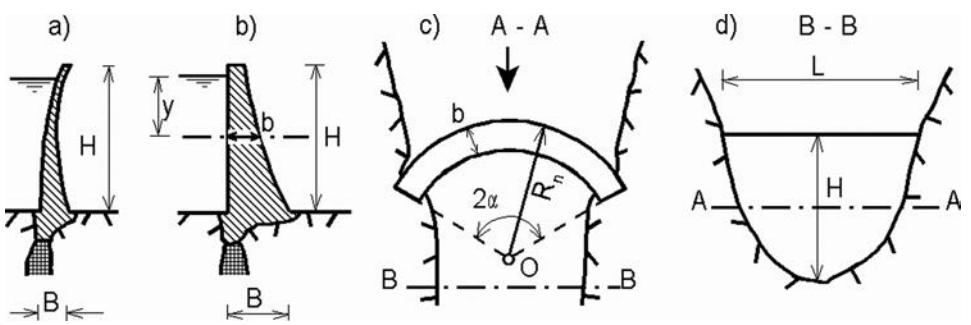

Figure 20.1 Schematic presentation of a true arch dam (a) and an arch-gravity dam (b).

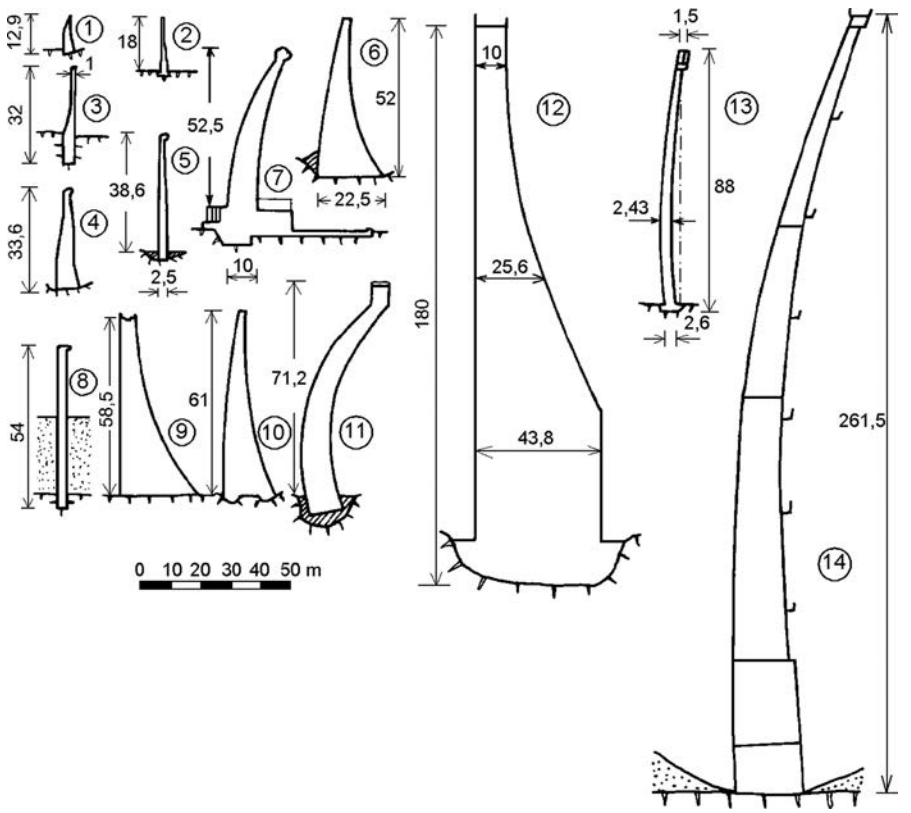

Figure 20.2 Cross-sections of some arch dams. (1) Diablo (USA); (2) Venda Nova (Portugal); (3) Amsteg (Switzerland); (4) Ashland (USA); (5) Pabelon (Mexico); (6) Brock (Switzerland); (7) Quesque (France); (8) Bioge (France); (9) Jibson (USA); (10) Aloz (Spain); (11) Ossille (Italy); (12) Tignes (France); (13) Tolla (Corsique, France); (14) Vaiont (Italy).

Arch dams, depending on the ratio of their individual parameters, can be divided into two types:

(a) *True arch dams* (Fig. 20.1a), when $B < 0.3H$, in which almost the entire water pressure transfers to the banks; this type of dam is usually employed when the width of the dam site is $L \leq (2–2.5)H$.
(b) *Arch-gravity dams*, for which $B = (0.3–0.5)H$, when the dam takes on a part of the water pressure by means of its self-weight, while a part of it is transferred to the banks. This kind of dam is used when it is $L \leq 3.5H$.

When it is a question of a narrow dam site, composed of sound, hard, and firm rock, in terms of economy and the safety of the structure, arch dams have no competitors among the other types of dams. This is especially so with dams of greater height. In practice of the construction of arch dams, there are cases when the ratio L/H exceeds the value of 3.5 and reaches even the value of 10! However, those are rare, exceptional

examples, which do not influence the cited definition of the two basic types of arch dams.

In Chapter 16, it has been shown that sometimes gravity dams have a curved shape in plan, i.e. layout, aiming at a better adaptation to the ground topography and at increasing the sliding stability. It is important that such dams, in relation to the method of work and dimensions, have nothing in common with arch-gravity dams and must not be confused with them.

True arch dams can be divided into: (1) very thin arch dams, when $B < 0.1H$; (2) thin arch dams, when $B = (0.1–0.2)H$ and (3) thick arch dams, when $B = (0.2–0.3)H$.

According to *the method of jointing with the foundation,* we can distinguish arch dams that are elastically jointed with the foundation, dams with a contour (perimeter) joint, dams with joints, or with joint-cuts, constructed in the lower part of the dam, in the vicinity of the joint with the foundation.

In relation to height, there is no strict classification of arch dams. However, with regard to the nature of their work and problems encountered with these dams, they could be divided into *low dams* ($H < 40$ m), *medium dams* ($H = 40–100$ m) and *high dams* ($H > 100$ m). The high dams are of the greatest significance, since they are founded on sound, hard, and firm rock, in a narrow dam site, so that with them in its strongest form there is expressed the advantage of taking on the horizontal forces by means of a suitable structural form. Even though arch dams have a low representation within the overall number of large dams built in the world (only 4.4%), they dominate among the dams that are higher than 150 m (27%).

According to the method of passing through the flood flow waters in the course of the service of the hydraulic scheme, arch dams can be divided into *non-overflow dams* and *overflow dams*. In this, in addition to the surface overflow structure, for the same purpose it is also possible to construct large depth openings, provided with appropriate gates.

Regarding the material from which arch dams are constructed, they can be masonry, concrete, or reinforced concrete dams. In modern practice, masonry dams are not built at all, while reinforced concrete dams are found quite rarely. Lately (since 1990), roller-compacted concrete has also been used for arch dams, which has been in the last decade (and is also expected to be in the future) an irreplaceable material for the construction of gravity dams.

In comparison with gravity dams, the arch dams, owing to their smaller thickness, have two to four times smaller volume (per meter of the length). However, owing to the thinner construction, the unit price of the concrete is higher. Two factors play an important role in the work and the structure of arch dams: the topography, or geometry, of the dam site, and its geologic character.

If the profile of dam site has the form of a rectangle (Fig. 20.3a), then the span of the arches in the upper and in the lower horizontal sections will be approximately the same and the thickness must be increased from above downwards, owing to the increase of the hydrostatic pressure. In the case of a trapezoidal section (b), the spans, going downwards, decrease, which can compensate for the increase in the hydrostatic pressure without requiring thickening of the dam. This is even more so in the case of the triangular form of the cross-section (c). For the construction of arch dams, the most suitable are symmetrical profiles with a parabolic, trapezoidal, or triangular form. In practice there are very rarely found completely symmetrical profiles, owing to

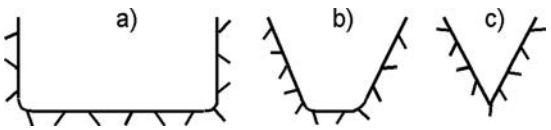

Figure 20.3 Various forms of dam site. (a) Rectangular form; (b) trapezoidal form; (c) triangular form.

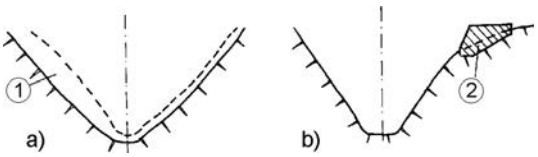

Figure 20.4 Improvement of the symmetry of profile. (1) Excavation; (2) concrete block.

which, almost regularly, there are performed certain adjustments, either with deeper excavation from one side (Fig. 20.4a), or with the execution of a mass concrete block in the upper part of the slighter incline (b). Looking in plan, the most suitable dam sites are those at the entrance of a narrow canyon, where the riverbed is constricted. At such places, we can build the most stable joint of arches with the rock in the banks (Fig. 20.1c).

The arch dam, especially if it is high, transfers very large forces to the abutments and foundation. Besides, under the effect of water pressure in the reservoir below the dam and through the banks, there can come about seepage flow with high gradients, due to the small width of the dam. All of this, in the case of insufficiently firm foundations, can cause deformations, which could lead to yielding of the constraining, i.e. fixing of the arches or else to their inadmissible overloading. Owing to that, of particular significance for arch dams is the quality and geological feature of the rock in the foundation and the banks of the dam site (Silveira et al., 1991). The rock must be hard and firm with a small number of fissures and with appropriate water-impermeability, constant in water and with filling in fissures, which is not susceptible to mechanical erosion under the effect of the seepage flow. Igneous rocks are the most suitable, but hard and firm sedimentary rocks (sandstones, limestones) can also be taken into consideration, of course without large fissures or tectonic faults. Even though lately there have been constructed some high arch dams on highly fissured foundations (by means of undertaking measures for their improvement), it should not be forgotten that the requirements for the rock in the foundation are much more rigorous than in the case of gravity dams, because the yielding of the abutments of the arch dam into the banks and foundation, would result in failure of the dam.

20.2 DEVELOPMENT OF ARCH DAMS THROUGH THE CENTURIES

Even though there are indications that arch dams were built even in the ancient Roman Empire, the first such discovered constructions go back to the end of the 13th century,

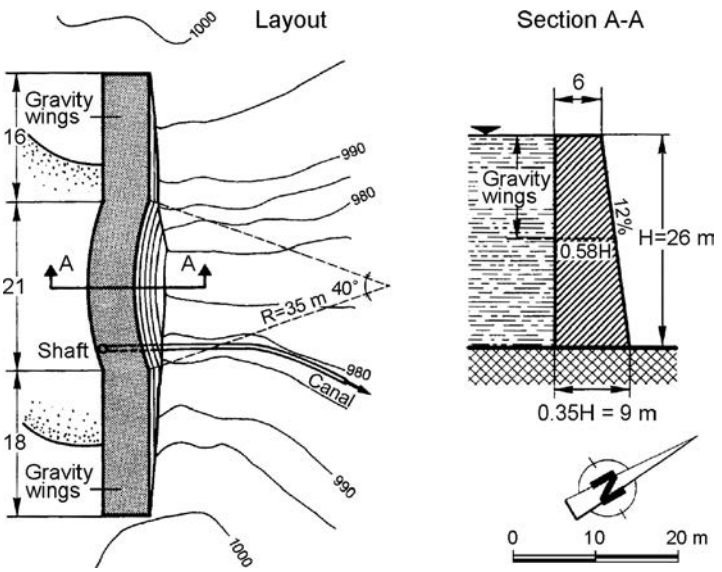

Figure 20.5 Layout and cross-section of Kebar dam, Iran (after Hartung & Kuros, 1987).

from which period there have been found three arch dams in the territory of today's Iran. Kebar is the best known among them, built of stone in mortar, constructed near the town of the same name, 160 km to the south of Teheran and 24 km to the south of the ancient town of Qom, in the period when the Mongolians ruled over Persia (1295–1349). The dam site is in a narrow canyon with a V-form, while the dam is 26 m high, with a total length of 55 m along the crest. Actually, the central part, 21 m in length, is arched with moderate curvature, continuing at the abutments in gravity wings (Fig. 20.5). The thickness of the crest amounts to 6 m, and up to 9 m in the lower part. The downstream face is slightly inclined towards the downstream course. The greater part of the upstream face is covered with sediment that has been deposited in the reservoir; however, according to the visible part, it seems that it is vertical along the entire height. The radius of curvature of the downstream face is equal along the entire height and it amounts to 35 m, so that, according to modern terminology, Kebar falls within the arch dams with a constant radius. In the upper part, the subsequent heightening is visible. In the banks, as well as in the riverbed, the dam is well encastered into the limestone rock. In the vicinity of the right-hand abutment in the dam's body, from the upstream face, there descends a spiral manhole, some ten meters deep. From the upstream face, it has several openings at various levels, as well as an outlet works at the bottom. In that way there was provided an intake of water in spite of the fact that the relatively small reservoir was progressively filled with sediment. It should be noted that the builders of the Kebar dam, despite the non-possession of experience with such structures, realized extraordinarily well that the dam site is ideal for at that time a new type of a dam – an arch dam (Smith, 1971; Hartung & Kuros, 1987).

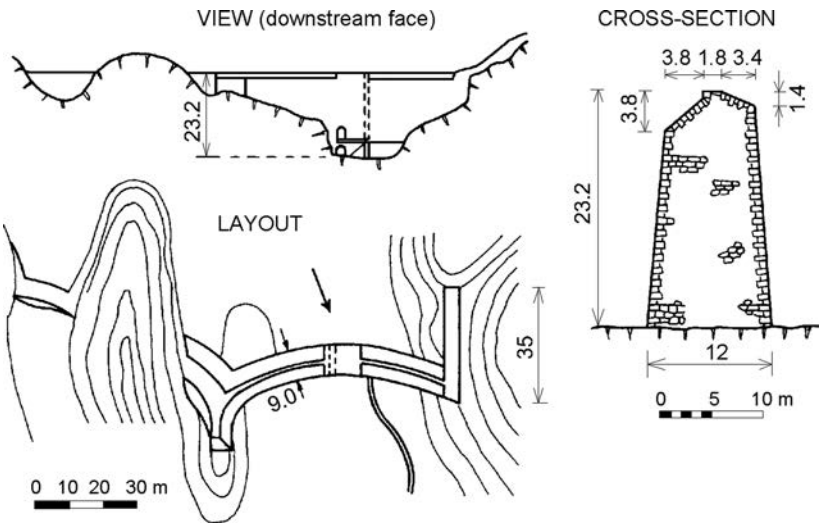

Figure 20.6 Elche dam, Spain, 16th century (after Smith, 1971).

Much larger than the Kebar dam, but rather less well known and investigated, is the Kurit dam, located some 620 km to the southeast of Teheran. It is more than twice as high as the Kebar dam and is the highest discovered dam (of all types) until the beginning of the 20th century. It is also located in a narrow canyon and also completely filled with sediment. A part of its vertical upstream face is heavily damaged, in which it is possible to see a type of masonry identical to that at Kebar, as well as a similar manhole (Schnitter, 1976).

At some 40 kilometres to the northwest of the Kurit dam, there is a smaller similar structure, which originates from the same period, which altogether rounds up this initial and isolated period of the building of arch dams, the occurrence of which is not yet sufficiently elucidated.

The oldest arch dam in Europe is the Elche dam, built in the 16th century in the vicinity of the city of the same name, in Spain (Fig. 20.6). It is also built in mortar and is 23.2 m high, with a cylindrical main arch, moderately curved. The upper part of the right-hand face rests on a concrete block, which is later on a measure frequently employed with arch dams, aimed at reducing the length of the dam. To the left, the main arch rests on a wing wall, which extends towards the reservoir storage space. All in all, this dam structure is intelligently adapted to the topographic conditions of the dam site (Smith, 1971).

Another true arch dam from the early period is the Ponte Alto dam (Northern Italy), located in an extremely narrow canyon, intended for flood protection. To begin with (1611–1613), it was constructed with a height of only 5 m, but in the period up to 1887 it was heightened seven times thus reaching its final height of 39 m. The thickness along the entire height is practically constant (Serafim & Clough, 1990).

In 1854 in France there was completed the Zola dam, 43 m high, which was designed by Francois Zola (1795–1847),[1] father of the well-known writer Emil Zola. It is an elegant structure, with a nice form, moderately curved – the first dam designed on the basis of an analysis of stresses. The analysis was conducted by treating the dam as an assembly of horizontal arches with the application of what is called the cylindrical formula, which was formulated by Navier,[2] , the creator of the statics of structures. Being designed in such a manner, the Zola dam, according to the stresses in its body, corresponds even to contemporary requirements and methods for dimensioning (Schnitter, 1976).

During the subsequent period in Europe and the USA there have also been constructed other arch dams; however, their development, due to the slow exchange of information, and also owing to the competition of the other types of dams (gravity, buttress, embankment dams), has evolved very slowly. Thus, in France, it has taken 80 years to elapse to construct another dam with a similar height as that of the Zola dam. A significant moment in the progress of arch dams was the abandonment of stone masonry and the transfer to the application of concrete.

Like other types of dams, arch dams experienced a rapid advancement in the second half of the 20th century. André Coyne built several much more daring structures (Le Gage, Tolla), of which there should be particularly noted the 90 m high Tolla dam (Corsica, 1961), with a maximum thickness of only 2.43 m. The extremely slender dams have shown to be risky, so that most of them, among them the Tolla dam, have been additionally strengthened. The very thin Le Gage dam, 46 m high, developed extensive cracking on both faces of the dam after first filling of the reservoir in 1955. Cracking continued to worsen for the next 6 years, and after the failure of Malpasset dam (December, 1959), Le Gage was abandon, and a new thicker arch dam was constructed upstream.

The development of methods for model investigation and the numerical methods of analysis have led to the present-day high degree of development of arch dams (Serafim & Clough, 1990). Table 20.1 presents data for arch dams, with a height of 200 meters and more, from which it can be seen that there are 26 such examples, which demonstrate the domination of this dam type when extremely high dams are considered. Two of them, one in final, and another one in beginning stage of construction, exceed the famous height of 300 m, reached by an embankment dam more than 30 years ago.

The oldest and at the same time the only dam built in Macedonia before World War II (1935–38), is the Matka (Saint Andrea) reinforced concrete arch dam (near Skopje), which still serves its purpose – forming an reservoir and a head for the production of electric power. It dams the gorge of the River Treska, at a narrow dam site with a V-form, composed of sound and impermeable rock. The dam consists of 10 arches with different radii of curvature (Figure 20.7), each 3 m high. The thickness of the lowermost arch is 1.6 m, while that of the uppermost is 1.0 m. Below the lowermost arch, in the foundation, there has been constructed a massive concrete foundation, Figure 20.9.

---

[1]Francois Zola died two months after the commencement of the construction of his dam.
[2]*Louis C.M. Navier* (1785–1836).

Table 20.1 Arch dams higher than 200 m.

Dam	*Country*	*Built (year)*	*Height [m]*	*Crest length [m]*	*Volume of the dam $m^3 \times 10^3$*	*Volume of the reservoir $m^3 \times 10^6$*
1. Bakhtiari	Iran	U.C.	315		3100	4845
2. Jinping I	China	(2014)	305	569	7425	7760
3. Xiaowan	China	2010	292	902		15,043
4. Xiluodu	China	2013	278	700	13,055	12,670
5. Inguri	Georgia	1980	272	680	3960	1100
6. Vaiont	Italy	1960	262	190	360	150
7. Mauvoisin	Switzerland	1957	250	520	2030	211.5
8. Laxiwa	China	2009	250	460	3682	1079
9. Deriner	Turkey	2012	249	720	3400	1970
10. Ertan	China	1999	240	775	4138	6170
11. El Cajón	Honduras	1984	234	282	1600	7085
12. Chirkey	Russia	1978	233	338	13,580	2780
13. Goupitan	China	2009	232.5	557		6451
14. Karun 4	Iran	2010	230	440	1650	2190
15. Luzzone	Switzerland	1963	225	600	1330	108
16. Contra	Switzerland	1965	220	380	660	105
17. Mratinje	Montenegro	1976	220	268	742	880
18. Glen Canyon	USA	1966	216	475	3747	33,304
19. Ermenek	Turkey	2009	210	132		4582
20. Zimapan	Mexico	1994	207	122	220	996
21. Karun 3	Iran	2005	205	462		2970
22. Dez	Iran	1962	203	380	480	3460
23. Karun 1	Iran	1976	203	380		3139
24. Almendra	Spain	1970	202	567	2186	2649
25. Berke	Turkey	2000	201		735	427
26. Kölnbrein	Austria	1977	200	626	1580	205

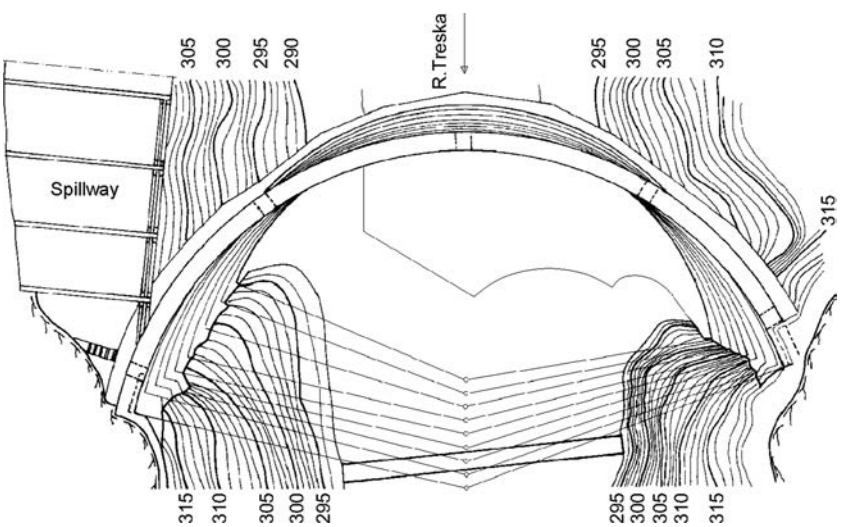

Figure 20.7 Plan of the Matka (Saint Andrea) dam, $H = 30$ m (Macedonia).

The concrete, of which arches have been carried out, contained 325 kg of high-strength low-setting cement. It is interesting to note the careful treatment of the joints between arches. Between individual arches there have been carried out horizontal joints with several coatings of bitumen and a thin zinc sheet. For achieving water-impermeability, there has been built in a copper sheet of 0.5 mm, which has penetrated some 25 cm into the neighbouring arches. As an additional measure for improving the water-impermeability of the dam, the upstream face has been coated with an insulation mixture on the basis of bituminous emulsion, upon which there has then been carried out a protective layer of cement mortar over a wire mesh, fixed into the dam's body. On the right-hand side there have been constructed a spillway structure and an outlet works, while on the left-hand side there has been constructed the intake structure to the power house of the near-dam electric power plant. The dam in which there have been incorporated 3000 m^3 of concrete and 150 t of reinforcing steel, impounds a reservoir of 3.55 million m^3. Miladin Peinar, professor at the University of Belgrade, later on an academician, designed it. The sound, hard and firm rock in the foundation and also the rather solid and reliable construction of the dam, have enabled it to be in service up to the present day (Fig. 20.8), surviving without damage the strong Skopje earthquake of 26 July 1963 (YCOLD, 1970, 1971; Thomas, 1976).

Since World War II, five other arch dams of small to medium height have been constructed in Macedonia:

1. *Lipkovo* (1958), $H_s = 40$ m, on the River Lipkovska, in the vicinity of Kumanovo;
2. *Gratche* (1959), $H_s = 43$ m, on the River Kochanska, in the vicinity of Kochani;
3. *Mladost* (1961), $H_s = 34$ m, on the River Otavica, near Veles;
4. *Ratevska Reka* (1970), $H_s = 53$ m, on the river of the same name, in the vicinity of the town of Berovo;
5. *Glazhnja* (1971), $H_s = 80$ m, on the River Lipkovska, near Kumanovo.
6. *Saint Petka* (2012), $H_s = 64$ m, on the River Treska, near Skopje.

In Macedonia, it is feasible to construct other arch dams, and, regarding the design, the greatest progress has been made in the case of the Chebren dam on the River Crna, in Mariovo, within a hydropower scheme. This dam has a feasible height of about 190 m; however, the realization of this expensive project in such a form can hardly be considered in the near future, owing to the questionable economic effects (high cost in relation to the possible generation of electric power). There are conditions for this structure to be effective and rational within a pumped-storage scheme as an upper reservoir of the possible storage reservoir *Galishte*, also located on the River Crna, between Chebren and the existing reservoir Tikvesh, with an additional smaller reservoir just downstream of Chebren.

20.3 METHODS OF DESIGNING ARCH DAMS

20.3.1 Basic design

Arch dams consist of a number of horizontal arches, constructed in such a way as to ensure favorable conditions for the work both of the arches themselves and their abutments in the banks, at a minimum volume of concrete and embedment into the

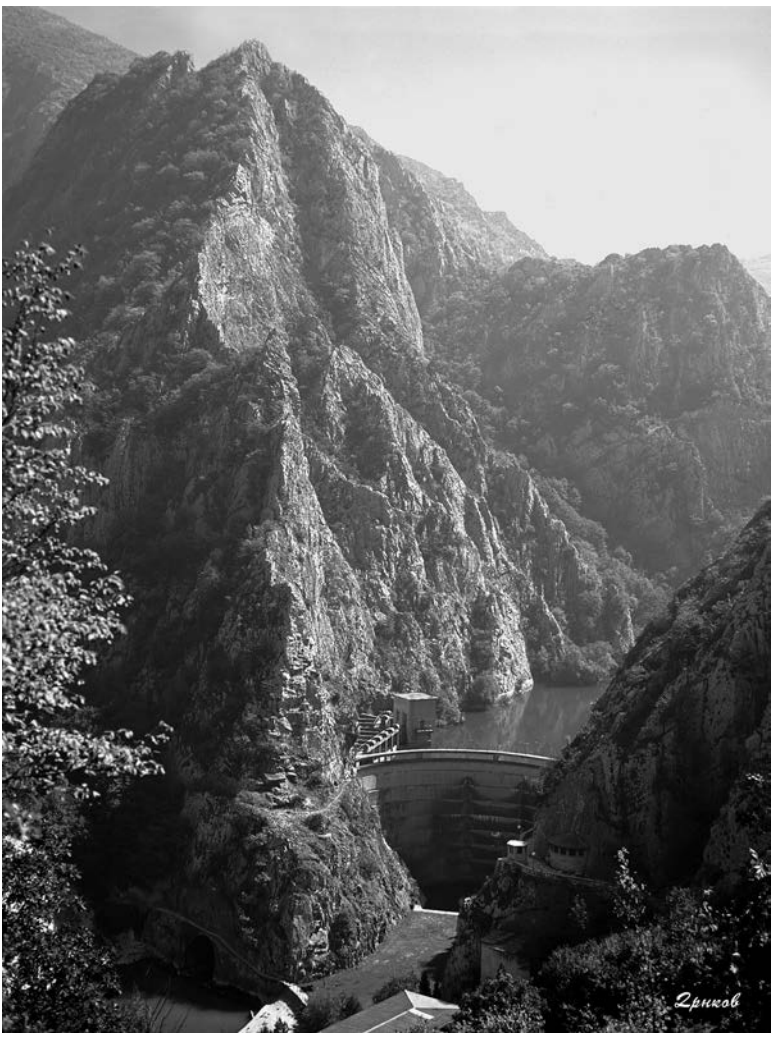

Figure 20.8 Matka dam.

rock. At the same time, in engineering the dam there should be observed two basic principles: (1) the structure should be simple, and all surfaces should change uniformly, i.e. gradually, without abrupt changes in any direction; and (2) one should always take into consideration that, in spite of the fact that the dam consists of a number of horizontal arches, the construction still represents a continuous medium. That is why the behaviour of the dam as a whole must be analysed, whenever there is to be performed any change in the shape of any part of the dam.

In principle, the stresses in the arches are increasingly smaller for a smaller radius of the arch R and for a larger central angle 2α. The central angle is, in practice, limited to 133°, since for its further increase, or what is obtained with the increase of the

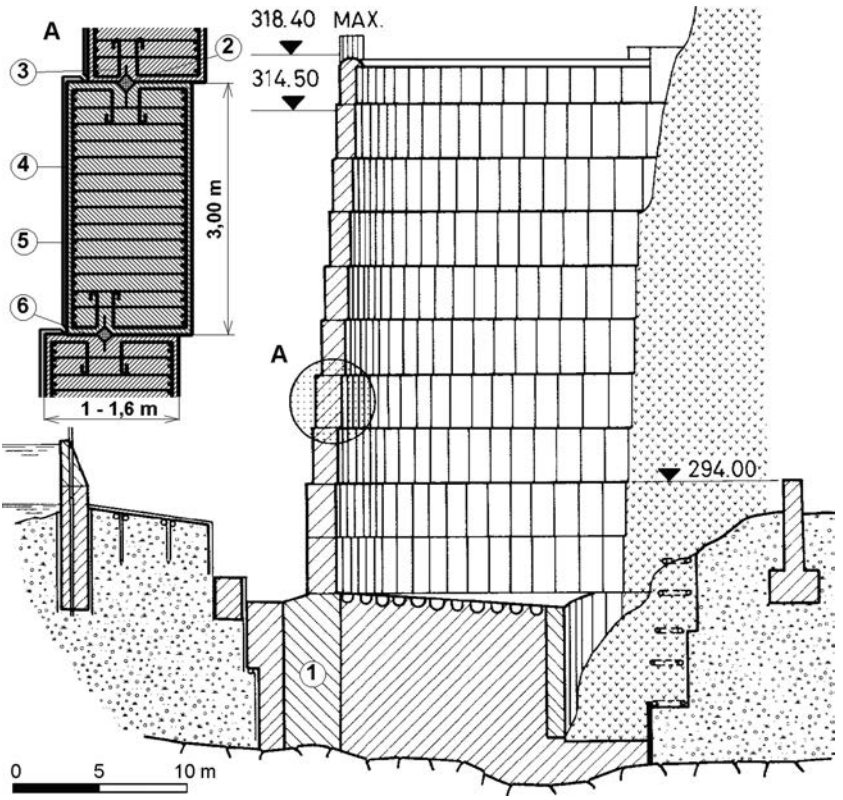

Figure 20.9 Cross-section of the Matka dam, along with a detail of the joint between arches (A). (1) Concrete foundation; (2) clay filling; (3) waterstop of copper sheet; (4) insulation of bituminous coating; (5) protective layer of reinforced mortar; (6) insulation coating and a thin zinc sheet.

bearing capacity of the arch, cannot compensate for its larger length (Zhu, 2001). There are two basic constructions of arch dams:

(1) With a constant external radius R_n along the height of the dam, and with a constant or variable central angle $2a$; the internal radii R_v, at this, decrease, going from the crest towards the foundation; that is to say, the thickness of the dam $b = R_n - R_v$ increases (Fig. 20.10a).
(2) With a constant central angle (along the height), but with a variable radius R (Fig. 20.10b).

The first method may be employed if the profile of the dam site has the form of a rectangle, so that the thickness of the arches going downwards increases approximately in proportion to the height. An example of such a construction is the 180 metres high Tignes dam (France) with an external radius of 150 m and a central angle of 125° (Fig. 20.11).

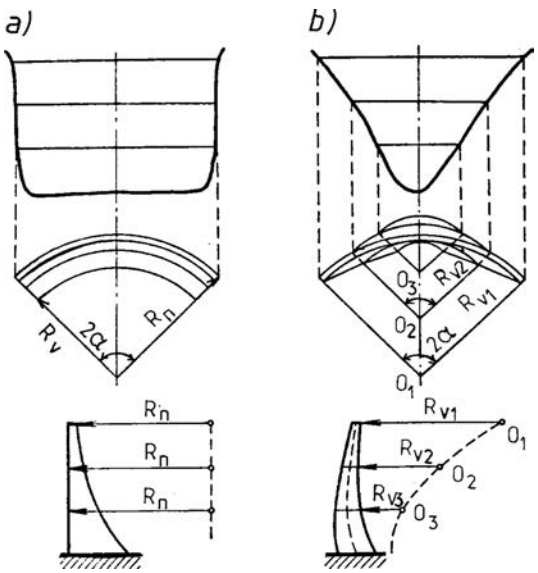

Figure 20.10 The two basic designs of arch dams.

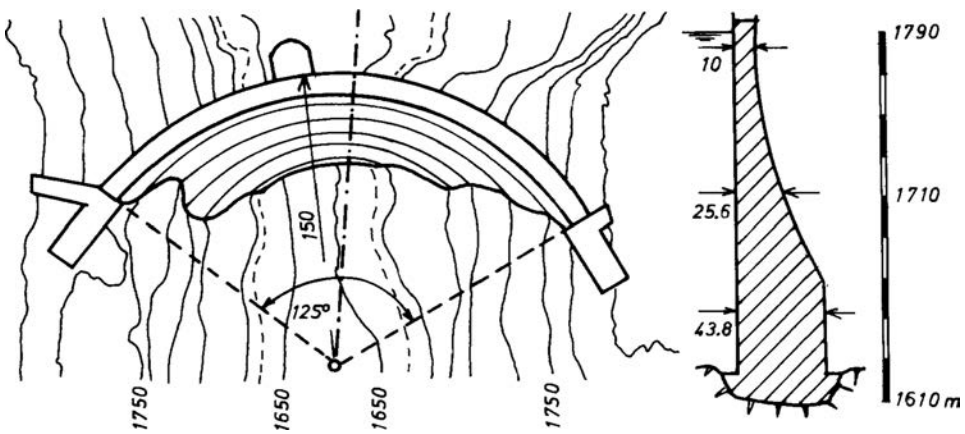

Figure 20.11 Tignes dam (France). (a) Plan; (b) cross-section.

In Macedonia such a construction has been employed for the Lipkovo and Gratche dams. The Lipkovo dam, 40 m high above the lowest point of the foundation and 29.5 m above the ground, has a ratio $H{:}L = 1{:}5$. It impounds a reservoir space of 2.25 million m^3, which serves for irrigation and water supply. It has been constructed in geologically very favourable conditions, in a profile consisting of a diabase. The relatively wide dam site, when it is a question of an arch dam (Figs. 20.12, 20.13), has imposed a construction of the type with a constant radius and a central angle – 59 m and 140°, respectively. The central part of the dam is an overflow part, with nine

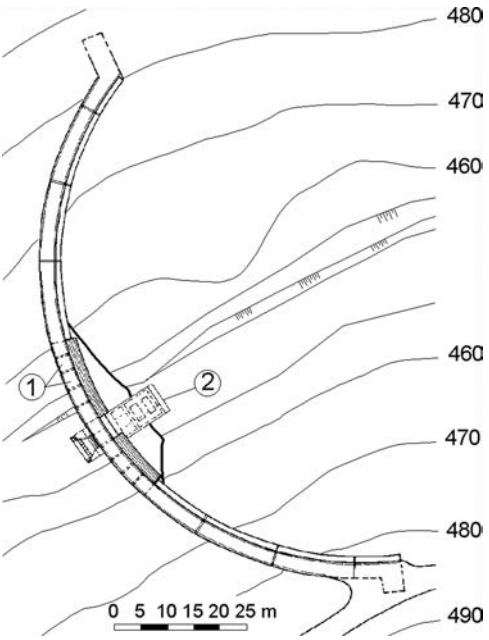

Figure 20.12 Lipkovo dam (plan).

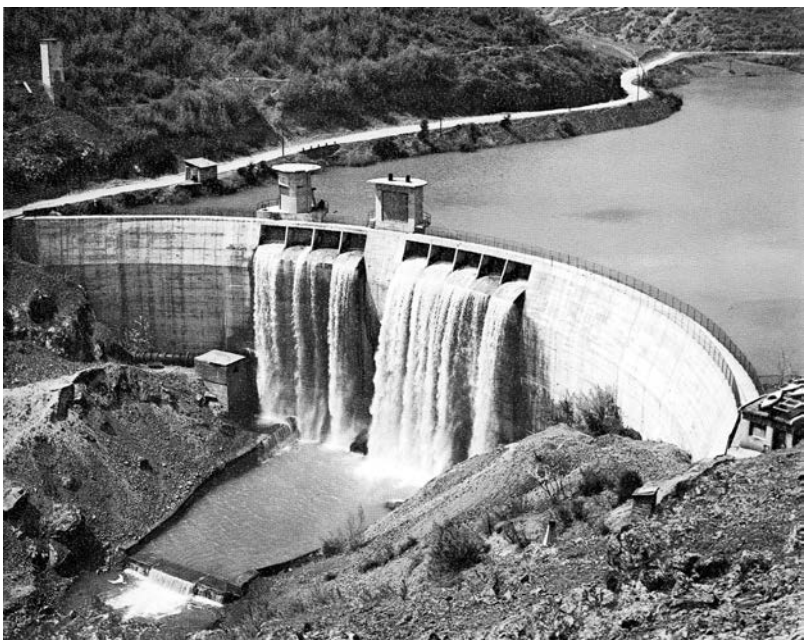

Figure 20.13 Lipkovo dam, view at the spillway under operation.

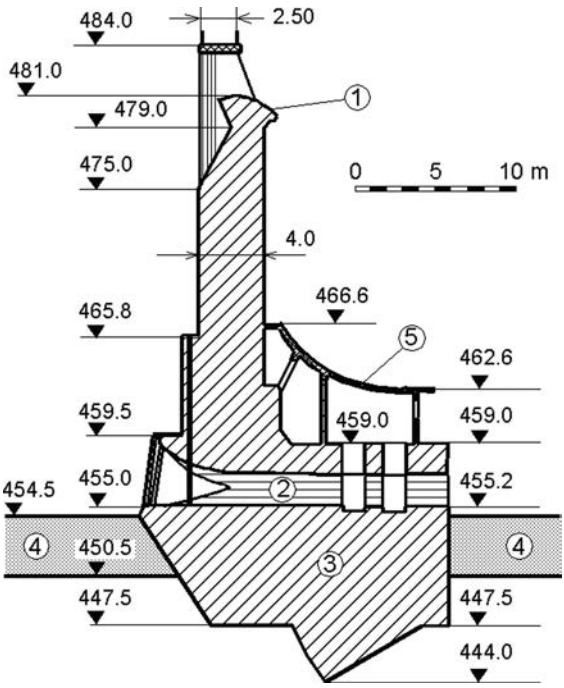

Figure 20.14 Lipkovo dam (cross-section).

uncontrolled spillway spans (1), each 4 m wide, with a total capacity of 152 m^3/s. In the lower part below the spillway, a bottom outlet has been constructed (2).

In the upper part, which is vertical, the dam has a constant thickness (4 m), while in the lower part the thickness increases going towards the bottom (Fig. 20.14; YCOLD, 1970, 1971). In the channel of the river, the founding has been performed over a massive concrete block (3), which cuts off the sediment stratum (4). The gate chamber of the bottom outlet is protected against the effect of the overflow stream from the intermediate overflow spans by means of an appropriate shaping of the structure (5).

In the dam's body there have been placed 13,000 m^3 of concrete, in blocks 2 m wide, and 8 m long. The water-impermeability of the vertical joints has been accomplished by means of the embedment of copper plates (upstream and downstream).

The Gratche dam has been constructed on the Kochanska River, which flows through a canyon with very steep banks. The foundation is composed of crystalline schists, decomposed at the surface in a zone of several metres. The height of the dam above the ground amounts to 29 m, while, above the highest point of the foundation, it is 43 m. The part which is above the ground (1) is a thin reinforced concrete construction in the river bed, founded above a massive concrete block (2) which cuts into the thick layer of river sediment, (3, Fig. 20.15). At the crest, 150 m long, the dam is 1 m wide. Going downwards, the thickness increases and, near the concrete block, it amounts to 3.45 m. The massive concrete block in the foundation is 6.45 m wide and

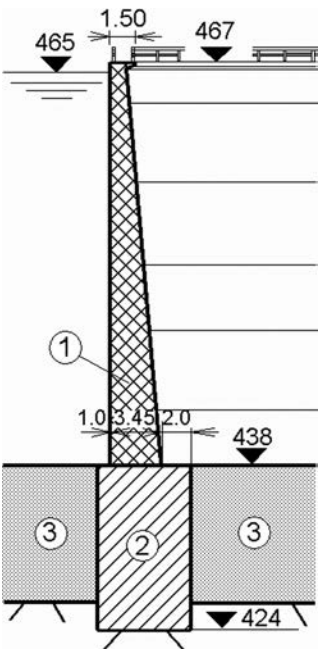

Figure 20.15 Gratche dam, cross-section (Macedonia).

14 m deep. It plays the role of a plug through the deposited sediment material, while at the same time serving also as a foundation of the dam.

In the horizontal sections of this dam, as in other dams constructed in Macedonia, there is a constant thickness. In a vertical section, the upstream face is vertical. The radius of curvature of the horizontal arches varies very little – from 64.35 to 50.75 m, so that it can be considered constant. The central angle ranges within limits from 136° to 96°. In the dam's body there have been incorporated 12,000 m^3 of concrete, with an average reinforcement of 40 kg reinforcing steel per 1 m^3 of concrete.

In plan the dam, which forms a storage space of 2.4 million m^3, is presented in Figure 20.16, in which it is possible to see the steep banks and the relatively wide riverbed of the Kochanska River.

The spillway is completely separated from the dam's body and consists of four spillway spans, each of them 7 m wide (Fig. 20.17). The total overflow capacity amounts to 120 m^3/s. The bottom outlet works accommodated in the central part of the dam have been provided with two gates, which are located in a small structure, immediately downstream of the dam. The pipe of the bottom outlet has a diameter of 1000 mm.

The second design concept, i.e. construction, is more suitable for a trapezoidal and triangular profile of a dam site at which, going downwards, there is a decrease of the span of arches and, with a change of the radius, there is obtained a much more economical construction. In the case of this design concept, one should pay attention to providing overlapping between the adjacent arches; that is to say, the lower arch

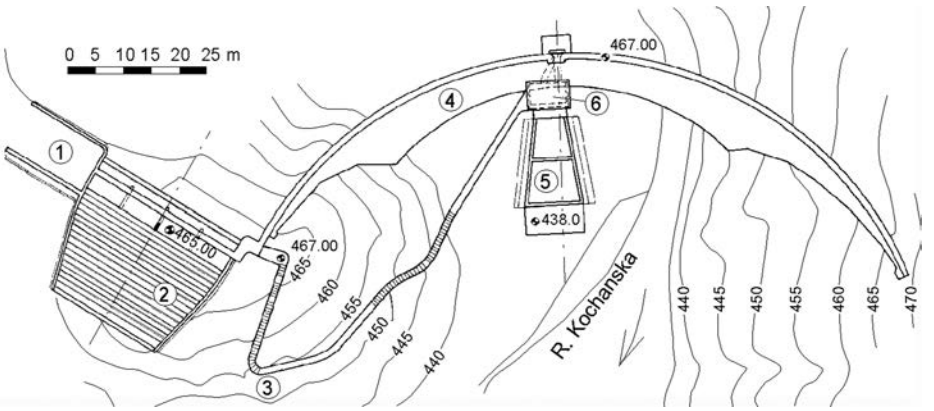

Figure 20.16 Gratche dam, layout. (1) Plateau; (2) *spillway*; (3) roadway; (4) the dam's body; (5) stilling basin at the bottom outlet; (6) gate chamber at the bottom outlet.

Figure 20.17 Gratche dam, with the spillway on the *right* side.

along its entire length should overlap the upper one by at least one third of its width. In this, it is difficult to retain a constancy of central angle along the entire height and, therefore, some variations are tolerated, i.e. allowable, so that in the bottom part of the dam it may drop to as low as 80° (Fig. 20.18).

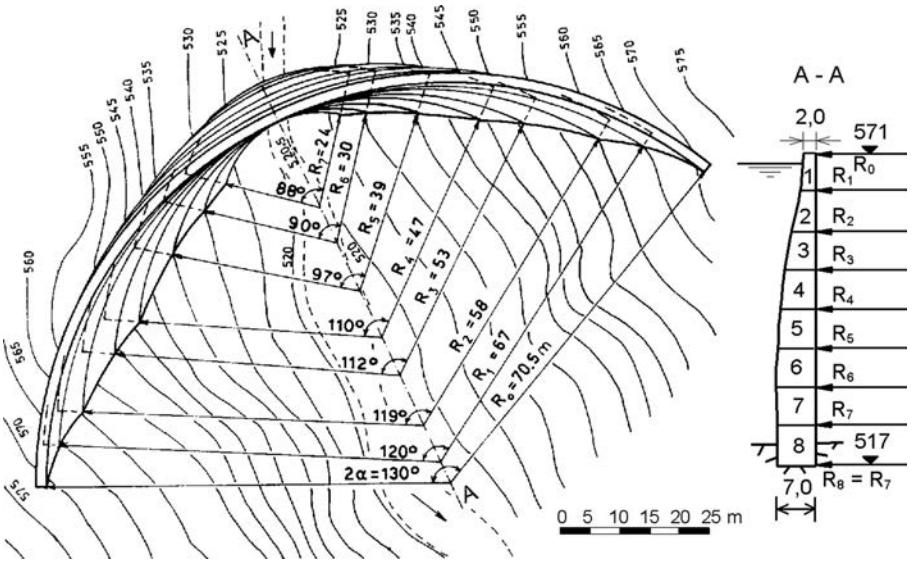

Figure 20.18 Design concept of an arch dam with a vertical downstream face in the highest section.

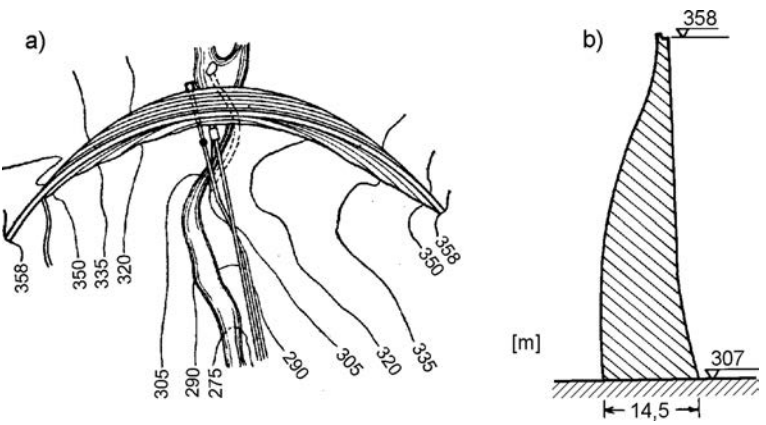

Figure 20.19 Salmon dam (Alaska). (a) Plan; (b) cross-section.

According to the second design method (construction), introduced into practice by Lars Jorgensen with his design for the Salmon dam (Fig. 20.19) in 1913, there were constructed a number of dams, in which there have been used different variations of the method. The simplest case appears when the downstream face of the highest section is vertical (in the river bed). That is a construction when all the arches pass through the section of the vertical plane, in which there lie the centres of the radii, with the dam (Fig. 20.18). Possible widening towards the downstream face is sometimes accomplished only in the lower part of the dam, such as in the example in Figure 20.19.

Of the arch dams constructed in Macedonia according to this method, the Matka dam has been constructed, in the vicinity of Skopje, which has already been discussed in section two of this chapter. The central angle is constant (varies from 155° to 148°), while the variations of the radii are shown in Figure 20.7.

20.3.2 Arch dams with double curvature

In the practice of designing and constructing of arch dams, besides the above-cited basic types, one may also find more complex types, with a distorted form, dictated by the conditions for adapting the dam to the ground, or else by static or hydraulic conditions. These dams have a double curvature; that is to say, in this case, both the upstream and the downstream faces of the cross-section are curved. For ensuring better static work, the dam is often overhung with the lower part towards the water. There are many examples of this kind of construction, and one of them is illustrated in Figure 20.20. Below the overhung part of this dam (at the upstream face), there have been constructed retaining buttresses (1). By means of such an overhung construction there is achieved a prevention of dangerous tensile stresses in the lower part of the upstream face, owing to the effect of self-weight. In some cases, with these kinds of dams, there have appeared tensile stresses in the downstream face in the course of construction, and, because of that, at the upstream face we execute supports in the form of buttresses, separated by means of joints from the basic profile. On the right bank, next to the dam, there is located a free overfall spillway.

The Mauvoisin Dam (Switzerland) has also been carried out by using double curvature and it is one of the highest arch dams in the world ($H = 237$ m, $L/H = 2.2$), built in the period 1951–57, Figure 20.21. This dam, which has shown exceptional behaviour during a service period of some 30 years, in the period of 1989–91 has been raised an additional 13.5 m, by adding an arch concrete element, 14 m wide at the bottom, and 12 m wide at the crest, in order to increase the volume of the storage reservoir. This heightening had been planned even in the course of dam's construction, owing to which a 14 m wide crest was constructed at that time. During this heightening, there were placed an additional 80,000 m^3 of concrete; that is to say, about 4%

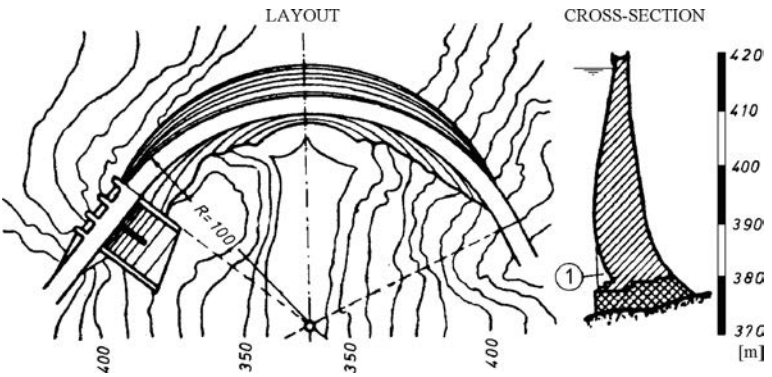

Figure 20.20 Mareges dam, France, 1935 ($H = 89$ m).

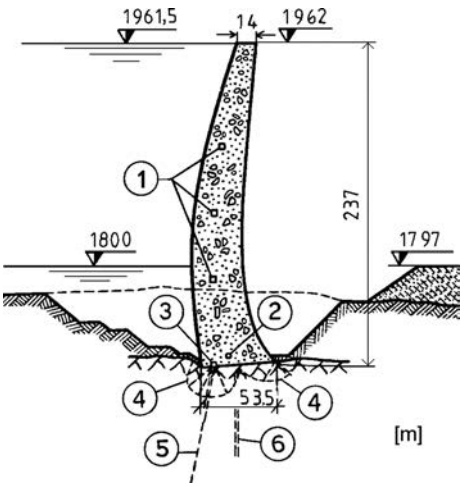

Figure 20.21 Mauvoisin dam. (1) Inspection galleries; (2) drainage gallery; (3) grouting gallery; (4) zones of consolidation grouting; (5) grout curtain; (6) drainage holes.

of the volume of the existing dam, while in an appropriate way there have also been upgraded the spillway structure and bottom outlet, and new approaches have been made as well (Urech & Gilg, 1988).

In designing and constructing the above described heightening, it was necessary to take account of two essential facts: (1) the new part of the dam could not have direct contact and support in the abutments, owing to the special structures located close to the abutment; and (2) construction works had to be performed at the working level of the storage reservoir, which reached 1910 mwl. The first condition imposed a construction of the additional structure with sufficient bearing capacity, without direct contact with the rock. Further on, due to the water loading in the zone of the former crest, there were to be expected tensile stresses in the new concrete at lowering of the water level of the storage reservoir. These requirements led to a structural heightening, as shown in Figure 20.22.

The execution and treatment of the joint covers the following works: removing the concrete forming the old crest, cleaning and wetting the contact surface, placing a layer of 5 cm cement mortar for achieving an improved bond between the new and the old concrete, and placing the new concrete all within one hour's time. The concreting was performed in blocks 18 m wide, with concrete containing 250 kg cement per m^3 of concrete, without additional cooling, in five bench levels 2.7 m high. Between each bench level, there has been placed a 3-cm mortar layer for an improved bond. Water-stops have been incorporated as is shown in Figure 20.22, while the joints were grouted in the summer of 1991.

Figure 20.23 shows the longitudinal section of the Mauvoisin dam, along with the layout scheme of the instrumentation and equipment for surveillance, adapted to the heightening (Straubhaar et al., 1994).

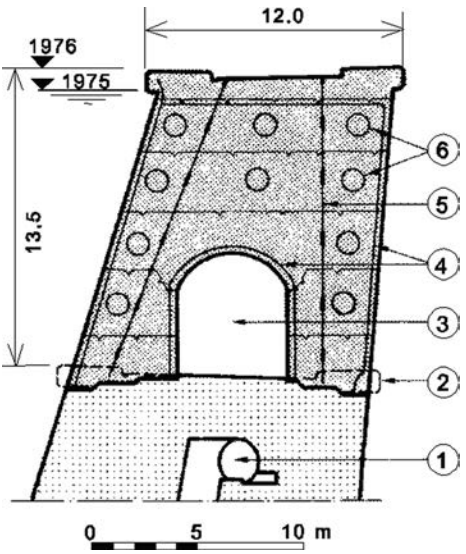

Figure 20.22 Mauvoisin Dam, detail of the heightening. (1) Inspection gallery; (2) removed concrete; (3) access gallery; (4) waterstops; (5) grouting pipes; (6) spherical wedges (Straubhaar et al., 1994).

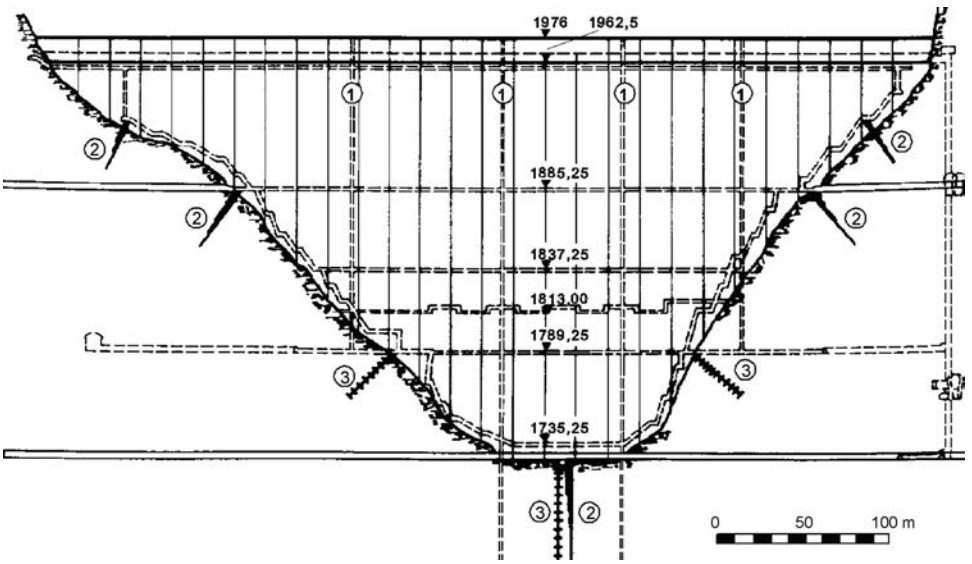

Figure 20.23 Longitudinal section of Mauvoisin Dam. (1) Plummet direction; (2, 3) devices for measuring displacements and dilatations in the rock (after Straubhaar et al., 1994).

The inverted overhang of the dam (towards downstream) is employed when we intend to construct a spillway over the crest of the dam. In that way, we can move the place of falling of the spillway flow away from the foundation of the dam (Fig. 20.24; Grishin et al., 1979). The construction of a dam with a double curvature, with an overhang of the upper part of the dam towards the downstream face, is also anticipated for improving the conditions for static work, in order to prevent vertical tensile stresses at the upstream face in the vicinity of the foundation, i.e. at the downstream face, in the upper third of the dam. Such an unusual construction has been employed for Boundary dam, Figure 20.25 (USA, 1967; USBR, 1977a).

The dam contains a dual system of spillways – a surface spillway in the banks, as well as a deep spillway in the dam's body. The height of the dam amounts to 104 m, while the width varies between 9.8 m at the foundation and 2.4 m at the crest, which means that it is a question of a very thin dam. In the designing and dimensioning of such an arch dam, which, in a certain horizontal section contains a considerable number of openings provided with gates, one should bear in mind that the arches immediately below and above the openings take on the greatest part of the loading from the gates.

Among the arch dams constructed in Macedonia, four have a double curvature – the Mladost, Glazhnja, Ratevska River, and Saint Petka dams (YCOLD, 1970, 1971).

The Mladost dam has been constructed on the River Otavica, a left tributary of the River Vardar. It impounds a reservoir storage space of 8 million m^3, intended mainly for irrigation. The dam site is narrow, but asymmetrical, composed of crystallized limestone. In spite of the tectonic fissures, the stratification of the rocks is vaguely manifested and it is rather compact rock. Over massive concrete blocks, the dam is jointed with the banks (Fig. 20.26). In the zone of the river bed, there has been accommodated an uncontrolled spillway over the dam, with a capacity of 76 m^3/s, below which there have been centrically set up bottom outlet works.

The height of the dam above the ground amounts to 27 m, while the structural height is 34 m. It was originally planned for the overflow section of the dam's crest

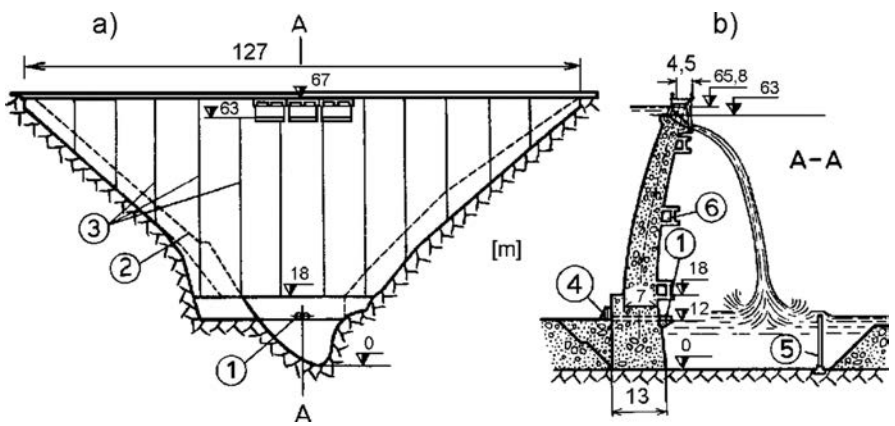

Figure 20.24 Lajanurskaya dam, Russia, ($H = 67$ m). (a) View towards the upstream face; (b) cross-section A–A. (1) pipes of the bottom outlet; (2) line of original ground; (3) temperature-deformation joints; (4) screen at the entrance to the bottom outlet; (5) arch reflective wall; (6) cantilevered service bridges.

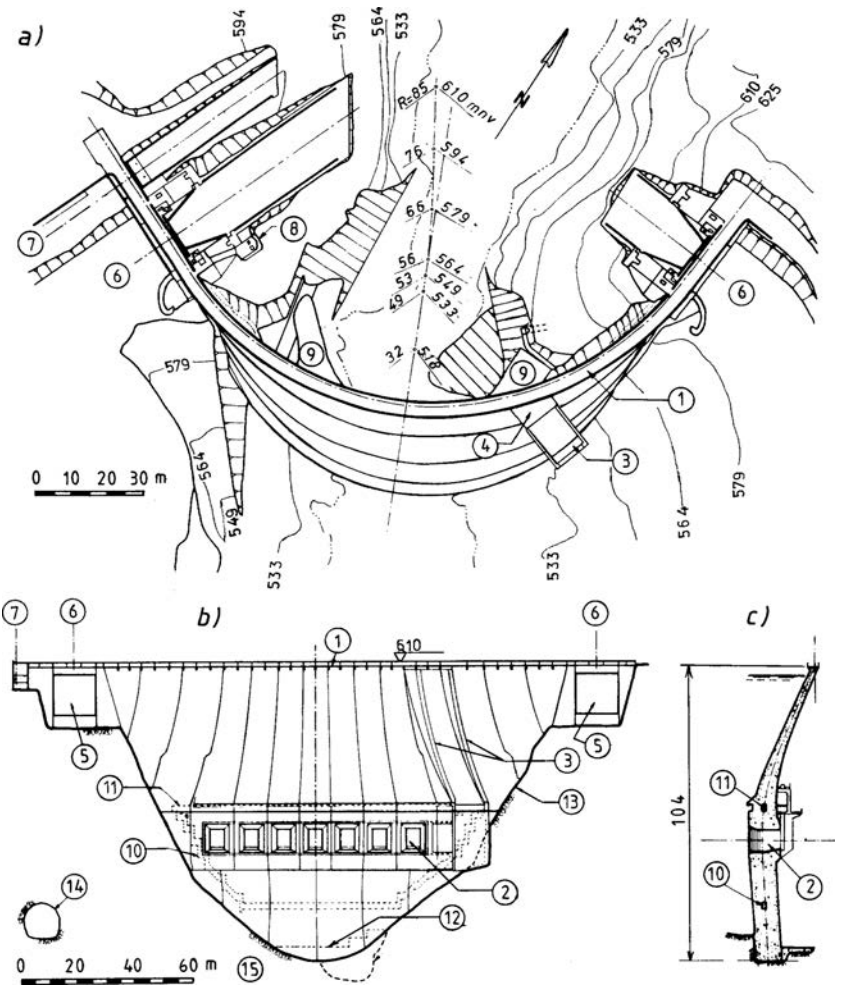

Figure 20.25 Boundary dam (USA). (a) Plan; (b) view of the downstream face; (c) cross-section. (1) Roadway over the crest; (2) outlet openings, b × h = 5.2 × 6.4 m; (3) overhaul gate with movable frame; (4) platform for elevator, at elevation 610; (5) spillway; (6) axis of the segment gate, 15.2 × 13.4 m; (7) axis of the gate for discharge of ice, etc., at maintaining the reservoir storage, 7.9 × 2.4 m; (8) access lift; (9) access bridge; (10) foundation gallery; (11) handling gallery; (12) contour of concrete plug; (13) line of excavation; (14) diversion tunnel; (15) bedrock – gray and dolomite limestone.

to be at an elevation of 245 mwl, while that of the non-overflow section at an elevation of 247 mwl. However, unusual for this kind of structure, only one year after the completion of the construction works, it was decided that the overflow part would be heightened by two metres, while the non-overflow part by one metre, aiming at obtaining a significantly larger available storage capacity by a relatively small intervention.

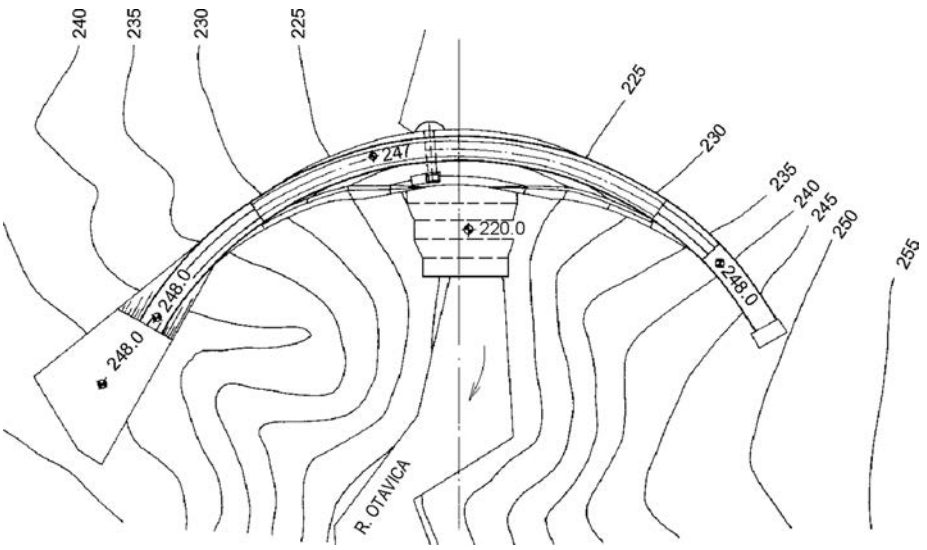

Figure 20.26 Mladost dam, layout.

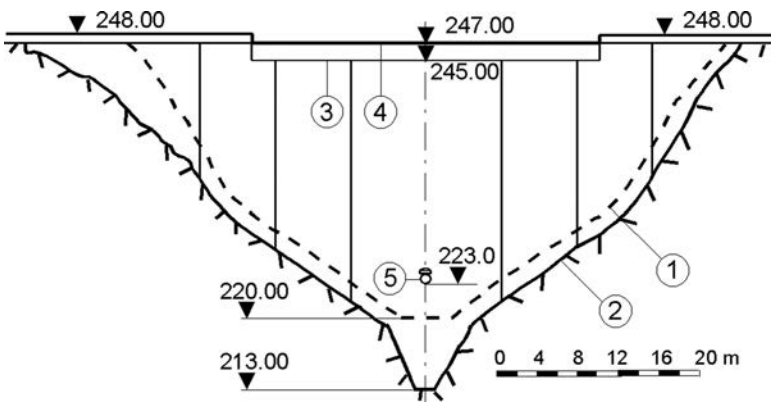

Figure 20.27 Mladost dam, *longitudinal* section. (1) Line of ground; (2) line of foundation; (3) original level of the crest of the overflow section of the dam; (4) spillway crest of the dam after the banking, i.e. heightening for higher freeboard; (5) bottom outlet.

This 'operation' may best be understood in the sketch of the longitudinal section of the dam (Fig. 20.27 – Thomas, 1976; YCOLD, 1970, 1971).

The dam is a thin, i.e. slender, double-curved reinforced-concrete structure, with a thickness that varies from 0.8 m at the crest to 4 m at the foundation (Fig. 20.28). In a horizontal section, the arches are of a constant thickness. The radius of curvature varies from 19.39 m to 27.92 m. In the foundation there has been placed a cylindrical concrete block with a radius of curvature of 19.39 m, 4 m thick. The dam is reinforced

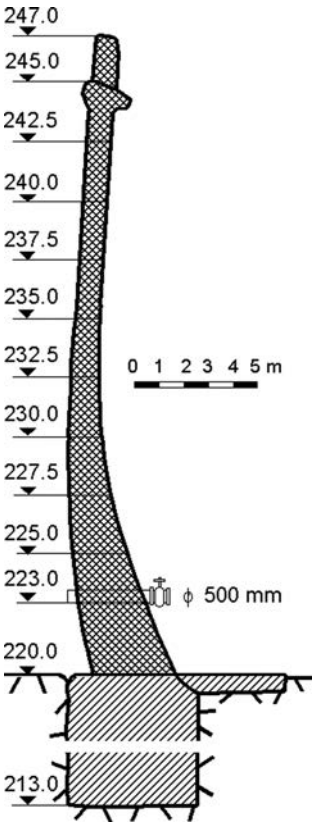

Figure 20.28 Mladost dam, cross-section.

on average with 25 kg of reinforcing steel per m^3 of concrete in order to reduce the time of construction avoiding vertical joints. The concreting has been performed in blocks 1.5 m high, with placing the concrete in layers of 30 cm along the entire length of the arches. Following the contact with the rock, surface grouting has been performed.

The Glazhnja dam, built in 1971 (Figs. 20.29 and 20.30) is located 5 km upstream of the Lipkovo dam. With its structural height of 80 m (71.5 m above the ground), it is the highest concrete dam in Macedonia. The dam impounds a reservoir storage of 22 million m^3, which serves for accomplishing a quality regulation of the waters of the Lipkovska River. The length of the dam at the crest amounts to 344 m. In its central part there has been carried out an uncontrolled spillway with discharge capacity of 175 m^3/s. Just downstream of the dam it has been formed a stilling basin for calming down the energy of the overflowing stream, in to which, also, the water of the bottom outlet is discharged. The concrete mixture was prepared with aggregate crushed limestone, while concreting has been carried out in blocks of 1.5×14 m.

The third arch dam constructed in Macedonia by using double curvature, is the Ratevska River dam, on the river of the same name, in the vicinity of Berovo.

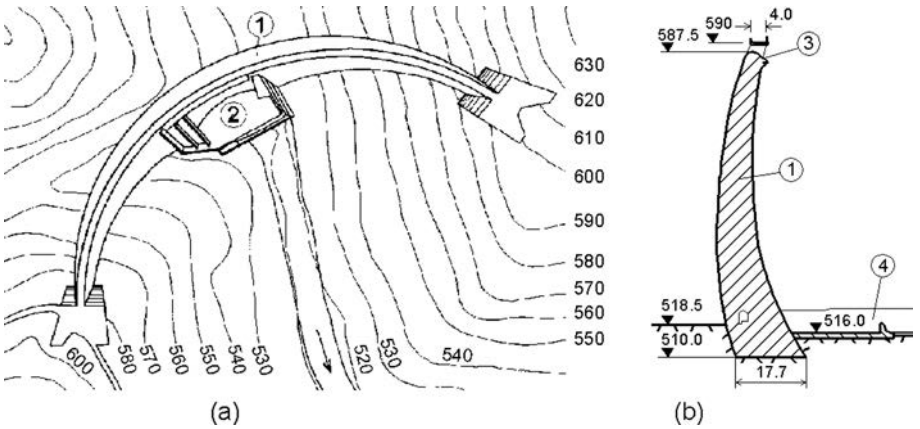

Figure 20.29 Glazhnja dam. (a) Plan; (b) cross-section; (1) dam's body; (2) overflow section with stilling basin; (3) overflowing crest; (4) stilling basin.

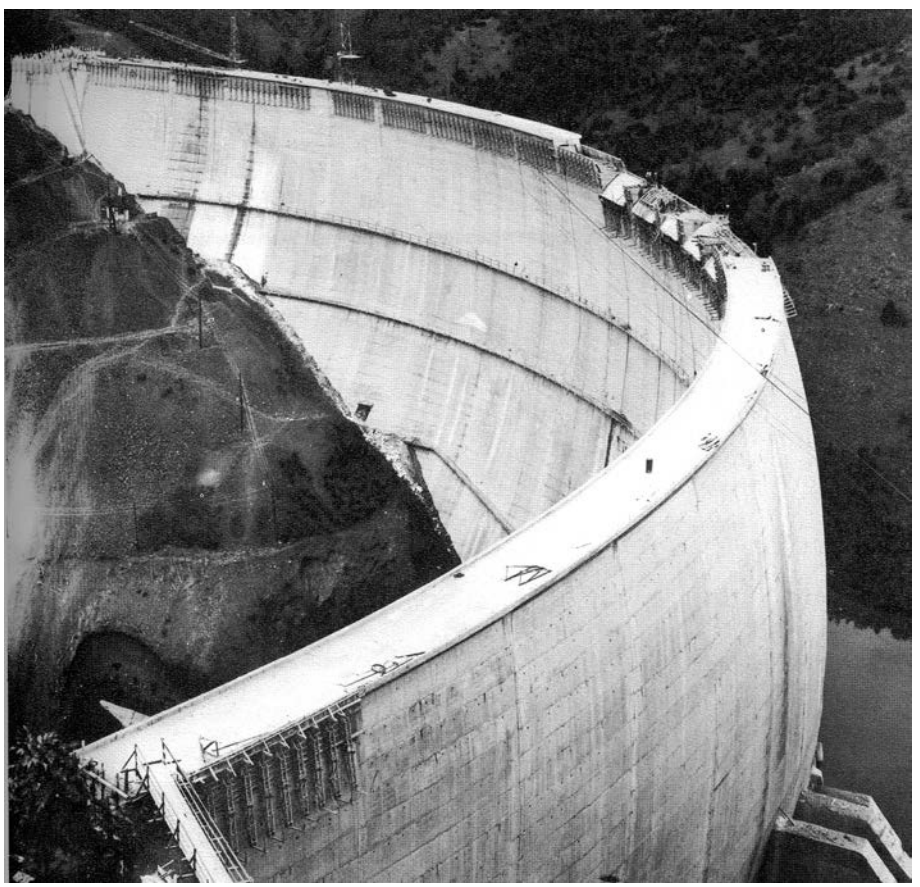

Figure 20.30 Glazhnja dam, nearing completion (1971).

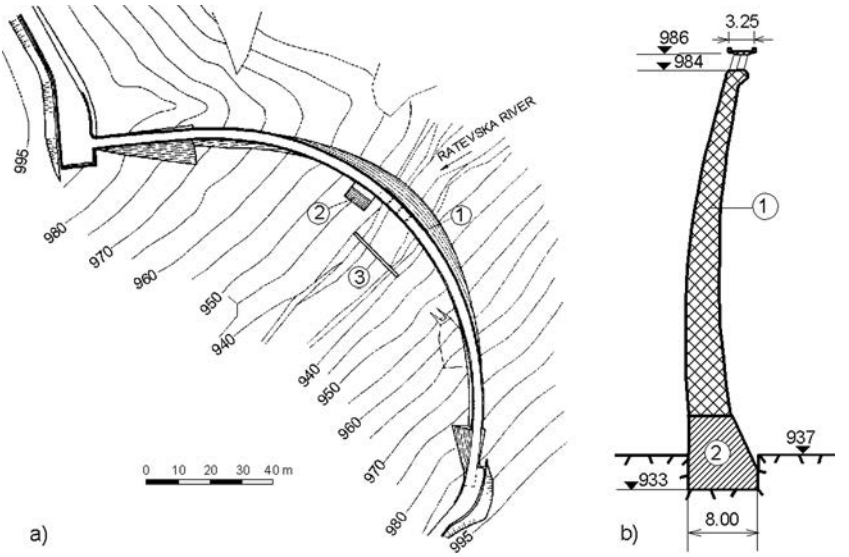

Figure 20.31 Ratevska River dam. (a) Layout: (1) spillway; (2) bottom outlet; (3) transverse concrete sill. (b) Section through the overflow part: (1) dam's body; (2) concrete foundation block.

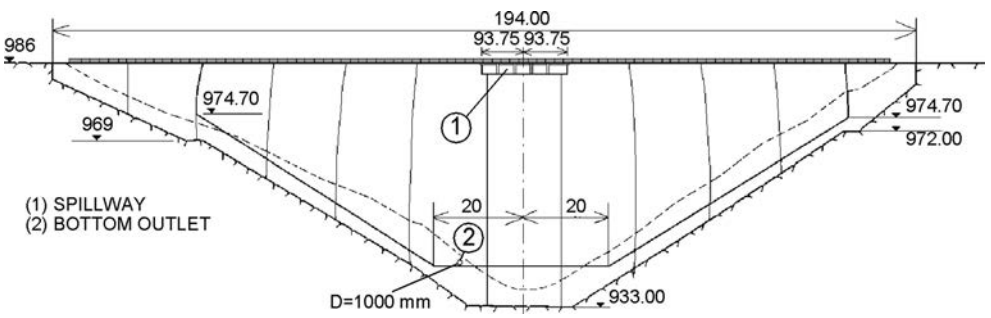

Figure 20.32 Ratevska River dam, longitudinal section.

It impounds a reservoir with a volume of 10.5 million m^3, intended for irrigation. The dam site foundation is composed of gneiss, while the lack of symmetry from a topographical viewpoint has been corrected with massive concrete blocks in both banks (Figs. 20.31a, 20.32). The length of the arch part of the dam along the crest amounts to 144 m, that of the gravity sections measures 34 m (in the right-hand bank), with 16 m in the left-hand bank. In the central part there has been constructed an uncontrolled spillway with a capacity of 70 m^3/s, while to the right of it there is a bottom outlet with pipe diameter amounting to 1000 mm. In the riverbed there has been placed a concrete beam, which forms a basin for stilling the energy of the overflow jet, (3, Fig. 20.31a).

The height of the dam above ground is 49 m, while the structural height is 53 m. It is 1.5 m wide at the crest, and the thickness increases 8 cm per each metre. The gravity

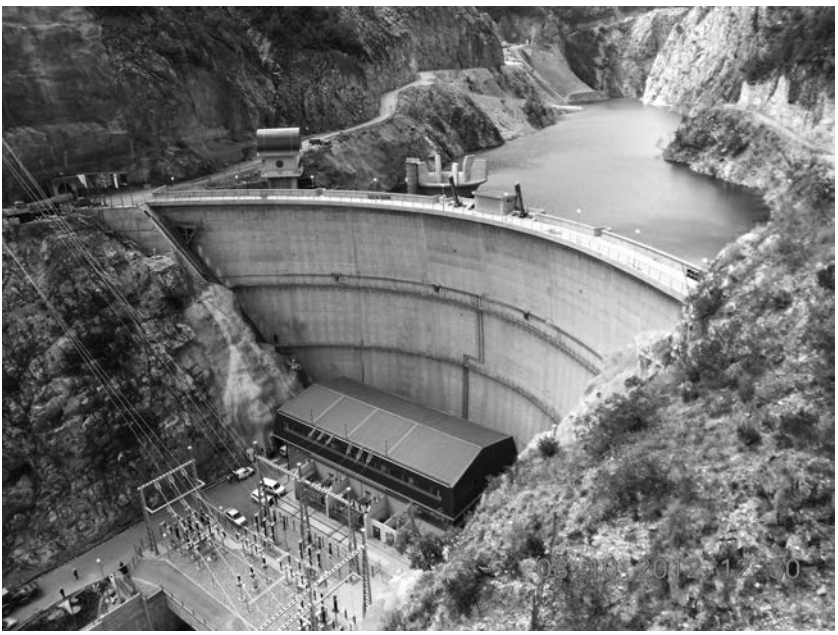

Figure 20.33 Dam Saint Petka (R. Macedonia, $H_s = 64$ m), during first reservoir filling.

blocks at the crest are 3 m wide and they have a trapezoidal cross-section. The dam's body is divided by means of vertical joints at each 16 m. A concrete foundation has been built in the base of the dam (2, Fig. 20.31b). The radii of curvature of the central line of arches are from 79.25 to 37.07 m, while the central angles are from 104° to 65°.

Below the dam, there has been added contact grouting, as well as a deep grout curtain. The contact grouting is composed of boreholes 1.5 m long, while the deep grout curtain is a two-rowed one, up to 30 m deep.

It is characteristic that first two arch dams with double curvature built in R. Macedonia (Mladost and Glazhnja) are inclined towards the upstream face, although both have an overflow part. This means that advantage has been given to the stability of the dam, in relation to the conditions for overflowing.

Fourth double curvature arch dam in R. Macedonia is Saint Petka, commissioned in 2012. It is located in the narrow value of the Treska river, between existing dams Matka and Kozyak (see Chapter 1, Fig. 1.8) The purpose of the dam is electricity production (36.4 MW installed capacity) as a second cascade of the hydro-system Treska, which is now completed. The dam has a structural height of 64 m, and it is 115 m long. The dam is 10 m thick at the base (elevation 300 m.a.s.l.) and 2 m in the crest (elevation 364 m.a.s.l.). Total dam volume is 32,500 m^3. By means of 9 vertical joints the dam body is divided in blocks, 9.5 m to 14 m wide. As a concrete aggregate limestone was used, separated in six fractions, with maximum grain size of 100 mm. The concrete mixture was prepared with 280 kg/m^3 Portland cement, with low water/cement ratio. The concreting was performed by means of steel formwork,

2 m high. The concrete was placed in layers of 40–50 cm and compacted by vibrators. The dam is founded on relatively strong and compact limestone. The contact dam-foundation, as well as the properties of the surface zone of the rock, was improved by 15 m deep consolidation grouting. To improve the watertightness of the foundation a grout curtain 35 to 78 m deep was performed, partly in one row, partly in three rows. To avoid conflict with other structures in the very narrow dam site, a shaft spillway was provided with a discharge capacity of 1200 m^3/s.

20.3.3 Form of arches in plan and adaptation to ground conditions

The most often employed form of arches in the plan is a circular one, with a constant thickness (Fig. 20.34a). This form is the simplest for execution; however, in relation to its adaptation to the topography of the ground, as well as from a static viewpoint, it is not always the most favourable. In circular arches with constant thickness, stresses increase towards the restraint (fixity), and sometimes the thickness of the end zones also increases (Fig. 20.34b). If there is a need for reducing the stresses in the rock, then in the zone of restraint it is possible to perform local thickening of the arch (Fig. 20.34c).

In order to obtain a more uniform distribution of stresses and more properly to utilize the topographical conditions of the dam site, arch dams with more complex arches are constructed, composed of parts of circular lines, drawn from a number of centres (Fig. 20.34d), or in the form of part of a parabola, hyperbola, ellipse, or other compound curve (Fig. 20.34e). In narrow canyons with a triangular form, there are recommended arches with a central curvature with a smaller radius and a peripheral curve with a larger radius (Fig. 20.34f), in which there is obtained a more uniform

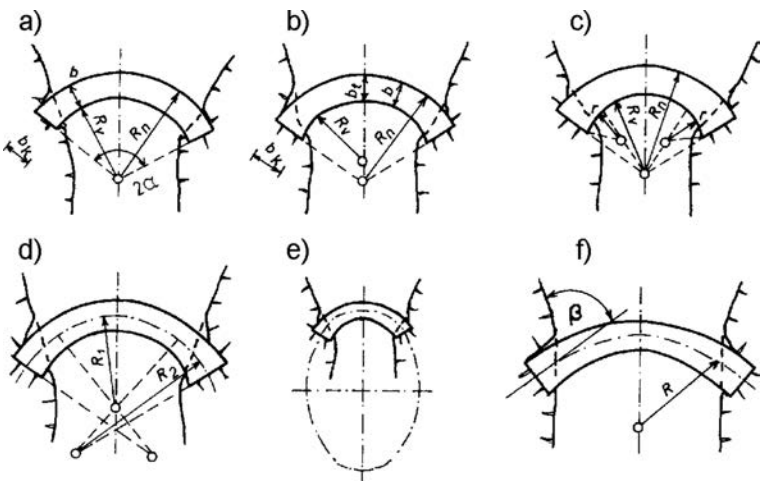

Figure 20.34 Forms of arches in plan. (a) Circular arch with constant thickness; (b) circular arch that thickens gradually towards the constraint; (c) circular arch with local thickening at the constraint; (d) arch with variable thickness *and* circular axis, drawn from three centres; (e) elliptical arch; (f) arch with slight curvature in the vicinity of restraint.

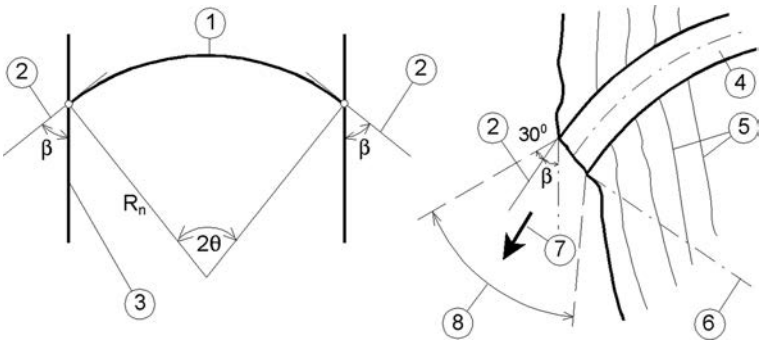

Figure 20.35 Entrance angle of the horizontal force of the arch into the abutment (after Novak et al., 2001). (1) Upstream face of dam; (2) line of tangent; (3) assumed spreading of contour of hard and firm rock; (4) arch; (5) contour of hard and firm rock; (6) radial line; (7)horizontal force transferred from arch to abutment; (8) zone of distribution of force at an angle of approximately 60°.

distribution of stresses and better restraint in the bank, at a larger angle β, which must not be smaller than 30°.

Generally speaking, the angle at which the arch transfers the horizontal component of loading to the bank is of enormous importance for the proper work of an arch dam. Namely, it must be transferred to the abutment at a safe angle, which would not cause overloading or instability of the abutment. The scheme for insertion of the horizontal component of loading into the abutment, for any arch, that is to say; for an arbitrary horizontal section, is shown in Figure 20.35. It is assumed that the horizontal force is distributed from the arch to the abutment in a zone forming an angle of approximately 60°, as is shown in the figure. Spreading out in the abutment, the force must not fall in the same line close to the contour of the hard, firm rock or lead to a considerable discontinuity in the rock, which could lead to instability of the abutment. In general, this condition makes for an entrance angle $\beta = 45°$ to 70°. The horizontal radius of the arch, and thus the stresses, as well as the volume of the arch, is a function of the entrance angle β. The optimum value of the angle β can be determined by a careful analysis of the geological composition and the strength characteristics of the rock in the foundation.

Very often, dam sites, which, according to their geological composition and the ratio *L/H*, correspond to the requirements for an arch dam, have certain irregularities in their form, which complicate the structural solution of the dam. This question has already been discussed (Fig. 20.4), while Figure 20.36 presents several parameters within which, if in the design and construction of the dam we stick to the natural configuration of the profile, there would come about abrupt changes in the spans of the arches, the result of which would be the occurrence of a concentration of stresses in particular parts of the dam.

Measures that can be taken in such a case are the following: (a) levelling of the convex parts of the bank by excavation into the rock; (b) execution of massive concrete blocks for constricting the profile; (c) execution of a concrete plug in the narrow lower

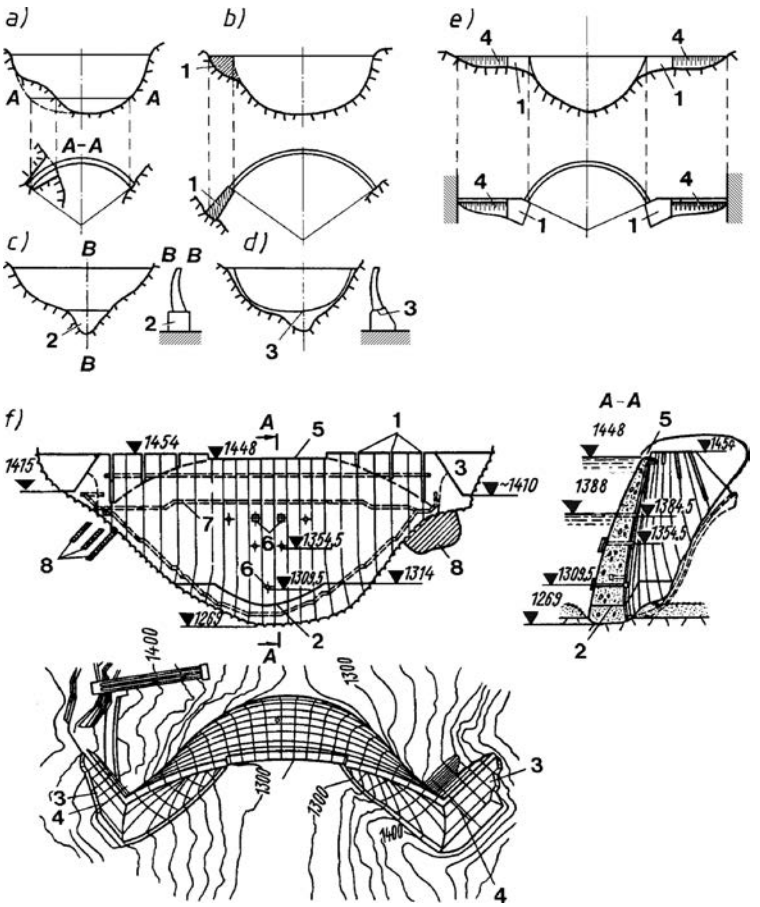

Figure 20.36 Schemes of arch dams in cases of complex form of dam site (a–e) and Kurobe dam, Japan, $H = 186$ m (1964), example of a dam with wing gravity blocks (f) (after Grishin et al., 1979). (a–e): (1) Concrete block; (2) concrete plug; (3) contour joint; (4) wing gravity blocks. (f): (1) vertical joint-cuts, sealed at the end; (2) partial contour joint; (3)wing gravity blocks; (4) constructional joints between the dam and wing blocks; (5) spillway; (6) temporary (construction) spillway openings; (7) outlet works; (8) deranged zones, strengthened in the course of construction.

part, which serves as an artificial foundation; (d) execution of a concrete foundation massif along the entire length of the dam, usually separated from the dam's body by means of a contour joint, which provides a more uniform distribution of stresses in the whole structure; and (e) execution of a combination of an arch dam in the middle and massive parts at the ends, in cases when the dam site abruptly widens in the upper part.

Figure 20.37 presents an example of an arch dam, the arches of which are constructed from two centres. This construction is suitable for an asymmetrical canyon.

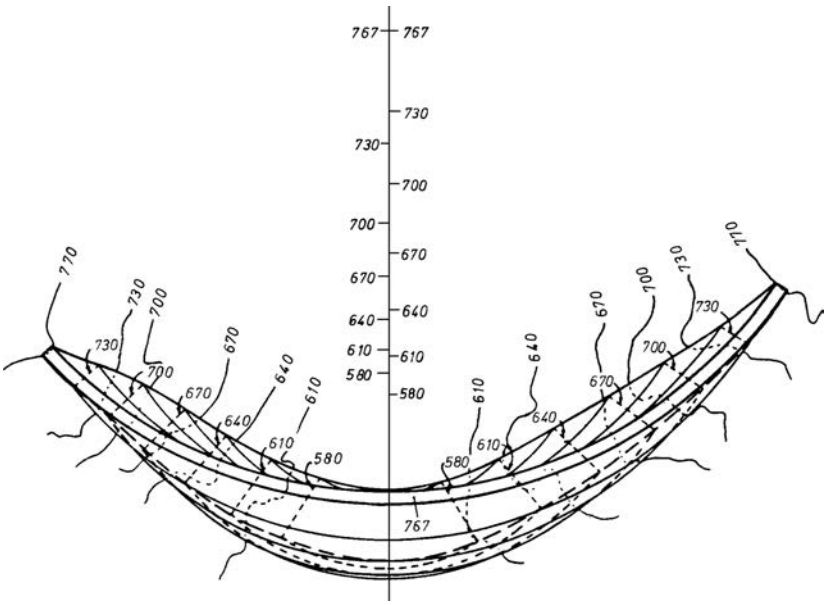

Figure 20.37 Arch dam with arches of constant thickness, constructed from two centres (after USBR, 1977a).

A horizontal arch is constructed together with a circular arch, drawn from a different centre for the left and the right side. In order to maintain continuity, both groups of centres must lie in one vertical referent plane. In the presented example, the radius of the axis of the dam's crest is equal for both the left and for the right side, but in a general case, it could be different; that is to say, the centres of the left side and those of the right side need not necessarily coincide. In the case of this construction, the individual arches are of a constant thickness (Golzé, 1977; USBR, 1977a).

The arches constructed from two centres, in case of need, can be of a variable thickness, i.e. at one and the same side, the internal and external radius of the arch can be drawn from different centres. In this case, as well, continuity is maintained, in which all centres lie in one and the same vertical plane. An example of such a construction is given in Figure 20.38.

There are even more complex constructions for arch dams. A three-centred (or elliptical) dam is constructed with arches at which both the external side and the internal side are constructed with a set of three different radii. Usually, the radius is shorter in the central part of the arch, and is longer in the vicinity of the joint with the bank. Arches may also, in this case, be of constant or variable thickness (Golzé, 1977; Serafim & Clough, 1990; USBR, 1977a).

Polycentric dams consist of arches constructed from a number of centres, so that in practice, one may obtain exactly the required form of the arches, that is to say, of the dam as a whole.

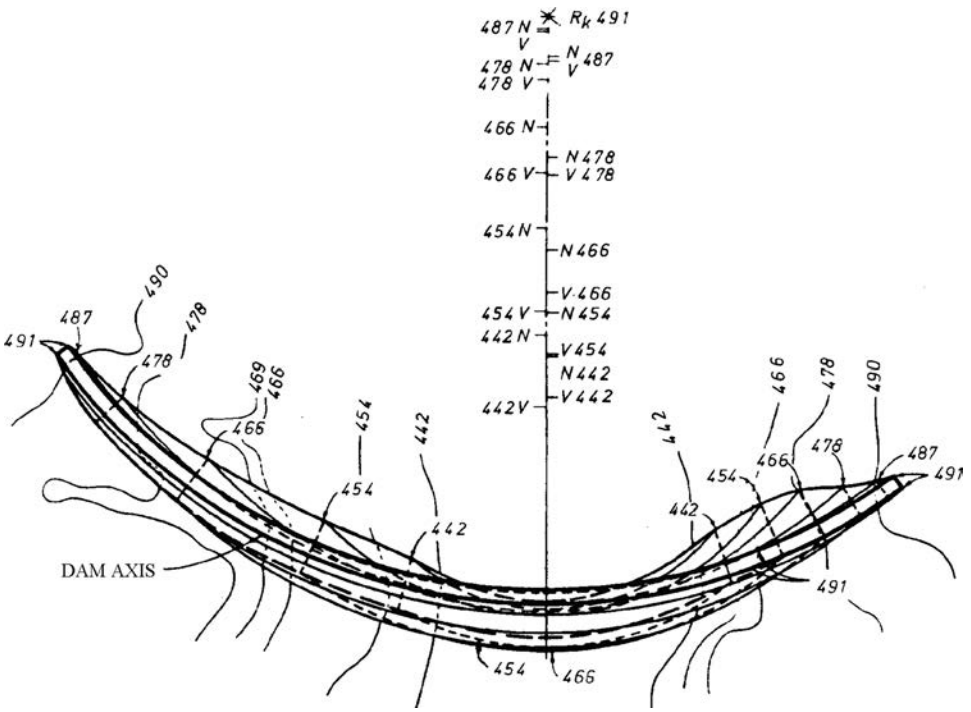

Figure 20.38 Arch dam with arches of variable thickness, constructed from two centers: $N = E$ = external radius, and $V = I$ = internal radius (after USBR, 1977a).

20.4 STRUCTURAL DETAILS OF ARCH DAMS

Crest of the dam. In the non-overflow section of the dam, this is constructed with a thickness of 1.5 m to 4 m. The freeboard of the crest is performed in the same way as for gravity dams. The overflow section is shaped hydraulically and, depending on whether overflow is free (uncontrolled) or controlled (with gates), we obtain an appropriate form and width of the crest, which has been illustrated through examples of arch dams, given in the various sections of Chapter 20. If a roadway is to pass over the dam, then most often, special cantilevered extensions are constructed on the crest.

Overfall spillway. In constructing an arch dam, one should always analyze the possibility of executing a spillway over its body, which, in many cases, is more economical than a spillway in the bank.

Owing to the small thickness of arch dams, it is not possible to achieve shaping of the overflow part, as in the case of gravity dams by means of taking away the water to the downstream surface of the ground (an exception to this are the thicker arch-gravity dams). This taking away of the water, similar to massive dams, can be achieved by constructing a special slab, supported on walls, as is shown in the example in Figure 20.39a. A spillway with a free overfall of water (free overfall or straight drop spillway) following the overflow through a specially shaped crest, which enables throwing off

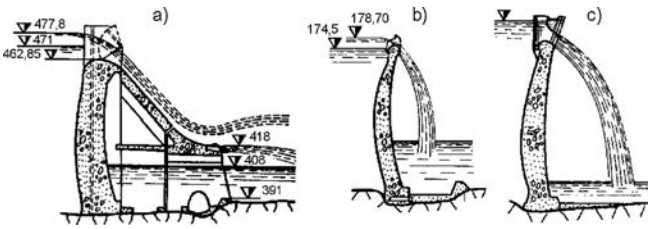

Figure 20.39 Overflow dams in Portugal (after Grishin et al., 1979). (a) Picote, 1958, $H = 100$ m; (b) Bouca, 1955, $H = 65$ m; (c) Salamonde, 1953, $H = 78$ m. (1) slab; (2) retaining wall.

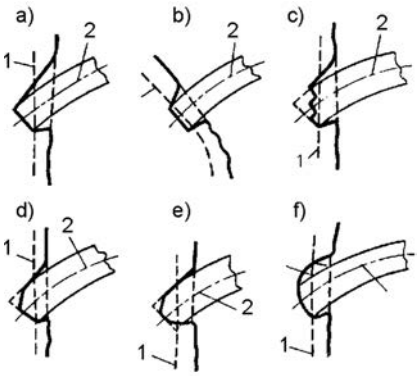

Figure 20.40 Achieving composite construction of horizontal arches and bank. (1) Boundary of sound rock; (2) axis of arch.

the jet farther away from the dam, is more economical (Fig. 20.39b). The overflow depth of the water layer in such a case amounts to 2–4 m. Instead of a spillway over an open surface, the overflow may be performed through an opening, positioned a little below the maximum water level (Fig. 20.38c). In this way, it is possible to increase the overflow capacity of the spillway (higher spillway depth of water); there is also avoided the need for a bridge over the spillway. The foundation in front of the dam upon which the water jet falls, is strengthened (usually with concrete), or else a stilling basin may be added, as is shown in the example in Figure 20.24.

With arch dams, in some cases, there are also made deep openings for evacuation of flood flow waters, while depth outlet structures and intake structures are customary with every arch dam, in which the zone around the opening is reinforced. Gates on the water-conveying structures are most often located at the downstream side of the dam, while only a protective trash rack is sufficient at the upstream side of the dam.

Achieving composite construction of the dam with the bank and foundation. Achieving a composite action of the horizontal arches and the rock in the bank is most frequently performed in a radial plane (Fig. 20.40a, b). Such a joint is safe and requires minimum excavation into the rock. In the case of thicker arches, especially if in the zone of the joint they form a more acute angle with the chord, then it is more rational to build a step like joint (Fig. 20.40c), in which case the individual steps have

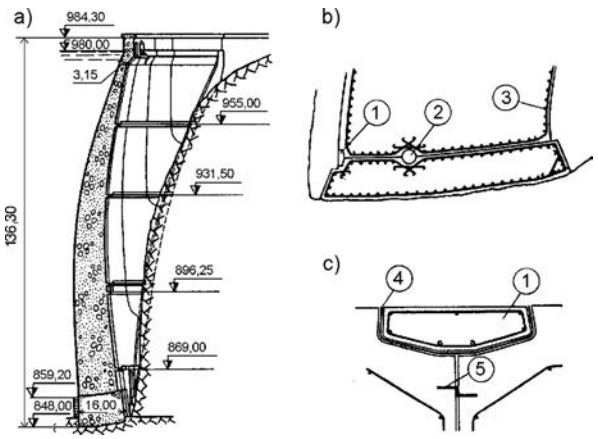

Figure 20.41 Lumiei dam (Italy), $H = 136.3$ m, $L/H = 1.12$ (after Grishin et al., 1979). (a) Cross-section; (b) contour joint; (c) detail for sealing a joint. (1) Reinforced concrete block; (2) drainage; (3) reinforcement; (4) insulation layer; (5) copper plate, 10 mm.

a radial direction. In such a case, there is a danger of concentration of stresses in the zone of the joint, and that is why other forms of joint are also employed, with slight variations (Fig. 20.40d–f).

The dam can achieve composite construction with the banks and foundation, as well as with a concrete foundation, separated from the dam's body by means of a contour joint. In such a case, the arch dam rests on the foundation through a suitably shaped seat, inclined towards the force's upstream side, in order to facilitate the resultant force's being perpendicular. An example of a structural shaping of a contour joint is given in Figure 20.41, as used in the Lumiei dam (Italy), standing 136.3 m high. In a similar way, one may achieve composite construction with a concrete plug or with a massive block in the bank.

An arch dam must be carefully jointed with the foundation. The fissured and weakened surface layer of the rock should be removed, while the remaining significant fissures should be cleaned and filled with concrete. In case of need, the foundation should be strengthened by means of grouting to a depth of 10–30 m, depending on the condition of the rock and the height of the dam.

As with other types of dams, we also include a grout curtain – here across the entire foundation and banks. The grout curtain is constructed close to the upstream side and can be either vertical or inclined towards the water (Fig. 20.42a–c). The second position is better, since it reduces the seepage area below the dam and increases the stability of the foundation. In selecting the position of the grout curtain, it is also necessary to take into consideration the distribution of stresses in the interface dam – foundation. Namely, the grout curtain must not be positioned in the zone of tension (if any), in which case it should be shifted somewhat downstream (Fig. 20.42d). The depth of the curtain depends on the condition and quality of the rock. Behind the grout curtain there is constructed a vertical drainage, with a drainage gallery, which can, at

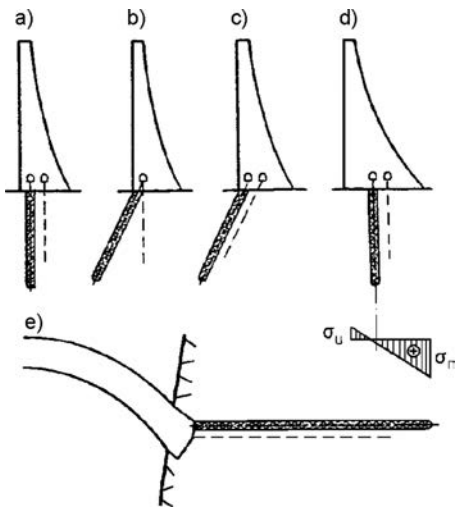

Figure 20.42 Positions of grout curtain and vertical drainage.

the same time, also be a grouting gallery (b). The grout curtain and drainage should also be extended into the banks, outside the dam (Fig. 20.42e).

Structural joints. In order to prevent fissures due to temperature variations in the concrete, or possible minor settlements, during construction the dam is divided into blocks separated by vertical (radial) joints, which, for providing monolithism of the dam, are filled during the lowest possible temperature of construction. Artificial cooling of the blocks may also be used for that purpose. The spacing between the structural joints ranges from 7 to 15 m, rarely more.

According to the method of filling, we can distinguish two types of joints: those which are concreted, and those which are cemented. The first are wider – 0.7–1.2 m (Fig. 20.43a) and they are filled with a special dense concrete. Cemented joints are used more frequently. They are of small width, sufficient for dilatation of the blocks and, according to their structure, they are analogous with the joints used in massive dams (Fig. 20.43b). In the course of constructing the dam, in the joints are placed perforated pipes or pipes with special valves, which serve for the grouting of joints with cement grout, squeezed under pressure. In performing this process, the arches to some extent are loaded under pressure, and that reduces tensile stresses, which would occur in the dam in the course of its service. There is a deficiency of thin joints – during their filling, an insight into the quality of the accomplished water-impermeability is prevented.

Combined joints are used in some cases (Fig. 20.43c). Those are wide joints (1–1.5 m), which are first concreted, and then cemented. This leads to accomplishing better water-impermeability. In cases of arch-gravity dams, in addition to the transverse (radial) joints, in the lower, wider part, there are also constructed longitudinal joints of the same structure.

Waterstops (rubber or sheet metal) that are employed with arch dams, according to their structure, are identical to those used for gravity concrete dams.

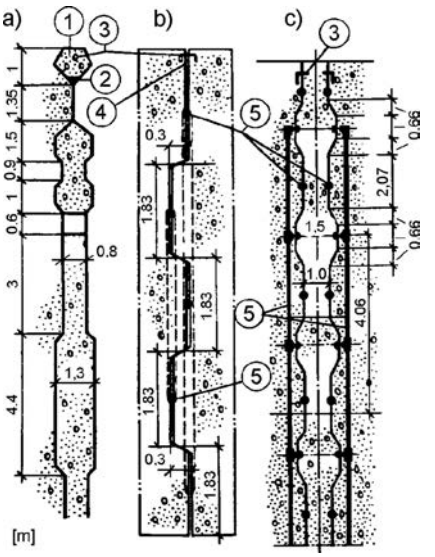

Figure 20.43 Structural joints for arch dams. (1) Reinforced concrete dowel; (2) bituminous sealing compound; (3) metal waterstop; (4) asphalt filling; (5) grouting pipes.

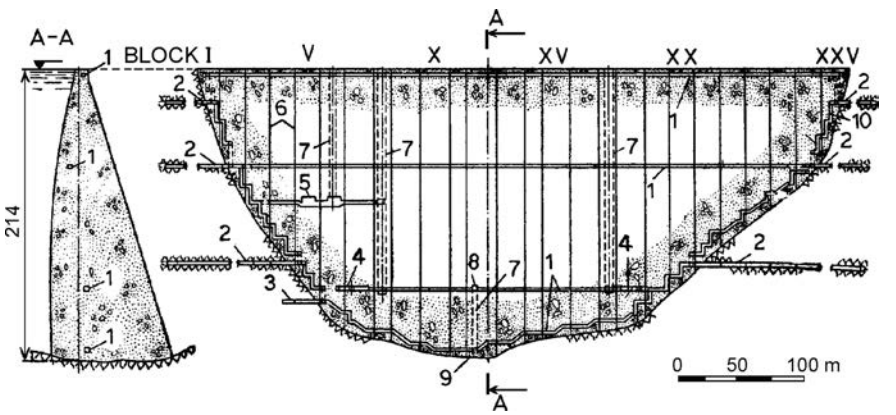

Figure 20.44 Glen Canyon dam (USA). (1) Inspection galleries; (2) tunnel in bank; (3) exit from gallery; (4) access galleries to power house; (5) gallery for gates of outlet structure; (6) joints; (7) manhole; (8) pumping station; (9) pit for collecting filtrated water; (10) stairway.

Figure 20.44 presents a cross-section (a) and longitudinal section (b) of the Glen Canyon arch-gravity dam (USA), completed in 1966, and standing 216 m high. By means of vertical joints, the dam is divided into 26 blocks, up to 28 m wide.

The old Matka dam also serves as an additional example of the treatment and closure (sealing) of joints (Fig. 20.9).

Inspection galleries. For controlling the behaviour of the dam in the course of its service, inspection galleries are constructed at a vertical spacing of 15–40 m. A similar function is played by the cantilevered service bridges at the downstream side, which, with very thin dams, are also the only means of communication.

Materials for arch dams. In modern practice, arch dams are exclusively built of concrete, which must be water-impermeable and have a corresponding strength. In the case of arch dams, there occur high stresses: compressive stresses up to 13 MPa and tensile stresses up to 3 MPa. During the last 20 years, apart from the conventional concrete, roller-compacted concrete was also used for construction of some arch dams (see section 20.5).

Reinforcing for concrete arch dams is accomplished only in the zones of high local stresses, as, for example, around outlet and overflow openings, galleries, etc. Reinforcing is also added across the surfaces of the structural joints, for instance in contour joints (Fig. 20.41), in the uppermost arches for taking on the stresses caused by seismic forces, and in some other sensitive places, depending on the structure of the dam and the local conditions of the dam site.

20.5 ROLLER-COMPACTED CONCRETE ARCH DAMS

Following the successful application of roller-compacted concrete for construction of gravity and arch-gravity dams, research was carried out in China at the end of 1980s and the beginning of 1990s with the aim of investigating the possibility of applying RCC to the construction of arch dams. As a result, after the complement of the two RCC arch-gravity dams in South Africa in 1988 and 1990 respectively, the first RCC arch-gravity dam *Puding* in Guizhou Province ($H = 75$ m, $L = 196$ m, ratio $B/H = 0.38 > 0.3$) in China was successfully completed in June 1993.

There were different opinions on the applicability and feasibility of thin RCC arch dams because although the concrete cost is low, a large construction yard is still needed. Therefore money-saving aspect is rather questionable. But RCC arch dams were still attractive for Chinese engineers as this technique can save cement. Thereafter, the first RCC arch dams were constructed: *Wequanpu* dam (1994, $H = 49$ m, $L = 188$ m, $B/H = 0.28$) and *Xibinxi* dam built in Fujian Province (1995, $H = 63.5$ m, L = 93 m, $B/H = 0.19$). These two projects have proved both the safety and economy of the pure RCC arch dam (Jiazheng & Jing, 2000).

Xibinxi dam was designed in 1993 with a new shape based on simulation calculations made during the above-mentioned research works. The dam is 63.5 m high, with a maximum thickness at the base of 12 m (Figs. 20.45 and 20.46). Thus the thickness-to-height ratio is 0.19 which is near the upper limit ($B{:}H = 0.2$) for a thin arch dam (see section 20.1). The dam site is very narrow, having a ratio L/H of 1.47. Xibinxi dam is designed as a single center circle arch dam with upstream slope 1:0.082 (Fig. 20.46, section A-A). The overflow part of the dam is constructed by conventional concrete, which is also applied for the contact layer between the RCC and foundation. The dam was built on weak weathered and jointed sandstone. The dam site is located in a rainy area with mean annual air temperature of 18°C. There is a transverse joint in the upper part of the dam, located at about two-thirds of the dam's height, but there are no other through joints in the lower part of the structure. The dam was rapidly built to

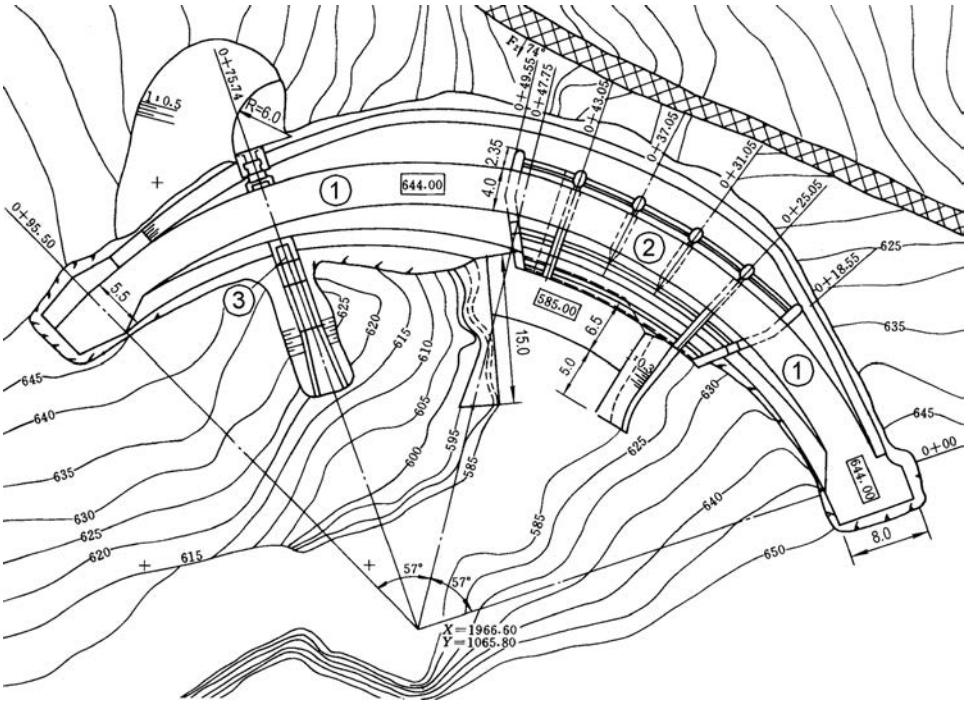

Figure 20.45 Plan of Xibinxi dam (China, 1995, $H = 63.5$ m), one of the first pure RCC arch dams (after Jiazheng & Jing, 2000). (1) RCC arch dam body; (2) overflow part of the dam; (3) outlet.

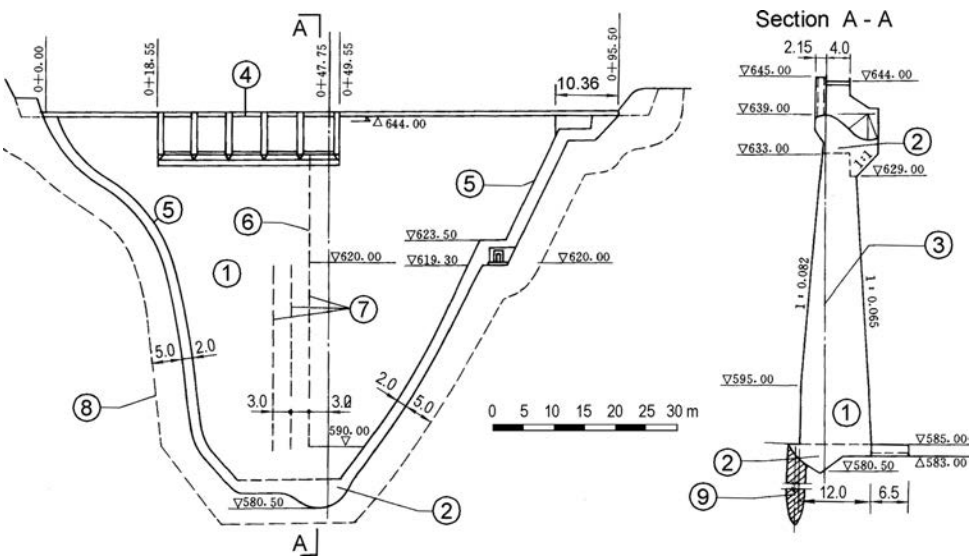

Figure 20.46 Longitudinal section and cross-section (A–A) of the Xibinxi dam (after Jiazheng & Jing, 2000). (1) RCC arch dam body; (2) conventional vibrated concrete; (3) vertical dam axis; (4) overflow part of the dam; (5) joint on upstream face; (6) construction joint; (7) joint on downstream side; (8) downstream excavation line; (9) grout curtain.

Table 20.2 Roller-compacted concrete arch dams constructed in China.

RCC arch dam	Built [year]	Height H [m]	Length L [m]	Ratio B/H	Dam volume $[m^3 \times 10^3]$ RCC	Dam volume $[m^3 \times 10^3]$ Total	Cement + pozzolan $[kg/m^3]$	Reser. vol. $[m^3 \times 10^6]$
Wenquanpu	1994	48	176	0.28	55	63	110 + 68, 69 + 85	7
Xibinxi	1995	63.5	93	0.19	25	33	80 + 120, 79 + 105	9
Sishanping	1995	56	147			18		3
Fengxiangxia	1998	60	158			770		8
Kengxiashan	1998	34	80					1
Wajin	1999	47	235			240		7
Shankou No 3	2001	57	179		90	119	105 + 86, 63 + 80	48
Shimenzi	2001	109	176	0.27	188	211	93 + 110, 62 + 110	80
Shapai	2002	132	250	0.24	365	392	115 + 91	18
Nankengyuan	2003	34	114					1
Junxi II	2003	69	192					6
Linhekou	2003	100	311	0.28	229	293	74 + 111	147
Wangkang	2004	56	155			38	15	
Shanggou	2004	39	176					1
Liubo	2004	70	258		130	168		51
Yujianhe	2005	81	180		105	155		11
Zhaolaihe	2005	107	206		166	254	84 + 126, 126 + 103	70
Qilinguan	2005	77	132		45	55		14
Niuqiao	2007	62	201			710		26
Longqiao	2007	95	156		135	160		26
Shaba	2008	87	149		67	90		99
Xuanmiaoguan	2008	80	243		75	95		41
Xiaqiao	2008	68	213		172	226		49
Maobaguan	2008	66	120		81	106		2
Saizhu	2008	72	160		107	115		3
Huanghuazhai	2008	110	275		280		52 + 96	1748
Bailianya	2009	104	348	0.25	485	560	72 + 108	453
Weihou	2009	82						133
Qingxi	2009	81						98
Tianhuaban	2009	113	160		182	360		79
Dahuashui	2010	135	306		550	650	81 + 81, 94 + 94	277
Yunlonghe No 3	2010	135	119		182	207		44
Yunkou	2010	119	152			205		
Yangjiayuan	2010	68						78
Sanliping	2012	133	185					499
Qinglong	2012	140						28
Nankanghe No 2	2012	68						31
Shankouyan	2013	99						105
Linxihe	2013	74	146					52
Luntan	2013	90	377					180

Note: *B* is the maximum thickness of the dam.

two-thirds of its eventual height for flood protection. In the cementitious material high fly ash content was used, with a view to obtaining a low-temperature, high-strength RCC. This allowed continuous placement without relying on heat loss through the concrete surfaces. To reduce tensile stress and to integrate any cracks into the structure,

artificial joints were provided at the upstream abutment and downstream arch crown aimed to release stresses caused by temperature and water pressures (Liu et al., 2002).

The roller-compacted concrete at the Xibing dam in a quantity of 25,000 m^3 was placed in only six months in 1995. During the same year, the reservoir was impounded, and for the sake of increasing power production, for four years the dam continuously impounded flood waters which brought the reservoir level higher than the exceptional water level. After that no cracks have been found. Some defects between the layers occurred during construction, most likely as a result of inadequate construction equipment and the prolonged concrete placement time. The influence of these defects on the transfer of arch stress is not considered significant, but the defects were grouted, however, to prevent leakage later.

After this beginning, let us say experimental, but successful period from 1990 to 1995, Chinese dam engineers have been encouraged to build new RCC arch dams. Thus, up to 2013 around 40 dams of this type have been completed in different provinces, under different geological, seismic and climate conditions. Some data of these dams, available to the author, are shown in Table 20.2. It can be seen that 12 of these dams are higher than 100 m, the highest reaching 140 m. Some of these dams were constructed in unfavorable conditions, for example the *Shimenzi* dam. This 109 m-high dam was constructed in a very cold area of North Xinjiang (the annual mean temperature is 4.1°C) and on weak foundations (argillo-calcareous cemented conglomerate, with elastic modulus of only 4 GPa). Limited by the carrying capacity of the rock, the maximum thickness of the dam base was enlarged to 30 m. Thus, the width-to-height ratio is 0.27, and the dam belongs to the thick arch dam type.

Generally, it can be said that regarding the composition of the concrete mixture and cementitious content the well-established rules at RCC gravity dams have been followed. The same is valid for the methods applied for improvement of the dam watertightness. To prevent cracks caused by changing of temperature transversal joints are used. The spacing width between joints varies with the region and climate, in the range from 16 to 80 m. Before the reservoir impounding grouting of joints was performed to ensure the structure to work as a whole. In recent time a special grouting system have been introduce to repeat the grouting of joints if these are again opened under the influence of the higher temperature in dam body than the stable temperature field.

20.6 STATIC ANALYSIS OF ARCH DAMS

From a static viewpoint, arch dams represent a spatial structure with variable curvature and thickness in the vertical, and sometimes also in the horizontal direction, with complex geometric and static boundary conditions. Because of that, obtaining an exact solution is practically impossible or else it is associated with significant mathematical difficulties. That is why it is understandable that approximate methods are used, with many simplifications.

In analysing arch dams there are taken into consideration the same forces as in the case of gravity dams, in which seepage uplift is taken into consideration only with arch-gravity dams. Of particular importance are temperature variations (Castellanos & Martin, 1995; ICOLD, 1994a; Meyer & Mouvet, 1995), which, in the case of a

statically indeterminate system of the arch dam, can cause significant forces which can derange the monolithism of the structure. In the case of arch dams, significant forces can be generated by possible deformations of the bank and the bottom of the reservoir, originating in the vicinity of the dam under the effect of water pressure. The seismic forces, as well, should be taken into consideration, and they are especially dangerous if they have a direction transverse to the river valley.

The methods which are used for the static analysis of the arch dams, in most cases, have the function of checking-up the stresses and deformations for some assumed dimensions of the structure. The most frequently used methods, along with short descriptions, are presented in the continuation.

20.6.1 Method of independent arches

According to this method, the concrete vault of the arch dam, by means of horizontal planes, is divided into a number of horizontal arches, in which it is assumed that they work independently of one another. The calculation of each individual arch may be performed (under the assumption that arches are thin) according to the well-known *cylinder formula*:

$$b = R_n - R_v = \frac{h\gamma_w R_n}{\sigma_p} \tag{20.1}$$

where h = height of the water column of the considered arch; and σ_p = permissible compressive stress in the concrete.

With an assumed thickness of the arch b, the compressive stress in the thin arch σ_h, (according to this method, the arch is treated as a ring) will be:

$$\sigma_h = \frac{h\gamma_w R_n}{b} \tag{20.2}$$

By means of formulae (20.1) and (20.2), there has been taken into consideration only the force of the hydrostatic pressure of water, so that the obtained solution is extremely rough, and it can be used only in the initial stage of designing. Another essential deficiency of this method is that it does not take into consideration the mutual interaction of arches and the restraint of the dam in its foundation and abutments.

An extremely simplified assumption for discrete, independent horizontal arches, which are free of any mutual interaction, is clearly indefensible. The other assumption, which further on simplifies the problem, stating that the radial deformations are uniformly distributed along the length of the arch, is also indefensible; first, owing to the restraint of the arch into the banks, and, second, owing to the fact that the span of the arch will get a certain increase due to the elastic deformations of the abutments. In fact, the deflection of the arch leads to a reduction in the value of σ_h in the vicinity of the arch crown and its progressive increase at the abutments.

Theoretically, the thickness of the arches, due to the cited reasons, should decrease towards the crown and increase towards the abutments. In practice, it is customary on every determined level to take a constant thickness of the arch, when it is a question of dams with a single curvature. This, clearly, leads to maximum tangential stresses

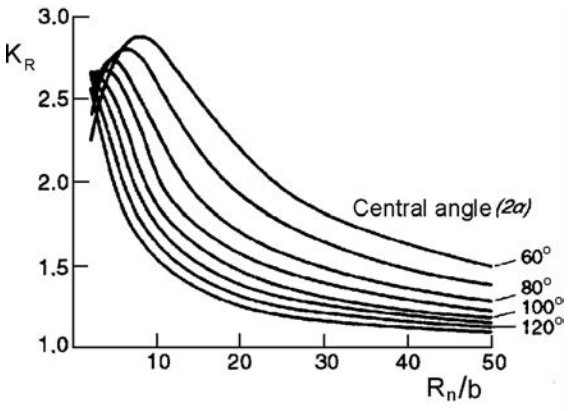

Figure 20.47 Correction factor for calculation of stresses in arch abutments (after Novak et al., 2001).

in both abutments. If we assume that, with the loading, there does not come about a reaching of the bearing capacity of the abutments, then one can calculate the normal compressive stress in them by introducing the correction factor K_R:

$$\sigma_h = \frac{K_R h \gamma_w R_n}{b} \tag{20.3}$$

The factor K_R is a function of the central angle 2α as well as of the ratio R_n/b. Figure 20.47 yields curves from which it is possible to read out the value of the correction factor, as a function of the cited elements.

The question of the magnitude and distribution of stresses in the arch abutments is of great importance for the stability and the safe work of the dam, as a whole. It can effectively be solved only with the application of modern methods.

The calculation of thin arches can be more accurately performed in accordance with the methods from the theory of structures, as statically indeterminate systems. This calculation reduces to determination of the unknown quantities, X_1 and X_2, from the canonic equations:

$$\begin{aligned} X_1\delta_{11} + X_2\delta_{12} + \delta_{1p} &= 0 \\ X_1\delta_{21} + X_2\delta_{22} + \delta_{2p} &= 0 \end{aligned} \tag{20.4}$$

while, the determination of the normal forces, N, and moments, M, in sections of the arch, according to the formulae:

$$\begin{aligned} N &= N_p + X_2 \cos\alpha \\ M &= M_p + X_1 + X_2 y \end{aligned} \tag{20.5}$$

as well as the normal stresses from the expression for eccentric pressure:

$$\sigma = \frac{N}{F} \pm \frac{M}{W} \tag{20.6}$$

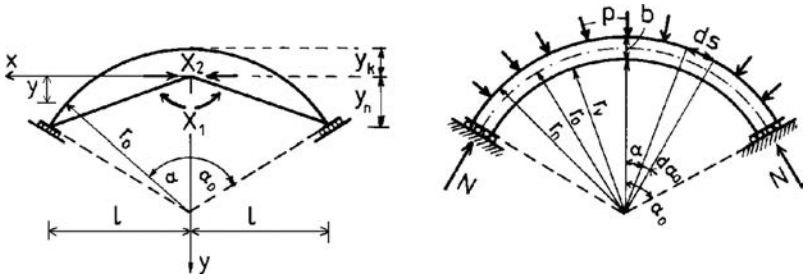

Figure 20.48 Scheme for calculation of a thin arch.

For thin arches, for which $r_0/b > 3$, the unit displacements and displacements caused by loadings, are determined according to the formula:

$$\delta = \int_0^s \frac{M_i M_k}{EJ} ds + \int_0^s \frac{N_i N_k}{EF} ds \tag{20.7}$$

In calculating the arches for the effect of water pressure p, the statically indeterminate system should suitably be transformed into a basic statically determinate system, in the form of a freely supported arch, by inserting the statically indeterminate values of $M_a = X_1$ and $N_a = X_2$ in the elastic centre of the rigid cantilevers (Fig. 20.48a). And since $\delta_{12} = \delta_{21}$, then in such a case, it follows (Fig. 20.48b):

$$N_p \sin \alpha_0 = \int_0^{\frac{s}{2}} p \cos \alpha \, ds = \int_0^{\alpha_0} p r_n \cos \alpha \, d\alpha = p r_n \sin \alpha_0 \tag{20.8}$$

If we substitute $N_p = p r_n$ and $M_p = 0$, it follows:

$$M_a = 0; \qquad N_a = \frac{r_n \int_0^s \cos \alpha \, ds}{\int_0^s \frac{y^2}{EJ} ds + \int_0^s \frac{\cos^2 \alpha}{EF} ds} = A \cdot p \tag{20.9}$$

where A is the coefficient which is obtained from the boundary conditions.

By means of formulae (20.6), (20.8), and (20.9), and taking $F = b$ (two-dimensional treatment of the problem), and $W = b^2/6$, we obtain the expression for stresses:

$$\sigma = \left(\frac{r_n + A \cos \alpha}{b} \pm \frac{Ay}{e^2} \right) p = \sigma'_a p \tag{20.10}$$

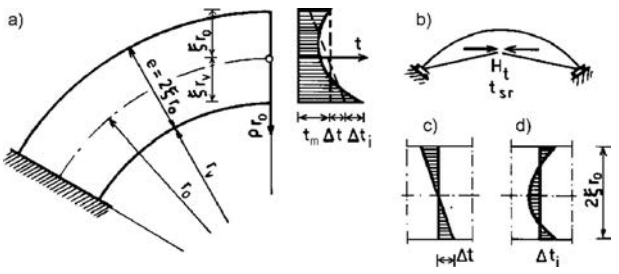

Figure 20.49 Schemes for calculation of temperature stresses in the arch. (a) Temperature distribution across arch thickness; (b) scheme for determination of stresses due to t_m; (c) due to Δt; (d) due to Δt_i.

The expression in brackets, denoted with σ'_a yields the unit stresses in the arch (at $p = 1$). For a certain angle α or ordinate y, σ'_a depends only on the geometric parameters of the arch.

According to this method, in the calculations we can also introduce the influence of temperature variation; in the case of thin, restrained (fixed) beams, this is very important. Temperature variations in the arch appear due to the effect of temperature on the environment-water in the reservoir and the surrounding air. In a general case, the diagram for distribution of temperature across the thickness of the arch can be represented with the expression (Fig. 20.49):

$$t_i = t_m + \frac{\Delta t}{\xi}\rho + \Delta t_i \tag{20.11}$$

where t_m is the mean temperature of the arch across its thickness; Δt_i are the ordinates of the curvilinear part of the diagram of temperature; $\xi = (r_n - r_v)/2r_0$ is the relative thickness of the arch; ρ the relative coordinate that varies from $-\xi$ to $+\xi$, in which $r_n = r_0(1 + \xi)$; and also, $r_v = r_0(1 - \xi)$.

In the determination of t_m, there also must be taken into consideration the temperature at closing of the joints, which can be achieved by means of artificial cooling.

The temperature across the thickness of the arch t_m can vary both uniformly and non-uniformly. A uniform variation of temperature causes stresses and deformations in the arch analogous to the uniform pressure of the water, with the difference that, at temperature deformations, there is no external loading, so that it is $N_p^t = 0$ and $M_p^t = 0$, and what occurs is only the force H_t with a direction towards the elastic centre. In this, the force H_t in relation to the force H_p, caused by the uniform water pressure, behaves like the deformation of an element of the arch ds, caused by the temperature Δds_t and due to the pressure of water Δds_p:

$$\frac{H_t}{H_p} = \frac{\Delta ds_t}{\Delta ds_p} = \frac{EF}{N_p \alpha_t t_m} \tag{20.12}$$

where α_t is the coefficient of temperature expansion.

Substituting $N_p = p \cdot r_n$, $F = b$ and using the formula (20.9), it follows:

$$H_t = AE\alpha_t \frac{b}{r_n} t_m \tag{20.13}$$

By means of a known force H_t we can determine the moments and normal forces in any section, through the relationships:

$$M_t = H_t y; \quad N_t = H_t \cos \alpha \tag{20.14}$$

while stresses can be determined with the expression:

$$\sigma_{tav} = \frac{N_t}{b} \pm \frac{M_t}{W} \tag{20.15}$$

The sign '+' relates to the upstream side in which, at an increase of temperature there occurs compression, while for a drop in temperature, there occurs tension. At the downstream side, the stresses will have an inverted sign.

A non-uniform change in temperature Δt, tends to cause buckling deformations in the section of the arch (Fig. 20.49c). In the case of a rigid joint between the arch and the rock, deformations cannot occur; therefore, the magnitude of stresses will be:

$$\sigma_{\Delta t} = E\,\alpha_t \frac{\Delta t}{\xi} \rho \tag{20.16}$$

For mean values of E and α_t, it will be $E\alpha_t = 0.2$ MPa and so, at the external side of the arch ($\rho = \pm\xi$), the stresses will be:

$$\sigma_{\Delta t} = \pm 0.2 \Delta t \quad [\text{MPa}] \tag{20.17}$$

At the side with a higher temperature we have $+\Delta t$ and compressive stresses, while at the opposite side $-\Delta t$, and tensile stresses. Such stresses will appear in any section along the length of the arch, and it is particularly important that they be calculated where they have a negative reflection on the summary stresses.

Temperature stresses caused by the curvilinear part of the diagram Δt_i (Fig. 20.49d) may be determined with the general expression:

$$\sigma_{\Delta t_i} = \frac{E\,\alpha_t}{1 - \nu} \Delta\, t_i \tag{20.18}$$

in which ν is Poisson's ratio.

20.6.2 Method of central cantilever

This method takes into consideration the restraint of the dam in its foundation in such a way that the dam is divided not only into horizontal arches, but also into vertical cantilevers, restrained in the lower part of the foundation shown by vertical dashed lines (Fig. 20.50). In that, it is assumed that a part of the hydrostatic pressure is taken on by the system of arches, while another part is taken on by the system of cantilevers.

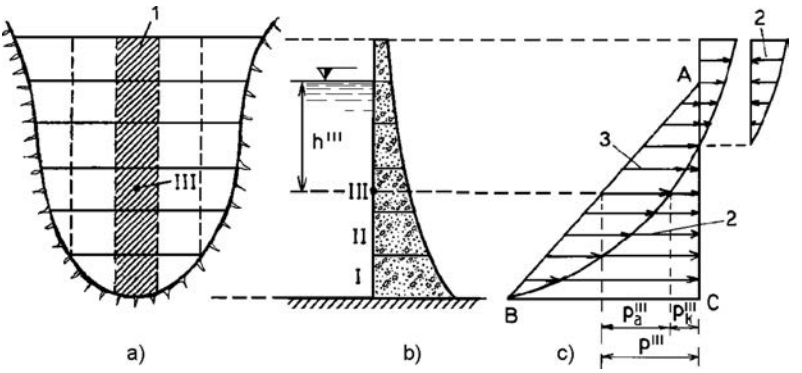

Figure 20.50 Scheme for the central cantilever method. (a) Longitudinal section; (b) cross-section; (c) distribution of hydrostatic pressure. (1) Central cantilever; (2) diagram of hydrostatic pressure falling off to the central cantilever; (3) to the arch.

In that way, the hydrostatic pressure, shown by the diagram ABC in Figure 20.50c, should be distributed between the arches and cantilevers adequately to their rigidity, so that, at all points in the vault, the deflections of the arches and deflections of the cantilevers should be equal.

For simplification, only the central cantilever is analysed, which is in the highest section (hatched part in Fig. 20.50a), and which is examined together with all arches. If, for example, at the central point of arch III, there acts the hydrostatic pressure $p^{III} = \gamma_w \cdot h^{III}$, then that pressure should be distributed between the central cantilever and the arch III, as is shown in Figure 20.50c. The arch is assigned the value p_a^{III}, and to the cantilever p_k^{III}, in which:

$$p^{III} = p_a^{III} + p_k^{III} \tag{20.19}$$

Now, it is possible to make up the equations of deflections for the arch III, as well as for the central cantilever, and then, with their equalizing, we can obtain the values of p_a and p_k, for a previously assumed section of the dam. In that way, it is possible to obtain the values of p_a^I, p_a^{II}, p_a^{III} ... and p_k^I, p_k^{II}, ... By means of such obtained pressures, we calculate the stresses in various places in the dam.

As can be seen from Figure 20.50c, in the lower part of the dam, the greater part of the hydrostatic pressure is taken on by the cantilevers, while in the upper part, it is taken on by the arches. In the upper part of the dam, in equalizing the deflections, the loading should be undertaken with the opposite course (direction).

In using the central cantilever method, it is also possible to take into consideration the forces due to self-weight of the cantilever and also due to temperature variations. Let us now examine the joint work of an arch and a cantilever due to temperature effects, under the influence of which there occur temperature stresses in the arch $\sigma_{t_m}^a$, $\sigma_{\Delta t}^a$ and $\sigma_{\Delta t_i}^a$, caused respectively by t_m, Δt and Δt_i as well as in the cantilever $\sigma_{\Delta t_i}^c$ due to Δt_i. At the same time there appear temperature displacements in the arch w_t^a due to t_m and of the cantilever w_t^c due to Δt (Fig. 20.51). And since, because of the

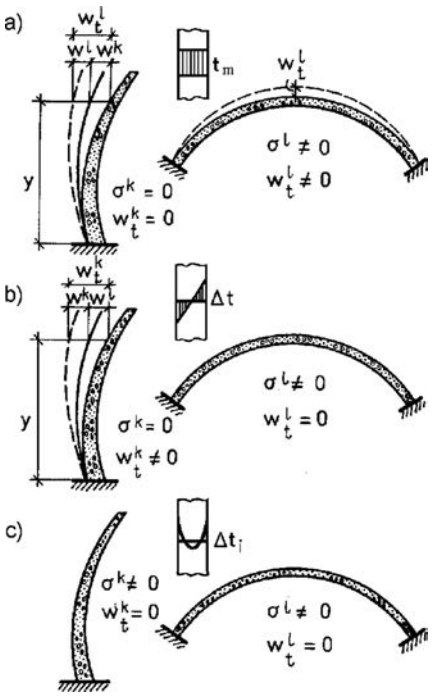

Figure 20.51 Schemes for temperature deformations in elements of an arch dam (after Grishin et al., 1979). (a) Due to t_m; (b) due to Δt; (c) due to Δt_i.

restraint of the arch dam, displacements cannot freely develop, between the arches and cantilevers there occur forces of reciprocal action $p_t^a = -p_t^c$, causing additional stresses, σ^a in the arches and σ^c in the cantilever. In that way, the temperature stresses in the arches will be:

$$\sigma^a = \sigma^a_{t_m} + \sigma^a_{\Delta t} + \sigma^a_{\Delta t_i} + \sigma^a_t \tag{20.20}$$

while in the cantilever they will be:

$$\sigma^c = \sigma^c_{\Delta t_i} + \sigma^c_t \tag{20.21}$$

The stresses $\sigma^a_{t_m}$, $\sigma^a_{\Delta t}$ and $\sigma^a_{\Delta t_i}$ are determined in the same way as in the method of independent arches, while $\sigma^c_{\Delta t_i}$ according to the formula:

$$\sigma^c_{\Delta t_i} = \frac{E\alpha_t}{1-\nu}\Delta t_i \tag{20.22}$$

The stresses σ^a_t and σ^c_t can be determined from the condition for joint work of the arches and cantilevers, by solving the differential equation for bending of a cantilever:

$$[EJ(y)w^{c''}(y)]'' = p_c(y) \tag{20.23}$$

where $p_c(y)$ is the load on the cantilever. In this specific case it will follow:

$$p_t^c + p_t^a = 0; \quad w_t^a - w_t^c = w^c - w^a \tag{20.24}$$

where w_t^a and w_t^c are the deflections of the arch and the cantilever in their section due to the forces of reciprocal action between the arches and the cantilever; w_t^c is the temperature displacement of the independent cantilever in the section y. It is assumed that the deflection will have a positive sign if it is directed towards the downstream side.

The forces of mutual action between the arches and the cantilever are determined by means of the expression:

$$p_t^c = -p_t^a = -kw^a = k(w_t^a - w_t^c) - kw^c \tag{20.25}$$

where k is the coefficient of elasticity of the foundation.

Accordingly, the differential equation can be written in the following form:

$$[EJ(y)w^c(y)]'' + k(y)w^c(y) = k(y)[w_t^a(y) - w_t^a(y)] \tag{20.26}$$

or, by performing substitution,

$$p_t(y) = k(y)[w_t^a(y) - w_t^a(y)] \tag{20.27}$$

it is finally obtained

$$[EJ(y)w^{c\prime\prime}(y)]'' + k(y)w^c y = p_t(y) \tag{20.28}$$

By solving the above differential equation[3], it is possible to obtain the deflections and loads due to temperature effects, with the following inter-relationships:

$$w^a = w^c - (w_t^a - w_t^c) \tag{20.29}$$

and,

$$p_t^a = kw^a; \quad p_t^c = -p_t^a \tag{20.30}$$

From the obtained loads, it is now possible to calculate the stresses σ_t^a and σ_t^c in the arches and in the cantilever.

20.6.3 The trial-load method

The Trial-Load Method originated in the USA even before World War II, and in the subsequent period it has been improved and upgraded. This is a three-dimensional method, which is based on the assumption that, by means of horizontal and vertical radial planes, the dam is divided into arches and cantilevers, upon which loads are distributed, so that the deflection of the arches and cantilever is equal at every joint

[3]The solution is given in the specialized professional references, while the differential equation (20.28) is analogous to the differential equation which describes the action of the hydrostatic pressure.

point in all the arches and all the cantilevers, not only in the central cantilever, as was a case in the previous method. Furthermore, the method assumes that the distribution of loads is such as to cause equal deflection of the arches and cantilevers in all directions. Complete analysis by means of this method is obtained with a proper distribution of the radial loads, tangential loads, and bending loads between the arch elements and cantilever elements, as long as an agreement is obtained for all three axial and three rotational displacements of all jointing points between the elements of the arches and the cantilevers. The method is very accurate; that is to say, its accuracy is limited only by the precision of the basic data and assumptions, as well as by the number of selected horizontal and vertical sectional planes, which is confirmed with a comparison of results from calculations and observations on already constructed dams.

Until the appearance of powerful computing machines, the trial-load method had a significant disadvantage in that we could come to the solution only following a hard and long-lasting work. Lately, there have been developed computer programs, by means of which the analysis can be performed rapidly and, at the same time, not too expensively. A number of computer programs have been developed lately, by means of which, not only is there performed static and dynamic analysis, but also it is possible to perform other phases of the design – plotting in layout, working out of sections, calculation of the volume of excavation or volume of concrete, etc. Probably, there soon will appear programs that will be able to work out a complete design for an arch dam. Yet, that will take place only with the aid of engineers, since sound engineering reason, by means of which the computing machine is directed, operated and controlled, by means of which it is made judgement for the advantages and disadvantages of particular solution, will never lose its significance. One of the first such programs has been developed in the USA – ADSAS (Arch Dam Stress Analysis System) – which makes possible analyzing cylindrical, two-centred and three-centred arch dams, by taking into consideration the following loads: (1) water pressure from the upstream side; (2) pressure of the tailrace; (3) pressure due to ice; (4) pressure due to sediment; (5) forces owing to temperature variations; (6) radial and tangential loads caused by the dynamic response from an earthquake; and (7) self-weight of the dam, as well as other dead loads (Golzé, 1977).

20.6.4 The Finite Element Method

The Finite Element Method, with all of its advantages as described in Chapter 8 on embankment dams, represents the most powerful method for static and dynamic analysis of arch dams, also. In this, satisfactory results may also be obtained by means of a nonlinear two-dimensional analysis; however, owing to the small thickness of the structure, it is recommended, whenever possible, that there be performed a three-dimensional analysis, even though this is several times more expensive and requires a powerful computing system. Lately there have been made significant efforts for developing appropriate and effective software, and, in doing so, significant results have been accomplished. In a sophisticated three-dimensional form, the Finite Element Method indeed yields great possibilities for a complete analysis of arch dams, all of which leads to attaining their stable and rational structure.

The discretization also encompasses the foundation up to a certain depth, as well as parts of the foundation upstream, downstream and nearby the dam. If the dam site is symmetrical (in geometrical regard and in relation to the features of the rock in the

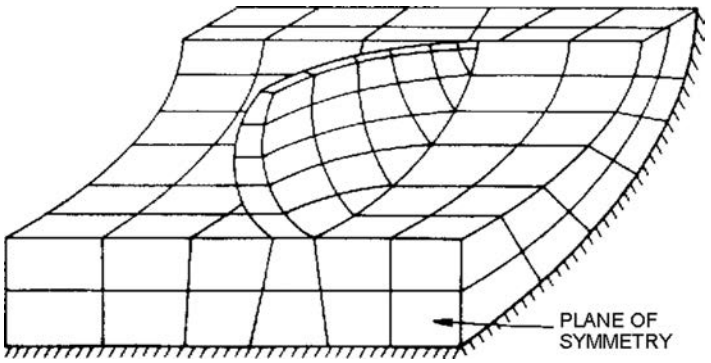

Figure 20.52 Space discretization of one half of a symmetrical arch dam along with its foundation.

foundation), then one half of the dam is examined, Figure 20.52. Nowadays in the three-dimensional analysis there are also inserted special jointing elements for including the behaviour of the interface concrete-rock in the foundation and abutments of the dam, which yields an even more precise and more realistic analysis (Clough & Zienkiewicz, 1987; Lichun & Shuhong, 2000; Swoboda & Lei, 1994).

Similarly to gravity dams, arch dams are constructed as a system of monolithic blocks separated by joints. The joints are later grouted under high pressure to form a complete monolithic structure in compression. Using the standard finite element discretization procedure, the monolithic arch structure is idealized as an assemblage of finite elements of appropriate shapes and types. In principle, any reasonably accurate 3-D element and mesh arrangement may be used. In practice, however, isoparametric solid and shell elements of various types are best suited for the analysis of arch dams. Such elements are included in the commercial software packages, specially aimed at arch dam analyses, or for general structural analyses. The curved surfaces of an arch dam are directly represented by curved isoparametric elements. The element nodes on the surfaces of the dam should be arranged on a grid of vertical and horizontal lines in order to appropriately relate to the arches and cantilevers.

The foundation model should include the significant geological features of the rock and should also extend to a distance at which the interaction with the dam becomes negligible. A foundation model which extends to infinity or extends to finite distance, but includes wave-transmitting boundaries, is also available in contemporary software.

It should be noted that during the last 30 years computer programs for arch dam shape optimization have been developed. In these programs the finite element method, as well as the trial load method, is incorporated for calculation of stresses, because the thickness of arch dams is primarily determined by the stresses in the dam body (Pan and He, 2000).

In modern practice, one can observe an increasingly distinct tendency for the Finite Element Method to be applied, not only in the designing of new arch dams, but also in the service of existing ones. Complex models are made by means of which we can simulate the historical loading and behavior of the dam, obtained on the basis of data from observations in the course of construction and operation. Such a complex model

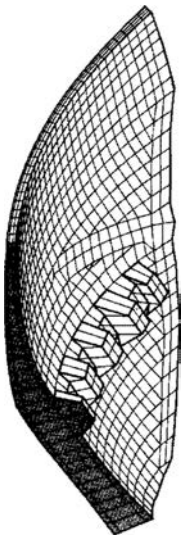

Figure 20.53 (Sharma et al., 1994).

has also been worked out and applied for a dam with an unusual construction, the Boundary dam, which has already been discussed in this chapter. In this model, the thin dam has been discretized using a three-dimensional mesh with three rows of elements (hexahedrons) in the cross-section along the entire length of the structure (Fig. 20.53). Of course, by means of discretization, an appropriate part of the foundation has also been encompassed. The mesh is so constructed as to make possible easy insertion of the actual values of temperature, measured by means of the built-in instruments, as well as the entire former history of the loading, originating from auscultation. Also, there has been simulated a fissure, originating in the course of service. The entire structure, along with the foundation, has been modeled with 5188 elements and 8061 nodes, which is one of the indicators of the complexity of the whole undertaking (Sharma et al., 1994).

20.6.5 The experimental method

The state of stresses for arch dams can be investigated efficiently on models in reduced scale. This method is very expensive and is usually employed for checking-up and improving the structure of a dam, calculated according to some of the described methods. It is possible to consider the application of this method when it is a question of a larger arch dam, with a more complex construction. Even though the beginnings of model investigation of concrete dams date back to the first decade of the 20th century, the method experienced its real development in the period 1950–1965, applied precisely to complex arch dams. It is often used in Italy, Portugal, Switzerland, Austria, France, and the USA – countries in which there have been constructed a large amount of arch dams.

The model investigation method has two main deficiencies – it is relatively expensive and is very non-elastic in practice. Namely, the investigation of the effect of the change of geometry on the construction, on certain constructional details (for instance the joints) or else on some important parameter, may require working out of a completely new model. Due to these, as well as also to other reasons, the Finite Element Method in the last thirty years has pushed back the experimental method, to a great extent. In this period, it can be said that a combined method has been developed, in which the numerical Finite Element Method and the experimental method are combined and supplemented, as a very fortunate and effective combination. The mathematical model most often requires data, which can be taken out from the physical model, so that there exist conditions for this hybrid model to develop further.

The physical models *in reduced scale* are designed and tested in accordance with the *laws of similarity*, that is to say the conditions that have to be satisfied in order to obtain the required similarity between the model and the prototype. The ratio of a certain variable in the prototype and the corresponding variable in the model represents a *scale factor (proportion factor)*. In the case of arch dams (and in general with concrete dams), the simulation of the external hydrostatic load, which will satisfy the requirements of the appropriate *laws of proportioning*, requires application of a liquid with high density. In practice, for this purpose, an elastic bag filled with mercury is most often used (Fig. 20.54) in which one should take into account the ratio of the density of mercury to water of 13.6, in relation to the other factors of the proportioning (ANCOLD, 1991).

The material from which the model is worked out should have characteristics which make possible a real representation of the stresses–deformations relationship, as well as a relatively low value of the modulus of elasticity, in order to improve the model of deformations and to enable the application of loading with mercury on a model with

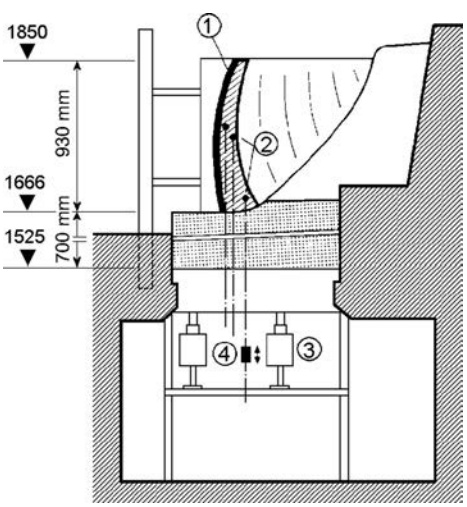

Figure 20.54 Installation for model investigation of Zillergründl dam (Austria) (after ANCOLD, 1991). (1) Bag filled with mercury; (2) fixed spots for simulating dead load in independent blocks; (3) hydraulic press; (4) device for controlling the dead load.

controllable dimensions. The material, also, should have high compressive and tensile strengths, in order to reduce the risk of cracks. It must have proper workability in order to enable a proper shaping of the dam's profile. Among the materials, which have successfully been used for such a purpose, are *microconcrete, plastics* and compounds based on *mortar*. Compounds of especially well composed mortar, with an addition of chemically inert filler, have turned out to be particularly efficient, since they possess the following positive characteristics: (1) isotropy and homogeneity; (2) uniform elasticity in the range of the expected stresses; (3) Poisson's ratio, approximately equal to that of concrete and rock – 0.15 to 0.22; (4) elastic properties that do not depend on time; and (5) strength and modulus of elasticity that can precisely be controlled. Typical values of the main engineering properties of such a compound are $E = 0.7 \times 10^3$ to 5.0×10^3 MN/m^2 and $\nu = 0.20$. The compressive strength lies within the limits of 2.0–20.0 MN/m^2, with a tensile strength amounting to 12% to 25% of the compressive strength. By means of the compound mortar-filler, it is also possible to simulate the rock masses in the foundation and the banks.

The scale of the model most often ranges within the limits 1:50 to 1:100, in which one should take into consideration that a sufficient part of the foundation and the abutments be encompassed, in order to make it possible correctly to simulate the interaction between the concrete construction and the natural foundation. The stresses and deformations are recorded by means of special built-in instruments. Special complex techniques and methods have been developed for simulating the loads due to self-weight, for presenting the joints, and also for inserting the temperature effect.

This page intentionally left blank

Chapter 21

Dynamic stability of concrete dams

21.1 EARTHQUAKE EFFECTS ON CONCRETE DAMS

Concrete dams that are built in areas of potential hazard of a strong earthquake, should be carefully analysed by taking into consideration the complex seismic influences. Until the mid-sixties, all dams were analysed in accordance with the pseudostatic method, with the insertion of the inertial forces from the concrete mass and the mass of water, as has been described in Chapter 4. Even though greatly simplified, this method has been deemed sufficient, to which a contribution has also been made by the fact that there had not been recorded any case of a failure of a concrete dam owing to an earthquake. That fact has also contributed to the opinion that concrete dams, above all arch dams and gravity dams, possess a high degree of resistance to seismic forces.

In the former practice, there has only been one concrete dam which has failed under the effect of an earthquake. Also in only a small number of cases have there been recorded serious damages (CEE, 1990; Knight & Mason, 1992, ICOLD, 2001, Nuss et al., 2012). Characteristic cases in that respect are the examples with the *Hsinfengkiang* buttress dam (China, also known as *Xinfengjiang Dam*) and the *Koyna* gravity dam (India), which experienced earthquake damage in the 1960s; it is deemed that these earthquake effects were of an induced type, occurring as a consequence of the changes caused by the filling of their large reservoirs[1]. In the case of the two cited dams, the damage was sufficiently great as to necessitate repairing and strengthening of these structures. These two cases will be discussed in Section 21.3 of this chapter.

The only concrete dam to fail was *Shih Kang Dam* in Taiwan, a 21.4 m high gravity dam, containing an 18-bay gated spillway with a crest length of 357 m. The dam is located directly over a branch of the fault caused by the M 7.6 Chi Chi earthquake on September 21, 1999. The main Che-Lung-Pu fault located 300 m away from the dam was known at the time of the design of the dam, but not the branch that ruptured under the dam. The fault rupture caused extensive damage to three spillway bays on the right side of the structure. The ground movement raised the left part of these bays about 11 m and the right side by about 2 m. Thus, there was a vertical differential movement of about 9 m in this area. There was also a diagonal horizontal offset through the dam body dam of about 7 m. A peak horizontal ground acceleration of 0.51*g* and

[1]More on reservoir-triggered earthquakes (earlier known as reservoir-induced earthquakes) can be found in Chapter 33.

a peak vertical acceleration of 0.53*g* were recorded some 500 m from the dam site. The remaining portion of the dam adjacent to the damaged area separated from its foundation bedrock. Six gates of the spillway were inoperable after the earthquake. While an appreciable part of the dam failed, due to the upstream topography as well as the gates and piers falling into the passageway, the discharge of the reservoir water was limited to 100–200 m^3/sec. As such, the earlier assumption was proved, namely that a concrete gravity dam is safer than an earth dam in such a fault movement due to its inherent stability after damage (Zienkiewicz et al., 1986).

Another example of a concrete dam damaged by an earthquake is *Sefid Rud Dam* in Iran, located some 200 km north-west of Tehran. The dam is a 106 m high buttress structure, completed in 1962, designed to withstand an earthquake of 0.25*g* peak horizontal ground acceleration (PHGA). Sefid Rud Dam suffered appreciable damage due to severe shaking from the M 7.7 Manjil Earthquake of June 21, 1990. It is assumed that the epicentre of the earthquake was close to the dam site. The estimated PHGA at the dam site was back-calculated to be 0.71*g* based on the nearest record 40 km away where a PGA of 0.56*g* was recorded. The dam suffered several types of damage, including: horizontal cracks about 18 m below the dam crest where the inclined buttress intersected the vertical section; minor displacement both in the upstream and downstream direction in a few of the 23 dam blocks; minor damage and displacement of all the gates; varying types of damage at the dam crest. Repairs were made in 1991 by grouting the cracks and installing prestressed anchors in the cracked areas. The dam remains in service at this time. It was reported that 40,000 people died due to the earthquake and another 60,000 people were injured. The neighbouring towns of Manjil and Rudbar were almost completely destroyed (Nuss et al., 2012).

In general, concrete dams, especially arch dams, have performed extremely well when subjected to earthquake motions, even when shaken by forces exceeding their design loading. However, only a relatively small number of concrete dams have been severely shaken by actual earthquakes – perhaps two hundred, but only about twenty such dams have experienced peak horizontal ground accelerations (PHGA) recorded, or estimated, greater than 0.3*g*. Some characteristic examples, apart from the three already mentioned such dams, will be presented in brief (ICOLD, 2001, Nuss et al., 2012).

Lower Crystal Springs Dam is a 47 m high curved gravity dam completed in 1890, located 32 km south of San Francisco, California. The dam was built with interlocking concrete blocks on a rock foundation. It withstood the 1906 San Francisco earthquake with a magnitude of M 8.3, with an estimated PHGA of 0.52 to 0.68*g* without a single crack in spite of the fact that the reservoir was almost full, while the distance from the route of the fault, at the point where sliding of 2.4 m was recorded, was only 350 m. It must be emphasized that the stability of this dam exceeds the stability of typical gravity dams owing to the curved form in plan, as well as to the stronger cross-section, in connection with the plan for a subsequent heightening, which has never been realized (CEE, 1990; Knight & Mason, 1992).

Williams Dam is a 21 m high gravity dam completed in 1895 in California, and was the closest dam to the epicentre of the M 7.1 Loma Prieta earthquake of October 17, 1989. The dam is located about 10 km north of the epicentre which had a focal depth of 18.5 m and just south of Austrian Dam, an embankment dam that settled up to 90 cm during the event. Inspections following the earthquake indicated no damage to the

concrete dam that was located 0.8 km from the San Andreas Fault which ruptured at that time. It was estimated that the dam was shaken by a peak horizontal acceleration of 0.6*g*.

Gohonmatsu Dam is a concrete gravity dam in Japan, built in 1900 of concrete rubble masonry with a structural height of 33 m and a crest length of 110 m. The epicenter of the January 17, 1995 Kobe earthquake was 15 km away from the dam. The PHGA was 0.83*g*. The only damage was hairline cracks in the concrete parapet on the dam crest.

Mingtan Dam is a concrete gravity dam in Taiwan with a structural height of 82 m. Being 12 km away, the Chi Chi earthquake induced PHGA at the dam estimated between 0.4 to 0.5*g*. There was no reported damage to the dam.

Kasho Dam (Japan, $H = 46.4$ m completed in 1990) is the second concrete dam, (the first being Pacoima Dam), in which acceleration greater than 2.0*g* was recorded at the dam crest. This concrete gravity dam was shaken by the October 6, 2000 Western Tottori earthquake (M 7.3). The epicentre of the earthquake was 3 km from the dam. At the time of the earthquake, the reservoir was 5.8 m below normal level. Peak accelerations of 0.54*g* horizontal and 0.49*g* vertical were measured in the lower inspection gallery located 9 m above the base of the dam and 2.09*g* in an elevator shaft at the dam crest. From plumb line readings in the dam body the main shock produced a relative displacement of 28 mm towards the right abutment and 0.7 mm in the upstream direction. The maximum displacement was 29 mm. There was no damage to the concrete gravity dam.

Takou Dam (Japan) is a 77 m high concrete gravity dam with a crest length of 322 m. During the March 11, 2011 Tohoku earthquake (M 9.0) main shock, a power failure occurred and the accelerographs were out of function. But when the dam was hit by an aftershock of magnitude M 7.1 on March 17, the accelerograms were recorded. The PGA values at the foundation were 0.38, 0.29 and 0.27*g* in the upstream to downstream direction, the cross-canyon direction, and the vertical direction, respectively. Peak accelerations at the crest in the same directions were 1.79, 2.04 and 1.33*g*, respectively. The significant amplitude at the crest of the dam in the cross-canyon direction is noticeable. PHGA during the main shock is estimated to have been 0.4*g*. The water level in the reservoir during the main shock was 33 m below the crest elevation. The dam was not damaged.

Pacoima Dam (California, USA, completed 1929) is a 113 m high concrete arch dam, 180 m long. It has been shaken by two major earthquakes, the February 9, 1971 San Fernando earthquake of M 6.6 and then the January 17, 1994 Northridge earthquake of M 6.8. The epicentre of 1971 earthquake was 6.4 km north of the dam site, with a focal depth of approximately 13 km. Ground accelerations recorded by an accelerograph located on the left abutment 16 m above the dam crest showed high frequency peaks of 1.25*g* on both horizontal components and a maximum of 0.70*g* vertical at this location. That large acceleration is presumed to have been related to the local narrow ridge topography, and to the shattered condition of the bedrock at the location of the strong motion instrument. Despite the very high intensity of the shock and the established weak left abutment, an inspection of the dam showed that no cracks had developed in the dam body, and no differential movement had occurred between adjacent blocks. The main damage was a separation of the arch dam from the left massive block of 1 cm at the crest and extending downwards about 16 m. After this

event, an extensive seismic instrumentation system was installed and the upper rock mass of the left abutment was secured to more competent rock below by means of 35 rock anchors. The epicentre of the 1994 Northridge earthquake was 18 km southwest of the dam at a focal depth of 17 km. Strong motion records indicate a PHGA of 0.53*g* at the base of the dam, while an instrument at the upper left abutment measured a peak acceleration of 1.58*g* due to the topographic amplification in the canyon. Peak horizontal accelerations greater than 2.3*g* were recorded at the dam crest. Despite being subjected to high accelerations, the arch dam behaved well. The main damage was an opening of the contraction joint between the arch dam and the thrust block at the left abutment of approximately 50 mm. A downward movement of about 13 mm indicates that the thrust block and underlying rock mass may have moved away from the dam. Minor horizontal cracking of concrete at the left end of the dam, and several minor horizontal and vertical block offsets at the joints occurred. The earthquake provided for the first time evidence of opening and closing of vertical contraction joints during an earthquake. The water level at this event was 4.1 m higher than the water level during the 1971 earthquake.

Ambiesta Dam (1956), a 59 m high cupola arch dam in northern Italy, was shaken during the 1976 Friuli earthquake (M 6.5), with the epicentre 22 km from the dam. The dam has a crest length of 145 m, a crest thickness of 2.8 m, and a base thickness of 7.8 m. Ground acceleration of 0.33*g* was recorded at the right abutment. The dam suffered no damage, confirming results of previous physical model studies, which had indicated that substantially greater accelerations (0.75*g* or greater) would be required to cause damage to the structure.

Rapel Dam is a double curvature arch dam built in 1968 in Chile. The dam is 111 m high, with a length at the crest of 116.5 m between the two massive blocks in which large spillways are positioned. The dam at the foundation is 18.54 m wide, while it is 5.5 m wide at the crest. At the downstream face, in the lower part, immediately next to the dam the powerhouse of the hydroelectric power station is attached. During its design (1960), the effect of an earthquake was introduced into the calculations with an acceleration of 0.12*g* in the upstream-downstream direction, by the application of a pseudostatic method. In order to prevent overhanging of the dam towards the upstream face in an earthquake with a downstream-upstream direction at a state of an empty reservoir, there was anticipated an aseismic belt, i.e. a band of steel reinforcement consisting of 144 steel reinforcing bars Ø36 mm, placed at a distance of 36 m below the crest. On March 3, 1985, the magnitude M 7.8 Santiago earthquake occurred about 90 km offshore at a depth of 33 km. Measured peak free-field accelerations near the dam were 0.31*g* in the cross-canyon direction, 0.14*g* in the upstream to downstream direction, and 0.11*g* vertical. The arch dam did not experience any damage and the measured displacements were within the usual, allowable limits, but the spillway walls cracked and there was leakage at the wall of the right spillway. The upper part of one intake tower also cracked and separated from the dam body. This dam was shaken again by the M 8.8 Maule earthquake on February 27, 2010 while its reservoir was full. The maximum PHGA recorded by an accelerograph located on the dam was 0.207*g*. Seepage again increased along the right abutment; this time from a normal 13 l/sec to 40 l/sec (Serafim & Clough, 1990; Nuss et al., 2012).

Techi Dam ($H = 183$ m, $L = 290$ m) is a doubly-curved arch dam in Taiwan. The epicentre of the Chi Chi earthquake of 1999 was 85 km from the dam. PHGAs were

estimated between 0.3 and 0.5*g* at the base of the dam with 0.86*g* measured near the crest. There was no damage to the dam body with no signs of vertical joint movements. After the shake seepage increased, but returned to normal within days of the event.

Shapai Dam (Sichuan Province, China, $H = 132$ m, completed in 2002)[2] is the first roller-compacted concrete arch dam shaken by a major earthquake. The dam is located 32 km from the Wenchuan earthquake fault that occurred on May 12, 2008[3]. The earthquake magnitude was 8.0 and the PHGA at the dam site was estimated to be 0.25 to 0.50*g*, while the dam was designed to cope with acceleration of 0.1375*g*. With a nearly full reservoir at the time of the earthquake, the dam remained undamaged. The major problems were caused by rockfall: the grouting and drainage galleries were flooded due to rockfall blocking the outlets, and there was a complete failure of a penstock. One of the spillway gantries was slightly damaged, but all gates were functional after the shaking. The power house was badly damaged when large rocks rolled down the steep mountain site knocking holes in the building walls.

Matka, (R. Macedonia, $H = 38$ m, see Chapter 20, Section 20.2) is a reinforced arch dam, in operation since 1938. It was 10 km away from the epicentre of July 26 1963 Skopje earthquake (M 6.1), and it was not damaged.

Poiana Usului Dam, in Romania, a buttress dam ($H = 82$ m, $L = 500$ m, founded on sandstones, commissioned in 1972) was located about 60 km away from the epicentre of the 1977 Romanian earthquake (M 7.2), and performed satisfactorily.

The high level of seismic safety of concrete dams was confirmed during the high intensity earthquakes in the area of L'Aquila in April 2009. The main shock of 6 April with magnitude of 5.9 impacted 16 concrete dams, mostly of gravity type, up to 93 m high, but not one was damaged (Caruana et al., 2010).

Japan experienced several severe earthquakes in the first decade of the 21st century, but no dams collapsed. When the magnitude of the shake exceeded $M = 6.7$ and the distance from the epicentre was less than 30 km, some of embankment dams suffered moderate damage, but concrete dams were not damaged in any case (Matsumoto, 2010).

Overall, the performance of concrete dams during true earthquakes, especially of arch dams, has been satisfactory, and such dams could be implied to be more earthquake-resistant than embankment dams. This is perhaps because concrete dams may have been built to design standards higher than used for some of the earlier embankment dams.

Positive experiences gained with the already constructed dams, should not, however, lead to a general conclusion that this kind of construction is safe during earthquakes, since until now there is no very high concrete dam, let us say higher than 150 m, which has been subjected to a maximum earthquake at a state of a full reservoir. On the contrary, there is justification for the tendency that all existing dams, constructed in seismically potentially active regions, as well as those anticipated for construction, be examined by means of advanced dynamic analyses for a maximum earthquake to which they could be exposed.

---

[2]For more data on the Shapai dam, see Table 20.2, Chapter 20.

[3]The consequences of the Sechuan earthquake were terrible: 87,000 people were killed and about 675,000 were injured.

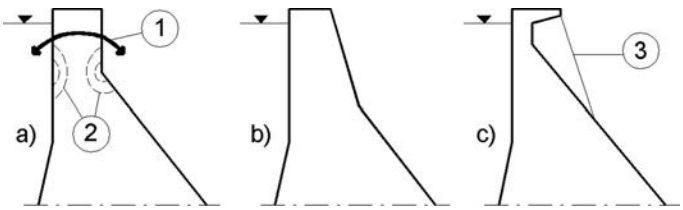

Figure 21.1 Seismic effect in the crest zone of a gravity dam (after Novak et al., 2001). (1) High inertia effects due to mass of the crest and the roadway; (2) upstream and downstream zones of high stress with a possibility of cracks; (3) piers supporting the roadway.

The basic objective, which is imposed in the aseismic design of concrete dams, is to make a structure that would be able to withstand a maximum earthquake without the occurrence of large, uncontrolled cracks. With higher dams, it is also necessary to investigate the danger of resonance, even though in practice it is rather reduced with the effect of damping.

If we imagine a gravity concrete dam with an idealized triangular cross-section, with a height H [m] and width of the base B [m], constructed in concrete with a modulus of elasticity $E = 14\,\text{GN/m}^2$, then the natural frequency of vibration f_n [Hz] will be approximately:

$$f_n \approx \frac{600B}{H^2} \tag{21.1}$$

or, by means of another approximate expression:

$$f_n \approx \frac{\sqrt{E}}{0.012H} \tag{21.2}$$

The analysis of equations (21.1) and (21.2) indicates that a resonance with frequency of vibrations due to an earthquake amounting to 1–10 Hz, is possible to take place only in the case of larger dams, with a very low probability of its happening in the whole cross-section. However, concrete dams have vulnerable spots, susceptible to damages during the effect of inertial forces. In that respect, the discontinuities in the profile, in which high local stresses can take place, are particularly sensitive.

Such is the case with the zone near the crest in the case of gravity dams, in which the high inertial effect of the mass of crest and roadway can lead to a concentration of high stresses and cracks, (Fig. 21.1a). Case (b) illustrates a rather rigid structure of the upper part of the dam, which is satisfactory for an earthquake of medium intensity, while (c) illustrates a case for extremely unfavourable conditions (Novak et al., 2001).

21.2 METHODS FOR DYNAMIC ANALYSIS OF CONCRETE DAMS

Like embankment dams, concrete dams should also be analysed for two types of earthquakes – an *operating basis earthquake (OBE)* and a *maximum credible earthquake*

(MCE).[4] In this, one should take into consideration that performing a dynamic analysis for concrete dams is not any simpler than in relation to the embankment dams. Although a concrete dam is constructed of a homogeneous, hard material, there occur a number of problems, which greatly aggravate or complicate the analysis. The most significant among them are:

1. The dam should obligatorily be analysed as a joint system with the foundation below it and around it;
2. Concrete dams of mass concrete, being constructed in blocks, with joints between them, do not, in fact, represent a homogeneous, but rather a discrete system;
3. The water in the reservoir plays a significant role during an earthquake, while the method of its true simulation is very complex (Lotfi, 2001);
4. Arch and buttress dams should obligatorily be treated by means of a three-dimensional analysis, which additionally aggravates the problem.

In general, a proper study of the response of concrete dams to earthquake ground motions requires three basic steps:

- Selecting earthquake ground motions at the site;
- Modeling the concrete dam, flexible foundation, and reservoir, and performing a transient analysis; and
- Analyzing and evaluating the dynamic response, including the assessment of dam stability.

The earthquake ground motions are characterized in terms of peak ground acceleration, velocity, or displacement values, and seismic response spectra or acceleration time histories. For the evaluation of concrete dams, the response spectrum and time-history representation of earthquake ground motions should be used.

The concrete in the dam body exhibits complex nonlinear mechanical behaviour under dynamic loading conditions. The concrete has low tensile strength and during severe earthquakes the unreinforced concrete masses in the dam body are likely to undergo cracking. Considerable research has been invested in the development of numerical techniques for the nonlinear fracture analysis of concrete, which can be grouped into two categories: the fracture-mechanics-based approach and the continuum-damage-mechanics-based approach. Continuum damage mechanics has provided an elegant way of simulating crack formation and propagation by way of stiffness degradation and recovery. In the fracture mechanics approach, a typical concrete cracking model is generally composed of three components: a condition for determining the onset of crack initiation, a method for crack representation, and a criterion for crack propagation. The crack initiation and propagation criteria can be based either on strength of material or on theory of fracture mechanics. Typical strength-of-material-based crack initiation and propagation criteria include the maximum principal stress criteria and the maximum principal strain criteria, which assume that a crack will be initiated when the computed maximum principal stress or strain at the crack-tip exceeds the strength of the material. On the other hand,

[4]For more details see Chapter 9, Section 9.2.2.

fracture-mechanics-based crack initiation and propagation criteria can be generally divided into two groups: linear elastic fracture mechanics criteria and nonlinear fracture mechanics criteria. Linear elastic fracture mechanics allows the stress to approach infinity at the crack tip. However, since infinite stress cannot exist in real materials, a certain range of plastic zone should develop at the crack tip. In concrete, this plastic zone is termed the fracture process zone. The fracture behaviour of concrete is greatly influenced by this fracture process zone and should be described by nonlinear fracture mechanics criteria. Reviews of the fracture-mechanics-based approach and the continuum-damage-mechanics-based approach numerical techniques can be found in the literature (de Borst, 2002; Bazant, 2002; Bhattacharjee & Leger, 1992; van Mier, 2013).

In the seismic evaluation of concrete dams, the foundation rock is typically treated as a continuous viscoelastic half space (USSD 2008). However, rock masses are naturally discontinuous, inhomogeneous, anisotropic, inelastic, and fractured porous media. Traditionally, nonlinear fractured rock masses are treated as equivalent elastoplastic continua described by yielding criteria such as the Mohr-Coulomb model, the Drucker-Prager model, and the Hoek-Brown model (Hoek, 1983; Hoek & Brown, 1997). Recently, the constitutive models of rocks are more rigorously accounted for by contact mechanics, fracture mechanics, and damage mechanics principles (Jing, 2003).

A commonly utilized approach to include the hydrodynamic pressure effect resulting from the reservoir water is the well-known added mass technique introduced in 1933 by Westergaard. In modern practice it is considered inadequate and oversimplified. Darbre (1998) modified the added mass model with the incorporation of damping to the added mass effect, in which incompressible water masses are attached in series to the dam through viscous dampers. A more rigorous approach for the constitutive modelling of the reservoir water is the use of the finite element method (FEM) or boundary element method (BEM) based on either a pressure-based formulation or a displacement-based formulation, as well as with the application of what are called liquid finite elements. But one can say that investigations of seismic dam-reservoir interaction are still far from being finalized, despite the evident progress (Chopra & Chakrabarti, 1981; Clough & Zienkiewicz, 1987; CEE, 1990; Guan et al., 1994; Asteris & Tzamtzis, 2003; Gao et al., 2011; Zeydan, 2013, Popovici et al., 2013).

Equations of motion representing an effect of the earthquake, as well as the response of the structure, are given in textbook references for dynamics of structures, as well as in the textbook references on dams, for example (Clough & Zienkiewicz, 1987; Golzé, 1977). For solving the problem, during the last forty years or so, satisfactory techniques have been developed, incorporated in the general computer software for analysis of structures, as well as in the special programmes aimed at concrete dam analysis.

The analytical procedures, by means of which it is possible to express the response of the dam during an earthquake, which have been developed so far, are applicable to both the linear and non-linear systems. In general, the critical conditions during an earthquake, in which there is a probability of damages to the structure, are not a linear mechanism of response, but a nonlinear one. In other words, in order to predict whether the concrete dam would fail or not during an earthquake, one should apply a nonlinear procedure. Taking into consideration the complexity of the nonlinear procedure, the great authority in this field, Clough, recommended for analysis with a

design earthquake applying calculations with a linearly elastic response of the structure. In such a case, the criterion for the endurance of the structure will be the comparison of the calculated stresses with the strength of the material. In the case of action of a maximum credible earthquake, in which considerable damage to the structure is expected, nonlinear analysis is indispensable, while a criterion will be whether there will come about drawdown of water from the reservoir through the damaged dam. If the water remains in the reservoir, the behaviour of the dam is satisfactory (Serafim & Clough, 1990).

Throughout the world there is a lot of work going on regarding the improvement of the methods for conducting nonlinear analysis. The rapid advancement of computer technology has made the speed and capacity of computers, as well as the cost of computing time, not a problem or a limiting factor any longer. The main problem in this case, is still the insufficient knowledge in connection with the nonlinear properties of the concrete, which is used for dam construction. It is known that the mechanical properties of the concrete vary in the course of time, as they also vary due to the temperature and moisture content. Furthermore, the strength and stiffness of the concrete vary, depending on the speed with which loads are applied. In that way, the properties of the material, when it is a question of an earthquake, can considerably differ from the results obtained with customary traditional laboratory investigations. That is why appropriate extensive dynamic investigations are indispensable in order to determine the properties of the material, which will correspond to the execution of the nonlinear dynamic analysis. This is why linear dynamic analysis, as well as some other simplified procedures, is still popular (Yamaguchi et al., 2004; Wieland et al., 2008; Wieland & Ahlehagh, 2013; Furgani & Nuti, 2013);

21.2.1 Linear analysis and response of the structure

When the behaviour and stability of the concrete dam during an earthquake is assessed, in many cases it is rational to assume that, during an earthquake with a weak to medium intensity, the response of the structure will be linear. This means that it is expected that deformations of the dam will be directly proportional to the amplitude of the earthquake applied to the foundation. The assumption of a linear response of the structure essentially simplifies the formulation of the mathematical model, which represents the dam, the water in the reservoir, and the rock in the bedrock, as well as the procedure for determination of the response. The results of the linear analysis serve as a presentation of the general characteristics of the dynamic response, in which the amplitude of the calculated displacements and strains indicates whether there is a reality in the assumption of linearity. During a strong earthquake, it is probable that the calculated deformations will exceed the elastic bearing capacity, i.e. strength of the concrete, and will mean damage to the dam, which can be determined only by means of a more complex nonlinear analysis.

Realizing that the pseudostatic procedure in contemporary practice has extremely limited possibilities, both the designers and researchers of dams have worked on developing a realistic presentation of the response of a concrete dam to an earthquake. The first significant successes in this respect were accomplished in the late sixties, with the application of the Finite Element Method. Even at that time, there were developed three-dimensional models throughout the world, by simulating the foundation

as a flexible one; however, without mass. The water in the reservoir has been represented as a mesh of noncompressible liquid elements. Later on, the models have been developed by improving the earthquake input into the analysis, so that it has a spatial variation in the interface dam-foundation, while the water is represented as being compressible. The conclusions of the intensive investigations in this field, performed in the seventies and eighties, lead to the following statements (Clough & Zienkiewicz, 1987; CEE, 1990; Serafim & Clough, 1990):

1. The response of concrete dams increases intensively with the interaction with the water in the reservoir. The contribution of the hydrodynamic force is especially significant at the response of the vertical component of the earthquake.
2. The hydrodynamic effect has a greater role in the case of arch dams, while a smaller role with gravity dams.
3. The assumption of noncompressibility of the water usually leads to errors for an earthquake with an upstream-downstream action. For a vertical action and for an action that is transverse to the river valley, it is very likely that this assumption will not play an essential role.
4. The hydrodynamic waves are absorbed by the rock in the foundation and by the sediment layer in the reservoir. This effect can be obtained only if the water of the reservoir is treated as compressible. The neglecting of this effect leads to an unreal enhancement of the response of the structure.
5. The neglecting of the dynamic interaction of the dam with the deformations of the rock in the foundation also leads to an overestimate of the dynamic response of the dam.

Therefore, the general conclusion is that the dam-water interaction in the reservoir, also including here the compressibility of the water, as well as the absorption of the pressure due to seismic waves within the boundaries of the reservoir, then the dam-rock interaction in the foundation, should all be taken into consideration in the analysis of the response of concrete dams due to the effect of an earthquake. Throughout the world there have been developed a number of programs, which include the above-cited effects, while treating the problem as a two-dimensional one. They are applicable to dams of roller-compacted concrete in wide valleys, as well as to gravity dams made of mass concrete with even vertical joints between the blocks. The first one usually has no joints, while in the second ones, the blocks have a tendency to vibrate, independently of one another. In the case of dams with uneven joints and regarding dams located in narrow canyons, the three-dimensional model yields much better results. There have also been developed a number of three-dimensional models, mainly especially adapted for the analyses of arch dams.

21.2.2 Nonlinear analysis and the response of the dam

As has been said in the previous section, anticipation of damage to a concrete dam owing to a strong earthquake is possible only by means of a nonlinear analysis. In order to make such an analysis possible, it is necessary to possess as precisely determined parameters for the materials and components of the system as possible, which are characterized by nonlinear stresses-deformations relationships, used in an appropriate

nonlinear procedure for obtaining the response of the structure. The entire procedure for performing nonlinear analysis can be boiled down to the following points:

1. Defining the seismic input;
2. Determining the behaviour of the materials and components of the system owing to the action of dynamic loads;
3. A mathematical model by means of which the nonlinear behaviour will be represented;
4. An efficient numerical procedure for the calculation of the nonlinear response of the system;
5. Criteria for acceptable behaviour and assessment of the mode of failure of the dam.

As was already mentioned, concrete exhibits a complex nonlinear stress-strain relationship, dependent on the degree and history of loading. The nonlinear behaviour of mass concrete becomes significant when stresses reach the compressive strength or a relatively low tensile strength. Concrete dams are dimensioned so as to take on the primary loads causing compressive stresses, in which the tensile stresses either do not appear at all, or they are minimum.

A strong earthquake can cause significant dynamic stresses in the dam body, both compressive and tensile, while the combination of static and dynamic stresses can exceed the range of the linear response of the concrete, especially when it is a question of tensile stresses. Experiments have shown that the concrete exhibits linear behaviour under cyclic loading up to compressive stress, which amounts to 50–60% of the compressive strength.

The tensile stresses caused by an earthquake have to be taken on by the concrete, since the dam's body, generally speaking, is not reinforced. Linear analyses indicate that the strength limit during an earthquake can be exceeded at a number of spots in the dam's body (in the case of gravity dams, it is in the upper part and in the toes, with indications occurrence of cracks).

As the stresses in the dam reach the tensile strength, microcracks, which are always present in the concrete, unite and show a tendency to form cracks across the surface. In the case of moderate earthquakes, the dynamic forces open and close the cracks in the course of a cycle of vibration, which, finally, can end up without any consequences for the dam. After an earthquake, the static forces will convert the tensile stresses into compressive stresses, leaving the cracks in a closed position. During the appearance and expansion of cracks, caused by an earthquake, there comes about a dissipation of energy, so that the amplitude of the dynamic response of the structure decreases if the dam remains stable. During a strong motion of the earth, it is possible for the cracks to expand across the entire section of the dam, which potentially leads to dynamic instability, as well as to uncontrolled leakage of water. In this, by means of analysis one should assess whether at a maximum credible earthquake, the dam will be stable or not (CEE, 1990).

With the real modelling of the cracks due to tension in the mass concrete, it is necessary to encompass the variation of the properties of the material in the dam's body, simulate the gradual construction of the dam, as well as the effect of pore pressure on the occurrence of cracks. This means that the variation of the concrete

strength in various zones can have an influence on the location of the tensile crack. Also, the structural joints can make influence the location of cracks. The pore pressure in the saturated concrete has an influence on the state of stresses, as well as on the occurrence and expansion of cracks, especially in the lower part of the dam and in the joint with the rock in the foundation. In general, in the analysis we take into consideration only the static pore pressure, while the response of the structure to an earthquake is determined by taking into consideration the dynamic total stresses; that is to say, we assume that the pore pressure does not change during cyclic loading.

The earthquake response of the gravity dam-reservoir system is affected by the behaviour at the interfaces between contacting materials, which was clearly demonstrated by Asteris & Tzamtzis (2003). In a nonlinear seismic response analysis of a realistic gravity dam-reservoir system they employed interface elements with the function of allowing large relative displacements to occur between adjacent blocks and to permit the transfer of shear stresses across the interfaces. The results of the analyses show that the response of concrete gravity dam-reservoir systems is significantly affected by the behaviour at the interfaces of the various discontinuities present in real systems. The authors emphasised that constitutive and strength properties of multi-axially loaded mass concrete under dynamic conditions need to be properly defined before any nonlinear response analysis procedure can reliably predict the extent of damage that may be caused during an intense ground motion and evaluate its implications to the safety of concrete dams. Furthermore, reliable data on the properties of joint materials have to be evaluated from experiments under dynamic loading conditions because such data are essential for an accurate prediction of system response.

The behaviour of the rock in the foundation below the dam is typically nonlinear, owing to the fact that the rock, almost always, is fissured and discontinued. The nonlinear behaviour of the rock has an influence on the static and dynamic response of the dam. For example, during a strong earthquake the forces acting on the abutments of arch dams significantly increase which, in the case of a certain weaker zone, can lead to failure of the abutment owing to an exceeding of the shearing strength. The question of stability of the foundation is also very important in the case of gravity dams, and it is aggravated by the fact that a thorough analysis of the potential danger of failure in the foundation is often not possible, because the information on the rock condition is limited, especially in the case of old, existing dams. This question should never be neglected, because practice shows that most of the accidents with concrete dams have been initiated in the foundation (CEE, 1990; Hinks & Charles, 1992; Knight & Mason, 1992; Saini, 1992).

The nonlinear response of concrete dams, to a considerable extent, depends on the characteristics of the soil movement, as, for example, on the duration of the tremor and the amplitude of variation of the velocity of movement, which particularly influences the expanding of the tension cracks and the compactness of the joints. A considerable increment of variation of the velocity of foundation movement, typical of the zone close to the epicentre, sends an impulse to the dam, which can cause the occurrence and expansion of cracks, so that it also influences the stability of the dam if cracks expand excessively. For these reasons, a real assessment of the stability, based on nonlinear analysis, would require a detailed seismotectonic study of the dam site, as well as the development of appropriate records of the movement of the foundation, specific to the particular dam site.

The nonlinear mechanism, which has already been discussed, and which is connected with the occurrence, widening and expansion of tension cracks in the concrete, loss of compactness in the joints and the hazard of failure in the foundation, is a result of the vibration of the dam as a response to an earthquake. It must be said that complete sliding of the dam and its overturning – traditional criteria for an assessment of the stability – in a general case are not likely to appear as a consequence of an earthquake (CEE, 1990).

A realistic nonlinear analysis for the response of a concrete dam to an earthquake requires the use of a mathematical model, in which there have been included the expansion and widening of the cracks due to tension in the concrete, cyclic displacements of the joints and the abutments, as well as the deformability of the rock in the bedrock. In this, it is indispensable to perform a nonlinear analysis of the response of the structure, since the above-cited elements are a consequence of the nonlinear relationship between displacements and the resisting forces. A rigorous nonlinear analysis must encompass the effects of the dam-water and dam-foundation interaction, along with nonlinear models of the concrete in the dam, joints, and the foundation. At this moment, the Finite Element Method is considered to be the best method above all, owing to the possibility for presentation of an arbitrary geometry of the system, as well as the variation of the behaviour of the materials, dicretization of the water in the reservoir and the rock in the foundation (Popovici, 2002, Asteris & Tzamtzis, 2003; Gao et al., 2011; Dakoulas et al., 2013).

When the concrete dam exhibits a nonlinear response to a strong earthquake, the principle of superposition will not be valid any longer, so that the equations of motion are solved in the time domain, in a number of time steps. In this, a lot of clumsy and difficult calculations are performed, which, until recently, have often exceeded the capacities of the computing systems. That is why, in a number of models various modifications have been introduced – such as, for example, division of the structure into linear and nonlinear substructures – in order to simplify and speed up the procedure. The significant development in the speed and power of computers has put an end to the need for such modifications.

The question of using two-dimensional or three-dimensional analysis is raised here, as well. In general, in the cases of arch dams and buttress dams one should necessarily use a three-dimensional analysis (Gudushauri, 1990; Nuss et al., 1994; Popovici et al., 2000), while in the case of gravity dams a two-dimensional analysis will also satisfy, bearing in mind the limitations that have already been mentioned (JCOLD, 2000; Wieland & Ahlehagh, 2013).

21.2.3 Dynamic analysis of RCC and hardfill dams

Most of the material presented in the previous sections of this chapter concerns the concrete dams made of conventional mass concrete. RCC dams and hardfill dams (see Chapter 18) have some specific features which should be taken into consideration when performing a dynamic analysis.

The earthquake behaviour of a RCC gravity dam is very similar to that of conventional gravity dams. However, there are some differences. In the case of conventional mass concrete the material properties are isotropic within a concrete cantilever. In RCC dams the tensile strength in a lift joint may be a fraction of that of the isotropic mass

concrete, which means that in case of a strong earthquake horizontal cracks can form along any of these interfaces. Opening of any vertical contraction joints can also occur. As gravity type dams are designed to carry the loads by cantilever action (not by arch action), the formation of vertical cracks or the opening of contraction joints are not critical issues. If a horizontal crack is formed, which is inclined towards the upstream face of an arch gravity dam then a detached concrete block may slide progressively into the reservoir during earthquake shaking, which could represent a critical situation. As a matter of fact, cracks and joint openings may not be detrimental to the earthquake safety of a RCC dam (Wieland & Brenner, 2004).

One of the main characteristics of RCC dams is its construction in the horizontal lifts with low height. Thus, there exists a large number of horizontal joints at narrow spacing through the whole dam section. However, from the point of view of dynamic stability of concrete blocks separated by cracks and joints, horizontal cracking planes of RCC dams are less problematic as compared to inclined cracks, which may occur in conventional concrete dams. Numerical simulations have shown that the sliding movement along a crack with an upstream inclination of 15° is about one order of magnitude larger than that of a perfectly horizontal crack (Wieland & Malla, 2000). It may be concluded that RCC dams are well suited to resist strong ground shaking. The lower compressive strength of RCC compared to that of conventional mass concrete is not a problem for the seismic safety of RCC dams, as cracking is governed by the tensile stresses developed in the dam body and the low dynamic tensile strength along lift joints and contraction joints (Wieland & Brenner, 2004).

The seismic behaviour of Pervari Dam with a maximum height of 180 m, designed as RCC type in Turkey, has been examined by performing finite difference analyses utilizing the FLAC computer program. The time-history analyses were performed for an operating basis earthquake (OBE) and a maximum design earthquake (MDE) with peak ground accelerations of 0.11*g* and 0.38*g* respectively (Yıldız & Gürdil, 2012).

A typical symmetrical trapezoidal hardfill dam on rigid foundation, 70 m in height, 10 m wide in the crest, with upstream and downstream slope of 1V:0.7H, has been studied and analysed in China, based on microscopic damage theory and the finite element method, and using the Weibull distribution to characterize random distribution of the mechanical properties of materials, failure modes and seismic dam safety. The main conclusions were (Xiong et al., 2013):

- During an earthquake with an intensity of 8 degrees, the seismic responses of the hardfill dam simulated with a microscopic damage model are generally consistent with those obtained by a linear elastic model.
- The symmetrical trapezoidal 70 m-high hardfill dam remains at a low stress level, undamaged or slightly damaged during an earthquake with an intensity of 8 degrees. However, stress values of different microscopic elements show a lot of variation, due to inhomogeneity of the hardfill material.
- During earthquakes, there are damaged areas in both upstream and downstream parts of the hardfill dam because its symmetrical section is under alternating inertial forces. But the upstream part of the dam body experiences more serious damage than the downstream one. With the increase of the earthquake peak acceleration, tensile cracks occur at dam surfaces and then extend to inside the dam body.

Therefore, under seismic conditions, the failure pattern of the hardfill dam is the tensile fracture of the upstream regions and the dam toe.

- Compared with the traditional gravity dam, the trapezoidal hardfill dam has better seismic performance and greater seismic safety.

21.3 KNOWLEDGE GAINED FROM PRACTICE AND EXPERIMENTS

21.3.1 Knowledge gained from case studies

In the first section of this chapter, it has been elaborated that only one concrete dam (more precisely its spillway part) has failed due to an earthquake. Some characteristic examples have been presented in brief. Also it was noted that there is no recorded evidence of a very strong earthquake in the most unfavourable conditions (Knight & Mason, 1992; Nuss at al., 2012). The closest to such a case was the abovementioned Koyna gravity dam (India), 103 m high, with an almost full reservoir during the earthquake, (Fig. 21.2).

The motion of the foundation, caused by an earthquake with a seismic focus in the vicinity, which is believed to have been triggered by the load of the reservoir, was of a magnitude of 6.5. The maximum acceleration amounted to 0.49*g* in the direction of the river, while the duration of the strong tremor lasted for four seconds. Through a certain number of non-overflow blocks, at a level of 36 m below the crest, where the downstream face changes the inclination, there have occurred significant horizontal cracks; however, the gravitational stability was not deranged, even though the water was at 25 m above the cracks. Damages to the most of the structural joints are an indication that the blocks have vibrated individually (CEE, 1990).

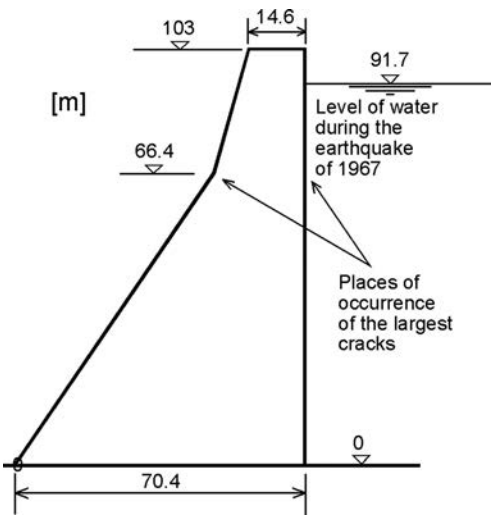

Figure 21.2 Cross-section of Koyna Dam, along with presented water level during the earthquake of 1967 and zones of major cracks.

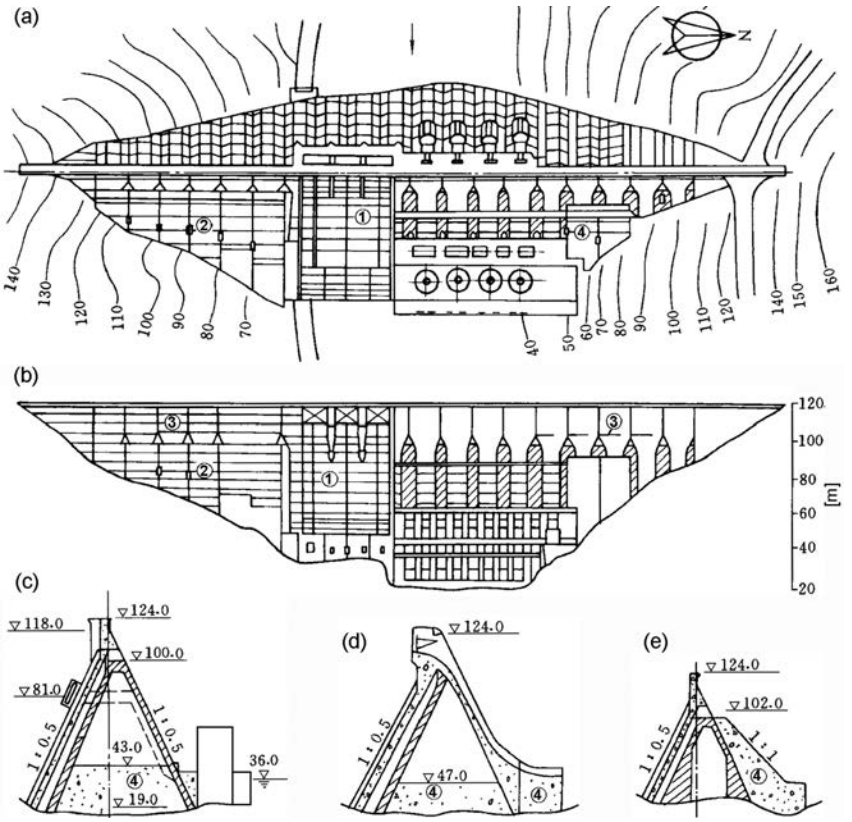

Figure 21.3 Hsinfengkiang (or Xinfengjiang) buttress dam (after Jiazheng & Jing, 2000). (a) Plan; (b) longitudinal section; (c) section through penstock; (d) section through overflow dam part; (e) section through right-bank dam part; (1) overflow dam part; (2) right-bank dam part; (3) cracks; (4) massive concrete.

There was another similar experience in 1962 with the 105 m high Hsinfengkiang (or Xinfengjiang) buttress dam completed in 1959 in Kwanatung Province, China. The total storage capacity formed by this dam is very large −11.5 billion m^3. The dam has nineteen 18-m wide diamond-head buttresses flanked by gravity dam sections. The dam crest width is 5 m, and crest length is 440 m. The Basic intensity of the reservoir area with a recurrence period of about 500 years was designated as VI. Before impounding of the reservoir, no destructive earthquakes were recorded in this region. During a period of 25 years before impounding, only four earthquakes of intensity V–VI occurred in the nearby countries. Taking into account the extreme importance of the dam, it was decided on the basis of experts' experiences to strengthen the dam in time to meet the requirement of resisting an earthquake of intensity VIII, and the dam was strengthened in 1961. For this dam the critical problem was that the buttresses were opened at downstream face and thus did not have enough lateral stiffness to resist the action of axial earthquake components. So concrete-supporting walls were

constructed along all buttresses throughout the whole length of the dam to improve its structural integrity. On March 19, 1962, about two and a half years after impounding of the reservoir, a magnitude M 6.1 earthquake, believed to be reservoir-triggered, impacted the dam. Owing to the timely strengthening, during the major shock although a local crack appeared at the top part of the dam, the strengthened dam withstood this strong earthquake with respect to the overall stability. A horizontal crack 82 m long developed on the right side of the downstream face at an abrupt change in cross-section (Fig. 21.3). A few smaller cracks developed on the left side of the dam at the same elevation as the crack on the right side.

After the major shock more extensive research works were carried out continuously. From July 1961 to December 1978 the monitoring network recorded more than 330,000 shocks. Based on the results of continued research, a second stage strengthening was carried out. The extensive research works on Xinfengjiang reservoir-triggered earthquakes have laid the foundation for seismic investigation of concrete dams in China (Jiazheng & Jing, 2000).

21.3.2 Laboratory and field experiments

What would be interesting both for designers and researchers, namely a recorded time history of the response of a concrete dam, is mainly available only for weaker tremors. That is why researchers, mostly in the USA and Japan, have performed numerous numerical analyses aiming at reproducing the response of dams experiencing stronger tremors. For the same purpose there have also been performed a lot of experiments with artificially-caused vibrations in already constructed dams, with a smaller or higher degree of success, owing to the different difficulties which are met in the execution of a field test.

Since some idealizations and assumptions as well as uncertainties in selecting parameters are hard to avoid in a dynamic analysis of such a sophisticated system as a dam, special emphasis has been placed on the dynamic model test to improve and verify the analytical procedure and its results. Interesting in this respect are the experiments on linear elastic models, performed in various countries, aiming at determining the resonant frequencies, as well as the model of vibration of designed or constructed concrete dams. One of the advantages of the laboratory tests for linear models is the possibility of performing a modelling of the effect of the compressibility of water on an appropriate scale. The model investigations are especially beneficial when we investigate the nonlinear aspects of the response of the dam (cracks, opening of joints). In that, it is indispensable to use special materials and a shaking platform. The main difficulty in conducting these complex tests is that the experiment performed on a reduced model is done so at normal gravity weight, while the strength and stiffness of the model material must be reduced in relation to that of the prototype. Nonlinear laboratory tests are often performed in Japan, Russia, Italy, Portugal and China, but in the textbook references there has not been published sufficiently detailed information on that matter. In the USA, this kind of model investigation is less widespread. There is known the investigation of a unit gravity monolith of the Koyna Dam, in which there occurred a crack similar to the real one, which occurred during the earthquake of 1967 (Fig. 21.4; CEE, 1990).

A number of shaking tables have been set up in China, the most advanced of which is the large triaxial earthquake simulator installed in the China Institute of

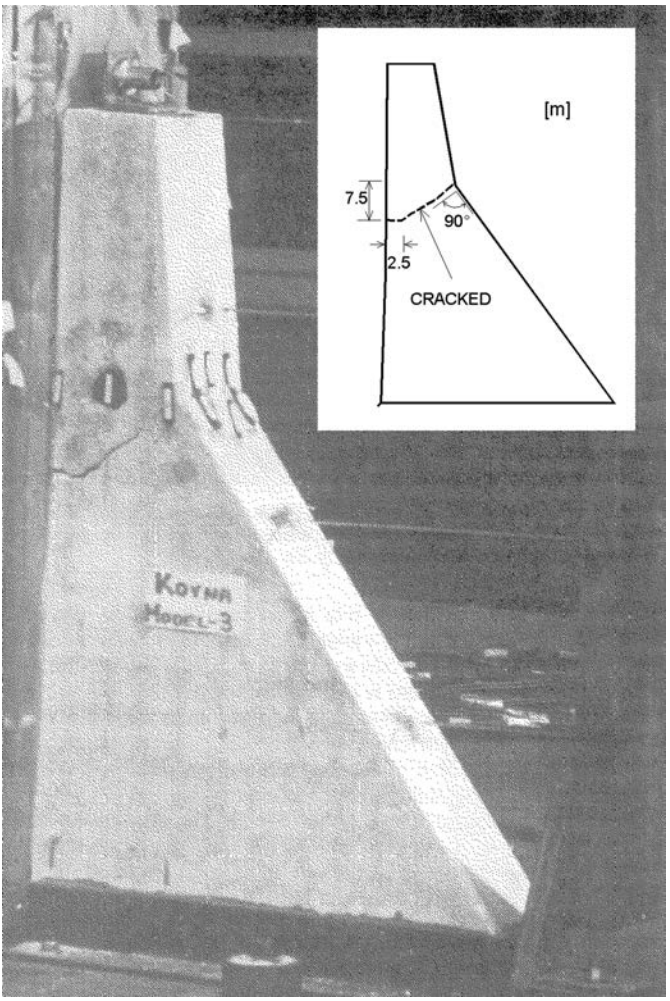

Figure 21.4 Model of a unit gravitational monolith of the Koyna Dam; the crack is a result of a test on a shaking platform, with the inclusion of a two-dimensional model of the reservoir (after CEE, 1990).

Water Resources and Hydropower Research (IWHR). The performance specifications and main features of the table in IWHR are:

- Size of table: 5×5 m;
- Frequency range: 0.1–120 Hz;
- Direction of excitation: 2 horizontal and vertical simultaneously with 6 degrees of freedom;
- Maximum displacement: ±40 mm (horizontal), ±30 mm (vertical);
- Maximum velocity: ±400 mm/s (horizontal), ±300 mm/s (vertical);
- Maximum acceleration: $\pm 1.0g$ (horizontal), $\pm 0.7g$ (vertical).

As the basic requirement for similarity is that the quantities governing behaviour of the system must be retained in the same relative magnitudes in the model as occur naturally in the prototype, the requirements of similarity laws from the modelling theory specified for dams have been investigated. The ratio between the physical quantities of prototype and model is defined as similarity constant C. By the principle of similarity theory the similarity constants of the main quantities of possible significance in defining the system behaviour must satisfy additional relationships. Details are given by Jiazheng & Jing (2000).

The shaking-table experiments employing physical models of concrete dams also require the introduction of limiting assumptions, with regard to both the properties of the model structure, reservoir water and foundation rock and the nature of the simulated boundary conditions. For these reasons it is believed that the better evidence by far about the dynamic behaviour of dams is that obtained from in-situ field vibration experiments. Field vibration experiments, using either ambient or different forced input excitation, are very useful in verifying the mathematical model of the dam system mainly at low-response amplitudes. Particularly, if the compressibility of the reservoir water and the absorption effect of the silt deposit as well as the non-uniform input mechanism and radiation damping of the foundation are studied, the field vibration experiment will be the unique approach for verifying the developed analytical procedures (Jiazheng & Jing, 2000).

21.4 RECOMMENDATION FOR DESIGN AND CONSTRUCTION OF CONCRETE DAMS IN SEISMICALLY ACTIVE AREAS

Based on experiences gained from case studies, dynamic analyses and laboratory and filed experiments, the following recommendation can be given for design and construction of gravity and buttressed concrete dams in potentially seismically active areas (ICOLD, 2001; Wieland & Ahlehagh, 2013):

- Maintenance of low concrete placing temperatures to minimize initial, heat-induced tensile stresses and shrinkage cracking.
- Development and maintenance of a good drainage system.
- Providing well-prepared lift surfaces to maximize bond and tensile strength.
- Utilization of shear keys in the construction joints over the height of the dam.
- Minimizing of discontinuities in the dam body, such as parapet walls, thrust blocks, piers etc., to avoid or to decrease local stress concentrations.
- Increasing the crest width to reduce the consequences of local through-cracking.
- The quality of concrete at the top dam portion should be properly raised.
- Avoiding a break in slope on the downstream faces of gravity dams to eliminate local stress concentrations.
- Provide a smooth and gradual change in the configuration of the dam.
- Account for the effect of the amplification of the earthquake action at the dam crest and strengthening the top portion of the dam properly without increasing its inertial force (reinforcement of crest zone).
- Enlarging of wedge at upstream heel of the dam to increase shear resistance.

- Constructing of grout curtain closer to the upstream face of the dam to minimize uplift pressures.
- Installing of geotextile at upstream face of the dam where cracks along horizontal lift joints are possible in order to eliminate any uplift forces acting on detached concrete blocks.
- Increasing of slope angle (towards downstream) of lift joints and/or the dam-foundation contact.
- Application of measures to increase the stability of buttress dams in the longitudinal direction (parallel to the dam axis). For this purpose, the downstream faces of the buttresses should be connected as a whole, and the heads of the buttresses should also have sufficient contact surfaces between each other.

There is an opinion that arch dams have higher resistance against earthquakes than other concrete dams. Anyhow, some recommendations can be made:

- Development of a design with regular and smooth geometry (symmetry is desirable, but not essential).
- Maintenance of continuous compressive loading along the foundation, by its appropriate shaping.
- Limiting the crest length to height ratio, to assure that the dam does not distort excessively in the higher modes of vibration during earthquake shaking.
- Providing contraction joints with adequate interlocking.
- Improving the dynamic resistance and consolidation of the foundation rock by extensive foundation benefaction, consisting of excavation and replacement with concrete of lesser quality rock, shears, cavities, etc., and grouting.
- Provision of well-prepared lift surfaces to maximize bond and tensile strength.
- Increasing the crest width, to reduce the incidence of local cracking.
- Minimizing mass in the upper portion of the dam.

An important general guideline, applicable for all concrete dam types, is: if significant movement along a fault crossing the dam site is accepted as a reasonable possibility during the lifetime of the dam, the best advice is to select an alternative site, less exposed to geodynamic hazard (Wieland et al., 2008).

Of special interest is also the performance of combined structures under seismic conditions, such as various combinations of concrete and earth-rockfill structures. Of particular interest are dams where the earth or earth-rock structures are wrapped around the end of a gravity dam or concrete spillway structure. Of concern are the dynamic interaction and differential displacement of the adjacent earth and concrete structures. Each structure will have a different response and displacement, which should be analyzed to determine the dynamic compatibility of the two different structures during earthquake shaking. Sloping of the concrete interface to maintain a normal embankment loading against the concrete and the use of plastic soils and wider filter zones in the embankments are special design considerations for the interface area (ICOLD, 2001).

Chapter 22

Monitoring and surveillance of concrete dams

22.1 MONITORING, SURVEILLANCE, AND INSTRUMENTATION OF CONCRETE DAMS – GENERAL

The objective of surveillance, monitoring, and instrumentation of concrete dams is the same as that for embankment dams. Of primary importance in surveillance and monitoring are data, on the basis of which it is possible to judge the safety of the dam; of secondary importance, is the information that might be used in designing other dams.

In the case of concrete dams we keep under observation the temperature in the dam's body, strains and deformations, opening of joints, stresses (for arch dams also in the foundation) as well as the uplift pressure of pore water, filtrated into the concrete and the foundation. Here also there are two main methods for performing measurements: (1) by means of precise instruments that measure displacements of permanent bench marks, set up on the surface of the dam, galleries, vertical shafts, tunnels in the abutments and in the measuring wells in the foundation; (2) by means of instruments that are incorporated into the dam's body and the appurtenant structures by means of which the above-cited measurements are carried out; in case of need, instruments are incorporated both into the base of the dam and into the concrete-rock interface (Goguel & Mpala, 1992). Figure 22.1 shows an example of installed instruments of both types in the case of an arch dam (Golzé, 1977; USBR, 1977a).

Regarding the location of the instruments, similar principles are valid as for the embankment dams – the surveillance, i.e. monitoring, should encompass the zones with maximum expected values of stresses, deformations, and points at which they have previously been calculated, in order for it to be possible to carry out comparisons of the expected values and the actual ones.

The abundance of the instruments depends on the type, size, and complexity of the structure that is under observation. Higher and more complex structures require more instruments. In the case of arch dams, as more sophisticated and more sensitive structures, it is necessary to perform more complex surveillance, in comparison with gravity dams and buttress dams. The number of instruments should be so selected as to ensure that a clear picture of the law is obtained, according to which there have been distributed stresses, deformations and temperatures in the dam's body as a whole, as well as in its foundation and in some particularly important elements. However, the number of instruments installed is of less importance than the selection of appropriate equipment, its proper installation at critical locations, and correct interpretation of the resulting data within a well-planned surveillance programme.

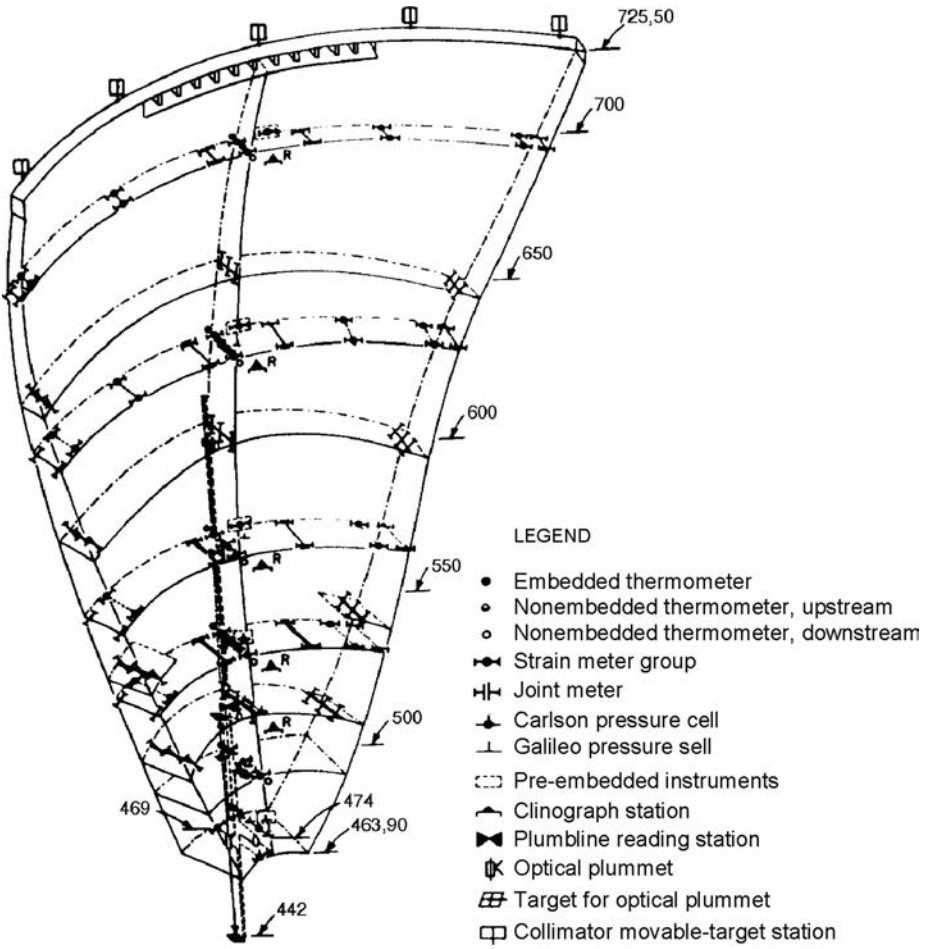

Figure 22.1 Instruments installed in an arch dam (after Golzé, 1977; USBR, 1977a).

22.2 MONITORING BY PRECISE SURVEY METHODS

By means of survey methods, it is possible to perform precise survey regarding deformations of the dam and its foundation. Using optical or electronic distance measuring equipment or lasers, relative vertical and horizontal movement of securely established surface stations can be determined. Measurements are also performed by means of plumblines, tangent line collimation, precise levelling, tape gages, and triangulation of deflection targets on the face of the dam. The relative movement and tilt of adjacent monoliths may also be determined via relatively simple mechanical or optical joint-meters.

The plumbline is a suitable and relatively simple device for measuring deformations caused by forces of water and also due to temperature variations. Weighted plumblines and float-supported plumblines are used. The first one consists of a weight near the

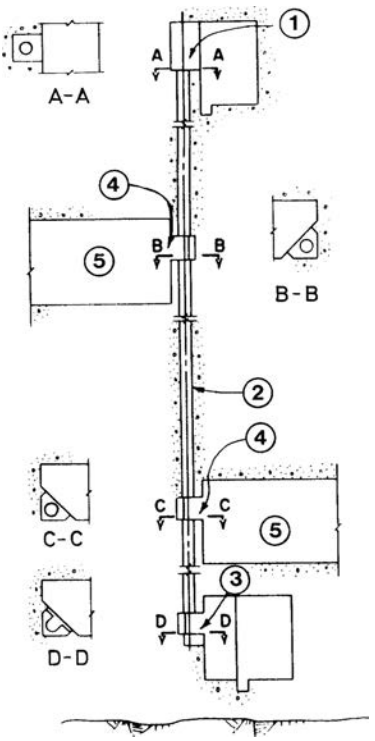

Figure 22.2 Scheme for a typical plumbline well (after USBR, 1976; Golzé, 1977). (1) Suspension chamber; (2) well, Ø30.5 cm; (3) reading station at the bottom; (4) reading stations at various levels; (5) adit.

base of the dam suspended by a wire and dropped down through a vertically-formed well from the dam's crest. For the float-supported plumbline, a float is installed in a tank at the top of the dam, connected with a wire to an anchor in the vicinity of the base of the dam. The measurements are performed at measuring stations, located in horizontal openings at various levels of the dam, in order to obtain a deflection along its entire height. A typical scheme of a well with measuring stations is presented in Figure 22.2. The measurements are performed by means of a sliding micrometer, provided either with a peep sight or with a microscope, set up in the measuring stations. The measured displacements indicate deformation of the structure with respect to the fixed end of the plumbline (USBR, 1976).

The installation of a plumbline is very often used in gravity dams, as well as in arch-gravity dams. In the case of arch dams, especially of double-curvature arch dams, the execution of a vertical well for a plumbline is usually not possible. And, with exactly this type of dam, the deflection of the crest in relation to the foundation is an important datum for an assessment of the dam's behaviour. Formerly, other methods were used for solving this problem, as, for example, with the installation of clinometers. Lately, we have performed direct measurement of displacements in an

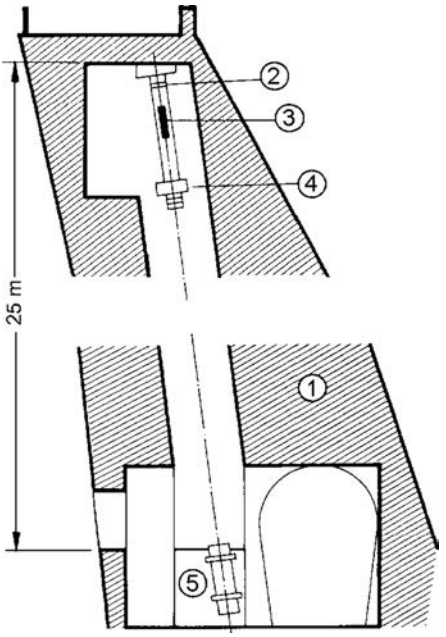

Figure 22.3 Laser plumbline installed in Zillergründl arch dam, Austria (ANCOLD, 1991). (1) Dam's body (concrete); (2) bearing part; (3) laser tube; (4) modulating and focusing element; (5) receiver.

inclined shaft, by utilizing a controlled monochrome light beam, as in the Zillergründl Dam (Austria), Figure 22.3. In the inclined shaft there has been installed a bearing device (2), which contains a laser tube (3) and which terminates with an element for directing and focusing the alignment (4). At the base, above the measuring mark, there is set up a receiver of the measuring signal (5) emitted from the laser tube. In that way, a teletransmission of the measuring signal is possible. The emitter of the signal in the upper part of the dam, as well as the receiver at the base, i.e. foundation, are watertight. This modern device measures displacements within the limits of ± 40 mm, with an accuracy of 0.2 mm (ANCOLD, 1991).

For determining deformations of particular points of the dam, in relation to reference points outside the dam, we employ collimation, then triangulation measurements, as well as levelling measurements.

Collimation measurements are performed with a theodolite at measuring points at the dam's crest. At one of the abutments, a pier for the instrument is constructed, set up at a higher level than that of the crest, while at the opposite abutment, approximately at the same level, there is set up a reference target. These two points are located so that the line of sight between them passes through locations on the dam's crest where measurements are to be made. In the case of arch dams, owing to the curvature of the crest, more targets and/or piers are necessary (Fig. 22.4; Golzé, 1977).

The deviation of the movable target from the line of sight yields the displacement of the appropriate point at the dam's crest. Three to four measuring points are usually

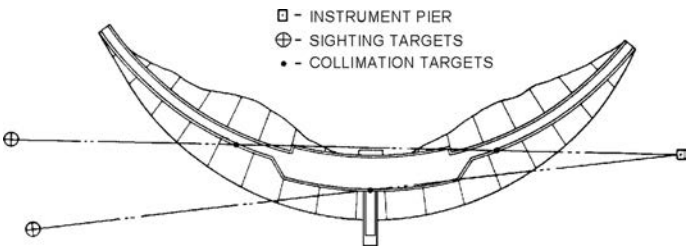

Figure 22.4 Layout for collimation measurements used for an arch dam (after Golzé, 1977).

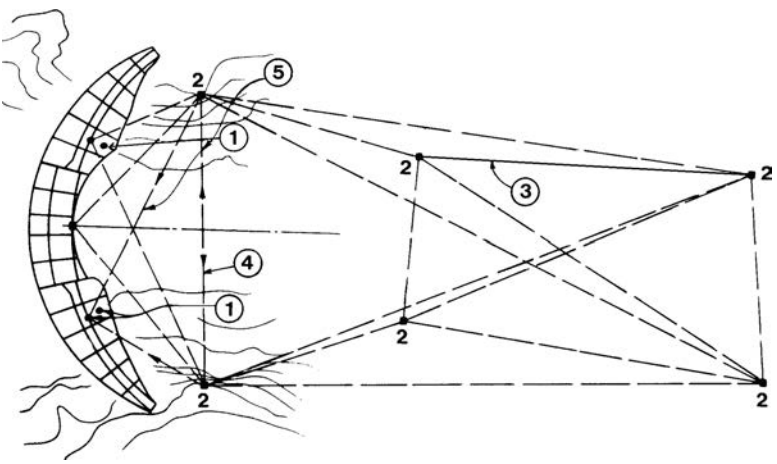

Figure 22.5 Layout for triangulation measurement (after Golzé, 1977). (1) Measuring targets on dam surface; (2) theodolite piers; (3) measured base line; (4) computed base line; (5) sight lines.

located, and the results are combined with the results obtained from measurements by means of a plumbline.

More abundant data for displacements are obtained by means of triangulation measurements. For that purpose, a system of triangulation targets is placed on the surface of the dam (the crest and downstream face), as well as on the appurtenant structures. This system requires a net of instrument piers and a base line downstream of the dam (Fig. 22.5; Golzé, 1977). The instrument piers should be positioned so as to make possible collimation from each pier to as many measuring targets as possible. The number of piers is dictated by the nature and topography of the surrounding ground. Measurements must be carried out by means of precise instruments and methods, performed by well-trained, experienced and skilled surveyors. The results show deformations of the dam, in relation to the targets outside its body, and deformations of the canyon downstream of the dam, in the direction of the river flow and perpendicular to it.

Levelling measurements serve for determination of the vertical displacements of points of the structure in relation to off-dam references, positioned sufficiently far

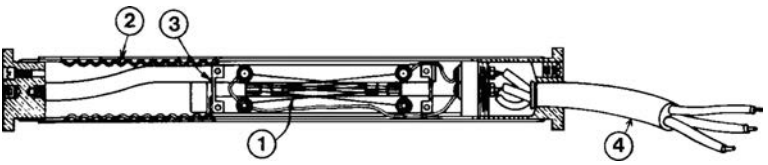

Figure 22.6 The Carlson Resistance Meter (after Golzé, 1977). (1) Music wire coils; (2) bellows; (3) steel spring; (4) conductor rubber covered cable.

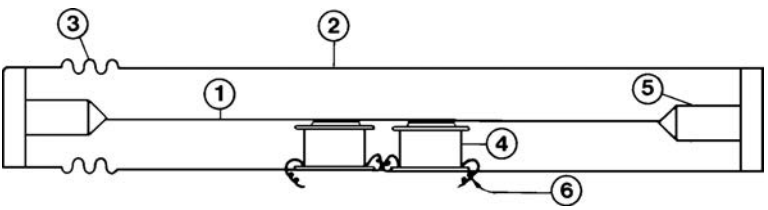

Figure 22.7 Scheme of vibrating wire instrument (after Golzé, 1977). (1) Vibrating wire; (2) case; (3) bellows; (4) electric magnet; (5) chuck; (6) lead.

away from the zone in which we can expect settlements caused by the structures of the hydraulic scheme, as well as the water in the reservoir. Similarly to triangulation measurements, levelling measurements also require the use of precise instruments and methods.

22.3 SURVEILLANCE WITH EMBEDDED INSTRUMENTS

A lot of surveillance instruments are produced in the world, intended for embedding in the body of concrete dams. These instruments are permanently developed and improved. Therefore, in the following only the principal and most often used instruments, as typical representatives of particular groups of instruments, will be described.

Various types of instruments are used for measuring temperature in individual zones of the dam's body. In the USA the most popular such instrument is the *Carlson elastic wire instrument*. This is a dual-purpose instrument in which a main element is an elastic music wire coil (1; Fig. 22.6). The instrument takes advantage of the fact that the electrical resistance of steel wire varies directly with the temperature. This instrument can also be used for measuring tensile stresses, since the changes in the electric resistance in the wire are also in direct dependence on the tension in the wire. In practice, this instrument has turned out to be a safe and stable instrument even in long-lasting service (Golzé, 1977).

In Europe, they very often use an instrument with a vibrating wire (Fig. 22.7). This instrument makes use of the fact that an increase in tension increases the frequency of vibration of the wire when plucked. The frequency is measured by use of a magnetic circuit. The measurements can be made by electrical readouts.

For determination of stresses in a given location of the dam's body, a group of 12 strain meters are usually embedded, of which 11 are connected to one support and

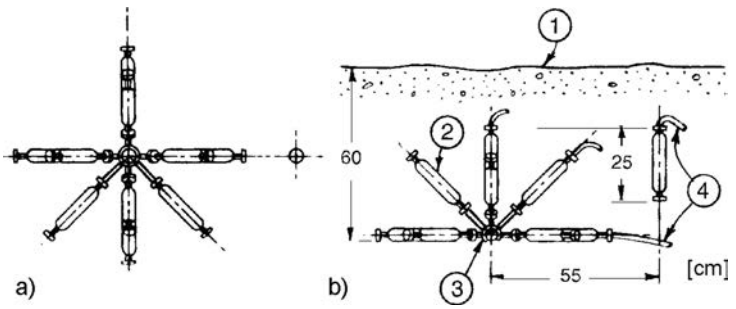

Figure 22.8 Group (cluster) of 12 strain meters (after Golzé, 1977; USBR, 1977b). (a) Plan; (b) elevation. (1) Upper boundary of layer; (2) strain meters; (3) strain meter spider (support); (4) electrical cables.

incorporated in the form of a cluster, as is shown in Figure 22.8. The twelfth strain meter is set up vertically in the vicinity of the cluster. Nine strain meters give complete information on strains in all directions, while three strain meters serve as a reserve, as well as for a check-up on the obtained results. Depending on the requirements and needs, it is also possible to incorporate a smaller number of strain meters, which, in the particular location, will yield data on only certain, especially interesting, directions. Then, on the basis of the obtained data on strains, it is possible to calculate stresses, based on the known dimensions and characteristics of the strain meters.

A *Carlson Stress Meter* is used for the determination of compressive stresses. Its main elements are two flat steel plates, with a diameter of 15.7 cm, connected with a layer of mercury, about 0.5 mm thick (Fig. 22.9). The central part of the upper plate has a very reduced thickness and it behaves as a diaphragm. The external pressure, acting on the plates, causes appropriate pressure in the mercury, which causes deflection of the diaphragm towards the external side, by means of which there comes about an activation of the device for measuring strains. This consists of two threads of steel wire, placed on sheaves (pulleys), connected by means of a steel frame. The deflection of the diaphragm tensions the wire from one of the threads, while loosening the other, in equal proportion. The variation in tensioning changes the electric resistance of the two threads, which can be measured by means of Wheatstone's bridge, while the variation of the resistance is a measure of the deflection of the diaphragm. The resistance is not dependent on change in the temperature, since it equally influences the two coils (Golzé, 1977; Hanna, 1985; Sing & Sharma, 1976).

The Carlson Stress Meter is usually employed for special purposes, such as, for example, for the determination of the vertical stresses at the base, i.e. foundation, and for comparison of results obtained by means of a strain meter. It is also used with arch dams for determination of the horizontal compressive stress in the thin elements in the vicinity of the crest. The Carlson Stress Meter is used not only with concrete dams, but also with embankment dams (Sing & Sharma, 1976).

Appropriate instruments are used for measurement of the opening of joints, which are similar to the strain meters; however with a wider measuring range, owing to the greater expected displacements. That is why the sensitivity and accuracy of these

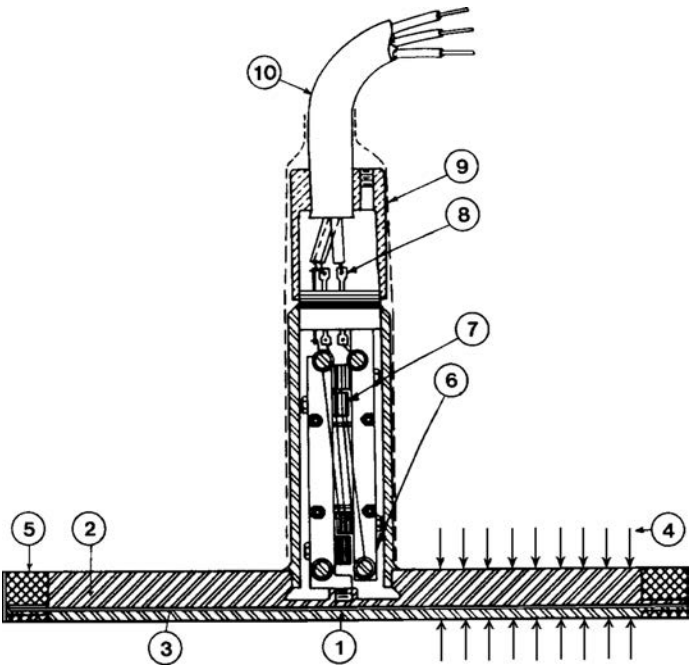

Figure 22.9 Carlson Stress Meter (after Golzé, 1977). (1) Internal plate; (2) external plate; (3) mercury film; (4) stress being measured; (5) compressible material; (6) steel bar; (7) ceramic spool; (8) glass insulated terminals; (9) fabric cover; (10) conductor cable.

instruments has been reduced. This type of instrument can also be embedded in a borehole in the foundation, immediately below the dam, with the task of measuring deformations in the rock foundation.

At some concrete dams in Europe they also carry out measurements of the rotation of some reference axis in relation to certain horizontal or vertical planes. Such measurements are performed at selected places in the galleries, by means of two types of instruments: clinometers and inclinometers. *Clinometers*, used for measuring changes of the angles in relation to the horizontal plane, are more often employed than *inclinometers*, used for measuring the angle of rotation in relation to the vertical (Hanna, 1985).

Tiltmeters have been popular in concrete dams during the last few decades. These are very precise instruments. During the initial period, they were used for a determination of the changes of the level of two points. The first such instruments consisted of a glass tube, which contained an electrolyte. At the end of the tube, as well as in the middle in the electrolyte, partially submerged electrodes have been set up. The resistance between the central and end electrode varies with the inclination of the tube. In that way, by means of installing appropriate measuring devices, it is possible to record very small changes of the inclination in regard to the horizontal. Also, there are some tiltmeters that operate with water. They are sensitive and are used by geologists for recording small strains in the earth's crust, caused by seismic activities. They have also been used for monitoring the displacements of rock masses.

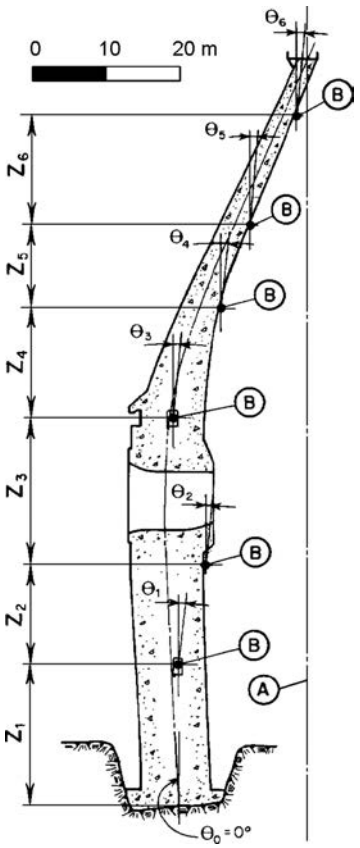

Figure 22.10 Installed tiltmeters in the central section of the Boundary Dam, USA (after Sharma et al., 1994). (A) Reference axis; (B) tiltmeters.

Modern tiltmeters are automatic and by means of their high accuracy we can measure angle rotation. They are installed on the concrete surfaces of the dam or into galleries, with appropriate anchoring into specially made and prepared boreholes. Every tiltmeter by means of cables is connected to receiving units, which are, further on, connected with stations for recording, as well as with alarm units, which are activated while recording abnormal behaviour of the dam. Modern systems of tiltmeters are automated in relation to collecting data, remote control, etc. Such a completely automated system of 20 *biaxial* tiltmeters was installed towards the end of 1992 (a number of years after its start-up in service) at the Boundary arch dam (USA), whose unusual structure has already been considered in the chapter on arch dams. Biaxial tiltmeters are intended for measuring the vertical angle deflection, parallel and perpendicular to the appropriate planes, which are radial in relation to one reference cylinder, the axis of which (*A*) is presented in the central section (Fig. 22.10; Sharma et al., 1994).

Six tiltmeters have been installed into the gallery of the Boundary Dam, while others were put in place across the downstream slope. Owing to its inclination towards

the downstream side, that has not been at all simple to carry out[1]. The manufacturer of the tiltmeters has supplied system software for automatic reading, i.e. recording, of data at intervals determined by the user. The output data consist of values of the angle of deflection and the angle of inclination, measured in relation to the radial surface of the tiltmeter. And since the vertical section through the plane of tiltmeters is not uniform, and also due to the three-dimensional effect, there has been developed a special method for accurate calculation of the horizontal deflection based on the data obtained from the measurements. By using the method of the least squares, the following formula has been developed:

$$D(k) = \sum_{i=1}^{k} \left[A(i) + \frac{\Theta(i) + \Theta(i-1)}{2} Z(i)B(i) \right] \tag{22.1}$$

where, $D(k)$ is the deflection at a particular location of the tiltmeter k; $A(i)$ and $B(i)$ are the constants of the tiltmeter; $\Theta(i)$ is the angle deflection measured with the tiltmeter; and $Z(i)$ is the vertical distance between the subsequent tiltmeters.

The obtained data are compared with the values that have been calculated by using the Finite Element Method, in which the model for calculations is permanently calibrated and adjusted on the basis of the measured data. The final objective of the users of the dam was to obtain complete coincidence of the calculated data and measured data, which implies obtaining a model with a completely true and authentic presentation of the behaviour of the dam.

In the case of gravity concrete dams, it is also necessary to measure the value of the uplift pressure in the concrete–rock interface and in the dam's body, occurring owing to the penetration of water through cracks in the foundation and concrete, due to a badly constructed grout curtain or due to poor functioning of the drainage. For that purpose there is installed a system of pipes in several blocks in the contact of the dam and the foundation, while the uplift is determined by means of measuring instruments or with a whistle. Also, piezometers can also be embedded, especially in smaller dams, of similar construction to those used for embankment dams. In the case of soil foundations, the uplift can also be measured with built-in cells for measuring pore pressure, which can be embedded at selected locations and in the dam's body, for measuring the pore pressure in the concrete.

22.4 AUTOMATIZATION AND COMPUTERIZATION OF MONITORING

Along with the development of computer technology, there have been created broad possibilities for the automated and continuous keeping under observation of the behaviour of dams through networking the measuring instruments with precise microcomputers (Pircher, 2001). Such an automated centralized system for reading out, i.e. recording, has been developed by the company TELEMAC for giving out results and it can be used both with embankment dams and with concrete dams. The standard scheme of that electronic system is presented in Figure 22.11.

[1]During construction a company specialised in mountaineering techniques and construction sites with special difficulties of access was brought in.

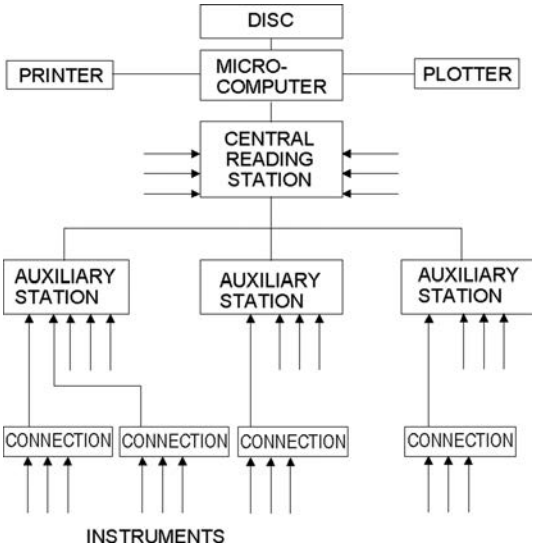

Figure 22.11 TELEMAC system for automated centralized monitoring.

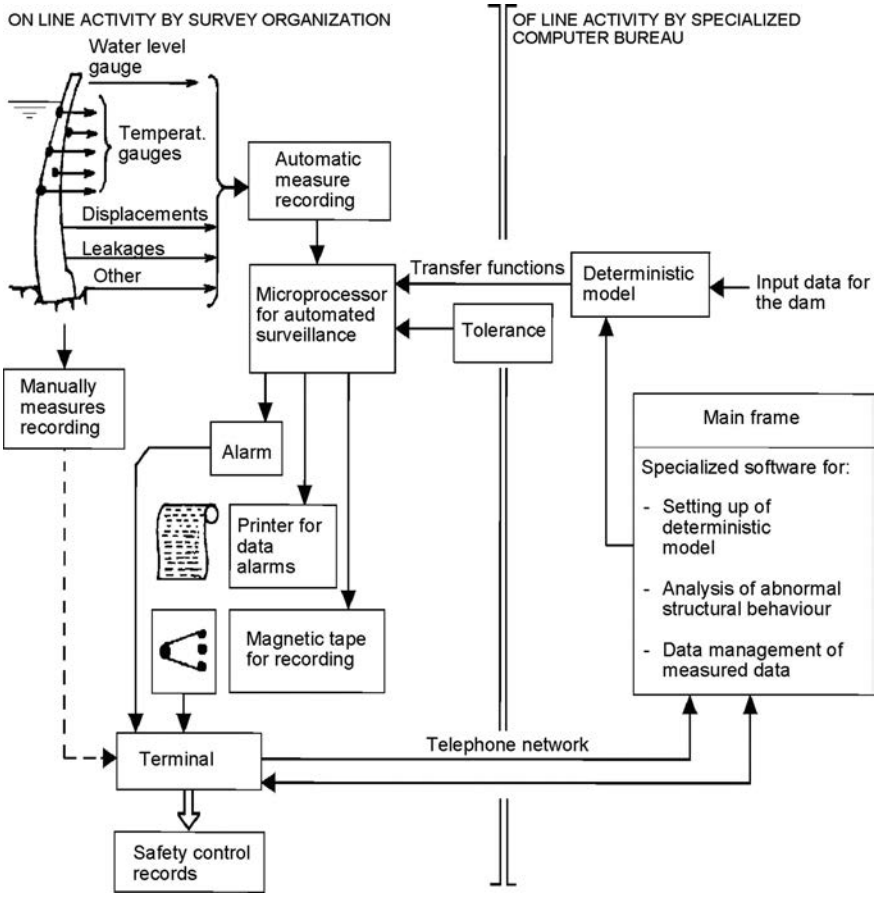

Figure 22.12 Microprocessor-aided monitoring system in Italian dams (after Hanna, 1985).

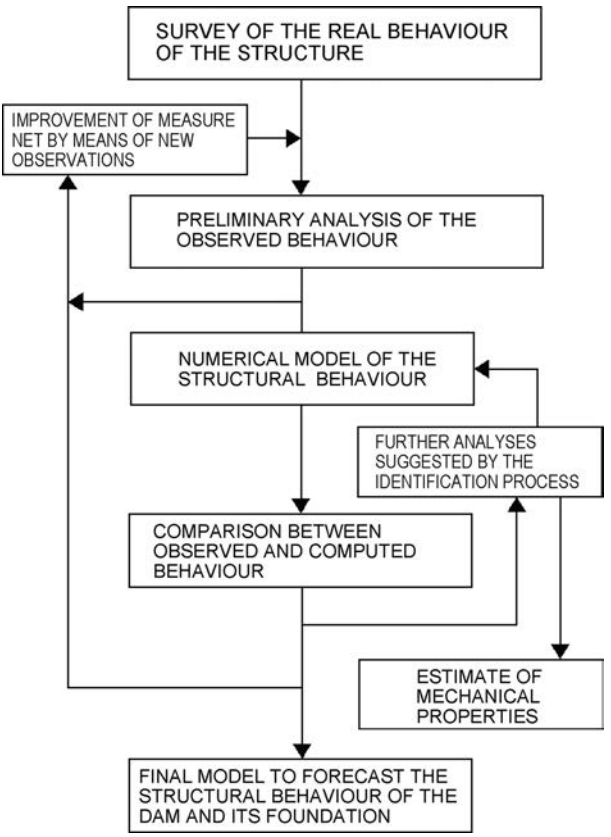

Figure 22.13 Conceptual scheme of arch dam analysis and behaviour monitoring (after Hanna, 1985).

Through relays in the auxiliary stations, it is possible in an automated way to observe the instruments that are controlled by a microcomputer, which can also convert the electrical signals into units of strains, stresses, and temperature. The microcomputer is also able to process the obtained data, as well as to alarm should there come about an exceeding of the specified values (Hanna, 1985).

The Italian National Energetic Agency has developed a microprocessor system for monitoring of concrete dams, as well as a rational interpretation of the obtained results, the principle of which is explained in the flow chart in Figure 22.12. The system works continually 24 hours a day and it carries out recording of all measured parameters, as well as the diagnosis any abnormal behaviour of the dam. It immediately calculates the differences between the expected and obtained values of parameters, then compares the differences with the allowable values and, at the same time, it sorts out data for subsequent calculations and investigations in specialized computer offices. In that way, the data from measurements are obtained in the fastest way and can immediately be used for control static calculations with true authentic input parameters. In the case of arch dams in Italy, on the basis of results obtained regarding the real behaviour of

a constructed dam structure as well as the rock in the foundation, in case of need, they perform upgrading and enriching of the network for observations, while at the same time, permanently perform numerical, static, and dynamic calculations, until they come to the final model, by means of which it will be possible to predict the behaviour of the dam and its foundation. Then the parameters of that model are taken for comparison with the results obtained from measurements. The flow chart of such a system is illustrated in Figure 22.13.

In Austria automatization and computerization of the monitoring of dams is also performed. It is characteristic that Austria possesses many dams, located in distant mountainous regions, hardly accessible in winter conditions. That is why, in general, the reading-out of the instruments in that country is recorded at a central, remote station, which, when obtaining a value that exceeds the allowable one, reacts with an optical or acoustic signal. Such modern system having display options available on any personal computer in the Company Network, is described by Kofler (2010).

This page intentionally left blank

Part 4

Hydromechanical equipment and appurtenant hydraulic structures

This page intentionally left blank

Chapter 23

Mechanical equipment and appurtenant hydraulic structures – general

23.1 HYDROMECHANICAL EQUIPMENT – GENERAL

23.1.1 Introduction

Within the composition of a hydraulic scheme, there are very often constructed water-conveying structures, either general or specific ones, which serve for conveyance of the water from one place to another. In order to enable their functioning, it is compulsory to use hydro-mechanical equipment, which serves for closing and opening of the openings of the water-conveying structures. In that way, in the case of hydraulic schemes with a dam, it is possible to realize a controlled discharge of water, as well as to regulate the level of the headwater, and also a controlled intake, conveying and utilization of water for certain objectives.

In the cases of hydraulic schemes with a dam, as well as with isolated water-conveying structures, the following basic kinds of hydro-mechanical equipment are used:

1. *Gates* and *valves*, which serve for straightforward closing and opening of the openings for the passage of water;
2. *Fixed parts* of the gates and valves, that is to say stationary metal parts, embedded in the concrete dam's body;
3. *Mechanisms for lifting and lowering* the gates and valves (hoists, cranes, hydraulic mechanisms), by means of which we can achieve handling of the gates and valves;
4. *Service bridges*, upon which are installed stationary mechanisms for lifting of the gates and valves or along which cranes operate.

The hydraulic engineer should be acquainted with the hydromechanical equipment in order to be able to carry out its proper selection in designing the hydraulic scheme (Araoz, 1994), to determine the over-all dimensions of the equipment and other necessary parameters, all in order to determine more precisely the cost, prior to working out a special design for the equipment. In this, of particular interest are the gates and valves for the spillway structures and the outlet works structures of dams. The preliminary as well as the construction design for the gates and valves, as well as the remaining hydromechanical equipment, are performed by specialized companies, most often by those that will manufacture the equipment.

23.1.2 Classification of gates and valves

The gates and valves, which are used with every hydraulic scheme with a dam, and are the most significant part of hydro-mechanical equipment, can be divided in different ways.

According to the *position of the opening* in relation to the level of headwater, the gates and valves are divided into: (a) surface (crest) gates, which serve for closing the surface openings; and (b) high-head or submerged gates and valves, which are set up at the beginning, at the intermediate part or at the end of the water-conveying structure below the water level. In contrast to the surface gates, the high-head gates and valves operate under high pressure.

According to their *purpose,* i.e. function, gates and valves can be: (a) basic or service, i.e. operational, which are used permanently during the service of the structure; (b) maintenance (overhaul) gates and valves – for covering the opening during an overhaul of the service, gate or valve; (c) emergency gate or valve, for closing the opening in case of an emergency which threatens to cause catastrophic consequences; and (d) temporary gates or valves, which serve for covering the openings during the execution of works. In certain cases, it is worthwhile and useful to combine the functions of the gates or the valves, for example, to use an overhaul-emergency gate or valve or some other combination.

According to *the material of which they are made*, we can differentiate: (a) steel gates and valves, which are the most widespread types owing to their significant strength, as well as the suitable conditions for fitting and erection; (b) aluminium alloy gates or valves, which possess a smaller mass and are resistant to corrosion; (c) reinforced concrete gates, with very limited application due to their large mass (this deficiency could be overcome with the application of prestressed concrete structures, i.e. members); however, for the time being there have been no significant results achieved in this field; (d) wooden gates or valves, which are used mainly for openings with pressure heads up to 5 m and spans up to 4 m; and (e) fabric gates, either rubberised or synthetic.

According to the *way of transmission water-pressure*, we can differentiate gates or valves: (a) that transfer the pressure to the parting walls or piers; (b) that transfer the pressure to the sill of the structure; (c) that transfer the pressure to the sill and to the parting walls (or piers), i.e. to the whole structure; (d) that transfer the pressure to the part of the structure at the perimeter of the deep opening; or (e) that do not transfer the pressure of the water to the structure or the element.

According to the *mode of operation*, the gates and valves can be: (a) with a possibility of regulation; that is to say, able to operate with partial opening (regulating gates and valves); and (b) without such a possibility for regulation (non-regulating gates and valves).

According to the *type of movement*, the gates and valves can translate, rotate, roll, or float. The translation can be transverse to the flow or parallel to it. To achieve movement, it is possible to use mechanisms with electrical, hydraulic, or manual drive, and we can also utilize the force of the water pressure.

Depending on the *water passage* in relation to the leaf position, the following situations are possible: (a) discharge over the leaf; (b) discharge under the leaf; or (c) discharge over and under the leaf.

Depending on the *skin plate (waterproof lining) shape*, gates may be: (a) flat; or (b) radial.

Various kinds of gates and valves are used in practice, but this book will examine only the most frequently used ones. In examining these elements, a classification will be utilized according to the *position of the opening* in relation to the level of headwater and also according to the *way of transfer of the water pressure* to the structure.

23.1.3 Forces acting on gates and valves

In order to perform proper dimensioning of the gates and valves, it is essential as accurately as possible to anticipate and take into consideration all forces acting upon them and for various possible conditions of work. In general, the following basic, i.e. primary, forces act on the gates and valves:

- *Hydrostatic pressure* of water and *sediment* (*silt*) *pressure*. These forces are assumed in the same way as in the dimensioning of dams.
- *Static pressure of ice*. This force is most often not taken into consideration, since in most cases, there have been taken measures in service aiming at reducing that action.
- *Self-weight* of the gate or valve. In the first approximation, the weight of the gate or valve is calculated by means of empirical formulae and diagrams for various kinds of gates and valves, depending on the width of opening and the height of the gate or valve. Finally, the weight of the gate or valve is obtained after the completion of the design for its metal or other kind of construction, depending on the materials anticipated for the execution of the gate or valve.
- *Forces due to temperature variations, wind pressure* and *waves*, *seismic pressure of water*, and *hydrodynamic pressure of water*, as well as *dynamic pressure of ice* are taken into consideration in certain cases, if they have considerable values for the given conditions. Among the forces, cited in this group, of particular importance are the *hydrodynamic forces*. They are in close relation with the conditions of flow in the zone of the gate or valve. In this, the most important factors that influence the conditions of flow, and which can be constructed either above or under the gate, are the geometry of the water-conveying structure upstream and downstream of the gate or valve, and the geometry and position of the gate (valve), as well as its additional elements, such as waterstops, supports, etc., whether the flow is submerged or unsubmerged, etc. In cases where it appears to be appropriate, these forces will be considered and examined in the following chapters, with particular kinds of gates or valves.

23.2 MECHANISMS FOR LIFTING AND LOWERING OF THE GATES AND VALVES. SERVICE BRIDGES

In describing the most important individual gates and valves, in brief and within the necessary extent, we shall discuss the specific qualities of the mechanisms for handling the equipment, that is to say, for lifting and lowering the gates and valves, which are

essential for the particular kind of gate or valve. In general, the mechanisms for lifting and lowering the gates and valves can be divided into two groups:

1. When there is utilized pressure of the water, which is conveyed in a special chamber;
2. When the movement is performed mechanically.

The mode of operation of gates and valves, which move by means of water pressure, will be described in the forthcoming chapters, where appropriate kinds of gates or valves will be examined.

The gates and valves with mechanical operation, which have the widest application, move, i.e. dislocate, in two ways: either with stationary or with mobile mechanisms. The stationary mechanisms, which service only one gate or valve, have the following advantages in relation to the mobile (movable) ones, which can be moved and, thus, service a number of gates and valves: (1) they enable fast and easy handling of the gate (valve); (2) we can relatively easily carry out adaptation for remote control; and (3) there is relatively simple handling of the gates and valves which require use of force for their lowering. If the overflow part of the dam consists of a number of spans, for instance 7–8 and more, then movable mechanisms are usually more economical. Besides, movable mechanisms enable movement, i.e. dislocation, of gates from one opening to another, transportation of the overhaul-emergency gates along the length of the dam, as well as their use for other needs in the course of construction and service of the dam.

The gates, regardless of whether they are serviced by stationary of movable mechanisms, are fastened with clips, which can be vertical, inclined, or (more rarely) horizontal. We distinguish elastic clips, in the form of steel ropes and chains, as well as rigid clips, in the form of a metal lever with a screw (for small gates or valves), as a complex lever without a screw, consisting of a number of hinge-like (articulated) connected parts, or in the form of straight or arch-toothed levers (as in the case of radial gates).

The stationary devices for moving the gates in smaller systems, are constructed in the form of mechanisms with a screw (Fig. 23.1), while in the case of larger ones, appropriate hoists are used, operated by means of: manual, electric, or hydraulic drives. The weight of individual mechanisms, which influences their cost, depends on the size of the force which is required for lifting, on the type of the gate (valve), and the speed of movement, which usually amounts to about 2 m/min. The least weight of the mechanisms for lifting is required by the radial (tainter) and cylinder gate (see the two forthcoming chapters on gates).

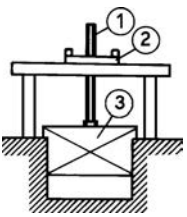

Figure 23.1 Mechanism with screw. (1) Lever with screw; (2) revolving part; (3) gate (valve).

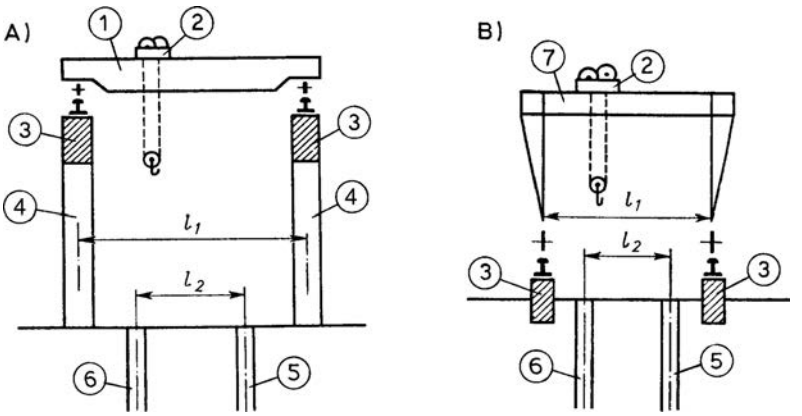

Figure 23.2 Schematic presentation of bridge crane (A) and portal crane (B). (1) Bridge crane; (2) hoist able to move along the crane bridge; (3) crane load-bearing girder; (4) column; (5) recess for service gate; (6) recess for overhaul gate; (7) portal crane.

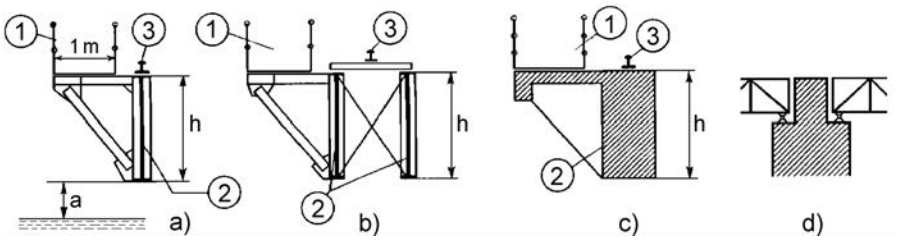

Figure 23.3 Service bridges. (1) Steel service bridge; (2) crane girder; (3) rail.

Regarding mobile hoisting mechanisms, when it is a question of small gates, ordinary hoists may be employed, which move from one span (opening) to another. In the case of larger gates, which are most frequently flat or radial, there are employed cranes that move on rails. Hoists are mounted on the cranes, and they can move along the span of the crane. In the case of dams, bridge cranes are employed (more rarely; Fig. 23.2A), as well as portal cranes (B) (Grishin et al., 1979; Chugaev, 1985).

The crane should be so constructed and positioned as to enable complete opening and, in case of need, also drawing out of the gate from the recesses. The span of the crane, upon which a hoist moves, should enable servicing not only of the service gates but also of the overhaul-emergency gates. Portal cranes, although more expensive than bridge ones, are employed much more frequently, since they do not require posts or columns.

In addition to the transit bridges, what are called service bridges are also constructed, upon which we set up stationary and mobile mechanisms for the handling of the gates, which also serve for official communication. The spans of these structures are equal to the width of the spans (openings) that are covered with the gates. Figure 23.3 presents schemes of cross-sections of service bridges, among others metal ones

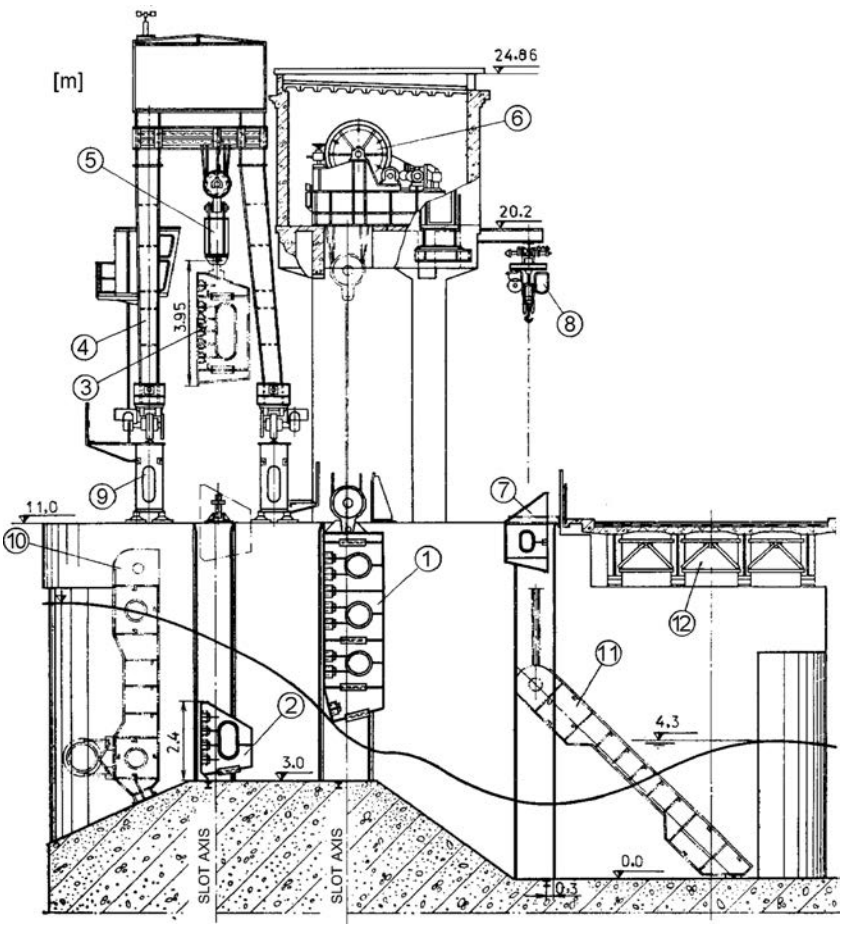

Figure 23.4 Hydro-mechanical equipment in an overflow dam (after Seleznev et al., 1982). (1) Service gate; (2) lower part and (3) upper part of upstream overhaul gate; (4) portal crane; (5) tackling part of the crane; (6) stationary moving mechanism; (7) downstream overhaul gate; (8) hoist; (9) crane girder; (10, 11) floating gates; (12) bridge.

(a, b) and reinforced concrete ones (c), along with a possible solution for resting the bridge on the parting wall (or pier) (d). The bridge or the crane girder should be elevated above the maximum level of the water by a value of a, in order to make possible unobstructed passage of ice and other floating solids (Fig. 23.3a; Chugaev, 1985).

As an illustration of possible positioning of gates and other hydro-mechanical equipment for various purposes, Figure 23.4 presents the cross-section of an overflow concrete dam, after its reconstruction (Seleznev et al., 1982).

23.3 INSTALLATION AND SERVICE OF GATES AND VALVES

In the selection of the type, construction and dimensions of the gates and valves, it is also necessary to take into account the conditions for their workmanship, and

possibilities for transportation, as well as for the experience, skill and fitness of the contractor of the works.

Metal gates and valves, as a rule, are manufactured in specialized factories, while only small ones can be made in a workshop. Wooden and reinforced concrete gates are most often made on the construction site. Gates, which, according to their dimensions, allow transportation by railway or roadway, are transported in an assembled state from the factory to the construction site. If that is not possible, then transportation is achieved in assembling (fit-up) units, that is to say in parts (elements) of the structure, which can relatively easily be assembled at the construction site. As a rule, we should try and endeavour the biggest part of the work on the execution of the gate to be performed in the factory. In this respect, plain gates (for more details see the forthcoming two chapters regarding the most important types of gates) can be set up in the span of the opening, as a whole, by means of cranes and hoists. In the same way, it is also possible to erect roller gates, flap gates, and sometimes also to construct radial gates. Sector gates and bear-trap gates are assembled directly into the openings, which extends the time of erection work on the dam, and that can influence the selection of the type of gate.

In order to make it possible for gates to be always ready for operation, it is necessary to periodically control and check them, along with the mechanisms for their moving, to replace the worn-out parts, clean, and lubricate the turning (rotating) parts, and to paint the parts susceptible to corrosion. For safe operation under winter conditions, it is necessary to undertake special measures in order for there not to come about freezing of the water immediately near the gate and, thus, its being thrown out of operation.

The control of mechanisms for manoeuvring the gates can be local (when the operator is immediately near the gate, i.e. a distance up to 1 km), tele-guided, and automatic control. Automatic control ensures the required position of the gate, depending on the level of the headwater or the tail water. That enables the closing of the gate in emergency situations. The automatization of the gates is achieved by the application of appropriate electrical equipment or by means of gates that react automatically to the pressure of water, which is more favourable from a service (operation) aspect, especially for rivers in which high flood waters may abruptly break out.

23.4 APPURTENANT HYDRAULIC STRUCTURES

23.4.1 Definition, function and capacity

For proper and safe service of a dam, it is indispensable, within its framework, to anticipate various *appurtenant hydraulic structures*, which can be general or special ones. While the special structures serve a certain water economics branch, the general (or common) structures serve a number of branches (see Chapter 1). Among the general hydraulic structures, the most significant are *the spillway* and *outlet works* which, almost without exception, are constructed in every hydraulic scheme with a dam.

The spillway structures have the task of evacuating flood waters from the reservoir at an assigned maximum level of the headwater and conveying them downstream in a safe manner. The structure and the type of the spillway works depend primarily on

the quantity of the flood water that should be evacuated, and the type and location of the dam, as well as on the size, function, and way of utilizing the reservoir.

The outlet works serve to empty the reservoir (completely or to a certain level) in case of need for repairs to the structures within the framework of the hydraulic scheme or when there is danger of a failure of the dam, as well as for discharging water from the reservoir for satisfying sanitary and water management requirements downstream of the hydraulic scheme. The above-described function of the outlet works dictates that it should be positioned low in relation to the crest of the dam, that is to say, close to the foundation. That is why, usually, it is called a bottom outlet. The construction and position of the bottom outlet depend, first of all, on the type of the dam, the purpose of the reservoir, and the quantity and depositing of silt. The level of the entrance edge of the outlets is most often dictated by the level of the dead storage in the reservoir, i.e. by the conditions for discharging the minimum quantity of sanitary water, or for satisfying the biological minimum in the river downstream of the dam.

In designing the spillway and outlet works, in addition to the governing water, it is also necessary to take account of all other elements which influence their dimensions, structure and convenience during construction as well as their behaviour during service (Singh & Varshney, 1995).

The maximum water quantity which should be evacuated by means of the spillway structures is determined depending on the significance and size of the dam (Fahlbusch, 1999; Rissler, 2001). There has been a widely accepted practice for the spillways of large dams to be dimensioned for flood water with a probability of 0.01% occurrence for embankment dams and 0.1% for concrete dams. This rule, which has lately been accepted and applied here, was subject to serious revision. Namely, ICOLD records failed dams higher than 15 m (ICOLD, 1974). The reasons for a failure of 216 such dams are presented in the diagrams in Figure 23.5. From the last diagram, containing data for all kinds of dams together, it can be seen that overflowing over the crest, which is mainly a consequence of an insufficient spillway capacity, is the most frequent reason for failures of dams. Owing to that in the USA, as well as in all other developed countries, an obligation has been introduced: for all more significant dams, the

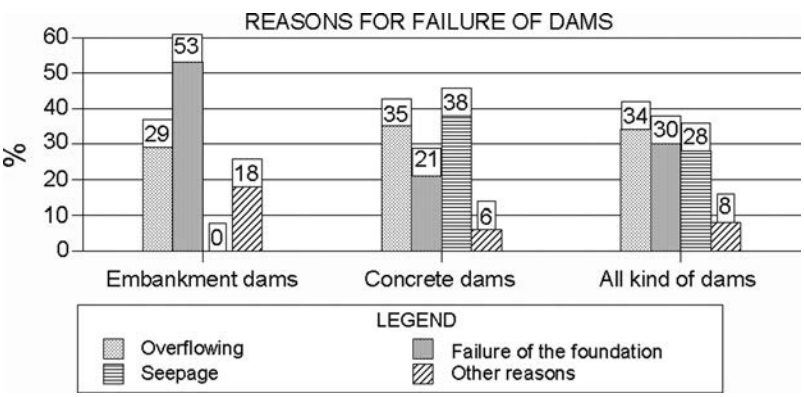

Figure 23.5 Reasons for failure of dams (not including failures occurring in the course of construction and caused by military actions).

spillway structures should be dimensioned for the probable maximum flood – PMF (USCOLD, 1988). This tendency has spread to an increasing number of countries, and even already constructed dams are subject to revisions (Solvik & Skoglund, 1994). Various methods have been developed in hydrology for determination of the PMF (Lafitte, 1989, 1992; Reinius, 1989). Some well-known experts in the field of hydrology and hydraulic structures have been against the application of PMF water for dimensioning of spillways, for example Yevgjevic (2001).

The assumption of the maximum water quantity (the design flood) which will be evacuated via the spillway structure is an extremely complex problem and it should emerge from a detailed study, worked out separately for each specific case, and not with a linear application to water with a certain probability of occurrence (Talbot, 1994). In the analysis one should particularly take into consideration the location of the dam, type of dam, procedure which is used for determination of design flood and the availability with measurements upon which the applied procedure is based. For illustration of the factors that influence the solution of this question and for a possible way of their being taken into consideration, Table 23.1 gives the recommendations which, in that respect, the Institution of Civil Engineers (UK) issues (Novak et al., 2001).

The capacity of the outlet works is determined on the basis of the time which is necessary for emptying the reservoir and the necessity for sanitary water for satisfying the biological minimum in the river downstream of the dam. While the second condition gives a certain fixed quantity of water that should be conveyed through the outlet works, the first one – time necessary for emptying the reservoir – is determined for each hydraulic scheme separately, depending on local conditions. In that respect, a number of factors are influential: type and size of dam, volume of reservoir storage space, pressure at which the hydraulic scheme works, the possibility during emptying the reservoir of also using water-conveying structures constructed for other purposes, i.e. functions, and conditions existing in the watercourse downstream of the hydraulic scheme, etc. In some cases, the time of emptying can be 2–3 days; in other cases, 2–3 weeks, while a month or two may be needed.

The capacity of the bottom outlet is in direct dependence on the dimensions of the water-conveying part and the size of gates, as well as on the maximum pressure head at which it operates. One should take account of the fact that, in the case of high-head hydraulic schemes, in case of need for discharging significant quantities of water, in the bottom outlet there can occur high velocities, which brings a danger of cavitation and cavitational erosion (Galjperin et al., 1977; see Chapter 4).

23.4.2 Classification of spillways and bottom outlets

The spillway structures, or *spillways*, can be divided into two major groups: (a) spillways *in the dam's body* (1, Fig. 23.6), and (b) spillways *outside the dam's body* (2, 3, Fig. 23.6). The type and structure of the spillways depend on the type of dam, as well as on the local topographical, geological, and hydrologic conditions.

According to their structure, spillways are divided into a number of types that are found in the two major groups of spillways or in only one of them. Thus, for example, according to the position of the inlet (intake) or the entrance part, spillways can be surface (crest) spillways or high-head (submerged) spillways, which are found

Table 23.1 Flood, wind and wave standards by dam category, *Institution of Civil Engineers, UK* (after Novak et al. 2001).

Dam category	*Potential effect of a dam breach*	*Initial reservoir condition standard*	*Reservoir design flood inflow*		*Concurrent wind speed and minimum wave surcharge allowance*
			General	*Minimum standard if overtopping is tolerable*	
a	Where a breach could endanger lives in a community	Spilling long-term average inflow	Probable maximum flood (PMF)	10,000-year flood	Mean annual maximum hourly wind speed Wave surcharge allowance not less than 0.6 m
b	Where a breach – could endanger lives – could result in extensive damage	Just full (i.e. no spill) flood	10,000-year	1000-year flood	
c	Where a breach would pose negligible risk to life and cause limited damage	Just full (i.e. no spill)	1000-year flood	150-year flood	Mean annual maximum hourly wind speed
d	Special cases where no loss of life can be foreseen as a result of a breach and very limited additional flood damage would be caused	Spilling long-term average inflow	150-year flood	Not applicable	Mean annual maximum hourly wind speed Wave surcharge allowance not less than 0.3 m

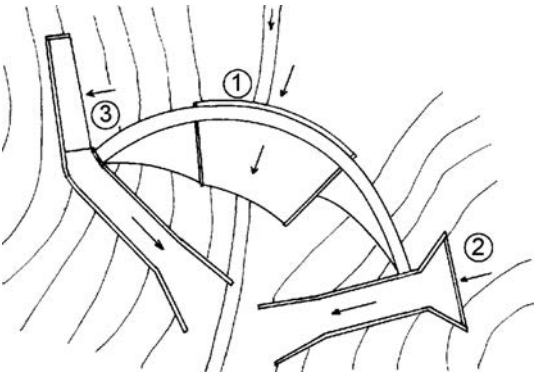

Figure 23.6 Spillways in dam's body (1) outside dam's body (2, 3).

more rarely, and mainly in concrete dams. According to the method of runoff of the overflow water, spillways can be open, closed, or combined. In practice, surface spillways through the dam's body (in cases of concrete dams) and outside the dam's body are most often used. Mainly, they are: free overfall (ogee or chute) spillway, side-channel spillway, shaft (morning glory) spillway, and siphon spillway. The overfall (ogee) spillway is positioned along the crest of concrete dams, while the frontal spillway is positioned in the bank near the dam. In this case, the spillway jet retains the direction of the flow approximately as is the direction of the natural river flow. The side-channel spillway is always constructed immediately next to the dam and, in this case, the overflowing of the spillway jet is approximately perpendicular to the direction of the flow of the dammed watercourse. The shaft (morning glory) spillway is characterized by a shaft in which the spillway jet overflows and then, through a tunnel, is evacuated downstream of the dam. The siphon spillway has a specific structure and mode, i.e. manner of work. It can be executed both through the body of a concrete dam and also independently of the dam, in a separate concrete block. All of these, as well as other significant spillways, will be considered in more detail in the forthcoming chapters.

The overflowing of water over a spillway crest can be free or else controlled, in which case the spillway is provided with gates. In the case of free overflowing, the level of the spillway coincides with the normal water level in the reservoir, while the elevation of the maximum water level is obtained when we add the overflow height at overflowing of the maximum water quantities to the elevation of the normal level (Fig. 23.7). The volume between these two levels can be used only for transforming the flood wave. Reducing the overflowing height Hp can be performed by increasing the length of the spillway. However, by constructing a controlled spillway, in which the spillway can be set up at a level that is lower than the normal level, we can achieve a reduction of the length of the spillway (Hager, 1988). Controlled spillways are usually more economical than free overflowing spillways, while they are more difficult for utilization and less safe owing to the danger of breakdown to some of the mechanisms. The control of controlled spillways can be performed manually, or by means of remote control or automatically, depending on the level of water in the reservoir. If certain

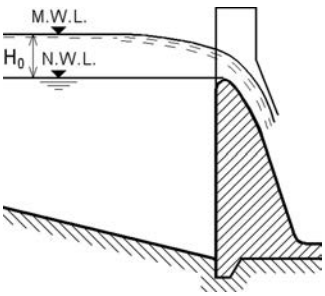

Figure 23.7 Free overflowing spillway.

local conditions – possible seismic activity, distrust of the capability for professional maintenance and control of the equipment, difficulties in the approach - throw suspicion on the safe and efficient service of the gates, then it is better to carry out an uncontrolled gate (Ionescu, 2000; Quintela et al., 2000).

The bottom outlet, similar to the spillway structures, can be positioned through the dam's body or outside the dam's body. The first solution is regularly employed with concrete dams, while the second solution is employed with embankment dams. Only in the case of small embankment dams that impound reservoirs with a small capacity, there are used outlet works through the dam's body since, in such cases, it is possible to achieve rational dimensions of the outlet, with possibilities of minimizing the danger of contact seepage along the length of the water-conveying part of the outlet structure.

In designing the spillway and bottom outlet works structures, it is also necessary to analyze the possibility of their combined work, that is to say, for joining their functions into one structure, as well as the possibility and conditions for utilizing the outlet for evacuation of the waters in the course of constructing the hydraulic scheme. In such a jointing, as a rule, we achieve a more economical solution; however, we should pay attention in order not to reduce the functionality. In the following chapters, in appropriate places, this question will also be examined.

23.5 EVACUATION OF OVERFLOWING WATERS VIA A CHUTE SPILLWAY

In general, spillway structures, regardless of whether they have been located through the dam's body or outside the dam's body, consist of three parts: overflow part, water-conveying part and terminals part. In considering various kinds of spillway structures, here we shall analyse the characteristics of particular types of spillway parts. The water-conveying part is very important, because it has to conduct the overflowing water from the upper level to the lower level working, in complex hydraulic and sometimes also static conditions. It can be an underground structure, in the form of a tunnel or a gallery (Marheim et al., 1994), or else a surface structure, in the form of a channel with a considerable gradient, called a chute. The chute spillway is regularly employed in the cases of overflow concrete gravity dams, and sometimes also with other types

of overflow dams. In the case of spillways located outside the dam's body, the chute is the most frequently used structure for the conduction of overflowing waters. In such cases, depending on the layout of works within the hydraulic scheme, it can achieve a considerable length, which aggravates or complicates the conditions for its operation.

The flow in the chute is always supercritical, from which there emerge four major phenomena that influence its structure. They are: potential danger of cavitation, occurrence of interference waves, translatory waves and aeration of the flow (Visockiy, 1977; Abbasoglu & Okay, 1992; Novak et al., 2001).

Some consideration has been given to cavitation and damage arising therefrom in Chapter 4, and we shall also refer to this dangerous phenomenon and the measures that are undertaken for its prevention at appropriate places in the subsequent text (Galjperin et al., 1977; ICOLD, 1977; Prusza, 1994).

The interference waves (also called cross-waves) are shock waves that appear at all places where the supercritical flow comes into contact with the changes in the cross-section, direction, inclination, or else, collides with a parting pier or similar structural element. Those are stationary waves, with a position depending on the discharge. Their main consequence is the raising of the water level and consequently, the need for higher side walls of the chute, because the water has a tendency to run-up at places of contact between the wave and the side walls. The hydraulic treatment of the question is given in the specialized textbook references (Novak et al., 2001). Interference waves can also cause difficulties at the dissipation of the overflowing jet, but this rarely takes place, because the waves disappear immediately when there is aeration of the flow. The danger of the appearance of interference waves can be reduced to a minimum by means of careful shaping of each change in the form of the channel and also by means of a rather slight change of the direction and the inclination of the flow.

Translatory waves occur in certain situations and, as their name indicates, they move along with the flow, straight towards the terminal structure. They also raise the level of the overflowing water and, sending non-stationary impulses into the terminal structure, may even cause its failure. They appear at chute inclinations from 0.02 to 0.35 within which boundaries the chute inclinations most often vary. They may be avoided by the construction of an artificial unevenness, i.e. roughness, along the surface of the chute; that, however, increases the danger of cavitation. The best way of preventing the danger of the occurrence of translational waves is to design the chute in such a way that the ratio between the depth of water and the wetted perimeter is greater than 0.1 for the maximum discharge, assuming that at low discharge the waves are not a threat to the safety of the completed structure.

Aeration of the flow is the most significant consequence in the supercritical flow. Although it is useful, from the aspect of cavitation and dissipation of the energy of the overflowing water, it must be taken seriously into consideration because it enhances the price of the chute, owing to the need for additional heightening of the side walls, which particularly comes to the fore in the case of long tailraces (Rutschmann & Volkart, 1988). The transition from critical flow at the crest – through a supercritical non-uniform, non-aerated flow into a non-uniform partially and completely aerated flow – and, finally, into a uniform aerated flow, is schematically presented in Figure 23.8. The aeration of the flow starts at the point at which the turbulent boundary layer

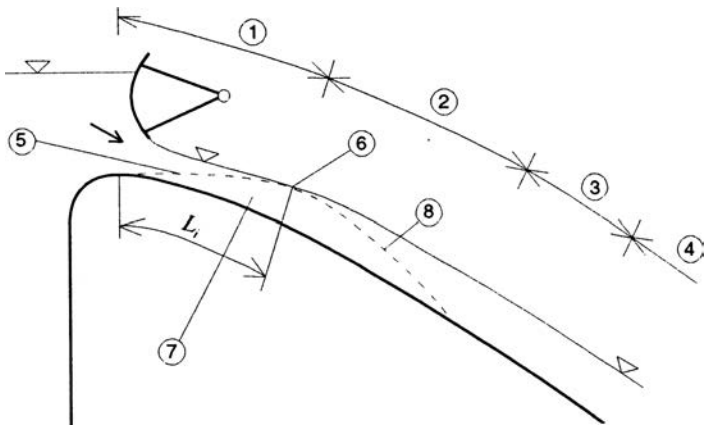

Figure 23.8 Changes of the flow in a chute spillway (after Novak et al., 2001). (1) Non-aerated flow; (2) partially aerated flow; (3) completely aerated flow; (4) uniform aerated flow; (5) boundary layer; (6) starting point of aeration of the flow; (7) fully turbulent zone; (8) interface between aerated and non-aerated flow.

penetrates the full depth of the flow (6, Fig. 23.8). Approximately, the position of that point can be determined by means of the Hickot's equation (Novak et al., 2001):

$$L_i = 14.7q^{0.53} = 15\sqrt{q} \tag{23.1}$$

where q is the unit discharge.

The depth y of the non-aerated non-uniform flow is determined by means of well-known methods in hydraulics. There are a number of empirical methods for the assessment of the depth of the aerated flow. In accordance with some of them, we can determine the depth y_a of the aerated uniform flow (4, Fig. 23.8). Denoting the average concentration of air as $C = Q_a/(Q_a + Q)$ (Q_a is the flow of air, while Q is the flow of water), and the ratio of the flow of water in relation to the flow of the mixture of water and air as $\rho_1 = Q/(Q_a + Q)$ (i.e. $C = 1 - \rho_1$), for a rectangular open channel it follows:

$$\rho_1 = \frac{Q}{Q_a + Q} = \frac{y_0}{y_a} \tag{23.2}$$

where y_0 is the depth of the uniform non-aerated flow.

Wood (Novak et al., 2001) defines C, introducing the depth y', at which the concentration of air is 90%:

$$C = 1 - \frac{y_0}{y'} \tag{23.3}$$

For a quick evaluation of y_a, we can utilize the following approximate equation:

$$y_a = c_1 y_c = c_1 \sqrt[3]{\frac{q^2}{g}} \tag{23.4}$$

with the coefficient c_1 within the limits $0.32 < c_1 < 0.37$ or

$$\frac{y_a - y_0}{y_0} = 0.1\sqrt{0.2\,Fr^2 - 1} \tag{23.5}$$

By experiments, it has been verified (Novak et al., 2001) that the ratio of the aerated factor of friction λ_a, in relation to the non-aerated λ, reduces with the increase of the concentration of air approximately with the expression:

$$\frac{\lambda_a}{\lambda} = 1 - 1.9C^2 \tag{23.6}$$

for $C < 0.65$. For $C > 0.65$, λ_a/λ is a constant amounting to 0.2.

For the concentration of air in the flow, the textbook references also give some other expressions for a rough lining:

$$C = 0.7226 + 0.743 \log\left(\frac{m}{q^{1/5}}\right) \tag{23.7}$$

for $0.16 < m/q^{1/5} < 1.4$ (m is the inclination of the chute). For a smooth lining:

$$C = 0.5027\left(\frac{m}{q^{2/3}}\right)^{0.385} \tag{23.8}$$

where $0.23 < m/q^{2/3} < 2.3$.

There are also other empirical methods by means of which, with an accuracy sufficient for practical purposes, it is possible to calculate the aerated depth of the flow. Therefore, by means of the described method we can calculate the aerated depth y_a, assuming that in the lower part of the chute the aerated flow is uniform. In practice, the aerated flow becomes uniform a great distance away from the overflowing part, especially if the specific overflowing quantity is significant ($q > 50\,m^2/s$). From the aspect of preventing cavitation, the minimum required saturation of the flow with air, in the interface with the lining, is 70%. Equations (23.4)–(23.8) imply an average concentration of air in the flow.

In order to achieve protection from cavitation in cases when there is no aeration of the flow, we can apply artificial aeration by means of the execution of aerators along the length of the spillway chute (Abbasoglu & Okay, 1992). These aerators can have the form of offsets in relation to the direction of the bottom, of transverse grooves in the bottom or ramps, Figure 23.9. They are usually carried out as a combination of two or three of the cited forms. The most often employed combination is that of offset with a ramp. The air is brought to the surface of the bottom of the spillway chute automatically through aeration pipes immediately when it comes to a separation of the flow, which causes a drop in pressure below the atmospheric one. The number

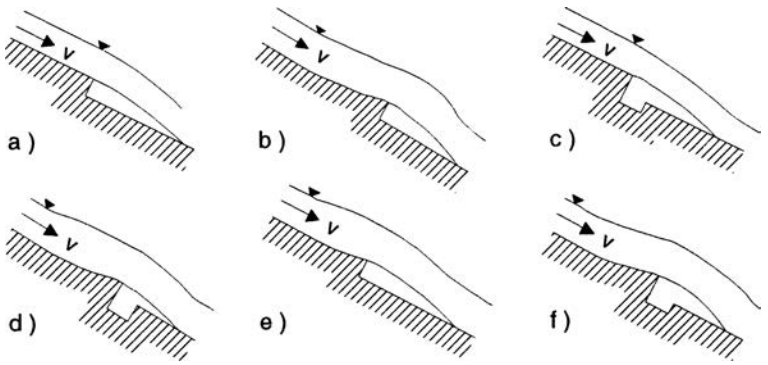

Figure 23.9 Possibilities for aeration of a spillway chute. (a) Offset in relation to the bottom; (b) ramp; (c) offset with air groove; (d) ramp with air groove; (e) ramp and offset; (f) ramp and offset with air groove.

of aerators should be selected so that it ensures a sufficient concentration of air in the flow, taking into consideration that the air bubbles disappear towards the surface. Approximately, the distance between the aerators in metres can be assumed to be equal to the average velocity of the flow (in m/s).

23.6 ENERGY DISSIPATION OF THE SPILLWAY JET

The water which is conducted via the spillway structures, possesses enormous energy, since in a relatively short path, it is transferred at a certain, often considerable, difference in elevation. In fact, the magnitude of this energy depends on the specific overflow quantity of water q, as well as on the difference between the water level upstream and downstream. Prior to the discharge of the overflowing water in the watercourse downstream of the dam, there must be achieved dissipation of the energy, in order not to lead to destruction of the surrounding ground. In the case of high dams, with large overflowing quantities, the magnitude of the energy that has to be dissipated may be enormous. For instance, in the case of the Tarbella Dam (Pakistan), it has the power of 40,000 MW, which is 20 times higher than the planned generating capacity of the hydroelectric power plant within the framework of the hydraulic scheme. That imposes the need, in designing the hydraulic schemes, to approach this question with particular seriousness, particularly owing to the fact that the way of energy dissipation of the spillway jet has an influence also on the environment (Provorova, 1995; Novak et al., 2001).

The transfer of water from the reservoir downstream into the watercourse, may be connected with various hydraulic phenomena, such as the transition into supercritical flow – non-aerated and aerated flow, free overfall flow, entrance into the stilling basin by leaving the supercritical flow, and the occurrence of turbulence of the flow, etc. Even though the spillway structures, as a rule, encompass a special structure for dissipation of the energy, the process of energy dissipation of the overflowing jet, in practice

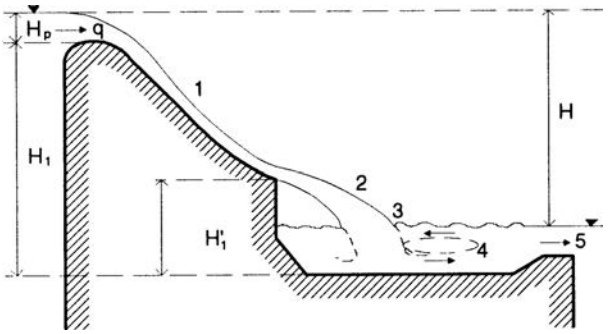

Figure 23.10 The five stages of energy dissipation (after Novak et al., 2001).

begins at the surface of the spillway and can advance in five separate phases, with a possible combining, or with the absence of some of them, as is shown in the example of overflowing over the body of a concrete dam (Fig. 23.10):

1. Dissipation of energy at the spillway surface;
2. Dissipation in the zone of free fall of the jet;
3. An impact into the downstream pool;
4. Dissipation of energy in the stilling basin;
5. Dissipation at the discharge into the riverbed.

The loss of energy at the surface of the spillway can be expressed as:

$$e = \frac{\xi \alpha v'^2}{2g} \tag{23.9}$$

where v' is the supercritical velocity at the end of the spillway structure, α is a Coriolis coefficient, while ξ is the head loss coefficient, dependent on the velocity coefficient φ (the ratio between the real and theoretical velocity), given with the expression:

$$\xi = \frac{1}{\varphi^2} - 1 \tag{23.10}$$

The ratio between the energy loss e and the total energy E, that is to say, the relative energy loss, is:

$$\frac{e}{E} = \frac{\dfrac{\xi v'^2}{2g}}{\dfrac{v^2}{2g} + \dfrac{\xi v'^2}{2g}} = \frac{\xi}{1+\xi} = 1 - \varphi^2 \tag{23.11}$$

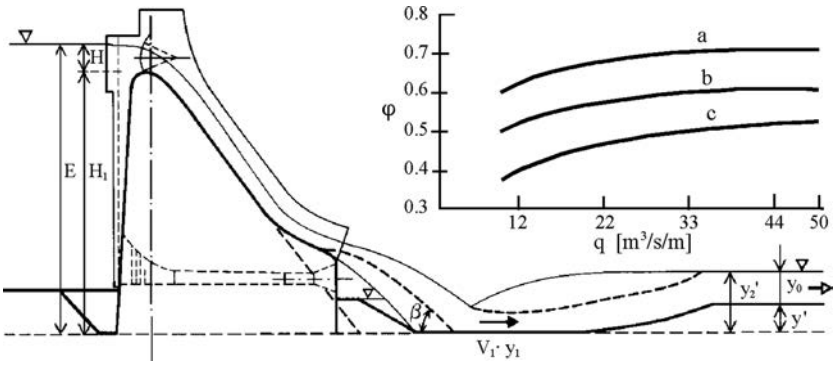

Figure 23.11 Comparison of three different constructions of the terminal part of the spillway (after Novak et al., 2001).

For the ratio $H_1/H_p < 30$, and for a smooth spillway surface, the velocity coefficient φ_1, regarding the part of the overflowing surface, will be:

$$\varphi_1 = 1 - \frac{0.0155\ H_1}{H_p} \tag{23.12}$$

For a given H_1, φ_1 decreases with the increase H_p. Thus, for $H_1/H_p = 5$, $\varphi_1 = 0.92$ the relative head loss is 15%, while for $H_1/H_p = 25$, $\varphi_1 = 0.61$, while the head loss is 62%.

The value of ξ could be increased and thus the value of φ be decreased, with the application of a rough spillway surface, or with embedment of ribs or blocks. In that way, the danger of cavitational erosion is increased, so that the artificial increase of the roughness must be handled very carefully and following detailed studies. This is the reason for that measure not being employed very often.

With most modern constructions of spillway structures, an increased dissipation of the spillway jet is achieved with a free overfall of the jet by shaping the terminal part of the spillway so as to enable it to project the spillway jet in the form of a "ski-jump" (Fig. 23.11), or by means of the execution of a special concrete block with an appropriate form, downstream of the spillway (Fig. 23.12).

The construction with a ski-jump was first applied by André Coyne in 1935 and later on it has been improved and perfected through detailed model studies (Billoré, 1991). It can be very economical in suitable geological and morphological conditions, and especially in cases when it is positioned above the power house of the hydroelectric plant, and when it is integrated in the dam's body. The head loss in the projected spillway jet is not very large – some authors estimate it to be a maximum of 12%. If the jet is divided into several smaller jets that collide with one another, or if a solution is applied with two separate jets colliding with each other, then the dissipation of energy is significantly increased.

In the case of a ski-jump, the greatest energy loss takes place in the third stage – at the impact of the jet with the water pool formed downstream. In this, the loss is greater if the jet has been dispersed and intensively aerated prior to the impact. The

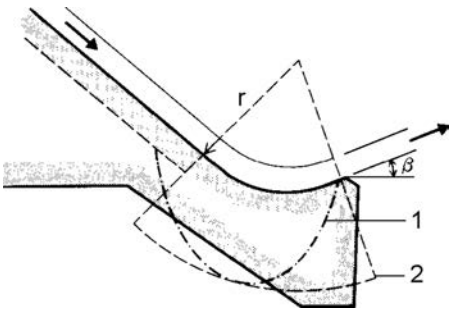

Figure 23.12 Flip bucket (after Novak et al., 2001). (1) Diagram of pressure obtained experimentally; (2) theoretical diagram of pressure.

total energy loss in the first three stages of the energy dissipation can be expressed with the velocity coefficient φ_{1-3}, which can be determined through model investigations, which yield very good ratios for the relative advantages and deficiencies of different solutions. Generally speaking, φ_{1-3} is a function of the ratio H_1'/H_1, (Fig. 23.10), and of q and of the geometry of the spillway. Figure 23.11 presents a comparison of the values of φ_{1-3} for three different constructions: (a) terminal part of a spillway structure with a stilling basin; (b) ski-jump spillway; and (c) ski-jump spillway with splitters at the exit end which split the jet, thus improving the intake of air and dissipation of energy (Novak et al., 2001).

The right upper part of the diagram in Figure 23.11 presents the dependence of φ on q for the three considered constructions. It is evident that in all cases, φ increases with the increase of q; that is to say, with the increase of the specific flow quantity, there is a decrease in the energy loss. Breaking of the jet, as it has been determined experimentally, is accomplished at a distance L from the spillway crest, which can be determined by means of the expression (23.13), in which q is expressed in m^2/s:

$$L = 5.89\, q^{0.319} = 6(q)^{1/3} \quad [\text{m}] \tag{23.13}$$

The concrete block in the form of a flip bucket (Fig. 23.12) is, in fact, a variant of the ski-jump construction, which is used at the termination of a spillway chute or a tunnel by means of which the water is taken away downstream, at a smaller or greater distance from the dam. The geological and topographical conditions of the surrounding ground also play a significant role in its location and application. As in the previous case, the structure of this completed work within the framework of the spillway structure has been developed by means of model investigations. Key parameters for the engineering of the flip bucket are the approach velocity and depth, radius of curvature r, and the exit angle β of the downstream edge. In designing the flip bucket, which is treated as a massive concrete block, the problem is most frequently analyzed as a planar one, in which there must be taken into consideration all forces, including also the hydrodynamic pressure of the water jet. In the case of a circular curvature of the flip bucket, the experimental investigations indicate a non-uniform distribution of pressure (1, Fig. 23.12), which deviates from the theoretical one (2). In the case of low spillway

quantities, the flip bucket works similarly to a stilling basin, with discharge of the water along the downstream edge and wall and, owing to that, the foundation and the zone immediately downstream to the flip bucket should be protected against erosion in an appropriate way.

The trajectory of the jet projected with flip bucket, for velocities smaller than 20 m/s, to a great measure depends on the air resistance, while for a velocity of 40 m/s the length of projection can be reduced by a value up to 30% of the theoretical value $(v^2/g)\sin 2\beta$. The designer always endeavours that the zone of impact of the jet into the ground be as far away from the flip bucket as possible, in order to protect the structure from retrogressive erosion. In practice, there have been developed and are used, different constructions of more complex flip buckets, which give a three-dimensional shape to the jet, all in order to direct it towards certain a side, i.e. direction.

The most often used structure for energy dissipation of the spillway jet is the stilling basin in which there takes place a conversion of the supercritical flow into a steady flow, compatible with the regime of the river downstream. The simplest, and most often the best, method for achieving this transmission is through a submerged jump, formed in a simple stilling basin (in fact, a channel) with a rectangular cross-section. Taking into consideration the designations of Figure 23.13 and equations (23.9) and (23.10), it may be written as:

$$E = y_1 + \frac{\alpha q^2}{2g\varphi^2 y_1^2} \tag{23.14}$$

$$y_2 = \frac{y_1}{2}\left(-1 + \sqrt{1 + 8\frac{q^2}{g y_1^3}}\right) \tag{23.15}$$

where y_2 is the coupled depth at the hydraulic jump. Then, the depth of the stilling basin is given by the expression:

$$y' = y_2' - y_0 = \sigma' y_2 - y_0 \tag{23.16}$$

while the length will be

$$L = K(y_2 - y_1) \tag{23.17}$$

where σ' and K are coefficients derived from laboratory and field investigations.

When we apply the equations (23.14)–(23.17), we start with a known unit discharge q, to which there corresponds an appropriate depth y_0 in the channel of the river downstream. The coefficient φ is assumed, while the value of E is not known at the beginning, so that it is best if the calculations, according to the equations (23.14)–(23.17) are performed according to an iterative procedure, assuming in the beginning that $y' = 0$. This calculation, suitable for several different discharges, may lead to these five cases:

(a) $y_2 > y_0$ for the entire range of values for q;
(b) $y_2 = y_0$ for the entire range of values for q;
(c) $y_2 < y_0$ for the entire range of values for q;

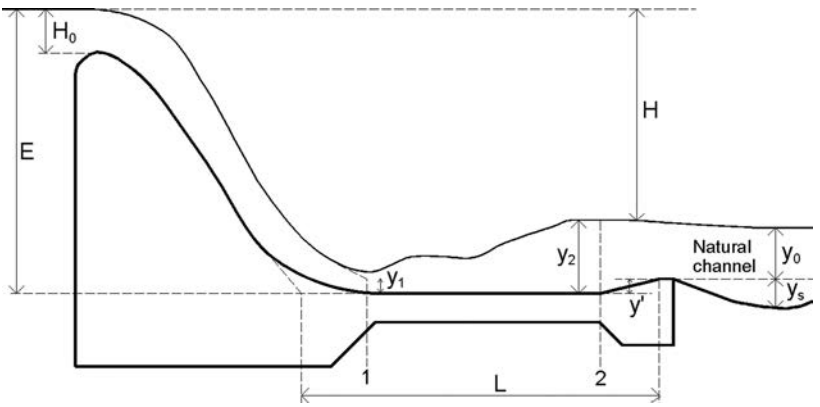

Figure 23.13 Definition sketch for hydraulic jump stilling basin.

(d) $y_2 > y_0$ only at high discharges;
(e) $y_2 > y_0$ only at low discharges.

Case (a) most often takes place, and it indicates that a stilling basin is necessary for all discharges in order to obtain a submerged jump. Case (b) is possible only theoretically and, for safety, here again we would deal with it as in case (a). For case (c), a stilling basin would not be necessary. For case (d), the stilling basin would be dictated only by the maximum discharges (as in case a); while in case (e), it would be dictated by the discharge yielding the greatest difference between y_2 and y_0 ($Q_d < Q_{max}$); that can result in the execution of a small stilling basin.

When the calculation with an initial value $y' = 0$ indicates that a stilling basin is necessary, then the procedure is repeated for a new value of E, equation (23.14), by lowering the energy level below the line of the river bed. The values of coefficients σ' and K in equations (23.16) and (23.17) range within the limits $1.1 < \sigma' < 1.25$ and $4.5 < K < 5.5$, in which the lower value for K is used for $Fr_1 > 10$, while the higher value for $Fr_1 \leq 3$ (Fr_1 is the Froude number in the section 1). The equations (23.15) and (23.17), as well as the entire described procedure, relate only to a stilling basin with a horizontal bottom. The value of φ in the expression (23.14) corresponds to φ_{1-3}, that is to say, to the total losses between the spillway crest and the entrance into the stilling basin.

The loss of energy in the fourth and the fifth stages of the process of dissipation of energy can be represented as:

$$e_{4,5} = \frac{(y_2 - y_1)^3}{4y_2y_1} \tag{23.18}$$

Downstream of the jump, at the discharge from the stilling basin, there still exists considerable remaining energy, mainly due to the high turbulence of the flow, which may be expressed as:

$$e = (\alpha' - \alpha)\frac{v_0^2}{2g} \tag{23.19}$$

where α' is the increased value of the Coriolis coefficient, caused by a high degree of turbulence and a non-uniform distribution of velocity; while for $3 < Fr_1 < 10$, it will be $2 < \alpha' < 5$, while $\alpha \cong 1$.

From the equations (23.18) and (23.19), it follows that:

$$\frac{e_4}{e_{4,5}} = 1 - \frac{e_5}{e_{4,5}} \approx 1 - 4(\alpha' - 1)\frac{1 + \sqrt{1 + 8Fr_1^2}}{\left[-3 + \sqrt{1 + 8Fr_1^2}\right]^3} \tag{23.20}$$

The equation (23.20) indicates that the efficiency of dissipation of the energy in the jump in the stilling basin decreases with the increase in the Froude number, in which there remains up to 50% of the energy for dissipation downstream of the stilling basin at low Froude numbers.

Regardless of whether the flow at the entrance to the stilling basin is aerated or not, during the hydraulic jump there comes about an interception, i.e. intake of a significant quantity of air. The main consequence of the presence of air in the jump is the need for construction of higher side walls in the stilling basin. On the other hand, the highly turbulent nature of the hydraulic jump causes high fluctuations of the pressure on the side walls, especially at the bottom of the stilling basin, which can lead to cavitation, along with all its harmful consequences. Another, maybe the biggest, danger, which aggravates, complicates, and makes the construction of the stilling basin slab more expensive, is the force of uplift, to which attention has been paid in Chapter 17. Protection against vibrations, caused by the turbulence of flow, also leads to a more massive stilling basin slab, if possible anchored in the foundation. If the stilling basin is utilized for the discharging of waters from the bottom outlet, then there exists a danger of abrasion of the concrete under the effect of the sediment (silt), when the flow occurs with a velocity greater than 10 m/s.

Although the most common stilling basin, with a simple sill at the end, based on the principle of a hydraulic jump, usually works efficiently, in certain cases there are also used other types of stilling basins that they are more economical and more efficient. In the USBR, they have developed standardized constructions of stilling basins with chute blocks at the entrance and baffle blocks in the central part, along with a specially shaped downstream end sill. Such a construction is indicated in Figure 23.14 (USBR, 1976, 1977). It is advisable for a natural velocity of $v < 18$ m/s and $q < 18.5$ m^2/s. Owing to the effect of the baffle blocks, it has a smaller length than a usual stilling basin; however, the dimensions, construction, and position of the baffle blocks must be selected with particular attention in order not to lead to the occurrence of cavitational erosion.

The plain and slotted roller bucket, as has already been mentioned, are frequent alternatives to stilling basins (of course, in certain geological, topographical, and hydrological conditions). Constructions presented in Figure 23.15, have also been developed in the USA (USBR, 1976, 1977). In addition to the extensive model investigations of structures for the dissipation of the energy of the overflowing jet, observations on numerous such constructions have also contributed to their development. One such investigation relates to the results from observations of 370 dissipators of energy, constructed throughout the world after 1950. It includes stilling basins in rock and without

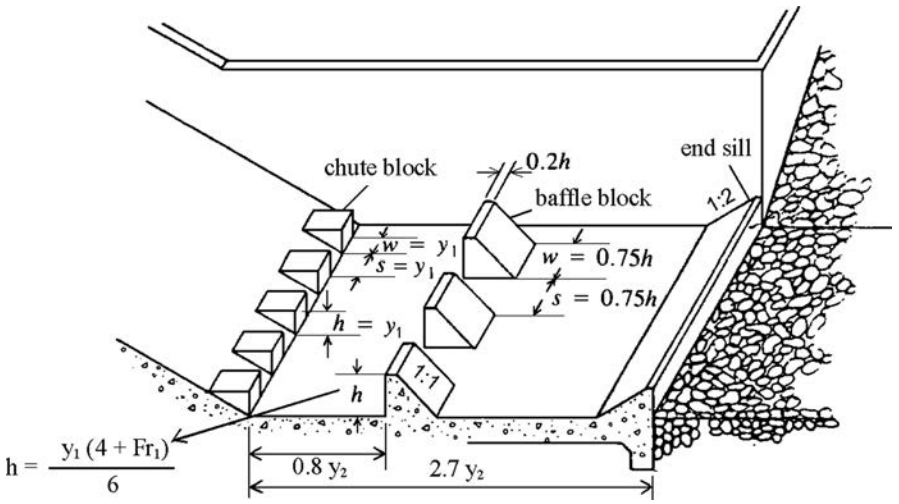

Figure 23.14 Stilling basin with chute blocks and baffles (USBR, Type III).

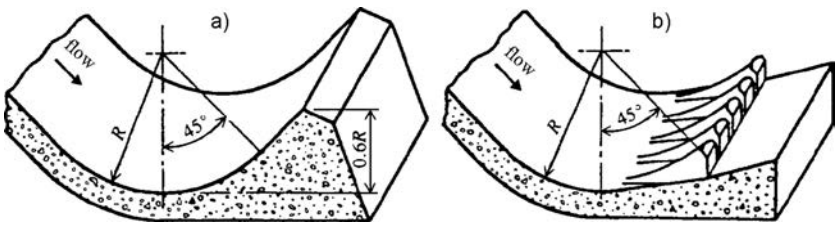

Figure 23.15 Plain and slotted roller bucket, developed in the USA (after Novak et al., 2001).

protection, ordinary stilling basins, stilling basins with chute blocks and baffle blocks, as well as various constructions of flip buckets, including here also a dissipator with a free trajectory of the jet. The results of the investigation, summarized in Figure 23.16 confirm that for successful functioning of the stilling baffle basin, it is necessary to have a certain minimum pressure, that is to say, an approach velocity; however, the area of their application is limited to pressure heads of up to 30 m, due to the possible problems of cavitation. Stilling basins in which there is developed a simple hydraulic jump have also been used for pressure heads greater than the 50 m indicated in the figure. In such a case, it is necessary to pay great attention in designing and during construction. In order to work properly, the various types of flip buckets require a minimum pressure head of 10 m.

It has been mentioned that during the discharge of water from the stilling basin into the downstream river channel, the flow still possesses some remaining energy. Owing to that, and also due to the non-uniform distribution of velocities in the profile, there always comes about certain local erosion downstream of the stilling basin. The elimination of this occurrence requires additional investments in the execution of an

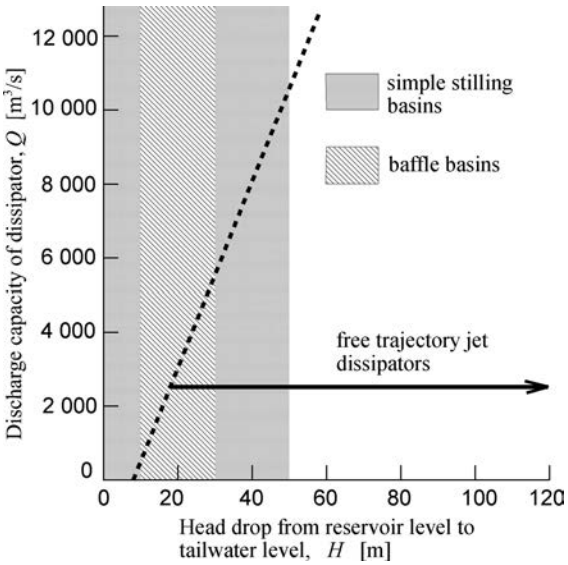

Figure 23.16 (after Novak et al., 2001).

appropriate construction (riseberm), which has also been discussed in Chapter 17. The size and shape of the erosion hole, which can be formed downstream of the stilling basin, depends on the hydraulic parameters, the geology of the ground and the geometry of the river channel. For calculation of the depth of that hole (Fig. 23.13), the following formula can be used, obtained on the basis of model investigations and a limited number of field observations (Novak et al., 2001):

$$y_s = 0.55\left[6H^{0.25}q^{0.5}\left(\frac{y_0}{d_{90}}\right)^{1/3} - y_0\right] \tag{23.21}$$

where d_{90} is the appropriate diameter of grains of the sediment material that is formed by the river bed. The investigations on which this equation has been based indicate that a stilling basin reduces the potential erosion by 50%.

When the jet is projected with a ski-jump ending of the spillway or with a flip bucket directly in the river channel, then a pit, is excavated (completely or partially) in natural rock into which the jet falls and forms a plunge pool. Sometimes, we leave the jet to excavate for itself the pit with its own energy. For calculation of the depth of the plunge pool, we can apply the simplified Martins formula (1975):

$$y'_s = 1.5q^{0.6}H^{0.1} \tag{23.22}$$

where $y'_s = y_s + y_0$.

Further work developed what is referred to as the Mason formula (Mason, 1989):

$$y_s = \frac{3.27 \cdot q^{0.60} H^{0.05} y_0^{0.15}}{g^{0.30} d^{0.10}} \tag{23.23}$$

where q is unit flow [m^2/s]; H is head drop from reservoir elevation to tail water elevation [m]; y_0 is tail water depth [m]; g is acceleration caused by gravity [m/s^2]; and d is bed material particle size [m], see Figure 23.13. From the same research Mason concluded that the head drop H is a proxy for the degree of aeration in the pool and that an alternative form of expression is:

$$y_s = \frac{3.39 \cdot q^{0.60} (1+\beta)^{0.30} y_0^{0.16}}{g^{0.30} d^{0.06}} \tag{23.24}$$

where β is the volumetric air-to-water ratio in the plunge pool, defined as:

$$\beta = 0.13\left(1 - \frac{v_c}{v}\right)\left(\frac{H}{t}\right)^{0.446} \tag{23.25}$$

where t is the jet thickness; and v_c the minimum velocity required for air entrainment (1.1 m/s).

A review of different practices and formulae, as well as a summary of prototype experiences with trajectory jet plunge pool erosion are given by Malik & Munir (2011).

Recently, computational fluid dynamics models have been developed that attempt to predict plunge pool development in three dimensions, but it is always essential that the results are cross-checked against real prototype data (Mason, 2011).

23.7 SELECTION OF TYPE OF SPILLWAY STRUCTURE

The type of spillway structure is selected by taking into consideration a number of factors, the most important being: (1) type and height of dam; (2) quantity of flood waters for evacuation during service and construction of the structure, i.e. works; (3) general layout of the works, organization of the works, and method of passing of the construction waters; (4) topographical, geological, and hydrogeological conditions in the zone of the hydraulic scheme; (5) utilization particularities of possible solutions for the spillway structure; and (6) data from technical and economic comparisons of the possible variants.

For certain other conditions in a hydraulic scheme with an embankment dam, an overfall (ogee) spillway in the bank alongside the dam is the most economical one, if there is a slight inclination of the bank. The side-channel and shaft (morning glory) spillway structures are rational in cases of rock foundations and steep inclinations of banks. The siphon spillway is efficient for floodwater waves, which come in rapidly, and with reservoirs with relatively low retentive capacity.

In the case of gravity concrete dams, the most rational is the application of a spillway over the dam's body, while in the case of other concrete dams a number of

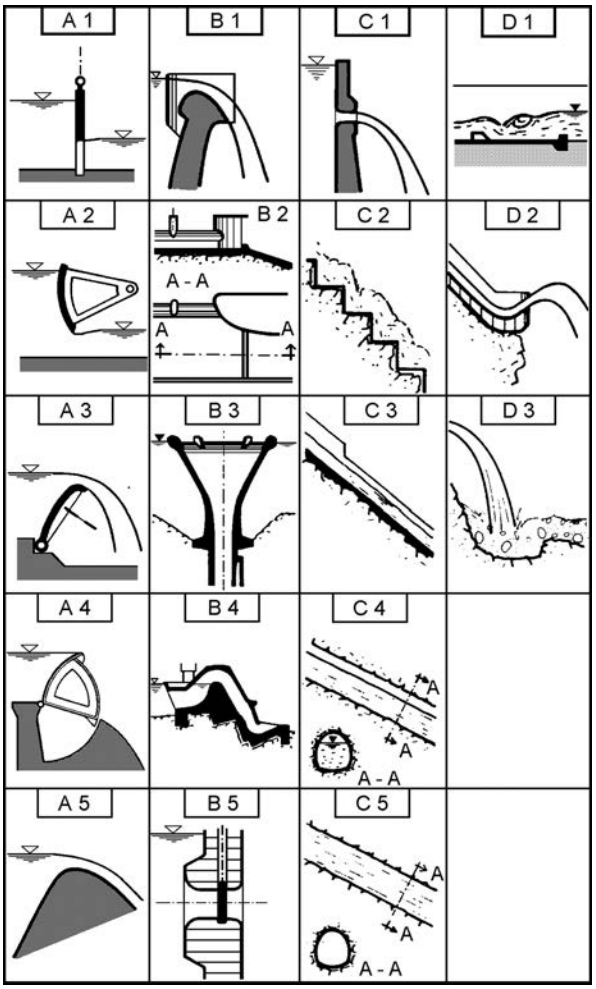

Figure 23.17 Most frequently used elements in spillway structures. (A) Regulation gates: (1) plain gate; (2) radial (tainter) gate; (3) plain gate; (4) sector (drum) gate; (5) uncontrolled spillway. (B) Spillway: (1) over the dam; (2) side-channel; (3) shaft; (4) siphon; (5) deep (high-head). (C) Conducting: (1) free fall; (2) cascade; (3) chute; (4) free-flow tunnel (non-pressure); (5) pressure tunnel. (D) Terminal elements: (1) stilling basin; (2) flip bucket; (3) water pool.

solutions are possible, which should be analyzed and compared prior to making a final decision.

If we take into consideration the most frequently used methods for regulating the overflowing quantities (A, Fig. 23.17), the most frequently used types of spillways (B), as well as the possible ways for conducting the overflowing waters (C), and stilling of the flow (D), then, theoretically, there exist $5 \times 5 \times 5 \times 3 = 375$ possible combinations of individual elements. Bearing in mind that a certain number of the combinations are

not possible, and another certain number of combinations have no practical meaning, there still remain some 60 combinations which can be considered for application. Taking into consideration all the above-mentioned factors, which influence the selection of the type of spillway structure, as well as the advantages and deficiencies of certain types, the engineer has a responsible obligation to select an optimal solution for each specific case. In this, it is necessary to bear in mind that *everybody who causes potential danger is obliged to undertake everything that is in man's power in order to keep it under control.*

It must be admitted that the construction of a dam with an reservoir also causes changes to the environment, which involves a larger or smaller potential danger in the case of failure of the dam, while on a well-selected and designed spillway, to a great extent, depends the safety of the dam during its long service period which, usually, amounts to about 100 years, or much more for well-maintained structures and works.

This page intentionally left blank

Chapter 24

Surface (crest) gates

24.1 BASIC SCHEMES OF SURFACE (CREST) GATES

Surface (*crest*) *gates* are used for controlling the inlet parts of water conveyance structures that serve for intake of water at the surface, without water pressure. In the cases of hydraulic schemes with dams, these gates are mainly used with surface spillways, aiming at controlled discharge of floodwaters. A number of different surface (crest) gates may be differentiated, of which the basic ones are presented in Figure 24.1:

(a) *Plain gate*. During closing or opening, the gate (1) moves along vertical gate slots (2), provided in the sidewalls or piers; it is also sometimes called *a sluice gate*.
(b) *Stop-log gate*. It is formed by making up, i.e. laying down horizontal beams (1), also into gate slots (2).
(c) *Radial* (*tainter*) *gate* (1). The cross-section has the shape of a circular segment; it rotates in relation to a horizontal axis (2).
(d) *Roller gate* (1). Has the form of a cylinder; this gate moves by rolling along an inclined toothed track (2), placed in the gate slots.
(e) *Sector gate*. Has the shape of a circular sector in cross-section. It is hinged downstream, i.e. it has a downstream axis of rotation. The sector gate, during the opening of the gate (1), by rotating around the axis (2), descends into the gate slot (3).
(f) *Drum gate*. Differs from the previous type according to its axis of rotation, which in this case is located upstream, i.e. the drum gate is hinged upstream.
(g) *Bear-trap gate*. Increased water pressure is created in the provided space (5), at which parts of the gate (1) and (2), rotating in relation to the axis (3) and (4), raise and close the opening.
(h) *Floating gate* (1). Has the shape of a prismatic floating element; by floating, it simply staggers, i.e. toddles, to the place of closing by means of its weight. It dams the opening (h_1) or else the axis (2) is positioned in the hinges (3) that are provided in the side walls or piers. Furthermore, the gate is filled with water, during which process it turns around its hinges taking up the position (4) and covering the opening (h_2).
(i) *Flashboard* (*Poiré gate*). Consists of a series of planar vertical trusses (1), set up transversely to the river; these trusses can rotate in the bearing (2) around the horizontal axes. The span between the trusses (1) ranges from 1 to 1.5 m and they

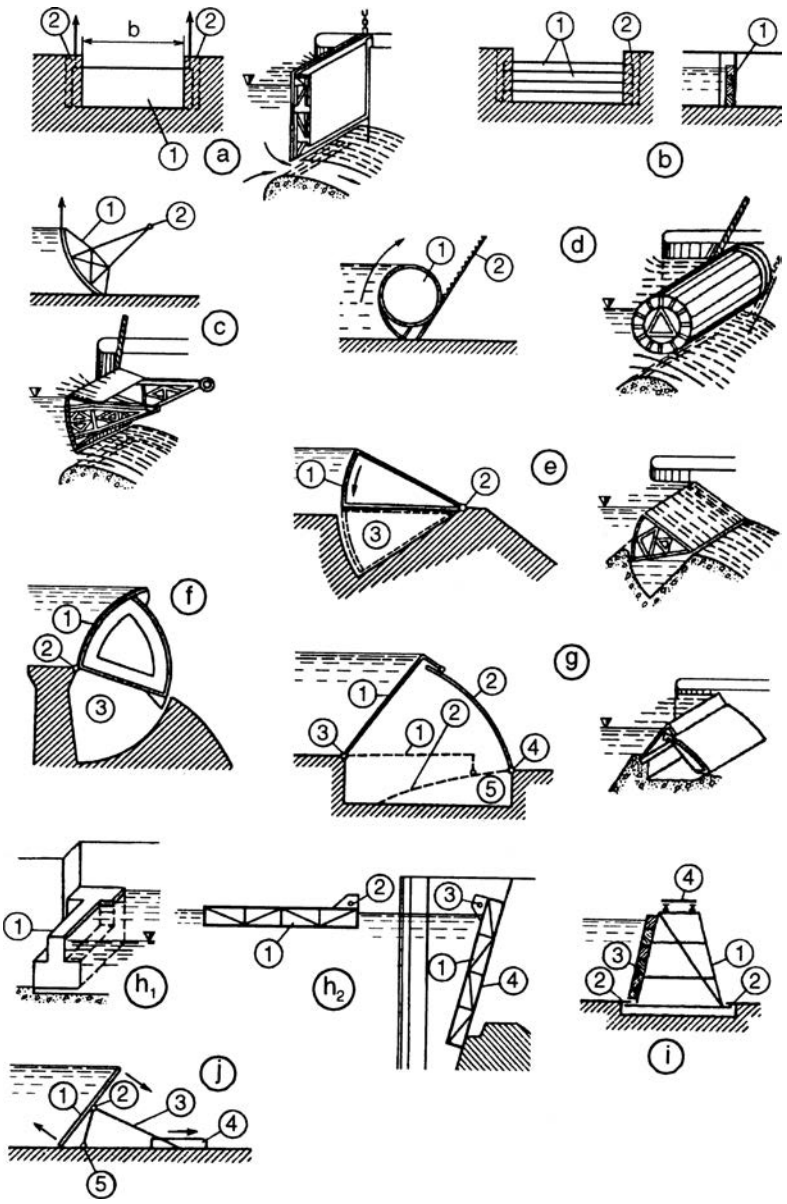

Figure 24.1 Schematic presentation of basic types of surface (crest) gates (after Grishin et al., 1979).

are closed with wooden planks, i.e. logs (3), or else with special shutters. At the topside there is mounted a bridge (4) that holds the trusses in a vertical position. Above the trusses, there is fastened a beam, the end of which is connected with a hoist that is mounted on a post. Following dismantling of the bridge (4), the hoist

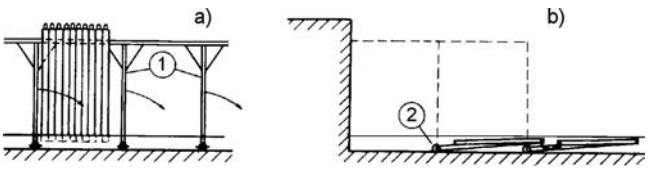

Figure 24.2 Poiré gate; (a) longitudinal section; (b) cross-section.

releases the beam and trusses rotating in the bearing (2), they go down on the bottom (Fig. 24.2a, b) and so the opening is free. For closing the span, the hoist, by means of the beam, raises the trusses into a vertical position, then the bridge is again mounted and the spans between trusses are covered. In earlier times, such a gate was used on navigable rivers as a movable dam for a temporary raising of the water level, as well as for improving the conditions of navigation. Nowadays it serves as an overhaul bulkhead or barrier. There is no limitation in relation to the width of the opening that is to be closed.

(j) *Strutted-flap gate*, formed of a series of shields (1), which rotate in relation to the axes, (2) and (5). For opening span, the strut (3) is taken out of the bearing (4) and so the shield (1) lies on the bottom. This gate is applied in cases similar to those of the gate cited under item (i).

(k) *Flap gate*. This type of gate consists of straight or curved retaining surfaces that rotate around a horizontal axis, fixed to the gate sill (see section 24.3.2).

(l) *Inflatable fabric gates*, manufactured from special fabric or rubber. They work by being filled with air or water (see section 24.3.4).

By means of opening the gates, we let water, ice, and other floating solids through the span, as well as sediment. These different kinds of surface (crest) gates work under different conditions and do not have same abilities when it is a question of the discharge rate of flow, i.e. capacity for water, floating solids, and sediment.

For discharging water, there are usually employed gates without regulation or with regulation of discharge waters. With the second type, we differentiate gates that work by means of lifting when, during partial opening, the discharge is allowed under the gate and the gates that are opened by lowering, so that overflowing takes place over the gate. In the first case, a better regulation of the level of the headwater is obtained. There also exist combined gates, with a possibility of discharging water both from the upper and the lower side.

Ice and other floating solids are suitably discharged by means of the gates over which overflowing is achieved. The gates that are lifted for this purpose should be capable of complete opening. If during the service period there is a need to discharge sediment through the openings, which travels on the bottom, then gates that are capable of lifting have the advantage.

A classification of gates has been made in Chapter 23. In the continuation, we shall examine the most important kinds of surface (crest) gates, divided according to the way of transferring the water pressure.

24.2 SURFACE (CREST) GATES TRANSFERRING WATER PRESSURE TO SIDE WALLS OR PIERS

24.2.1 Ordinary plain metal gates

Ordinary plain gates consist of a metal load-bearing structure, covered at the upstream side with a watertight lining, usually made of steel plate.

In a simple case, the load-bearing structure consists of beams, as is shown in Figure 24.3, as follows: horizontal beams – *bars* or *chords* (1) and vertical bearers, i.e. stanchions (4). The horizontal beams and vertical stanchions cross each other, in which all the vertical stanchions, except the end ones (2), are intersected by the horizontal beams into individual parts. The horizontal beams are integral, and non-intersected, i.e. continuous.

The water stopping seals (6) and (7) cover the gaps between the metal gate and the concrete parts of the structure at the bottom, as well as laterally. The lifting forces act on the end vertical stanchions, onto which the water pressure is transferred through the horizontal beams. For lifting the gate, the end stanchions move along special stationary rail tracks, embedded into gate slots (Grishin et al., 1979).

The above-described scheme of gate falls into the group of what are called *multi-beam gates,* which are rarely employed, and then only for a relatively low value of the ratio *b/H*. For usual ratios of *b/H that* are employed nowadays, a *two-beam plain gate* is employed (Fig. 24.4).

The load-bearing structure of the two-beam gate consists of various horizontal and vertical elements, as well as of inclined joints, so that it forms a space truss that works under complex conditions and so cannot accurately be statically calculated.

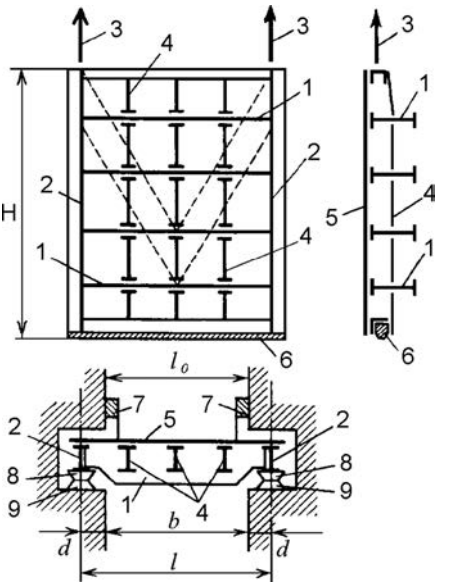

Figure 24.3 Ordinary plain gate. (1) Beams; (2) end vertical stanchions; (3) lifting forces; (4) vertical stanchion; (5) waterproof lining; (6) bottom water stopping seal; (7) lateral water stopping seal; (8) beam with a length of H; (9) stationary rail track.

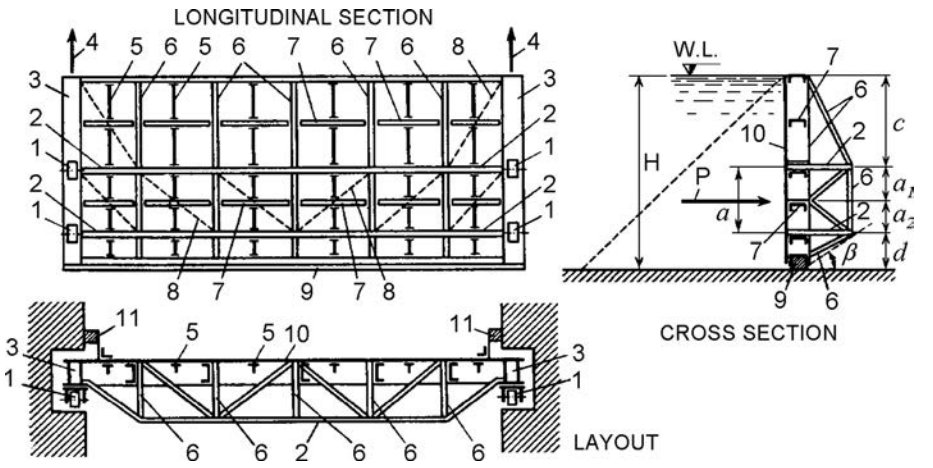

Figure 24.4 Scheme of ordinary two-beam plain gate. (1) Supporting movable part; (2) main beam; (3) end vertical stanchions; (4) lifting forces; (5) auxiliary vertical stanchions; (6) transverse vertical truss; (7) auxiliary beam; (8) lifting truss; (9) sealing at the bottom; (10) waterproof lining; (11) lateral sealing.

Figure 24.5 Cross-section of end vertical stanchions.

In order to enable the beam to be equally loaded by the force of the hydrostatic pressure, in the bottom part they are spaced at smaller distances. The gate, in order to be more stable, is set up on four supporting movable structural systems. The distance $a = a_1 + a_2$ between appropriate beams should be as large as possible since, in doing so, we reduce the height c of the cantilevered part of the gate, which should not be larger than $(0.4–0.45)H$. The distance d should be sufficiently large so that, during lifting of the gate, the water flowing under the gate does not happen to strike the lowest bar (chord) and so does not generate a vacuum. The angle β should not be smaller than 30°, that is to say, d must not be smaller than $(0.12–0.15)H$.

The end vertical stanchions (3) serve for fastening onto the supporting movable mechanism. The ends of the beam are fastened into the vertical stanchions and, at those points, the beam transfers the hydrostatic pressure to the stanchions. The length of the vertical stanchions is equal to the height of the gate. They can be made of one wall or two walls (Fig. 24.5a, b) in which the distance between the walls *(a)* must not be smaller than 0.5 m. The lining is made of steel plate, of a thickness as is necessary for taking on the hydrostatic pressure, increased by 1 mm, because of the possibility

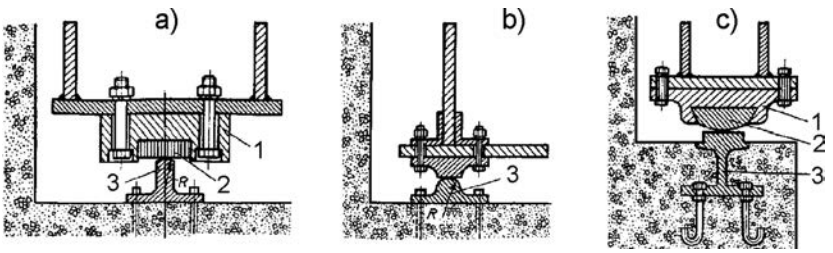

Figure 24.6 Supports that work by sliding. (a) With inserted pad of wood or plastic; (b, c) with steel elements. (1) Bearing; (2) inserted pad; (3) rail.

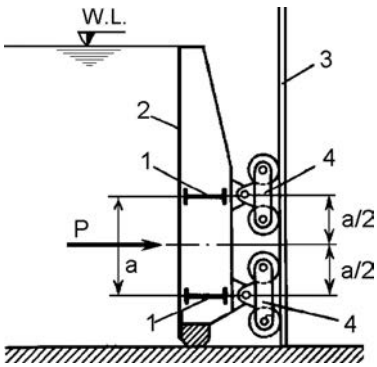

Figure 24.7 Wheeled supporting movable part. (1) Main beam; (2) waterproof lining; (3) rail (in gate slot); (4) wheels.

of corrosion. Usually, the thickness of the lining is 8 to 20 mm. The individual metal elements of the gate are interconnected by means of welding.

Depending on the construction of the supporting movable parts, we differentiate plain gates, which operate by sliding, and wheeled gates (also called *Stoney* gates), or gates operating by rolling on cylinders. The supports working by sliding (Figs. 24.6, 24.7) are made of wood, metal or synthetic materials.

Wheeled gates are employed for reducing the power of the mechanisms for lifting. With the wheeled gate, the resistance to movement consists of friction during rolling of the wheel along the rail and of friction between the wheel and its axis. The force T, which resists the movement, is as follows: $T = fP = 0.1P$ (P = force of the hydrostatic pressure on the gate that works by sliding). The number of wheels is four (Fig. 24.7) and endeavours should be made to position them in such a way as to be uniformly loaded. The diameter of the wheels usually amounts to between 0.3–1.0 m.

Gates on rolling cylinders (Fig. 24.8) have supporting stanchions (1) that rest on cylinders in the gate slots (7), connected by a frame (5). The force for lifting (2) transfers onto the frame by means of a steel rope (3), by means of a wheel (4), and thereby there is enabled rolling of the cylinders (7) across the surface of the concrete wall (6).

The gaps between the gate and the concrete construction must be hermetically sealed. For that purpose – at the end of the gate, and sometimes also on the concrete

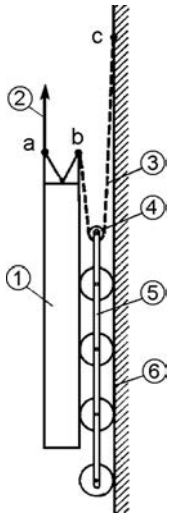

Figure 24.8 Rolling cylinders.

construction – there are constructed seals that are made of rubber, and also of elastic steel, or very rarely, of wood. The rubber for this purpose should comply with rigorous technical specifications. As a protection against wearing and also for reducing the force of friction, the surface of sliding of the rubber is sometimes covered with a metal plate. According to their method of working, one can differentiate two types of seals:

1. Seals that separate from the surface of the dam during movement of the gate;
2. Seals that slide across the surface of the dam, as, for example, in the case of lateral sealing of the plain gate. Figure 24.9 presents constructional solutions for sealing at the bottom (*A*) and sides, i.e. flanks (*B*), in the case of plain gates.

The mass of the movable part of the ordinary plain gate may be determined approximately with the empirical formula, after *Berezinsky*:

$$m = 0.055F\sqrt{F}\ [t] \tag{24.1}$$

where $F = bH$ is the area of the opening which is covered, i.e. spanned, by the gate, in m^2.

The weight of the gate G may also be expressed as dependent on the width of the opening b (m) and the force of the hydrostatic pressure P (kN), by means of the formula:

$$G = k(Pb)^n \tag{24.2}$$

For sliding gates where $Pb > 200$ kNm, it will be $k = 0.12$ and $n = 0.71$; and where $Pb > 270$ kNm, it will be $k = 0.09$ and $n = 0.73$.

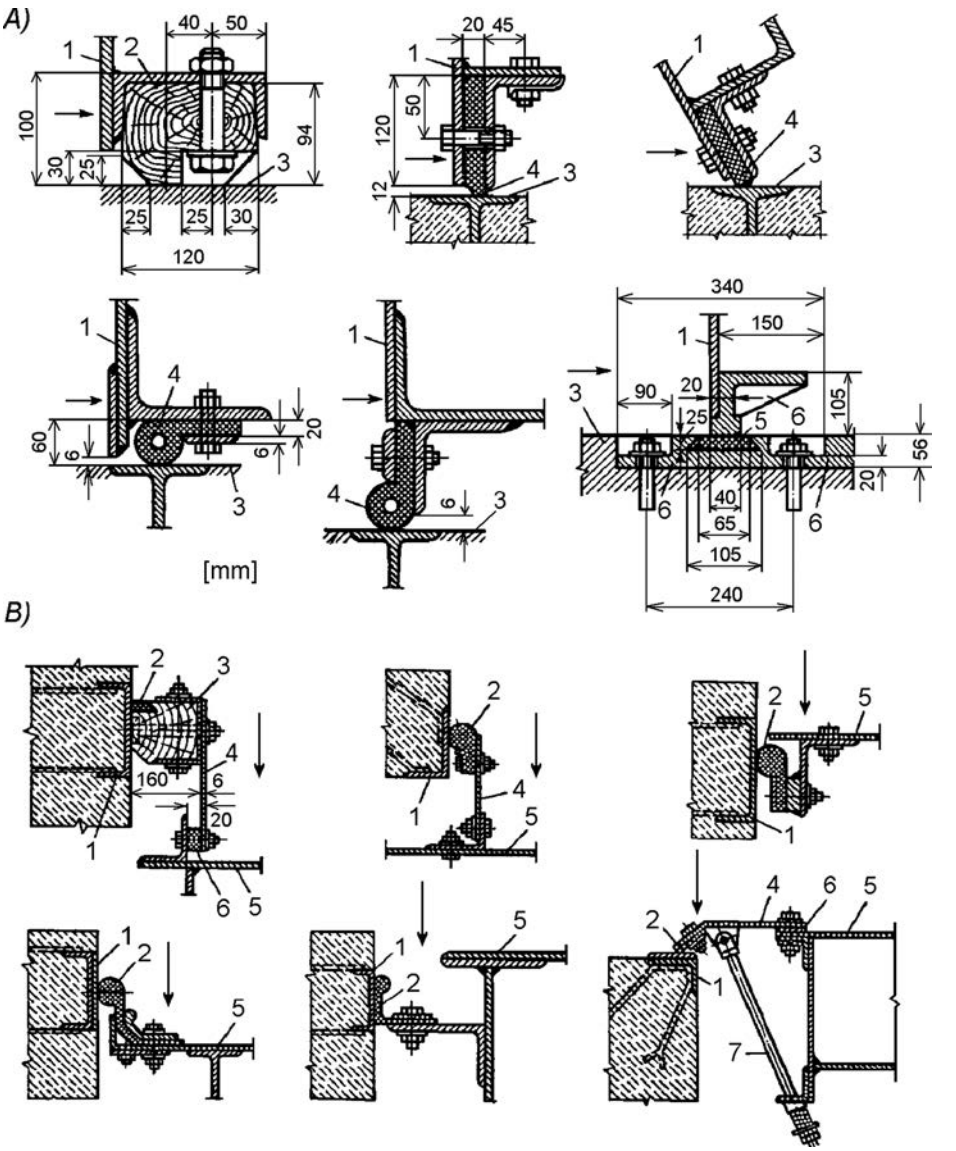

Figure 24.9 Sealing at bottom (A) and sides, i.e. flanks (B) for plain gates (after Grishin et al., 1979). (A): (1) lining; (2) wooden beam; (3) overflowing seal; (4) rubber; (5) filling of soft alloy; (6) steel casting. (B): (1) part embedded in the wall; (2) rubber; (3) wood; (4) elastic steel plate; (5) lining; (6) inserted rubber pad; (7) regulating screw.

The force which is required for lifting of a plain gate in still water is determined with the expression:

$$S\uparrow = n_1 G \tag{24.3}$$

where n_1 is the coefficient of safety, owing to the inaccuracy in the determination of G; and if G has been determined on the basis of a worked out design, then $n_1 = 1.1$. The uplift force is disregarded in this calculation.

If it is a question of flowing water, then, in addition to the weight of the gate G, it is also necessary to take into consideration the following forces: resistance to movement T caused by friction in the supporting movable parts, force of friction T_z in the seals, and vertical water pressure upon the gate G_0 (if any), as well as the suction force P_{vac}, which appears below the bottom seal. In that way, the force $S\uparrow$ is determined according to the following formula:

$$S\uparrow = n_1 G + n_2(T + T_z) + G_0 + P_{\text{vac}} \tag{24.4}$$

where n_2 is the coefficient of safety, due to inaccuracy in the determination of the forces T and T_z; so, it can be assumed that $n_2 = 1.2$.

The magnitude of the force T depends on the construction of the supporting movable parts, while T_z and P_{vac} are determined with the following formulae:

$$T_z = f\,P_z \tag{24.5}$$

$$P_{\text{vak}} = p_{\text{vak}}\omega \tag{24.6}$$

where P_z is the force of pressure of the lateral seals on the surfaces of sliding; f is the appropriate coefficient of friction; ω is the area of the horizontal projection of the bottom surface of the gate, upon which a vacuum can appear; and p_{vac} is the magnitude of the vacuum that can be assumed to be equal to 5–6 N/cm^2.

In some particular cases, during calculation of $S\uparrow$, one should also take into consideration the influences of ice and sediment.

For approximate calculations, we can apply the following simple formula:

$$S\uparrow = 1.5G \tag{24.7}$$

The force for lowering the gate $S\downarrow$ in flowing water is calculated from the expression:

$$S\downarrow = n_2(T + T_z) + W - n_1' G \tag{24.8}$$

where n_1' is the coefficient of safety, analogous to n_1 (but here it is assumed to be less than one ($n_1' = 0.9$); W *is* the vertical component of the water pressure upon the gate, taking into consideration the uplift (if it turns out that W is directed downwards, then it is taken with the sign of $-$).

If so calculated, force $S\downarrow$ has a negative sign, and it means that the gate does not require a force for forced lowering.

Ordinary plain gates can be used at the crest of the dam with any cross-section, for a height of opening of 7–8 m and for a width of 15–16 m. In this, they do not require any considerable length of flat surface of the spillway sill. They can be easily lifted from the gate slots by mean of a crane, in the case of need for overhaul.

The deficiencies of plain gates are the following: (1) ice can be let through only at complete opening of the span, which leads to loss of water; (2) the force required

for lifting the gate is significant, which is reflected in the cost of the mechanisms for lifting; and (3) high side walls may be required (Chugaev, 1985; Grishin et al., 1979).

24.2.2 Special plain gates

Some of the deficiencies of ordinary plain gates can be eliminated with special types of plain gates. One of them is the double plain gate, which consists of two independent parts, (Fig. 24.10). When lowering the upper part, there is the possibility of letting through floating solids (ice and the like); by lifting the bottom part, we can discharge the sediment that has been deposited in front of the gate. During water discharge, at the same time both above and under the gate, there are created favourable conditions for dissipating the energy of the flow.

Figure 24.11 shows the development of the construction of double gates, as used in Switzerland, Germany, and France. Construction under examples (a), (b), and (c) require execution of double gate slots and rails on each side, as well as separate mechanisms for the lifting of both parts. Illustration (d) presents a gate in the form of a shield, while illustration (e) presents a Γ-form gate, which is more favourable than the previous ones. Double gates also have some deficiencies – complex construction and installation, a necessity for horizontal sealing between the upper and lower section, and wide gate slots.

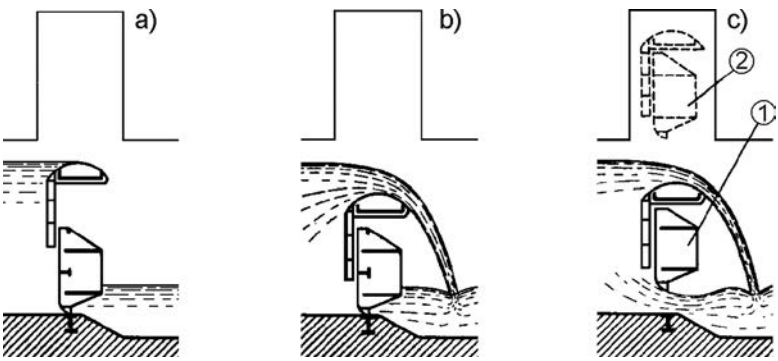

Figure 24.10 Schematic presentation of a Γ-shape double gate. (a) opening closed; (b) the upper part put down; (c): (1) discharge both from upper and lower side; (2) gate raised.

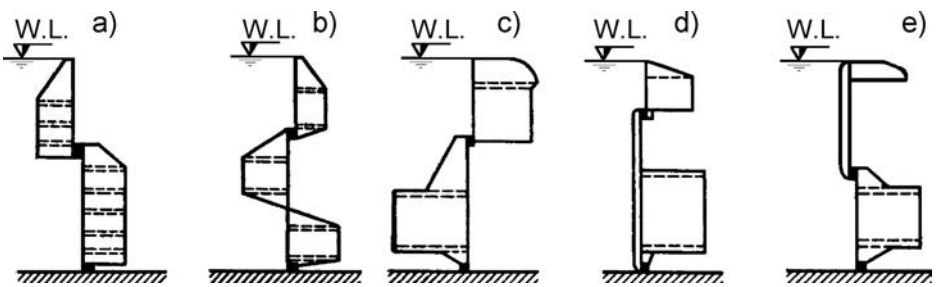

Figure 24.11 Development of the construction of double plain gates.

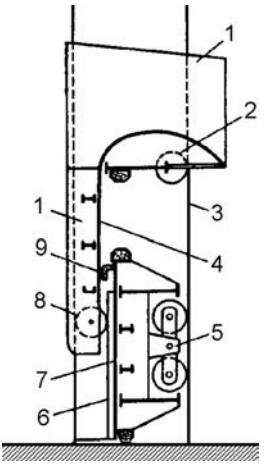

Figure 24.12 Double plain gate. (1) Plate; (2), (8) wheels of the upper part; (3) rail in the gate slot; (4) plate lining at the upper part; (5) beam with wheels of the lower part; (6) rail of the plate lining of the lower gate part; (7) lining at the lower part; (9) seal between the upper and the lower parts.

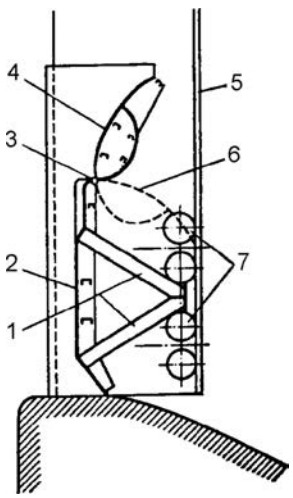

Figure 24.13 Plain gate with a flap. (1) Truss; (2) plate lining; (3) hinge; (4) flap; (5) rail in a gate slot; (6) flap in lowered position; (7) wheels (in the slot).

Double gates can be constructed at $H > 7$ m and $b > 15$ m, and the span that may be covered with them reaches to $b = 30$ m at H up to 20 m. The width of gate slots amounts to 5 m. Figure 24.12 presents a Γ-form double plain gate (Grishin et al., 1979).

Another kind of plain gate is the gate with a flap in the upper part (Fig. 24.13). It is employed for small heights ($H \leq 8$ m) when double gates are not rational. The flap (4)

turns in relation to the axis (3), opening the upper part of the span, thus enabling overflowing of the water. In addition, by lifting it is possible also to discharge water from the bottom side. These gates have been much used lately, especially in Western Europe. They have proved to be better than those with a Γ- form and may cover spans up to 40 m.

24.2.3 Stop-log gates

Stop-log gates are plain gates composed of a number of sections. They are employed as emergency gates or overhaul gates (only in the case of small dams can they be used as service gates). The simplest such gate is formed by means of laying down oak planks, i.e. beams, which, at the ends, penetrate into the gate slots. Their application is limited to smaller spans.

Figure 24.14(a, b) shows stop-log gates for opening spans with a width up to 8 m. They are difficult to lower into flowing water; therefore, they are used only as overhaul gates. In the case of openings wider than 8 m, it is possible to use metal flashboard gates (Fig. 24.14c), forming a plain gate with a number of sections. The lifting and

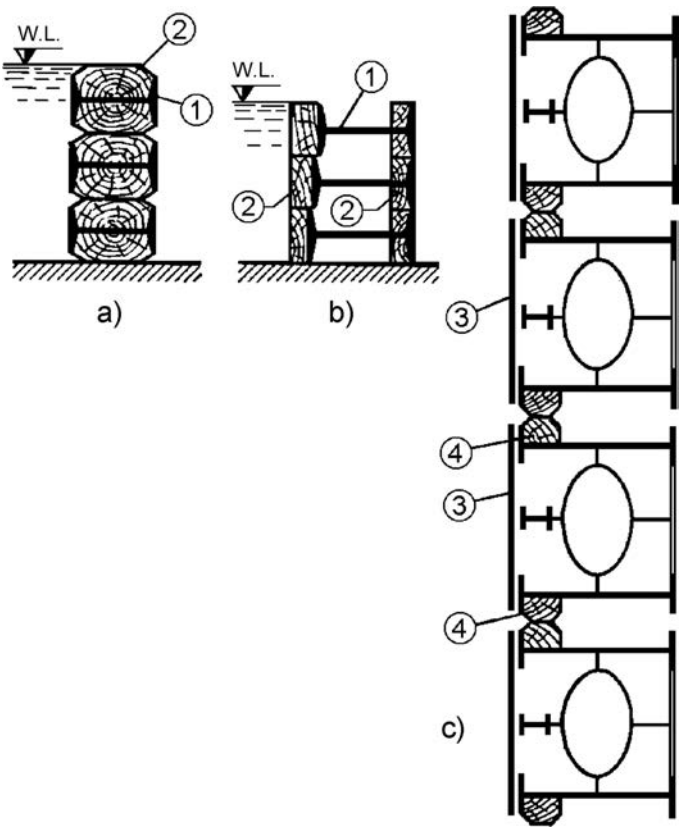

Figure 24.14 Steel stop-log gates (a) For spans up to 8 m (after Grishin et al., 1979); (b, c) sectional gate. (1) Steel beams; (2) wood; (3) metal lining; (4) seal (wood or rubber).

lowering of the sections of such a gate is performed by means of a holding beam that travels in gate slots the same as the gate itself, while a portal crane can be utilized for servicing. Individual sections may have supporting movable parts that work by sliding or rolling. The height of individual sections is from 2 to 3 m (Grishin et al., 1979).

24.2.4 Radial gates

Radial gates have a broad application since they require a smaller lifting force than plain gates. The ordinary radial gate (Fig. 24.15) contains the following basic elements: (1) lining constructed along a circular curve with a radius $R = (1–2.5)H$; (2) space load-bearing structure upon which the line rests, and which is constructed as a space truss as with the plain gates, but with a radius of curvature R; (3) supporting legs, by means of which the hydrostatic pressure is transferred to the supporting hinges (4); and (5) short reinforced concrete or metal cantilevers, overhung from the side walls, upon which the supporting hinges are set up (4). The short cantilevers are made in order to avoid the gate slots, in which the gate span is reduced and also the thickness of the side walls is reduced.

With the application of the force S, the gate can rotate around the axis of the supporting hinges (4), and thus, release the opening. The force of the self-weight G is moved away from the centre of the supporting hinge by the value $a_1 = 0.8R$. In order to determine the lifting force S, one should derive an equation of the moments of all forces in relation to (4). The most significant among these forces are the following: (1) the lifting force S; (2) self-weight G; (3) the friction force T_z in the lateral seals (6); (4) the suction force P_{vac}, which acts from downward to the gate; and (5) the friction force in the supporting hinges, dependent on the hydrostatic pressure, with a lever

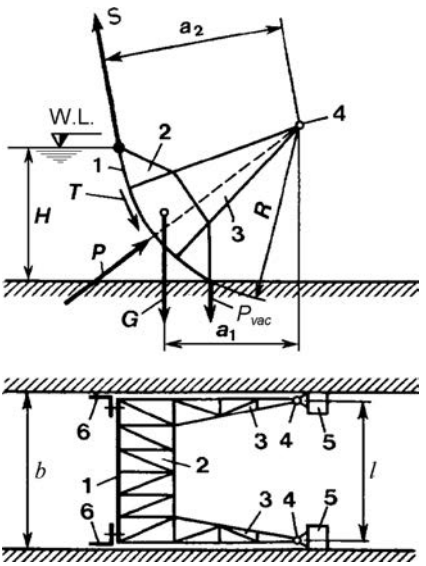

Figure 24.15 Ordinary radial gate.

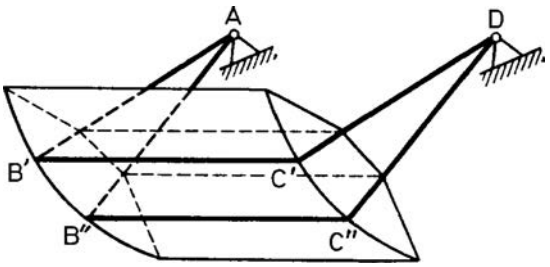

Figure 24.16 Scheme of a radial gate.

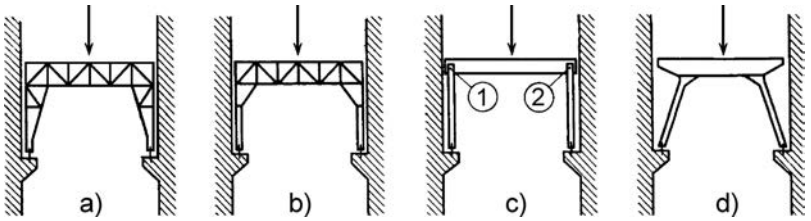

Figure 24.17 Structural schemes of the load-bearing part of radial gate and supports.

arm equal to the radius of the hinge r. The above-mentioned moment equation yields $S = 0.8G$; that is to say, S is twice as small as in the case of a plain gate.

The weight of the radial gate for the first approximation, prior to working out the design, may be determined from diagrams (given in textbook references) or by means of empirical formulae, for instance, after Berezinsky:

$$G = 0.15\, F\sqrt[4]{F}\ [t] \tag{24.9}$$

where F is the area of the opening in m^2.

It is also possible to use the expression (24.2), in which for $Pb > 150$ kNm, it will be $0.11 < k < 0.15$ and $n = 0.07$.

The basic elements of a radial gate are two (sometimes three) rectangular frames ABCD, which rest on hinges A and D (Fig. 24.16). The frames are mutually interconnected, so that there is obtained a rigid, trussed, load-bearing structure (Fig. 24.17). In the members of such a structure there appear relatively significant bending moments. In order to reduce these moments, we can use constructions with relatively elastic supporting legs (Fig. 24.17b) while for small gates ($b \leq 10$ m, $H \leq 7$ m) there are made vertical hinges (1, Fig. 24.17c), at the places of connection of the gate with its supporting legs. Lately, they have been making gates with inclined supporting legs (Fig. 24.17d), in which the bending moments of the beam are considerably reduced, while in the supporting legs those moments are almost completely eliminated.

The metal structure of the gate is made in the form of a trussed system or with beams of a certain section. The examples in Figure 24.18 shows two different systems

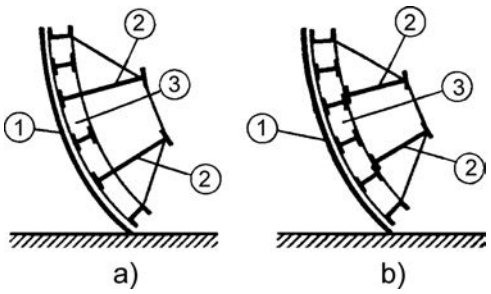

Figure 24.18 Two systems of beam cells. (1) Lining; (2) main beam; (3) beam cell.

of beam cells of a radial gate, while in Figure 24.19 A, B, and C present various alternatives of its structural shaping.

The supporting hinges should be set up above the water level. The hinges may have such a position that the lining of the gate would be to the left of the vertical, passing through the bottom seal (Fig. 24.19), which is more often the case. The height of the side walls may be reduced by positioning the hinges at the end of the wall (Fig. 24.19). The supporting hinges can be spherical, cylindrical, or conical and are dimensioned by means of static calculations.

Spherical hinges are very complex of execution and are very rarely used. *Cylindrical* hinges are produced in three types, Figure 24.20: (a) in the form of a beam on two supports; (b) in the form of a cantilever system of beams and (c) in the form of a cantilever beam for a given supporting leg, Figure 24.22. *Conical* hinges (d) are made in the form of a cantilever.

Manoeuvring of radial gates is achieved by means of stationary mechanisms for lifting and lowering, in which two mechanisms are usually employed, set up at both sides of the gate. In this, the operation of the mechanisms should be synchronized in an appropriate manner, in order to prevent distortion of the gate. Chains and thick ropes are usually employed for lifting and lowering.

Sealing of gaps in a radial gate does not differ essentially from that in a plain one. Figure 24.21 shows a scheme of structural shaping of lateral sealing.

In terms of the ability for covering, that is to say, bridging, radial gates are employed for widths of openings of 40 m and a height of 14 m. Lately, the height has reached up to 20 m, with a tendency for reducing the ratio *b*/*H* (Chugaev, 1985; Daniell & Taylor, 2000; Davis & Sorensen, 1969; Grishin et al., 1979; Novak et al., 2001; Erbisti, 2004).

The radial gate and the plain gate are similar in relation to the weight and dimensions of the openings for which they are employed, while the radial gate has the following advantages: (1) smaller force required for lifting; (2) more favourable for winter conditions since the hinges are positioned above the water; (3) opening performed faster; (4) side walls lower and thinner; (5) smaller vibrations during flowing; and (6) it can also be constructed as a gate with automatic action.

Radial gates also have certain deficiencies in relation to plain ones: (1) they cannot be relocated from one opening to another; (2) they cannot be used as gates in the

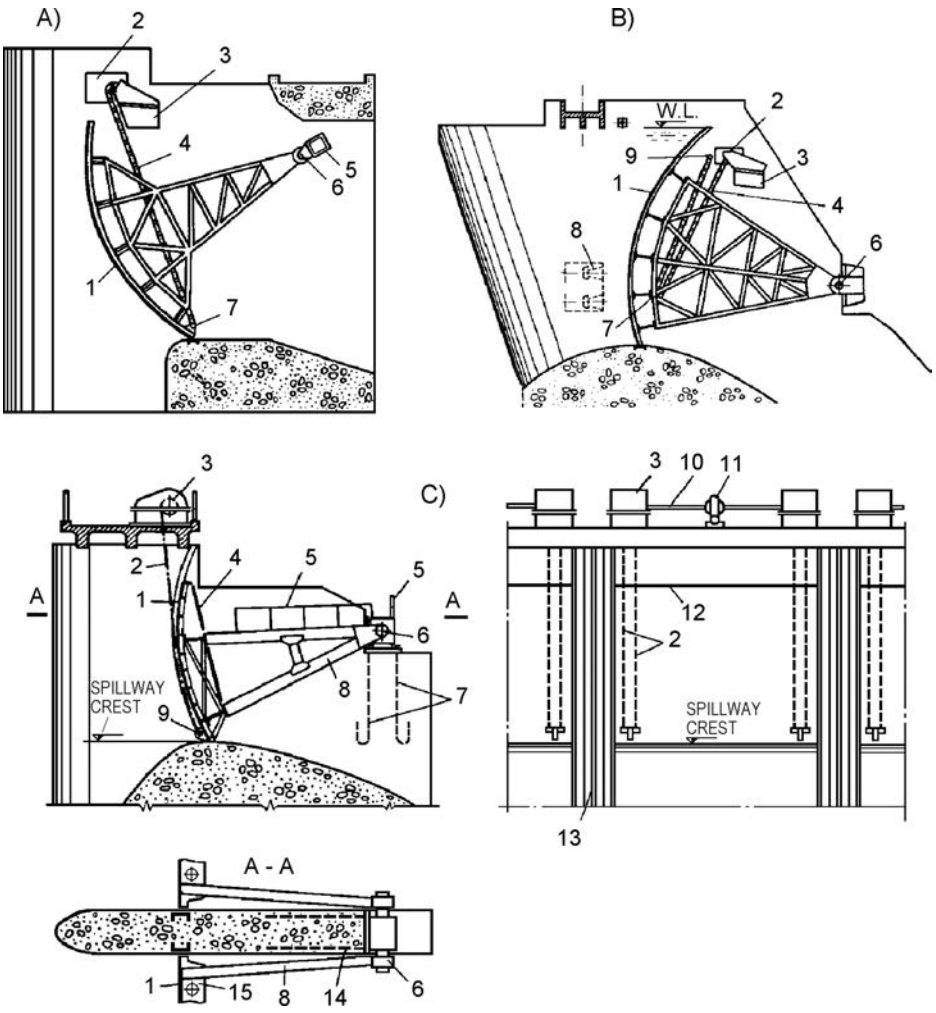

Figure 24.19 Constructional schemes of radial gates with inclined supporting legs. (A, B): (1) Waterproof lining; (2) place for fixing the lifting mechanism; (3) space for placing of the chain; (8) fixing of the anchoring reinforcement of the hinge; (9) fastening the chain into the side wall. (C): (1) Lining; (2) chain or thick rope; (3) hoist; (4) downstream lining; (5) fence; (6) hinge; (7) anchors of the hinge; (8) supporting leg; (9) fixing of the rope; (10) shaft; (11) engine; (12) crest of gate; (13) deformation joint in the side wall; (14) horizontal anchors of the hinge; (15) bar (beam).

course of execution of construction works; and (3) they have greater length of the side walls.

In order to enable passing through of ice, as well as smaller overflowing water quantities without raising the entire gate, we construct special radial gates, with a specific part – a flap, in the upper part (Fig. 24.23). The flap lowers and lifts by means

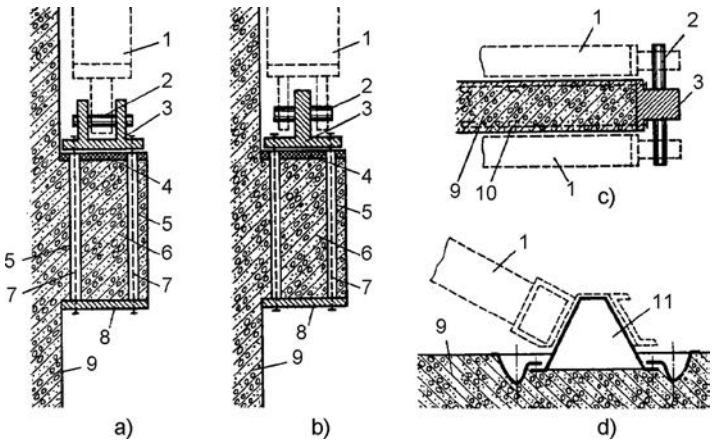

Figure 24.20 Scheme of supporting hinges (after Grishin et al., 1979). (1) Supporting leg; (2) fixed cylindrical axis; (3) steel stationary part of the hinge; (4) levelling layer of cement mortar; (5) pipe; (6) reinforced concrete cantilever; (7) anchor bolt, carried through the pipe (5); (8) steel plate, $\delta = 14$–20 mm; (9) side wall; (10) anchors; (11) fixed steel casting of the conical hinge.

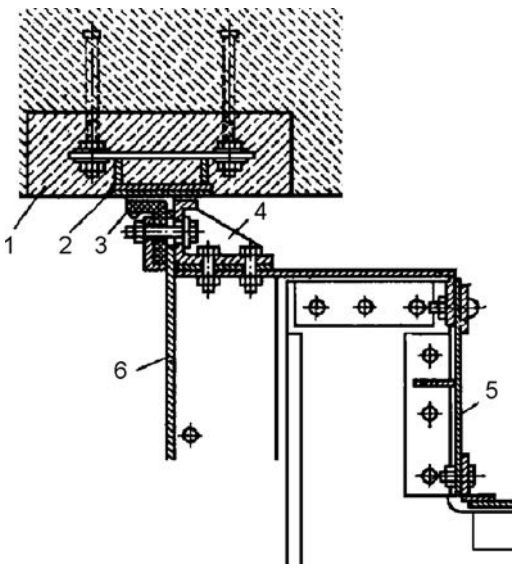

Figure 24.21 Constructional shaping of a lateral seal in a radial gate. (1) Concrete; (2) guide member, embedded in concrete; (3) rubber seal; (4) stiffening element; (5) lining of the gate at the downstream side; (6) lining of the gate at the upstream side.

of a special mechanism, for instance with a hydraulic drive, which is usually set up on a metal construction on the gate itself. In the zone of the flap, the overflow opening is somewhat constricted, in order to protect the supporting legs against the overflowing waters.

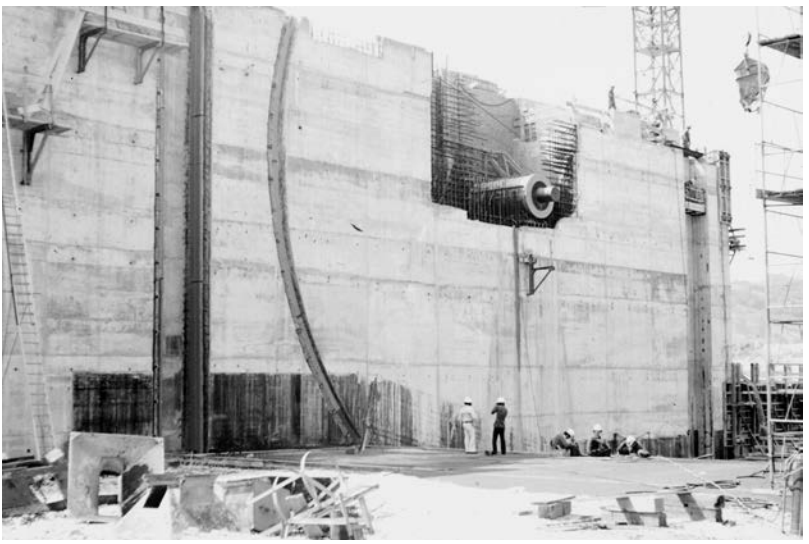

Figure 24.22 Hinge and rail (in gate slot) for the radial gate at a dam on the River Rhone (France), under construction (1979).

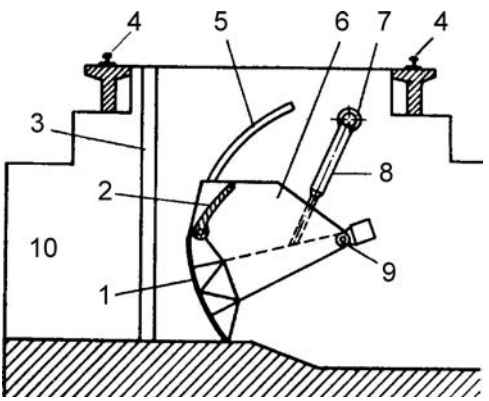

Figure 24.23 Radial gate with overflowing flap. (1) Lining of gate; (2) overflowing flap; (3) slot for overhaul gate; (4) rails; (5) guide member embedded in concrete; (6) metal liners for constricting the opening in zone of flap; (7) fixing of hoist to the side wall; (8) hydraulic hoist; (9) supporting hinge; (10) side wall.

24.2.5 Roller gates

The roller gate is a cylinder of a considerable diameter, which closes the opening. The cylinder can roll along a toothed inclined rail track, fastened in the gate slots in the side walls, which enables handling of the gate. We differentiate three basic schemes of the cross-section of the roller gate, Figure 24.24: (a) in the form of a cylinder; (b) cylinder with a bottom shield; and (c) cylinder with a front shield. In the last case,

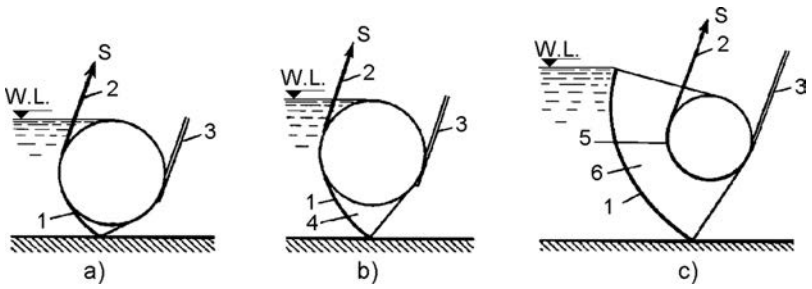

Figure 24.24 Schemes of cross-sections of roller gates. (1) Lining that takes on the hydrostatic pressure; (2) elastic rope; (3) rail track (in gate slot); (4) bottom shield; (5) lining; (6) front shield.

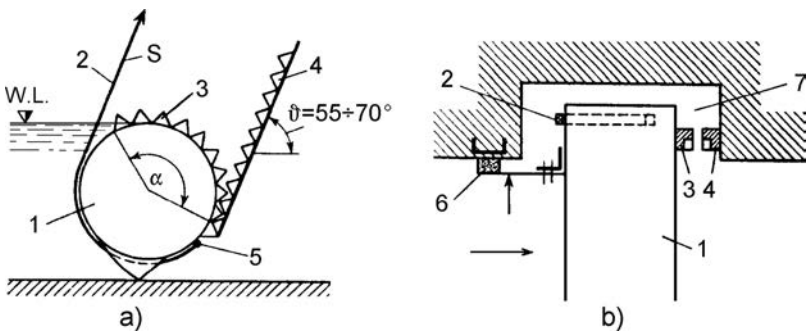

Figure 24.25 Scheme for the supporting parts of the roller gate (after Grishin et al., 1979). (a) Cross-section; (b) layout. (1) Roller gate; (2) elastic rope; (3) toothed wheel rim; (4) toothed rail track; (5) fixing of the rope to the gate; (6) seal; (7) gate slot.

the hydrostatic pressure is taken on directly by the lining (1) of the front shield (6), while the cylinder plays the role of a load-bearing structure.

Toothed wheel rims (3, Fig. 24.25), are fastened at the ends of the gate, while in the gate slots on the side walls there are fastened rail tracks (4) at an angle of 55 to 70°, in relation to the horizontal, provided with a toothed track. By means of the force *S*, the gate rolls along the rail track; only stationary hoists service the roller gates.

Roller gates are constructed of metal. The load-bearing structure, in the form of a cylinder, is constructed in the following way: transversely to the cylinder, at distances of 1.5 to 2 m, diaphragms are placed (2, Fig. 24.26); horizontal beams (3) are placed along the length of diaphragms; and a lining (1) is constructed along the external contour of the cylinder (a steel plate with a thickness of 10 to 15 mm). The end diaphragms that rest upon the rail tracks, which are placed into the gate slots, are made with a reinforced construction, or else two diaphragms are placed next to one another.

The diaphragm can also have a different shape and construction; for instance, triangular (4) (in section), as is shown in Figure 24.27. This figure also shows the construction of the lower shield (3) and of the toothed wheel rim (1), the teeth of which go into the stationary toothed rail track (2), placed into the gate slot.

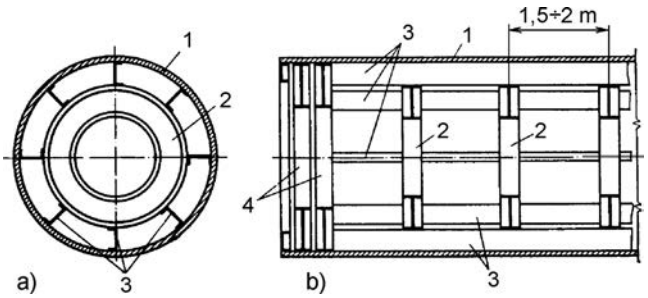

Figure 24.26 Construction of the load-bearing part of the roller gate (after Grishin et al., 1979). (a) cross-section; (b) longitudinal section. (1) Lining; (2) transverse diaphragm; (3) longitudinal beams; (4) supporting diaphragms.

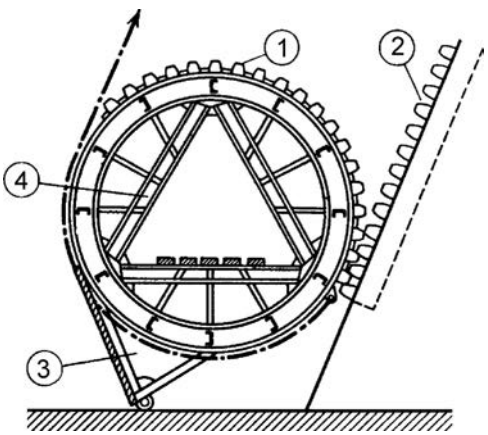

Figure 24.27 Construction of a roller gate with bottom shield and triangular diaphragm.

The construction of the seals for roller gates differs from that of plain gates and radial gates. One of the solutions for lateral sealing with the application of an elastic metal plate (5), which closes and seals the gate slot, is presented in the example in Figure 24.28.

The dimensions of the load-bearing parts of the gate are determined by means of static calculations, considering its different elevation positions. For the first approximation, the diameter of the cylinder can be taken as $d = (1/8)b$. This diameter is rarely greater than 5 m. The spans that are covered with the roller gates reach 45 m, and even 50 m. The height H can reach up to 13 m. The height of the bottom shield is equal to $(0.4–0.5)H$. For greater values of H, the gates, as a rule, are made with a front shield. The depth of the gate slot is greater and amounts to 1–2 m. The side walls for this gate are not thinner than 5 m.

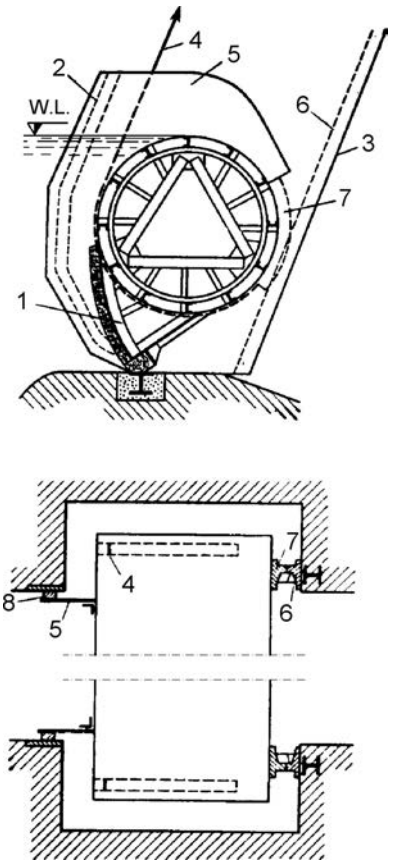

Figure 24.28 Roller gate with bottom shield. (1) Shield; (2) boundary of lateral seal; (3) boundary of gate slot; (4) chain; (5) metal plate covering gate slot; (6) rail track in gate slot; (7) wheel rim; (8) seal.

For the first approximation, the weight of the steel gate covering an opening F [m^2], can be determined according to the formula after *Berezinsky*:

$$G = 0.5\,F + 0.2\,F\sqrt{F} \tag{24.10}$$

In addition to the gates described above, there are also roller gates of a special type (Fig. 24.29): (a) descended type; (b) with overflowing flap; and (c) with longitudinal load-bearing construction in the form of a drum, but not with a circular-cylindrical form, aiming at achieving greater stiffness. The supports of such gates have a circular-cylindrical form, in order to be able to roll along the rectilinear rail track that is embedded in the gate slot.

Roller gates have the following advantages in relation to plain gates and radial gates: (1) covering a greater area; (2) simple supporting parts; (3) their mechanisms

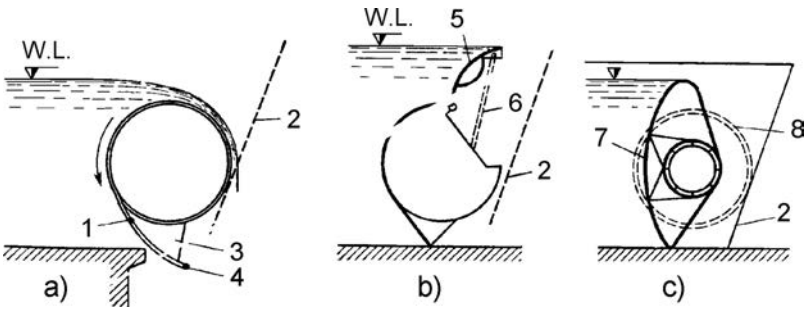

Figure 24.29 Special types of roller gates (after Grishin et al., 1979). (1) second lining; (2) rail track in gate slot; (3) bottom shield; (4) basic seal; (5) flap; (6) lever arm of hydraulic hoist; (7) lining; (8) circular-cylindrical part in gate slot.

for lifting and lowering are not expensive, $S = (0.3–0.5)G$; (4) they have a significant stiffness; and (5) they do not require service bridges.

The deficiencies of the roller gates are: (1) high cost, which is a reason for their rare application; (2) side walls with considerable dimensions; and (3) the level of headwater is relatively difficult to regulate (Chugaev, 1985; Grishin et al., 1979).

24.3 SURFACE (CREST) GATES TRANSFERRING THE WATER PRESSURE TO THE GATE SILL

These gates are not subjected to bending as are those that lie on side walls, and this simplifies their construction and enables covering of great spans of openings.

24.3.1 Sector and drum gates

Sector and drum gates are gates that have a cross-section in the form of a sector with a lining, fixed to the sill of the dam on a horizontal axis. Rotating in a circle, they may be partially or completely lowered into a special gate slot. They can operate with a hydraulic drive, which is the most frequent case, or else with a mechanical drive. Sector gates have a downstream axis of rotation, while drum gates are hinged at the upstream side.

24.3.1.1 Sector gate

This kind of a gate is presented in Figure 24.30. Under the action of the water pressure, it turns in relation to the axis (6), descends into the chamber (7), so the water overflows over the downstream lining (5). The basic elements of such a gate are the upstream lining (4), drawn from the axis of rotation (6), with a radius R and downstream flat lining (5), along which the water discharges downstream. It is usually assumed $R = (1.4–1.6)H$.

The hydraulic handling is achieved in the following way: the pipeline (1) relates the headwater with the chamber (7, Fig. 24.30); when the water through the pipeline

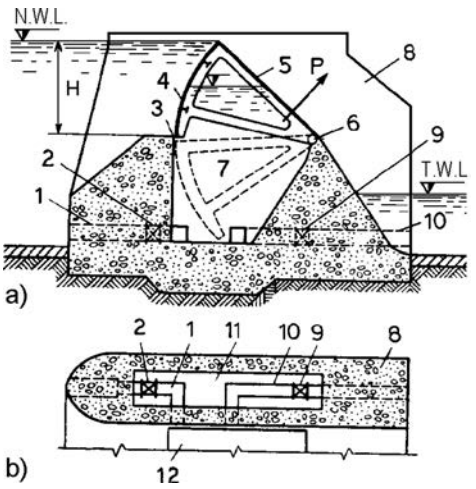

Figure 24.30 Sector gate with downstream axis of rotation (6). (a) Cross-section; (b) horizontal section. (1), (10) Pipelines with flaps (2) and (9); (3) bottom seal; (4) lining (circular-cylindrical); (5) flat lining; (6) horizontal axis; (7) and (11) chamber; (8) side wall; (12) the gate in plan.

(1) enters the chamber, there is an increase in the pressure and the water level in the chamber; the force of hydrostatic pressure P increases and the gate starts rising; the other pipeline (10) relates the chamber with the tailwater and, when water discharges, the level in the chamber decreases, and the pressure also decreases and the gate drops down. The degree of span opening of the dam depends on the water level in the chamber. The side walls (8), in this case, serve for the placement of the pipelines. Their width can amount to as much as 6 m. The chamber must be hermetically isolated, i.e. sealed, which is achieved by means of appropriate seals at the sides, as well as along the axis (6).

The construction of the gate consists of planar trusses (1, Fig. 24.31) spaced at distances from 1.25 to 3 m, in which each truss is fastened to the concrete by means of a hinge. The supporting hinges are put in place below each truss or are continuous along the entire length of the gate.

The sealing of the sector gates should be achieved with high precision and responsibility, in order to protect the chamber against losing pressure, as well as against filling with sediment. The lateral seals have a construction like that of radial gates, while bottom sealing is performed by means of an elastic plate, in combination with rubber or wooden elements. The axis of rotation is continuous, or sealing may be achieved with an elastic plate along with rubber elements.

The weight of the movable element of the gate, in kg per 1 m^2 of the opening, can be approximately obtained from the expression:

$$g = 135 + 129\sqrt{H} + 54H \tag{24.11}$$

The above-described sector gate requires a significant widening of the dam's crest. It can cover openings up to 65 m and a height up to 11 m. The basic advantages of these

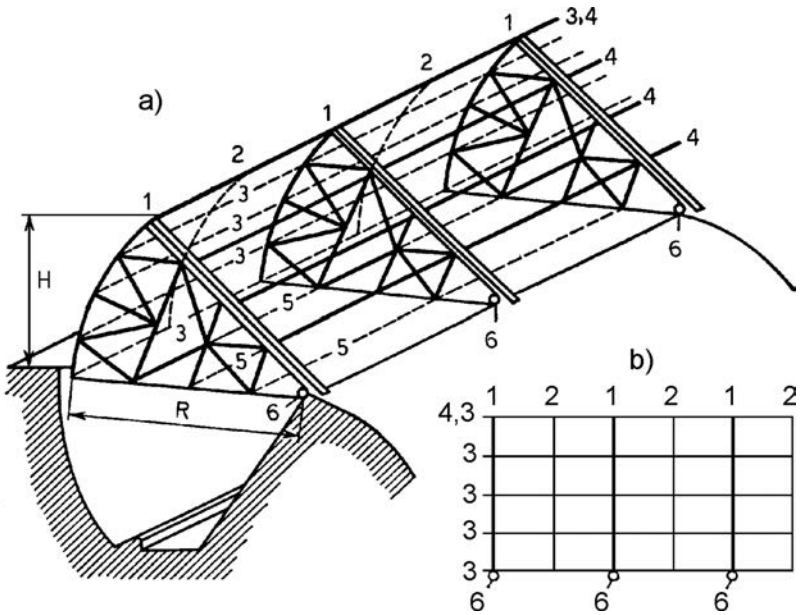

Figure 24.31 Construction of a steel sector gate with downstream axis of rotation (a), and layout of the basic elements of the construction (b) (after Grishin et al., 1979). (1) Planar truss; (2) auxiliary curvilinear support; (3) beam; (4) upper horizontal beams; (5) lower horizontal beams; (6) hinges.

gates are: (1) they make possible accurate and fast regulation of the level of headwater; (2) the height of the side walls is not significant; and (3) they are stiff and enable covering of significant spans. The main deficiencies are their complex construction, high cost, and the considerable width required in the crest of the dam.

24.3.1.2 Drum gate

This kind of gate is hinged at the upstream side, as is presented in Figure 24.32. A drum gate is formed of transverse curvilinear frames (3) spaced at a mutual distance of 1 m. The steel lining (2) covers the frame on all sides; in addition, there are also provided lateral watertight linings, at both end frames. Thus, a float member has been made, in the interior of which there is formed a closed air space (4). The principle of hydraulic action of this kind of gate is the same as in the previous case.

The above-described type of gate is very compact and rigid. It is applied in relatively high dams, when there is no danger of penetration of sediment into the chamber (8). The chamber is not submerged by the tailwater. The ratio of the radius of curvature of the gate vis-à-vis the height is assumed to be $R/H = 1$. When the gate is completely closed, it forms a vacuum-free overflowing surface, with a coefficient of discharge $m = 0.44–0.45$. In the upper part of the gate there is a shield (9), by means of which we increase the moment of the force of hydrostatic pressure from the upstream side, in relation to the point (5) in order to reduce the value of the reaction at that point.

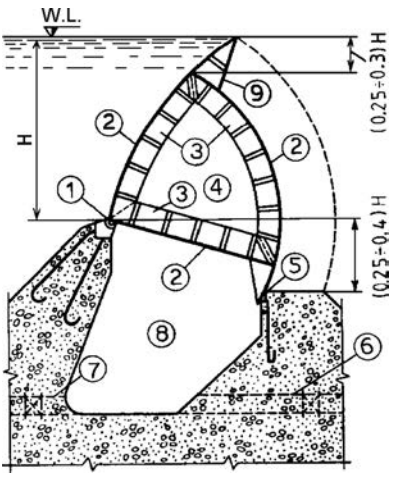

Figure 24.32 Drum gate. (1) Hinge with sealing, located at the upstream side; (2) lining; (3) three-sided curvilinear space frame; (4) closed air space; (5) seal; (6, 7) pipelines with valves; (8) chamber; (9) shield.

The height of the shield amounts to (0.25–0.30)H. The axis of rotation is positioned above the gate sill for a value of (0.25–0.40)H.

This gate is heavier in relation to a sector gate, and its weight (kg per 1 m^2 of the opening) can be approximately determined according to the empirical formula, after *Toranovsky* (Chugaev, 1985; Grishin et al., 1979):

$$g = 255 + 217\sqrt{H} + (50\text{–}80)H \tag{24.12}$$

24.3.2 Flap gates

Flap gates consist of flat or curvilinear watertight surfaces rotating around a horizontal axis, fixed to the sill. Two types have been made lately (Fig. 24.33): (A) with a longitudinal beam and (B) in the form of a lens. They can be applied to higher dams and to lower sills. The work of these gates can easily be automated. They can cover spans of up to 50 m, at a height of up to 7 m. As mechanisms for lifting, there are usually employed hoists or stationary mechanisms with hydraulic drive.

Figure 24.34 shows two flap gates with hydraulic drive, the mechanism of which is located in the dam's body. Example (A) presents a gravity dam with a gate 20 m long and 5.35 m high. The overflow, which is 80 m long, has four such gates incorporated into it. Each of them at the ends has two supports, i.e. struts, which are connected, hinge-like, with the cylinders of the hydraulic hoists.

Example (B) presents the gate of an overflowing span with dimensions 12 × 3.1 m in the case of an arch-gravity dam. The hydraulic drive is centrally accommodated – below the middle of the flap – while the required stiffness of the gate is provided by means of transverse ribs.

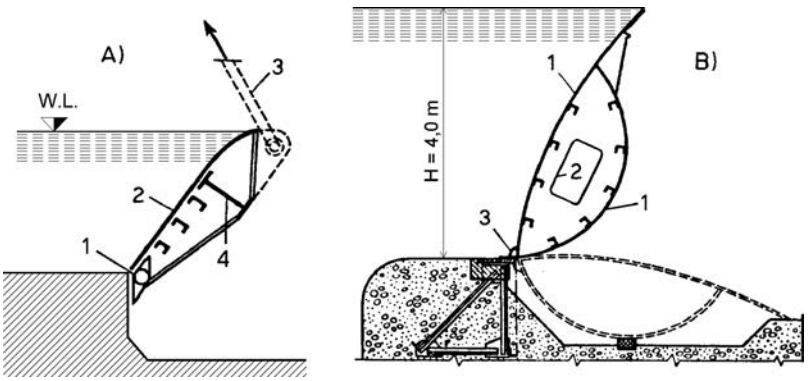

Figure 24.33 Flap gates (after Grishin et al., 1979). (A) With a longitudinal beam (4): (1) hinge with sealing; (2) lining; (3) thick rope. (B) in the form of a lens: (1) lining; (2) diaphragm; (3) hinge.

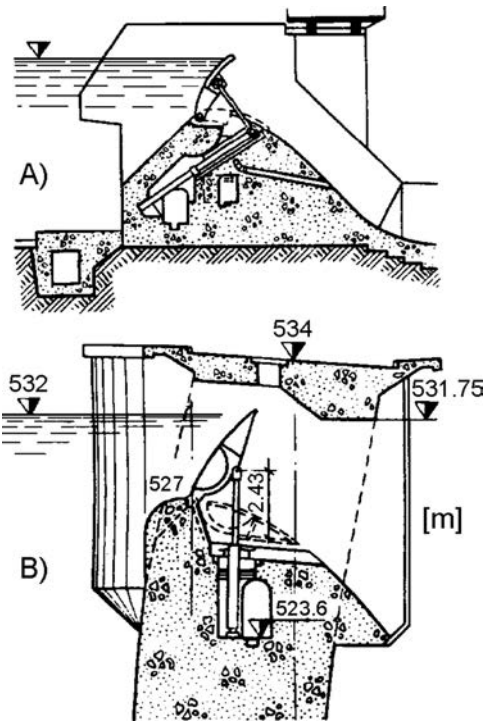

Figure 24.34 Flap gate with hydraulic drive.

Balanced flap gates, in which balancing is achieved by means of a counterweight or hydraulically, are more rarely employed. Hydraulically balanced flap gates rotate about a horizontal axis, which is placed in the middle part of the gate and, at a certain pressure of the headwater, they turn about their axis, thus enabling overflowing.

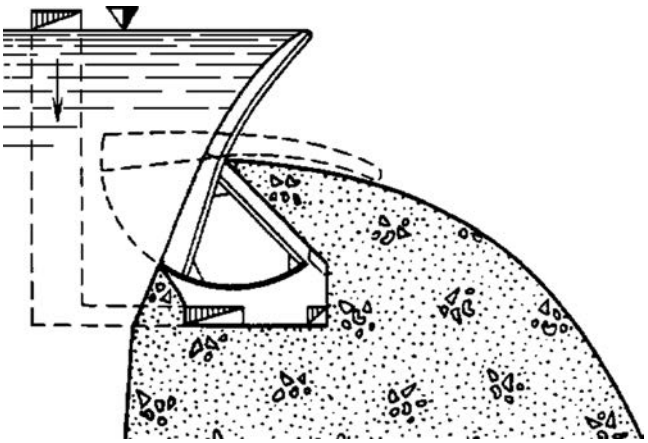

Figure 24.35 Balanced flap gates.

A more complicated type of such a gate is that in which the movement is achieved by pressure variation in the chamber below the flap by means of supplying water (Fig. 24.35), similarly to the sector gates.

The favourable features of flap gates are the following: simple to manoeuvre, accurate in regulating the water level, passing through of floating bodies without a significant loss of water, possibility of covering considerable widths. Their deficiencies are: the need for execution of a recess, i.e. slot in the sill, complicated erection, and overhaul.

24.3.3 Bear-trap gates

The movable parts of these gates consist of two flaps which, rotating around a horizontal axes, form a kind of roofed structure in a raised condition which, in a lowered condition, is accommodated in a gate slot within the sill of the structure (Fig. 24.36). The upstream flap or the downstream flap has at the end a short extension, perpendicular to the plane of the flap. The downstream flap has a curved surface. The chamber, which is formed by the gate, is filled with water from the upper level and imposes pressure on the flaps.

In the position as shown in Figure 24.36b, forces due to mater pressure W_1, W_2 and W_3 act on the flaps, as well as weights G_1 and G_2, and then reactive forces – the reaction N in the interface of the flaps C, which is transferred by means of wheels, reacts in the supporting hinges A and O, as well as friction in hinges A, C and O. If we neglect the forces of friction, then equations of moments are obtained, which express the equilibrium conditions for the flaps. For the upper flap it is:

$$W_1 a_1 - W_2 a_2 + G_1 b_1 - N n_1 = 0 \tag{24.13}$$

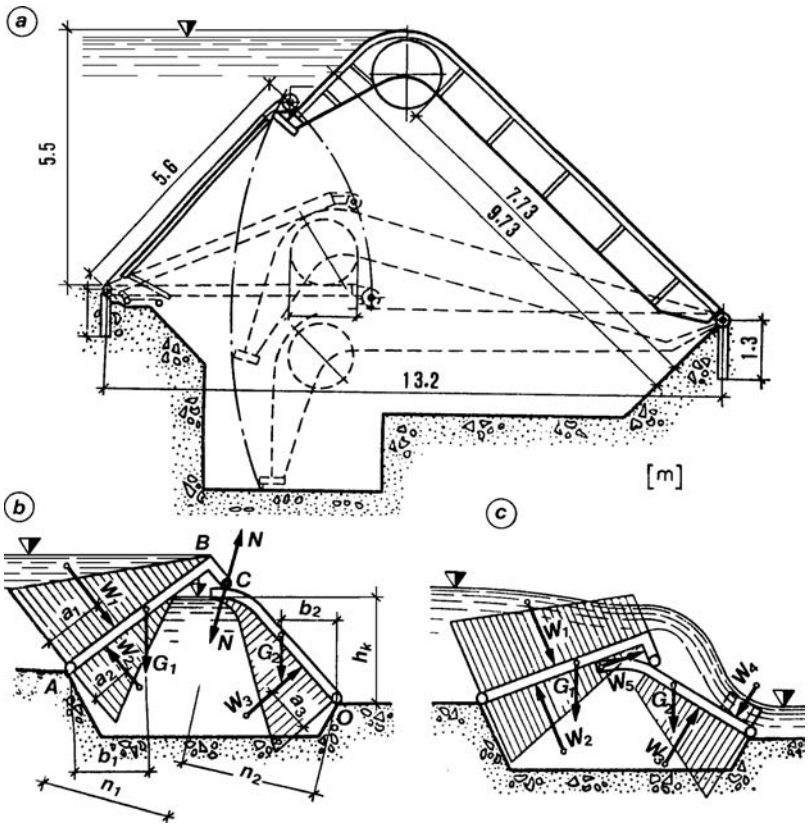

Figure 24.36 Example of a bear-trap gate (after Grishin et al., 1979). (a) Cross-section; (b, c) schemes of force action.

while for the lower one it is:

$$W_3 a_3 - G_2 b_2 - N n_2 = 0 \tag{24.14}$$

The lever arms of forces a_2, a_3, n_1, n_2 and forces W_2 and W_3 can be expressed through h_k – the height of the water in the chamber above the hinge O. For known W_1, G_1, G_2, b_1 and b_2, by means of the expression (24.13), we can find the value of h_k at equilibrium, that is to say, to determine the water level in the chamber.

In an intermediate position of the gate (Fig. 24.36c), there are changes in the values of the forces W_1, W_2, W_3, G_1 and G_2, as well as changes in the values of their lever arms. New forces appear: W_4, the force due to water that flows over the flap, and W_5, the force due to water pressure from the side of the chamber on the extension of the upper flap. Analogous to the previous case, it is possible to determine the necessary pressure in the chamber.

The bear-trap gates cover openings up to 45 m wide, at heights of 6–7 m. The gate can descend within 2–10 minutes, lets through ice and other floating bodies, i.e. solids,

and provides accurate regulation of the level of headwater; however, it requires a wide crest sill of the dam, is of complex construction, is difficult for installation, and sensible to freezing and to penetration of sediment.

24.3.4 Inflatable gates

Gates made of synthetic fabrics or rubber, filled with liquid or air, form an inflated gate that is anchored into the sill of the dam. The fabric can be single-layer or multi-layer; it is made of synthetic fibres with rubberised protection on one side or both sides. The strength of fabric used exceeds 100 kN/m^2. By means of these gates, we can cover wide openings. In the USA, by means of a gate made of fabric, there have been covered, i.e. bridged, four spans of 134 m each, at a pressure head of 3.17 m. There is also known an inflated gate, which, at a pressure head of 6 m, bridges an opening 28 m wide. Lately, in Serbia, gates have been employed of this kind for the regulation of the River Nishava. These constructions have a low mass, are easy to transport, simple to install and low-cost. They also have deficiencies – danger of damage and limited durability (up to 10 years) – which are compensated for by their simplicity and economy.

Inflated gates are fixed to the sill by means of one or two lines of anchors (Fig. 24.37a, b). The gate is kept in a raised position by means of water pressure – non-freezing liquid, or else air. Filling and emptying can be performed freely or under pressure, in which it is necessary to have a liquid reservoir on the pier or on the side wall. Fluid supply and off-take is achieved through pipelines in the sill or on the piers (Chugaev, 1985; Grishin et al., 1979).

In calculations, we determine the shape of the gate, which depends on the internal pressure, as well as on the quantity of the overflowing water; strength, i.e. bearing capacity, is also examined.

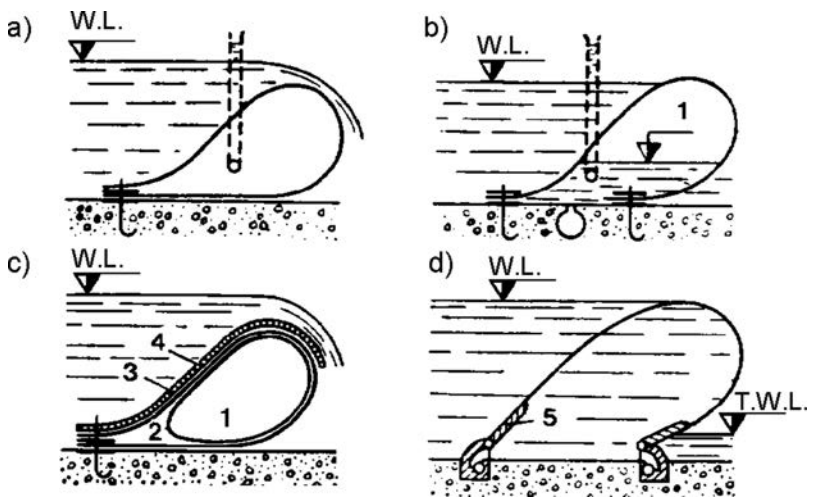

Figure 24.37 Schemes and examples of structural solutions for inflated gates made of fabric. (1) Air; (2) internal lining; (3) lining for fixing; (4) protective lining; (5) metal part, fastened onto a hinge.

This page intentionally left blank

Chapter 25

High-head gates and valves

25.1 GENERAL CHARACTERISTICS – CLASSIFICATION

The high-head gates and valves differ from surface (crest) gates in that they are always under water, and they close the opening from all sides and do not allow overflowing of water at the upper side. In the case of dams, they are employed with outlet works, supply structures, intake structures, and also with deep or high-head spillway structures. The submersion of the gate or valve may be from several metres up to several dozens of metres. The characteristic service features of high-head gates and valves are such that they are subjected to a high water-pressure, while they are less accessible for control in comparison to surface gates, and handling them is less frequent. Velocities of flow in the water-conveyance structures or conduits, which are closed by these high-head gates and valves, are considerable and they can reach 30 m/s. The above-cited features impose the need for the construction of these gates and valves to be firm and stable, while the operation safe even in the hardest conditions of service. In order to be protected from coarse objects and solids, rough trash racks are usually placed in front of them. And since they close important structures, the high-head gates and valves are manufactured as either double type, one after another, or an overhaul-emergency gate or valve is anticipated, in addition to the service gate or valve.

Owing to the high velocities, to the slots or recesses or due to change of the profile, behind the gate or valve there appear whirls as well as a vacuum, which cause vibrations and cavitational erosion. In order to avoid such an unfavourable effect, behind the gate or valve we regularly provide an aeration pipe, for bringing in air (Fig. 25.1). The section of the aeration pipe is assumed to be about 10% of the cross-section of the water-conveying structure behind the gate or valve. If the gate (valve)

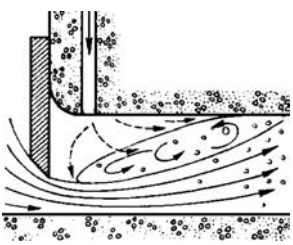

Figure 25.1 Aeration pipe behind the gate.

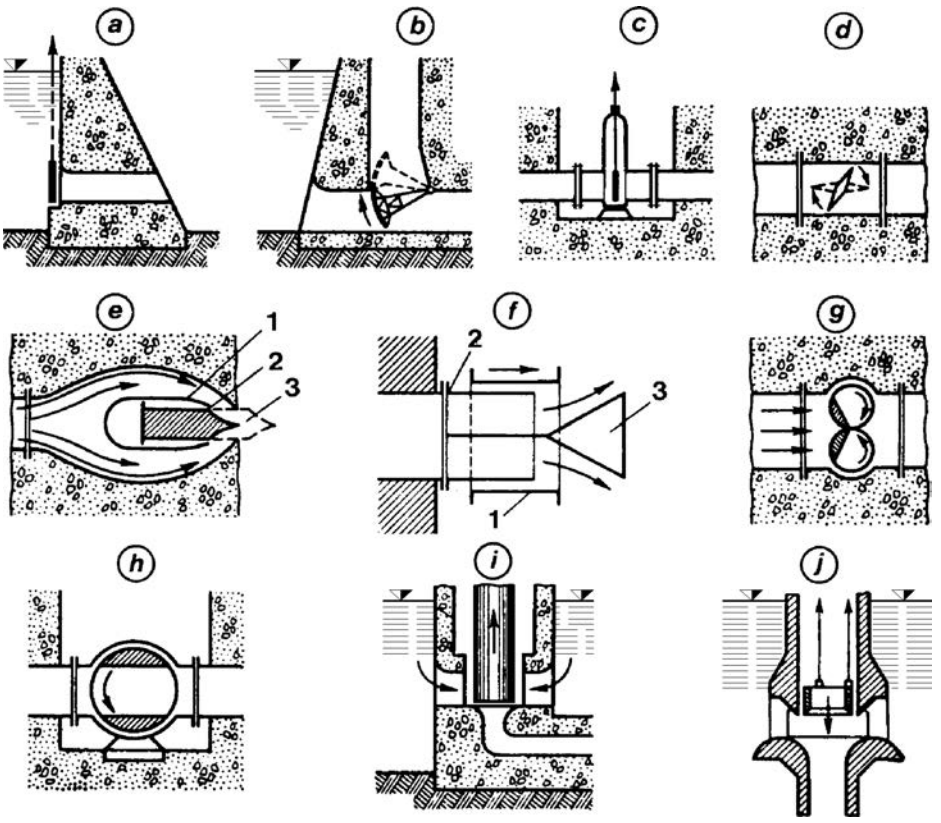

Figure 25.2 Service types of high-head gates and valves (after Grishin et al., 1979).

is placed at the outlet of the water-conveyance structure and discharge is carried out directly into the atmosphere, then the above-described phenomena do not take place. In addition to the provision of an aeration pipe, as a supplementary measure, we usually apply a lining of metal at the zone of the gate (valve) (Davis & Sorensen, 1969; Grishin et al., 1979; Sagar, 1995).

The main characteristic for classification of the high-head gates (valves), as with surface gates, is the method of transferring the water pressure to the structure.

Gates that transfer the water pressure to the structure *directly through their support* are (Fig. 25.2): (a) *plain* high-head gates, analogous to surface gates and (b) *radial* high-head gates.

Valves transferring the pressure *through the shell* encasing the valve, are (Fig. 25.2): (c) a *plain valve*, which dams the opening; (d) a *disc-like* or *butterfly* valve that rotates about a horizontal or about a vertical axis; (e) a *needle* valve, which has a wedge emerging from the cylinder (1) and covers the opening (3) by means of a needle part (2); (f) a *cone dispersion* valve; by moving the cylinder (1), it covers the opening between

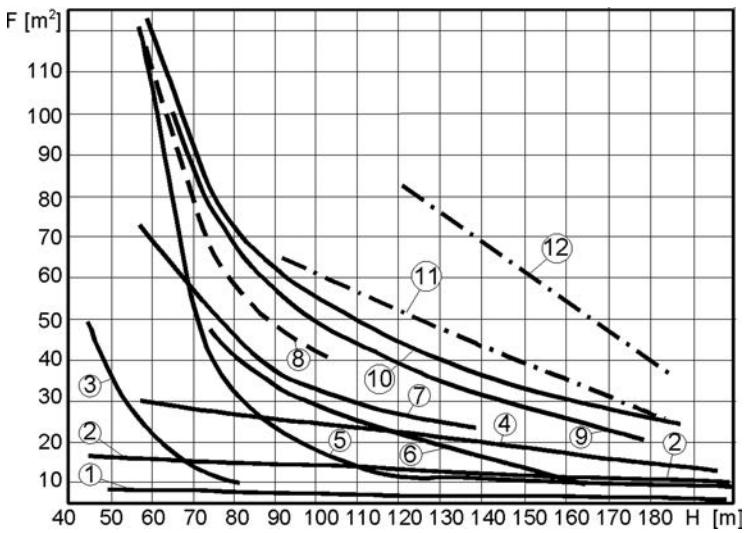

Figure 25.3 Approximate curves for the range of applications of high-head gates and valves in various countries (after Grishin et al., 1979). (1) Cone dispersion valve; (2) needle valve; (3) plain friction gates; (4) disc-like (butterfly) valves; (5) plain gates on wheels, which are used in Russia; (6) plain gates on cylinders; (7) radial gates; (8) plain gates on wheels that are used outside Russia; (9) plain sliding gates, emergency-overhaul type; (10) plain overhaul and construction gates; (11) diaphragm gates; (12) hydraulically balanced valves.

the stationary cylinder (2) at the end of the water-conveyance structure and the cone (3); (g) a *cylindrical* valve or (h) a *ball* valve. The disc-like (butterfly) valve, cylindrical valve and the ball valve can work only if they are completely open or completely closed, that is to say they cannot regulate the discharge.

The balanced valves, which do not transfer the pressure to the structure, can be (Fig. 25.2): (i, j) cylindrical balanced valves, with balanced pressure of the water; or (k) balanced valves with pressure chamber.

The diagrams in Figure 25.3 present the approximate curves which indicate the areas of actual application of various types of high-head gates and valves.

The existence of so many different types of high-head gates and valves is connected with the fact that, in front of the hydraulic gates and valves, there are imposed a number of different requirements, depending on the purpose and service particularities. For each specific case, we select the type and structure of gate (valve) that will best correspond to all requirements and conditions. European dam gates are characterized by the application of a broad spectrum of high-head gates and valves, while in the USA the number of these gates (valves) that are used is much smaller. For reducing costs on gates (valves) and for shortening the necessary time for their procurement, in most countries they produce typified gates and valves with standard dimensions, calculated for certain pressures.

25.2 HIGH-HEAD GATES TRANSFERRING PRESSURE TO THE STRUCTURE DIRECTLY THROUGH THEIR SUPPORTS

25.2.1 Plain high-head gates

Plain high-head gates have the simplest construction, while at the same time there is a possibility for the execution of the most compact gate-system, which has led to their broad application. They are the most widespread gates and are used either as service gates or as overhaul-emergency gates. They are made of steel or of prestressed concrete. They can move by *sliding*, on *wheels* or on *cylinders*, or else on *teeth*. The drive is usually from hydraulic servomotors. At higher water velocities, their application is limited to pressure heads up to 50 m.

Sliding plain gates are suitable for low-pressure heads and for small openings; otherwise, the resistance due to friction becomes very significant. They close very well; however, they require a considerable lifting force. If behind such a gate there is another one, which equalizes the pressure in front of and behind the gate, then it can also be used at significant pressures. Schematic presentation of a sliding plain gate is shown in Figure 25.4.

The front gate of the two is an emergency gate, while the other is a service gate. Both move by means of hydraulic servomotors, accommodated in a gallery (1). The speed of gate movement, in such cases, usually amounts to 0.3 m/min. The gallery above the gates should have dimensions that will enable pulling out of the gates, as well as their storage, in case of need.

Sliding gates have broad application. In the USA, they manufacture them in series for pressure heads up to 87 m, with dimensions 1.2/1.8 and 1.8/3.0 m. With such dimensions, when the height is 1.5–2 times greater than the width, the supporting parts are less loaded, and there is less bending of the gates, while the movement is more uniform (Davis & Sorensen, 1969).

For larger openings and high-pressure heads, gates on wheels or teeth are often used. The service and the emergency gate are of the same type, and in front of them there are slots for an overhaul gate (Fig. 25.5). If there is more than one water-conveyance structure and, if there are constructed slots for overhaul gates, then the emergency gates usually drop off. The lifting mechanisms are installed on the crest of the dam, while lifting and lowering is performed by means of chains or ropes. In case of need for inspection and overhaul, the gate may be pulled outside, which is a significant advantage. On the other hand, possible vibrations of the gate can damage the long steel ropes. Owing to the significant loads that these gates take on from a structural viewpoint, they are shaped as a multi-bar construction.

The position of the sealing contour has a vital influence on the magnitude of the force that is required for lifting plain high-head gates. If it is positioned at the upstream side (Fig. 25.6a), the vertical forces due to the atmospheric pressure Pa, acting on the gate from above and from below, are practically balanced. If the seal is placed at the downstream side (Fig. 25.6b), then from the upper side there acts the force due to water pressure in the shaft, while from the lower side there acts the force due to the water pressure, with a direction depending on how much the gate has been open. If the opening is closed, it acts upwards, and if it is partially open – it acts upwards or downwards, depending on the contour of the bottom seal (Grishin et al., 1979).

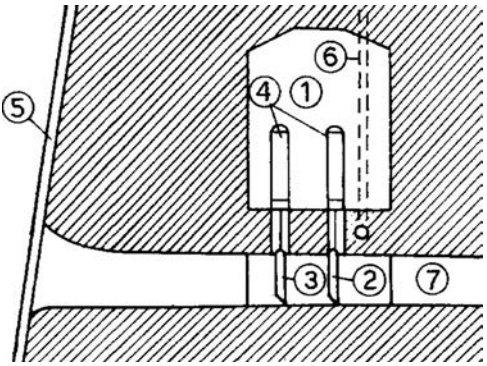

Figure 25.4 Schematic of a sliding plain gate. (1) Gallery; (2) service gate; (3) overhaul-emergency gate; (4) hydraulic mechanisms for lifting; (5) slot for overhaul gate; (6) aeration pipe; (7) conduit.

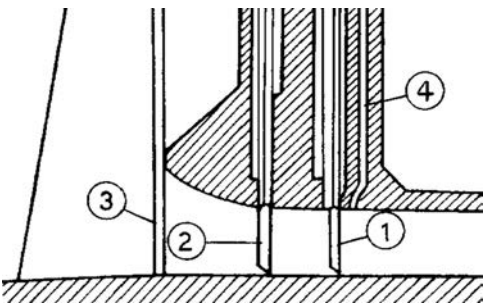

Figure 25.5 Schematic presentation of plain gates on wheels. (1) Service gate; (2) emergency-overhaul gate; (3) slot for overhaul gate; (4) aeration pipe.

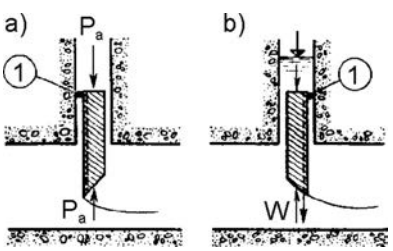

Figure 25.6 Position of seal (1) at plain high-head gate. (a) Upstream position; (b) downstream position.

The most favourable hydraulic conditions are created when, in front of the gate there comes about a constriction of the flow, and behind the gate, separation from the walls, which is achieved with the construction of a part that constricts in front of the gate (Fig. 25.7a). The constriction of the stream facilitates the aeration of the zone of separation, which is obligatory in fighting cavitational erosion. The separation of the

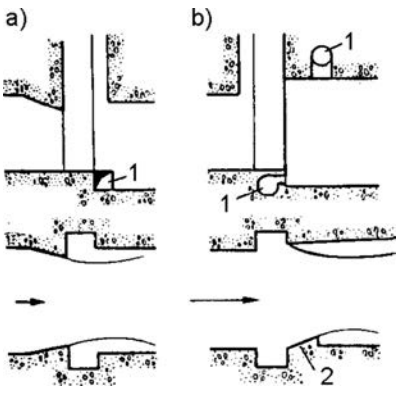

Figure 25.7 Variant of constructional forming of the water-conveyance structure at the part of the gate. (a) Constriction in front of the gate; (b) separation of the flow from the walls at the expense of widening of the water-conveyance structure or execution of a bumper. (1) Aeration channels; (2) bumper.

flow from the bottom of the water-conveyance structure behind the gate is ensured by lowering the bottom of the conduit. The separation of the flow from the walls behind the gate is achieved by widening the water-conveying structure behind the gate or by the construction of a bumper (2, Fig. 25.7b).

In order to prevent flowing of water when the gate is completely closed, seals are placed along its perimeter – a bottom seal, a lateral seal, and a top seal, as with the surface plain gates. Of the numerous different types of such seals that usually employ wooden beams and steel or rubber shapes with different sections, several are presented in Figure 25.8. In designing such seals, one should clearly differentiate two cases: when the gate is placed in front of the opening, and when it is placed behind the opening. In the first case, the headwater presses the gate towards the perimeter of the opening, so that the conditions for work of the seal are more favourable; in contrast to the second case, when it is more difficult to achieve proper sealing (Chugaev, 1985; Grishin et al., 1979).

The rubber seals, proved to be good when medium pressure heads, as a rule, have shown more weaknesses and deficiencies during work under high pressure heads, when greater strength is required, and there is a necessity of covering larger gaps between the structure and the surface to be sealed, a necessity of low coefficient of friction, and high sealing properties, etc. However, rubber is a noble material for such a purpose and it is not a simple matter to discard it. Therefore, in the case of gates working under high-pressure heads, there is usually employed special, harder rubber, with greater dimensions of the section. Two-rowed seals are also employed, such as for instance in the case of the *Sayano-Shushenskaya* hydroelectric power plant (Fig. 25.9). In particularly serious and difficult cases, it is also possible to use multi-rowed seals (Seleznev, 1988).

For pressure heads greater than 120 m even the hardest rubber experiences plastic deformations. In such a case, as the seals with the greatest prospects have proven to be seals made of high-strength polyethylene, which is stiffer than rubber and has a

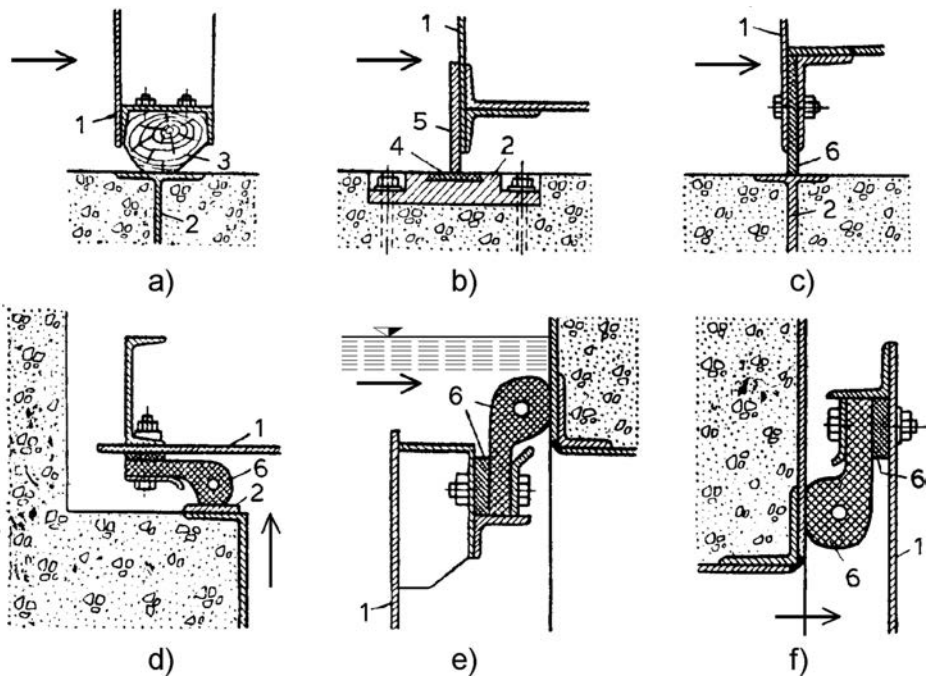

Figure 25.8 Examples of sealing high-head plain gates. (a, c) Bottom sealing; (d) lateral sealing; (e) top sealing, when gate is installed in front of opening; (f) top sealing, when gate is installed behind opening. (1) Lining of gate; (2) built-up part; (3) wooden beam; (4) alloy; (5) metal plate; (6) hard rubber.

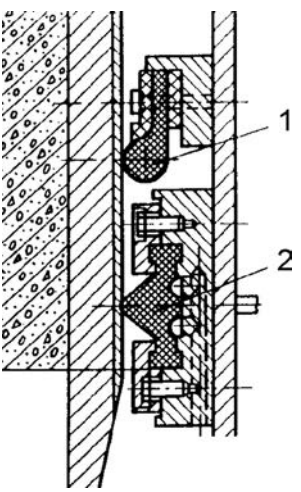

Figure 25.9 Two-rowed seal (after Seleznev, 1988). (1, 2) Rubber seals of two types.

smaller coefficient of friction. Polyethylene seals are made by casting under pressure in special molds. They are easy for working out and are mutually jointed by means of welding. With lowering of the temperature, in the case of polyethylene seals, the ability for sealing decreases to a lower extent in relation to rubber seals (Seleznev, 1988).

25.2.2 Radial (tainter) high-head gates

The radial (tainter) high-head gates, from a structural point of view, do not differ much from surface gates. Usually, they are employed as working gates. Their primary advantage, in relation to plain gates is, as with surface gates, the necessity for an essentially smaller force for lifting. In addition, radial high-head gates have a favourable form at the upstream part and ensure good hydraulic conditions for discharging, and do not require obligatory use of slots or recesses, while their supports are protected against the direct action of water and sediment. Greater stiffness of the structure ensures smaller vibration of the gate. Their deficiencies are their complex construction and high cost. Lately, the range of application of radial high-head gates has extended to higher-pressure heads thanks to, above all, the perfection of the supporting hinges. A sketch of the cross-section of a high-head radial gate, along with a stop-log overhaul gate in front of it, is given in Figure 25.10.

In order to ensure proper sealing of the gate along the perimeter of the opening and also to achieve hermetical sealing, there are used radial gates with eccentric support (Fig. 25.11). During lifting or lowering, the gate first of all separates from the perimeter of the opening by means of the eccentric shaft, so that, during lifting, what is overcome is only the moment of the force due to the weight of the gate and that of the friction in the axis of rotation. The radial displacement of the gate amounts to 30–35 mm.

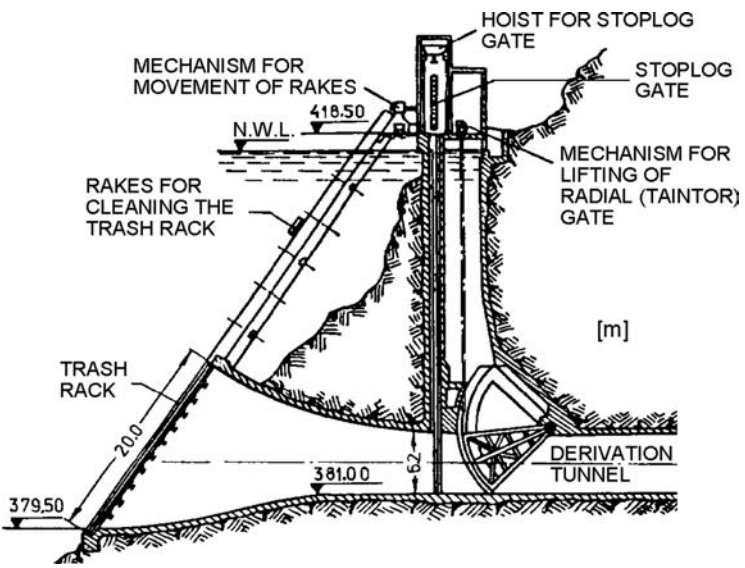

Figure 25.10 High-head radial gate.

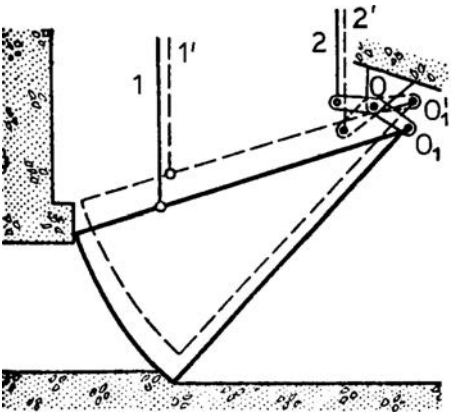

Figure 25.11 Kinematic scheme of radial gate with eccentric supports (after Grishin et al., 1979). (O) axis of the support; ($O_1 O'_1$) position of the axis of rotation when the gate is closed, i.e. sealed, and when it does not close (seal). (1) Lever arm of the service mechanism; (2) lever arm of the eccentric shaft.

Figure 25.12 gives an example of a gate with eccentric support, which has been employed for the headrace tunnel of the Nurek dam (Tajikistan), for a pressure head of 110 m. Manoeuvring with this gate is enabled by means of four hydraulic servo-mechanisms, two of which serve for lifting and lowering of the gate and the other two serve for turning the eccentric shaft (Grishin et al., 1979).

Inverse gates, in which the axis of rotation is located at the upstream side, have also been used lately. If this kind of gate is installed at the beginning of the water-conveying structure (Fig. 25.13a), then the supports and legs are always under water. It is more favourable when it is installed at the end of the water-conveying structure, as shown in Figure 25.13b (Seleznev, 1988).

The diagrams in Figure 25.14 give us an idea of the range of application of high-head, plain, and radial gates for pressure heads greater than 40 m.

In Russia, they have worked out a design of a radial gate with a *spherical lining,* for a pressure head of 200 m, intended for the regulation of the discharge, at a cylindrical water-conveying structure of a diameter 4.45 m (Fig. 25.15). The centre of the spherical lining coincides with the point at which there intersects the axis of rotation and the axis of the water-conveying structure, which enables obtaining a flat contour of sealing. The spherical form of the lining enables focusing of the water stream along the axis of the water-conveying structure. It is deemed that such a construction of the gate will reduce the danger of cavitation. Also, in this case, prior to manoeuvring with the gate, the seals separate from the contour. As deficiencies of this gate may be quoted the difficulties faced during the mechanical treatment of the spherical lining (Seleznev, 1988).

An interesting construction is *the double radial gate* (Fig 25.16). In this case, the hydraulic loading is divided into two longitudinal structures, placed one over the other. During opening of the water-conveying structure, the lower segment fits into the lower gate slot (recess), while the upper one fits into the shaft above the opening. The control

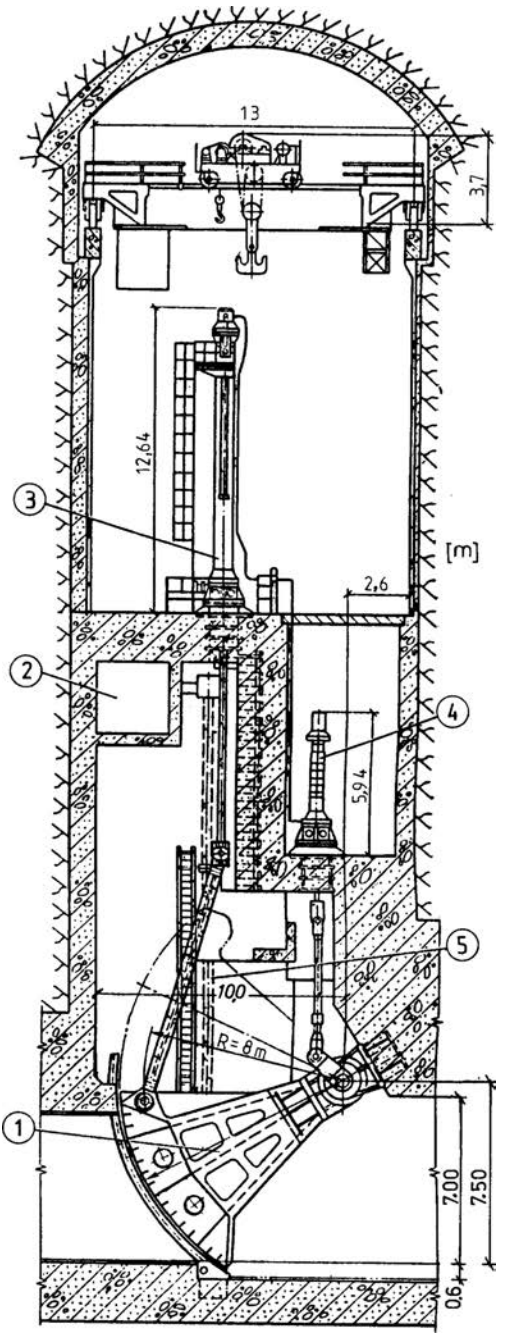

Figure 25.12 Gate house with a service radial gate at the Nurek hydroelectric power plant (after Grishin et al., 1979). (1) Radial gate; (2) aeration channel; (3) servo-mechanism of the gate; (4) servo-mechanism of the eccentric shaft; (5) air pipe.

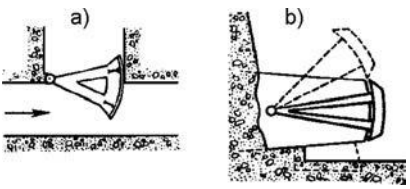

Figure 25.13 Inverse radial gate. (a) At the beginning of the water-conveying structure; (b) at the end.

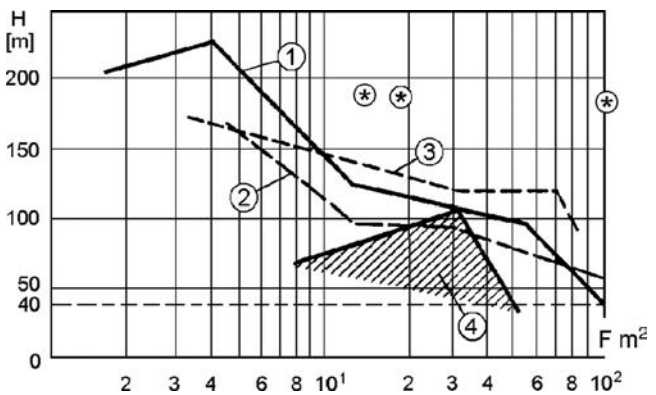

Figure 25.14 Range of application of high-head plain gates and radial gates (after Grishin et al., 1979). (1) Plain sliding service and emergency-overhaul gates; (2) plain emergency-overhaul gates on wheels; (3) plain crawler emergency-overhaul gates; (4) radial gates; (*) service, emergency-overhaul and overhaul plain gates at the Ingurskaya Dam (Georgia).

of the gates is achieved by means of hydraulic mechanisms that are accommodated in the lateral gate slots of the gatehouse. The synchronized closing of the two segments ensures concentration of the flow along the middle of the height of the opening. We should avoid relatively small openings, in which it is likely expansion of the flow stream in plan, with a possibility of cavitation phenomena at the lateral walls (Seleznev, 1988).

25.2.3 Diaphragm gate

The diaphragm gate is a double plain gate with an incision into one of the sections. The incision into the diaphragm section is overlayed by the other section, like a shutter, located either at the upstream or at the downstream side of the diaphragm (Fig. 25.17). At a certain stage of service, i.e. operation, the diaphragm can be fastened to the concrete structure (Fig. 25.17a). There is also a variant with a double diaphragm with a bottom gate slot, i.e. recess (g). The diaphragm and shutter may rest on independent fixed parts and be serviced by independent mechanisms. There is also a possibility of a variant of the gate construction resting on the shutters of the diaphragm, as well as a variant with lifting of the two sections with only one mechanism.

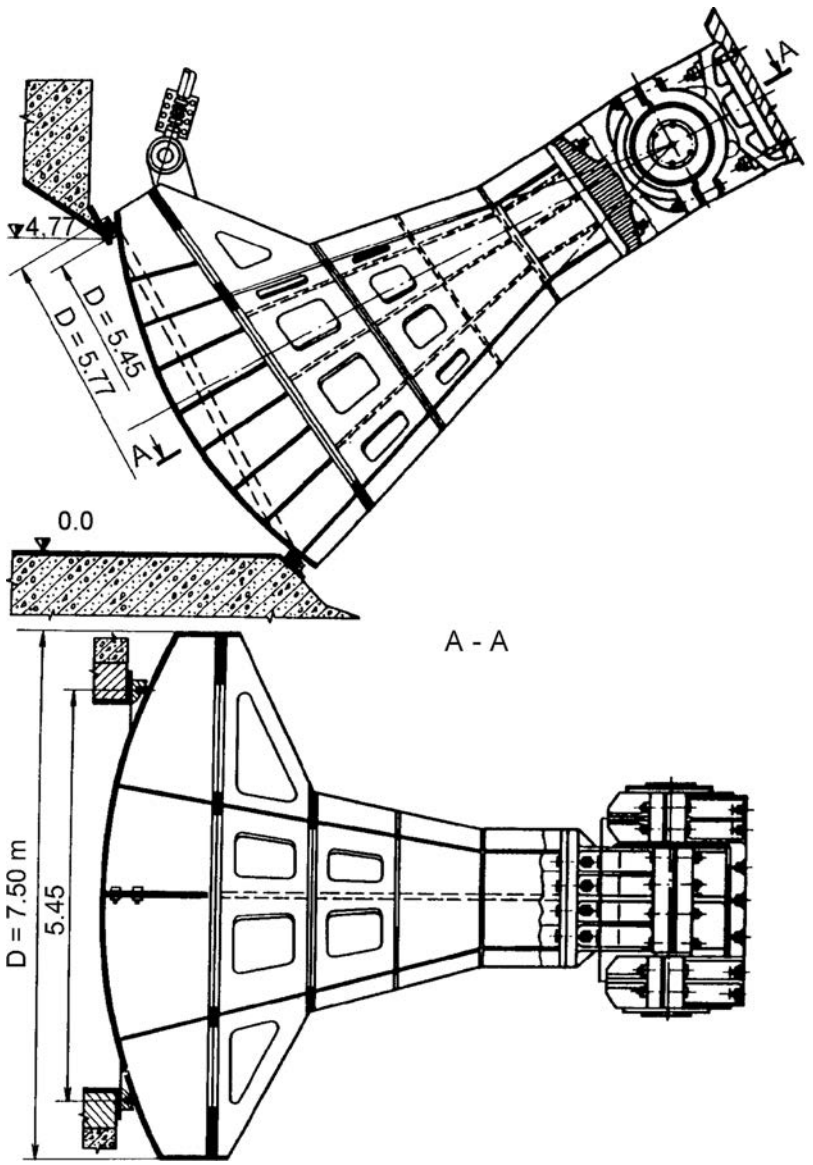

Figure 25.15 Radial gate with spherical lining (Seleznev, 1988).

In practice, in cases with water-conveyance structures that serve for discharging water in the course of construction of the hydraulic complex, a case can be found when regulation of the discharge is not necessary, only a reduction within certain limits. In such a case, the execution of a diaphragm without shutters (b) is also possible.

In applying the diaphragm gate, the water stream is separated from the wall of the water-conveying structure and conditions are met for its strong aeration, which

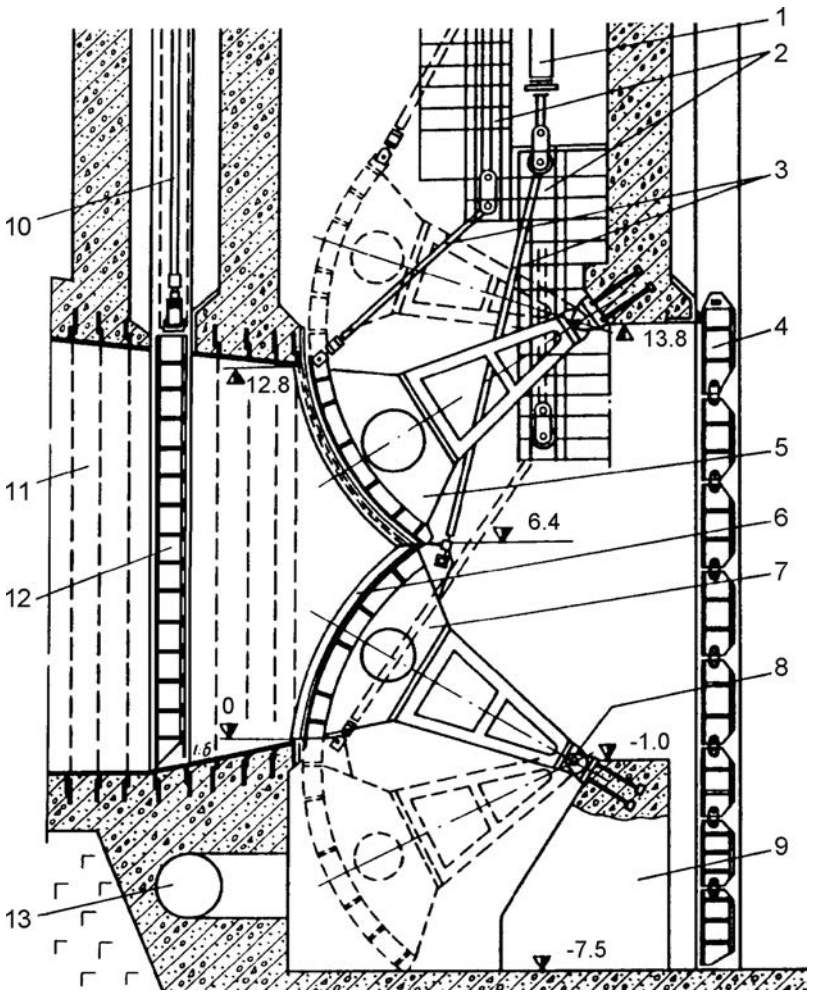

Figure 25.16 Double radial gate (Seleznev, 1988). (1) Hydraulic mechanism of service gate; (2) directional lever; (3) lever; (4) overhaul gate; (5) upper segment; (6) deflector; (7) lower segment; (8) supporting hinge; (9) lateral post; (10) hydraulic mechanism for emergency-overhaul gate; (11) confusor liner; (12) emergency-overhaul gate; (13) aeration pipes.

eliminates the danger of cavitation. This gate is employed in cases of structures intended for evacuation of water in the course of construction of the hydraulic complex.

The dimensions of the incision into the gate are chosen and based on conditions for passing the water through at a full opening. The shape of the incision depends on the conditions of the service and it can be circular, elliptical, or rectangular, while longwise can be conical or cylindrical.

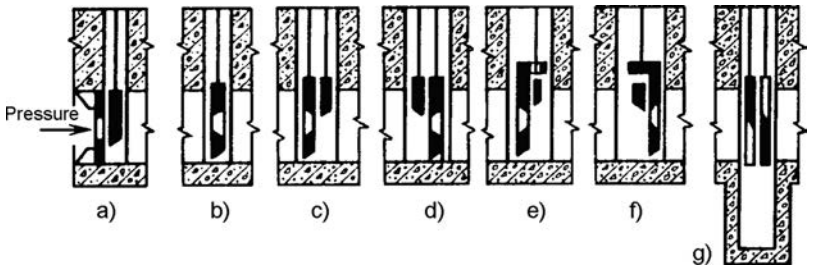

Figure 25.17 Variants of diaphragm gates (after Seleznev, 1988). (a) Section with diaphragm fixed to the concrete; (b) diaphragm that lets through non-regulated discharge; (c, d) both sections have independent mechanisms; (e, f) both sections have a joint mechanism; (g) double diaphragm with bottom gate slot (recess).

25.3 VALVES TRANSFERRING THE PRESSURE THROUGH THE SHELL ENCASING THE VALVE

25.3.1 Waterworks valve types

These high-head valves have a broad application in underground and open conduits with a diameter up to 1600 mm. The shell, made of cast iron, or steel, for cases with higher pressures (1, Fig. 25.18), has two flanges (2) at which the pipes are jointed (3). By turning the steering wheel (4), which is connected with a vertical valve spindle (5) upon which a screw has been cut out, discs (6) are lowered or lifted and, thus, the pipeline is open or closed. During lowering of the valve spindle, it presses the wedge (7) that is positioned between discs and sticks them onto the sealing rings (8). When the valve spindle is raised, along with it there are lifted both the discs and the wedge, so that they come into position outside the pipeline, in the upper part of the shell.

In cases of larger diameters (over 800 mm), the force and time required for handling become rather significant. Should such a case arise, electrical mechanisms are employed. In certain cases, the valve spindle can be very long, sometimes reaching the top of the tower valve-house, above the water level of the reservoir.

In order to reduce the dimensions of the valve (thus reducing the cost and also facilitating and speeding up the handling), there is performed a reduction of the diameter of the pipeline by means of conical parts (Fig. 25.19). In this, there appear increased losses of pressure during flowing through the pipeline. When the valve is closed, the force P, which presses the discs, should be taken on by means of a massive concrete block, to which the pipeline is fastened by means of steel jointing clips.

These valves are usually mounted in pairs (one behind the other), so that the first one serves as a service valve, while the second serves as an overhaul valve.

In cases of waterworks type valves, instead of discs, it is also possible to apply flat rectangular gate valves, with an area up to 6 m^2. These are called *gate valves*, which differ from the ordinary plain gates in that they transfer the pressure to the valve shell in which they are accommodated. They are most frequently employed for pressure heads up to 50 m, but also for much higher-pressure heads, in which, in order to enable

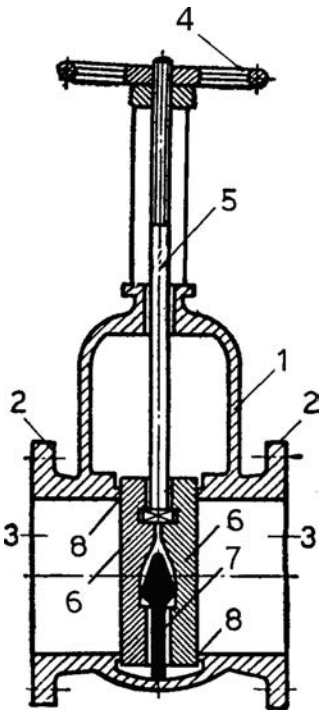

Figure 25.18 Waterworks valve type. (1) Shell of the valve; (2) flange; (3) pipe joint; (4) steering wheel; (5) valve spindle; (6) disc; (7) wedge; (8) sealing ring.

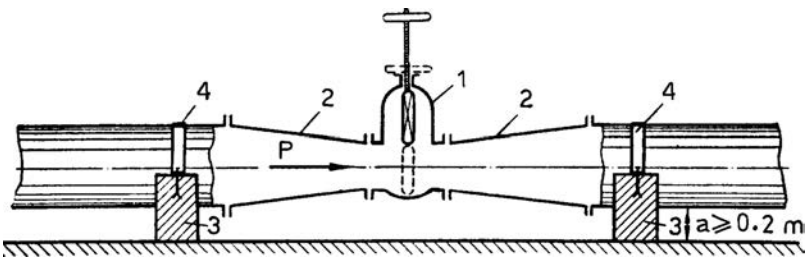

Figure 25.19 Reducing the diameter of the pipeline at the valve. (1) Shell of the valve; (2) conical pipe; (3) concrete block; (4) steel pipe-jointing clip.

easier manoeuvre, there are applied bypass pipes that serve for equalizing the pressure at both sides of the gate valve. They move by means of a hydraulic drive or by means of an electromotor. The gate valves can be left open when they are mounted on steel pipeline conduits, or else they are embedded into the concrete mass of the dam, and may also be accommodated in a separate underground chamber, Figure 25.20 (Grishin et al., 1979).

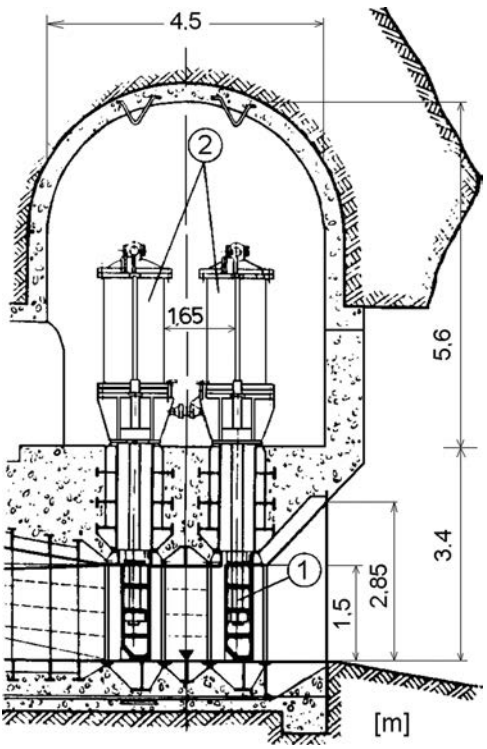

Figure 25.20 Rectangular gate valves, a service type and an overhaul type, at the outlet of a spillway conduit (tunnel), with pressure head of 209 m. (1) Movable part; (2) mechanism for lifting (hydraulic).

25.3.2 Disc-like or butterfly valves

The disc-like or butterfly valve consists of a cast circular disc (1) that rotates around a vertical or a horizontal axis (2) (Fig. 25.21). The disc may have the form of a lens (Fig. 25.21a, b) or be flat (c, d) (Chugaev, 1985; Davis & Sorensen, 1969; Grishin et al., 1979). Handling with the valve is achieved by turning the end of the axis (which emerges outside the shell), by means of a hydraulic or mechanical drive. If the disc is installed eccentrically in relation to the control mechanism (Fig. 25.21b), it is possible to close the water-conveyance structure even in a case of a defect of the control system. The disc-like valve is intended to work at completely open or closed position, since at a partially open valve, there would come about intensive vibration due to the formation of a significant whirlpool zone (3) which could even lead to a failure of the structure. The coefficient of resistance of the valve in the form of a lens, when it is completely open, amounts to $\xi = 0.26$. The deficiency of this valve is that it is difficult to achieve watertightness with the seal along the perimeter of the disc's body, which, usually, consists of a rubber hose inflated with air.

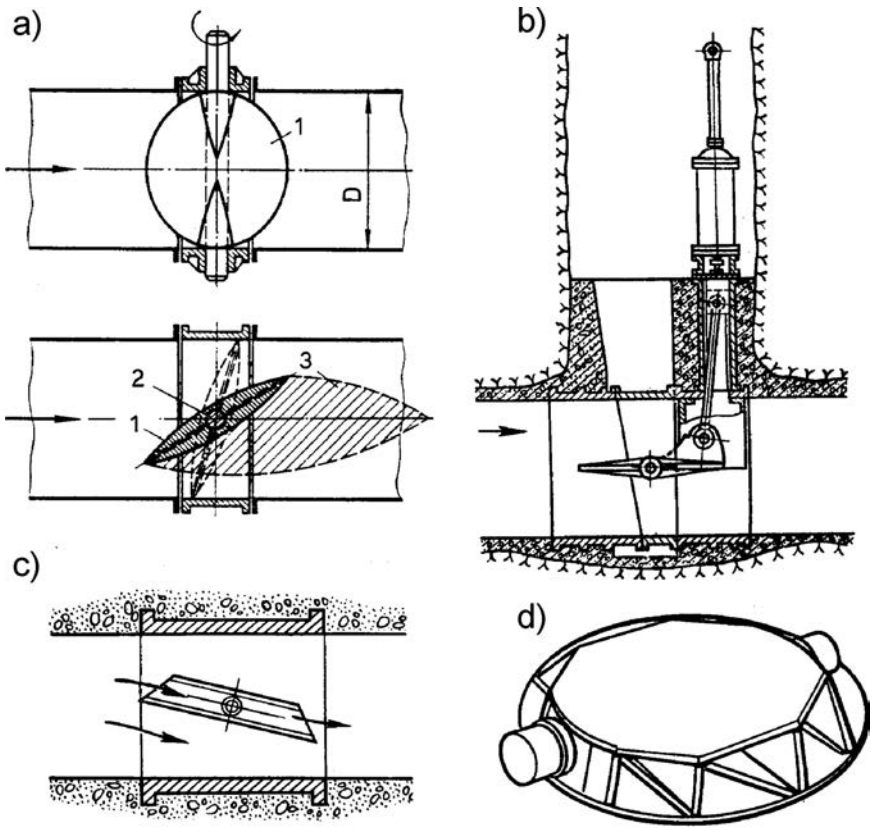

Figure 25.21 Disc-like or butterfly valves (after Grishin et al., 1979). (a) Scheme of a valve in the form of a lens (layout and section); (b) valve control with hydraulic mechanism; (c) flat disc-like valve; (d) structure of a flat disc. (1) Disc; (2) axis; (3) whirlpool zone.

As an improved construction, there appears the disc composed of two flat plates, placed on ribs (Fig. 25.21c, d). Such a disc is twice as lightweight as that in the form of a lens, while it has the same coefficient of resistance.

Disc-like valves are usually employed as emergency valves. As service valves, they are used at outlets with a diameter up to 3.5 m, at pressure heads of 50–150 m. The diameter of these valves is, in practice, also limited by the possibilities and convenience of their transportation. For pressure heads up to 30 m, a disc-like valve can also operate as a regulating type.

In the USA as early as the 1920s, there was employed a butterfly disc-like valve with a diameter of 8.2 m, at a pressure head of 27 m. In the case of the highest arch dam that has been constructed so far, Ingurskaya (Georgia), they have applied discs with a diameter of 6 and 5 m, at a pressure head of 120, or 175 m, as emergency valves on the derivation (supply) tunnel. The *Chervakska* hydroelectric power plant (Russia) has a built-in disc-like valve of a diameter 5 m, for a pressure head of 223 m.

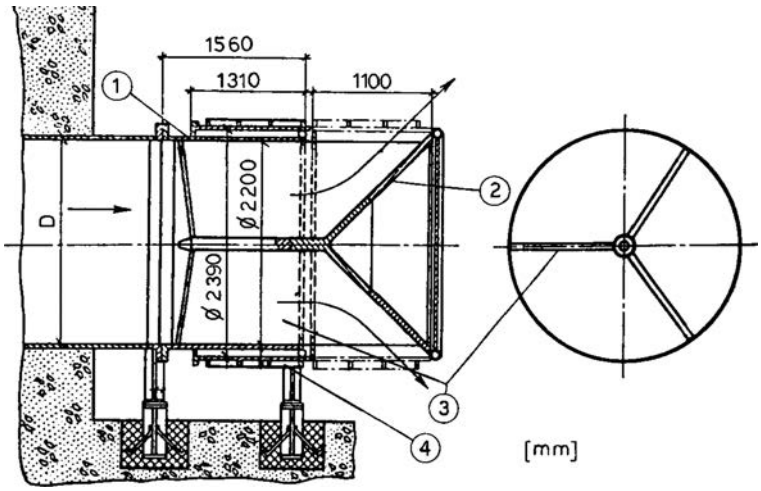

Figure 25.22 Cone dispersion valve D = 2200 mm, for pressure heads up to 150 m.

25.3.3 Cone valve

Cone valve, also known as Howell-Bunger valve[1], consists of a stationary part (1, Fig. 25.22), a conical screen (2) fixed on a cross (3), and a movable cylinder (4) that covers the circular opening between the stationary part and the screen. The water jet, in the case of an uncovered circular opening, projects divergently in the form of a cone. The displacement of the cylinder is achieved by means of a hydraulic or electrical drive. The cone dispersion valve is located at the end of an outlet spillway conduit. The coefficient of discharge with this kind of valve amounts to 0.91 (Creager et al., 1961; Grishin et al., 1979). A large experimental study was performed recently in Italy with the aim of characterizing the dissipation efficiency of different shaped Howell-Bunger valves. An empirical equation for estimation of the discharge coefficient is proposed. One of the conclusions is that specific models, both physical and numerical, are needed for optimal design and correct hydraulic characterization of these valves (Renna et al., 2013).

A cone valve is particularly efficient in controlling flow at outlet works and in dissipating energy in medium to high head conditions. The manufacture of this kind of valve is relatively simple; however, at openings amounting to 62–69% of the cross-section, a vacuum zone forms at the outlet part. For elimination of this phenomenon, there has been proposed a construction with a curvilinear shape of the outlet part.

In the former USSR, where this kind of valve was broadly used as a regulating valve for hydraulic works, there have been utilized cone dispersion valves with the greatest diameter of 2200 mm, for a pressure head of 150 m. A known example of a

[1]This valve was originally introduced by C. H. Howell and H. P. Bunger in 1935 and has been widely used throughout the world since the 1940s.

cone dispersion valve has been used in the USA, with a diameter of 0.3 m for a pressure head of 244 m.

25.3.4 Needle valves and spherical valves

These valves are used for regulating discharges through high-head openings. They let water through at a partial opening, without the appearance of vibrations or cavitation. The essence of a needle valve consists of the following (Fig. 25.23): the valve's body joins the outlet pipe, in whose interior is placed the valve itself, which is composed of a stationary and a movable cylinder. The movable (internal) cylinder is a kind of a bottomless piston, i.e. ram. This ram can move, at closing – under the effect of water pressure in the space (1), while at opening – under the effect of the pressure in the space (2). A part of the cylinder, turned towards the opening, and called a needle, is achieved with a sharp pointed profile. In a drawn position, the needle closes the opening. The coefficient of resistance of a needle valve at a completely open position amounts to 0.20. With this kind of a valve, the water jet is convergent (Brien & Klein, 2001; Creager et al., 1961; Davis & Sorensen, 1969; Grishin et al., 1979).

The spherical valve is a modification of the needle valve. The movable cylinder has no sharp needle part and closing is performed directly with the cylinder (3, Fig. 25.23c, d).

The needle valves and spherical valves are usually mounted at the end of outlet works or spillway structures (Fig. 25.23e). In cases of small diameters, they can work at any pressure head of the hydraulic scheme.

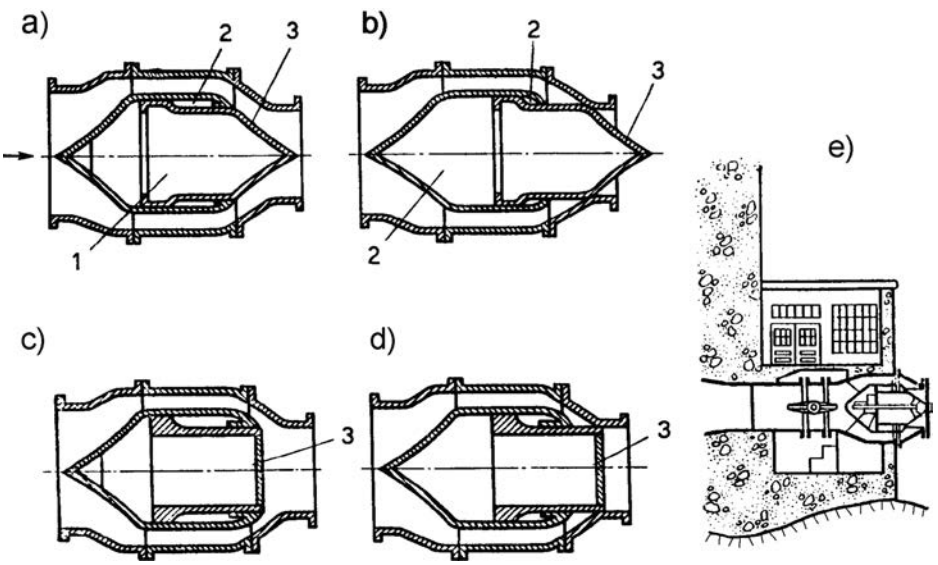

Figure 25.23 Schematic presentation of needle valves and spherical valves (after Grishin et al., 1979). (a, b) Needle valve in open and closed position; (c, e) spherical valve. (1, 2) Chambers under pressure; (3) movable part.

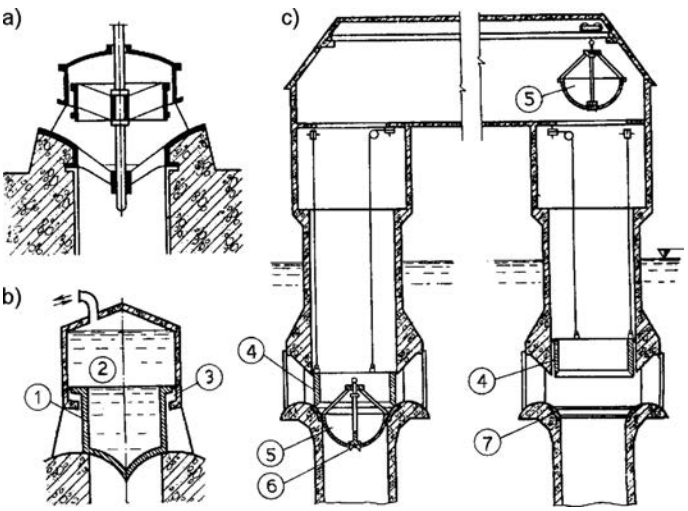

Figure 25.24 Cylindrical balanced valves (after Grishin et al., 1979). (a) With mechanical action; (b) with hydraulic action; (c) in the hydraulic scheme Schiffenen in Switzerland. (1) Cylinder; (2, 3) chambers; (4) service valve; (5) overhaul valve; (6) spillway intake; (7) sealing.

25.4 CYLINDRICAL BALANCED HIGH-HEAD VALVES

Cylindrical valves are installed at openings in towers or in special shafts, and the axis of the valve is vertical. The water pressure acting upon the valve in a radial direction is balanced so that the valve does not transfer the water pressure to the structure. There are various constructions of these valves: *unsubmerged cylindrical valve* (Fig. 25.2i, j), *submerged cylindrical valve,* Figure 25.24a, b (Grishin et al., 1979).

In the case of a submerged valve with a hydraulic action, the chamber (3) is permanently connected with the headwater. When water from the upper level penetrates, into the chamber (2), the cylinder (1) will go down, since the force acting on the cylinder downwards is greater than the force acting in the chamber (3) upwards (Fig. 25.24b). For lifting of the cylinder, the water from the chamber (2) descends downstream. When the cylinder is raised, the water penetrates the circular edge of the tower opening. In order for it not to happen that the forces of friction prevent the lowering of the valve, it is loaded with ballast (for instance, the metal cylinder is filled with concrete).

Cylindrical valves are applied with the intake structures and outlet works, i.e. structures. There are executed valves with a diameter of up to 10 m, which cover, i.e. bridge, openings higher than 3 m, at a pressure head of up to 100 m.

Figure 25.24c presents the towers of the intakes for the hydroelectric power plant of the hydraulic complex Schiffenen in Switzerland (with an arch dam, $H = 47$ m, completed 1963), with cylindrical and with spherical valves. The axes of the towers are at 16 m distance from each other, as well as from the upstream side of the arch dam. In the right tower, the inlet is open, while in the left tower the overhaul valve has been mounted. Within this hydraulic scheme, an analogous solution has also been accepted for the spillway structure.

Chapter 26

Spillways passing through the dam's body

26.1 CREST SPILLWAYS

26.1.1 Crest spillways at concrete dams

Crest spillways are most often found with mass concrete dams. They are also constructed with other kinds of concrete dams. A dam with an overflow section through its own body is the most economical solution for the evacuation of floodwaters in the course of service of the hydraulic scheme. Figure 26.1 shows sketches of the most frequently used spillways through the body of concrete dams. Illustrations (a) and (b) presents spillways with the practical profile that is most often applied in practice. These spillways ensure uniform overflowing of water without dynamic impacts. Types (c) and (d) are spillways with a free overfall jet (nappe), employed for an arch and buttress dam. Type (e) is a spread profile of a spillway with a practical profile that is employed with weaker foundations, as well as the application of gates requiring a wider crest, while type (f) is a spillway with a wide crest sill.

The spillway can be located in the central part of the dam, where the river channel is, or else somewhat aside, towards the bank, which depends on the conditions in the foundation, as well as on the layout of other works within the framework of the hydraulic scheme.

The length of the spillway sill, i.e. overflow crest, is selected so that for an assumed height of the overflow jet, the spillway should have the required discharge capacity, which is calculated with the expression:

$$Q = \varepsilon m b \sqrt{2g} H_0^{\frac{3}{2}} \tag{26.1}$$

where, Q is the overflow water quantity, ε the coefficient of lateral contraction, caused by the side walls and piers, being approximately $\varepsilon = 0.90$–0.95; m is the coefficient of discharge, which ranges from 0.35 for broad-crested spillways, to 0.42 for thin-wall spillways; 0.45 for vacuum-free profiles, and up to 0.50 for vacuum profiles; b is the width of spillway; $H_0 = H_p + v_0^2/(2g)$, H_p is the overflow height; and v_0 is the approach velocity, for $v_0 \leq 1$ m/s it can be taken $H_0 = H_p$.

The value of the specific overflowing quantity q (m^3/s per metre) depends on the length of the spillway, on which further on there depend the dimensions of all the structures, i.e. members, within the framework of the spillway structure. More rational dimensions of the works are obtained for higher specific discharges; however,

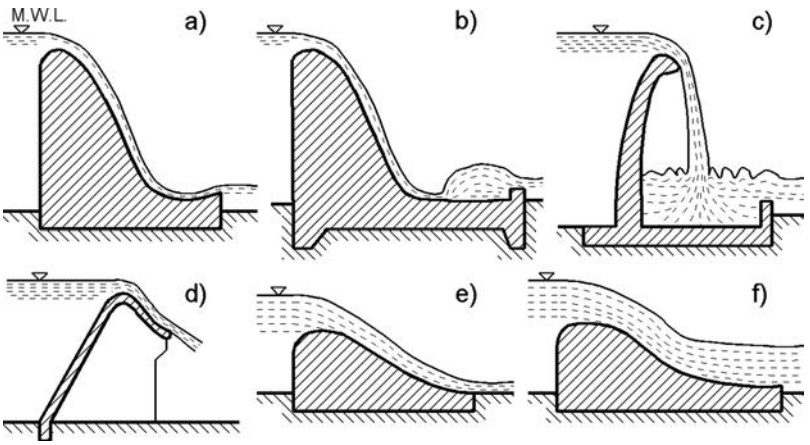

Figure 26.1 Spillways passing through the body of concrete dams.

q_{max} is limited by the geological conditions in the foundation. For soil (non-rock) foundations, it is recommended not to exceed 40 m^2/s, while for rock foundations, 90 m^2/s is the norm. There exist cases when spillways over a dam have been constructed with $q = 120\ m^2/s$ and more.

For the construction of spillway structures and for transferring the waters through the spillway chute over the body of a massive dam, as well as for the dissipator of energy, considerations have been given in the chapter on gravity concrete dams in which, as a rule, the spillway structures are constructed in the dam's body. Also, in the examination of buttress and arch dams, there have been discussed the possibilities of the construction of a spillway in the dam's body which, owing to the construction of these dams, is not as simple as it is with gravity dams. In the continuation there will be described two more examples of the execution of a spillway over the body of such dams.

Figure 26.2 presents the cross-section of the overflow part of the Stoney Gorge buttress dam, USA, 1928 (Fig. 26.3 Chugaev, 1985), while Figure 26.4 presents the overflow part of the Couesque arch dam (France), 65 m high, with overflow water $Q_{max} = 2700\ m^3/s$ (Ganev et al., 1965). The spillway has two openings in whose sides there have been constructed deflectors of the water stream that cause mutual collision of the water stream from both overflowing spans and self-dissipation of energy. In that way, the absorption pool, takes on more economical dimensions.

In cases when the power house of the hydroelectric plant is constructed in the body of a concrete dam, if a spillway is to be constructed over the dam, the overflow jet is projected through a flip bucket, located at the end of the spillway chute, over the power house, as is the case with the Monteynard gravity dam, as described in the chapter on hydraulic schemes.

Dams are very often constructed as combined dams – of embankment parts into the banks and a gravity overflow part in the zone of the river channel. This combination is particularly practical when it is a question of watercourses with a wide channel of

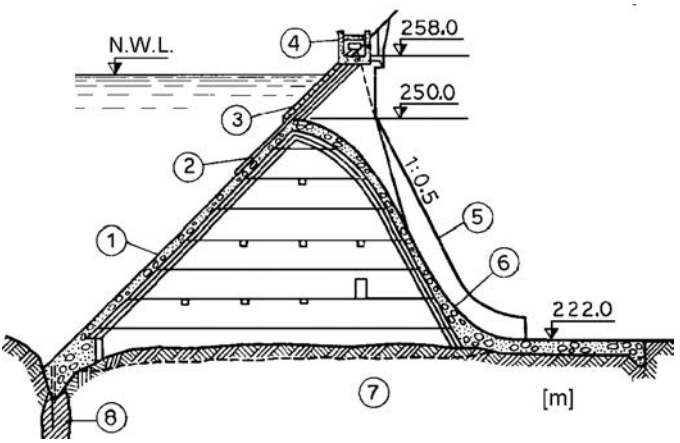

Figure 26.2 Spillway of Stoney Gorge Dam (USA). (1) Flat slab deck; (2) guide member for the gate; (3) plain gate; (4) control gate-house; (5) side wall; (6) spillway surface; (7) conglomerate; (8) grout curtain.

Figure 26.3 General view of the Stoney Gorge buttress dam (after Grishin et al., 1979).

the river, abundant with water. In this, the spillway structures, in essence, do not differ from the already described spillway structures used for gravity dams, in that sometimes, owing to the high flood overflow waters, it is necessary to undertake essential measures for protection of the river bed (channel) downstream of the spillway structures.

A characteristic example of an overflow gravity concrete part in the riverbed at an exclusively abundant water current is the spillway that has been constructed for the Tucurui hydroelectric plant, on the River Tocantis, in Brazil (Fig. 26.5), with a capacity of 100,000 m^3/s. It consists of 23 overflow spans provided with radial gates each 20 m

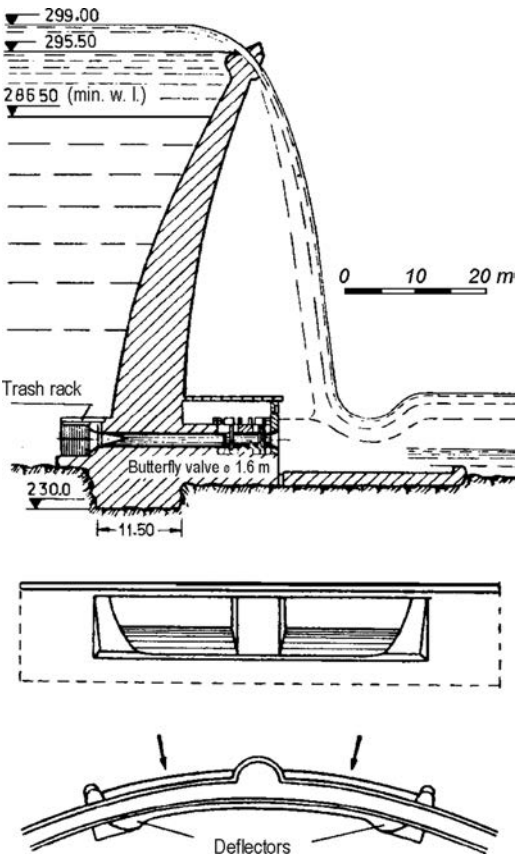

Figure 26.4 The overflow part of the Couesque Dam (after Ganev et al., 1965).

wide and 21.5 m high, so that the maximum unit overflow quantity amounts to more than 200 m^2/s. The side (parting) walls (22 in all) are each 5 m thick. The downstream side of the dam is shaped as a non-vacuum profile and, by means of side walls, it is divided into three large and four small overfall spans for the sake of more convenient control of the spillway structure at different overflow quantities. As is usual with this kind of combined dam, the overflow gravity part is separated from the adjacent power house of the hydroelectric plant by means of lateral walls, with a carefully constructed joint, in order to prevent penetration of water along the contact (Rios & Barbalho, 1988).

Owing to the favourable geology of the foundation, the stilling of the overflow jet is accomplished by its projecting over a flip bucket into a stilling basin, excavated into the natural ground, without lining, with a floor level of 70 m lower than the level of the flip bucket, (Fig. 26.6). The lining of the ground with a concrete slab has been constructed only in the zone immediately next to the dam (behind the flip bucket) in order to avoid scouring of the ground at low overflow waters that are projected at a small distance.

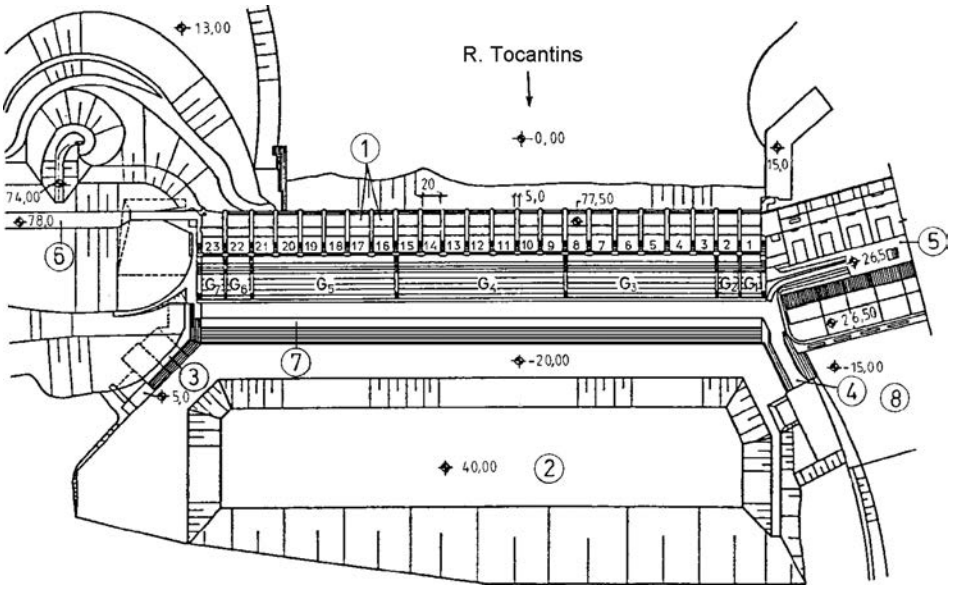

Figure 26.5 Layout of overflow part of Tucurui Dam (Rios & Barbalho, 1988). (1) Radial gates; (2) stilling basin, made by excavation into the ground; (3) right lateral wall; (4) left lateral wall; (5) power house of the hydroelectric plant; (6) embankment dam; (7) concrete facing slab; (8) tail race.

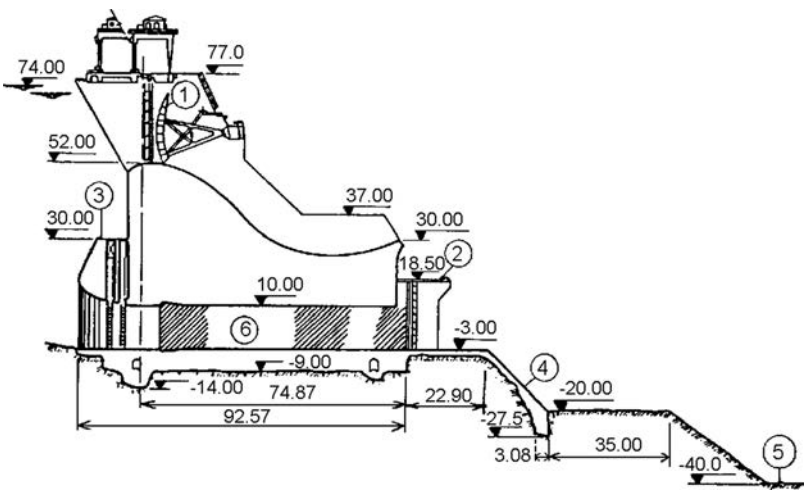

Figure 26.6 Cross-section through spillway structures of Tucurui Dam (Rios & Barbalho, 1988). (1) Radial gate; (2) bridge (downstream); (3) bridge (upstream); (4) slab; (5) stilling basin; (6) gallery.

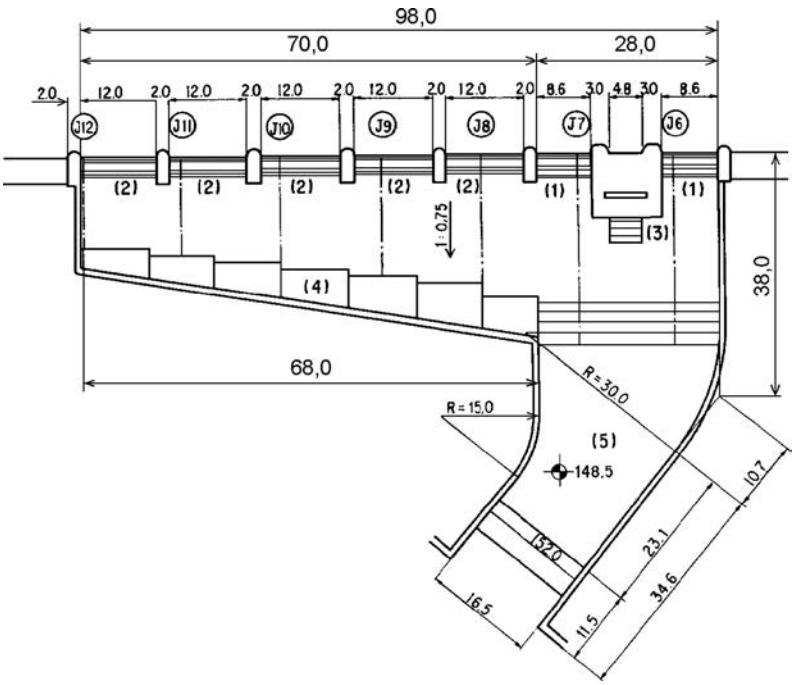

Figure 26.7 Spillway structures for Benoki Dam, Japan (after Takasu & Yamaguchi, 1988). (1) Uncontrolled overflow spans; (2) uncontrolled overflow spans at a level 70 m higher than (1); (3) regulated spillway under low pressure; (4) channel below dam's toe; (5) stilling basin.

In the case of such abundant water currents, in spite of the great retentive capacity of the reservoir, there often comes about overflowing. In such conditions, the above-described spillway structure has worked in a normal way.

In cases of gravity dams with uncontrolled crest spillways, sometimes, for a better stilling of the overflow water current, we do not undertake its direct offtake in the direction of the overflowing, but, through a channel that is constructed at the downstream toe, it is led towards one of the ends of the overflow dam where the stilling basin has been located, as shown in the example in Figure 26.7. The overflowing spans (1), over the stilling basin are located at a level that is 70 m lower than the level of the spill-crest of the overflow spans (2). Thus it is achieved, for smaller overflow waters, that the spillway, even though uncontrolled, works in only one smaller part, while at significant overflow waters in the stilling basin there is already a certain discharge, thereby achieving favourable hydraulic conditions for dissipation of energy. In addition, the spillway structure of the cited example is also provided with a regulated spillway at low pressure (3) (Takasu & Yamaguchi, 1988).

Thanks to technological advances in the construction of RCC dams over the past three decades, stepped spillways have gained significant interest among researchers and dam engineers. The main advantage of stepped chutes over conventional smooth spillway, in addition to the construction economy, is the significant energy dissipation

along the chute as a result of the macro-roughness of the step, and the reduced cavitation risk because of the greatly reduced flow velocities and the large amount of air entrainment. But the aeration produces flow bulking, and therefore requires higher sidewalls. Another disadvantage of steeped chute spillways is that in principle, wide crest is usually required because the unit discharge q is limited to 25–30 m^2/s owing to the risk of cavitation damage. In Chapter 18 some examples of RCC dams with stepped spillways are described and discussed in brief. The relatively complex question on hydraulic calculations and dimensioning of stepped chutes are discussed in detail by Chanson (2002), and some results of research works are given by Boes & Minor (2002).

26.1.2 Crest spillways at embankment dams

In general, spillways are practically not made over the body of embankment dams. Indeed, a number of attempts have been made for low embankment dams to be carried out as overflow dams, in two cases: (1) when the cost of the spillway structure has been very high in relation to the cost of the dam; (2) in reparation and rehabilitation of dams, over whose body there has come about overflowing of water because of the insufficient capacity of the spillway structures (Solvik & Skoglund, 1994). We should pay special attention to this second case, since it is deemed that throughout the world there have been carried out a number of small dams with insufficient capacity of the spillway structures. With quite a number of them it could turn out that it would be simpler and more economical for the dam's body to be prepared for accepting a thin overflow jet, rather than to carry out an extension of the capacity of the spillway structures. Namely, with an analysis of cases of embankment dams lower than 15 m, at which there has come about overflowing, i.e. overtopping over the crest, it can be concluded that in the case of a well-compacted embankment, a short-time overflowing, of less than 0.6 m, causes only minor damages. In cases of larger overflowing depths or in cases of an overflow with duration of several hours, there comes about a failure of the dam. The mechanism of failure is such that first of all there comes about erosion of the dam's downstream toe which, further on, extends upwards, towards the slope and, at a longer duration of the overflowing, this leads to the entire failure of the dam. It has been established that an embankment of coherent material is much more resistant to scour and erosion effects of the overflow jet than an embankment made of incoherent material.

In practice, there have been made numerous attempts in different ways to protect earthfill dams against the scouring and erosion effects of an overflow jet of less than 0.60 m. At quite small overflow quantities and a short duration of the overflow, grassing of the surface can be sufficient, but one should undertake such a measure extremely cautiously. Better results are obtained in combination with a layer of geotextile below the layer of grassed soil. Lining of the crest with concrete slabs or concrete blocks, with large rock pieces, possibly strengthened with reinforcement of steel bars and execution of gabions, are efficient, but expensive, measures. The most economical material and that with the greatest prospects for preparing earthfill dams to withstand a minor overtopping is, certainly, roller-compacted concrete, by means of which we line the crest and the downstream slope, as is shown in the example in Figure 26.8 (Powledge & Sveum, 1988). RCC has become a popular method to increase spillway capacity

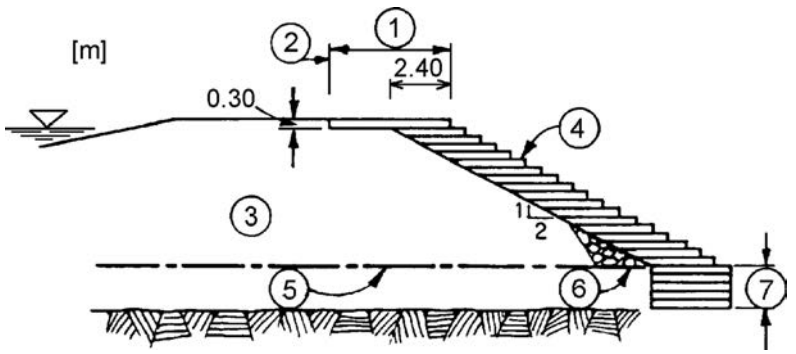

Figure 26.8 A typical section of an earthfill dam with a crest and downstream slope faced with roller-compacted concrete (after Powledge & Sveum, 1988). (1) Variable; (2) lining of the crest from the point with critical depth; (3) earthfill embankment; (4) roller-compacted concrete; (5) upper boundary of the earth material in the base; (6) drainage; (7) excavation and roller-compacted concrete in the river bed up to firm and sound rock.

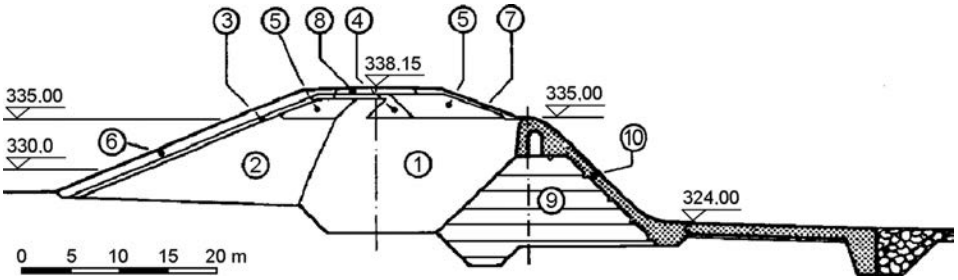

Figure 26.9 Spillway over an embankment dam (design) (after Minor & Schmidiger, 1988). (1) Clay core; (2) upstream dam-body part made of sandy gravel; (3) filter layer made of gravel; (4) filter layer made of sandy gravel; (5) fine gravel; (6) rockfill; (7) protection of the downstream slope; (8) roadway; (9) roller-compacted concrete; (10) conventional concrete.

and to provide overtopping protection for earthen dams in the United States. Since the mid-1980s, RCC has been successfully used on more than 100 earthen dams to armour the downstream slopes and the crests of dams, thereby allowing overtopping of the dams. The reasons for the popularity of RCC among designers and owners include: simplicity, speed of construction, strength and durability, and economic advantages over alternative methods (Dolen & Fares, 2008).

Over the body of embankment dams there can be considered the construction of what is called *an erosion* spillway. It is a standby or emergency spillway that is positioned higher than the main spillway and works as its addition, with a small height of the overflow jet – only in the occurrence of maximum overflow flood waters. Its uppermost part is constructed of incoherent erosion material, while the maximum overflow current destroys it and, later on, it is reconditioned. In this, the most effective results are achieved if the downstream part of the dam's body is of combined roller-compacted concrete and mass concrete, as shown in the example in Figure 26.9. The

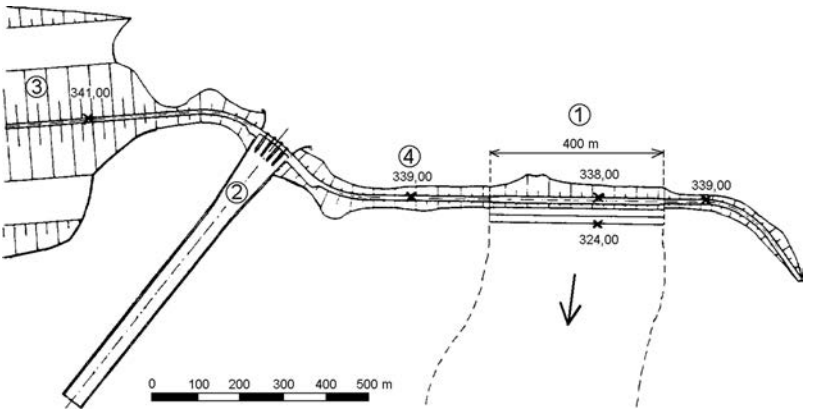

Figure 26.10 Plan of erosion auxiliary spillway (after Minor & Schmidiger, 1988). (1) Erosionspillway; (2) main spillway; (3) main dam; (4) auxiliary dam.

presented dam is intended to serve as an auxiliary spillway, in addition to the main spillway. The overall length of the overflow part amounts to 400 m and, by means of massive concrete lateral walls, is protected against lateral erosion. The upper part of the dam (over elevation 335) is erodible, i.e. susceptible to erosion, while the downstream part (below that elevation) is protected, since it is constructed of a combination of roller-compacted concrete and ordinary concrete. By means of a concrete slab, there has also been achieved protection of the ground downstream of the dam. The upper part (above elevation 335) is cut by a thin, inclined section of the clay core, placed between sections of water-permeable sandy gravel (5), which goes on also over the thin core in a layer of 0.5 m. A retaining body (2) of sandy gravel is anticipated upstream of the core. The roadway over the crest consists of a pavement of connected concrete blocks, over a sand bedding. The thin section of the core has been given an inclined position in order to form an upper impermeable layer if, one day, the adjacent downstream filter layer becomes eroded (at maximum overflowing) (Minor & Schmidiger, 1988).

The main spillway structure in this dam consists of an ogee free overfall spillway with five overflow spans (2, Fig. 26.10), provided with gates, with an elevation of the spillway of 317.50 mwl. When all the gates are open, the main spillway lets through the probable maximum flood of 12,400 m^3/s, at an elevation of the water in the reservoir of 337.85. The auxiliary erosion spillway is anticipated for a case if one of the five gates breaks down; that is to say, if one of the spilling spans remains closed, when overflowing over the auxiliary spillway will begin when the water in the reservoir exceeds the elevation 338.00. The overflowing quantity in the auxiliary spillway will come to 4000 m^3/s at an overflow height of the stream of 0.70 m, when the erosion part of the spillway will be carried off and so it will be necessary for it to be renovated. During normal work of the main spillway, the auxiliary spillway has the role of a non-overflow dam. It is evident that the probability of activating of the auxiliary spillway is practically insignificant, which justifies its construction.

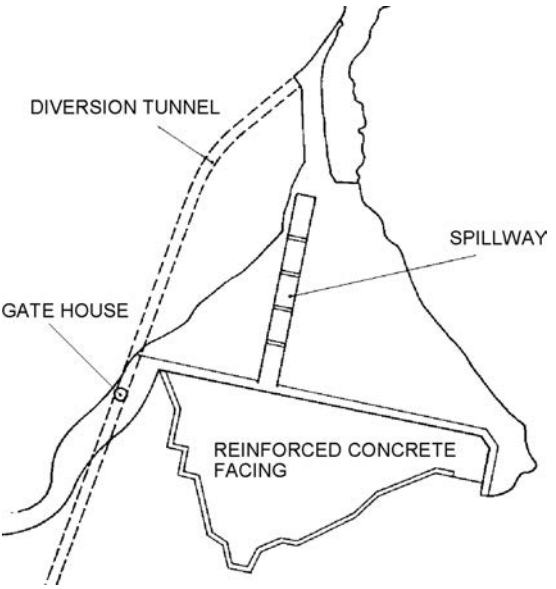

Figure 26.11 Spillway over embankment dam with reinforced concrete facing (layout).

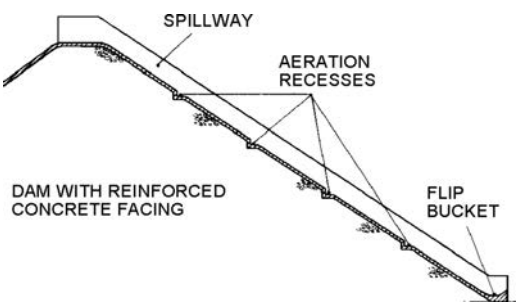

Figure 26.12 Spillway over embankment dam with reinforced concrete facing (cross-section).

A new possibility has been indicated lately for the execution of spillway structures over the body of embankment dams. Namely, with the development of new methods for the construction of rockfill dams with reinforced concrete facing, it can be considered that there have been bridged the main obstacles for the execution of a spillway over the body of such dams. In modern practice, rockfill dams with reinforced concrete facing are constructed with careful selection, zoning and compaction of the filling material, by means of which the subsequent deformations of the embankment (see Chapter 12) are reduced to the least possible measure. In addition, already constructed facing across the upstream slope gives favourable conditions, in one part, through the crest and the downstream slope, to shape up a spillway structure.

Such an example is presented in Figures 26.11 and 26.12. Practically, it consists of a concreted part over the crest, a spillway chute and a terminal flip bucket. In the spillway

chute there have been left transverse aeration recesses for preventing cavitation. This kind of spillway is suitable for smaller amount of overflow water, as well as a spillway that is supplementary to the main one.

26.2 HIGH-HEAD SPILLWAY STRUCTURES

Spillway structures in the dam's body, constructed as high-head spillways, are exclusively employed in concrete dams. Their advantage is the fact that they have a much greater discharge capacity than surface spillway structures for an equal area of the opening; however, they, of course, require appropriate gates or valves. High-head spillway structures are constructed much more rarely than surface ones, because of the following disadvantages: (1) gates or valves are more loaded and they must be of stronger construction; (2) control of these gates or valves is more difficult; (3) their access for revision is more difficult, as is their maintenance and overhaul.

For high-head spillways, when they are subjected to a pressure head greater than 50 m, we say that they work under high pressure. In terms of the construction and the position of the gates and valves, there are different kinds of high-head spillway structures. In relation to the position of the service gate or valve, they are divided into two groups: (1) when the gate (valve) is placed at the entrance of the spillway; and (2) when it is placed at the exit of the spillway. There is also the possibility of a third position of the service gate or valve – in the central part of the water conveyance structure (conduit) – however, it is virtually not to be found in the high-head spillway structures (though it is frequently employed at bottom outlets).

In the first case, depending on the depth at which the spillway opening has been positioned, the flow can be constructed freely, along the bottom, or else the water stream can fill the entire section of the offtake part.

Free flow along the bottom takes place when the spillway opening is not positioned deeply below the crest of the dam, while the bottom of the offtake part follows the trajectory of the water jet (1, Fig. 26.13a, d – Visockiy, 1977; Grishin et al., 1979):

$$y = x\tan\beta + \frac{x^2}{4\varphi^2\cos^2\beta H} \tag{26.2}$$

If we solve this equation in a system with the equation of the straight line of the downstream slope of the dam:

$$y = x\tan\alpha - H \tag{26.3}$$

we will find the position of the point K at which the trajectory joins at the bottom as a tangent to the downstream slope:

$$\begin{aligned} x_k &= \frac{2H}{\tan\alpha - \tan\beta} \\ y_k &= H\left(\frac{2\tan\alpha}{\tan\alpha - \tan\beta} - 1\right) \end{aligned} \tag{26.4}$$

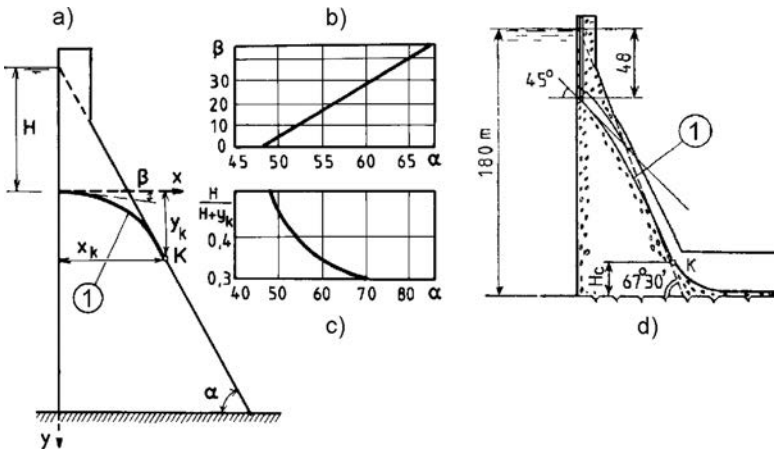

Figure 26.13 High-head spillway with flow along the bottom. (a) Design calculation scheme; (b, c) auxiliary graphs; (d) example of application (practically limiting case). (1) Trajectory of the water jet, i.e. line of the bottom of the offtake part of the spillway.

The analysis of the reciprocal relationship of the angles α and β (Fig. 26.13b) indicates that the thinner the dam is in relation to its height, the greater value for β should be selected, in order to enable the water stream along the bottom to join with the downstream slope without a directional break, i.e. change. In that way, while with gravity dams on rock foundation, at which most frequently $\alpha = 54°–57°$, the entrance angle β varies from 10° to 20°, in the case of arch-gravity dams, at which it is $\alpha \geq 60°$, the angle β reaches the value from 30° to 45°. Owing to this, it can be said that, in the case of the thinner arch-gravity and arch dams, this kind of a spillway is practically impossible. Another limiting factor for the application of this type of spillway is the low level of utilization of the pressure (Fig. 26.13c), which fact can create an unjustified increase in the number and dimensions of the spillway structures. From the diagram it can be seen that for $\alpha = 50°$ there is used 1/2, while for $\alpha = 65°$ there is used only 1/3 of the pressure built up by the dam.

It is more common to use high-head spillways that work under higher pressure, located in the lower part of the dam. Beside the greater rate of flow, i.e. discharge capacity, in relation to the previously described ones, they have the advantage that, if located quite low, they can at the same time also serve as a bottom outlet for emptying the reservoir, and sometimes also for evacuation of the construction waters during the staged construction of the dam.

Figure 26.14 presents an example of a high-head spillway under pressure with gates in the initial part. The twelve high-head openings are provided with plain service gates and with overhaul gates and, as an addition for small overflow quantities, there are also constructed two surface overflow spans. The overall quantity of overflow water that can be evacuated with this 99.5 m high dam, amounts to 4500 m^3/s. Handling with these gates is achieved by means of a portal crane from the dam's crest (Grishin et al., 1979).

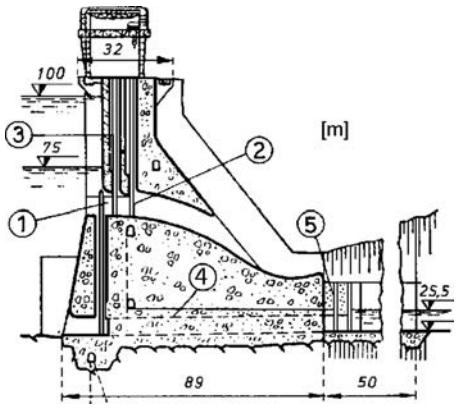

Figure 26.14 High-head spillway for Sanmenxia Dam (China, 1962). (1) Twelve high-head openings; (2) service gate; (3) overhaul gate; (4) gallery for letting through the construction waters; (5) slots for gates.

The Sayano-Shushenskaya arch-gravity dam, 245 m high, on the River Yenissei, is one of the most significant dams in the Russia. It impounds a storage space of 31.3 km^3, of which 15.3 km^3 is live storage (up to a depth of 40 m below the normal level). The dam is constructed on a relatively wide dam site ($L/H = 4.56$); the length at the crest is 1070 m, while its body incorporates 9×10^6 m^3 of concrete. Within the framework of the hydraulic scheme there is built the most powerful hydroelectric plant in the Russia, with installed power of 6400 MW. Owing to the long period of construction of the delicate hydraulic scheme (construction works began in 1960, while the last and third stages were completed in 1978), and the necessity of giving passage to the maximum waters over such a long period, there has also been anticipated and realized construction and work on spillway structures in three stages (Fig. 26.15). In that way, there have been constructed three high-head spillways under a high pressure head: the first one with an entrance (intake) at 61 m, while the second one at 152 m below the normal water level, used after the second stage of construction of the hydraulic scheme, and the third one very near to the bottom, which served for evacuation of waters in the first construction stage (Fig. 26.15). In all cases, the gates are positioned at the intake part.

The service spillway structure (following the completion of the hydraulic scheme) consists of 11 equal sections, each of them having three characteristic parts: (1) a short intake part under pressure, with a plain service gate on rollers; (2) a pipeline offtake part, i.e. conduit, with a vertical curve, without pressure; and (3) an open free flow channel (spillway chute), in which the water reaches a velocity of up to 60 m/s at the entrance to the stilling basin. Each section has a discharge capacity of 1200 m^3/s, with a high specific discharge along the spillway chute of 200 m^2/s. For the protection of the spillway elements against cavitation, there have been anticipated several constructional details for aeration of the flow both at the closed and the open parts.

The stilling basin after the spillway chute has a length of 142 m, a width at the beginning of 130.6 m, and a width at the end of 112 m, measured along the upper side

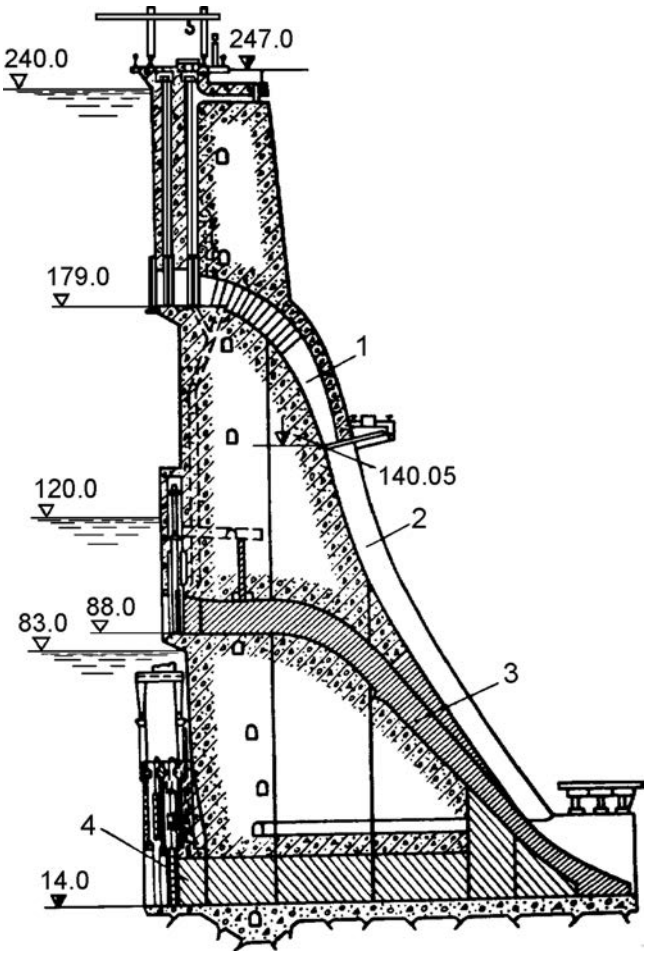

Figure 26.15 Section through the high-head spillways of the Sayano-Shushenskaya Dam (Russia). (1) Service high-head spillway, pipeline conduit part; (2) open spillway chute; (3) high-head spillway for stage II of construction; (4) outlet for the first construction stage.

of the reflection wall, 29 m high. When it does not work, the stilling basin empties by means of a pump station, specially installed for that purpose. In the course of works on the spillway structures, in spite of all the measures undertaken, certain damage to the stilling basin took place, which is frequently the case with the spillway structures of the hydraulic schemes constructed on rich water currents, when there often comes about overflowing of significant quantities of water. The damage has been repaired, while the operation of the spillway structures, as well as of all structures within the framework of the hydraulic scheme, is permanently checked and analyzed (Moroz & Shatravskiy, 1994; Rozanov & Kubeckiy, 1994).

Figure 26.16 presents a gate-house of the service spillway. The entrance part is rounded, and hydraulically shaped and it supports the overhaul gate (1). Behind it,

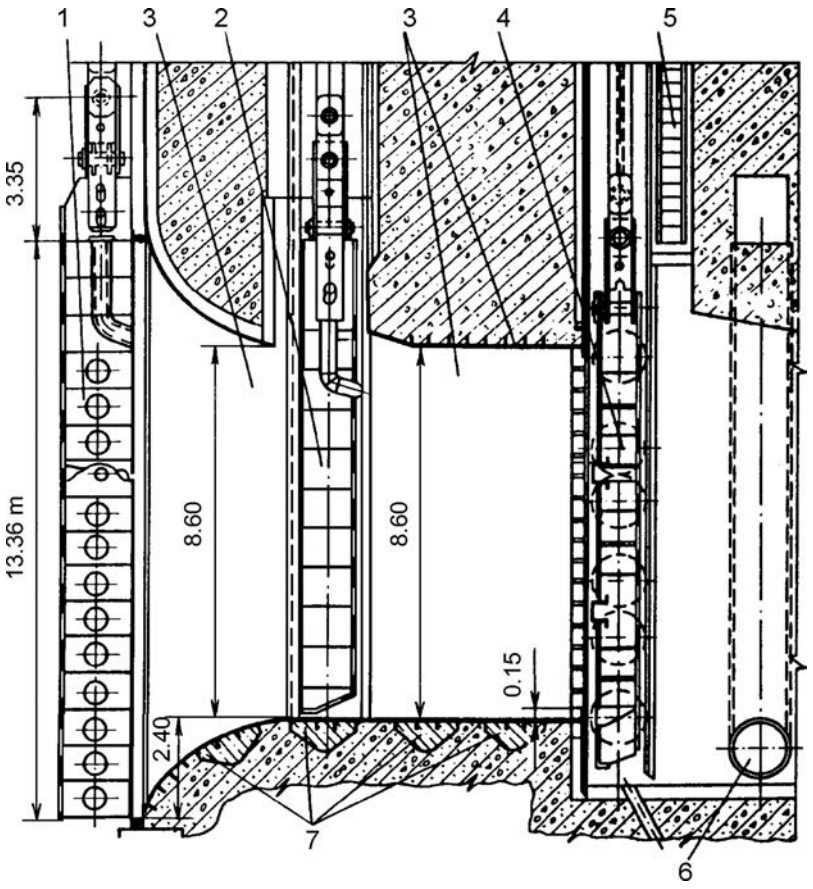

Figure 26.16 Intake with gate-house of the higher service spillway of Sayanoya-Shushenskaya gravity dam ($H = 61$ m). (1) Overhaul gate, leaning onto the intake; (2) emergency-overhaul plain gate (5.8×8.6 m); (3) steel lining for protection against cavitation; (4) service gate, plain, wheeled (5.4×8.6 m); (5) stairway and aeration pipes; (6) exit opening (outlet) of aeration pipe; (7) blocks, concreted into the sill.

there is placed an emergency overhaul gate (2), plain, that moves by sliding. Further on, there comes the service gate (4), which is also plain and moves on wheels. The entire zone of the gate-house, as well as the pipe offtake in the dam in continuation, is lined with steel (3) for the sake of protection against possible cavitation. Then, the overflow water is taken off along the slope of the dam by means of a steep spillway chute.

The valves at the end of the high-head spillway structure are used with arch dams at which, owing to their small thickness, it is not possible to construct a valve house in the form of a gallery in the dam's body, or slots or recesses in the crest. An example of such a spillway, formed with an embedded steel pipe with a diameter of 5.0 m,

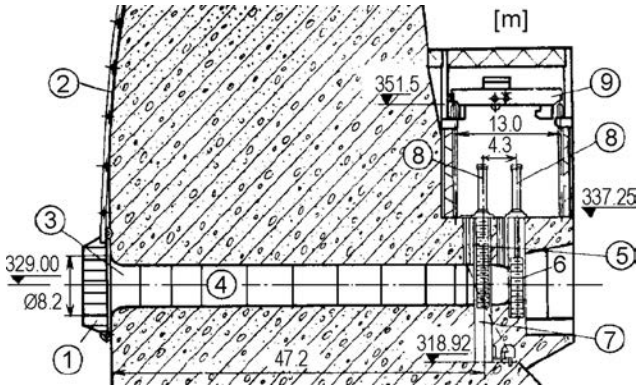

Figure 26.17 High-head spillway of Ingurskaya arch dam. (1) Overhaul gate, controlled from the crest; (2) lever for lifting; (3) widening of the pipeline; (4) pipeline, $\phi > 5$ m; (5) emergency-overhaul valve and (6) service valve; (7) case of the valve; (8) hydraulic hoist; (9) crane.

provided with three plain gates (overhaul, emergency-overhaul, and service), is presented in Figure 26.17. It is constructed within the highest arch dam constructed in the former USSR – the Ingurskaya Dam. This kind of solution eliminates the danger of cavitational erosion in the offtake, which, along the entire length, works under a regime of constant pressure. In winter periods to manoeuvre with the valves can be aggravated due to ice, but it is possible for this danger to be avoided by placing the exit portal below the minimum level of the tailwater. The overflowing jet falls into a stilling basin immediately downstream of the dam and, thus, dissipation of energy is accomplished on account of intensive aeration and mixing of the water streams in the zone of the tailwater (Bronstein, 1994).

In practice, several attempts have been made with arch dams, instead of using a plain service gate on the spillway structure, to use a radial gate, owing to its well-known and already described favourable features and advantages which, above all, are reflected in their easier manoeuvre, which is especially important with high-head spillways. At the beginning, these attempts were accepted with suspicion and reservation; practice, however, has proved the contrary.

An example of a successfully engineered and constructed high-head spillway with radial service gates in the exit part, can be found in the Cahora Bassa arch dam, constructed in 1975 on the River Zambezi (Fig. 28.18), designed and constructed by German specialists. The dam has a structural height of 163.5 m, while the high-head spillway consists of eight openings with a reverse gradient, in order to achieve projecting of the overflow water jet at a safe distance from the toe of the dam. For forming a place for the leaning of the plain overhaul-emergency gates and the service radial gate, from the upstream and from the downstream side of the dam, there have been constructed cantilevered overhangs. Stationary hydraulic hoists are used for handling the service gates; they are accommodated at the downstream side of the dam; a portal crane from the dam's crest is used for manoeuvre of the overhaul-emergency gates. The capacity of the spillway is 14,000 m^3/s, while a spillway hole is constructed for

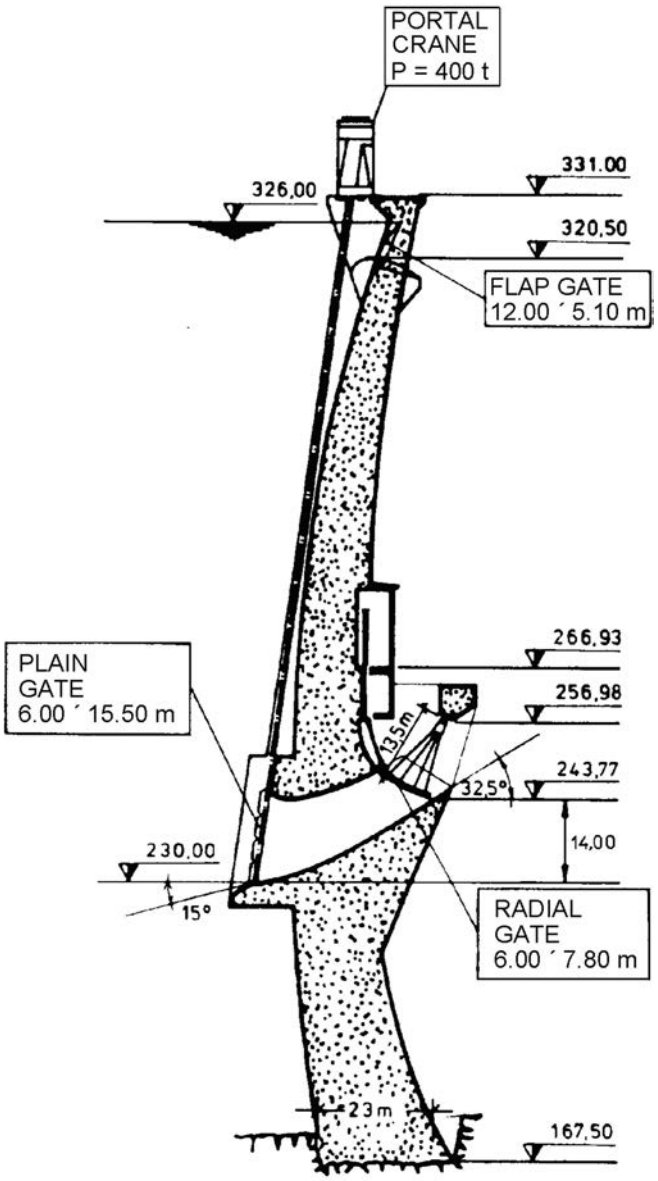

Figure 26.18 Cross-section through one of the high-head spillway openings of Cahora Bassa Dam.

small overflow quantities, located immediately below the dam's crest, provided with a flap gate (Grishin et al., 1979). In the course of long time service, on a number of occasions there has come about overflowing of significant quantities of water, in which the spillway structure has functioned well.

This page intentionally left blank

Chapter 27

Spillways outside the dam's body

27.1 INTRODUCTION

Spillway structures located outside the dam's body are employed within the framework of hydraulic schemes with non-overflow dams. Those are, mainly, embankment dams, and in certain topographic and other conditions, their use is also rational and justifiable with concrete dams, above all, arch dams and buttress dams.

Depending on the ground, and the geological and hydrological conditions of the dam site, there are possibilities for numerous combinations in the technical shaping and in the construction of spillway structures built outside the dam's body. A vital characteristic, according to which their classification is made, is the construction of the spillway part, according to which the following most important types of spillway structures can be differentiated: overfall (or ogee) spillway, side-channel spillway, shaft (or morning glory) spillway, and siphon spillway. Of importance as well, is the manner of offtake of the overflow waters, which may be surface, by means of a channel that has a slope greater than the critical one, or underground, by means of a tunnel. One can often encounter a combined offtake, i.e. diversion of the overflow waters, with an outlet tunnel and a spillway chute. The water current of the overflow waters possesses significant energy that must be dissipated prior to the discharge of the water into the natural river channel downstream of the dam. Such dissipation of the water energy can be accomplished in a special structure – a stilling basin – or else the water jet can be projected to a safe distance from the main structures, i.e. works, by means of a special terminal structure of the outlet part of the spillway structure, which has been discussed in Chapter 23.

27.2 OVERFALL (OGEE) SPILLWAY STRUCTURE

The overfall (or ogee) spillway structures are placed in the slight banks near the dam (Fig. 27.1). They consist of four basic parts (Chugaev, 1985; Grishin et al., 1979; Nedriga et al., 1983; Rozanov et al., 1985):

1. Approach channel;
2. Spillway of frontal (overfall) type;
3. Outlet or diversion part;
4. Terminal part.

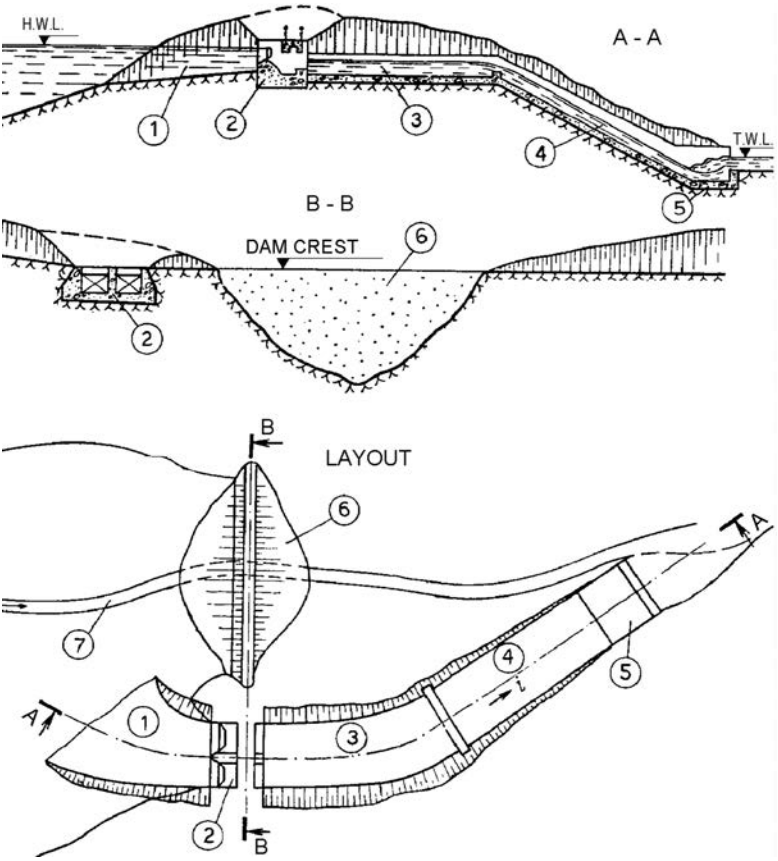

Figure 27.1 Ogee spillway structure with surface outlet (after Grishin et al., 1979). (1) Approach channel; (2) spillway; (3) outlet part I; (4) outlet part II; (5) terminal part; (6) embankment dam; (7) river bed (channel).

The *approach channel* should ensure uniform supply or inflow of water towards the spillway. In plan, it usually has a curvilinear form and variable width (1, Fig. 27.1). Most often, the bottom is horizontal and, in the case of rock foundations, is not faced, the same as the slopes. In the case of a soil foundation, protection is performed by means of facing, i.e. lining; however, only in the zone that is in front of the spillway structure. The cross-section is constructed in a trapezoidal form and with inclinations of the slopes 1:1.5–2.5 for soil foundation and 1:0.5 for rock foundation.

The *spillway part* is a weir, i.e. a low overflow concrete dam, with a spill-crest set up perpendicular to the initial part of the outlet structure and approximately parallel to the dam. The spill-crest is constructed rectilinearly and, in certain cases, it can have a curvilinear or even more complex form, in order to provide a longer overflow front in certain unfavourable topographical conditions.

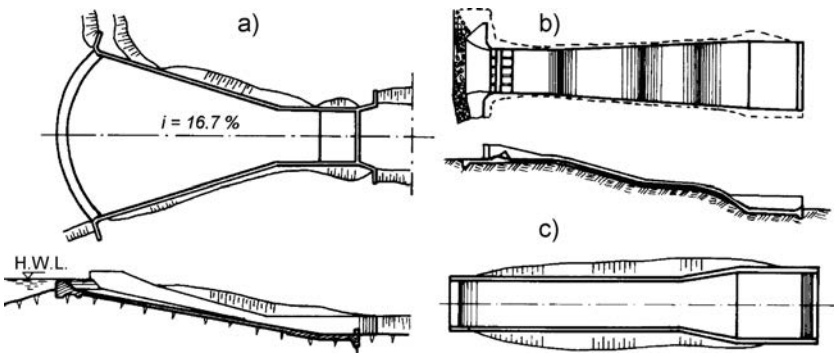

Figure 27.2 Spillway chute with variable width (after Grishin et al., 1979). (a) Contracting towards the downstream side; (b) widening towards the downstream side; (c) widening only in the terminal part.

The outlet (offtake) part consists of a spillway chute (4), by means of which the water is conveyed to the terminal part of the structure. If that is dictated by the topographic conditions, the outlet part can also encompass a transitional channel (3) with a slope smaller than the critical one, which supplies the water into the spillway chute. A transitional channel is constructed when the ground, immediately after the spillway, has a very mild slope. The bottom and sides of the channel have a concrete or reinforced concrete lining, with a thickness that depends on the size of the channel and the geological characteristics of the foundation.

The *spillway chute* is a channel with a longitudinal gradient greater than the critical one. Most frequently, the inclination ranges from 5 to 25%, and can also be greater, especially in cases of firm and sound rock. For better adaptation to the ground, one same spillway chute can have a number of sections with different gradients. The width of the spillway chute can be either constant or variable, in which it can decrease (Fig. 27.2a) or increase (b) towards the downstream side. Often, its widening is not performed along the entire length of the spillway chute, but only at the section that is immediately in front of the terminal part of the spillway structure (c). The necessity of designing the spillway chute with a variable width is usually imposed by the conditions for dissipation of the water energy in the terminal part, while in the case of long spillway chutes, the contraction sometimes leads to reduction of the extent of works, and thus, to a reduction in costs (Mazhbiz & Bulanov, 1990).

From a constructional point of view, the spillway chute is a concrete or reinforced concrete channel with a rectangular or a trapezoidal cross-section (Fig. 27.3a–f). One should endeavour that the channel be embedded into the ground, while the sides can be formed as either ordinary linings (a, d-f), or else in the form of retaining walls of a certain type, usually separated from the bottom by deformation joints. In the case of channels with smaller dimensions, and also with reinforced concrete channels, the lateral walls and the bottom are constructed as a monolithic unity. On a soil foundation, the bottom is executed in the form of slabs, with a thickness of from 30 to 80 cm, while the sides have a thickness of 20–40 cm if they are not constructed as retaining walls.

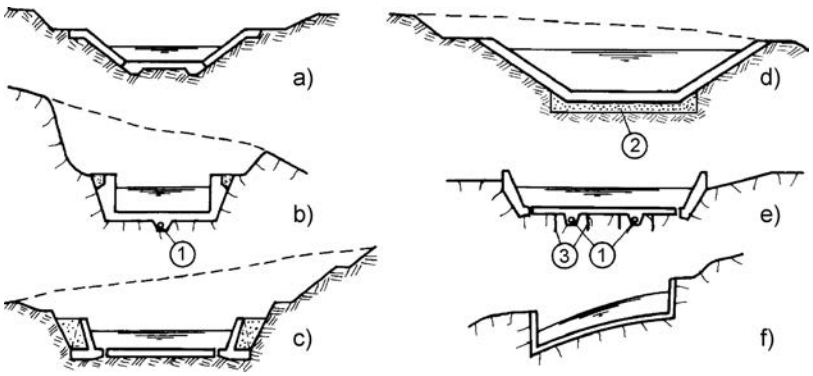

Figure 27.3 Cross-sections of the spillway chute (after Grishin et al., 1979). (a, c, d) In the case of a soil foundation; (b, e, f) in the case of a rock foundation. (1) Drainage; (2) drainage layer of sand; (3) anchors.

Longitudinally, the walls and the bottom are divided by deformation joints at each 20–25 m. In certain cases, with firm and sound rock, the lining can also be left out or constructed with vertical walls of minimum thickness. In cases of weaker rock, the side walls are constructed with an inclination of 1:0.3–0.5, while the concrete lining is of a thickness of from 20 to 40 cm and can be anchored into the foundation (Fig. 27.3e).

The shape of the cross-section of the spillway chute and the ratio of the width versus the height depend on the geological and topographical conditions of the ground and on the amount of overflowing water. Wider, but shallower channels, are applied to soil foundations. The hydraulic dimensioning is performed in accordance with the rules for non-uniform flow in open channels, and for maximum overflow waters (see Chapter 23). The sidewalls are heightened above the water level by 0.5 m.

Static dimensioning is achieved for the most adverse conditions of loading, that is to say, for a full channel, without the action of lateral earth pressure, and for an empty channel, with the action of lateral earth pressure.

The longitudinal axis of the spillway chute in plan should best be in a straight line but, in many cases, the ground conditions impose the need for its curvature. In such a case, for ensuring normal working of the spillway chute, and under conditions of the action of centrifugal forces, a need can arise for sloping the bottom also in the transverse direction (Fig. 27.3f). The use of a curve spillway chute in certain topographic conditions facilitates an essential reduction of the extent of construction works.

In cases of spillway chutes with a greater width at the initial part and with a curved spill-crest, for the sake of increasing the stability of the water flow in the transverse section and for more uniform change of depth in the curved sections, longitudinal parting walls are constructed, as shown in the examples in Figures 27.4–27.6.

In order to reduce the velocity of flow, low sills are constructed in certain parts of the spillway chute, which helps towards an artificial increase of the roughness of the bottom-as in the example presented in Figure 27.7. Low sills, or baffle blocks, can be constructed on sections with smaller velocity owing to the danger of these additional elements being damaged (or carried off) by the rapid water jet (Rozanov et al., 1985).

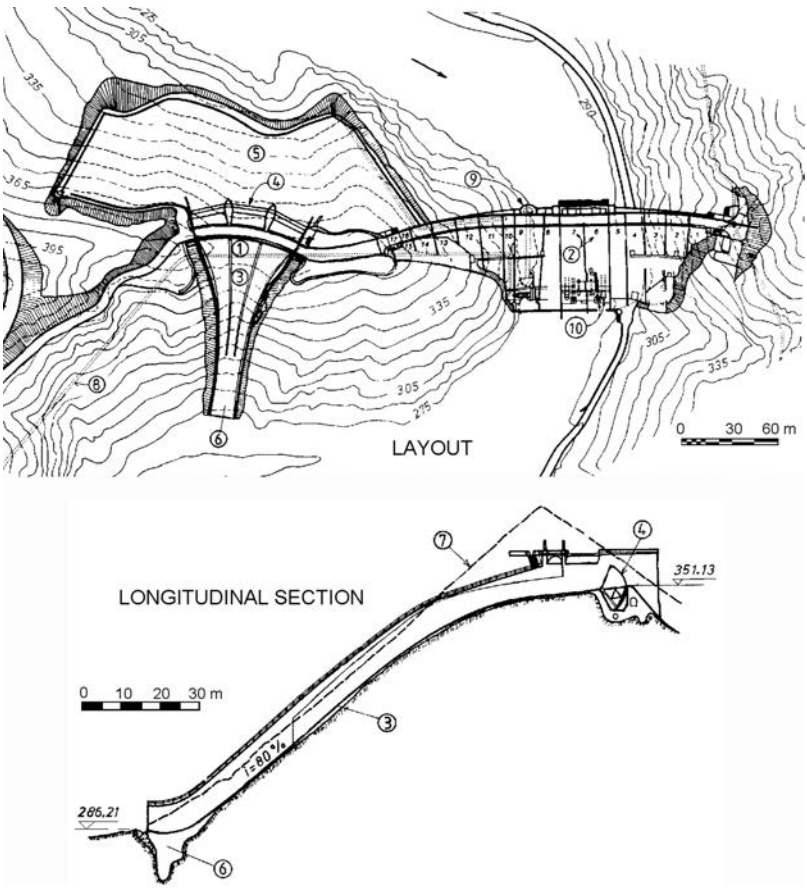

Figure 27.4 Controlled spillway structure with a curved spill-crest and sidewalls in the spillway chute for the Morris Dam (USA, 1934) (1) Spillway; (2) blocks into which gravity dam is divided; (3) spillway chute; (4) drum gate; (5) concreted bottom in approach part; (6) flip bucket; (7) ground boundary along axis of spillway chute; (8) tunnel conduit (D = 11 m); (9) intake tower for water supply; (10) needle valve.

When the need arises for a greater width, the spillway chute can be constructed as a twin type, which is presented in the example of the controlled spillway within the framework of a hydraulic scheme with arch dam (Fig. 27.8).

For reducing the effect of the seepage water along the length of the spillway chute, one should construct drainages below the bottom and behind the sidewalls. This will be most efficient if the drainage is executed from a layer of sand, with a thickness of 20 to 40 cm, with perforated pipes at the ends.

In cases of significant longitudinal inclination of the ground, for instance greater than 25%, and relatively small specific discharge (up to 15 m^2/s), instead of a spillway chute it is possible to use a cascade outlet of water (Fig. 27.9). The cascades are constructed in the form of a number of steps with equal dimensions, formed with

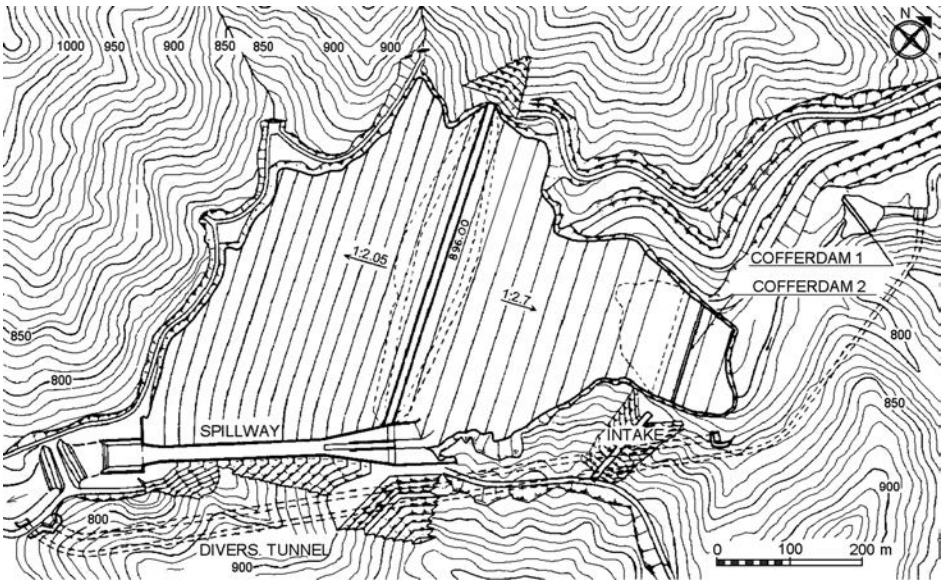

Figure 27.5 The hydraulic scheme with Naramata embankment dam (Japan), completed in 1990, $H = 158$ m. The spillway is partially controlled; the widened part of the spillway chute is separated by a sidewall; capacity 1650 m^3/s.

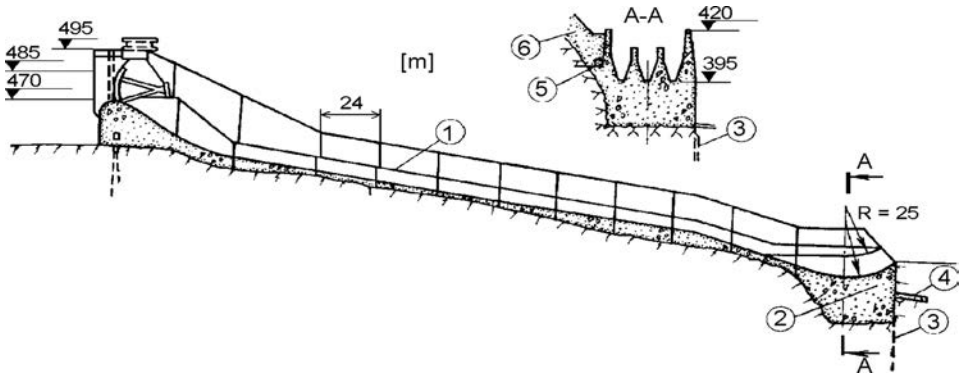

Figure 27.6 Spillway chute with sidewalls. (1) Upper edge of training walls; (2) terminal structure in the form of a massive block for projecting the water jet; (3) grout curtain; (4) concrete slab with thickness of 1 m; (5) drainage pipe; (6) earthfill.

longitudinal (lateral) and transverse walls. The dimensions of the stairs, as well as the height of the reflection sills, are determined by means of hydraulic calculations from the condition for complete dissipation of the energy. The most frequently used step rise is 4–6 m, while the velocity of flow in the multiple-stage cascade usually amounts to (2–3) m/s (Grishin et al., 1979).

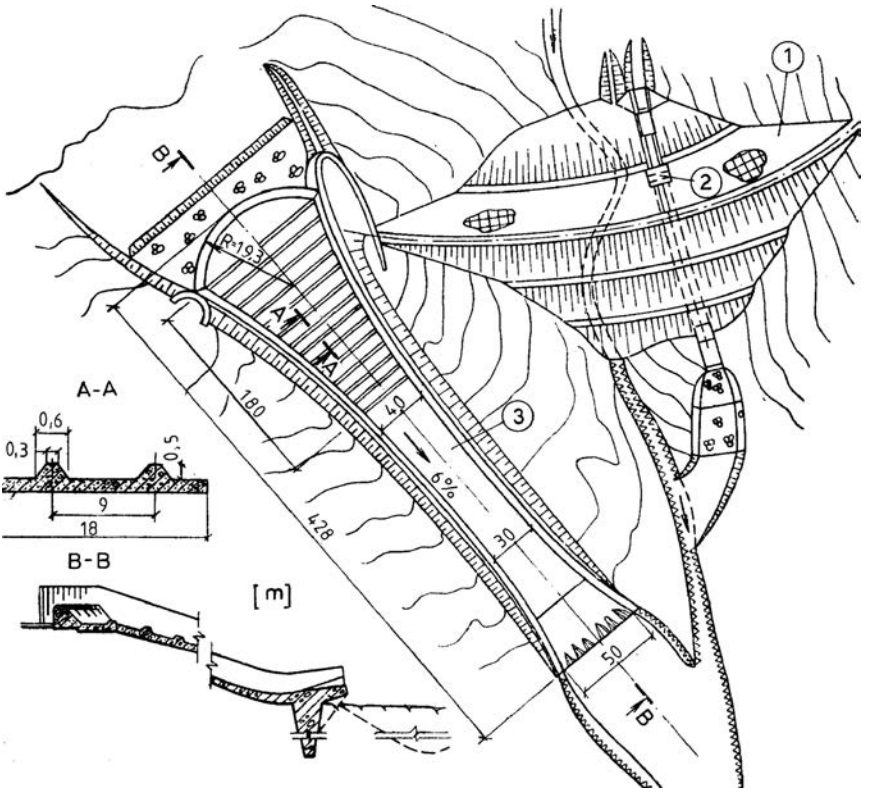

Figure 27.7 Ogee spillway of the hydraulic scheme *Carlos Manuel de Cespe* (Cuba), 1967, with a capacity of 3660 m^3/s. (1) Dam ($H = 52$ m, $L = 850$ m); (2) valve house at the bottom outlet; (3) spillway chute at the spillway structure with transverse low sills in the upper part.

Should the ground conditions not allow the construction of a surface outlet of the overflow waters, then a tunnel outlet can be employed, in which the flow is performed freely, without pressure (Fig. 27.10). This solution is employed in cases of hydraulic schemes with lower pressure heads. The terminal structure here also can be constructed in the form of a stilling basin – overground (a) or underground (b) – or else in the form of a flip bucket (c). Between the circular or rounded section of the tunnel and the rectangular section of the terminal structure, a special transition should be constructed.

The *terminal part* of the spillway structure is designed in such a way as to enable dissipation of the energy of the water current and to ensure a steady flow in the river channel downstream of the works. In rare cases, in favourable geological conditions and when the spillway is distant from the dam, as shown in the example in Figure 27.11, we can discharge water into the river channel directly from the spillway structure, without a special terminal structure (CNCOLD, 1979). In all other cases, after the spillway there is anticipated either a stilling basin for dissipation of the energy (Fig. 27.12a, b), or else a structure for projecting, i.e. throwing off, the water stream at a certain distance (c, d). Upon the stilling basin slab, if the velocity at the end of the

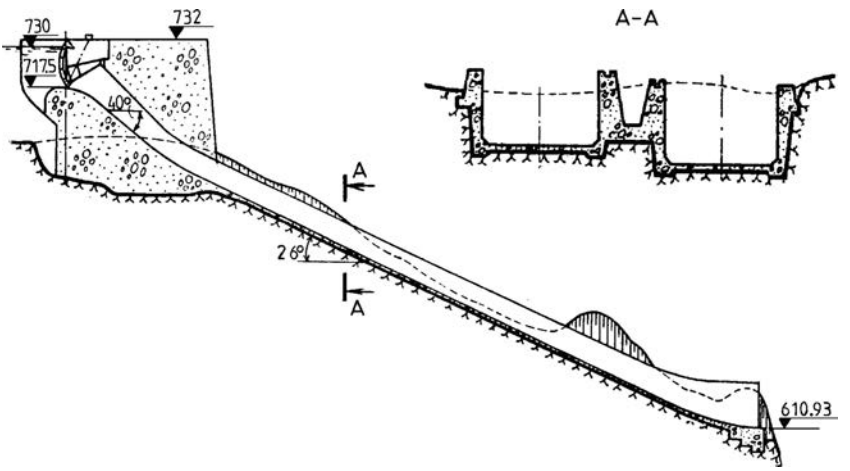

Figure 27.8 Spillway structure with a twin chute.

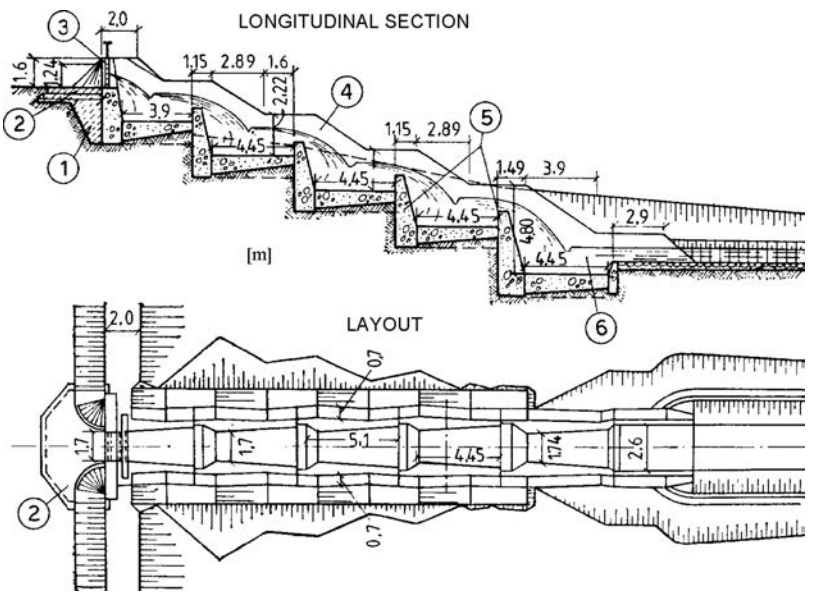

Figure 27.9 Examples of multiple-stepped cascade (after Grishin et al., 1979). (1) Clay-concrete; (2)blanket; (3) plain gate; (4) side wall; (5) sill; (6) basin.

spillway structure is less than 15 m/s, we can carry out baffle blocks for better dissipation of the energy. The solution presented in Figure 27.12a has the deficiency that the stilling basin slab is subjected to a significant force of uplift from the underground water, so that special measures are required for the elimination of the effect of water

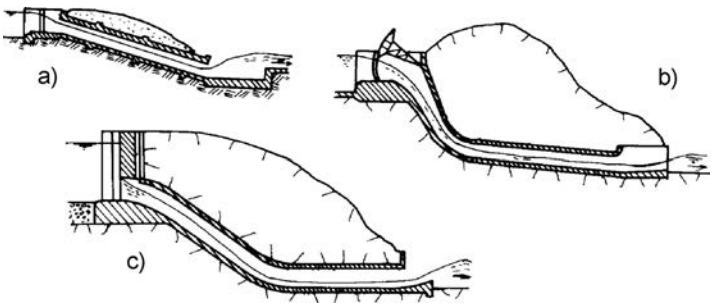

Figure 27.10 Ogee outlet of waters with a no-pressure tunnel.

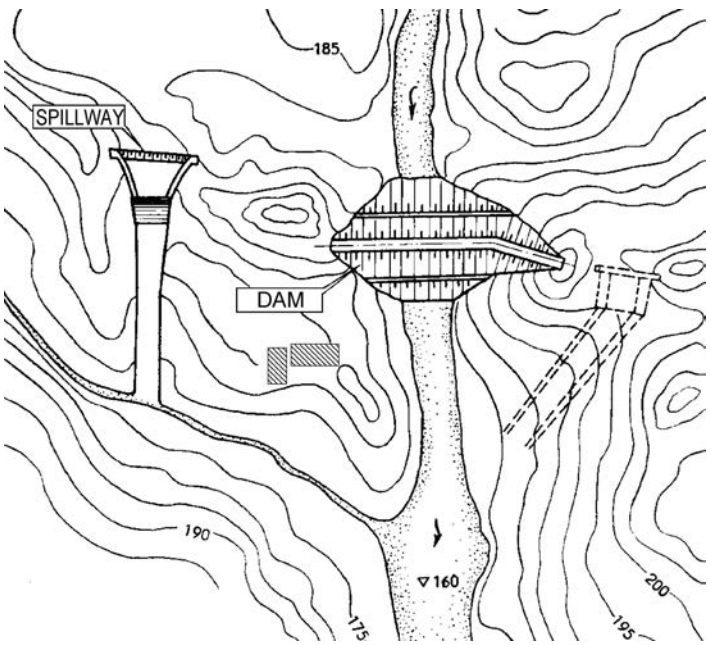

Figure 27.11 Layout of works within a hydraulic scheme in China, with an overfall chute spillway.

seepage. The illustration (1) in the sketch shows the deficit of pressure, denoted with arrows directed upwards (Chugaev, 1985).

Very often the terminal part is constructed in the form of a structure that projects, i.e. throws off, the water jet at a certain distance (Fig. 27.12c, d). In this, the dimensions of the plunge pool, into which the jet falls, depends on the specific water discharge q, which is thrown off from the end section of the structure (see Chapter 23, section 23.6). In order to reduce q, the terminal part of the spillway chute is widened, or else the structure for projecting is widened. For better sprinkling of the water jet, the projecting structure can be given a curvilinear form in plan, as well as in its cross-section, as is

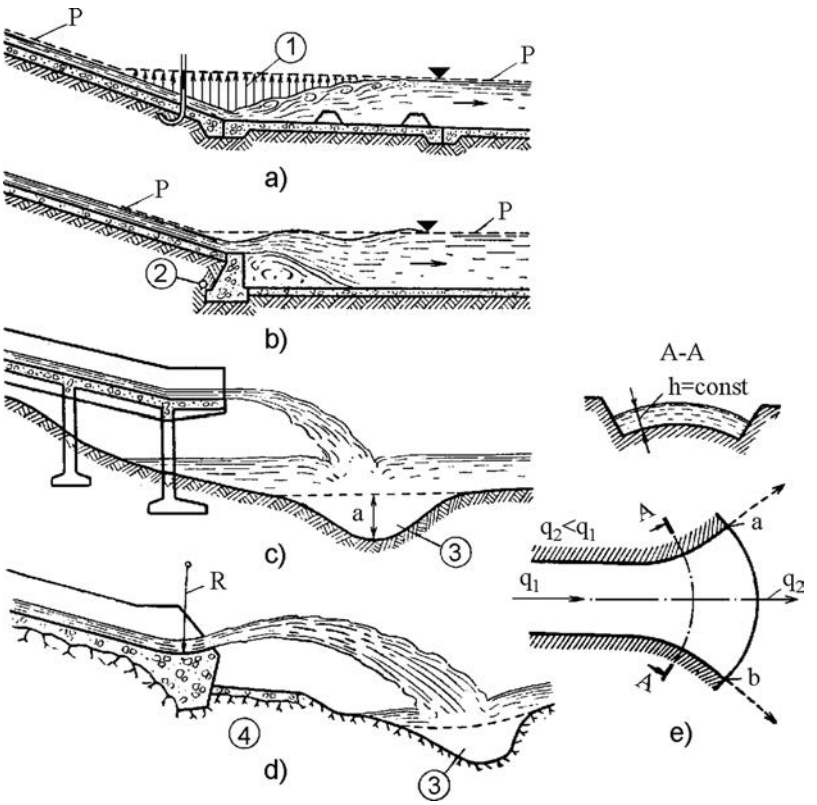

Figure 27.12 Terminal (end) part of the spillway structure (after Grishin et al., 1979). (a, b) With a stilling basin; (c, d) with a structure for projecting the flow jet. (1) Deficit of pressure; (2) drainage; (3) plunge pool; (4) rock in foundation.

shown in Figure 27.12e. In this way, the specific water discharge is reduced and remains constant along the length of the line a, b. Sometimes, baffle blocks are constructed in the terminal part, or some kind of orientating elements.

The terminal structures are dimensioned according to the methods that are known in hydraulics. The same applies to the dimensions of the plunge pool, as well as for the throwing off of the water jet, in which one should also take into consideration aeration, owing to which the distance of the projecting of the water jet is reduced.

27.3 SIDE-CHANNEL SPILLWAY

The side-channel spillway, schematically presented in Figure 27.13, is characterized by the fact that the spill-crest is placed in the direction of flow of the river and of the outlet structure, that is to say, approximately perpendicular to the axis of the crest of the dam. The following parts fall within the composition of the side-channel spillway: (1) overflow part, which is shaped as an ogee-crest spillway or else as a broad-crested

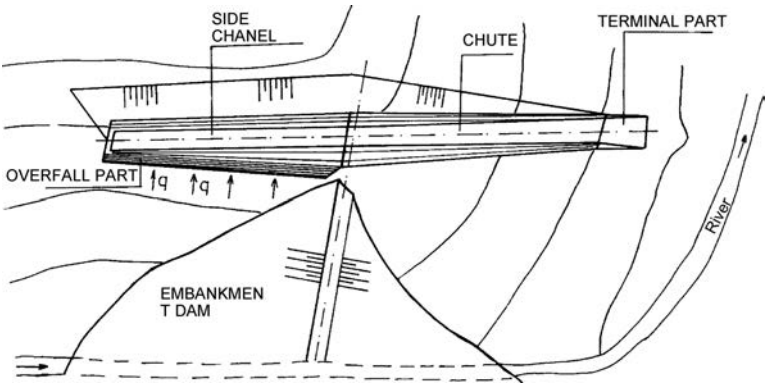

Figure 27.13 Schematic presentation of a side-channel spillway.

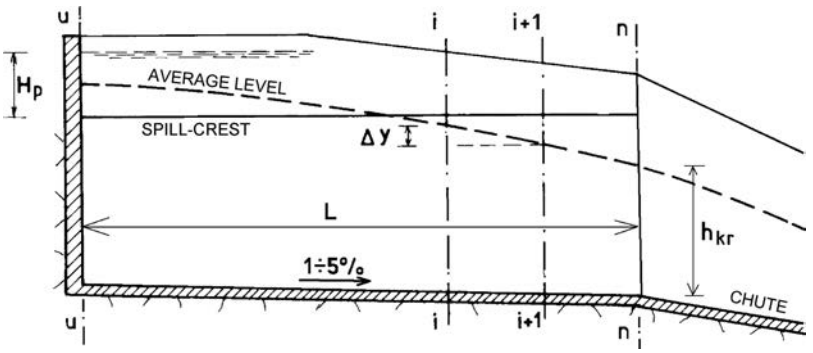

Figure 27.14 Scheme of longitudinal section along the axis of a side channel.

weir; (2) side channel, which collects the overflow water; (3) outlet part, most often in the form of a spillway chute or, more rarely, as an tunnel; and (4) terminal part.

The *overflow part* can be either controlled or free (Torres et al., 2000). Free spillways are for smaller quantities of overflow waters, while the controlled ones are for Q_{max}, up to 8000 m^3/s at an overflow height of 8 m. If the gates are of automatic action, then they are employed for Q_{max}, up to 6000 m^3/s with an overflow height up to 2 m. From a structural point of view, a side-channel overflow part does not differ from a smaller overflow concrete gravity dam.

The *side channel* is parallel to the spill-crest and is a trapezoidal channel with a bottom width and depth, which increases from the upstream end towards the downstream end. The side facing of the spillway has an inclination of 1:(0.5–0.6), while the opposite side is carried out with an inclination of 1:0.5 for rock foundations (as is the case with the side channel of the Turiya dam, Figure 27.22), while it is somewhat slighter for weaker foundations. The longitudinal slope of the bottom of the side channel should range from 1 to 5%. For reducing the seepage uplift pressure, drainage is

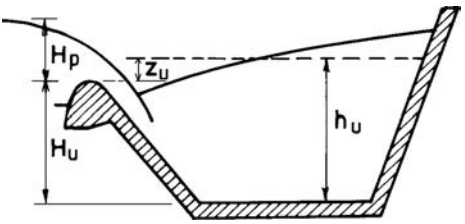

Figure 27.15 General cross-section of a side channel.

carried out below the bottom of the concrete channel. As a characteristic of the flow in the side channel, there appears the variable water flow longitudinally as well as the occurrence of whirlpool motion, which has a negative influence on the regime of flow and the discharge capacity of the side channel. Owing to that, it is necessary to pay special attention to the hydraulic dimensioning, in which there have to be fulfilled a number of conditions. In the case of side-channel spillways with significant capacity, model investigations are also necessary during their dimensioning.

The hydraulic dimensioning of the side channel can be performed by means of the expression for the head-losses in a section between the sections i and $i+1$ (Fig. 27.14):

$$\Delta y = \frac{Q_i(V_i + V_{i+1})}{g(Q_i + Q_{i+1})}\left[(V_{i+1} - V_i) + \frac{V_{i+1}(Q_{i+1} - Q_i)}{Q_i}\right] \tag{27.1}$$

where, Δy is the difference in mean water levels in two adjacent sections i and $i+1$; V_i and V_{i+1} are the velocities of flow in sections i and $i+1$, respectively; and Q_i and Q_{i+1} are the corresponding discharge quantities (USBR, 1977).

Solving the equation (27.1), that is to say, the determination of delevelling of the flow in two adjacent sections is determined by trial and gradual approximation, and the problem is suitable for programming even on a pocket computer. The accuracy of solution is high, if we choose a sufficiently small interval, the size of which depends upon the specific overflow water quantity, on the width of the side channel, as well as on the longitudinal slope.

Dimensioning of the side channel begins from the end cross-section, where the beginning of the outlet of the side-channel spillway structure is. Here the mean depth of water should be equal to the critical one. In order to obtain economical dimensions of the side channel, the level of the bottom of the side channel should be selected in such a manner that, in the first half, the mean water level would be above the spill-weir, while in the second half, below it (Fig. 27.14). In order to ensure non-submersion of the most upstream section u-u, the following condition should be complied with (Fig. 27.15):

$$z_u = 0.5H_p \tag{27.2}$$

In order to ensure a steady flow along the channel, without unacceptable influence on the lateral water catchments and the change of the direction of the water flow, it

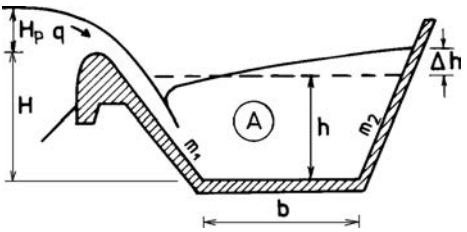

Figure 27.16 Cross-section of a side channel.

is necessary in each section, and especially at the downstream end, for the following condition to be fulfilled:

$$\varphi = \frac{qH}{\sqrt{gAh^3}} < 0.15 \tag{27.3}$$

where h is the average depth of water in the cross-section; and $A = b \times h + \frac{1}{2}h^2(m_1 + m_2)$ is the area of the live cross-section (Fig. 27.16 – Hajdin, 1967).

Rising of the water level Δh over the mean level at the downstream side of the spillway is calculated from the expression:

$$\Delta h = \frac{qH}{\sqrt{gAh}} \tag{27.4}$$

obtained on the basis of experimental investigations. The lateral lining is given freeboard above the obtained water level by another 0.50 m. If, on the basis of assumed parameters, it turns out that the condition (27.3) has not been satisfied, then certain changes are implemented, in which variations in H_p, H, and b are possible. In addition, the economy of the solution depends on the ratio of the parameters H and b.

If the spillway structure is founded on a soil foundation, then the side channel is made shallower, as well as wider, as shown in the example in Figure 27.17. The best thing is if the entire channel is made by excavation. Owing to the low load-bearing capacity of the soil foundation, the spill-weir should have a considerable width. A layer of sand is compulsory below the channel, for elimination of the uplift which, when the need arises, can be extended also below the massive concrete weir. In order to reduce the extent of the excavation, the off-take channel, immediately after the side channel, enters the dam's body, so that the joint must be safeguarded with a massive retaining wall, Figure 27.17c.

The outlet and the terminal part of the side-channel spillway, in relation to the construction, do not differ from the corresponding parts used in an ogee spillway.

In the continuation, there will be given some examples of constructed dams with side-channel spillways, founded on rock foundations.

Figure 27.18 presents the layout of the Futaba embankment dam (Japan) along with the appurtenant hydraulic structures, completed in 1987. The dam is founded on andesite, is 61 m high, and has a water-impermeable element in the form of asphaltic

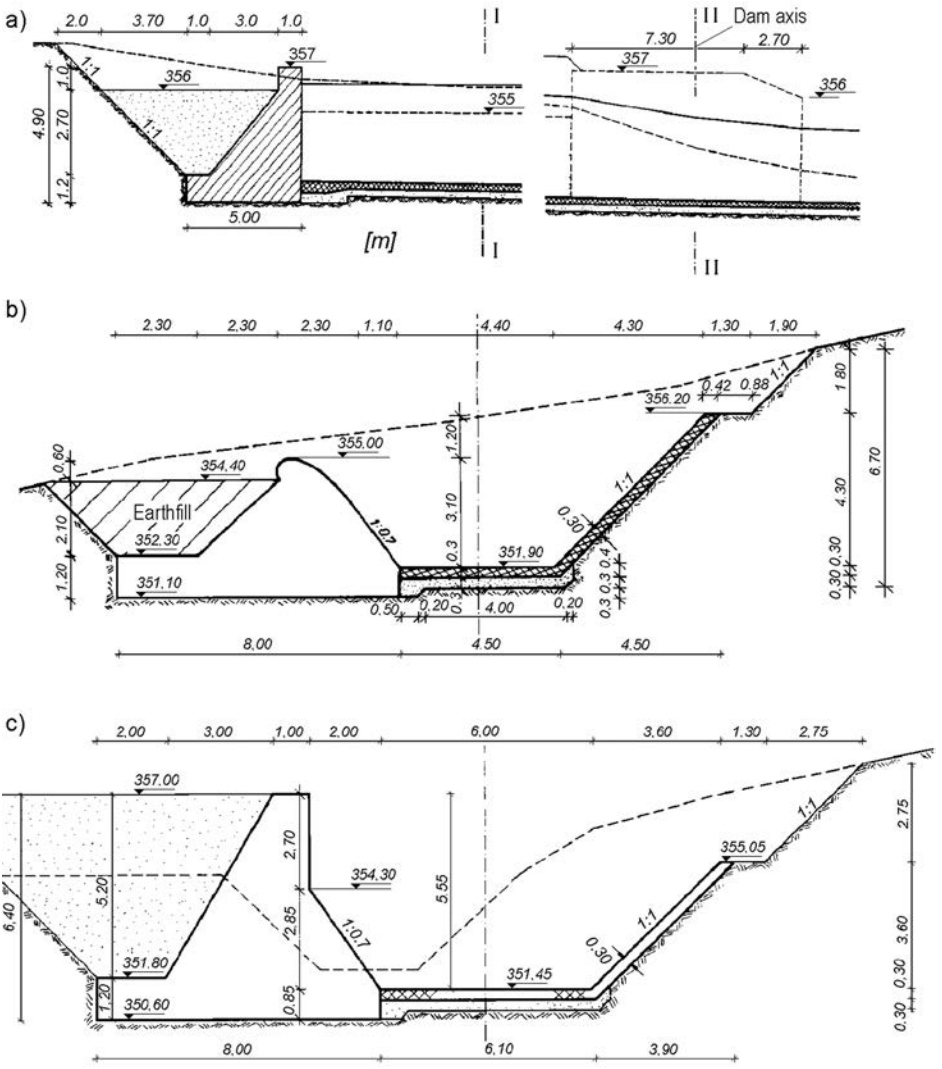

Figure 27.17 Longitudinal section through the collecting and initial part of the outlet channel. (a) and cross-sections I–I and II–II (b and c), in a side-channel spillway structure on soil foundation.

facing (lining). The side-channel spillway is constructed as an uncontrolled spillway, with a capacity of 780 m^3/s, entirely in a straight alignment. The hydraulic scheme is intended for irrigation (JNCOLD, 1991).

Figure 27.19 illustrates a plan of the hydraulic scheme of the Vodocha earth–rock dam (Macedonia), along with an uncontrolled side-channel spillway structure, with a length of the side channel of 40 m. The capacity of the spillway structure is 140 m^3/s. One part of the outlet channel is constructed in a curve. Before the end, the spillway

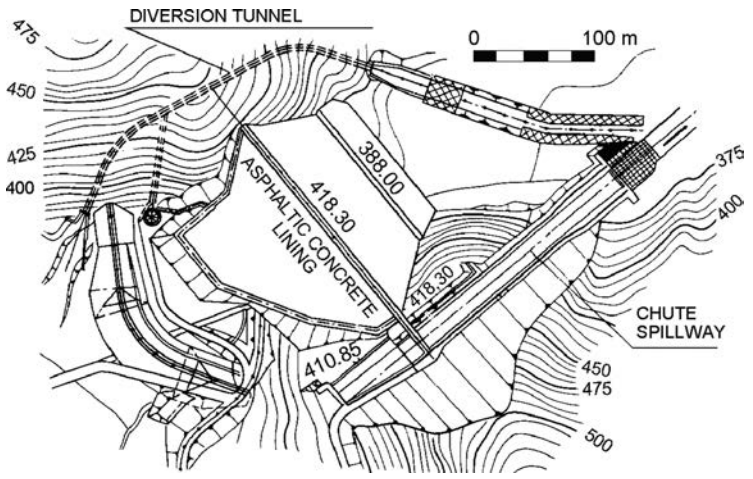

Figure 27.18 Futaba Dam (Japan), along with appurtenant hydraulic structures, including an uncontrolled side-channel spillway structure (JNCOLD, 1991).

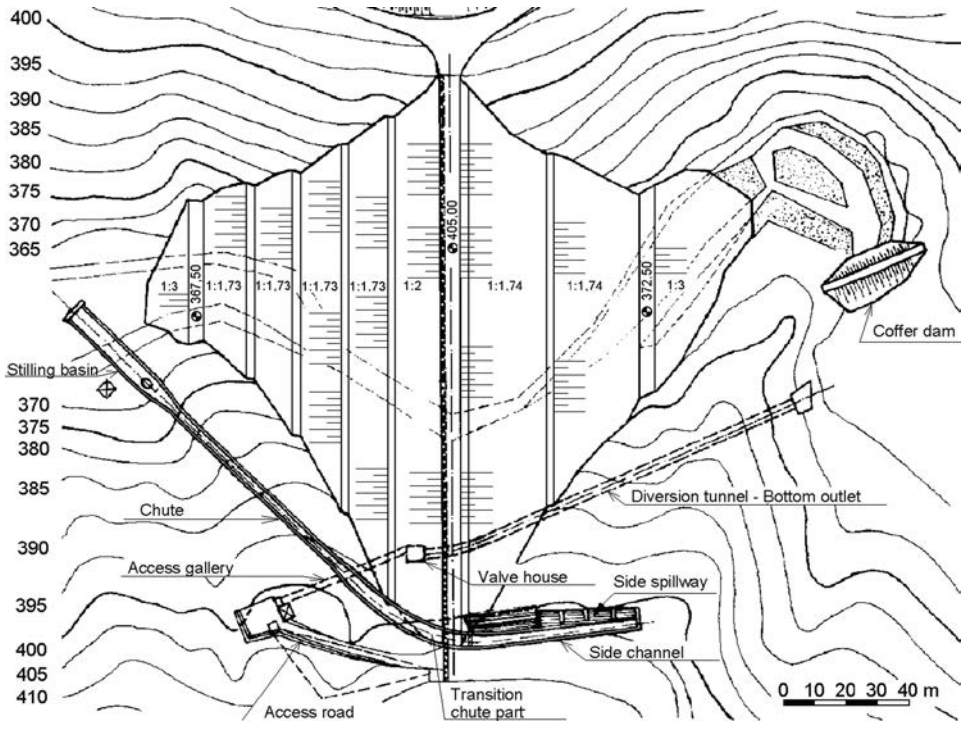

Figure 27.19 Vodocha hydraulic scheme (Macedonia), with a side-channel spillway.

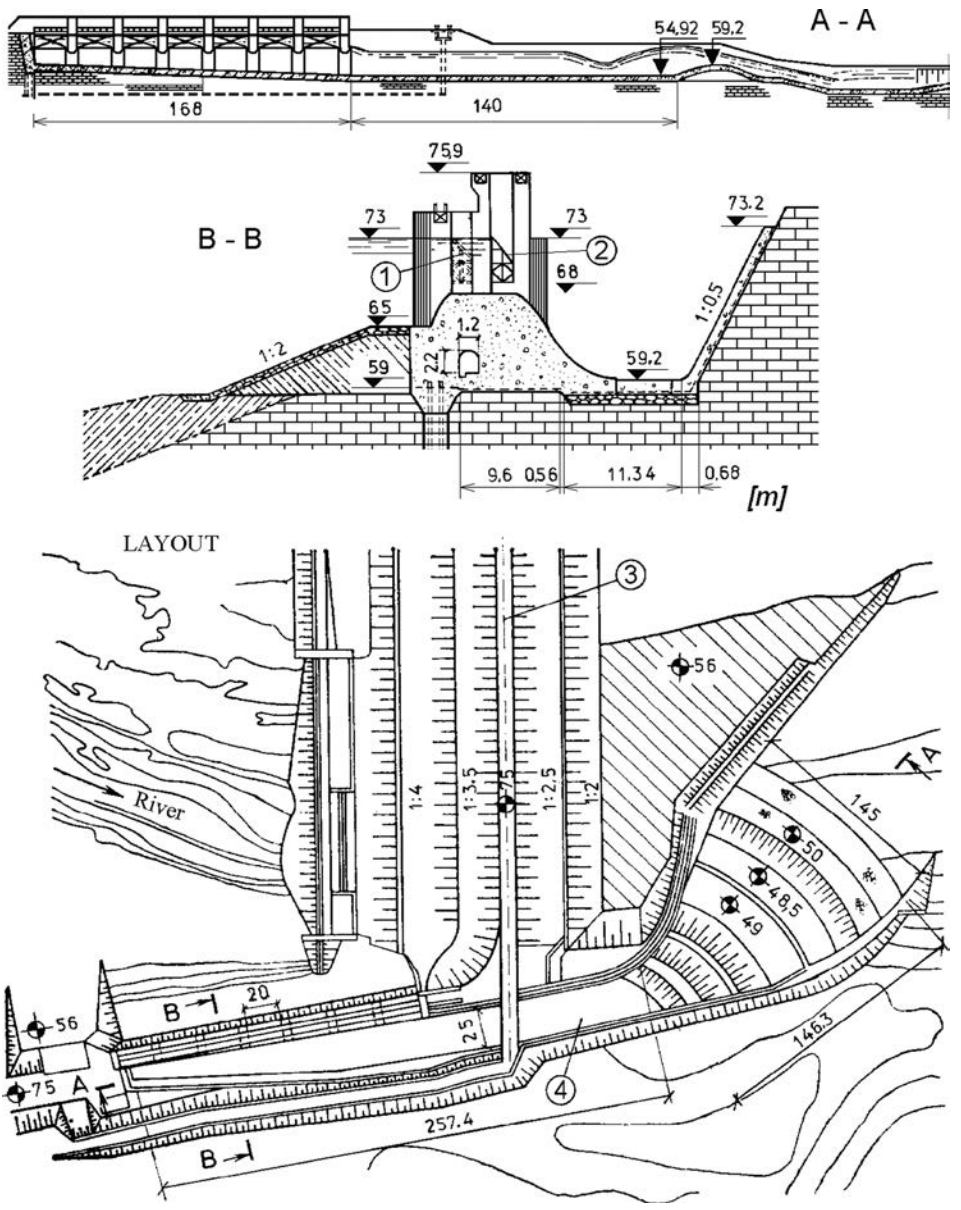

Figure 27.20 Controlled side-channel spillway structure (after Grishin et al., 1979).

chute is widened and, as a terminal structure, there has been constructed a stilling basin for dissipation of water energy. By means of parting walls, the spill-weir is divided into four spans, in order to ensure a more uniform inflow of water and better conditions for flow in the side channel (YCOLD, 1970).

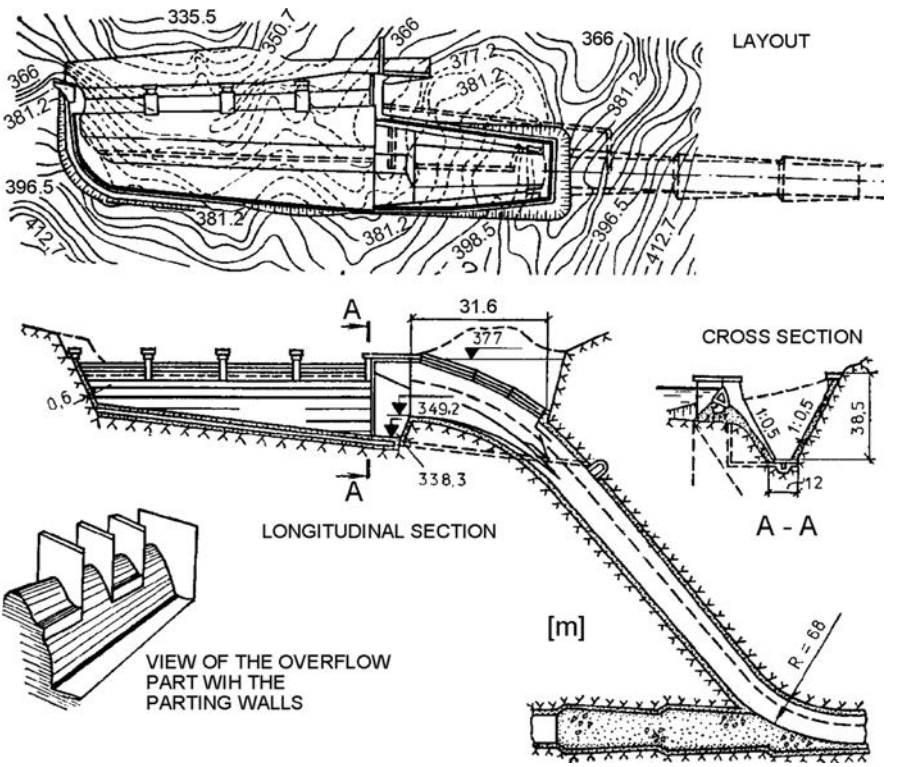

Figure 27.21 Side-channel spillway structure with a tunnel outlet used in the *Boulder* (*Hoover*) hydraulic scheme in the USA, along with arch-gravity dam.

A controlled side-channel spillway structure with a broad-crested weir is presented in Figure 27.20. Seven overflow spans have been anticipated, each 20 m wide, while the height of the overflow jet amounts to 5 m. The outlet tunnel is relatively short, while the stilling basin has a slight curve, with an irregular section and shape of the bottom (Rozanov et al., 1985).

In certain cases, when it is dictated by ground conditions, it is possible to carry out a side-channel spillway structure with a tunnel (instead of a surface) outlet. Such an example is shown in Figure 27.21. The spillway is uncontrolled, divided into four sections, while the bottom of the side channel has a longitudinal slope, which is greater than the one recommended, when it is a question of surface offtake. The horizontal part of the outlet tunnel was used as a diversion tunnel in the course of construction of the hydraulic scheme. The flow in the tunnel is free, without pressure, which is the more frequent case with this kind of structure.

The side-channel spillway structure is suitable for application in cases of steep banks of the dam site over the dam's crest. In such a case, a frontal ogee spillway with a longer spill-crest will not be an economical solution due to the significant excavation necessary. It is most often used in cases of hydraulic schemes with an embankment

Figure 27.22 Side-channel of Turiya dam (Macedonia).

dam, but it can also be found as an appurtenant hydraulic structure with arch dams and arch-gravity dams.

27.4 SHAFT (MORNING GLORY) SPILLWAY

27.4.1 Shaft spillway with circular funnel crest

The basic part in the shaft spillway structure is a vertical or slightly inclined shaft (Fig. 27.23). The water in the shaft discharges down over the spill-crest that is in the form of a circle, an incomplete circle (Fig. 27.28), or of some other shape in plan. The upper part of the shaft is sometimes carried out in the form of a tower. The shaft spillway structure is used for the evacuation of large quantities of water (up to 6000 m^3/s) within medium and high head hydraulic schemes over a rock foundation.

The basic parts of the shaft spillway are: surface overflow part, in the form of a funnel (1 in Fig. 27.24); vertical or slightly inclined shaft (2); air inlet for the aeration of the flow, in order to prevent cavitation (3); outlet tunnel (4) and terminal part (5). Sometimes, the outlet tunnel continues into the surface spillway chute, followed by the terminal part of the spillway structure.

In cases of a shaft spillway structure with a circular funnel intake, the circular overflow part is most often constructed as a vacuum-free profile that follows the coordinates of the lower boundary of the water current, which drops freely into the shaft. A vacuum profile is sometimes used, which has a higher value of the discharge coefficient, or else it can have a flat overflowing crest. The overflowing part gradually joints

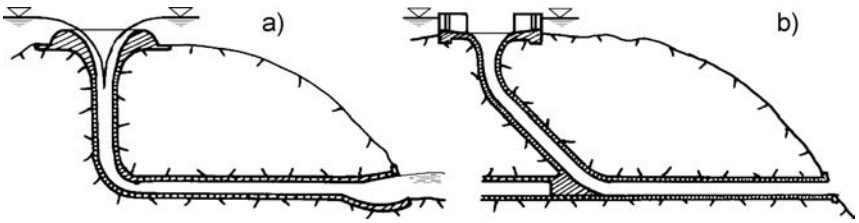

Figure 27.23 Shaft spillway. (a) Uncontrolled, with vertical shaft; (b) controlled, with inclined shaft.

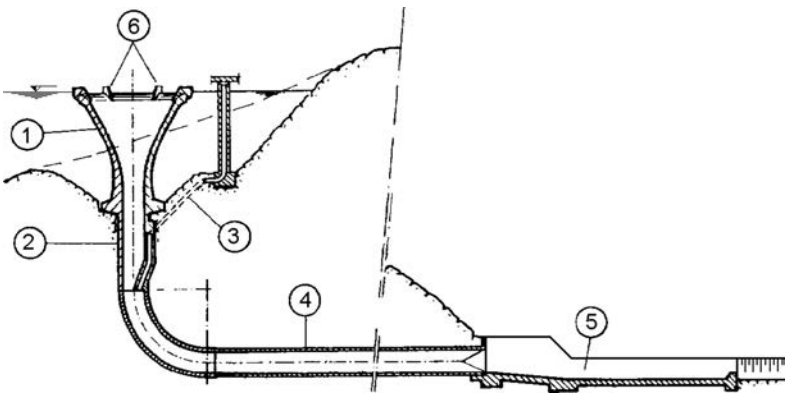

Figure 27.24 Schematic presentation of a shaft spillway. (1) Funnel; (2) shaft; (3) air inlet; (4) off-take tunnel; (5) terminal part; (6) rectifiers.

with the shaft, forming a funnel intake in the upper part. Submersion of the crest is not permissible, since it leads to reduction of the discharge capacity. The whirlpool movements of the water overflowing into the funnel inlet reduce the discharge capacity of the spillway and, for neutralization of the effect of this phenomenon, directing or heading walls or ribs (6) are constructed on the crest of the spillway. For providing uniform admittance of water, the ground around the circular funnel inlet is excavated up to a certain depth.

The height of the overflow jet over the spill-crest most frequently ranges within limits from 1 to 4 m while, with controlled shaft spillway structures, it can reach up to 8 m. The shaft spillways are mainly constructed as uncontrolled ones.

The vertical shaft with a circular cross-section is designed so that the wall follows the shape of the overflowing jet. Otherwise, a vacuum would occur in the shaft, and that can cause dangerous cavitational erosion to the lining. In any horizontal cross-section of the shaft, at a depth y below the maximum level of the headwater, the mean velocity should be:

$$v = \varphi\sqrt{2gy} \approx 0.9\sqrt{2gy} \tag{27.5}$$

where φ is a velocity coefficient containing the losses of pressure on the path from the headwater to the examined cross-section; these losses, to a greatest extent, consist of the local losses in the approach part and the funnel inlet.

The area of the live cross-section of the vertical stream, i.e. current, at a depth y, is:

$$F = \frac{Q}{v} \tag{27.6}$$

and it is recommended for the area of the horizontal section of the shaft, at a depth y, that it be from 10–20% greater, because of possible aeration of the water current:

$$F_0 = (1.1 \div 1.2)F = \frac{(1.1 \div 1.2)Q}{0.9\sqrt{2gy}} \tag{27.7}$$

By means of the above expression, we can obtain the contour of the shaft along the entire height, in which the section is reduced, going downwards. In practice, the shaft is designed as a cylindrical member in its lower part, gradually uniting with the funnel inlet. Details of the hydraulic dimensioning of the constituent elements of shaft spillway structures can be found in the specialized hydraulics textbook references.

When the shaft cuts into the ground, which appears to be a frequent case with steep inclinations of the bank, the whirlpool movement of the overflowing jet is rather manifest, which leads to a significant reduction of the overflow water quantity. In such cases, we can construct anti-whirlpool walls and piers, in combination with excavation around the spillway shaft structure, in order to provide a better approach for the overflowing water. The elements of such a construction are presented in Figure 27.25. The contour of the excavation, which can be either vertical or inclined, depending on the quality of rock, is defined with the equation of parabola:

$$z = \frac{4x(l - x)a}{l^2} \tag{27.8}$$

where $a = 1.75D_c = \text{const}$. For obtaining optimum performance in the working of the spillway structure, there should also be satisfied $l > 6D_c$ and $0 < n < 0.5$ (Fig. 27.25 – Mojs, 1970).

The outlet tunnel in plan should be designed as rectilinear. The shaft and the tunnel unite by means of a circular vertical curve with a radius:

$$R = (2.5 \div 4)D \tag{27.9}$$

where D is the diameter of the tunnel. The diameter of the tunnel is a function of the geological-engineering and hydrological conditions, as well as of the economical-technical solution of the spillway structure. In practice, there have been constructed tunnels with a maximum diameter of 15 m. Air should be brought in at the end of the bend, similarly to what has been described in the case of high-pressure gates and valves. The tunnel has either a concrete or a reinforced concrete lining.

In relation to the position of the level of the tailwater, the outlet tunnel, generally speaking, may be constructed for four different flow regimes, as shown in Figure 27.26

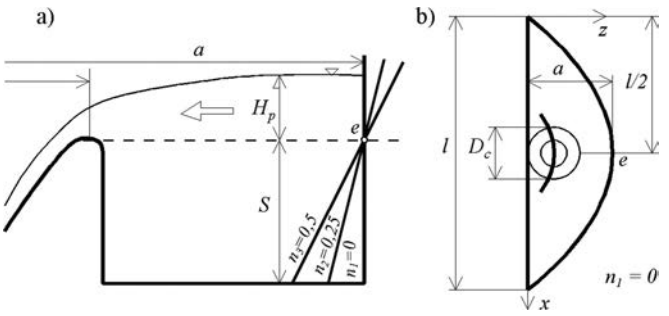

Figure 27.25 Shaft spillway structure, positioned in a side cut in the bank.

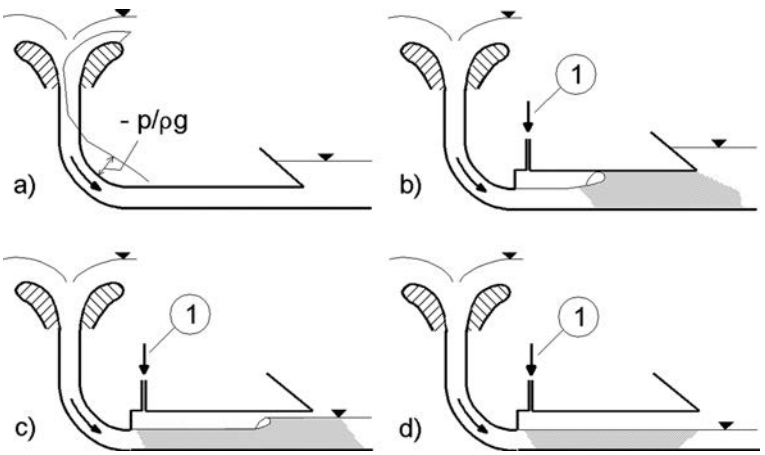

Figure 27.26 Configuration of the tunnel of a shaft spillway (after Novak et al., 2001). (1) Air inlet (shaded zones of the flow are aerated).

(Novak et al., 2001). From the point of view of stability of the flow in the tunnel and prevention of vibrations, the most favourable is the solution shown in the illustration (d). It is very important for the transition of the shaft into the tunnel to be well aerated, in order not to lead to the occurrence of a vacuum. The area of the cross-section of the pipe serving as an air inlet should amount to about 1/10 of the area of the cross-section of the tunnel.

In many cases, the diversion tunnel is used as an outlet tunnel for the shaft spillway structure, details of which can be found in Chapter 30. Such a combined solution should be avoided in cases of high-head plants, when the lowering of the outlet tunnel down to the level of the river channel is not obligatory, but it is possible to obtain a solution by positioning the tunnel at a higher elevation extending, i.e. lengthening the outlet tunnel with a surface spillway chute, Figure 27.30, in which we obtain lower velocities of flow in the tunnel and that is more favourable from the aspect of the service conditions.

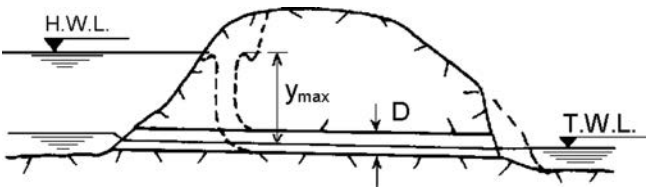

Figure 27.27 Schematic presentation of the combination of a shaft spillway structure and a diversion tunnel.

Figure 27.28 The shaft spillway of Globochica dam (Macedonia).

In order for it to be possible to apply a shaft spillway structure, it is necessary to have a certain minimum available value of y_{max} (Fig. 27.27). The shaft spillway structure would be inapplicable in the case if it were:

$$y_{max} < \left[15\left(\frac{Q}{1000}\right)^{0.4} + 2.5D\right] \tag{27.10}$$

where Q is expressed in m^3/s, while D and y_{max} are in metres.

The terminal section of the shaft spillway structure, in most cases is constructed in the form of a stilling basin, and more rarely as an object for throwing off the spillway jet.

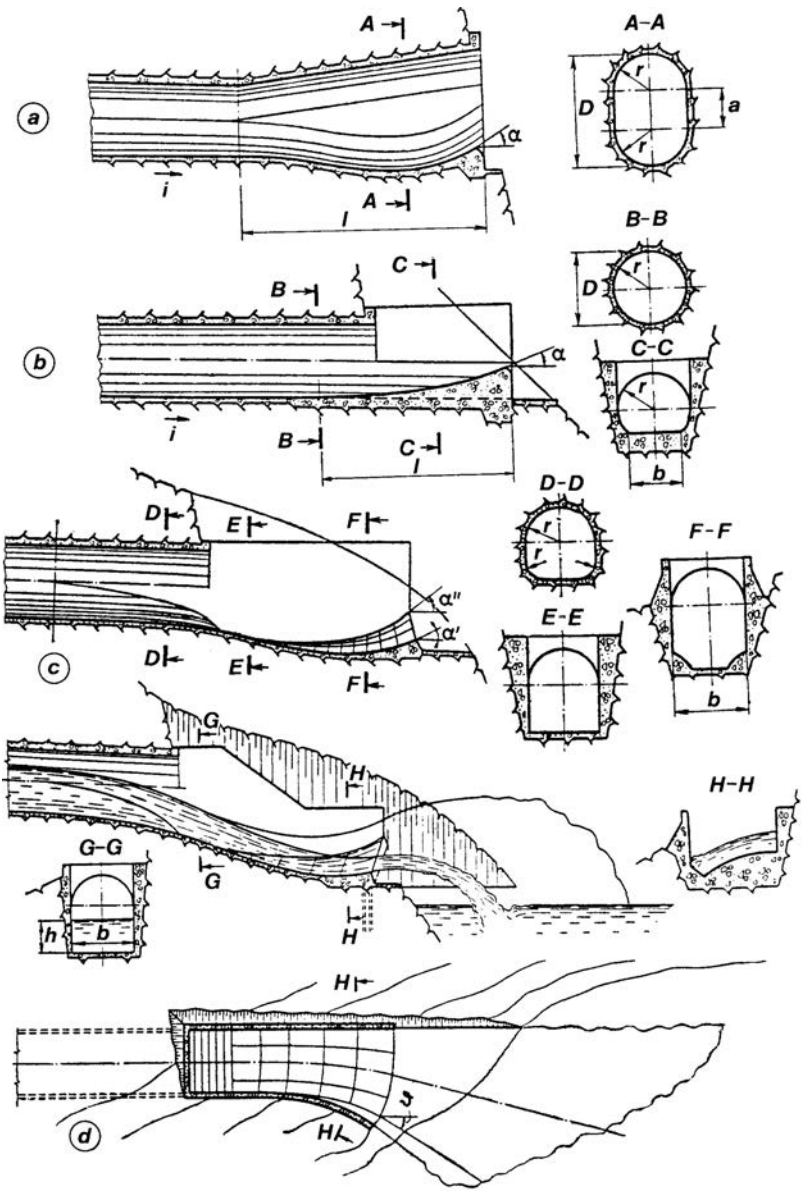

Figure 27.29 Possible alternatives for the construction of the terminal section of the outlet tunnel. (a)Elliptical; (b) cylindrical; (c) combined; (d) asymmetrical.

Possible alternatives for the construction of the terminal part are shown in Figure 27.29. The terminal part can also be constructed in the form of a stilling basin, with a previous transition part, by means of which there is a transfer from the circular cross-section of the tunnel into the rectangular cross-section of the stilling basin (Grishin et al., 1979; Chugaev, 1985).

Figure 27.30 The exit of the outlet tunnel and the surface chute of Globochica dam (Macedonia).

Figure 27.31 The shaft spillway at Shpilje dam (Macedonia).

The shaft spillway is very frequently used throughout the world, and in Macedonia as well (Figs. 27.31, 27.33). By way of illustration of the application of an uncontrolled spillway structure, there will be presented the spillway structure of the Tikvesh earth-rock dam on the Crna River (Macedonia), completed in March 1968, (YNCOLD, 1970), Figures 27.32 and 27.34. With its structural height of 113.5 m

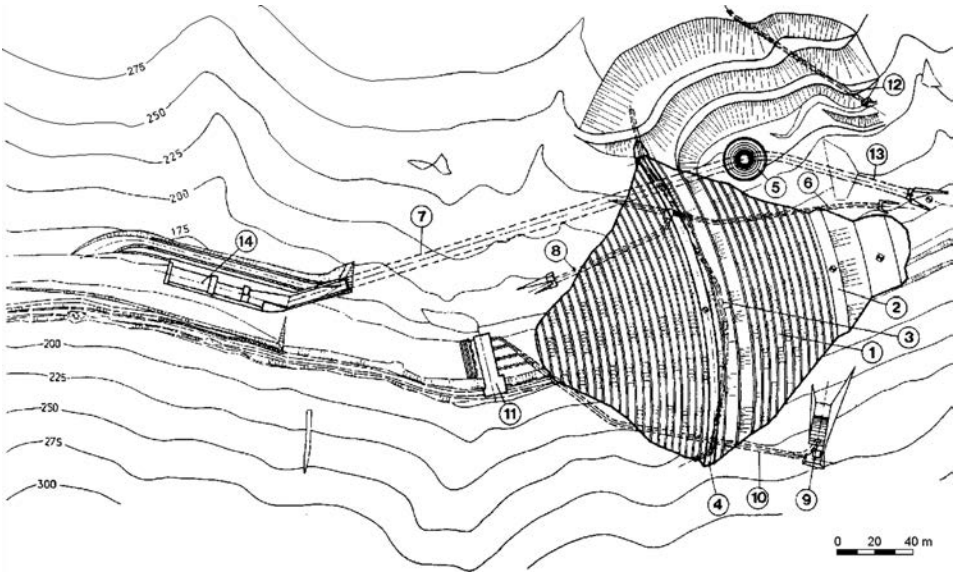

Figure 27.32 Site plan of the Tikvesh hydraulic scheme. (1) Dam; (2) cofferdam; (3) grout curtain; (4) dam axis; (5) spillway shaft; (6) bottom outlet; (7) outlet tunnel; (8) access gallery; (9) intake; (10) supply tunnel; (11) power house; (12) irrigation tunnel; (13) diversion tunnel.

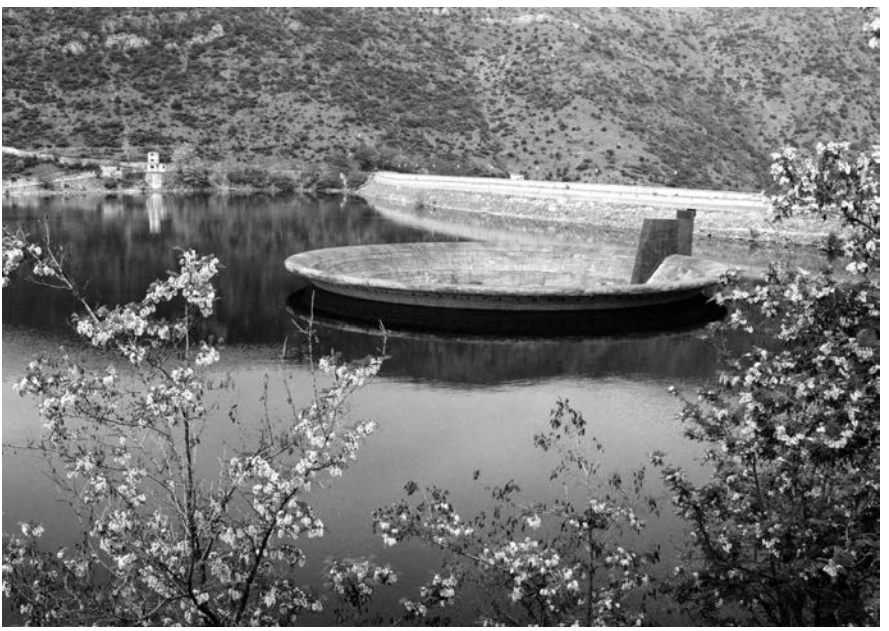

Figure 27.33 The shaft spillway of Tikvesh dam (Macedonia).

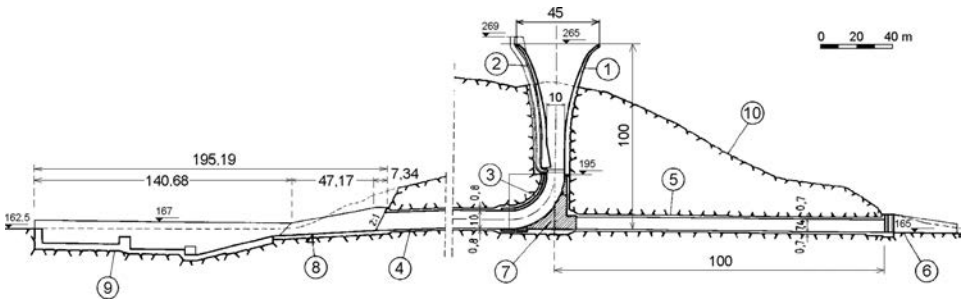

Figure 27.34 Longitudinal section through the spillway structure of the Tikvesh hydraulic scheme. (1) Shaft *spillway*; (2) air inlet; (3) strengthening of the lining in the shaft bend; (4) outlet tunnel (converted from the diversion tunnel); (5) diversion tunnel (closed); (6) water intake of the diversion tunnel (7) concrete plug for filling of the diversion tunnel; (8) surface chute; (9) stilling basin, shaped with model investigations; (10) ground line.

when it was constructed the Tikvesh dam was the highest dam in Macedonia, and it used to be the highest embankment dam in former Yugoslavia. It is founded on sedimentary rocks with surface and depth appearances that indicate tectonic faults. It impounds a live storage of 240 million m^3, which enables irrigation of 18,300 hectares of agricultural land in the Tikvesh Plain and an annual output of more than 200 GWh electric energy. The spillway structure has a capacity of 2150 m^3/s and consists of a circular shaft spillway with a diameter of 45 m, (1), Figure 27.34, an outlet tunnel with a diameter of 10 m (2), which ends up in a stilling basin (3), the shape of which has been determined by means of model investigations. The outlet tunnel in the course of the construction of the hydraulic scheme was used as a diversion tunnel for the evacuation of construction waters ($Q_{constr} = 630\ m^3/s$). In spite of the air inlet, i.e. supply of air (2), in the shaft bend, owing to the significant velocities of the flow, cavitation, and ageing of the concrete, the tunnel lining has been damaged and rehabilitation is necessary. This example is one more negative experience of jointing several water conveyance structures into one conduit structure, at such a high-head hydraulic scheme. In worldwide practice after 1970, such examples are not found any longer, since the negative experiences gathered in the previous period are sufficiently clear for drawing conclusions.

A shaft spillway can also be combined with the bottom outlet; that is to say, the bottom outlet can be jointed with the outlet tunnel of the shaft spillway structure, as is shown in the example in Figure 27.35. The joint between the two tunnels should be constructed at as small an angle as possible, with rounded contacts. The bottom outlet is handled through an underground gate chamber which, together with the approach tunnel (or gallery), should be properly isolated against penetration of water. One should take into consideration that these kinds of combinations increase resistances to the flowing in the outlet structures and aggravate their construction and service (Minor & Schmidiger, 1988).

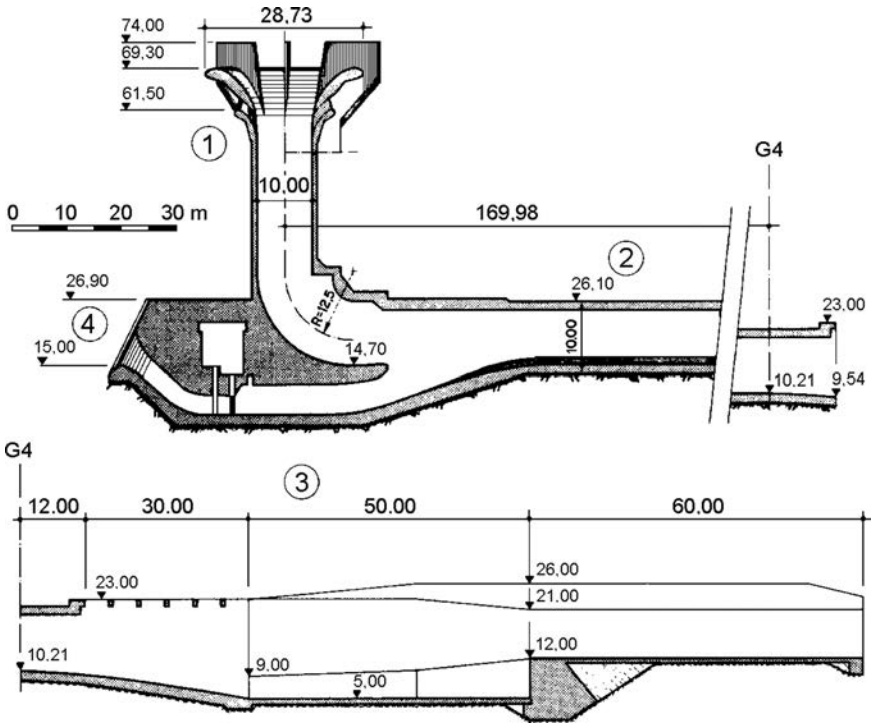

Figure 27.35 The spillway structure, along with the bottom outlet of the Oued El Makhazine dam (Morocco), 1979, $H = 67$ m, $Q = 1540$ m^3/s (Minor & Schmidiger, 1988). (1) Shaft spillway (2) outlet tunnel; (3) stilling basin; (4) bottom outlet with gate chamber.

27.4.2 Special types of shaft spillways

For improving the conditions of operation of the shaft spillway structures, for better adaptation to the topographic conditions of the ground, as well as for increasing of the overflow capacity, special types of shaft spillway structures are employed. A shaft spillway structure with an *incomplete circular funnel* is constructed next to the steep bank and does not require excavation of the ground to a greater extent or execution of anti-whirlpool constructional elements. An example of such a type of shaft spillway is shown in Figure 27.28, while a possible construction of this kind of spillway with controlled overflowing is presented in Figure 27.36a. The *spiral shaft spillway* (Fig. 27.36b) has an inlet part in the form of a spiral chamber into which the water overflows directly, or else is brought up through an approach channel. The overflow jet in the spiral chamber takes on a whirlpool flow, and an air core forms along the axis of the shaft, thanks to which the spillway works in a stable manner at any overflow quantities. It has been employed for $Q_{max} = 180$ m^3/s, with a diameter of the shaft of 6.0 m, and it is deemed that there can be obtained an economical and, from a structural viewpoint, favourable solution even for much greater quantities (Chugaev, 1985; Galant et al., 1995; Grishin et al., 1979).

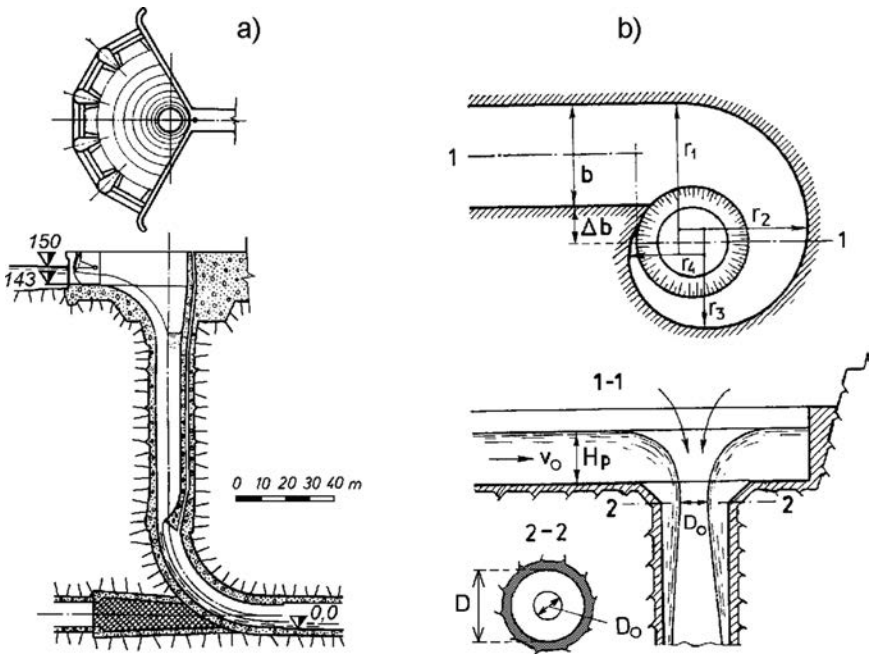

Figure 27.36 Shaft spillway with incomplete circular funnel intake (a) and spiral shaft spillway (b).

The shaft spillway structure with *duck bill* crest, *labyrinth,* or other special shape, makes it possible to obtain a long overflow front that ensures overflowing of significant quantities of water without considerable heightening of the maximum level of the headwater above the normal one, even if the specific discharge may be decreased owing to interference to flow (Blanc & Lempérière, 2001). The tendency for achieving this goal leads to different, often unusual, constructions of the spillway part. In the example, shown on Figure 27.37, the spillway can give passage to a maximum water quantity of 500 m^3/s. In this, the overflow height amounts to only 1.2 m. The spillway tunnel, of a diameter of 6 m, in the course of construction of the hydraulic scheme received water from the diversion tunnel which, afterwards, was transformed to serve as a bottom outlet, which is controlled by a tower-gate chamber (Chugaev, 1985; Thomas, 1976).

27.4.3 Tower spillway

Spillway structures in the form of a *tower* have certain similarities with the shaft spillway structure (Fig. 27.38 – Chugaev, 1985). In such cases, instead of a shaft, a tower is constructed in the upper part, above the ground, while the shaft is constructed only in the lower part, which is shorter than the upper one, above the ground. The tower must be so constructed as to eliminate the possibility of rising to the surface under the effect of the uplift water-pressure, which, as a rule, makes the construction

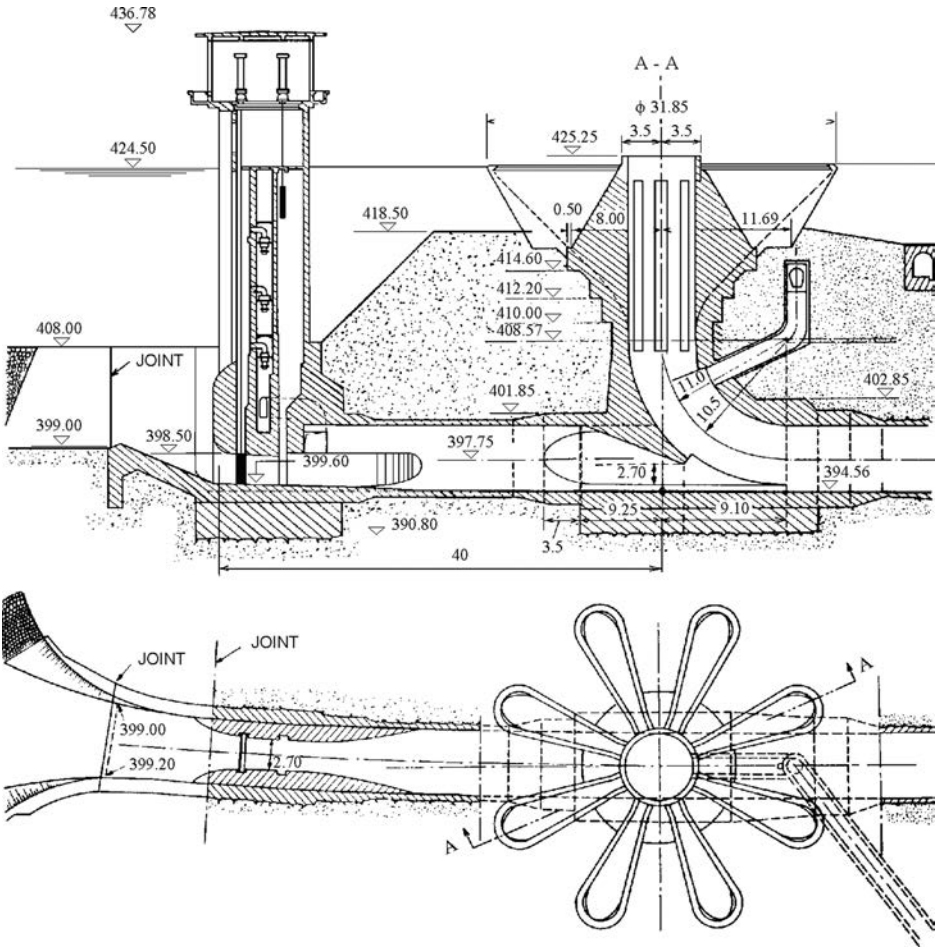

Figure 27.37 Spillway structure of the Sarno embankment dam (Algeria) (after Thomas, 1976).

of the works more expensive. Here again, an outlet tunnel is used as an outlet structure (Fig. 27.38a).

The solution with a spillway tower can also be applied when it is a question of a spillway through the body of an embankment dam, (Fig. 27.38b). In such a case, a gallery (3) is used as an outlet structure, which is constructed prior to the application of the filling of the dam's body. The construction illustrated under (b) is employed for small overflow quantities and, in practice, it is rarely encountered. During its design, it is necessary to take into account the danger of nonuniform settlements of the tower and the outlet gallery, as well as of preventing contact seepage between the concrete and the earthfill embankment. This problem will be more extensively examined in the chapter on outlet works.

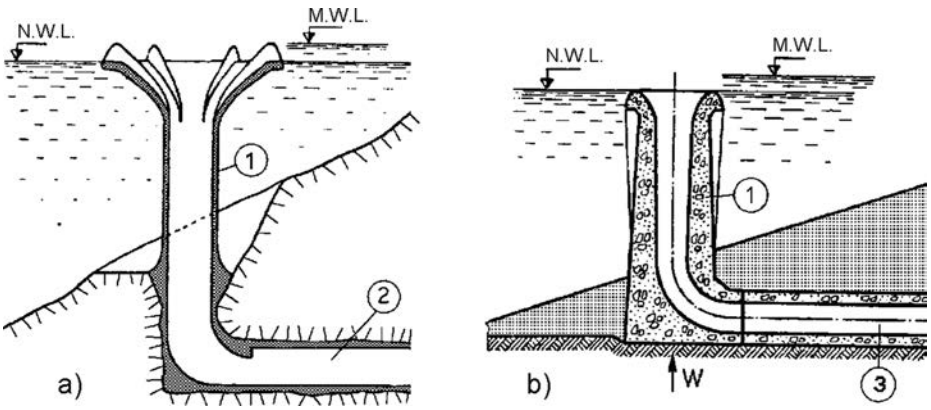

Figure 27.38 Spillway structure in the form of a tower with offtake in the form of an outlet tunnel (a) and gallery through the dam's body (b). (1) Tower; (2) tunnel; (3) gallery.

27.5 Labyrinth spillway

A spillway crest in the form of a *labyrinth*, consisting of a broken line, is considered to be a very efficient way of increasing the overflow capacity, at a fixed width of the spillway. The model investigations indicate that, in spite of the complex character of the flow through such a spillway, according to the cost it can be competitive with the other possible solutions (Yildiz & Üzücek, 1996). The labyrinth spillway is used to concentrate discharge into a narrow chute, where space does not permit a linear ungated crest. It generally minimizes approach excavation, whereas the concrete weir is more complicated to construct. An adequate foundation is necessary for economical construction of this kind of spillway. Labyrinth spillways have been built with a wide range of sizes and discharge capacities and are well suited for rehabilitation of existing spillway structures when increased spillway capacity is needed. The discharge coefficients of these spillways are usually (but not always) somewhat smaller than those of conventional spillways.

A typical layout of a labyrinth spillway is shown in Figure 27.39. The number of spillway cycles should be determined on the basis of the magnitude of the upstream head, the effect of nappe interference, and the economics of the design. Under normal operating conditions, the vertical aspect ratio w/P for each labyrinth cycle should be 2.5 or greater. Discharge capacity is a function of the head over the crest (H_t), the height of the crest wall (P), the shape of the crest (Fig. 27.39C), the angle of the labyrinth (α), the number of cycles, and the length of the side leg (L1 – an actual length; L2 – an effective length of side leg). Knowing the design discharge Q and the maximum head, the required effective length L can be determined from the following equation (Tullis et al., 1995):

$$Q = \frac{2}{3} C_d L \sqrt{2g} H_t^{\frac{3}{2}} \tag{27.11}$$

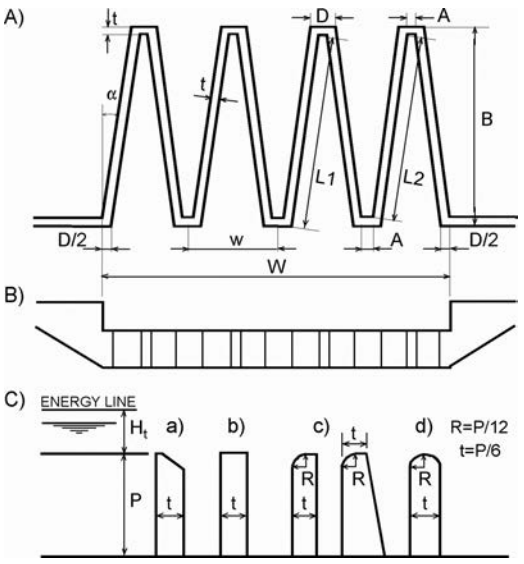

Figure 27.39 Layout (A), upstream view (B) and possible shapes of the spillway crest (C) of a typical labyrinth spillway weir (after Tullis et al., 1995). (a) Sharp crest; (b) flat; (c) ¼ round; (d) ½ round.

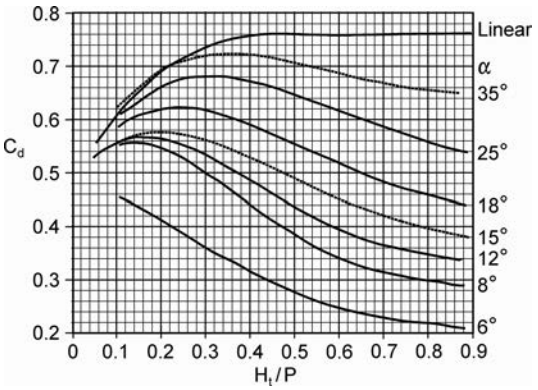

Figure 27.40 Crest discharge coefficient C_d for labyrinth spillways (after Tullis et al., 1995).

where the discharge coefficient C_d can be derived from the diagram shown in Figure 27.40; for $\alpha = 8°$, and $H_t/p = 0.8$, $C_d = 0.30$. Then, fixing the apex A, the number of cycles in the labyrinth N can be determined from the formula

$$L = 2N(A + L2) \tag{27.12}$$

where $L2$ is sized to produce an integral number N.

To find the most economical labyrinth size, other trial sizes can be determined by assuming different angles α (other than 8°) or by varying H_t/p (it should be ≤ 0.9). It is important to note that the costs of the other spillway elements, like the approach channel, spillway chute and terminate structure, may influence the ultimate selection of labyrinth geometry.

After the selection of the labyrinth size, follows detail as: $t = P/6$, $R = P/12$, and $A = (1 \text{ to } 2t)$. The suitable crest shape is quarter-round. The width of the spillway chute downstream is equal to the width of the labyrinth W. To avoid the submergence effect, the supercritical flow condition should be maintained at the chute crest downstream from the labyrinth, and the chute slope must be supercritical for the entire flow range (Tullis et al., 1995).

Traditional labyrinth spillways, mainly constructed with vertical walls and a trapezoidal layout, have been used for more than 70 years. They are rather simple structures, but relatively expensive, requiring a massive (wide) base and a high quantity of reinforced concrete.

Since 1998 many studies and model laboratory test have been performed, mainly in France, with the aim of improving the shape of the labyrinth spillway and thus to make it more rational and more economical. The result is a new type of labyrinth spillway, named *piano key weir* spillway. Most solutions of this spillway type are based on a rectangular layout on a narrower crested weir than present at a classical labyrinth spillway, and one or two overhangs (upstream and downstream) of the "piano key" spillway part. This improved type has found application in the upgrading of existing free-flow spillways, but also as a free-flow spillway added to a gated spillway and as a free-flow spillway for new dams (Lempérière, 2000; Blanc & Lempérière, 2001; Lempérière & Ouamane 2003; Hughes, 2010; Lempérière et al., 2012; Pinchard et al., 2013; Laugier et al., 2013).

On the labyrinth-shaped top of the spillway fusegates are often applied. Since their first use in 1991 (Lemperière, 1992) fusegates have been installed in many countries, mainly during the reconstruction or enlargement of the capacity of existing spillways. Actually, fusegates are a type of surface gate. Their height can be up to 75% of the free spillway head and they can pass moderate floods as a spill over their labyrinth-shaped top. For higher floods, at precisely determined reservoir level, the independent free-standing units turn about a downstream sill, when a bottom chamber filled through an inlet well generates an uplift pressure beneath the unit. After the flood has receded the overturned units can be replaced by new ones. When they require frequent replacement, the fusegates become uneconomical. There are ideas for improvement and rationalization of the fusegates for application at piano key weir spillways (Lempérière et al., 2012).

27.6 SIPHON SPILLWAYS

Siphon spillway structures fall within the series of spillway structures with automatic action and they operate as uncontrolled structures. They can be constructed in a separate concrete block, outside the dam's body, but also they can be constructed in the body of concrete dams (Fig. 27.41a–c), as well as in the form of a tower with an outlet gallery below the body of embankment dams (d) (Grishin et al., 1979).

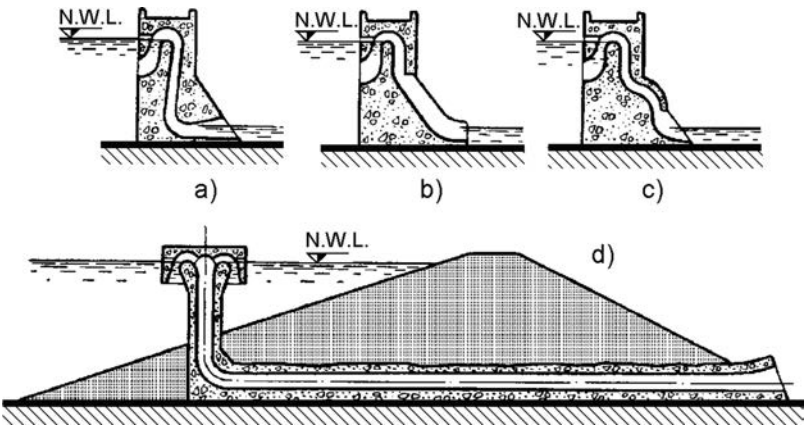

Figure 27.41 Examples of siphon spillway structures.

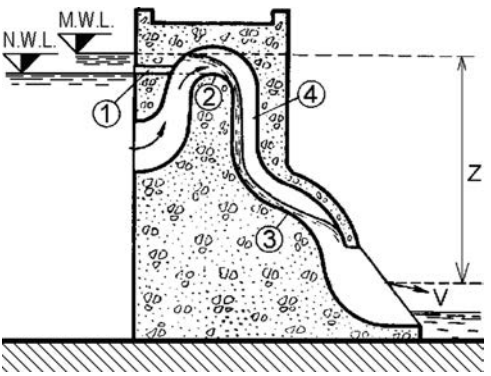

Figure 27.42 Siphon spillway – principle of work.

The siphon spillway is a closed conduit in the form of an inverted U, which consists of an inlet part, a short upper leg, throat, air pipe, lower (downstream) leg, and outlet. The principle of work of the siphon spillway can be clarified in the scheme presented in Figure 27.42. Point 2 is at the elevation of the normal water level in the reservoir, where the air vent is also located (1). When there is heightening of the level of the headwater above the normal water level, the air vent is submerged, at which there begins overflowing of water over the crest of the spillway structure (2). At the beginning, the overflowing water quantity is insignificant and so the overflowing over the crest of the throat is free, as it is over an ordinary weir. With its increase (and the increase of the level of headwater), the velocity in the siphon also increases and, at point 3, in the lower leg, the water current reflects from the concrete and strikes into the wall of the opposite side of the siphon, in which a closed air zone (4) forms in it. Following the elapse of a short time interval, the air of this zone is sucked up by the

water stream, at which the siphon is filled and begins to work under head Z, which means that the exit velocity of the siphon is:

$$v = \varphi\sqrt{2gZ} \tag{27.13}$$

The beginning of the work of the siphon with a full capacity normally takes place when the level of headwater reaches about one-third of the height of the throat. In that way, a vacuum is created in the upper part of the siphon.

In the equation (27.11), the velocity coefficient φ can be expressed as:

$$\varphi = \frac{1}{\sqrt{\xi_1 + \xi_2 + \xi_3 + \xi_4}} \tag{27.14}$$

where ξ_1, ξ_2, ξ_3 and ξ_4 are head-loss coefficients for the entry, bend, and exit, as well as friction losses in the siphon.

At drawdown of the level of headwater, there comes about an inverse process. When the air vent (1) is released, through it the air enters the zone of the vacuum and the siphon empties, while the water in the reservoir remains at the normal level.

Similar to other spillway structures, the siphon spillway can also consist of several conduits set up in parallel. The area of the inlet cross-sections of the siphon conduits is usually 2–3 times greater than the area of the cross-section in the throat, at the crest (point 2). Dimensions of a rectangular cross-section of the siphon conduit usually range within the following limits: height $a = 1.5$–2 m; width $b = (1.5$–$3.0)a$; and radius of curvature in the upper part over the point 2: $r \geq (1.5$–$2.5)a$. The width $h_{\min}$, at which the siphon begins to work, is:

$$h_{\min} = (0.16\text{–}0.20)a \tag{27.15}$$

The siphon spillway must be well-conceived, designed, and constructed in order to work properly and effectively, without harmful associated phenomena, of which cavitation may be especially inconvenient. That is why, especially when it is a question of siphons that work under a high-head – for instance >10 m – it is necessary to carry out precise hydraulic calculations, supported by model investigations.

The downstream part of the siphon conduit is sometimes executed with constriction at the exit, in order to reduce the value of the vacuum in the uppermost part. In this, the value Z can obtain a value up to 40 m. The specific discharge of siphon spillway structures ranges up to 25 m^3/s per metre of the spillway front.

An exceptionally interesting example of a siphon spillway has been carried out within the Burgkhammer concrete dam ($H = 22$ m), Germany, which has been in service since 1932. It consists of 6 siphon pipes installed in a 21 m long concrete block. Each span is 3 m wide, 1.8 m high, and at the end there has been performed a constriction to 2.8 m (width) and 1.2 m (height), Figures 27.43 and 27.44 (Bollrich, 1994). Besides the siphon spillway, which has a capacity of $6 \times 50 = 300\ m^3/s$, the hydraulic scheme also has a controlled spillway over the dam, with a capacity of $2 \times 110 = 220\ m^3/s$.

From the cited elevations in Figure 27.43 one can notice that the siphon works under an exceptionally high head for this kind of construction, from 15.10 to 16.00 m.

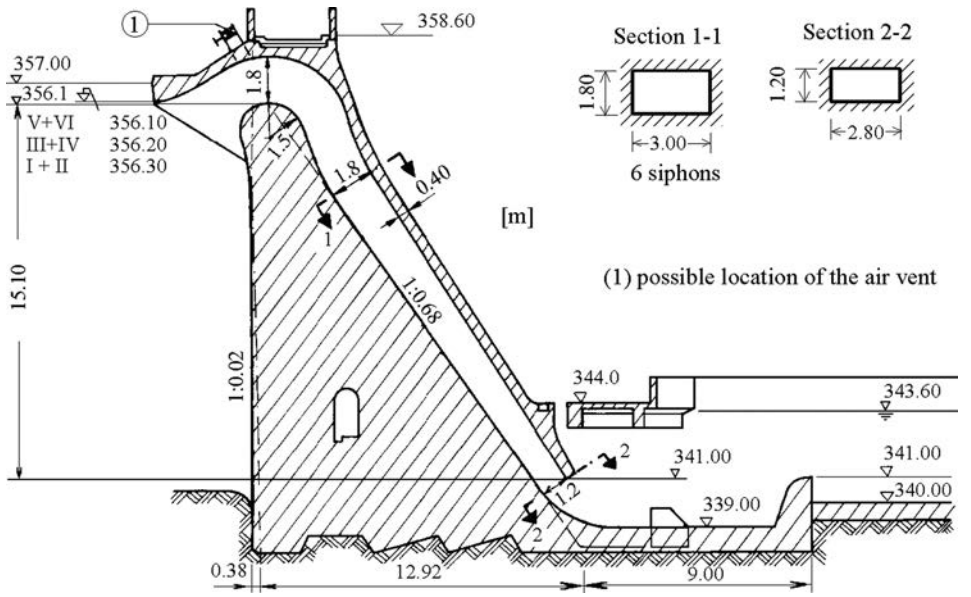

Figure 27.43 Siphon spillway structure of the Burgkhammer dam, Germany (Bollrich, 1994). (1) Possible location of the air vent.

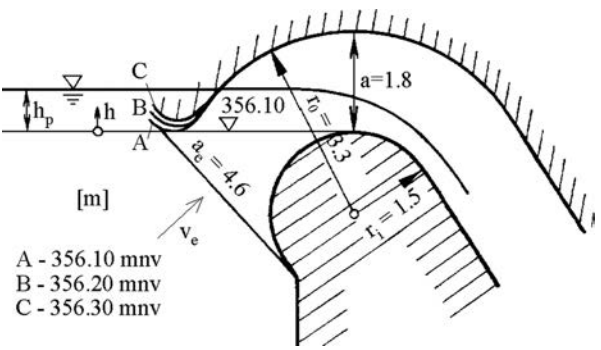

Figure 27.44 Overflowing into the siphon prior to its activation (Bollrich, 1994).

In order to avoid simultaneous overflowing at full capacity, the inlets of the six conduits have been positioned in pairs, at intervals of 10 cm above the overflow crest (the elevations are 365.10, 365.20, and 365.30 mwl). The siphon is activated in such a way that it is kept submerged at the downstream end by means of an overflow weir, with a crest at an elevation of 341.00 mwl.

Owing to the high-head under which it operates, the siphon is permanently investigated, especially from the aspect of the danger of the occurrence of cavitation. As a result of these investigations, it has been proposed to include a short aeration pipe

as an air vent (1), controlled with a valve, which would normally be kept in a closed position. The required cross-section of the aeration pipe would be 0.2 m^2, which corresponds to a pipe with a diameter of 500 mm, and that is 3.7% of the cross-section of the siphon pipe. This air vent would enable reduction of the discharge, Q, to any value; that is to say, the siphon spillway would be made a regulated one; however, the installation of such a vent in the reinforced concrete wall of the six siphons would be very complicated. Also, there remains the danger of errors in handling with the valves.

In brief, siphon spillways have the following advantages:

- They can give passage to significant quantities of water, without noticeable heightening of the level of headwater above the normal one;
- The inclusion in work and the exclusion from work is performed automatically, without having a need for expensive mechanical equipment (gates and mechanisms for lifting);
- They are an excellent alternative as an additional spillway structure when it is necessary to perform an increase in the installed overflow capacity.

At the same time, the siphon spillway structures also have certain disadvantages:

- In the usual case, it is not possible to regulate the discharge – the siphon conduit, starting with its work, lets through a full discharge as long as it is switched off from work;
- Letting through of ice and floating solids is difficult;
- In areas with low temperatures, there exists a danger of freezing of the air vent and the inlet of the conduit;
- In switching on and switching off the siphon pipes, vibrations in the structure can take place.

Chapter 28

Bottom outlet works

28.1 BASIC ASSUMPTIONS ON DESIGNING BOTTOM OUTLET WORKS

Bottom outlet works within hydraulic schemes with a reservoir are constructed in order to ensure conveyance of water from the reservoir into the lower part, downstream of the dam, in order to facilitate lowering of the level of the reservoir, or else to ensure water for the biological minimum flow in the riverbed, downstream of the works. In cases of small dams and reservoirs, the bottom outlet structures often also serve for intake of water for some user as well, most often for irrigation. As has been said in the general part, in Chapter 23, an outlet structure is also called a *bottom outlet*, owing to the fact that the intake of water is constructed at a low level, close to the foundation of the dam. In Chapter 23, there have been set out the basic issues regarding outlet structures, including the question of design water.

According to their position in relation to the dam, bottom outlet works are classified in two groups:

1. Outlet structures passing through the dam's body;
2. Outlet structures that are placed in the bank, outside the dam's body.

The outlet structures, in cases of hydraulic schemes with a concrete dam, regularly fall within the first group, while in cases of hydraulic schemes with an embankment dam, they can be of both the first and the second type. When there are questions of bottom outlet works of the first group, a steel or reinforced concrete conduit pipe is employed, while in the second group, it is a pressure tunnel or, in more rare cases, completely or partially, by means of flow under a free water table.

Outlet structures most often work periodically and, in more rare cases, they can also work permanently if they serve for the provision of the biological minimum flow in the river channel, downstream of the hydraulic scheme. In this second case, it is necessary for the outlet structure to consist of a minimum of two conduits, in order to enable exclusion of one of them in case of need for overhaul in the course of service.

An important question in designing the outlet works is the arrangement and type of valves and gates (Kipping, 2001). Each outlet structure must be provided with two gates or valves – a service (basic) and an overhaul gate or valve. Regarding the arrangement, type and method of handling the valves and gates, due attention is paid at relevant places in the two forthcoming sections.

The bottom outlet structure works under variable head-pressure and should be designed so as to facilitate emptying of the reservoir for a certain period of time, that is to say, give passage to the anticipated quantity of water at given elevations of the headwater and tailwater. In connection with that, appropriate hydraulic calculations should be constructed, by means of which the following questions will be successfully solved:

- Determination of the discharge capacity of the outlet structure;
- Prevention of the possibility of cavitation;
- Shaping of the elements so that there would result the least possible hydraulic resistances and hydrodynamic forces;
- Anticipation and dimensioning of air inlet;
- Defining the flow regime at different discharge quantities, different levels of headwater and tailwater, different openings of the service gate or valve;
- Dimensioning for the terminal structure;
- Determination of the conditions for creating composite action of the flow at the transition into the natural channel;
- Determination of deformations of the soil or the rock at the part of the riverbed that is immediately next to the terminal structure.

In designing the bottom outlet structure, of particular significance is the question of fighting the occurrence and the harmful effect of cavitation. It has been proved that, already at a velocity of the flow of 11 m/s, a normal unevenness of a concrete surface of 3 mm can cause cavitation (Novak et al., 2001). In order to prevent the occurrence of cavitation, it is necessary to undertake appropriate measures, which will be discussed later. In cases of greater and more complex structures, a necessary measure is the construction of a model or prototype on which appropriate investigations and measurements will be performed.

28.2 BOTTOM OUTLET WORKS IN CONCRETE DAMS

The material of which concrete dams are constructed, as well as the nature of their construction, enables relatively simple solving of the question of designing the bottom outlet structure. In the cases of gravity and arch concrete dams, the bottom outlets consist of steel pipes embedded into the dam's body, each provided with two valves (Fig. 28.1). It is recommended that a minimum of two pipes be used in order to achieve greater safety in service. Also, in cases of buttress dams, steel pipes are employed, positioned in the opening between the buttresses. Examples can be found when the pipes have been embedded in the buttresses. The bottom outlets in concrete dams consist of the following elements: (1) inlet part; (2) outlet part; (3) gates or valves; and (4) dissipator of energy (possibly).

A rough trash rack is installed at the inlet part, through which the maximum velocity of flow should not be greater than 1 m/s. It is made of strong metal bars and is raised higher than the upper edge of the opening. The trash rack can be a plane; however, it is better curved, in order to ensure access of water not only from the head, but also laterally. Behind the trash rack there slots for an overhaul gate. The inlet into the pipeline conduit is widened and rounded in order to reduce the local head losses.

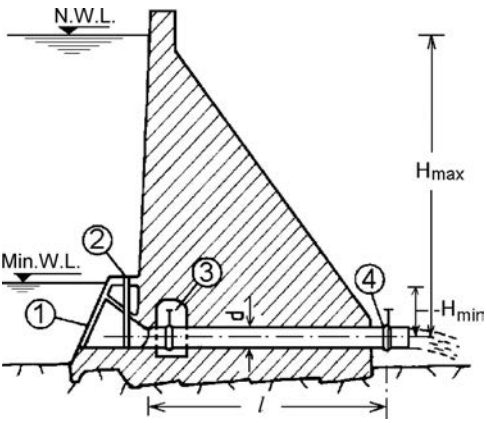

Figure 28.1 Scheme of outlet with a mass dam. (1) Rough trash rack; (2) slots for standby or emergency valve; (3) valve chamber; (4) regulating valve.

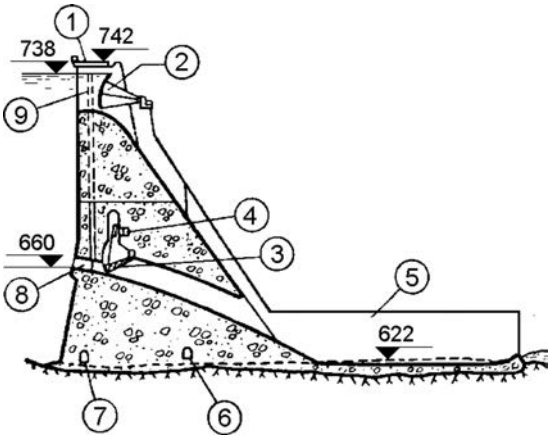

Figure 28.2 Outlet and spillway of the Libby dam (1973). (1) Bridge; (2, 3) radial gate; (4) gallery; (5) training wall; (6) drainage gallery; (7) grouting gallery; (8) three outlet openings; (9) two spillway openings.

Two valves, or gates, are usually constructed: a basic (or service) one, installed at the beginning, and an auxiliary or regulating one, located at the exit (outlet). In some cases, both valves (gates) are placed close each other.

At the end of the pipeline conduit, a stilling basin for dissipation of energy is carried out, Figures 28.2 and 28.3, while in the case of sound rock the water jet can be discharged with a free fall and with previous sprinkling over appropriate types of high-head valves. In cases of overflow dams, it is rational if the outlet structures are positioned below the spillway, in order to utilize the dissipator of energy of the spillway structure, as is in the example of the Libby Dam (USA), 129 m high, Figure 28.2.

Figure 28.3 The terminal part of the bottom outlet of the Gratche dam (Macedonia).

The discharge capacity through the outlet is determined with the expression for free discharge:

$$Q = \mu F\sqrt{2gH_{\max}};$$

$$\mu = \frac{1}{\sqrt{1 + \Sigma\xi_1 + \frac{\lambda l}{d}}} \tag{28.1}$$

where F is the cross-section of the conduit; $\Sigma\xi_1$ are the total local losses; and λ is the coefficient of friction, while other factors are seen in Figure 28.1.

28.3 BOTTOM OUTLET WORKS IN EMBANKMENT DAMS

The type and construction of the outlet structure within the hydraulic scheme with an embankment dam is dependent on the topographic and geological conditions, and the structure of the dam, as well as on the quantity of water that has to be discharged. These outlets are constructed as: (a) a pipe or gallery below the embankment of the dam or (b) as a tunnel in the bank, outside the dam's body, which is the much more frequent case. The first type is utilized in hydraulic schemes with an earthfill dam with a low pressure head and consists of one or more pipe conduits, provided with valves or gates, with a structure for intake of water and control of the valves or gates in the form of a tower, or with a chamber in the form of a gallery. The solution with a tower is much more widespread, because it is safer from the aspect of service.

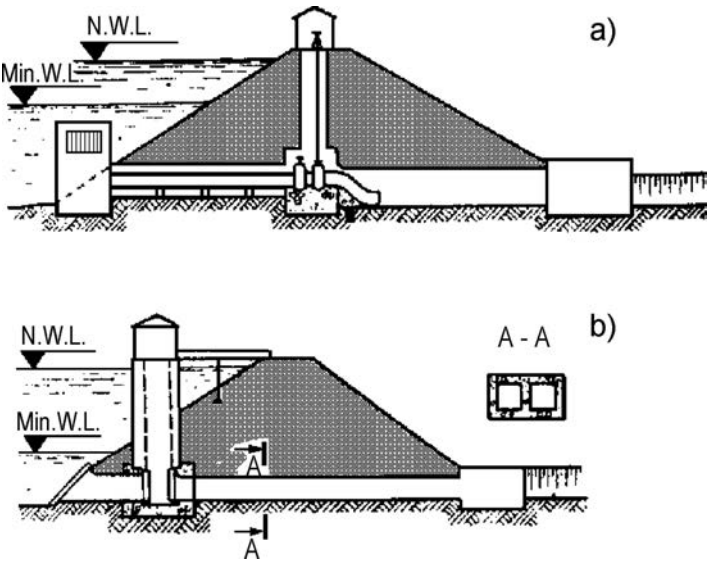

Figure 28.4 Tower-gate/valve chamber in the central part of the dam (a), and in the initial part of the dam (b).

The conduits are constructed as reinforced concrete galleries or as steel pipe conduits, lined with reinforced concrete. The tower-gate/valve chamber can be located in the central part of the dam, or else in the initial part (Fig. 28.4a, b). In the first case, the approach to the tower is simpler; however, the greater part of the conduit is permanently under water. Very often, the gallery for the bottom outlet is utilized for giving passage to the water in the course of the construction of the hydraulic scheme, for which a greater cross-section is necessary. In such cases, usually in the gallery, there is embedded a steel pipe on which the valves are mounted. In the example 28.4a, the pipe has been embedded from the intake structure to the tower; however, it is more often positioned between the tower and the terminal structure. The pipe rests on concrete supports at each 5–6 m.

The tower is most often constructed with a planned circular cross-section, with an internal diameter that is determined depending on the diameter of the conduits and the dimensions of the control mechanisms for the valves and gates, but not smaller than 2.5–3 m. Often, the thickness of the tower wall gradually decreases from below upwards and it should not be less than 20 cm.

Reinforced concrete galleries, in which the flow takes place under pressure, are designed with a circular internal cross-section, and on the external side in the upper part with a circular section, while flat in the base, all in order to achieve a uniform transfer of stresses in the foundation (Fig. 28.5). The lateral walls at the external side are made vertical, or slightly inclined, in order to achieve better composite action with the embankment, without the occurrence of "hanging" and noticeable differentiated settlements. At the external side, it is good to carry out waterproofing based on bitumen or else with epoxy resins on the wall. By means of joints, the gallery is divided at

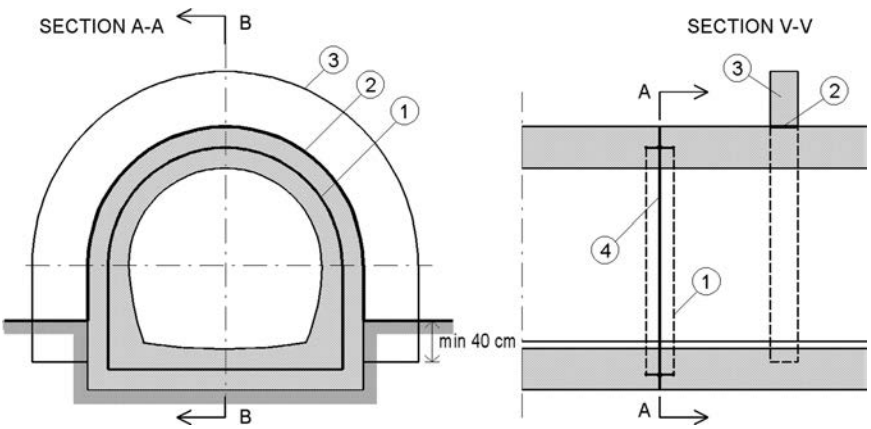

Figure 28.5 Reinforced concrete water-conveyance gallery. (1) Rubber waterstop seal; (2) waterproofing; (3) reinforced concrete cutoff collar; (4) joint.

each 10–15 m. Rubber waterstop seals are incorporated into the joints, while the reinforcement extends from one section into another.

The preparation of the foundation in the zone in which the water-conveyance conduit will be laid must be equivalent to the preparation of the foundation for the dam itself. In order to improve the connection between the pipe or gallery conduit and the foundation and also in order to reduce contact seepage, reinforced concrete *cutoff collars* are constructed (also called *diaphragms*) along the zone of contact of the water-conveyance conduit with the impervious material of the dam's body (3, Fig. 28.5). Most frequently, the cutoff collars are 60–90 cm high and 30–40 cm wide. They are positioned at distances 7–10 times the height, along the length of the part of the pipe conduit that lies in the impervious zone (USBR, 1977). For water-conveyance conduits set up on a soil (non-rock) foundation, the cutoff collar should completely surround the pipe conduit. In cases of a rock foundation, it is sufficient for it to be founded in the rock at a depth of a minimum of 40 cm (Fig. 28.5). In order to avoid concentration of stresses in the wall of the water-conveyance conduit, the cutoff collar should be separated from the pipe conduit. This is most often achieved with the execution of a layer of asphalt mastic in the interface (2, Fig. 28.5); sometimes the cutoff collars are constructed on the joint itself.

The conduit can also be made out of prefabricated elements. Elements of prestressed concrete are especially suitable for that purpose, owing to their low mass. At the small Buchinci dam (near Skopje, Macedonia), the bottom outlet has been constructed with prefabricated prestressed concrete pipes ϕ80 cm, with a wall thickness of only 6.5 cm. One pipe comes into another, while the water-impermeability of the joints is achieved with simple incorporation of rubber rings. During testing under pressure, two times the pressure of the hydraulic scheme, none of the joints has shown water leakage, while the thin concrete lining showed leakage at only 2–3 spots, which have been repaired with a coating of epoxy resin.

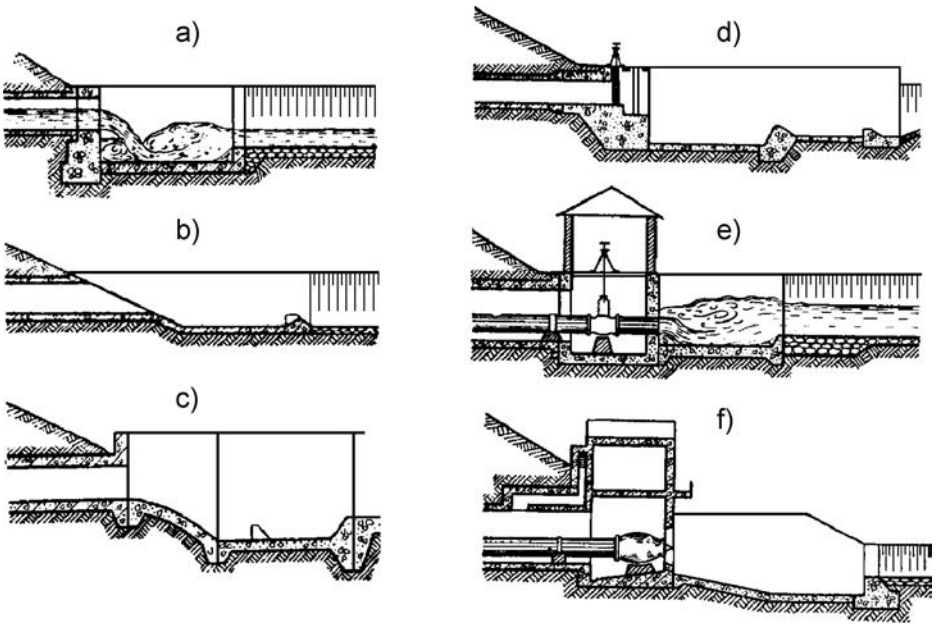

Figure 28.6 Schemes of the terminal part of outlet works (Grishin et al., 1979).

The internal dimensions of the galleries with a free water table are determined from the condition for letting through the construction waters, for which purpose the gallery is regularly used in the course of dam construction. Furthermore, an influence on the dimensions is also made by the conditions for placement of the pressure pipe conduits within the framework of the bottom outlet. The space should be so planned as to enable unobstructed placement and maintenance of the pipeline conduits and equipment. The bottom is most often flat, while the pipeline conduits lie on especially prepared concrete seating. When deformations are expected, we should anticipate joints spaced at distances of 10–15 m along the length of the gallery. Devices for taking on deformations are anticipated in the joint and are called *compensators;* anti-seepage measures are also undertaken. For the accommodation of the compensators that, most often, consist of two concave metal sheets, the section of the gallery is thickened by 0.8–1 m.

Possible solutions for the exit (outlet) part of the bottom outlet with a tower, or with a gallery, as well as a valve chamber, are presented in Figure 28.6a–c. Those are, in fact, structures for energy dissipation in the form of a stilling basin. In accordance with the specific conditions, the designer will decide which type to adopt. Instead of in the initial or in the central part, the handling with the bottom outlet can be performed through a valve chamber at the end of the gallery, i.e. of the pipeline conduit. In such a case, the terminal part of the bottom outlet, in which discharge and stilling of the flow jet is performed, may be constructed as shown in Figure 28.6d–f. Sometimes, such a solution is dictated by economy and by the possibility of employing a certain type of valve (cone, or needle), which is fitted at the end of the pipeline conduit.

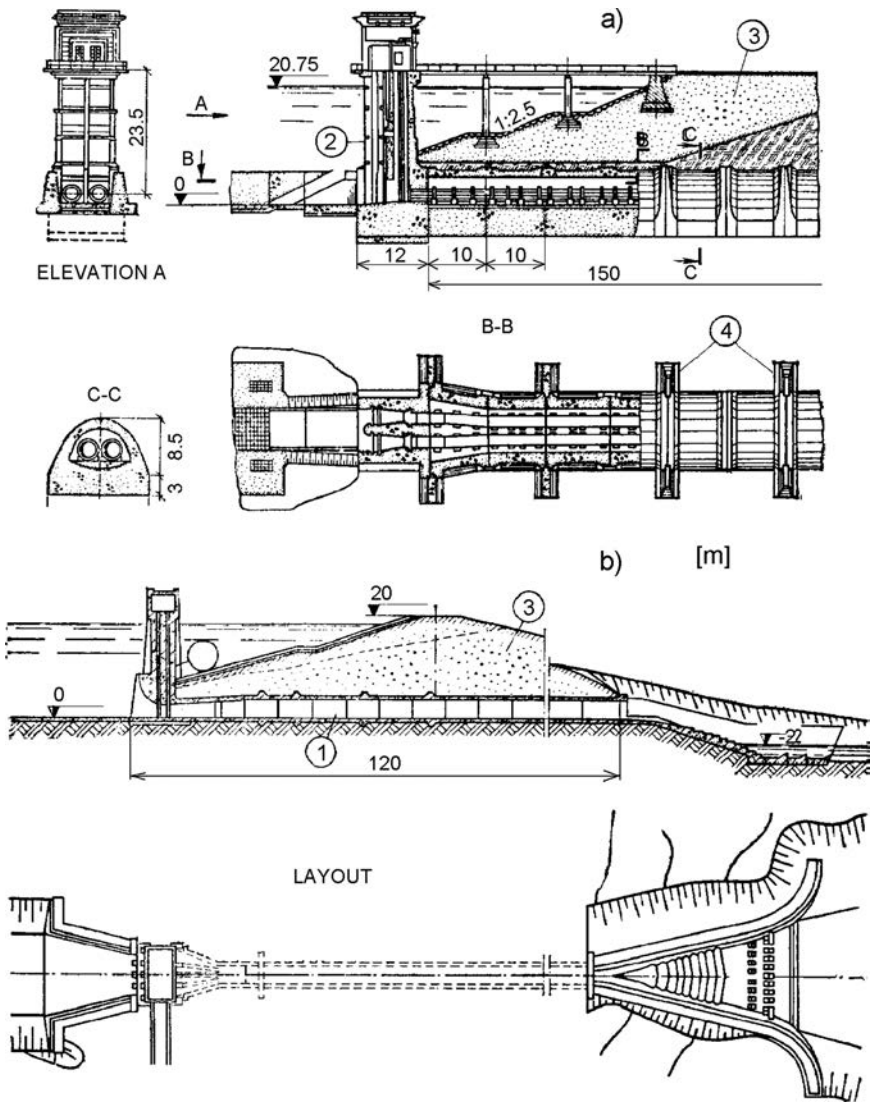

Figure 28.7 Outlet structure with a tower and gallery in which there are installed steel pipes (a) and reinforced concrete pipe (b) (after Grishin et al., 1979). (1) Reinforced concrete pipe; (2) tower; (3) embankment dam; (4) reinforced concrete cutoff collars.

Practical examples of a bottom outlet below the body of an earthfill dam, with a tower-gate chamber in the inlet part, are presented in Figure 28.7 (Nedriga et al., 1983). In the example (a), in the reinforced concrete gallery there are parallelly installed two steel pipes, fixed to concrete supports by means of steel pipe-jointing clips. At each 20 m around the gallery, there have been constructed reinforced concrete cutoff collars, intended to lengthen the path of the contact seepage. In the example (b) the

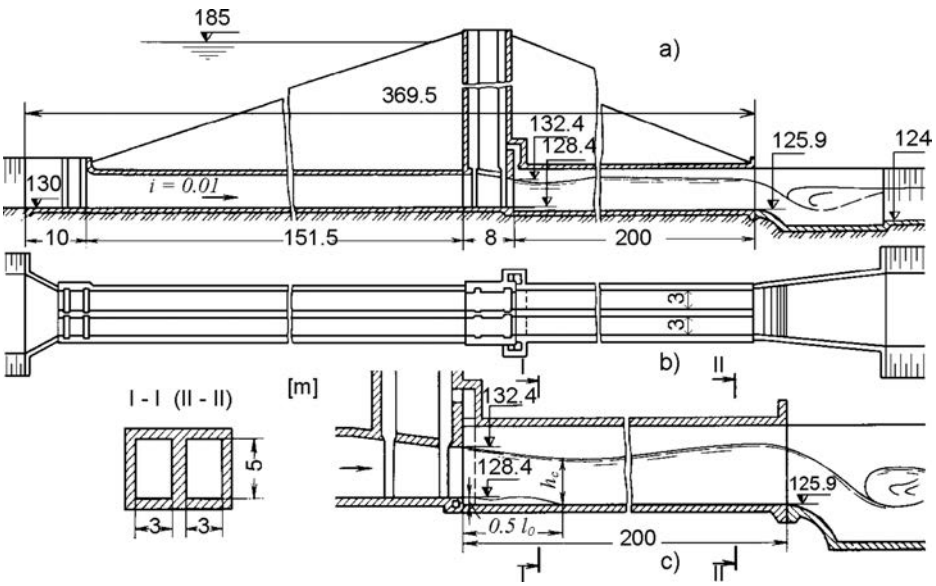

Figure 28.8 A bottom outlet structure in form of a gallery (after Lapshenkov, 1989).

bottom outlet structure consists of a reinforced concrete pipeline ($D = 5$ m), divided by means of joints at each 8 m, in order to achieve a certain adaptation for possible differentiated displacements of the soil (non-rock) foundation under loading of the dam. In the zone of the gates, the cross-section of the pipeline has been reduced, and in front of the stilling basin there has been constructed a spillway chute with a toothed bottom, intended for better stilling of the flow. The approach to the tower has been solved by means of a bridge, in the first case from the crest of the dam, while in the second case from the bank.

Figure 28.8 shows an example of a bottom outlet structure in the form of a gallery located under the dam, in which the control is constructed by means of a central tower. The flow from the entrance (intake) of the conduit to the tower, that is to say to the gates, is under pressure, and from the tower to the terminal structure, in the form of a stilling basin – under a free water table. The outlet is dimensioned for a maximum discharge of 560 m^3/s, at an elevation of the headwater of 185 mwl, with a possibility, at a minimum elevation of 140 mwl, to let through a biological minimum of 15 m^3/s. In order to avoid cavitations in the slots (recesses) of the plain gates, there has been anticipated contraction in the chamber for closing, so that the height of the conduit is reduced from 5 to 4 m. The height of the outlet part of the conduit is determined from the condition for operation under a free water table. The area of the aeration pipe for air supply behind the working gate, has been adopted so that it is no smaller than of 4% of the area of the conduit and, with the application of the coefficient of safety of 1.5, it amounts to 2 m^2 (Lapshenkova, 1989).

The outlet structures located *outside the dam's body* are constructed in the form of a tunnel, which, most often, works under pressure; another solution is possible

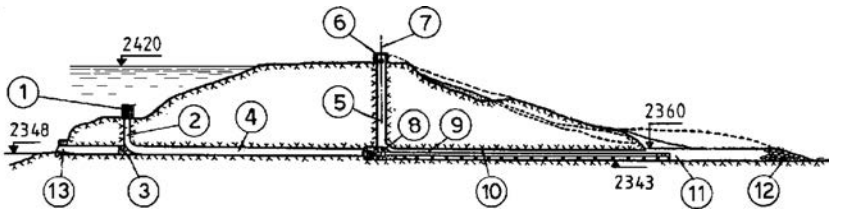

Figure 28.9 Outlet structure for the Green Mountain dam (USA), built in 1943 (the diversion tunnel has been transformed into a bottom outlet). (1) Trash rack at the intake of the outlet; (2)intake shaft of the bottom outlet, $D = 4.1$ m; (3) concrete plug of the diversion tunnel; (4) tunnel, $D = 5.5$ m; (5) shaft for controlling the bottom outlet, $D = 6.0$ m; (6)mechanism for lifting the gates; (7) axis of the dam; (8) gate chamber; (9) welded steel pipelines (two), $D = 2.5$ m, installed in the tunnel; (10) tunnel with a horseshoe cross-section; (11) channel; (12) tipped rockfill; (13) intake into the diversion tunnel.

where steel pipes are installed in a tunnel. The solution with the installation of pipes in the tunnel is particularly frequently used in cases when the diversion tunnel, which serves for the evacuation of the construction waters, transforms into a bottom outlet structure. Such solution, with a shaft from which to control the gates, is presented in Figure 28.9 (Chugaev, 1985).

The control of the gates or valves, in addition to the solution from a shaft, can also be performed from a tower, constructed in front of the entrance into the tunnel from a gate/valve house at the end, or else from a special chamber constructed above the tunnel, as is presented in the example in Figure 28.10. A gate or a valve in the front part or in the central part of the outlet has the advantage that the entire part, or the greater part, of the conduit can be closed and become accessible for revision and for maintenance.

The entrance (intake) part into the bottom outlet should also be well conceived, engineered, and constructed, since it should respond to a number of requirements: (1) at a minimum water level of the reservoir, the outlet must not suck in floating bodies (ice or waste, muck, scrap material), while at the water surface an air bellmouth must not be formed; (2) branches, ice, and other objects must not be retained on the protecting trash racks, since they reduce the inlet area; (3) approaching water must not cause deformations in the reservoir, because of washing out of the soil, etc.; and (4) head-losses at the intake should be minimal. In order to fulfil the first condition, the minimum distance of the upper edge of the intake into the outlet, up to the water level must be (Fig. 28.11a):

$$s_{\min} = (0.54 \div 0.72)v\sqrt{D} \tag{28.2}$$

where D is the diameter of the opening [m]; and v is the mean velocity of water at the intake [m/s]. In any case, it should be $s_{\min} > v^2/(2g)$; it must also be greater than the thickness of the expected ice.

If an entrance part (intake) has been constructed without a gate and without a protective trash rack, then an approach channel should be excavated in front of the

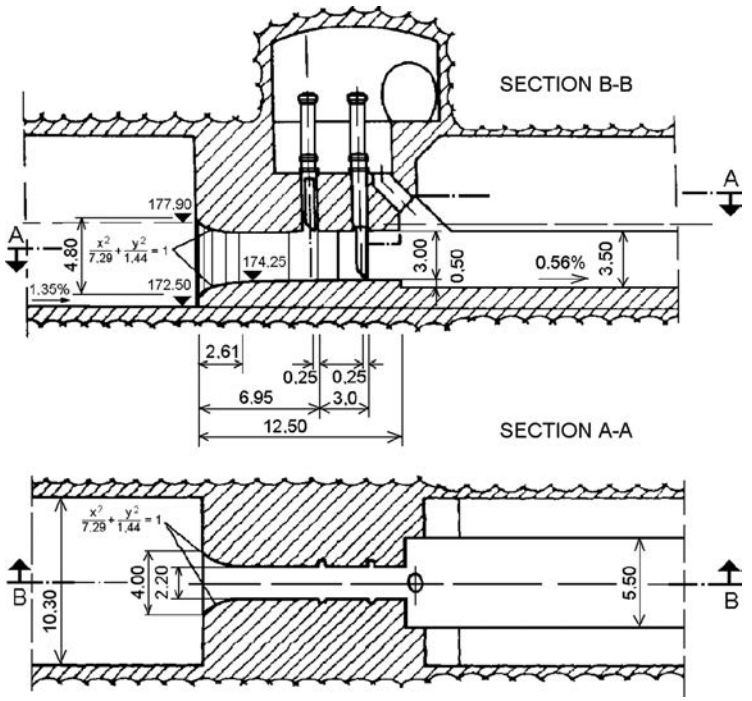

Figure 28.10 Gate-house with plain gates at the bottom outlet structure, Agios Nikolaos dam, Greece.

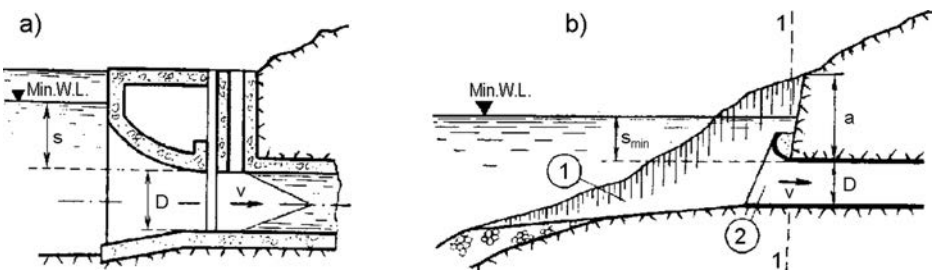

Figure 28.11 Scheme of intake into the outlet (a) and construction of an uncontrolled intake. (1) Approach channel; (2) entrance part (intake) into the tunnel.

entrance (1, Fig. 28.11b). Starting from the section 1–1, the outlet structure is constructed as a tunnel type of structure, and that is the place where the cost per 1 m open excavation becomes equal to the cost per 1 m length of the tunnel. In this, the following condition should additionally be fulfilled: the thickness of the rock mass *a* should be sufficient in order not to derange the unity of the rock. The minimum value of *a* usually amounts to (7–8) m. Widening of the entrance (2) is important in order

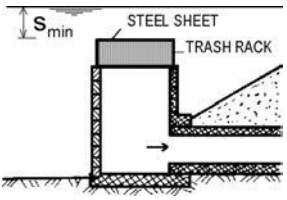

Figure 28.12 An intake structure of a bottom outlet at small embankment dams.

Table 28.1 Values of the relative cavitations resistance n for different materials, obtained experimentally, at a velocity of flow $v = 30$ m/s and $\beta = 0.675$ (Nedriga et al., 1983)

Material	*n*
1. Waterproof concrete, 30 MPa, with coarse infilling of gravel, $d_{max} = 40$ mm	1
2. Hydraulic concrete with compressive strength $R > 30$ MPa, max 60 MPa, with coarse infill of gravel or of gritting material $d_{max} = 40$ mm, $W/C = 0.38 - 0.42$	15 – 20
3. Cement solutions, $R < 70$ MPa	30 – 50
4. Shot-crete, $W/C = 0.35$; $R = 50$ MPa	≤15
5. Polymer solutions based on monomers, $R = 70 - 100$ MPa	≤150
6. Polymer coverings based on:	
epoxies,	≤500
nairite, polyurethane	≤1000
7. Steel	
ordinary	500 – 700
special, stainless	>1000

to reduce losses of pressure. In cases of a soil foundation, the approach channel, at greater approach velocity, should be stabilized with an appropriate lining.

In most cases, the entrance part is protected with a trash rack installed in an inclined position along the slope of the bank and provided with rabbles or rakes for cleaning, as is shown in Figure 25.10 (Chapter 25), or else a space trash rack is constructed, as shown in Figure 28.9. In cases of an outlet structure under an earthfill dam with uncontrolled intake, the simplest thing would be to construct a small, rectangular, reinforced concrete tower with a steel trash rack in the upper part, (Fig. 28.12). The tower would be open at the front side in order to enable the water to penetrate into the pipeline conduit in the course of construction of the hydraulic scheme. A trash rack should be incorporated during adaptation of the pipeline conduit into a bottom outlet, while the opening of the tower at the front side should be closed with a stoplog gate made up of oak planks, i.e. beams, placed in the gate slots.

In solutions of outlet structures with a pressure tunnel, particular attention should be paid to cavitations. The concrete on the internal side of the lining should be as even as possible, while the structure of the bottom outlet should be such that the velocity

of flow should not exceed certain critical values. At a velocity greater than 15 m/s, there is a necessity for careful analyses regarding the danger of cavitations. A velocity of flow greater than 25 m/s is not by any means recommended. The analyses should commence with a determination of the coefficient of cavitations σ, in accordance with the recommendations laid down in Chapter 4, as well as the critical value σ_{cr}, thus defining the relationship $\beta = \sigma/\sigma_{cr}$. Details regarding the determination of σ_{cr} may be found in professional textbook references (Nedriga et al., 1983).

Besides the execution of as even internal concrete surfaces as possible, the most widespread measure is a supply of air in the zones in which a vacuum is expected, which has already been discussed at several places in this book. When it is deemed that, in spite of the cited measures, it would not be possible to completely eliminate the danger of cavitations, then it will be necessary to use (completely or partially) materials that are resistant to cavitations. For the application with bottom outlets, there can be considered materials as described in Table 28.1.

From Table 28.1, it is evident that steel linings and polymer coverings can drastically improve the cavitations resistance of the linings; however, they are very expensive, therefore, their selective use is recommended, in combination with other measures.

This page intentionally left blank

Chapter 29

Special hydraulic structures

29.1 INTRODUCTION

Special hydraulic structures are intended for performing certain functions within the hydraulic scheme for the needs of some water economy branches. The special structures can be for amelioration (channels, pumping stations, etc.); hydroelectric power plants (power houses, pumped storage hydroelectric power plants, intake structures, derivation (supply) channels and tunnels, etc.); water transport (channels, ship navigation locks and lifts, etc.); structures for fishery economy (fish bypasses, i.e. fish ladders and lifts, etc.); water supply; for fighting floods and erosion of the soil; for utilization of underground waters (underground intake structures, etc.); for sedimentation of waste materials and other purposes. More detailed enumeration of special hydraulic structures has been given in Chapter 1. Since the majority of the above-mentioned special hydraulic structures have been analyzed in other specialized fields of hydraulic engineering, and in order to enable an easier pursuance of the forthcoming chapters in which problems regarding the designing of hydraulic schemes are treated, here we shall only treat in brief those issues, the knowledge of which is indispensable in composing hydraulic schemes.

29.2 TRANSPORT STRUCTURES

Transport structures are constructed within hydraulic schemes of navigable rivers and they serve for the conveyance of navigation vessels from one level to another. Ship navigation locks and lifts are used for that purpose.

A *ship navigation lock* consists of a chamber in which the navigation vessel stays during its transfer from one level to another. The lock chamber is formed of two longitudinal walls and two gates, which can be opened and closed, in order to enable entrance of the navigation vessel into the lock chamber and its exit from it (Fig. 29.1). The conveyance of the navigation vessel from one level to another consists of a series of operations. For instance, during movement of the ship in an upstream direction and, under the assumption that the water level in the lock chamber coincides with the level of the tail-water (lower reach), the sequence of operations is as follows: (1) opening the gates at the downstream side; (2) the ship then enters the lock chamber from the lower approach channel; (3) closing the gates at the downstream side; (4) the chamber is filled with water from the upper level through special openings, so that the water

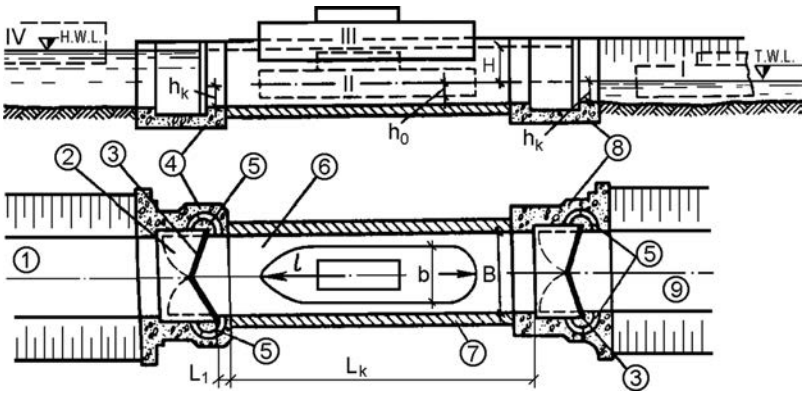

Figure 29.1 Scheme of a ship navigation lock with one lock chamber. (I–V) Positions of the navigation vessel (1) Upper approach channel; (2) space for movement of the lock gate doors; (3) lock gate door; (4) upstream head; (5) openings for giving passage to water; (6) lock chamber; (7) longitudinal wall of the lock chamber; (8) downstream head; (9) lower approach channel, h_0 = draught of navigation vessel.

level in it is equalized with the level of the headwater (upper reach); (5) opening the upstream gates; and (6) the ship is taken out into the upper approach channel. Now the ship navigation lock is ready to receive a navigation vessel and, with an inverted sequence of operations, to move it down to the lower level.

Ship navigation locks should be sufficiently spacious in order to be able to accept the traffic that is expected in the course of the service life of the structure. In Russia, the ship navigation locks are made with lock chambers 11 to 30 m wide, and 50 to 290 m long, with a minimum depth of water of $h_k = 1–5.5$ m. The head of the hydraulic scheme ranges up to 40 m. In the case of greater heights, they use ship navigation locks with two or more chamber locks, or else lifts. In the USA, they make lock chambers with dimensions in plan 17×122 m up to 33.5×366 m. The minimum depth is taken to be at least 1 m greater than the maximum draught of the navigation vessel that will use the ship navigation lock (Grishin et al., 1979).

In respect of their construction, ship navigation locks can be made of mass concrete, reinforced concrete, and without or in combination with steel sheet piling. In cases of ship navigation locks with a low or with a medium head ($H < 12$ m), as well as with small to medium dimensions in plan ($B = 12–24$ m, $L = 190–230$ m), the ship navigation locks have a prismatic form with vertical walls, constructed of anchored steel sheet piling (Fig. 29.2a), of reinforced concrete prefabricated elements, or as an open frame that is cast *in situ* (Fig. 29.2b). With this kind of ship navigation lock, the filling and emptying is performed directly, through the lock gate doors. Indirect filling and emptying of the ship lock chamber is employed in cases of high-pressure heads ($H > 12$ m) and small dimensions in plan ($B = 12$ m). That is most suitably realized by means of long water-supply conduits that are located either in the side (lateral) walls (Fig. 29.2c), or in the bottom (Fig. 29.2d). At the upstream and downstream ends of the ship navigation lock, the longitudinal water supply conduits are provided

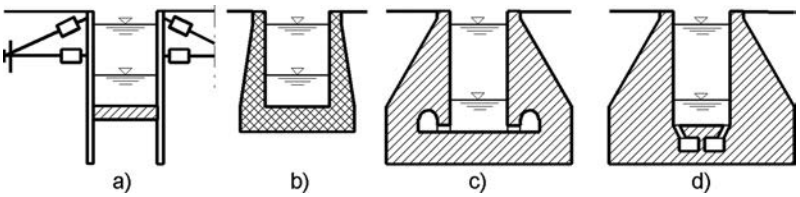

Figure 29.2 Cross-section of ship navigation locks (after Novak et al., 2001). (a) Anchored steel sheet piling; (b) reinforced concrete semi frame; (c) gravity walls with lateral longitudinal filling water conduits; (d) gravity walls with bottom water conduits.

with gates (plain gates or radial, gates), that must be accommodated below the lowest possible water level (Novak et al., 2001).

The total time that is necessary for filling or emptying the lock chamber usually amounts to 20 to 40 minutes, to which one should also add the time for handling of the gates (from 2 to 8 minutes), as well as the time necessary for manoeuvre with the navigation vessels, all in order to obtain the total time for the lockage, i.e. carrying over in one full cycle.

During every lockage (carrying over) there comes about a transfer of water from the upper level to the lower level, in a quantity that can be approximately calculated from the expression:

$$V = BLH \tag{29.1}$$

where B is the width of lock chamber at the top; L is the length of lock chamber; and H is the pressure of the ship navigation lock.

Within the composition of the ship navigation lock, there also come approach channels, in which the navigation vessels wait to be carried over. Their length should not be smaller than $1.2L_k$. In order to ensure appropriate service conditions, the ship navigation lock should be set up in straight alignment with a length of:

$$L \geq nL_k + 2l_c + \Sigma l_g \tag{29.2}$$

where n is the number of lock chambers; l_c the length of the ship caravan that is carried over; and Σl_g is the sum of concrete piers, which do not come into the useful length of the lock chambers.

The location of ship navigation locks within the hydraulic scheme depends on the dimensions of the structure, i.e. works, on topographical, geological, and other conditions. As a rule, ship navigation locks are moved away from the powerhouse and from the spillway structures (Fig. 29.3, 29.4, 29.5). The scheme illustrated in Figure 29.3a is possible when the bank is not very steep and allows for the execution of a derivation (supply) channel, upon which the ship navigation channel is set up, in the vicinity of which there are constructed places for anchorage of the navigation vessels waiting to enter the lock chamber. The entrance and the exit of the derivation channel are denoted with lighthouses. In the scheme illustrated in Figure 29.3b, the derivation channel is constructed further away from the weir, at a place at which the foundation

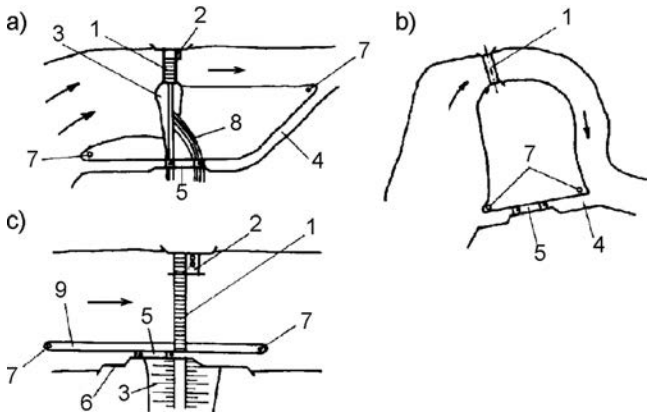

Figure 29.3 Schemes for siting of ship navigation lock within a hydraulic scheme. (1) Spillway; (2) power house; (3) embankment dam; (4) derivation channel; (5) navigation lock; (6) approach channel; (7) lighthouse; (8) roadway; (9) training wall.

Figure 29.4 The ship navigation lock at one concrete gravity dam on River Rhone (France), under construction (1979).

is suitable for the execution of excavation for this kind of structure. When there are no suitable conditions for execution of a derivation (supply) channel, we apply the scheme shown in Figure 29.3c, in which the ship navigation lock is separated from the overflow part of the dam by means of a parting (side) wall, and a distant entering the reservoir, so that the entrance to the approach channel would be moved away from the overflow (Grishin et al., 1979).

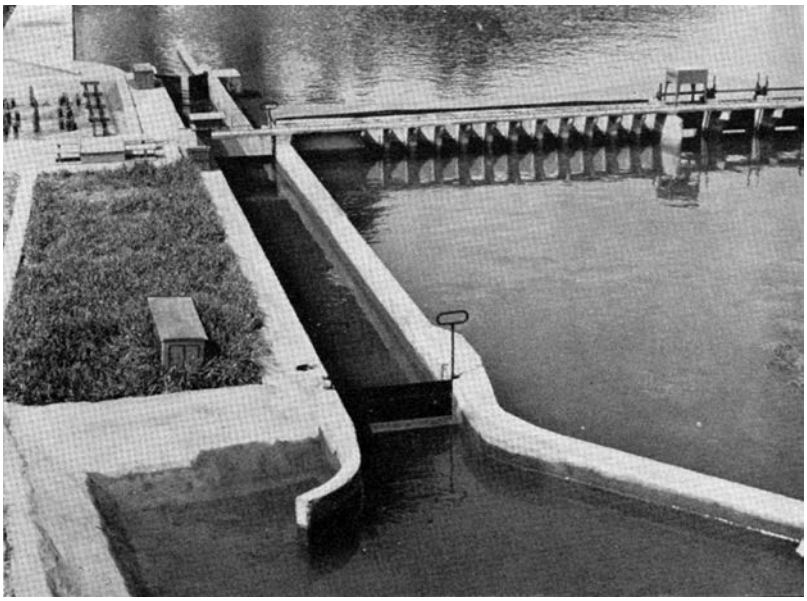

Figure 29.5 Two-staged ship navigation lock of Gjerdap I Dam on Danube, Serbia (model).

In those hydraulic schemes that are aimed at power generation, where water consumption for navigation must be minimized, high heads are overcome by means of either two-stage locks, like in the Gjerdap scheme on the Danube river (Fig. 29.5), or three-stage locks as in the Dnieprogress scheme on the Dniepr river. Recently the largest system of locks in the world was constructed for the famous Three Gorges Project on the Yangtze River in China. The so-called *whole cascade system of locks* was applied, using a cascade of 5 locks next to a 183 m high concrete gravity dam with a total head of about 110 m. Each lock chamber measures $280 \times 34 \times 5$ m and can accommodate a 10,000 ton barge fleet.

Water can be efficiently saved by using *thrift locks*. In thrift locks, considerable reduction of water consumption is achieved by conveying, by gravity, part of the water during lock emptying to thrift basins, to be returned again by gravity to the lock during its subsequent filling. Thrift basins are usually constructed next to the lateral lock wall, and every basin is connected with the lock by its own conduit, provided with two-way gates. Up to four basins give a rational solution regarding the reduction of water consumption and the handling time. Thrift locks are used for heads of up to 30 m (Novak et al., 2001).

Another way to save water is by using lifts. A *ship lock lift* is a hydraulic structure by means of which, and in which, the navigation vessel is moved from one level into another, along with the movable chamber, in which there is a constant water level. It is employed with hydraulic schemes with a medium to high-pressure head. In contrast to the ship navigation locks, it does not spend water, and in cases of high pressure heads, there is a shorter time of handling.

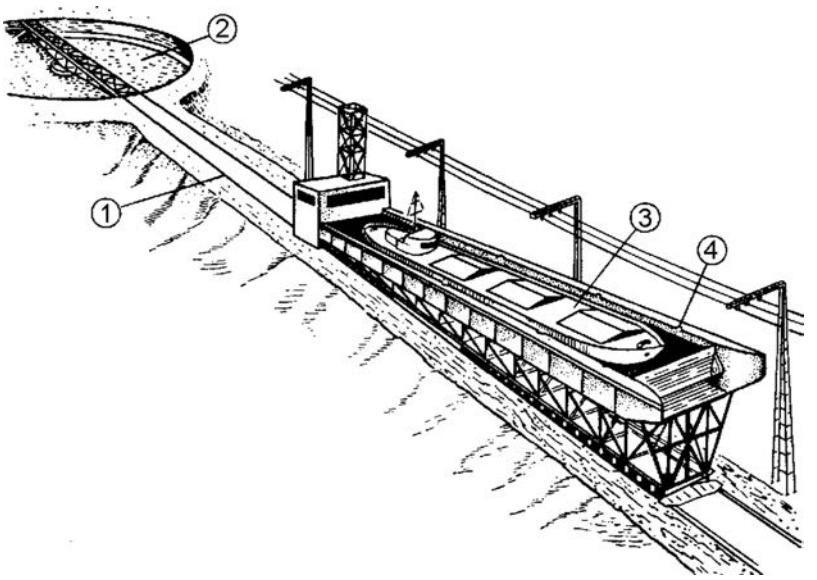

Figure 29.6 Inclined ship navigation lift within the *Krasnoyarsk* hydraulic scheme. (1) Rails; (2) turning structure; (3) navigation vessel; (4) lock chamber.

According to the way of action, the ship lifts are divided into mechanical lifts, hydraulic lifts, and floating lifts and, according to the direction of movement, they are divided into vertical lifts and inclined lifts. Figure 29.6 presents an inclined ship lift, constructed within the *Krasnoyarsk* hydraulic scheme (Russia). By means of toothed wheels, the lock chamber moves along guide rails that have been fastened upon an inclined foundation slab. It works at a pressure head of 100.8 m, while the dimensions of the chamber are $90 \times 18 \times 2.2$ m. The mass of the lock chamber together with water and a navigation vessel amounts to 6500 t. The speed of lifting amounts to 1 m/s, so that one continuous double cycle takes 80 minutes. This kind of solution has proved to be twice as inexpensive as would be the construction of a multi-stage ship navigation lock (Grishin et al., 1979).

29.3 HYDRAULIC STRUCTURES FOR THE ADMISSION AND PROTECTION OF FISH

River hydraulic structures in many cases derange the conditions for the development, life, and even the survival of the ichthiofauna. Here we should mention the closure of the migration routes of fish, the change of regime of their spawning (high upper level, while the lower level is also changed in relation to the natural river regime), drawing of the young fish into the intake structures, and their injury with various other structures and fast navigation vessels, etc. For reducing the negative effect of hydraulic schemes under pressure on the fishery economy, it is necessary to undertake the following measures: (1) to ensure giving passage to the fish during their migration

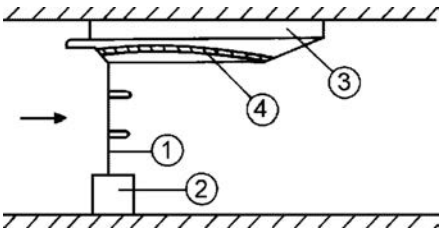

Figure 29.7 Fishway in parting (side) wall. (1) Overflow dam; (2) power house; (3) ship navigation lock; (4) fishway.

period in both directions; (2) to develop simulated breeding of fish, and to stock the reservoir with lake fish.

For ensuring the migration of the fish in the river hydraulic schemes, according to their purpose, we can differentiate two groups of special structures: (1) structures for admitting i.e. giving passage to, fish; and (2) structures for the protection of fish. Within the framework of the two basic groups, and according to the character of the work and structural particularities, there is performed a division into subgroups: (a) structures for admission, in which the fish surmount the elevation difference by themselves; (b) structures, in which there is performed lockage (transfer) of the fish into the upper level by means of special lock channels or by means of special containers – mechanical or floating ones; (c) structures within the framework of the hydraulic scheme which can be adapted for giving passage to the fish in the migration period, such as ship locks, etc.; and (d) protective structures.

The position of the structures for giving passage to the fish, within the framework of the hydraulic scheme, depends on a number of factors. It is solved individually in each particular case. Still, some general principles can be established. In cases of valley hydraulic schemes with a low or medium pressure head, as a rule, the structures for admission of the fish, that is to say, the fish-passing facilities, consist of fishways, located in the parting walls (Fig. 29.7).

The fishway is a channel connecting the upstream end with the downstream end of the dam. The walls and the bottom of the channel are of such roughness, that the velocity of flow should be less than 2 m/s, and this velocity is acceptable to the fish. There is a relationship between the roughness of the wall and the bottom, on the one hand, and the slope of the channel, on the other hand. The inclinations of the fishways range from 5 to 20%. The artificial roughness is achieved by means of partitions or weirs – complete ones (according to the system of the Belgian engineer Denil, which has been abandoned lately), or incomplete ones, some of which are presented in Figure 29.8.

Fish ladders consist of a channel with a ladder-type bottom and partitions (2) forming a series of basins (1) and cascades between them (Fig. 29.9). Openings are left in the partitions (5) for the passage of the fish. The basins serve for the rest of the fish following their passage through the openings. The dimensions of the fishways, number of steps, size of cascades, the form and position of the openings are solved for each particular case individually, depending on the required discharge and the type of

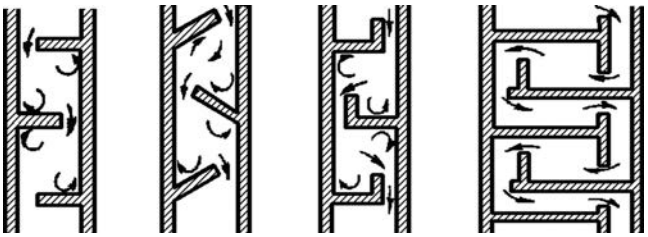

Figure 29.8 Types of incomplete transverse partitions.

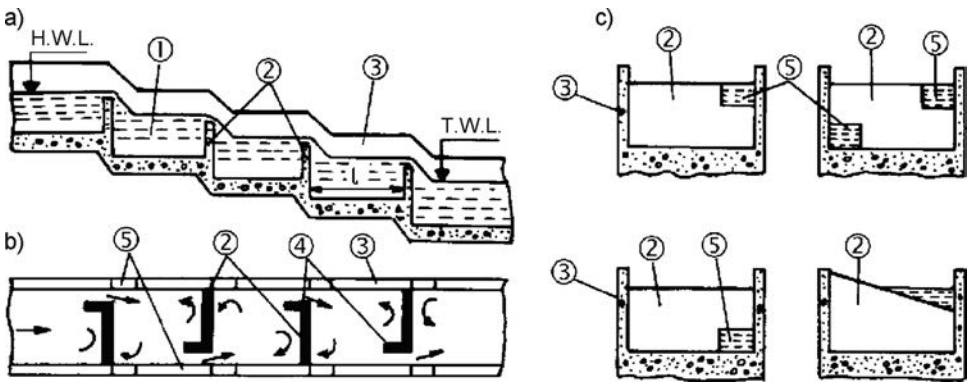

Figure 29.9 Scheme of a fish ladder (stepped fish bypass, i.e. fishway) (after Grishin et al., 1979). (a) Longitudinal section; (b) plan; (c) positions of the openings. (1) Basin; (2) transverse partitions; (3) longitudinal walls; (4) protective partitions; (5) openings.

fish. Fish ladders are the most widespread in practice. They are employed for hydraulic schemes with a pressure head up to 30 m.

In the case of hydraulic schemes with derivation hydroelectric power plants, there are two possible solutions (Fig. 29.10): (a) in the case of an open derivation without pressure, fishways are made both at the dam and at the hydroelectric power plant; and (b) in the case of a closed derivation, fishways are constructed only at the dam, while the approach of the fish into the power intake should be prevented by means of protective structures.

In cases of hydraulic schemes with a high pressure head and a short derivation (supply), the entrance of the structure for giving passage to the fish is constructed close to the powerhouse, while the transport can further on be performed by means of an aerial ropeway.

The fish lifts perform mechanical lifting of the fish in a special net or else in a chamber filled with water. The principle of work of the fish lifts is analogous to that of the ship lifts. In addition to these types, there are also hydraulic and floating structures for lifting the fish.

In cases of hydraulic schemes on large rivers that are rich in fish, it is necessary to anticipate two or more structures for conveyance of the fish, as is shown in the

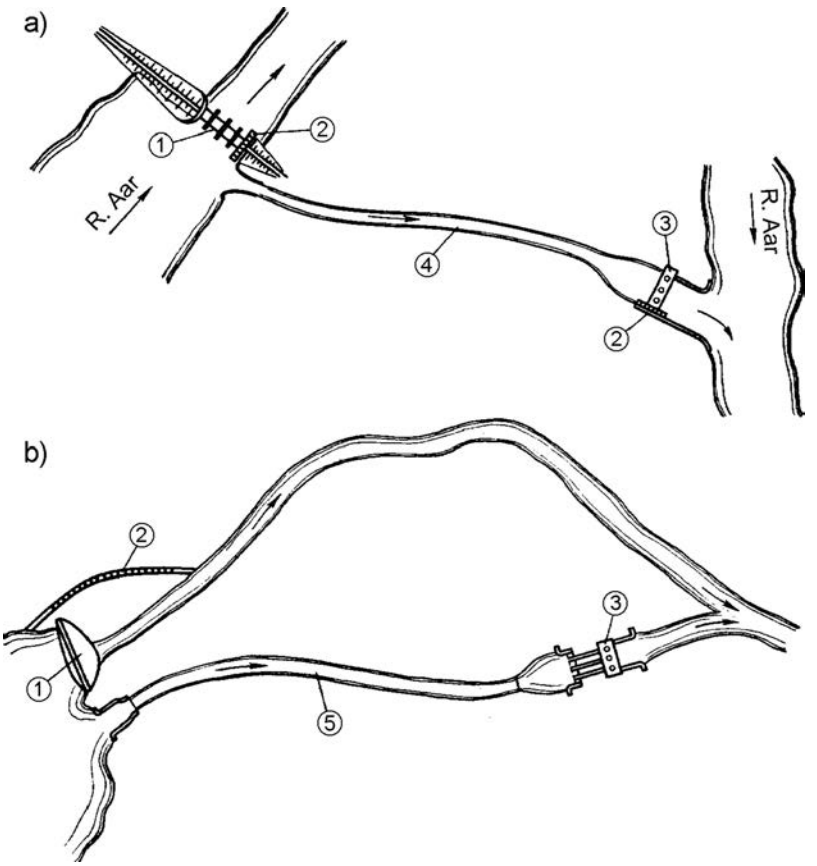

Figure 29.10 Position of fishways in derivation (diversion) hydraulic schemes. (a) Derivation without pressure; (b) derivation with pressure (1) Dam; (2) fishway; (3) power house; (4) channel; (5) tunnel.

example in Figure 29.11. The fish may be conveyed from one water level to another by means of a special structure (2) working together with a directing structure (5), with a ship navigation lock (3), and with an individual shipping vessel (4) (Grishin et al., 1979).

In relation to the suitability for the application of particular solutions, it may be concluded that for a pressure head up to 30 m, the passage of the fish should be performed through fish ladders (stepped fishways) or through floating structures. For greater elevation differences, it is more rational to use fish locks and fish lifts with either mechanical of hydraulic action. A lift with hydraulic action is shown in Figure 29.12, and consists of three basic elements: a lower chamber (1), an upper chamber (2) and an inclined gallery (3). Both chambers have openings, provided with chamber gates. Lifting of the fish begins at the opened chamber gates of the lower chamber, when water is admitted from the reservoir into the upper chamber. The water discharges along the

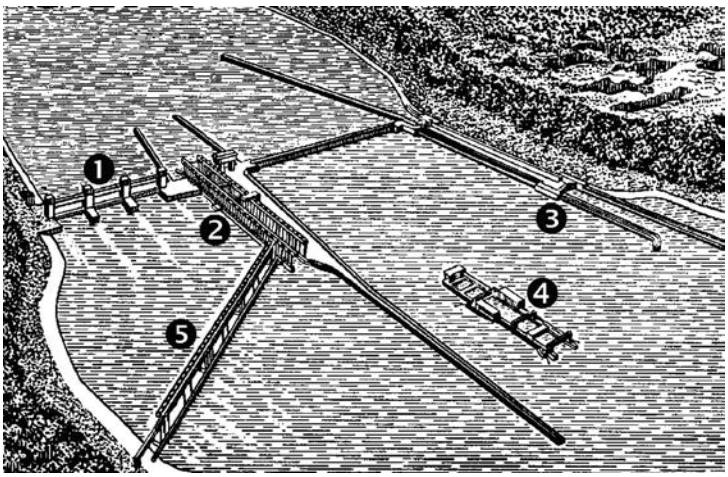

Figure 29.11 Layout of structures at a hydraulic scheme on a large plain-land river. (1) Overflow dam; (2) structure for giving passage to the fish; (3) ship navigation lock; (4) floating vessel for conveyance of the fish; (5) directional structure.

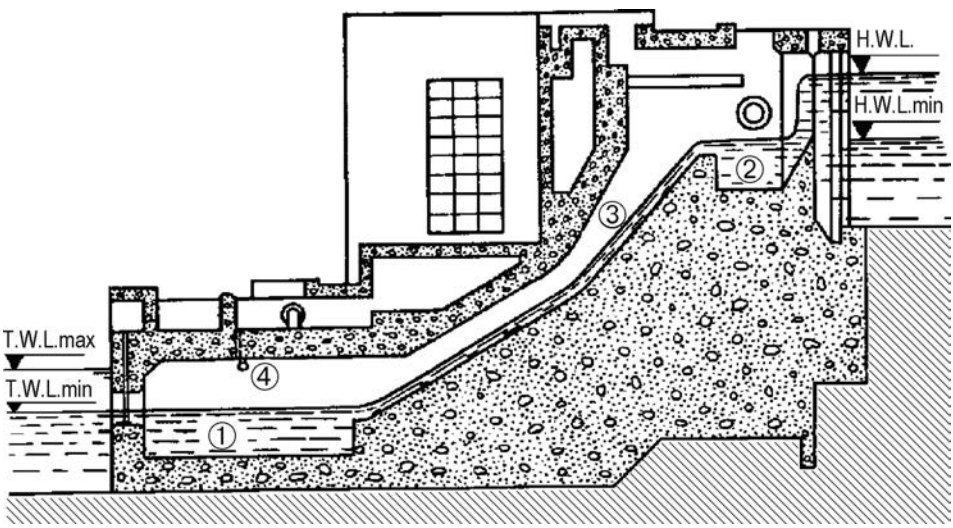

Figure 29.12 Fish lift structure with hydraulic action (after Grishin et al., 1979).

inclined gallery and through the lower chamber into the tailwater, and that attracts the fish and directs the fish towards the lower chamber. Then the lower chamber is closed and, following the complete filling of the inclined gallery with water, the outflow pipe is activated (4); thus there takes place a flow of water through the system and this makes the fish climb into the upper chamber, from which they swim into the reservoir through the flat rectangular gate. Afterwards, there is an automatic rising of the gate

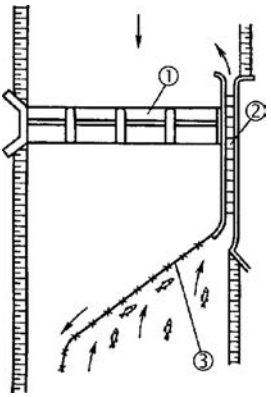

Figure 29.13 Directing net. (1) Dam; (2) fishway; (3) directing net.

of the lower chamber and so the lift empties. The hydraulic fish lift has a number of advantages in comparison to other kinds of structures for giving passage to the fish: it may be employed in hydraulic schemes with a low and medium pressure head for all types of fish, the conveyance of the fish can be performed both upward and downward, while they do not expend too much of energy on overcoming the elevation difference (Grishin et al., 1979).

The structures for the protection of the fish have the task of preventing the fish entering into the intake structures and other dangerous places. The structures that direct the fish towards the entrance of the conveyance structures consist of nets or screens made of metal or made of man-made fibres, fixed to stiff supports (Fig. 29.13). The deficiency of such a structure is the fact that it requires cleaning, maintenance, and overhaul (Grishin et al., 1979).

In cases of the modern hydraulic schemes, they most often use partitions with electrical action, the application of which is based on the irritating effect of the electric field on the body of the fish. Lately, they have made attempts for the movement of the fish in the zone of hydraulic structures to be controlled by means of optical, acoustical, and chemical means; however, there are not yet sufficient data on such achieved effects.

In order to prevent the fish migrating towards the downstream side coming into the power intake of the hydroelectric power plant and so passing through the turbines, different types of protective nets or screens have been tried out in practice. Major criteria for their design are the dimensions of the meshes, i.e. openings, as well as the approach velocity of the water. In the USA, they apply the following criteria:

Length of fish [mm]	*Approach velocity [m/s]*	*Network mesh (openings) [mm]*
<60	0.12	3.2
>60	0.24	6.4

The solution in the design for protection by means of a net or screen depends on the size of the turbines and the reservoir. In cases of small hydroelectric power

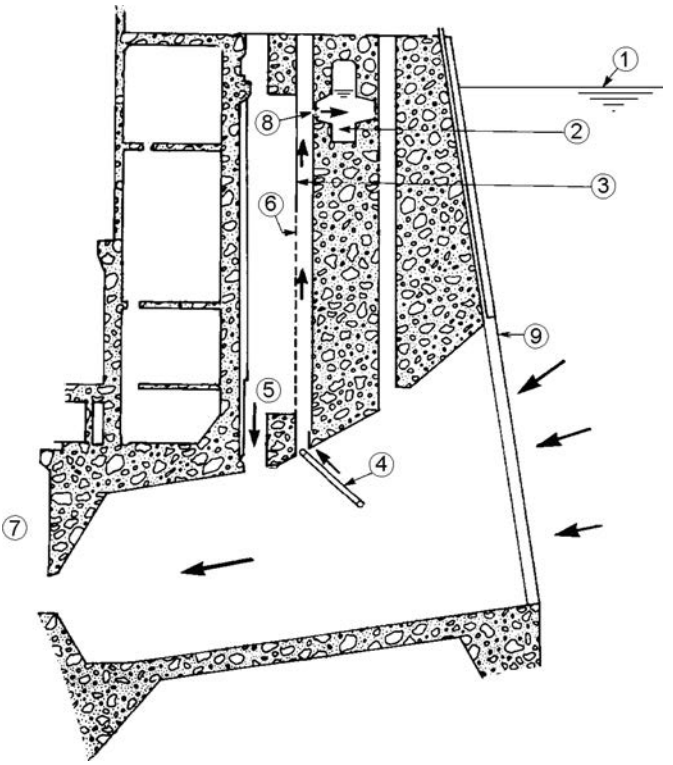

Figure 29.14 Directing screen (Cassidy, 1991). (1) Level of headwater; (2) bypass gallery; (3) path from the chamber toward the gallery; (4) directing screen; (5) chamber; (6) perforated plate; (7) turbine space; (8) opening; (9) grille at the entrance of the intake.

plants, the nets are placed across the entire front of the turbine power intake, with an inclination towards the flow, in order to direct the fish outside the zone of the power intake, towards the bypass channel.

In cases of large hydroelectric power plants, the entire coverage of the power intake is not economical owing to its considerable dimensions and the significant discharge quantity. In such cases there have been investigated and applied nets, i.e. screens, which, partially, cover the power intake (⅓–½). Figure 29.14 presents such a newer installation developed in the USA (Cassidy, 1991), along with a directing net (4), rotating by ≈45°. By means of the net, the fish, moving along the flow, are directed upwards into the opening that leads into chamber (5), which, by means of a perforated plate (6), is divided into two vertical chambers. A part of the water flow entering the vertical chamber discharges into the downstream part through the perforated plate, thus concentrating the fish in the first part. The remaining water, that contains the fish, directed here by means of the net or screen, moves upward and passes through an opening of Ø200 mm (8) into a bypass gallery. The water, along with the fish, is conveyed through the gallery longitudinally down the dam into a channel which, by means of a curve, leads downstream of the dam.

The directing screen must be analyzed in detail from a hydraulic viewpoint, in order to respond to a number of requirements. First of all, it must exhibit sufficient resistance to the flow in order to direct the water upwards, into the chamber. On the other hand, too large a resistance would force the flow to turn downwards, around the screen, and it would also strike the fish out around the screen. Furthermore, the velocity, which is perpendicular to the screen, must be sufficiently small for the young fish not to be in a position to impact into the screen and thus to be injured. The components of the velocity, perpendicular and parallel to the screen, are designed so that the fish would only be directed without injury.

In cases of hydraulic schemes with a high-pressure head, there has not yet been found a completely satisfactory solution for giving passage to the ichthiofauna. The adaptation of other special structures of the hydraulic scheme, for instance the ship navigation locks for the passage of the fish, should be deemed as a parallel solution, without excluding the construction of a main structure.

This page intentionally left blank

Chapter 30

River diversion during the construction of the hydraulic scheme

30.1 RIVER DIVERSION DURING THE CONSTRUCTION OF DAMS AND APPURTENANT HYDRAULIC STRUCTURES – GENERAL

One of the characteristics of the river hydraulic schemes is the essential need, in the course of the entire period of construction, to divert the river water from the dam site, i.e. to give passage to that water. This is ensured by means of a series of individual structures: cofferdams (temporary dams), embankments, channels, and tunnels, as well as by utilizing the permanent works of the hydraulic scheme, temporarily, for this purpose, as well.

The maximum quantity of water that is to be diverted in the course of the construction of the hydraulic scheme is called *construction water*. It is determined by means of a technical-economical analysis. It is evident that if we assume a smaller quantity of water that has to be diverted, that is to say, against which the construction foundation pit is to be protected, the costs will be lower, while the risk of flooding of the construction pit will be greater. Or, *vice versa* the larger the quantity of such construction water, the smaller the risk to the safety of the construction pit. The usual practice for the construction water is to assume the water with a return period that is 3–5 times longer than the period that has been anticipated for the construction of the hydraulic scheme. Of course, here as well, the specific conditions prevailing at the dam site are of great importance in making decisions.

In selecting the scheme for diverting, i.e. letting through, the construction waters, one must take account of: the hydrological, topographical, and geological, as well as the construction and economy conditions of the locality anticipated for construction, the utilization of the river in the course of construction and other water economy needs (navigation, rafting, and floating of logs), etc. A poor solution for giving passage to the construction water leads to slowing down the construction of the hydraulic scheme, while the danger of damage is increased. A detailed working out of the issue for letting through the construction waters is essential during the execution of dams at large plain-land rivers, especially if they are constructed upon a soil (non-rock) foundation.

Depending on the width of the river at the dam site and the quantity of construction water, in the course of construction of the hydraulic scheme the river waters can be evacuated in three main ways: (A) without diversion from the parent river channel, in which the major and permanent concrete works are constructed; (B) with diversion of the river from the parent river channel and its conveyance through channels, tunnels or pipelines; or (C) combined, when part of the permanent major works

are constructed without diverting the water, while another part with diversion of the water. By means of the combined method of diversion of construction water, the main permanent structures of the hydraulic scheme are constructed according to a certain construction sequence, i.e. some of them without diversion of the river, while others with diversion of the river, or else one and the same structure is constructed at certain periods with river diversion, while without river diversion at other periods. In some cases, it is rational to widen the river channel by clearing one of the banks, and this has been employed with abundant watercourses, with lowland rivers, or semi-plains rivers.

30.2 CONSTRUCTION OF THE STRUCTURES WITHOUT RIVER DIVERSION FROM THE PARENT RIVER CHANNEL

With the application of this method, the execution of the hydraulic structures can be achieved in a construction (foundation) pit, protected with a cofferdam, or else without damming of the construction pit, by using construction of the underground parts of the works with methods of underground construction, while the overground parts are constructed in the dry, giving passage to the waters through the parts of the structures that have been erected during the first stage of construction.

30.2.1 Method with damming of the construction (foundation) pit

In applying this method, damming of the construction pit is usually performed in two stages. In the beginning, we build the structures within the construction pit, located in the river channel, protected with the cofferdams from the first stage (Fig. 30.1). The longitudinal cofferdam (1) is constructed first, along the course of the water or inclined at a small angle, followed by the construction of the upstream cofferdam (8) and downstream (5) cofferdam, perpendicular to the river valley. One part of the main permanent works (the powerhouse and a part of the concrete dam (Fig. 30.1) are constructed in the construction pit and they contain openings for giving passage to the water during the construction of the major permanent works of the second stage. In the course of constructing the structures of the first stage, we also construct the longitudinal protection cofferdam of the second stage (4, 7), associated to the previously executed works (toward the parting wall 6). Then the downstream cofferdam (5) is removed or dismantled and the downstream part of the works is submerged; what follows is the removal of the upstream cofferdam (8) and so the water is admitted through the structures constructed during the first stage, and through the river channel. Next, there follows the construction of the downstream cofferdam (3) and the upstream transverse cofferdam (2), by means of which the space between the cofferdams has been protected, while waters are admitted through the openings of already constructed parts of structures of the first stage. The main permanent structures are constructed under the protection of the cofferdams of the second stage and, when their construction stage reaches a sufficient extent, we remove the cofferdams of the second stage. In order to facilitate passage of the construction waters of the second stage, the openings that have been constructed in the first stage are walled-up according to a certain sequence.

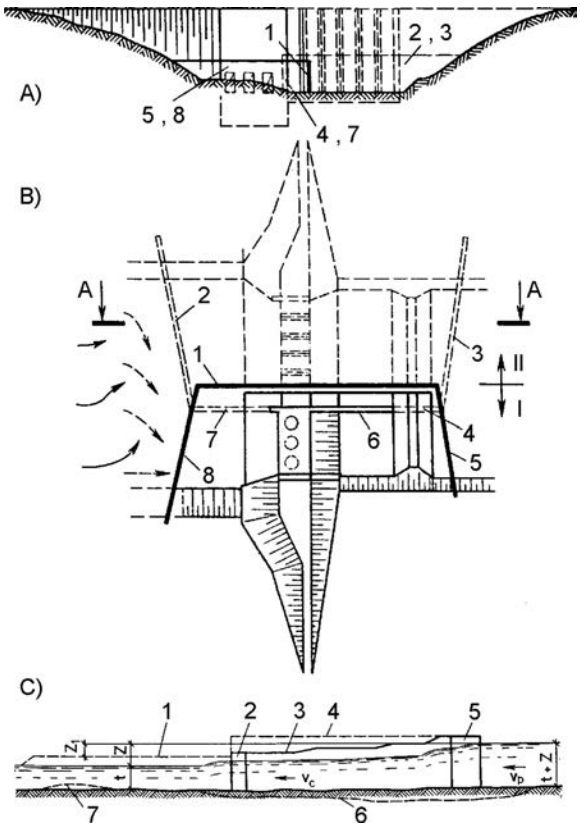

Figure 30.1 Diversion of waters by means of sectional cofferdams (A and B) and the influence of cofferdams on the water level of the river (C).

The structures coming out of the boundaries of the cofferdams are usually constructed under water.

The above-described method with cofferdams, constructed in two sections, is employed for rivers abundant with water and for the construction of concrete works. The cofferdams are most often 10–15 m high, but they can also exceed 30 m. Within the contracted river channel, if there is a rock foundation, the velocity of the water can amount to 8–10 m/s (Grishin et al., 1979).

The reduction of the cross-section of the river channel, with the execution of the cofferdams, causes a slowing down of the water in front of the cofferdam, as well as increasing of the velocity of flow in the contracted part, at the expense of which there is a possibility of erosion of the river channel and the cofferdam at that part. In that, we assume that along the length of the river channel (section A–A, Fig. 30.1C) there will not come about erosion (6) and sedimentation (7) of the washed-out particles, then the headwater can approximately be determined according to the formula:

$$Z = \frac{v_c^2}{\varphi^2 2g} - \frac{v_p^2}{2g} \tag{30.1}$$

where v_p and v_c are the mean velocities in front of the cofferdam and in the contracted section of the river channel, respectively, and φ is the coefficient of contraction, $\varphi = 0.75–0.90$ (lower values relate to cofferdams that have an approximate rectangular form in plan, Figure 30.2a, while the higher values relate to a trapezoidal form and to the existence of structures for directing the flow, Figure 30.2b, c. If there comes about erosion (6) of the riverbed, which is especially intensive during the first flooding, there follows sedimentation of the material (7) downstream of the cofferdams and a rising of the water level (1), the expense of which there is a decrease in the value of Z, which now becomes Z_1. In this case, a need may arise for increasing the height of the cofferdams (4 instead of 3, Fig. 30.1C).

The selection of the extent of contraction of the river channel is best performed by means of model investigations of several alternatives. In practice, this contraction amounts to 30–65%, in which one should endeavour that the following conditions be fulfilled: the velocity v_c should not damage the cofferdams, passage of ice should be facilitated, conditions for navigation should be provided ($v_c < 2$ m/s), and rafting and floating of logs ($y_c < 3$ m/s) should be possible.

The erosion of the foundation, as well as washing away and scouring of the cofferdams, may be reduced by the execution of particular cofferdams with a form that would alleviate the flow and also by means of the addition of dykes that direct the flow (Fig. 30.2b, c), and by shaping up the river channel by means of excavation (c) (Grishin et al., 1979).

For the protection of the construction pit various types of cofferdams can be applied, including straight, arched and buttressed concrete walls. Typical cross-sections

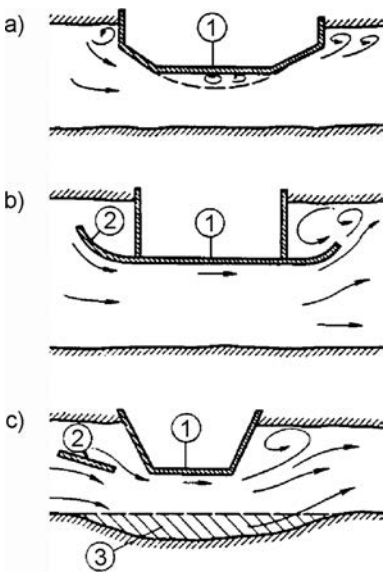

Figure 30.2 Methods for improving the conditions for flow in the contracted river channel (after Grishin et al., 1979). (1) Cofferdams; (2) directional embankments; (3) excavation.

Figure 30.3 Construction of parting wall on the river *Aar,* in the vicinity of Zürich, under the protection of a steel sheet piling partition.

of cofferdams made from different materials are briefly described in section 30.3.1 and shown in Figure 30.9. Some of them are similar to the regular dams, some are typical temporary structures.

For cofferdams aimed at protecting the construction pit of concrete dams, we can also employ ordinary steel sheet piling beams, driven in such a way that, partially or completely, they encircle a part of the structure in the river channel. Such an example is given in Figure 30.3, which presents the encircled part of the foundation pit in the course of construction of a dam on the River *Aar*, in the vicinity of Bern (Switzerland) in 1979. The water penetrating from the foundation and through the joints of the steel sheet piles is drawn out by means of pumps.

30.2.2 Method without damming of the construction pit

When applying this method, the structures are constructed, partially or completely, directly in the water. In the practice of dam construction, methods employing *caissons* and *wells* have also found application; methods using caissons and wells are much more complex in comparison with the method of damming (of the construction pit); however, they enable a faster construction and commissioning and starting-up of the works into service. Wells are cheaper than caissons, but they may be used only when the foundation allows work under water, without drying out. Caissons are used for

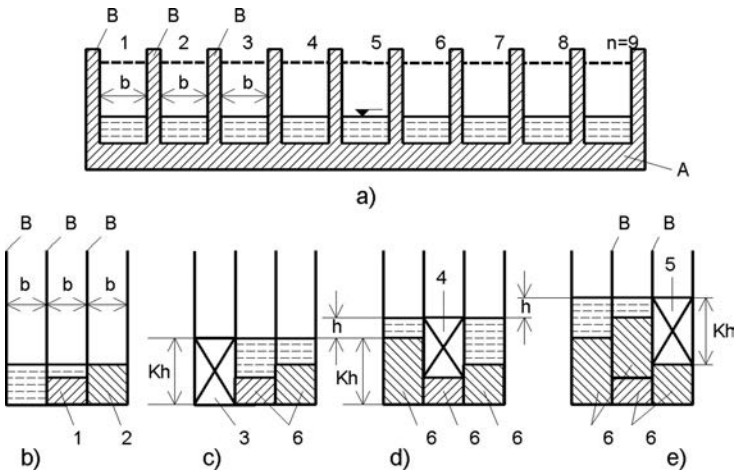

Figure 30.4 Scheme for the method of overflowing openings (a) and concreting of one three-stage section (b–e) (after Chugaev, 1985). (1) Concreted following the first placement of the gate; (2) concreted following the second placement of the gate; (3–5) the third, fourth, and fifth placement of the gate (always at the lowest sill); (6) concreted parts of the openings.

sinking foundations up to depths of 30–35 m, and this limitation does not exist with wells[1].

Another method in this group, which can be combined with the method of caissons and wells, is the *method of overflow openings*. Let us suppose that, by using one of the above-mentioned methods, there has been constructed the foundation part (A) of a concrete overflow dam up to the level of the temporary sill (Fig. 30.4a), as well as the parting walls (B) up to their final height. The overfall parts of the dam (each between two parting walls) may be constructed during a period of the state of low waters, i.e. when it is $Q_{const} = Q_{min}$, with a simultaneous diversion of the construction waters through the incomplete dam, in the following way: one part of the incomplete openings (spans) are covered with gates and, under their protection, they are concreted; at the same time, the construction waters are discharged through the other incomplete openings (Chugaev, 1985).

Let us suppose that the number of incomplete openings (spans) is n. We group them into equal sections of k openings, so that the number of sections will be $n_0 = n/k$. The number of openings in one section (k) is taken to be 2–4. All sections are concreted in the same way, in which only one gate services each section. As an illustration, let us follow through the concreting of one three-stage section (Fig. 30.4b–e). Following the two initial positions of the gate (a), concreting is further utilized as in the sketches b–e, during which time the construction waters overflow through the ungated openings. The elevation difference h is called *a pace of concreting*. From the sketches, it can be seen that, after each dislocation of the gate, the headwater rises by the value of h.

[1]These problems are covered in greater detail in professional textbook references dealing with questions of foundation engineering.

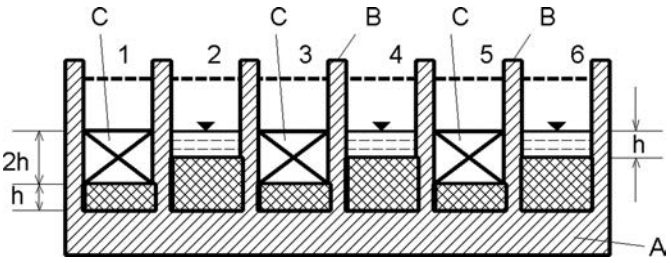

Figure 30.5 Scheme for concreting of a two-stage section (after Chugaev, 1985). (A) Foundation part of the dam; (B) parting walls; (C) gates.

The height of the layer that is concreted behind the gate amounts to $k \times h = 3 \times h$, with the exception of the two initial layers, which are lower (a).

If the sections are two-stage ones ($k = 2$), concreting is achieved alternately – by even or odd openings (Fig. 30.5). When the odd openings are covered with gates, the water overflows over the even openings, and vice versa.

During giving passage to the water, the openings most often work as an unsubmerged broad-crested weir, in which individual parameters are related with the following formula:

$$h = N\left[\frac{Q}{nmb\sqrt{2g}}\right]^{\frac{2}{3}} \tag{30.2}$$

where $N = (k/(\Sigma p^{3/2})^{2/3}$; m is the discharge coefficient; p are integers from 1 to $(k-1)$ inclusive; b is the clear span (opening) between parting walls; and Q is the total overflowing quantity through all openings.

During the application of this method, in the stage of design, it is necessary to determine the elevation of the temporary sill, h, n, k, and height of gates in the course of construction process, in which different variants are possible, so that the optimum solution should be selected. In this, one should take into consideration all factors influencing the rationality of the solution. For instance, if there is an increase in k (at known n and b), then there is a decrease in h, as well as the height and the number of gates; along with it, there is also an increase in the number of dislocation of the gates, etc.

For orientation, h ranges from 1 to 1.5 m; the height of the gate is taken to be:

$$h_z = kh + d \tag{30.3}$$

where d is a reserve, which can be taken as 0.5 m. The spans (openings, i.e. widths) are covered with gates that range up to 15 m. Various metal or else stop-log or stop-plank reinforced concrete gates are used, which may also serve as a formwork that will remain in the dam's body. The gates are placed in gate slots, at the upstream side in the parting walls, while, at more considerable depths of the tailwater, also from the downstream side.

30.3 CONSTRUCTION OF THE STRUCTURES WITH RIVER DIVERSION FROM THE RIVER CHANNEL

The method of construction of structures by means of diversion of the river from the river channel is usually employed with narrow river channels, as well as with steep banks during the construction of hydraulic schemes with a medium and with a high-pressure head. This method is very often used in practice. In the first place, the water conveyance structure is constructed; it serves for diversion of the construction water. This structure may be a tunnel (Fig. 30.6), channel, or pipeline. Then, the river channel is dammed by means of a cofferdam, as a rule at lower discharges.

A diversion tunnel is most often used as a water conveyance structure. The diameter of the tunnel and the height of the cofferdam, are determined by means of an economical and technical analysis, with provided passage to the construction waters, whose probability of occurrence is once in 5–25 years. For the period of recurrence it is usually taken to be 3–5 times longer than the period that has been anticipated for the construction of the structures that are being protected. The economical and technical analysis is conducted in such a way that for several values of the diameter of the tunnel we calculate the required height of the cofferdam, which increases, with the reduction of the diameter. For the appropriate diameters, we then calculate the cost of the diversion tunnel as well as the cofferdam. The summary values yield a curve of the joint cost for the two structures, from which one can read out the optimum value for the diameter of the tunnel, Figure 30.7. This value can undergo certain corrections if a cofferdam of a determined height cannot be executed sufficiently fast. The minimum diameter of the tunnel can be 2 m, while the maximum one 15 m. In a case of need, we can anticipate two diversion tunnels. The distance between the toes of the embankment dam and the cofferdam should be at least 10–20 m.

At the downstream side, the foundation pit is protected against the diverted water by means of a smaller auxiliary dam. The cofferdams and the auxiliary dams are frequently designed in such a way that, following the construction of the hydraulic scheme, they remain within the dam's body. The diversion tunnel, in many cases, is rearranged as a permanent structure; it then serves as a conveyance structure for overflowing waters or as a bottom outlet. One should take into consideration that the

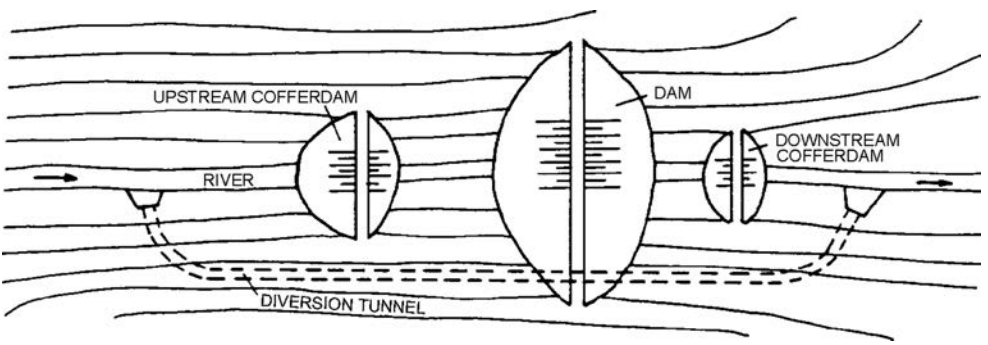

Figure 30.6 Protection of the construction pit with auxiliary dams and diversion of waters by means of a diversion tunnel.

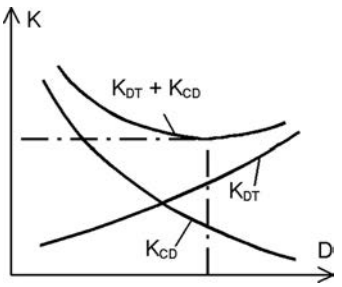

Figure 30.7 Diagram for determining the diameter of the diversion tunnel.

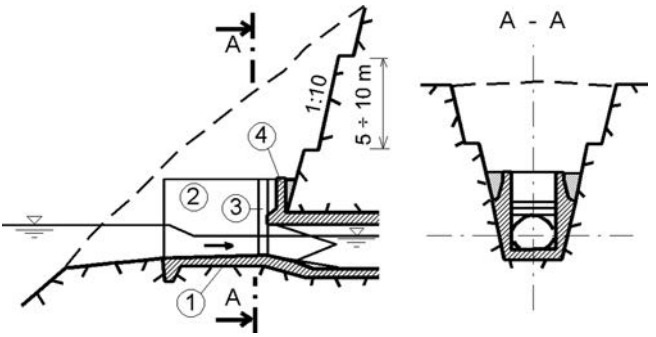

Figure 30.8 Entrance portal of a diversion tunnel.

diversion tunnel and the cofferdams are constructed at the commencement of the construction of the hydraulic scheme, i.e. when the construction site is not yet equipped, worked out, and developed to a maximum, so that the working activities on the execution of these structures as permanent structures, usually have a higher unit cost than they would if they were constructed later on, together with the other major permanent structures.

The entrance portal of the tunnel is formed in excavation, for instance as shown in Figure 30.9. The inclination of the slopes of the rock depends on its quality and it can be very steep – up to 1:10. If the slope is very high, it can be moderated by means of berms at each measure 5–10 m. The space in front of the tunnel is widened, while the bottom (1) and sides (2) are concreted. Slots (3) are left in the sidewalls for an overhaul gate. At the entrance, the tunnel is concreted to a greater height (4), while the part between concrete and rock is filled with soil material. The exit portal, that is to say, the terminal part of the diversion tunnel, is designed in a way similar to the case of the intake tunnel of a shaft spillway structure.

The diversion of waters by means of channels or pipelines, which are placed in the river channel next to the riverbanks, may be achieved only with smaller quantities of construction waters.

In the cases of small dams, a customary practice is for the evacuator of the waters in the course of construction to use the pipeline of the bottom outlet, which is used at the beginning of the construction of the dam, along with a temporary shaped-up

entrance part and terminal part. At the completion of construction, we perform its final shaping-up into a bottom outlet, with the finishing of the entrance (inlet) and the exit (outlet) structure and placement of gates and other hydromechanical equipment. We evacuate the waters in the course of construction of most small dams in our country in this way.

30.3.1 Types of cofferdams

In selecting the type and dimensions of the cofferdams, as well as the form of the construction (foundation) pit, it is necessary to take into consideration the following elements: (1) the distance from the cofferdam to the foundation of the structure, should not be smaller than 10 m; (2) the form in plan of the construction pit should be such as to make possible easy access and descent into it, as well as a good connection with the roadways that are used in the course of construction; (3) the shape and dimensions of the construction pit should ensure safe installation of cranes and of other construction plants and equipment.

Figure 30.9 presents several types of cofferdams, which are most frequently used for the protection of the dam construction pit. When it is a question of an embankment cofferdam (a, b) made of water-impermeable material, it is rational that the water-impermeable element be utilized in the form of an impervious facing, as is shown in the

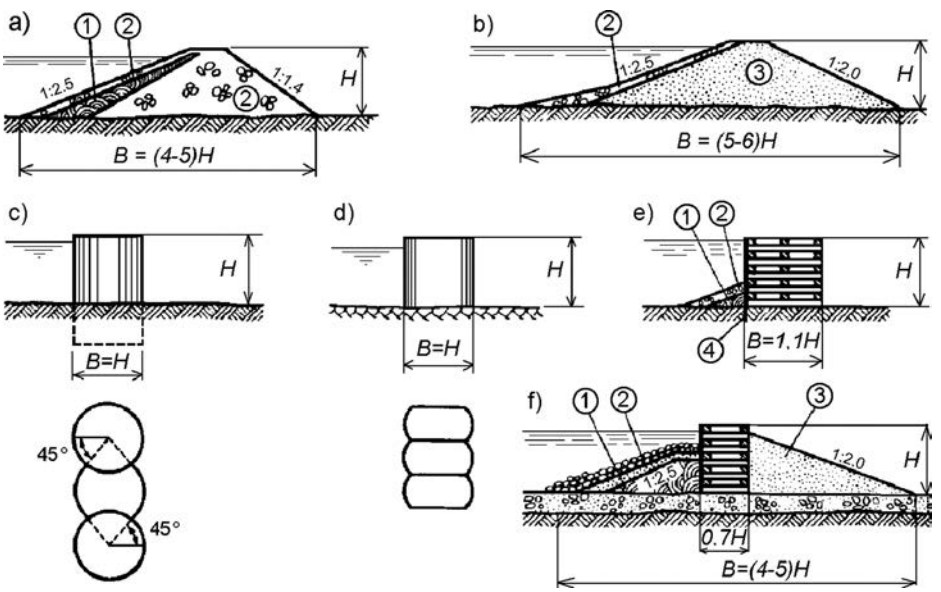

Figure 30.9 Cross-sections of cofferdams (after Grishin et al., 1979). (a) Rockfill cofferdam with earthen facing; (b) sand cofferdam; (c) cylindrical oval cofferdam made of steel sheet piling; (d) segmental oval cofferdam made of steel sheet piling; (e) cofferdam with a wide wooden grille; (f) cofferdam with a narrow wooden grille. (1) Earthen water-impermeable part; (2) rockfill; (3) sand; (4) wooden timber piling.

drawings, since the facing is constructed upon the completed dam's body, irrespective of it. The construction of a core would slow down the construction and can be justified only if such a cofferdam were to be incorporated into the body of the main dam. In that way, it would become a permanent structure. Also, homogeneous earthfill cofferdams of poorly permeable material are often constructed, especially when it is a question of a hydraulic scheme with a smaller dam. Concrete cofferdams are constructed less frequently. They are mainly found in cases of hydraulic schemes with an arch dam, especially in the form of a small, simple arch dam. Steel sheet piling (c, d) is used in countries with a developed steel production, while the employment of wood (e, f) is limited to dam sites that are located in regions that are rich in this natural raw material.

Recently an internal geomembrane was installed as impervious core at the Gibe III cofferdam in Ethiopia, 50 m high, aimed to protect the construction pit of the highest RCC dam in the world ($H = 240$ m, under construction). The construction of the cofferdam was preceded by the construction of a 20 m high pre-cofferdam, incorporated into the final cofferdam. For details see Chapter 14, section 14.2.2, Figures 14.43 and 14.44. In the appropriate places in this book the reader can find other examples of constructed cofferdams.

This page intentionally left blank

Part 5

Hydraulic schemes

This page intentionally left blank

Chapter 31

Composition of structures in river hydraulic schemes

31.1 DEFINITION AND CLASSIFICATION OF HYDRAULIC SCHEMES

As has been defined in Chapter 1, a *hydraulic scheme* is a group of hydraulic structures that are interconnected in their conditions of joint work, i.e. operation, as well as their location. According to *location*, hydraulic schemes may be:

- River hydraulic schemes;
- Channel hydraulic schemes;
- Marine hydraulic schemes;
- Lake hydraulic schemes;
- Fishpond hydraulic schemes.

This book is examining river hydraulic schemes. According to their *primary function*, river hydraulic schemes are divided into water-intake hydraulic schemes (serving various water economy branches – such as irrigation, water supply, energetics, etc.), energy hydraulic schemes, transport hydraulic schemes, fishery economy hydraulic schemes, and hydraulic schemes for regulation of river flow and its utilization for various purposes, etc. Frequently, the hydraulic schemes have a complex purpose or function; that is to say, they serve the needs of two or more water economy branches.

The hydraulic schemes may be:

- Without pressure, i.e. without a pressure-head (for instance, a river harbour);
- Under pressure, i.e. under a pressure-head H. The hydraulic schemes that are under pressure are further divided into low-head hydraulic schemes (H less than 10 m), medium-head ($H = 10$–50 m), and high-head, when it is $H > 50$ m.

The low-head hydraulic schemes are built on plain-land rivers in order to facilitate water-intake, as well as water transport, while in the middle course of the river and the upper course of the river for water intake. The medium-head and high-head hydraulic schemes are usually multi-purpose, i.e. multi-functional.

A complex of hydraulic structures, usually united in several hydraulic schemes and associated with a joint function, is called *a water economy system*, or a *hydrosystem*. Thus, there are hydroelectric power systems, hydroamelioration, water-supply systems, and navigation systems, etc. There are also complex hydrosystems that satisfy the

needs of a number of water economy branches. There are a number of such hydrosystems in the Republic of Macedonia, for instance, the *Mavrovo* hydroelectric power system, the *Strezhevo* hydroamelioration system, the *Tikvesh* complex hydrosystem, and others.

31.2 GENERAL CONDITIONS AND PRINCIPLES FOR THE COMPOSITION OF HYDRAULIC SCHEMES

In designing the hydraulic schemes, as a rule, we start from the condition of a complex utilization of the river flow intended for provision of sufficient water for various economic branches. Owing to that, within the composition of the hydraulic scheme, together with the dam and other general structures, it is usually necessary to also anticipate different special hydraulic structures, and that causes complications to a larger or a smaller extent in composing the hydraulic scheme.

Various factors also influence the composition of the structures and their configuration within the hydraulic scheme, such as topographical and geological conditions in the zone of the hydraulic scheme, the quantity of water in the river, the pressure head, the conditions for the execution of individual structures, and the conditions for utilization of the hydraulic scheme, etc.

The *topographical conditions* in the zone of the hydraulic scheme should provide the minimum length of the structures under a pressure head without significant submerging of agricultural and industrial areas. Also, it is important in the vicinity of the dam site to have a flat area with the necessary conditions for migration of the population from the areas that are to be submerged. The land contours of the locality should also allow for construction of the essential network of roads.

The *geological feature* of the foundation and banks should correspond to the requirements in relation to the load-bearing capacity, as well as in relation to the seepage properties. One should especially take account of whether the foundation is suitable for founding of the concrete works.

In relation to *conditions for construction*, it is necessary to take into consideration that, for rational composing of the hydraulic scheme, there must be ensured the following conditions: safe passage for the construction waters in the course of the entire period of construction of the hydraulic scheme; the concrete structures should be placed compactly, without greater contact surfaces with the embankment structures; the available local material should be used to a maximum, without deranging the surrounding natural environment; ensuring the possibility of the maximum mechanization of the construction process, with the application of the most modern plant and equipment; and to take into consideration the possibility for staged execution and utilization of the hydraulic scheme, so that during the execution of the forthcoming stage, the structure should normally be in service without lowering the normal water level of the previous stage.

In terms of *service requirements*, the structures of the hydraulic scheme should be compact, and they should perform their function in the most effective way. Both upstream and downstream of the hydraulic scheme, it is necessary to provide a favourable hydraulic regime, especially in the letting through of high floodwaters. The courses and values of the velocities of flow should ensure a gradual access of water

towards the water conduits, without any washing-out and scouring of the banks in the zone of the structures or sedimentation of silt in the upstream part. All of the structures should be connected with roadways and should also be accessible for overhaul.

Composing the hydraulic schemes is a rather complex engineering task and it is of an individual nature, so that the final solution is adopted on the basis of a technical and economical comparison of a number of possible variants, giving preference to the solution in which each structure performs its function in the best possible way, without causing difficulties during the construction and operation, while the hydraulic scheme, as a whole, should require minimum funds for both its construction and service. In this, account should be taken of the following fundamental principles:

- Each structure, as a member of the hydraulic scheme, should be suitable to the intended function;
- Each structure, through operation, should facilitate proper functioning of the hydraulic scheme as a whole;
- The structures, in the fulfilment of their functions, should not interfere with or disturb each other;
- The hydraulic scheme should function as a compact unity;
- Each structure should satisfy the requirements for safety;
- The most appropriate materials should be selected for construction;
- The economy of individual structures, as well as of the hydraulic scheme as a whole, should be satisfied to the maximum;
- In designing the hydraulic scheme and the individual structures within its framework, it is obligatory to employ the latest world achievements in both the theory and the practice of the relevant fields;
- The structures should be at a satisfactory level in relation to their aesthetic appearance.

When composing hydraulic schemes, and especially in composing complex ones, it is also necessary to take into account the possibility of *development and expansion* in the future, with an increase of the head, construction of a ship navigation lock, new intake, or with an increase of the installed power, if it is a question of a hydroelectric power plant.

Besides the above-cited assumptions, in composing the hydraulic scheme we should endeavour that the *aesthetic appearance* of the hydraulic scheme be harmonized as much as possible with the natural scenery of the surrounding ground. Another important factor is the preservation of natural, cultural, and historical rarities, including here the potential sites, anticipated for excavation. Nor should one forget the possibilities that the construction of the hydraulic scheme could change the thermal regime of the watercourse, even the microclimate in the surrounding region which, also, could have a negative impact on the environment. In the end, during construction of large reservoirs, one should also take into consideration the possibility that the significant loading from the water could cause changes in the seismic characteristics of the surrounding area.

Existing, as well as future, hydraulic schemes on the watercourse, influence the composition of the hydraulic scheme and the dimensions of the primary structures.

For instance, the construction of new reservoirs in fact decreases the probability of significant variations of inflow in the existing reservoir, downstream of them.

31.3 CHARACTERISTICS OF RIVER HYDRAULIC SCHEMES FOR DIFFERENT WATER ECONOMY BRANCHES

River hydraulic schemes, intended for only one water economy branch, have the following basic characteristics:

(a) *Hydroelectric power complex*. It has the task of providing conditions for intake of water and for forming smaller or larger reservoirs. By means of the intake structures, water is captured from the reservoir and, by means of the supply conduits, it is brought to the hydroelectric power plant where, with the appropriate head, it is used for the generation of electric power. Such a hydraulic scheme forms a unity with the other essential structures – the spillway structure, the outlet, etc., as well as with the distribution power structures and the transmission lines, by means of which distribution of the electric power is performed.

(b) *Amelioration hydraulic scheme*. This is composed of a group of structures, the task of which is to drain the excess water from a certain amelioration area, or else to bring water for irrigation in such a quantity and time schedule so as to compensate for the natural shortage of water. In the first case, it is a question of an amelioration hydraulic scheme for dewatering, i.e. drainage, while in the second case it is a question of a hydraulic scheme for irrigation. The hydraulic scheme for irrigation possesses an intake structure with or without a weir, as well as water-conduits for bringing the water into the amelioration area where, by means of a distribution network, water is brought to the plants. Most frequently, the required quantities of water for irrigation are provided by forming an appropriate reservoir space by means of the construction of a dam with the necessary appurtenant hydraulic structures. In that way, accumulation of water is made possible, as well as its distribution according to the demands for irrigation.

As examples of hydraulic schemes for irrigation, one may point out Futaba (Japan) and Vodocha (Macedonia) the hydraulic schemes of dams, with layouts as presented in Figures 27.18 and 27.19 (Chapter 27).

The Futaba dam (an embankment dam with upstream asphalt facing, 60 m high) forms a reservoir with an available storage capacity of more than 9 million m^3. The intake of water for irrigation is achieved by means of a tower, accommodated next to the left bank. By means of the tower, the water may be intercepted from a number of levels in order to facilitate intake of warm water from the surface (the variation of the water level in the reservoir amounts to 23 m). From the intake tower, the water, by means of a short tunnel, enters the diversion tunnel, and then is taken away to the surface, i.e. by land for irrigation, by gravity through the river channel.

The Vodocha embankment dam in Macedonia, 48 m high, accumulates water from the rivers Vodocha and Trkanya and forms a reservoir with an available storage capacity of 25.12 million m^3, intended for the irrigation of 4200 hectares of land in the Strumica Plain. Also, in this case, the diversion tunnel has been changed into a bottom outlet, which also serves for the intake of water for irrigation. For that purpose, in the zone of the grout curtain, below the core, a valve chamber has been constructed,

provided with a butterfly valve and a cone valve. The dimensions of the valves are Ø 800 mm and they should provide closing and accurate regulating of discharges at partial opening. The maximum necessary water quantity for irrigation is 2.3 m^3/s, while the capacity of the bottom outlet is 18 m^3/s.

(c) *Hydraulic scheme for water transport*. This is a group of structures that should make possible navigation, loading, reloading, and unloading of goods, as well as protection of navigation vessels in the course of stationing, i.e. berthing. Usually, the structures for the accomplishment of all of these tasks cannot be concentrated in one single place, so they are stretched out along the length of the river course. In this way, it is possible to carry out fragmentation of the hydraulic scheme for water transport into smaller hydraulic schemes with certain specific purposes, for example, for facilitating navigation, for loading, reloading and unloading of goods, and for stationing (berthing) of navigation vessels in the course of the winter (during ice blocking). We can especially distinguish hydraulic schemes also serving for the rafting and floating of logs. The structures of the hydraulic scheme for navigation should be so composed and configurated as to enable the creation of a navigable depth and elements of the waterway route, which will make possible unobstructed travel of the relevant navigation vessels. For that purpose, it is necessary to construct regulating structures or elements (sills, baffle piers, etc.). In cases of rivers that are canalized, it may be necessary to construct a whole series of steps that help slow down the water, and each step, with its appurtenant hydraulic structures, is deemed as a separate hydraulic scheme. At places where a man-made navigable channel is constructed, they carry out a whole set of local hydraulic schemes, mutually and functionally interconnected. Such hydraulic schemes encompass structures that serve for the formation of a reservoir and depth (various types of dams), structures for lockage transferring of navigation vessels from one level into another, as well as structures for the supply of channels with water.

In the case of this kind of hydraulic scheme, we should also mention the harbour hydraulic schemes, where there belong structures such as wharves or quays, transport storages with devices and equipment for loading and unloading, moles, etc.

(d) *Hydraulic scheme for water supply*. This is a group of structures with a joint purpose, and that is to provide the necessary quantities of water for the water supply of a certain area, settlement, or industrial facility. The structures that belong to such a hydraulic scheme are intake structures, supply structures (conduits), and the system for distribution and control of the water. Therefore, this kind of hydraulic scheme may also encompass structures for the formation of a reservoir for provision of reserves of the necessary water quantities. The water for water supply usually requires purification, i.e. water treatment, which is performed in filtering water treatment plants, in the vicinity of the consumers or else near the intake structures. Depending on their position, they either belong to the hydraulic scheme near the intake or to a hydraulic scheme in the area of utilization.

(e) *Hydraulic scheme for water retention*. This is a group of structures with a dam forming a reservoir and other necessary appurtenant hydraulic structures. The reservoir encompasses the flood waves of the floodwaters and protects the area against floods downstream of the hydraulic scheme. The efficiency of such a hydraulic scheme increases with its approach to the area that is to be protected. Such a hydraulic scheme usually has other objectives, too. If it serves only for retention, which is a rare case, then its composition is relatively simple, with an overflow structure of smaller

capacity in relation to other hydraulic schemes. The requirements in respect of water-impermeability of the dam and its foundation are rather rigorous, while the bottom outlet may also consist of an uncontrolled water conduit.

(f) *Hydraulic scheme for sediment retention*. This hydraulic scheme consists of a dam forming a reservoir that serves for the sedimentation of silt or waste products of certain industrial processes. The reservoir for such a purpose is so dimensioned as to be filled with sediment and waste materials within a certain time period. In that, the construction of the dam may be achieved in stages, following the filling of a certain volume of the reservoir space.

(g) *Hydraulic schemes for other purposes*. In addition to the above-described roles, there also exist other hydraulic schemes – for sewerage works of inhabited places and industrial facilities, for protection against torrents and downpours (consisting of a series of structures – weirs, cascades, drain flume and channels, and gutters, etc.), for the needs of the fishery economy, for sport and recreation, etc.

In most cases, the hydraulic schemes have a complex purpose and function; that is to say, they are constructed in order to serve the needs of two or more water economy branches. In this, such water economy branches should be mutually combined in such a manner as not to lead to any significant obstacles in the utilization of the hydraulic scheme, while the combination and the regime of utilization of the water should be such as to obtain the maximum effect and level of utilization of the capacities.

Within the former presentations, there have already been given layouts of some multipurpose compound hydraulic schemes. The hydraulic scheme at the Naramata earth–rock dam (Japan, Fig. 27.5), is anticipated to serve for retention, irrigation, water supply, and provision of a biological minimum in the river channel, downstream of the hydraulic scheme. The dam is 158 m high and it impounds a storage reservoir of 85 million m^3, with a variation of the water level of 88 m.

One of the highest embankment dam in Macedonia, Tikvesh (Fig. 27.32), forms a reservoir for irrigation, as well as generation of electric power. The hydroelectric power plant is a near-dam type of plant, with an intake and tunnel supply, accommodated in the left bank. The intake and the supply conduit for irrigation, with an installed discharge capacity of 12 m^3/s, are on the right bank. The hydroelectric power plant has an installed discharge of 60 m^3/s during the first stage (1968), increased to 120 m^3/s during the second construction stage.

31.4 AESTHETIC SHAPING OF HYDRAULIC SCHEMES

The hydraulic schemes with a dam that form an artificial lake (Fig. 31.1), in many cases represent in themselves attractive tourist and recreation facilities. With the development of tourist traffic, many visitors and chance travellers and guests visit the hydraulic schemes. In that way, there is an enhanced need for as much aesthetic shaping of the dams and appurtenant structures, as possible all in order to highlight their natural beauty.

The type of dam that is constructed within the hydraulic scheme plays an essential role in the aesthetic shaping of hydraulic schemes. For embankment dams, it is characteristic that, within their body, there is placed an enormous quantity of local material, exploited from borrow pits in the vicinity of the dam. That is why, for such structures,

Figure 31.1 Water impounded into a lake in itself represents an aesthetic experience: the storage lake that provides water for the cooling of the first nuclear power plant in Switzerland (built in 1954) makes the scenery pleasant and mitigates the unpleasant feeling that you are in the vicinity of a dangerous structure.

it is of essential importance, immediately after completion of the construction of the hydraulic scheme, to level, grass, and plant the zones of the borrow pits. Similar treatment is also required in the stockpiling areas with material from excavation from the dam's foundations and the appurtenant hydraulic structures. Another question is that of temporary structures for workshops, storage of materials, stationary plant, and equipment, as well as residential and administration buildings, which serve during the course of the construction of the works. They should be dismantled and taken away, and if any of them remains and is made into a permanent structure, then it should be accordingly reconstructed and adapted. In developed countries, special attention is paid to this question, and maybe the greatest attention is paid in Japan. In the case of recently completed Japanese hydraulic schemes, as well as in the older ones, it is not possible to notice that only a few days earlier there had been a large construction site at that place, with many temporary structures, borrow pits, and stockpiling areas of local materials. The embankment dam that usually dominates over the other structures within the hydraulic scheme, should have a nicely shaped crest and downstream slope, which harmonizes best in the surrounding landscape if it is grassed.

The situation is different in the case of concrete dams. In that case, there are no residues from the enormous borrow pits of local materials. However, that is why the grey concrete should be shaped in such a manner as not to be in contrast with the surrounding ground. Usually, the best harmonization with the surrounding scenery is achieved with arch and arch-gravity dams owing to their characteristic shape, smaller dimensions, and narrow dam site, which often correspond well with concrete. Buttress

dams, because of their fragmented structure and exuberant form also, without special making up, cause a pleasant aesthetic feeling.

Gravity concrete dams look rather rough and heavy and that is why they require greater attention to their aesthetic shaping and for concordant harmonization with the environment. According to the investigations of Japanese dam constructors, there have been defined 13 aesthetic elements of a hydraulic scheme with a dam, presented in Figure 31.2, the example of a hydraulic scheme with a gravity concrete dam (Sasaki et al., 1991).

In connection with those elements and the general considerations of the aesthetic requirements, attention should be drawn to the following issues, which compose the philosophy of the aesthetic shaping of hydraulic schemes:

- Achievement of harmony between nature and the structure. With appropriate, usually simple, measures, it is possible to achieve coordination between nature and the structures. Those measures may be an inventive selection of colours and materials, as well as regeneration of the landscape at places where it has been damaged owing to the artificial interventions. For example, the artificial fillings of earth look harmonious with the landscape if they are covered with vegetation, while slopes in the ground, formed by excavation, require levelling and cutting-in, which will enable a slight transition from the dam toward the natural ground.

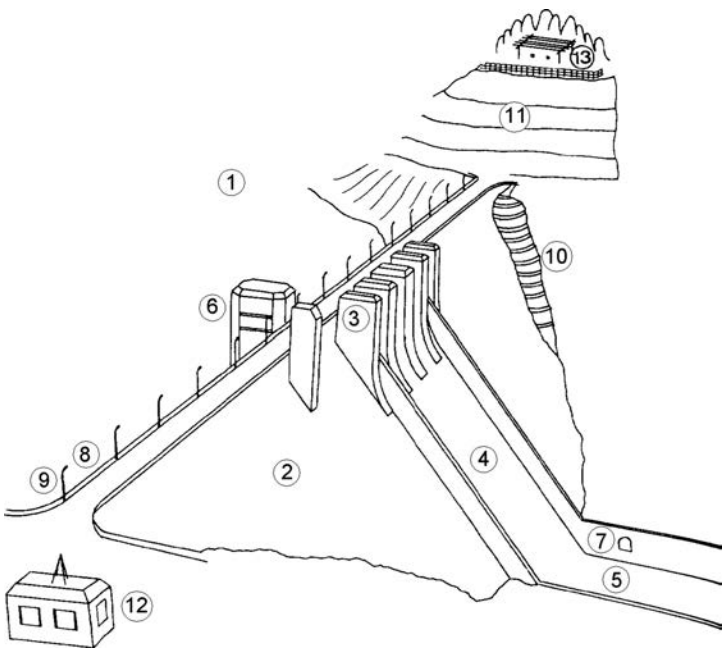

Figure 31.2 Aspects of aesthetic shaping of a hydraulic scheme with a concrete dam. (1) General view; (2) downstream side of the dam (without spillway); (3) training wall of the spillway; (4) spillway chute; (5) stilling basin; (6) intake structure; (7) conduit for water supply; (8) fence; (9) lighting devices and equipment; (10) step-like shaped rock; (11)slope of excavation and construction site for temporary works; (12) control house; (13) surveillance platform.

Geometric continuity of the dam, rounded joints with the appurtenant hydraulic structures, rounded edges of the crest, and training walls, etc. – also make a contribution to improved harmony with the landscape.

- The configuration of the dam and other structures should be as simple as possible. With a simple construction of the dam's body, and without sharp transitions, we may emphasize its beauty. In order to achieve that, one should avoid emphasized details of the appurtenant hydraulic structures and simplify the overall configuration. The mechanical equipment, whenever possible, should be invisible from outside.
- Materials and colours should be as consistent as possible. In terms of coordination of colours and materials, again the greatest possibility for disharmony comes from the hydromechanical equipment, such as the large gates, etc. A possible measure is their accommodation in the interior of the dam or 'masking' with concrete, all in order to improve the compatibility between materials and the configuration, thus creating an impression of integrity.
- The horizon of the crest should be flat. A dam is a beautiful, mechanically stable structure and its general silhouette should be preserved to the maximum. For that purpose the overflowing part, which in gravity dams is most frequently located in the middle of the dam, should be of a limited height of the gates and the training walls, in order not to break the horizon of the crest too much.
- The appurtenant hydraulic structures should be configurated in a systematized manner. The appurtenant hydraulic structures, as well as their components, should be set up by observing certain regulations – symmetry, equal mutual distances, etc., in order to maintain the equilibrium of the entire configuration of the hydraulic scheme and to maintain its rhythm. In this respect, one should pay attention to the arrangement of the elements of the spillway, gate chambers, and lighting devices and equipment.

31.5 RIVER HYDRAULIC SCHEMES WITHOUT PRESSURE HEAD

To this group of hydraulic schemes there belong all kinds of river intakes that serve for intake of water without anticipating any weir in the river channel. The water is diverted from the parent river channel, at the natural level in the river. This kind of hydraulic scheme is formed in the lower course of the river, and it most often serves the needs of amelioration, water supply, and water transport.

According to the conditions for diverting the waters from the river into the channel, we may differentiate an intake with regulating of the quantities of water and an intake without such regulating. In cases of unregulated intakes, the quantity of intercepted water depends on the level of the river. In cases of regulated intakes, the water is transferred into the channel by means of regulators or by means of pumping stations, so that the required quantity of water can be captured at any level of the river.

Each significant intake of water from the river changes its hydrological regime; that is to say, it changes the arrangement of velocities and courses of the flow, and the travelling of sediment and ice. In designing the intake, we should create such a regime of diverting the water into the intake as would prevent penetration of silt or

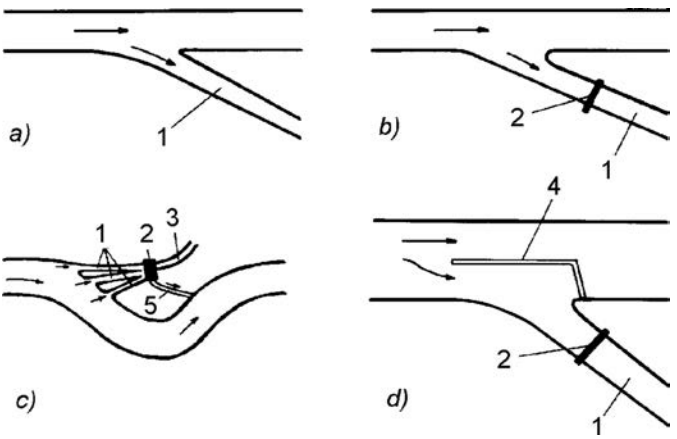

Figure 31.3 Hydraulic schemes for an intake without a pressure head. (1) Channel; (2) regulating structure; (3) primary channel; (4) directing wall; (5) weir.

various floating objects into the water conduits. These conditions should be fulfilled at a variable water level of the river and at possible deformations of the river channel.

The location and composition of the hydraulic scheme without a pressure head is determined by means of analyzing a series of factors, such as the conditions and quantity of water that has to be captured, climatic conditions of the region, topographical, geological, and hydrogeological conditions of the examined river section, etc. More precisely, the location of the intake without a pressure head is selected on a section of the river where the discharge is stable, in a channel without shallow spots or river islands, and with a stable line of the bank.

The basic schemes of the plan of intakes without a pressure head are presented in Figure 31.3. The simplest intake, which is primarily used for irrigation, is a part of an open channel, which comes out of the river channel at a certain angle in relation to the longitudinal axis (Fig. 31.3a). Placement of a regulating structure at the beginning of the channel (2, Fig. 31.3b) facilitates obtaining better conditions for work of the intake, giving passage to regulated quantities of water.

On rivers with unstable banks and with great quantities of sediment, they sometimes make intakes with a number of exit channels, with regulating structures at each channel or else with a joint one as shown in Figure 31.3c. This kind of structure ensures an uninterrupted inflow of water to the consumer and, in the case of some of the channels being thrown out of operation, owing to infilling with sediment or due to scouring of the river bank.

Another kind of intake without a pressure head is the frontal intake, at which a directing wall is constructed in the river channel, and directs the water into the channel (Fig. 31.3d). The directing wall is similar to low embankments and are constructed with local materials. Such a construction improves the approach of the water towards the channel, while at the same time it decreases the quantity of sediment in the channel.

31.6 LOW-HEAD HYDRAULIC SCHEMES

The low-head hydraulic schemes are constructed on low-lying (plains) rivers, in order to improve the conditions for navigation, rafting, and floating of logs or else intake of water, as well as in the upper course of rivers, in which case the water is intercepted and used for irrigation, or else for power generation, usually through derivation power facilities. In addition to the dam and other primary structures, within the composition of such hydraulic schemes there also belong special structures – ship navigation locks, intake structures and, in case of need, a hydroelectric power plant (if it is a question of navigation and a power hydraulic scheme). It is often also necessary to anticipate a structure for giving passage to fish.

In composing low-head hydraulic schemes, the transport and power facilities are usually positioned at different banks, which have already been discussed in Chapter 29 (Figs. 29.2 and 29.5), since the work of these structures is not mutually connected. One should endeavour that the powerhouse be constructed during the first stage of construction of the hydraulic scheme, since it requires a longer time period for mounting of the equipment. It is favourable to construct the ship navigation lock at the same time as the powerhouse, at which it would be very convenient to separate the derivation (supply) channel if that is allowed by the local conditions. The placement of the powerhouse and the ship navigation lock at the same side creates certain difficulties in the utilization of the hydraulic scheme; however, it eases the execution of the concrete works located within a hydraulic scheme. In such a case, a special bridge will have to be constructed over the ship navigation lock, in order to enable transport of the heavy equipment to the place of mounting (Fig. 31.4).

In case of insufficient width of the river, a part of the structures are inserted into the bank, within an excavated part. In such cases, we can save space with locating the hydroelectric generating sets in the training walls of the overflow dam.

In the upper courses of a river, the overflow part of the dam is usually constructed in the form of a concrete sill with plain or radial gates, or else with a free over-fall. In the transport hydraulic schemes in the low-lying (plains) rivers, at pressure heads up to 4 m, we may use movable dams in the form of a gate with mobile trusses or else in the form of an inflatable gate (Chapter 24). For higher-pressure heads on this kind of

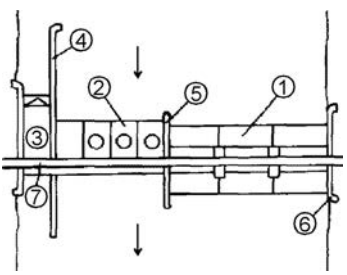

Figure 31.4 Hydraulic scheme under a low-pressure head. (1) Overflow dam; (2) powerhouse; (3) ship navigation lock; (4) longitudinal directing wall; (5) training wall; (6) waterfront side wall; (7) bridge over the ship navigation lock.

dam, there are great losses of water among the numerous elements, so that it would be suitable to employ low concrete sills, provided with plain gates, radial gates, bear-trap gates, or sector gates.

31.7 MEDIUM-HEAD RIVER HYDRAULIC SCHEMES

Hydraulic schemes under a medium pressure head are built on lowlands rivers in broad river valleys, rich in water where, as a rule, there is a soil foundation, or else on mountain rivers with relatively steep banks, narrow river channels, and a semi-rock or rock foundation. These hydraulic schemes are mainly intended for energy generation purposes. They often have transport structures, while the intake structures are usually of the pressure head type. The following primary structures are usually

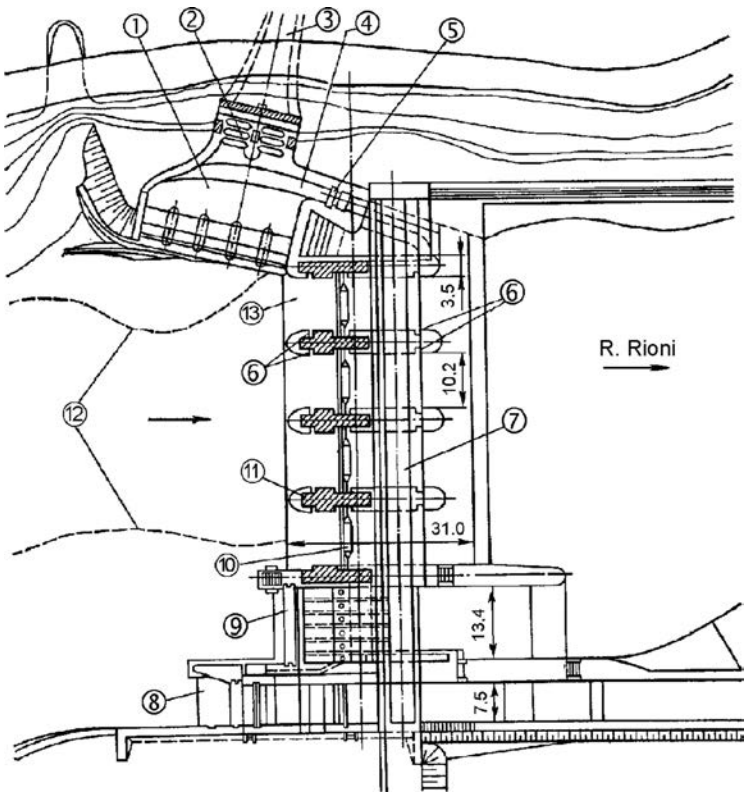

Figure 31.5 Hydraulic scheme on the River Rioni (Georgia), $H = 12$ m. (1) Sedimentation tank (chamber) for coarse sediment; (2) gates in front of the entrance into the tunnel; (3) derivation (supply) tunnel for hydroelectric power plant; (4) channel for washing out of the sediment; (5) gates or valves on the channel for washing out; (6) gate slots for flashboard (stop log) gates; (7) bridge; (8) rafting structures (for floating logs); (9) siphon spillway; (10) gates; (11) training walls; (12) natural river channel; (13) weir.

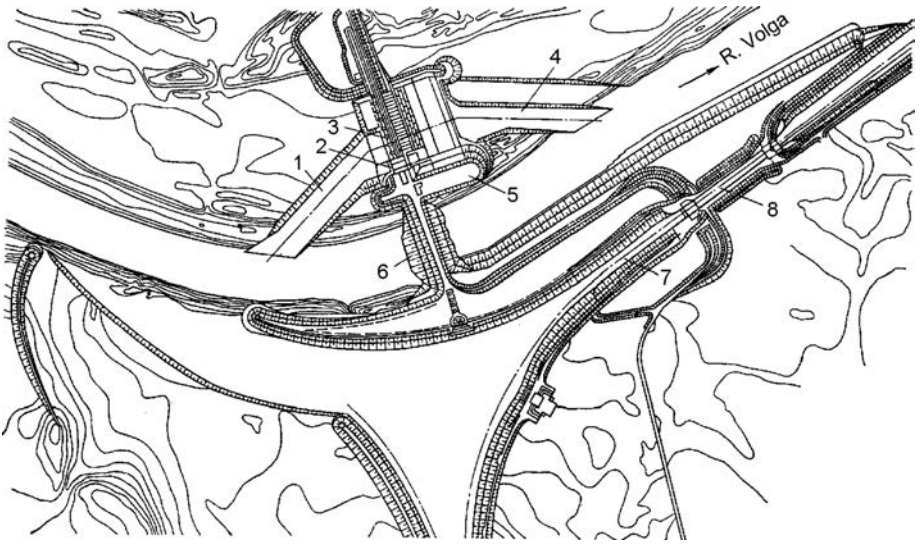

Figure 31.6 Ivankovskiy hydraulic scheme on the River Volga (Russia), $H_k = 20$ m. (1) Access channel; (2) powerhouse; (3) overflow dam; (4) tail race; (5) substation; (6) earthfill dam; (7) navigable channel; (8) ship navigation lock.

constructed: concrete overflow dam, powerhouse, and a ship navigation lock, while the remaining part of the water-retaining structure may be constructed as an embankment dam.

In composing a hydraulic scheme of the first type on a low-lying (plains) river in a broad valley, there are two basic schemes: (1) when the overflow dam is constructed in the river channel by applying the method of sectional cofferdams; and (2) when the overflow part is located in the broader part of the river valley, while the river valley is dammed with an embankment dam, constructed in water.

As an example for the first scheme, we may cite the hydraulic scheme on the River Rioni (Georgia), with a pressure head of 12 m, constructed in the period from 1928 to 1934 (Fig. 31.5). All structures within the hydraulic scheme are accommodated in the river channel. The purpose and function of the hydraulic scheme is to create conditions for the intake of water, which, afterward, by means of a derivation (supply) tunnel, is transferred to the powerhouse (Chugaev, 1985).

An example of the second scheme is the *Ivankovskiy* hydraulic scheme on the River Volga (Russia), with a height of the dam of 20 m, built during the period 1933–1937 (Fig. 31.6). This hydraulic scheme is for transport and energetic purposes. The power house is accommodated in the concrete part of the dam, while the navigation is achieved through a channel, accommodated next to the opposite bank and provided with a ship navigation lock (Chugaev, 1985).

In addition to the above-described two basic schemes, a combined scheme is also possible – when, in the river channel of a broad valley river, we construct a combination of an embankment and concrete dam, in which is accommodated the hydroelectric

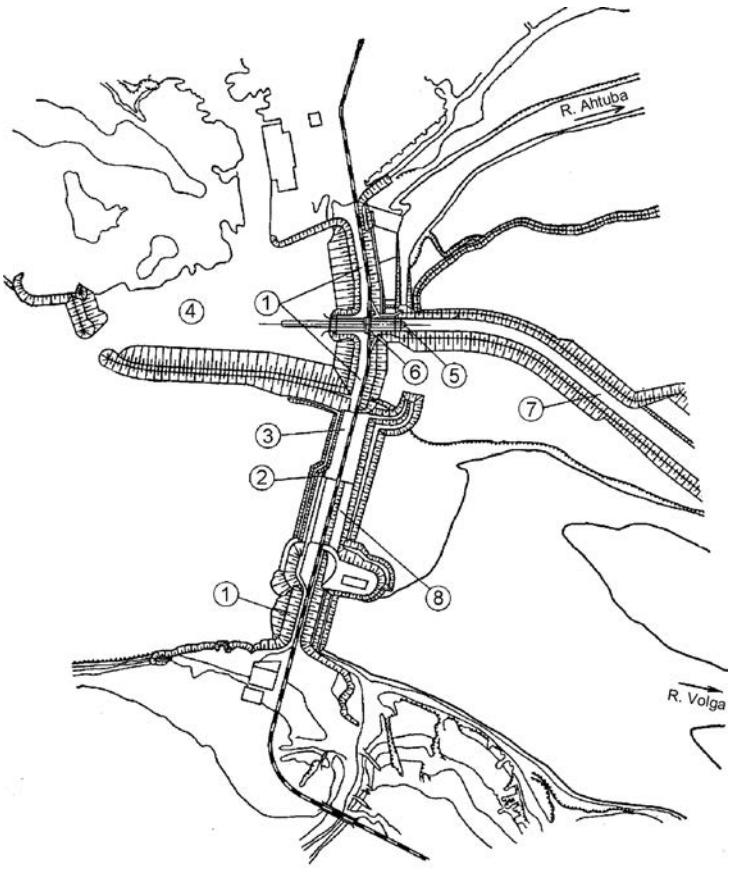

Figure 31.7 The Volgograd hydraulic scheme (Russia), $H_k = 33$ m. (1) Embankment dam; (2) fish lift facility; (3) concrete overflow dam; (4) harbour; (5) ship navigation lock; (6) hydroelectric power plant between the ship navigation locks; (7) downstream access channel; (8) hydroelectric power plant.

power plant, as is the case with the Volgograd hydraulic scheme (Fig. 31.7), with a dam 33 m high, built in the period 1951–1961 (Chugaev, 1985).

In cases of medium-head hydraulic schemes, the principle of locating the transport and power structures, i.e. facilities, is the same as in the low-head hydraulic schemes.

The composing of the medium-head hydraulic schemes applied on mountain rivers on a rock foundation does not differ in principle from the composing of high-head hydraulic schemes, which will be described in the following chapter.

Chapter 32

High-head river hydraulic schemes

According to their locality, high-head river hydraulic schemes ($H > 50$ m) can be classified into two basic groups: (I) *on mountain rivers*, in deep and relatively narrow valleys, with a foundation and banks consisting of rock; and (II) *on semi-lowland and lowland rivers*, rich in water, with a foundation also consisting of rock. The following structures belong to the group of high-head river hydraulic schemes: high dams, spillway structures, structures for protection of the construction pit and conveyance and diversion of construction waters, powerhouse with an intake for a hydroelectric power plant and a tail race, and intakes for irrigation and water supply. Ship navigation lifts and more rarely, ship navigation locks, can also be considered as high-pressure head river hydraulic schemes of the second type.

32.1 HIGH-HEAD RIVER HYDRAULIC SCHEMES ON MOUNTAIN RIVERS (TYPE I)

In composing the structures in narrow dam sites, two basic solutions are possible: (1) A concrete dam is constructed – a gravity dam or arch dam – and the spillway is completely accommodated within the dam or partially in one of the banks, while the powerhouse is set up either in the dam's body or immediately next to it, or else under the ground; (2) An embankment dam is constructed (rarely a concrete dam), and all spillway and water conveyance structures (conduits) – open type or tunnel type – are located in the banks, while the powerhouse is usually an underground type, or else is set up on the river banks, a little away from the dam.

The selection of the solution of the hydraulic scheme is determined through an economical and technical comparison of the possible alternatives, in which the basic factor is in the wealth of water in the river, and the width of the dam site. In the case of a narrow valley and great quantities of water for evacuation, it is more likely that a scheme with an arch or with a gravity dam will be a rational one, while for medium and small flood waves, the application of an embankment dam would be economical. In any case, the economical and technical analysis is obligatory, taking into consideration the characteristics of the locality and the available local materials.

As an example of the solution quoted under (1) for hydraulic schemes of the first type, Figure 32.1 presents the layout of the structures within the hydraulic scheme, formed by the Shimaigawa Dam (Japan), built in the period 1976–1981. The ratio of the length of the gravity dam along the crest vis-à-vis the height of 2.7:1 indicates that it

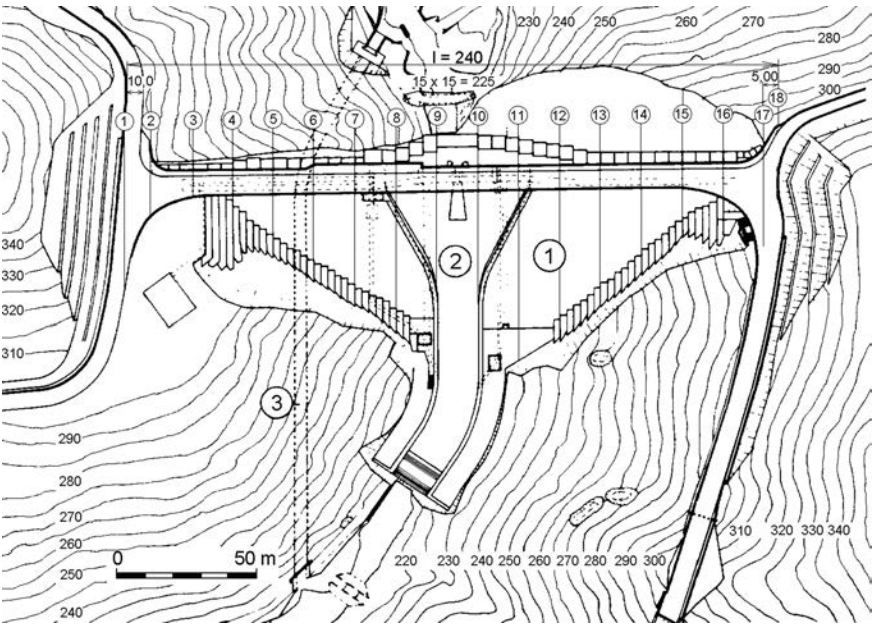

Figure 32.1 Hydraulic scheme at Shimaigawa Dam (Japan), Type I, solution 1 (JNCOLD, 1991). (1) Gravity dam; (2) spillway structure; (3) diversion tunnel.

is a question of a decidedly narrow dam site. The dam, 89 m high, impounds a reservoir storage space of 20 million m^3, which is used for retention of flood waves, water supply and the provision of a biological minimum in the river channel. The spillway is an ogee free overfall spillway, uncontrolled, located in the central part of the dam, with a capacity of 750 m^3/s. The spillway is 53 m wide, while the spillway chute contracts and ends up in a stilling basin, 35 m long. The protection of the construction pit has been achieved by means of an upstream and downstream earthfill cofferdam, while the diversion of construction water is by means of a tunnel, driven through the right bank. In the central part of the dam, below the spillway, there have been constructed an upper and a lower intake and outlet structure with pipes of Ø1200 mm and Ø800 mm (JNCOLD, 1991).

Another characteristic and pictorial example of solution 1 is the hydraulic scheme at the Monteynard Dam (Southeastern France), Figure 32.2, one of the numerous steps on the River Drac[1]. The Drac is a steep river, with a longitudinal slope of 1% and with a catchment area at *Monteynard* of 2000 km^2, it has excellent conditions for the generation of hydroelectric power. It is a tough and wild mountain river, which, flowing through a series of deep and narrow canyons, carries and deposits significant quantities of stone, and it can also be raised and swollen with enormous quantities of water, almost instantaneously. The dam site, also, is very tough, with fissured rock across almost vertical hillsides, from which stones down. Under such conditions it

[1]This dam has already been discussed in Chapter 26, section 26.1.

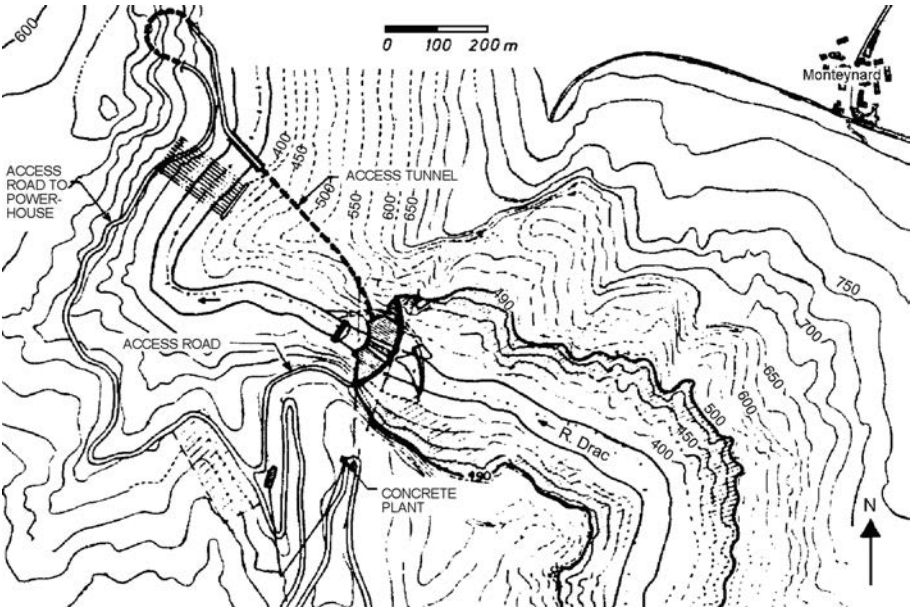

Figure 32.2 General layout of structures in the Monteynard hydraulic scheme (Type I, solution 1).

was concluded that the best solution would be that of an arch-gravity concrete dam, with a powerhouse incorporated in its body, Figures 32.3, 32.4. The dam, with a height of 150 m and a crest length of 210 m, impounds a reservoir storage space of 240 million m^3, of which 150 million m^3 are formed between the elevation 450 and 490 m height above sea level and it is used for the generation of hydroelectric power. The flooded area amounts to 620 hectares, mainly uncultivated land, while and under the water level there also remain some fifteen houses of the nearby village of Savelle.

The upstream side of the dam is vertical, carried out with a circular curve, with a radius of curvature of 120 m, Figure 32.3, while the downstream side is carried out in a terraced form so that the entire structure has been made easily accessible for maintenance purposes (Fig. 32.4). A roadway 5.2 m wide passes over the crest of the dam. The depression, in which the powerhouse has been accommodated, has a middle line in the form of a circular arch, with a length of 81 m and a radius of 67.5 m.

The dam foundation and the zone of the hillsides was thoroughly investigated by means of a tunnel, dug out especially for that purpose under the river channel and into the steep hillsides of the dam site, while the elastic properties of the rock material were determined by means of geophysical investigations. The total quantity of material excavated for the foundations of the dam, amounted to 76,000 m^3, while the concrete placed in the dam's body amounted to 455,000 m^3.

The protection of the construction pit was achieved by means of the most frequently employed method, characteristic for this kind of solution, with an upstream cofferdam and a downstream cofferdam, as well as a diversion of construction water by means of a diversion tunnel, located in the left bank.

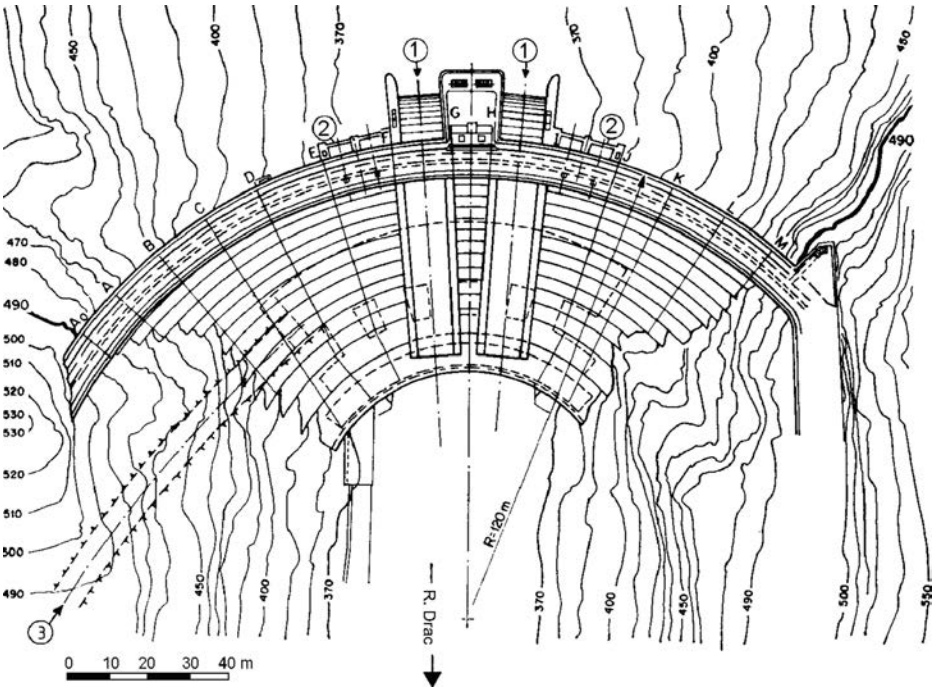

Figure 32.3 Locality plan of Monteynard Dam (France). (1) Spillway; (2) intake; (3) access tunnel.

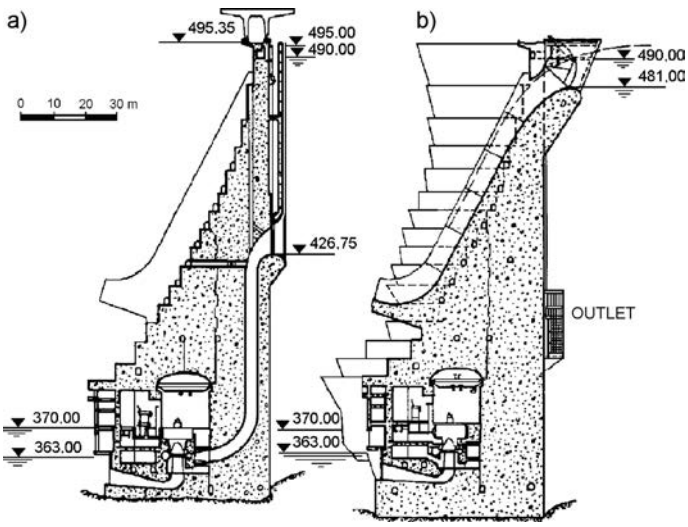

Figure 32.4 Cross-section through one of the supply conduits in the powerhouse (a) and through one of the spillways (b) of Monteynard Dam.

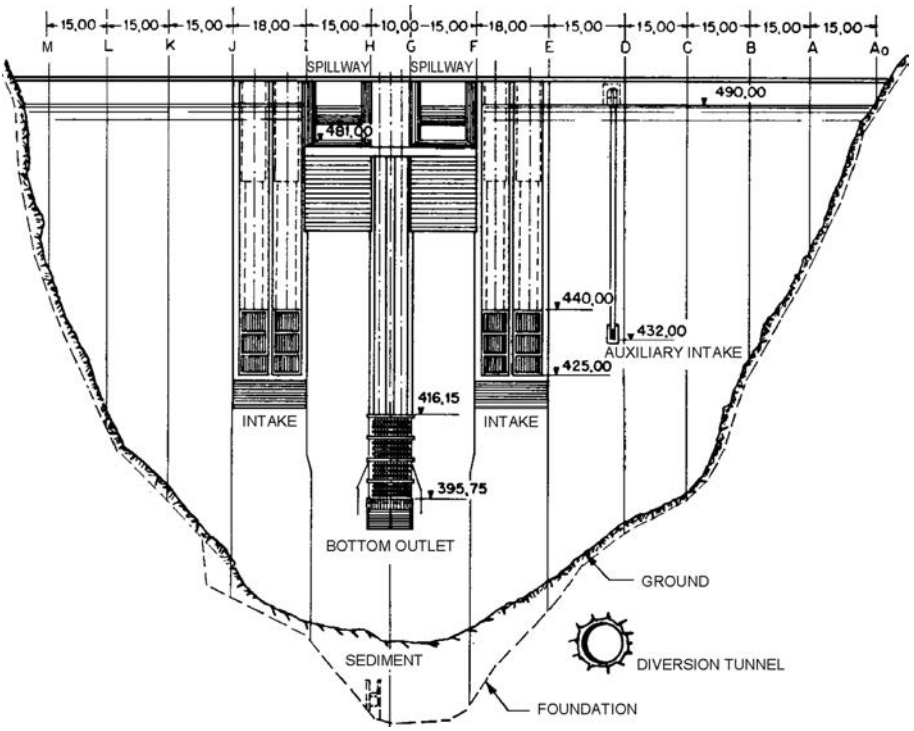

Figure 32.5 View of the upstream side of Monteynard Dam.

The spillway was carried out over the dam and it consists of two separated spans, the water is projected into the river channel downstream through two flip buckets, located over the space of the powerhouse (Fig. 32.4). Each overflow opening evacuates 625 m^3/s at a normal water level, so that the spillway has a capacity as much as is the maximum known discharge through the River Drac. If we add the other structures for discharge and for intake of water, as well as the retentive capacity of the reservoir, then it can be concluded that it is capable of receiving a flood wave of a total of 3000 m^3/s.

The two outlets have their entrance over the roof of the powerhouse, Figures 32.4, 32.5, thus leaving a dead storage capacity of 5,000,000 m^3 over the existing river channel; in the course of time, this space is expected to be filled with sediment. The outlets are carried out as steel pipes set in concrete, with a diameter of 2.5 m and a length of 37 m each, provided with double valves. The projecting of the water jet is performed in a line with the axis of the river channel, so that there is no danger of damaging the banks.

As an addition to the outlet structures, through the filling of the diversion tunnel there has been set back a pipe with a diameter of 3.2 m that has a valve at the downstream end, which is controlled by a servomotor. This facilitates emptying of the reservoir even below the elevation of the dead storage capacity until its filling the sediment.

Four intakes for water have been carried out from the upstream side – one for each turbine, provided with plain gates (3 m × 9 m), controlled by a servomotor with chains. The entrance into the intakes is protected by a steel trash rack (15 m × 6 m), with bars spaced at 3 cm. The trash racks have been in three separate sections, in order to be lighter for pulling up from the crest, for the purpose of cleaning, maintenance, or replacement. Also, the trash racks can be replaced with a stop-log gate, during execution of works on maintenance of the main gates. Each intake is provided with a steel pipeline, with a diameter of 4.10 m, which descends through the concrete, vertically to its turbine. The pipelines are not provided with valves. The powerhouse is accommodated in an opening in the dam, with a form that follows the curve of the downstream side of the dam, Figure 32.3, 32.4. Four units with Francis turbines have been accommodated in it; with an installed discharge capacity of 75 m^3/s each. At a head of 127 m, they can develop power of 80 MW each. Owing to the exceptionally difficult field conditions, two years were necessary (1954–56) to build the structures for the protection of the construction pit and for diversion of the river, while the construction of the main structures went on in the next five years.

In practice, there have been constructed a great number of hydraulic schemes of the *Type I*, *solution* 2. The hydraulic scheme with the highest embankment dam constructed so far in the world – *Nurek* – belongs among them. The dam, 300 m high, filled with sand-gravel material, with a central core made of loam, impounds a reservoir of 4.5 billion m^3 of water, which is used for generation of hydroelectric power and for irrigation. No structures have been carried out in the dam's body. In the right bank there has been carried out a powerhouse with a power of 2700 MW, together with intakes and supply conduits of a tunnel type (Figs. 32.6, 32.7).

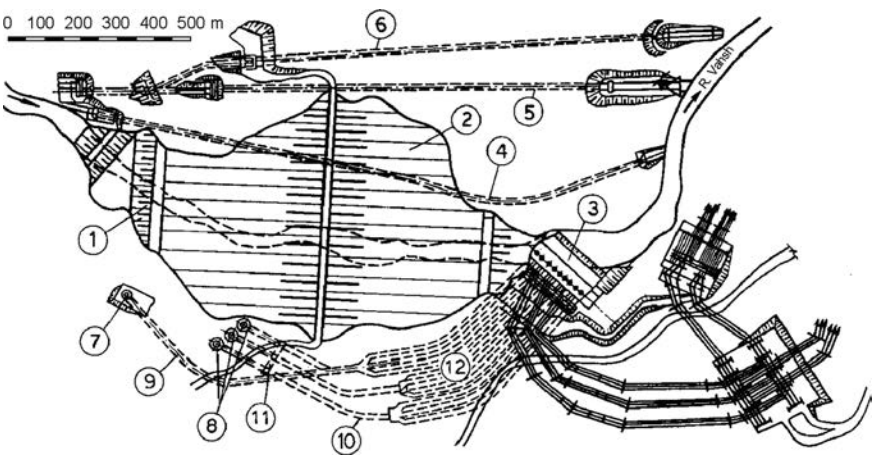

Figure 32.6 Locality plan of the structures of the *Nurek* hydraulic scheme (Tajikistan). (1) Cofferdam; (2) dam; (3) powerhouse; (4, 5) diversion tunnels; (6) overflow tunnel; (7) temporary intake; (8) permanent intakes; (9) supply tunnel for the first-commissioned generating sets; (10) supply tunnels; (11) space for emergency-overhaul gates or valves; (12) supply conduits for the turbines.

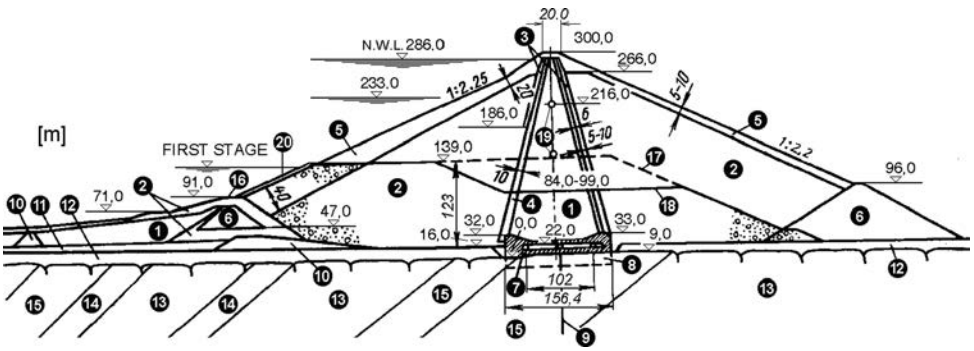

Figure 32.7 Nurek Dam, $H = 300$ m (the highest embankment dam in the world). (1) Core made of loam; (2) sand-gravel material; (3) two-layered filter, 0–5 mm and 0–40 mm; (4) filter 0–40 mm; (5) coarse stone; (6) rockfill; (7) concrete foundation with gallery; (8) zone of consolidation grouting (up to 20 m); (9) grout curtain; (10) auxiliary cofferdam; (11) earthfill; (12) river sediment; (13) sandstone; (14) aleurolites (siltstone); (15) sandstone with aleurolites; (16) cofferdam; (17) designed profile of the dam in the first stage; (18) realized profile in the first stage; (19) gallery for surveillance instrumentation; (20) temporary facing.

Three tunnels have been dug out in the left bank. Two of them are deeper and of the dimensions 10.0×11.5 m with a length of 792 m each. During the construction of the dam they were used for diversion of the construction water, while the third tunnel, set up at a higher level, during the utilization of the dam can evacuate flood water, to the amount of 2,040 m^3/s. The dam and the hydroelectric power plant were built in two stages, so that the dam in the first stage was 143 m high, while the hydroelectric power plant worked with three generating sets (commissioned for work in 1973). That dictated the elevation position of the intakes for the first three generating sets and the utilization of the two lower tunnels for diversion of flood flow during the service of the hydraulic scheme in the first stage. The Nurek hydraulic scheme has been built in tough geological and topographical conditions, and it was successfully completed in 1981 (Rozanov, 1983).

The *Oroville* hydraulic scheme, completed in 1967 on the Feather River in California, USA, Figure 32.8, also belongs to this group. Within the framework of the hydraulic scheme, there is also an earth-rock dam, 235 m high (see also Fig. 11.12) that forms a reservoir storage space of over 4 billion m^3 water, which is utilized for hydroelectric power, as well as for flood control. This type of dam and its cross-section were selected following extensive preliminary investigations of the technical and economical aspects of a number of possible different types of dams: a concrete gravity dam, multiple-arch dam, rockfill dam with a core, and gravel embankment dam with vertical or sloping core (Golzé, 1977; Moyseev & Moyseev, 1977; Thomas, 1976).

The powerhouse of the hydroelectric power plant, with an installed capacity of 1200 MW, is located on the left bank and is constructed as an underground structure (Fig. 32.8). One half of the generating sets are reversible; that is to say, they are used within the framework of the work of the pumped storage facility. On the right bank

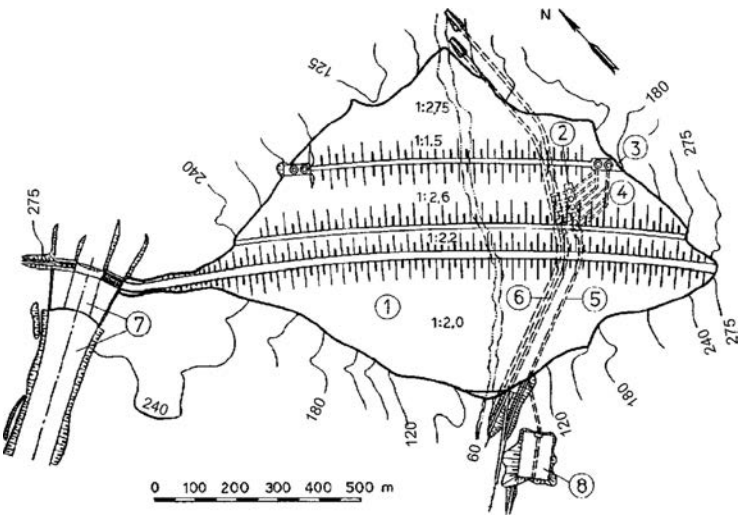

Figure 32.8 Location plan of the Oroville hydraulic scheme. (1) Earth–rock dam; (2) underground powerhouse; (3) intake tower; (4) supply conduits; (5) access tunnel; (6) diversion tunnels; (7) spillway structure; (8) distribution facility.

next to the dam where the ground becomes slight, there is set up a chute spillway with eight openings, controlled by radial gates with dimensions 12.8×5.2 m, and with a discharge capacity of 4250 m^3/s. By means of a spillway chute, the water is conveyed into a smaller, secondary watercourse, far away from the dam. The construction pit has been protected by means of a cofferdam over 90 m high, incorporated into the dam's body, while the construction water has been diverted by means of two tunnels with diameters of 10.7 m each. In the period of service, these are partially employed for diversion of the water from the turbines of the hydroelectric power plant.

Another example of a hydraulic scheme of Type I is at the *Green Mountain* embankment dam (USA), 94 m high, constructed in 1943 at an altitude of over 2300 m (Fig. 32.9). The spillway is an ogee-crest chute type of spillway, located at the left side of the dam. The chute channel is placed next to the contour of the downstream part of the dam with the ground, so that water is discharged directly into the direction of the river channel. This solution of the spillway structure is possible with smaller spillway water quantities. The protection of the construction pit is achieved by means of a cofferdam, incorporated into the dam's body, while diversion of the construction water is by means of a diversion tunnel, driven through the right bank.

The diversion tunnel was modified into a supply tunnel for the hydroelectric power plant, by extending the appropriate structures (new entrance structure and valve chamber). The powerhouse has been constructed by cutting into the right bank, behind the downstream end of the dam (Chugaev, 1985).

Another interesting example of hydraulic schemes of Type I is the *Alicura* hydroelectric power project on the river Rio Limay (Argentina), with an embankment dam

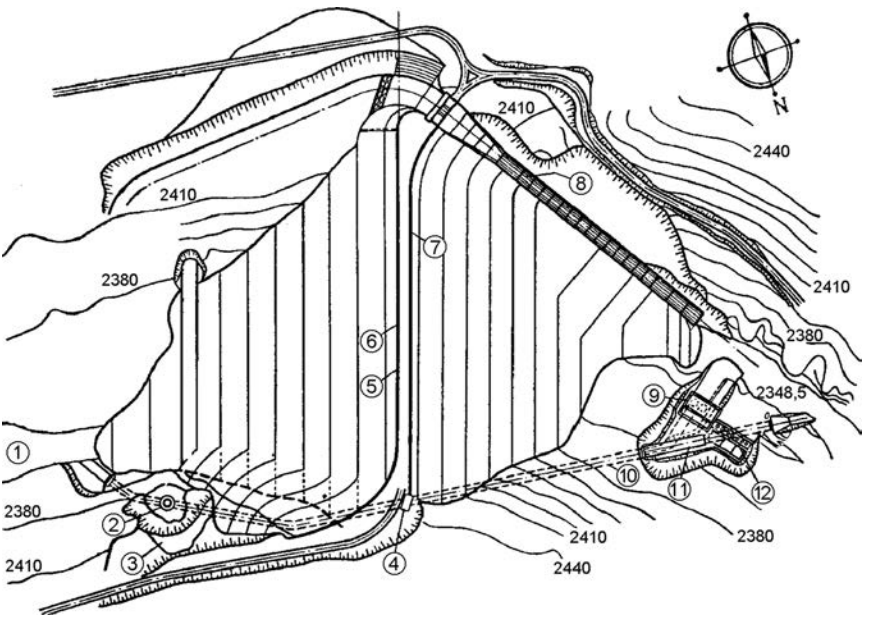

Figure 32.9 Layout of the hydraulic scheme of the Green Mountain dam (USA), $H = 94$ m. (1) River channel; (2) tower with trash rack; (3) slope in the rock; (4) gate chamber; (5) axis of the dam; (6) concrete parapet wall; (7) concrete fence; (8) spillway chute; (9) powerhouse; (10) supply tunnel; (11) intake tunnel; (12) substation.

120 m high (Fig. 32.10), with a length along the crest of 800 m, and total built-in filling material of 18 million m^3. The available storage capacity of the reservoir amounts to 2.4 billion m^3. The construction water is diverted by means of two tunnels, with a diameter of 9.0 m each, a length of 628, i.e. 893 m, and a total discharge capacity of 1200 m^3/s. The second diversion tunnel was modified and is now a bottom outlet, controlled from a valve chamber in the form of a gallery, by means of two plain valves 3.5×2.2 m. The capacity of the bottom outlet is high – 600 m^3/s – and, due to the significant velocities, measures have been undertaken for protection against vibrations and cavitational erosion.

An original solution has been applied in the case of the spillway structure and the intake of this hydroelectric power plant, Figures 32.11 and 32.12. Namely, the steep left river slope, near the crest of the dam, changes over into a slope with a very slight inclination. On that part, next to the dam, a channel has been dug out, with a bottom 33 m below the crest of the dam, by means of which the water is brought to the widening in the form of a basin, protected with concrete lateral lining, and located downstream of the longitudinal axis of the dam. In that space, there has been placed an overfall spillway with three radial gates 10×13.8 m, a spillway chute, and a stilling basin with a capacity of 3000 m^3/s, as well as an intake for the hydroelectric power plant, to which water is brought by means of four surface pressure pipelines, each with a diameter of 6.50 m and a length of 224 m.

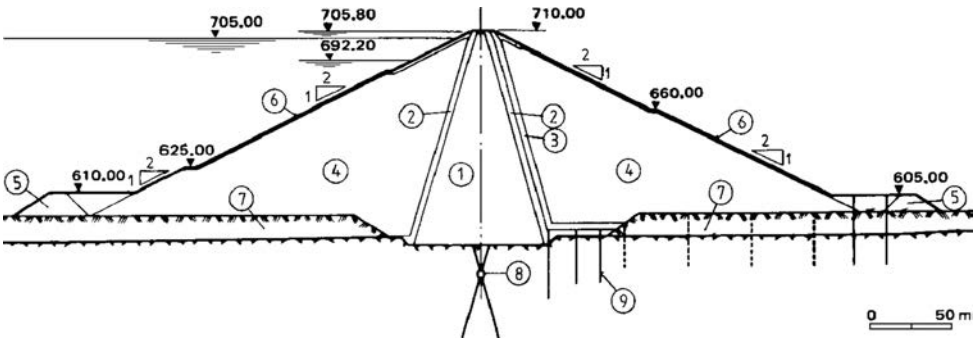

Figure 32.10 Cross-section of the Alicura Dam (Argentina). (1) Core; (2) filter layers; (3) drainage; (4) retaining bodies; (5) cofferdams; (6) protective layer of coarse stone; (7) sediment; (8) grouting gallery; (9) drainage boreholes.

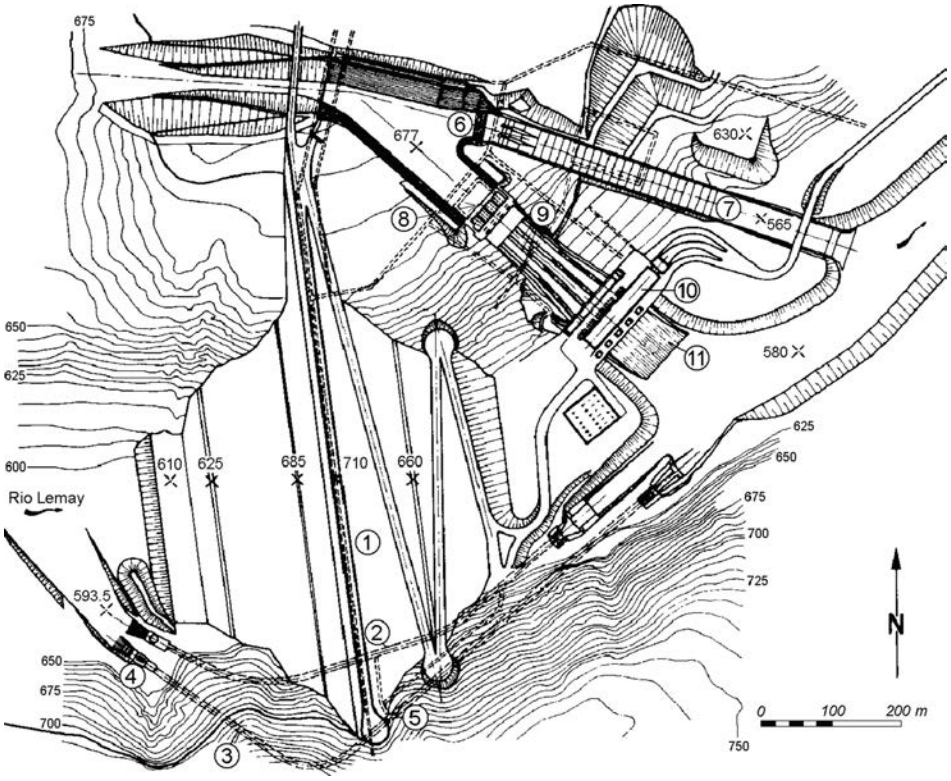

Figure 32.11 Layout of the hydraulic scheme at the Alicura Dam. (1) Dam. (2) diversion tunnel No. 1; (3) diversion tunnel No. 2; (4) intake of bottom outlet; (5) valve chamber of the bottom outlet; (6) spillway; (7) stilling basin; (8) intake for the hydroelectric power plant; (9) supply pipe conduits under pressure; (10) powerhouse; (11) tail race.

Figure 32.12 Alicura high-head hydraulic scheme (Argentina).

The powerhouse is located in the left bank, a little away from the end of the dam. It is provided with four Francis turbines with an installed discharge of $4 \times 237 = 948\ m^3/s$ and installed power of $4 \times 250 = 1000$ MW. The hydraulic scheme was built in five years and was commissioned for working operation in 1984.

In composing hydraulic schemes of Type I, solution 2, the shaft spillway is very often employed as a spillway structure. An example of such a solution is the *Tikvesh* hydraulic scheme (Figs. 27.32–27.34), as well as the hydraulic scheme at the dam *Globochica* (Macedonia), on the River Crn Drim (Figs. 32.13, 32.14) (YCOLD, 1970, 1971). The rockfill dam with a wide clay core, 95 m high and a length at the crest of 196 m, dams the profoundly narrow profile and forms a pressure head for the derivation hydroelectric power plant with an installed power of 42 MW. The dam site consists of limestone in thin highly-fissured layers, very permeable, so that below the core there has been constructed a multiple-row grout curtain, with a total quantity of built-in grouting mixture of 4500 tons. The uncontrolled shaft spillway has a capacity of $1100\ m^3/s$ and is located on the right bank. The diameter of the shaft amounts to 36 m, while that of the intake tunnel is 9 m. The terminal part has a surface spillway chute and a flip bucket for projecting the water jet, both of which are moved away from the downstream dam toe. The protection of the construction pit is performed by means of a cofferdam, incorporated into the body of the main dam, and the river stream (construction water was $300\ m^3/s$) was diverted to a tunnel with a diameter of 5.70 m, also located on the right bank. The diversion tunnel is modified into a bottom outlet with a cross-section 1.35×2.80 m, controlled from a gate/valve house that is accommodated in an underground chamber. The intake and derivation (supply) tunnel are located on the right bank. The construction of the hydraulic scheme was completed in 1965.

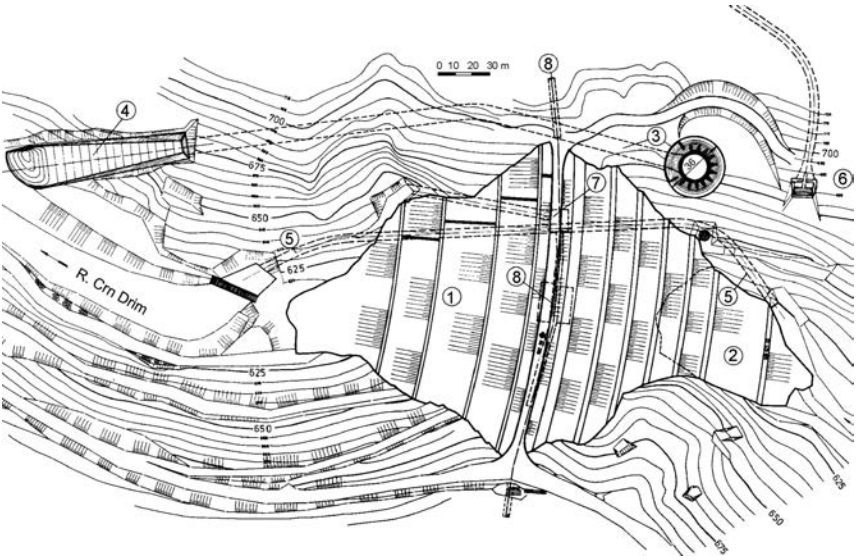

Figure 32.13 Hydraulic scheme for the Globochica Dam (Macedonia). (1) Earth–rock dam; (2) cofferdam; (3) spillway; (4) spillway chute with flip bucket; (5) diversion tunnel, modified into a bottom outlet; (6) intake with tunnel supply; (7) underground valve chamber; (8) grouting gallery.

Figure 32.14 *Globochica* high-head hydraulic scheme (Macedonia).

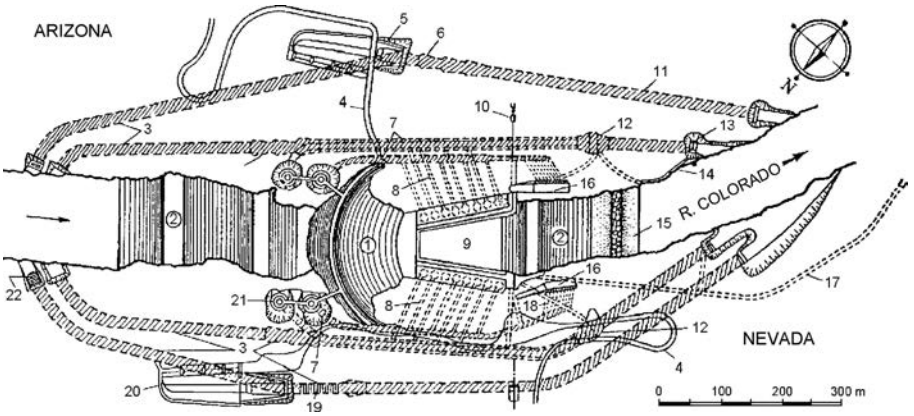

Figure 32.15 Layout of the hydraulic scheme of the Hoover Dam on the Colorado River (USA), completed in 1936, $H_k = 223$ m. (1) Dam; (2) cofferdam; (3) diversion tunnel, $D = 15.25$ m; (4) roadway; (5) side-channel spillway; (6) concrete plug; (7) steel pipeline, $D = 9.15$ m; (8) supply pipe conduits, $D = 4$ m; (9) powerhouse; (10) cable; (11) outlet tunnel of the spillway, $D = 15.25$ m; (12) outlets into the concrete plug of the tunnel, with six needle valves, $D = 1.8$–2.0 m; (13) Gate; (14) Off-take; (15) blanket; (16) spillway into the canyon wall (6 needle valves, $D = 2$ m); (17) access tunnel to the powerhouse; (18) headings; (19) temporary outlet; (20) side-channel spillway; (21) intake in the form of a tower; (22) trash rack.

Solution 2 is also employed in hydraulic schemes with a concrete dam. The *Hoover* hydraulic scheme, constructed on the Colorado River (USA), is an arch-gravity dam 223 m high, which is constructed in a narrow profile (Fig. 32.15). Owing to that, as well as owing to the significant quantity of water that flows through the river, all intakes and spillway structures are accommodated in the rock banks. The hydroelectric power plant is a near-dam type and is located on both banks, while the supply of water is performed through supply tunnels, also driven into the banks (Creager et al., 1955; Grishin et al., 1979).

A hydraulic scheme of Type I, solution 2, but now with a true arch dam, is presented in Figure 32.16. The diversion of flood waters has been solved with an uncontrolled curvilinear side-channel spillway, located in the steep left bank. There is a noticeable concentration of a large number of appurtenant hydraulic structures on both the left and right bank (Chugaev, 1985).

32.2 HIGH-HEAD HYDRAULIC SCHEMES ON MIDDLE AND LOW PARTS OF RIVERS

In composing high-pressure head hydraulic schemes of Type II, one should take into account the fact that the high flood water in rivers with a broad river channel imposes the construction of an overflow concrete dam in the river channel. The remaining part of the profile is dammed with a concrete non-overflow dam, or else with an embankment dam, if it is possible to execute an economical joint between the works

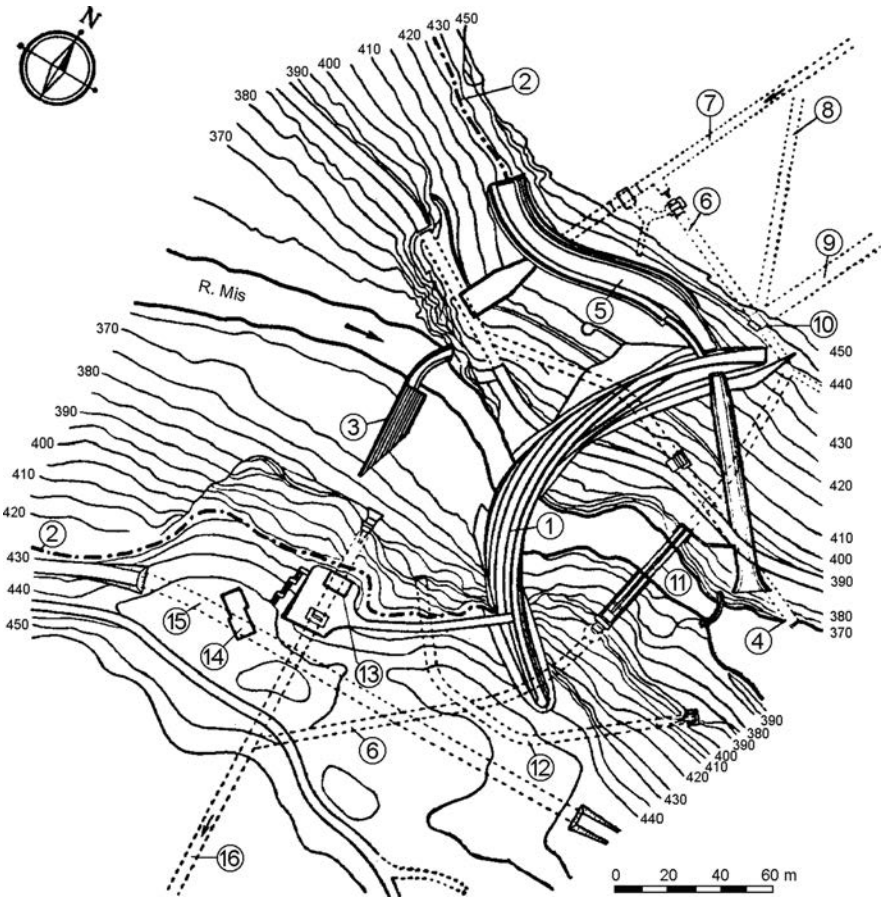

Figure 32.16 Layout of the hydraulic scheme *Mis* (S. Giuliana), Italy, built in 1962, $H_k = 91$ m. (1) Dam; (2) contour of water; (3) cofferdam; (4) diversion tunnel; (5) side-channel spillway; (6) side (lateral) outlet; (7) tunnel for transferring of waters from the river of Stanga; (8), (9) levelling chamber; (10) levelling reservoir; (11) bridge – pipeline; (12) high-head spillway; (13) controlling desk; (14) store house; (15) tunnel on the new route; (16) tunnel for transferring of waters into another reservoir.

of heterogeneous material. The powerhouse is most often located just behind the concrete dam, but may also have other positions, depending on the ground conditions. Transport structures (ship navigation locks or lifts) could suitably be located in the rock banks.

A typical example of a hydraulic scheme in a broad river valley, rich in water, is the hydraulic scheme at the *Bratskaya* hydroelectric power plant (Russia) on the River Angara, shown in Figure 32.17 (Grishin et al., 1979).

In cases of hydraulic schemes of Type II, there are examples when one of the banks is steep, while the other one is very slight, so that the dam site is rather wide, as is the case of the Angostura Dam (USA), 59 m high, built in 1949. The river channel and the

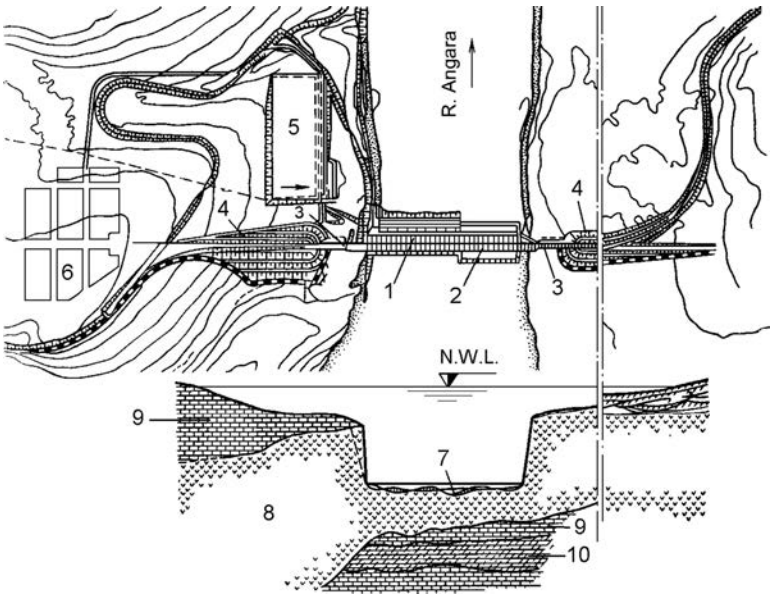

Figure 32.17 Hydraulic scheme at the *Bratskaya* hydroelectric power plant (Russia). (1) Non-overflow part of the dam and powerhouse behind it; (2) overflow part of the dam; (3) parts of the concrete dam in the banks; (4) embankment parts of the dam; (5) substation; (6) inhabited place; (7) sediment; (8) diabase; (9) sandstone; (10) alternately, aleurolites (siltstones) and sandstones.

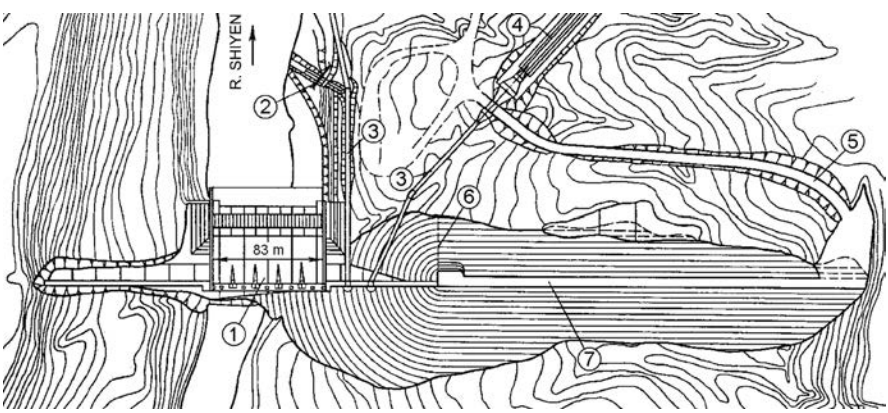

Figure 32.18 Hydraulic scheme at Angostura Dam (USA). (1) Gravity overflow dam; (2) powerhouse of the hydroelectric power plant; (3) pipeline; (4) channel; (5) roadway; (6) terminal part of the concrete dam; (7) embankment dam.

steep left bank are dammed with an overflow mass dam, while the slight right bank has an embankment dam. The hydroelectric power plant is accommodated in the right bank next to the river channel, some hundred metres away from the dam (Fig. 32.18) (Chugaev, 1985).

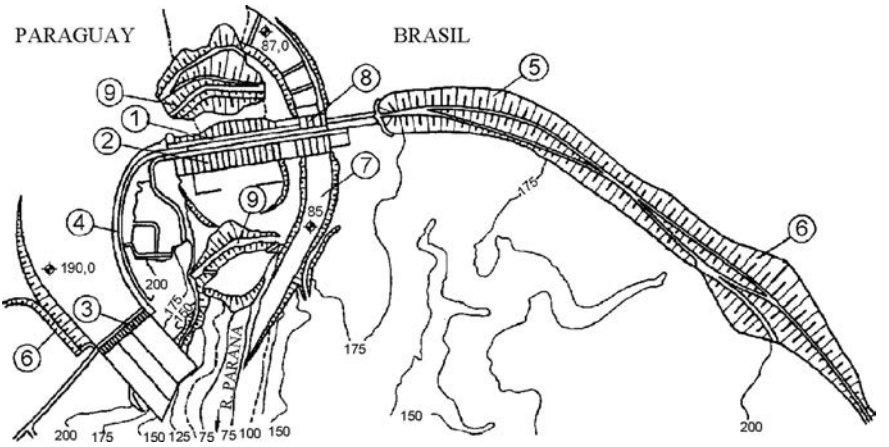

Figure 32.19 Layout of the *Itaipu* hydraulic scheme, *Itaipu.* (1) Main dam; (2) powerhouse of the hydroelectric power plant; (3) overflow dam; (4) right saddle dam (buttress dam); (5) earth–rock dam on the left bank; (6) earthfill dam; (7) bypass channel; (8) outlet; (9) cofferdam.

Especially complex and interesting are the hydraulic schemes of Type II, in the case of damming of a river exceptionally rich in water in its middle or lower course. In such a case, for achieving a high-head, a very long dam would be necessary, usually consisting of several dam types, as well as a spillway with an exceptionally significant capacity that works frequently with high overflow water. The most characteristic example in that respect is the *Itaipu* hydraulic scheme on the 1200 km long river Parana, located on the border between Brazil and Paraguay, immediately in front of the three-border point with Argentina. The most significant structure within the framework of the hydraulic scheme is the main dam (1, Fig. 32.19), accommodated in the river channel, with a maximum height of 196 m. In selecting the type of the dam, there have been analyzed alternatives with an arch-gravity dam, earth–rock dam, and hollow gravity concrete dam. The last type has been adopted owing to the convenience it offers for accommodation of the 960 m long near-dam, i.e. run-of-river type of hydroelectric power plant (local development), and for evacuation of significant quantities of construction water – 30,000 m^3/s.

By means of wide joints, the main dam is divided into 30 sections, of which 14 sections are in the river channel. Each section is 34 m wide (the width of the other sections amounts to 17–24 m), which leaves room for openings in these sections for giving passage to the construction water. In the six central sections, with a height of from 170 to 196 m, there have been accommodated power intakes for the hydroelectric power plant, which feed the supply conduits ($D = 10.5$ m) for the generating sets, passing across the downstream slope, and faced with concrete. Altogether, 20 generating sets have been anticipated[2], with a total power of 14,000 MW, so that *Itaipu* is one of the most powerful hydroelectric power plant in the world.

[2]The hydraulic scheme Itaipu was commissioned in 1985, but the two last units were installed in 2002.

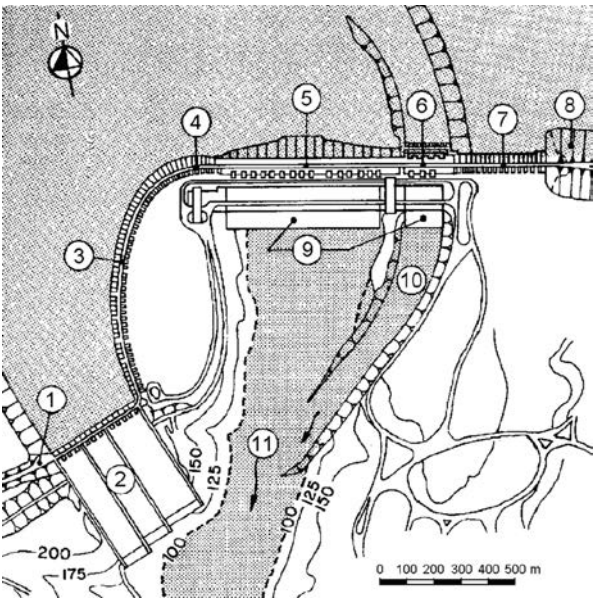

Figure 32.20 Layout of the main structures of the *Itaipu* hydraulic scheme (Schulman et al., 1988). (1) Earthfill dam; (2) overflow dam; (3) right saddle dam and (4) right connecting dam – buttress dam, $H_{max} = 65$ m; (5) main dam – hollow gravity dam, $H_{max} = 196$ m, $L = 610$ m; (6) outlet for construction waters; (7) left connecting dam (buttress dam); (8) earth–rock dam, $L = 4300$ m, $H_{max} = 70$ m; (9) powerhouse; (10) bypass channel; (II) the river Parana.

An overflow concrete dam has been constructed on the right bank for the evacuation of flood water, and then moved away from the main dam and the hydroelectric power plant about 1.2 km downstream. The river basin of a smaller tributary into the main river has been utilized for the siting of that overflow concrete dam, which reduces to a minimum the excavation works, and thus, there is also avoided interaction with the hydroelectric power plant, (Fig. 32.20 – Schulman et al., 1988).

The overflow dam is divided into three fields with separate spillway chutes, as well as flip buckets, Figures 32.21–32.23. The access channel is deepened to the elevation of 190 m, between the right saddle concrete dam and the excavated lateral slope of the channel, protected with rockfill, and a concrete lateral lining. The spillway is a massive gravity structure with an elevation of the foundation of 180 m, while the spillcrest is at an elevation of 200 m, and the highest part is at an elevation of 225 m. The structure is provided with 14 radial gates, fastened to the 5 m thick parting walls. The three spillway chutes are mutually divided by means of concrete walls, anchored into the foundation by means of steel bolts. The three sections of the spillway chute are at different levels for better adaptation to the rock contour and for reducing the excavation. The spillway chutes are 377 to 417 m long, the intermediate one and the right one are each 95 m wide, while the left spillway chute is 145 m wide and encompasses six overflow openings (the other two encompass four overflow openings

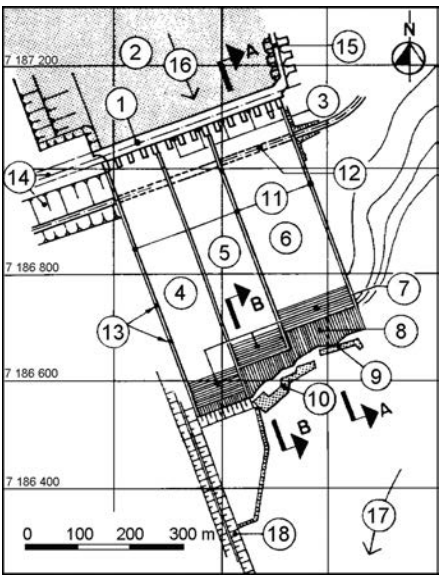

Figure 32.21 *Itaipu*, plan of the spillway structure (Schulman et al., 1988). (1) Axis of the spillway; (2) access channel; (3) radial gates $14 \times 20\,m \times 20\,m$; (4) right spillway chute, $L = 417\,m$, $b = 95\,m$; (5) central spillway chute, $L = 387\,m$, $b = 95\,m$; (6) left spillway chute, $L = 377\,m$, $b = 145\,m$; (7) flip bucket; (8) downstream protection; (9) protective wall (1985); (10) protective wall (1986); (11) training walls; (12) vehicle tunnel; (13) openings for aeration galleries; (14) right earthfill dam; (15) right saddle concrete dam; (16) water flow; (17) the river Parana; (18) slope.

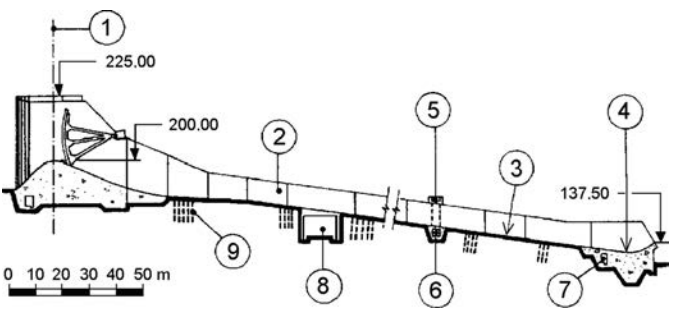

Figure 32.22 *Itaipu*, section A–A (through the spillway structure) (after Schulman et al., 1988). (1) Axis of the spillway structure; (2) training walls; (3) spillway chute; (4) flip bucket; (5) air vent; (6) aeration gallery; (7) drainage gallery; (8) vehicle tunnel; (9) anchors.

per spillway). The bottom of the spillway chutes consists of a 1 m thick concrete slab, with double reinforcement.

The energy of the spillway jet is dissipated by projecting it over a flip bucket at the end of each spillway chute. Downstream of the massive blocks, the slopes are protected

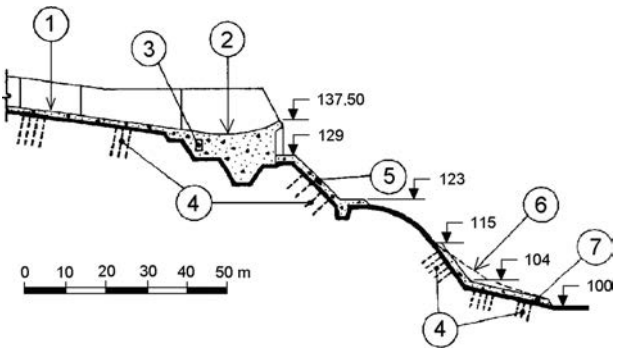

Figure 32.23 *Itaipu*, spillway structure – section B–B (after Schulman et al., 1988). (1) Spillway chute; (2) flip bucket; (3) drainage gallery; (4) anchor bolts; (5) slabs for the protection of slopes; (6) line of the rock; (7) protective wall.

with concrete slabs, firmly founded and anchored in the rock. Further downstream, the slopes are covered with two layers of shot-crete, with a steel net that is anchored into the rock, with three-metre long bolts, spaced at distances of 2 m. The spillway capacity of the two narrower spillways is 17,700 m^3/s each, while the capacity of the left spillway – the broader one – is 26,560 m^3/s, at an elevation of the reservoir of 223.24 m. Prior to the selection of such a construction of the spillway, there were conducted a number of investigations on hydraulic models, in order to ensure efficient diversion, i.e. conveyance, of the waters and to obtain a solution with minimum erosion of the ground downstream. The following regulations for handling the spillway have emerged from those investigations:

- With each spillway chute, the gates are opened beginning from the ends toward the middle, in order to avoid significant forces and submersion of the training walls.
- All of the gates of a spillway chute open equally, and closing is performed with a reversed sequence.
- In order to reduce to a minimum the erosion downstream of the structure, they first allow overflowing through the left spillway chute; then the central spillway chute is activated, in order to work together with the left one. In cases of high overflow water, the right spillway chute may also be activated. The exclusion is performed in a reversed sequence.The minimum initial lifting of the gates amounts to: 1.00 m for the gates of the left spillway chute, 2.75 m for the gates of the central spillway chute, and 0.75 m for the gates of the right spillway chute.

The *Itaipu* hydroelectric power plant works predominantly as a run-off type of plant, so that the reservoir is maintained full, in order to ensure a constant and maximum high-head for the production of electric power. The variation of the level is limited to only 0.6 m between the normal maximum level of the reservoir of 220 and the normal minimum level of 219.4 m. The spill crest is at a level of 200 m, so that by

means of the gates they can control the discharge of water from the uppermost 20 m of the reservoir. During a flood wave, the gates open successively and uniformly, in order to maintain the normal level for as long as possible. The uniform handling with the gates is also necessary for another reason: for the needs of navigation downstream of *Itaipu*, hourly fluctuations of the level of the Parana River must not be greater than 0.5 m, and the daily ones not greater than 2.0 m. Even before the completion of the *Itaipu* hydraulic scheme, it was subjected to significant flood water a number of times, while the maximum one recorded in 1983, reached 40,000 m^3/s and caused minor damage to the spillway structure owing to cavitation. The damage has been successfully repaired with epoxy mortars, prior to the commissioning for service of the hydraulic scheme in 1985 (Torales et al., 1994).

32.3 PUMPED-STORAGE HYDRAULIC SCHEME

Pumped storage hydropower is a modified use of conventional hydropower technology to store and manage energy or electricity. Let us examine this special type of high-head hydraulic scheme in the example of the *Cortes La Muela* pumped storage plant (Spain), Figure 32.24. It consists of the following structures: lower reservoir (1), with powerhouse (2), upper reservoir (3), with intake (4) and supply conduit (5) to the powerhouse. In cases of pumped storage plants, in the powerhouse there are placed units which can work both as turbines and as pumps, by means of which, during the

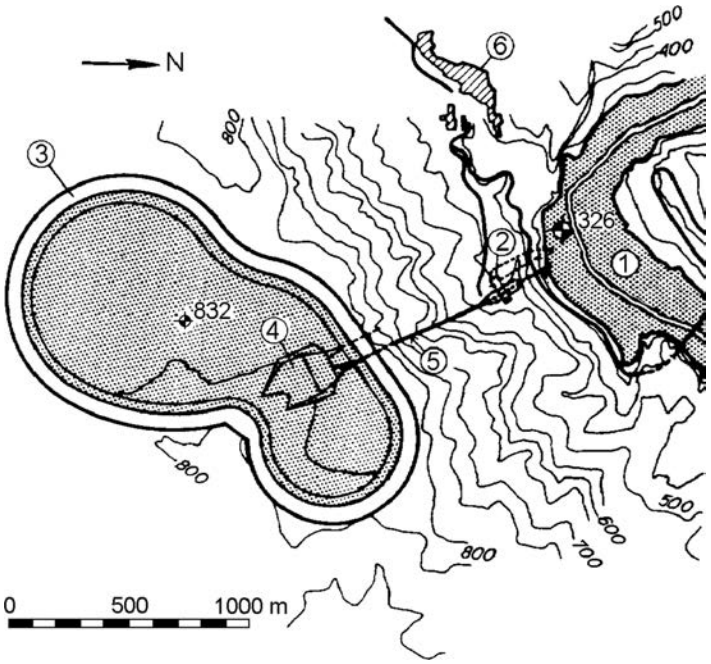

Figure 32.24 Hydraulic scheme of the *Cortes La Muela* pumped storage plant (Spain) (Navalon & Gaztanaga, 1988). (1) Lower reservoir (*Cortes*); (2) powerhouse; (3) upper reservoir (*La Muela*); (4) intake; (5) supply conduit; (6) settlement.

night period, water is pumped out from the lower reservoir into the upper reservoir and it is later on used for generation of electric power at peak periods, when it is most needed. In that way, for each spent kWh energy, they obtain about 0.7 kWh, so that these plants in the total balance appear as consumers of energy. In fact, they spend "barren" energy in the period in which there is more available than is necessary, and they generate "quality" power in the period of the day when there is a maximum demand for energy.

The lower reservoir, along with the dam and the appurtenant hydraulic structures, is composed and configurated in accordance with the principles for composing high-head or medium-head hydraulic schemes. The upper reservoir can also, be formed by damming a watercourse, but is more often carried out as a man-made reservoir, surrounded on all sides by means of embankment, at a suitable place above the lower reservoir, as is the case in the examined example of the *Cortes – La Muela* hydraulic scheme, Figure 32.25. An important condition that these reservoirs have to fulfill is

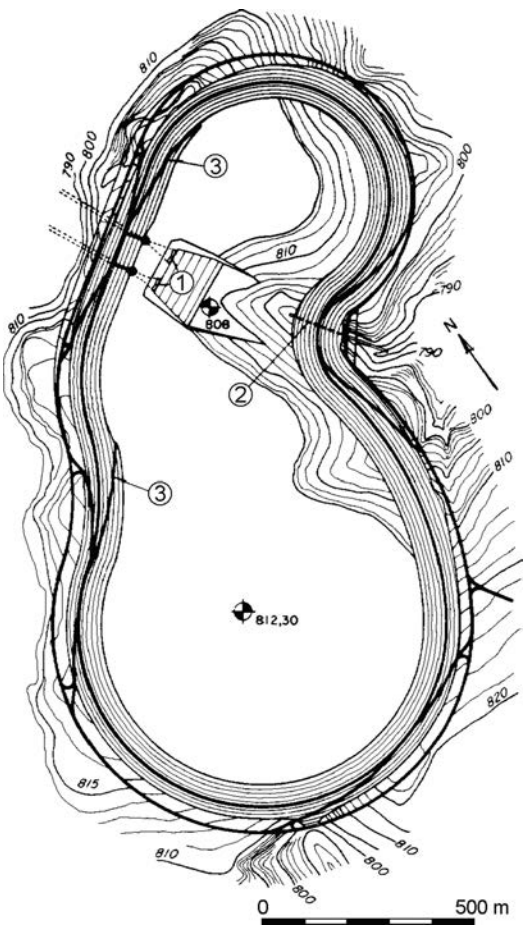

Figure 32.25 Plan of the upper reservoir (*La Muela*) (Navalon & Gaztanaga, 1988). (1) Intake structure; (2) bottom outlet; (3) access road.

low water-permeability, because they are supplied with expensive water, pumped from the lower reservoir. That is why these reservoirs, as a rule, are carried out with a water-impermeable lining across the slopes of the embankment as well as across the bottom of the reservoir. For that, the most frequently employed material is asphalt-concrete, owing to its exceptionally high impermeability and economical execution (see on this issue also the chapter on reservoirs). Another particularity of the upper reservoir is that, as a rule, it does not require a spillway, but only a bottom outlet, because the catchment area of the upper artificial reservoir is usually negligible.

The *Cortes – La Muela* hydraulic scheme is built in Eastern Spain, near the city of Valencia. The lower reservoir has been formed with two arch-gravity dams, while the upper one is an artificial reservoir that was formed on the Muela de Cortes plateau, with an embankment lined with asphaltic concrete facing, which extends also across the bottom of the reservoir. The elevation difference between the two reservoirs is about 600 m, at a horizontal distance of only 900 m, which provides ideal conditions for a pumped storage plant. The installed power of the combined plant amounts to 870 MW.

For shaping the upper reservoir, rock excavation has been performed to a quantity of 3.6 million m^3 and also an embankment 4.5 km long has been constructed, with inclinations of the internal slope 1:1.6, and of the external slope 1:1.4, with an elevation of the crest of 834.5 m. In plan, the reservoir consists of two circles connected with straight lines and circular tangents, without edges and angles, in order to facilitate continuous execution of the facing. The bottom is mainly horizontal, at an elevation of 812.30 m, joined with the slope by means of a circular curve, with a radius of 20 m (Navalon & Gaztanaga, 1988).

The volume of the reservoir is 23×10^6 m^3, while the area of the asphaltic concrete facing is 1.102×10^6 m^2, of which 887,000 m^2 belong to the flat bottom and 215,000 m^2 belong to the slope. Two access roads are located along the embankment slope, on which lightweight trucks may approach any zone of the reservoir in the case of possible need for repairs. The construction of the hydraulic scheme was completed in 1987, the initial filling was done in 1988, and the plant was commissioned for trial work in the middle of 1989.

The bottom outlet (Fig. 32.26) is accommodated below the embankment, at the existing stream, where the natural ground was the lowest. Although in the reservoir there is practically no natural inflow, which means that there is no need for a spillway,

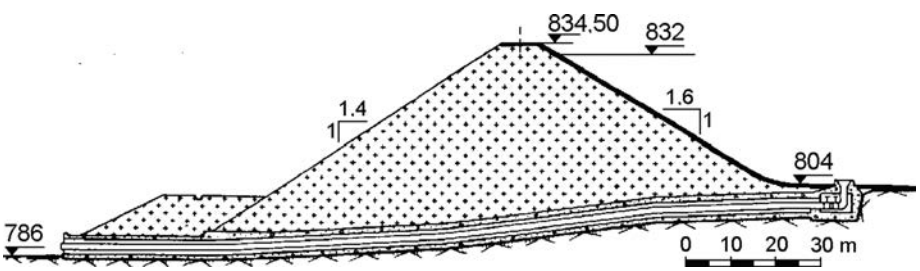

Figure 32.26 Bottom outlet of the upper reservoir (Navalon & Gaztanaga, 1988).

still, for safety, the crest of the embankment in the zone of the stream is lower by 50 cm, enabling some spilling in eventual extreme situations.

From the very beginning of the realization of La Muela project, a second stage was planned, and its construction started in 2006, under the name La Muela II. It contains a new penstock which connects the existing intake with a new cavern power plant. La Muela II has been equipped with four additional Francis pump-turbine units, similar to those installed at La Muela I. The completed Cortes – La Muela project (the commissioning is planned for 2013) will have a capacity of 1280 MW in the pumping mode, and a generating capacity of 1720 MW (Bravo & Gaztañaga, 2012).

The first pumped storage project came online in Europe in the early 1900s and in the U.S.A. around 1930, but pumped storage hydropower has provided significant benefits to the energy power supply system during its primary development in the 1960s, 1970s, and early 1980s, in parallel with the construction of a large number of nuclear power stations. Pumped storage technology has advanced significantly since its original introduction and now includes improved efficiencies with modern reversible pump-turbines, as well as improved tunnelling construction methods and design capabilities. The pump-turbine generator efficiency has increased by 5% in the last three decades, resulting in energy conversion or cycle efficiencies of about 80%.

Globally, there are more than 300 pumped storage plants in the world, with a combined generating capacity of around 140,000 MW, located mainly in the highly-developed countries (Fig. 32.27). Approximately 50 such schemes have an installed capacity in the range of 1000 to 3000 MW. As is the case with all types of hydraulic schemes, modern pumped-storage hydropower project costs can vary based on site-specific conditions. A feasible project site would include an approximate cost estimate range from $1500 per kilowatt to $2500/kW, based on an estimated 1000 MW sized project. As a rule, smaller projects are less effective. In connection with the stimulation of the renewable energy production there is still significant interest in developing pumped-storage projects, or in upgrading the existing ones. But many pumped-storage

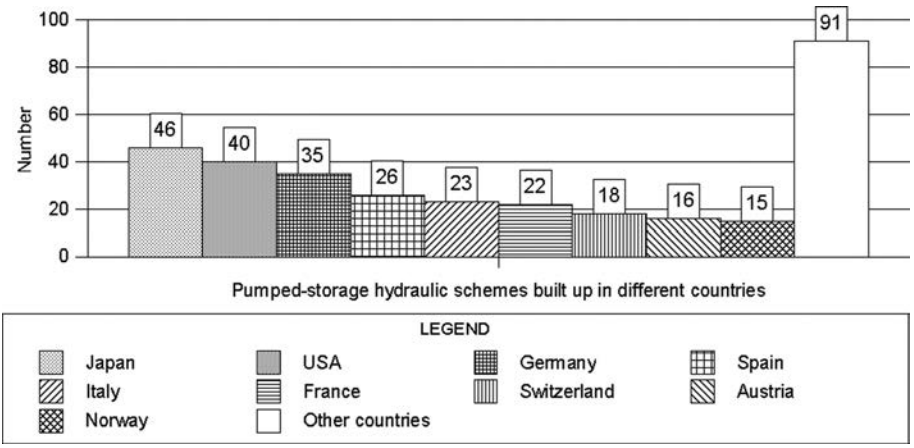

Figure 32.27 Number of pumped-storage hydraulic schemes built up (or under construction) in different countries up to 2001.

developers today face significant environmental misconceptions, mainly connected with the construction of large dams, especially in developed countries. Enhanced awareness of the impacts of construction of large dams and storage reservoirs on the river systems limits the construction of large high-head hydraulic schemes and forces the engineers to work directly with the environmental community to try to reduce or mitigate project impacts.

Chapter 33

Reservoirs

33.1 INTRODUCTION

The term *reservoir* implies a storage space formed when a watercourse is dammed and, afterwards, completely or partially filled with water. The reservoir may then be utilized for one, two, or more purposes and functions (Fig. 33.1). It is almost always more economical and more efficient for two or more functions to be combined within the construction of one reservoir, rather than to construct individual structures for each purpose and function.

By means of a hydraulic scheme with a dam and a reservoir, it is possible to satisfy different needs if the reservoir storage space has been properly selected and planned and if, within the framework of the hydraulic scheme, there have been anticipated all the necessary structures for its rational exploitation, i.e. service. Detailed studies are needed for utilization of a multi-purpose reservoir, which analyze the individual functions, the most suitable extent and range for each of the functions, optimum management, control, and many other aspects, after which we may obtain the resultant extent of the reservoir.

The above-described analyses are based on the hydrologic, technical, and economic aspects of the problems encompassed in the design. Continuing in the following two chapters, other aspects will be discussed, which are also important for the efficient designing of reservoirs – constructional questions, migration of population, relocation of individual structures, utilization of the reservoir for sport and recreation as a secondary function, auxiliary works, cleaning of the reservoirs, and problems related to the protection of the environment.

It is necessary to point out that these quoted questions, connected with the formation, safety, and service of the reservoir, are closely related to its size. In cases of large reservoirs, most of the cited aspects gain in weight and importance. Many reservoirs of enormously large volume, measured with hundreds of billions of m^3 space, have been built throughout the world. In Macedonia, the above problems have no such weight or significance, since our biggest reservoirs do not exceed a volume of 500 million m^3. Nevertheless, all of the listed aspects should be carefully analyzed at the stages of design, construction, and service of each hydraulic scheme with a reservoir.

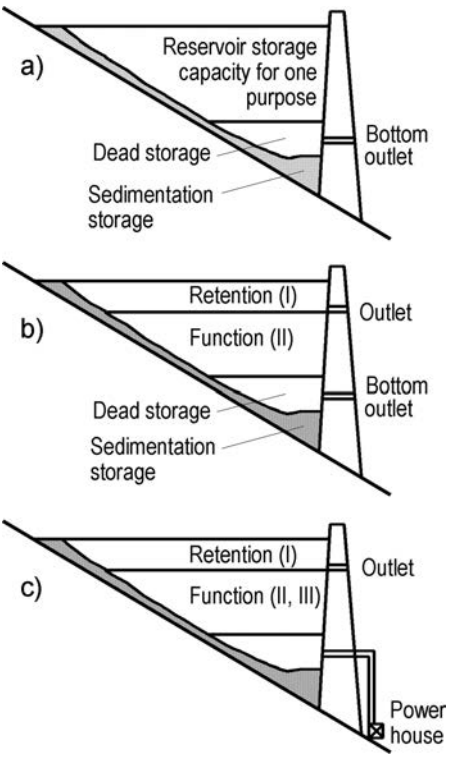

Figure 33.1 Utilization of the storage space in the reservoir for one (a), two (b), or more (c) functions.

33.2 FORMATION AND SAFETY OF RESERVOIRS

In designing hydraulic schemes, usually the structure of the dam and its appurtenant hydraulic structures that facilitate functioning of the hydraulic scheme are of the utmost importance. Of no less importance is the safe construction of the reservoir itself, that is to say, the provision of its ability to safely hold the designed volume of water, at least in the course of the anticipated operational life of the reservoir. In that, it is necessary not only that the reservoir be safe, but also that the water at any given moment should be available for utilization. The most important factors in considering these questions are the stability of the banks of the reservoir, the water-impermeability of the ground, water absorption in the soil, evaporation, and sediment accumulation. This means that, not only the dam site but also the entire site of the reservoir requires a thorough investigation and analysis. Hydraulic engineers should closely cooperate with geologists, in order to obtain the appropriate information for the assessment of their location of the reservoir. The initial information is obtained from the existing geological maps, while in the subsequent stages we carry out surface and underground investigations, in which case we also use the data of already collected investigation works (for instance, for the needs of mining or in the discovery of underground water).

33.2.1 Stability of reservoir banks

The stability of the banks of the reservoir and their water-impermeability usually remain in close mutual correlation. The seepage of water through a part of the bank of the reservoir storage space could be the first step towards caving-in and failure of the corresponding part, which leads to a reduction of the volume of the reservoir. A considerable caving-in and failure of a hillside mass could greatly reduce the storage capacity of the reservoir, and even lead to overtopping of the water over the dam. Therefore, the consequences of possible caving-in and failure of a part of the bank depend on the size of the caved-in and failed mass in comparison to the volume of the reservoir, so that they might be insignificant, but they may also be catastrophic, in which case, the considered dam site should be abandoned.

When potential landsliding cannot be ignored, without endangering safety and the dam site is such that it should not be abandoned, certain measures for adaptation may be examined, by means of which we could safely use the reservoir. For instance, in easier cases, the limitation of the variation of the water level, as well as of the speed with which that variation takes place, could be sufficient. If such simple measures are not sufficient or cannot be applied, then we should undertake more straightforward measures for elimination of the danger of the potential landslide, such as, for example, interception and conveyance of the rain water from the critical zone, execution of drainage for the elimination of the uplift pressure along the length of the potential surface of sliding (Forrester, 2001), anchoring of the unstable rock masses for the parent formation, and execution of retaining walls.

Stabilization of the ground may also be achieved by means of strengthening, or else with replacement of the weak material. Grouting is a frequently used remedy, while the replacement of the material, if it were of a significant extent, would certainly be very expensive. Probably the best solution is the simple filling in of earth or rock mass at the lower end of the potential landslide, especially if it is a location that may be used as a stockpiling area for the material from the excavation of individual structures within the framework of the hydraulic scheme. In certain instances, it might be necessary to apply unloading, even with complete removal of the material, which could be justifiable when that material could be used for filling some of the structures within the framework of the hydraulic scheme. There are frequently taken measures that represent a combination of two or more of the described measures.

In practice, there have been recorded numerous cases of caving-in and failure of the banks of a reservoir, occurring due to sliding (Sakamoto et al., 1994) or due to erosion of the material. Some of them have taken place at the beginning of the utilization, while others have taken place after a number of years of normal operation. In the case of a reservoir in the USA, after a continuous utilization lasting a number of years, and at a high water level, there came about sliding of a part of the bank, after the water level had a rapid drawdown to an unusually low level.

A well-known example of the sliding of a part of the bank was recorded at the Vaiont reservoir (Italy) formed with an arched dam with a double curvature (Fig. 33.2), 265.5 m high, 190.5 m long at the line of the crest. The dam is 3.4 m wide at the crest, while 22.71 m at the base. The two concrete supports are reinforced with 300 prestressing anchoring cables 55 m long, since a part of the fissured rock mass is unfavourably oriented in relation to the orientation of the pressure of the dam. The dam has been constructed in a narrow canyon, featuring dolomitic limestone.

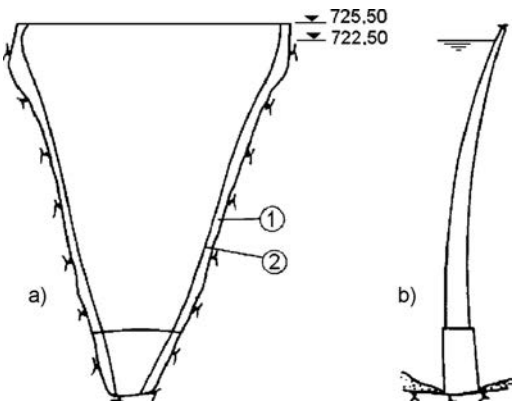

Figure 33.2 Vaiont dam, Italy (after ICOLD, 1974). (a) Elevation; (b) transverse section. (1) Concrete support; (2) interface of the dam with the concrete support.

The idea to build a dam at this place was an old one and planning of the project began in 1920. The excavation works began in 1956, while concreting began two years later. Filling of the reservoir commenced in March 1960 and, all of a sudden, during the same autumn, there came about a movement of the ground in the left bank of the reservoir, close to the dam, when there was noticed surface sliding of a mass of 700,000 m^3. Along the length of the perimeter of the fissure with a W shape, the rock mass 2000 m long and 1200 m wide started creeping with a maximum speed of 4 cm a day (Fig. 33.3). As a consequence, the water level in the reservoir was slowly lowered and, a few weeks later, the creeping ended, which can be seen on the diagram in Figure 33.4 (ICOLD, 1974).

In the winter of 1961, immediately after a bypass tunnel had been constructed around the sliding zone, the water level again increased. Even at the maximum level, reached in 1960 (77 m below the crest), there did not come about new displacements. The mass again began creeping at a water level of 50 m below the crest, at a low speed of less than 0.2 cm a day, which increased to 1 cm a day at a water level of 26 m below the crest. The water level again slowly decreased and, four months later, the creep stopped. The next heightening of the water level occurred in the summer of 1963, when the mass began creeping again, now with a speed less than 1 cm a day, at a level of 50 m below the crest. At a level of 15 m below the crest, the creep speeded up and the slow emptying of the reservoir did not reduce the speed of sliding which, on 8 October 1963, reached a value of 20 cm a day. The following day the creeping changed into a sudden sliding, with a speed of 2500 cm/s. The rock mass of about 250 million m^3 was displaced horizontally by 400 m, including also here the 90 m wide canyon and it forced out 40 million m^3 of water, which had been elevated to a level 260 m higher than the level of the reservoir and so the water overtopped the dam, flowing downstream along the canyon of the River Piave, which spread devastation along its way. It swept away the town of Longarone and three villages, carried off more than 2000 inhabitants and created inestimable damage. The dam, even though an overflow jet of 100 m high overtopped the dam, has remained intact.

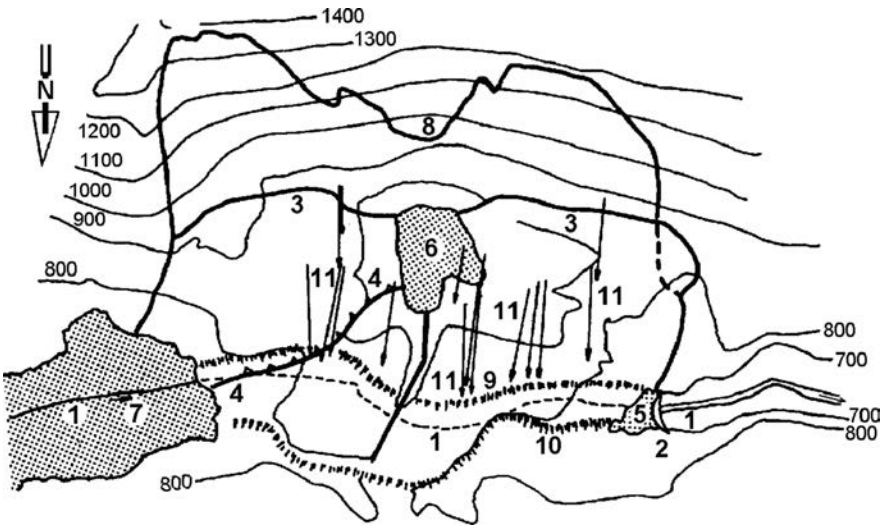

Figure 33.3 Location plan of the landslide of the Vaiont reservoir (after ICOLD, 1974). (1) River Vaiont; (2) dam; (3) south boundary of the landslide; (4) fault; (5) remaining western lake; (6) remaining central lake; (7) remaining eastern lake; (8) boundary of the fissure in 1963; (9) slope of the rock prior to sliding; (10) slope of the rock after sliding of the mass; (11) displacements of certain points.

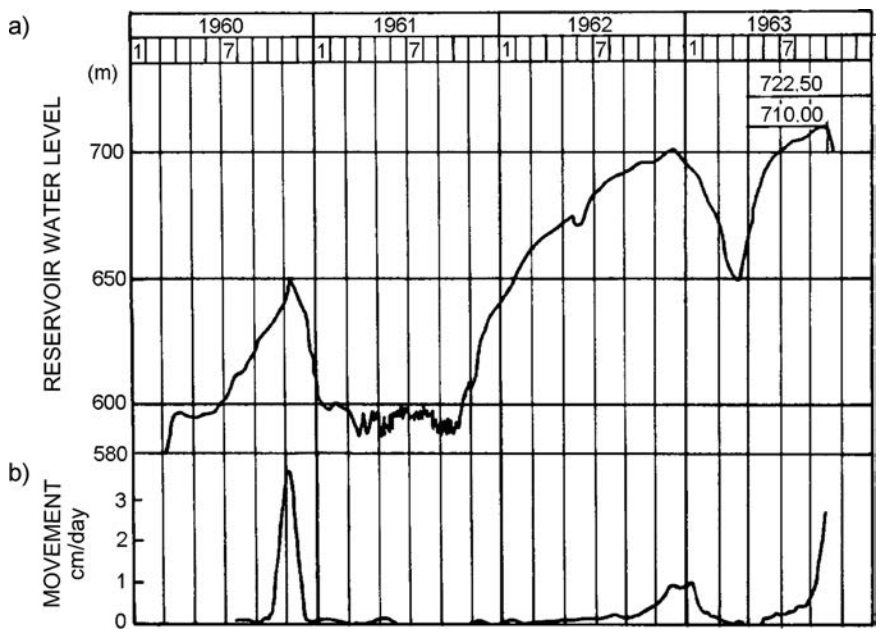

Figure 33.4 Diagram of water level in the Vaiont reservoir (a) and speed of movement of the control points (b) (after ICOLD, 1974).

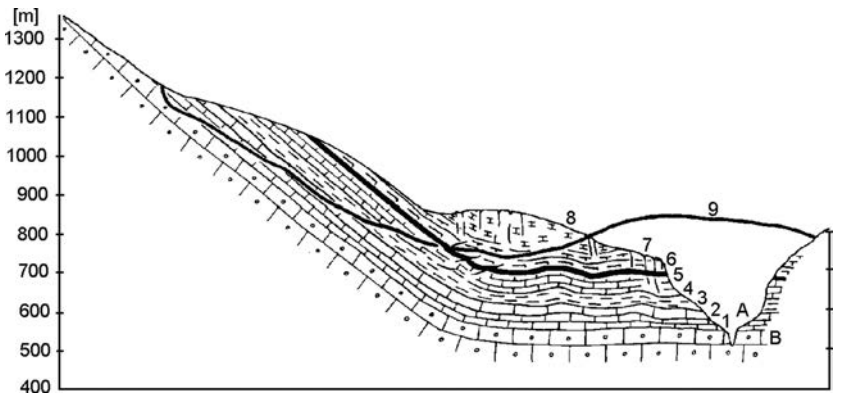

Figure 33.5 Reconstructed geological section of the hillside of the Vaiont reservoir (ICOLD, 1974). (A) Vaiont canyon; (B) Dogger (Middle Jurassic) – Malm (Upper Jurassic) formations; (3–5) formations of Lower Cretaceous Age; (6–8) formations of Upper Cretaceous Age; (9) edge of the rock after sliding.

In this case, it is obviously a question of significant omissions on the part of the geologists. Namely, the geological investigations of the reservoir storage space that began in 1928 were intensified in 1956, but only the latest investigations of 1959 indicated the possibility of the sliding of a mass of several million m^3, as it has been concluded "under certain, not very probable circumstances". It has appeared that the exploratory holes, bore pits, and test wells had been too shallow to give all the necessary data, and the obtained results had not been evaluated properly. Namely, the strata in the upper part of the hillside that slipped, are inclined by almost 50°, while in the deeply cut-in canyon of the Vaiont stream they are almost horizontal (Fig. 33.5). The rock in that part consists of calcareous deposits from the Upper Jurassic formation (Triassic period, Dogger or Middle Jurassic period, Malm or Upper Jurassic period), up to limestone and marly limestone from the Lower and Upper Cretaceous Age. The strata are from 1 m, up to several centimetres thick, and they are broken by means of two mutually perpendicular systems of fissures. The layered surfaces are infilled with interbeds or an intercalation of heavy soil material and, after the sliding, there were found large quantities of sandy-clay heavy soil materials on the plane of sliding. Precisely the strength of that material was relevant for the stability of the Vaiont hillside, and not the strength of the rock through the mass or through the rough uneven surfaces, which the preliminary investigation works had not taken into account.

33.2.2 Water-impermeability of the reservoir

Losses of water from the reservoir, owing to insufficient water-impermeability of the ground, may originate in two possible ways: through seepage or through leakage. In the former, there comes about a small loss of water through the pores of the earth material, and in the latter, there come about considerable losses, originating through very porous material or through fissures and cracks. The leakage may endanger the stability of the banks of the reservoir and, of course, that has to be prevented. The

seepage is not harmful if it does not essentially influence the balance of the reservoir and if it does not over saturate the surrounding agricultural land. In the contrary case, measures should be taken for its reduction, and, if these measures are irrational, then we should abandon the dam site.

The dam site usually is the lowest point of the reservoir and that is why it is also a potential zone for the greatest seepage. In some ways, this is a fortunate circumstance, since at the dam site they perform the most intensive investigation works, and also they treat the foundation in the most cautious way, in order to ensure the stability and safety of the dam, which leads to automatic cutting down of seepage.

In dealing with this problem, it is of greatest importance to find out the path of the leakage or that of the unacceptable seepage, for which there are different techniques at one's disposal, starting with the use of colour or other kinds of substances, down to the application of radioactive route markers. Also, it is useful to observe and track the registration of the level of underground water through observation wells. All the quoted methods make a contribution in the design stage to the assessment of possible losses of water owing to seepage during the exploitation (use) of the hydraulic scheme.

In many cases grouting can be helpful, by means of which it is possible to form a grout curtain, or else a three-dimensional impermeable zone. The grouting can be applied as either an independent measure, or else in combination with other measures, by means of which we can reduce losses of water. If unacceptable losses are anticipated and it is a question of a small reservoir with limited optional possibilities, it could be justifiable to line the banks and the bottom with a water-impermeable liner. For this purpose we can use concrete, geosynthetics, and especially compacted earth and various kinds of asphalt (Cavallin, 1988). The application of linings is especially frequent in cases of pumped storage reservoirs, where the water has a high price (GSCLD, 1988; Huth et al., 1988; Jappelli et al., 1988; Smith et al., 1988; Scuero & Vaschetti, 2013).

One of the latest examples of the execution of lining across the entire upper reservoir is the *Cortes – La Muela* pumped storage plant, as described in Chapter 32. The *La Muela* reservoir rests on limestone and on marmorean limestone, highly fissured and karstified, with vertical joints, so that the foundation may be assessed as being water-permeable. Because of that, it has been necessary to face the entire internal surface of the reservoir. In selecting the material for facing, a clay lining was immediately rejected, since there was no appropriate material in the vicinity of the reservoir, and therefore, a number of artificial materials were analyzed. Following detailed analyses, it was concluded that the two basic requirements: (1) high water-impermeability; and (2) economy, would best be fulfilled by linings of factory-made bitumen-polyester membrane and of asphaltic concrete. The first-mentioned lining, owing to its weaker adhesion with the foundation, was suitable for the bottom of the reservoir, while the second one was suitable for the slopes. In the end, it was decided that the entire lining be made of asphaltic concrete, in which not only technical but economic factors participated in making the decision (Navalon & Gaztanaga, 1988).

The structure of the lining is shown in Figure 33.6. As bedding to the lining, both at the bottom and on the slopes, there has been applied a layer of crushed stone, with dimensions of the rock pieces up to 150 mm, and with a minimum thickness of 30 cm. One may then distinguish two different constructions: at the bottom and across the slopes. At the bottom, upon the crushed stone, there has been applied a base course (binder), with a thickness of 6 cm, which ensures an even surface for the

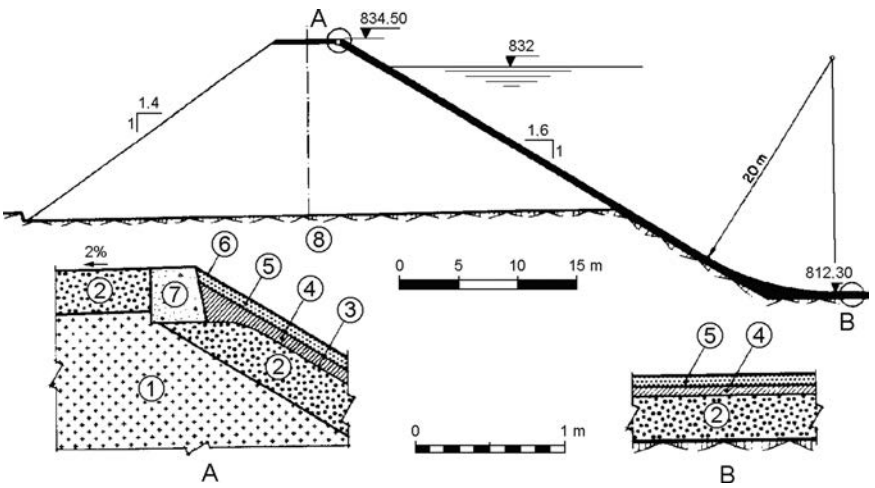

Figure 33.6 Cross-section and details of lining at the La Muela reservoir, Spain (Navalon & Gaztanaga, 1988). (1) Rockfill, limestone; (2) layer of crushed stone; (3) surface treatment with bituminous emulsion; (4) base course (binder); (5) asphaltic concrete layer; (6) bituminous mastic; (7) concrete block; (8) rock foundation.

impermeable asphaltic concrete layer, with a thickness of 7 cm, applied in strips 6 m wide. The asphaltic concrete has been designed to contain 3% free voids in a compacted condition and to yield a coefficient of permeability lower than 10^{-9} cm/s.

Across the slopes, the structure of the lining consists of the following elements: (1) surface treatment of the layer of crushed stone by means of cationic bituminous emulsion, proportioned in a quantity of 2 kg/m^2; (2) base course (binder), 7 cm thick; (3) asphaltic concrete layer, 7 cm thick, in strips 5 m wide; and (4) surface protection with a coating of bituminous mastic in a quantity of 2 kg/m^2.

Crushed limestone has been used as an aggregate for preparing the asphalt concrete mixture; this aggregate has been obtained from the excavations for the reservoir. Sand has been used from the river channel while, for filler, there has been used mainly cement mixed with some rock flour from the limestone. In the asphalt concrete layer, placed along the slopes, a small amount of asbestos has been added.

At places where the lining extends over concrete structures, such as, for example, in the vicinity of the intake structure, the interface has been coated with bitumen, in order to provide a better bond. When applying the latest strip, the previous one has been cooled, and they have used additional heating of the joint by means of infrared rays, followed by repeated compaction.

In the course of construction, a detailed control has been performed on both disturbed and undisturbed samples of the material in the lining, in which special attention has been paid to water-impermeability. The entire lining, with an area of 1.102×10^6 m^2, was installed from May 1986 until October, 1987.

In cases of very large reservoirs, a complete lining does not come into consideration, while one could take into consideration lining some of the smaller, more critical zones. Sometimes, we might solve the problem with the execution of an upstream blanket,

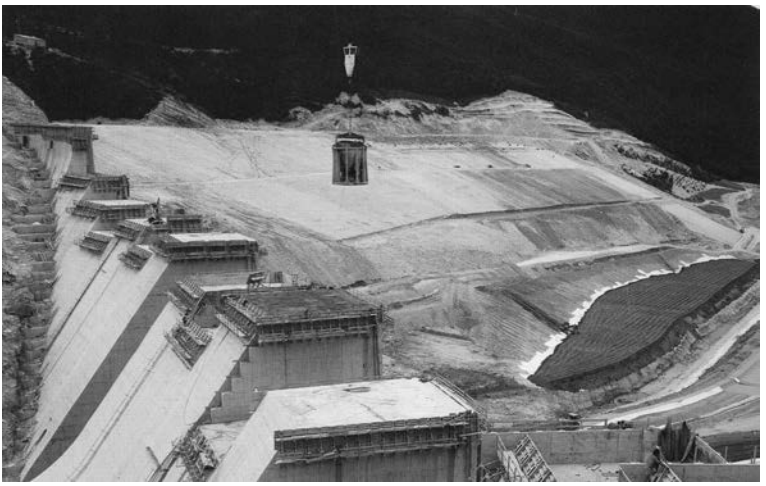

Figure 33.7 The Castreccioni dam (Italy), with upstream waterproofing works (construction stage).

as an extension to the dam. A typical example of such an approach is the hydraulic scheme with the Castreccioni dam (Italy), built up on the river Musone in 1985 for irrigation purposes. The reservoir, with storage of 37.3 million m^3, was formed by a 67 m high concrete gravity dam. The problem of the high permeability of the carstified foundation was solved by placing of wide clay blanket just upstream of the dam, 5 m thick (Fig. 33.7). Furthermore, the banks were covered by PVC geomembrane (1.2 mm thick) placed between two layers of geotextile. The lining of the banks was protected partially by concrete slabs, gravel, and rockfill (Fig. 33.8). Special attention was paid to the joint of the reservoir waterproofing system with the concrete dam, as well as to the drainage system of the bank lining. This well-designed and executed waterproofing system has worked successfully for more than 25 years.

33.2.3 Seismicity of the ground in the zone of the reservoir

A number of regions in the world are potentially susceptible to destructive earthquakes, among them the Republic of Macedonia, which is close to the second seismic belt in the world (along the coast of the Pacific), which starts in Northern India, and then passes through Pakistan, Turkey, Greece, and Italy. An earthquake in the vicinity of a dam, may cause damage, even failure, if, during the designing process, the forces due to the earthquake have not been examined in an appropriate way, and that has already been discussed in Chapters 4, 9, and 21. An earthquake may cause direct damage to the dam (cracks and fissures, deformations, or sliding of slopes), or else indirect damage through high waves formed in the reservoir, either from the shake or due to sliding of the banks. And, since it is not possible to predict when, where, or with what magnitude an earthquake will occur, it is necessary during the first stage of designing to assess the seismic risk at the dam site and the reservoir storage space by means of existing seismic maps. In the subsequent stages, especially in cases of large hydraulic

Figure 33.8 The Castreccioni dam (Italy), with linings on both banks, protected by concrete slabs or rockfill.

schemes, it is necessary to perform detailed and thorough seismological and geological investigations, by means of which we may determine the risk from earthquakes more precisely.

Since the 1960s, attention has been drawn by the relationship between the loadings with water of large reservoirs vis-à-vis the increase of seismic activity in the zone of the reservoir (Nikonov, 1993; Saxena et al., 1988; Vladut, 1993). For instance, the earthquakes that have damaged the 91.5 m high Koyna gravity concrete dam in India, and the 90 m high Hsinfengkiang buttress dam in China are deemed to have been caused by the filling of the reservoirs. In both cases, following the filling of the reservoirs, there was recorded a series of tremors in the vicinity of the hydraulic schemes, before the strong earthquakes that caused damage on 11 December 1967, and on 19 March 1962. A number of tremors have also been recorded in the vicinity of the reservoir, formed with the 107 m high Kariba dam, on the River Zambezi, for the first time filled in August 1963, with 133 billion m^3 of water. Between 14 August and 8 November 1963, in the vicinity of the reservoir, nine earthquakes of intensities from 5.1 to 6.1 degrees, according to the Richter scale, took place. Filling of the reservoir commenced in December 1958, while the first tremors were felt in 1961. There were recorded 155 tremors in 1962, 135 tremors in the first seven months of 1963, while in the period between 14 August and 30 September the same year, there were recorded as many as 750 small tremors. The literature also takes note of other cases of earthquakes associated with the filling of large reservoirs. However, it should be noted that in cases of a number of large reservoirs there has not been noticed any seismic activity, or else if there has been a tremor, such as in the example of the Oroville hydraulic scheme

in California, it has been deemed as not being related to the reservoir (Golzé, 1977; Paskalov, 2001).

It has not been clarified, and it is still being investigated, what the connection is between the loading of the reservoir and the occurrence of earthquakes. An early hypothesis was that the loading of the water in the large reservoirs was the reason for occurrence of so called *reservoir-triggered seismicity* (RTS). Later on, it was believed that the loading of the reservoir is only a motive mechanism by means of which there is caused a release of the existing stressed state in the Earth's crust. Confirmation of this was that the Koyna hydraulic scheme, as well as others, at which tremors have occurred after the filling of the reservoir, is located in a zone that is not marked as a highly seismic one. At the same time, in distinctly highly seismic California, there have not been observed any stronger tremors associated with the filling of large reservoirs.

The newest hypothesis says that the pore pressure of the reservoir water permeated into the rock reducing its effective stresses and causing the drop of shear resistance. As is more commonly recognized, the effect of added weight of impounding water on the stresses is negligible in comparison with the stresses imparted by the weight of rock at the location of the hypocenter (Houqun et al., 2010).

In connection with this problem and for the purpose of recording tremors, it is recommended to install a network of three stations in the vicinity of large reservoirs, five years prior to the commencement of filling. If during filling of the reservoir there comes about increased seismic activity, the network should be extended. One of the seismograph stations should be installed as permanent, while the others may be temporary stations.

By gathering much practical and investigative experience, the problem of the relationship between the loading of the reservoir and possible earthquakes, will also become clearer. In the meantime, engineers have to appraise whether or not we should build a hydraulic scheme with a large reservoir in certain regions. In that, it is clear that the decision will also depend on whether in the vicinity there is a larger inhabited place or whether the reservoir is located in a remote, isolated zone. The reader can find more details regarding RTS in ICOLD Bulletin 137 (2011).

33.2.4 Water absorption of the ground in the zone of the reservoir

Part of the water from the reservoir storage space is absorbed into the surrounding ground and it fills the voids in the earth mass or the rock mass in the zone of the reservoir. It is supposed that this water will remain in the surrounding mass. In contrast to the filtrated and runout water, this water theoretically is not lost; however, in practice, it should still be deemed as lost water if it is not available for use. In the case of very large reservoirs with a slow lowering of the water level, the water that is accumulated in the banks could be used, while in cases of small reservoirs the fluctuations of the water table are usually faster than the reverse flowing (return of filtrated water from banks to the reservoir).

The position of the underground water table has a considerable influence on the accumulation of water in the banks. If the ratio between the existing current flow vis-à-vis the underground water is such that the underground water feeds the current

flow, then the accumulation in the bank will be brought to a minimum. On the contrary, the loss due to the accumulation of water in the banks may be a problem.

The accumulation of water in the ground surrounding the reservoir storage space is not a phenomenon that can be prevented or modified, but it should be evaluated in the studies on justifiability of the realization of the project even in determining the annual available water. The evaluation of this water falls into the competence and responsibility of hydrogeologists.

33.2.5 Evaporation

In addition to losses of water from the reservoir into the surrounding terrain, losses also take place into the atmosphere, in the following two ways: directly, through evaporation and, indirectly, through the transpiration of plants.

Evaporation depends on the climate, as well as on the shape of the reservoir. Reservoirs with a small water surface area in relation to the volume of the water, suffer small losses due to evaporation. In addition, when assessing these losses, one should also take into consideration the conditions of the blowing of the wind, temperature, and humidity. For reducing evaporation from the reservoirs, we may use chemical retarders against evaporation, which effect its decrease and form a monomolecular film on the surface of the water. However, even the best of these agents have deficiencies, while the greatest ones are their weakness regarding the effect of wind, as well as their high cost.

With regard to losses due to transpiration, certain types of plants, known under the name of *phriatophytes*, are especially significant consumers of water. They are grown in areas with high underground water, spread fast, and have roots that can reach a depth of up to 23 m. Phriatophytes consume up to 100% more water than most agricultural crops. It has been estimated that in the western part of the USA alone, they consume 31 million m^3 of water, and that is approximately the amount from losses due to direct evaporation. In the action for the extermination of these harmful plants, one may use both physical and chemical measures, followed by substitution with plants that have a smaller need for water.

33.2.6 Sediment accumulation

The slope of the free water surface, velocity of flow, and also the transport capacity of the flow, decrease proportionally with the approach to the hydraulic scheme and to the dam. As a result, the sediment that is carried by the current is partially settled on the bottom, sorting itself according to its size. The lowest part of the reservoir, called *dead storage space*, is used for sediment accumulation. The sedimentation is especially intensive at hydraulic schemes in mountain rivers that regularly have a powerful current. Besides the watercourse, for sedimentation into the reservoirs, a contribution is also made by scouring or failure of the banks, originating as a consequence of the effects of waves.

In the beginning, the sediment settles mainly in the upper part of the reservoir, in that in the initial part there settle the coarsest particles, and in the direction of the course, finer and finer ones. That is presented in Figure 33.9, in which the curve ab_1c_1 confines a volume of sediment settled in time t_1, while $d_1 > d_2 > d_3 > d_4$, where d is

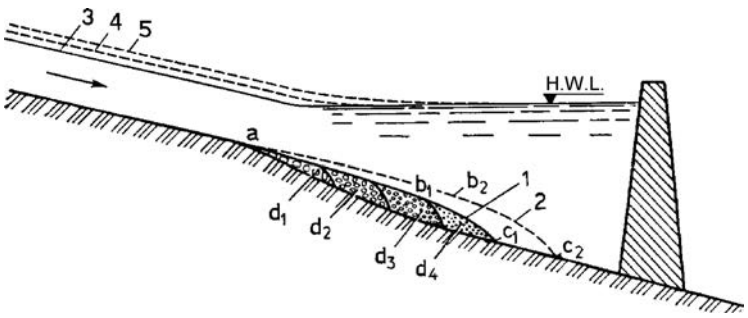

Figure 33.9 Scheme for reservoir infilling with sediment. (1) Surface of the sediment settled in time t_1; (2) the same as 1, but in time t_2; (3) water level in natural conditions; (4, 5) water level after time t_1, and t_2, respectively.

diameter of the fractions in the sediment. In the course of time, the area of the settled sediment approaches to the dam (curve ab_2c_2, which represents the sediment settled in time $t_2 > t_1$.

The time which is necessary for infilling of the reservoir with sediment may approximately be determined by means of the formula (Grishin et al., 1979):

$$T = \frac{V}{\rho \frac{V_{av}}{\gamma_1}\left(1 + \frac{\beta}{\gamma_2}\right) + V_b} \tag{33.1}$$

where V is the volume of the reservoir; ρ is the average annual muddiness of the river; V_{av} the average annual flow through the river; γ_1, γ_2 the unit weight of the floating sediment and bed load, i.e. sediment; V_b is the quantity of sediment owing to caving-in, scouring, and failure of the banks; and β is the ratio of the volumes of the floating sediment and the bed load, i.e. sediment.

By means of the proposed formula, we may calculate the total quantity of sediment that is found in the watercourse that feeds the reservoir. In fact, a part of the floating sediment is given passage through the outlets and through the overfall structures in the course of utilization of the hydraulic scheme, so that the real time for infilling of the reservoir is somewhat smaller than the estimated one. Many other formulae are also used in practice, usually different ones for different kinds of sediment, by means of which, depending on the authenticity and credibility of the input parameters, we may carry our more or less precise calculations of the expected quantities of sediment (Skrilnikov, 1988; Ando et al., 1994).

As was shown, dam construction can considerably alter the flow behaviour from fluvial to lacustrine, with deposition of incoming solid particles. Depending on the overall conditions in the catchment area upstream of the dam, a reservoir can silt up in various rates. If no measures are taken for decreasing the transport of sediment, the reservoir may rapidly be infilled with sediment, as in the case of the Gumati I hydraulic scheme, on the River Rioni (Georgia), see Figure 33.10. In this case, 10–11 years after the commissioning of the dam practically the whole reservoir was filled with sediment.

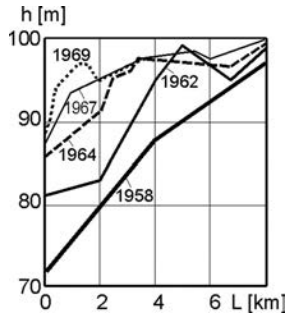

Figure 33.10 Transverse profile of the Gumati I reservoir, Georgia (after Grishin et al., 1979). *h* – water level at the dam; *L*, distance from the dam.

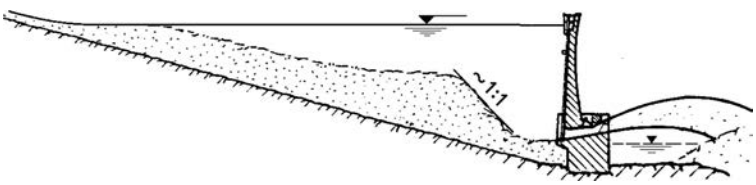

Figure 33.11 Limited effect of the bottom outlet for evacuation of sediment (Vischer & Rutschmann, 1988).

Different measures may be undertaken in order to reduce settling of the sediment in the reservoir (Alam, 2001, 2002; Jacobsen, 2003). The most efficient measure, and the most expensive, is the protection of the entire catchment area by means of a forestation, in order to prevent erosion of the ground. Another often used measure is to build obstacles upstream of the reservoir and in the upper part of the reservoir aimed to stop the turbidity current and to force it to settle down its solid load. Cleaning of the sediment from the bottom could be economical in cases of small reservoirs, while washing out through low-positioned outlet structures has yielded limited results, especially for quite small and narrow reservoirs. Namely, in cases of large reservoirs with usual dimensions of the outlet structures, it is possible to evacuate the sediment only from a small width and length of the reservoir, in the vicinity of the outlet, since, during the flowing of water through the bottom outlet, there comes about a washing out of sediment of only a small volume, in the form of a funnel, with an inclination 1:1, in a narrow zone around the opening, as is shown in Figure 33.11.

Recently an experimental study was launched with the aim of developing an alternative efficient method to release sediment from a reservoir at hydro-power schemes. The concept is based on the release of the fine sediment through the headrace tunnel and turbines in the area upstream of the power intakes. Specific jet arrangements should provide the energy and generate the optimal circulation needed to maintain the sediment in suspension and enhance its entrainment into the power intakes during turbining sequences. The authors of the study believe that the experimental results of

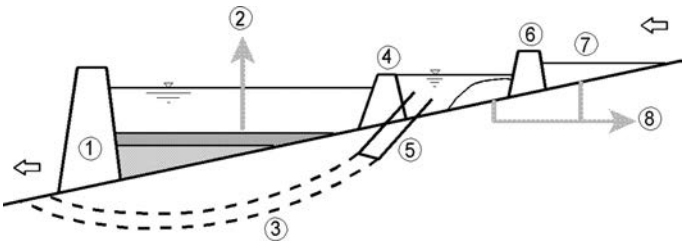

Figure 33.12 Concept for the protection of the Miwa reservoir (Japan) against infilling with sediment (after Ando et al., 1994). (1) Miwa dam; (2) cleaning of sediment from the reservoir by means of pumping; (3) bypass tunnel; (4) dam for separation; (5) open bypass channel; (6) dam for retaining of the coarse sediment; (7) coarse sediment; (8) dredging and conveyance of the coarse sediment.

the new method for releasing sediment through the water intake are very promising even though no test at natural scale has been performed so far (De Cesare et al., 2011).

In some countries, for example in Japan, they approach the questions associated with the infilling of the reservoirs with sediment, very thoroughly. In this highly developed country there have been constructed about 700 reservoirs with a volume larger than a million m^3 of water and infilling with sediment is a serious problem for many of them. Cleaning of the reservoirs with the application of heavy plant and equipment is a frequently employed measure, especially when there is a possibility for the sediment to be utilized as construction material at some nearby construction site[1] (Roovers, 1989; and Takebayashi & Takasu, 1994).

In some cases, they employ scheme measures, such as, at the reservoir formed with the Miwa gravity concrete dam, which serves for retention of floodwaters, irrigation, generation of hydroelectric power, and providing a biological minimum in the river. The measures taken for the protection of the Miwa reservoir against infilling with sediment consist of cleaning out of the sediment and prevention of its entering the reservoir. The scheme of the protective measures is shown in Figure 33.12. From the figure it can be clearly seen the conception adopted. Upstream of the main dam (1) there have been constructed two auxiliary dams. One of them (6), serves for retaining the coarser sediment, of which only a part passes and settles downstream, directly next to the dam. The other auxiliary dam (4) serves for separation of the first auxiliary dam from the main dam. This dam is an overflow dam, but it is also provided with a bypass channel (5), which goes into a bypass tunnel (3), by means of which one part of the flood waters is taken away directly downstream of the main dam, without entering the main reservoir storage space. In that way, we may decrease the quantity of sediment and reduce it to finer fractions, so that its occasional cleaning by pumping would be possible (2). The coarse sediment (7), retained by the auxiliary dam (6) and settled

[1]In Japan, as in other highly developed countries, space for stockpiling of waste materials is very limited, especially if there are significant quantities, when longer transport time would be very expensive.

downstream of it, is dredged and conveyed from the auxiliary reservoirs (Ando et al., 1994).

The solution with sediment conveying bypass tunnel was applied recently in the case of the Solis reservoir in Switzerland. The original reservoir volume, aimed for electricity generation, was 4.1×10^6 m^3, formed by an arch dam, 61 m in height, located in a narrow river canyon. Since the construction of the reservoir in 1986, high sediment input from upstream mountain torrents has led to major aggradations, filling nearly half of the original reservoir volume. It was decided to construct a sediment bypass structure consisting of a guiding structure, an intake with a skimming wall, a bypass tunnel, and an outlet. The total length of all structures is 973 m, with a constant inclination of 1.9%. The intake structure is located 450 m upstream of the dam. The bypass tunnel cross-section has an arch shape and is 4.4 m wide and 4.7 m high. A 100 m-long outlet structure is provided on an embankment to convey the sediment-laden flow back from the tunnel end to the river bed downstream of the dam. The construction of the sediment bypass structures started in 2011 and it was planned to be operational in the spring of 2012 (Auel et al., 2011).

Another interesting case is the sedimentation of the reservoir of the highest concrete gravity dam in the world, *Grande Dixence* ($H = 285$ m, 1961), located in the heart of the Swiss Alps, a key structure of the eponymous hydroelectric scheme. The concession for the use of the waters is attributed to the Grande Dixence society for 80 years and will end 31-12-2044. The dam does not have any spillway structure, because 8/9 of the water comes from the diverted catchment areas and 2/3 of the water is pumped, and it is possible to control the water inflow in the reservoir. The water from melting glaciers contains sediments of various sizes. A share of these sediments settles down in the reservoir.

About 400 m upstream of the Grande Dixence dam lies the older hollow gravity Dixence dam, 87 m high, built in 1935, with a crest at an elevation of 2241 m.a.s.l., Figure 33.13. This dam is underwater and can be seen only during April–May, when the level of the Grande Dixence reservoir is lower than its crest. To allow the water to flow through the dam, two orifices have been built in both upstream and downstream faces, designed to discharge 55 m^3/s. The upstream orifice is at an elevation of 2196 m. When the Grande Dixence reservoir level is below 2241 m.a.s.l., the whole discharge flows through the orifices, entraining fine sediments in the reservoir space between the two dams, with an average settling rate of 50 cm/year. The problem of sedimentation has been recognized since the start of the service period. In 1969, just four years after the beginning of the exploitation of the whole scheme, the bottom outlet was upraised by 18 m with metal pipe segments, because the sediment level had already reached its entrance. At the above-mentioned average speed, the sediments reached the dam bottom outlet in 2011 and the water intake will be reached in 2018.

To overcome the problem, since 2006 many solutions for the sediment management of the Grande Dixence reservoir have been analyzed, including: construction of a bypass tunnel, dredging, yearly flushing by using the bottom outlet, abandonment of the bottom outlet, construction of a new bottom outlet, and turbining the water with suspended load. Finally, a solution with permanent storage upstream of the old Dixence dam by creating a new higher located orifice and by plugging the existing one was accepted as feasible and most economical. The sediment storage capacity gained through this intervention on the old dam was estimated to be enough for at least the

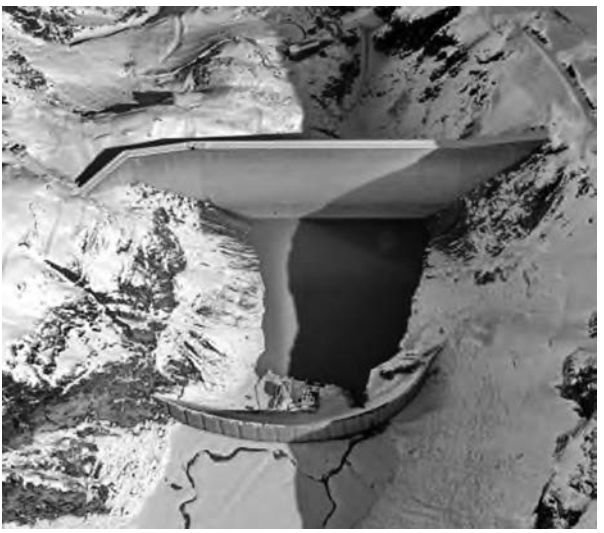

Figure 33.13 Grande Dixence dam (1961, $H = 285$ m), and older Dixence dam (1935, $H = 87$ m) located 400 m upstream (Bretz, 2013).

coming century. The new flow section is designed for a discharge of 130 m^3/s, instead of the previous 55 m^3/s. The new upstream orifice is located 5 m above the existing one, which enables to store sediments until 2050 at least. The downstream orifice is resized from 4 m up to 10 m in height. At the end of the construction of the new upstream orifice, the existing one was plugged with concrete.

To be insured of favourable conditions for execution of the works the water level in the reservoir was lowered during the winter 2010/2011 by turbining. In February 2011, the works on-site started with the security measures: setting up a cable car between the 2 dams, installing life lines and a guardrail on the crest of the old Dixence dam. Works on-site finished in April 2011, having lasted 41 days, with only 3 days of interruption because of bad weather (Bretz, 2013).

Finally, not all effects of sedimentation are necessarily harmful. In some cases, the settled sediment in front of the dam may play the role of a natural blanket and, in that way, reduce the losses due to seepage.

33.3 RESETTLEMENT OF POPULATION AND RELOCATION OF STRUCTURES

With the construction of reservoirs, especially large ones, there comes about a submerging of inhabited places, arable agricultural land areas, woodlands, economic, commercial, transport and other structures, etc., and land is also occupied with the construction of various structures within the framework of the hydraulic scheme. In that way, an obligation is imposed, even at the stage of preparation of the design: to

solve often scheme questions regarding the resettlement of the population and relocation of structures, along with solving the property and legal relationships and problems, and that requires more time. There should exist coordination between the engineers and the competent services and governing authorities, aimed at proper classification, describing, and assessing the requisitioned property, as well as defining the program and progress time schedule for the resettlement and relocation of individual structures or facilities. Certain new locations or sites, which would be in the vicinity of the former ones, should be previously examined and, if possible, the securing of better or at least, as good, conditions.

The Three Gorges Project on the Yangtze River (construction period 1993–2009) is the key backbone project in developing and harnessing of the Yangtze River, and also is the largest multipurpose project in development and comprehensive utilization of a river resource in the world. The realization of this grandiose project could make great composite benefits such as flood control, power generation, and navigation and will greatly affect and promote the economic development in the Yangtze valley. Because of the gigantic scale of the project, a lot of major technical, scientific, and environmental problems have been solved. Perhaps the biggest among them was the problem of the resettlement – more than one million people were resettled. The pilot work for development-oriented resettlement in Three Gorges Project began from 1985 and entered ordinary implementation period in 1993. In 1997, the first period of resettlement arrangement was smoothly finished and satisfied the demand of the river closure. From 1993 to the end of 1999, the State arranged a total of $1.72 billion US of resettlement compensation investment of Three Gorges Project, which consisted of various newly built kinds of houses of 13.13 million m^2, moved or closed 543 industries, rebuilt 675 kms of highway, installed 998 kms of power transmission and lines, resettled 219,000 people, and created resettlement conditions for 69,000 people. The living conditions of the resettled people have been improved and the economy of Three Gorges reservoir region is continually and healthily advancing (CYTGPDC, 2000).

From an engineering aspect, of particular interest is the question of relocation of transport structures or systems – railways and roadways. In cases of large reservoirs, they bear the major amount of cost for relocation of those works. Appropriate attention should be paid to this question, since the construction and the handover to utilization of the relocated sections of transport facilities must be done so on time and also must be synchronized with the construction and commissioning to service of the hydraulic scheme.

Sometimes, flooding, i.e. submerging, may also involve various significant works and installations (monuments, old bridges, churches, archaeological sites, graveyards, necropolises), which are of local or broader social and public significance. The possibilities of their partial or entire relocation should be timely and thoroughly analyzed with the competent authorities and interested parties, taking into account that emotions are also regularly involved in negotiations about such sensitive questions. Examples of such relocations may frequently be found, and maybe the most characteristic are the works that were undertaken during the construction of the high Aswan Dam in Egypt. With funds from the Egyptian government, enriched by international donations, there have been relocated a number of ancient works and monuments, even an old temple, carved into a hill, has been removed from the zone of the reservoir.

33.4 SPORTS AND RECREATIONAL FACILITIES

In designing hydraulic schemes, we usually anticipate a larger or smaller number of auxiliary structures that alleviate and ease or improve and enhance the utilization of the main works. Here, one may count the access roads and tunnels, bridges, and various kinds of buildings. Within the framework of the reservoir itself, of particular importance are the sporting and recreational facilities that may be anticipated when this is allowed by the main function of the hydraulic scheme (Elahovskij, 1990).

Facilities that make sport and recreation possible are more and more often inserted into the water economics plans. Even though, in designing the sports and recreational zones, one should consult experts from the appropriate fields, civil engineers should be acquainted with the basic principles of these fields.

In order to ensure possibilities for recreation, it is necessary to build beaches and strands, grounds for outings, picnics, and camping, pathways for walking and jogging, and to create possibilities for kayaking. As auxiliary structures for the provision of the above-quoted activities, we should also obligatorily include access roads and parking lots, sanitary facilities, works for collecting waste, and a water-supply network for drinking water, etc.

Beaches and strands must be located only on appropriate ground consisting of suitable earth material, which, at the same time, is a stable material. In this, of great importance is the accessibility of the areas for outings, picnics and camping, widespread sand, quality of water, and the temperature, and the blowing of wind and formation of waves, as well as the variations of the water level in the reservoir. The slope of the bottom under the water should desirably be from 5 to 8%, and not more than 15%, while outside of the water, the ground should not be steeper than 25%. The water-supply network should provide 10 to 60 litres per person per day, depending on the type of sanitary facilities and on whether there have been provided showers. The sanitary facilities should not be more than 120 metres away from the normal water level. The parking lot should be some 150 metres distant from the beach or strand. For ensuring the security of bathers and swimmers, there have to be anticipated observation towers with life-guards every 100 m, as well as floating marks that restrict the space for swimming.

A typical example of a thought-out utilization of a reservoir for sport and recreation is the Rutland reservoir (England, UK), within the framework of the hydraulic scheme, the main function of which is the water supply of inhabited places, commissioned into operation in 1977 (Figs. 33.14, 33.15). The exclusive shape of the reservoir, with two branches, separated by the Hambleton peninsula, with a lot of branching and outspread banks and an exceptionally quiet environment, have facilitated the forming of a copious sports and recreational centre, with well thought-out and located different contents. In that, there have been preserved to a maximum the nature reservations, with an endeavour at their successful harmonization into the additionally constructed contents. The basic function and working regime of the reservoir do not at all derange the secondary utilization of the reservoir for sport and recreation. This hydraulic scheme can also serve as an example for the enhancement of the natural environment in the realization of significant civil engineering undertakings. Namely, along with flooding and submerging the lands within the reservoir, there were been chopped down or moved about 40,000 trees, while at the perimeter of the lake there have been

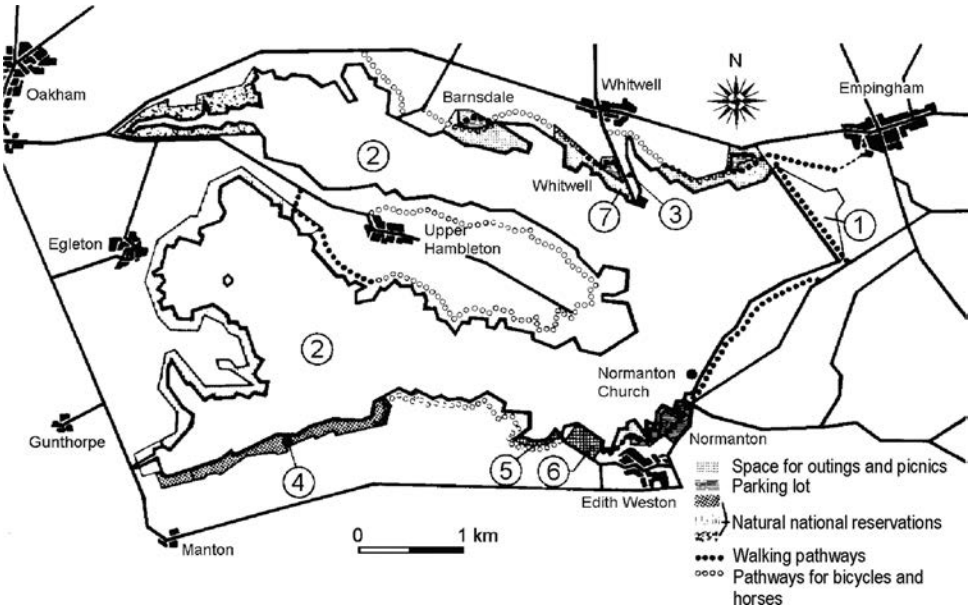

Figure 33.14 Location of the recreational-sporting facilities at the Rutland reservoir, England, UK (after Langford, 1979). (1) Embankment dam; (2) branches of the reservoir; (3) rescue centre; (4) information centre; (5) offices of the race centre; (6) kayaking club; (7) Whitwell peninsula.

Figure 33.15 The Empingham dam, which forms the Rutland reservoir.

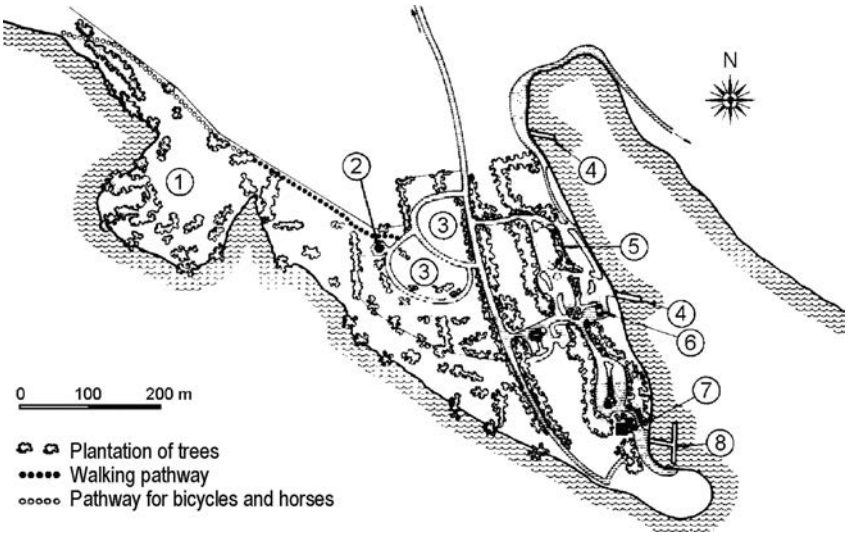

Figure 33.16 Layout plan of the Whitwell peninsula, Rutland, England, UK (after Langford, 1979). (1) Free grassed area; (2) sanitary facility; (3) public parking lot; (4) ramp; (5) pond for small boats; (6) rescue centre; (7) administration building; (8) pontoon.

planted 200,000 new trees of different kinds – oaks, ash, beech, limes, maples, as well as trees tolerating and enduring water, planted at the edges of the reservoir (Langford, 1979).

Typical details for solving certain space issues is given in Figure 33.16, in which the small Whitwell peninsula is presented (marked with 7 in Fig. 33.14). A public parking lot has been built in the central part of the peninsula, while the western part has been reserved for walking, resting, and recreation.

This page intentionally left blank

Chapter 34

Negative effects of hydraulic schemes and environmental protection

34.1 TYPES OF NEGATIVE EFFECTS ON THE ENVIRONMENT

Every project for a hydraulic scheme, thought-out and rationally constructed, brings benefits, above all economic benefits, as well as social benefits. There can also be expected certain benefits from the refinement and enhancement of the environment. There are some structures and works within the framework of the hydraulic scheme, especially the dam and the reservoir, which also cause, to a smaller or greater extent, negative effects on the environment. That is why in the designing, even at the stage of determining the technical-economic feasibility of the hydraulic scheme, we should examine several alternative solutions for the dam and the reservoir in order to utilize all possibilities for keeping to the least possible measure of negative effects (Golzé, 1977; Razvan, 1992).

In some places, up until the 1960s and, in some regions even up into the 1970s, practically minimum or even no attention was devoted to the question of the influence of dams on the environment and environmental protection, even when it has been a question of grandiose projects. Such is the example, for instance, with the Glen Canyon dam, constructed on the Colorado River (USA), at 25–26 km before the entrance into the Grand Canyon, one of the seven natural wonders of the world (Matter & Wegner, 1994). Or, similarly, the Kariba dam, completed in 1959, which, with the damming of the River Zambezi, has formed at that time the largest artificial lake in the world, with an area of 5400 km^2, as a symbol of progress (Marshall, 1994). Another similar example is the Nurek reservoir, within the framework of the highest embankment dam in the world, that began with its filling in the middle of the 1970s (Beylinson et al., 1990). The newest and most significant example in this field is the Three Gorges project on the Yangtze River, recently constructed (CYTGPDC, 2000; Jiazheng & Jing, 2000).

A dam and a reservoir can cause great or small negative effects in a number of different ways that can be divided into the following four categories:

(a) Changing the land into the area of the reservoir;
(b) Change of the flow downstream of the dam;
(c) Damming the migration paths of fish and wild animals;
(d) Change in the surrounding landscape and the microclimate.

Within the above-enumerated four categories, one may further influence fragmentation of the negative effects, some of which are inevitable but may be moderated to

a certain degree, while others may be avoided by means of undertaking appropriate measures. In the continuation, the most important aspect of the already mentioned categories will be briefly explained.

34.1.1 Changing the land into the area of the reservoir

34.1.1.1 Loss of living space for fish and water plants

After the filling of the reservoir, there comes about the submerging of the watercourses in its zone, by means of which some living environment is lost, to which there belonged spawning places, shelters for fish, and the entire network, e.g. variety of food resources, for the existing types of animals. With the filling of the reservoir, there will probably come about a replacement of different kinds of fish and other kinds of water animals. The effects of these changes should be analyzed for each specific case separately.

34.1.1.2 Loss of living space for wild animals

Some kinds of animals live on grazing and cropping of the vegetation alongside the watercourses, but that is partially lost with the submersion following the construction of the hydraulic scheme. Some kinds of vegetation flourishing alongside watercourses adapt in order to survive a short period under water, for instance, during the retention of a flood wave in a reservoir. Reduction of the effect of this loss can be achieved by preparing and enabling other areas for grazing, cropping, and browsing; however, that may be costly and it is not certain whether it will yield the desired effects.

34.1.1.3 Loss of access to mineral and ore deposits

One of the aims of environmental protection is the preservation of sources and occurrences of ores and mineral wealth for future generations. If a certain existing mine in the zone of the reservoir is closed down because of the execution of the hydraulic scheme, the loss is calculated in the cost at its economic value. However, if there are ore deposits in the zone of the reservoir, which, at the moment, are not utilized commercially but have potential value for the future, then their flooding and submerging may be deemed as causing damage to the environment. Such a problem requires serious analysis by taking into consideration the possible need for exploitation, i.e. utilization, of the given mineral in the future, as well as its spread and occurrence at other locations.

34.1.1.4 Loss of areas of a mountain valley

The reservoir storage space in a mountain valley may take hold of the only flat land, or else the greater part of the existing flat ground over a significant length. In such a case, the flat land is of significance for various future users that would appear as a consequence of the growth of population. The economic cost of such a loss at the moment of its consideration and examination may not express the real future value.

34.1.1.5 Submerging locations of historical or archaeological value

The most important archaeological discoveries made so far, with some exceptions, are located at relatively high locations. Namely, in ancient times valuable monuments

have been built on higher ground. A lot of ancient civilizations inhabited the areas in river valleys and along the waterways, and in precisely those kinds of places there have been discovered numerous ancient objects. In most cases, a visit by an archaeologist to the site of the planned reservoir is sufficient to give an answer to the question whether or not the ground, anticipated for submerging, is of archaeological value. Existing small objects could be moved to appropriate museums, while large and significant archaeological remains may be a serious obstacle for changing the location into a reservoir. The most characteristic case of this is the construction of the Aswan Dam on the River Nile, for which a number of large ancient Egyptian monuments were removed to a location higher than the elevation of the new reservoir, in spite of the enormous cost of such an undertaking. Perhaps it is worth mentioning that in the case of the Aswan dam the cost of construction was recovered in only two years. The dam has made a significant contribution to the economic survival of Egypt, having protected the country from both droughts and floods (Tortajada et al., *Eds*, 2012).

Submerging of historical places with a reservoir may be a moderate, or even a heavy, loss for the environment. With the construction of an appropriate museum, the loss could be moderated and eased. However, in a case of a very important historical site, it is certain that this would obstruct and prevent the construction of the hydraulic scheme. An example of such a case is the South Fork River near Coloma in California (USA). This site has extraordinary physical and economical conditions for water utilization; however, since the reservoir storage space would have to take in a historical site from the gold rush, the project has been abandoned and replaced by an alternate, much more expensive solution.

34.1.1.6 Submerging of exceptional geological formations

The anticipated reservoir could submerge (completely or partially) exceptional geological formations and topographical creations – waterfalls, large springs (ordinary or geothermal), rare open rocks, caves, and caverns. These kinds of places, if they have been denoted as national parks or monuments of geological significance, will certainly be an obstacle to the construction of the reservoir. An example of this is the National Park within the framework of the Grand Canyon on the Colorado River in the USA (Golzé, 1977).

34.1.1.7 Generation of conditions for reservoir triggered earthquakes

In the previous chapter, we have discussed and examined the possibility of the occurrence of earthquakes in the immediate vicinity of constructed large artificial reservoirs. There have been presented examples of strong, reservoir triggered earthquakes that have damaged some dams. Here, we shall add the example of the reservoir within the Nurek dam. The Nurek hydraulic scheme is located in a zone in which an earthquake with an intensity of eight degrees is possible. Scheme seismological investigations have been performed since 1955, which means some 20 years prior to filling the reservoir. They indicate an increase by 30% of the number of weak earthquakes in the period after filling of the reservoir, which means a small increase in seismicity. In that way, the release of energy happens gradually and more uniformly, which can be assessed as a favourable effect (Beylinson, 1990).

34.1.2 Change of the flow downstream of the dam

34.1.2.1 Reduction of the living space for fish and plants

In some of the previous chapters and parts, presentations have made of the negative effect of hydraulic schemes on the life of the fish and measures that are being undertaken to ease and modify this situation. Under natural conditions, the watercourse sometimes weakens very much, and it can even dry up completely; this natural phenomenon leads to a great loss of water space. Any project regularly anticipates a provision of a permanent minimum flow downstream of the water accumulated in the reservoir. That is a certain compensation for the negative effect, caused by the reduction of the flow downstream of the hydraulic scheme during a longer period of the year. There are different opinions on how great the flow downstream of the dam should be in order to avoid a serious negative effect on the living world. In most projects, it is recommended that for maintaining the water life downstream of the reservoir, it would be necessary to discharge a flow to the amount of from 10% to 1/3 of the multi-annual average of the natural flow.

34.1.2.2 Reduction of the transport capacity of the watercourse

Watercourses transport different quantities of sediment, depending on the discharge of water: a great amount of sediment is transported during flooding, and small amounts are transported during low discharges. The situation changes with the construction of a dam and reservoir: the sediment settles in the reservoir, while the transport capacity of the watercourse downstream is reduced, owing to the reduced discharge of water. Theoretically, the situation may be improved by the occasional sudden evacuation of a large quantity of water through the bottom outlet with a great capacity; however, this problem has not yet been sufficiently investigated. Up until now, in this field there has been achieved only very limited success, and that has already been discussed in the previous chapter. In the case of the Nurek hydraulic scheme, in the course of 15 years of observations after its commissioning, it has been noticed that the tailwater is permanently clear, which indicates that the sediment has completely settled in the reservoir. During 18 years of service, some 1.8×10^9 m^3 sediment has settled in the reservoir, also including some 40×10^6 m^3 material from the erosion of the banks. In that way, the dead storage space has already been filled (0.7×10^9 m^3), as well as a part of the available live storage capacity (1.1×10^9 m^3). This effect has a negative reflection on the quality of water in the reservoir and leads to loss of space; however, it has a positive effect on the quality of water downstream of the reservoir.

34.1.2.3 Change of the water quality

The most important parameters for the quality of water which are of significance for the environment, and upon which the dam and reservoir have an influence, are the following: temperature, muddiness, contents of oxygen, contents of dissolved mass, and contents of organic matter.

Certain biologists are of the opinion that the quality of water in watercourses flowing under natural conditions is an optimum one since, during a long period of time, the water flora and fauna has adapted to the natural conditions and any change in those conditions would cause a negative effect on the environment. An objection

can be put to such an opinion, because the quality of water, as well as the quantity of water, may not completely remain constant owing to the changes of the weather from one year to another, as well as the conditions within the catchment area. As direct reasons for variation of the quality of water, we may denote the changeability of rainfall and intensity of the surface runoff, fires caused by lightning within the catchment area, as well as the proportion between the quantity of underground water within the catchments area vis-à-vis the surface runoff. The water animal species survive in spite of these changes; this is due to their ability to adapt to non-uniform living conditions. In the continuation, there will be described the above-mentioned basic effects that a reservoir has on the quality of water.

The temperature of water in a reservoir is variable depending on the depth. The water is warmest at the surface, while colder in the depths. The water discharged into the natural (river) channel downstream of the dam may be either colder or warmer, in comparison to that prior to the construction of the reservoir, depending on the position of the entrance of the outlet structure. Most frequently, this structure is located at a considerable depth and the discharged water is colder than the natural course. This may be improved with an outlet structure with entrance parts at various elevations.

A significant change has been noticed in the temperature of water in the River Vahsh, dammed by the Nurek dam. Thus, at the entrance into the reservoir in the winter period, the temperature of the water varies from 0°C to 3.5°C, while the temperature of the tailwater, owing to the thermo-regulating effect of the reservoir, does not go down below 7°C. This phenomenon has a favourable effect on the agricultural lands downstream of the dam.

With the natural regime of flow, the water (at high discharges) is turbid and muddy, while at low discharges it has a tendency to become clear. When the water has been accumulated, the bed load, i.e. sediment, settles along the bottom, where the finer particles will need a longer period for sedimentation. Usually, the water that is discharged from the reservoir has low turbidity and muddiness, but there are exceptions. During high floodwaters, the reservoir will be completely filled with very murky and turbid water, while the deeper parts will remain turbid and muddy for a longer period. In that way, the discharge of such turbid water may also be extended in the droughty season, when the natural courses are clear. There are cases when the reservoir is small in relation to the inflow of water so that the accumulated water is almost permanently turbid and murky, especially in the deepest part, near the dam. Regarding turbidity and murkiness, another phenomenon has been noticed in cases of reservoirs. The water slowly inflows into the reservoir, but non-uniformly so that, near the bottom, it is denser, owing to the lower temperature and greater quantity of suspended sediment. This kind of water can flow through the reservoir and through the outlet, while the higher, warmer, and less turbid water has a tendency to be still. When such an occasion comes about, the water that is discharged downstream is even more turbid. An outlet with different elevations of water intake may help in regulating the turbidity of the discharged water, just as has been the case with temperature.

The oxygen, dissolved in the accumulated water, could be used in the process of explication or breaking down of the organic matter in the water. The exhaustion of the oxygen is probably, in the deepest parts of the reservoir, where there is the smallest possibility for the reaeration of the water. The quantity of used oxygen depends on the

quantity of organic matter inserted into the reservoir and that will be greater in cases of catchment areas with vigorous vegetation.

Dissolving of the mineral matter in the natural water takes place with the softening by soaking of the soil and the rock with the flowing water. The dissolution is the greatest when the discharge is minimal and the entire inflow comes from underground springs, while it is the least when there are high inflows with the greatest quantity of water inflowing from the surface due to rainfall and thawing of snow. The reservoir enables mixing of one water with another, so that the water discharged downstream varies less, in relation to the quantity of dissolved mineral matter. In cases of shallow reservoirs, with a large surface of the water surface, the concentration of dissolved minerals increases owing to the considerable evaporation. This effect is greater when the water has been kept in the reservoir for a longer period.

One of the effects of the contents of organic matter has been mentioned in examination of connection with the oxygen content. The decomposition of the organic matter enriches the water with nutritious particles, in which there is no essential difference whether the process takes place in the reservoir or in a watercourse under natural conditions. Such decomposition causes gases, which have a higher concentration in the accumulated water under pressure and which enter the outlet conveyance structures or conduits, to cause local pollution. At locations with an extreme concentration and decomposition of organic matter in the reservoir, by aerating the water at the outlet, the gases will be eliminated and the oxygen will be renewed faster than it would be in the natural way, under conditions a longer distance from the downstream course.

At the end of presentation of the part on the quality of water, it can be said that all possible negative effects on the environment, caused by the change of the quality of water with the construction of the reservoir, may be avoided or eased and moderated by undertaking appropriate preventive measures.

34.1.3 Damming the migration paths of fish and wild animals

34.1.3.1 Blocking the migratory fish paths

Some rivers are important fish paths for migration of fish from the sea to their spawning places in the mountainous parts of watercourses, and vice versa. Many dam sites are located on such watercourses and they interrupt the migratory path of the fish. In this, the least obstacles are presented by low overflow dams (weirs, etc.) and ship navigation locks. High dams and large reservoirs are a barrier difficult to overcome, and this has already been considered earlier in this book.

34.1.3.2 Blocking the migratory paths of animals

Tall game, as well as other wild animals, move, i.e. migrate, in their search for food from highland areas, in which they stay and live during summer periods, toward lowland areas, where they spend winters. These migration paths could be cut off by a dam and a reservoir. And, while the animals could swim across small lakes, large reservoirs present a serious obstacle. The negative effect is greatest when the animals, attempting to migrate, are caught on a peninsula between two major anabranches of a reservoir.

34.1.4 Change in the surrounding landscape and the microclimate

34.1.4.1 Unsightly excavations and stockpiles

From the aspect of the aesthetics of a hydraulic scheme, it will be ideal if all materials necessary for the construction of the dam are obtained from the surface of the reservoir. However, this is most frequently not the case, and that is why borrow pits are opened in the immediate vicinity and remain visible after the filling of the reservoir. These areas, along with stockpiles of material that has been excavated from the foundations of the dam and its appurtenant structures, if not treated in an appropriate way, will permanently deface the appearance of the environment. The treatment consists of levelling and planting with appropriate cover vegetation. For better results, it could to be necessary for the ground to be covered with a layer of fertile soil, which will help the growth of vegetation. Borrow pits should be levelled and arranged so as to drain their water. With the plan for developing the environment of the hydraulic scheme, it is necessary to anticipate landscaping certain areas, filled with excavated material, to be rearranged into parking lots for vehicles and equipment.

34.1.4.2 Unsightly banks of the reservoir below the maximum level

Since the reservoirs are utilized at different water levels, a part of the banks will be visible whenever the reservoir is not full. Reservoirs for the flood control, as well as the upper part of multipurpose reservoirs, are filled up to the maximum level only occasionally and, for long time intervals (for instance, once in several years) and for a short duration, so that on the exposed ground there could flourish and prosper vegetation of low plants during the period between two submerging. Other reservoirs often fluctuate and the exposed surfaces are usually stripped, without vegetation, which gives a bad aesthetic impression. An exception may be beaches and strands, as well as reservoirs in barren and arid areas, where the appearance at the boundary between the water and the ground makes the view more interesting.

34.1.4.3 Abandoned temporary works that have served in the course of construction

The settlement that has been used in the course of construction, storage, and working areas, if they have been abandoned and left in semi-demolished condition after the completion of the hydraulic scheme, may seriously deface and distort the environment[1]. That is why it is quite logical that a certain percentage of the cost of the hydraulic scheme be spent on removing these works, as well as clearing up the environment. In some cases, in favourable conditions, the existing settlement may be rearranged for utilization in the course of the service of the works.

---

[1]This is not the case with the remains of abandoned mining settlements to which a historical significance has been attributed, but such does not apply to the settlement that has been used during the construction of a dam. The historical witness to the construction of the dam is the dam itself.

34.1.4.4 Distortion and defacing of the environment with access roads that serve the construction of the works

Temporary works that are used in the course of construction of the hydraulic scheme are often built without taking into account the aesthetic view of the environment. The situation is especially worsened and aggravated if, at the end of the construction period, they are abandoned and left in a semi-demolished condition. Such roads will further on be subjected to increased erosion due to inappropriate drainage and will lead to progressive damage of the surrounding ground. This negative effect of temporary roads is unavoidable in only a very small number of cases. One of the important preventive measures is the construction of an appropriate drainage system, with permanent or semi-permanent construction, regardless of the fact that the roads will be utilized only temporarily.

34.1.4.5 Cleaning of the reservoir

If the dam site of the future reservoir contains structures that have been built by man – houses and other buildings – they are usually dismantled and the material is taken out of the reservoir storage space to be sold. Cutting down and replacement of trees and coarse types of bushes and shrubs takes up a main part of the essential cleaning of the reservoir. Some of the trees may be used for commercial purposes as timber material and, for that purpose, they are cut and transported. The trees that cannot be utilized for such a purpose, as well as bushes, should be cut and removed in the best possible way, usually by means of burning. In this, the smoke leads to temporary pollution of the air, which is usually a small negative effect in comparison with that caused by forest fires.

34.1.4.6 Changes in the microclimate

Large reservoirs, with their accumulated water mass, have their own influence on the change in the microclimate, changing the humidity and temperature of the air. These changes, as a rule, are confined within a limited space around and above the zone of the reservoir but it may be harmfully reflected on the existing natural regime of the living world, as well as on any ancient monuments, especially churches and monasteries that are rich in old frescoes. The change of the microclimate may also be positive, which is characteristic of large reservoirs located in arid regions and in areas with harsh or fierce climatic conditions. Such is the case with the Nurek reservoir. The created aquatory, i.e. water area, with an area of 100 km^2, a volume of 10.5 km^3, and a mean depth of 160 m, could not but have an influence on the microclimate. That influence has affected certain low-lying areas around the reservoir while, in the case of the steep banks, it has been reflected up to a height of some 50 metres above the water level. The temperature of the air in the summer period has decreased by 1–1.5°C, with a simultaneous increase in the humidity by 15–20%. The accumulated heat is radiated from the middle of October, and in the winter period the temperature of the air drops to below 0°C (Beylinson, 1990).

34.2 SOCIAL AND ECOLOGICAL MONITORING

Various movements struggling for the preservation of the natural environment throughout the world have greatly expanded during the last decade, and this has assumed threatening proportions in relation to the prospects and the outlook for the construction of dams, thus slowing down the construction of many significant works. In that, we can differentiate two characteristic cases: when a project intrudes into and encroaches upon the interests and feelings of the population of a broader region, which may encompass two or more countries, and when the residents of a particular locality are affected.

The first case appears very often in practice since, in many cases, large hydraulic schemes are constructed on borderline rivers; thus, they touch and affect the interests of at least two countries. Such works and structures are especially sensitive in terms of their influence on the environment, also having an emphasis on the social and political aspects. In that respect, the Gabchikovo-Nadzhimaros complex hydrosystem on the River Danube is highly characteristic; it is a joint project between Hungary and the former Czechoslovakia. Following many organized protests and demonstrations, especially by Hungarian immigrants in the USA who claimed that the hydrosystem will considerably derange the natural ecoequilibrium in the broad zone alongside the Danube, Hungary unilaterally suspended the commenced construction in 1989 (Borsos, 1991).

In relation to the second case, of considerable importance are the opinion and the mood and temper of the local population in the region encompassed by the project, which takes an active part in solving the social and ecological problems, together with the hydraulic engineers and other specialists. Here, it is indispensable to have mutual confidence and to compromise in solving disputable questions. One of the efficient ways for effectuating the above-mentioned cooperation is to conduct *socio-ecological monitoring*, which implies *a specific scheme of activities, including systematic observation of the structure from a technical aspect, from the aspect of the influence on the environment, and from a social aspect, analysis of the results of the observations, elaboration of the management solutions, all in order to ensure an optimum condition of the structure and prevention of adverse* (*extreme*) *situations*. Namely, earlier on designers in practice analyzed only the structures while, later on, the structures together with their mutual effect with the natural environment were analyzed, gradually widening the circle of relevant tangential questions. In modern practice, it is also necessary to include consideration and examination of the social sphere, that is to say, the interest of the local population and the authorities, by taking into consideration their economic, ethnic, and cultural traditions.

The structure will be optimal if it contributes to providing the most favourable technical, social, and ecological conditions, which implies: safe, economical, and profitable working, the prosperity and health of the population, and absence of degradation of vegetation and the animal world, as well as the surrounding landscape and scenery.

The difference in principle that separates monitoring from the usual observations is its inclusion into the management system. Namely, following the assessment of the technical, natural, and social condition of the structure by comparing the actual and specified values of the indicative indices, management decisions are undertaken, i.e. we undertake management and control decisions. In other words, we carry out correction

of the existing activity and, if it is necessary, we implement a correction of the specified indicators. The social and ecological monitoring may be done independently, but may also be a constituent element of the system for general monitoring and surveillance, as in the example of the Katunskaya hydroelectric power plant in Russia (Kayakin & Mulina, 1993). An expert system may also join this social and ecological monitoring system, and it will be utilized in decision-making in the system of management.

34.3 ENVIRONMENTAL PROTECTION – SELECTION OF A SOLUTION WITH MINIMUM NEGATIVE EFFECTS ON THE ENVIRONMENT

In designing the hydraulic scheme, one should endeavour to come to an optimum solution, taking into account that it is necessary to satisfy the technical and economic requirements. At the same time, one should take into account that the design should be prepared so that all negative effects on the environment are reduced to a minimum. The solution of the task of assessing and forecasting the influence of the hydraulic scheme on the environment is characterized by indeterminacy, owing to the lack of quantitative information, and also by its multi-criterion nature because of the necessity of taking into consideration contradictory factors. Throughout the world there have been elaborated special methods and procedures for solving the assigned task, based on the assessment of experts – specialists in various fields: water engineering, hydrology, amelioration, biology, sociology, etc. (Hrisanov et al., 1990). Owing to the specificity of the conditions prevailing at each dam site, it is not possible to give a general approach for solving the problem. In the continuation, we shall describe a simpler method for the selection of alternative solutions, which, in any specific case, would require certain modifications.

In the first step, it is necessary to discover and investigate the different important qualities of the environment near the watercourse or the system of watercourses within the framework of the hydraulic scheme being analyzed and to arrange them according to their importance.

In the second step, one should assess the conditions in the environment that would prevail in the future, without the realizing of the project. These could be the same conditions as at the moment of examination – improved or else worsened. The future conditions could be improved, for instance, if there is a plan for reducing existing pollution of the watercourse, while they could worsen in various ways.

In the following step, we should make a decision that will optimally satisfy the technical and economic requirements, without taking into consideration negative effects on the environment, which will only be enumerated and described.

Then, we should work out an alternative solution in which the stress would be put on minimizing the all-important negative effects. If this alternative, which causes minimum harm to the environment, indicates a significant reduction of the planned aims or a noticeable increase in relation to the optimum economic and technical solution, then we must examine a third solution, which would represent a compromise between the two extreme alternatives. There, we should endeavour to avoid or minimize the most important negative effects on the environment, with the simultaneous achievement of all or most of the potential requirements of the optimum economic-technical

alternative. Since the last alternative makes concessions and a compromise towards the environment, it will be more expensive than the economically optimum one.

As a result of the assessment of the alternative solutions, we should then make a summary survey that will indicate the relevant values of the influence on the environment, fulfilment of the basic requirements of the design, and cost and funds that have to be spent on maintenance of the environment, in the event that the planned design is not implemented. The conclusion will give a basis for achieving an agreement and for making a decision on the final selection of a solution.

In the continuation, we shall present an example that illustrates the idea of examination and analysis of three alternative solutions (Golzé, 1977). Figure 34.1 presents a simplified river system at the same time leaving out its small tributaries. The river possesses different environmental qualities, two of which are of primary importance:

- A noticeable part of the river has aesthetic and/or recreational values;
- The main course of the river is a migratory fish path, while one of the upper sections is a space for spawning of fish (Fig. 34.1a).

The future conditions of the environment might be a little worse or a little better than the presented ones, depending on the activities that will be undertaken alongside the river and within the catchment area. Sketch (b) presents one of the possible alternate solutions. There is inserted in it a large reservoir on the main watercourse, which enables utilization of a greater part of the discharge through the river and will also enable a high degree of protection against flooding of the downstream areas. It is certain that this alternative is optimal from an economic point of view; however, at the same time it causes significant negative effects on the environment. The high dam blocks the fish migration paths, seriously reducing one important economic branch on the examined watercourse. The aesthetic and recreational part is of reduced length. Indeed, the reservoir might contribute certain possibilities for recreation and the raising of certain kinds of fish, but those effects are weak when compared to the losses. Sketch (c) indicates a project according to which the negative effects on the environment are minimized. A distant reservoir has been anticipated, located at a place where its utilization would cause only negligible negative effects on the environment. The low dam on the main watercourse, by means of which diversion of the water has been made possible, is provided with a fish pathway, so that migration of the fish has not been seriously obstructed. The main disadvantage of this kind of solution is that a smaller amount of water will be used in comparison to the previous case, owing to the limited capacity of the structures for diversion and supply of water. In addition to this, there are no possibilities for the protection against flooding of the part downstream of the low dam. Also, the unit cost of the water, obtained with such a solution, is very high.

Sketch (d) indicates how we may economically improve the previous solution and, at the same time retain, or even improve, most of the values relating to the protection of the environment. One or more reservoirs have been added to the above two upper watercourses, with the function of enabling a partial regulation of the flow, i.e. discharge, in the stretch leading to the low diversion dam, which enables the transfer of greater quantities of water into the remote reservoir. The water will accumulate in the upper reservoirs and it will be retained at a time when the available discharge exceeds the capacity of the structures for diversion and supply of the water into the distant

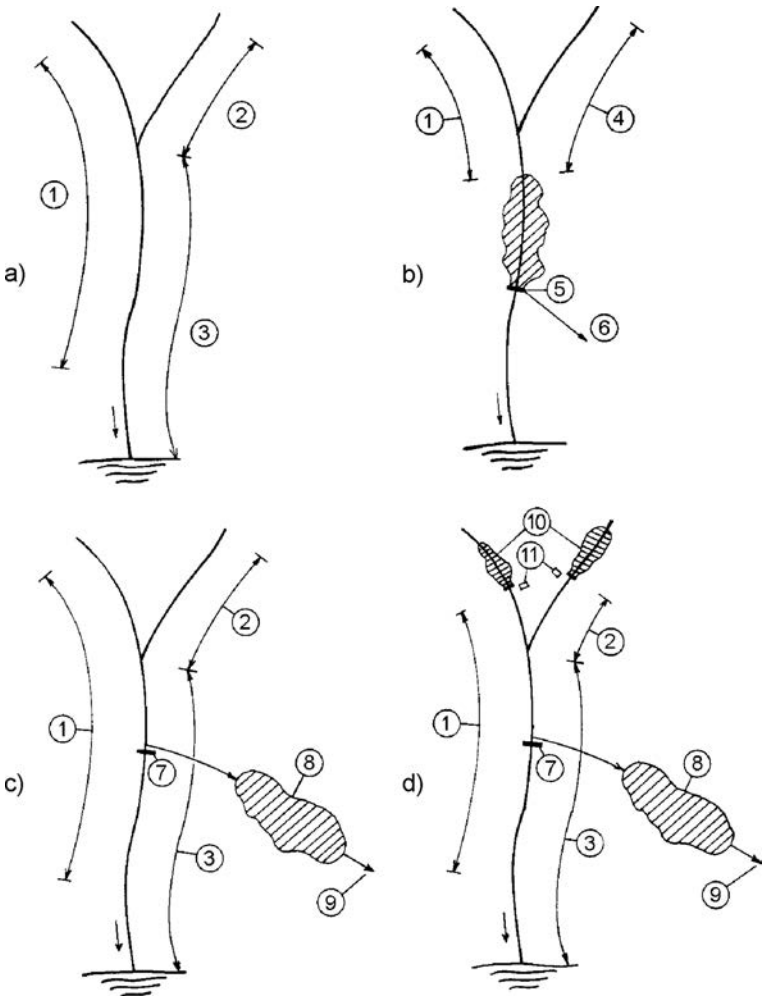

Figure 34.1 Alternative solutions of a river system (after Golzé, 1977). (1) Part with aesthetic and/or recreational values; (2) spawning-place for fish; (3) migration path for the fish; (4) space for the fish that do not migrate; (5) obstacle on the fish migration path; (6) direction of users of the accumulated water; (7) low dam with a fish path; (8) distant reservoir; (9) direction of users; (10) upper reservoirs; (11) spawning-places (newly constructed).

reservoir, while it will be discharged, i.e. evacuated, in the course of a drought season. This will increase the quantity of water in the river upstream of the low dam, which represents an improvement of the conditions of the environment in that sector. In order to moderate and ease the loss caused by the upper reservoirs, we should construct new spawning-places for the fish. In that way, the solution (d) represents a compromise by means of which the derangement of the environment has been reduced to a minimum, while the gain from the project has not been seriously reduced (Golzé, 1977).

Chapter 35

Restoration and reconstruction of hydraulic schemes

35.1 NEED FOR RESTORATION AND RECONSTRUCTION

After the construction and commissioning into service of a dam, in most cases, one can say that the hydraulic scheme has been completed. What remains is for the user intensively and carefully to follow its work and to maintain it in a proper and correct condition in the course of its service life. With a certain number of hydraulic schemes, sooner or later after completion, there comes a need for performing restoration and reconstruction of the dam, and/or of its individual appurtenant structures and elements. The need for restoration appears owing to three reasons:

- Incorrect or inadequate technical solutions in the design that have led to irregular and improper work of the dam and/or the appurtenant structures;
- Damage to the dam and/or appurtenant structures due to influences that could not be anticipated, that is to say, there had been a very low probability of their occurrence;
- Ageing of the structures and artificial materials of which they have been made, originating as a result of external influences and long-lasting service conditions.

The need for reconstruction of the hydraulic schemes may be due to two reasons:

- *Change in design criteria*. Namely, in the course of time, some of the design criteria become more rigorous, while there develop more accurate and rigorous methods of analysis, which, when applied to hydraulic schemes in service, might reveal some of their weaknesses and deficiencies. The most important role here is played by the criteria and methods for the static and dynamic analysis of dams, for determination of the flood waters, i.e. the capacity of the spillway structures, and the criteria for and comprehension of the biologic minimum in the river, as well as for the protection of the environment.
- *Increased needs of the users of the hydraulic scheme*. This reason is very frequent and it is considered and examined in a number of hydraulic schemes, because there is a permanent increase in the needs of water for the population and for the economy. At the same time, by means of reconstruction we might realize only an increase in the installed capacity of the plant or the structure, that is to say, of the capacity for intake of water, although it is also possible to carry out an increase in the pressure-head of the hydraulic scheme and the volume of the available storage capacity of the reservoir, which is, however, a very complex task. One should

take into consideration that reconstruction of the hydraulic scheme may be much simpler and more painless if it is planned well in advance, that is to say, if it has been anticipated even in the original deign for the hydraulic scheme. Such reconstruction is applied with increasing frequency in modern practice and, in fact, it is a staged execution of the hydraulic scheme. Its advantage is that, as a rule, the high investments that are necessary for the realization of the hydraulic scheme are distributed over a longer period of time, correlated with the increase of the demands for water. However, even in that case, during the reconstruction, i.e. during the staged execution, one should overcome and surmount various difficulties, especially if during its realization there must not be interrupted the utilization of the hydraulic scheme.

35.2 RESTORATION OF DAMS AND HYDRAULIC SCHEMES

One of the most frequent reasons for restoration of dams is the inappropriate construction of the dam, which is most often manifested in its static and dynamic instability and/or in its high water-permeability. The effects of these two manifestations – insufficient stability and high water-permeability – are often interwoven and mutually enhanced. Numerous examples of damage and restoration of dams that have originated as a consequence of an improper structure and yielding of the foundation are given by Thomas (1976). In the continuation we shall deal with some more recent examples in which there have been described interesting original solutions, associated with the application of modern methods and materials.

The analyses of damage in the case of concrete dams indicates that, in the initial years of their service, there occur 45% of the troubles, i.e. accidents or difficulties, while only 5% after 30 years. For example, in Spain, well-known for the construction of numerous concrete dams, the greatest number of problems (35–40%) originate from the design and construction (Agulló et al., 1995).

In the case of concrete dams, a frequent reason for restoration is damage to the concrete, originating as a consequence of its inadequate composition, chemical action of the water, and ageing of the concrete. As a result of the damage, there occurs increased seepage through the dam's body, which, usually is of a progressive nature and can, in extreme cases, endanger the stability of the structure. In such cases, modern materials are used in the restoration with increasing frequency – geomembrane in combination with geotextile.

In the case of the Publino Dam (Italy), 40 m high and a double curvature arch dam, 250 m long at the crest, built in 1951 for generation of hydroelectric power, in 1988 there was noticed significant damage to the concrete across the surface of the upstream side. For the prevention of further damage and the occurrence of a considerable loss of water, a decision was made to undertake preventive restoration measures. The restoration has been accomplished with the placement of an impermeable facing of geocomposite, consisting of a 2.5 mm thick flexible PVC-geomembrane, factory-welded upon polyester geotextile. The strips have been produced with sufficient length for covering the entire height of the dam, without horizontal joints. The vertical joints and mechanical anchors have been covered with an additional strip of

the same material. The solution has turned out to be efficient and economical (Zuccoli et al., 1989).

The highest dam in Italy (in operation) is Alpe Gera ($H = 174$ m, $L = 528$ m), a gravity dam within a hydroelectric power plant, constructed in the period from 1958 to 1964, with a total volume of concrete of 1,700,000 m^3. Specific construction technology has been used during execution of its works, which resembles the methods used on the future dams made of roller-compacted concrete. Namely, they have used a leaner mix than the ordinary one[1], while the placement of the concrete has been performed in layers of 70 cm, from one bank to another, at a time interval of several hours. Joints have been cut while the concrete had not yet hardened. Taking into consideration the composition of the concrete, as well as the great number of horizontal joints, the designers have anticipated steel facing at the upstream side, thus separating the static function of the concrete from its function of water-impermeability.

The facing consisted of steel plates of dimensions 2025 – 2030 × 1380 mm, 3 mm thick, welded at the shorter side to steel sections, embedded into the concrete. At the constructional joints in the concrete (at 12.17 m intervals) and in the middle of each block (at 6.085 m) Ω-joints have been embedded, in order to enable dilatation of the steel. The plates overlapped on the longer side, where the welding has taken place. The facing has been protected against corrosion, by means of cathodic protection, galvanization, and with a vinyl-acrylic coating, from the crest to the elevation of the minimum level. Immediately behind the steel facing drainage pipes have been installed for evacuation of infiltrated water, which have worked in combination with a series of boreholes into the rock, drilled from a gallery along the foundation.

In the course of utilization, the lower part of the facing, which had not been protected with coating, has been heavily damaged by corrosion, with occurrences of holes with a diameter of 3 mm. The coated part has behaved better, even though here, as well, local swellings have been noticed. Comprehensive investigations regarding the measures necessary for restoration have been performed and in 1987 a trial protection of PVC-composites was installed at several places . After five years of observations, the behaviour of the trial protection was assessed to be satisfactory, so that in 1993 they began with the installation of a facing made of geomembrane at the most damaged sections. The restoration has been limited to the part of the facing between elevations of 2040.23 and 1990.56 mwl (Fig. 35.1).

This kind of restoration method had previously been employed on a number of other dams and it has been based on achieving water-impermeability, by means of PVC-membranes with very low permeability and drainage of possibly penetrated water – with geotextile attached to the membrane. The geomembrane has been anchored to the steel facing by means of welded vertical steel sections, spaced at distances of 6085 mm, accurately along the line of the Ω-sections of the steel facing, in order to enable the geomembrane, with its constituent components, to follow freely the displacements in the dam's body. All perimeter anchors have been well sealed, in order to ensure water-impermeability of the entire zone. The new facing has consisted of specially modified geocomposite strips with a width of 6.25 m (standard width of geocomposites and

[1]This has been done because it has been known that in cases of Italian dams, the strength of concrete has been with a low level of utilization, which, as a matter of fact, is a general phenomenon with gravity dams made of conventional concrete.

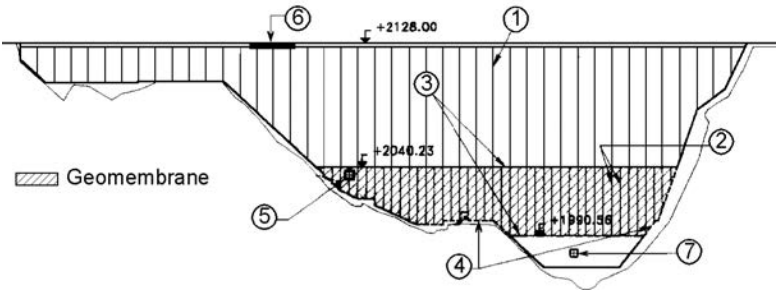

Figure 35.1 Upstream side of the Alpe Gera Dam with the renovated section (Fanelli et al., 1995). (1) Vertical constructional joints; (2) vertical profiles (sections); (3) perimeter sealing of the existing steel; (4) perimeter sealing of the existing concrete foundation; (5) supply tunnel; (6) overflow; (7) outlet.

membranes that are used in Italy is 2.05 m, while until then, the largest employed width had been 3.70 m) and they consist of a 2 mm thick PVC-geomembrane, jointed with polyester geotextile of 400 g/m^2. The strips descend from the crest, unwind, and are fastened by means of vertical steel sections. The installation occurred during the summers of 1993 and 1994. Prior to the installation of the geomembrane, the infiltrated water through the steel facing had varied from 40 to 50 l/s, with a tendency to a progressive increase. Following the restoration, the total infiltrated water is less than 10 l/s, and almost all of it originates from the steel facing, from the elevation above 2040.23 mwl. In the zone covered with the geomembrane, the loss of water is practically zero (Fanelli et al., 1995).

During the last 15 years PVC-geomembranes have been widely used for restoration or improvement of the watertightness of all types of concrete dams, as well as of CFRDs (Vaschetti & Scuero, 2009).

An interesting case of restoration, by means of which the static stability of the dam has been improved and, at the same time, the water-permeability reduced to a permissible level, has been performed on the Kölnbrein Dam (Austria), 200 m high, a very thin arch dam. The rock in the foundation consists of gneiss, and an important characteristic of the dam site is the 150 m wide flat bottom, which contributes to the increase of the length of the dam to 626 m. An enormous total force of water acts on the dam (54 GN). The storage lake impounds a volume of 200×10^6 m^3, while the hydraulic scheme was built during the period 1971–1977. During the first reservoir filling in 1977, there occurred cracks at the upstream toe of the dam, at an elevation of the water of 42 m below the normal elevation, in the central part of the dam (Fig. 35.2). Through the cracks there penetrated 200 l/s of water into the lowest inspection gallery. At the same time, the uplift-pressure in the foundation reached the water level into the reservoir. Owing to that, it was believed that the grout curtain had been damaged. Soon afterwards, there were taken a number of consecutive measures, in order to reduce the uplift, as well as the infiltration of water, which measures include:

- 1979: strengthening of the grout curtain by means of grouting with cement grout. Decrease of the uplift by means of drilled drains;

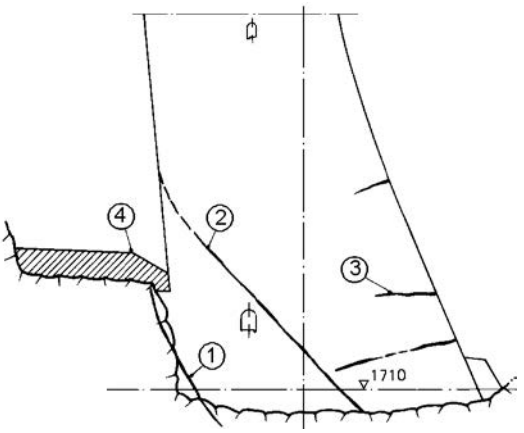

Figure 35.2 Lower part of the Kölnbrein Dam with cracks (Lombardi, 1991). (1) First group of cracks; (2) second group of cracks; (3) downstream cracks; (4) concrete blanket.

- 1980–1981: grouting with polyurethane rubber. Freezing of the central part of the dam during filling of the reservoir;
- 1981–1983: execution of a concrete blanket, covered with PVC sheets at the bottom of the dam site, immediately next to the dam;
- 1984–1985: PVC sheets had to be renewed and to be extended to the upstream face of the dam. The grout curtain was grouted again, parallel to the occurrence of new cracks, which led to a temporary increase of the infiltrated water, which reached up to as much as 1000 l/s. The level of the water was limited, for safety reasons, to 1880–1885 mwl (normal level is 1902).

In spite of the fact that, by means of the listed measures, the hydraulic scheme has been maintained in operational condition, it was evident that it was necessary to perform a thorough restoration, i.e. rehabilitation and strengthening, of the dam as soon as possible.

The reasons for the cracks in this dam are very complex and it is difficult to explain them in a simple fashion. It is a question of a force of circumstances in which a number of factors play a role, such as the height and construction of the dam, width of the foundation, and great total loading due to water, etc.

The purpose of the more radical measures was to increase the stability of the dam in the zone of the cracks and to ensure utilization of the reservoir in the future without restrictions. The extensive analyses led to a conclusion that it was necessary to construct a mass arch-gravity structure downstream of the dam, which would take one part of the load due to water (12 GN) and would reduce the shear forces in the cantilevers of the dam. At the same time, the connection of the new structure with the dam must not be very rigid. A solution for such contradictory requirements (stability in relation to rigidity) was found in the execution of a joint with a variable opening between the massive block and the dam. During filling of the reservoir, the joint would close progressively from the bottom upward. In order to ensure regulation of the

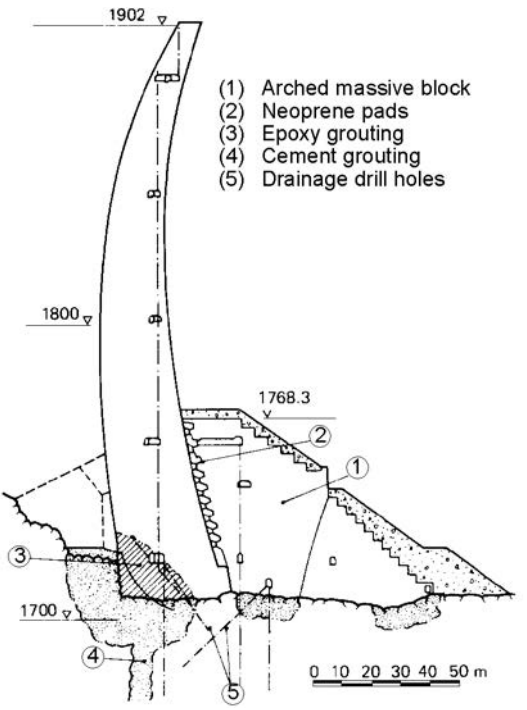

Figure 35.3 Section through the Kölnbrein Dam and the arched massive block (Lombardi, 1991).

opening when the dam is not loaded, there have been employed over 600 neoprene boards, specially produced for this purpose, by means of which they have filled the open joint. The design has precisely specified the points for closing of each of those 600 shims (pads), depending on the level of water. In that way, there has been established a contact with the dam aiming at commencement of transfer of the load onto the massive block. Thus, the neoprene shims have become a major element of the solution for strengthening of the dam (Fig. 35.3). Another important measure that has been undertaken has been the filling of the cracks by means of grouting, which measure ensures the monolithism of the structure, without transfer and concentration of forces, as well as water-impermeability of the foundation and of the lower part of the dam. Not less significant has been the sequence of grouting, performed in seven stages, denoted from M to R, (Fig. 35.4; Table 35.1). The drainage system was executed in the last stage (T). The works on the restoration and rehabilitation were built during the period 1989–1994 (Lombardi, 1991).

In most developed countries, during the last two decades, the criteria for the stability of concrete gravity dams have been tightened up, so that a lot of such older dams do not satisfy those criteria and have a low stability. This is due to the former limited knowledge of the properties of the materials, the behaviour of the dam, and theaction of loads. In addition to the execution of elements by means of which the dam

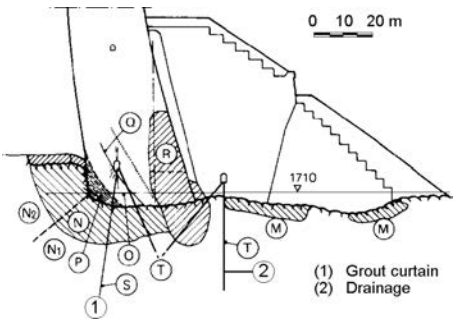

Figure 35.4 Seven stages of grouting (M to R) and additional drainage (T) (Lombardi, 1991).

Table 35.1 Seven stages of grouting (M-R) and additional drainage (T).

Zone	*Definition*	*Grout mix*	*Reservoir level*	*Purpose*
M	rock under massive block	cement	has not been conditioned	consolidation
N	rock upstream	cement	average	consolidation
O	concrete upstream	epoxide resin	has not been conditioned	possible anchoring
P	concrete, cracks group I	epoxide resin	average	strengthening, impervious
Q	concrete, cracks group II	epoxide resin	average	strengthening, impervious
S	grout curtain	epoxide resin	average	impervious, strengthening
R	concrete/rock downstream	epoxide resin	has not been conditioned	1990
T	drainage downstream		after grouting	reduction of uplift

is additionally loaded from the downstream side, in practice they also use the method of *vertical prestressing*, which does not increase the overall dimensions of the dam.

The prestressing method gives an additional vertical load with a resultant line of action close to the upstream side. For that purpose, it is necessary to install highly prestressed steel cable, anchored at the crest, and at a certain depth of the foundation, Figure 35.5. For that reason an indispensable condition for prestressing is the existence of hard and firm rock, capable of taking on the high loading from the anchor.

Strengthening by means of prestressing is achieved by making holes through the dam and the foundation, provided at certain distances. Cables are inserted into these holes and are anchored in the foundation by means of grouting, as is shown in Figure 35.5. The cables are conducted through installation at the crest, where they are prestressed to the required stress level, prior to their final anchoring, i.e. fixing. The prestressing force is thus distributed from the top anchor. The whole operation should be carefully performed in order to avoid excessive local stress in the concrete around the anchor.

Prestressing also provides the possibility of efficient and economical heightening of gravity dams (Fig. 35.6). This method is more efficient than expanding and widening

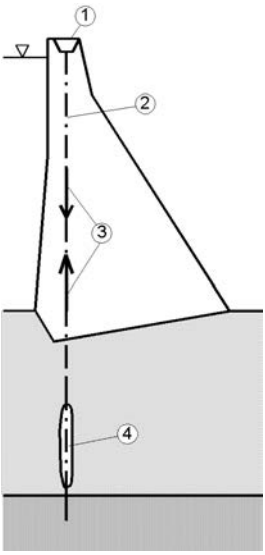

Figure 35.5 Strengthening of the dam by means of vertical prestressing. (1) Anchoring at the crest; (2) prestressed cable in the hole; (3) prestressing force; (4) grouted anchorage in firm rock.

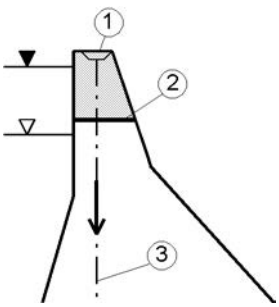

Figure 35.6 Prestressing at dam heightening. (1) Anchoring into the new concrete crest; (2) joint between the old and the new concrete; (3) prestressed cable.

of the dam's body downstream, since by this means, among other things, it is possible to avoid the problems associated with the joint between the old and new concrete.

In recent practice, prestressing has been used for the strengthening of the Elder Dam, Germany (Fig. 35.7). For that purpose, in the dam's body there have been incorporated specially designed prestressing anchors, with a capacity of 4500 kN, at mutual spacings of 2.25 m, fixed, i.e. anchored, at 23 m below the dam by means of grouted anchoring, with a length of 10–14 m. In order to provide the required space for the fixing devices, the entire crest of the dam has had to be replaced with a new crest, also including here the upper gallery (Fig. 35.7). The whole work on the restoration and rehabilitation was completed during the period 1992–1994 (Rissler, 1994).

In the cases of embankment dams, they often carry out restorations and rehabilitations to a smaller or larger extent, but it is difficult to classify these according

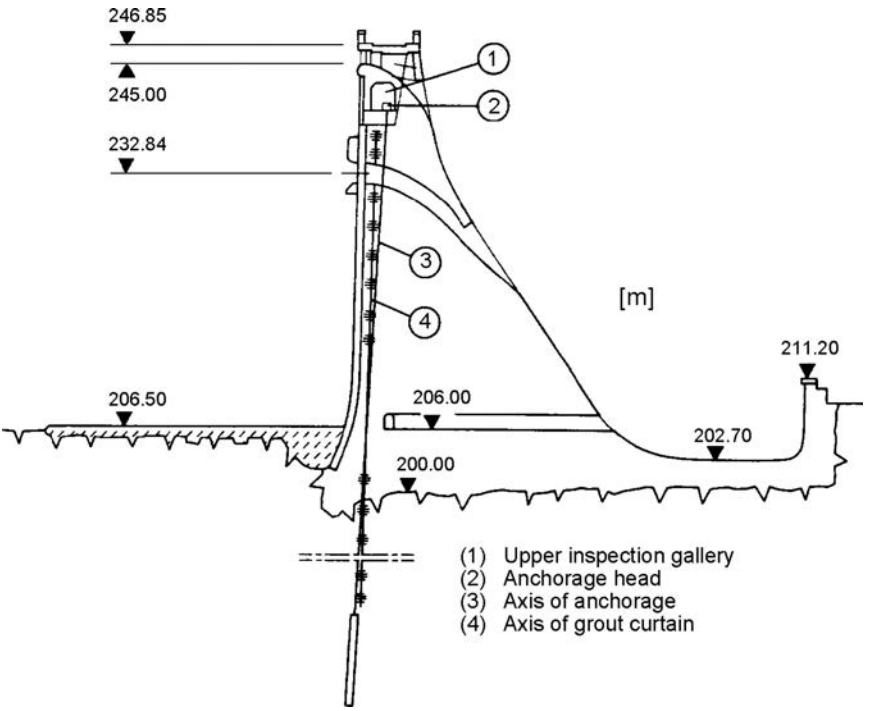

Figure 35.7 Increasing the stability of the Elder Dam by means of prestressing (after Rissler, 1994). (1) Upper inspection gallery; (2) anchorage head; (3) axis of anchorage; (4) axis of grout curtain.

to any determined rule, since they regularly bear the specific nature of the problems involved. In most cases, the purpose of the restorations and rehabilitations has been to eliminate problems associated with increased seepage through the dam's body or through the foundation. In that, the character of the problem, as well as the method of restoration or rehabilitation, strictly depends on the type of the embankment dam, that is to say, on the type of the impervious element. There are a number of cases of restoration or rehabilitation of impervious elements in the form of a facing, as well as execution of additional impermeable elements. In appropriate chapters of this book devoted to individual kinds of embankment dams, it is possible to find examples of solving of problems arising with dams in service. Restoration or rehabilitation of embankment dams aimed at improving their static or dynamic stability is very rarely found in practice, especially if that is not associated with increased seepage.

35.3 RECONSTRUCTION OF HYDRAULIC SCHEMES

The reconstruction of hydraulic schemes with a dam most frequently anticipates heightening of the dam and that is probably the most difficult and the most expensive operation in reconstructing hydraulic schemes. The heightening is achieved in order

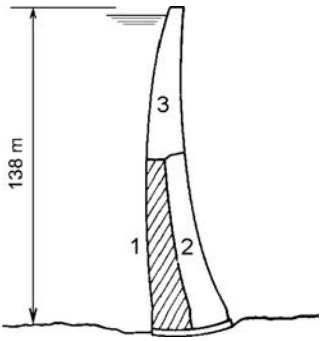

Figure 35.8 Frera Dam, three stages.

to increase the reservoir storage space and the gain from the hydraulic scheme. This kind of undertaking is not at all easy and during its realization one needs to solve a lot of problems associated with the interaction of the heightening of the dam with the appurtenant hydraulic structures and other structures, by means of which it is possible to ensure the functioning of the hydraulic scheme (spillway, outlet structures, intake structures, and powerhouse, etc). In that, the realization of the heightening, as a rule, is simpler if it has been planned during the construction of the works (that is to say, at stage I), although even in such a case, a lot of difficulties may occur. The simplest case is the heightening of arch dams, which it is possible to see in the examples of dams such as the Mladost Dam (Macedonia), and especially the Movoisen Dam (Switzerland) that have been described in Chapter 20. The point is that, if the heightening has been planned, that is to say, if the crest has sufficient width to receive a new arch upon itself, then the new construction is undertaken only upward, without a need for modification of the existing dam's body. If the heightening is significant in relation to the height of the dam in the first stage, then it is possible to apply staged construction with increasing the entire cross-section of the dam, as shown in the example in Figure 35.8. In heightening concrete gravity dams, it is necessary to widen or expand the whole dam, except if the increase is small, where we can solve the problem with overbuilding (extending) of the crest by means of local widening only at the upper part, or else we may employ prestressing, which has already been discussed (Fig. 35.6).

As an example of heightening of a gravity dam, we might cite the Porsuk Dam (Turkey), constructed in 1948, 29 m high (Fig. 35.9). After 20 years, it was heightened by 18 m, aiming at satisfying the increased demand for water supply and irrigation. Prior to application of the concrete of stage II, they formed a rough, stepped surface at the downstream side of the dam (see detail in Fig. 35.9) (Thomas, 1976).

Heightening of embankment dams is performed less frequently than is the case with concrete dams, mainly because of two reasons: (1) heightening essentially widens the cross-section of the dam, which has significant influence on the appurtenant structures and, in general, on all structures within the hydraulic scheme; and (2) the joint of the old with the new impervious element is usually not easy to perform. In cases of earthfill dams and earth–rock dams, the situation may additionally be aggravated and complicated if, during the reconstruction, the reservoir needs to be maintained in filled

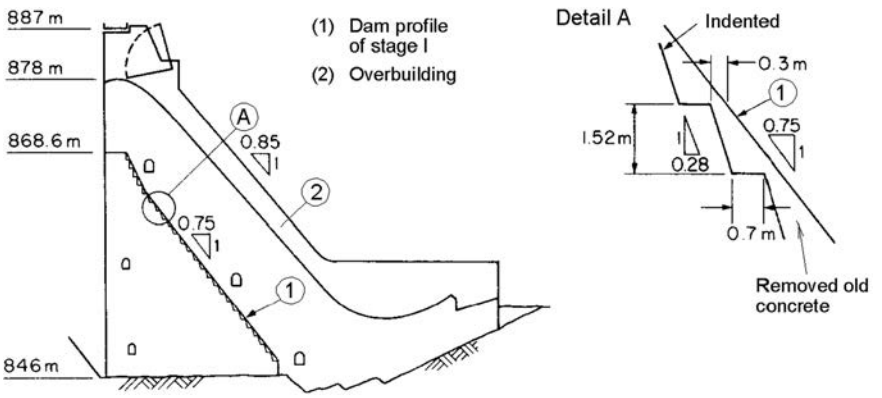

Figure 35.9 Heightening of the Porsuk Dam (Thomas, 1976).

condition, because the high moisture aggravates the conditions for execution of the joint of the existing earthfill impervious embankment, or element, with the new one.

One possibility, by means of which we might avoid the second deficiency, is to construct a dam with a completely new impervious earthen element, in which the existing dam would be completely incorporated into the new dam's body (Fig. 35.10a). An earth–rock dam, with a thick central core, can be heightened by means of widening the embankment toward the downstream side and extension of the core with a sloping part (Fig. 35.10b), while in the case of a dam with a thin sloping core, the overbuilding of the impervious element may be performed with the execution of a horizontal blanket, which will extend into a new sloping core (Fig. 35.10c). With this kind of construction we might avoid significant differentiated displacements in the joints between the old and the new impervious elements. In that, the fill below the core should be placed with proper compacting, especially in the zone (4), which should be compacted in thin layers, for instance 0.5 m (Thomas, 1976).

When heightening of an earth–rock dam is planned, we should also think about the possibility of the impervious element made of earthen material being extended by means of artificial materials. For that purpose, in practice they often use asphalt concrete and geosynthetics.

An interesting and original solution was employed in the heightening of the Breitenbach Dam (Germany), constructed in 1977–1978. In the first stage, completed in 1956, an earth–rock dam was constructed, 29 m high, with a sloping clay core. It had been anticipated for the dam to be heightened later on by 12.5 m, according to the plan shown in Figure 35.11. In this, the original conception for heightening was changed following analyses conducted in 1975, mainly because of the fact that, during execution of the works, it required a draw-down of the level of the reservoir to an elevation of 347.00 mwl, which would essentially reduce the only source of water supply for an entire area. It was concluded that under such conditions the heightening could be successfully achieved by means of an asphalt concrete diaphragm used as a waterproof element, jointed with the loam core with a horizontal asphalt concrete layer (Fig. 35.12).

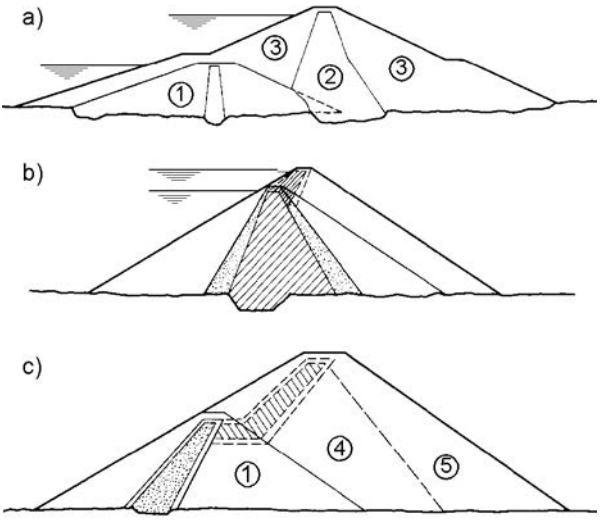

Figure 35.10 Heightening of earth–rock dams (Thomas, 1976). (1) Existing dam; (2) new core; (3) rockfill; (4) rockfill compacted in thin layers; (5) rockfill compacted in thicker layers (1–2 m).

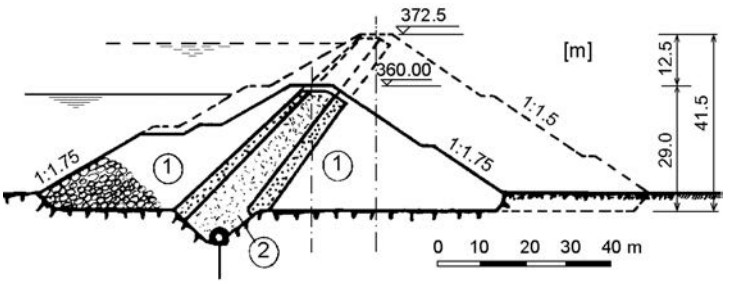

Figure 35.11 Breitenbach Dam (Germany), with the first design for heightening (after Weinhold & Haug, 1988). (1) Rockfill; (2) clay core.

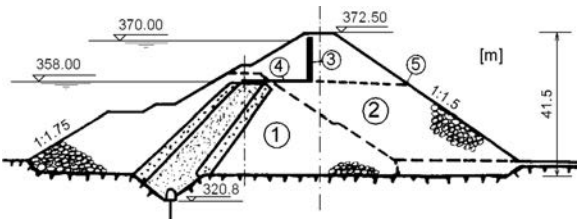

Figure 35.12 Breitenbach Dam with heightening (after Weinhold & Haug. 1988). (1) First stage, 1956; (2) second stage, 1977–1978; (3) asphalt concrete diaphragm; (4) horizontal asphalt concrete layer; (5) control pipes.

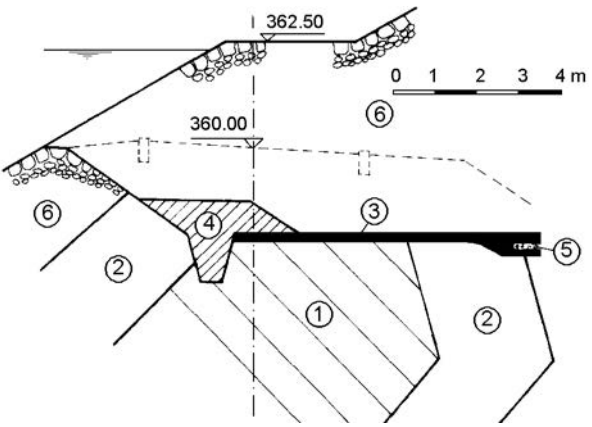

Figure 35.13 Breitenbach Dam, joint of the horizontal asphalt concrete layer with the clay core (Weinhold & Haug, 1988). (1) Core made of loam; (2) transition zone; (3) horizontal asphalt concrete layer; (4) special clay; (5) drainage layer; (6) rockfill.

Such a technical solution imposed a need for careful design and construction of the joint between the existing and the additional waterproof elements. Especially sensitive is the bond of the horizontal asphalt concrete layer with the loam core, since it must be water-proof, capable of transferring shearing stresses, and able to withstand an expected settlement of 40 cm. Following experiments performed on models scaled 1:1, there was engineered a joint which is presented in Figure 35.13. The experiments showed that it is feasible to place asphalt concrete with high temperature, over loam, which contains 10–14% moisture. The joint between the asphalt concrete and the loam has a low water-permeability – equal to that of the loam, while the angle of friction of the joint is 5° smaller than that of the loam. This example indicates that the staged construction of a dam can be rather complicated and take a significant amount of additional funds, in comparison to the construction in one stage (Weinhold & Haug, 1988).

Sometimes the reconstruction of a hydraulic scheme is done in order to increase the retentive capacity of the reservoir. Such is the case with the Pactola Dam (USA), at which a decision on heightening was taken following the heavy floods of 1972, when it was concluded that the retentive capacity of the reservoir was insufficient. The reconstruction was achieved with heightening of the dam and with widening of the spillway in order to be able to accept the maximum probable water. The dam was 67 m high, while the length at the crest was 381m. In addition, there were constructed two more embankments, 32 m and 20 m high, with a curved crest 1006 m long, which all together has ensured a reservoir of 122×10^6 m^3, intended for recreation and retention of flood waves. The spillway consisted of a 73 m wide channel, cut into the rock in the left bank of the main dam, between the dam and the auxiliary embankment. The core (Fig. 35.14) was constructed with sandy clay. Following this reconstruction, the spillway has been widened by 56 m, while the dam and the embankments have been

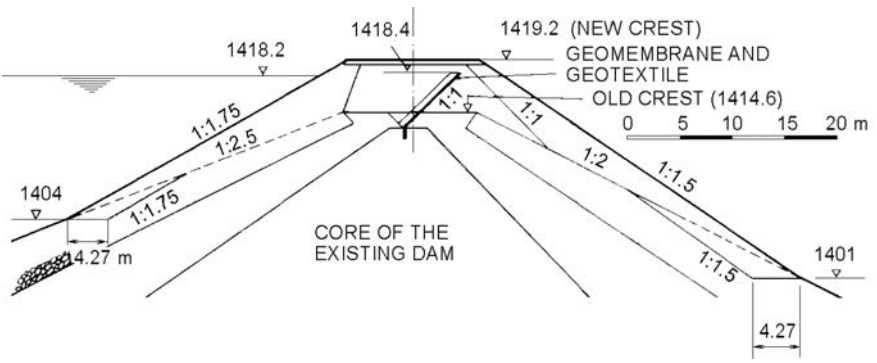

Figure 35.14 Detail of the crest of the Pactola Dam (after Lippert & Hammer, 1989).

heightened by 4.6 m, so that the new length of the crest of the dam, along with the two embankments, has increased to 1568 m. The design solution and construction have been aggravated and obstructed by the following limiting factors: (1) steep banks alongside the main dam; (2) dimensions of the road passing across the crest of the dam and embankments; (3) requirement for the road to remain open to traffic during reconstruction; and (4) balancing the quantity of material that was excavated from the spillway and the material necessary for heightening of the dam.

As the best solution, they accepted the geomembrane as a waterproof element in the heightened part. Namely, using the geomembrane avoids opening a borrow pit for clay, there is a decreased need for processed filter material (which would have to be brought from a considerable distance), there is a reduction in the construction time and, finally, there are savings of some $1.5 million.

From the laboratory-tested four types of geomembrane, they selected a geomembrane 1 mm thick, combined with geotextile. The geomembrane starts in the middle of the crest of the existing core, where it is embedded in a vertical trench, 90 cm deep. The trench, 15 cm wide, has been filled with lean concrete in order to ensure a good joint between the embankment and the geomembrane. In the zones of the joint of the geomembrane with the banks of metamorphic rock, there was cut a trench, 60 cm deep, and 23 cm wide, filled with lean concrete, in which the membrane has been anchored by means of bolts. The membrane is laid at an inclination 1:1 upon compacted fine-grained rockfill. The longer side of the geomembrane has been embedded in the direction of the axis of the embankment, so that the number of vertical joints has been reduced. The works were executed between April 1985 and November 1987, in a period somewhat longer than the anticipated one, owing to different unforeseen difficulties that had to be overcome in the course of construction (Lippert & Hammer, 1989).

Relatively simple is the heightening of the rockfill dams with a facing, which, because of that, is suitable for staged execution. In that respect, as an example we shall point to the Pindari Dam, with a reinforced concrete facing, built in the period 1966–1968 in Australia. It has been heightened from the original 40.4 m to 85 m, so that the reservoir has been enlarged from $37 \times 10^6 m^3$ to $312 \times 10^6 m^3$, and thus

they have gained additional water for irrigation of the cotton fields but they have also increased the safety against floods. The original dam was 488 m long, with inclinations of the slopes of 1:1.3. The concrete facing had been conservatively designed so as to facilitate subsequent heightening. The foundation slabs varied in width from 7 m at the maximum section, to 3 m at the banks. The thickness of the slabs of the facing varied from 760 to 488 mm, according to the formula $d = 488 + 0.066H$, where H is the vertical distance from the crest. The reinforcing ratio was 0.52% (minimum) in vertical and longitudinal direction. The slabs had been located continuously, with vertical joints spaced at 18.29 m. All expansion joints, including the perimeter, were sealed with a 250 mm wide PVC-waterstop. A grout curtain was constructed throughout the upstream foundation of the facing.

The spillway structure consisted of a rectilinear channel, driven through the rock and unlined, located in the left bank, immediately next to the dam. The spillway was 88.4 m wide and 300 m long, so that it could let through 6700 m^3/s of water. With the design for reconstruction, the floodwaters were analyzed with new methods, so that the maximum probable flood, which, in the reconstruction, has been adopted as the governing one, is much greater than the capacity of the old spillway. With the design for reconstruction there were also set in motion other questions looking for a solution. For illustration of the complexity of the whole operation, in the continuation there will be listed the major activities anticipated with the reconstruction of the Pindari hydraulic scheme:

- Heightening of the dam from 44.5 to 85 m;
- Extension of the heightened part of the dam through the existing spillway;
- Construction of a new spillway, capable of giving passage to the maximum probable water;
- Construction of an auxiliary outlet through the left bank, utilizing the diversion tunnel, in order to ensure greater capacity for evacuation of water;
- Adaptation of the access to the existing outlet to the new circumstances;
- Updating and adding up of the hydromechanical and electric equipment of the existing outlet for adaptation to the increased volume of the reservoir;
- Construction of a new road to replace the old one that had passed over the crest.

The major elements of the hydraulic scheme before and after the reconstruction are presented in Figure 35.15. The heightening of the dam was achieved with an extension of the facing with the same inclination as in the original dam and expansion of the embankment towards the downstream side. The heightening was constructed by stages, in a number of sequences, aiming at giving safe passage to the flood waters, so that the part over the old spillway was constructed in the last stage. The new cross-section of the heightened dam is presented in Figure 35.16a, while the section of the part over the old spillway (which is completely new) is presented in Figure 35.16b. A typical section of the heightening of the facing in the zone of the joint with the existing facing is presented in Figure 35.17. Static and dynamic analyses were performed for a thus constructed new dam. For a maximum probable earthquake, with a maximum acceleration of 0.39 g, they have obtained the expected settlement of the crest in the highest section, amounting to 51 cm.

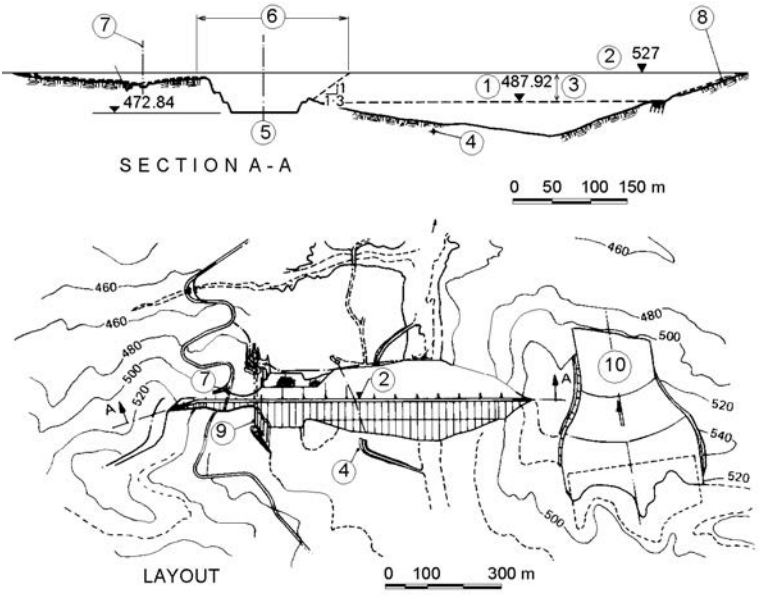

Figure 35.15 Layout of the structures of the Pindari hydraulic scheme (after Lenehan, 1992). (1) Existing crest of the dam; (2) crest of the heightened dam; (3) heightening of the dam; (4) existing outlet tunnel; (5) axis of the existing spillway; (6) extension of the dam over the existing spillway; (7) axis of the drainage channel; (8) preparation of the foundation for the new embankment; (9) new outlet; (10) new spillway.

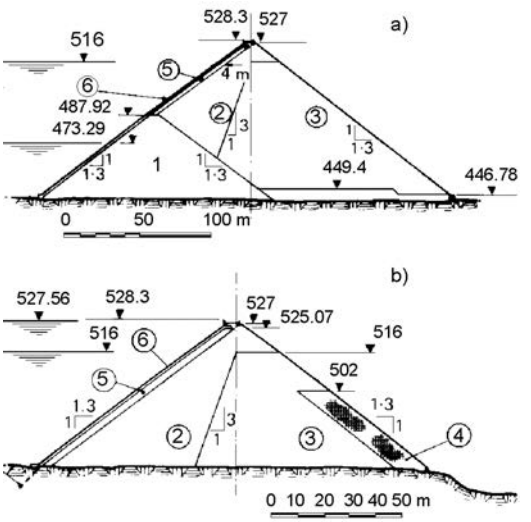

Figure 35.16 Cross-section of the heightened dam (a) and of the part above the old spillway (b) (after Lenehan, 1992). (1) The old dam; (2) well compacted rockfill; (3) compacted rockfill; (4) selected compacted rockfill, strengthened with reinforcement; (5) compacted gritting material; (6) new facing.

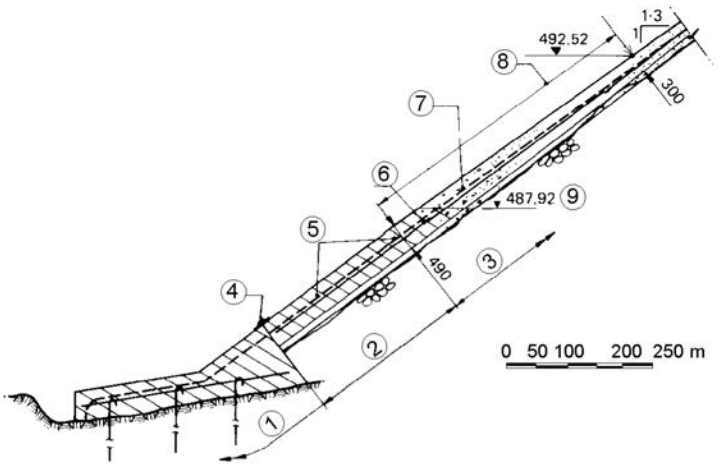

Figure 35.17 Typical section through the heightening of the facing (after Lenehan, 1992). (1) Existing foundation slabs; (2) slabs of the existing facing; (3) slabs of the new part of the facing; (4) filling of the perimeter joint; (5) existing PVC-waterstops; (6) existing reinforcement; (7) new PVC-waterstop; (8) transition zone in which there is a transition of the thickness of the facing at 30 cm, of which the thickness remains constant up to the crest; (9) existing crest.

The complete works on the reconstruction of the hydraulic scheme, including relocation of the public road that passed over the old dam, investigations and design, and acquisition of land (expropriation), as well as measures for the protection of the environment, have amounted to costs of $57 million US (Lenehan, 1992). The entire reconstruction was completed in 1995.

This page intentionally left blank

References

ABBREVIATIONS

ANCOLD: Austrian National Committee on Large Dams, Vienna
ASCE: American Society of Civil Engineers, New York, NY, USA
CBDB: Brazilian Committee on Dams
CEE: Committee on Earthquake Engineering, Washington
CFRD: Concrete Faced Rockfill Dams
CGJ: Canadian Geotechnical Journal, Canada
CNCOLD: Chinese National Committee on Large Dams, Beijing
CYTGPDC: China Yangtze Three Gorges Project Development Corporation
GSCLD: Group of the Swiss Committee on Large Dams
ICOLD: International Commission on Large Dams, Paris, France
IJNAMG: International Journal for Numerical and Analytical Methods in Geomechanics
IJNME: International Journal for Numerical Methods in Engineering
ISSMFE: International Society for Soil mechanics and Foundation engineering, Cambridge, UK
JGE: Journal of Geotechnical Engineering, ASCE, USA
JHE: Journal of Hydraulic Engineering, ASCE
JNCOLD: Japanese National Committee on Large Dams, Tokyo
JSE: Journal of Structural Engineering, ASCE, USA
JSMFD: Journal of Soil Mechanics and Foundation Division
JSSMFE: Japanese Society of Soil Mechanics and Foundation Engineering
MACOLD: Macedonian Committee on Large Dams
SLOCOLD: Slovenian Committee on Large Dams
USBR: United States Bureau of reclamation, Denver, Co., USA
USCE: United States Corps of Engineers, Vicksburg, Miss., USA
USCOLD: United States Committee on Large Dams, Denver, Co., USA
USSD: United States Society on Dams, USA
WP&DC: Water Power and Dam Construction, UK
YCOLD: Yugoslav Committee on Large Dams

Abadjiev, B.C. 1994. Safety assessment and stability improvement of the upstream slope of earth dams. *XVIII ICOLD Congress, Q.68, R. 20,* Durban.

Abbaso, C. & Okay, G. 1992. TURKEY – The remedial structures on the spillway of Keban dam. *WP&DC*, December.

Abdel-Ghaffar, M.A. & Elgamal, M.A.-W. 1987. Elasto-Plastic Seismic response of 3-D Earth Dams: Theory. *JGE, ASCE*, Vol. 113, No. 11, Nov.

Abdel-Ghaffar, M.A. & Scott, F.R. 1979a. Analysis of Dam Response to Earthquakes. *JGE, ASCE*, Vol. 105, No. 12, Dec., 1379–1405.

Abdel-Ghaffar, M.A. & Scott, F.R. 1979b. Shear Moduli & Damping Factors of Earth Dam. *JGE, ASCE*, Vol. 105, No. 12, Dec.

Adikari, N.S.G. & Parkin, K.A. 1982. Deformation Behaviour of Talbingo Dam. *IJNAMG*, Vol. 6.

Agulló, L., Aguado, A. & Fernández-Cánovas, 1995. A Survey of Damage Causes & Repair Techniques in Spanish Concrete Dams. *Dam Engineering*, Volume VI, Issue 3, September, Reed Business Publishing.

Ajrapetjan, R.A. 1979. Prevention of cracking of embankment dams. *Gidrotehnicheskoe stroiteljstvo* (in Russian). Energiya, Moskva, No. 1.

Akhtarpour, A. & Khodai, A. 2009. Nonlinear Numerical Evaluation of Dynamic Behavior of an Asphaltic Concrete Core Rockfill Dam (A Case Study). *JSEE*, Vol. 11, No. 3.

Akhtarpour, A., Khodaii, A., Ebrahimi, A. & Zohourian 2011. Evaluation of Dynamic Response of an Asphaltic Concrete Core Rockfill Dam Using Newmark Approach (a Case Study). Lucerne 2011.

Alam, S. 2001. A critical evaluation of sedimentation management design practice. *Hydropower & Dams*, International Hydropower Association. Issue One: 54–59.

Alam, S. 2002. Improving sedimentation management using multiple dams & reservoirs. *Hydropower & Dams*, International Hydropower Association. Issue One: 63–68.

Alarcon-Guzman, A., Leonards, A.G. & Chameau, L.J. 1988. Undrained Monotonic & Cyclic Strength of Sands *JGE, ASCE*, Vol. 114, No. 10, Oct.

Allende, M., Rivas, P. & Pascual V. 2012. Construction of the Enciso RCC dam. *Hydropower & Dams*, Issue Five, 2012, pp. 83–87.

Alonso, E. & Gens A. (eds). 2011. *Unsaturated Soils*, Taylor & Francis Group, London.

Alonso, E. & Cardoso R. 2010. Behaviour of materials for earth & rockfill dams: Perspective from unsaturated soil mechanics. *Proceedings of the 8th ICOLD European Club Symposium*, 22nd–23rd September 2010, Innsbruck, Austria.

Alonso, E.E. & Oldecop, L.A. 2000. Fundamentals of rockfill collapse. *Proceedings of the Asian Conference on Unsaturated Soils* (Unsat-Asia 2000), (Rahardjo, Toll & Leong ed.) Singapore, Balkema, Rotterdam. pp. 3–13.

Alonso, E.E. & Pinyol, N.M. 2008. Unsaturated soil mechanics in earth & rockfill dam engineering. *Proc. Unsaturated Soils: Advances in Geo-Engineering*. Eds. Toll, D.G., Augarde, C.E., Gallipoli, D. & Wheeler, S.J. pp. 3–32.

Alonso, E.E., Gens, A. & Josa, A. 1990. The constitutive model for partially saturated soils. *Géotechnique*, Vol. XL, Number 3, September, London.

Alonso, E.E., Olivella S. & Pinyol M.N. 2005. A review of Beliche Dam, *Géotechnique* 55, No. 4, pp. 267–285.

Alonso-Franco, M. 2003. RCC dams in Spain. Present & future. *4th International Symposium on Roller Compacted Concrete RCC Dams*, Madrid, Noviembre 2003.

ANCOLD 1991. *Dams in Austria*. Vienna: Austrian National Committee on Large Dams.

Ando, N., Terazono, K. & Kitazume, R. 1994. Sediment removal project at Miwa dam. *ICOLD, XVIII Congress, Q*. 69, *R*. 27, Durban.

Andriolo, F.R. 1998. *The use of roller compacted concrete, Part I, II & III*. Sao Paulo, Brazil.

Arai, Katsuhiko & Tagyo, Keiichi 1985. Determination of Noncircular Slip Surface Giving the Minimum Factor of Safety in Slope Stability Analysis. *Soils & Foundations*, The Japanese Society of Soil Mechanics & Foundation Engineering, Vol. 25, No. 1, March.

Araoz, A. 1994. Deterioration of the outlet mechanisms of dams – causes & protective measures. *ICOLD, XVIII Congress, Q. 71, R. 19*, Durban.

Arnevik, A., Kjaernsli, B. & Walbo, S. 1988. The Storvatn Dam, a rockfill dam with a central core of asphaltic concrete. *ICOLD, XVI Congress, Q. 61, R. 9*, San Francisco.

Arulanandan, K. & Perry, B.E. 1983. Erosion in relation to Filter design Criteria in Earth dams. *JGE, ASCE*, Vol. 109, No. 5, May.

Arulanandan, K., Anandarajah, A. & Abghari, A. 1983. Centrifugal Modelling of Soil Liquefaction Susceptibility. *JGE, ASCE*, Vol. 109, No. 3, March.

ASCE 1987. Concrete face Rockfill Dam – Special Memorial Issue (J. Sherard), *JGE, ASCE* Vol. 113, No. 10, Oct.

Asman, I. & Bratianu, G. 2013. Project for rehabilitation of Belci Dam after the 1991 failure. *9th European Club Symposium*, 10–12 April, 2013, Venice, Italy, B.14.

Asteris, G.P. & Tzamtzis, D.A. 2003. Nonlinear Seismic Response Analysis of Realistic Gravity Dam-Reservoir Systems. *International Journal of Nonlinear Sciences & Numerical Simulation*, Freund Publishing House Ltd., 4 (2003) pp. 329–338.

Astete, J., San Martin, L. & Alvarez, L. 1992. CHILE – The Santa Juana CFRD for irrigation in northern Chile. *WP&DC*, April.

Atkinson, H.J. 1973. Elasticity & plasticity in soils. *Géotechnique*, Vol. XXIII, Num. 4, December, London.

Auel, C., Boes, R., Ziegler, T. & Oertly, C. 2011. Design & construction of the sediment bypass tunnel at Soils, *The International Journal of Hydropower & Dams*, Volume Eighteen, Issue 3, pp. 62–66.

Aufleger, M., Dornstädter, J., Strobl, T., Perzlmaier, S., Conrad, M. & Goltz, M. 2007. 10 Jahre verteilte faseroptische Temperaturmessungen im Wasserbau. In Prof. Peter Rutschmann (ed.); *Proceedings of the 7th ICOLD European Club Dam Symposium*, September 17–19, Freising, Germany.

Aufleger, M., Perzlmaier, S., Dornstädter, J., & Schewe, L. 2005. A leakage detection system for concrete faced rockfill dams. In Chen Qian (ed.); *Proceedings on symposium on concrete faced rockfill dams*, September 19–26, Yichang, China.

Baker, R. & Gorber, M. 1978. Theoretical analysis of the stability of slopes. *Géotechnique*, Vol. XXVIII, Number 4, Dec. London.

Baldovin, G., Baldovin, E. & Fiamberti, A. 1994. Rehabilitation & waterproofing of the upstream facing of Ceresole Reale dam. *ICOLD, XVIII Congress, Q. 68, R. 87*, Durban.

Barrachina, L.J. & Blasco, M.L. 1988. An unpredicted high flood at La Baells dam on the 7th & 8th November 1982. *ICOLD, XVI Congress*, *Q. 63, R. 66*, San Francisco.

Basmaci, E. 1991. Foundation behaviour of Ataturk dam on first filling. *ICOLD, XVII Congress, Q. 66, R. 57*, Vienna.

Batmaz, S. 2003. Cindere dam-107 m high Roller Compacted Hardfill Dam (RCHD) in Turkey. In: Berga L, Buil J.M, Jofre C., et al. eds. *Proceedings of the 4th International Symposium on Roller Compacted Concrete Dams*, Madrid, Spain, 2003. 121–126.

Bayat, O.H. & Choi S.H.P. 1988. Design of Siah-Bishe concrete face rockfill dams. *ICOLD, XVI Congress, Q. 61, R. 60*, San Francisco.

Bazant, P.Z. 2002. Concrete fracture models: testing & practice, *Engineering Fracture Mechanics*, 69, pp. 165–205.

Beach, A., Gill, R. & Van Emmerick, P. 1991. Advances in face slab construction techniques for CFRDs. *WP&DC*, January.

Bejlinson, M.E., Kolichko, A.V. & Sherman, S.M. 1990. Nurek reservoir & the environment. *Gidrotehnicheskoe stroiteljstvo* (in Russian). Energoatomizdat, Moskva, No. 11.

Bell, G.F. 1980. *Engineering geology & Geotechnics*. London: Newnes-Butterworths.

Belloni, L. & Tanzini M. 1992. THAILAND – Behaviour of the Chiew Larn dam during construction. *WP&DC*, March.

Belloni, L., Ulisse C. & Valenti D. 1988. Behaviour of an asphalt membrane under seismic loading. *ICOLD, XVI Congress, Q. 61, R. 56*, San Francisco.

Bento, J., Dias, L.J. & Pina, B.A.C. 1995. Monitoring of Large Dams: Inferring Knowledge from previous Incidents. *Dam Engineering*, Volume VI, Issue 4, December, Reed Business Publishing.

Berra, M. & Bertacchi P. 1991. Alkali-aggregate reaction in concrete dams. *WP&DC*, April.

Berrill, B.J. & Davis, O.R. 1985. Energy Dissipation & Seismic Liquefaction of Sands: revised Model. *Soils & Foundations*, JSSMFE, Vol. 25, No. 2, June.

Bhattacharjee, S.S. & Léger, P. 1995. Fracture Response of Gravity Dams due to Rise of the reservoir Elevation. *Journal of Structural Engineering*, ASCE, Vol. 121, No. 9, Sep.

Bhattacharjee, S.S.& Leger, P. 1992. Concrete constitutive models for nonlinear seismic analysis of gravity dams – state-of-the-art, *Canadian Journal of Civil Engineering*, 19, pp. 492–509.

Billoré, J. 1991. André Coyne: a review of his ideas & their application today. *WP&DC*, June.

Blanc, P. & Lempérière, F. 2001. Labyrinth spillways have a promising future. *Hydropower & Dams*, International Hydropower Association. Issue Four: 129–131.

Blinder, S., Toniatti, B.N. & Ribeiro, S. 1992. Brazil – Construction progress & behavioural monitoring of Segredo dam, *WP&DC*, April.

Boes, R. & Minor, E.H. 2002. Hydraulic design of stepped spillways for RCC dams. *Hydropower & Dams*, Volume Ninth, Issue 3, pp. 87–91.

Bollrich, G. 1994. Hydraulic investigation of the high-head siphon spillway of Burgkhammer. *ICOLD, XVIII Congress, Q. 71, R. 2*, Durban,

Borovoy, A.A. 1976. Technical progress in the design & construction of large dams (in Russian). *Energiya*, Moskva.

Borsos, B. 1991. HUNGARY/CZECHOSLOVAKIA – Socio-political aspects of the Bös-Nagymaros barrage system, *WP&DC*, May.

Boscardin, D.M., Selig, T.E. Lin, R.-S. & Yang, G.-R. 1990. Hyperbolic Parameters for compacted Soils, *JGE, ASCE*, Vol. 116, No. 1, Jan.

Boulanger, W.R. & Hayden, R.R. 1995. Aspects of Compaction Grouting of Liquefiable Soil, *JGE, ASCE*, Vol. 121, No. 12, Dec.

Boulanger, W.R. & Seed, B.R. 1995. Liquefaction of Sand under Bidirectional Monotonic & Cyclic Loading, *JGE, ASCE*, Vol. 121, No. 12, Dec.

Boulanger, W.R., Bray, D.J., Merry, M.S. & Mejia, H.L. 1995. Three-dimensional dynamic response analyses of Cogswell Dam, *CGJ*, Vol. 32, No. 3, June.

Brauns, J., Degen, P.F. & Armbruster, H. 1988. The leakage problem with thin dam seals, *ICOLD, XVI Congress*, *Q. 61, R. 8*, San Francisco.

Bravo Carvera, H. & Gaztañaga, M.J. 2012. The design of Spain's La Muela II pumped-storage plant, *The International Journal of Hydropower & Dam*, Volume Nineteen, Issue 5, pp. 39–42.

Bremen, R. & Bertola, F.P. 1994. Increasing the spillway capacity of the Contra dam. *ICOLD, XVIII Congress, Q. 68, R. 27*, Durban.

Bretz, V.N. 2013. Sediment management at Grande Dixence dam. *9th European Club Symposium*, 10–12 April, 2013, Venice, Italy, D. 13.

Bridle C. R. & Vaughan R. P. 2005. The Perfect Filter Approach in Reducing Uncertainty in the Safety Evaluation of Internal Erosion in Embankment Dams. 73rd Annual Meeting of ICOLD, Tehran, Iran, May 1-6, 2005.

Bridle, C. R. 1988. Selection & design of the waterproofing element for Queen's Valley Dam, Jersey, Channel Islands. *ICOLD, XVI Congress*, *Q. 61, R. 35*, San Francisco.

Brien, J. & Klein, P. 2001. Design, Development, & manufacture of needle valves as bottom discharge valves for dams such as for the reservoir Möhnetalsperre (Ruhrverband Essen). *Modern Techniques for Dams-Financing, Construction, operation, Risk Assessment; Proc. workshop, Vol. I, Dresden, 14 October 2001*. Dresden.

Bronstein, V.I. 1994. State of Ingurska Dam & its foundation (in Russian). *Gidrotehnicheskoe stroiteljstvo*, Energoatomizdat, Moskva, No. 2.

Brown, A.J. 1988. Use of soft rockfill at Evretou Dam, Cyprus. *Geotechnique* 38, No. 3, 333–354.

Buchas, J. & Buchas, F. 1991. Argentina plans second generation of RCC dams. *WP&DC*, April.

Burland, B.J. 1990. On the compressibility & shear strength of natural clays. *Géotechnique*, Vol. XL, Number 3, September, London.

Burns, Fred 1994. Reservoir & stream effects of water chemistry changes caused by roller compacted concrete. *ICOLD, XVIII Congress, Q. 69, R. 44*, Durban.

Butakov, A.N. 1995. Formulae for calculation of discharge coefficient at spillways (in Russian). *Gidrotehnicheskoe stroiteljstvo*, Energoprogress, Moskva, No. 9.

Cambiaghi, A. & Rimoldi, P. 1991. The use of Geosynthetics in Embankment Dams: an Overview. *Idrotechnica*, 2, March–April.

CARPI 1996. World's highest embankment dam with a geosinthetic liner near competition. *Hydropower & Dams*. Volume Three, Issue Five.

Caruana, R., Catalano, A. & Spogli, G. 2010. Behaviour of the Dams Involved in Seismic Sequence Occurred in April 2009 in Abruzzo (Italy). *Proceedings of the 8th ICOLD European Club Symposium*, 22nd–23rd September 2010, Innsbruck, Austria, pp. 473–480.

Casagrande A. 1948. Research on stress-deformation and strength characteristics of soils and soft rocks under transient loading (Soil mechanics series), Harvard University, Graduate School of Engineering, p. 132.

Casinader, R. & Rome, G. 1988. Estimation of leakage through upstream concrete facings of rockfill dams. *ICOLD, XVI Congress*, *Q. 61, R. 17*, San Francisco.

Cassidy, J.J. 1991. Intercepting downstream migrating juvenile anadromous fish at hydroelectric dams. *ICOLD, XVII Congress, Q. 64, R. 18*, Vienna.

Castellanos, P.I.J. & Martin, M.E. 1995. Stresses & Movements in Arch Gravity Dams due to Thermal Action of the Environment. *Dam Engineering*, Volume VI, Issue 4, December, Reed Business Publishing.

Cathie, D.N. & Dungar, R. 1978. Evaluation of finite element predictions for constructional behaviour of a rockfill dam. *Proceedings, The Institution of Civil Engineers*, London, Sept., part 2.

Cavallin, E.J. 1988. Hydraulic asphalt concrete for impervious upstream facing: Morro reservoir. *ICOLD, XVI Congress*, *Q. 61, R. 32*, San Francisco.

CBDB, 2009. *Main Brazilian Dams III – Design, Construction & Performance*, Brazilian Committee on Dams, Jaragua do Sul – SC, Brazil, p. 436.

Cedergren, R.H. 1973. Seepage Control in Earth dams. In *Embankment-Dam Engineering*, Casagrande Volume, New York: John Wiley & Sons.

CEE, 1990. *Earthquake Engineering for Concrete Dams: Design, Performance, & Research Needs*. Washington: National Academy Press.

Chandler, W.H. 1990. A model for the deformation & flow of granular materials. *Géotechnique*, Vol. XL, Number 3, September, London.

Chang, S.C. & Whitman, R. 1988. Drained Permanent deformation of Sand due to Cyclic Loading. *JGE, ASCE*, Vol. 114, No. 10, Oct.

Chanson, H. 2002. *Hydraulics of stepped chutes & spillways*. A.A. Balkema Publishers, Swets & Zeitlinger B. V., Lisse, The Netherlands.

Chappell, A.B. 1990. Rock Mass Characterization for Dam Foundations. *JGE, ASCE*, Vol. 116, No. 4, April.

Charles, A.J. & Penman, M.D.A. 1988. The behaviour of embankment dams with bituminous watertight elements. *ICOLD, XVI Congress*, *Q. 61, R. 38*, San Francisco.

Charles, A.J., Tedd, P. & Wright E. C. 1994. Safety assessment & legislation for reservoirs in Great Britain. *ICOLD, XVIII Congress, Q.* 68, *R.* 71, Durban.

Charlie, A.W., Scott, E. C., Siller, J.T., Butler, W.L. & Doehring, D.D. 1995. Estimating liquefaction potential of sand using the Piezovane. *Géotechnique*, Vol. XLV, Number 1, March.
Cheung, Y.K., Yeo, M.F. 1979. *A Practical Introduction to Finite Element Analysis*. London: Pitman Publishing Limited.
Chonggang, S. 1991. Roller compacted concrete dams in China. *WP&DC*, November.
Chopra, A.K. & Chakrabarti, P. 1981. Earthquake Analysis of Concrete Gravity Dams including Dam-Water-Foundation Rock Interaction. *Earth. Eng. & Struc. Dynamics*, Vol. 9, pp. 363–383.
Chopra, K.A. 1967. Earthquake Response of Earth Dams. *JSMFD, ASCE*, March.
Chowdhury, N.R. 1978. *Slope Analysis*. Amsterdam – Oxford – New York: Elsevier Scientific Publishing Company.
Chraibi, A.F. & Zakaria, A. 2003. Marocco's 120 m-high Sidi said RCC dam, *The International Journal of Hydropower & Dams*, Volume Ten, Issue 6, 2003, pp. 58–61.
Christian, T.J., Ladd, C.C. & Baecher B.G. 1994. Reliability Applied to Slope Stability Analysis. *JGE, ASCE*, Vol. 120, No. 12, Dec.
Chu, J. 1995. An experimental examination of the critical state & other similar concepts for granular soils. *CGJ*, Vol. 32, No. 6, December.
Chugaev, R.R. 1985. *Hydraulic structures*, Part I & II (in Russian). Moskva: Agropromizdat.
Chugh, K.A. 1981. Multiplicity of Numerical Solutions for Slope Stability Problems. *IJNAMG*, Vol. 5, No. 3, July–September.
Clayton, I.R.C., Steinhagen, M.H. & Powrie, W. 1995. Terzaghi's theory of consolidation, & the discovery of effective stress. *Proceedings of The Institution of Civil Engineers*, *Geotechnical Engineering*, October.
Clough, W.R. & Woodward, J. Richard III, 1967. Analysis of Embankment stresses & deformations. *JSMFD, ASCE*, July.
Clough, W.R. & Zienkiewicz, C.O. 1987. Finite Element Methods in Analyses & Design of Dams. *ICOLD, Bulletin 30a*, Paris, Jan.
CNCOLD, 1979. *Dam Construction by the Chinese People*. Beijing: The Chinese National Committee on Large Dams.
Collins, F.I., Gunn, M.I.C., Pender, J.M. & Yan, W. 1988. Slope Stability Analyses for Materials with a Non-linear Failure Envelope. *IJNAMG*, Vol. 12, No. 5, September–October.
Cooke, J. Barry 1984. Progress in Rockfill Dams, *JGE, ASCE*, October.
Cooke, J.B. & Sherard, J.L. 1987. Concrete Face Rockfill Dam: I Assessment; II Design. *Journal of Geotechnical Engineering*, ASCE, v. 113. No. 10.
Cooke, J.B. 1991. The concrete-faced rockfill dam. *WP&DC*, January.
Cooke, J.B. 1992. Development of the high concrete faced rockfill dam. *WP&DC*, April.
Cooke, J.B. 2000a. The high CFRD Dams. In J. Barry Cooke Volume-Concrete Face Rockfill Dams. *ICOLD*, Beijing.
Cooke, J.B. 2000b. The plinth of The CFRD Dam. *Proceedings, International Symposium on Concrete Faced Rockfill Dams*. !8 September, Beijing, China: 21–28.
Coyne, André 1943. *Leçons sur les Grandes Barrages*. Paris: École Nationale des Ponts et Chaussées.
Craig, F.R. 1978. *Soil Mechanics*, Second Edition. England: Van Nostrand Reinhold Company Ltd.
Creager, William, Justin Joel, Hinds Julian 1955. *Engineering for Dams*, Volume I, II & III. New York: John Wiley & Sons.
Cruz, T.P., Materon, B. & Manoel, F. 2009. *Concrete face rockfill dams*, Oficina de Textos, Sao Paulo, p. 448.
CYTGPDC, 2000. Proceedings of China Yangtze Three Gorges Project. *For 2000 ICOLD*. Beijing.
Daddazio, P.R., Ettouney, M.M. & Sandler, S.I. 1987. Nonlinear Dynamic Slope Stability Analysis. *JGE, ASCE*, Vol. 113, No. 4, April.

Daicho, A. 1988. Design & monitoring of Tataragi Dam. *ICOLD, XVI Congress*, Q. 61, R. 14, San Francisco.
Dakoulas, P. & Gazetas, G. 1987. Vibration Characteristics of Dams in Narrow Canyons. *JGE, ASCE*, Vol. 113, No. 8, August.
Dakoulas, P., Thanopoulos, Y., Anastassopoulos, C. & Dimou, C. 2013. Seismic Performance & Safety Evaluation of Tavropos Arch Dam. *9th European Club Symposium*, 10–12 April, 2013, Venice, Italy, B.66.
Daniell, W.E. & Taylor, C.A. 2000. The seismic safety evaluation of a radial flood gates. *XX ICOLD Congress, Q.79, R. 9*, Beijing, Volume IV: 123–132.
Danilevsky, A. 1992. Dams built by controlled blasting. *WP&DC*, July.
D'Appolonia, E. 1990. Monitored Decisions. *JGE, ASCE*, Vol. 116, No. 1, Jan.
Darbre, R. G. 1998. Phenomenological two-parameter model for dynamic dam-reservoir interaction, *Journal of Earthquake Engineering*, 2, pp. 167–176.
Davis, V.C. & Sorensen, E.K. 1969. *Handbook of applied hydraulics*. New York: McGraw-Hill Book Company.
Day, A.R. & Potts, M.D. 1994. Zero Thickness Interface Elements – Numerical Stability & Application. *IJNAMG*, Vol. 18, No. 10, October.
De Alba, P., Seed, H.B., Retamal, E. & Seed, B.R. 1988. Analyses of Dam Failures in 1985 Chilean Earthquake. *JGE, ASCE*, Vol. 114, No. 12, Dec.
De Borst, R. 2002. Fracture in quasi-brittle materials: a review of continuum damage based approaches, *Engineering Fracture Mechanics*, 69, pp. 95–112.
De Cesare, G., Schleiss, J.A. & Althaus Jenzer, I.M.J. 2011. Innovative approaches to sediment management, *The International Journal of Hydropower & Dams*, Volume Eighteen, Issue 3, pp. 68–73.
Desai, S.C. & Christian, T.J. 1977. *Numerical Methods in Geotechnical Engineering*. New York: McGraw-Hill Book Company.
Desai, S.C. & Salami, R.M. 1987. Constitutive Model for Rocks. *JGE, ASCE*, Vol. 113, No. 5, May.
Desai, S.C. 1979. *Elementary Finite Element Method*. Prentice-Hall, Inc.
Desai, S.C., Pham, V.H. & Sture, S. 1981. Procedure, Selection & Application of Plasticity Models for a Soil. *IJNAMG*, Vol. 5, No. 3, July–September.
Di Prisco, C., Matiotti, R. & Nova, R. 1995. Theoretical investigation of the undrained stability of shallow submerged slopes. *Géotechnique*, Vol. XLV, Number 3, Sept.
Diacon, A., Stematiu, D. & Mircea, N. 1992. ROMANIA – An analysis of the Belci dam failure. *WP&DC*, September.
Dimitrov, N., Jedelhauser, P. & Sierotzki, K. 1994. Belmeken rockfill dam – safety assessment. *ICOLD, XVIII Congress, Q. 70, R. 4*, Durban.
Dobrynin, S.N., Kuznecov, O.M., Tihonova, T.S. & Jurinova, T.N. 1994. Mathematical modeling for prediction the behaviour of hydraulic structures based on data gained by monitoring (in Russian). *Energoatomizdat*, Moskva, No. 2, 1994.
Dolen, P.T. & Abdo, Y. 2008. Roller-compacted Concrete for Dam Safety Modifications. *Brazilian International RCC Symposium*, IBRACON, September, 2008.
Doležalová, M. 1994. On Overestimation of Displacements in Numerical Calculation of Zoned Dams. *IJNAMG*, Vol. 18, No. 1, January.
Dornstädter, J. & Heinemann, B. 2010. In Situ Detection of Internal Erosion. *Proceedings of the 8th ICOLD European Club Symposium*, 22nd–23rd September 2010, Innsbruck, Austria, pp. 481–485.
Dornstädter, J. 2013. Leakage Detection in Dams – State of the Art. *Proceedings of the International Symposium: Dam engineering in Southeast and Middle Europe – Recent experience and future outlooks*, 16th October 2013, Ljubljana, Slovenia, pp. 77–86.
Drescher, A. & Christopoulos C. 1988. Limit Analysis Slope Stability with Nonlinear Yield Condition. *IJNAMG*, Vol. 12, No. 3, May–June.

Duncan, J.M. & Chang, C.Y. 1970. Nonlinear analysis of stress & strain in soils. *J Soil Mechanics & Foundation Division*, ASCE, pp. 1629–1653.
Dungar, R. 1978. An efficient method of fluid-structure coupling in the dynamic analysis of structures. *IJNME*, Vol. 13, 93–107.
Dungar, R. 1988. Computer modelling of embankment dams: response to earthquake. *WP&DC*, June.
Dungar, R. 1988. Evaluating pore pressures in embankment dams. *WP&DC*, Jan.
Dunstan, M.R.H. & Santos, O.F. 2001. The interrelationship between design & construction for efficient RCC dams. *Modern Techniques for Dams-Financing, Construction, operation, Risk Assessment*; Proc. workshop, Vol. I, Dresden, 14 October 2001. Dresden.
Dunstan, M.R.H. 2012. New development in RCC dams, *The International Journal of Hydropower & Dam*s, Volume Nineteen, Issue 5, pp. 50–54.
Eadie, S.H. & McGregor, R.I. 1988. The application of a geomembrane at Nigeria's Isanlu dam. *WP&DC*, June.
Eisenstein, Z. & Law, S. 1977. Analysis of Consolidation Behaviour of Mica Dam. *JGE, ASCE*, August.
Eisenstein, Z. & Naylor, J.D. 1986. Static Analysis of Embankment Dams. *ICOLD, Bulletin* 53, Paris.
Elahovskij, S.B. 1990. Water-power reservoirs & recreation (in Russian). *Gidrotehnicheskoe stroiteljstvo*, Energoatomizdat, Moskva, No. 1.
Elgamal, M.A.W. & Abdel-Ghaffar, M.A. 1987. Elasto-Plastic Seismic response of 3-D Earth Dams: Application, *JGE, ASCE*, Vol. 113, No. 11, Nov.
Elgamal, M.A.W., Scott, F.R., Succarieh, F.M. & Yan, L. 1987. La Villita Dam Response during Five Earthquake including Permanent Deformation. *JGE, ASCE*, Vol. 113, No. 10, October.
Erbisti, C.F.P. 2004. *Design of hydraulic gates*. A.A. Balkema Publishers, Swets & Zeitlinger B. V., Lisse, The Netherlands.
Fabian, E. & Ditter, K. 1988. Criteria for judgment of the aging behaviour of asphaltic surface linings & their influence on the repair & regeneration of pumped-storage reservoirs. *ICOLD, XVI Congress*, *Q. 61, R. 21*, San Francisco.
Fahlbusch, E.F. 1999. Spillway design floods & dam safety. *Hydropower & Dams*, International Hydropower Association. Issue Four: 120–127.
Failer, E. & Abong, D.M. 1995. The 2400MW Bakun hydroelectric project. *WP&DC*, November.
Fanelli, C.G., Scuero, M.A. & Vaschetti, G. 1995. PVC membrane protects Italy's highest dam. *WP&DC*, November.
Fanelli, M. & Paolina, R. 1994. Application of the Lomabrdi & Lomabardi-Fanelli criteria to some arch-gravity dams. *ICOLD, XVIII Congress, Q. 68, R. 65*, Durban.
Fauchet, B., Carrère, A. & Tardieu, B. 1992. Poroplasticity: modelling of pore pressure effects in concrete & rocks. *WP&DC*, July.
Feizi-Khankandi, S., Ghalandarzadeh, A., Mirghasemi, A.A. & Höeg, K. 2009. Seismic Analysis of the Garmrood Embankment Dam with Asphaltic Concrete Core. Soils & Foundations, Japanese Geotechnical Society. Vol. 49 No. 2, April 2009, pp. 153–166.
Feizi-Khankandi, S., Mirghasemi, A.A., Ghalandarzadeh A. & Höeg, K. 2008. 2D Nonlinear Analysis of Asphaltic Concrete – Core Embankment Dams. *The 12th International Conference of International Association for Computer Methods & Advances in Geomechanics* (IACMAG), Goa, India.
Fell Robin, MacGregor Patrick & Stapledon David 1992. *Geotechnical Engineering of Embankment Dams*. Rotterdam/Brookfield: A. A. Balkema.
Filho Rocha Pedricto 1995. Slab Deflection of a Concrete Faced Rockfill Dam. *Dam Engineering*, Volume VI, Issue 3, September, Reed Business Publishing.
Filov, V., Pishtachev, C. & Avramov, G. 1972. *Channals* (in Bulgarian). Sofia: Tehnika.

Finn Liam, D.W. 1991. Estimating how embankment dams behave during earthquakes. *WP&DC*, April.
Finn Liam, D.W. et al. 1991. Dam on liquefiable foundation: safety assessment & remediation. *ICOLD, XVII Congress, Q. 66, R. 30*, Vienna.
Finn Liam, D.W., Miller S.I. R. 1976. Nonlinear analysis of earth structures. *IJNAMG*, Vol. 1, pp. 194–201.
Flemme, W., Baztan, A.J. & Funk, E. 1990. Repairs to the Martin Gonzalo dam. *WP&DC*, November.
Forbes, A.B. 1988. The development & testing of roller compacted concrete for dams in Australia. *ICOLD, XVI Congress*, *Q. 62, R. 6*, San Francisco.
Forbes, A.B. 2008. RCC – New Developments & Innovations. *1st Brazilian International RCC Symposium*, IBRACON, September, 2008.
Forrester, K. 2001. *Subsurface Drainage for Slope Stabilization.* Reston, Virginia: ASCE
Foster, M.A. & Fell, R. 2001. Assessing embankment dam filters that do not satisfy design criteria. *Journal of Geotechnical & Geoenvironmental Engineering*, 127 (5) pp. 398–407.
Foster, M.A. 1999. The probability of failure of embankment dams by internal erosion & piping. *PhD Thesis*. School of Civil & Environmental Engineering, The University of New South Wales, Sydney.
Franco, A.M. & Pena, S.A. 1988. Plinths in dams with watertight facing. Design, construction & performance. *ICOLD, XVI Congress*, *Q. 61, R. 48*, San Francisco.
Fredlund, G.D. 2006. Unsaturated Soil Mechanics in Engineering Practice. *Journal of Geotechnical & Geoenvironmental Engineering*, Vol. 132, No. 3, March, pp. 286–321.
Fredlund, G.D., Xing, A., Fredlund, M.D. & Barbour, S.L. 1995. The relationship of the unsaturated soil shear strength to the soil water characteristic curve. *Canadian Geotechnical Journal* 33, pp. 440–448.
Freer, R. 1994. Safety of concrete & masonry dams in the UK. *WP&DC*, September.
Furgani, L. & Nuti, C. 2013. Evaluation of Dams Seismic Response. *9th European Club Symposium*, 10–12 April, 2013, Venice, Italy, B.57.
Galant, M.A., Zhivotovskij, B.A., Novikova, I.S., Rodionov, V.B. & Rozanova, N.N. 1995. Spiral shaft spillways – properties & hydraulic conditions (in Russian). *Gidrotehnicheskoe stroiteljstvo*, Energoprogress, Moskva, No. 9: 16–22.
Gallacher, D. 1988. Asphaltic central core at the Megget Dam. *ICOLD, XVI Congress*, *Q. 61, R. 39*, San Francisco.
Galljperin, S.R. et al. 1977. *Cavitation at hydraulic structures* (in Russian). Moskva: Energiya.
Ganev, Ivan et al. 1965. *Dams and Reservoirs* (in Bulgarian). Sofia: Tehnika.
Gao, Y., Jin, F., Wang, X. & Wang, J. 2011. Finite Element Analysis of Dam-Reservoir Interaction Using High-Order Doubly Asymptotic Open Boundary. *Hindawi Publishing Corporation, Mathematical Problems in Engineering*, Volume 2011, Article ID 210624.
Garcia, D.J. 1988. The asphalt facing of the rockfill section of the Negratin Dam and its joint with the concrete section. *ICOLD, XVI Congress*, *Q. 61, R. 44*, San Francisco.
Garga, K.V., Hansen D. & Townsend, R.D. 1995. Mechanisms of massive failure for flowthrough rockfill embankments. *CGJ*, Vol. 32, No. 6, December.
GCOLD, 2001. *Dams in Germany.* Verlag Glückauf GmbH.
Georgiannou, N.V., Burland, B.J. & Hight, W.D. 1990. The undrained behaviour of clayey sands in triaxial compression and extension. *Géotechnique*, Vol. XL, Number 3, September.
Ghaboussi, J. & Wilson, L.E. 1973. Seismic Analysis of Earth Dam-Reservoir Systems. *JSMFD, ASCE*, October.
Ghaboussi, J., Wilson, L.E. & Isenberg, J. 1973. Finite Element for Rock Joints and Interfaces. *JSMFD, ASCE*, October.
Giovagnoli, M., Schrader, E. & Ercoli, F. 1992. HONDURAS – Concepcion dam: a practical solution to RCC problems. *WP&DC*, February.

Girod, K., Seifert, S., Teichmann, P. & Turbing, M. 1994. Evaluation of safety of a rockfill dam with concrete core on the basis of measurement, test, and calculation results. *ICOLD, XVIII Congress, Q. 68, R. 6*, Durban.

Giroud, P.J. 1989. Comment – Are geosynthetics durable enough to be used in dams? *WP&DC*, February.

Goguel, B. & Mpala S.A. *ZAMBIA/ZIMBABWE – Monitoring and maintenance at Kariba dam*, *WP&DC*, June 1992.

Goh, C.T.A. 1994. Seismic Liquefaction Potential Assessed by Neural Networks. *JGE, ASCE*, Vol. 120, No. 9, Sept.

Goh, C.T.A. 1996. Neural-Network Modelling of CPT Seismic Liquefaction Data. *JGE, ASCE*, Vol. 122, No. 1, January.

Goljdin, L.A., Rasskazov, N.L. 1987. Design of embankment dams (in Russian). *Energoatomizdat*, Moskva.

Goltz, M., Aufleger, M., Dornstädter, J. & Mangarovski, O. 2011. Distributed fiber optic temperature measurements in embankment dams with central core – new benchmark for seepage monitoring. *Proceedings of the Symposium SLOCOLD-MACOLD*, Skopje, 17 November 2011, pp. 123–132.

Golzé Alfred 1977. *Handbook of Dam Engineering*. New York: Van Nostrand Reinhold Company.

Gonzalez, V.J. & Rodrigues, F.S. 1988. Bituminous concrete faced rockfill dam – A Portuguese case. *ICOLD, XVI Congress*, *Q. 61, R. 41*, San Francisco.

Goodman, E. Richard 1995. Block theory and its application, Thirty-fifth Rankine Lecture. *Géotechnique*, Vol. XLV, Number 3, September.

Goodman, E., Taylor, L. & Brekke, L.A. 1968. *Model for the Mechanics of Jointed Rocks*, *JSMFD, ASCE*, Vol. 94, May.

Goubet, A. & Guérinet, M. 1992. FRANCE – Experience with the construction of the Riou dam. *WP&DC*, February.

Griffiths, V.D. & Prevost, H.J. 1988. Two- and three-dimensional dynamic finite element analyses of the Long Valley Dam. *Géotechnique*, Vol. XXXVIII, Number 3, Sept.

Griffiths, V.D. *Failure* 1990. Criteria Interpretation Based on Mohr-Coulomb friction. *JGE, ASCE*, Vol. 116, No. 6, June.

Grishin, M.M. et al. 1979. *Hydraulic structures*, Part 1 & 2 (in Russian). Moskva: Vyshaya shkola.

GSCLD 1988. Long-term behaviour of bituminous and cement concrete facings of compensation reservoirs in Switzerland. *ICOLD, XVI Congress*, *Q. 61, R. 18*, San Francisco.

Guan, F., Moore, D.I. & Lin, G. 1994. Transient response of ReservoirnDamnSoil Systems to Earthquakes. *IJNAMG*, Vol. 18, No. 12, December.

Gudushauri, I.I. 1990. Methods of seismic calculation of arch and buttress dams based on spectral theory. (in Russian). *Gidrotehnicheskoe stroiteljstvo*, Energoatomizdat, Moskva, No. 9.

Guocheng, J. & Zengkai, Z. 2000. High Concrete Face Rockfill Dams in China. *Proceedings, International Symposium on Concrete Faced Rockfill Dams.* !8 September, Beijing, China: 1–20.

Haas, H., Haug, W. & Schonian, E. 1988. Asphalt surface linings on dams with steep slopes in comparison to concrete surface linings. *ICOLD, XVI Congress*, Q. 61, R. 10, San Francisco.

Hager, H.W. 1988. Discharge characteristics of gated standard spillways. *WP&DC*, January.

Hajdin, G. 1967. Influence of the lateral spilling to the flow of the side channel. *Transactions*, Institute "Jaroslavčerni", Belgrade, No. 43.

Hanna, H.T. 1985. *Field Instrumentation in Geotechnical Engineering*, First Edition, Trans. Tech. Pub. USA.

Hansen, D.K. & Forbes, A.B. 2012. Thermal induced cracking performance of RCC dams. *6th International Symposium on Roller-Compacted Concrete (RCC) Dams*, Zaragoza, 23–25 October 2012.

Hansen, D.K. 1988. RCC'88 will review recent developments. *WP&DC*, February.
Hao, Y.L. & He, S.B. 2008. Design of the Yele Asphalt Core Rockfill Dam, *Dam Construction in China – State of the Art*, CHINCOLD.
Hardin, O.B. 1983. Plane Strain Constitutive Equations for Soils. *JGE, ASCE*, Vol. 109, No. 3, March.
Hartung, F. & Kuros, G.R. 1987. Historische Talsperren im Iran, in Garbrecht, Günther, *Historische Talsperren 1*, Stuttgart: Verlag Konrad Wittwer, pp. 221–274.
Hasegawa, T. & Kikusawa, M. 1988. Long-term observation of asphaltic concrete facing dam. *ICOLD, XVI Congress*, *Q. 61, R. 13*, San Francisco.
Hayashi, M., Komada, H. & Fujiwara, Y. 1973. Three dimensional dynamic response and earthquake resistant design of rock fill dam against input earthquake in direction of dam axis. *Fifth World Conference on Earthquake Engineering*, Rome.
Heigerth, G., Melbinger, R., Obernhuber, P. & Tschernutter, P. 1994. Assessing and improving the safety of existing dams in Austria, *ICOLD, XVIII Congress, Q. 68, R. 58*, Durban.
Helper, E.T. & Scott, A.G. 1992. USA – Increasing the capacity of the Roosevelt dam, *WP&DC*, May.
Herzog, M.A. Max 1989. Spatial Action of Straight Gravity Dams in Narrow Valleys, *JSE, ASCE*, Vol. 115, No. 3, March.
Hinks, L.J. & Charles A.J. 1992. Engineering guide to seismic risk to dams. *WP&DC*, March.
Hird, C.C., Pyrah C.I., Russell & Cinicioglu, F. 1995. Modelling the effect of vertical drains in two-dimensional finite element analyses of embankments on soft ground. *CGJ*, Vol. 32, No. 5, October.
Höeg, K. 1992. NORWAY – An evaluation of asphaltic concrete cores for embankment dams. *WP&DC*, July.
Höeg, K. 1993. Asphaltic Concrete Cores for Embankment Dams. Stikka Press, Norway, ISBN 82-546-0163-1.
Hoek, E. & Brown, T. E. 1997. Practical estimates of rock mass strength. *International Journal of Rock Mechanics and Mining Sciences*, 34, pp. 1165–86.
Hoek, E. 1983. Strength of jointed rock masses, 1983 Rankine Lecture, *Géotechnique*, Vol. XXXIII, pp. 187–223.
Holanda, G.F. 1994. Built in Brazil – RCC Dams of the 1990s. *WP&DC*, November.
Hollingworth, F. & Geringer, J.J. 1992. South Africa – Cracking and leakage in RCC dams. *WP&DC*, February.
Hollingworth, F., Druyts, M.W.H.F. & Maartens, W.W. 1988. Some South African experiences in the design and construction of rollcrete dams. *ICOLD, XVI Congress*, Q. 62, R. 3, San Francisco.
Honjo, Y. & Veneziano, D. 1989. Improved filter Criterion for Cohesionless Soils. *JGE, ASCE*, Vol. 115, No. 1, Jan.
Houkun, C., Zeping, Xu & Ming, Li. 2010. The relationship between large reservoirs and seismicity. www.waterpowermagazine.com, January, 2010, pp. 29–33.
Hrabowski, W. & Rzadkowski, B. 1988. Behaviour of earth dams in Poland during operation, *ICOLD, XVI Congress*, *Q. 61, R. 7*, San Francisco.
Hrisanov, N.I., Kerro, N.I. & Koljnik, G.A. 1990. Complex expert evaluation of the impact of hydraulic structures to the environment (in Russian). *Gidrotehnicheskoe stroiteljstvo*, Energoatomizdat, Moskva, No. 3.
Hryciw, D.R., Vitton, S. & Thomann, G.T. 1990. Liquefaction and Flow Failure During seismic Exploration. *JGE, ASCE*, Vol. 116, No. 12, December.
Hughes, K.A. 2010. A Simple Labyrinth Weir Installation at a Dam in a National Park in the UK. *Proceedings of the 8th ICOLD European Club Symposium*, 22nd–23rd September 2010, Innsbruck, Austria, pp. 515–520.

Hughes, K.A. 2010. A Simple Experience with a 'new means' of Leakage Detection. *Proceedings of the 8th ICOLD European Club Symposium*, 22nd–23rd September 2010, Innsbruck, Austria, pp. 509–514.

Hunter, G. & Fell, R. 2003. The deformation behaviour of embankment dams. *UNICIV Report No. R-416*, February 2003, the University Of New South Wales, Sydney, Australia.

Huth, P., Ditter, K. & Heidbrink, W. 1988. New placing techniques for asphaltic concrete linings at the Geeste storage reservoir. *ICOLD, XVI Congress*, *Q. 61, R. 11*, San Francisco.

Ibanez de Aldecoa, R. & Ortega, F. 2013. International RCC Symposium reviews design and construction technology (conference report). *Hydropower & Dams*, Issue Three, 2013, pp. 116–122.

Ibanez de Aldecon, R., Polimon, J., De Cea, C.J., Yague Cordova, J. & Berga, L.C. 2012. 30 years of RCC dam construction in Spain: From complexity to simplicity. *Hydropower & Dams*, Issue Five, 2012, pp. 60–67.

ICOLD 1974. Lessons from Dam Incidents. *Complete Edition*, Paris, 1974.

ICOLD 1977. Spillways for Dams. *Bulletin 58*, Paris.

ICOLD 1982. *Bituminous concrete Facings for Earth and Rockfill Dams*, Committee on Materials for Large Dams, *Bulletin 32*, Paris.

ICOLD 1988. Embankment dams with impervious upstream facings: an overview of Italian practice. *Working Group, Italian Committee on Large Dams*, *ICOLD, XVI Congress, Q. 61, R. 23*, San Francisco.

ICOLD 1993. Rock materials for rockfill dams. *Bulletin 92*, Paris.

ICOLD 1994a. Numerical Analysis of Dams. Third Benchmark Workshop, Theme A1 *Non linear analysis of joint behaviour under thermal and hydrostatic loads for an arch dam*, September, Gennevilliers, France.

ICOLD 1994b. Numerical Analysis of Dams. Third Benchmark Workshop, Theme A2 *Evaluation of critical uniform temperature decrease for a cracked buttress dam*, September, Gennevilliers, France.

ICOLD 1994c. Numerical Analysis of Dams. Third Benchmark Workshop, Theme B1 *Evaluation of pore pressure and settlements of an embankment dam under static loadings*, September, Gennevilliers, France.

ICOLD 1994d. Numerical Analysis of Dams. Third Benchmark Workshop, Theme B2 *Dynamic analysis of an embankment dam under a strong earthquake*, September, Gennevilliers, France.

ICOLD 1996. A guide to Tailings Dams and impoundments – Design, construction, use and rehabilitation. *Bulletin 106*, Paris.

ICOLD 1999. *Embankment dams with bituminous concrete facing*. Committee on Materials for Large Dams, *Bulletin 114*, Paris.

ICOLD 2001. Design features of dams to resist seismic ground motion – guidelines and case studies. *Bulletin 120*, Paris.

ICOLD 2001. Design Features of Dams to Resist Seismic Ground Motion – Guidelines and Case Studies. Bulletin 120, Paris.

ICOLD 2003. Roller-compacted concrete dams – State of the art and case histories. *Bulletin 126, Paris*.

ICOLD 2010. Selecting seismic parameters for large dams. Guidelines, Rev. of Bulletin 72 (1989).

ICOLD 2010a. Geomembrane sealing systems of dams – Design principles and review of experience. *Bulletin 135*, Paris.

ICOLD 2011. Reservoir and seismicity – State of knowledge. *Bulletin 137, Paris*.

Idel, K.H. 1979. Connection of impervious surface of asphaltic material with concrete structures such as control galleries and bottom outlets, *XIII ICOLD*, New Delhi.

Ionescu, S. 2000. The safety assessment of fill dams with gated or ungated spillways. *XX ICOLD Congress, Q.79, R. 14*, Beijing, Volume IV: 197–208.

Ishihara, K. 1984. Post-earthquake failure of a tailings dam due to liquefaction of the pond deposit, Proceedings, Vol. 3, *International Conference on Case Histories in Geotechnical Engineering*, Rolla, Missouri, USA; May 1984.

Ishihara, K. 1996. *Soil Behaviour in Earthquake Geotechnics*. Oxford: Clarendon Press.

Ishii, K. & Kamiji, M. 1988. Design for asphaltic concrete facings of Sabigawa Upper Dam. *ICOLD, XVI Congress*, Q. 61, R. 19, San Francisco.

Jacobsen, T. 2003. Sediment handling technologies: experience from case studies. *The International Journal of Hydropower and Dams*, Volume Ten, Issue 6, 2003, pp. 84–87.

Jairaj, V., Wesley, D.L. 1995. Construction of a chimney drain using bio-polymer slurry at Hays Creek dam. *WP&DC*, February.

Janbu, N. Slope Stability Computations 1973. In *Embankment-Dam Engineering*, Casagrande Volume, New York: John Wiley & Sons.

Jansen, B.R. 1988. *Advanced Dam Engineering*. New York: Van Nostrand Reinhold.

Jansen, B.R. 1990. Estimation of embankment dam settlement caused by earthquake. *WP&DC*, December.

Jappelli, R., Marzocchi, L. Fantoma, D., Musso, A., Federico, F. & Mariani, M. 1988. Impervious facings and large central drain for the embankment dams of a pumped-storage plant. *ICOLD, XVI Congress*, *Q. 61, R. 25*, San Francisco.

Jeyapalan, K.J., Duncan, M.J. & Seed, B.H. 1983. Analyses of Flow Failures of Mine Tailings Dams. *JGE, ASCE*, Vol. 109, No. 2, Feb.

Jeyapalan, K.J., Duncan, M.J. & Seed, B.H. 1983b. Investigation of Flow Failures of Tailings Dams. *JGE, ASCE*, Vol. 109, No. 2, Feb.

Jiazheng, P. & Jing, H. 2000. *Large Dams in China. A Fifty – Year Review.* Beijing: China Water Power Press.

Jing, L. 2003. A review of techniques, advances and outstanding issues in numerical modelling for rock mechanics and rock engineering, *International Journal of Rock Mechanics & Mining Sciences*, 40, pp. 283–353.

JNCOLD 1982. *Dams in Japan.* Tokyo: Japanese National Committee on Large Dams.

JNCOLD 1991. *Dams in Japan.* Japanese National Committee on Large Dams, No. 12, Tokyo.

Johannson, S. & Sjödahl, P. 2007. Experiences from seepage monitoring using distributed temperature sensing in optical fibers. In Prof. Peter Rutschmann (ed.); *Proceedings of the 7th ICOLD European Club Dam Symposium*, September 17–19, Freising, Germany.

Johansson, S. 1997. Seepage monitoring in embankment dams. *Doctoral Thesis*, Royal Institute of Technology, Stockholm, ISBN 91-7170-792-1.

Judek, T.R. & Bechai, M. 1988. Use of sheet piles and geotextile system as the impervious core in rockfilled dams. *ICOLD, XVI Congress*, Q. 61, R. 46, San Francisco.

Justo, J. L. & Saura, J. 1983. Three-dimensional analysis of Infiernillo dam during construction and filling of the reservoir. *Int. J. Numer. Anal. Methods Geomech*. 7, No. 2, pp. 225–243.

Justo, J.L. & Durand, P. 2000. Settlement-time behaviour of granular embankments. *Int. J. Numer. Anal. Methods Geomech*. 24, pp. 281–303.

Justo, L.J., Canete, P., Manzanares, L.J., Del Campo, J. & De Porsellinis, P. 1988. The upstream facing of Martin Gonzalo rockfill dam, *ICOLD, XVI Congress*, Q. 61, R. 45, San Francisco.

Kajakin, V.V. & Mulina, A.V. 1993. Socio-environmental monitoring at hydraulic works (in Russian). *Gidrotehnicheskoe stroiteljstvo*, Energoatomizdat, Moskva, No. 3.

Kalkani, C.E. 1989. Analysing seepage in an earth dam. *WP&DC*, February.

Karasawa, S., Shimazu, Y., Shirakawa, N. & Kuwashima, T. 1994. *A consideration on the behaviour of zoned rockfill dams*, *ICOLD, XVIII Congress, Q*. 68, *R*. 52, Durban.

Kawai, J., Aoe, J., Aoki, Y. & Tani, T. 1994. Seismic behaviour characteristics and safety evaluation of Nagara dam (zoned earth dam). *ICOLD, XVIII Congress, Q. 68, R. 53*, Durban.

Keming, C., Dafeng, F. & Shiyuan, Y. 1992. CHINA – The design of the Tianshenqiao concrete faced rockfill dam. *WP&DC*, April.

Kenney, T.C. & Westland, J. 1993. Laboratory study of segregation of granular filter materials. *Filters in Geotechnical and Hydraulic Engineering* (Eds: Brauns, Heibaum & Schuler). Balkema, Rotterdam, pp. 313–319, ISBN 9054103426.

Khalid, S. 1992. R*ockfill dams – finite element analysis to determine stresses and deformations in membrane type rockfill dam.* Central Board of Irrigation and Power, New Delhi, Rotterdam: A.A. Balkema.

Khalid, S., Singh, B., Nayak, C.G. & Jain, P.O. 1990. Nonlinear Analysis of Concrete Face Rockfill Dam. *JGE, ASCE*, Vol. 116, No. 5, May.

Khan, H.I. 1983. Failure of an Earth Dam: A Case Study. *JGE, ASCE*, Vol. 109, No. 2, Feb.

Khor, H.C. & Woo, K.H. 1989. Investigation of Crushed Rock Filters for Dam Embankment. *JGE, ASCE*, Vol. 115, No. 3, March.

Kikusawa, M. & Hasegawa, T. 1985. Analysis of Model Embankment Dam by Shaking Table Test. *Soils and Foundations*, The Japanese Society of Soil Mechanics and Foundation Engineering, Vol. 25, No. 1, March.

Kikusawa, M. 1990. Seismic stability analysis of rockfill dams, *Géotechnique*, Vol. XL, Number 2, June.

Kipping, W. 2001. Valves for bottom outlets of dams. Modern Techniques for Dams-Financing, Construction, operation, Risk Assessment; Proc. workshop, Vol. I, Dresden, 14 October 2001. Dresden.

Kjærnsli, B., Moum, J. & Torblaa, I. 1966. Laboratory test on asphaltic concrete for an impervious membrane on the Venemo rockfill dam. Norwegian Geotechnical Institute, Publication No. 69, Oslo, pp. 17–26.

Knight, J.D. & Mason, J.P. 1992. Lessons from the effects of earthquakes on dams. *WP&DC*, March.

Kofler, B. 2010. Automated Monitoring, Strategy and Procedure employed by Verbund-Austrian Hydro Power. *Proceedings of the 8th ICOLD European Club Symposium*, 22nd–23rd September 2010, Innsbruck, Austria, pp. 531–535.

Kokalanov, G. & Tančev, L. 1988. Finite element analysis of embankment dams. *Engineering modelling*, No. 1, Split.

Konrad, J.-M & Watts, D.B. 1995. Undrained shear strength for liquefaction flow failure analysis. *CGJ*, Vol. 32, No. 5, October.

Konrad, J.-M. 1990a. Minimum Undrained Strength of Two Sands. *JGE, ASCE*, Vol. 116, No. 6, June.

Konrad, J.-M. 1990b. Minimum Undrained Strength versus Steady-State Strength of Sands. *JGE, ASCE*, Vol. 116, No. 6, June.

Kulhawy, F., Duncan, J. 1972. Stresses and movements in Oroville Dam. *JSMFD, ASCE*, July.

Kulhawy, F., Gurtowski, T. 1976. Load Transfer and Hydraulic Fracturing in Zoned Dams, *JGE, ASCE*, Sept.

Kutzner, C. 1991. New criteria for rock grouting in Dam Engineering, ICOLD. *XVII Congress, Q. 66, R. 18*, Vienna.

Kutzner, C. 1997. *Earth and rockfill dams.* Rotterdam: A.A. Balkema.

Kuusiniemi, R., Loukola, E. & Maijala, T. 1994. Dam safety measures in Finland. *ICOLD, XVIII Congress, Q. 68, R. 73*, Durban.

Kuusiniemi, R., Pöllä, J. & Rathmayer, H. 1992. FINLAND – Internal erosion at the Uljua earth dam. *WP&DC*, March.

Laá Gomez, G. 1992. Experience with RCC dams in Spain. *WP&DC*, September.

Lafitte, R. 1989. Comment – Dam safety in relation to floods. *WP&DC*, April.

Lafitte, R. 1992. Comment – Progress in dam safety in relation to flood risks. *WP&DC*, Sept.

Lafuente, I.R., Pascual, Q.M. 2012. RCC dams in Spain's Ebro basin. *Hydropower & Dams*, Issue Five, 2012, pp. 76–81.

Langford, R.P. 1979. Leisure and sports Facilities at Rutland Water. *Journal of the Institution of Water Engineers and Scientists*, Vol. 33, No. 2, March, London.

Lapshenkov, S.V. 1989. *Design of hydraulic structures for undergraduate study and final work*. Moskva: Agropromizdat.

Larsen, S. 1994. Dam safety assessment in Norway. *ICOLD, XVIII Congress, C.16*, Durban.

Laschienov, J.S., Ryzhov, A.V., Rasskazov, N.L. & Zhelankin, G.V. 1994. Problems arising from staged construction of embankment dams. *ICOLD, XVIII Congress, Q. 70, R. 54*, Durban.

Laugier, F., Vermeulen, J., Pralong, J. & Blancher, B. 2013. Overview of new innovative labyrinth piano key weir spillways (PKW). *9th European Club Symposium*, 10–12 April, 2013, Venice, Italy, B.33.

Le Bel, Gérard 1981. Upstream Facing Interface with Foundation and Abutments. *ICOLD*, Bulletin 39, Paris.

Le Coroller, A., Bienaime, C., Herment, R., Poupart, M., Huynh, P., Crepel, M.J., Modaressi, A. & Bard, E. 1988. Approche par un modèle de calcul aux éléments finis du comportement des écrans internes en béton bitumineux. *ICOLD, XVI Congress*, *Q. 61, R. 54*, San Francisco.

Lee, H.F. & Foo, L.S. 1990. Undrained cyclic loading on a saturated dense sand stratum. *Géotechnique*, Vol. XL, Number 3, September, London.

Lefebvre, G., Duncan, J. & Wilson, E. 1973. Three-Dimensional Finite Element Analyses of Dams. *JSMFD, ASCE*, July.

Lempérière, F. & Ouamane, A. 2003. The Piano Keys weir: a new cost-effective solution for spillways, *The International Journal of Hydropower and Dams*, Volume Ten, Issue 5, 2003, pp. 144–149.

Lemperière, F. 1992. Overspill fusegates. *Water Power & Dam Construction*, 44, July, pp. 47–48.

Lempérière, F. 1999. Risk analysis: what sort should be applied and to which dams? *Hydropower and Dams*, International Hydropower Association. Issue Four: 128–132.

Lempérière, F. 2000. More cost data may help to optimize spillways, *The International Journal of Hydropower and Dams*, Volume Seven, Issue 4, 2000, pp. 132–138.

Lempérière, F., Vigny, J-P. & Ouamane, A. 2012. Promising future for P.K. Weirs, *The International Journal of Hydropower and Dam*, Volume Nineteen, Issue 2, pp. 90–93.

Lenehan, R.J. 1992. AUSTRALIA – The enlargement of the Pindari dam. *WP&DC*, April.

Leps, M.T. 1989. USA – The influence of possible fault offsets on dam design. *WP&DC*, April.

Leshchinsky, D. & San, K.-C. 1994. Pseudostatic seismic Stability of Slopes: design Charts. *JGE, ASCE*, Vol. 120, No. 9, Sept.

Leshchinsky, D. 1990. Slope Stability Analysis: Generalized Approach, *JGE, ASCE*, Vol. 116, No. 5, May.

Lewis, W.R. & Schrefler, A.B. 1998. *The Finite Element Method in the Static and Dynamic Deformation and Consolidation of Porous Media* (Second Edition). England: John Wiley & Sons Ltd.

Li, C.G. & Desai, S.C. 1983. Stress and Seepage Analyses of Earth Dams. *JGE, ASCE*, Vol. 109, July.

Lippert, L.T. & Hammer, G.G. 1989. USA – The use of a geomembrane in heightening the Pactola dam. *WP&DC*, February.

Liu Guang Ting, Peng Hui Li & Xie Shu Nan. 2002. RCC arch dams: Chinese research and practice, *The International Journal of Hydropower and Dams*, Volume Nine, Issue 3, 2002, pp. 95–98.

Ljather, V.M., Li, A.T. & Ivashenko, I.N. 1984. Earthquake stability of Nurek Dam (in Russian). *Gidrotehnicheskoe stroiteljstvo*, Energoatomizdat, Moskva, No. 12.

Lombardi, G. 1991. AUSTRIA – Kölnbrein dam: an unusual solution for an unusual problem. *WP&DC*, June.

Londe, P. & Lino, M. 1992. The faced symmetrical hardfill dam: a new concept for RCC dams. Water Power & Dam Construction, February 1992, pp. 19–24.

Long, T.J. & Bandeira, M.O. 2009. Construction of the Bakun dam: the world's second highest CFRD, *The International Journal of Hydropower and Dams*, Volume Sixteen, Issue 1, 2009, pp. 46–52.

Lotfi, V. 2001. Frequency domain analysis of concrete gravity dams including hydrodynamic effects. *Dam Engineering*, Volume XII, Issue 1, May, Reed Business Publishing: 33–53.

Low, B.-K. 1989. Stability Analysis of Embankments on Soft Ground. *JGE, ASCE*, Vol. 115, No. 2, Feb.

Majmaii, M. & Haj-Hasani, R.H. 1992. The evaluation of earth dam heightening problems. *WP&DC*, March.

Makdisi, I. Faiz & Seed, H.B. 1978. Simplified Procedure for Estimating Dam and Embankment Earthquake-Induced Deformations, *JGE, ASCE*, Vol. 104, No. 7, July.

Makdisi, I.F. & Seed, H.B. 1979. Simplified Procedure for Evaluating Embankment Response. *JGE, ASCE*, Vol. 105, No. 12, Dec.

Malik, I.Y. & Munir, J. 2011. Computation of plunge pool scour using different approaches. *The International Journal of Hydropower and Dams*, Volume Eighteen, Issue 5, pp. 84–91.

Mansouri, A.T., Nelson, D.J. & Thompson, G.E. 1983. Dynamic Response and Liquefaction of Earth Dams. *JGE, ASCE*, Vol. 109, No. 1, Jan.

Marachi, D.N., Chan, K.C. & Seed, B.H. 1972. Evaluation of Properties of Rockfill Materials. *JSMFD, ASCE*, January.

Marcuson, III F.W., Hadala, F.P. & Ledbetter, H.R. 1996. Seismic Rehabilitation of Earth Dams, *JGE, ASCE*, Vol. 122, No. 1, January.

Marheim, A., Hverven, V., Johansen, M.P., Lysne, K.D. & Jenssen, L. 1994. The unlined spillway tunnels at Virdnejavri Dam *ICOLD, XVIII Congress, Q. 71, R. 18*, Durban.

Marshall, E.B. 1994. Environmental impact assessment of major hydroelectric projects in the middle Zambezi river system. *ICOLD, XVIII Congress, Q. 69, R. 13*, Durban.

Martin, II R.G. & Clough, W.G. 1994. Seismic Parameters from Liquefaction Evidence. *JGE, ASCE*, Vol. 120, No. 8, August.

Marulanda, A., Amaya, R. & Ramirez, A.C. 1991. Colombian experience with concrete face rockfill dams. *WP&DC*, January.

Marulanda, A., Castro, A. & Rubiano, N.R. 2002. Miel I: a 188 m-high RCC dam in Colombia, *The International Journal of Hydropower and Dams*, Volume Nine, Issue 3, 2002, pp. 76–81.

Maslov, N.N. 1987. *Basic Engineering Geology and Soil Mechanics*. Moscow: Mir Publishers.

Mason, P.J, Hughes, R.A.N. & Molyneux, J.D. 2008. The design and construction of a faced symmetric hardfill dam. *Hydropower & Dams*, Issue Three, 2008, pp. 90–94.

Mason, P.J. 1989. Effects of Air Entrainment on Plunge Pool Scour. ASCE, *Journal o Hydraulic Division*, Vol. 115, No. 3.

Mason, P.J. 2011. Plunge pool scour: an update. *Hydropower & Dams*, Volume Eighteen, Issue 6, pp. 123–124.

Materon, B., Pitanga W. & Arfelli E. 1992. BRAZIL – Construction planning for the Xingó CFRD. *WP&DC*, April.

Matsumoto, N. 2010. The Resent Earthquakes and Dam Safety in Japan. *Proceedings of the 8th ICOLD European Club Symposium*, 22nd–23rd September 2010, Innsbruck, Austria, pp. 571–576.

Matsumoto, N., Yamabe, K., Sakamoto, T. & Hojo K. 2000. Seismic Response Analysis of CFRD. *Proceedings, International Symposium on Concrete Faced Rockfill Dams*. !8 September, Beijing, China: 351–360.

Matsumoto, N., Yoshida, H. & Kasai, T. 2011. Performance of the Ishibuchi CFRD during the Miyage earthquake, *The International Journal of Hydropower and Dams*, Volume Eighteen, Issue 1, pp. 52–55.

Matter, A.M. & Wegner, D. 1994. Assessing effects of Glen Canyon Dam on the Colorado River in Glen and Grand canyons for restoration and mitigation. *ICOLD, XVIII Congress, Q. 69, R. 47*, Durban.

Mattsson, H., Hellström, J.G.I. & Lundström, S.T. 2008. On Internal Erosion in Embankment Dams. *A literature survey of the phenomenon and the prospect to model it numerically*. Luleå University of Technology, pp. 54.

Mayne, W.P. 1985. A Review of Undrained Strength in Direct Simple Shear. *Soils and Foundations, JSSMFE*, Vol. 25, No. 3, Sept.

Mazhbic, G.L. & Bulanov, E.P. 1990. Hydraulic research of the spillway with chute channel (in Russian). *Gidrotehnicheskoe stroiteljstvo*, Energoatomizdat, Moskva, No. 11.

McLean, C.A. & Gribble, D.C. 2005. *Geology for Civil Engineers*. Second Edition, Taylor & Francis e-Library.

Mejia H.L., Seed B.H. & Lysmer J. 1982. Dynamic Analysis of Earth Dams in Three Dimensions. Journal of Geotechnical Engineering Division, Proceedings ASCE, Vol. 108, GT12, December, 1982.

Mejia, H.L. & Seed, H.B. 1983. Comparison of 2-D and 3-D Dynamic Analyses of Earth Dams. *JGE, ASCE*, Vol. 109, No. 11, Nov.

Mejia, H.L., Seed, H.B. & Lysmer, J. 1982. Dynamic Analyse of Earth Dams in Three Dimensions. *JGE, ASCE*, Vol. 108, No. 12, Dec.

Mendez, F. & Perez, A. 2007. The behaviour of a very high CFRD under first reservoir filling, *The International Journal of Hydropower and Dams*, Volume Fourteen, Issue 2, 2007, pp. 44–49.

Meyer, T. & Mouvet, L. 1995. Behaviour Analysis of the Vieux-Emosson Arch Gravity Dam under Thermal Loads. *Dam Engineering*, Volume VI, Issue 4, December, Reed Business Publishing.

Milligan, V. 2003. Some uncertainties in embankment dam engineering. *Journal of Geotechnical and Geoenvironmental Engineering*, ASCE, 129 (9), pp. 785–797.

Minor, E.H. & Schmidiger, R. 1988. Selection of spillway type giving special attention to safety aspects. *ICOLD, XVI Congress*, *Q. 63, R. 20*, San Francisco.

Misselhorn, G., Nel, P. & Wrigley, D. 1995. Plastic dams save screens. *WP&DC*, April.

Mitovski, S. 2013. Private communication.

Moiseev, I., Yakovlev, N., Goldin, A., Gorelic, G. & Radchenko, V. 1988. Rockfill dams with asphalt concrete diaphragms. *ICOLD, XVI Congress*, *Q. 61, R. 62*, San Francisco.

Mojs, P.P. 1970. *Shaft spillways* (in Russian). Moskva: Energiya.

Montañez-Cartaxo, E.L. 1992. MEXICO – The perimetric joint design for Aguamilpa dam. *WP&DC*, April.

Mori, T.R. & Pinto, De S.N. 1988. Analysis of deformations in concrete face rockfill dams to improve face movement prediction. *ICOLD, XVI Congress*, *Q. 61, R. 2*, San Francisco.

Moroz, A.J. & Shatravskij, A.I. 1994. Condition of the conduits at Sayano-Shushenska hydraulic scheme and questions concerning to their service (in Russian). *Gidrotehnicheskoe stroiteljstvo*, Energoatomizdat, Moskva, No. 4.

Moutafis, I.N. 2009. Face symmetrical hardfill dams – a review. *Proceedings of the Workshop: Advanced Methods and Materials for Dam Construction*, MACOLD, 3rd–4th September 2009, Skopje.

Moyseev, I. & Moyseev, S. 1977. *Rock-fill dams* (in Russian). Moskva: Energiya.

Nackler, K. & Tschernutter, P. 1992. AUSTRIA – Austria's second highest central asphaltic membrane at Feistritzbach dam. *WP&DC*, July.

Nagataki, S., Fujisawa, T. & Kawasaki, H. 2008. State of art of RCD dams in Japan. *1st Brazilian International RCC Symposium*, IBRACON, September, 2008.

Najmaii, M. & Haj-Hasani, R.H. 1992. The evaluation of earth dam heightening problems. *WP&DC*, March.

Nakai, T. 1985. Finite Element Computations for Active and Passive Earth Pressure Problems of Retaining Wall. *JSSMFE, Soils and Foundations*, Vol. 25, No. 3, Sept.

Nakamura, Y., Okumura, T., Narita, K. & Ohne, Y. 2004. Improvement of Impervious Asphalt Mixture for High Ductility against Earthquake Excitation. *Proceedings, 4th International Conference on Dam Engineering, Nanjing*, China; October 2004.

Navalon, N. & Gaztanaga, M.J. 1988. The lining of La Muela Upper Reservoir. *ICOLD, XVI Congress*, Q. 61, R. 51, San Francisco.

Naylor, D.J., Maranha das Neves, E., Mattar, D. & Veiga Pinto, A.A. 1986. Prediction of construction performance of Beliche dam. *Geotechnique*, Vol. 36 (3), pp. 359–376.

Naylor, D.J., Maranha, J.R., Maranha das Neves, E. & Veiga Pinto, A.A. 1997. A back-analysis of Beliche dam. *Geotechnique*, Vol. 47 (2), pp. 221–233.

Naylor, D.J., Tong, S.L. & Shahkarami, A.A. 1989. Numerical modelling of saturation shrinkage. *Proc. Numerical models in Geomechanics NUMOG III*, (Pietruszczak & Pande ed.) Amsterdam, Elsevier. pp. 636–648.

Nedriga, V.P. et al. 1983. *Hydraulic structures* (in Russian). Moskva: Strojizdat.

Neidert, H.S. & Toniatti, B.N. 1991. Design and construction of the Segredo concrete-faced rockfill dam. *WP&DC*, January.

Nejad, G.B., Phillip, S., Hossein, T. & Murphy, S.. 2010. Seismic Deformation Analysis of a Rockfill Dam with a Bituminous Concrete Core. *Materials Science and Engineering* 10 (2010) 012106.

Newmark, M.N. & Rosenblueth, E. 1971. *Fundamentals of earthquake engineering*. Prentice-Hall, INC.

Ng, T.-T. & Dobry, R. 1994. Numerical Simulations of Monotonic and Cyclic Loading of Granular Soil. *JGE, ASCE*, Vol. 120, No. 2, Feb.

Nichiporovich, A.A. 1973. *Embankment dams* (in Russian). Moskva: Strojizdat.

Nielsen, M.N. 1989. CANADA – Enhancing the safety of Strathcona dam. *WP&DC*, April.

Nikonov, A.A. 1993. Induced earthquakes during the reservoir filling (two examples from Tajikistan) (in Russian). *Gidrotehnicheskoe stroiteljstvo*, Energoatomizdat, Moskva, No. 3.

Nishigori, T. & Takimoto, J. 1991. Foundation treatment for alluvial deposits at Tadami dam. *ICOLD, XVII Congress, Q. 66, R. 24*, Vienna.

Nobari, E.S. & Duncan, J.M. 1972. Effect of reservoir filling on stresses and movements in earth and rockfill dams, *Report TE-72-1*, University of California, Department of Civil Engineering.

Nonveiller, Ervin 1979. *Soil Mechanics and Foundation Engineering* (in Croatian). Zagreb: Školska kniga.

Nonveiller, Ervin 1983. *Embankment dams* (in Croatian). Zagreb: Školska knjiga.

Nonveiller, Ervin 1989. *Grouting – theory and practice* (in Croatian). Zagreb: Školska knjiga.

Novak, P., Moffat, B.I.A., Nallury, & Narayanan, R. 2001. *Hydraulic Structures*, London: Spon Press.

Nuss, K.L., Matsumoto, N, Kenneth, D. Hansen, D.K. 2012. Shaken, But Not Stirred – Earthquake Performance of Concrete Dams, *United States Society on Dams*, April 2012.

Nuss, K.L., Payne, L.T. & Muller, C.B. 1994. Dynamic structural analyses of a multiple arch Bartlett dam – Phoenix, Arizona – USA. *ICOLD, XVIII Congress, Q. 68, R. 60*, Durban.

Oberti, G. 1991. The interconnection between concrete dam and foundations. *ICOLD, XVII Congress, Q. 66, R. 42*, Vienna.

Obrezkov, S.S. 1993. Asphaltic concrete cores at embankment dams (in Russian). *Gidrotehnicheskoe stroiteljstvo*, Energoatomizdat, Moskva, No. 11.

Ohmachi, T. 1994. Assessment of ultimate earthquake stability of rockfill dams with vertical clay core. *ICOLD, XVIII Congress, Q. 68, R. 50*, Durban.

Ohmachi, T. 2011. Change in the dynamic properties of a central clay core rockfill dam subhected to intense earthquake shaking, *The International Journal of Hydropower and Dams*, Volume Eighteen, Issue 1, pp. 47–51.

Okusa, S. & Anma, S. 1980. Slope failures and tailings dam damage in the 1978 Izu-Ohshima-Kinkai earthquake. Journal of Engineering Geology, No. 16.

Oldecop, L.A. & Alonso, E.E. 2001. A model for rockfill compressibility. *Géotechnique*, 51 (2), pp. 127–140.

Oldecop, L.A. & Alonso, E.E. 2007. Theoretical investigation of the time-dependent behaviour of rockfill. *Géotechnique*, 57 (3), pp. 289–301.
Orehov, V.G. 1990. Improvement of the calculation of the strength and the stability of high concrete dams (in Russian). *Gidrotehnicheskoe stroiteljstvo*, Energoatomizdat, Moskva, No. 9.
Paskalov, Trifun 2001. *Earthquake* (in Macedonian). Skopje: DINGD "Nashe Delo".
Patokov, Ivan et al. 1986. *Hydraulic structures* (in Bulgarian). Sofia: Tehnika.
Penman A.D.M. 2003. Major challenges in tailings dams, *The International Journal of Hydropower and Dams*, Volume Ten, Issue 3, 2003, pp. 92–97.
Penman, A. & Charles, A. 1973. Constructional Deformations in Rockfill Dam. *JSMFD, ASCE*, February.
Penman, A.D.M. & Charles, J.A. 1979. The Influence of their Interfaces on the Behaviour of Clay Cores in Embankment Dams. *ICOLD, XIII Congress, Q. 48, R. 39*, New Delhi.
Penman, A.D.M., Burland, J.B. & Charles, J.A. 1971. Observed and predicted deformations in a large embankment dam during construction. *Proceedings*, The Institution of Civil Engineers, London, May.
Penman, A.D.M., Saxena, K.R. & Sharma, V.M. 1999. *Instrumentation, Monitoring and Surveillance – Embankment Dams*. Rotterdam: A.A. Balkema.
Perez, H.J., Johannesson, P. & Stefansson, B. 2007. The Kárahnjúkar CFRD in Iceland instrumentation and first impoundment dam behavior. In: Proccedings, III Symposium on CFRDs-Honoring J. Barry Cooke, Florianópolis.
Pietruszczak, S. & Pande, N. G. 1996. Constitutive Relations for Partially Saturated Soils Containing Gas Inclusions. *JGE, ASCE*, Vol. 122, No. 1, January.
Pilarczyk, W.K. 2000. *Geosynthetics and Geosystems in Hydraulic and Coastal Engineering*. Rotterdam: A.A. Balkema.
Pinchard, T., Farges, L.J., Boutet, M.J., Lochu, A. & Laugier, F. 2013. Spillway capacity upgrade at Malarce dam: construction of an additional piano key weir spillway (PKW). *9th European Club Symposium*, 10–12 April, 2013, Venice, Italy, B.40
Pinto, De N.L. 2009. The design an construction of extra high CFRDs, *The International Journal of Hydropower and Dams*, Volume Sixteen, Issue 3, pp. 41–44.
Pinto, De S.N. & Mori, T.R. 1988. A new concept of a perimetric joint for concrete face rockfill dams. *ICOLD, XVI Congress*, *Q. 61, R. 3*, San Francisco.
Pinto, De S.N.L. 2008. Very high CFRDs: Behaviour and design features, *The International Journal of Hydropower and Dams*, Volume Fifteen, Issue 4, pp. 43–49.
Pinto, V.A., De Melo, G.F. & Ramos, M.C. 1988. Design criteria of upstream concrete facing rockfill dams. *ICOLD, XVI Congress*, *Q. 61, R. 47*, San Francisco.
Pircher, W. & Schwab, H. 1988. Design, construction and behaviour of the asphaltic concrete core wall on the Finstertal dam. *ICOLD, XVI Congress*, Q. 61, R. 49, San Francisco.
Pircher, W. 1993. 36000 dams and still more needed. *WP&DC*, May.
Pircher, W. 2001. Trends in dam surveillance. *Hydropower and Dams*, International Hydropower Association. Issue Three: 81–84.
Poceski, A. 1992. *Mixed Finite Element Method*. Berlin: Springer-Verlag.
Polimon, J., Jinsheng, J. & Berga, L. 2012. Zaragoza RCC Symposium will review technology and achievements. *Hydropower & Dams*, Issue Five, 2012, pp. 56–58.
Popovici, A. 2002. *Dams for water storage*, Vol. II (in Romanian). Teditura Technica, Bucureşti, p. 660.
Popovici, A., Ilinca, C. & Vârvorea R. 2013. Study on arch dam – reservoir seismic interaction. *12th International Benchmark Workshop on Numerical Analysis of Dams*, Graz, 2–4 October 2013.
Potts, M.D., Dounias, T.G. & Vaughan, R.P. 1990. Finite element analysis of progressive failure of Carsington embankment. *Géotechnique*, Vol. XL, Number 1, March.

Powledge, R. & Sveum, L.D. 1988. Overtopping embankment dams – an alternative in accommodating rare floods? *ICOLD, XVI Congress*, *Q. 63, R. 35*, San Francisco.
Provorova, T.P. 1995. Hydraulic calculation of energy disipation structures (in Russian). *Gidrotehnicheskoe stroiteljstvo*, Energoprogress, Moskva, No. 10, 1995.
Prusza, Z. 1994. Design and construction measures to avoid cavitation in a large spillway. *ICOLD, XVIII Congress, Q. 71, R. 15*, Durban.
Quintela, A.C., Pinheiro, A.N., Afonso, J.R. & Cordeiro, M.S. 2000. Gated spillways and free flow spillways with long crests. Portuguese dams experience. *XX ICOLD Congress, Q.79, R. 12*, Beijing, Volume IV: 171–190.
Radchenko, V.G. & Semenkov, V.M. 1993. Geomembranes at embankment dams (in Russian). *Gidrotehnicheskoe stroiteljstvo*, Energoatomizdat, Moskva, No. 10.
Rahardjo, H. & Fredlung, G.D. 1995. Experimental verification of the theory of consolidation for unsaturated soils. *CGJ*, Vol. 32, No. 5, October.
Rampino, C., Mancuso, C. & Vinale, F. 2000. Experimental behaviour and modelling of an unsaturated compacted soil. *Canadian Geotechnical Journal*, 37, pp. 748–763.
Razvan, E. 1992. The environmental impact of large dams. *WP&DC*, October.
Reinius, E. 1988. Stresses and cracks in the rock foundation of an earthfill dam. *WP&DC*, June.
Reinius, E. 1989. Statistical estimation of extreme flood flows using confidence intervals. *WP&DC*, April.
Renna, M.F., Zenocchini P., Guerini A., Fratino U. & Pagano A. 2013. Analyzing experimental data on Howell-Bunger valves. *Hydropower & Dams*, Volume Twenty, Issue 2, pp. 90–94.
Renner, J. 1994. Experiences in monitoring systems for dams with impervious core. *ICOLD, XVIII Congress, Q. 68, R. 4*, Durban.
Reséndiz, D., Romo, M. & Moreno, E. 1982. El Infiernillo and La Villita Dams: Seismic Behaviou. *JGE, ASCE*, Jan.
Rissler, P. 1994. Rehabilitation of existing gravity dams in Germany with respect to safety philosophy and economy. *ICOLD, XVIII Congress, Q. 68, R. 5*, Durban.
Rissler, P. 2001. Dimensioning of the design flood as part of a reservoir safety concept. *Hydropower and Dams*, International Hydropower Association. Issue Four: 98–105.
Roosta, M.R. & Alizadeh, A. 2012. Simulation of collapse settlement in rockfill material due to saturation. *International Journal of Civil Engineering*, Vol. 10, No. 2, June 2012, pp. 93–99.
Roovers, M. 1989. The removal, treatment and use of sediment from reservoirs. *WP&DC*, March.
Roth, H.W., Bureau, G. & Brodt, G. 1991. Pleasant Valley Dam: an approach to quantifying the effect of foundation liquefaction. *ICOLD, XVII Congress, Q. 66, R. 64*, Vienna.
Routh, D.C. 1988. The investigation, identification and repair of the asphaltic concrete facing of Winscar dam. *ICOLD, XVI Congress*, *Q. 61, R. 36*, San Francisco.
Rowe, P.W. 1963, Stress-dilatancy, earth pressure and slopes, *J. soil mech. and found. Div.*, ASCE, 89 (5), pp. 37–61.
Rozanov, N.N. 1983. *Embankment dams* (in Russian). Moskva: Strojizdat.
Rozanov, N.P. & Kubeckij, V.L. 1994. Condition of the dam and foundation of Sayanoshushenska dam and measures for improvement of its safety (in Russian). *Gidrotehnicheskoe stroiteljstvo*, Energoatomizdat, Moskva, m2, 1994.
Rozanov, N.P. et al. 1985 *Hydraulic structures* (in Russian). Moskva: Agropromizdat.
Rutschmann, P. & Volkart, P. 1988. Spillway chute aeration. *WP&DC*, January.
Sagar, A.T.B. 1995. ASCE Hydrogates Task Committee Design Guidelines for High-Head Gates. *JHE, ASCE*, Vol. 121, No. 12, Dec.
Saini, S.S. 1992. Seismic stability analysis of Dudhganga dam. *WP&DC*, March.
Sakamoto, T., Kuwahara, K., Nakamura, K. & Itoh, A. 1994. Research for and planning of measures against landslides around reservoirs. *ICOLD, XVIII Congress, Q. 68, R. 54*, Durban.
Salmon, M.G. & Hartford, D.N.D. 1995. Risk analysis for dam safety – part I. *WP&DC*, March.

Salmon, M.G. & Hartford, D.N.D. 1995. Risk analysis for dam safety – part II, WP&DC. April.
Sandilands, N.M. & Findlay, J.V. 2000. Development of a risk based approach to dam safety management. *XX ICOLD Congress, Q.76, R. 10*, Beijing, Volume I: 133–149.
Sarkaria, S.G. & Andriolo, R.F. 1995. Special factors in design of high RCC gravity dams, Part II. *WP&DC*, August.
Sarkaria, S.G. & Andriolo, R.F. 1995. Special factors in design of high RCC gravity dams, Part I. *WP&DC*, April.
Sarma, K.S. 1973. Stability Analyses of Embankments and slopes. *Géotechnique*, Vol. XXIII, Number 3, September, London.
Sarma, K.S. 1979. Stability Analysis of Embankments and Slopes. *JGE, ASCE*, Vol. 105, No. 12.
Sasaki, S., Kazusa, S. & Yanagawa, J. 1991. Aesthetic design on dam. *ICOLD, XVII Congress, Q. 64, R. 18*, Vienna.
Saville, T. Jr., Mc Clendon, E.W. & Cochran, L.A. 1962. Freeboard allowances for waves in inland reservoir, *Proc. ASCE*, New York, *Journal of the Waterways and Harbour Division*, WW2, May.
Savinov, O.A. et al. 1986. Earthquake stability of Nurek dam – some aspects (in Russian). *Gidrotehnicheskoe stroiteljstvo*, Energoatomizdat, Moskva, No. 5.
Saxegaard, H. 2012. Private communication.
Saxena, K.S., Ger, M.A. & Sengupta, A. 1988. Reservoir Induced Seismicity n A New Model. *IJNAMG*, Vol. 12, No. 3, May–June.
Scavia, C. 1995. A method for the study of crack propagation in rock structures. *Géotechnique*, Vol. XLV, Number 3, September, London.
Schenk, V. 1988. Monitoring aspects of two embankment dams with bituminous impervious elements in the Federal Republic of Germany. *ICOLD, XVI Congress*, *Q. 61, R. 42*, San Francisco.
Schewe, L. 1990. Design and construction of concrete facings for embankment dams. *WP&DC*, March.
Schmid, R. & Frohnauer, R. 2001. Asphalt sealing in hydraulic structures – modern technique based on long experience. Modern Techniques for Dams-Financing, Construction, operation, Risk Assessment; Proc. workshop, Vol. I, Dresden, 14 October 2001. Dresden.
Schnitter, J.N. 1976. The evolution of the arch dam. *WP&DC*, Oct.
Schnitter, J.N. 1994. *A History of Dams*. Rotterdam: A.A. Balkema.
Schober, W. 1988. A study on the behaviour of embankment dams with diaphragms. *ICOLD, XVI Congress*, *Q. 61, R. 53*, San Francisco.
Schober, W. 1991. Concrete core diaphragm wall with bituminous slip layer. *Innovations in fill dam sealing elements*, University of Innsbruck.
Schober, W., Hupfauf, B. & Hechenblaickner, K. 1994. The prestressed dam – a new approach to safety in embankment dams. *ICOLD, XVIII Congress*, C.17, Durban.
Schrader, H.E. & Namikas, D. 1988. Performance of roller compacted concrete dams. *ICOLD, XVI Congress*, *Q. 62, R. 19*, San Francisco.
Schrader, K.E. 2004. Roller-Compacted Concrete: Understanding the Mix. *HRW*, December 2004.
Schulman, L.R., Krauch, W.H., Zaleski, M.J., Szpilman, A., Emerson, M.W. & Piasentin, C. 1988. Itaipu project spillway behaviour during the maximum recorded flood. *ICOLD, XVI Congress*, *Q. 63, R. 74*, San Francisco.
Scuero, A. & Vaschetti, G. 2013. PVC geomembranes in pumped storage schemes. *9th European Club Symposium*, 10–12 April, 2013, Venice, Italy, B.1.
Scuero, M. A. & Vaschetti, L.G. 2011. Geomembrane systems for watertighness of new fill dams. *Proceedings of the 6th International Conference on Dam Engineering*, 15 – 17 February 2011, Lisbon, Portugal, pp. 1119–1138.
Seed, B.H., Idriss, M.I. & Arango, I. 1983. Evaluation of Liquefaction Potential Using Field Performance Data. *JGE, ASCE*, Vol. 109, No. 3, March.

Seed, H.B. 1973. Stability of Earth and Rockfill Dams during Earthquakes. In *Embankment-Dam Engineering*, Casagrande Volume, New York: John Wiley & Sons.
Seed, H.B. 1979. Considerations in the earthquake-resistant design of earth and rockfill dams. *Géotechnique*, Vol. XXIX, Number 3, March, London.
Seed, H.B. 1987. Design Problems in Soil Liquefaction. *JGE, ASCE*, Vol. 113, No. 8, August.
Seed, H.B., Makdisi, I.F. & Alba De Pedro 1978. Performance of Earth Dams during Earthquakes. *JGE, ASCE*, Vol. 104, No. 7, July.
Sehgal, K.C. 1996. Design Guidelines for Spillway Gates. *JHE, ASCE*, Vol. 122, No. 3, March.
Seid-Karbasi, M. & Byrne P.M. 2004. Embankment dams and earthquakes. *Hydropower & Dams*, Issue Two, 2004.
Seleznev, S.V. 1988. *New structures of high-head gates* (in Russian). Moskva: Energoatomizdat.
Seleznev, S.V., Klimov, S.M. & Vaulina O.B. 1982. Some particularities of the exploitation of the mechanical equipment of the hydraulic scheme Krasnoyarsk (in Russian). *Gidrotehnicheskoe stroiteljstvo*, Energoizdat, Moskva, No. 2.
Sembenelli, G.P. &, Sembenelli, G. 2013. New Developments in Upstream Polymer Liners for Granular Dams. *9th European Club Symposium*, 10–12 April, 2013, Venice, Italy, B52.
Serafim, L.J. & Clough, W. R. 1990. *Arch Dams*. Rotterdam: A. A. Balkema.
Serafim, L.J. & Coutinho-Rodrigues, M.J. 1989. Statistics of dam failure: a preliminary report. *WP&DC*, April.
Serafim, L.J. 1988. New development in the construction of concrete dams. *ICOLD, XVI Congress*, *Q. 62, GR*., San Francisco.
Serrano, M.T., Soria, L.J. & Mieza, A. 1988. Behaviour of Sallente dam. *ICOLD, XVI Congress*, C.16, San Francisco.
Shalaby, M.A. 1991. Foundation soil consolidation for High Aswan Dam. *ICOLD, XVII Congress, Q. 66, R. 3*, Vienna.
Sharma, D.H., Nayak, C.G. & Maheshwari, B.J. 1976. Generalization of sequential Nonlinear Analysis – A study of Rockfill Dam with Joint Elements. *Proceedings of the Second Intern. Conference on Numerical Methods in Geomechanics*, Blacksburg, Vol. II.
Sharma, D.H., Nayak, C.G. & Maheshwari, B.J. 1979. Nonlinear Analysis of a high Rockfill Dam with earth Core. *ICOLD, XIII Congress, Q.48*, New Delhi.
Sharma, P.R., Jackson, E.H., Hastig, D.J. & Davis, L.W. 1994. Deterministic forecasting model and retrofit instrumentation for safety monitoring of Boundary dam. *ICOLD, XVIII Congress, Q*. 68, *R*. 62, Durban.
Sheng, D., Fredlund, D.G. & Gens, A. 2008. A new modeling approach for unsaturated soils using independent stress variables. *Canadian Geotechnical Journal*, 45, pp. 511–534.
Shenouda, K.W. 1991. Comparison between observed and calculated settlement of High Aswan Dam. *ICOLD, XVII Congress, Q*. 66, *R*. 46, Vienna.
Sherard L.J. 1973. Embankment Dam Cracking. In *Embankment-Dam Engineering*, Casagrande Volume, New York: John Wiley & Sons.
Sherard, J., Woodward, R., Gizienski, S., Clevenger, W. 1963. *Earth and Earth-Rock Dams*. John Wiley & Sons, Inc.
Sherard, L.J. 1986. Hydraulic Fracturing in Embankment Dams. *JGE, ASCE*, Vol. 112, No. 10, Oct.
Shroff, V.A. & Shah, L.D. 1993. *Grouting Technology in Tunnelling and Dam Construction*. Rotterdam: A.A. Balkema.
Shuljman, G.S. 1976. *Earthquake stability of hydraulic structures calculating the influence of the reservoir* (in Russian). Moskva: Energiya.
Sieber, H.U. 2000. Hazard and risk assessment considerations in German standards for dams – Present situation and suggestions. *XX ICOLD Congress, Q.76, R. 43*, Beijing, Volume I: 669–690.
Silveira, F.A., Pina, B.A.C., Costa, P.A.C. & Direito, T.F. 1991. Influence of foundation heterogeneity on safety of arch dams. *ICOLD, XVII Congress, Q. 66, R. 76*, Vienna.

Sing, B., Sharma, D.H. 1976. *Earth and Rockfill Dams*. Meerut: Sarita Prakashan.
Singh, B. & Varshney S.R. 1995. *Engineering for Embankment Dams*, Rotterdam-Brookfield: A. A. Balkema.
Skermer, N.A. 1973. Finite Element Analysis of El Infiernillo Dam. *CGJ*, Vol. 10, No. 2, May.
Skryljnikov, V.A. 1988. Calculation of reservoir sedimentation (in Russian). *Gidrotehnicheskoe stroiteljstvo*, Energoatomizdat, Moskva, No. 8.
Smith, C. L., Macpherson, H. H. & Oechsel, G. R. 1988. Long term performance asphalt lined Upper reservoir Seneca pumped storage station. *ICOLD, XVI Congress*, *Q.61, R. 27*, San Francisco.
Smith, Norman 1971. *A History of Dams*. London: Peter Davies.
Smith, Norman 1992. *The Heritage of Spanish Dams*. Spanish Committee on Large Dams, Madrid.
Sobrinho, A.J, Xavier, V.L., Albertoni, C.S., Correa, C. & Fernandes, R. 2007. Performance and concrete face repair at Campos Novos, *The International Journal of Hydropower and Dams*, Volume Fourteen, Issue 2, 2007, pp. 39–42.
Solvik, Ø. & Skoglund, M. 1994. Some leakage and overtopping problems regarding rockfill dams with central core. *ICOLD, XVIII Congress, Q. 68, R. 48*, Durban.
Søreide, O.K., Nordal, S. & Bonnier, P.G. 2002. An implicit friction hardening model for soil materials. In: Mestat (ed.), *Numerical Methods in Geotechnical Engineering* (NUMGE), pp. 155–161.
Soriano, A., Sanchez, F. J. & Serrano, C. 1990. Simulation of wetting deformations of rockfills. *Proc. 2nd Eur. Conf. on Numer. Methods in Geotech. Engng*, Santander, pp. 495–517.
Squier, L.R. 1970. Load Transfer in Earth & Rockfill Dams. *JSMFD, ASCE*, Jan.
Stark, D.T. & Olson, M.S. 1995. Liquefaction Resistance Using CPT and Field Histories. *JGE, ASCE*, Vol. 121, No. 12, Dec.
Stark, D.T., Ebeling, M.R. & Vettel, J.J. 1994. Hyperbolic Stress-Strain Parameters for Silts. *JGE, ASCE*, Vol. 120, No. 2, Feb.
Stematiu, D., Popescu, R. & Luca, E. 1991. Contact clay problems during the erection of Maru dam. *WP&DC*, April.
Stephenson, David 1978. Drawdown in embankments. *Géotechnique*, Vol. XXVIII, Number 3, September, London.
Stephenson, David 1979. *Rockfill in Hydraulic Engineering*. Elsevier Scientific Publ. Comp.
Sterenberg, J. 1992. The RCC technique: a perfect integration in the field of gravity dams, *WP&DC*, February.
Straubhaar, R., Feuz, B. & Haegeli, H. 1994. Rising of Mauvoisin Dam general aspects and treatment of the interface between the old and new section. *ICOLD, XVIII Congress, Q. 70, R. 3*, Durban.
Sutherland, B.H. 1988. Uplift resistance of soils. *Géotechnique*, Vol. XXXVIII, Number 4, December, London.
Swoboda, G. & Lei, Y.X. 1994. Simulation of Arch DamnFoundation Interaction with a new friction Interface Element. *IJNAMG*, Vol. 18, No. 9, January.
Taboada-Urtuzuastegui, V.M. & Dobry, R. 1995. Centrifuge modeling of earthquake-induced lateral spreading in sand, *Journal of Geotechnical Engineering*, ASCE, 124 (12).
Takahi, K., Kimoto, E. & Kanwo, S. 1991. Design and construction of an earthfill dam on sandy foundation. *ICOLD, XVII Congress, Q. 66, R. 22*, Vienna.
Takasu, S. & Yamaguchi, J. 1988. Principle for selecting type of spillway for flood control dams in Japan. *ICOLD, XVI Congress*, *Q. 63, R. 19*, San Francisco.
Takebayashi, S. & Takasu, S. 1994. Historical development and design method of reservoir sediment flushing facilities in Japan, *ICOLD, XVIII Congress, Q. 71, R. 28*, Durban.
Talbot, R.J. 1994. Earth spillway performance and damage assessment – a ten year study. *ICOLD, XVIII Congress, Q. 71, R. 29*, Durban.

Tančev, L. & Kokalanov, G. 1988. Application of joint elements at analysis of embankment dams with finite element method (in Macedonian). *Proceedings*, Faculty of Civil Engineering, Skopje.

Tančev, L. & Kokalanov, G. 1989. Deformations and stability of an embankment dam constructed in several stages (in Macedonian). *XIV Congress of YNCOLD*, Part 1, Struga.

Tančev, L. & Kokalanov, G. 1995. Application of joint elements at finite element analysis of embankment dams. *Second International conference on Computational Methods in Contact Mechanics*, Ferrara.

Tančev, L. & Milevski, S. 2009. Long-term behaviour of Tikvesh Dam. *Proceedings of the 2nd International Conference on Long Term Behaviour of Dams*, 12th–13th October 2009, Graz, Austria, pp. 911–916.

Tančev, L. 1981. Asphaltic concrete linings at embankment dams (in Macedonian). *Association of Civil Engineers of Macedonia*, Bulletin No. 8 and 9, Skopje.

Tančev, L. 1982. Choice of impervious element at embankment dams (in Macedonian). *Proceedings*, Faculty of Civil Engineering, University "St. Cyril and Methodius", Skopje.

Tančev, L. 1985. Embankment dams with asphaltic concrete core, Part I an II (in Macedonian). Faculty of Civil Engineering, Skopje, *Proceedings*, Skopje.

Tančev, L. 1989. *Static analysis of embankment dams* (in Macedonian). Skopje: Studentski zbor.

Tančev, L. 1992. *Hydraulic structures* (in Macedonian). Skopje: University "St. Cyril and Methodius".

Tančev, L. 1995. Dam project management – an extremely complex process (in Macedonian). *First Macedonian symposium of project management*, Struga, September.

Tančev, L. 1996. Some aspects of dam's legislation (in Macedonian). *First symposium for water economy*, Struga, March.

Tančev, L., Kokalanov, G. & Petkovski, L. 2007. Three Dimensional Analysis îf Kozyak Dam, *Fifth International Conference on Dam Engineering*, Lisbon, 14–16 February 2007, pp. 585–693.

Tančev, L., Kokalanov, G., Poceski, A., Petkovski, L. & Manchevski, D. 1991. *Static and dynamic analysis of Gradec dam* (in Macedonian). Skopje: Faculty of Civil engineering.

Tanchev, L., Petkovski, L. & Mitovski, S. Dam construction practice in Macedonia – past, present, future, *Proceedings of the Symposium SLOCOLD-MACOLD*, Skopje, 17 November 2011.

Tanchev, L., Petkovski, L., Mihajlovski, S. & Mitovski, S. Knezevo Dam – a key structure of the Hydro-System Zletovica, *Proceedings of the Workshop: Advanced Methods and Materials for Dam Construction*, MACOLD, 3rd–4th September 2009, Skopje, pp. 55–77.

Taylor, W. D. 1948. *Fundamentals of Soil Mechanics*. London: John Wiley & Sons.

Tejteljbaum, I.A., Meljnik, G.V. & Savvina, A.V. 1975. Cracks in the cores and screens at earth-rock dams (in Russian). Moskva: Strojizdat.

Teleshev, V.I. 1982. Methods of construction of high concrete dams and their improvement (in Russian). *Gidrotehnicheskoe stroiteljstvo*, Energoizdat, Moskva, No. 10.

Terzaghi, K. 1960. From Theory to Practice in Soil Mechanics. John Wiley & Sons Inc, p. 425.

Thomas, H.H. 1976. *The Engineering of Large Dams*. Part I and II, John Wiley & Sons.

Torales, A.M., Villalon, O., Szpilman, A., Cardozo, F., Rosso, A.J., Piasentin, C. & Fiorini, S.A. 1994. Itaipu spillway deterioration and maintenance after 10 years of operation. *ICOLD, XVIII Congress, Q. 71, R. 38*, Durban.

Torres, C.J., Moran, C.J. & Martinez, M.E. 2000. Factors to be considered when deciding lateral spillways with or without gates. Special consideration to labyrinth spillway type. *XX ICOLD Congress, Q.79, R. 5*, Beijing, Volume IV: 67–76.

Tortajada, C., Altinbilek, D. & Biswas, K. A. (Eds). 2012. *Impacts of Large Dams: A Global Assessment*. Springer, p. 407.

Tørum, A. 1994. Stability of upstream face of rockfill dams against wind generated waves. *ICOLD, XVIII Congress, Q. 68, R. 37*, Durban.
Truscott, G.E. & Traves, H.N. 1988. Two rockfill dams with thin gunite faces – 30 years experience. *ICOLD, XVI Congress*, *Q. 61, R. 16*, San Francisco.
Tschernutter, P 2009. Influence of Soft Rock-Fill Material as Dam Embankment with a Central Bituminous Concrete Membrane. *Proceedings of the 2nd International Conference on Long Term Behaviour of Dams*, 12th–13th October 2009, Graz, Austria, pp. 305–310
Tschernutter, P. 1988. Experience gained with asphaltic concrete facings on high-level embankment dams of the Fragant group of power schemes. *ICOLD, XVI Congress*, Q. 61, R. 59, San Francisco.
Tsokodayi, M.C., Mazvidza, Z.D. & Gurukumba, K. 1996. Securing spillways at the Kariba Dam. *WP&DC*, January.
Tullis, J. P., Amanian, N. & Waldron, D. 1995. Design of Labyrinth Spillways, *Journal of Hydraulic Engineering*, ASCE 121 (3): March 1995.
Uddin, N. & Gazetas, G. 1995. Dynamic response of Concrete-Faced Rockfill Dams to Strong Seismic Excitation. *JGE, ASCE*, Vol. 121, No. 2, Feb.
Urech, M. & Gilg, B. 1988. Conditions for a successful raising of a concrete arch dam as illustrated for the 250 m high Mauvoisin arch dam in Switzerland. *ICOLD, XVI Congress, Q. 62, R. 13*, San Francisco.
USBR 1976. *Design of Gravity Dams* Denver, USA.
USBR 1977a. *Design of Arch Dams*. Denver, USA.
USBR 1977b. *Design of small Dams*. Washington, USA.
USBR 2011. *Design standard No. 13, Embankment Dams*, Chapter 4: Static Stability Analysis, U.S. Department of the Interior, Bureau of Reclamation, October 2011.
USCOLD 1988. *Development of Dam Engineering in the United States*. San Francisco, USA.
USSD 2008. *Numerical models for seismic evaluation of concrete dams: review, evaluation and interpretation of results*, Denver, Colorado.
Vaid, P.Y. & Thomas, J. 1995. Liquefaction and Postliquefaction Behaviour of Sand. *JGE, ASCE*, Vol. 121, No. 2, Feb.
Vallejo, E.L. 1995. Fractal analysis of granular materials. *Géotechnique*, Vol. XLV, Number 1, March, London.
Valstad, T., Selnes, B.P., Nadim, F. & Aspen, B. 1991. Seismic response of a rockfill dams with an asphaltic concrete core. *WP&DC*, April.
Van Asbeck, F.W. 1962. *Le bitume dans les travaux hydrauliques*, Paris.
Van Mier, M.G. Jan 2013. *Concrete fracture: a multiscale apptoach*. CRC Press, Taylor & Francis Group. p. 357.
Vaschetti L.G. & Scuero A. 2009. Use of geomembranes for new construction and rehabilitation of h draulic structures, *Proceedings of the Workshop: Advanced Methods and Materials for Dam Construction*, MACOLD, 3rd–4th September 2009, Skopje.
Vaughan, P. R. & Soares, H. F. 1982. Design of filters for clay cores of dams. *Transactions of the American Society of Civil Engineers*, 108 (6T, 1) pp. 17–321.
Vaughan, R.P. 1994. Assumption, prediction and reality in geotechnical engineering. *Géotechnique*, Vol. XLIV, Number 4, December, London.
Vaughan, R.P., Johnston A.T. & Chalmers, W.R. 1991. *Foundation conditions at the reconstructed Carsington Dam*, *ICOLD, XVII Congress, Q. 66, R. 82*, Vienna.
Veiga Pinto, A.A. 1983. Previsao do comportamento estrutural de barragens de aterro. *Thesis*, LNEC, Lisbon.
Veltrop, A.J. 1991. Water, dams and hydropower in the coming decades. *WP&DC*, June.
Verruijt, A. 2012. *Soil Mechanics*. Delft University of Technology, Netherlands.
Vick, G.S. 1990. *Planning, Design and Analysis of Tailings Dams*. Bi Tech Publishers Limited, p. 369.

Vischer, D. & Rutschmann, P. 1988. Spillway facilities: topology and general safety questions. *ICOLD, XVI Congress*, *Q. 63, R. 23*, San Francisco.
Vladut, T. 1993. Environmental aspects of reservoir induced seismicity. *WP&DC*, May.
Volpe, L.R., Ahlgren, S.C. & Goodman, E.R. 1991. Selection of engineering properties for geologically variable foundations, *ICOLD, XVII Congress, Q. 66, R. 59*, Vienna.
Vrymoed, J. 1981. Dynamic FEM Model of Oroville Dam. Journal of Geotechnical Engineering Division, Proceedings ASCE, Vol. 107, GT8, August, 1981.
Vysockiy, I.L. 1977. *Control of high-speed flow at spillways* (in Russian). Moskva: Energiya.
Wahlstrom, E.E. 1974. *Dams, Dam Foundations, and Reservoir Sites*. Amsterdam-Oxford-New York: Elsevier Scientific Publishing Company.
Walz, H.A. 1989. Automated data management for dam safety evaluations. *WP&DC*, April.
Wang, W. & Höeg, K. 2010. Developments in the design and construction of asphalt core dams. *Hydropower & Dams*, Volume Seventeen, Issue Three, pp. 83–91.
Wang, Y., Chen, J. & Shen, Y. 1988. Xibeikou concrete face rockfill dam. *ICOLD, XVI Congress, Q. 61, R. 57*, San Francisco.
Wark, J.R. & Mann, B.G. 1992. AUSTRALIA – Design and construction aspects of New Victoria dam. *WP&DC*, February.
Weinhold, R. & Haug, W. 1988. The influence of large deformations on asphaltic cores and membranes – examples of the rockfill dams of Breitenbach and Prims reservoirs. *ICOLD, XVI Congress*, *Q. 61, R. 22*, San Francisco.
Wieland, M. & Ahlehagh, S. 2013. Dynamic stability analysis of a gravity dam subject to the safety evaluation earthquake. *9th European Club Symposium*, 10–12 April, 2013, Venice, Italy, B.63
Wieland, M. & Brenner, P. R. 2004. Earthquake aspects of roller compacted concrete and concrete-face rockfill dams. *13th World Conference on Earthquake Engineering*, Vancouver, Canada, August 1–6, 2004, Paper No. 3399.
Wieland, M. & Malla S. 2000. Earthquake Safety of an Arch-Gravity Dam with a Horizontal Crack in the Upper Portion of the Dam. *Proceedings, 12th World Conference on Earthquake Engineering*, Auckland, New Zealand, Jan. 31 – Feb. 4, 2000.
Wieland, M. 2010. CFRDs in highly seismic regions. *International Water Power & Dam Construction*, March 2010.
Wieland, M. 2011. Seismic Safety of Large Storage Dams. *High-level Forum on Safe Construction and Risk Management of High Dams and Large Reservoirs*, Beijing, August 2011.
Wieland, M., Aemmer, M & Ruoss, R. 2008. Designs aspects of Deriner dam. www.waterpowermagazine.com, July 2008, pp. 19–34.
Wilson, D.S. 1973. Deformations of Earth and Rockfill Dams. In *Embankment-Dam Engineering*, Casagrande Volume, New York: John Wiley & Sons.
Wilson, M.E. 1977. *Engineering Hydrology*, London and Basingstoke: The Macmillan Press LTD.
World Atlas 2012. *The International Journal of Hydropower and Dams*, Aqua-Media International Ltd.
WP&DC 1989. *Geosynthetics in dam construction*, February.
WP&DC, *Handbook 2000*, Reed Business Publishing.
Wright, S.G., Kulhawy, H.F. & Duncan, M.J. 1973. Accuracy of Equilibrium Slope Stability Analyses. *JSMFD, ASCE*, October.
WU Meng Xi, DU Bin, YAO Yuan Cheng & HE Xian Feng. 2011. An experimental study on stress-strain behavior and constitutive model of hardfill material. *Science China, Physics, Mechanics and Astronomy*, November (2011) Vol. 54, No. 11, pp. 2016–2024.
Xavier, V.L., Albertoni, C.S., Pereira, F.R. & Antunes, J. 2008. Behaviour and treatment of Campos Novos dam during second impounding, *The International Journal of Hydropower and Dams*, Volume Fifteen, Issue 4, pp. 53–58.

Xiong K., Weng H. Y., & He L. Y. 2013. Seismic failure modes and seismic safety of hardfill dam. Water Science and Engineering, Apr. 2013, Vol. 6, No. 2, pp. 199–214.
Xiurun, G. 1981. Non-Linear Analysis of a Joint Element and its Application in Rock Engineering. *IJNAMG*, Vol. 5, No. 3, July–September.
Yamaguchi, Y., Hall, R., Sasaki, S., Matheu, E., Kanenawa, I. K., Chudgar, A. & Yule, D. 2004. Seismic performance evaluation of concrete gravity dams. *13th World Conference on Earthquake Engineering*, Vancouver, Canada, August 1–6, 2004, Paper No. 1068.
Yang, Q., Sun, Z. & Ding, P. 1988. Asphalt concrete facing for rockfill dams built by directional blasting. *ICOLD, XVI Congress*, *Q. 61, R. 58*, San Francisco.
YCOLD 1970. *Dams in Macedonia*. Skopje: Yugoslav Committee on Large Dams.
YCOLD 1971. *Dams in Yugoslavia*. Belgrade: Yugoslav Committee on Large Dams.
Yegian, K.M., Ghagraman, G.V. & Harutiunyan, N.R. 1994. Liquefaction and Embankment failure Case Histories, 1988 Armenia Earthquake. *JGE, ASCE*, Vol. 120, No. 3, March.
Yevgjevic, V. 2001. Private communication.
Yildiz, D. & Üzücek, E. 1996. Modelling the performance of labyrinth spillways. *Hydropower and Dams*, Issue Three.
Yıldız, E & Gürdil, F.A. 2012. Review on Seismic Design of Concrete Gravity or RCC Dams with Design Examples. *15 World Conference on Earthquake Engineering*, Lisboa.
Yildiz, I. & Yildiz, G. 1994. Modification of Kürtün Dam project as a result of foundation problems encountered during construction. *ICOLD, XVIII Congress, Q. 70, R. 11*, Durban.
Youd, L.T. & Bennett, J.M. 1983. Liquefaction Sites, Imperial Valley, California. *JGE, ASCE*, Vol. 109, No. 3, March.
Youd, L.T., Idriss, I.M., Andrus, R., et.al. 2001. Liquefaction resistance of soils, summary report from the 1996 NCEER and 1998 NCEER/NSF workshops on evaluation of liquefaction resistance of soils. *Journal of Geotechnical and Geoenvironmental Engineering*, ASCE, 127 (10).
Zeghal, M. & Elgamal, A.-W. 1994. Analysis of Site Liquefaction Using Earthquake Records. *JGE, ASCE*, Vol. 120, No. 6, June.
Zeping Xu, 2009. Numerical Analysis and its Aoolications, *in the book: Concrete Face Rockfill Dams* (Cruz, T.P., Materon, B. & Manoel, F. 2009).
Zeping Xu, 2009. Performance of the Zipingpu CFRD during the Wenchuan earthquake, *The International Journal of Hydropower and Dams*, Volume Sixteen, Issue 3, pp. 89–82.
Zeydan, A.B. 2013. Seismic Dam-Reservoir Interaction of Concrete Gravity Dams. *9th European Club Symposium*, 10–12 April, 2013, Venice, Italy, B.62.
Zhu, B. 2001. Optimum central angle of arch dam. *Dam Engineering*, Volume XII, Issue 1, May, Reed Business Publishing: 21–31.
Zhu, Bofang & Xu, Ping 1995. Thermal Stresses in Roller Compacted Concrete Gravity Dams, *Dam Engineering*, Volume VI, Issue 3, September, Reed Business Publishing.
Zienkiewicz, C.O. 1977. *The Finite Element Method*, third edition. England: McGraw-Hill Book Company.
Zienkiewicz, C.O., Clough, W.R. & Seed, B.H. 1986. Static Analysis of Embankment Dams. *ICOLD, Bulletin 52*, Paris.
Zuccoli, Scalabrini, C. & Scuero, A. 1989. ITALY – The use of a geomembrane for an arch dam repair. *WP&DC*, February.

This page intentionally left blank

This page intentionally left blank

This page intentionally left blank

Dams and Appurtenant Hydraulic Structures, now in its second edition, provides a comprehensive and complete overview of all kinds of dams and appurtenant hydraulic structures throughout the world.

The reader is guided through different aspects of dams and appurtenant hydraulic structures in 35 chapters, which are subdivided in five themes:

I. Dams and appurtenant hydraulic structures – General;
II. Embankment dams;
III. Concrete dams;
IV. Hydromechanical equipment and appurtenant hydraulic structures;
V. Hydraulic schemes.

Subjects treated are general questions, design, construction, surveillance, maintenance and reconstruction of various embankment and concrete dams, hydromechanical equipment, spillway structures, bottom outlets, special hydraulic structures, composition of structures in river hydraulic schemes, reservoirs, environmental effects of river hydraulic schemes and reservoirs and environmental protection. Special attention is paid to advanced methods of static and dynamic analysis of embankment dams.

The wealth of experience gained by the author over the course of 35 years of research and practice is incorporated in this richly-illustrated, fully revised, updated and expanded edition. For the original Macedonian edition of **Dams and Appurtenant Hydraulic Structures**, Ljubomir Tanchev was awarded the Goce Delchev Prize, the highest state prize for achievements in science in the Republic of Macedonia.

This work is intended for senior students, researchers and professionals in civil, hydraulic and environmental engineering and dam construction and exploitation.

Ljubomir Tanchev is a retired Professor in Dams and Hydraulic Structures (Faculty of Civil Engineering at the Ss. Cyril and Methodius University in Skopje, Republic of Macedonia). In addition, he has been involved in many hydraulic engineering projects as a designer, consultant, and supervisor. Since June 2013 he is Honorary President of the Macedonian Committee on Large Dams (MACOLD).

CRC Press
Taylor & Francis Group
an **informa** business
www.crcpress.com

6000 Broken Sound Parkway, NW
Suite 300, Boca Raton, FL 33487
Schipholweg 107C
2316 XC Leiden, NL
2 Park Square, Milton Park
Abingdon, Oxon OX14 4RN, UK

ISBN 978-1-138-00006-3
9 781138 000063
an **informa** business